TRANSITION METAL-CATALYZED ENANTIOSELECTIVE C-ALKYLATION OF NITROALKANES AND TRIFLUOROMETHYLATION OF NITROALKANES

by

Vijayarajan Devannah

A dissertation submitted to the Faculty of the University of Delaware in partial fulfillment of the requirements for the degree of Doctor of Philosophy in Chemistry & Biochemistry

Spring 2018

TRANSITION METAL-CATALYZED

ENANTIOSELECTIVE C-ALKYLATION OF NITROALKANES

AND TRIFLUOROMETHYLATION OF NITROALKANES

by

Vijayarajan Devannah

Approved: _____

Brian J. Bahnson, Ph.D.
Chair of the Department of Chemistry & Biochemistry

Approved: _____

George H. Watson, Ph.D.
Dean of the College of Arts and Sciences

Approved: _____

Ann L. Ardis, Ph.D.
Senior Vice Provost for Graduate and Professional Education

I certify that I have read this dissertation and that in my opinion it meets the academic and professional standard required by the University as a dissertation for the degree of Doctor of Philosophy.

Signed: _____

Donald A. Watson, Ph.D.
Professor in charge of dissertation

I certify that I have read this dissertation and that in my opinion it meets the academic and professional standard required by the University as a dissertation for the degree of Doctor of Philosophy.

Signed: _____

Charles G. Riordan, Ph.D.
Member of dissertation committee

I certify that I have read this dissertation and that in my opinion it meets the academic and professional standard required by the University as a dissertation for the degree of Doctor of Philosophy.

Signed: _____

John T. Koh, Ph.D.
Member of dissertation committee

I certify that I have read this dissertation and that in my opinion it meets the academic and professional standard required by the University as a dissertation for the degree of Doctor of Philosophy.

Signed: _____

Christopher J. Kloxin, Ph.D.
Member of dissertation committee

ACKNOWLEDGMENTS

I would like to thank my advisor, Professor Donald A. Watson, for his expert guidance and training thoughtout these past five years. Thank you for providing your expert opinions and suggestions, constructive criticisms and challenging projects to pursue. In addition to the wealth of chemistry knowledge that you passed on to me, thank you for teaching me the value of thinking critically as scientist and an individual.

I would like to thank the members of my thesis committee Professor Charles Riordan, Professor John Koh and Professor Christropher Kloxin for helpful conversations and for investing in me by serving as my thesis committee.

To my undergraduate mentors, Dr. V.S. Srinivasan, Dr. K. Najarajan, Dr. V. Subramanian, and Mr. L.R. Ganesan. your passion and devotion to undergraduate teaching was crucial in my desire to continue my education. It was from you that I learned the intellectual curiosity that I consider one of my strongest assets as a scientist and teacher. My special thanks to my undergraduate teachers N. Elangovan, R. Ramesh Kumar and V. Gopalakrishnan for being so helpful hand whenever needed. I would like to thank Mr. V. Thiagarajan who taught me physics and mathematics in my undergraduate school.

Special thanks to Mr. Ian Campbell, Dr. David Norton and Mr. Robert Gleeve at GlaxosmithKline R&D at Stevenage and Harlow, United Kingdom. The opportunity and support you all provided me was what fostered my passion for practicing synthetic organic chemistry.

I owe much of my success to my co-workers, especially those working on nitroalkane alkylation projects, Dr. Gildner, Dr. Gietter-Burch, Dr. Shimkin, Dr. Rezazadeh, and Dr. Sharma for helping me so much on several projects throughout my Ph.D. career. Dr. Vulovic and Dr. Shimkin for being a great co-workers and helpful mind whenever needed. My special thanks to Katerina Korch, Feiyang Xu, Sarah Krause and Michael Wisthoff for being great colleagues.

I would like to thank all the Watson group members of my class year: Scott Schuler, William Reid and Andrew Cinderella. We all began our PhD journey together and I could have never done it without all of you. You are all the wonderful lab mates and friends I could have asked for. I thank you all making me a better person and chemist. I look forward to all of you enjoying tremendous success in your life.

To the managers of our department facilities and to the department staff members, thank you for helping with everything and dropping what you are doing when something was needed. A special thank you to Dr. Steve Bai, John Famiglietti, Susan Cheadle, Glenn Yap, Pat McMohan and Rick Beard. Your friendship and assistance so many times have been invaluable.

To my siblings Rekha Karupaiah, Jothi Deepak, brother K. Vinayagam and my friends. I would not have come this far without your support and encouragement.

To Mohana, none of this possible without your endless love and patience. We have overcome many struggles together, and I can’t wait to start our life together.

This thesis is dedicated to my mom Saraswathi Devannah and to the memory of dad N. Devannah. Thank you for your unending support and always believe in my ability to accomplishing great things.

TABLE OF CONTENTS

LIST OF TABLES x
LIST OF FIGURES xii
ABSTRACT xxii

Chapter

1 INTRODUCTION 1

1.1 Nitroalkanes as Versatile Functional Group 1

1.1.1 Henry Reaction 2
1.1.2 The Nitro-Mannich Reaction or aza-Henry Reaction 5
1.1.3 Michael Addition 10
1.1.4 Allylation of Nitroalkanes 14

1.1.4.1 Allylation of Unactivated Nitroalkanes 14
1.1.4.2 Allylation of Activated Nitroalkanes 17
1.1.4.3 Intramolecular Allylation of Nitroalkanes 21

1.1.5 Arylation of Nitroalkanes 23
1.1.6 Miscellaneous Reaction of Nitroalkanes 27

1.1.6.1 The Suzuki-Miyaura Reaction of Nitroarenes 27
1.1.6.2 The Buchwald-Hartwig Amination of Nitroarenes 29

1.1.7 Reduction of Nitroalkanes to Amines 31
1.1.8 Hydrolysis of Nitroalkanes to Carbonyls (The Nef Reaction) 34
1.1.9 Denitration of Nitroalkanes 37

1.2 Early Efforts Towards C-Alkylation of Nitroalkanes Using Alkyl Electrophile 41

1.2.1 Early Reports of *O*-alkylation over *C*-alkylation 42
1.2.2 Mechanistic Studies for *C*-alkylation of Nitroalkanes 42
1.2.3 Katritzky's Pyridinium Salts in the C-Alkylation of Nitroalkanes 45
1.2.4 Alkyl Metal Complexes to *C*-Alkylate Nitroalkanes 46

1.3 Radical Cross-Coupling Reactions Using Base Metal Catalysis 48

1.3.1 Nickel Catalyzed Cross Couplings of sp^3 Halides 48
1.3.2 Iron Catalyzed Cross Couplings of sp^3 Halides 54
1.3.3 Cobalt Catalyzed Cross Couplings of sp^3 Halides 58
1.3.4 Copper Catalyzed Atom Transfer Radical Addition 61

REFERENCES 65

2 TRIFLUOROMETHYLATION OF SECONDARY NITROALKANES 73

2.1 INTRODUCTION AND BACKGROUND 73
2.2 Medicinal Importance of Trifluoromethyl Groups 77
2.3 Importance of α-(Trifluoromethyl)amines 81
2.4 Previous Syntheses of α-Perfluoronitroalkanes: 84
2.5 Previous Syntheses of α-(trifluoromethyl)nitroalkanes: 86
2.6 Copper Mediated Radical Trifluoromethylation Reaction using Electrophilic Trifluromethylating Reagent: 89
2.7 Development of Reaction Conditions 95
2.8 Scope of Trifluoromethylation of Secondary Nitroalkanes 97
2.9 Synthesis of Vinyl Trifluoromethylalkenes 102
2.10 Synthesis of α-(trifuoromethyl)amines 103
2.11 Mechanistic Studies 104

2.11.1 Radical Probing Experiment 104
2.11.2 Deprotonation Studies – ^{1}H NMR Spectroscopy 105
2.11.3 Interaction of DBU with Umemoto's Reagent – ^{1}H NMR study. 107
2.11.4 ^{1}H NMR Monitoring of Trifluoromethylation of Secondary Nitroalkane: 111
2.11.5 ^{1}H NMR monitoring of Trifluoromethylation of Secondary Nitroalkane (optimal reaction condition): 116
2.11.6 Proposed Mechanism 118

2.12 Conclusion 119
2.13 Experimental Section 120

2.13.1 General Experimental Details 120
2.13.2 Instrumentation and Chromatography: 121
2.13.3 Synthesis of Novel Nitroalkane Starting Materials: 122
2.13.4 General Protocol for the Synthesis of α-Trifluoromethylnitroalkanes: 132
2.13.5 Crystal Data and Structure Refinement for 2.74, 2.80, 2.84: 153

REFERENCES 155

3 NICKEL CATALYZED ENANTIOSELECTIVE *C*-ALKYLATION OF NITROALKANES WITH α-BROMOAMIDES: SYNTHESIS OF β-NITROAMIDES 160

3.1 Introduction 160
3.2 Nickel-Catalyzed Enantioselective Reactions Using α-Halocarbonyls As Electrophiles 161
3.3 Discovery and Optimization of Enantioselective Nickel-Catalyzed *C*-Alkylation of Nitroalkanes with α-bromoamides 163
3.4 Initial Experiments with DBU as the Base 165

3.4.1 Electronic Effect in the Nickel-Catalyzed *C*-Alkylaiton of Nitroalkanes 166
3.4.2 Origin of Enantioselectivity in the Nickel-Catalyzed *C*-Alkylation of Nitroalkanes 167
3.4.3 Examination of Chiral 1,2-diamine Ligands Under DBU Conditions 168
3.4.4 Activated Secondary Alkyl Electrophile as Coupling Partners 169

3.5 Identification of Metal Alkoxide Bases and Optimization 174
3.6 Optimization of Reaction Conditions using *N*-Benzyl-*N*-Phenyl Amide as a Model Substrate 178

3.6.1 Examination of Diverse Chiral Bidentate Nitrogen Ligands 179
3.6.2 Effect of α-Alkyl Substitution in the Electrophile 183
3.6.3 Identification of Et_2Zn as the Internal Reductant 184
3.6.4 Identification of Single Component Pre-catalyst 187
3.6.5 Effect of Temperature 191

3.7 Reaction Scope with Respect to Nitroalkanes 193
3.8 Reaction Scope with Respect to Electrophile and Amide Backbone 194
3.9 Preliminary Results 197
3.10 Down Stream Functionalization of Alkylated Products 198
3.11 Investigation of Reaction Mechanism 203
3.12 Other Nickel-Catalyzed C-Alkylation of Nitroalkanes Reactions 213
3.13 Conclusion 217
3.14 Experimental Section 217

3.14.1 General Experimental Details 217
3.14.2 Instrumentation and Chromatography 218
3.14.3 Procedure for Initial Experiments with DBU as Base: 219

3.14.4 Synthesis of β-nitroamide: 220
3.14.5 Synthesis of Novel Chiral 1,2 Diamine Ligands: 222
3.14.6 General Protocol for Synthesis of Previously Unknown α-bromo amides: 237
3.14.7 Synthesis of Radical clock substrate 3.79 246
3.14.8 Synthesis of Starting Nitroalkanes 248
3.14.9 Synthesis of the single-component pre-catalyst 3.48 249
3.14.10 General Protocol for Asymmetric Alkylation of Nitroalkanes 250
3.14.11 Procedure for Stereoconvergence in the Nickel Catalyzed Enantioselective *C*-Alkylation of Nitroalkanes: 297
3.14.12 Determination of Stereochemistry of β-nitroamides 299
3.14.13 Crystallographic Details: 301

REFERENCES 303

Appendix

A SPECTRAL DATA FOR CHAPTER 2 307
B SPECTRAL DATA FOR CHAPTER 3 429
C PERMISSION LETTERS 752

LIST OF TABLES

Table 1.1: Action of Leaving Group on C-Alkylation of Nitroalkanes 43

Table 1.2: Effect of Radical Inhibitor on *C*-Alkylation of Nitroalkane 44

Table 2.1: Comparison of the Oral Bioavailability of Sitagliptin and its Non-Fluorinated Analogs 81

Table 2.2: α-Trifluoromethylamines as Amide Isosteres in Cathepsin K Inhibitors 82

Table 2.3: Comparison of CF_3 Replacements in Cathepsin K inhibitors 82

Table 2.4: Comparison of CF_3 Replacements in JAK2 Inhibitors 83

Table 2.5: Comparison of CF_3 Replacements in Taxoid 84

Table 2.6: Optimization of Reaction Condition for the Trifluoromethylation of Secondary Nitroalkanes 96

Table 2.7: Optimization of Trifluoromethylating Reagent 97

Table 2.8: Effect of Radical Scavengers on the Formation of α-(trifuoromethyl)nitroalkane **2.62** 105

Table 2.9: Chemical Shift of **2.61** and **2.96** in ^{1}H NMR 106

Table 2.10: Yield of **2.61** and **2.96** over Time using DBU 107

Table 2.11: Chemical Shift of **2.9**, **2.9·DBU**, dibenzothiophene and fluoroform in ^{1}H NMR 110

Table 2.12: Chemical Shift of **2.61**, **2.62**, **2.9·DBU** and **2.101** in ^{1}H NMR 113

Table 3.1: Comparing Copper and Nickel Catalyst with Diamine ligand 163

Table 3.2: Investigating Nickel Catalysts in the *C*-Alkylation of Nitroalkanes 164

Table 3.3: Discovery of DBU as the Base in the Nickel-Catalyzed Enantioselective *C*-Alkylation of Nitroalkanes 165

Table 3.4: Examining Electronic Effect in the Nickel-Catalyzed C-Alkylation of Nitroalkanes 166

Table 3.5: Inconsistent Results Using DBU as the Base 171

Table 3.6: Investigation of Metal Alkoxide Bases 174

Table 3.7: Optimization of Solvent and Catalyst Loading 176

Table 3.8: Role of Smaller Counter-Anion Bases 179

Table 3.9: Comparison of "methyl" vs "ethyl" Substitution in the α-Bromoamide **3.33** 183

Table 3.10: Survey of Internal Reductant for Ni(II) to Ni(0) 185

Table 3.11: Reducing the Loading of MeMgCl and Et_2Zn 186

Table 3.12: Comparison of Efficiency of $Ni(COD)_2$ and Ni(II)/Et_2Zn Catalytic System 187

Table 3.13: Comparison of Single Component Pre-Catalyst **3.48** and Multi-Component Catalyst **3.30** 189

Table 3.14: Investigation of Internal Reductants using Single Component Pre-catalyst **3.48** 190

Table 3.15: Role of Temperature 193

Table 3.16: Diastereoselective Michael Addition of Enantioenriched β-Nitroamide **3.47** 199

Table 3.17: Synthesis of Enantioenriched Quaternary α-Trifluoromethylnitroalkane (**3.73**) 201

Table 3.18: Study of Product ee and Catalyst ee 206

Table 3.19: Revisiting Internal Reductant Screen 207

Table 3.20: Effect of Catalyst Loading 208

LIST OF FIGURES

Figure 1.1: Henry Reaction and its Synthetic Applications 2

Figure 1.2: Pioneering Studies of Asymmetric Henry Reaction by Shibasaki and Coworkers 3

Figure 1.3: Shibasaki's Synthesis of (-)-pindolol using Asymmetric Henry Reaction 4

Figure 1.4: Gong's Copper Catalyzed Enantioselective Nitro-Aldol Reaction of Enal 4

Figure 1.5: Gong's Synthesis of Azatricyclic Framework using Enantioselective Henry Reaction 5

Figure 1.6: aza-Henry Reaction and its Synthetic Applications 6

Figure 1.7: Anderson's First Diastereoselective aza-Henry Reaction 7

Figure 1.8: Pioneering Studies of Enantioselective aza Henry Reaction by Shibasaki and Coworkers 8

Figure 1.9: Duan's Bifunctional Phase-Transfer Catalyzed Enantioselective and Diastereoselective aza-Henry Reaction of Amidosulfones 9

Figure 1.10: Wang's Synthesis of anti-HIV drug DPC 083 Using nitro-Mannich Reaction with Thiourea Catalyst **1.31** 10

Figure 1.11: The Nitro-Michael Reaction and its Synthetic Applications 11

Figure 1.12: Kohler's Early Study of Conjugate Addition Reaction Using Nitroalkane as Nucleophiles 11

Figure 1.13: Watson's Diastereoselective Michael Reaction Using β-nitrocarbonyls as Nucleophiles 12

Figure 1.14: Watson's Proposed Model for Observed Diastereoselectivity 13

Figure 1.15: Miaura's Enantioselective Conjugate Addition Reaction Using Organocatalyst **1.43** 14

Figure 1.16: Aleksandrowicz and Wade's Pioneering Studies of Allylation of Unactivated Nitroalkanes 15

Figure 1.17: Helmchen's Pioneering Studies of Asymmetric Allylic Alkylation of Nitroalkanes 15

Figure 1.18: Trost's Studies of Asymmetric Allylic Alkylation of Nitroalkanes 16

Figure 1.19: Helmchen's Studies of Asymmetric C-Allylation of Nitroalkanes Using Iridium Catalysis 17

Figure 1.20: Wade and Genet's Pioneering Studies of Allylation of Activated Nitroalkanes 18

Figure 1.21: White's Palladium Catalyzed Allylic C–H Alkylation of Activated Nitroalkanes 19

Figure 1.22: Ooi's Palladium Catalyzed Allylation of Nitroalkanes Using Chiral Ion-Paired Ligands 19

Figure 1.23: Tunge's Deacylative Allylation of Nitroalkane Using Palladium Catalysis 20

Figure 1.24: Tsuji's Initial Report on Intramoleculare Allylation of Nitroalkanes 21

Figure 1.25: Tunge's Decarboxylative Intramolecular Allylation of Nitroalkanes 21

Figure 1.26: Tunge's Proposed Mechanism for the Decarboxylative Intramolecular Allylation of Nitroalkanes 22

Figure 1.27: Rajappa's Intramolecular Allylation of Nitroalkanes under Palladium Catalysis 23

Figure 1.28: Muratake's Pioneering Studies on Palladium Catalyzed Intramolecular Arylation of Nitroalkanes 24

Figure 1.29: Buchwald's Palladium Catalyzed Intermolecular Arylation of Nitroalkanes 25

Figure 1.30: Kozlowski's Palladium Catalyzed Intermolecular Arylation of Nitromethane 26

Figure 1.31: Kozlowski's Palladium Catalyzed α-arylation of arylnitromethane 26

Figure 1.32: Kozlowski's Palladium Catalyzed One-Pot Diarylation of nitromethane 27

Figure 1.33: Wu and Shinde's Studies on Rhodium and Copper-Catalyzed Cross Coupling of Nitroarenes.....28

Figure 1.34: Sakaki's Groundbreaking Studies on Palladium-Catalyzed Suzuki-Miyuara Cross Coupling of Nitroarenes and Boronic Acids.....29

Figure 1.35: Nakao's First Example of Palladium Catalyzed Buchwald Hartwig Amination of Nitroarenes 29

Figure 1.36: Nakao's Stoichiometric Studies in Palladium Catalyzed Buchwald Hartwig Amination of Nitroarenes 30

Figure 1.37: Nakao's Proposed Mechanism Palladium Catalyzed Buchwald Hartwig Amination of Nitroarenes 30

Figure 1.38: Pedro's Synthesis of (*S*)- (+)-Solatol using Nitroalkane Reduction.....32

Figure 1.39: Johnston's Synthesis of (–)-nutlin using Sodium Borohydride Reduction of Nitroalkanes in the presence of Cobalt Chloride 33

Figure 1.40: Orlandi's Metal-Free Reduction of Nitroalkane Using Trichlorosilane and Tertiary Amine.....33

Figure 1.41: Oxidative and Reductive Conditions for the Nef Reaction 35

Figure 1.42: Fuji's Synthesis of Spirotryprostatin B Using Reductive Nef Reaction..36

Figure 1.43: Hayashi's Synthesis of Beraprost Using Oxidative Nef Reaction.....36

Figure 1.44: Kornblum's First Radical Denitration of Nitroalkanes.....37

Figure 1.45: Ono and Tanner's Trialkyltin Reagents for Denitration of Nitroalkanes.....38

Figure 1.46: Dixon's Synthesis of Paroxetine Using Radical Denitration of Nitroalkanes.....39

Figure 1.47: Yamaguchi's Stereoretentive Denitration of Nitroalkanes.....39

Figure 1.48: Fu's Trialkyltin Reagent Catalyzed Reduction of Nitroalkanes to Alkanes 40

Figure 1.49: Fu's ^{119}Sn NMR Studies 40

Figure 1.50: Fu's Proposed Mechanism for the Bu_3SnH Catalyzed Reduction of Nitroalkane to alkane 41

Figure 1.51: Alkylation of Nitroalkanes 42

Figure 1.52: Hass and Bender's Study of Nitroalkane Alkylation 42

Figure 1.53: Kornblum's Proposed Radical Chain Mechanism for *C*-Alkylation of Nitroalkanes 44

Figure 1.54: Katritzky's Alkylation of Nitronates with Pyridinium Salts and Proposed Mechanism 45

Figure 1.55: Russell's Alkylation of Nitroalkanes Using Alkylmercury Halides and Proposed Mechanism 46

Figure 1.56: Branchaud's Alkylation of Nitroalkanes Using Alkylcobalt Complex and Proposed Mechanism 47

Figure 1.57: Proposed Base Metal Catalyzed to C-Alkylate Nitroalkanes via Radical – Anion Coupling 48

Figure 1.58: Suzuki, Knochel and Kambe Studies on Cross-Coupling of Primary Alkyl Electrophile Using Pd or Ni Catalysis 49

Figure 1.59: Fu's Pioneering Studied on Nickel-Catalyzed Negishi Cross Coupling of Secondary Alkyl Electrophile Using Tridentate PyBOX Ligand 50

Figure 1.60: Fu's Pioneering Studied on Nickel-Catalyzed Negishi Cross Coupling of Secondary Alkyl Electrophile Using Tridentate PyBOX Ligand 51

Figure 1.61: Baran's Nickel-Catalyzed Negishi Cross Coupling of Redox-Active Esters 52

Figure 1.62: Baran's Radical Probe Studies Negishi Cross Coupling of Redox-Active Esters 53

Figure 1.63: Baran's Proposed Mechanism on Negishi Cross Coupling of Redox-Active Esters 53

Figure 1.64: Weix's Nickel-Catalyzed Reductive Cross Coupling of RAEs and Aryl Iodides 54

Figure 1.65: Kochi's Early Study on Alkyl-Alkyl Cross Coupling Using Iron Catalysis 55

Figure 1.66: Chai's Initial Studies on Iron-Catalyzed Kumada Reaction 55

Figure 1.67: Chai's Radical Probing Studies on Iron-Catalyzed Kumada Reaction 56

Figure 1.68: Nakamura's First Example of Iron-Catalyzed Asymmetric Reaction between α-chloroesters and Aryl Grignard Reagents 56

Figure 1.69: Nakamura's Proposed Mechanism on Iron-Catalyzed Asymmetric Reaction between α-chloroesters and Aryl Grignard Reagents 57

Figure 1.70: Baran's Iron-Catalyzed Cross Coupling of Redox-Active Esters with Alkyl Zinc and Magnesium Reagents 58

Figure 1.71: Chai's Initial Studies on Cobalt-Catalyzed Kumada Reaction Using Alkyl Halides 59

Figure 1.72: Kambe's Advancement in the Cobalt-Catalyzed Alkyl-Alkyl Cross Coupling Using 2° and 3° Alkyl Grignard Reagents 59

Figure 1.73: Kambe's Radical Probing Studies 60

Figure 1.74: Walsh and Bian's First Example of Cobalt-Catalyzed Asymmetric Kumada Cross Coupling between α–bromoesters and Aryl Grignard Reagents 60

Figure 1.75: Kharasch Seminal Report on Atom Transfer Radical Addition 61

Figure 1.76: Tsuji's Seminal Report on ATRC Reaction and The Proposed Mechanism 62

Figure 1.77: Nishikata's Copper Catalyzed Radical Alkenylation Reaction 64

Figure 2.1: Copper-Catalyzed *C*-Alkylation of Nitroalkanes with Benzyl bromide 74

Figure 2.2: Proposed Mechanism for *C*-Benzylation of Nitroalkanes 74

Figure 2.3: Copper-Catalyzed C-Alkylation of Nitroalkanes with α-Halocarbonyl Compounds 75

Figure 2.4: Copper-Catalyzed C-Alkylation of Nitroalkanes with α-Bromonitriles .76

Figure 2.5: Trifluoromethylation of Secondary Nitroalkanes using Umemoto's Reagent 77

Figure 2.6: Comparison of K_i Value of Prozac® and its Derivatives 78

Figure 2.7: Mechanism of Inhibition of Thymidylate Synthase by Trifluridine.....79

Figure 2.8: Structure Comparison of Vitamin D_3 and Falicalcitral.....80

Figure 2.9: Umemoto's Synthesis of α-Perfluoronitroalkanes 85

Figure 2.10: Feiring's Synthesis of α-perfluoronitroalkanes using Photolytic Condition 85

Figure 2.11: Knunyant's Synthesis of α-(trifluoromethyl)nitroalkanes.....86

Figure 2.12: Scope of Togni's α-(trifluoromethyl)nitroalkanes of α-Nitroesters.....87

Figure 2.13: Limitations of Togni's Trifluoromethylation of α-Nitrocarbonyls. 88

Figure 2.14: Togni's Diastereoselective Studies of Trifluoromethylation of α-Nitroesters using Phenyl Menthol Chiral Auxillary 88

Figure 2.15: Togni's Preliminary Enantioselective Studies of Trifluoromethylation of α-Nitroesters using Cu-BOX Complex. 89

Figure 2.16: Xiao's Trifluoromethylation of Heteroaryl Iodides with (S)-(Trifluoromethyl)diphenylsulfonium Triflate.....90

Figure 2.17: Xiao's Proposed Mechanism for the Generation of $CuCF_3$ Intermediate 90

Figure 2.18: Buchwald's Copper Catalyzed Enantioselective Oxytrifluoromethylation of Alkenes using Togni's Reagent 91

Figure 2.19: Buchwald's Radical Probe Studies in the Oxytrifluoromethylation of Alkenes 92

Figure 2.20: Proposed Mechanism of Buchwald's Oxytrifluoromethylation of Alkenes 93

Figure 2.21: Fu's Radical Sandmeyer Trifluoromethylation of Anilines using Umemoto's Reagent 94

Figure 2.22: Fu's Radical Probe Studies in the Trifluoromethylation of Anilines 94

Figure 2.23: Proposed Mechanism of Fu's Radical Trifluoromethylation of Anilines 95

Figure 2.24: Scope of the Trifluoromethylation of Secondary Nitroalkanes 98

Figure 2.25: Proposed Model for Observed Diastereoselectivity and Crystal Structure of **2.74** 99

Figure 2.26: Determination of Relative Stereochemistry of Trifluoromethylated Henry Reaction Substrate and Crystal Structure **2.84** 100

Figure 2.27: Crystal Structure of **2.80** 101

Figure 2.28: Competitive Alkene Formation and Role of Base 102

Figure 2.29: Synthesis of Vinyl Trifluoromethylalkene 103

Figure 2.30: Preparation of α-(trifuoromethyl)amines 104

Figure 2.31: Deprotonation Event between **2.61** and DBU 105

Figure 2.32: ^{1}H NMR Monitoring of Deprotonation of **2.61** [0.05] M CD_2Cl_2, –25 °C, Compared to Spectra of Reagents and Products Under the same conditions 106

Figure 2.33: Ratio of Compound **2.61** and Nitronate Anion **2.96** over Time 107

Figure 2.34: Yu's Radical Trifluoromethylation of Heteroarenes with Umemoto's Reagent 108

Figure 2.35: Yu's Proposed EDA complex **2.97** 108

Figure 2.36: Proposed Mechanism of Yu's Trifluoromethylation of Heteroarenes via (EDA) Complex **2.97** 109

Figure 2.37: Interaction Between Umemoto's Reagent **2.9** and DBU 110

Figure 2.38: ^{1}H NMR Study of Interaction Between Umemoto's reagent **2.9** and DBU, [0.05 M] CD_2Cl_2, –25 °C, Compared to Spectra of Reagents and Products Under the Same Conditions. 111

Figure 2.39: Trifluoromethylation of **2.61** at –25 °C in CD_2Cl_2 [0.05 M] 112

Figure 2.40: ^1H NMR Monitoring of Trifluoromethylation of **2.61** [0.05 M] CD_2Cl_2, –25 °C, Compared to Spectra of Reagents and Products Under the Same Conditions. 114

Figure 2.41: Kinetic Profile of Trifluoromethylation of **2.61** [0.05 M] CD_2Cl_2 and Change of **2.61, 2.62, 2.101** and **2.9·DBU** over Time. 115

Figure 2.42: Trifluoromethylation of **2.61** at –25 °C in CD_2Cl_2 [0.1 M] 116

Figure 2.43: ^1H NMR Monitoring of Trifluoromethylation of **2.61** [0.1 M] CD_2Cl_2, –25 °C, Compared to Spectra of Reagents and Products under The Same Conditions. 117

Figure 2.44: Kinetic Profile of Trifluoromethylation of **2.61** [0.1 M] CD_2Cl_2 and Change of **2.61, 2.62, 2.101** and **2.9·DBU** over Time 118

Figure 2.45: Proposed Mechanism for Nitroalkane Trifluoromethylation 119

Figure 3.1: Copper-Catalyzed Enantioselective *C*-Alkylation of Nitroalkanes 160

Figure 3.2: Fu's Pioneering Studies on Enantioselective Cross-Coupling Between α-bromoamide and Alkylzinc Reagents. 161

Figure 3.3: Fu's Enantioconvergent Cross-Coupling via a Radical Intermediate 162

Figure 3.4: Fu's Studies on Enantioselective Cross-Coupling Between α-Chloroamide and Organoboron Reagents. 163

Figure 3.5: Hammett Plot of Enantioselective as a Function of Ligand Electronics 167

Figure 3.6: Role of N–H bonds in the Enantioselective *C*-Alkylation of Nitroalkanes 168

Figure 3.7: Steric Effect in the 3,5-position of Chiral 1,2 diamines 169

Figure 3.8: First Example of Nickel-catalyzed Enantioselective C-Alkylation of Nitroalkanes Using Racemic Secondary Alkyl Electrophile 170

Figure 3.8: Epimerization Studies 172

Figure 3.9: Rationalization for Epimerization of β-nitroamide **3.28** 173

Figure 3.10: Proposed Metal Alkoxide Base in the Nickel-Catalyzed Enantioselective *C*-Alkylation of Nitroalkanes 173

Figure 3.11: Identification of Electron Deficient Ligand **3.30** 177

Figure 3.12: Examination of Amide Backbone in the Nickel-Catalyzed Enantioselective *C*-Alkylation of Nitroalkanes 178

Figure 3.13: Diverse Chiral Bidentate Nitrogen Ligands in the Nickel-Catalyzed *C*-Alkylation of Nitroalkanes 181

Figure 3.14: Examination of Electron Deficient Chiral Diamine Ligands 182

Figure 3.15: Poor Reactivity of Functionalized Nitroalkane **3.46** 188

Figure 3.16: Preparation of Single Component Pre-catalyst **3.48** 188

Figure 3.17: Reaction Set Up in the Glove Box Using Cooling Unit 192

Figure 3.18: Scope of Nitroalkanes in the Nickel-Catalyzed Enantioselective C-Alkylation of Nitroalkanes 194

Figure 3.19: Scope of Electrophiles in the Nickel-Catalyzed Enantioselective *C*-Alkylation of Nitroalkanes 195

Figure 3.20: Scope of Amide Backbone in the Nickel-Catalyzed Enantioselective *C*-Alkylation of Nitroalkanes 196

Figure 3.21 ^{1}H NMR spectra of 3.54 *syn* and *anti* diastereomers 197

Figure 3.22: Preliminary Results in the Nickel-Catalyzed Enantioselective *C*-Alkylation of Nitroalkanes 198

Figure 3.23: Theoretical Enantioselectivity of Michael Addition based on Relative Ratio of Stereoisomers 200

Figure 3.24: Tsuji-Trost Allylation Reaction of Enantioenriched β-Nitroamide 202

Figure 3.25: Reduction of Alkylated Products 202

Figure 3.26: Radical Probe Studies in the Nickel-Catalyzed Enantioselective *C*-Alkylation of Nitroalkanes 203

Figure 3.27: Stereoconvergence in the Nickel-Catalyzed Enantioselective *C*-Alkylation of Nitroalkanes 205

Figure 3.28: Enantiomeric excess of the catalyst Vs enantiomeric excess of the *syn* diatereomer **3.69** 206

Figure 3.29: Enantiomeric excess of the catalyst Vs enantiomeric excess of the *anti* diatereomer **3.69** 207

Figure 3.30: Proposed Mechanism for the Generation of Low-Valent Ni Species and Alkyl Radical 210

Figure 3.31: Proposed Outer Sphere Mechanism for the Nickel-Catalyzed Enantioselective *C*-Alkylation of Nitroalkanes 211

Figure 3.32: Proposed Inner Sphere Mechanism for the Nickel-Catalyzed Enantioselective *C*-Alkylation of Nitroalkanes 213

Figure 3.33: Copper-Catalyzed *C*-Alkylation of Nitroalkanes 214

Figure 3.34: Proposed C-alkylation of Nitroalkanes with Unactivated Alkyl Halides Under Nickel Catalysis 214

Figure 3.35: Sample Scope of Nickel-Catalyzed C-alkylation of Nitroalkanes Using Unactivated Alkyl Halides 216

Figure 3.36: X-ray Structure of Single Component Precatalyst (***R,R***)- **3.48** 250

Figure 3.37: Stereochemistry of Major Diastereomer **3.62**.....299

Figure 3.38: Stereochemistry of Minor Diastereomer **3.54**.....300

Figure 3.39: Relative and Absolute Stereochemistry of **3.78**.....301

ABSTRACT

This dissertation focused on the development of new methods to synthesize enantioenriched complex nitroalkanes using transition metal catalysis. Nitroalkanes are useful intermediates in several C–C bond forming reactions and serve as precursors for several functional groups including amines and carbonyls. Despite this rich chemistry, the seemingly simple *C*-alkylation of nitroalkanes with alkyl electrophiles (such as alkyl halides) has remained a highly challenging task due to competing *O*-alkylation. Using the advent of transition metal catalysis our group has addressed this century old problem.

In this regard, I was involved in four main projects during my graduate career. Chapter 1 describes the synthetic utility of nitroalkanes in organic synthesis and include a summary of base metals known to undergo C–C bond forming reactions using simple alkyl electrophiles via a radical mechanism.

Chapter 2, describes the development of metal-free trifluoromethylation of secondary nitroalkanes using commercially available reagent reagent 5-(trifluoromethyl)dibenzothiophenium triflate (Umemoto's reagent). These conditions provide high yielding access to fully substituted α-(trifluoromethyl)nitroalkanes and I showed that these compounds can be easily converted into medicinally relevant α-(trifluoromethyl)amines.

Chapter 3, describes the discovery and development of the first nickel-catalyzed conditions for the enantioselective synthesis of β-nitroamides using racemic α-bromoamides as electrophiles. In this work, I showed the stereocenter alpha to the

nitro group could be controlled and I also showed that the enantioenriched β-nitroamides can be used as a handle for further C–C bond forming reactions such as conjugate addition, trifluoromethylation and Tsuji-Trost allylation to set a fully substituted NO_2 stereocenters without erosion of enantiomeric excess and producing the product with excellent diastereoselectivity.

Chapter 3, also describes the development of a first, nickel-catalyzed *C*-alkylation of nitroalkanes using unactivated alkyl iodides. This method allowed the preparation of a diverse array of complex nitroalkanes using simple starting materials. Significantly, this system allows for the alkylation of primary, secondary, and tertiary alkyl iodides without the requirement of radical stabilizing groups.

Preliminary results in the copper and nickel catalyzed enantioselective *C*-alkylation of nitroalkanes using additional radical stabilizing substrate classes such as benzyl bromide and α-bromoketones will be discussed in detail in Appendix D and E.

Chapter 1

INTRODUCTION

1.1 Nitroalkanes as Versatile Functional Group

Nitroalkanes are one of the most useful building block in organic synthesis.[1] They take part in a variety of C–C bond forming reactions such as the Michael addition,[2] Henry reaction,[3] and aza-Henry reaction.[4] They can also be converted easily to alkyl amines, carbonyls, amides, or alkanes. Nitroalkanes are also known to react in transition metal-catalyzed reactions to form C–C bonds through arylation or allylation reactions.[5,6] Recently, nitroarenes have been shown to react in palladium catalyzed reactions to form C–C bonds using aryl boronic acids or C–N bonds using arylamines.[7] Additionally, they serve as radical precursors and synthons for heterocycles in cycloaddition reactions.[1] Despite the prolific use of nitroalkanes in organic synthesis, the carbon alkylation of nitroalkanes with simple alkyl halides remains undeveloped. For the first time, our group has developed a copper-catalyzed method for the C-alkylation of nitroalkanes using a wide variety of simple alkyl electrophiles (see chapter 2 section 2.1 for discussions).[8]

The following section of this chapter will introduce the utility of nitroalkanes in organic synthesis and include a summary of base metals known to undergo C–C bond forming reactions using simple alkyl electrophiles via a radical mechanism.

1.1.1 Henry Reaction

In 1895, L. Henry discovered that aldehydes and ketones were easily combined with nitroalkanes to afford β-nitroalcohols in the presence of a base.[9] The aldol condensation between carbonyl compounds and nitroalkanes (nitro-aldol reaction) has become a significant tool in the formation of C–C bonds and referred to as the Henry reaction. The β-nitroalcohols are easily converted into useful synthetic intermediates (Figure 1.1). For example, reduction of the nitro group affords β-aminoalcohols (**1.1**), dehydration gives nitroalkenes (**1.2**), oxidation of secondary alcohol affords α-nitroketones (**1.3**), and radical denitration gives secondary alcohols (**1.4**).[1]

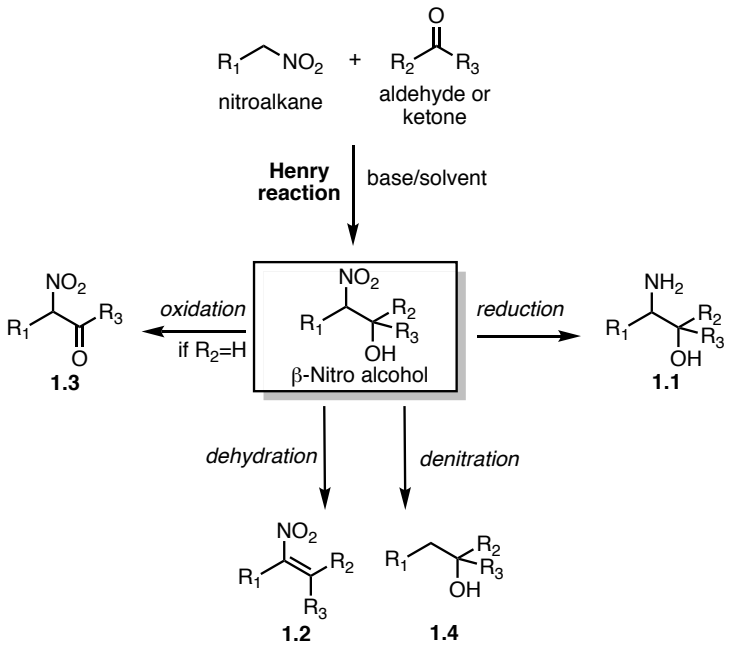

Figure 1.1: Henry Reaction and its Synthetic Applications

Controlling absolute and relative stereochemistry in the Henry reaction was difficult due to the reversible nature of the reaction and the facile epimerization of the

carbon center α to the nitro substituent. Extensive research efforts have been directed towards the discovery and development of an asymmetric version of the Henry reaction. In 1992, Shibasaki and coworkers reported the first asymmetric version of the nitro-aldol reaction using a $La(BINAP)_3$ complex (**1.5**) as catalyst to afford β-nitroalcohol (**1.6**) in good yield and excellent enantioselectivity (Figure 1.2, top). The heterobimetallic complex (**1.5**) possess both Lewis acidic and basic sites, which activates nitro compound and aldehyde substrate independently to forge the C–C bond with excellent enantioselectivity. They also controlled the relative stereochemistry in the Henry reaction using prochiral nitroalkane and chiral catalyst (**1.7**), which possesses a triethylsilane (TES) group in the BINOL backbone. Using this modified mixed metal alkoxide complex (**1.7**), β-nitroalcohol (**1.8**) was produced in excellent diastereoselectivity and enantioselectivity (Figure 1.2, bottom).[10] Later, Shibasaki successfully utilized asymmetric Henry reactions with chiral catalyst (**1.5**) in the synthesis of the effective β-blocker (-)-pindolol (**1.9**) (Figure 1.3).[11]

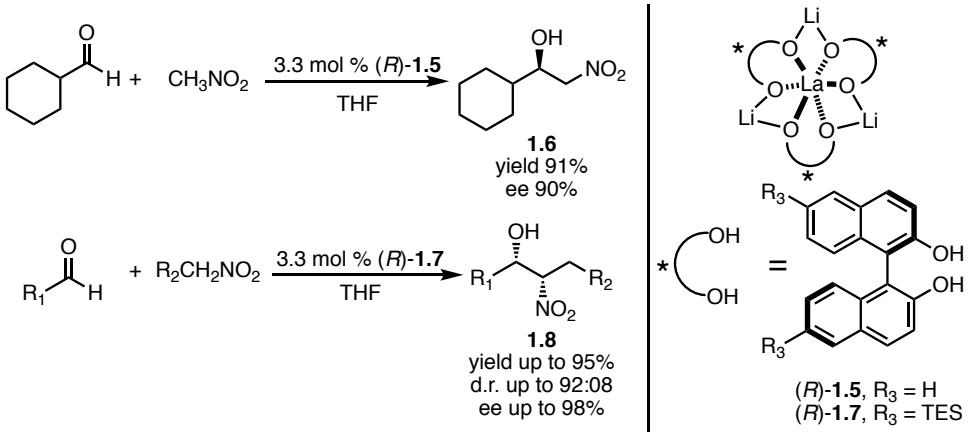

Figure 1.2: Pioneering Studies of Asymmetric Henry Reaction by Shibasaki and Coworkers

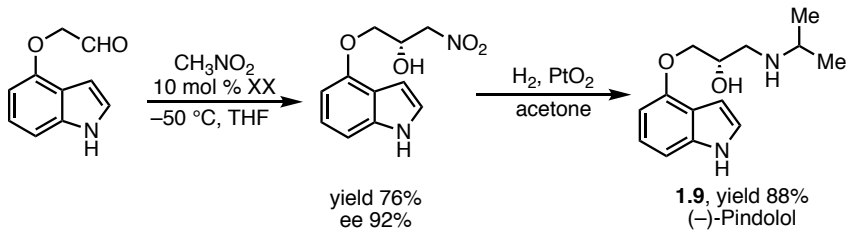

Figure 1.3: Shibasaki's Synthesis of (-)-pindolol using Asymmetric Henry Reaction

Considering the significance of asymmetric C–C bond forming reactions in organic synthesis, Henry reactions are discussed extensively in research communications and review articles.[3,12] These reviews cover syntheses of β-nitroalcohols and their applications in organic synthesis. A more recent review published in 2011 summarizes literature on the nitro-aldol reaction published up to 2011.[13] Few recent examples of Henry reactions are discussed below.

In 2013, Gong and coworkers reported the mild, copper-catalyzed enantioselective Henry reaction of enals with nitromethane (Figure 1.4). Using a C_1-symmetric chiral diamine (**1.10**) and copper (II) catalytic system, a variety of cyclic and acyclic α,β-unsaturated aldehydes undergo the Henry reaction to afford β-nitroalcohol (**1.11**) with excellent yield and enantioselectivity.[14] However, nitroalkanes other than nitromethane were not investigated.

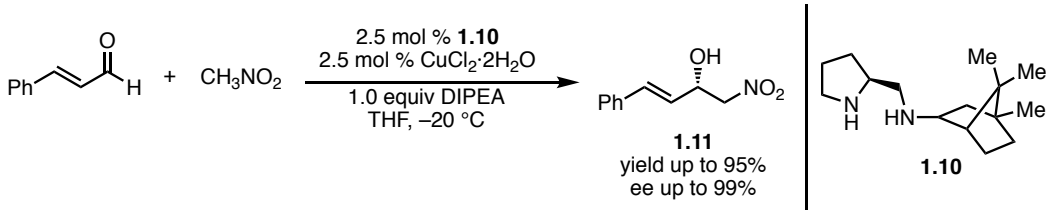

Figure 1.4: Gong's Copper Catalyzed Enantioselective Nitro-Aldol Reaction of Enal

Furthermore, synthetic utility of this asymmetric protocol was demonstrated by its application in the synthesis of chiral azatricyclic hexahydrochromeno[4,3-b] pyrrole scaffold, which is a prevalent pharmocophore in medicinal chemistry (Figure 1.5).[15] For example, the enal (**1.12**) was reacted with nitromethane under copper-catalyzed conditions to afford product (**1.13**) in 96% ee. The nitro alcohol was sequentially reduced to the amine and protected as the tolyl sulfonamide. The amino alcohol (**1.14**) underwent intramolecular iodolactamization to afford azatricyclic framework (**1.15**).

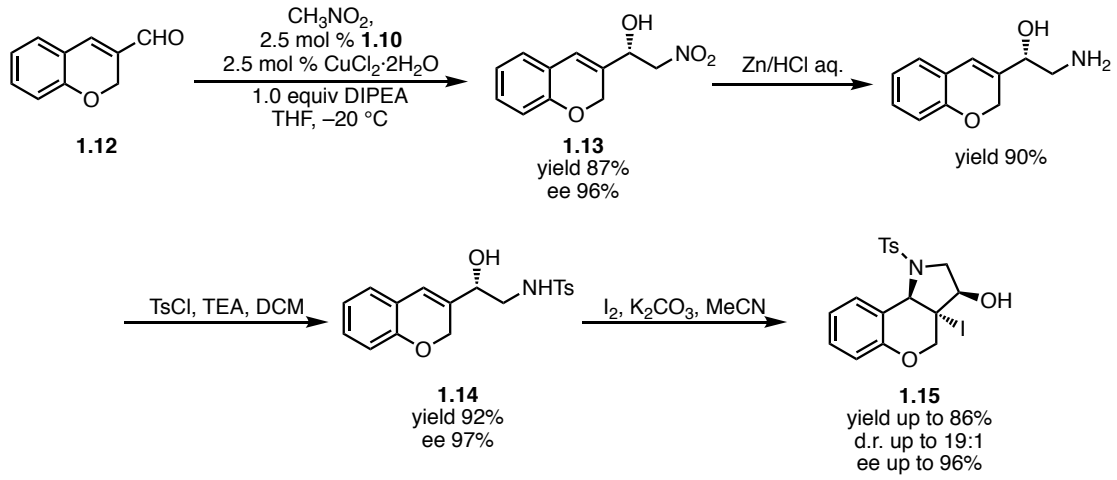

Figure 1.5: Gong's Synthesis of Azatricyclic Framework using Enantioselective Henry Reaction

1.1.2 The Nitro-Mannich Reaction or aza-Henry Reaction

The addition of nitronate anion to an imine electrophile to form a C–C bond is known as the nitro-Mannich (or aza-Henry) reaction. The first report of this transformation was published by L. Henry in 1896.[16] This reaction allowed access to β-nitroamines, which are easily converted into useful synthetic intermediates (Figure

1.6). For example, reduction of the nitro group affords 1,2-diamines (**1.16**), hydrolysis gives α-aminocarbonyls (**1.17**), and radical denitration gives monoamines (**1.18**). [1]

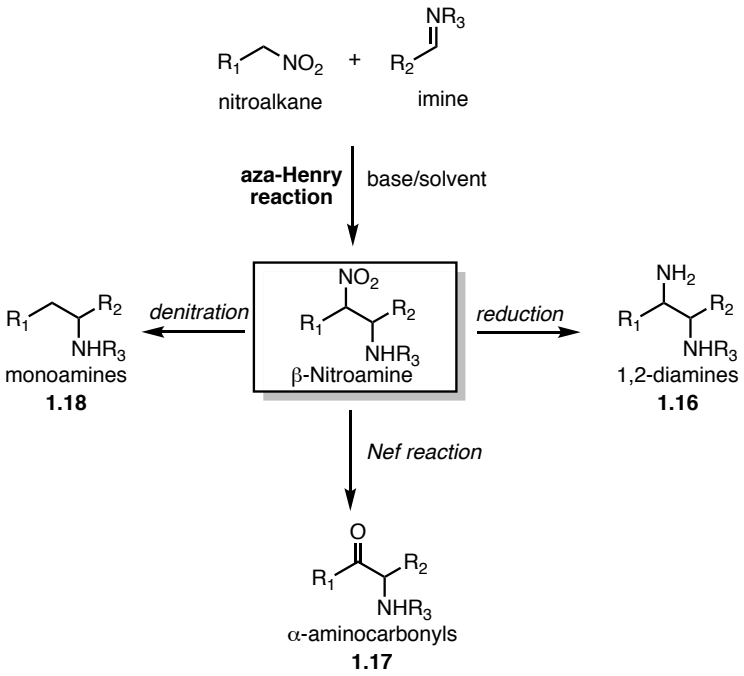

Figure 1.6: aza-Henry Reaction and its Synthetic Applications

The significant interest in nitro-Mannich began with the development of the first acyclic diastereoselective reactions reported by Anderson and his coworkers in 1998 (Figure 1.7).[17] The author treated lithium nitronates with protected imines (**1.19**) in the presence of acetic acid to produce nitro-Mannich products (**1.20**) with excellent *anti* diastereoselectivity and yield. Due to the instability of (**1.20**), the group synthesized 1,2-diamines (**1.21**) by reduction of the nitro group and removal of the amine protecting group. The author also suggests that the addition of a nitronate anion to an imine is thermodynamically unfavored due to the difference in pKa values

between the nitronate anion (pK_a 9) and the anion of the nitro-Mannich product (**1.20**) (pK_a 35). Hence, acetic acid is crucial for the reaction to occur.

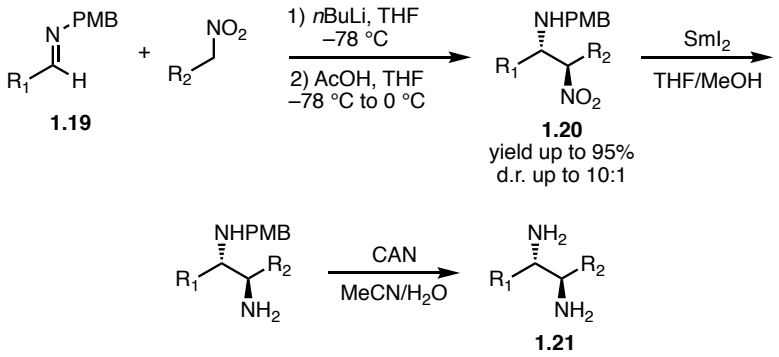

Figure 1.7: Anderson's First Diastereoselective aza-Henry Reaction

In 1999, Shibasaki and coworkers reported the first enantioselective version of the nitro-Mannich reaction between coordinating N-phosphinoyl imines (**1.22**) and nitromethane. Heterobimetallic (**1.23**) afforded β-nitroamine (**1.24**) in good yield and excellent enantioselectivity (Figuare 1.8, top).[18] Interestingly, the complex prepared in a 1:1:2 ratio of $Yb(O^iPr)_3$, KO^tBu, and (R)-binapthol did not catalyze the reaction, however the same component mixed in 1:1:3 ratio afforded excellent results. The heterobimetallic complex (**1.23**) possesses Lewis acidic and Bronsted basic sites, which activates both the nitro compound and the imine substrate, hence no base is required for the reaction. Using LDI-TOF mass spectra studies, the authors reported that active catalyst was a complex formed by [YbK(binaphthoxide)$_2$] and (R)-binapthol. However, nitroalkanes other than nitromethane were not suitable coupling partners. This lack of scope was attributed to the smaller size of the binding pocket of

the catalyst which does not have sufficient space to accommodate both electrophilic and nucleophilic coupling partners.

The same group later showed that the catalyst derived from (R)–ALB AlLi[(R)-binaphthoxide]$_2$ (**1.25**) and KO^{t}Bu was an efficient catalyst for a variety of nitroalkanes.[19] Using this BINOL-based catalyst system, β-nitroamines (**1.26**) were produced with good to excellent enantioselectivity (Figure 1.8 below).

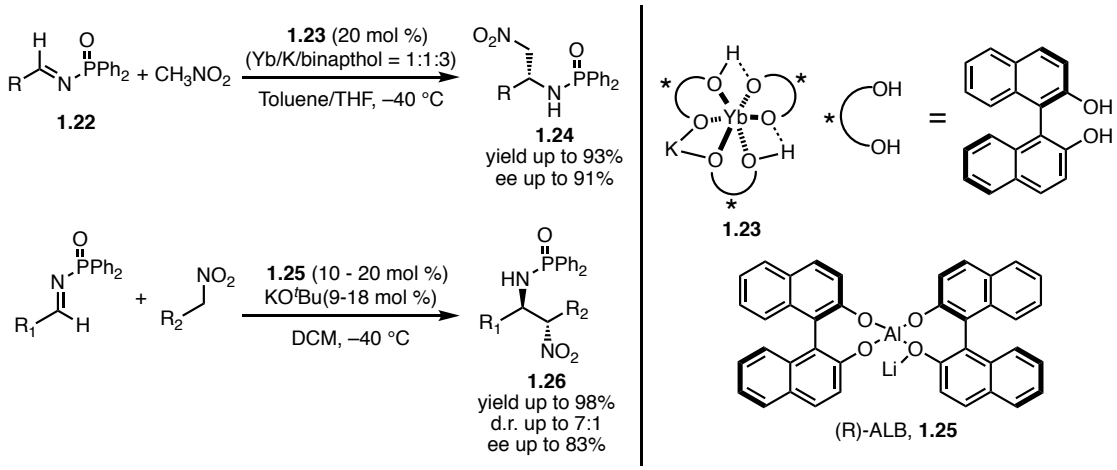

Figure 1.8: Pioneering Studies of Enantioselective aza Henry Reaction by Shibasaki and Coworkers

Selected aspects of the nitro-Mannich reactions have been appeared in reviews on related subjects. These include reviews on multimetallic multifunctional catalysts,[20] asymmetric addition to C=N bonds,[21] organocatalysis,[22] N-acylimines,[23] and synthesis of α,β-diamino acids.[24] Considering the significance of aza-Henry reactions there are several reviews reported on the literature.[25] More recent reviews summarize literature

on the nitro-Mannich reaction and its applications in organic synthesis published up to 2013.[4] More recent examples of nitro Mannich are discussed below.

In 2017, Duan and coworkers reported the mild, bifunctional phase-transfer catalyst to catalyze the diastereo- and enantioselective aza-Henry reaction of β,γ-unsaturated nitroalkenes (**1.27**) with amidosulfones (**1.28**). Using a bifunctional phase-transfer catalyst (**1.29**) derived from cinchona alkaloids, a variety of substrates afford nitro-Mannich products (**1.30**) with excellent diastereo- and enantioselectivity (Figure 9).[26]

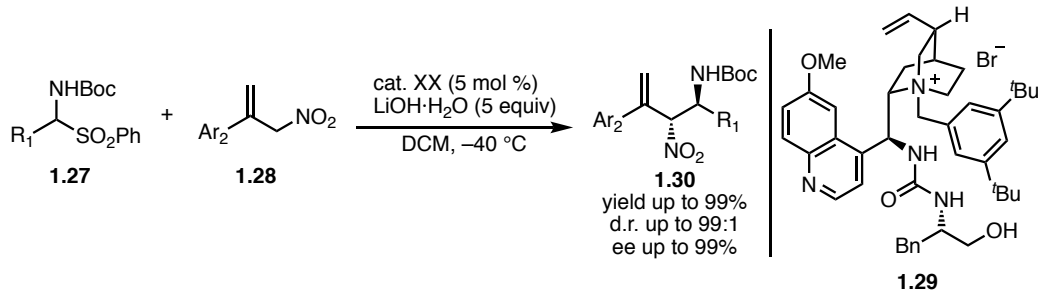

Figure 1.9: Duan's Bifunctional Phase-Transfer Catalyzed Enantioselective and Diastereoselective aza-Henry Reaction of Amidosulfones

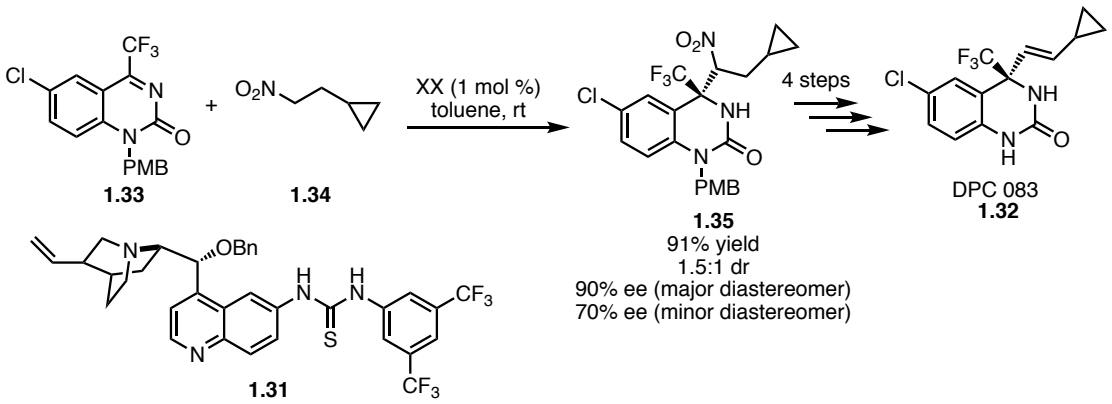

Figure 1.10: Wang's Synthesis of anti-HIV drug DPC 083 Using nitro-Mannich Reaction with Thiourea Catalyst **1.31**

In 2011 Wang and coworkers utilized thiourea (**1.31**) as a catalyst for the nitro-Mannich reaction of cyclic trifluorometthyl ketimines in the synthesis of the anti-HIV drug DPC 083 (**1.32**).[27] The nitro-Mannich reaction between cyclic ketimine (**1.33**) and nitroalkane (**1.34**) afforded β-nitroamine (**1.35**) in 91% yield and 90% ee (major diastereomer) albeit in poor diastereoselectivity. Completion of the synthesis of DPC 083 (**1.32**) was accomplished in further four steps (Figure 1.10).

1.1.3 Michael Addition

Nitroalkanes are a convenient source of stabilized carbanions that react with electron deficient olefins giving the corresponding γ-nitro substituted 1,4-adducts with high regioselectivity. The γ-nitro substituted products are useful synthetic intermediates which can be derivatized into useful functional groups such as amine, carbonyl, etc. (Figure 1.11).[1]

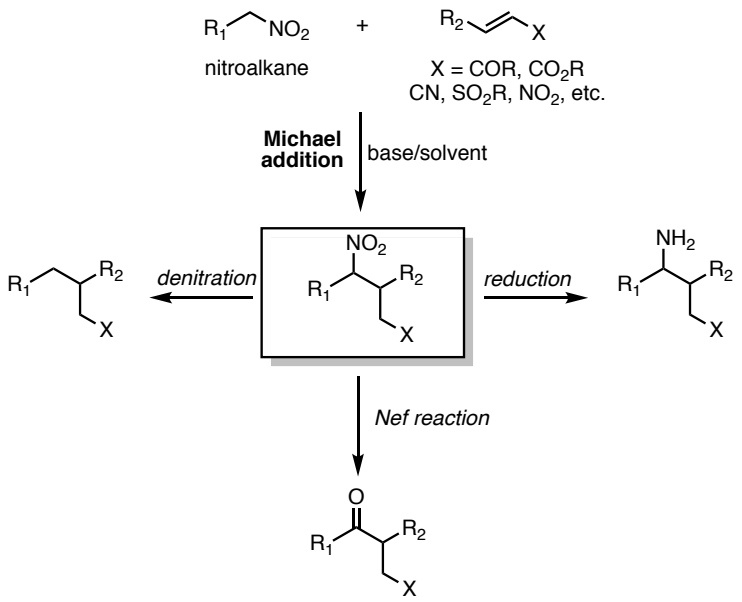

Figure 1.11: The Nitro-Michael Reaction and its Synthetic Applications

In 1916, Kohler and coworkers published the first example of nitroalkane reacting with chalcone (**1.36**).[28] Sodium methoxide is the base in the reaction, which is generated by combining sodium and methanol. Nitromethane reacts with α,β-unsaturated carbonyls to afford γ-nitroketone (**1.37**) in excellent yield (Figure 1.12). Even though only a few examples of primary and secondary nitroalkanes were studied, this was an important step in the development of conjugate addition reactions using nitroalkane nucleophiles.

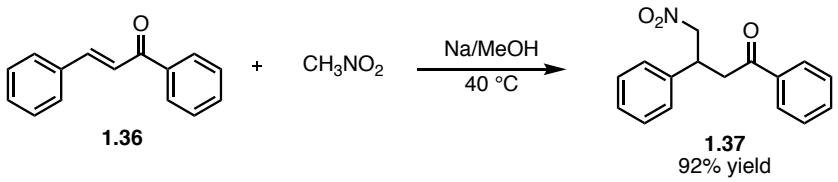

Figure 1.12: Kohler's Early Study of Conjugate Addition Reaction Using Nitroalkane as Nucleophiles

Nitroalkanes in Michael additions have been extensively used in organic synthesis and have been reviewed.[2] This review covers syntheses of γ-nitrocarbonyl products and their applications in organic synthesis. The asymmetric organocatalytic synthesis of γ-nitrocarbonyls through Michael reaction has been extensively reviewed more recently.[29] A few recent examples of Michael addition using nitroalkanes as nucleophiles are discussed below.

In 2015, Watson and coworkers reported a highly diastereoselective Michael reaction using α-substituted, β-nitrocarbonyls as nucleophiles to afford functional group rich stereodiads containing fully substituted nitrogen-bearing centers.[30] Good to excellent diastereoselectivity was observed. For example, a mixture of diastereomers of Weinreb amide (**1.38**) reacts with methyl acrylate to afford fully substituted nitroalkane (**1.39**) with excellent yield and diastereoselectivity. This transformation tolerates various types of carbonyls on the nucleophile as well as a wide range of Michael acceptors (Figure 1.13).

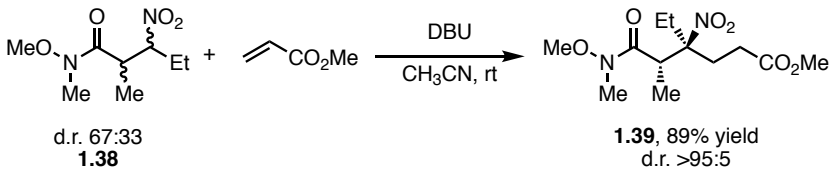

Figure 1.13: Watson's Diastereoselective Michael Reaction Using β-nitrocarbonyls as Nucleophiles

The author proposes internal hydrogen bonding in the nitroalkane tautomer imparts the observed relative stereochemistry of the observed products. A rapid reversible deprotonation of the diastereomeric mixture of nitroalkane (**1.38**)

establishes a tautomer (**1.40**). Intramolecular hydrogen bonding to the adjacent carbonyl organizes compound (**1.39**). From this common intermediate, the Michael acceptor likely reacts away from the alkyl group (Figure 1.14). This model is consistent with the observed diastereoselectivity in these transformations.

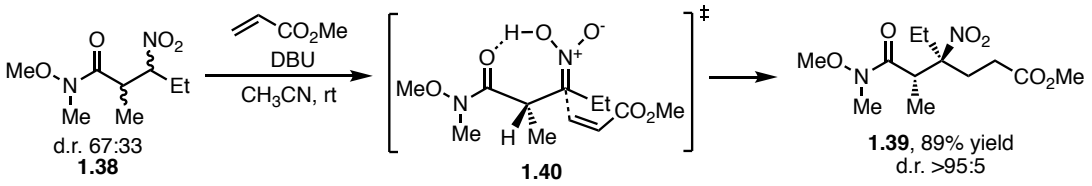

Figure 1.14: Watson's Proposed Model for Observed Diastereoselectivity

In 2017 Miaura and coworkers reported an enantioselective catalytic conjugate addition of nitroalkanes (**1.41**) to α,β-unsaturated ketones (**1.42**) using a novel sulfonamide-thiourea organocatalyst (**1.43**).[31] The author prepared a variety of enantioenriched γ-nitrocarbonyl products (**1.44**) using this protocol in excellent enantioselectivity (Figure 1.15). However, the scope with respect to nitroalkane is very limited. Nitroalkanes other than nitromethane, nitroethane, and 2-nitropropane were not investigated. Further, scope with respect to the Michael acceptor is limited to aromatic enones. A wide range of Michael acceptors were not studied under these catalytic conditions.

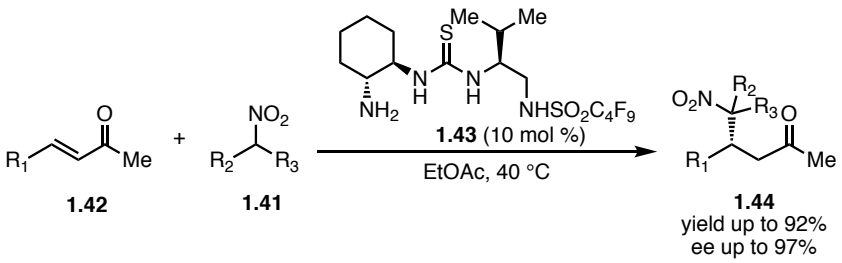

Figure 1.15: Miaura's Enantioselective Conjugate Addition Reaction Using Organocatalyst **1.43**

1.1.4 Allylation of Nitroalkanes

In the early 1970's Tsuji and coworkers reported the palladium-catalyzed telomerization of butadiene using nitroalkanes as nucleophiles towards the synthesis of many natural products.[32] Since then, palladium catalysis has served as a broad platform for the allylation of nitroalkanes using allylic electrophiles.

1.1.4.1 Allylation of Unactivated Nitroalkanes

In 1982, Aleksandrowicz and coworkers reported the first example of the allylation of nitroalkanes using allylic chlorides, acetates, phenyl ethers and alcohols in the presence of palladium catalysts (Figure 1.16, top).[6] In the same year, Wade and coworkers published similar reactions of (phenylsulfonyl)nitromethane, primary nitroalkanes, phenyl nitromethane, and α-nitro esters using cinnamyl acetates as electrophiles (Figure 1.16, bottom).[33] These reactions often yielded a mixture of regioisomers (**1.45** and **1.46**) resulting from attack of nitronate anion at both electrophilic sites of the π-allyl intermediate.

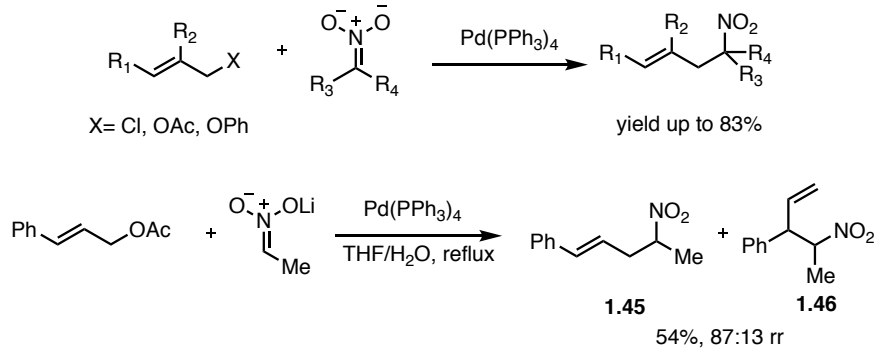

Figure 1.16: Aleksandrowicz and Wade's Pioneering Studies of Allylation of Unactivated Nitroalkanes

In 1996, Helmchen and coworkers published the first example of enantioselective allylic alkylation reaction using nitromethane as a nucleophile.[34] Using symmetrical 1,3-disubstituted allylic carbonates (**1.47**) as allylating agents in combination with 4,5-dihydrooxazoles (**1.48**) as ligands, excellent yields and enantioselectivities were obtained (Figure 1.17). Under these catalytic conditions, overalkylation competes with monoalkylation, depending on the stoichiometry of nitromethane employed. Even though only nitromethane was employed as a nucleophile, this was an important step in the asymmetric allylic alkylation of nitroalkanes.

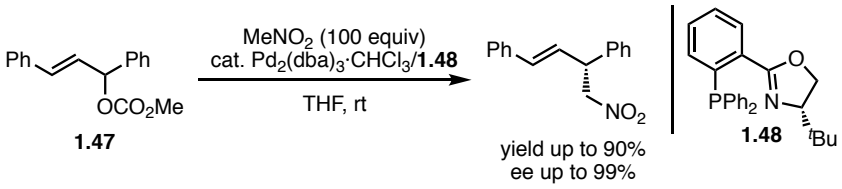

Figure 1.17: Helmchen's Pioneering Studies of Asymmetric Allylic Alkylation of Nitroalkanes

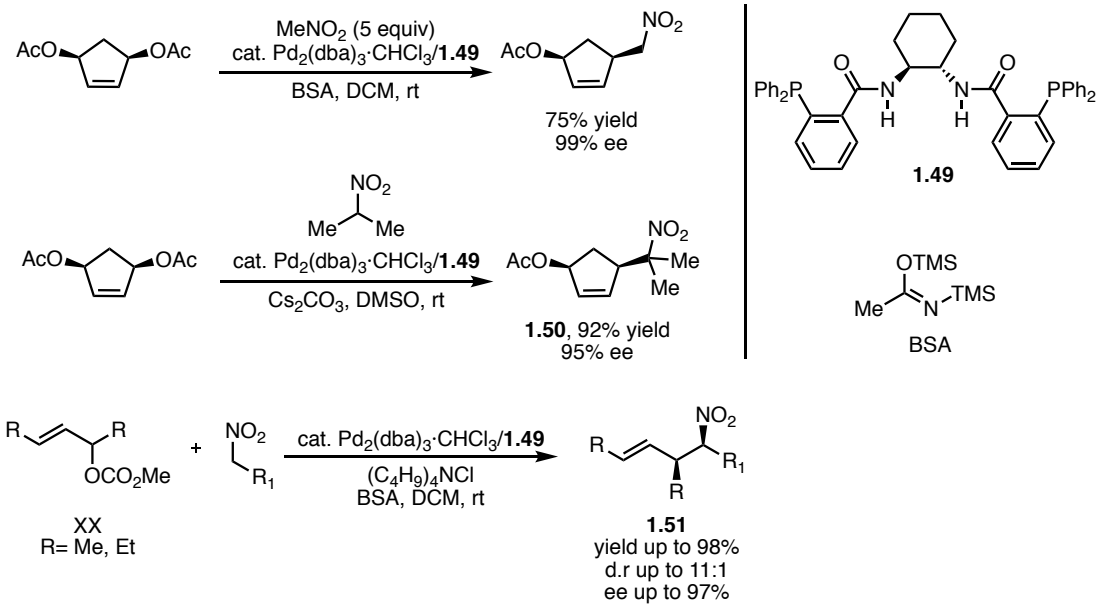

Figure 1.18: Trost's Studies of Asymmetric Allylic Alkylation of Nitroalkanes

In 2000, Trost and coworkers expanded the scope of allylic electrophiles such as meso-diesters, cycloalkenyl carbonates and acetates.[35] Utilizing ligand (**1.49**), nitromethane and 2-nitropropane were alkylated under different conditions providing highly enantioenriched nitroalkanes (**1.50**) (Figuare 1.18). Soon thereafter, the method was expanded to substituted nitroalkanes. In this case, symmetrical substituted 1,3-dialkyl allylic carbonates were employed as allylating agents.[36] Homoallylic nitroalkanes (**1.51**) were obtained with good diastereoselectivity and uniformly excellent enantioselectivity (Figure 1.18 bottom).

In 2006, Helmchen and coworkers showed that iridium catalysis can also promote C-allylation of nitroalkanes when using monosubstituted allylic carbonates (**1.52)**.[37] Utilizing phosphoramidite ligand (**1.53**), both unactivated nitroalkanes and activated ethyl nitroacetate were coupled with excellent efficiency. Because

nitromethane did not undergo efficient coupling, ethyl nitroacetate (**1.54)** was used as a nitromethane surrogate, as it could be easily decarboxylated to afford the nitromethylated product (**1.55**) in a two-step process. Couplings with ethyl nitroacetate were not diastereoselective, however this is inconsequential because of the subsequent removal of the ester group.

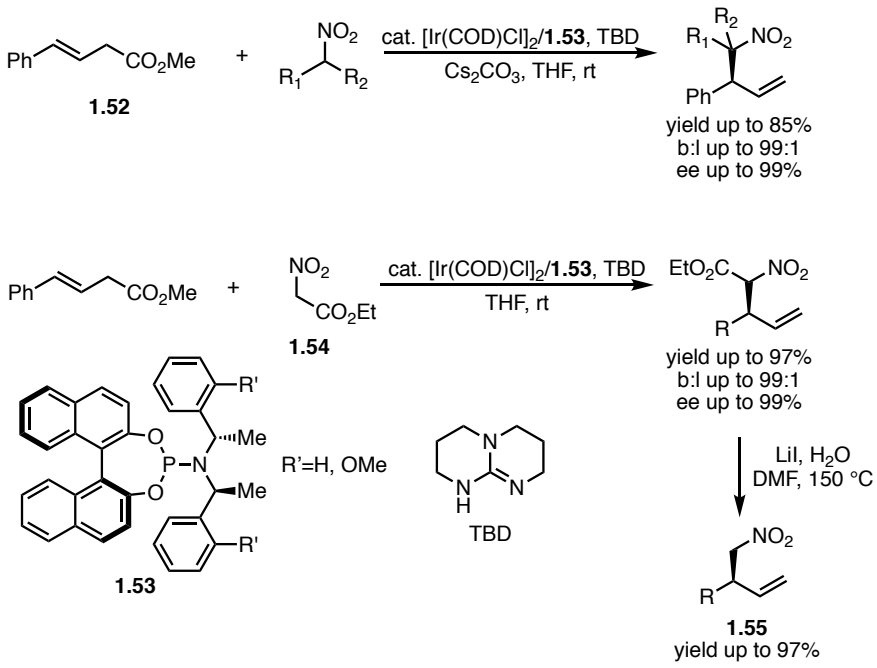

Figure 1.19: Helmchen's Studies of Asymmetric C-Allylation of Nitroalkanes Using Iridium Catalysis

1.1.4.2 Allylation of Activated Nitroalkanes

This section will cover methods for the allylation of "activated" nitroalkanes. This class include those nitroalkanes possessing highly acidic α-protons such as α-nitroesters, α-nitroketones and α-nitrosulfones (pKa ~ 5). As with the allylation of nitroalkanes, the Wade group was instrumental in early studies of α-nitrosulfone

allylation. In 1981, they reported that the lithium salt of (phenylsulfonyl) nitromethane (**1.56**) was allylated using various monosubstituted allylic acetates (**1.57**) with excellent regioselectivity for the linear products.[38]

In 1984, Genet and coworkers pioneered the studies on the allylation of α-nitroacetates (**1.58**). They were allylated using allylic acetates, phenyl ethers, and carbonates (**1.59**) (Figure 1.20).[39] These methods were utilized in various efforts toward the synthesis of complex ergoline alkaloids.[40]

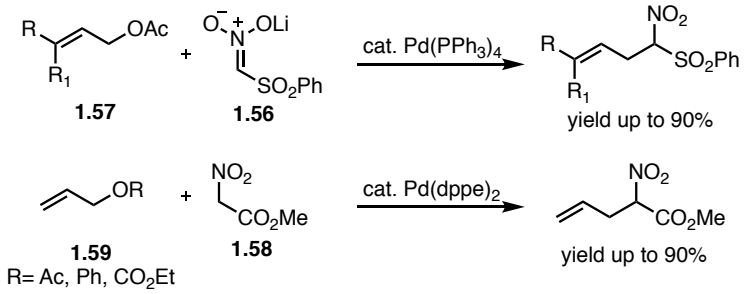

Figure 1.20: Wade and Genet's Pioneering Studies of Allylation of Activated Nitroalkanes

In 2008, White and coworkers reported alkylation of nitroacetates with allylbenzene derivatives. This was achieved through palladium-catalyzed C–H activation (Figure 1.21).[41] This protocol is highly attractive because it precludes the necessity of pre-oxidized electrophiles like allylic acetates and carbonates. By utilizing 2,6-dimethylbenzoquinone (DMBQ) and DMSO as a π-acceptor ligand, nitroacetates were smoothly coupled with allylbenzene in good branched to linear ratios (**1.60**) without the need for prefunctionalized electrophiles.

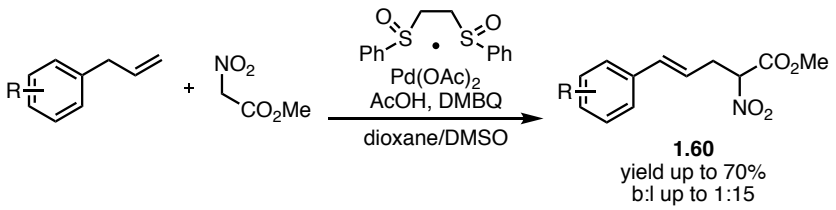

Figure 1.21: White's Palladium Catalyzed Allylic C–H Alkylation of Activated Nitroalkanes

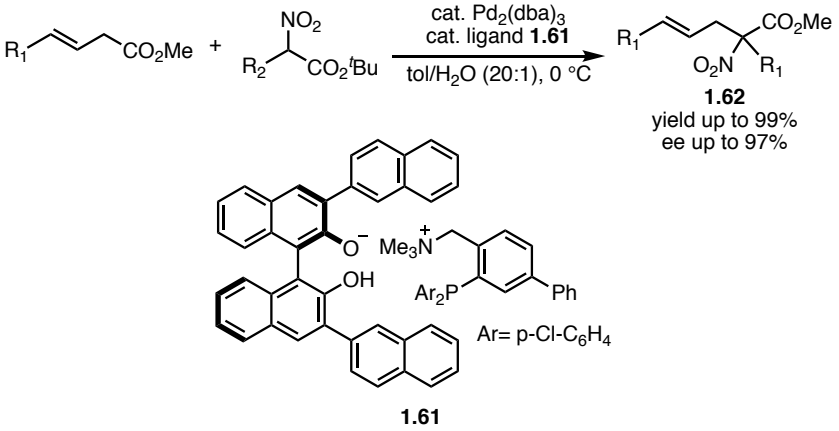

Figure 1.22: Ooi's Palladium Catalyzed Allylation of Nitroalkanes Using Chiral Ion-Paired Ligands

In 2012, Ooi and coworkers published the enantioselective allylation of nitroacetates with cinnamyl carbonates using novel chiral ion-paired ligands (**1.61**).[42] While most chiral, non-racemic ligands used in asymmetric catalysis consist of a single chiral molecule bearing coordinating groups, the authors found that an achiral ammonium phosphine ionically bound to a chiral binaphtholate anion could impart excellent levels of stereocontrol. This new class of ligand was shown to promote the allylation of nitroacetates with cinnamyl carbonates in excellent yield and

enantioselectivity (**1.62**). The products from the reaction could be easily derivatized into α,α-disubstituted amino acid derivatives (Figure 1.22).

In 2011, Tunge and coworkers reported that α-nitroketones can undergo three component unsymmetrical bisallylation under palladium catalysis (Figure 1.23 top).[43] A variety of homoallylic nitroalkanes could be synthesized using this novel strategy with excellent yield. This reaction proceeds by initial allylation of the α-nitroketones (**1.63**) to afford (**1.64)**, followed by transfer of the acyl group to an exogenous alcohol (**1.65**), which is accompanied by nitronate anion formation. The resultant nitronate anion (**1.66**) undergoes a second Tsuji-Trost type allylation with the newly formed allylic acetate to provide unsymmetrical bisallylated nitroalkanes (**1.67**) (Figure 1.23 bottom).

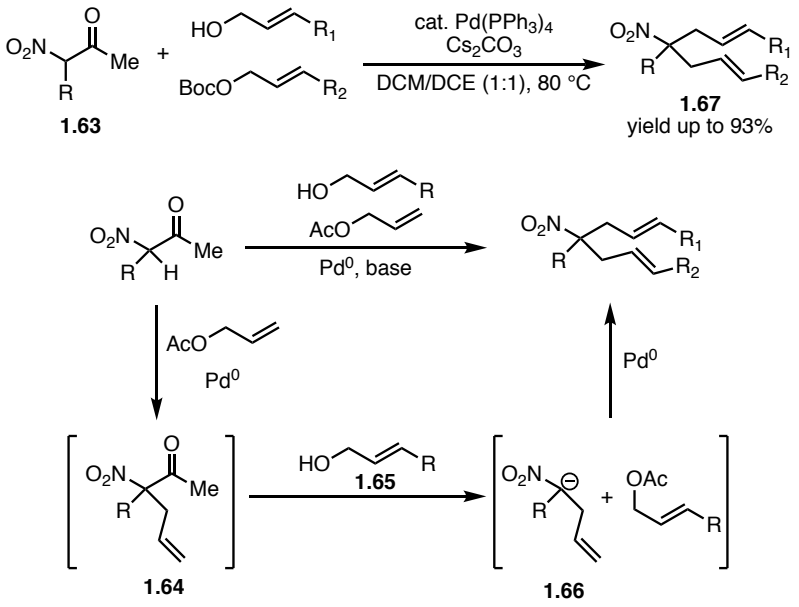

Figure 1.23: Tunge's Deacylative Allylation of Nitroalkane Using Palladium Catalysis

1.1.4.3 Intramolecular Allylation of Nitroalkanes

In 1987, Tsuji and coworkers pioneered the studies on the intramolecular decarboxylative allylation of carbon nucleophiles. The author showed that α-nitro allyl esters could undergo *C*-allylation under decarboxylative palladium catalysis.[44] Only a single example was reported and a significant amount of *O*-allylation product was observed. Although the selectivity could be enhanced at low temperatures, *O*-allylation could not be avoided (Figure 1.24).

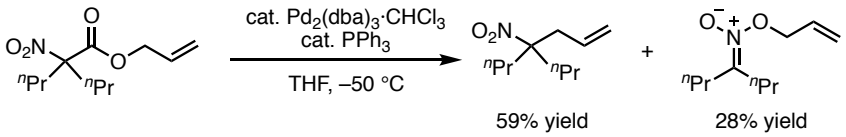

Figure 1.24: Tsuji's Initial Report on Intramoleculare Allylation of Nitroalkanes

In 2010, Tunge and coworkers reinvestigated the decarboxylative allylation of nitroalkanes, and showed that *O*-allylation could be suppressed and *C*-allylated products (**1.68**) could be formed in excellent yields under mild reaction conditions (Figure 1.25).[45]

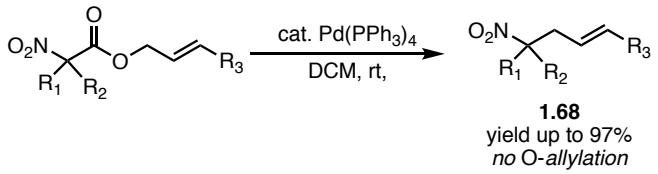

Figure 1.25: Tunge's Decarboxylative Intramolecular Allylation of Nitroalkanes

Examination of the reaction mechanism revealed that *O*-allylation proceeds in certain cases, but the process is reversible via a bimolecular palladium π-allyl (**1.69**) reformation from the *O*-allylated nitronate intermediate (**1.70**). To suppress the *O*-allylated nitronate, which produces aldehyde (**1.71**) byproduct, increasing the reaction concentration allowed irreversible *C*-allylation to favor. Thus, the desired products (**1.72**) were formed with excellent yields and selectivity (Figure 1.26).

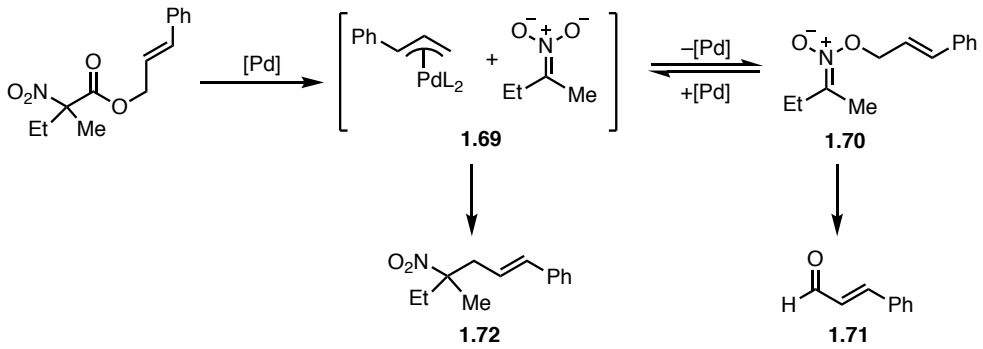

Figure 1.26: Tunge's Proposed Mechanism for the Decarboxylative Intramolecular Allylation of Nitroalkanes

In another example of an intramolecular allylation, Rajappa and coworkers have shown that allyl groups can be transferred from pendant allyl esters without undergoing decarboxylation.[46] For example, α-nitroamide (**1.72**) undergoes Michael addition to allyl acrylate, affording α-nitrocarbonyl (**1.73**) bearing a pendant allyl ester. Under the palladium catalysis conditions, the allyl group is transferred to palladium, forming a π-allyl complex. The α-nitro carbon is deprotonated by DBU, and combines with π-allyl fragment to afford (**1.74**) in good yield (Figure 1.27). The

products formed were used in the synthesis of *N*-hydroxypyroglutamylproline ester derivatives.

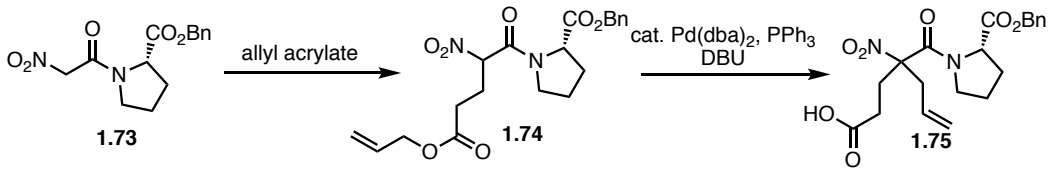

Figure 1.27: Rajappa's Intramolecular Allylation of Nitroalkanes under Palladium Catalysis

1.1.5 Arylation of Nitroalkanes

The chemistry of arylation of nitroalkanes has progressed more slowly when compared to allylation of nitroalkanes. Early examples of arylation of nitroalkanes include reactions of nitronate anions with aryllead acetates,[47] iodonium salts,[48] triarylbismuth reagents,[49] and arenes in the presence of manganese salts.[50] While these early studies provided proof of concept, an ideal method would avoid the need for stoichiometric arylmetal reagents. Palladium catalysis has proven to be the strategy for achieving this goal.

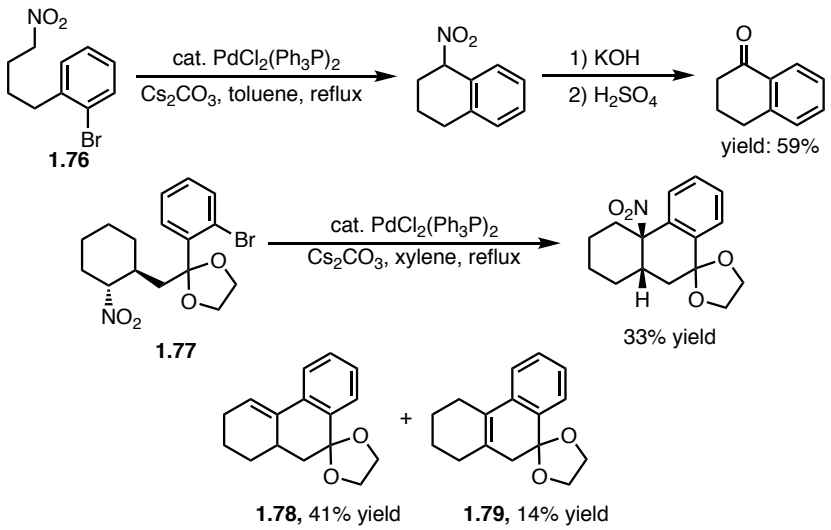

Figure 1.28: Muratake's Pioneering Studies on Palladium Catalyzed Intramolecular Arylation of Nitroalkanes

In 1998, Muratake and coworkers reported the first intramolecular arylation of nitroalkanes using palladium catalysis.[51] The scope of the reaction was not studied thoroughly, but both primary and secondary nitroalkanes (**1.76** and **1.77**) were shown to undergo cyclization in synthetically useful yields, albeit with significant amount of byproducts (**1.78** and **1.79**), formed due to the competing elimination reaction (Figure 1.28).

In 2000, Buchwald and coworkers, explored to the more useful intermolecular arylation of nitroalkanes. By utilizing electron rich, sterically encumbered biaryl phosphine ligand (**1.80**), excellent yields of benzylic nitroalkanes (**1.81**) were produced using a variety of complex primary nitroalkanes with aryl bromides and aryl chlorides.[5a,b] Significantly, nitroalkanes bearing esters and terminal olefin functional groups were effectively arylated and no competing enolate arylation or Heck-type reaction was observed. Although this protocol showed broad generality of primary

nitroalkanes, secondary nitroalkanes and nitromethane were not suitable coupling partners reaction (Figure 1.29).

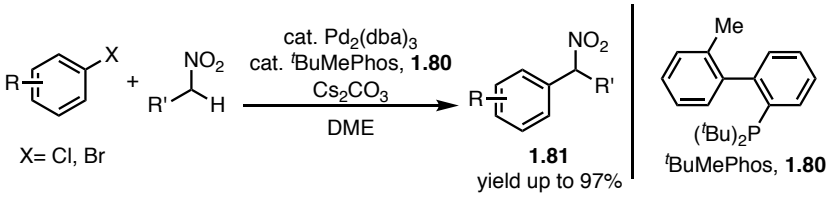

Figure 1.29: Buchwald's Palladium Catalyzed Intermolecular Arylation of Nitroalkanes

Subsequently, Kozlowski and coworkers reported that the arylation of nitromethane with pseudohalides and aryl halides could be achieved though judicious choice of ligand.[5d] The authors utilized electron rich, slightly less sterically encumbered Xphos (**1.83**) compared to Buchwald's ligand (**1.80**). The generality of the nitromethylation reaction was broad, allowing access to a variety of benzyl nitroalkanes (**1.82**) in good yield (Figure 1.30). Although these studies required the use of nitromethane as solvent, subsequent modification used only 2-10 equivalents of nitromethane, minimizing the safety concerns that typically accompany reactions using large quantities of nitromethane.[5e]

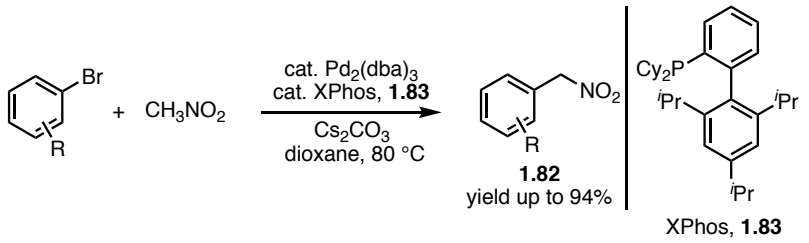

Figure 1.30: Kozlowski's Palladium Catalyzed Intermolecular Arylation of Nitromethane

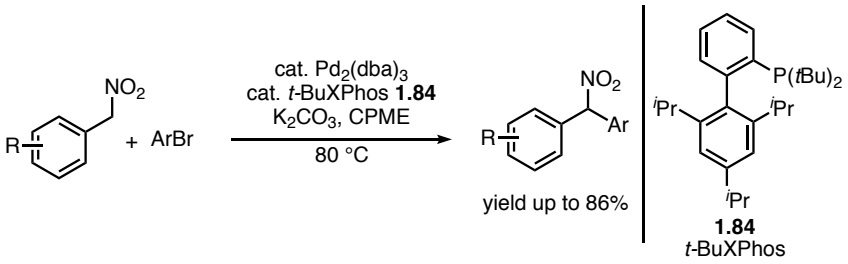

Figure 1.31: Kozlowski's Palladium Catalyzed α-arylation of arylnitromethane

In 2015, Kozlowski and coworkers developed palladium catalyzed conditions for the α-arylation of arylnitromethane (Figure 1.31). Using high-throughput experimentation techniques, *t*-BuXPhos (**1.84**)was identified as the optimal ligand for this strategy.[52] Some of the diaryl nitromethane products are unstable under the reaction condition, a one pot diarylation/Nef reaction sequence was developed to afford benzophenone in good yields. However, some diarylnitromethanes were observed to be stable and isolated in good yield. Finally, the authors also demonstrated that the orthogonal conditions for the mono- and diarylation can be done in a one-pot diarylation of nitromethane (Figure 1.32).

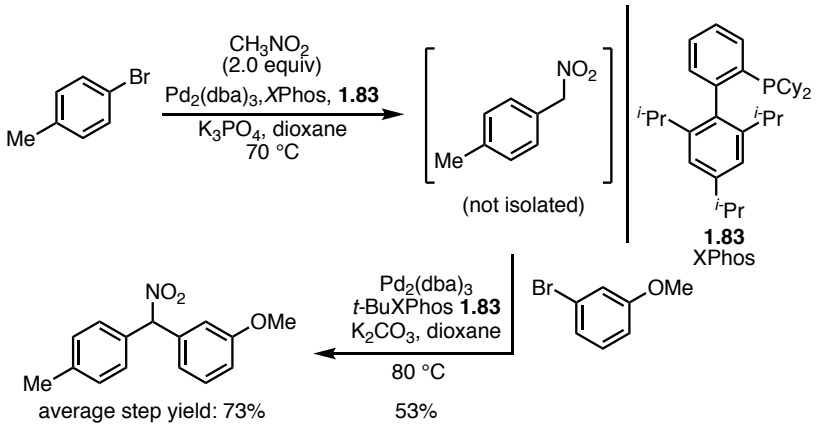

Figure 1.32: Kozlowski's Palladium Catalyzed One-Pot Diarylation of nitromethane

1.1.6 Miscellaneous Reaction of Nitroalkanes

1.1.6.1 The Suzuki-Miyaura Reaction of Nitroarenes

Nitroarenes are highly versatile, cheap, common aromatic building blocks in organic synthesis. They can be easily prepared from nitration of the parent arenes. In 2011, Wu and coworkers showed a rhodium catalyzed C–O bond forming reaction using nitroarenes (Figure 1.33, top).[53] Additionally, an analogous copper catalyzed C–S cross coupling of nitroarenes was described by Shinde and coworkers in 2013 (Figure 1.33, bottom).[54] Although these methods represent a good synthetic tool, they suffer from limited substrate scope and electron withdrawing groups are necessary for the excellent yields of the coupling products. However, these pioneering studies show that nitroarenes can undergo nucleophilic aromatic substitution in which the NO_2 group serves as a leaving group under rhodium and copper catalysis.

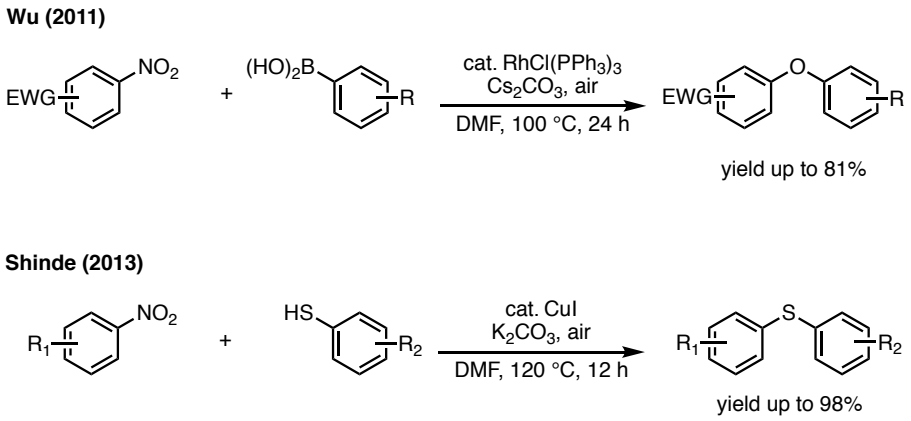

Figure 1.33: Wu and Shinde's Studies on Rhodium and Copper-Catalyzed Cross Coupling of Nitroarenes

In 2017, Sakaki and coworkers described a palladium-catalyzed C–C bond forming reaction using nitroarene and aryl boronic acids. After extensive optimization, the authors discovered electron rich, sterically encumbered biarylphosphine Brettphos (**1.84**) as the optimal ligand for this transformation.[7b] In addition, K_3PO_4 in the presence of 18-crown-6 and a trace amount of water was found to be crucial for the success of the transformation. Under the optimized reaction condition, a wide array of nitroarenes underwent this Suzuki-Miyuara coupling affording biaryl compounds in excellent yields (**1.85**) (Figure 1.34). Several heterocyclic substrates were tolerated under this reaction conditions. Furthermore, electron-rich, electron-deficient, and sterically encumbered boronic acids are compatible with this protocol.

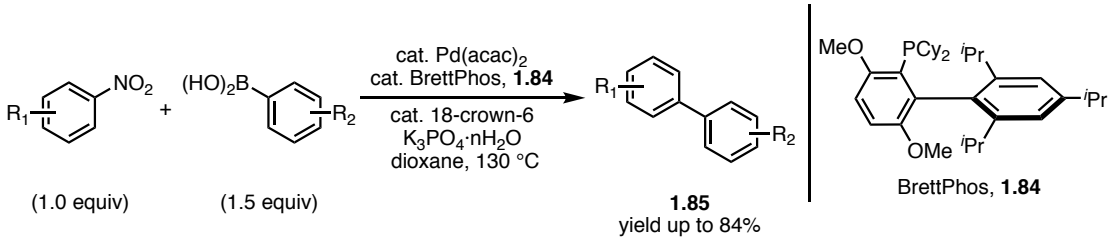

Figure 1.34: Sakaki's Groundbreaking Studies on Palladium-Catalyzed Suzuki-Miyuara Cross Coupling of Nitroarenes and Boronic Acids

1.1.6.2 The Buchwald-Hartwig Amination of Nitroarenes

In 2017, Nakao and coworkers described the first example of palladium catalyzed Buchwald Hartwig amination of nitroarenes. By utilizing biarylphosphine Brettphos (**1.84**) as the optimal ligand, a wide array of nitroarenes (**1.85**) with diverse electronic properties were found to be excellent substrates for this C–N bond forming reaction. In addition to secondary amines, primary amines (**1.86**) could also be converted into aniline derivaties in excellent yield (**1.87**) (Figure 1.35).[7a]

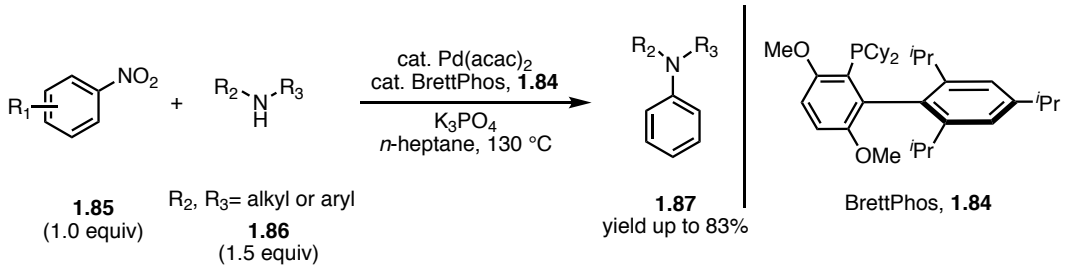

Figure 1.35: Nakao's First Example of Palladium Catalyzed Buchwald Hartwig Amination of Nitroarenes

To gain insight into the reaction mechanism, the authors performed stoichiometric studies. Treatment of $(COD)_2Pd(CH_2TMS)_2$ (**1.88**), BrettPhos (**1.84**),

and nitroarene in THF at 60 °C afforded the oxidative addition complex (**1.89**). X-ray structure clearly shows that the electron rich Pd^0 oxidatively added into Ar–NO_2 bond (Figure 1.36).

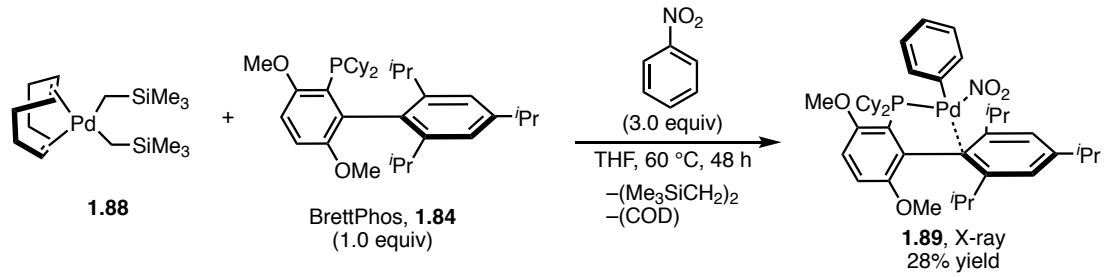

Figure 1.36: Nakao's Stoichiometric Studies in Palladium Catalyzed Buchwald Hartwig Amination of Nitroarenes

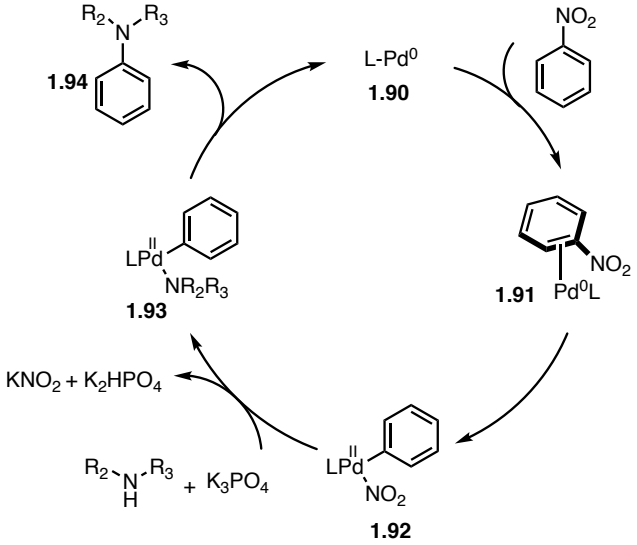

Figure 1.37: Nakao's Proposed Mechanism Palladium Catalyzed Buchwald Hartwig Amination of Nitroarenes

The author proposes a mechanism for the Buchwald-Hartwig amination of nitroarenes which is described in figure (1.37). Nitroarene reacts with Pd(0) complex (**1.90**) to form η^2 arene palladium (0) complex (**1.91**), followed by oxidative addition of the C–NO_2 bond to afford (**1.92**). Subsequently, the amine reacts with (**1.92**) in the presence of base to afford aryl Pd amide (**1.93**), which undergoes reductive elimination to give aryl amine (**1.94**). The arene ligand can then exchange to regenerate the active catalyst (**1.90**).

1.1.7 Reduction of Nitroalkanes to Amines

The reduction of a nitro group represents a versatile and powerful way to access amino group in a molecule.[1] There are a variety of methods developed to reduce aliphatic and aromatic nitro compounds to amines.[55] The most frequently employed methods involve catalytic hydrogenation using palladium on carbon (Pd/C) or Raney nickel. Other common methods include Zn/AcOH or HCl, $NiCl_2/NaBH_4$, $CoCl_2/NaBH_4$, $HCOONH_4$ in the presence of Pd/C.

In 2010, Pedro and coworkers reported the enantioselective synthesis of (*S*)-(+)-sotalal, a member of the class III β–blockers, using catalytic enantioselective Henry reaction to afford β-nitroalcohol (**1.95**). Hydrogentation in the presence of palladium on carbon reduces (**1.95**) to amine (**1.96**) in near quantitative yield (Figure 1.38).[56]

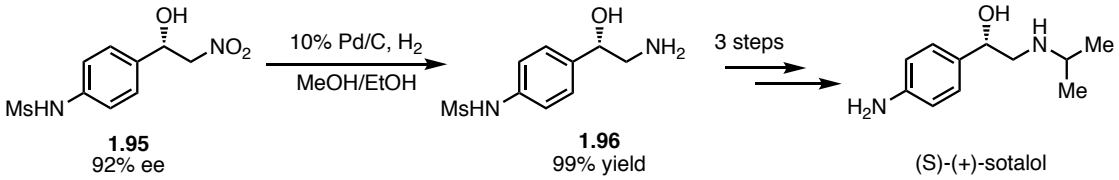

1.95
92% ee

1.96
99% yield

(S)-(+)-sotalol

Figure 1.38: Pedro's Synthesis of (*S*)- (+)-Solatol using Nitroalkane Reduction

The reduction of nitroalkanes can be stereoretentive. Products from the nitro-aldol reaction (section **1.1.1**), aza-Henry reaction (section **1.1.2**), Micheal addition (section **1.1.3**) or allylation (section **1.1.4**) can all be reduced and retain the stereochemistry at the nitro center; as a result, this transformation can be utilized in late stage total synthesis.

In 2011, Johnston and coworkers published the enantioselective synthesis of (–)-nutlin, using catalytic enantioselective aza-Henry reaction to β-nitroamine (**1.97**).[57] The authors used the combination of sodium borohydride with cobalt chloride as a mild and efficient reducing agent of nitroalkanes through the *in situ* formation of cobalt hydride (Figure 1.39). The reduction of (**1.97**) affords diamine (**1.98**) with stereoretention and good yield. Further functional group transformation afforded (**1.99**) (–)-nutlin, a potent cis-imidazoline small molecule inhibitor of p53-MDM2 which is used as a probe in cell biology and drug development.

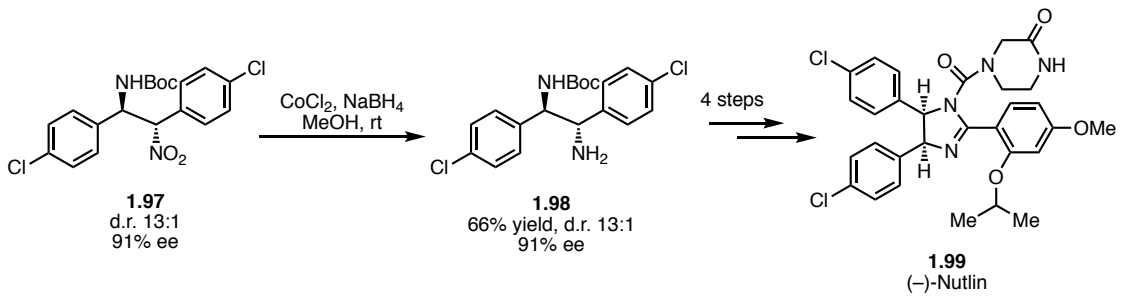

1.97
d.r. 13:1
91% ee

1.98
66% yield, d.r. 13:1
91% ee

1.99
(–)-Nutlin

Figure 1.39: Johnston's Synthesis of (–)-nutlin using Sodium Borohydride Reduction of Nitroalkanes in the presence of Cobalt Chloride

In 2015, Orlandi and coworkers reported a mild, metal-free reduction of both aromatic and aliphatic nitro groups to amines using the combination of trichlorosilane and tertiary amine (Figure 1.40). The scope of the reaction was broad and highly functional group tolerant, providing product with excellent yield.[58] This metal-free reduction was employed in the reduction of nitrolactone (**1.100**) in the total synthesis of aliskiren.[59] Remarkably, the mild procedure afforded enantiopure aminolactone (**1.101**) in 99% yield without altering the stereochemical integrity of the four stereocenters of the molecule (**1.101**).

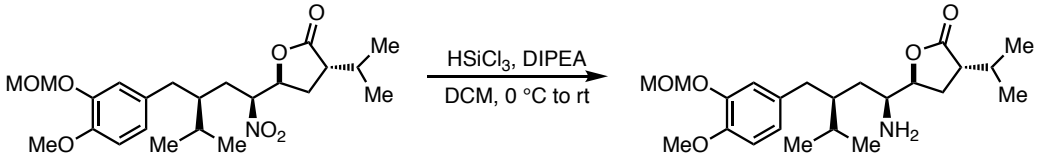

1.100
>99% ee

1.101
99% yield
>99% ee

Figure 1.40: Orlandi's Metal-Free Reduction of Nitroalkane Using Trichlorosilane and Tertiary Amine

1.1.8 Hydrolysis of Nitroalkanes to Carbonyls (The Nef Reaction)

In 1893, M. Konovalov showed that the treatment of potassium salt of 1-phenylnitroethane with dilute acid (AcOH, H_2SO_4) afforded 1-phenylnitroethane and acetophenone.[60] In 1894, J.U. Nef systematically studied the acidic hydrolysis of sodium salt of nitroalkane and demonstrated the generality of this transformation, the conversion of nitroalkanes into the corresponding carbonyl compounds is known as the Nef reaction.[61] The harsh acidic reaction conditions developed by Nef made the reaction incompatible with sensitive functional groups, thus limiting the scope of the transformation. Furthermore, when the pH>1, byproducts such as oximes and hydroxynitroso compound can be formed. To make the reaction more chemoselective and functional group tolerant, oxidative and reductive conditions have been developed for the Nef reaction (Figure 1.41). Nef reactions have been extensively studied in organic synthesis and reviewed, and they will not be discussed here in detail.[62] Few recent examples of the Nef reaction are discussed below.

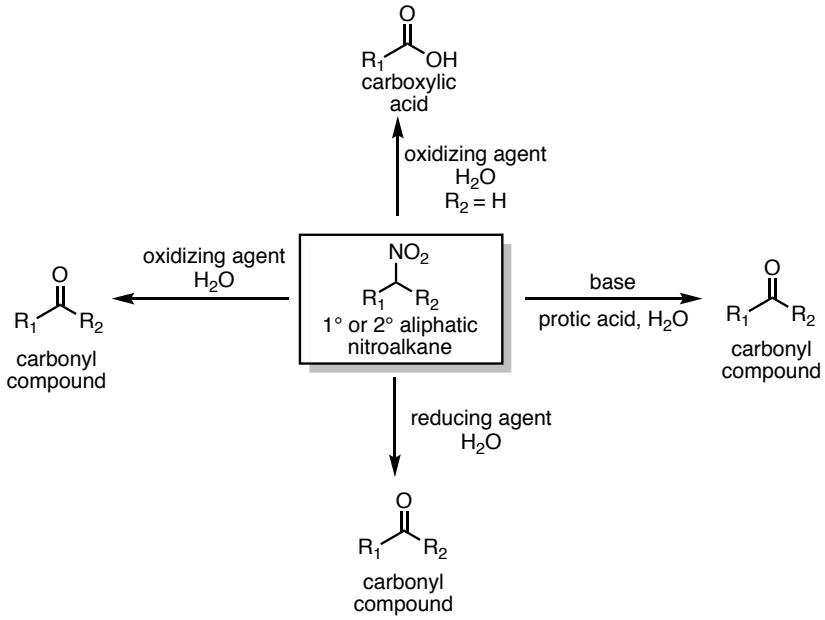

Figure 1.41: Oxidative and Reductive Conditions for the Nef Reaction

Reductive conditions for Nef reactions have been used in the total synthesis of several natural products. Among the reductive methods for accessing carbonyls from nitroalkanes, the McMurry method using $TiCl_3$ is the most commonly used. The total synthesis of Spirotryprostatin B was accomplished by Fuji and coworkers using the McMurry method.[63] The conversion of the nitroolefin (**1.102**) to the corresponding aldehyde (**1.103**) was carried out under reductive conditions using excess $TiCl_3$ in aqueous solution. The initially formed aldehyde oxime was hydrolyzed *in situ* by the excess ammonium acetate.

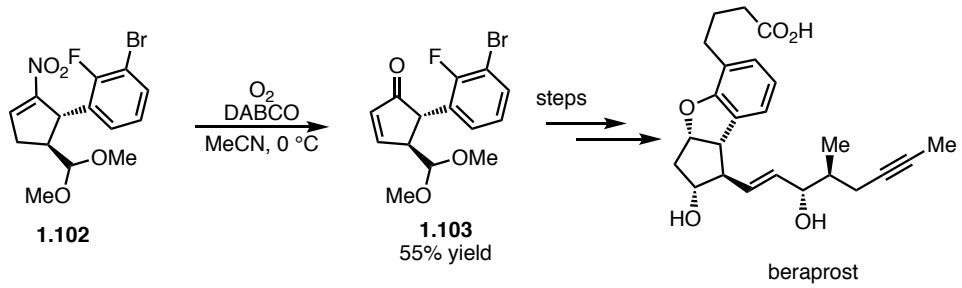

Figure 1.42: Fuji's Synthesis of Spirotryprostatin B Using Reductive Nef Reaction

Oxidative Nef conditions use oxidizing agents, such as potassium permanganate ($KMnO_4$), *m*-choroperbenzoic acid (*m*-CPBA), hydrogen peroxide (H_2O_2), or Oxone®.[64] The oxidative method allows conversion of primary nitroalkanes into aldehydes or carboxylic acids, while the secondary nitroalkanes are converted into ketones.

In 2017, Hayashi and coworkers reported an elegant example of oxidative Nef reaction in the enantioselective synthesis of Beraprost.[65] Nitrolefin (**1.104**) is oxidized to α,β−unsaturated ketone (**1.105**) using oxygen as the oxidant and 1,4-diazabicyclo [2.2.0].

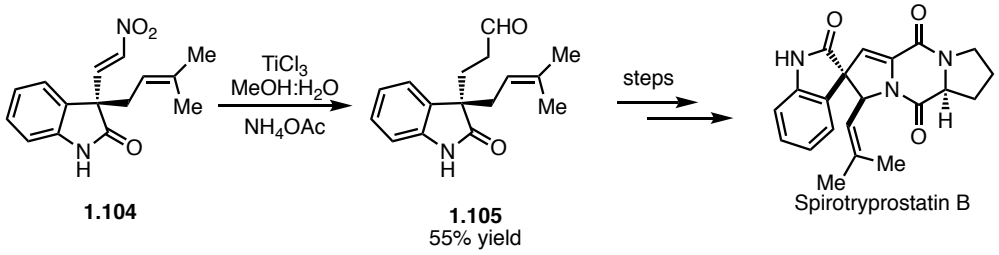

Figure 1.43: Hayashi's Synthesis of Beraprost Using Oxidative Nef Reaction

1.1.9 Denitration of Nitroalkanes

The replacement of a nitro functional group by hydrogen is a relatively novel transformation as compared with other traditional functional group transformations (See section **1.1.7** and **1.1.8**). The ease and functional group compatibility of denitration methods make this strategy a powerful one for natural product synthesis. In 1979, Kornblum and coworkers reported the first radical denitration to afford aliphatic chain (**1.107**).[66] The tertiary nitroalkane (**1.106)** was treated with sodium salt of methyl mecaptan to cleave the carbon-nitrogen bond to afford denitrated product (**1.107**) via radical mechanism in excellent yields (Figure 1.44). However, the scope was limited to tertiary nitroalkanes; secondary nitroalkanes shows little reactivity and primary nitroalkanes were unreactive. Also, toxic HMPA was used as solvent, which negatively impacts the practicality of this approach.

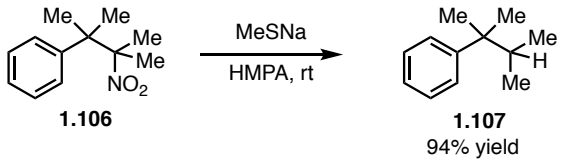

1.106 **1.107**
94% yield

Figure 1.44: Kornblum's First Radical Denitration of Nitroalkanes

In 1981, Ono and Tanner reported independently that tributyltin hydride (Bu_3SnH) is more versatile for denitration of nitroalkanes than sodium salt of methyl mecaptan.[67] Tanner demonstrated that the excess Bu_3SnH and catalytic benzoyl peroxide was efficient for the conversion of tertiary nitroalkanes (**1.108**) into denitrated product (**1.109**) in good yield. Tanner proposed a radical mechanism, as the

reaction was completely inhibited by the addition of strongly electron withdrawing m-dinitrobenzene (Figure 1.45 top).

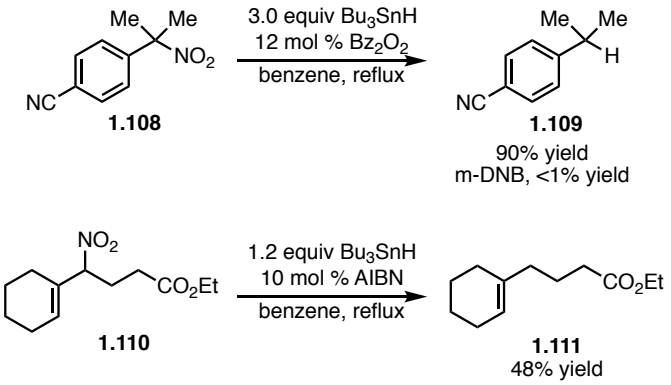

Figure 1.45: Ono and Tanner's Trialkyltin Reagents for Denitration of Nitroalkanes

In 1981 Ono and coworkers reported the first reduction of secondary nitroalkanes (**1.110**). The secondary nitroalkane (**1.110**) was treated with catalytic amount of radical initiator such as 2,2-azobisisobutyronitrile (AIBN) and stoichiometric Bu_3SnH to cleave the carbon-nitrogen bond to afford denitrated product (**1.111**) via radical mechanism in good yields (Figure 1.45, bottom).

The synthetic utility of denitration with trialkyltin reagents is demonstrated in the synthesis of (*3S*, *4R*)-paroxetine, a serotonin inhibitor used in the treatment of depression, by Dixon and coworkers.[68] Denitration of nitroamide (**1.112**) affords product (**1.113**) in good yield and without erosion of ee (Figure 1.46). The Yamaguchi group reported complete stereoretention in the cleavage of C–N bond of the stereochemically pure Michael addition compound (**1.114**) (Figure 1.47).[69] With the

synthetically useful stereoselective methods developed for Henry reaction, aza-Henry reaction, and Michael addition, this method enhances the utility of the resultant products as chiral intermediates for further derivatization.

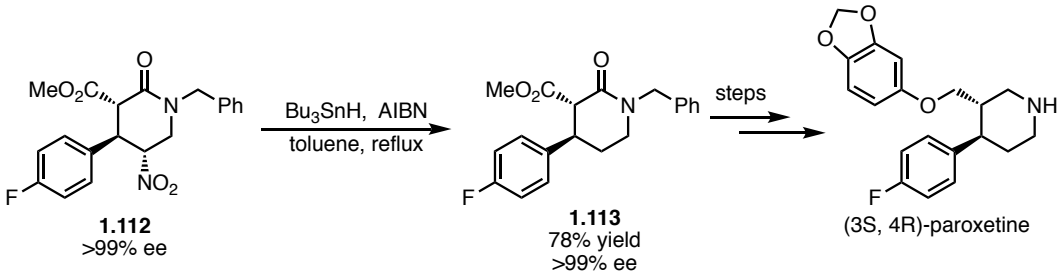

Figure 1.46: Dixon's Synthesis of Paroxetine Using Radical Denitration of Nitroalkanes

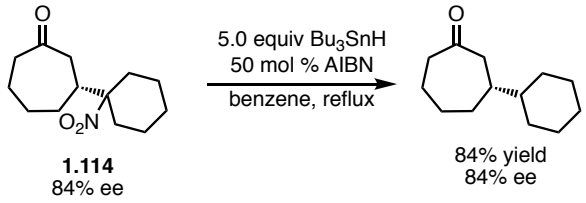

Figure 1.47: Yamaguchi's Stereoretentive Denitration of Nitroalkanes

Even though the radical-mediated reduction of nitroalkanes to alkanes with stoichiometric Bu_3SnH has been extensively used in the organic synthesis, due to stoichiometric and super stoichiometric amounts of Bu_3SnH, inherent toxicity of tributyl tin compounds, as well as purification issues associated with Bu_3SnH reagent, methods have been developed that use catalytic quantities of trialkyltin in the presence of silicon hydride reductant. In 1998, Fu and coworkers reported an efficient method

using a catalytic amount of tributyl tin and phenyl silane as a reductant.[70] This new catalytic method is effective for the reduction of tertiary nitroalkanes and activated secondary nitroalkanes and is compatible with several functional groups including acetals, esters, ketones, ethers nitriles and mesylates (Figure 1.48).

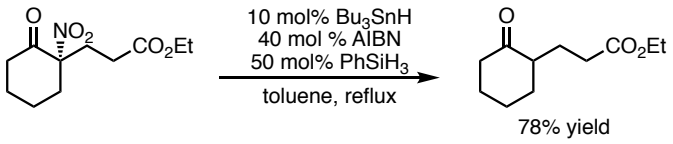

Figure 1.48: Fu's Trialkyltin Reagent Catalyzed Reduction of Nitroalkanes to Alkanes

The proposed mechanism involves the reaction of nitroalkane (**1.115**) with Bu_3SnH produces alkane (**1.116**) and Bu_3SnONO (**1.117**). In the regeneration step of the catalytic cycle, phenyl silane (**1.118**) reduces Bu_3SnONO to Bu_3SnH to turn over the catalytic cycle (Figure 1.50). The evidence supporting the reduction step comes from ^{119}Sn NMR studies (Figure 1.49).

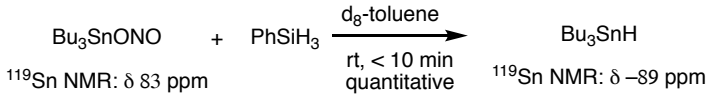

Figure 1.49: Fu's ^{119}Sn NMR Studies

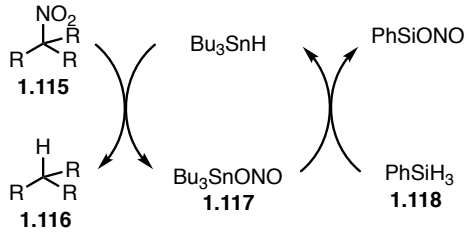

Figure 1.50: Fu's Proposed Mechanism for the Bu_3SnH Catalyzed Reduction of Nitroalkane to alkane

1.2 Early Efforts Towards C-Alkylation of Nitroalkanes Using Alkyl Electrophile

Although several reactions of nitroalkanes are known, such as the Henry reaction (section **1.1.1**), conjugate additions to α,β–unsaturated carbonyls (section **1.1.2**), and palladium-catalyzed allylation (section **1.1.4**) and arylation reactions (section **1.1.5**), the alkylation of nitroalkanes with alkyl halide electrophiles to form a new C–C bond remains a highly challenging task. This is because the nitronate anion undergoes alkylation at oxygen leading to unstable nitronic esters, which break down to give an oxime and carbonyl compound (Figure 1.51). Given the variety of the existing methods of forming new C–C bonds with nitroalkanes, the ability to selectively C-alkylate nitroalkanes with alkyl electrophile would fill a significant gap in the existing scientific literature. Despite the apparent value and seeming simplicity of such a *C*-alkylation method for nitroalkanes with simple alkyl electrophiles, reports as early as 1908 have described failed attempts to perform such a general transformation.

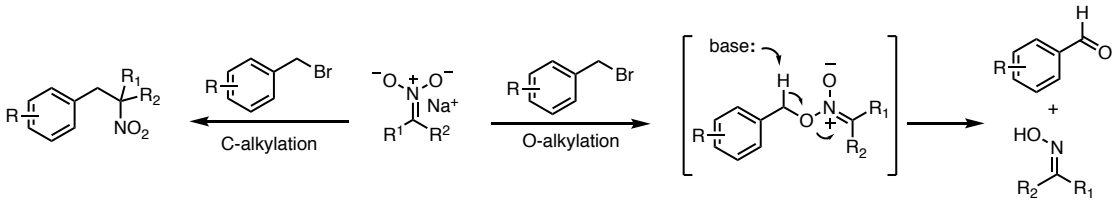

Figure 1.51: Alkylation of Nitroalkanes

1.2.1 Early Reports of *O*-alkylation over *C*-alkylation

In 1949, when Hass and Bender first investigated the reaction between the sodium salt of 2-nitropropane and various benzylic halides, the O-alkylation products were predominantly observed.[71] However, an exception occurred when the electron deficient *p*-nitrobenzyl chloride was employed, exclusively providing the C-alkylated product (**1.119**) (Figure 1.52).

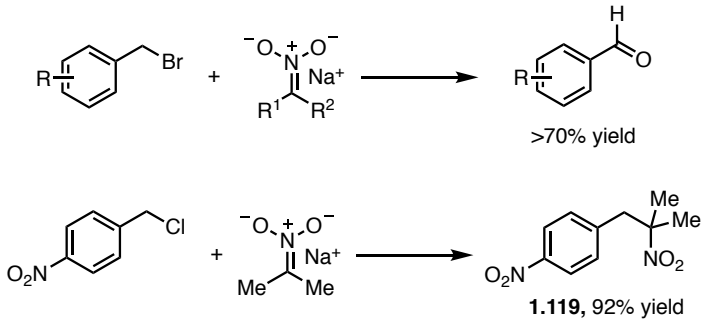

Figure 1.52: Hass and Bender's Study of Nitroalkane Alkylation

1.2.2 Mechanistic Studies for *C*-alkylation of Nitroalkanes

In 1975, Kornblum and coworkers proposed a radical anion mechanism to explain the initial report by Hass and Bender.[72] The author observed a trend between the formation of C-alkylation product (**1.119**) and the leaving group on the starting

material (**1.120**). The better leaving groups favor O-alkylated product (**1.121**) via typical S_N2 mechanism, and the less effective leaving groups favor C-alkylation product (**1.119**) *via* a radical mechanism (Table 1.1).

Table 1.1: Action of Leaving Group on C-Alkylation of Nitroalkanes

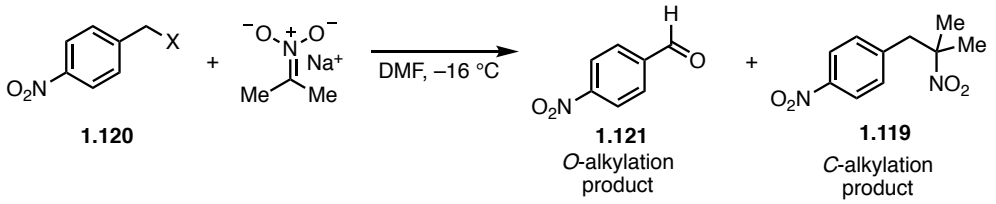

1.120 | **1.121** *O*-alkylation product | **1.119** *C*-alkylation product

Entry	X	Yield 1.121	Yield 1.119
1	Cl	1%	95%
2	OTs	32%	40%
3	Br	65%	17%
4	I	81%	7%

To gain insight into the radical nature of the *C*-alkylaiton of nitroalkanes, Kornblum and coworkers exposed the reaction to known radical inhibitor, *p*-dinitrobenzene.[73] Adding catalytic amount of *p*-dinitrobenzene affords *O*-alkylated product (**1.121**). The control experiment without *p*-dinitrobenzene affords the *C*-alkylated product (**1.119**) (Table 1.2). Based on this experiment, Kornblum proposed the mechanism as shown in Figure 1.53. In this mechanism, single electron transfer (SET) from the electron rich nitronate anion (**1.123**) to the electron deficient arene (**1.122**) afforded the radical anion intermediate (**1.124**). This radical intermediate decomposes to expel chloride and a benzylic radical (**1.125**). This benzylic radical then undergoes radical-anion coupling with the nitronate anion (**1.123**) to form the

radical anion of the product (**1.126**), which reduces another equivalent of the benzyl chloride, thus propagating the chain reaction and generating the *C*-alkylated product (**1.119**).

Table 1.2: Effect of Radical Inhibitor on *C*-Alkylation of Nitroalkane

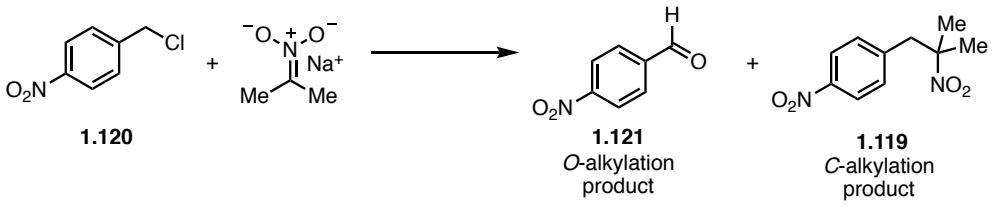

Entry	Additive	Yield 1.121	Yield 1.119
1	none	6%	92%
2	*p*-dinitrobenzene	88%	6%

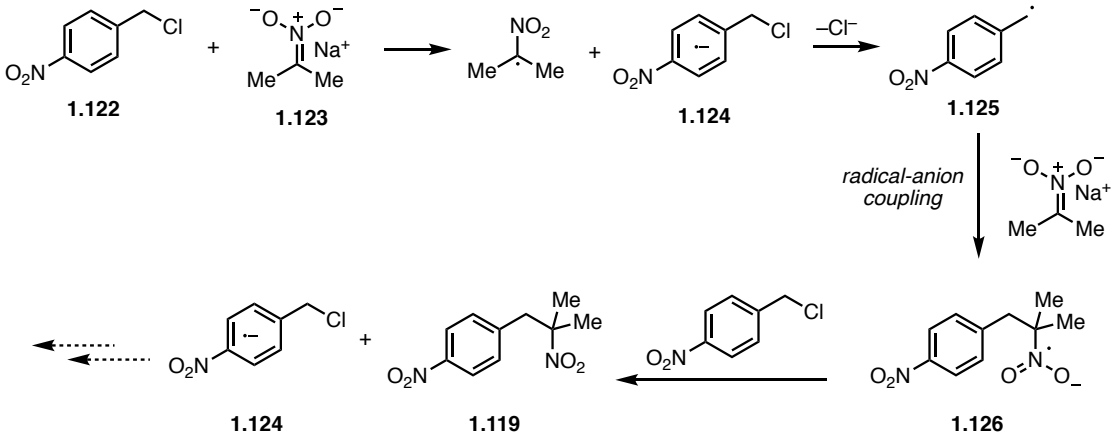

Figure 1.53: Kornblum's Proposed Radical Chain Mechanism for *C*-Alkylation of Nitroalkanes

1.2.3 Katritzky's Pyridinium Salts in the C-Alkylation of Nitroalkanes

To explore other methods to C-alkylate nitroalkanes, in 1981 Katritzky and coworkers showed that *N*-alkyl pyridinium salts or quinolium salts (**1.127**) alkylate a variety of nitronate anions (Figure 1.54, top).[74] Although this method is compatible with both primary and secondary nitroalkanes, the functional group tolerance was not studied. Furthermore, the multistep synthesized pyridinium salts used in this reaction are used stoichiometrically and they are not recoverable after the reaction.

Unlike Kornblum's radical chain mechanism for C-alkylation of nitroalkanes, this process is not a radical chain reaction. Instead, Katritzky suggests the intermediacy of a charge-transfer complex (**1.129**) between the nitronate anion and the pyridinium salt. This charge-transfer complex undergoes homolytic bond cleavage to afford triphenylpyridine (**1.130**), an alkyl radical, and an α–nitro radical (**1.131**), which recombines to provide the C-alkylated product (**1.132**) (Figure 1.54, bottom).[75] Interestingly, the addition of known radical scavengers such as *p*-dinitrobenzene does not the inhibit the reaction.

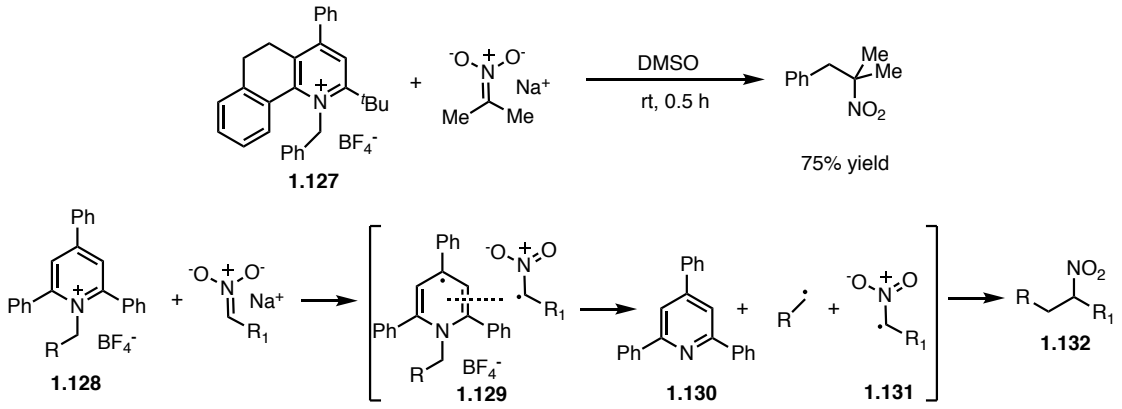

Figure 1.54: Katritzky's Alkylation of Nitronates with Pyridinium Salts and Proposed Mechanism

1.2.4 Alkyl Metal Complexes to *C*-Alkylate Nitroalkanes

Russell and coworkers showed that alkylmercury halides can be used to *C*-alkylate nitroalkanes. By utilizing photolytic conditions, tertiary alkyl mercury chloride or secondary alkyl mercury chloride (**1.133** and **1.134**) could be treated with secondary nitronate anions to afford *C*-alkylated product (Figure 1.55).[76] The product (**1.135** and **1.136**), which possesses two fully substituted carbon centers, can be accessed in synthetically useful yields. However, the toxicity of the alkylmercury reagents impedes their use in synthesis. The author proposed a radical anion coupling mechanism. Under the visible light irradiation, alkylmercury halides (**1.133**) generates an alkylradical (**1.137**). Subsequently, this alkyl radical undergoes radical anion coupling with the nitronate anion to afford *C*-alkylated product (**1.135**) (Figure 1.55, bottom).

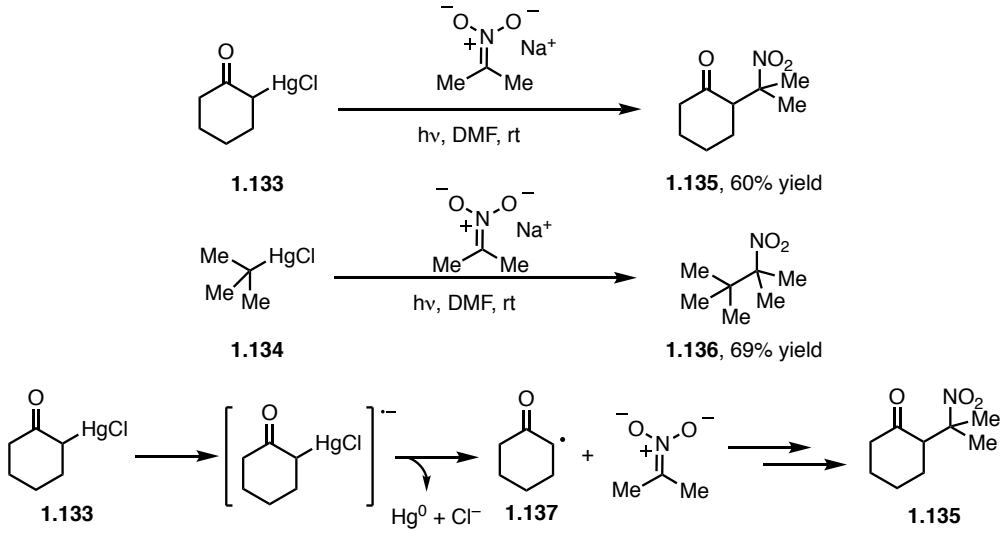

Figure 1.55: Russell's Alkylation of Nitroalkanes Using Alkylmercury Halides and Proposed Mechanism

Branchaud and coworkers have shown that alkylcobalt complex (**1.138**) can also be used to *C*-alkylate nitroalkanes. By utilizing photolytic conditions, primary alkylcobalt complex could be treated with primary nitronate anions to afford desired product (**1.139**) (Figure 1.56 top).[77] Simple nitroalkanes such as nitromethane and 1-nitropropane were shown to participate in the reaction, although functionalized nitroalkanes were not studied. Furthermore, the requirement to synthesize the alkylcobalt reagent and the photolytic conditions limits the scalability and impedes its use in the synthesis. Under visible light irradiation, the alkylcobalt complex decomposes to form alkyl radicals, which undergo coupling with nitronate anions to afford product (**1.140**) upon oxidation (Figure 1.56 bottom). This reaction, as well as above examples, (section **1.2.1, 1.2.2, 1.2.3**) displays the high propensity of alkyl radicals to combine with nitronate anions to form *C*-alkylated products.

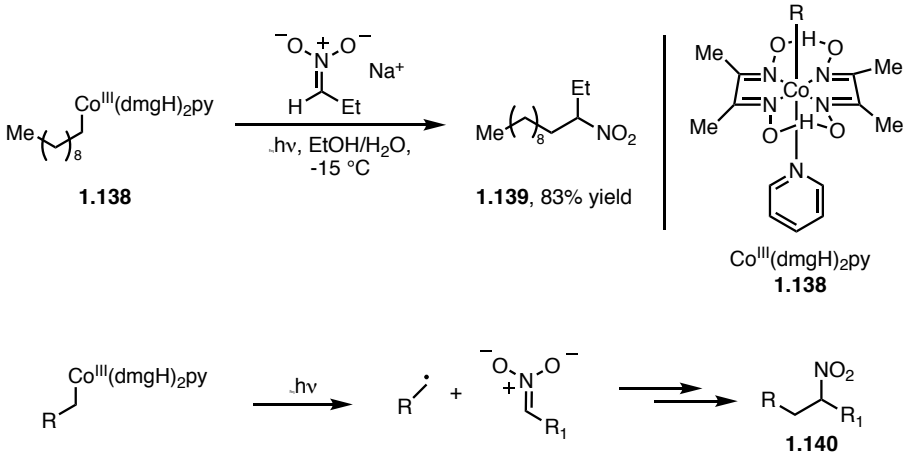

Figure 1.56: Branchaud's Alkylation of Nitroalkanes Using Alkylcobalt Complex and Proposed Mechanism

1.3 Radical Cross-Coupling Reactions Using Base Metal Catalysis

Even though the methods described in section 1.2 to *C*-alkylate nitroalkanes suffered from harsh reaction conditions, utilized toxic reagents, and the starting materials required multistep synthesis, they are proposed to undergo radical-anion coupling as the key step in the C–C bond forming event. A wide variety of useful and elegant chemistry has been developed over the past several decades using radical intermediates.[78] A review of literature suggests that first-row transition metals such as nickel,[79] iron,[79b,80] cobalt,[81] and copper[78a,82] are known to generate transient radicals when exposed to alkyl halides. We hypothesized that such a radical based process might form the basis for a general, catalytic approach to successful C-alkylation of nitroalkanes.

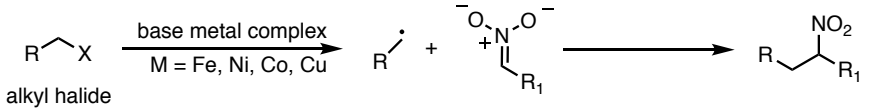

Figure 1.57: Proposed Base Metal Catalyzed to C-Alkylate Nitroalkanes via Radical – Anion Coupling

1.3.1 Nickel Catalyzed Cross Couplings of sp^3 Halides

Nickel is by far the most versatile metal for the cross coupling of simple alkyl halides and it has drawn a lot more attention in recent years than palladium. This is due to low cost, accessibility to various oxidation states such as Ni (0), (I), (II), (III) (which allows different modes of reactivity and radical based mechanisms), and a slower β-hydride elimination step. Specifically, the energy barrier to the Ni–C bond rotation prior to β-hydride elimination is often significantly higher for nickel than for comparable palladium species.[83]

Nickel-catalyzed cross couplings of alkyl electrophiles in organic synthesis and the involvement of alkyl radical intermediates have been extensively reviewed.[79a,84] The seminal reports and recent advancements in the nickel catalyzed alkyl electrophile cross coupling will be discussed.

In 1992, Suzuki and coworkers published the first palladium catalyzed C(sp^3) – C(sp^3) cross coupling reaction using primary alkyl iodide and alkyl boranes, but significant amounts of elimination and reduction products were also formed (elimination: reduction: desired product, 9:27:50) (Figure 1.58 top).[85] Knochel then reported that nickel catalysts could be used to successfully couple primary alkyl iodides with alkylzinc reagents using a tethered alkene[86] or exogenous electron-deficient alkene (Figure 1.58 bottom).[87] Kambe reported an olefin-assisted Kumada coupling of primary alkyl halides and tosylates, proposed to proceed via a bis(η^3-allyl) nickel catalyst formed by the coupling of two equivalents of butadiene (Figure 1.58 middle).[88]

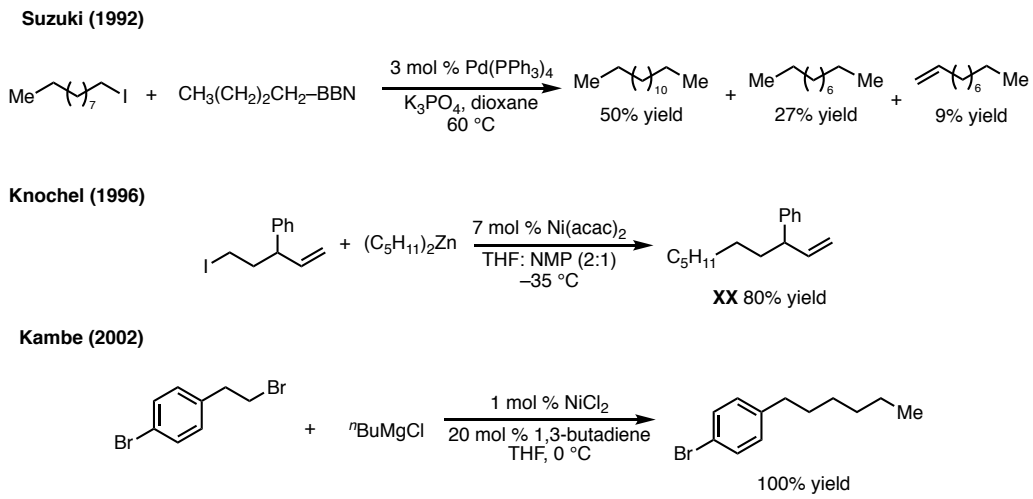

Figure 1.58: Suzuki, Knochel and Kambe Studies on Cross-Coupling of Primary Alkyl Electrophile Using Pd or Ni Catalysis

In 2003, Fu and coworkers reported the nickel-catalyzed cross-coupling of secondary alkyl bromides with β-hydrogens (**1.141**) and alkylzinc reagents (**1.142**). The chelating tridentate PyBOX nitrogen ligand (**1.143**) was essential, perhaps by slowing the rate of β-hydride elimination, which requires an open coordination site. The transition from previously used primary alkyl halides to secondary alkyl halide is ground-breaking, because it opened the door way to asymmetric synthesis of tertiary stereocenters (Figure 1.59).[89]

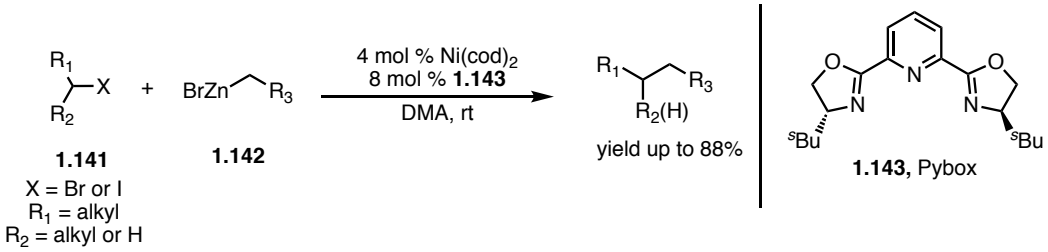

Figure 1.59: Fu's Pioneering Studied on Nickel-Catalyzed Negishi Cross Coupling of Secondary Alkyl Electrophile Using Tridentate PyBOX Ligand

Following extensive mechanistic studies by Vicic, it is hypothesized that a Ni^{I} species (**1.144**) undergoes transmetallation with alkylzinc reagent to form a Ni^{I}-alkyl species (**1.145**). Single-electron transfer (SET) from (**1.145**) to the alkyl halide generates a solvent-caged Ni^{II}-alkyl intermediate and an alkyl radical (**1.146**).[90] Upon recombination, a Ni^{III} dialkyl species (**1.147**) is formed, which after reductive elimination, affords the cross coupled product (**1.148**) and the active Ni^{I} catalyst (**1.144**) (Figure 1.60). The proposed radical mechanism was supported by the inhibition of the product formation when radical scavengers were added to the reaction, fragmentation of cyclopropyl bearing substrates results in olefinic products,

and dimerization of alkyl radicals. The synthesis and isolation Ni ^{I}(terpy)(CH_3) mono methyl complex were performed and the complex was found to be active intermediates in this reaction.[91]

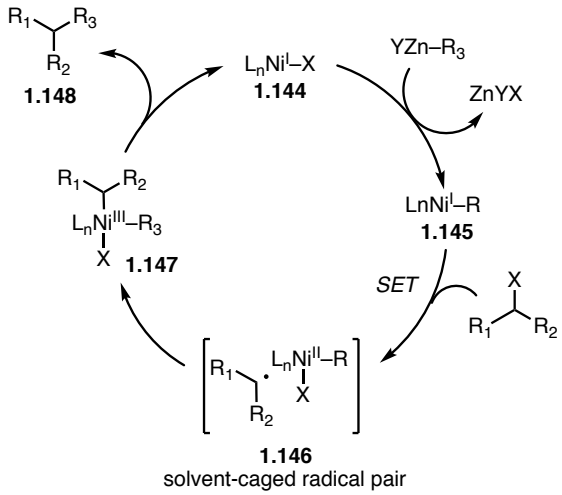

Figure 1.60: Fu's Pioneering Studied on Nickel-Catalyzed Negishi Cross Coupling of Secondary Alkyl Electrophile Using Tridentate PyBOX Ligand

Recently, the Baran and Weix group have shown that redox-active esters (RAEs) are also potential alkylating agent in nickel-catalyzed cross coupling and reductive cross couplings, respectively. These methods take advantage of utilizing alkyl carboxylic acids, which are not only cheap, abundant feedstock chemicals, but are also present in many complex bioactive molecules, giving rise to opportunities for late-stage functionalization. In their seminal report, Baran and coworkers investigated the Negishi cross coupling of alkylzinc halides (**1.149**) with a variety of electronically and sterically diverse, secondary RAEs (**1.150**) (Figure 1.61).[92] The enantioenriched redox-active ester (**1.151**) loses chiral integrity and a cyclopropyl acetic acid

derivative (**1.152**) ring-opens under the reaction conditions suggesting the intermediacy of alkyl radical during the catalytic cycle (Figure 1.62).

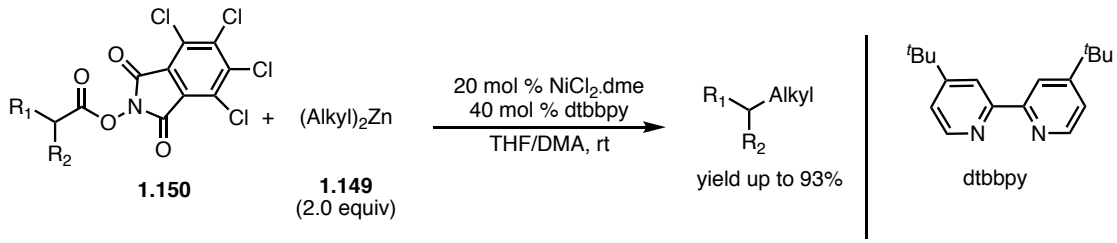

Figure 1.61: Baran's Nickel-Catalyzed Negishi Cross Coupling of Redox-Active Esters

Based on these studies, they proposed a $Ni^{I/III}$ catalytic cycle in which an active Ni^{I} species (1.153) undergoes a transmetallation with the alkylzinc halide to form alkyl-nickel species (1.154). This species can then undergo oxidative addition via single-electron transfer, thus generating an alkyl radical. This newly formed alkyl radical can then recombine with Ni^{II} species (1.155) to form high-valent Ni^{III} species (1.156). Upon reductive elimination, the desired product (1.157) is produced and the catalytically active, electron rich, low-valent Ni^{I} valent specis (1.153) is regenerated (Figure 1.63). Since this seminal report, several other cross couplings using RAEs have also been demonstrated, including Negishi or Kumada alkylations and Suzuki-Miyura arylations.[93]

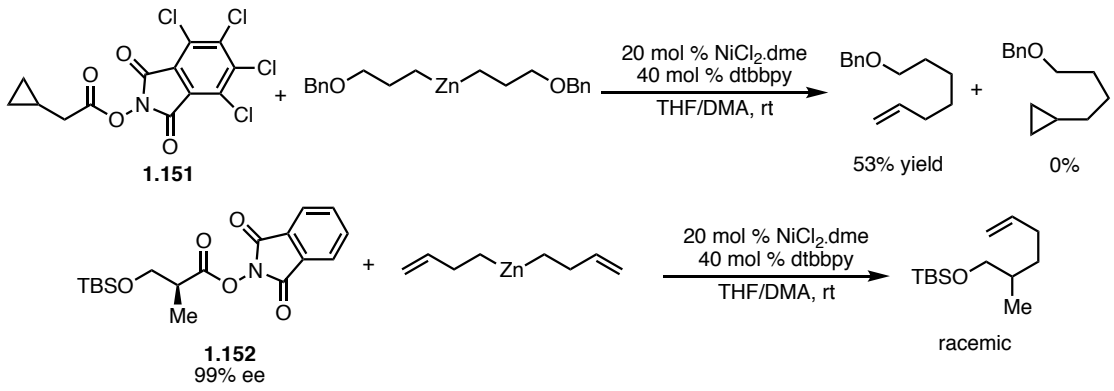

Figure 1.62: Baran's Radical Probe Studies Negishi Cross Coupling of Redox-Active Esters

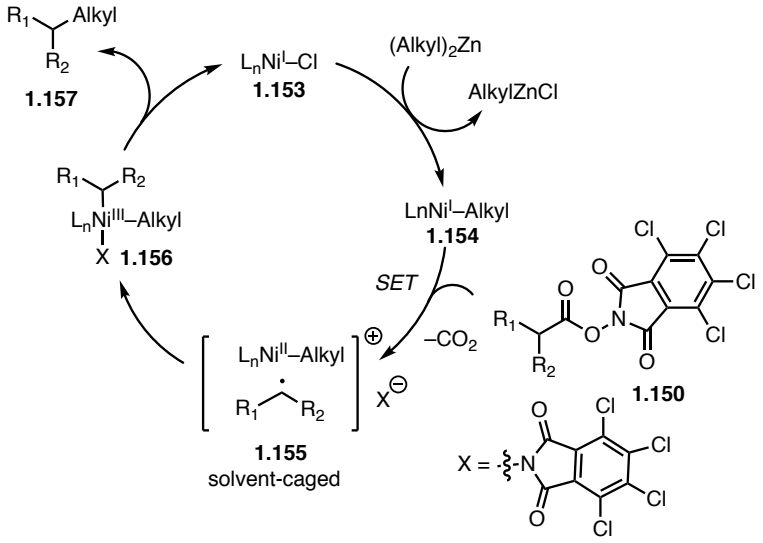

Figure 1.63: Baran's Proposed Mechanism on Negishi Cross Coupling of Redox-Active Esters

Alternatively, Weix has shown that RAEs can serve as alkyl electrophiles in a nickel-catalyzed reductive coupling with aryl iodides. The reaction exhibits broad scope in both the RAEs and aryl electrophile, affording the primary or secondary alkyl arenes (**1.158**) in excellent yields (Figure 1.64).[94] Even though the authors have not

proposed a mechanism but suggested that a radical-chain bimetallic mechanism may be operative.

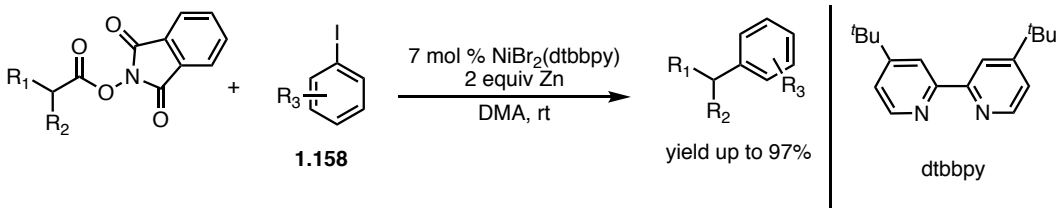

Figure 1.64: Weix's Nickel-Catalyzed Reductive Cross Coupling of RAEs and Aryl Iodides

1.3.2 Iron Catalyzed Cross Couplings of sp^3 Halides

Iron compounds offer many advantages over other transition metals catalysts such as nickel, palladium, rhodium, etc. as iron is extremely cheap, abundant, nontoxic and environmentally benign. Iron-catalyzed reactions have been utilized in organic synthesis and it has been extensively reviewed.[80] As with nickel catalysis, a variety of different alkyl-alkyl cross coupling reactions using iron catalysis have also been developed.[78a,79b,84b,95] The seminal reports and recent advancements in the iron-catalyzed alkyl electrophile cross coupling and the radical intermediate involvement will be discussed.

In 1971, Kochi and coworkers reported the first alkyl electrophile cross coupling using iron catalysis. For example, simple alkyl halides (**1.159**) were treated with Grignard reagents (**1.160**) in the presence of catalytic amounts of $FeCl_3$ to form new C–C bonds in modest yields (Figure 1.65). Several byproducts such as homocoupling of alkyl halide and hydrogen atom abstraction were observed; accordingly, Kochi proposed a radical based mechanism.[96]

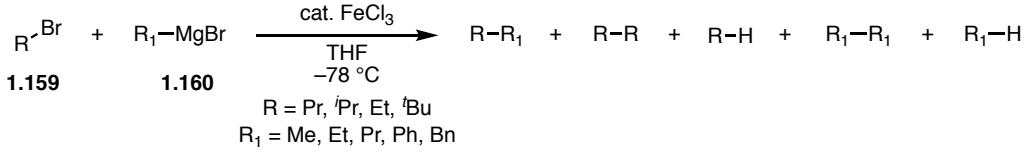

Figure 1.65: Kochi's Early Study on Alkyl-Alkyl Cross Coupling Using Iron Catalysis

In 2007, the Chai group published the first synthetically useful alkyl-alkyl cross coupling of Grignard reagents with unactivated alkyl halides using Xantphos (**1.161**) as the optimal ligand for iron(II) acetate (Figure 1.66).[97]

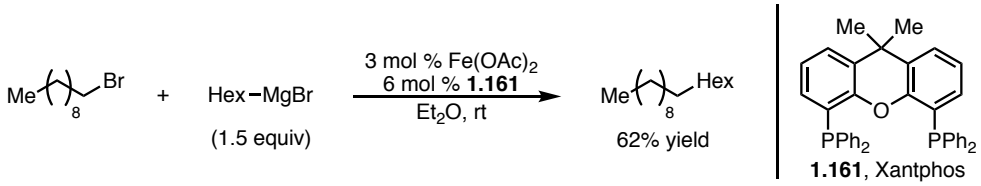

Figure 1.66: Chai's Initial Studies on Iron-Catalyzed Kumada Reaction

To investigate the mechanism of the reaction, the authors performed radical probing experiments. For example, when the substrate (**1.162**), which bears a cyclopropyl ring, was treated with Grignard reagent (**1.163**), the ring-opened product (**1.164**) was formed in modest yield (Figure 1.67). The desired product (**1.165**) was formed in less than 5% yield. This experiment suggests the intermediacy of an alkyl radical generated under the reaction conditions.

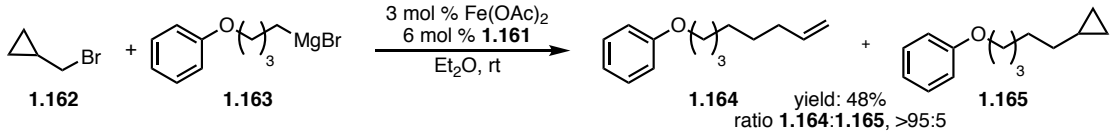

Figure 1.67: Chai's Radical Probing Studies on Iron-Catalyzed Kumada Reaction

In 2015, Nakamura and coworkers reported the first iron-catalyzed enantioselective cross coupling reaction between Grignard reagents and α-chloroesters.[98] The author showed a variety of racemic α-chloroesters (**1.166**) were coupled with aryl Grignard reagent in the presence of a catalytic amount of $Fe(acac)_3$ and a chiral bisphosphine ligand (**1.167**), affording the products (**1.168**) in high yield and good enantioselectivity (Figure 1.68).

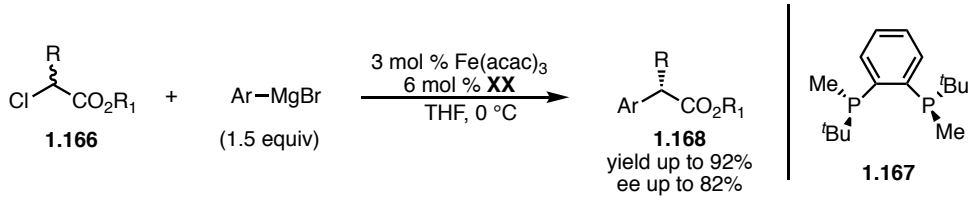

Figure 1.68: Nakamura's First Example of Iron-Catalyzed Asymmetric Reaction between α-chloroesters and Aryl Grignard Reagents

The authors proposed a bimetallic radical chain mechanism, the cycle begins with Fe(II) species (**1.169**), which is generated from the partial reduction of $Fe(acac)_3$ in the presence of ligand (**1.167**) (Figure 1.69). This species (**1.169**) abstracts a halogen atom from the substrate (**1.166**) to form alkyl radical intermediate (**1.170**) and iron species (**1.171**). The alkyl radical (**1.170**) reacts with another divalent iron species (**1.169**) to form high valent Fe(III) species (**1.172**). Upon reductive elimination,

desired product (**1.168**) and a low valent Fe(I) species (**1.173**) is produced. This Fe(I) species (**1.173**) conproportionates with the Fe(III) species (**1.171**) to form catalytically active Fe(II) species (**1.169**). The intermediacy of alkyl radical was supported by the observation of ring opened product from the substrate bearing cyclopropyl ring.

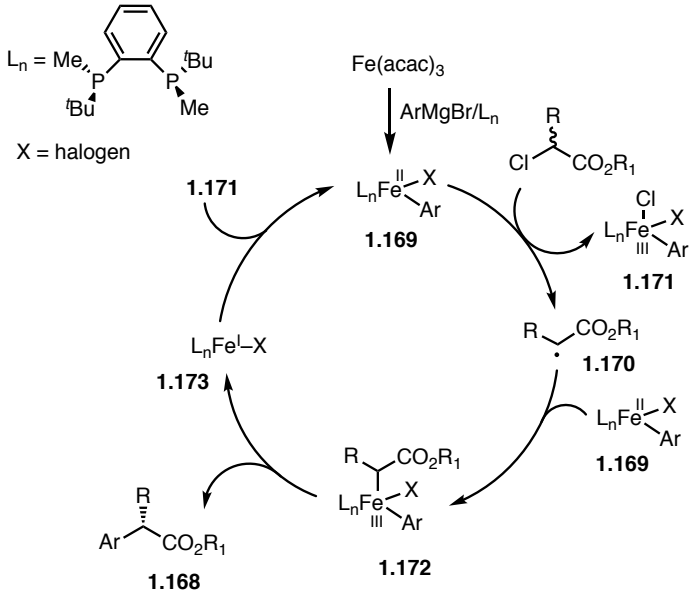

Figure 1.69: Nakamura's Proposed Mechanism on Iron-Catalyzed Asymmetric Reaction between α-chloroesters and Aryl Grignard Reagents

In 2016, Baran and coworkers reported that redox-active esters (RAEs) serve as alkyl electrophiles in an iron-catalyzed reaction with alkylzinc and alkylmagnesium reagents. A variety of electronically and sterically diverse, secondary and tertiary RAEs (**1.174**) could be treated with alkylzinc or alkylmagnesium reagents to afford cross-coupled products (**1.175**) in good yields (Figure 1.70).[99] Like alkyl halides, this transformation is catalyzed via *in situ* generated low-valent Fe-species. Based on the

preliminary mechanistic studies, the author proposed a radical mechanism that proceeds through a stepwise oxidative addition *via* single electron transfer.

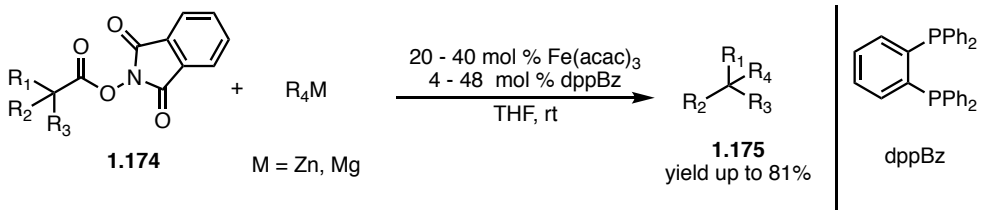

Figure 1.70: Baran's Iron-Catalyzed Cross Coupling of Redox-Active Esters with Alkyl Zinc and Magnesium Reagents

1.3.3 Cobalt Catalyzed Cross Couplings of sp^3 Halides

Cobalt catalyzed reactions have been extensively utilized in organic synthesis and have been reviewed accordingly.[81] As with nickel and iron catalysis, a variety of different alkyl-alkyl cross coupling reactions using cobalt catalysis have also been developed.[78a,84b] The seminal reports and recent advancements in the cobalt-catalyzed alkyl electrophile cross coupling will be discussed.

In 2008, the Chai group published the seminal report on cobalt-catalyzed alkyl-alkyl cross coupling of alkylmagnesium reagents.[100] By utilizing $CoCl_2$.2LiI in the presence of excess tetramethylethylenediamine (TMEDA), the cross coupling between primary and secondary alkyl halides (**1.176**) and alkyl Grignard reagents (**1.177**) was achieved in good yields (Figure 1.71). However, tertiary alkyl halide was not a competent cross coupling partner, thus limiting the synthetic utility of the process. The authors hypothesized the reaction proceeds via a radical pathway.

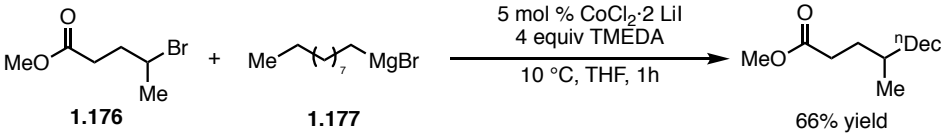

1.176 **1.177**

Figure 1.71: Chai's Initial Studies on Cobalt-Catalyzed Kumada Reaction Using Alkyl Halides

In 2013, Kambe and coworkers, advanced the alkyl-alkyl cross coupling reaction using Co catalysis by utilizing 2° and 3° alkyl Grignard reagents.[101] A variety of products (**1.178 and 1.179**) bearing sterically congested quaternary carbon centers were synthesized in excellent yield using this process (Figure 1.72).

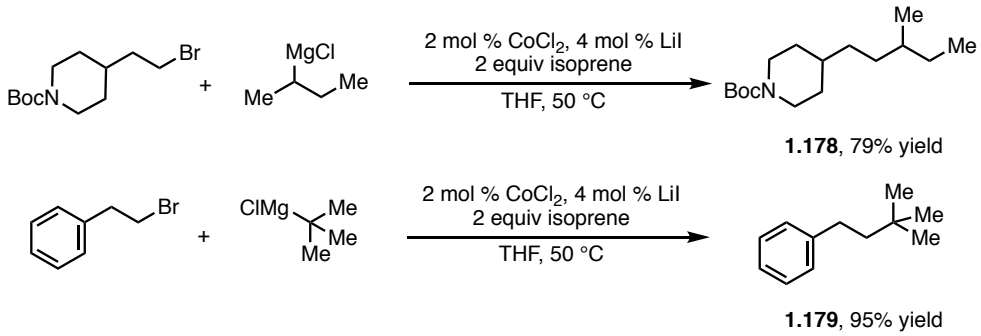

Figure 1.72: Kambe's Advancement in the Cobalt-Catalyzed Alkyl-Alkyl Cross Coupling Using 2° and 3° Alkyl Grignard Reagents

Kambe proposes a two-electron mechanism and rules out a radical mechanism for the transformation based on the radical probing experiments. When the substrate (**1.180**) was treated under reaction conditions, cyclized product (**1.181**) was not formed regardless of the nature of the Grignard reagent utilized (Figure 1.73 top).

Furthermore, by utilizing a cyclopropyl-bearing substrate (**1.182**), no ring opened product (**1.183**) was observed (Figure 1.73 bottom).

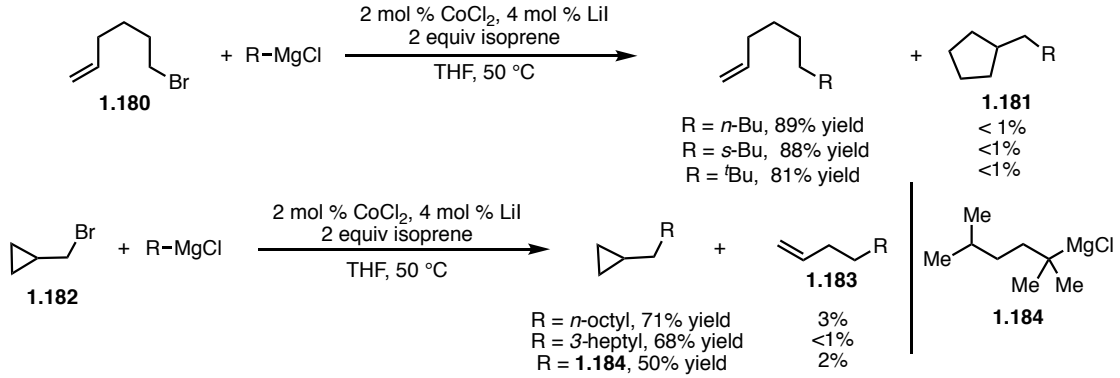

Figure 1.73: Kambe's Radical Probing Studies

In 2014, the Walsh and Bian group reported the first cobalt-catalyzed enantioselective cross coupling reaction between Grignard reagent and an α-bromoester.[102] The author showed a variety of racemic α-bromoesters (**1.185**) were coupled with aryl Grignard reagent (**1.186**) in the presence of catalytic amount of CoI_2 and a chiral bisoxazoline ligand (**1.187**), affording the products (**1.188**) in high yield and good enantioselectivity (Figure 1.74).

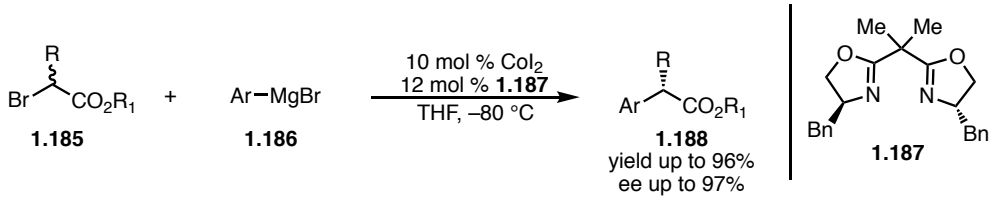

Figure 1.74: Walsh and Bian's First Example of Cobalt-Catalyzed Asymmetric Kumada Cross Coupling between α–bromoesters and Aryl Grignard Reagents

1.3.4 Copper Catalyzed Atom Transfer Radical Addition

Copper complexes were known to undergo a variety of radical based reactions and they have successfully been utilized in natural product synthesis along with other first row transition metals.[103] Even though several radical reactions are known for copper catalysis, the most utilized and relevant transformation to the chemistry discussed in chapter 3 and to copper-catalyzed *C*-alkylation of nitroalkanes developed in our group is atom transfer reactions.[82,104]

The Kharasch addition was first discovered in 1945 as a means of adding halogenated methanes to olefins by using light or radical initiators.[105] Today, this process, commonly referred to as atom transfer radical addition (ATRA) and it goes via radical mechanism. Catalytic amount of diacetyl peroxide initiates a radical-chain mechanism by decomposition of methyl radical (**1.189**) and peroxide radical (**1.190**). These radical species abstract a hydrogen atom from (**1.191**), forming a stabilized radical (**1.192**). This radical species (**1.192**) adds across the olefin, forming a new C–C bond (**1.193**). The product distribution is very poor because the product (**1.193**) can undergo a variety of additional reactions (Figure 1.75).

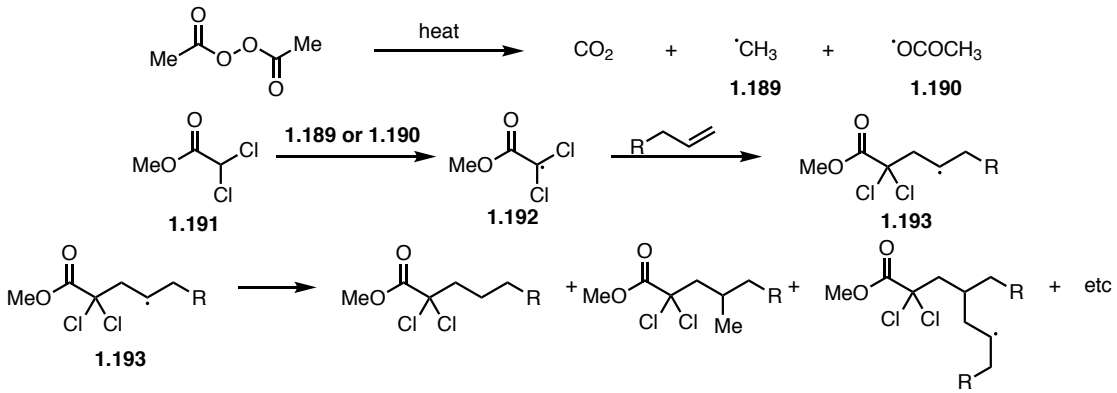

Figure 1.75: Kharasch Seminal Report on Atom Transfer Radical Addition

Intramolecular transition metal-catalyzed ATRA or atom transfer radical cyclisation (ATRC) reaction is an attractive tool because it enables the synthesis of functionalized ring systems that can be used as a precursor for complex molecule synthesis. In 1990, the Tsuji group reported the first successful example of copper mediated ATRC reaction in the synthesis of trichlorinated γ-lactones from readily available alkenyl trichloroacetates.[106] The proposed mechanism involves abstraction of a chlorine atom (**1.194**) by Cu(I) salt to generate stabilized alkyl radical (**1.195**) and Cu(II) species. The radical (**1.195**) adds across the double bond to generate primary radical (**1.196**), which abstracts a chlorine atom from Cu(II) species to regenerate active Cu(I) species and product (**1.197**) (Figure 1.76).

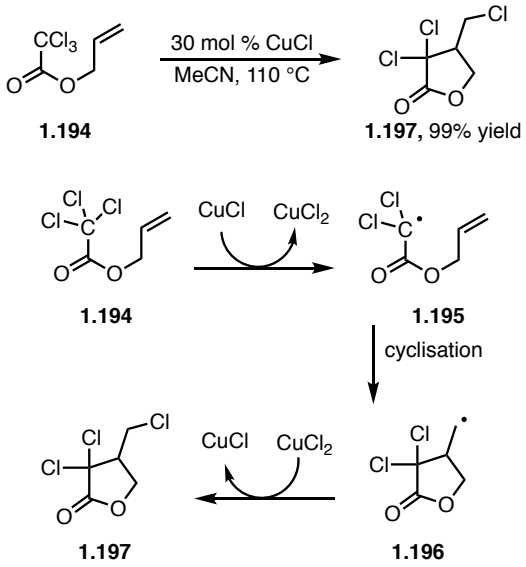

Figure 1.76: Tsuji's Seminal Report on ATRC Reaction and The Proposed Mechanism

Recently, Nishikata and workers reported the copper-catalyzed radical alkenylation using activated tertiary alkyl halide (**1.198**) and styrene derivatives. This reaction provides an efficient synthesis of tertiary-alkylated products (Figure 1.77).[107] The activated tertiary bromide substrate (**1.198**) is known to undergo atom transfer reactions when exposed to Cu salts and the author's proposed mechanism begins with atom transfer reaction between Cu(I) salt and (**1.198**) to generate Cu(II) and stabilized tertiary radical (**1.199**). Evidence of this step arises from the reaction in the presence of TEMPO which does not afford the desired product (**1.200**). Instead, tertiary-alkylated TEMPO adduct was obtained, which suggests the intermediacy of radical species (**1.199**). This radical (**1.199**) adds across the double bond to give a new radical intermediate (**1.201**), which abstracts a bromide atom from Cu(II) to give intermediate (**1.202**) and regenerate the active Cu(I) species to complete the catalytic cycle. The brominated intermediate (**1.203**) undergoes –HBr elimination with the amine to afford the desired product (**1.200**).

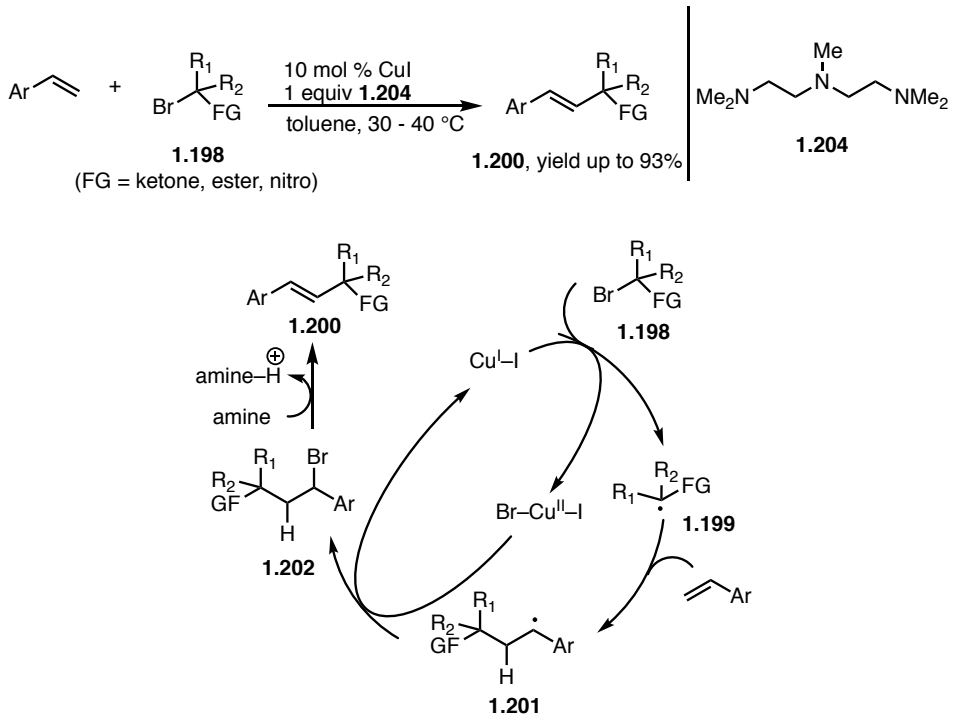

Figure 1.77: Nishikata's Copper Catalyzed Radical Alkenylation Reaction

Matyjaszewski pioneered the mechanistically similar atom transfer radical polymerization reaction, which affords polymers of different lengths from simple monomers using copper catalysis. This has been extensively reviewed and will not be discussed here.[104a,b,108]

REFERENCES

(1) Ono, N. *The Nitro Group In Organic Synthesis*; John Wiley And Sons: New York, 2001.

(2) Ballini, R.; Bosica, G.; Fiorini, D.; Palmieri, A.; Petrini, M. *Chem. Rev.* **2005**, *105*, 933.

(3) (a) Palomo, C.; Oiarbide, M.; Laso, A. *Eur. J. Org. Chem.* **2007**, *2007*, 2561. (b) Boruwa, J.; Gogoi, N.; Saikia, P. P.; Barua, N. C. *Tetrahedron: Asymmetry* **2006**, *17*, 3315. (c) Luzzio, F. A. *Tetrahedron* **2001**, *57*, 915.

(4) Noble, A.; Anderson, J. C. *Chem. Rev.* **2013**, *113*, 2887.

(5) (a) Fox, J. M.; Huang, X.; Chieffi, A.; Buchwald, S. L. *J. Am. Chem. Soc.* **2000**, *122*, 1360. (b) Vogl, E. M.; Buchwald, S. L. *J. Org. Chem.* **2001**, *67*, 106. (c) Metz, A. E.; Berritt, S.; Dreher, S. D.; Kozlowski, M. C. *Org. Lett.* **2012**, *14*, 760. (d) Walvoord, R. R.; Berritt, S.; Kozlowski, M. C. *Org. Lett.* **2012**, *14*, 4086. (e) Walvoord, R. R.; Kozlowski, M. C. *J. Org. Chem.* **2013**, *78*, 8859.

(6) Aleksandrowicz, P.; Piotrowska, H.; Sas, W. *Tetrahedron* **1982**, *38*, 1321.

(7) (a) Inoue, F.; Kashihara, M.; Yadav, M. R.; Nakao, Y. *Angew. Chem., Int. Ed.* **2017**, *56*, 13307. (b) Yadav, M. R.; Nagaoka, M.; Kashihara, M.; Zhong, R.-L.; Miyazaki, T.; Sakaki, S.; Nakao, Y. *J. Am. Chem. Soc.* **2017**, *139*, 9423.

(8) (a) Gildner, P. G.; Gietter, A. A. S.; Cui, D.; Watson, D. A. *J. Am. Chem. Soc.* **2012**, *134*, 9942. (b) Gietter, A. A. S.; Gildner, P. G.; Cinderella, A. P.; Watson, D. A. *Org. Lett.* **2014**, *16*, 3166. (c) Shimkin, K. W.; Gildner, P. G.; Watson, D. A. *Org. Lett.* **2016**, *18*, 988.

(9) Henry, L. C. R. *Acad. Sci. Ser. C.* **1895**, *120*, 1265.

(10) (a) Sasai, H.; Suzuki, T.; Arai, S.; Arai, T.; Shibasaki, M. *J. Am. Chem. Soc.* **1992**, *114*, 4418. (b) Sasai, H.; Tokunaga, T.; Watanabe, S.; Suzuki, T.; Itoh, N.; Shibasaki, M. *J. Org. Chem.* **1995**, *60*, 7388.

(11) Sasai, H.; M.A. Yamada, Y.; Suzuki, T.; Shibasaki, M. *Tetrahedron* **1994**, *50*, 12313.

(12) Palomo, C.; Oiarbide, M.; Mielgo, A. *Angew. Chem., Int. Ed.* **2004**, *43*, 5442.

(13) Blay, G.; Hernández-Olmos, V.; Pedro, J. R. *Synlett* **2011**, *2011*, 1195.

(14) Zhou, Y.; Zhu, Y.; Yan, S.; Gong, Y. *Angew. Chem., Int. Ed.* **2013**, *52*, 10265.

(15) Bolognesi, M. L.; Bartolini, M.; Cavalli, A.; Andrisano, V.; Rosini, M.; Minarini, A.; Melchiorre, C. *J. Med. Chem.* **2004**, *47*, 5945.

(16) Henry, L. C. R. *Bull. Acad. R. Belg.* **1896**, *32*, 33.

(17) Adams, H.; Anderson, J. C.; Peace, S.; Pennell, A. M. K. *J. Org. Chem.* **1998**, *63*, 9932.

(18) Yamada, K.-i.; Harwood, S. J.; Gröger, H.; Shibasaki, M. *Angew. Chem., Int. Ed.* **1999**, *38*, 3504.

(19) Yamada, K.-i.; Moll, G.; Shibasaki, M. *Synlett* **2001**, *2001*, 0980.

(20) (a) Shibasaki, M.; Kanai, M. *Chem. Pharm. Bull.* **2001**, *49*, 511. (b) Shibasaki, M.; Matsunaga, S.; Kumagai, N. *Synlett* **2008**, *2008*, 1583.

(21) Friestad, G. K.; Mathies, A. K. *Tetrahedron* **2007**, *63*, 2541.

(22) (a) Akiyama, T.; Itoh, J.; Fuchibe, K. *Adv. Synth. Catal.* **2006**, *348*, 999. (b) Doyle, A. G.; Jacobsen, E. N. *Chem. Rev.* **2007**, *107*, 5713. (c) Ting, A.; Schaus, S. E. *Eur. J. Org. Chem.* **2007**, *2007*, 5797. (d) Takemoto, Y. *Chem. Pharm. Bull.* **2010**, *58*, 593.

(23) Petrini, M.; Torregiani, E. *Synthesis* **2007**, *2007*, 159.

(24) Arrayas, R. G.; Carretero, J. C. *Chem. Soc. Rev.* **2009**, *38*, 1940.

(25) (a) Westermann, B. *Angew. Chem., Int. Ed.* **2003**, *42*, 151. (b) Marqués-López, E.; Merino, P.; Tejero, T.; Herrera, R. P. *Eur. J. Org. Chem.* **2009**, *2009*, 2401.

(26) Lu, N.; Bai, F.; Fang, Y.; Wei, Z.; Cao, J.; Liang, D.; Lin, Y.; Duan, H. *Adv. Synth. Catal.* **2017**, *359*, 4111.

(27) Xie, H.; Zhang, Y.; Zhang, S.; Chen, X.; Wang, W. *Angew. Chem., Int. Ed.* **2011**, *50*, 11773.

(28) Kohler, E. P. *J. Am. Chem. Soc.* **1916**, *38*, 889.

(29) (a) Roca-Lopez, D.; Sadaba, D.; Delso, I.; Herrera, R. P.; Tejero, T.; Merino, P. *Tetrahedron: Asymmetry* **2010**, *21*, 2561. (b) Serdyuk, O. V.; Heckel, C. M.; Tsogoeva, S. B. *Org. Biomol. Chem.* **2013**, *11*, 7051. (c) Tsakos, M.; Kokotos, C. G. *Tetrahedron* **2013**, *69*, 10199.

(30) Gietter-Burch, A. A. S.; Mitrut, R. E.; Watson, D. A. *Org. Lett* **2015**, *17*, 5468.

(31) Kawada, M.; Nakashima, K.; Hirashima, S.-i.; Yoshida, A.; Koseki, Y.; Miura, T. *J. Org. Chem.* **2017**, *82*, 6986.

(32) Mitsuyasu, T.; Hara, M.; Tsuji, J. *Journal of the Chemical Society D: Chemical Communications* **1971**, 345.

(33) Wade, P. A.; Morrow, S. D.; Hardinger, S. A. *J. Org. Chem.* **1982**, *47*, 365.

(34) Rieck, H.; Helmchen, G. *Angew. Chem., Int. Ed. Engl.* **1996**, *34*, 2687.

(35) Trost, B. M.; Surivet, J.-P. *Angew. Chem., Int. Ed.* **2000**, *39*, 3122.

(36) Trost, B. M.; Surivet, J.-P. *J. Am. Chem. Soc.* **2000**, *122*, 6291.

(37) Dahnz, A.; Helmchen, G. *Synlett* **2006**, *2006*, 0697.

(38) Wade, P. A.; Hinney, H. R.; Amin, N. V.; Vail, P. D.; Morrow, S. D.; Hardinger, S. A.; Saft, M. S. *J. Org. Chem.* **1981**, *46*, 765.

(39) (a) Ferroud, D.; Genet, J. P.; Muzart, J. *Tetrahedron Lett.* **1984**, *25*, 4379. (b) Genet, J. P.; Ferround, D. *Tetrahedron Lett.* **1984**, *25*, 3579.

(40) Genet, J. P.; Grisoni, S. *Tetrahedron Lett.* **1986**, *27*, 4165.

(41) Young, A. J.; White, M. C. *J. Am. Chem. Soc.* **2008**, *130*, 14090.

(42) Ohmatsu, K.; Ito, M.; Kunieda, T.; Ooi, T. *Nature Chem.* **2012**, *4*, 473.

(43) (a) Grenning, A. J.; Tunge, J. A. *J. Am. Chem. Soc.* **2011**, *133*, 14785. (b) Grenning, A. J.; Tunge, J. A. *Angew. Chem., Int. Ed.* **2011**, *50*, 1688.

(44) Tsuji, J.; Yamada, T.; Minami, I.; Yuhara, M.; Nisar, M.; Shimizu, I. *J. Org. Chem.* **1987**, *52*, 2988.

(45) Grenning, A. J.; Tunge, J. A. *Org. Lett* **2010**, *12*, 740.

(46) Thomas, A.; Rajappa, S. *Tetrahedron* **1995**, *51*, 10571.

(47) Kozyrod, R.; Pinhey, J. *Aust. J. Chem.* **1985**, *38*, 713.

(48) Kornblum, N.; Taylor, H. J. *J. Org. Chem.* **1963**, *28*, 1424.

(49) (a) Barton, D. H. R.; Blazejewski, J.-C.; Charpiot, B.; Finet, J.-P.; Motherwell, W. B.; Papoula, M. T. B.; Stanforth, S. P. *J. Chem. Soc., Perkin Trans. 1* **1985**, 2667. (b) Barton, D. H. R.; Finet, J.-P.; Giannotti, C.; Halley, F. *J. Chem. Soc., Perkin Trans. 1* **1987**, 241. (c) Finet, J. P. *Chem. Rev.* **1989**, *89*, 1487. (d) Elliott, G. I.; Konopelski, J. P. *Tetrahedron* **2001**, *57*, 5683.

(50) Kurz, M. E.; Ngoviwatchai, P.; Tantrarant, T. *J. Org. Chem.* **1981**, *46*, 4668.

(51) Muratake, H.; Nakai, H. *Tetrahedron Lett.* **1999**, *40*, 2355.

(52) VanGelder, K. F.; Kozlowski, M. C. *Org. Lett.* **2015**, *17*, 5748.

(53) Zheng, X.; Ding, J.; Chen, J.; Gao, W.; Liu, M.; Wu, H. *Org. Lett.* **2011**, *13*, 1726.

(54) Bahekar, S. S.; Sarkate, A. P.; Wadhai, V. M.; Wakte, P. S.; Shinde, D. B. *Catal. Commun.* **2013**, *41*, 123.

(55) (a) Weis, C. D.; Newkome, G. R. *Synthesis* **1995**, *1995*, 1053. (b) Orlandi, M.; Brenna, D.; Harms, R.; Jost, S.; Benaglia, M. *Org. Process Res. Dev.* **2016**.

(56) Blay, G.; Hernández-Olmos, V.; Pedro, J. R. *Tetrahedron: Asymmetry* **2010**, *21*, 578.

(57) Davis, T. A.; Johnston, J. N. *Chem. Sci.* **2011**, *2*, 1076.

(58) Orlandi, M.; Tosi, F.; Bonsignore, M.; Benaglia, M. *Org. Lett* **2015**, *17*, 3941.

(59) Rossi, S.; Benaglia, M.; Porta, R.; Cotarca, L.; Maragni, P.; Verzini, M. *Eur. J. Org. Chem.* **2015**, *2015*, 2531.

(60) Konovalov, M. J. *Russ. Phys. Chem. Soc.* **1893**, 509.

(61) Nef, J. U. *Liebigs Ann. Chem.* **1894**, *280*, 263.

(62) (a) Petruš, L.; Petrušová, M.; Pham-Huu, D.-P.; Lattová, E.; Pribulová, B.; Turjan, J. *Monatshefte für Chemie / Chemical Monthly* **2002**, *133*, 383. (b) Ballini, R.; Petrini, M. *Tetrahedron* **2004**, *60*, 1017.

(63) Bagul, T. D.; Lakshmaiah, G.; Kawabata, T.; Fuji, K. *Org. Lett* **2002**, *4*, 249.

(64) Saville-Stones, E. A.; Lindell, S. D. *Synlett* **1991**, *1991*, 591.

(65) Umemiya, S.; Sakamoto, D.; Kawauchi, G.; Hayashi, Y. *Org. Lett* **2017**, *19*, 1112.

(66) Kornblum, N.; Carlson, S. C.; Smith, R. G. *J. Am. Chem. Soc.* **1979**, *101*, 647.

(67) (a) Ono, N.; Miyake, H.; Tamura, R.; Kaji, A. *Tetrahedron Lett.* **1981**, *22*, 1705. (b) Tanner, D. D.; Blackburn, E. V.; Diaz, G. E. *J. Am. Chem. Soc.* **1981**, *103*, 1557.

(68) Hynes, P. S.; Stupple, P. A.; Dixon, D. J. *Org. Lett* **2008**, *10*, 1389.

(69) Yamaguchi, M.; Shiraishi, T.; Igarashi, Y.; Hirama, M. *Tetrahedron Lett.* **1994**, *35*, 8233.

(70) Tormo, J.; Hays, D. S.; Fu, G. C. *J. Org. Chem.* **1998**, *63*, 5296.

(71) (a) Hass, H. B.; Bender, M. L. *J. Am. Chem. Soc.* **1949**, *71*, 1767. (b) Hass, H. B.; Berry, E. J.; Bender, M. L. *J. Am. Chem. Soc.* **1949**, *71*, 2290.

(72) Kornblum, N. *Angew. Chem., Int. Ed. Engl.* **1975**, *14*, 734.

(73) (a) Kornblum, N.; Pink, P.; Yorka, K. V. *J. Am. Chem. Soc.* **1961**, *83*, 2779. (b) Kerber, R. C.; Urry, G. W.; Kornblum, N. *J. Am. Chem. Soc.* **1964**, *86*, 3904.

(74) Katritzky, A. R.; De Ville, G.; Patel, R. C. *Tetrahedron* **1981**, *37*, 25.

(75) Katritzky, A. R.; Kashmiri, M. A.; De Ville, G. Z.; Patel, R. C. *J. Am. Chem. Soc.* **1983**, *105*, 90.

(76) (a) Russell, G. A.; Hershberger, J.; Owens, K. *J. Am. Chem. Soc.* **1979**, *101*, 1312. (b) Russell, G. A.; Guo, D. *Tetrahedron Lett.* **1984**, *25*, 5239.

(77) P.Branchaud, B.; Yu, G.-X. *Tetrahedron Lett.* **1988**, *29*, 6545.

(78) (a) Studer, A.; Curran, D. P. *Angew. Chem., Int. Ed.* **2016**, *55*, 58. (b) Yan, M.; Lo, J. C.; Edwards, J. T.; Baran, P. S. *J. Am. Chem. Soc.* **2016**, *138*, 12692. (c) Zard, S. Z. *Org. Lett* **2017**, *19*, 1257.

(79) (a) Hu, X. *Chem. Sci.* **2011**, *2*, 1867. (b) Jana, R.; Pathak, T. P.; Sigman, M. S. *Chem. Rev.* **2011**, *111*, 1417.

(80) Bauer, I.; Knölker, H.-J. *Chem. Rev.* **2015**, *115*, 3170.

(81) Cahiez, G.; Moyeux, A. *Chem. Rev.* **2010**, *110*, 1435.

(82) Clark, A. J. *Chem. Soc. Rev.* **2002**, *31*, 1.

(83) Lin; Liu, L.; Fu, Y.; Luo, S.-W.; Chen, Q.; Guo, Q.-X. *Organometallics* **2004**, *23*, 2114.

(84) (a) Netherton, M. R.; Fu, G. C. *Adv. Synth. Catal.* **2004**, *346*, 1525. (b) Rudolph, A.; Lautens, M. *Angew. Chem., Int. Ed.* **2009**, *48*, 2656. (c) Tasker, S. Z.; Standley, E. A.; Jamison, T. F. *Nature* **2014**, *509*, 299. (d) Biswas, S.; Weix, D. J. *J. Am. Chem. Soc.* **2013**, *135*, 16192. (e) Breitenfeld, J.; Ruiz, J.; Wodrich, M. D.; Hu, X. *J. Am. Chem. Soc.* **2013**, *135*, 12004.

(85) Ishiyama, T.; Abe, S.; Miyaura, N.; Suzuki, A. *Chem. Lett.* **1992**, *21*, 691.

(86) Devasagayaraj, A.; Stüdemann, T.; Knochel, P. *Angew. Chem., Int. Ed. Engl.* **1996**, *34*, 2723.

(87) Giovannini, R.; Knochel, P. *J. Am. Chem. Soc.* **1998**, *120*, 11186.

(88) Terao, J.; Watanabe, H.; Ikumi, A.; Kuniyasu, H.; Kambe, N. *J. Am. Chem. Soc.* **2002**, *124*, 4222.

(89) Zhou, J.; Fu, G. C. *J. Am. Chem. Soc.* **2003**, *125*, 14726.

(90) Anderson, T. J.; Jones, G. D.; Vicic, D. A. *J. Am. Chem. Soc.* **2004**, *126*, 8100.

(91) (a) Jones, G. D.; McFarland, C.; Anderson, T. J.; Vicic, D. A. *Chem. Commun.* **2005**, 4211. (b) Jones, G. D.; Martin, J. L.; McFarland, C.; Allen, O. R.; Hall, R. E.; Haley, A. D.; Brandon, R. J.; Konovalova, T.; Desrochers, P. J.; Pulay, P.; Vicic, D. A. *J. Am. Chem. Soc.* **2006**, *128*, 13175.

(92) (a) Cornella, J.; Edwards, J. T.; Qin, T.; Kawamura, S.; Wang, J.; Pan, C.-M.; Gianatassio, R.; Schmidt, M.; Eastgate, M. D.; Baran, P. S. *J. Am. Chem. Soc.* **2016**, *138*, 2174. (b) Qin, T.; Cornella, J.; Li, C.; Malins, L. R.; Edwards, J. T.; Kawamura, S.; Maxwell, B. D.; Eastgate, M. D.; Baran, P. S. *Science* **2016**, *352*, 801.

(93) (a) Wang, J.; Qin, T.; Chen, T.-G.; Wimmer, L.; Edwards, J. T.; Cornella, J.; Vokits, B.; Shaw, S. A.; Baran, P. S. *Angew. Chem., Int. Ed.* **2016**, *55*, 9676. (b) Edwards, J. T.; Merchant, R. R.; McClymont, K. S.; Knouse, K. W.; Qin, T.; Malins, L. R.; Vokits, B.; Shaw, S. A.; Bao, D.-H.; Wei, F.-L.; Zhou, T.; Eastgate, M. D.; Baran, P. S. *Nature* **2017**, *545*, 213. (c) Li, C.; Wang, J.; Barton, L. M.; Yu, S.; Tian, M.; Peters, D. S.; Kumar, M.; Yu, A. W.; Johnson, K. A.; Chatterjee, A. K.; Yan, M.; Baran, P. S. *Science* **2017**, *356*.

(94) Huihui, K. M. M.; Caputo, J. A.; Melchor, Z.; Olivares, A. M.; Spiewak, A. M.; Johnson, K. A.; DiBenedetto, T. A.; Kim, S.; Ackerman, L. K. G.; Weix, D. J. *J. Am. Chem. Soc.* **2016**, *138*, 5016.

(95) Sherry, B. D.; Fürstner, A. *Acc. Chem. Res.* **2008**, *41*, 1500.

(96) Tamura, M.; Kochi, J. *J. Organomet. Chem.* **1971**, *31*, 289.

(97) Dongol, K. G.; Koh, H.; Sau, M.; Chai, C. L. L. *Adv. Synth. Catal.* **2007**, *349*, 1015.

(98) Jin, M.; Adak, L.; Nakamura, M. *J. Am. Chem. Soc.* **2015**, *137*, 7128.

(99) Toriyama, F.; Cornella, J.; Wimmer, L.; Chen, T.-G.; Dixon, D. D.; Creech, G.; Baran, P. S. *J. Am. Chem. Soc.* **2016**, *138*, 11132.

(100) Cahiez, G.; Chaboche, C.; Duplais, C.; Giulliani, A.; Moyeux, A. *Adv. Synth. Catal.* **2008**, *350*, 1484.

(101) Iwasaki, T.; Takagawa, H.; Singh, S. P.; Kuniyasu, H.; Kambe, N. *J. Am. Chem. Soc.* **2013**, *135*, 9604.

(102) Mao, J.; Liu, F.; Wang, M.; Wu, L.; Zheng, B.; Liu, S.; Zhong, J.; Bian, Q.; Walsh, P. J. *J. Am. Chem. Soc.* **2014**, *136*, 17662.

(103) Evano, G.; Theunissen, C.; Pradal, A. *Nat. Prod. Rep.* **2013**, *30*, 1467.

(104) (a) Matyjaszewski, K.; Xia, J. *Chem. Rev.* **2001**, *101*, 2921. (b) Tsarevsky, N. V.; Matyjaszewski, K. *Chem. Rev.* **2007**, *107*, 2270. (c) Pintauer, T.; Matyjaszewski, K. *Chem. Soc. Rev.* **2008**, *37*, 1087.

(105) Kharasch, M. S.; Urry, W. H.; Jensen, E. V. *J. Am. Chem. Soc.* **1945**, *67*, 1626.

(106) Nagashima, H.; Seki, K.; Ozaki, N.; Wakamatsu, H.; Itoh, K.; Tomo, Y.; Tsuji, J. *J. Org. Chem.* **1990**, *55*, 985.

(107) Nishikata, T.; Noda, Y.; Fujimoto, R.; Sakashita, T. *J. Am. Chem. Soc.* **2013**, *135*, 16372.

(108) Matyjaszewski, K. *Macromolecules* **2012**, *45*, 4015.

Chapter 2

TRIFLUOROMETHYLATION OF SECONDARY NITROALKANES

2.1 INTRODUCTION AND BACKGROUND

Nitroalkanes are useful intermediates in several C–C bond forming reactions and serve as precursors for several functional groups including amines and carbonyls. Despite this rich chemistry, the seemingly simple *C*-alkylation of nitroalkanes with alkyl electrophiles (such as alkyl halides) has remained a highly challenging task.[1] This is because the nitronate anion undergoes alkylation at oxygen rather than carbon. This process generates a nitronic ester (**2.1**) which decomposes rapidly in the presence of base to give aldehyde and oxime (Figure 2.1).[2] As such, we sought to develop a mild catalytic protocol for the *C*-alkylation of nitronate anions with high selectivity over O-alkylation. My colleagues Dr. Peter Gildner and Dr. Amber Geitter Burch discovered the first catalytic conditions for the benzylation of nitroalkanes using the combination of a simple copper (I) salt and easily synthesized diketimine ligand (nacnac) (**2.2**).[3] This method provides access to a variety of complex homobenzylic Nitroalkanes (**2.3**) which can be readily transformed into medicinally relevant phenethylamine derivatives.

Our preliminary mechanistic hypothesis involves a stabilized radical intermediate generated via atom transfer from electron-rich Cu(I)-nacnac complex, followed by radical-anion coupling with nitronate anion to afford nitronate radical (**2.4**), and back transfer of an electron to the Cu(II) center to regenerate the catalyst and desired product (**2.3**) (Figure 2.2).

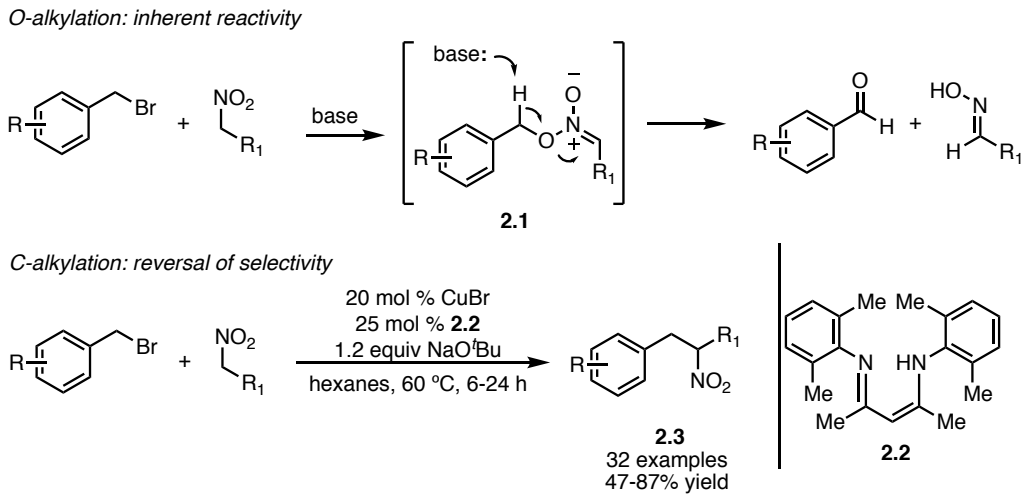

Figure 2.1: Copper-Catalyzed *C*-Alkylation of Nitroalkanes with Benzyl bromide

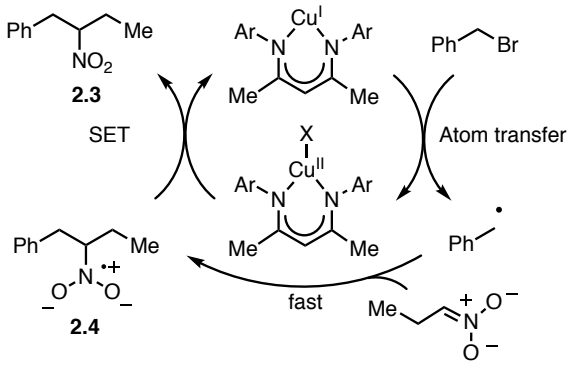

Figure 2.2: Proposed Mechanism for *C*-Benzylation of Nitroalkanes

Our studies on the benzylation of nitroalkanes showed that the reaction proceeds through an intermediacy of alkyl radicals. This suggests that the other alkyl halides bearing stabilizing group might serve as potential alkylating agents for nitroalkanes. Toward this end, our group investigated the use of the α-halocarbonyl scaffold (**2.5**), since these substrates have been shown to form alkyl radicals in transition-metal catalysis. This method can be utilized to access to a variety of β-

nitrocarbonyls (**2.6**).[4] The substrate scope is remarkably broad, tolerating various carbonyl groups including esters, amides, ketones and aldehydes in excellent yields. Additionally, the alkylation proceeds even in the presence of considerable steric congestion, forming products bearing contiguous quaternary centers in synthetically useful yields. The products can be easily derivatized into β-amino acids, compounds with considerable use in bioorganic chemistry, as the basis of peptoids.[5]

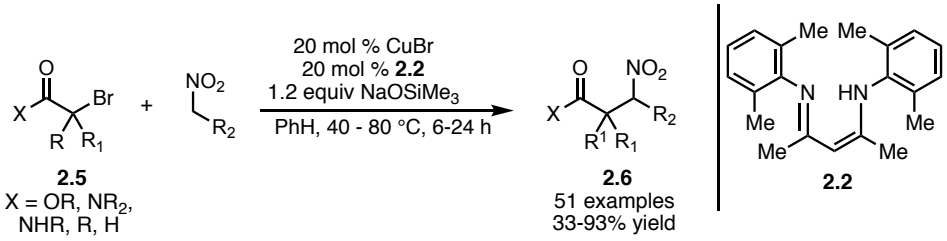

Figure 2.3: Copper-Catalyzed C-Alkylation of Nitroalkanes with α-Halocarbonyl Compounds

Our group's interest in the synthesis of highly nitrogen-rich compounds led us to consider nitrogen-containing groups that could be used to support neighboring radicals. Toward this end, my colleague Dr. Kirk Shimkin discovered a mild copper-catalyzed condition for the *C*-alkylation of nitroalkanes with α-bromonitrile (**2.7**)electrophiles.[6] This method provides access to a variety of β-cyanonitroalkanes (**2.8**), which are valuable synthetic building blocks due to their potential use as orthogonally masked 1,3-diamines. In addition, these products can also be derivatized into complex cyanoalkenes and 5-aminoisoxazoles in good yields.

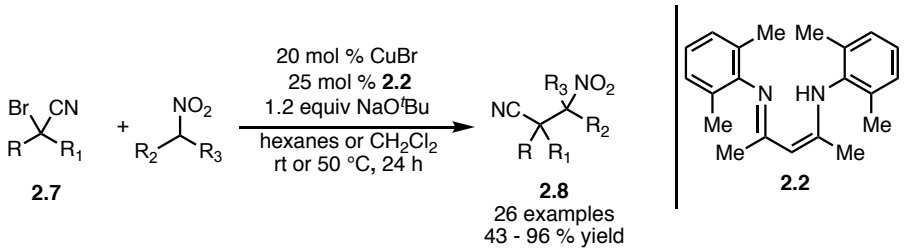

Figure 2.4: Copper-Catalyzed C-Alkylation of Nitroalkanes with α-Bromonitriles

Organofluorine compounds play an important role in pharmaceuticals, agrochemicals, liquid crystals, dyes, and polymers.[7] Trifluoromethyl groups in particular have been shown to impart unique physiological properties, including modulation of binding affinities, lipophilicity, metabolic stability, and bioavailability when incorporated into organic compounds.[8] Introduction of a trifluoromethyl group alpha to nitrogen results in favorable modulation of *in vivo* activity compared to their non-fluorinated analogs.[9] A rapid entry into such α-trifluoromethylamines can be achieved through the trifluoromethylation of nitroalkanes, followed by subsequent reduction of the nitro functional group. Based on our past studies, we envisioned that alkylation of a nitroalkanes with appropriate electrophilic trifluoromethylating agent would provide an elegant solution to this problem. Umemoto's reagent (**2.9**) was selected as an appropriate trifluoromethyl source because of its potential to form CF_3 radical under catalytic conditions. The fully substituted α-trifluoromethylnitroalkanes (**2.10**) obtained from this transformation can be derived into a variety of complex nitrogen-containing, medicinally-relevant α-(trifluoromethyl)amines **2.11** (Figure 2.5). This chapter will describe the development of trifluoromethylation of secondary nitroalkanes using Umemoto's reagent as electrophile.

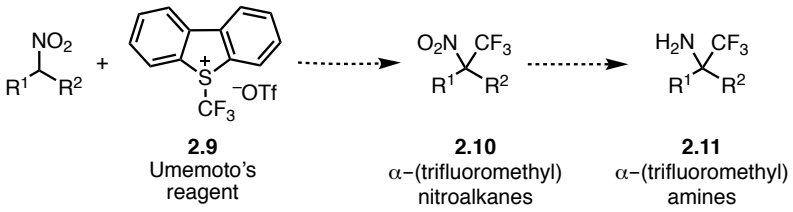

Figure 2.5: Trifluoromethylation of Secondary Nitroalkanes using Umemoto's Reagent

2.2 Medicinal Importance of Trifluoromethyl Groups

Trifluoromethylated molecules are increasingly targeted in the field of medicinal chemistry for a myriad of reasons (see section 2.1). Remarkably, a subtle structural change from a methyl group to a trifluoromethyl group often imparts pronounced improvements in drug-like qualities of a molecule. The antidepressant Fluoxetine (Eli Lilly), marketed as the racemate and commonly known as Prozac®, is a molecule containing an aryl trifluoromethyl group. Studies have shown that depression is linked to low levels of neuro-transmitter 5-hydroxytryptamine (5-HT), also known as serotonin. Fluoxetine acts by selectively inhibiting the reuptake of serotonin, allowing the neurotransmitter to activate its specific receptor. Structure-activity relationship studies showed that the presence of a trifluoromethyl group in the para position of the phenolic ring increases the potency for inhibiting 5-HT uptake by 6-fold, compared to the non-fluorinated parent compound (Figure 2.6).[10] It has been documented that the size of the trifluoromethyl group is almost double the size of the methyl group, and closer in size to an isopropyl group.[8a] Accordingly, it is hypothesized that the steric bulk of the trifluoromethyl group allows the aryl ring to adopt a conformation which favors binding to the 5-HT transporter.[11]

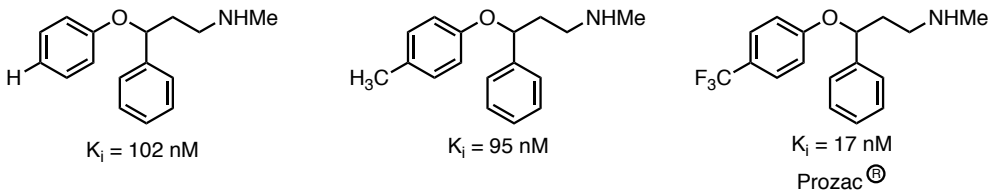

Figure 2.6: Comparison of K_i Value of Prozac® and its Derivatives

Another case study of the trifluoromethyl group's medicinal properties can be seen in the development of trifluridine. Trifluridine is an antiviral drug used in the treatment of eye infections. It is a suicide inhibitor, causing irreversible inhibition of thymidylate synthase (TS). TS is an enzyme that mediates the methylation of deoxyuridine monophosphate forming thymidine monophosphate, a key step in DNA biosynthesis. Inhibition of this enzyme causes apoptic cell death, which affects rapidly dividing cancer cells or viruses.

The drug acts by irreversibly forming a covalent bond with thymidylate synthase. The proposed mechanism involves the Michael addition of the nucleophilic group at the active site, followed by fluoride elimination to give difluoromethylene intermediate. The nucleophilic amine group at the active site further reacts with the intermediate to form an amide bond after the fluoride elimination and subsequent hydrolysis. The mechanism of inhibition of thymidylate synthase by trifluridine (Figure 2.7).[12]

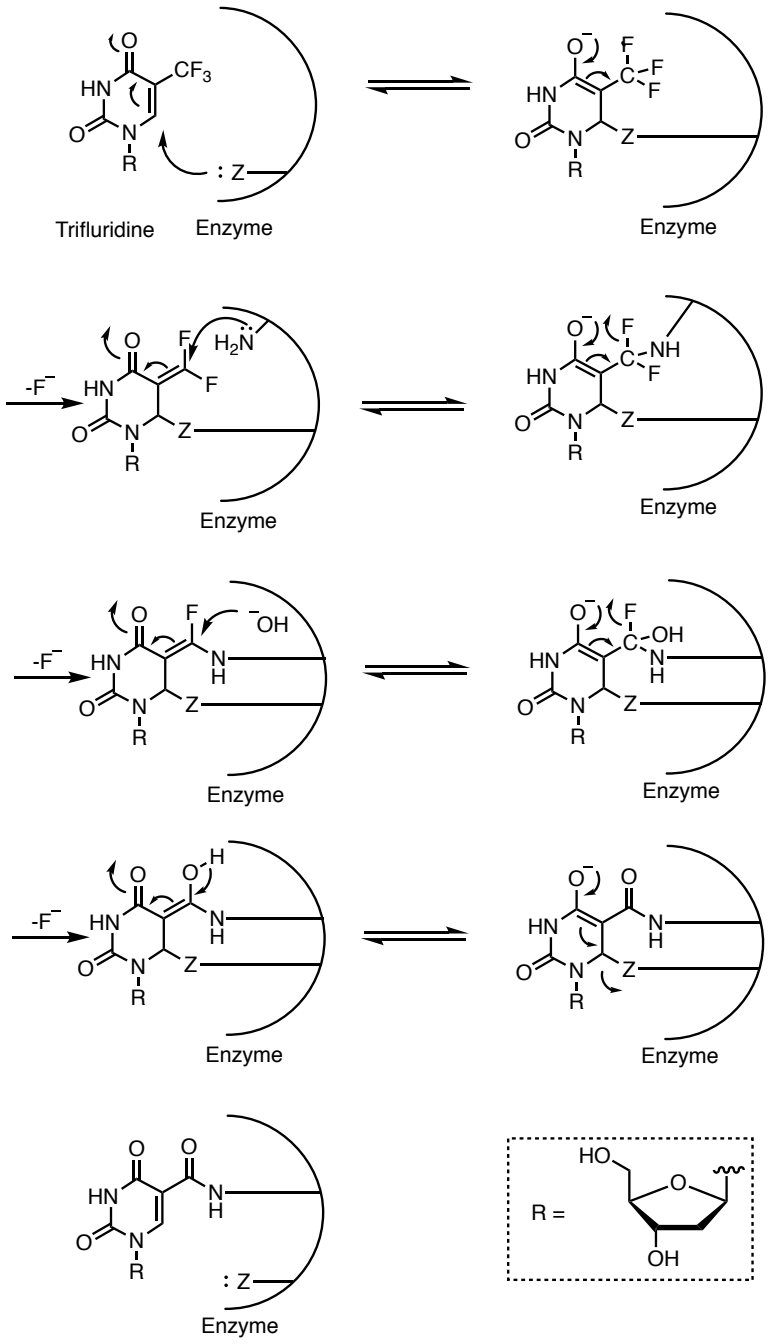

Figure 2.7: Mechanism of Inhibition of Thymidylate Synthase by Trifluridine

Suppressing the rate of oxidative metabolism by fluorine substitution is an important strategy in drug development. vitamin D_3 is used in the treatment of hyperthyroidism. Falicalcitral, a fluorinated analogue of vitamin D_3 exhibits increased metabolic stability compared to native vitamin D_3 (Figure 2.8). In this case, C–25 hydroxyl oxidation is blocked by the presence of trifluoromethyl substituents.[13]

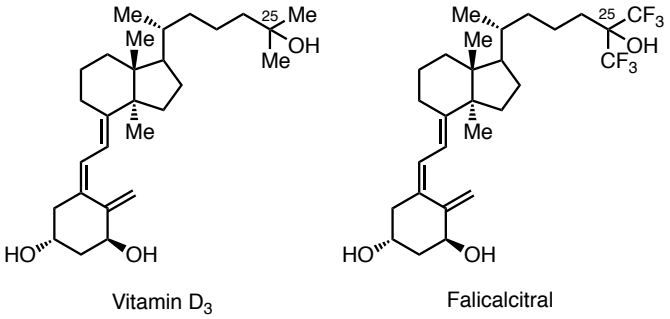

Figure 2.8: Structure Comparison of Vitamin D_3 and Falicalcitral

Enhancing the oral bioavailability by incorporating trifluoromethyl groups is another important strategy in drug discovery. Structure-activity relationship studies of Sitagliptin, a DPP-4 inhibitor used in the treatment of type 2 diabetes, showed that only the trifluoromethylated derivative possessed good oral bioavailability (Table 2.1).[14]

Table 2.1: Comparison of the Oral Bioavailability of Sitagliptin and its Non-Fluorinated Analogs

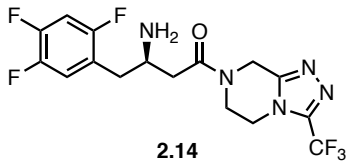

2.14
Sitagliptin

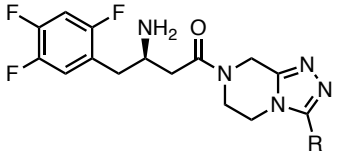

Compound	R	DPP-4 IC_{50} (nM)	Oral Bioavailability F (%)
2.12	H	68	3
2.13	C_2H_5	37	2
2.14	CF_3	18	76

2.3 Importance of α-(Trifluoromethyl)amines

As previously discussed, α-trifluoromethyl amines has been shown to favorably modulate the biological properties of numerous small molecules compared when to their non-fluorinated analogues. The following examples illustrate a pronounced effect on the potency of the drug candidates.

Replacement of amide bonds with suitable bioisosteres is an approach used in the medicinal chemistry. There are few examples of amide bond isosteres that preserve the geometry and basicity of the amide N-H bond; notably, trifluoromethylamines serve as competent bioisosteres for the amide group.[9a] Cathepsin K is a cysteine protease that is highly expressed in osteoclasts; accordingly, it is an important target for the treatment of osteoporosis.[15] Studies have shown that replacement of the amide carbonyl with a trifluoromethyl group enhances the potency of the Cathepsin K inhibitor (Table 2.2). Molecular modeling studies show that the non-basic nature of the α-trifluoromethylamine maintains the excellent hydrogen bonding to Gly66.[9a] Furthermore, structure-activity relationship studies show that the fluorinated analog is 1000 times more potent than the non-fluorinated analogues (Table 2.3).

Table 2.2: α-Trifluoromethylamines as Amide Isosteres in Cathepsin K Inhibitors

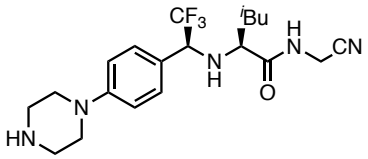

2.15

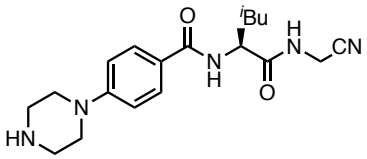

2.16

Compound	Cathepsin K IC_{50} (nM)
2.15	≤0.0015
2.16	0.015

Table 2.3: Comparison of CF_3 Replacements in Cathepsin K inhibitors

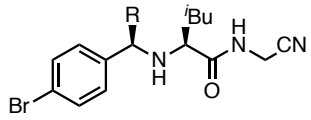

cathepsin K inhibitor

Compound	R	Cathepsin K IC_{50} (nM)
2.17	H	802
2.18	CH_3	988
2.19	CF_3	0.9

In 2011, researchers at Merck reported **2.19** as an inhibitor of Janus Kinase 2 (JAK2).[16] JAK2 has been linked to myeloproliferative disorders (MPDs), which are a group of disorders that cause red blood cells, white blood cells, and platelets to grow abnormally in bone marrow. These abnormalities have been linked to several different diseases, such as primary myelofibrosis and chronic myelogenous leukemia. With respect to JAK2 inhibitors, the installation of a trifluoromethyl group on the parent scaffold increased the inhibitory concentration by 25-fold, enhanced the enzymatic

selectivity, and improved the pharmacokinetic profile towards inhibition of JAK 2 (Table 2.4).

Table 2.4: Comparison of CF_3 Replacements in JAK2 Inhibitors

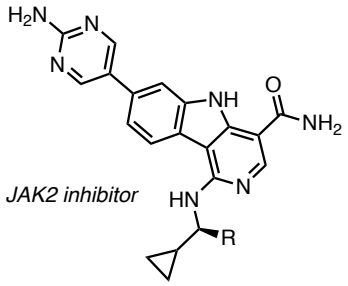

Compound	R	JAK2 IC_{50} (nM)
2.20	CH_3	11
2.21	CF_3	0.4

Taxol® is an anti-cancer drug used extensively in the treatment of breast and ovarian cancers. However, studies have shown that its use results in undesirable side effects.[17] Ojima and coworkers showed a second-generation, fluorine-containing taxoid which exhibits fewer side effects and improved activity against drug-resistant tumors.[18] Structure - activity relationship studies showed **2.22** to be 20-fold more potent than the phenyl analogue (**2.23)** (Table 2.5).[19] The new trifluoromethylated taxoid possesses excellent activity against several human cancer cell lines, A121 (ovarian carcinoma), A549 (non-small cell lung carcinoma), HT-29 (colon carcinoma), and MCF-7 (mammary carcinoma).

Table 2.5: Comparison of CF_3 Replacements in Taxoid

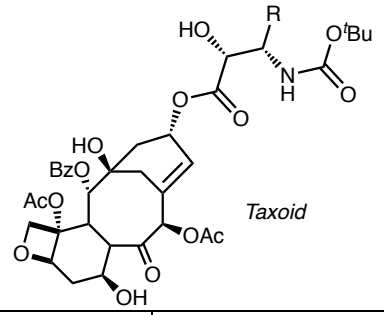

Compound	R	JAK2 IC_{50} (nM)
2.22	Ph	6.3
2.23	CF_3	0.3

2.4 Previous Syntheses of α-Perfluoronitroalkanes:

Two methods have been previously described to prepare α-perfluoronitroalkanes. Both methods utilized a perfluoroalkylating agent for the perfluoroalkylation of nitroalkanes. In 1981, Umemoto and coworkers described the perfluoroalkylation of an alkyl sodium nitronate salt using the perfluorinated hypervalent iodine reagent (**2.24**) (FITS).[20] Similarly, using the less reactive perfluoroalkylphenyliodonium sulfate (**2.25**) (FIS) was competent in the reaction, albeit in lower yield than (**2.24**). The high reactivity of (**2.24)** is attributed to the good leaving ability of the triflate group. Even though only two examples were studied using nitroalkanes as the nucleophiles, this was an important step in the development of perfluoroalkylation of nitroalkanes (Figure 2.9).

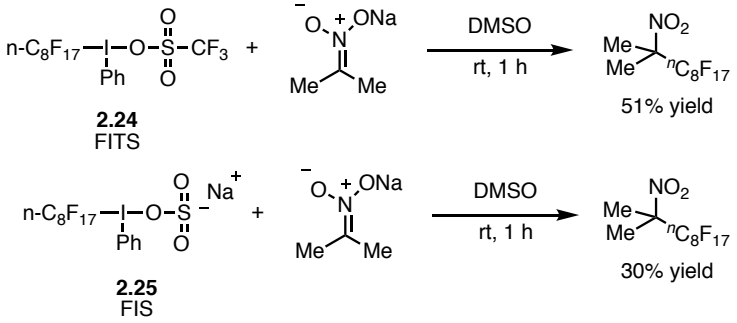

Figure 2.9: Umemoto's Synthesis of α-Perfluoronitroalkanes

In 1983, Feiring described the perfluoroalkylation of 2-nitropropane using perfluoroalkyliodides (**2.26**) as the perfluoroalkylating agent.[21] This method removes the need of FITS (**2.24**), which must be synthesized prior to use. The scope with perfluoroalkyliodides was limited, and only one nitroalkane was investigated. Several experiments suggest that the reaction proceeds via SRN1 mechanism. For example, the reaction gave low yield of the desired product when conducted in the dark and inhibited by radical scavengers. Second, electrochemical studies on 1-iodo-tridecafluorohexane revealed a reduction potential of -0.6 V vs SCE (in MeCN), which lies in the range of electron transfer from the nitronate anion. Finally, when 2° perfluoroalkyliodides are treated with nitronate anion, homodimers of perfluoroalkyl iodides were observed, suggesting the intermediacy of perfluoroalkyl radical species.[21]

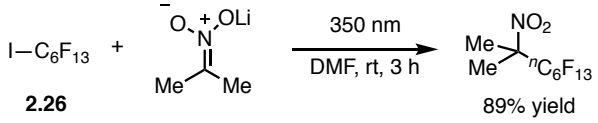

Figure 2.10: Feiring's Synthesis of α-perfluoronitroalkanes using Photolytic Condition

2.5 Previous Syntheses of α-(trifluoromethyl)nitroalkanes:

The method described in section 2.4 are effective to synthesize α-perfluoronitroalkanes, but are ineffective in synthesizing α-(trifluoromethyl)nitroalkanes. In 1963, Kununyants developed the first method to prepare simple α-(trifluoromethyl) nitroalkanes (**2.27**) by treating hydrogen fluoride and nitric acid with 1,1-difluoroethylene.[22] While this method established precedent for the synthesis of α-trifluoromethylnitroalkanes, the harsh reaction conditions utilized limits the general applicability of this transformation.

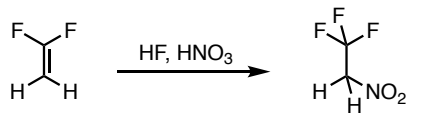

2.27, 58% yield

Figure 2.11: Knunyant's Synthesis of α-(trifluoromethyl)nitroalkanes

In 2007, Togni and his coworkers reported the first example of a transition metal-catalyzed reaction for the formation of α-(trifluoromethyl)nitroalkanes.[23] Using catalytic copper and Togni's reagent (**2.28**), activated α-nitroesters could be trifluromethylated in good yield (Figure 2.12). Notably, one example with an activated α-nitroamide was reported. Control experiments showed that no desired trifluoromethylated product was formed when copper (I) bromide dimethyl sulfide was omitted.

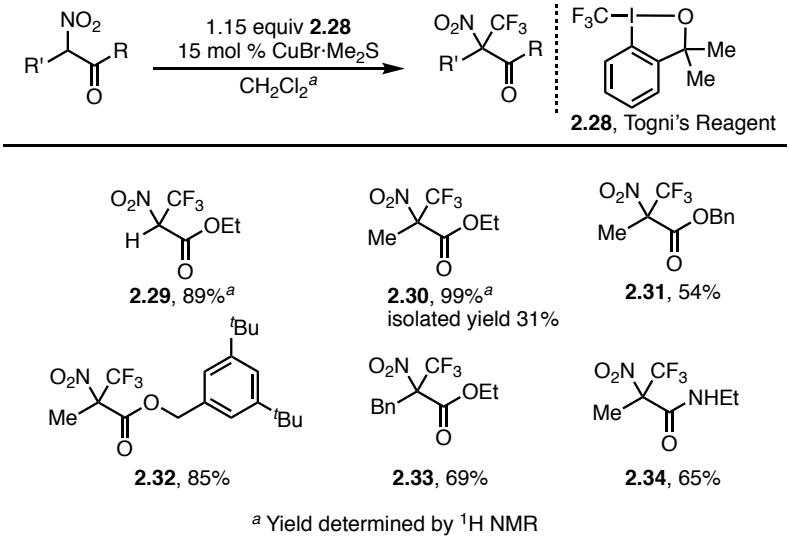

Figure 2.12: Scope of Togni's α-(trifluoromethyl)nitroalkanes of α-Nitroesters

This procedure, however, has several serious limitations (Figure 2.12). First, nitroalkanes bearing other activating group such as ketones and carboxylic acids were not suitable coupling partners. Second, any substitution α to the nitro carbon is not accessible and nitroalkanes possessing β-branching are not accessible, suggesting a serious steric limitation. Third, no functional group tolerance with respect to nitroalkanes was displayed using these reaction conditions (Figure 2.13). Finally, only α-nitrocarbonyls, which are a specialized class of activated nitroalkanes, were trifluoromethylated under the reaction conditions. α-Trifluoromethylation of unactivated nitroalkanes were not explored using these reaction conditions. It was also reported that the isolation of the products can be difficult. As shown in Figure 2.12, substrate (**2.30**) has ^{1}H NMR and isolated yield of 99% and 31% respectively, supporting the claim that the isolation was difficult. Togni attributed this discrepancy in yield to the high volatility of α-(trifluoromethyl)nitroalkane (**2.30**).

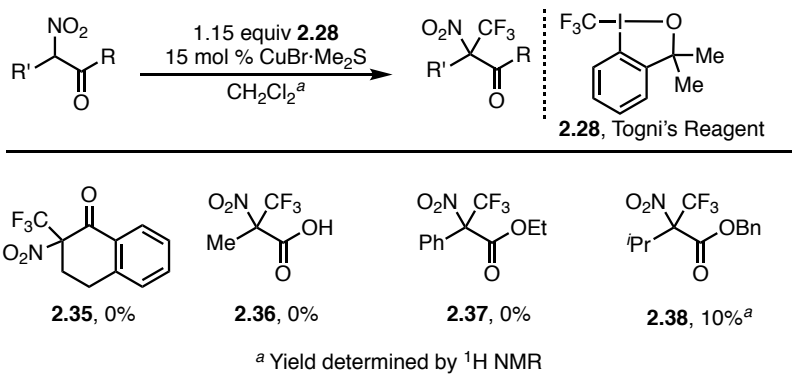

Figure 2.13: Limitations of Togni's Trifluoromethylation of α-Nitrocarbonyls.

Togni's group also investigated the possibility of developing an diastereoselective trifluoromethylation of chiral α-nitroesters (**2.39**). A doctoral thesis from Togni's group shows that formation of the C–CF3 bond could proceed diastereoselectively *via* remote stereo control. Using a menthol-derived chiral auxillary, diastereoselectivities of up to 6:1 were observed (Figure 2.14).[24]

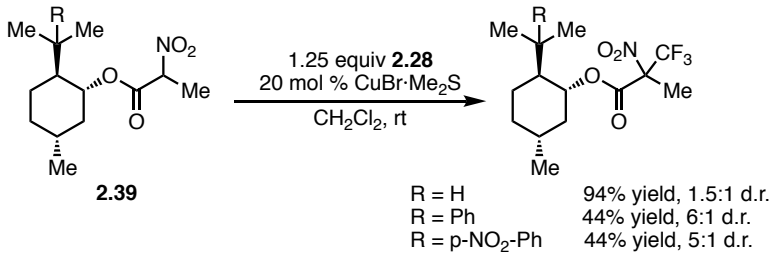

Figure 2.14: Togni's Diastereoselective Studies of Trifluoromethylation of α-Nitroesters using Phenyl Menthol Chiral Auxillary

As shown in Figure 2.15, the Togni group could desymmetrize the trifluoromethylation of α-nitroesters using a chiral Cu-BOX (**2.40**) complex.[25] After

survey of a variety of ligand scaffolds, the best results were obtained using chiral copper complex (**2.40**). Nitroalkane (**2.41**) was obtained in 24% ee (yield not reported). More discouragingly, attempts to extend to additional substrates such as (**2.42**), (**2.43**) and (**2.44**) afforded little to no ee. The lack of generality with nitroalkanes, limited substitution pattern accessible, lack of stereocontrol underscore the necessity for improved method for the preparation of α-(trifluoromethyl)nitroalkanes.

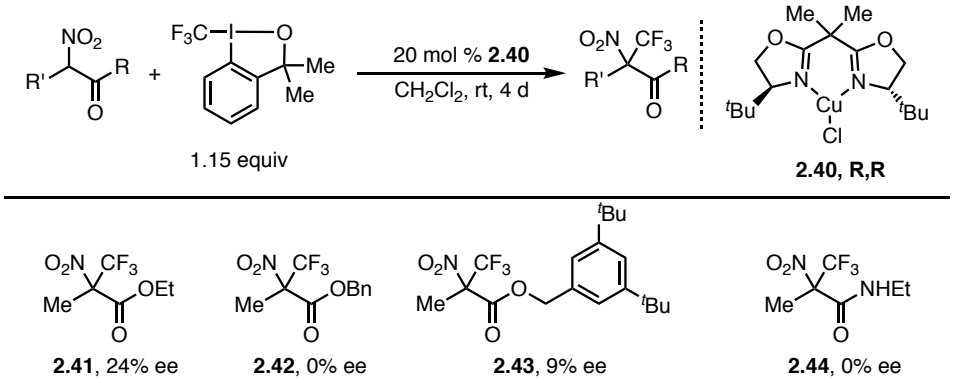

Figure 2.15: Togni's Preliminary Enantioselective Studies of Trifluoromethylation of α-Nitroesters using Cu-BOX Complex.

2.6 Copper Mediated Radical Trifluoromethylation Reaction using Electrophilic Trifluromethylating Reagent:

Trifluoromethylation reactions have been extensively studied in organic synthesis. Methods for their incorporation can be broadly classified as nucleophilic, electrophilic, free radical, or transition metal-catalyzed processes; they have been extensively reviewed and will not be discussed here in detail.[23b,26] Electrophilic trifluoromethylating reagents such as Togni's reagent (**2.28**) and Umemoto reagent (**2.9**) are easy to handle, stable at ambient conditions, and can be easily prepared.[27]

They have been reported to react with a wide variety of nucleophiles including keto derivatives, sulfides, arenes, enol silyl ethers, dicyanoalkylidenes, and alkynes.[28] Furthermore, they are known to generate CF_3 radicals in the presence of copper salts. A few recent examples are covered in the following section.

In 2011, Xiao and coworkers reported a mild procedure for the trifluoromethylation of heteroaryl iodides in the presence of copper using (S)-(trifluoromethyl)diphenylsulfonium triflate (**2.45**) (Figure 2.16).[29] The electrophilic trifluoromethylating reagent can be reduced by copper *via* single electron transfer (SET). The intermediate (**2.46**) rapidly decomposes to give a CF_3 radical, which reacts with copper to generate $CuCF_3$ (**2.47**). The formation of $CuCF_3$ is corroborated by ^{19}F NMR spectroscopy and ESI-MS studies (Figure 2.17).

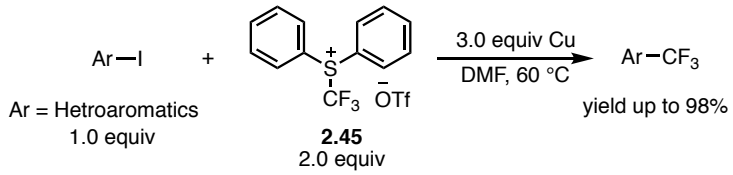

Figure 2.16: Xiao's Trifluoromethylation of Heteroaryl Iodides with (S)-(Trifluoromethyl)diphenylsulfonium Triflate

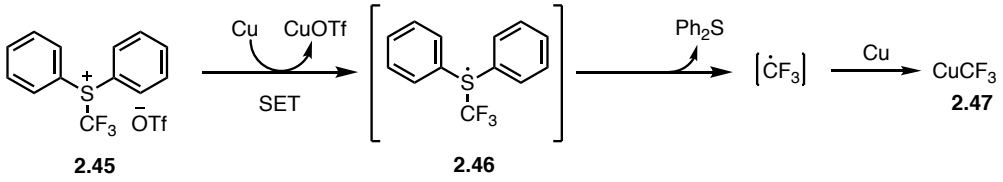

Figure 2.17: Xiao's Proposed Mechanism for the Generation of $CuCF_3$ Intermediate

In 2013, Buchwald and coworkers developed a mild method for the enantioselective oxytrifluoromethylation of alkenes using a Togni-type reagent (**2.48**) and chiral copper-based catalyst (**2.49**) system to afford lactones such as (**2.50**) in good yield and excellent enantioseletivity (Figure 2.18).[30]

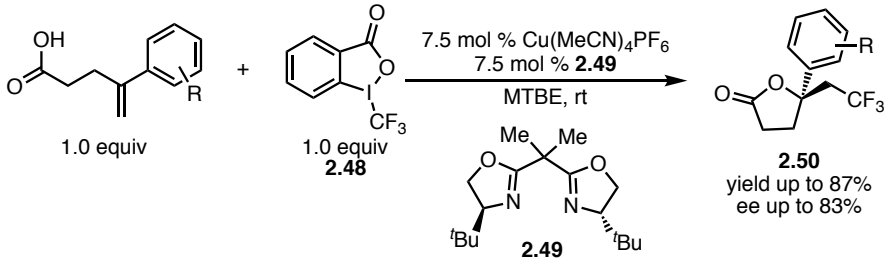

Figure 2.18: Buchwald's Copper Catalyzed Enantioselective Oxytrifluoromethylation of Alkenes using Togni's Reagent

To investigate the mechanism of the reaction, TEMPO was employed as a radical-capturing agent in the presence of catalyst to afford the TEMPO-CF_3 (**2.51**) adduct (Figure 2.19 bottom). When a cyclopropyl-bearing substrate (**2.52**) was subjected to standard reaction conditions, the ring-opened product (**2.53**) was observed (Figure 2.19 top).

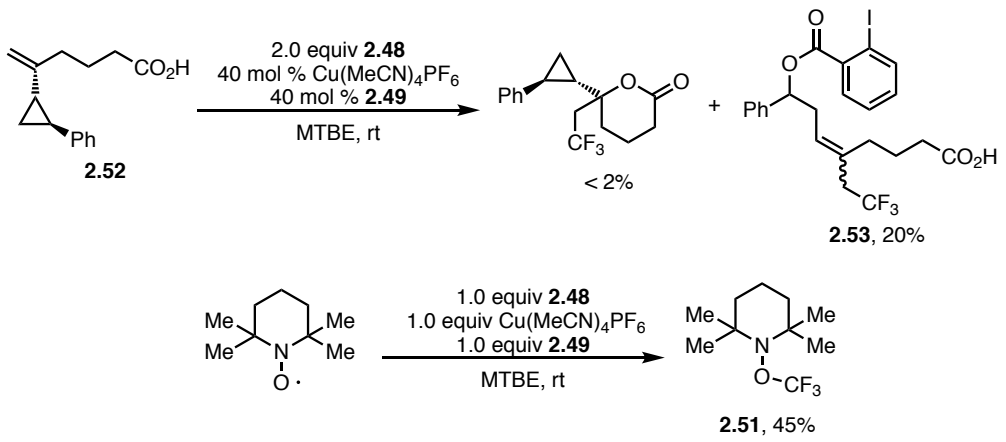

Figure 2.19: Buchwald's Radical Probe Studies in the Oxytrifluoromethylation of Alkenes

These experiments suggest the intermediacy of a CF_3 radical and an α-CF_3 alkyl radical intermediate formed under the reaction condition. Based on these results, the proposed mechanism involves single electron transfer between (**2.48**) and the Cu^I catalyst, generating a CF_3 radical and a Cu^{II} complex. The CF_3 radical then adds across the alkene to give (**2.54**), which undergoes enantioselective C–O bond formation *via* the Cu^{II} complex, thus affording the lactone (**2.50**) while regenerating the Cu^I catalyst (Figure 2.20).

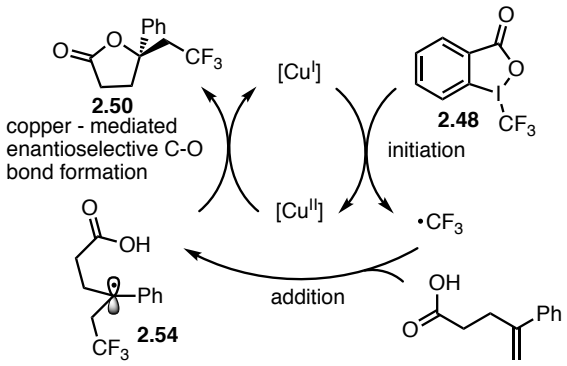

Figure 2.20: Proposed Mechanism of Buchwald's Oxytrifluoromethylation of Alkenes

In 2013, Fu and coworkers developed a copper-promoted Sandmeyer trifluoromethylation of aniline and its derivatives (**2.55**) using Umemoto's reagent (**2.9**) in good yield (Figure 2.21).[31] To gain insight into the formation of the CF_3 radical under the reaction conditions EPR studies were conducted. When Umemoto's reagent (**2.9**), copper metal, and TEMPO were combined, the EPR signal of TEMPO is suppressed and TEMPO-CF_3 (**2.51**) adduct was identified. This implies that copper facilitates the generation of the CF_3 radical under the reaction conditions. Furthermore, using 2-(allyloxy)aniline (**2.56**) as substrate yielded cyclized product (**2.57**); acyclic product (**2.58**) was not observed, suggesting the intermediacy of an aryl radical under the reaction conditions (Figure 2.22).

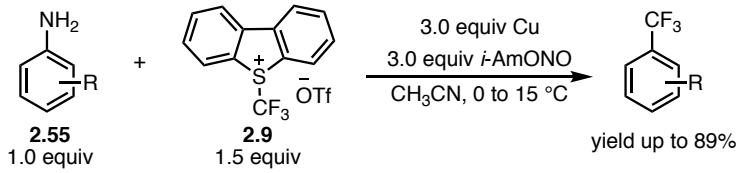

Figure 2.21: Fu's Radical Sandmeyer Trifluoromethylation of Anilines using Umemoto's Reagent

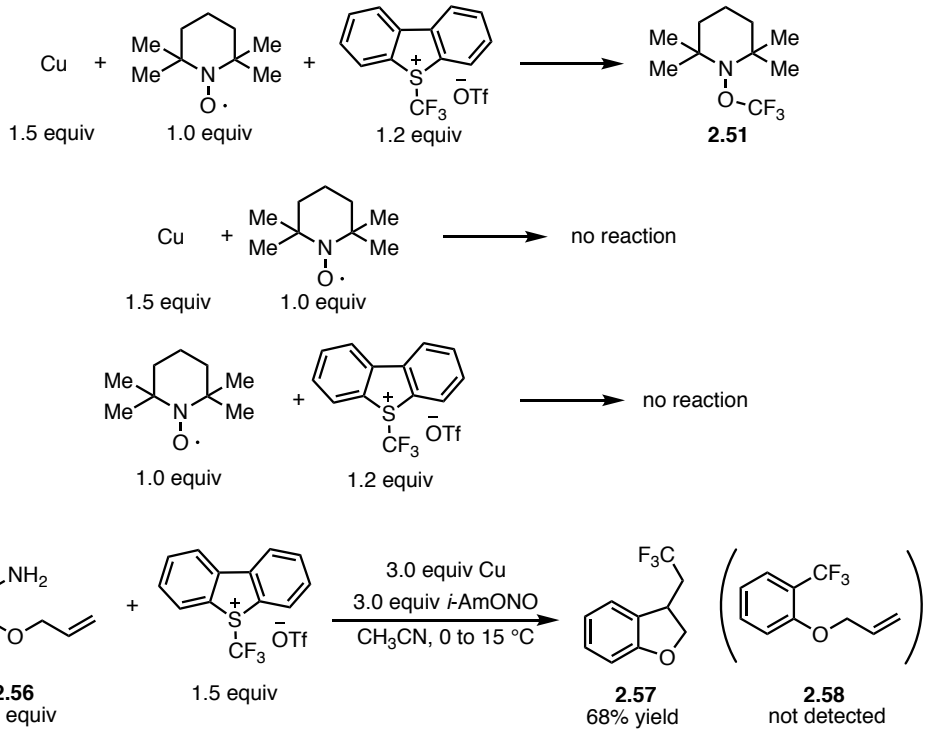

Figure 2.22: Fu's Radical Probe Studies in the Trifluoromethylation of Anilines

Based on these results, the author proposes copper-mediated SET in Umemoto's reagent (**2.9**) to generate the CF_3 radical. The CF_3 radical combines with Cu to give $CuCF_3$, which reacts with the aryl radical (**2.59**) generated from the aryldiazonium ion to give the desired product (**2.60**) (Figure 2.23).

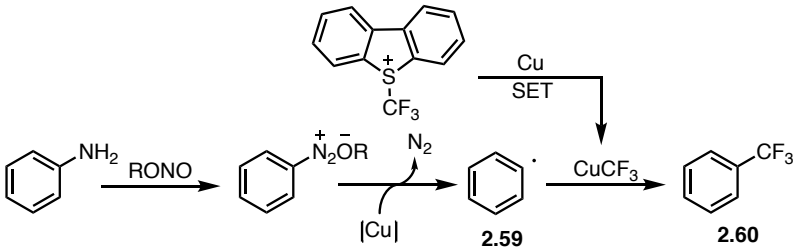

Figure 2.23: Proposed Mechanism of Fu's Radical Trifluoromethylation of Anilines

2.7 Development of Reaction Conditions

Our group was interested in developing a mild method to trifluoromethylate a diverse array of nitroalkanes to synthesize α-(trifluoromethyl)nitroalkanes, which can be easily converted into medicinally relevant α-(trifluoromethyl)amines. Given the likelihood for a radical-anion coupling mechanism in our C-alkylation chemistry using copper catalysis (see Section 2.1),[3-4,6] We believed we could access α-(trifluoromethyl) nitroalkanes by generating a CF_3 radical in situ using copper-diketimine catalyst.

My colleague Dr. Peter Gildner was the first to investigate this reaction. In preliminary studies, using Umemoto's reagent (**2.9**) as an electrophile,[27a,32] and secondary nitroalkane (**2.61**) as the model nucleophile, he observed a 22% yield of the desired product (**2.62**) in the presence of CuBr, diketimine ligand, and $NaOSiMe_3$ (Table 2.6, entry 1).

Table 2.6: Optimization of Reaction Condition for the Trifluoromethylation of Secondary Nitroalkanes

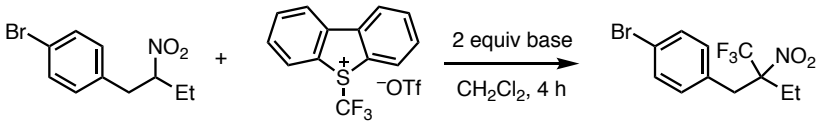

2.61 **2.9** **2.62**

Entry	Base	Additive	T (°C)	Yield 2.62[a]
1	$NaOSiMe_3$	20 mol % CuL[b]	40	22%
2	$NaOSiMe_3$	none	40	24%
3	DBU	none	40	52%
4	DBU	none	rt	58%
5	DBU	none	–25	90%
6	DBU	none	–50	91%

[a] 1.3 equiv **2.9**; yields determined by ^{1}H NMR using 1,3,5-trimethoxybenzene as an internal standard. [b] 20 mol % CuBr, 20 mol % bis-***N, N′***-(2,6-dimethylphenyl)-2,4-diiminopentane added to reaction.

After this preliminary result, my colleague Dr. Amber Gietter-Burch began optimization of the trifluoromethylation of secondary nitroalkanes using Umemoto's reagent. Through control experiments, she determined that the reaction did not require catalytic additives (Table 2.6, entry 2). Switching the base from sodium trimethylsilanolate to 1,8-Diazabicyclo[5.4.0]undec-7-ene (DBU) increased the yield to 52%. Finally, lowering the temperature from +40 °C to –25 °C afforded optimal amounts of the desired product (entry 3-5). Further decreasing the temperature did not afford an increase in yield (entry 6).

Finally, examination of trifluoromethylating reagents showed Umemoto's reagent was uniquely effective in the transformation (Table 2.7, entry 1). Togni's reagent did afford desired product, although the yield was lower (Table 2.7, entry 2). trifluoromethyl iodide and trimethyl(trifluoromethyl)silane (Ruppert's reagent) were ineffective, affording no yield of desired product under the optimized reaction conditions (Table 2.7, entry 3-4).

Table 2.7: Optimization of Trifluoromethylating Reagent

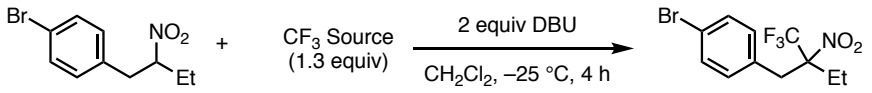

2.61 **2.62**

Entry	Trifluoromethylating Reagent	Yield 2.62[a]
1[b]	Umemoto's Reagent (**2.9**)	83%
2	Togni's Reagent (**2.28**)	31%
3[c]	CF_3I	0%
4	$TMSCF_3$	0%

[a] Yields determined by ^1H NMR using 1,3,5-trimethoxybenzene as an internal standard. [b] Isolated Yield. [b] Reaction performed under a balloon of CF_3I

2.8 Scope of Trifluoromethylation of Secondary Nitroalkanes

After Dr. Gietter-Burch optimized the reaction conditions, I joined with her to examine the scope of trifluoromethylation of secondary nitroalkanes. The reaction is general for a broad range of secondary nitroalkanes (Figure 2.24). The model substrate was isolated in 83% yield (**2.62**).[3] Other homobenzylic nitroalkanes (**2.63**) led to similar results. Both benzylic substrates (**2.64**-**2.67**)[33] and Michael reaction adducts (e.g., **2.68**-**2.71**) were also well-tolerated. Sterically demanding substrates could also be used; for example, even neopentylic substrates led to appreciable yields of products (**2.73**) containing vicinal fully substituted centers. In contrast to secondary substrates, primary nitroalkanes provide very little reactivity; for example, only traces of (**2.72)** were observed. Further studies will be directed at expanding the scope of the reaction to primary nitroalkanes.

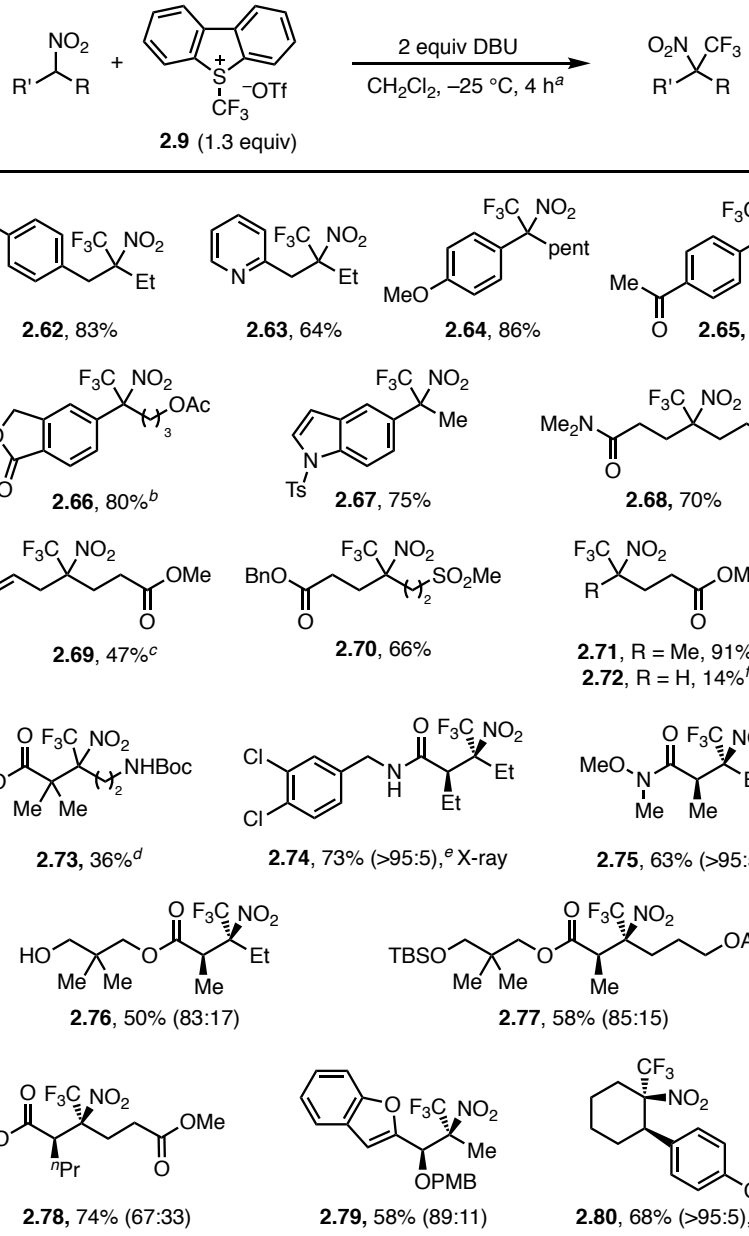

[a] Isolated yields unless otherwise noted. Diastereomeric ratios (dr) determined by ^{1}H NMR analysis of crude reaction. [b] 1.5 equiv of XX used. [c] 18 h. [d] 48 h. [e] 24 h. [f] Yield determined by ^{1}H NMR using 1,3,5-trimethoxybenzene as an internal standard.

Figure 2.24: Scope of the Trifluoromethylation of Secondary Nitroalkanes

Significantly, nitroalkanes bearing a tertiary stereocenter α to the nitro group proved to be excellent substrates.[4] In these cases, good to excellent levels of diastereoselection were observed. For example, amide (**2.74)** was formed with greater than >95:5 selectivity favoring the diastereomer shown (Figure 2.24). Similar selectivity was observed for the Weinreb amides (**2.75)**. Related ester products could also be prepared (**2.76-2.78**), albeit with slightly lower levels of diastereoselection. These results mirror the selectivity previously observed in Michael additions of β-nitrocarbonyls.[34]

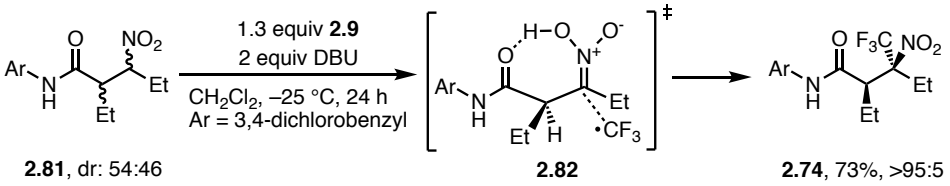

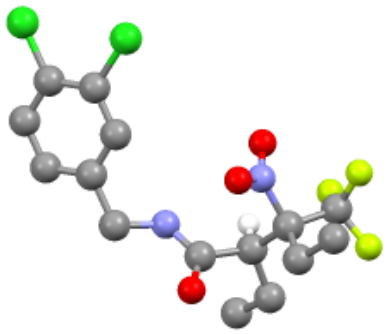

Figure 2.25: Proposed Model for Observed Diastereoselectivity and Crystal Structure of **2.74**

A rapid reversible deprotonation of the diastereomeric mixture of nitroalkane (**2.81)** establish a tautomer (**2.82)**. Intramolecular hydrogen bonding to the adjacent carbonyl organize compound. From this common intermediate, the CF_3 radical is expected to react away from alkyl group as shown (Figure 2.25). This model is consistent with the observed relative stereochemistry of the products. This model is also consistent with high diastereoselectivity observed for substrates bearing more basic carbonyl groups such as amides (**2.74**) and (**2.75**). On the other hand, esters (**2.76-2.78**), which bear a less basic carbonyl group than amides, produce slightly lower level of diastereoselection.

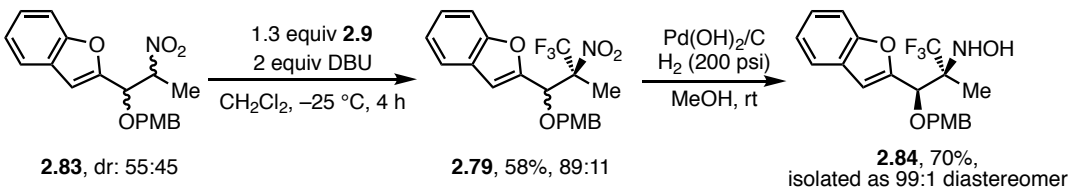

2.83, dr: 55:45

2.79, 58%, 89:11

2.84, 70%,
isolated as 99:1 diastereomer

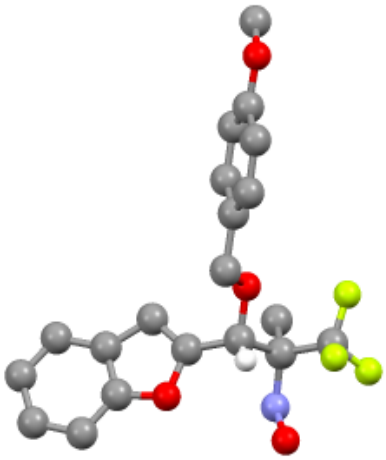

Figure 2.26: Determination of Relative Stereochemistry of Trifluoromethylated Henry Reaction Substrate and Crystal Structure **2.84**

Henry reaction products (**2.79**),[1a] as well as those from conjugate addition of nitroalkanes (**2.80**),[35] could both be trifluoromethylated with good to excellent levels of diastereoselectivity. In the latter case, stereoselectivity is consistent with addition of the CF_3 group away from the large aromatic ring (Figure 2.24 and 2.27).

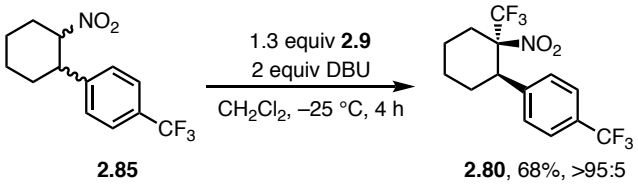

2.85 **2.80**, 68%, >95:5

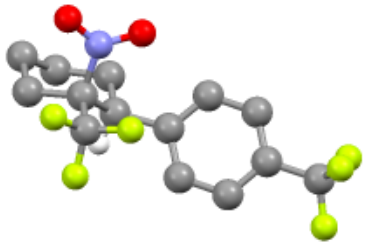

Figure 2.27: Crystal Structure of **2.80**

The functional group tolerance of the reaction is very high. In addition to those already mentioned, tolerated functional groups include aryl halides (**2.62** and **2.74**), heterocycles (**2.63**, **2.66**, **2.67**, and **2.79**), alkenes (**2.69**), aryl ethers (**2.64**), nitriles (**2.68**), ketones (**2.65**), protected and free alcohols (**2.76** and **2.77**), sulfones (**2.70**), and protic nitrogen functional groups (**2.73** and **2.74**).

2.9 Synthesis of Vinyl Trifluoromethylalkenes

The method does show some limitations with respect to nitroalkanes bearing acidic and sterically accessible β-protons. In such cases, elimination of an equivalent of nitrous acid from the trifluoromethylated product can be observed. For example, under standard conditions using DBU as base, the reaction of (**2.86**) did not lead to the trifluoromethylated nitroalkane (**2.87**) (Figure 2.28 top). Instead, the trifluoromethyl alkene (**2.88**) was observed in moderate yield. In some cases, the use of the bulkier base, tetramethylguanidine (TMG), enabled access to the desired product without significant elimination, albeit with less than ideal conversion and yield. In other cases, such as with ester (**2.89**), elimination could not be avoided regardless of the base used (Figure 2.28 bottom).

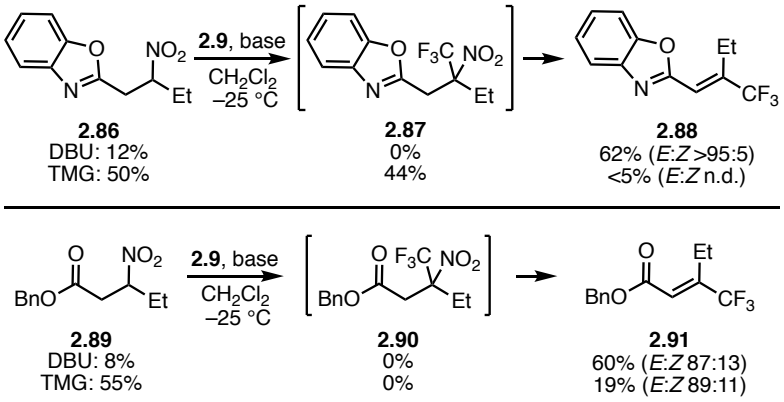

Figure 2.28: Competitive Alkene Formation and Role of Base

Interestingly, the trifluoromethylalkenes described in figure 2.28 all formed with significant selectivity for the E-isomer (as determined by $^{1}H–^{19}F$ Heteronuclear Overhauser Effect Spectroscopy, HOSEY NMR).[36] We attribute this selectivity to the

larger steric size of the CF_3 group compared to an n-alkyl group.[8a] Recognizing the possible utility of this process for preparing trifluoromethyl alkenes,[37] I investigated if this base promoted process can be triggered in less acidic products. Using substrate (**2.62**) as a model system, we found that exposure to KO^{t}Bu at 40 °C led to nearly quantitative yield of corresponding vinyl trifluoromethylalkene (**2.92**) with modest E:Z selectivity (Figure 2.29). This method potentially provides a mild, high yielding, two step synthesis of vinyl trifluoromethylalkenes from a variety of complex nitroalkanes.

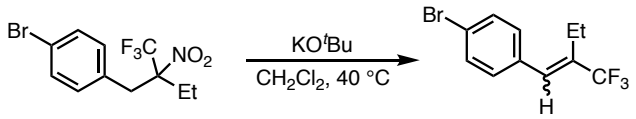

2.62 **2.92**, 93% (*E*:*Z* 72:28)

Figure 2.29: Synthesis of Vinyl Trifluoromethylalkene

2.10 Synthesis of α-(trifuoromethyl)amines

Trifluoromethylnitroalkanes are readily reduced to α-(trifluoromethyl)amines. As shown in Figure 2.30 (top and middle), both Zn/AcOH reduction and hydrogenolysis can be effective. However, we note that with α-aryl nitroalkanes, which are prone to denitration,[38] hydrogenolysis is the preferred method for reduction (Figure 2.30, bottom).

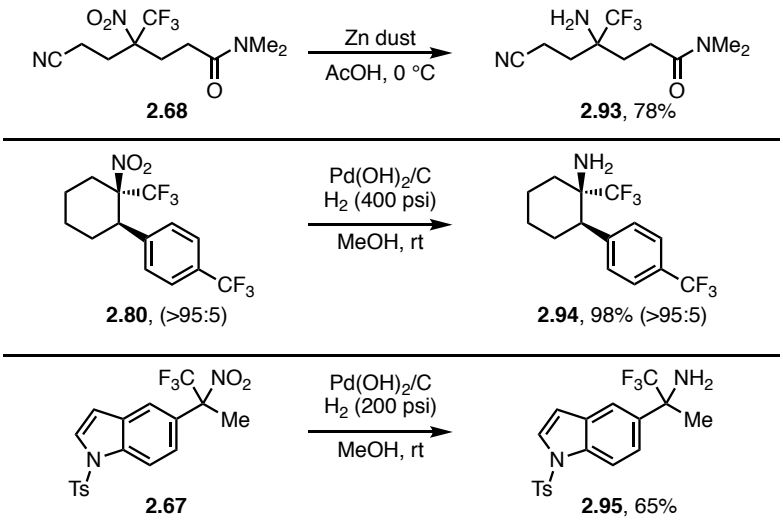

Figure 2.30: Preparation of α-(trifuoromethyl)amines

2.11 Mechanistic Studies

2.11.1 Radical Probing Experiment

I investigated the mechanism of trifluoromethylation of secondary nitroalkanes using Umemoto's reagent (**2.9**). Umemoto's reagent (**2.9**) is known to act as an either electrophilic or radical trifluoromethylating reagent.[26h] Additionally, nitronate anions have been shown to undergo a radical anion coupling mechanism.[39] Consistent with our earlier results,[3-4,6] preliminary mechanistic studies suggest that the reaction proceeds *via* a radical mechanism. As shown in (Table 2.8), when introducing a variety of known radical scavengers, the yield of α-(trifuoromethyl)nitroalkane (**2.62**) is greatly retarded (entries 2-4).[40]

Table 2.8: Effect of Radical Scavengers on the Formation of α-(trifuoromethyl)nitroalkane **2.62**

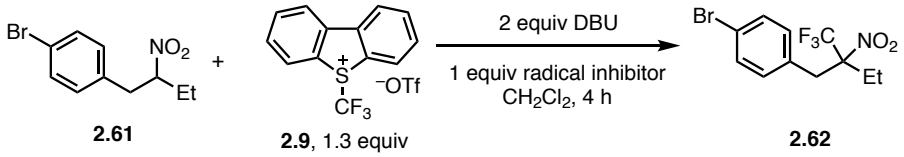

2.61 **2.9**, 1.3 equiv **2.62**

Entry	Radical Scavengers	Yield 2.62[a]
1	none	87%
2	1,2-dinitrobenzene	58%
3	TEMPO	0%
4	BHT	0%

[a] Yield determined by ^{1}H NMR using 1,3,5-trimethoxy benzene as an internal standard

2.11.2 Deprotonation Studies – ^{1}H NMR Spectroscopy

I performed several *in situ* ^{1}H NMR studies in CD_2Cl_2, which revealed many details of the reaction mechanism. First, combining DBU and nitroalkane (**2.61**) at low temperature reveals that a significant equilibrium concentration of nitronate anion (**2.96**) is produced (Table 2.9 and Figure 2.32). However, the deprotonation event is slow, taking about 10 minutes for a 2:1 mixture of DBU and (**2.61**) to reach equilibrium at –25 °C.

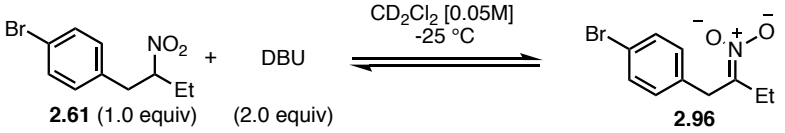

2.61 (1.0 equiv) (2.0 equiv) **2.96**

Figure 2.31: Deprotonation Event between **2.61** and DBU

The yields of starting material (**2.61**) and nitronate anion (**2.96**) were determined by integrating signals shown in the table below:

Table 2.9: Chemical Shift of **2.61** and **2.96** in ^{1}H NMR

Compound	^{1}H NMR signal
2.61	δ 7.42 (d, *J* = 8.1 Hz, 2H)
2.96	δ 7.33 (d, *J* = 8.1 Hz, 2H)

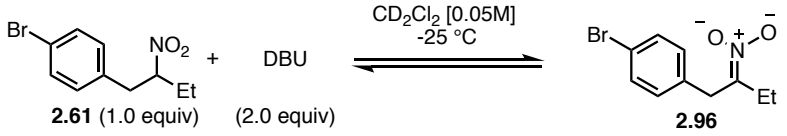

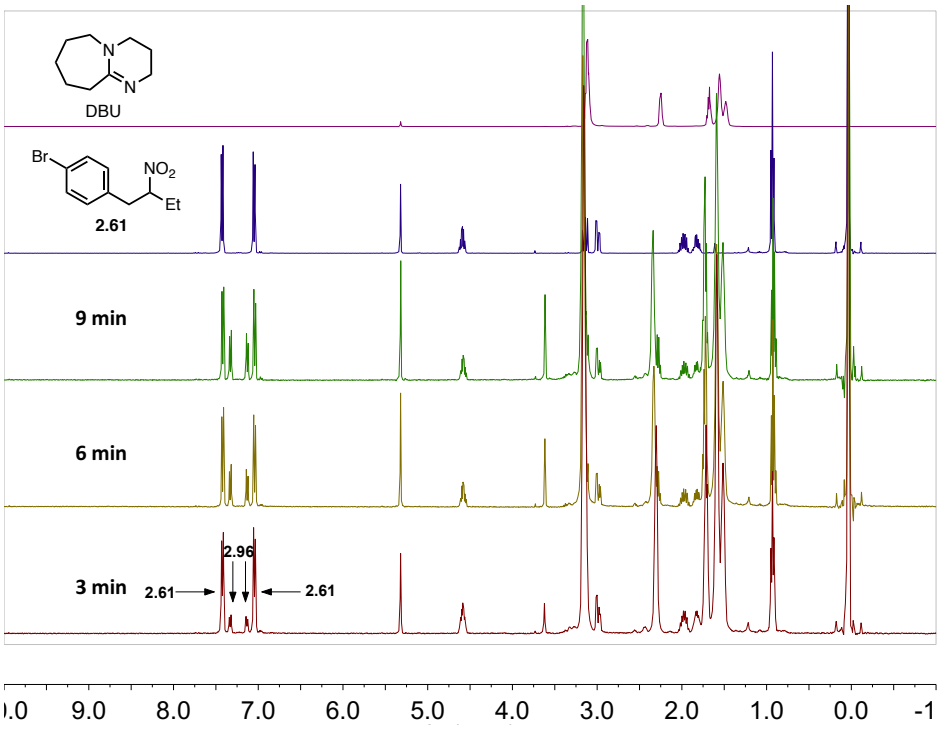

Figure 2.32: ^{1}H NMR Monitoring of Deprotonation of **2.61** [0.05] M CD_2Cl_2, –25 °C, Compared to Spectra of Reagents and Products Under the same conditions

Table 2.10: Yield of **2.61** and **2.96** over Time using DBU

Time(min)	Yield **2.61**[a]	Nitronate anion **2.96**[a]
0	100	0
3	86	16
6	74	30
9	68	35
12	65	37
15	66	37
18	65	37
21	64	37
24	65	37
27	67	36
30	69	36

[a]Yield determined by 1H NMR using hexamethyldisiloxane as an internal standard

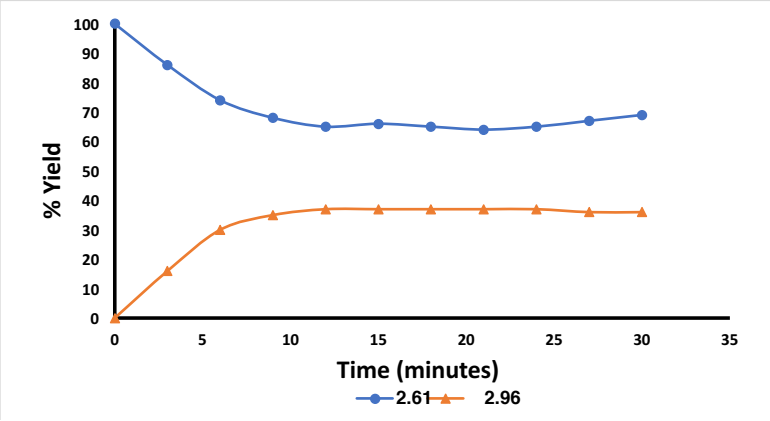

Figure 2.33: Ratio of Compound **2.61** and Nitronate Anion **2.96** over Time

2.11.3 Interaction of DBU with Umemoto's Reagent – ^{1}H NMR study.

In 2015, Yu and coworkers reported a mild condition for the direct C–H trifluoromethylation of heteroarenes using Umemoto's reagent *via* an electron-donor-acceptor (EDA) complex (Figure 2.34).[41] They showed that Umemoto's reagent (**2.9**)

forms electron-donor-acceptor (EDA) complexes with basic tertiary amines such as *N*-methylmorpholine (Figure 2.35).[41-42] Using ^{1}H NMR study, it was shown that combining Umemoto's reagent (**2.9**) and excess *N*-methylmorpholine produced a new set of signals which was attributed to the electron-donor-acceptor (EDA) complex (**2.97**). Although no structural spectroscopic evidence of complex (**2.97**) was reported, theoretical studies show that the formation of the EDA complex is thermodynamically favored. In addition, Electron Paramagnetic Resonance (EPR) studies suggest the intermediacy of trifluoromethyl radical generated in situ.

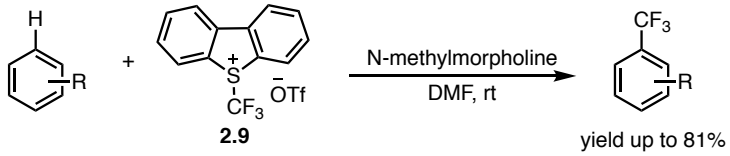

Figure 2.34: Yu's Radical Trifluoromethylation of Heteroarenes with Umemoto's Reagent

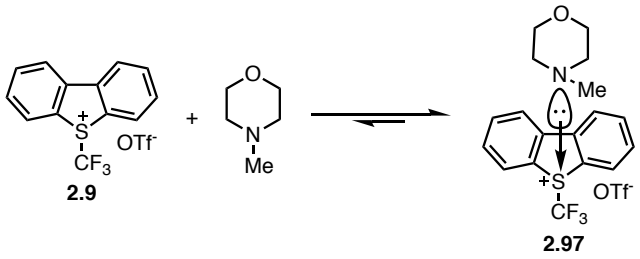

Figure 2.35: Yu's Proposed EDA complex **2.97**

Based on these results, the proposed mechanism involves the slow decomposition of complex **2.97** to the CF_3 radical and dibenzothiophene. The generated CF_3 radical adds to arene to give radical intermediate **2.98**, which can be

oxidized by either radical cation of *N*-methylmorpholine (path A) or by Umemoto's reagent **2.9** (path B) to give benzylic cation **2.99**, which upon deprotonation gives the desired product **2.100**.

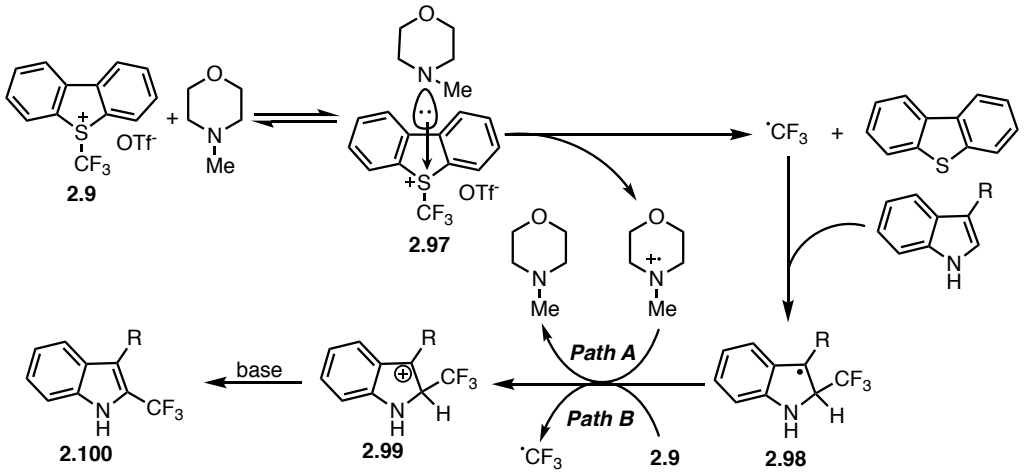

Figure 2.36: Proposed Mechanism of Yu's Trifluoromethylation of Heteroarenes via (EDA) Complex **2.97**

To understand possible interactions between DBU and Umemoto's reagent, I studied their reaction by ^{1}H NMR at –25 °C in CD_2Cl_2 in the absence of other reagents (Figure 2.37).

From the ^{1}H NMR spectra we observed the complete disappearance of Umemoto's reagent and formation of new adduct, bearing related aromatic signals. Prior studies have shown that (**2.9**) forms electron-donor-acceptor (EDA) complex with basic amine (see above) and we have tentatively assigned this as the EDA complex **2.9**·**DBU**. Traces of dibenzothiophene and fluoroform were also observed. The conversion happens within seconds, and the resulting solution is stable at –25 °C

for extended time (as judged by ^{1}H NMR). ^{1}H NMR signals are tabulated below (Table 2.11) (Figure 2.38).

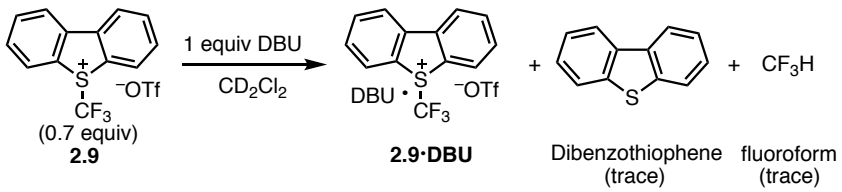

Figure 2.37: Interaction Between Umemoto's Reagent **2.9** and DBU

Table 2.11: Chemical Shift of **2.9**, **2.9·DBU**, dibenzothiophene and fluoroform in ^{1}H NMR

Compound	^{1}H NMR signal
dibenzothiophene	δ 8.19 (dd, *J* = 6.0, 3.2 Hz, 2H), 7.88 (dt, *J* = 7.1, 3.6 Hz, 2H), 7.53 – 7.42 (m, 4H)
CF_3H	δ 6.61 (q, *J* = 79, 1H)
Umemoto's reagent 2	δ 8.40 (d, *J* = 8.1 Hz, 2H), 8.23 (td, *J* = 7.8, 1.2 Hz, 2H), 8.03 (td, *J* = 7.7, 1.1 Hz, 2H) 7.82 (td, *J* = 7.9, 1.3 Hz, 2H)
2.9·DBU	δ 8.28 (d, *J* = 8.1 Hz, 2H) 8.23 (d, *J* = 7.8 Hz, 2H) 7.99 (t, *J* = 7.7 Hz, 2H) 7.79 (t, *J* = 7.8 Hz, 2H)

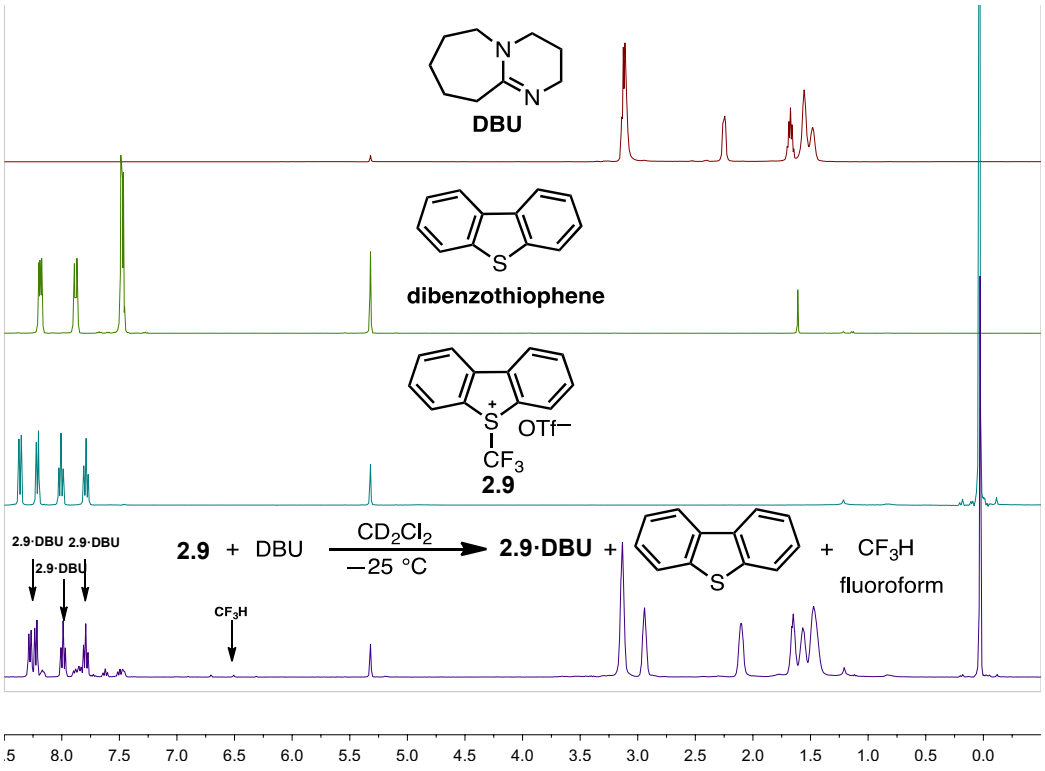

Figure 2.38: ^{1}H NMR Study of Interaction Between Umemoto's reagent **2.9** and DBU, [0.05 M] CD_2Cl_2, –25 °C, Compared to Spectra of Reagents and Products Under the Same Conditions.

From this data, I find that: (1) a DBU adduct of Umemoto's reagent can form; (2) the reaction kinetics are fast; (3) I was able to identify its ^{1}H NMR signals for use in the studies below.

2.11.4 ^{1}H NMR Monitoring of Trifluoromethylation of Secondary Nitroalkane:

I monitored trifluoromethylation of nitroalkane reaction using ^{1}H NMR at –25 °C in CD_2Cl_2 (Figure 2.39). Under the optimized reaction conditions [0.1 M], a very rapid reaction was observed that was too fast to adequately monitor by NMR. Spectra

traces from this reaction are shown below. Furthermore, the optimized reaction conditions are slightly heterogeneous for the first few minutes of the transformation, due to the saturation of Umemoto's reagent in methylene chloride at the reaction temperature. I was concerned that such heterogeneous behavior might obscure the reaction profile due to mass transport issues. To address both problems, I diluted the reaction (2-fold, to 0.05 M) for NMR studies. Under these conditions, the reaction slowed enough to allow better observation by transient NMR experiments, and was fully homogenous at the start of the reaction.

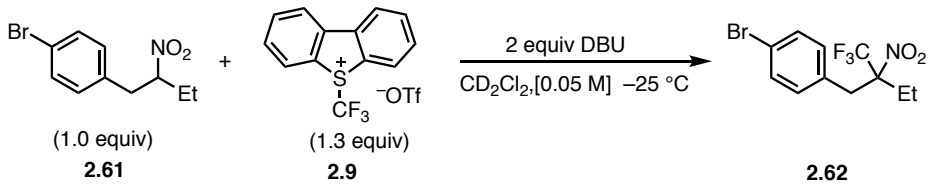

(1.0 equiv) **2.61** (1.3 equiv) **2.9** **2.62**

Figure 2.39: Trifluoromethylation of **2.61** at –25 °C in CD_2Cl_2 [0.05 M]

Data were collected periodically for the first 30 minutes then, collected for every 30 minutes.

Yields of starting material **2.61**, product **2.62**, **2.9·DBU** and **2.101** was determined by integrating signals shown in the table below:

Table 2.12: Chemical Shift of **2.61**, **2.62**, **2.9·DBU** and **2.101** in ^{1}H NMR

Compound	^{1}H NMR signal
2.61	δ 0.93 (t, *J* = 7.4 Hz, 3H)
2.62	δ 1.01 (t, *J* = 7.4 Hz, 3H)
2.101	δ 7.27 (d, *J* = 7.9 Hz, 2H)
2.9·DBU	δ 7.73 (t, *J* = 7.8 Hz, 2H)

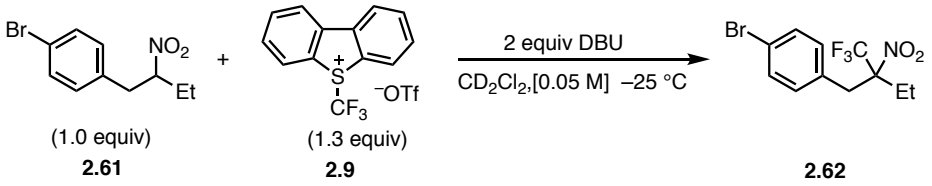

(1.0 equiv)
2.61

(1.3 equiv)
2.9

2.62

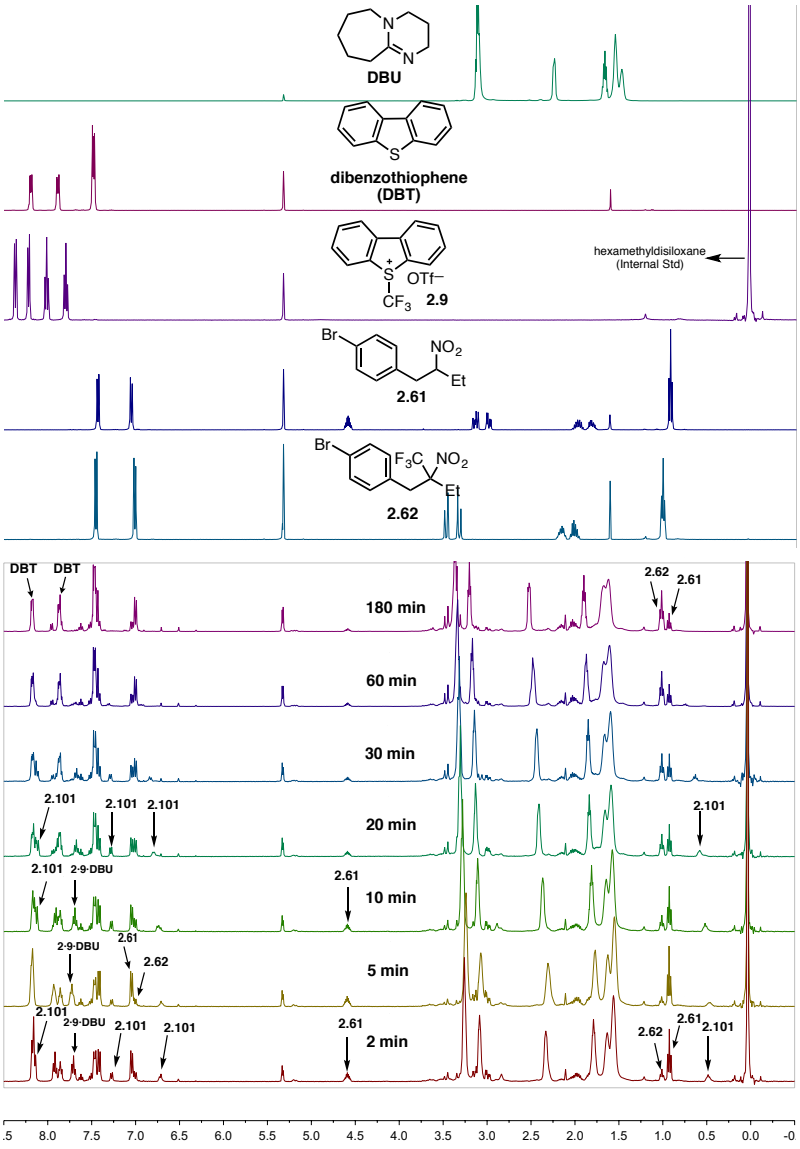

Figure 2.40: ^{1}H NMR Monitoring of Trifluoromethylation of **2.61** [0.05 M] CD_2Cl_2, –25 °C, Compared to Spectra of Reagents and Products Under the Same Conditions.

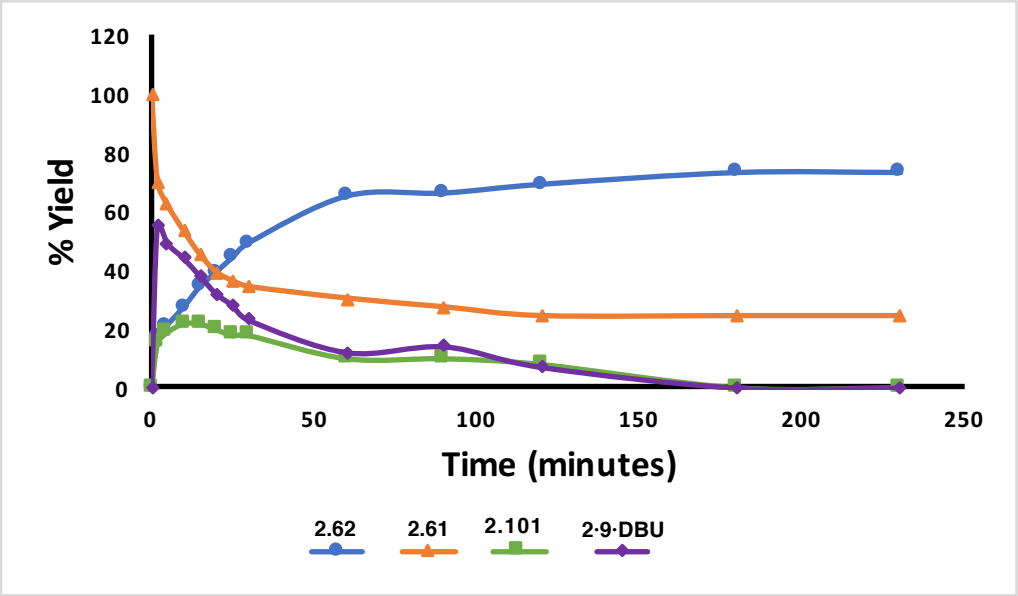

Figure 2.41: Kinetic Profile of Trifluoromethylation of **2.61** [0.05 M] CD_2Cl_2 and Change of **2.61, 2.62, 2.101** and **2.9·DBU** over Time.

From the ^{1}H NMR time study, I observed fast rate of formation of product (**2.62**) that slows considerably as the reaction progresses and the disappearance of starting material (**2.61**) (Figure 2.40). Under these conditions, two reactive intermediates are observed. First, a high concentration buildup of the peak at δ 7.73ppm (ca. 2 min) is observed that matches matches **2.9·DBU** at the beginning of the reaction, then gradually disappears at the end (Figure 2.41).

Second, another intermediate with ^{1}H NMR signals at δ 8.13, 7.27, 6.80, 0.6 ppm is observed. The concentration of these peaks increase and decrease together. These complex bears ^{1}H NMR signals that are relate to both the nitroalkane (**2.61**) and Umemoto's reagent (**2.9**), but are not identical to either. Based upon this spectra data,

we believe that this intermediate is the associated ion pair (**2.101**), where the nitronate anion has replaced triflate in Umemoto's reagent.

Based on our NMR study of DBU interaction with Umemoto's reagent we propose that the peak at δ 7.7ppm is adduct (**2.9·DBU**) which is formed between Umemoto's reagent and DBU and the peak at δ 8.13, 7.27, 6.80, 0.6 ppm is an ion pair (**2.101**), which is formed reversibly between (**2.9·DBU**) and nitronate anion (**2.96**).

2.11.5 ^{1}H NMR monitoring of Trifluoromethylation of Secondary Nitroalkane (optimal reaction condition):

The reaction at standard conditions showed similar overall features. Spectra traces from this reaction are shown below (Figure 2.42 and 2.43).

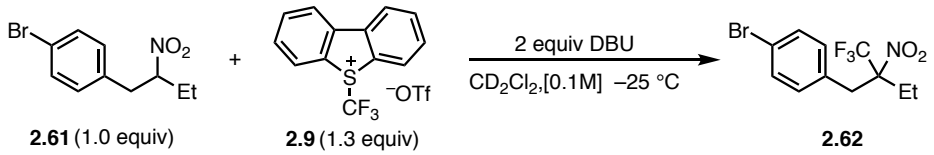

Figure 2.42: Trifluoromethylation of **2.61** at –25 °C in CD_2Cl_2 [0.1 M]

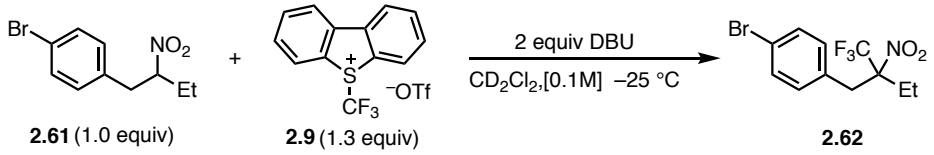

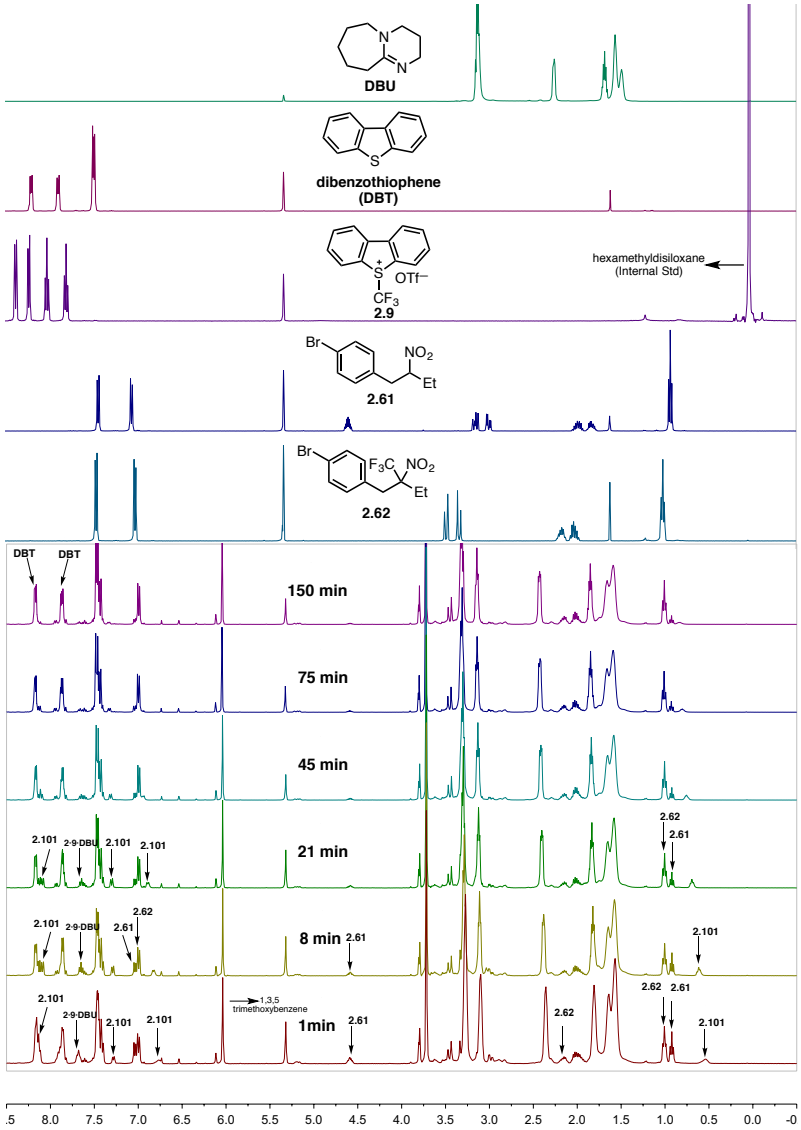

Figure 2.43: ^{1}H NMR Monitoring of Trifluoromethylation of **2.61** [0.1 M] CD_2Cl_2, –25 °C, Compared to Spectra of Reagents and Products under The Same Conditions.

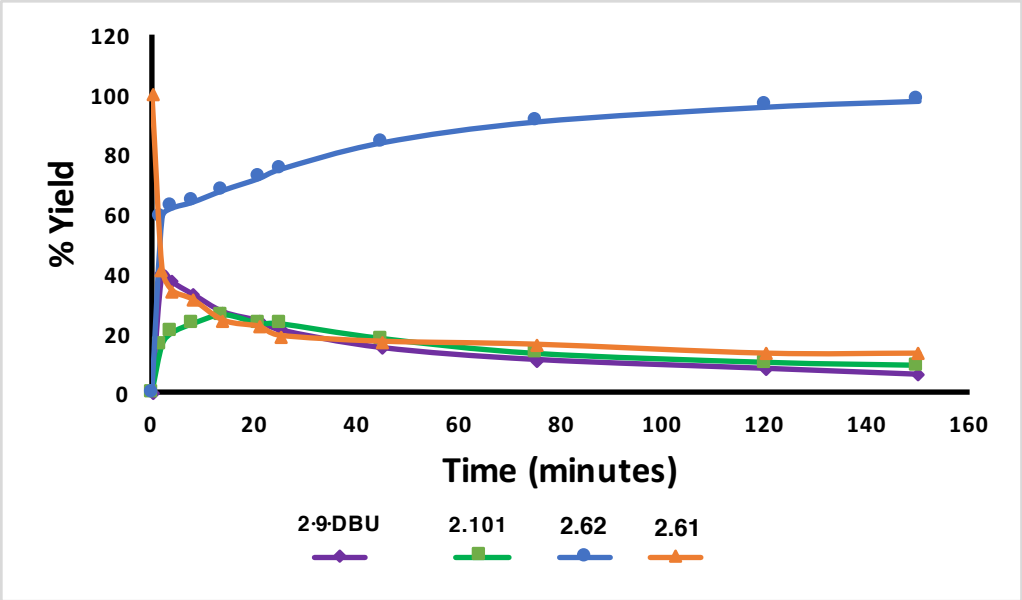

Figure 2.44: Kinetic Profile of Trifluoromethylation of **2.61** [0.1 M] CD_2Cl_2 and Change of **2.61, 2.62, 2.101** and **2.9·DBU** over Time

2.11.6 Proposed Mechanism

Based upon the observations of several ^1H NMR experiments (section **2.11.1-2.11.5**), we propose the following reaction mechanism (Figure 2.45). Early in the reaction, DBU and (**2.9**) form the EDA complex (**2.9·DBU**). As the nitronate anion (**2.96**) is formed, (**2.9·DBU**) is consumed and the ion pair (**2.101**) is formed. The salt complex (**2.101**) then undergoes slow decomposition to a nitronate radical (**2.102**), CF_3-radical, and dibenzothiophene *via* electron transfer. Rapid recombination of the two radicals results in the formation of the observed product (**2.62**). We cannot rule out the possibility of alternative radical-chain mechanism.

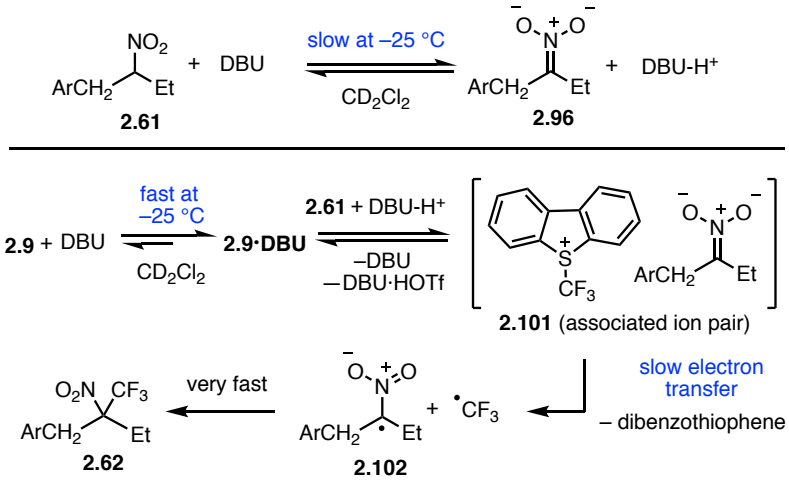

Figure 2.45: Proposed Mechanism for Nitroalkane Trifluoromethylation

2.12 Conclusion

In conclusion, we have developed mild reaction conditions for the trifluoromethylation of secondary nitroalkanes using a commercially available trifluoromethylating reagent. This procedurally simple protocol allows rapid access to highly complex quaternary α-trifluoromethylnitroalkanes in good yields and diastereoselectivity. The wide functional group tolerance highlights the power of this transformation as a method for late-stage installation of a trifluoromethyl group. In addition, we have demonstrated that these products can be reduced to medicinally interesting α-trifluoromethylamines. We have also shown that, in at least some cases, base-induced elimination of HNO_2 allows the products to be converted to highly substituted trifluoromethylalkenes with good levels of stereocontrol. Finally, I have conducted ^{1}H NMR mechanistic studies, which confirms the presence of two reactive intermediates proposed to be derived from Umemoto's reagent. Accordingly, these studies led to our proposed mechanism for the nitroalkane trifluoromethylation. This work was communicated in *Organic Letters* in 2017.

2.13 Experimental Section

2.13.1 General Experimental Details

Benzene, diethyl ether, dichloromethane, and dioxane were dried on alumina according to a published procedure.[43] Copper bromide, sodium methoxide and sodium trimethylsilanolate were purchased commercially; the bulk was stored in a N_2 filled glovebox; samples were removed from the glovebox and stored in a desiccator under air for up to two weeks prior to use. All hot glassware was oven dried for a minimum of two hours or flame-dried under vacuum prior to use. 4-nitrobutyl acetate,[44] methyl-4-nitrobutyrate,[45] N,N-dimethyl-4-nitrobutanamide,[46] (E)-N-((Z)-4-(2,6-dimethylphenylamino)pent-3-en-2-ylidene)-2,6-dimethylaniline,[47] 3-(tert-butyldimethylsilyloxy)-2,2-dimethylpropyl 2-bromopropanoate,[4] 3-(tert-butyldimethylsilyloxy)-2,2-dimethylpropyl 2-methyl-3-nitropentanoate,[4] 5-bromo-1-(p-toluenesulfonyl)-1H-indole,[48] benzyl-4-nitrobutanote,[49] 1-bromo-4-(2-nitrobutyl)benzene,[3] N-(3,4-dichlorobenzyl)-2-ethyl-3-nitropentanamide,[4] rac-2-(4-trifluoromethylphenyl)-1-nitrocyclohexane,[35] 4-acetyl-(1-nitropropyl)benzene,[33a] methyl 4-nitropentanoate,[50] 1-ethyl 6-methyl 3-nitro-2-propylhexanedioate,[4] ethyl-5-(tert-butoxycarbonylamino)-2,2-dimethyl-3-nitropentanoate,[4] N-methoxy-N,2-dimethyl-3-nitropentanamide,[4] 2-(2-nitrobutyl)pyridine,[3] and 2-(2-nitrobutyl)benzo[d]oxazole (**2.86**)[3] were synthesized according to published procedures. All other substrates and reagents were purchased in highest analytical purity from commercial suppliers and used as received. All NMR yields and diastereoselectivity are reported using 1,3,5-trimethoxybenzene as an internal standard. All reactions were set up using standard Schlenk technique. Reactions were heated with stirring in temperature controlled oil baths and cooled with stirring using

Cryo cooling units. “Double manifold” refers to a standard Schlenk-line gas manifold equipped with N2 and vacuum (ca. 0.1 mm Hg).

2.13.2 Instrumentation and Chromatography:

400 MHz ^{1}H, 101 MHz ^{13}C, and 376 MHz ^{19}F spectra were obtained on a 400 MHz FT-NMR spectrometer equipped with a Bruker CryoPlatform. 600 MHz ^{1}H and 151 MHz ^{13}C spectra were obtained on a 600 MHz FTNMR spectrometer equipped with a Bruker SMART probe. ^{13}C spectra were recorded using Attached Proton Test phase pulse sequence; carbons with an odd number of protons are phased down and those with an even number of protons are phased up.[51] All samples were analyzed in the indicated deutero-solvent and were recorded at ambient temperatures. Chemical shifts are reported in ppm. ^{1}H NMR spectra were calibrated using the residual protio-signal in deutero-solvents as a standard. ^{13}C NMR spectra were calibrated using the deutero-solvent as a standard. IR spectra were recorded on a Nicolet Magma-IR 560 FT-IR spectrometer as thin films on NaCl plates or using KBr pellets. Unless otherwise noted, column chromatography was performed with 40-63 μm silica gel with the eluent reported in parentheses. Where noted 5-20 μm silica gel was used to improve separation. Analytical thin-layer chromatography (TLC) was performed on precoated glass plates and visualized by UV or by staining with KMnO4. GCMS data was collected using an Agilent 6850 series GC and 5973 MS detectors. Low resolution ESI data was collected on a Thermo LCQ Advantage running in positive ion mode. High resolution MS data was obtained on a Waters GCT Premier spectrometer using chemical ionization (CI) or liquid injection field desorption ionization (LIFDI) or on a Thermo Scientific, Q Exactive model orbitrap using electrospray ionization (ESI).

2.13.3 Synthesis of Novel Nitroalkane Starting Materials:

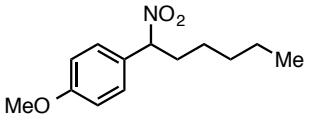

(**2.S1**) was synthesized by modification of a previously published procedure.[33a] A hot 200 mL Schlenk equipped with a magnetic stir bar and a rubber septum was attached to a double manifold and allowed to cool. Once cool, the flask was backfilled with N_2, the septum was removed and tris(dibenzylideneacetone)dipalladium(0) (129 mg, 141 μmol), BrettPhos (177 mg, 330 μmol), cesium carbonate (3.68 g, 11.3 mmol), and 4-bromoanisole (1.76 g, 9.42 mmol) were added. The septum was replaced, the flask was reattached to the double manifold and evacuated and backfilled with N_2 three times. Anhydrous dioxane (47 mL) and 1-nitrohexane (2.62 mL, 18.8 mmol) were added via syringe. The resulting heterogeneous solution was heated in an oil bath at 50 °C for 40 h. Once complete, the reaction was cooled to rt. Saturated NH_4Cl (10 mL) was added and the reaction was stirred for 10 minutes. Another 10 mL saturated NH_4Cl (10 mL) was added and the reaction was stirred for another 10 minutes. The reaction was then diluted with diethyl ether (25 mL), washed twice with brine (25 mL), dried over magnesium sulfate and concentrated *in vacuo*. The crude reaction was purified using flash silica gel chromatography (65:35 hexanes : ethyl acetate) to afford (**2.S1**) (1.83 g, 82%) as a yellow oil: ^{1}H NMR (400 MHz, $CDCl_3$) δ 7.40 (d, J = 8.7 Hz, 2H), 6.94 - 6.87 (m, 2H), 5.40 (dd, J = 8.6, 6.7 Hz, 1H), 3.81 (s, 3H), 2.51 - 2.38 (m, 1H), 2.05 (dt, J = 12.3, 6.5 Hz, 1H), 1.36 - 1.23 (m, 6H), 0.87 (t, J = 7.2 Hz, 3H); ^{13}C NMR (101 MHz, $CDCl_3$) δ 160.7, 129.2, 126.9, 114.3, 91.2, 55.4, 33.8, 31.2, 25.8, 22.4, 14.0; FTIR (cm^{-1}): 2957, 2860, 1550, 1253, 1179. HRMS (LIFDI) m/z calculated for $[C_{13}H_{19}NO_3]^+$: 237.1365; found: 237.1339.

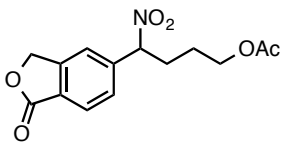

(**2.S2**) was synthesized by modification of a previously published procedure.[33a] A hot 100 mL Schlenk equipped with a magnetic stir bar and a rubber septum was attached to a double manifold and allowed to cool. Once cool, the flask was backfilled with N_2, the septum was removed and tris(dibenzylideneacetone)dipalladium(0) (110 mg, 120 μmol), BrettPhos (147 mg, 280 μmol), cesium carbonate (3.13 g, 9.60 mmol), and 5-bromophthalide (1.70 g, 8.0 mmol). The septum was replaced, the flask was reattached to the double manifold and evacuated and backfilled with N_2 three times. Anhydrous dioxane (30 mL) and nitroethane (855 μL, 12.0 mmol) were added via syringe. The resulting heterogeneous solution was heated in an oil bath at 50 °C for 24 h. Once complete, the reaction was cooled to rt. Saturated NH_4Cl (10 mL) was added and the reaction was stirred for 10 minutes. Another 10 mL saturated NH_4Cl (10 mL) was added and the reaction was stirred for another 10 minutes. The reaction was then diluted with diethyl ether (25 mL), washed twice with brine (25 mL), dried over magnesium sulfate and concentrated *in vacuo*. The crude reaction was purified using flash silica gel chromatography (80:20 hexanes : ethyl acetate) to afford (**2.S2**) (757 mg, 32%) as a thick orange oil: ^{1}H NMR (600 MHz, $CDCl_3$) δ 7.99 (d, J = 8.6 Hz, 1H), 7.64 (d, J = 7.3 Hz, 2H), 5.62 (dd, J = 9.1, 6.1 Hz, 1H), 5.36 (s, 2H), 4.19 - 4.08 (m, 2H), 2.68 - 2.58 (m, 1H), 2.23 - 2.13 (m, 1H), 2.06 (s, 3H), 1.78 - 1.63 (m, 2H); ^{13}C NMR (101 MHz, $CDCl_3$) δ 171.1, 170.1, 147.5, 140.2, 129.0, 127.4, 126.7, 121.7, 90.4, 69.6, 63.0, 31.0, 25.4, 21.0; FTIR (cm^{-1}): 2961, 1780, 1767, 1553, 1245, 1050; HRMS (LIFDI) m/z calculated for $[C_{14}H_{16}NO_6]^+$: 294.0978; found: 294.0983.

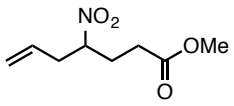

(**2.S3**) was synthesized by modification of a previously published procedure.[52] A hot 100 mL Schlenk equipped with a magnetic stir bar and a rubber septum was attached to a double manifold and allowed to cool. Once cool, the flask was backfilled with N_2, the septum was removed and bis(triphenylphosphine)palladium (II) chloride (386 mg, 550 μmol) and sodium methoxide (1.19 g, 22.0 mmol) were added. The septum was replaced, the flask was reattached to the double manifold and evacuated and backfilled with N_2 three times. Anhydrous methanol (22 mL) and methyl 4-nitrobutanoate (2.56 mL, 20.0 mmol) were added via syringe. The resulting yellow suspension was heated in an oil bath at 65 °C for 5 min, during which time the suspension turned brown. The reaction was cooled to rt and transferred to pre-cooled bath at 15 °C. allyl acetate (4.32 mL, 40 mmol) was added via syringe and the reaction was allowed to stir at 15 °C for 24 h. Once complete, the reaction was warmed to rt. The reaction was then diluted with diethyl ether (40 mL), washed thrice with brine (30 mL), dried over magnesium sulfate and concentrated in vacuo. The crude reaction was purified using flash silica gel chromatography (100:0 → 95:5 hexanes : ethyl acetate) to afford (**2.S3**) (552 mg, 15%) as a clear oil: ^{1}H NMR (400 MHz, $CDCl_3$) δ 5.78 - 5.63 (m, 1H), 5.20 - 5.16 (m, 1H), 5.15 (s, 1H), 4.67 - 4.57 (m, 1H), 3.69 (s, 3H), 2.77 - 2.64 (m, 1H), 2.60 - 2.48 (m, 1H), 2.49 - 2.29 (m, 2H), 2.30 - 2.18 (m, 2H); ^{13}C NMR (151 MHz, $CDCl_3$) δ 172.4, 131.2, 119.9, 87.0, 52.0, 38.0, 30.0, 28.1; FTIR (cm^{-1}): 2954, 2918, 2849, 1734, 1654, 1558, 993, 927 ; GC/MS (EI) 156.1 $(M\text{-}OCH3)^+$. HRMS (CI) m/z calculated for $[C_8H_{14}NO_4]^+$: 188.0923; found: 188.0917.

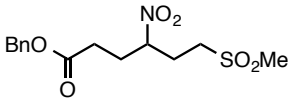

(**2.S4**) To a 50 mL round bottom equipped with a magnetic stir bar was added benzyl-γ-nitrobutanote (2.63 g, 12.7 mmol), dichloromethane (2.5 mL), water (21 mL), methyl vinyl sulfone (1.06 mL, 12.7 mmol) and sodium hydroxide (61.0 μg, 1.52 mmol). The biphasic reaction was vigorously stirred at room temperature for 4 days. Dichloromethane (20 mL) was added and the aqueous layer was extracted with dichloromethane (10 mL). The organic layers were combined, dried with magnesium sulfate and concentrated in vacuo. The crude reaction was purified using flash silica gel chromatography (70:30 benzene : ethyl acetate) to afford (**2.S4**) (513 mg, 12%) as a pale yellow solid: ^{1}H NMR (400 MHz, $CDCl_3$) δ 7.41 - 7.31 (m, 5H), 5.13 (s, 2H), 4.83 - 4.70 (m, 1H), 3.05 (t, J = 7.7 Hz, 2H), 2.94 (s, 3H), 2.56 - 2.42 (m, 3H), 2.42 - 2.24 (m, 2H), 2.23 - 2.12 (m, 1H); ^{13}C NMR (101 MHz, $CDCl_3$) δ 171.5, 135.5, 128.8, 128.6, 128.5, 85.5, 67.0, 50.7, 41.3, 30.0, 28.7, 26.0; FTIR (cm^{-1}): 2931, 1733, 1550, 1299, 1133; mp = 68-69 °C.ESI-MS: 352.3 $(M+Na)^+$ HRMS (ESI) m/z calculated for $[C_{14}H_{20}NO_6S]^+$: 330.10058; found: 330.09975.

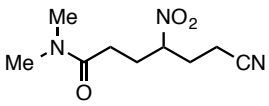

(**2.S5**) To a 200 mL round bottom flask equipped with a magnetic stir bar was added N,N-dimethyl-4-nitrobutanamide (5.23 mL, 40.0 mmol), acrylonitrile (2.62 mL, 40.0 mmol), dichloromethane (8 mL), sodium hydroxide (192 mg, 4.80 mmol), and water (67 mL). The flask was sealed with a polypropylene cap and stirred at room temperature for 42 h. The reaction was then diluted with dichloromethane (20 mL) and the organic layer was separated. The aqueous layer was extracted with dichloromethane (20 mL), dried over magnesium sulfate, and concentrated in vacuo. The crude reaction was purified using flash silica gel chromatography (18:80:2 hexanes : ethyl acetate : triethylamine)

to afford (**2.S5**) (1.65 g, 19%) as a white solid: ^{1}H NMR (400 MHz, $CDCl_3$) δ 4.74 (tt, J = 8.7, 4.4 Hz, 1H), 2.96 (d, J = 6.4 Hz, 6H), 2.50 - 2.33 (m, 5H), 2.28 - 2.12 (m, 3H); ^{13}C NMR (101 MHz, $CDCl_3$) δ 170.3, 117.9, 86.4, 37.1, 35.7, 29.6, 28.9, 28.8, 14.4; FTIR (cm^{-1}): 2938, 2248, 1645, 1550, 1150; mp = 53-55 °C; GC/MS (EI) 167.1 $(M-NO_2)^+$. HRMS (CI) m/z calculated for $[C_9H_{16}N_3O_3]^+$: 214.1192; found: 214.1192.

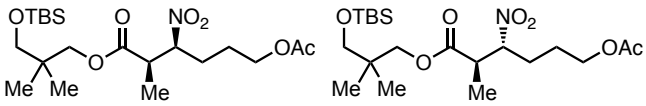

2.S6A **dr: 46 : 54** **2.S6B**

(**2.S6**) A hot 50 mL Schlenk equipped with a magnetic stir bar and a rubber septum was attached to a double manifold and cooled under vacuum.[4] Once cool, the septum was removed and CuBr (84.3 mg, 588 μmol), (E)-N-((Z)-4-(2,6-dimethylphenylamino)pent-3-en-2-ylidene)-2,6-dimethylaniline (180 mg, 588 μmol), and sodium trimethylsilanolate (429 mg, 3.82 mmol) were added. The septum was replaced, the flask was reattached to the double manifold and evacuated and backfilled with N2 three times. Anhydrous benzene (17 mL), 4-nitrobutyl acetate (663 mg, 4.12 mmol), and 3-(tert-butyldimethylsilyloxy)-2,2-dimethylpropyl 2-bromopropanoate (1.04 g, 2.91 mmol) were added via syringe. The reaction was heated to 60 °C with rapid stirring for 48 h. Once completed, the reaction was cooled to room temperature, the septum was removed and the reaction mixture was diluted with diethyl ether (50 mL). The crude reaction mixture was filtered through a plug of magnesium sulfate and concentrated in vacuo. NMR analysis revealed a 46:54 mixture of syn and anti-isomers. The crude reaction was purified by flash silica chromatography (90:10:1 hexanes: ethyl acetate: acetic acid) to afford a mixture of diastereomers of β-nitroester (**2.S6**) (760 mg, 60%) as a yellow oil: ^{1}H NMR (600 MHz, $CDCl_3$: mixture of diastereomers; useful diagnostic peaks for each compound are listed. See attached

spectra for details) δ **2.S6A**: 4.69 (ddd, J = 10.6, 9.2, 3.2 Hz, 1H), 2.99 (dq, J = 9.0, 7.0 Hz, 1H), 1.87 - 1.80 (m, 1H); **2.S6B**: 4.77 (td, J = 8.9, 3.6 Hz, 1H), 3.19 (p, J = 7.4 Hz, 1H); ^{13}C NMR (101 MHz, $CDCl_3$) δ **2.S6A**: 172.2, 89.8, 68.4, 63.2, 43.8, 29.0, 25.3, 21.6, 14.7; S6B: 172.5, 88.1, 68.5, 63.3, 42.5, 27.1, 24.8, 21.5, 13.5; FTIR (cm^{-1}): 2956, 1741, 1555, 1248, 1099, 776; GC/MS (EI) 376.3 $(M-C_4H_9)^+$; 329.1 $(M-C_4H_{10}NO_2)^+$. HRMS (CI) m/z, calculated for $[C_{20}H_{40}NO_7Si]^+$: 434.2574; found: 434.2575 and 434.2573.

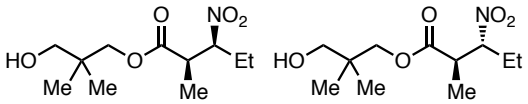

2.S7A **62 : 38** **2.S7B**

(**2.S7**) To a 500 mL round bottom flask with a stir bar was added 3-(tert-butyldimethylsilyloxy)-2,2-dimethylpropyl 2-methyl-3-nitropentanoate (800 mg, 2.22 mmol), THF (74 mL), and 3M HCl (55 mL). The flask was sealed with a polyethylene stopper and stirred vigorously at rt for 4.5 h. Once complete, the reaction was diluted with brine (20 mL) and extracted with ethyl acetate (3x, 35 mL). The organic layers were combined, washed with brine (1x, 20 mL), dried with magnesium sulfate, and concentrated in vacuo. NMR analysis revealed a 62:38 mixture of syn and anti-isomers. The crude reaction was purified by flash silica chromatography (60:40 hexanes: ethyl acetate) to afford alcohol (**2.S7**) (463 mg, 84%) as a clear oil: ^{1}H NMR (600 MHz, $CDCl_3$: mixture of diastereomers; useful diagnostic peaks for each compound are listed. See attached spectra for details) δ **2.S7A**: 3.05 - 2.96 (m, 1H), 0.93 (s, 6H); **2.S7B**: 3.20 (dq, J = 9.1, 7.3 Hz, 1H), 0.91 (apparent d, 6H); ^{13}C NMR (101 MHz, $CDCl_3$) δ **2.S7A**: 173.0, 91.5, 68.2, 43.5, 36.5, 25.5, 14.4, 10.6; **2.S7B**: 173.7, 89.8, 68.1, 42.0, 36.6, 24.0, 13.9, 9.5; FTIR (cm^{-1}): 3446, 2971, 1734, 1552, 1375; ESI-MS: 270.2 $(M+Na)^+$; HRMS (ESI) m/z, calculated for $[C_{11}H_{22}NO_5]^+$: 248.14925; found: 248.14849.

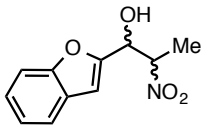

(**2.S8**) To a 100 mL round bottom flask equipped with a magnetic stir bar was added 2-benzofurancarboxaldehyde (4.15 mL, 34.2 mmol) and nitroethane (24.4 mL, 342 mmol). The reaction was cooled to 0 °C in an ice bath and tetramethylguanidine (216 μL, 1.71 mmol) was added dropwise via syringe. Once the addition was complete, the ice bath was removed and the flask was allowed to warm to rt where it was stirred for 12 h. The crude reaction was transferred to a seperatory funnel and diluted with brine (15 mL). The reaction was acidified with 5% HCl. The aqueous layer was extracted with ethyl acetate. The organic layer was dried with magnesium sulfate and concentrated in vacuo. NMR analysis revealed a 63:37 mixture of isomers. The crude reaction was purified via flash silica gel chromatography (93:7 hexanes : ethyl acetate) to afford α-nitroalcohol (**2.S8**) (6.60 g, 87%) as a yellow solid: ^{1}H NMR (400 MHz, $CDCl_3$: mixture of diastereomers; useful diagnostic peaks for each compound are listed. See attached spectra for details) δ **2.S8** (major): 6.81 (s, 1H), 5.22 (dd, J = 8.5, 6.2 Hz, 1H), 5.14 - 5.05 (m, 1H), 2.81 (d, J = 6.2 Hz, 1H), 1.49 (d, J = 6.8 Hz, 3H); **2.S8** (minor): 6.80 (s, 1H), 5.57 (t, J = 4.2 Hz, 1H), 5.01 (qd, J = 6.9, 3.6 Hz, 1H), 2.89 (d, J = 5.3 Hz, 1H), 1.62 (d, J = 6.9 Hz, 3H); ^{13}C NMR (101 MHz, CDCl3) δ **2.S8** (major): 155.1, 153.1, 127.5, 125.4, 123.5, 121.6, 111.7, 106.4, 86.1, 70.2, 16.5; **2.S8** (minor): 155.0, 153.8, 127.7, 124.9, 121.5,123.4, 111.5, 105.1, 84.7, 69.3, 12.9; FTIR (cm^{-1}): 3508, 3066, 2993, 1553, 1454, 753; mp = 68-70 °C; GC/MS (EI) retention time= 11.566, 174.0 $(M\text{-}HNO_2)^+$; retention time= 11.633, 173.9 $(M\text{-}HNO_2)^+$. HRMS (CI) m/z, calculated for $[C_{11}H_{12}NO_4]^+$: 222.0766; found: 222.0759 and 222.0755.

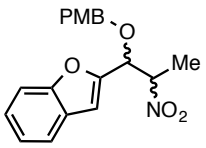

(**2.83**) A hot 100 mL round bottom flask equipped with a magnetic stir bar and a septum was attached to a double manifold and allowed to cool. Once cooled, the flask was backfilled with N_2, septum was removed and **2.S8** (2.00 g, 9.00 mmol) was added. The septum was replaced, the flask was reattached to the double manifold and evacuated and backfilled with N_2 three times. Anhydrous diethyl ether (45 mL) and 4-methoxybenzyl-2,2,2-trichloroacetimidate (3.33 g, 11.8 mmol) were added via syringe. The reaction was stirred for five minutes then trimethylsilyl trifluoromethanesulfonate (90.0 μL, 494 μmol) was added dropwise via syringe. Once addition was complete, the reaction was stirred at rt for 20 h. Once complete, the reaction was washed with $NaHCO_3$ (2x, 15 mL), 1M HCl (1x, 15 mL), and brine (1x, 15 mL). The reaction was dried with magnesium sulfate and concentrated in vacuo. NMR analysis revealed a 79:21 mixture of isomers. The crude reaction was purified via flash silica chromatography (95:5 hexanes : ethyl acetate) to afford (**2.83**) (358 mg, 12%) as a yellow solid: ^{1}H NMR (400 MHz, $CDCl_3$: mixture of diastereomers; useful diagnostic peaks for each compound are listed. See attached spectra for details) δ **2.83** Major: 4.53 (d, J = 11.4 Hz, 1H), 4.30 (d, J = 11.4 Hz, 1H), 3.79 (s, 3H), 1.36 (d, J = 6.8 Hz, 3H); **2.83** Minor: 4.63 (d, J = 11.3 Hz, 1H), 4.39 (d, J = 11.3 Hz, 1H), 3.81 (s, 3H), 1.65 (d, J = 6.8 Hz, 3H); ^{13}C NMR (101 MHz, $CDCl_3$) δ **2.83** Major: 159.6, 155.5, 151.2, 129.8, 128.6, 127.5, 125.4, 123.4, 121.5, 113.9, 111.8, 108.5, 85.3, 75.5, 71.0, 55.4, 16.4; **2.83** Minor: 159.7, 155.3, 152.5, 129.9, 128.8, 127.7, 125.0, 123.3, 121.5, 114.0, 111.7, 106.8, 84.4, 74.9, 71.8, 55.4, 13.7; FTIR (cm^{-1}): 2937, 2837, 1556, 1251, 1175; mp: 72-74 °C; GC/MS (EI) 235.0 $(M\text{-}C_7H_7O)^+$; 234.9 $(M\text{-}C_7H_7O)^+$. HRMS (LIFDI) m/z, calculated for $[C_{19}H_{19}NO_5]^+$: 341.1263; found: 341.1247.

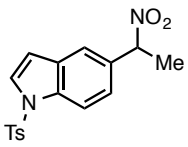

(**2.S10**) was synthesized by modification of a previously published procedure.[33a] A hot 100 mL Schlenk equipped with a magnetic stir bar and a rubber septum was attached to a double manifold and allowed to cool. Once cool, the flask was backfilled with N_2, the septum was removed and tris(dibenzylideneacetone)dipalladium(0) (82.0 mg, 90.0 μmol), BrettPhos (110 mg, 210 μmol), cesium carbonate (2.35 g, 7.20 mmol), and 5-bromo-1-(p-toluenesulfonyl)-1H-indole (2.09 g, 6.00 mmol). The septum was replaced, the flask was reattached to the double manifold and evacuated and backfilled with N_2 three times. Anhydrous dioxane (40 mL) and 4-nitrobutyl acetate (2.58 g, 16.0 mmol) were added via syringe. The resulting heterogeneous solution was heated in an oil bath at 50 °C for 24 h. Once complete, the reaction was cooled to rt. Saturated NH_4Cl (10 mL) was added and the reaction was stirred for 10 minutes. Another 10 mL saturated NH_4Cl (10 mL) was added and the reaction was stirred for another 10 minutes. The reaction was then diluted with diethyl ether (25 mL), washed twice with brine (25 mL), dried over magnesium sulfate and concentrated in vacuo. The crude reaction was purified using flash silica gel chromatography (65:35 hexanes : ethyl acetate) to afford (**2.S10**) (911 mg, 44%) as a thick yellow oil: ^{1}H NMR (400 MHz, $CDCl_3$) δ 7.99 (d, J = 8.6 Hz, 1H), 7.76 (d, J = 8.4 Hz, 2H), 7.63 (dd, J = 14.3, 2.6 Hz, 2H), 7.40 (dd, J = 8.7, 1.7 Hz, 1H), 7.24 (d, J = 8.1 Hz, 2H), 6.67 (d, J = 3.7 Hz, 1H), 5.68 (q, J = 6.9 Hz, 1H), 2.35 (s, 3H), 1.92 (d, J = 7.0 Hz, 3H); ^{13}C NMR (101 MHz, $CDCl_3$) δ 145.5, 135.4, 135.1, 131.1, 130.7, 130.2, 127.6, 127.0, 123.9, 120.8, 114.1, 109.0, 86.4, 21.8, 19.7; FTIR (cm^{-1}): 3144, 2989, 1550, 1373, 1175; HRMS (LIFDI) m/z calculated for $[C_{17}H_{16}N_2O_4S]^+$: 344.0831; found: 344.0845.

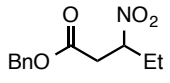

(**2.89**) A hot 150 mL high-pressure reaction vessel equipped with a magnetic stir bar and a Teflon cap and a Kontes cap was attached to a double manifold and cooled under vacuum. Once cool, the flask was backfilled with N_2, the Teflon cap was removed, and CuBr (940 mg, 6.55 mmol), (E)-N-((Z)-4-(2,6-dimethylphenylamino)pent-3-en-2-ylidene)-2,6-dimethylaniline (2.00 g, 6.55 mmol), and sodium trimethylsilanolate (2.06 g, 18.3 mmol) were added. The Teflon cap was replaced, the flask was attached to a double manifold, and evacuated and backfilled with N_2 five times. The Kontes cap was removed and replaced with a rubber septum, and anhydrous dichloromethane (77 mL), 1-nitropropane (1.52 mL, 17.0 mmol) and benzyl bromoacetate (2.10 mL, 13.1 mmol) were added via syringe. The Kontes cap was replaced and the resulting heterogeneous solution was submerged in an oil bath. The reaction was heated at 60 °C with rapid stirring for 21 h. Once completed, the reaction was cooled to room temperature, the septum was removed and the reaction mixture was diluted with diethyl ether (50 mL). The crude reaction mixture was filtered through a plug of Celite and concentrated in vacuo. The crude reaction was purified by silica gel flash chromatography (82:15:3 hexanes : benzene : ethyl acetate) to afford β-nitroester (**2.89**) (1.23 g, 40%) as a yellow oil: ^{1}H NMR (600 MHz, $CDCl_3$) δ 7.40 - 7.32 (m, 5H), 5.15 (s, 2H), 4.86 (dddd, J = 9.8, 7.5, 5.7, 4.5 Hz, 1H), 3.20 (dd, J = 17.3, 9.4 Hz, 1H), 2.73 (dd, J = 17.4, 4.3 Hz, 1H), 2.04 - 1.89 (m, 2H), 0.99 (t, J = 7.4 Hz, 3H); ^{13}C NMR (101 MHz, $CDCl_3$) δ 169.3, 135.3, 128.8, 128.7, 128.5, 84.4, 67.3, 36.8, 27.2, 10.0; FTIR (cm^{-1}):3066, 2975, 2883, 1738, 1552; GC/MS (EI) 107.0 $(M\text{-}C_5H_8NO_3)^+$. HRMS (CI) m/z calculated for $[C_{12}H_{16}NO_4]^+$: 238.1079; found: 238.1072.

2.13.4 General Protocol for the Synthesis of α-Trifluoromethylnitroalkanes:

General Protocol A: Synthesis of α-Trifluoromethylnitroalkanes: A hot 25 mL round bottom flask equipped with a magnetic stir bar and a rubber spectrum was attached via needle to a double manifold and cooled under vacuum. Once cooled, the flask was backfilled with N_2, the septum was removed, and nitroalkane (1 equiv) and 5-(trifluoromethyl)dibenzothiophenium trifluoromethanesulfonate (Umemoto's reagent **2.9**, 1.3 equiv) were added. The septum was replaced, the flask was reattached to a double manifold and evacuated and backfilled with N_2 three times. Anhydrous dichloromethane was added via syringe and the flask was lowered into a precooled –25 °C cooling bath and stirred. 1,8-Diazabicycloundec-7-ene (DBU, 2 equiv) was then added dropwise via syringe. The resulting homogenous solution was stirred at –25 °C for 4 h after which the flask was removed from the cooling unit and the septum was removed. The reaction mixture was washed with brine (1x), dried over magnesium sulfate, and concentrated in vacuo onto Celite. The product was purified by silica gel flash chromatography.

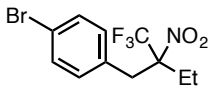

(**2.62**) According to general protocol A: 1-bromo-4-(2-nitrobutyl)benzene (257 mg, 1.00 mmol), Umemoto's reagent **2.9** (523 mg, 1.30 mmol) and anhydrous dichloromethane (10 mL) were combined under N_2 and cooled to –25 °C. DBU (299 μL, 2.00 mmol) was added dropwise and the reaction was stirred at –25 °C for 4 h. The reaction was worked up according to the general protocol and purified by flash silica gel chromatography (100:0 → 99:1 hexanes : ethyl acetate) to afford α-trifluoromethylnitroalkane **2.62** (270 mg, 83%) as a clear oil: ^{1}H NMR (600 MHz, $CDCl_3$) δ 7.45 (d, J = 8.3 Hz, 2H), 7.01 (d, J = 8.3 Hz, 2H), 3.51 (d, J = 14.7 Hz, 1H), 3.34 (d, J = 14.7 Hz, 1H), 2.22 (dq, J = 15.9, 8.4 Hz, 1H), 2.05 (dq, J = 14.8, 7.3 Hz, 1H), 1.08 (t, J = 7.4 Hz, 3H); ^{13}C

NMR (151 MHz, $CDCl_3$) δ 132.1, 132.0, 131.0, 122.6, 123.2 (q, J = 286 Hz), 94.3 (q, J = 25.9 Hz), 38.9, 26.1, 8.3; ^{19}F NMR (565 MHz, $CDCl_3$) δ -69.5; FTIR (cm^{-1}): 2987, 2957, 1561, 1490, 1195, 839, 812; GC/MS (EI) 278.0 $(M\text{-}NO_2)^+$. HRMS (CI) m/z calculated for $[C_{11}H_{11}NO_2BrF_3]^+$: 324.9925; found: 324.9930.

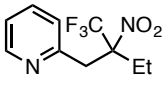

(**2.63**) According to general protocol A: 2-(2-Nitrobutyl)pyridine (180 mg, 1.00 mmol), Umemoto's reagent **2.9** (532 mg, 1.30 mmol), and anhydrous dichloromethane (10 mL) were combined under N_2 and cooled to –25 °C. DBU (299 μL, 2.00 mmol) was added dropwise and the reaction was stirred at –25 °C for 4 h. The reaction was worked up according to the general protocol and purified by flash silica gel chromatography (75:25 hexanes : ethyl acetate). A second column (50:50 hexanes : ethyl acetate) to remove trace dibenzothiophene afforded α-trifluoromethylnitroalkane **2.63** (158 mg, 64%) as a orange oil: ^1H NMR (600 MHz, $CDCl_3$) δ 8.55 - 8.51 (m, 1H), 7.64 (td, J = 7.7, 1.8 Hz, 1H), 7.20 (dd, J = 7.1, 5.3 Hz, 1H), 7.16 (d, J = 7.8 Hz, 1H), 3.83 (d, J = 14.8 Hz, 1H), 3.53 (d, J = 14.8 Hz, 1H), 2.41 - 2.26 (m, 2H), 1.10 - 1.06 (m, 3H); ^{13}C NMR (101 MHz, $CDCl_3$) δ 153.3, 149.6, 136.8, 124.8, 123.8 (q, J = 288 Hz), 122.8, 94.0 (q, J = 26.3 Hz), 39.6, 25.1, 8.6; ^{19}F NMR (565 MHz, $CDCl_3$) δ -71.3; FTIR (cm^{-1}): 2986, 2955, 1563, 1439, 1241, 1186; GC/MS (EI) 202.1 $(M\text{-}NO_2)^+$. HRMS (CI) m/z calculated for $[C_{10}H_{12}N_2O_2F_3]^+$: 249.0851; found: 249.0850.

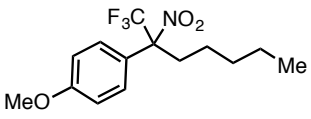

(**2.64**) According to general protocol A: **2.S1** (237 mg, 1.00 mmol), Umemoto's reagent **2.9** (523 mg, 1.30 mmol), and anhydrous dichloromethane (10 mL) were combined under

N_2 and cooled to –25 °C. DBU (299 μL, 2.00 mmol) was added dropwise and the reaction was stirred at –25 °C for 4 h. The reaction was worked up according to the general protocol and purified by flash silica gel chromatography (90:10 petroleum ether : benzene) to afford α-trifluoromethylnitroalkane **2.64** (263 mg, 86%) as a clear oil: ^{1}H NMR (600 MHz, C_6D_6) δ 7.03 (d, J = 8.8 Hz, 2H), 6.54 (d, J = 9.0 Hz, 2H), 3.16 (s, 3H), 2.41 - 2.30 (m, 2H), 1.43 (m, 1H), 1.31 (m, 1H), 1.09 - 0.96 (m, 4H), 0.75 (t, J = 7.2 Hz, 3H); ^{13}C NMR (101 MHz, $CDCl_3$) δ 160.7, 128.6, 123.8, 123.0 (q, J = 286 Hz), 114.2, 96.3 (q, J = 27.3 Hz), 55.5, 34.5, 31.9, 23.6, 22.3, 14.0; ^{19}F NMR (565 MHz, $CDCl_3$) δ -69.2; FTIR (cm^{-1}): 2960, 1563, 1518, 1263, 1180, 832. HRMS (LIFDI) m/z calculated for $[C_{14}H_{18}NO_3F_3]^+$: 305.1239; found: 305.1242.

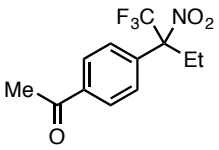

(**2.65**) According to general protocol A: 4-Acetyl-(1-nitropropyl)benzene (207 mg, 1.00 mmol), Umemoto's reagent **2.9** (532 mg, 1.30 mmol), and anhydrous dichloromethane (10 mL) were combined under N_2 and cooled to –25 °C. DBU (299 μL, 2.00 mmol) was added dropwise and the reaction was stirred at –25 °C for 4 h. The reaction was worked up according to the general protocol and purified by flash silica gel chromatography (99:05 → 90:10 hexanes : ethyl acetate) to afford α-trifluoromethylnitroalkane **2.65** (214 mg, 78%) as a clear oil: ^{1}H NMR (600 MHz, $CDCl_3$) δ 8.01 (d, J = 8.5 Hz, 2H), 7.43 (d, J = 8.3 Hz, 2H), 2.69 (hept, J = 7.8 Hz, 2H), 2.63 (s, 3H), 1.12 (t, J = 7.2 Hz, 3H); ^{13}C NMR (151 MHz, $CDCl_3$) δ 197.0, 138.3, 136.3, 128.8, 127.5, 122.7 (q, J = 285 Hz), 96.8 (q, J = 27.2 Hz), 28.2, 26.8, 8.7; ^{19}F NMR (565 MHz, $CDCl_3$) δ -68.7; FTIR (cm^{-1}): 2955, 1692, 1565, 1411, 1269, 1169, 824. HRMS (CI) m/z calculated for $[C_{12}H_{13}NO_3F_3]^+$: 276.0848; found: 276.0823.

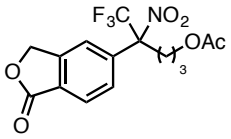

(**2.66**) According to general protocol A: **2.S2** (248 mg, 850 μmol), Umemoto's reagent **2.9** (532 mg, 1.30 mmol), and anhydrous dichloromethane (10 mL) were combined under N_2 and cooled to –25 °C. DBU (299 μL, 2.00 mmol) was added dropwise and the reaction was stirred at –25 °C for 4 h. The reaction was worked up according to the general protocol and purified by flash silica gel chromatography (65:35 hexanes : ethyl acetate) to afford α-trifluoromethylnitroalkane **2.66** (246 mg, 80%) as a white solid: ^{1}H NMR (600 MHz, $CDCl_3$) δ 8.03 (d, J = 8.2 Hz, 1H), 7.52 (d, J = 8.2 Hz, 1H), 7.45 (s, 1H), 5.38 (s, 2H), 4.13 (t, J = 6.1 Hz, 2H), 2.72 (dt, J = 10.6, 4.9 Hz, 2H), 2.08 (s, 3H), 1.96 - 1.86 (m, 1H), 1.77 - 1.67 (m, 1H); ^{13}C NMR (101 MHz, $CDCl_3$) δ 171.0, 169.6, 147.3, 137.5, 127.9, 127.9, 126.7, 122.4 (q, J= 286 Hz), 121.2, 96.2 (q, J= 28.1 Hz), 69.6, 63.2, 31.9, 23.6, 21.0; ^{19}F NMR (565 MHz, $CDCl_3$) δ –68.5; FTIR (cm^{-1}): 2960, 1773, 1739, 1567, 1240; mp = 109-110 °C; HRMS (LIFDI) m/z calculated for $[C_{15}H_{14}NO_6F_3]^+$: 361.0773; found: 361.0766.

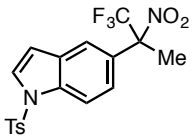

(**2.67**) According to general protocol A: **2.S10** (344 mg, 1.00 mmol), Umemoto's reagent **2.9** (523 mg, 1.30 mmol) and anhydrous dichloromethane (10 mL) were combined under N_2 and cooled to –25 °C. DBU (299 μL, 2.00 mmol) was added dropwise and the reaction was stirred at –25 °C for 4 h. The reaction was worked up according to the general protocol and purified by flash silica gel chromatography (80:20 hexanes : ethyl acetate) to afford **2.67** (309 mg, 75%) as a light yellow solid: ^{1}H NMR (400 MHz, $CDCl_3$) δ 8.02 (d, J = 8.9 Hz, 1H), 7.78 (d, J = 8.4 Hz, 2H), 7.64 (dd, J = 4.8, 2.9 Hz, 2H), 7.39 - 7.31 (m, 1H), 7.29 - 7.24 (m, 2H), 6.69 (d, J = 3.7 Hz, 1H), 2.37 (s, 3H), 2.26 (s, 3H); ^{13}C NMR (101 MHz, $CDCl_3$) δ 145.6, 135.4, 135.0, 130.9, 130.24, 127.9, 127.0, 126.6, 122.8 (q,

J = 283 Hz), 122.7, 120.3, 114.0, 108.9, 92.6 (q, J = 28.7 Hz), 21.8, 20.9; 19F NMR (376 MHz, $CDCl_3$) δ -72.3; FTIR (cm^{-1}): 3146, 2925, 1564, 1376, 1173, 1135; mp: 104-105 °C; HRMS (LIFDI) m/z calculated for $[C_{18}H_{15}N_2O_4SF_3]^+$: 412.0705; found: 412.0703.

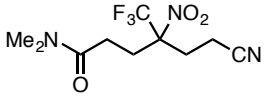

(**2.68**) According to general protocol A: **2.S5** (213 mg, 1.00 mmol), Umemoto's reagent **2.9** (523 mg, 1.30 mmol), and anhydrous dichloromethane (10 mL) were combined under N_2 and cooled to –25 °C. DBU (299 μL, 2.00 mmol) was added dropwise and the reaction was stirred at –25 °C for 4 h. The reaction was worked up according to the general protocol and purified by flash silica get chromatography (60:40 benzene : ethyl acetate) to afford α-trifluoromethylnitroalkane **2.68** (198 mg, 70%) as a white solid: ^{1}H NMR (400 MHz, $CDCl_3$) δ 2.98 (d, J = 10.7 Hz, 6H), 2.75 - 2.48 (m, 6H), 2.46 - 2.35 (m, 2H); ^{13}C NMR (101 MHz, $CDCl_3$) δ 169.3. 122.7 (q, J = 286 Hz), 117.4, 91.7 (q, J = 27.4 Hz), 37.1, 35.9, 28.8, 28.4, 27.0, 12.8 (q, J = 2.1 Hz); ^{19}F NMR (565 MHz, $CDCl_3$) δ -70.57; FTIR (cm^{-1}):2940, 2254, 1644, 1558, 1189; mp = 52-54 °C; GC/MS (EI) 235.1 $(M\text{-}NO_2)^+$; HRMS (ESI) m/z calculated for $[C_{10}H_{15}N_3O_3F_3]^+$: 282.10600; found: 282.10552.

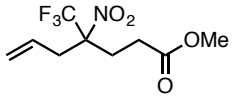

(**2.69**) According to general protocol A: methyl 4-nitrohept-6-enoate **2.S3** (187 mg, 1.00 mmol), Umemoto's reagent **2.9** (523 mg, 1.30 mmol) and anhydrous dichloromethane (10 mL) were combined under N_2 and cooled to –25 °C. DBU (299 μL, 2.00 mmol) was added dropwise and the reaction was stirred at –25 °C for 18 h. The reaction was worked up according to the general protocol and purified by flash silica gel chromatography (100:0 → 95:5 hexanes : ethyl acetate) to afford **2.69** (119 mg, 47%) as a clear oil: ^{1}H

NMR (600 MHz, $CDCl_3$) δ 5.69 (dd, J = 17.2, 7.5 Hz, 1H), 5.33 - 5.25 (m, 2H), 3.71 (s, 3H), 2.98 (dd, J = 14.9, 7.3 Hz, 1H), 2.90 (dd, J = 14.9, 7.3 Hz, 1H), 2.65 - 2.57 (m, 1H), 2.56 - 2.42 (m, 3H); ^{13}C NMR (151 MHz, $CDCl_3$) δ 171.8, 128.1, 122.7, 122.9 (q, J = 286 Hz), 92.5 (q, J = 26.8 Hz), 52.2, 37.6, 28.2, 27.3; ^{19}F NMR (565 MHz, $CDCl_3$) δ -71.1; FTIR (cm^{-1}): 3089, 2957, 1742, 1652, 1563, 1439, 1201, 936; GC/MS (EI) 224.0 $(M\text{-}OCH_3)^+$; HRMS (CI) m/z calculated for $[C_9H_{13}NO_4F_3]^+$: 256.0797; found: 256.0810.

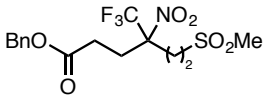

(**2.70**) According to general protocol A: benzyl 6-(methylsulfonyl)-4-nitrohexanoate **2.S4** (315 mg, 960 μmol), Umemoto's reagent **2.9** (500 mg, 1.24 mmol) and anhydrous dichloromethane (10 mL) were combined under N_2 and cooled to –25 °C. DBU (299 μL, 2.00 mmol) was added dropwise and the reaction was stirred at –25 °C for 4 h. The reaction was worked up according to the general protocol and purified by flash silica gel chromatography (95:5 → 80:20 hexanes : ethyl acetate) to afford α-trifluoromethylnitroalkane **2.70** (250 mg, 66%) as a clear oil: ^1H NMR (600 MHz, $CDCl_3$) δ 7.41 - 7.32 (m, 5H), 5.15 (s, 2H), 3.19 (dt, J = 12.9, 4.2 Hz, 1H), 3.12 (dt, J = 12.7, 4.3 Hz, 1H), 2.98 (s, 3H), 2.81 - 2.72 (m, 1H), 2.69 - 2.45 (m, 5H); ^{13}C NMR (151 MHz, $CDCl_3$) δ 170.7, 135.3, 128.8, 128.7, 128.5, 122.6 (q, J = 286 Hz), 91.5 (q, J = 27.4 Hz), 67.3, 49.0, 41.0, 28.2, 28.1, 25.0; ^{19}F NMR (565 MHz, $CDCl_3$) δ -70.8; FTIR (cm^{-1}): 3011, 1731, 1565, 1451, 1308, 1176, 755 ; ESI-MS 420.3 $(M+Na)^+$. HRMS (ESI) m/z calculated for $[C_{15}H_{19}NO_6F_3S]^+$: 398.0880; found: 398.0869.

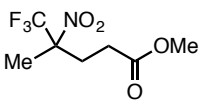

(**2.71**) According to general protocol A: Methyl 4-nitropentanoate (484 mg, 3.00 mmol), Umemoto's reagent **2.9** (1.57 g, 3.90 mmol) and anhydrous dichloromethane (30 mL) were combined under N_2

and cooled to –25 °C. DBU (897 μL, 6.00 mmol) was added dropwise and the reaction was stirred at –25 °C for 4 h. The reaction was worked up according to the general protocol and purified via silica gel flash chromatography (95:5 → 80:20 hexanes : ethyl acetate) to afford α-trifluoromethylnitroalkane **2.71** (624 mg, 91%) as a yellow oil: ^{1}H NMR (600 MHz, $CDCl_3$) δ 3.68 (s, 3H), 2.77 - 2.63 (m, 1H), 2.48 - 2.27 (m, 3H), 1.76 (s, 3H); ^{13}C NMR (101 MHz, $CDCl_3$) δ 171.6, 123.0 (q, J = 287 Hz), 90.0 (q, J = 29.1 Hz), 52.3, 28.7, 28.05, 17.6; ^{19}F NMR (565 MHz, $CDCl_3$) δ -75.7; FTIR (cm^{-1}): 2361, 1652, 1559, 1540, 1175; GC/MS (EI) 198.1 $(M\text{-}OCH3)^+$. HRMS (CI) m/z calculated for $[C_7H_{11}NO_4F_3]^+$: 230.0640; found: 230.0626.

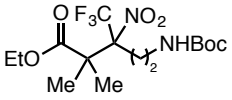

(**2.73**) According to general protocol A: Ethyl 5-(tert-butoxycarbonylamino)-2,2-dimethyl-3-nitropentanoate (318 mg, 1.00 mmol), Umemoto's reagent **2.9** (532 mg, 1.30 mmol), and anhydrous dichloromethane (10 mL) were combined under N_2 and cooled to –25 °C. DBU (299 μL. 2.00 mmol) was added dropwise and the reaction was stirred at –25 °C for 48 h. The reaction was worked up according to the general protocol and purified by flash silica gel chromatography (89:11 hexanes : ethyl acetate) to afford **2.73** (141 mg, 36%) as a pale yellow solid: ^{1}H NMR (400 MHz, $CDCl_3$) δ 4.76 (s, 1H), 4.13 (q, J = 7.1 Hz, 2H), 3.47 - 3.32 (m, 1H), 2.96 (ddt, J = 14.3, 10.3, 5.0 Hz, 1H), 2.65 - 2.40 (m, 2H), 1.49 - 1.34 (m, 15H), 1.23 (t, J = 7.1 Hz, 3H); ^{13}C NMR (101 MHz, $CDCl_3$) δ 171.6, 155.7, 123.1 (q, J = 287 Hz), 96.1 (q, J = 26.3 Hz), 79.9, 62.4, 49.2, 36.2, 32.0, 28.5, 23.3, 23.1, 13.8; ^{19}F NMR (565 MHz, $CDCl_3$) δ -62.6; FTIR (cm^{-1}): 3350, 2981, 1720, 1568, 1174; mp: 58-60 °C; ESI-MS: 409.1 $(M+Na)^+$. HRMS (ESI) m/z calculated for $[C_{15}H_{25}N_2O_6F_3Na]^+$: 409.15569; found: 409.15437.

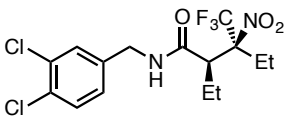

(**2.74**) According to general protocol A: N-(3,4-dichlorobenzyl)-2-ethyl-3-nitropentanamide (332 mg, 1.00 mmol), Umemoto's reagent **2.9** (532 mg, 1.30 mmol), and anhydrous dichloromethane (10 mL) were combined under N_2 and cooled to –25 °C. DBU (299 μL, 2.00 mmol) was added dropwise and the reaction was stirred at –25 °C for 24 h. The reaction was worked up according to the general protocol and purified by flash silica gel chromatography (75:25 hexanes : ethyl acetate). A second column (50:50 hexanes : ethyl acetate) to remove trace dibenzothiophene afforded α-trifluoromethylnitroalkane **2.74** (291 mg, 73%) as a light yellow solid: ^{1}H NMR (600 MHz, $CDCl_3$) δ 7.41 (d, J = 8.2 Hz, 1H), 7.32 (d, J = 1.7 Hz, 1H), 7.06 (dd, J = 8.2, 1.9 Hz, 1H), 5.84 (s, 1H), 4.32 (qd, J = 15.1, 5.8 Hz, 2H), 3.07 - 2.98 (m, 1H), 2.74 - 2.64 (m, 1H), 2.06 (dq, J = 14.7, 7.2 Hz, 1H), 1.93 (tq, J = 14.2, 7.2 Hz, 1H), 1.65 (dd, J = 12.8, 6.8 Hz, 1H), 1.09 (t, J = 7.2 Hz, 3H), 0.94 (t, J = 7.3 Hz, 3H); ^{13}C NMR (101 MHz, $CDCl_3$) δ 168.1, 137.6, 132.9, 131.9, 130.8, 129.8, 127.1, 122.7 (q, J = 287 Hz), 96.8 (q, J = 25.8), 54.0, 43.0, 21.9, 21.0, 12.6, 8.3; ^{19}F NMR (565 MHz, $CDCl_3$) δ -65.5; FTIR (cm^{-1}): 3297, 3088, 1658, 1563, 1201, 1088, 1032; 116-118 °C; ESI-MS: 401.2 $(M+H)^+$. HRMS (ESI) m/z calculated for $[C_{15}H_{18}N_2O_3Cl_2F_3]^+$: 401.06411; found: 401.06349; X-ray crystals were obtained by vapor diffusion (dichloromethane/ hexanes).

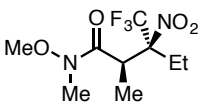

(**2.75**) According to general protocol A: N-methoxy-N,2-dimethyl-3-nitropentanamide (204 mg, 1.0 mmol), Umemoto's reagent **2.9** (532 mg, 1.30 mmol), and anhydrous dichloromethane (10 mL) were combined under N_2 and cooled to –25 °C. DBU (299 μL, 2.00 mmol) was added dropwise and the reaction was stirred at –25 °C for 4 h. The reaction was worked up

according to the general protocol and purified by flash silica gel chromatography (95:5 → 90:10 hexanes : ethyl acetate) to afford α-trifluoromethylnitroalkane **2.75** (172 mg, 63%) as a clear oil: ^{1}H NMR (400 MHz, $CDCl_3$) δ 4.05 (q, J = 7.1 Hz, 1H), 3.71 (s, 3H), 3.15 (s, 3H), 2.90 (ddd, J = 15.9, 7.5, 2.5 Hz, 1H), 2.16 (dd, J = 15.7, 7.6 Hz, 1H), 1.36 (d, J = 7.2 Hz, 3H), 1.11 (td, J = 7.4, 1.8 Hz, 3H); ^{13}C NMR (151 MHz, $CDCl_3$) δ 171.1, 123.1 (q, J = 287 Hz), 95.3 (q, J = 25.6 Hz), 61.6, 39.2, 32.4, 22.7, 13.8, 8.5; ^{19}F NMR (565 MHz, $CDCl_3$) δ -66.9; FTIR (cm^{-1}): 2985, 2951, 1670, 1565, 1203, 1179 ; GC/MS (EI) 226.1 $(M\text{-}NO2)^{+}$. HRMS (CI) m/z calculated for $[C_9H_{16}N_2O_4F_3]^{+}$: 273.1062; found: 273.1064.

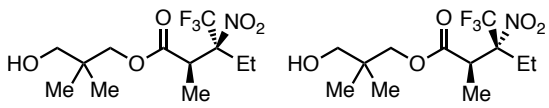

2.76A **83:17** **2.76B**

(**2.76**) According to general protocol A: 3-Hydroxy-2,2-dimethylpropyl 2-methyl-3-nitropentanoate **2.S7** (315 mg, 1.00 mmol), Umemoto's reagent **2.9** (523 mg, 1.30 mmol) and anhydrous dichloromethane (10 mL) were combined under N_2 and cooled to –25 °C. DBU (299 μL, 2.00 mmol) was added dropwise and the reaction was stirred at –25 °C for 4 h. The reaction was worked up according to the general protocol and concentrated in vacuo. NMR analysis of the crude reaction mixture revealed an 83:17 mixture of syn and anti isomers. The crude reaction was purified by flash silica gel chromatography (95:5 → 80:20 hexanes : ethyl acetate) to afford α-trifluoromethylnitroalkane **2.76** (157 mg, 50%) as a clear oil: The product was isolated as a mixture of diastereomers (dr: 88:12): ^{1}H NMR (600 MHz, $CDCl_3$: mixture of diastereomers; useful diagnostic peaks for each compound are listed) δ **2.76A**: 3.87 (d, J = 10.9 Hz, 1H), 3.72 (q, J = 7.2 Hz, 1H), 1.39 (d, J = 7.2 Hz, 3H); 17B: 3.60 (q, J = 7.1 Hz, 1H), 2.00 (d, J = 2.0 Hz, 1H), 1.31 (d, J = 7.2 Hz, 3H); ^{13}C NMR (151 MHz, $CDCl_3$) δ **2.76A**: 170.5, 122.8

(q, J = 287 Hz), 95.0 (q, J = 26 Hz), 68.1, 44.5, 36.2, 22.7, 21.5, 12.8, 8.5; **2.76B**: 170.3, 123,0 (q, J = 287 Hz), 95.2 (q, J = 26 Hz), 68.3, 43.9, 23.8, 13.0;^{19}F NMR (565 MHz, $CDCl_3$) δ **2.76A**: –66.8, **2.76B**: –67.1; FTIR (cm^{-1}): 3435, 2962, 1742, 1569, 1470, 1245, 1203, 824; GC/MS (EI) 212.0 $(M\text{-}C_5H_{11}O_2)^+$; 212.1 $(M\text{-}C_5H_{11}O_2)^+$. HRMS (CI) m/z calculated for $[C_{12}H_{21}NO_5F_3]^+$: 316.1372; found: 316.1364.

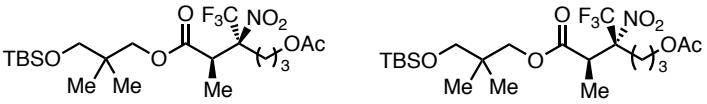

2.77A **85:15** **2.77B**

(**2.77**) According to general protocol A: **2.S6** (433 mg, 1.00 mmol), Umemoto's reagent **2.9** (523 mg, 1.30 mmol) and anhydrous dichloromethane (10 mL) were combined under N_2 and cooled to –25 °C. DBU (299 μL, 2.00 mmol) was added dropwise and the reaction was stirred at –25 °C for 4 h. The reaction was worked up according to the general protocol and concentrated in vacuo. NMR analysis of the crude reaction mixture revealed an 85:15 mixture of syn and anti isomers. The crude reaction was purified flash silica gel chromatography (100:0 → 95:5 hexanes : ethyl acetate) to afford α-trifluoromethylnitroalkane **2.77** (292 mg, 58%) as a clear oil. The product was isolated as a mixture of diastereomers (dr: 92:08): ^{1}H NMR (600 MHz, $CDCl_3$: mixture of diastereomers; useful diagnostic peaks for each compound are listed) δ **2.77A**: 3.81 (d, J = 10.6 Hz, 1H), 3.76 (q, J = 7.2 Hz, 1H), 1.40 (d, J = 7.2 Hz, 3H), 0.88 (s, 9H), 0.86 (d, J = 2.4 Hz, 6H), 0.03 (d, J = 5.2 Hz, 6H); 18B: 3.88 (d, J = 10.6 Hz, 1H), 3.61 (q, J = 7.2 Hz, 1H); ^{13}C NMR (151 MHz, $CDCl_3$) δ **2.77A**: 170.9, 169.8, 122.8, (q, J = 288 Hz), 94.2, (q, J = 26 Hz), 71.5, 63.8, 44.4, 43.9, 36.2, 26.1, 25.9, 23.2, 21.5, 21.4, 20.9, 18.3, 12.9, -5.5, -5.6; 18B: 71.4, 63.7, 43.9, 13.2; ^{19}F NMR (565 MHz, $CDCl_3$) δ **2.77A**: –67.2, **2.77B**: –67.5; FTIR (cm^{-1}): 2957, 2897,

1745, 1572, 1473, 1365, 1236, 838, 776; GC/MS (ESI) 524.3 $(M+Na)^+$. HRMS (ESI) m/z calculated for $[C_{21}H_{39}NO_7F_3Si]^+$: 502.2442; found: 502.24267.

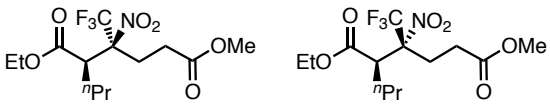

2.78A **67:33** **2.78B**

(**2.78**) According to the general protocol: 1-Ethyl 6-methyl 3-nitro-2-propylhexanedioate (275 mg, 1.00 mmol), Umemoto's reagent **2.9** (523 mg, 1.30 mmol), and anhydrous dichloromethane (10 mL) were combined under N_2 and cooled to –25 °C. DBU (299 μL, 2.00 mmol) was added dropwise and the reaction was stirred at –25 °C for 4 h. The reaction was worked up according to the general protocol and concentrated in vacuo. NMR analysis of the crude reaction mixture revealed a 67:33 mixture of syn and anti isomers. The reaction was purified by silica gel flash chromatography (100:0 → 95:5 hexanes : ethyl acetate) to afford α-trifluoromethylnitroalkane **2.78** (254 mg, 74%) as a yellow oil. The product was isolated as a mixture of diastereomers (dr: 73: 27): ^{1}H NMR (600 MHz, $CDCl_3$: mixture of diastereomers; useful diagnostic peaks for each compound are listed. See attached spectra for details): δ **2.78A**: 4.15 (q, J = 7.1 Hz, 2H), 3.71 (s, 3H), 3.44 (dd, J = 12.1, 2.4 Hz, 1H), 0.91 (t, 3H); 19B: 4.25 - 4.19 (m, 2H), 3.73 (s, 3H), 3.50 (dd, J = 12.0, 2.6 Hz, 1H), 0.95 (t, 3H); ^{13}C NMR (151 MHz, $CDCl_3$) δ **2.78A**: 172.0, 169.2, 122.7 (q, J = 286 Hz), 62.2, 50.3, 29.3, 28.5, 24.8, 21.3, 13.9, 13.7, 13.5; **2.78B**: 172.1, 169.5, 122.6 (q, J = 287 Hz), 62.1, 49.5, 29.9, 23.9, 28.6, 20.8, 14.0, 13.5; ^{19}F NMR (565 MHz, $CDCl_3$) δ **2.78A**: –66.2, **2.78B**: –68.1; FTIR (cm^{-1}): 2965, 2878, 1743, 1570, 1190; GC/MS (EI) 297.1 $(M-NO_2)^+$; 297.1 $(M-NO_2)^+$. HRMS (CI) m/z calculated for $[C_{13}H_{21}NO_6F_3]^+$: 344.1321; found: 344.1329.

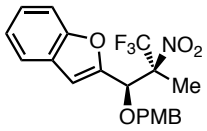

2.79A **89:11**

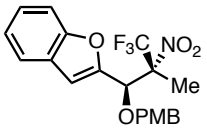

2.79B

(**2.79**) According to general protocol A: **2.83** (341 mg, 1.00 mmol), Umemoto's reagent **2.9** (523 mg, 1.30 mmol) and anhydrous dichloromethane (10 mL) were combined under N_2 and cooled to –25 °C. DBU (299 μL, 2.00 mmol) was added dropwise and the reaction was stirred at –25 °C for 4 h. The reaction was worked up according to the general protocol and concentrated in vacuo. NMR analysis of the crude reaction mixture revealed an 89:11 mixture of syn and anti isomers. The crude reaction was purified by flash silica gel chromatography (100:0 → 95:05 hexanes : ethyl acetate) to afford α-trifluoromethylnitroalkane **2.79** (236 mg, 58%) as a clear oil: ^{1}H NMR (600 MHz, $CDCl_3$: mixture of diastereomers; useful diagnostic peaks for each compound are listed) δ **2.79A**: 7.57 (d, J = 7.7 Hz, 1H), 7.50 (d, J = 8.3 Hz, 1H), 7.36 - 7.32 (m, 1H), 7.21 (d, J = 8.5 Hz, 2H), 7.15 (s, 1H), 6.88 (d, J = 8.6 Hz, 2H), 6.78 (s, 1H), 5.53 (s, 1H), 4.62 (d, J = 11.1 Hz, 1H), 4.42 (d, J = 11.1 Hz, 1H), 1.89 (s, 3H); **2.79B**: 7.54 (d, J = 8.4 Hz, 1H), 7.09 (d, J = 8.4 Hz, 2H), 6.85 (d, J = 8.6 Hz, 2H), 5.57 (s, 1H), 4.50 (d, J = 11.0 Hz, 1H), 4.27 (d, J = 11.2 Hz, 1H), 2.03 (s, 3H); ^{13}C NMR (151 MHz, $CDCl_3$) δ **2.79A**: 159.9, 155.6, 149.5, 130.1, 128.1, 125.5, 123.5, 122.7 (q, J = 287 Hz), 119.9, 111.8, 109.7, 109.3, 93.16, (q, J = 26.5 Hz), 74.5, 72.3, 55.4, 13.5; 20B: 159.8, 155.7, 149.3, 129.9, 128.0, 125.6, 109.7, 73.9, 71.6, 12.9; ^{19}F NMR (565 MHz, $CDCl_3$) δ **2.79A**: –72.0, **2.79B**: –73.2; FTIR (cm^{-1}): 2936, 2838, 1613, 1566, 1453, 1254, 751; GC/MS (EI) 409.0 $(M)^+$. HRMS (CI) m/z calculated for $[C_{20}H_{18}NO_5F_3]^+$: 409.1137; found: 409.1135.

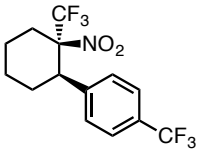

(**2.80**) According to general protocol A: rac-2-(4-Trifluoromethylphenyl)-1-nitrocyclohexane (410 mg, 1.50 mmol), Umemoto's reagent **2.9** (785 mg, 1.95 mmol), and anhydrous dichloromethane (15 mL) were combined under N_2 and cooled to –25 °C. DBU (448 μL, 3.00 mmol) was added dropwise and the reaction was stirred at –25 °C for 4 h. The reaction was worked up according to the general protocol and purified by flash silica gel chromatography (77:20:3 hexanes : benzene : ethyl acetate) to afford α-trifluoromethylnitroalkane **2.80** (333 mg, 65%) as a light yellow solid: ^{1}H NMR (400 MHz, $CDCl_3$) δ 7.55 (d, J = 8.2 Hz, 2H), 7.40 (d, J = 8.2 Hz, 2H), 3.33 (dd, J = 12.6, 3.8 Hz, 1H), 2.66 (d, J = 14.7 Hz, 1H), 2.38 (qd, J = 13.0, 3.7 Hz, 1H), 2.11 - 1.96 (m, 2H), 1.96 - 1.71 (m, 3H), 1.52 (ddp, J = 17.0, 8.7, 4.1 Hz, 1H); ^{13}C NMR (101 MHz, $CDCl_3$) δ 142.9, 130.2 (q, J = 35.5 Hz), 129.9, 125.3 (q, J = 3.64 Hz), 124.1 (q, J = 272 Hz), 122.9 (q, J = 284 Hz), 92.9 (q, J = 25.4 Hz), 46.4, 31.5, 29.1, 24.8, 20.6; ^{19}F NMR (376 MHz, $CDCl_3$) δ –62.7, –70.9; FTIR (cm^{-1}): 2947, 1561, 1328, 1161, 1123; mp = 43-45 °C; GC/MS (EI) 341.1 $(M)^+$. HRMS (CI) m/z calculated for $[C_{14}H_{13}NO_2F_6]^+$: 341.0871; found: 341.0850; crystals for X-ray analysis were obtained by slow evaporation of hexanes.

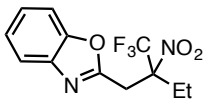

(**2.87**) A hot 25 mL round bottom flask equipped with a magnetic stir bar and a rubber spectrum was attached to a double manifold and cooled under vacuum. Once cooled, the flask was backfilled with N_2, the septum was removed, and 2-(2-nitrobutyl)benzo[d]oxazole (220 mg, 1.00 mmol) and Umemoto's reagent **2.9** (523 mg, 1.30 mmol) were added. The septum was replaced, the flask was reattached to a double manifold and evacuated and backfilled with N_2 three times. Anhydrous dichloromethane (10 mL) was added via syringe and

the flask was lowered into a precooled –25 °C cooling bath and stirred. 1,1,3,3,-Tetramethylguanidine (121 μL, 1.00 mmol) was then added dropwise via syringe. The resulting homogenous solution was stirred at –25 °C for 4 h, after which the flask was removed from the cooling unit and warmed to rt. The reaction mixture was washed with brine (1x), dried over magnesium sulfate, and concentrated in vacuo onto Celite. The product was purified by silica gel flash chromatography (100:0 → 95:5 hexanes : ethyl acetate) to afford α-trifluoromethylnitroalkane **2.87** (128 mg, 44%) as a pale yellow oil: ^{1}H NMR (400 MHz, $CDCl_3$) δ 7.74 - 7.68 (m, 1H), 7.56 - 7.50 (m, 1H), 7.41 - 7.32 (m, 2H), 3.99 (d, J = 16.0 Hz, 1H), 3.81 (d, J = 16.0 Hz, 1H), 2.54 (q, J = 7.5 Hz, 2H), 1.15 (dd, J = 7.4, 1.0 Hz, 3H); ^{13}C NMR (101 MHz, $CDCl_3$) δ 158.7, 150.8, 140.9, 125.7, 124.9, 122.8 (q, J = 291 Hz), 120.4, 110.9, 92.4 (q, J = 26.9 Hz), 30.39 (q, J = 1.41 Hz), 25.2, 8.45 (d, J = 1.66 Hz); ^{19}F NMR (376 MHz, $CDCl_3$) δ -72.9; FTIR (cm^{-1}): 2985, 1567, 1455, 1180, 1169; GC/MS (EI) 288.1 $(M)^+$. HRMS (CI) m/z calculated for $[C_{12}H_{12}N_2O_3F_3]^+$: 289.0800; found: 289.0794.

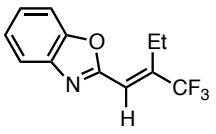

(**2.88**) According to general protocol A: 2-(2-Nitrobutyl)benzo[d]oxazole (220 mg, 1.00 mmol), Umemoto's reagent **2.9** (523 mg, 1.30 mmol), and anhydrous dichloromethane (10 mL) were combined under N_2 and cooled to –25 °C. DBU (299 μL, 2.00 mmol) was added dropwise and the reaction was stirred at –25 °C for 4 h. The reaction was worked up according to the general protocol and concentrated in vacuo. NMR analysis revealed a >95:5 mixture of E and Z isomers. The crude reaction was purified flash silica gel chromatography (100:0 → 98:2 hexanes : ethyl acetate) to afford vinyltrifluoromethylalkene **2.88** (147 mg, 61%) as a yellow oil: ^{1}H NMR (600 MHz, $CDCl_3$) δ 7.79 (d, J = 7.6 Hz, 1H), 7.57 (d, J = 7.7, 1H), 7.40 (pd, J = 7.2, 1.1 Hz,

2H), 6.96 (s, 1H), 2.97 (q, J = 7.5 Hz, 2H), 1.30 (t, J = 7.5 Hz, 3H); ^{13}C NMR (151 MHz, $CDCl_3$) δ 159.6, 150.4, 142.6 (q, J = 28.9 Hz), 141.9, 126.3, 125.1, 123.2, 120.8, 117.3 (q, J = 6.9 Hz), 110.9, 21.0, 13.2; ^{19}F NMR (565 MHz, $CDCl_3$) δ -68.3; FTIR (cm^{-1}): 2981, 2944, 2883, 1652, 1451, 1181, 745; GC/MS (EI) 241.1 $(M)^+$. HRMS (CI) m/z calculated for $[C_{12}H_{11}NOF_3]^+$: 242.0793; found: 242.0780. The relative stereochemistry of compound **2.88** was determined using a combination of 1D nOe and ^{19}F:^{1}H HOSEY correlations.[36] The results from these experiments is summarized in the tables and figures below:

1D nOe Correlation For **2.88**

Shift Irradiated (ppm)	1 D nOe Correlation Seen (ppm)
6.99	n/a

2D HOSEY Correlation for **2.88**: ^{1}H to ^{19}F

^{19}F Shift (ppm)	^{1}H Correlations Seen (ppm)
-68.3	1.23
-68.3	2.90
-68.3	6.88

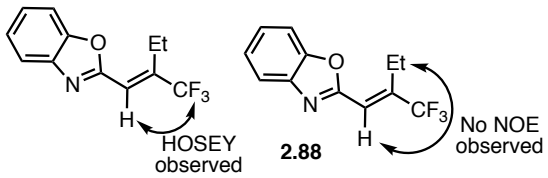

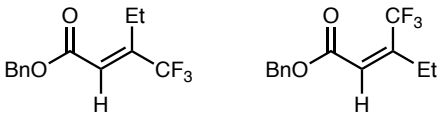

2.91A **88:12** **2.91B**

(**2.91**) According to general protocol A: **2.89** (238 mg, 1.00 mmol), Umemoto's reagent **2.9** (523 mg, 1.30 mmol), and anhydrous dichloromethane (10 mL) were combined under N_2 and cooled to –25 °C. DBU (299 μL, 2.00 mmol) was added dropwise and the reaction was stirred at –25 °C for 4 h. The reaction was worked up according to the

general protocol and concentrated in vacuo. NMR analysis of the crude reaction mixture revealed an 88:12 mixture of E and Z isomers. The crude reaction was purified flash silica gel chromatography (100:0 → 98:2 hexanes : ethyl acetate) to afford mixture of vinyltrifluoromethylalkene **2.91A** and **2.91B** (154 mg, 60%) as a clear oil. An analytically pure sample of product **2.91A** was obtained by column chromatography. Alkene **2.91B** was isolated contaminated with alkene **2.91A**. Diagnostic peaks for alkene **2.91A** are listed below: ^{1}H NMR (600 MHz, $CDCl_3$) δ 7.41 - 7.32 (m, 5H), 6.35 (s, 1H), 5.21 (s, 2H), 2.70 (q, J = 7.5 Hz, 2H), 1.17 (t, J = 7.5 Hz, 3H); ^{13}C NMR (151 MHz, $CDCl_3$) δ 164.5, 148.4 (q, J = 28.9 Hz), 135.5, 128.8, 128.7, 123.6 (q, J = 276 Hz) 121.5, (q, J = 6.20 Hz), 120.9, 66.9, 20.4, 13.4; ^{19}F NMR (565 MHz, $CDCl_3$) δ -69.2; FTIR (cm^{-1}): 3036, 2982, 1731, 1669, 1309, 1191, 696; GC/MS (EI) 258.1 $(M)^+$. HRMS (CI) m/z calculated for $[C_{13}H_{13}O_2F_3]^+$: 258.0868; found: 258.0896.

Alkene **2.91B** was isolated contaminated with alkene **2.91A**. Diagnostic peaks for alkene 27B are listed below: ^{1}H NMR (400 MHz, $CDCl_3$) δ 6.06 (s, 1H), 5.20 (s, 2H), 2.33 (qd, J = 7.3, 1.6 Hz, 2H), 1.13 (t, J = 7.3 Hz, 3H); ^{13}C NMR (151 MHz, $CDCl_3$) δ 164.8, 135.3, 128.8, 128.7, 128.6, 123.5, 67.4, 24.5, 11.8; ^{19}F NMR (565 MHz, $CDCl_3$) δ -63.5; GC/MS (EI) 258.1 $(M)^+$. HRMS (CI) m/z calculated for $[C_{13}H_{13}O_2F_3]^+$: 258.0868; found: 258.0859.

The relative stereochemistry for alkenes **2.91A** and **2.91B** was determined using 1D nOe and ^{1}H:^{19}F HOSEY. The results from these experiments is summarized in the tables and figures below:

1D nOe Correlation For **2.91A**

Shift Irradiated (ppm)	1 D nOe Correlation Seen (ppm)
6.38	n/a

2D HOSEY Correlation For **2.91A**: 1H to 19F

^{19}F Shift (ppm)	^{1}H Correlations Seen (ppm)
-69.2	1.17
-69.2	2.69
-69.2	6.34

1D nOe Correlation For **2.91B**

Shift Irradiated (ppm)	1 D nOe Correlation Seen (ppm)
6.10	2.35, 1.16
2.36	6.10, 1.16
1.16	2.36, 1.16

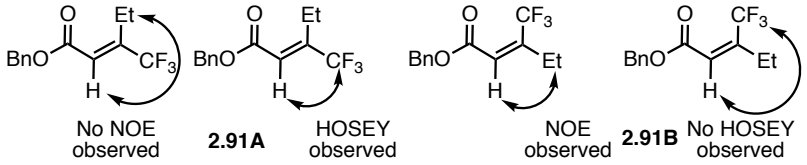

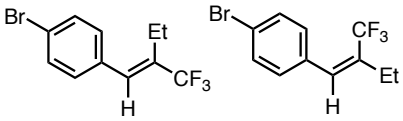

(**2.92**) A hot 25 mL round bottom flask equipped with a magnetic stir bar and a rubber spectrum was attached to a double manifold and cooled under vacuum. Once cooled, the flask was backfilled with N_2, the septum was removed, and 1-bromo-4-(2-nitro-2-(trifluoromethyl)butyl)benzene **2.62** (163 mg, 0.5 mmol), potassium tert-butoxide (84.0 mg, 0.75 mmol) and anhydrous dichloromethane (5 mL) were added and the reaction was stirred in an oil bath at 40 °C for 5 h. The reaction mixture was washed with NH_4Cl (1x15 mL), dried over magnesium sulfate, and

concentrated in vacuo. NMR analysis of the crude reaction mixture revealed an 72:28 mixture of E and Z isomers. The product was purified by silica gel flash chromatography (100 % hexanes) to afford a mixture of vinyltrifluoromethylalkene **2.92A** and **2.92B** (130 mg, 93%) as a clear oil. The product was isolated as a mixture of E:Z (72:28) isomers. ^{1}H NMR (600 MHz, C_6D_6: mixture of E and Z isomer; useful diagnostic peaks for each compound are listed; see attached spectra for details) δ **2.92A**: 7.14 - 7.10 (m, 2H), 6.72 (s, 1H), 6.55 (d, J = 8.4 Hz, 2H), 2.09 (q, J = 7.6 Hz, 2H), 0.90 (t, J = 7.5 Hz, 3H); **2.92B**: 6.78 (d, J = 8.3 Hz, 2H), 6.12 (s, 1H), 1.99 (qd, J = 7.4, 1.4 Hz, 2H), 0.86 (t, J = 7.4 Hz, 3H); ^{13}C NMR (151 MHz, $CDCl_3$) δ **2.92A**: 133.6, 133.2, 131.9, 130.8 (q, J = 6.5 Hz), 130.5, 124.9 (q, J = 274 Hz), 122.6, 19.8, 13.4; 28B: 134.4, 133.1, 132.7 (q, J = 3.9 Hz), 131.3, 130.2 (q, J = 2.5 Hz), 124.0 (q, J = 276 Hz), 122.1, 25.9, 13.1; ^{19}F NMR (565 MHz, $CDCl_3$) δ -59.4, -66.7. FTIR (cm^{-1}): 2975, 2942, 1653, 1489, 1251, 1161, 1115, 901; GC/MS (EI) 278.0 $(M)^+$. HRMS (CI) m/z calculated for $[C_{11}H_{10}F_3Br]^+$: 277.9918; found: 277.9909.

1D nOe Correlation For **2.92A**

Shift Irradiated (ppm)	1 D nOe Correlation Seen (ppm)
6.73	6.55

1D nOe Correlation For **2.92B**

Shift Irradiated (ppm)	1 D nOe Correlation Seen (ppm)
6.12	6.78, 1.99, 0.86

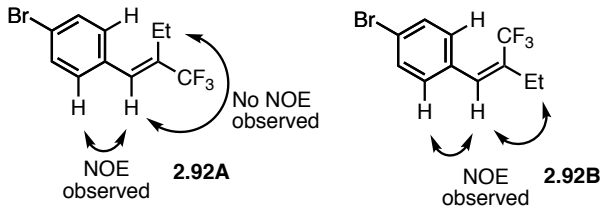

2D HOSEY Correlation For **2.92A**: ^{1}H to ^{19}F

^{19}F Shift (ppm)	^{1}H Correlations Seen (ppm)
-66.7	0.90
-66.7	2.09
-66.7	6.72

2D HOSEY Correlation For **2.92B**: ^{1}H to ^{19}F

^{19}F Shift (ppm)	^{1}H Correlations Seen (ppm)
-59.4	0.90
-59.4	1.99
-59.4	6.78

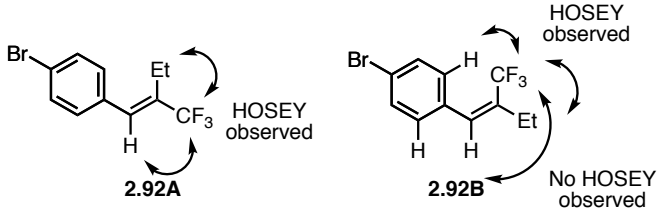

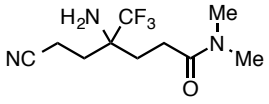

(**2.93**) To a 10 mL round bottom flask equipped with a magnetic stir bar was added α-trifluoromethylnitroalkane **2.68** (100 mg, 356 μmol) and acetic acid (1.19 mL). The flask was cooled to 0 °C in an ice bath and zinc dust (233 mg, 3.56 mmol) was added portionwise. Once addition of zinc was complete, the reaction was warmed to rt and stirred for 13 h. The crude reaction was filtered through Celite and diluted with ethyl acetate (10 mL). The reaction was washed with $NaHCO_3$ (3x, 10 mL). The aqueous layer was basified with 1 M NaOH. The water was removed in vacuo and the crude solid was washed with chloroform (25 mL). The mother liquor was concentrated in vacuo to afford α-trifluoromethylamine **2.93** (70.1 mg, 78%) as a light pink solid: ^{1}H

NMR (400 MHz, CDCl3) δ 3.02 (s, 3H), 2.93 (s, 3H), 2.82 - 2.70 (m, 1H), 2.70 - 2.57 (m, 1H), 2.58 - 2.45 (m, 2H), 2.36 - 2.05 (m, 4H); ^{13}C NMR (101 MHz, D_2O) δ 173.7, 156.0, 125.4 (q, J = 286 Hz), 73.3 (q, J = 27.7 Hz), 37.2, 35.5, 25.9, 24.2, 24.0, 21.7; ^{19}F NMR (376 MHz, $CDCl_3$) δ -76.7; FTIR (cm^{-1}): 3412, 2239, 1687, 1635, 1160; mp: 180-182 °C; ESI-MS: 268.1 $(M+OH)^+$. HRMS (ESI) m/z calculated for $[C_{10}H_{17}N_3OF_3]^+$: 252.13182; found: 252.13130.

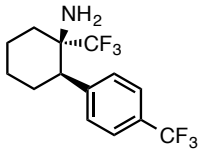

(**2.94**) To a 25 mL round bottom flask equipped with a magnetic stir bar was added α-trifluoromethylnitroalkane **2.80** (75.0 mg, 220 μmol), methanol (2.2 mL), and Pd/C (15.0 mg, 20 wt %) The flask was equipped with a rubber septum and a needle was inserted into the septum. The flask was placed in a Parr reactor and evacuated and backfilled with H_2 five times. On the last refill, the reactor was sealed at a H_2 pressure of 400 psi. The reactor was placed on a stir plate and the reaction was stirred at rt for 24 h. Once complete, the reactor was vented and the crude reaction was diluted with ethyl acetate and filtered through Celite and concentrated in vacuo to afford α-trifluoromethylamine **2.94** (66.8 mg, 98%) as a thick colorless oil. NMR analysis revealed a >99:1 mixture of syn and anti isomers: ^{1}H NMR (400 MHz, $CDCl_3$) δ 7.57 (d, J = 8.1 Hz, 2H), 7.34 (d, J = 8.1 Hz, 2H), 5.62 (s, 1H), 4.30 (s, 1H), 3.13 (dd, J = 13.0, 3.7 Hz, 1H), 2.57 (ddd, J = 13.4, 4.7, 3.0 Hz, 1H), 2.16 (qd, J = 13.2, 3.8 Hz, 1H), 2.00 - 1.87 (m, 1H), 1.83 - 1.39 (m, 5H); ^{13}C NMR (101 MHz, $CDCl_3$) δ 144.8, 129.5 (q, J = 30.2 Hz), 129.3, 127.0 (q, J = 288 Hz), 125.4 (q, J = 3.53 Hz), 124.2 (q, J = 273 Hz), 64.9 (q, J = 22.3), 46.3, 29.1, 26.3, 26.1, 20.3; ^{19}F NMR (565 MHz, $CDCl_3$) δ -69.5, -78.5; FTIR (cm^{-1}): 3307, 2943, 2865, 1166, 1120; GC/MS (EI) 310.1 $(M-H)^+$. HRMS (CI) m/z, calculated for $[C_{14}H_{16}NF_6]^+$: 312.1187; found: 312.1190.

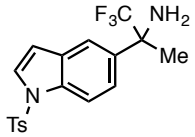

(**2.95**) To a 25 mL round bottom flask equipped with a magnetic stir bar was added α-trifluoromethylnitroalkane **2.67** (100 mg, 242 μmol), Pearlman's catalyst (10 mg, 10 wt %), and methanol (2.42 mL). The flask was equipped with a rubber septum and a needle was inserted into the septum. The flask was placed in a Parr reactor and evacuated and backfilled with H_2 five times. On the last refill, the reactor was sealed at a H_2 pressure of 200 psi. The reactor was placed on a stir plate and the reaction was stirred at rt for 16 h. Once complete, the reactor was vented and the crude reaction was diluted with ethyl acetate, filtered through Celite and concentrated in vacuo. The crude reaction was purified via flash silica chromatography (80:20 hexanes : ethyl acetate) to afford α-trifluoromethylamine **2.95** (60.1 mg, 65%) as a white solid: ^{1}H NMR (400 MHz, $CDCl_3$) δ 7.98 (d, J = 8.9 Hz, 1H), 7.81 - 7.75 (m, 3H), 7.59 (d, J = 3.6 Hz, 1H), 7.55 (d, J = 8.7 Hz, 1H), 7.24 (d, J = 8.3 Hz, 2H), 6.67 (d, J = 3.5 Hz, 1H), 5.48 (d, J = 3.5 Hz, 1H), 4.48 (d, J = 3.6 Hz, 1H), 2.35 (s, 3H), 1.79 (s, 3H); ^{13}C NMR (101 MHz, $CDCl_3$) δ 145.3, 135.3, 134.6, 131.4, 130.9, 130.1, 127.1, 127.0, 126.2 (J = 285 Hz), 123.7, 120.7, 113.5, 109.1, 66.5 (q, J = 23.7 Hz), 21.8, 18.8; ^{19}F NMR (376 MHz, $CDCl_3$) δ -74.1; FTIR (cm^{-1}): 3422, 2923, 1371, 1170, 1132; mp = 93-95 °C; HRMS (LIFDI) m/z calculated for $[C_{18}H_{17}N_2O_2F_3S]^+$: 382.0963; found: 382.1037.

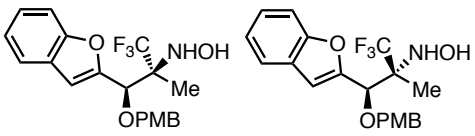

2.84A **93:07** **2.84B**

(**2.84**) To a 50 mL round bottom flask equipped with a magnetic stir bar was added α-trifluoromethylnitroalkane **2.79** (825 mg, 2.0 mmol), Pearlman's catalyst (165 mg, 20 wt %), and methanol (20.0 mL). The flask was equipped with a rubber septum and a needle was inserted into the septum. The flask was placed in a Parr reactor was purged with

H_2 five times. On the last refill, the reactor was sealed at a H_2 pressure of 200 psi. The reactor was placed on a stir plate and the reaction was stirred at rt for 20 h. Once complete, the reactor was vented and the crude reaction was diluted with ethyl acetate, filtered through Celite and concentrated in vacuo. NMR analysis of the crude reaction mixture revealed an 93:07 mixture of syn and anti isomers. The crude reaction was purified via flash silica chromatography (90:10 hexanes : ethyl acetate) to afford α-trifluoromethylhydroxylamine **2.84** (551 mg, 70%) as a white solid: ^{1}H NMR (600 MHz, $CDCl_3$) δ 7.60 (d, J = 6.0 Hz, 1H), 7.52 (d, J = 7.0 Hz, 1H), 7.32 (td, J = 8.4, 7.2, 1.4 Hz, 1H), 7.27 (d, 1H), 7.25 – 7.22 (m, 2H), 6.90 – 6.84 (m, 2H), 6.83 (s, 1H), 5.39 (d, J = 3.5 Hz, 1H), 5.20 (s, 1H), 4.65 (d, J = 3.4 Hz, 1H), 4.56 (d, J = 11.1 Hz, 1H), 4.37 (d, J = 11.1 Hz, 1H), 3.80 (s, 3H), 1.31 (s, 3H). ^{13}C NMR (151 MHz, $CDCl_3$) δ 159.6, 155.3, 153.4, 129.8, 129.3, 127.9, 126.5 (q, J = 288 Hz), 124.7, 123.3, 121.3, 113.9, 111.6, 107.4, 73.8, 71.9, 66.9 (q, J = 24 Hz), 55.4, 13.2. ^{19}F NMR (565 MHz, $CDCl_3$) δ -71.9; FTIR (cm^{-1}): 3282, 2937, 2837, 1612, 1585, 1514, 1613, 1566, 1453, 1251, 752; mp = 97-99 °C; HRMS (ESI) $(M-H)^+$ m/z calculated for $[C_{20}H_{21}NO_4F_3]$: 396.14357; found: 396.14172; Crystals for X-ray analysis were obtained by slow evaporation of diethylether.

2.13.5 Crystal Data and Structure Refinement for 2.74, 2.80, 2.84:

X-ray structural analysis for **2.74**, **2.80** and **2.84**: Crystals were mounted using viscous oil onto a plastic mesh and cooled to the data collection temperature. Data was collected on a Bruker-AXS APEX II DUO CCD diffractometer with Mo-Kα radiation (λ = 0.71073 Å) monochromated with graphite for **2.74** and **2.80**, and with Cu- Kα radiation (λ = 1.54178 Å) focused with Goebel mirrors for **2.84**. Unit cell parameters were obtained from 36 data frames, 0.5º ω, from three different sections of the Ewald

sphere. The systematic absences in the diffraction data are uniquely consistent with Pbca for **2.74**, P21/c for **2.80**, and P21/n for **2.84**. The data-sets were treated with multi-scan absorption corrections.[53] The structures were solved using direct methods and refined with full-matrix, least-squares procedures on F217. Four symmetry unique compound molecules were located in the asymmetric unit of 21 different from each only in C–C and C–N single bond rotations of the –CF3 and –NO2 groups, respectively. All non-hydrogen atoms were refined with anisotropic displacement parameters. The amine H-atoms in **2.74** and **2.84** were located from the electron density difference map and assigned an idealized fixed N-H distance of 0.87(2) Å with Uiso equal to 1.2 Ueq of the attached nitrogen atom. All other hydrogen atoms were treated as idealized contributions with geometrically calculated positions and with Uiso equal to 1.2, or 1.5 for methyl, Ueq of the attached atom. Atomic scattering factors are contained in various versions of the SHELXTL program library.[54] Structural information has been deposited with the Cambridge Structural Crystallographic Centre under depositary numbers CCDC 1411931 for **2.74**, CCDC 1411932 for **2.80**, and CCDC 1532771 for **2.84**.

REFERENCES

(1) (a) Ono, N. *The Nitro Group In Organic Synthesis*; John Wiley And Sons: New York, 2001. (b) Ooi, T.; Takada, S.; Doda, K.; Maruoka, K. *Angew. Chem., Int. Ed.* **2006**, *45*, 7606. (c) Dobish, M. C.; Johnston, J. N. *Org. Lett.* **2010**, *12*, 5744. (d) Grenning, A. J.; Tunge, J. A. *Org. Lett.* **2010**, *12*, 740. (e) Noole, A.; Lippur, K.; Metsala, A.; Lopp, M.; Kanger, T. *J. Org. Chem.* **2010**, *75*, 1313. (f) Noble, A.; Anderson, J. C. *Chem. Rev.* **2013**, *113*, 2887. (g) Qian, H.; Yu, X.; Zhang, J.; Sun, J. *J. Am. Chem. Soc.* **2013**, *135*, 18020. (h) Li, J.; Lear, M. J.; Kawamoto, Y.; Umemiya, S.; Wong, A. R.; Kwon, E.; Sato, I.; Hayashi, Y. *Angew. Chem., Int. Ed.* **2015**, *54*, 12986. (i) Manna, M. S.; Mukherjee, S. *J. Am. Chem. Soc.* **2015**, *137*, 130. (j) Schwieter, K. E.; Johnston, J. N. *Chem. Commun.* **2016**, *52*, 152. (k) Vara, B. A.; Johnston, J. N. *J. Am. Chem. Soc.* **2016**, *138*, 13794. (l) Inoue, F.; Kashihara, M.; Yadav, M. R.; Nakao, Y. *Angew. Chem., Int. Ed.* **2017**, *56*, 13307. (m) Yadav, M. R.; Nagaoka, M.; Kashihara, M.; Zhong, R.-L.; Miyazaki, T.; Sakaki, S.; Nakao, Y. *J. Am. Chem. Soc.* **2017**, *139*, 9423.

(2) Hass, H. B.; Bender, M. L. *J. Am. Chem. Soc.* **1949**, *71*, 1767.

(3) Gildner, P. G.; Gietter, A. A. S.; Cui, D.; Watson, D. A. *J. Am. Chem. Soc.* **2012**, *134*, 9942.

(4) Gietter, A. A. S.; Gildner, P. G.; Cinderella, A. P.; Watson, D. A. *Org. Lett.* **2014**, *16*, 3166.

(5) (a) Gellman, S. H. *Acc. Chem. Res.* **1998**, *31*, 173. (b) Seebach, D.; Gardiner, J. *Acc. Chem. Res.* **2008**, *41*, 1366.

(6) Shimkin, K. W.; Gildner, P. G.; Watson, D. A. *Org. Lett.* **2016**, *18*, 988.

(7) Kirsch, D. P. *Modern Fluoroorganic Chemistry: Synthesis, Reactivity, Applications*; Wiley-VCH: Weinheim, 2013.

(8) (a) Smart, B. E. *J. Fluorine Chem.* **2001**, *109*, 3. (b) Schlosser, M. *Angew. Chem., Int. Ed.* **2006**, *45*, 5432. (c) Müller, K.; Faeh, C.; Diederich, F. *Science* **2007**, *317*, 1881. (d) Hagmann, W. K. *J. Med. Chem.* **2008**, *51*, 4359. (e) Kirk, K. L. *Org. Process Res. Dev.* **2008**, *12*, 305. (f) Purser, S.; Moore, P. R.; Swallow, S.; Gouverneur, V. *Chem. Soc. Rev.* **2008**, *37*, 320.

(9) (a) Black, W. C.; Bayly, C. I.; Davis, D. E.; Desmarais, S.; Falgueyret, J.-P.; Léger, S.; Li, C. S.; Massé, F.; McKay, D. J.; Palmer, J. T.; Percival, M. D.; Robichaud, J.; Tsou, N.; Zamboni, R. *Bioorg. Med. Chem. Lett.* **2005**, *15*, 4741. (b) Aceña, J. L.; Sorochinsky, A. E.; Soloshonok, V. A. *Synthesis* **2012**, *44*, 1591. (c) Turcheniuk, K. V.; Kukhar, V. P.; Roschenthaler, G.-V.; Acena, J. L.; Soloshonok, V. A.; Sorochinsky, A. E. *RSC Advances* **2013**, *3*, 6693. (d) Mei, H.; Xie, C.; Han, J.; Soloshonok, V. A. *Eur. J. Org. Chem.* **2016**, *2016*, 5917. (e) Meyer, F. *Chem. Commun.* **2016**, *52*, 3077.

(10) Wong, D. T.; Bymaster, F. P.; Engleman, E. A. *Life Sci.* **1995**, *57*, 411.

(11) Roman, D. L.; Walline, C. C.; Rodriguez, G. J.; Barker, E. L. *Eur. J. Pharmacol.* **2003**, *479*, 53.

(12) Santi, D. V.; McHenry, C. S. *Proc. Natl. Acad. Sci. U. S. A.* **1972**, *69*, 1855.

(13) Tanaka, Y.; DeLuca, H. F.; Kobayashi, Y.; Ikekawa, N. *Arch. Biochem. Biophys.* **1984**, *229*, 348.

(14) (a) Kim, D.; Wang, L.; Beconi, M.; Eiermann, G. J.; Fisher, M. H.; He, H.; Hickey, G. J.; Kowalchick, J. E.; Leiting, B.; Lyons, K.; Marsilio, F.; McCann, M. E.; Patel, R. A.; Petrov, A.; Scapin, G.; Patel, S. B.; Roy, R. S.; Wu, J. K.; Wyvratt, M. J.; Zhang, B. B.; Zhu, L.; Thornberry, N. A.; Weber, A. E. *J. Med. Chem.* **2005**, *48*, 141. (b) Kim, D.; Kowalchick, J. E.; Edmondson, S. D.; Mastracchio, A.; Xu, J.; Eiermann, G. J.; Leiting, B.; Wu, J. K.; Pryor, K. D.; Patel, R. A.; He, H.; Lyons, K. A.; Thornberry, N. A.; Weber, A. E. *Bioorg. Med. Chem. Lett.* **2007**, *17*, 3373.

(15) (a) Li, C. S.; Deschenes, D.; Desmarais, S.; Falgueyret, J.-P.; Gauthier, J. Y.; Kimmel, D. B.; Léger, S.; Massé, F.; McGrath, M. E.; McKay, D. J.; Percival, M. D.; Riendeau, D.; Rodan, S. B.; Thérien, M.; Truong, V.-L.; Wesolowski, G.; Zamboni, R.; Black, W. C. *Bioorg. Med. Chem. Lett.* **2006**, *16*, 1985. (b) Gauthier, J. Y.; Chauret, N.; Cromlish, W.; Desmarais, S.; Duong, L. T.; Falgueyret, J.-P.; Kimmel, D. B.; Lamontagne, S.; Léger, S.; LeRiche, T.; Li, C. S.; Massé, F.; McKay, D. J.; Nicoll-Griffith, D. A.; Oballa, R. M.; Palmer, J. T.; Percival, M. D.; Riendeau, D.; Robichaud, J.; Rodan, G. A.; Rodan, S. B.; Seto, C.; Thérien, M.; Truong, V.-L.; Venuti, M. C.; Wesolowski, G.; Young, R. N.; Zamboni, R.; Black, W. C. *Bioorg. Med. Chem. Lett.* **2008**, *18*, 923. (c) O'Shea, P. D.; Chen, C.-y.; Gauvreau, D.; Gosselin, F.; Hughes, G.; Nadeau, C.; Volante, R. P. *J. Org. Chem.* **2009**, *74*, 1605.

(16) Lim, J.; Taoka, B.; Otte, R. D.; Spencer, K.; Dinsmore, C. J.; Altman, M. D.; Chan, G.; Rosenstein, C.; Sharma, S.; Su, H.-P.; Szewczak, A. A.; Xu, L.; Yin,

H.; Zugay-Murphy, J.; Marshall, C. G.; Young, J. R. *J. Med. Chem.* **2011**, *54*, 7334.

(17) Verweij, J.; Clavel, M.; Chevalier, B. *Ann. Oncol.* **1994**, *5*, 495.

(18) Ojima, I.; Slater, J. C. *Chirality* **1997**, *9*, 487.

(19) Ojima, I.; Slater, J. C.; Pera, P.; Veith, J. M.; Abouabdellah, A.; Bégué, J.-P.; Bernacki, R. J. *Bioorg. Med. Chem. Lett.* **1997**, *7*, 133.

(20) Umemoto, T.; Kuriu, Y. *Tetrahedron Lett.* **1981**, *22*, 5197.

(21) Feiring, A. E. *J. Org. Chem.* **1983**, *48*, 347.

(22) Knunyants, I. L.; German, L. S.; Rozhkov, I. N. *Bull. Acad. Sci. USSR, Div. Chem. Sci.* **1963**, *12*, 1794.

(23) (a) Kieltsch, I.; Eisenberger, P.; Togni, A. *Angew. Chem., Int. Ed.* **2007**, *46*, 754. (b) Charpentier, J.; Früh, N.; Togni, A. *Chem. Rev.* **2015**, *115*, 650.

(24) Koller, R., ETH, Swiss Federal Institute of Technology, Zurich, 2010.

(25) Kieltsch, I., ETH, Swiss Federal Institute of Technology, Zurich, 2008.

(26) (a) Ma, J.-A.; Cahard, D. *J. Fluorine Chem.* **2007**, *128*, 975. (b) Ma, J.-A.; Cahard, D. *Chem. Rev.* **2008**, *108*, PR1. (c) Studer, A. *Angew. Chem., Int. Ed.* **2012**, *51*, 8950. (d) Barata-Vallejo, S.; Lantaño, B.; Postigo, A. *Chem. - Eur.J.* **2014**, *20*, 16806. (e) Alonso, C.; Martínez de Marigorta, E.; Rubiales, G.; Palacios, F. *Chem. Rev.* **2015**, *115*, 1847. (f) Liu, X.; Xu, C.; Wang, M.; Liu, Q. *Chem. Rev.* **2015**, *115*, 683. (g) Ni, C.; Hu, M.; Hu, J. *Chem. Rev.* **2015**, *115*, 765. (h) Wang, S.-M.; Han, J.-B.; Zhang, C.-P.; Qin, H.-L.; Xiao, J.-C. *Tetrahedron* **2015**, *71*, 7949. (i) Yang, X.; Wu, T.; Phipps, R. J.; Toste, F. D. *Chem. Rev.* **2015**, *115*, 826.

(27) (a) Umemoto, T.; Ishihara, S. *J. Am. Chem. Soc.* **1993**, *115*, 2156. (b) Umemoto, T.; Ishihara, S. *J. Fluorine Chem.* **1998**, *92*, 181. (c) Macé, Y.; Raymondeau, B.; Pradet, C.; Blazejewski, J.-C.; Magnier, E. *Eur. J. Org. Chem.* **2009**, *2009*, 1390. (d) Matoušek, V.; Pietrasiak, E.; Schwenk, R.; Togni, A. *J. Org. Chem.* **2013**, *78*, 6763.

(28) Macé, Y.; Magnier, E. *Eur. J. Org. Chem.* **2012**, *2012*, 2479.

(29) Zhang, C.-P.; Wang, Z.-L.; Chen, Q.-Y.; Zhang, C.-T.; Gu, Y.-C.; Xiao, J.-C. *Angew. Chem., Int. Ed.* **2011**, *50*, 1896.

(30) Zhu, R.; Buchwald, S. L. *Angew. Chem., Int. Ed.* **2013**, *52*, 12655.

(31) Dai, J.-J.; Fang, C.; Xiao, B.; Yi, J.; Xu, J.; Liu, Z.-J.; Lu, X.; Liu, L.; Fu, Y. *J. Am. Chem. Soc.* **2013**, *135*, 8436.

(32) Zhang, C. *Org. Biomol. Chem.* **2014**, *12*, 6580.

(33) (a) Vogl, E. M.; Buchwald, S. L. *J. Org. Chem.* **2001**, *67*, 106. (b) Walvoord, R. R.; Kozlowski, M. C. *J. Org. Chem.* **2013**, *78*, 8859.

(34) Gietter-Burch, A. A. S.; Mitrut, R. E.; Watson, D. A. *Org. Lett.* **2015**, *17*, 5468.

(35) Hayashi, T.; Senda, T.; Ogasawara, M. *J. Am. Chem. Soc.* **2000**, *122*, 10716.

(36) Alam, T. M.; Pedrotty, D. M.; Boyle, T. J. *Magn. Reson. Chem.* **2002**, *40*, 361.

(37) (a) Kathiravan, S.; Nicholls, I. A. *Org. Lett.* **2015**, *17*, 1874. (b) Ramachandran, P. V.; Mitsuhashi, W. *Org. Lett.* **2015**, *17*, 1252.

(38) Fessard, T. C.; Motoyoshi, H.; Carreira, E. M. *Angew. Chem., Int. Ed.* **2007**, *46*, 2078.

(39) (a) Kornblum, N.; Swiger, R. T.; Earl, G. W.; Pinnick, H. W.; Stuchal, F. W. *J. Am. Chem. Soc.* **1970**, *92*, 5513. (b) Kornblum, N. *Angewandte Chemie International Edition in English* **1975**, *14*, 734.

(40) (a) Beckwith, A. L. J.; Bowry, V. W.; Ingold, K. U. *J. Am. Chem. Soc.* **1992**, *114*, 4983. (b) Bowry, V. W.; Ingold, K. U. *J. Am. Chem. Soc.* **1992**, *114*, 4992.

(41) Cheng, Y.; Yuan, X.; Ma, J.; Yu, S. *Chem. - Eur.J.* **2015**, *21*, 8355.

(42) Cheng, Y.; Yu, S. *Org. Lett.* **2016**, *18*, 2962.

(43) Pangborn, A. B.; Giardello, M. A.; Grubbs, R. H.; Rosen, R. K.; Timmers, F. J. *Organometallics* **1996**, *15*, 1518.

(44) Ballini, R.; Barboni, L.; Giarlo, G. *J. Org. Chem.* **2004**, *69*, 6907.

(45) Bobál, P.; Lightner, D. A. *J. Heterocycl. Chem.* **2001**, *38*, 527.

(46) Zhang, H.-Z.; Zhang, H.; Kemnitzer, W.; Tseng, B.; Cinatl, J.; Michaelis, M.; Doerr, H. W.; Cai, S. X. *J. Med. Chem.* **2006**, *49*, 1198.

(47) Budzelaar, Peter H. M.; Moonen, Nicolle N. P.; Gelder, René d.; Smits, Jan M. M.; Gal, Anton W. *Eur. J. Inorg. Chem.* **2000**, *2000*, 753.

(48) Zanon, J.; Klapars, A.; Buchwald, S. L. *J. Am. Chem. Soc.* **2003**, *125*, 2890.

(49) Newkome, G. R.; Kim, H. J.; Moorefield, C. N.; Maddi, H.; Yoo, K.-S. *Macromolecules* **2003**, *36*, 4345.

(50) Ballini, R.; Bosica, G. *Eur. J. Org. Chem.* **1998**, *1998*, 355.

(51) Patt, S. L.; Shoolery, J. N. *J. Magn. Reson.* **1982**, *46*, 535.

(52) Aleksandrowicz, P.; Piotrowska, H.; Sas, W. *Tetrahedron* **1982**, *38*, 1321.

(53) Apex3 software suite; Bruker AXS, I., Madison, WI, 2015.

(54) Sheldrick, G. *Acta Cryst.A* **2008**, *64*, 112.

Chapter 3

NICKEL CATALYZED ENANTIOSELECTIVE *C*-ALKYLATION OF NITROALKANES WITH α-BROMOAMIDES: SYNTHESIS OF β-NITROAMIDES

3.1 Introduction

As discussed in appendix **D**, I have discovered the first enantioselective copper-catalyzed *C*-alkylation of nitroalkanes using an α-bromoamide (**3.1**) as the alkyl electrophile. By utilizing a C_2 symmetric chiral 1,2 diamine ligand (**3.2**), we could produce enantioenriched β-nitroamides (**3.3**) with up to 72% ee and good yield (Figure 3.1). However, we are unable to achieve higher enantioselectivities, which led me to investigate catalysts derived from other first-row transition metals. Such complexes are known to generate transient radicals when treated with simple alkyl halides (see Chapter **1** section **1.3** for detailed discussions).[1] I was particularly cognizant of the recent advances in enantioselective nickel-catalyzed cross-couplings of racemic alkyl halides with carbon nucleophile.[2]

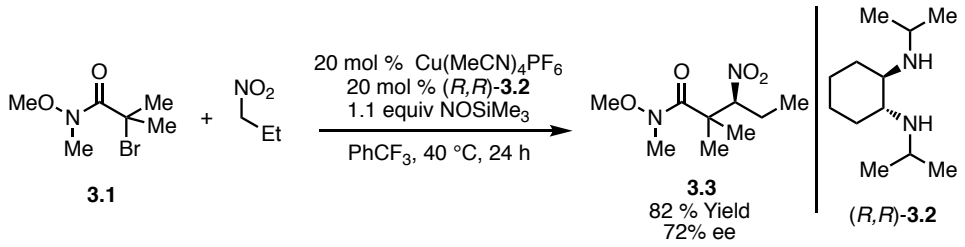

Figure 3.1: Copper-Catalyzed Enantioselective *C*-Alkylation of Nitroalkanes

3.2 Nickel-Catalyzed Enantioselective Reactions Using α-Halocarbonyls As Electrophiles

As discussed in Chapter **1** (section **1.3.1**) nickel is by far the superior metal for the cross coupling of simple alkyl halides with carbon nucleophiles.[3] Seminal reports from Fu and coworkers showed the nickel-catalyzed cross-coupling of secondary alkyl bromides with β-hydrogens and alkylzinc reagents (Chapter **1**, see section **1.3.1**). This report is ground breaking, because it opened the door to asymmetric synthesis of tertiary stereocenters.[4] Towards this end, the Fu group have published the first nickel-catalyzed enantioselective Negishi-type cross-coupling reaction between activated alkyl electrophiles such as the racemic secondary α-bromoamide (**3.4**) and organozinc reagent (**3.5**). Thus, a chiral nickel/pybox (**3.6**) catalyst achieves an array of alkyl-alkyl couplings with excellent enantioselectivity and excellent yield (**3.7**) (Figure 3.2).

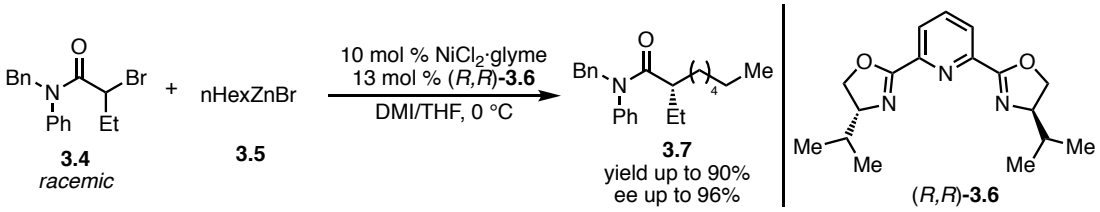

Figure 3.2: Fu's Pioneering Studies on Enantioselective Cross-Coupling Between α-bromoamide and Alkylzinc Reagents.

The fact that both yield and ee's are high suggests that this is not a kinetic resolution in which the chiral catalyst selectively reacts with one enantiomer of the electrophile and leaves the other enantiomer unreacted; instead, it is an

enantioconvergent reaction in which both enantiomers of the racemic starting material are converted into a single enantiomer of desired product (Figure 3.3).

Fu suggests that the electrophile probably undergoes a radical oxidative addition[5] in which both enantiomers of the racemic alkyl halide are converted through a common planar radical intermediate (**3.8**). This radical (**3.8**), combines with an enantiopure nickel catalyst (Cat*) to afford a single enantiomer of an alkylmetal complex (**3.9**), which proceed to form a single enantiomer of the desired product (**3.10**).[6]

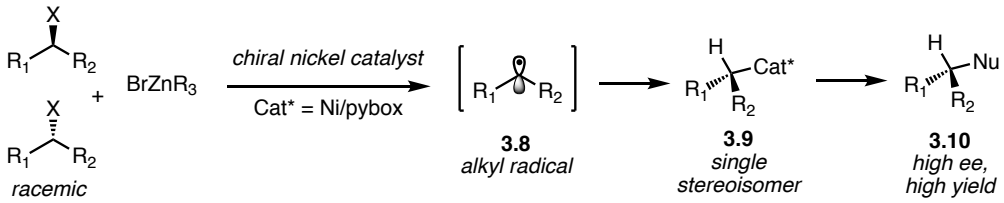

Figure 3.3: Fu's Enantioconvergent Cross-Coupling via a Radical Intermediate

In 2010, Fu and coworkers, reported the first nickel-catalyzed enantioselective cross-coupling between activated alkyl electrophile such as racemic secondary α-chloroamide (**3.11**) and organoboron reagent (Figure 3.4). By utilizing a chiral nickel/1,2-diamine (**3.12**) catalyst, a wide variety of tertiary α-arylcarbonyl compounds (**3.13**) can be synthesized with excellent enantioselectivities and yields.[7] In addition, the amide products can be easily transformed into enantioenriched α-arylcarboxylic acids without erosion of the ee. However, scope with respect to activated alkyl electrophile and nucleophiles is limited. α-Chloroamides other than

indoline amides and alkyl boronic acids are not suitable coupling partners under these reaction conditions.

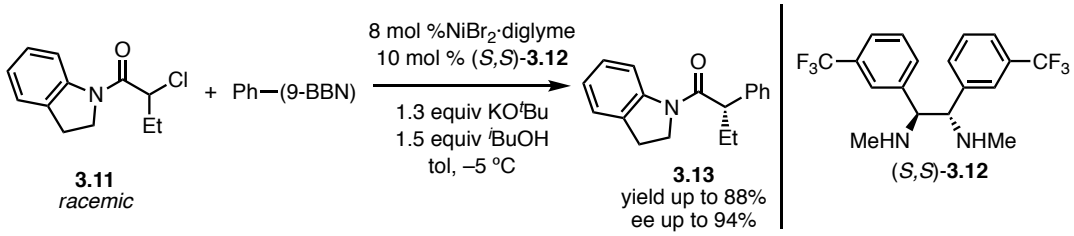

Figure 3.4: Fu's Studies on Enantioselective Cross-Coupling Between α-Chloroamide and Organoboron Reagents.

3.3 Discovery and Optimization of Enantioselective Nickel-Catalyzed *C*-Alkylation of Nitroalkanes with α-bromoamides

Early in the initial optimization of our *C*-alkylation conditions when using benzyl bromides and 1-nitropropane, Dr. Peter Gildner observed modest reactivity when using bis(1,5-cyclooctadiene) nickel (0) ($Ni(COD)_2$) and cyclohexyl 1,2-diamine (**3.14**) as a precatalyst. Ultimately, optimization was continued with the superior copper (I) bromide (Table 3.1) and further investigation of nickel catalyst in these systems was not pursued.

Table 3.1: Comparing Copper and Nickel Catalyst with Diamine ligand

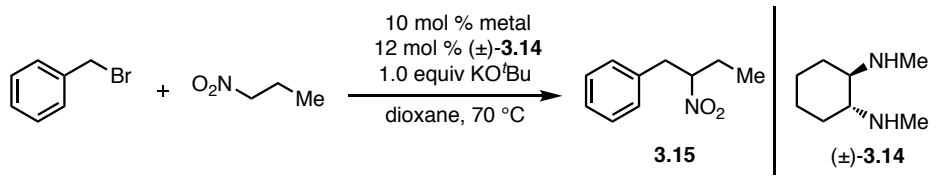

Entry	Metal	Yield 3.15

1	CuBr	43%
2	$Ni(COD)_2$	12%

However, the similar structure of the activated α-haloamide substrates in the enantioselective nickel-catalyzed work of the Fu group (section **3.2**) to the α-bromocarbonyls suitable for our *C*-alkylation conditions, as well as their use of chiral 1,2-diamines led me to further examine nickel as a potential catalyst in the enantioselective transformations.

Table 3.2: Investigating Nickel Catalysts in the *C*-Alkylation of Nitroalkanes

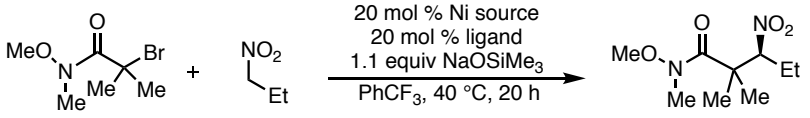

3.1 **3.3**

Entry	Ni source	Ligand	Yield 3.3[a]	ee 3.3[b]
1	$NiBr_2$·diglyme	3.16	22%	60%
2	$NiBr_2$·diglyme	3.17	12%	71%
3[c]	$NiBr_2$·diglyme	3.17	9%	73%
4	$Ni(COD)_2$	3.17	40%	63%

[a] Yields determined by ^1H NMR using 1,3,5-trimethoxybenzene as an internal standard.

[b] ee determined by HPLC using a chiral stationary phase [c] 40 mol % Zn powder added

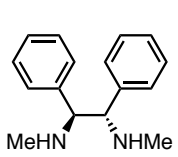

(*S,S*)-**3.16**

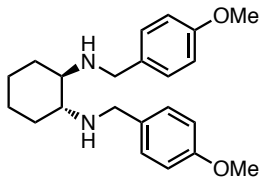

(*R,R*)-**3.17**

Towards this end, I used nickel (II) bromide with (*1R,2R*)-*N,N′*-dimethyl-1,2-diphenylethane-1,2-diamine (**3.16**) in the enantioselective *C*-alkylation of 1-

nitropropane with α-bromo Weinreb amide (**3.1**). Despite a modest yield I observed, (22%) of the C-alkylated product (**3.3**), significant enantioselectivity of 60% ee (Table 3.2, entry 1). Importantly, this is the first example of asymmetric nickel-catalyzed *C*-alkylation of nitroalkanes. Switching it to cyclohexyl 1,2-diamine ligand (**3.17)**, which had promise in the copper-catalyzed conditions, led to increased enantioselectivity with slightly diminished yield (entry 2). Addition of catalytic amount of zinc powder as a internal reductant to reduce Ni(II) to Ni(0) did not significantly alter the reactivity (entry 3).[8] However, using Ni(0) precatalyst such as $Ni(COD)_2$ led to improved yields with only slight decrease in the enantioselectivity (entry 4).

3.4 Initial Experiments with DBU as the Base

Optimizing the reaction condition with $Ni(COD)_2$ in conjunction with chiral diamine (**3.17**) as the ligand, I observed improved yields of β-nitroamides (**3.3**) when using the organic base 1,8-diazabicycloundec-7-ene (DBU) (Table 3.3 Entry 2). Lower temperatures led to increased reactivity and higher enantioselectivity (Table 3.3, Entry 3).

Table 3.3: Discovery of DBU as the Base in the Nickel-Catalyzed Enantioselective *C*-Alkylation of Nitroalkanes

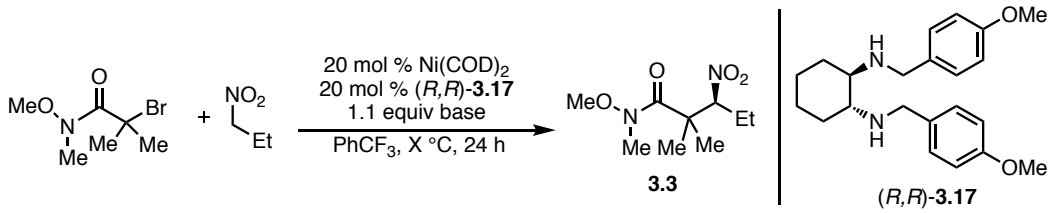

Entry	Base	T °C	Yield 3.3[a]	ee 3.3[b]
1	$NaOSiMe_3$	40	40%	63%
2	DBU	40	60%	62%

3	DBU	–20	78%	73%

[a] Yields determined by ^{1}H NMR using 1,3,5-trimethoxybenzene as an internal standard.

[b] ee determined by HPLC using a chiral stationary phase

3.4.1 Electronic Effect in the Nickel-Catalyzed *C*-Alkylaiton of Nitroalkanes

I carried out further optimization using DBU as the base as it produced the desired product **3.3** in 78% yield with 73% ee. The modular nature of the C_2-symmetric chiral 1,2-diamine allowed me to study the linear free energy relationship (LFER) for the enantioselective nickel-catalyzed *C*-Alkylation of nitroalkanes.

Table 3.4: Examining Electronic Effect in the Nickel-Catalyzed C-Alkylation of Nitroalkanes

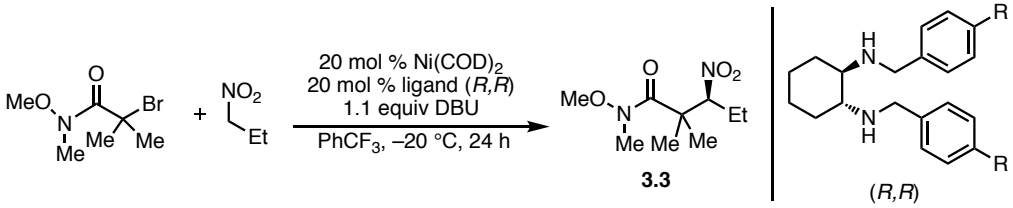

Entry	R	Ligand	Yield 3.3[a]	ee 3.3[b]	σ_{para}
1	MeO	3.17	72%	71%	–0.27
2	Me	3.18	78%	69%	–0.14
3	H	3.19	68%	64%	0
4	CF_3	3.20	77%	54%	0.53

[a] Yields determined by ^{1}H NMR using 1,3,5-trimethoxybenzene as an internal standard.

[b] ee determined by HPLC using a chiral stationary phase

Towards this end, LFER analysis revealed a correlation between ligand electronic variation and enantioselectivity (Table 3.4).[9] To quantify this electronic effect, Hammett σ-parameters, derived from the acidities of substituted benzoic acid were used.[10] The σ_{para} value of the substitutents in the chiral 1,2-diamine ligand was plotted against the enantioselectivity of the product (**3.3**) and the Hammett plot was

found to be linear with a negative ρ value, indicating that electron-donating ligand (**3.17**) gave high enantioselectivity and buildup of positive charge in the rate determining step was stabilized by the ligand (**3.17**) (Figure 3.5).

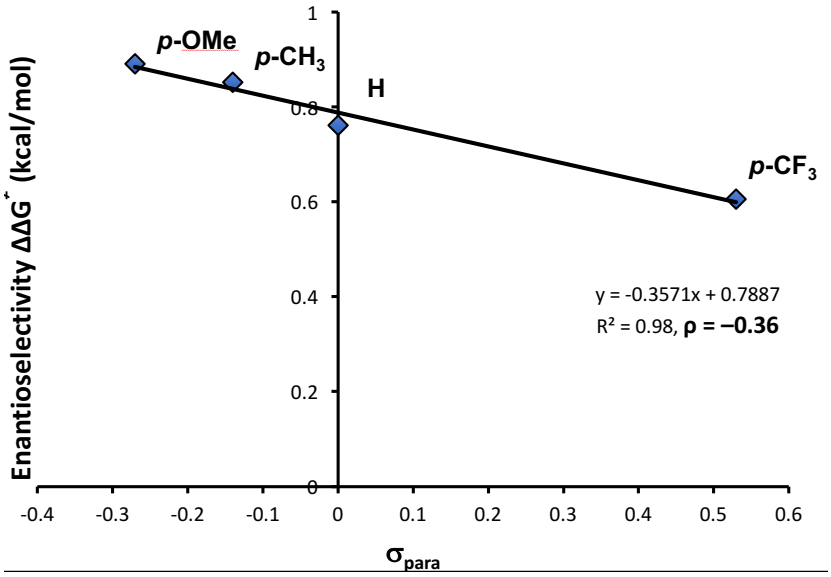

Figure 3.5: Hammett Plot of Enantioselective as a Function of Ligand Electronics

3.4.2 Origin of Enantioselectivity in the Nickel-Catalyzed *C*-Alkylation of Nitroalkanes

In an effort to understand the origin of enantioselectivity in the nickel-catalyzed *C*-alkylation reactions, I was wondering if the N–H bonds in the chiral 1,2-diamine ligand may be crucial for the observed enantioselectivity. To test this hypothesis, I designed and synthesized ligand (**3.21**) and (**3.22**) which has one and zero N–H bond, and tested this ligand in the enantioselective reaction. Although the ligand lacking N–H bonds provided similar level of catalytic activity (60% yield) only the ligand bearing N–H bond provided enantioselection. This potentially suggests that

the N–H bond of the chiral ligand is involved in the enantiodetermining step, by organizing the transition state via complex hydrogen bond with the substrates to produce good enantioselectivity (Figure 3.6).

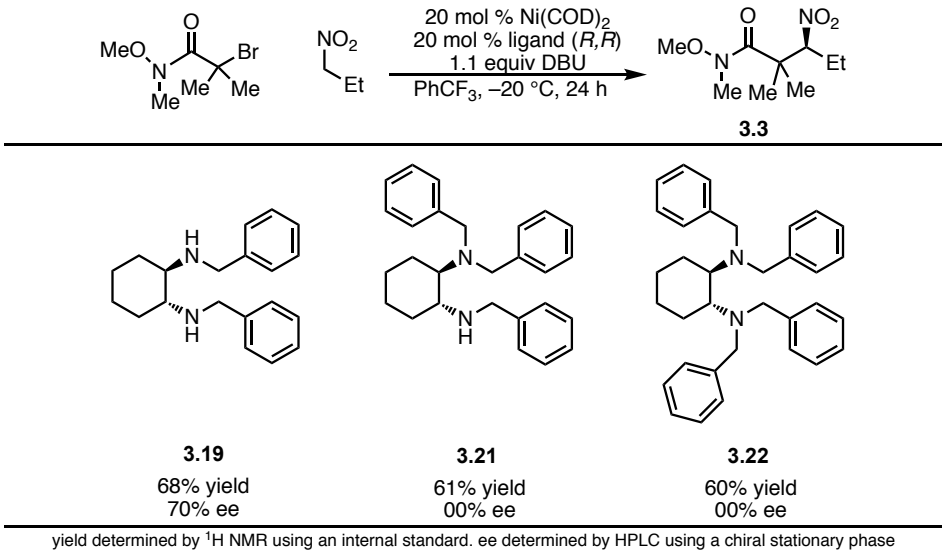

Figure 3.6: Role of N–H bonds in the Enantioselective *C*-Alkylation of Nitroalkanes

3.4.3 Examination of Chiral 1,2-diamine Ligands Under DBU Conditions

In order to increase the enantioselectiviy of the reaction, I studied the effect of substitution at the 3,5 position of the aryl ring in the chiral 1,2 diamines (**3.19**) under our nickel-catalyzed conditions using DBU as the base. The derivatives bearing electron donating group (Me, **3.23**) in the 3,5 position of the aryl ring provided products showing high enantioselectivity and comparable reactivity to the unsubstituted ligand (**3.19**). Interestingly, the sterically encumbered ligand (^{t}Bu, **3.24**) further enhanced the enantioselectivity and reactivity. However, further increasing the steric bulk (2,6-phenyl, **3.25**) did not increase the ee's. The chiral ligand (**3.24**) is the

optimal ligand for the *tert*-α-bromo Weinreb amide (**3.1**) substrate giving the product (**3.3**) in 80% ee with 78% yield.

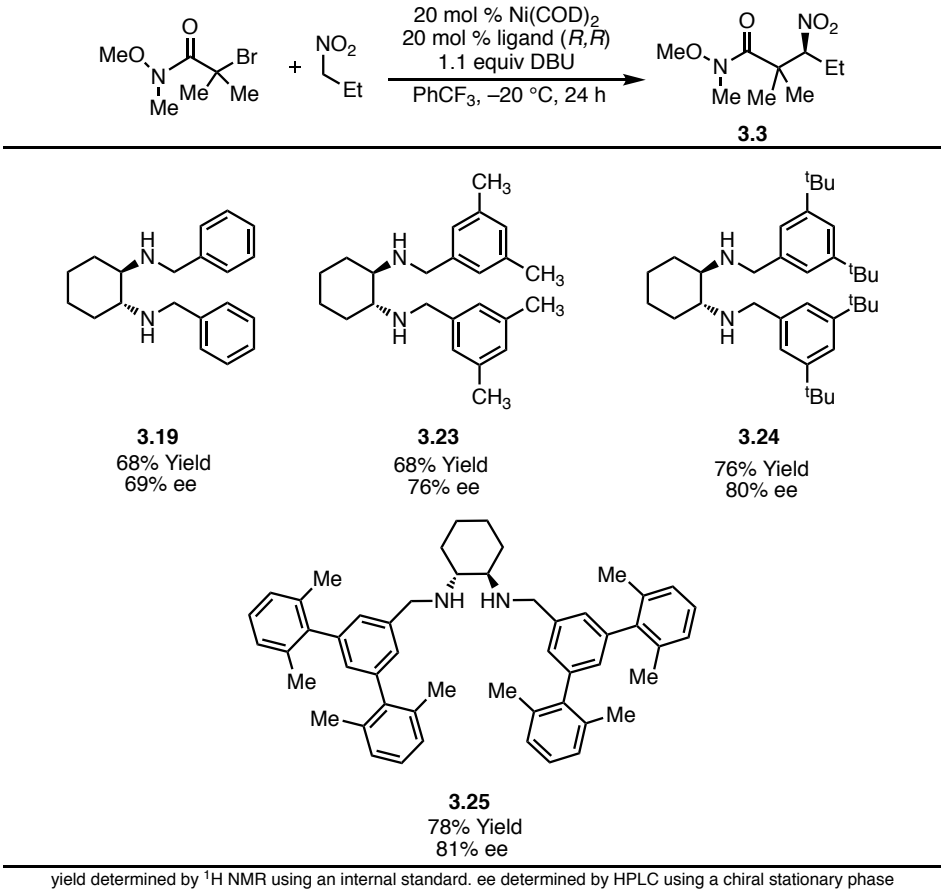

Figure 3.7: Steric Effect in the 3,5-position of Chiral 1,2 diamines

3.4.4 Activated Secondary Alkyl Electrophile as Coupling Partners

As discussed in section 3.4.3, chiral nickel/1,2-diamine catalyst (**3.24**) could differentiate the faces of the prochiral nitronate anion and couples with achiral *tert*-α-bromo Weinreb amide (**3.1**) giving 80% ee with 78% yield of the desired product (**3.3**). Next, I wanted to examine the alkylation of more interesting and useful racemic,

sec-α-bromo Weinreb amide (**3.26**) with achiral nitronate anion under the DBU conditions. This class of secondary alkyl electrophiles, when coupled with nitronate anion, sets two adjacent stereocenters and opens the door to control both absolute and relative stereochemistry of the desired β-nitroamide products. Significantly, the resulting enantioenriched β-nitroamides from the reaction can be used as nucleophiles in conjugate addition,[11] trifluoromethylation,[12] or Tsuji Trost allylation reactions[13] to set enantioenriched, congested, fully substituted nitrogen centers which cannot be access by nitro-Mannich reactions.[14]

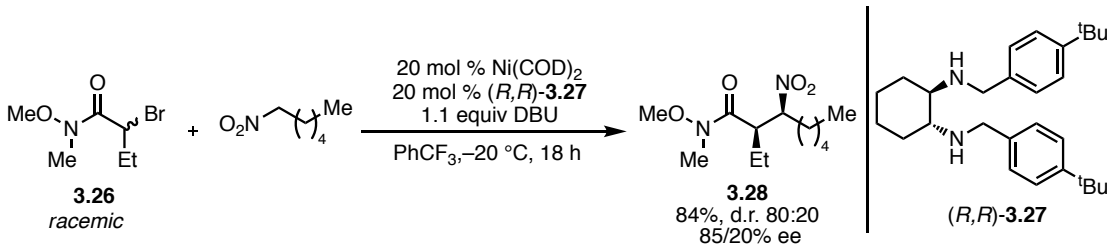

Figure 3.8: First Example of Nickel-catalyzed Enantioselective C-Alkylation of Nitroalkanes Using Racemic Secondary Alkyl Electrophile

Gratifyingly, the racemic sec-α-bromo Weinreb amide (**3.26**) couples with the prochiral 1-nitrohexane in the presence of chiral nickel/1,2-diamie catalyst (**3.27**) afforded (**3.28**) in 82% yield as a mixture of diastereomers (80:20 *syn:anti*). Enantioenrichment was observed for both the diastereomers with 85% ee for the major *syn* diastereomer and 20% ee for the minor *anti* diastereomer (Figure 3.8). Significantly, this is the first example where the chiral nickel catalyst controls both absolute and relative stereochemistry in the *C*-alkylation of nitroalkanes using racemic secondary activated alkyl electrophiles.

Even though the desired β-nitroamide (**3.28**) was produced in good diastereo- and enantioselectivity, the results were inconsistent. After several runs of the reaction, depicted in Table 3.5, the enantioselectivity and diastereoselectivity could not be reproduced, suggesting that β-nitroamide (**3.28**) was not stable under the reaction condition using DBU as the base (Table 3.5, entry 1-4).

Table 3.5: Inconsistent Results Using DBU as the Base

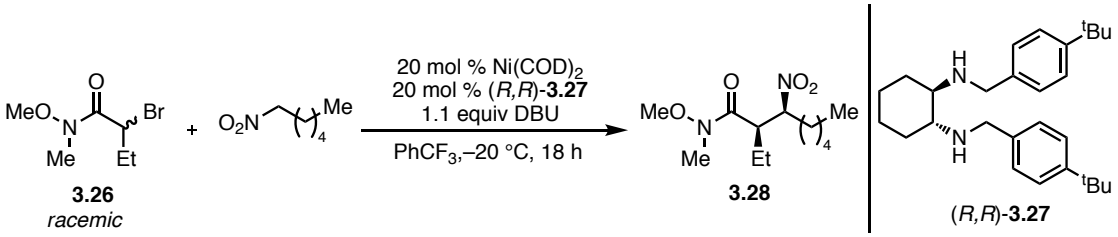

Entry	Run	Yield 3.28[a]	d.r 3.28 *syn:anti*	ee 3.28[b] *syn/anti*
1	A	62%	74:26	77/40%
2	B	64%	63:36	62/58%
3	C	65%	74:26	81/32%
4	D	69%	80:20	80/42%

[a] Yields determined by ^{1}H NMR using 1,3,5-trimethoxybenzene as an internal standard.

[b] ee determined by HPLC using a chiral stationary phase

In an effort to study the kinetic stability of the *syn* and *anti* diastereomers of β-nitroamide (**3.28**), I subjected the racemic, *syn* diastereomer (**3.28**) to our nickel-catalyzed enantioselective alkylation reaction using *tert*-α-bromo Weinreb amide (**3.1**) as electrophile and 1-nitropropane as nucleophile. Disappointingly, the racemic, *syn* diastereomer (**3.28**) was epimerized to mixture of diastereomers (*syn:anti* 61:39)

(Figure 3.8, top) and similar results were obtained on subjecting racemic, *anti* diastereomer (**3.28**) to the reaction conditions (Figure 3.8, bottom).

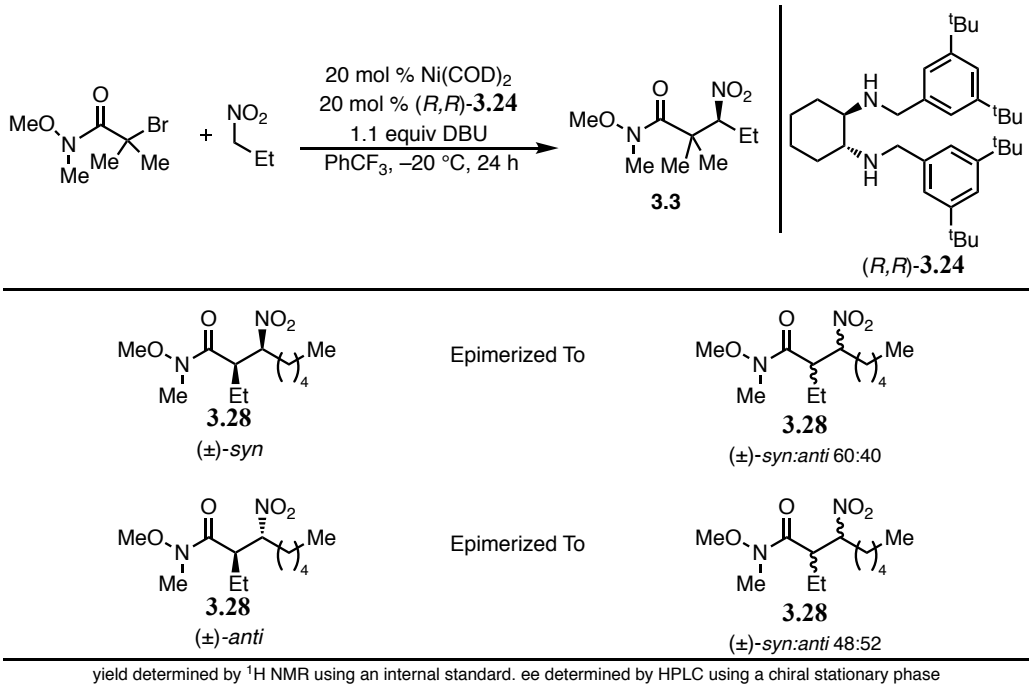

Figure 3.8: Epimerization Studies

Based on my previous deprotonation studies between DBU (pK'_a ~12 in H_2O) and nitroalkanes (pK_a ~10 in H_2O) using ^1H NMR spectroscopy, the deprotonation event is slow, taking about 10 minutes for a 2:1 mixture of nitroalkane and nitronate anion to reach equilibrium at –25 °C (see chapter 2, section 2.11.2 for more details) (Figure 3.9).[12] Under our working mechanistic hypothesis, there would be a significant concentration of soluble DBU base and soluble nitronate anion under the homogeneous reaction conditions. Presumably, the soluble DBU deprotonates the

formed enantioenriched β-nitroamide (**3.28**) slowly, consequently the products lose its configurational integrity.

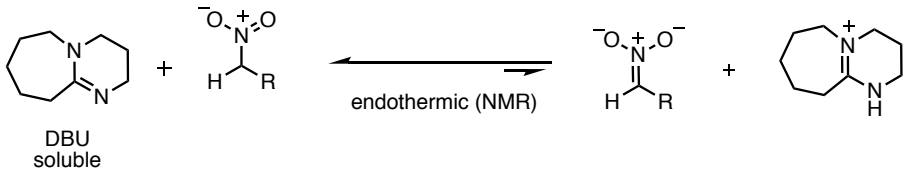

Figure 3.9: Rationalization for Epimerization of β-nitroamide **3.28**

To circumvent this epimerization issue, we reasoned that utilizing a much stronger base than DBU, such as metal alkoxides, might prove useful because the metal alkoxides (pK'_a ~17 in H_2O) would quantitatively deprotonates the nitroalkane (pK_a ~10 in H_2O) generating weakly basic metal nitronate anions which are sparingly soluble in the non-polar reaction media (Figure 3.10). Importantly, the heterogeneous reaction media might prevent the formed enantioenriched β-nitroamide (it would be in the solution phase) from epimerization as the weakly basic metal nitronate anion would be in the solid phase.

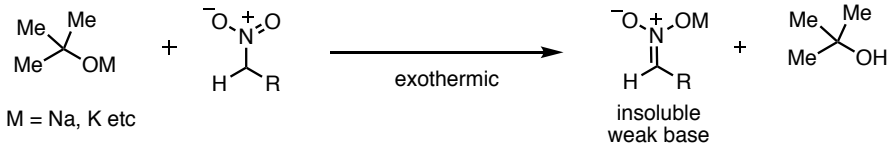

Figure 3.10: Proposed Metal Alkoxide Base in the Nickel-Catalyzed Enantioselective *C*-Alkylation of Nitroalkanes

3.5 Identification of Metal Alkoxide Bases and Optimization

Towards this end, I examined a few metal alkoxide bases under our nickel-catalyzed enantioselective *C*-alkylation conditions. The racemic, sec-α-bromo Weinreb amide (**3.26**) couples with the prochiral 1-nitrohexane in the presence of lithium *tert*-butoxide and nickel/1,2-diamine catalyst (**3.27**) affording (**3.28**) in 17% yield, 71:29 d.r with 0% enantioselectivity. By switching to a larger counter ion bearing metal alkoxide, such as sodium *tert*-butoxide, produces the product (**3.28**) in 31% yield with 49% ee and 77:23 d.r (Table 3.6 entry 2). Potassium *ter*t-butoxide was found to be more effective than sodium *ter*t-butoxide (Table 3.6 entry 3). It is interesting to note that lithium and sodium alkoxide did not induce enantioselectivity in the copper catalyzed enantioselective *C*-alkylation of nitroalkanes (Appendix **D**, section **D.7** and **D.8**) using chiral 1,3 diketimine ligand **D.15.**

Table 3.6: Investigation of Metal Alkoxide Bases

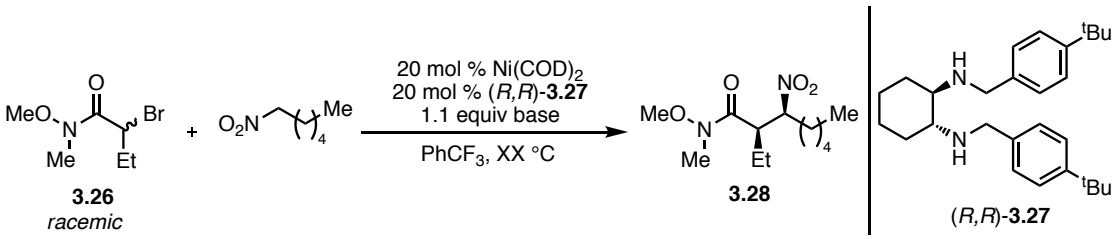

Entry	Base	T °C	Yield 3.28[a]	d.r 3.28 *syn:anti*	ee 3.28[b] *syn/anti*
1	LiO^{t}Bu	–20	17%	71:29	00/00%
2	NaO^{t}Bu	–20	31%	77:23	49/28%
3	KO^{t}Bu	–20	51%	75:25	58/32%
4	KO^{t}Bu	–20	53%	76:24	58/31%
5	KO^{t}Bu	rt	53%	80:20	77/40%

[a] Yields determined by ^{1}H NMR using 1,3,5-trimethoxybenzene as an internal standard.

[b] ee determined by HPLC using a chiral stationary phase

Significantly, the results were reproducible using potassium *ter*t-butoxide as the base and this suggests that the enantioenriched β-nitroamide (**3.28**) does not epimerize under the reaction conditions (Table 3.6 entry 4). Room temperature was found to be effective, giving product in 53% yield, 77% ee and 80:20 d.r. After the identification of potassium *ter*t-butoxide as the base, I wanted to extensively study the reaction conditions using a wide variety of ligand scaffolds, bases, solvents, different α-bromo carbonyls, etc to improve reactivity, diastereo- and enantioselectivity.

I screened several solvents under the new heterogeneous reaction condition using potassium *ter*t-butoxide as the base. The polar aprotic solvent such as dimethyl acetamide (DMA) gave poor diastereoselectivity of the desired product (**3.28**) (Table 3.7 entry 1), halogenated solvent such dichloromethane (DCM) gave slightly better d.r and enantioselectivity (Table 3.7 entry 2), non-polar solvents such as benzene increased the diastereoselectivity to 82:18 with comparable enantioselectivity to DCM. Finally, weakly coordinating solvent such as diethyl ether found to be optimal solvent affording 45% yield with 70% ee for the major *syn* diastereomers and 90:10 d.r (Table 3.7 entry 4). Further optimization was carried out using Et_2O as the solvent.

In our previous reaction conditions for the enantioselective *C*-alkylation reaction using DBU as the base, high catalyst loading was required. By reducing the catalyst loading, the enantioselectivity and reactivity significantly reduced. However, using potassium *tert*-butoxide as the base at lower catalyst loading, enantio- and diastereoselectivity were increased (Table 3.7 entry 5-7). Further optimization was carried out using 5 mol % $Ni(COD)_2$ as the precatalyst.

Table 3.7: Optimization of Solvent and Catalyst Loading

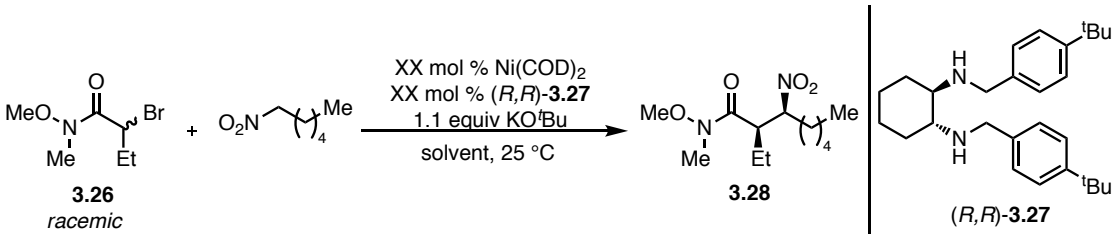

Entry	Solvent	Catalyst Loading	Yield 3.28[a]	d.r 3.28 *syn:anti*	ee 3.28[b] *syn/anti*
1	DMA	20 mol %	53%	55:45	56/24%
2	DCM	20 mol %	60%	67:33	70/30%
3	benzene	20 mol %	48%	82:18	70/28%
4	Et_2O	20 mol %	45%	90:10	70/52%
5[c]	Et_2O	20 mol %	51%	85:15	72/10%
6[c]	Et_2O	10 mol %	60%	87:13	76/10%
7[c]	Et_2O	5 mol %	53%	87:13	77/10%

[a] Yields determined by ^1H NMR using 1,3,5-trimethoxybenzene as an internal standard.

[b] ee determined by HPLC using a chiral stationary phase [c] (*R,R*)-**3.29** was used as ligand

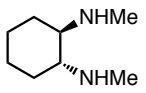

(*R,R*)-**3.29**

I performed a brief ligand study in the nickel-catalyzed enantioselective *C*-alkylation of nitroalkanes using newly identified base, solvent and catalyst loading. Towards this end, I found derivatives bearing electron donating group (Me, **3.23**) in the 3,5 position of the aryl ring provided products showing comparable enantioselectivity and yield and slightly higher diastereoselectivity than the unsubstituted ligand (**3.19**). Significantly, CF_3 group (**3.30**), which is sterically bigger than methyl group and also inductively electron withdrawing group increased the

enantioselectivity of the product (**3.28**) to 80% with 72% yield and 80:20 d.r. (Figure 3.11). It is interesting that in our previous copper (appendix **D** Section **D.11.2**) and nickel/DBU enantioselective condition (section 3.4.3), electron rich chiral 1,2 diamines found to be effective. However, with the new heterogeneous reaction condition with stronger metal alkoxide base electron deficient diamine ligand was found to effective. Further optimization of the nickel-catalyzed enantioselective reaction was carried out using electron deficient chiral diamine ligand **3.30**.

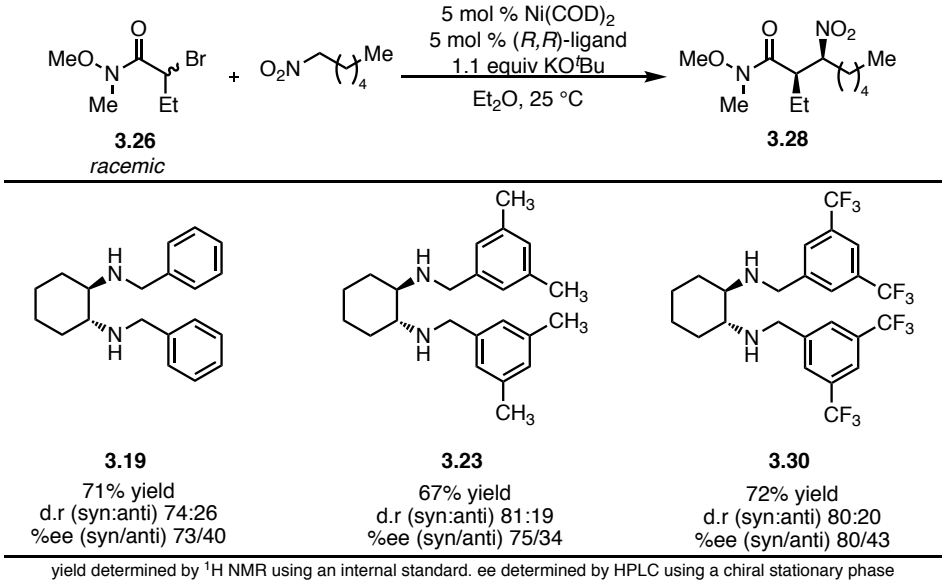

Figure 3.11: Identification of Electron Deficient Ligand **3.30**

Although Weinreb amides are synthetically useful, the enantioselectivity could not be achieved beyond 80% so I tested a few α-bromoamide bearing electronically different amide backbone. These studies found that β-nitroamides were produced in good enantioselectivity. For example, using 1-nitropropane as a nucleophile the

electron rich, secondary α-bromoamide (**3.31**) produced desired product (**3.32**) in 82% ee with 74:26 d.r and 74% yield. Significantly, the *N*-benzyl-*N*-phenyl amide (**3.33**) afforded (**3.34**) in 84% ee with 77:23 d.r and 84% yield (Figure 3.12). To further enhance the enantioselectivity, the *N*-benzyl-*N*-phenyl amide (**3.34**) was choosen as the optimal substrate for the further optimization.

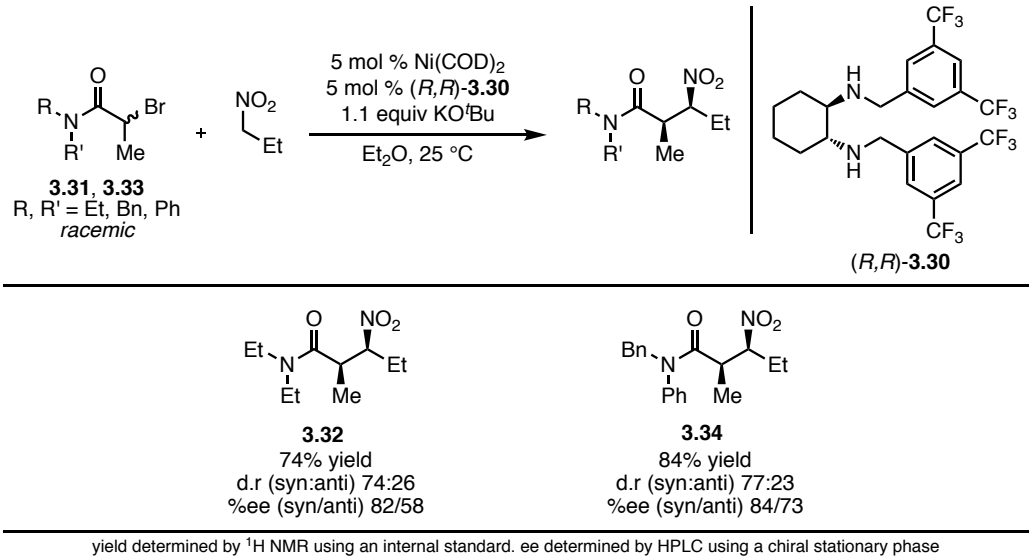

yield determined by ^{1}H NMR using an internal standard. ee determined by HPLC using a chiral stationary phase

Figure 3.12: Examination of Amide Backbone in the Nickel-Catalyzed Enantioselective *C*-Alkylation of Nitroalkanes

3.6 Optimization of Reaction Conditions using *N*-Benzyl-*N*-Phenyl Amide as a Model Substrate

After identifying *N*-benzyl-*N*-phenyl amide (**3.33**) as a model substrate, I was interested in examining the role of base under these new catalytic reaction conditions. Since potassium *tert*-butoxide produced 84% ee of the β-nitroamides (**3.34**) with the *N*-benzyl-*N*-phenyl amide (**3.33**), I screened several potassium bases which bear smaller anions than *tert*-butoxide. Potassium ethoxide produced (**3.34**) in 89% ee with

74:26 d.r and 85% yield (Table 3.8 entry 2). The potassium methoxide produced comparable results as the potassium ethoxide (Table 3.8 entry 3). Switching to LiOMe decreased the yield and enantioselectivity (Table 3.8 entry 4), however NaOMe produced 88% ee with 81:19 d.r and 74% yield (Table 3.8 entry 5). Although, potassium bases were found to be superior to NaOMe, I realized the yields with potassium bases were not consistent. Consequently, I choose NaOMe as the optimal base for further optimization.

Table 3.8: Role of Smaller Counter-Anion Bases

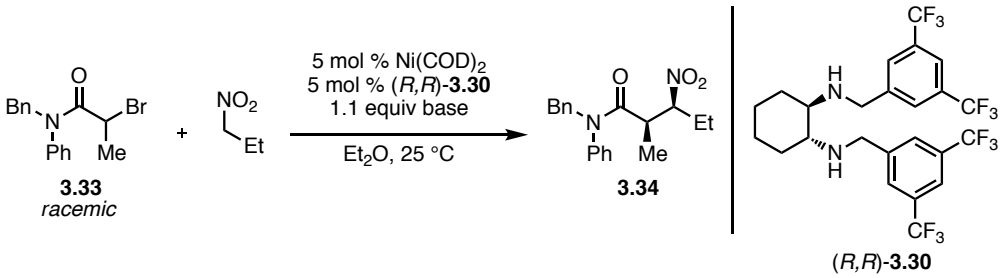

Entry	Base	Yield 3.34[a]	d.r 3.34 *syn:anti*	ee 3.34[b] *syn/anti*
1	KO^{t}Bu	84%	77:23	84/73%
2	KOEt	85%	76:24	89/77%
3	KOMe	87%	77:23	89/78%
4	LiOMe	17%	76:24	37/11%
5	NaOMe	74%	81:19	88/78%

[a] Yields determined by ^{1}H NMR using 1,3,5-trimethoxybenzene as an internal standard.

[b] ee determined by HPLC using a chiral stationary phase

3.6.1 Examination of Diverse Chiral Bidentate Nitrogen Ligands

After identifying Ni(COD)$_2$, NaOMe, Et$_2$O and *N*-benzyl-*N*-phenyl amide (**3.33**) amide as optimal reaction components for the enantioselective *C*-alkylation of

nitroalkanes, I next undertook extensive studies of ligand architecture to increase the enantioselectivity beyond 88%. Especially, I was interested in studying several chiral bidentate nitrogen ligands that haven't been examined under our new nickel-catalyzed enantioselective *C*-alkylation conditions. These classes of ligands have been extensively utilized in enantioselective C–C bond forming reactions[2b] and it has showed promising results in our earlier copper-catalyzed enantioselective *C*-alkylation of nitroalkanes (see Appendix **D** section **D.11.5** for more discussions).

Towards this end, using racemic, secondary amide (**3.33**) and 1-nitropropane as a model substrates several chiral bidentate nitrogen ligands have been tested under enantioselective *C*-alkylation reaction condition (Figure 3.13). The bis(oxazoline) BOX ligand (**3.35**) and pyBOX (**3.36**) ligands, which have been used in several enantioselective nickel-catalyzed radical reactions,[2a] were found to be ineffective. The C_2 symmetric chiral 1,2 diamine (**3.16**) gave 83% ee with 85:15 d.r albeit with low yield. The (*R,R*)-*N*,*N*'-ethylenebis(1-phenylethylamine) (**3.37**) gave excellent reactivity with 78% ee and 73:27 d.r. In contrast, the chiral cyclohexyl 1,2 diamine (**3.29**), gave 44% yield with slight increase in the enantio and diastereoselectivity compared to ligand (**3.16**). The benzyl substituted cyclohexyl diamine ligand (**3.19**) produced β-nitroamides (**3.34**) in 60% yield with similar enantio- and diastereoselectivity as ligand (**3.29**). After examining a variety of chiral bidentate nitrogen ligands, I found chiral 1,2 diamine scaffold (**3.19**) to be optimal ligand architecture for the nickel-catalyzed enantioselective *C*-alkylation of nitroalkanes for the synthesis of enantioenriched β-nitroamides.

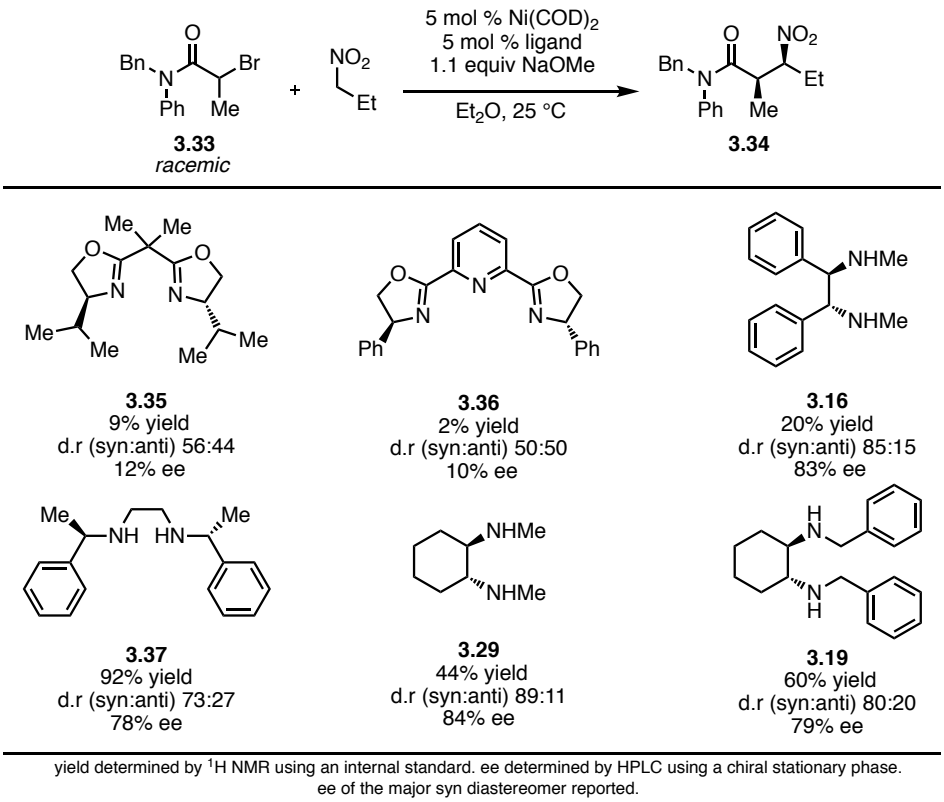

Figure 3.13: Diverse Chiral Bidentate Nitrogen Ligands in the Nickel-Catalyzed *C*-Alkylation of Nitroalkanes

As discussed in section 3.5 the new heterogeneous reaction condition with stronger metal alkoxide base and electron deficient diamine ligand (**3.30**) was found to be effective. To further enhance the enantioselectivity, I designed and synthesized several substituted derivatives of chiral diamine ligand (**3.19**) that bears electron withdrawing group in the phenyl ring. For example, the derivatives bearing electron withdrawing group (CF_3 **3.20** and **3.38**) in the *para* and *meta*-position gave similar diastereoselectivity and yield, however the ligand (**3.38)** which bears CF_3 group in the meta position gave slightly higher ee. The CF_3 substitution at the 3,5 position of the aryl ring produced 88% ee with 82:18 d.r and 74% yield (Figure 3.14).

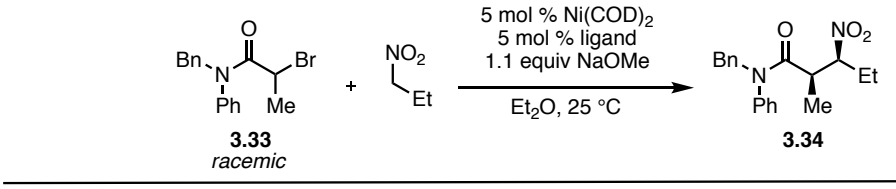

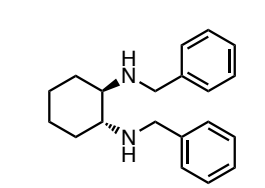

3.19
60% yield
d.r (syn:anti) 80:20
79% ee

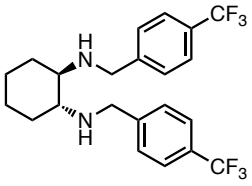

3.20
63% yield
d.r (syn:anti) 81:19
80% ee

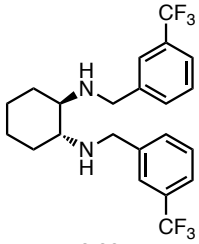

3.38
58% yield
d.r (syn:anti) 79:21
82% ee

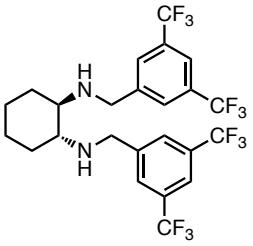

3.30
74% yield
d.r (syn:anti) 82:18
88% ee

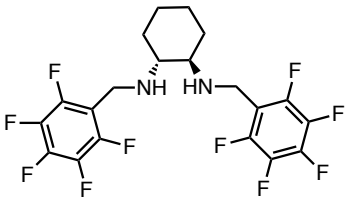

3.39
16% yield
d.r (syn:anti) 70:30
86% ee

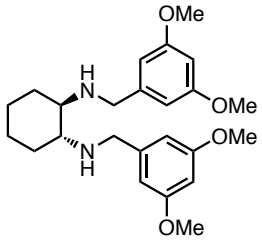

3.40
64% yield
d.r (syn:anti) 85:15
86% ee

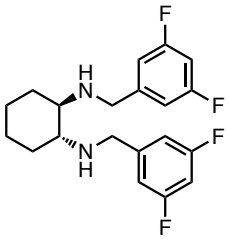

3.41
57% yield
d.r (syn:anti) 81:19
80% ee

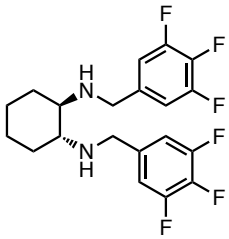

3.42
57% yield
d.r (syn:anti) 81:19
80% ee

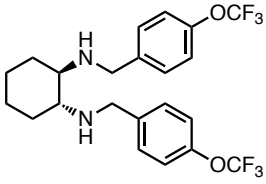

3.43
68% yield
d.r (syn:anti) 79:21
77% ee

yield determined by ^{1}H NMR using an internal standard. ee determined by HPLC using a chiral stationary phase.
ee of the major syn diastereomer reported.

Figure 3.14: Examination of Electron Deficient Chiral Diamine Ligands

However, extremely electron withdrawing pentafluoro ligand (**3.39**) was found to be ineffective producing (**3.34**) in 16% yield. Further tuning the ligands (**3.40**, **3.41**, **3.42**, and **3.43**) with several electron deficient groups in the aryl ring did not increase the enantioselectivity beyond 86%. Further optimization of the nickel-catalyzed enantioselective reaction was carried out using chiral diamine ligand (**3.30**).

3.6.2 Effect of α-Alkyl Substitution in the Electrophile

After identifying optimal ligand for the nickel-catalyzed enantioselective *C*-alkylation of nitroalkanes, I examined the scope of alkyl substitution at the *N*-benzyl-*N*-phenyl amide (**3.33**).

Table 3.9: Comparison of "methyl" vs "ethyl" Substitution in the α-Bromoamide **3.33**

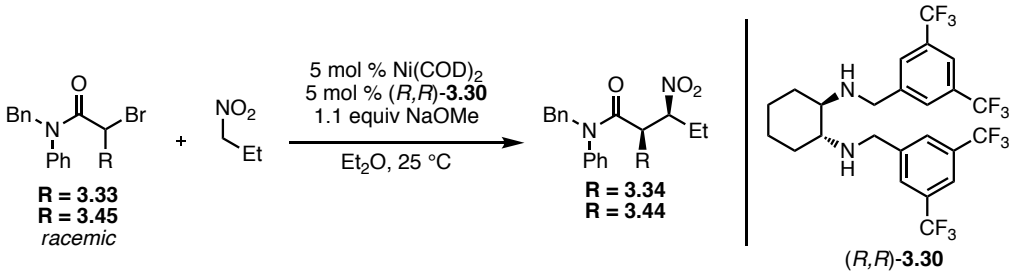

Entry	R	Product	Yield[a]	d.r *syn:anti*	ee[b] *syn/anti*
1	Methyl	3.34	74%	81:19	88/76%
2	Ethyl	3.44	34%	62:38	84/78%

[a] Yields determined by ^{1}H NMR using 1,3,5-trimethoxybenzene as an internal standard.

[b] ee determined by HPLC using a chiral stationary phase

To my disappointment, the catalytic condition was not effective for the α-bromoamide (**3.45**), which possess α-ethyl substitution. For example, the amide (**3.45**)

provided desired product (**3.44**) in 84% ee with 62:38 d.r albeit with low yield (Table 3.9 entry 2). In an effort to increase the yield of (**3.44**), I studied different ligand scaffold, bases, solvents etc with substrate (**3.45**), but the yield could not be improved beyond 45%.

3.6.3 Identification of Et_2Zn as the Internal Reductant

Our working hypothesis for the inefficiency of the catalyst is that, 1,5-cyclooctadience (COD) from the Ni(0) precatalyst may act as a competitive ligand leading to competitive non-enantioselective pathway. I reasoned that *in situ* generated Ni(0) pre catalyst may circumvent this problem and produces a more effective catalyst system than $Ni(COD)_2$ precatalyst. It has been well documented in several cross coupling reactions that internal reductants such as Zn, Mn, organometallic reagents, and organoborane reagents were known to reduce the Ni(II) to Ni(0)[8,15], and it is the low valent, electron rich Ni species that is involved in several alkyl electrophile cross-coupling reactions.[16]

Towards this end, I tested several internal reductants using Ni(II) precatalyst. The control experiment without added reductant did not furnish desired product (**3.44**), which suggests that Ni(II) is not active catalyst in the nickel-catalyzed enantioselective *C*-alkylation of nitroalkanes. Furthermore, Zn metal, Mn metal and Ph–Bpin were ineffective and they produced desired product in only trace amount (Table 3.10 entry 1-3). Significantly, MeMgCl and Et_2Zn both were found to be effective. For example, MeMgCl, gave product (**3.44**) in 76% yield with 57:43 d.r and 80%ee (Table 3.10 entry 5); Et_2Zn gave product (**3.44**) in 48% yield with 62:38 d.r and 40%ee (Table 3.10 entry 6). These results suggest that Ni(II) is reduced to low valent Ni species which catalyze the reaction.

Table 3.10: Survey of Internal Reductant for Ni(II) to Ni(0)

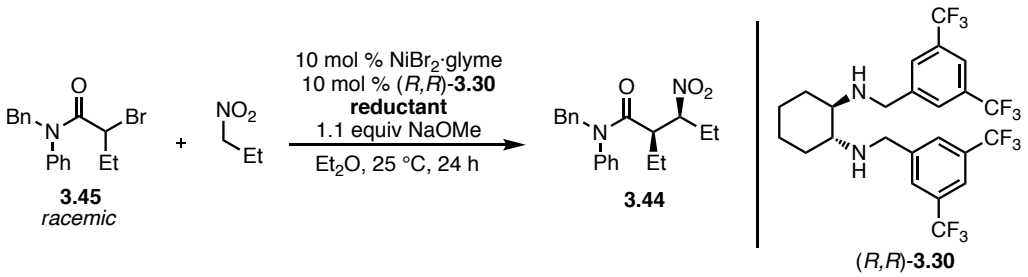

Entry	Reductant	Yield 3.44[a]	d.r 3.44 *syn:anti*	ee 3.44[b] *syn/anti*
1	none	<1%	-	-
2	Zn (3.0 equiv)	<1%	-	-
3	Mn (3.0 equiv)	<1%	-	-
4	Ph–Bpin (20 mol %)	12%	55:45	-
5	MeMgCl (20 mol %)	76%	57:43	80/74%
6	Et_2Zn (10 mol %)	48%	62:38	40/44%

[a] Yields determined by ^1H NMR using 1,3,5-trimethoxybenzene as an internal standard.

[b] ee determined by HPLC using a chiral stationary phase

Next, I reduced the loading of internal reductant to see if it helps in increasing both yield and enantioselectivity. Reducing the MeMgCl loading was detrimental to both the yield and enantioselectivity (Table 3.11 entry 1-3). However, reducing the Et_2Zn was found to be fruitful. For example, reducing Et_2Zn loading to 5 mol % increased the yield to 88% with 69% ee (Table 3.11 entry 4-5), further reducing Et_2Zn concentration increases the enantioselectivity. At 1 mol % Et_2Zn loading, desired enantioenriched β-nitroamides (**3.44**) was produced in 95% yield with 60:40 d.r and 84% ee for the major *syn* diastereomer (Table 3.11 entry 7).

Table 3.11: Reducing the Loading of MeMgCl and Et_2Zn

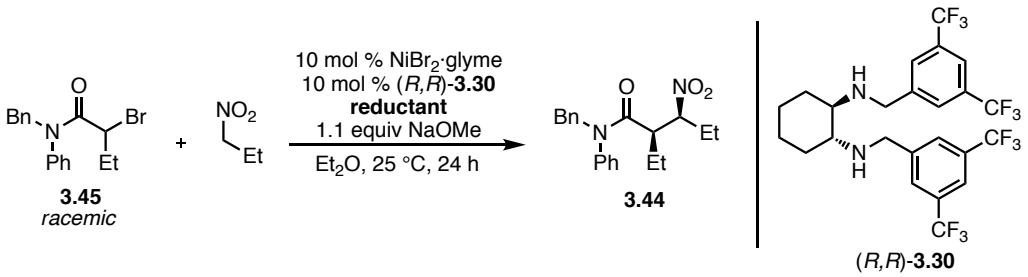

Entry	Reductant Loading	Yield 3.44[a]	d.r 3.44 *syn:anti*	ee 3.44[b] *syn/anti*
1	MeMgCl (20 mol %)	76%	57:43	80/74%
2	MeMgCl (10 mol %)	49%	59:41	80/81%
3	MeMgCl (5 mol %)	18%	60:40	82/82%
4	Et_2Zn (10 mol %)	48%	62:38	40/44%
5	Et_2Zn (5 mol %)	88%	58:42	69/--%
6	Et_2Zn (2.5 mol %)	89%	62:38	75/70%
7	Et_2Zn (1 mol %)	95%	60:40	84/82%

[a] Yields determined by ^1H NMR using 1,3,5-trimethoxybenzene as an internal standard.

[b] ee determined by HPLC using a chiral stationary phase

It is important to note that for the nickel-catalyzed enantioselective *C*-alkylation of nitroalkanes for the synthesis of the β-nitroamides, *in situ* generated Ni(0) pre-catalyst proved to be more efficient catalytic system than the Ni(0) precatalyst using $Ni(COD)_2$ (Table 3.12). Furthermore, high concentration of Ni(II) is necessary for the efficient catalytic system which will be discussed later. The $NiBr_2$·glyme/ Et_2Zn catalyst was used as catalyst for further optimization.

Table 3.12: Comparison of Efficiency of $Ni(COD)_2$ and Ni(II)/Et_2Zn Catalytic System

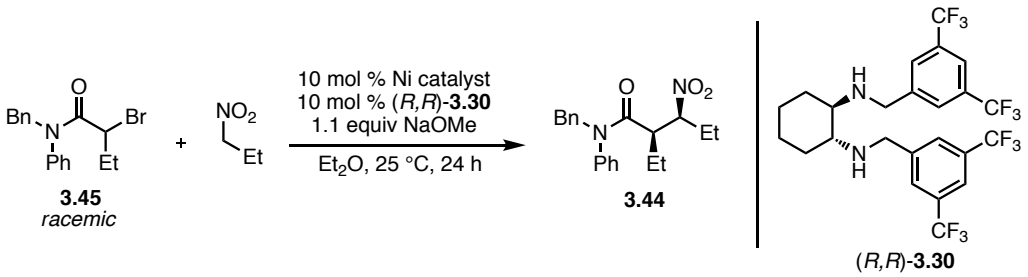

Entry	Ni Catalyst	Yield 3.44[a]	d.r 3.44 *syn:anti*	ee 3.44[b] *syn/anti*
1	$Ni(COD)_2$	34%	62:38	84/78%
2	$NiBr_2$·glyme/ Et_2Zn	95%	60:40	84/82%

[a] Yields determined by ^1H NMR using 1,3,5-trimethoxybenzene as an internal standard.

[b] ee determined by HPLC using a chiral stationary phase

3.6.4 Identification of Single Component Pre-catalyst

After identification of efficient Ni(II)/ Et_2Zn catalytic system, I examined the scope of nitroalkanes in the nickel-catalyzed enantioselective *C*-alkylation conditions. Disappointingly, even modestly functionalized nitroalkanes produced poor yields of **(3.47)**. By using 1-nitrohexene **(3.46)** as the nucleophile and racemic, secondary α-bromoamide **(3.33)** as the electrophile, **(3.47)** was produced in excellent 95:5 d.r with 86% ee of the *syn* diastereomer albeit with 25% yield.

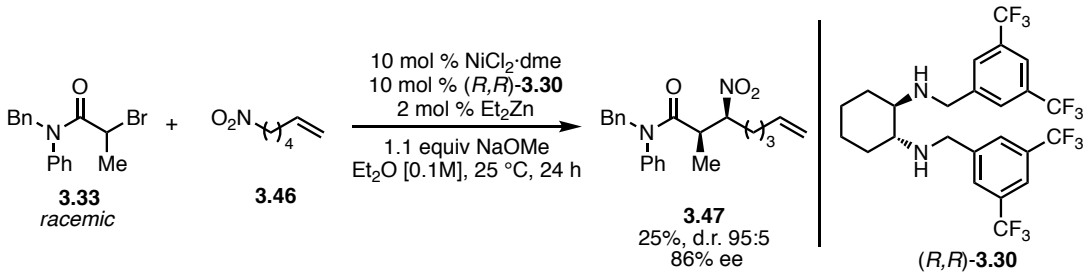

Figure 3.15: Poor Reactivity of Functionalized Nitroalkane **3.46**

We hypothesized that the functionalized nitroalkane coordinates with the active Ni species, and the rate of ligation of (**3.30**) with the Ni species would be slower. Consequently, sufficient concentration of active catalyst would not be present for the efficient catalytic turnovers. In an effort to address this limitation, We reasoned that single component pre-catalyst may be effective for the functionalized nitroalkanes. Towards this end, Dr. Rajgopal Sharma (postdoc) synthesized single component pre-catalyst (**3.48**) from Ni(II) species and ligand (**3.30**) in 85% yield (Figure 3.16).[17]

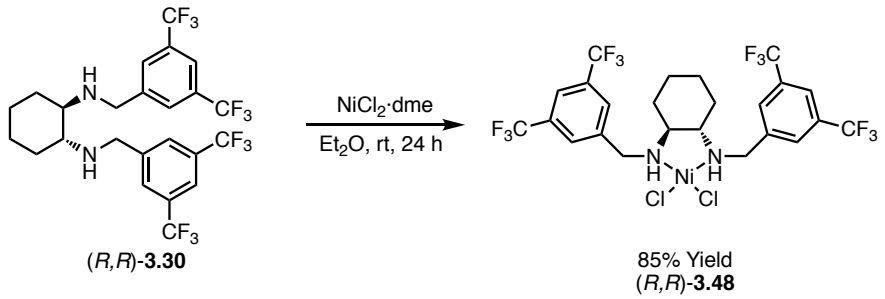

Figure 3.16: Preparation of Single Component Pre-catalyst **3.48**

After synthesizing pre-catalyst (**3.48**), I tested it in the nickel-catalyzed enantioselective reaction using functionalized nitroalkane (**3.46**). Gratifyingly, the single component pre-catalyst (**3.48**) was found to be effective. As shown in Table 3.13 entry 2, the catalyst (**3.48**), produced enantioenriched β-nitroamides (**3.47**) in 70% yield with 88:12 d.r and 86% ee.

Table 3.13: Comparison of Single Component Pre-Catalyst **3.48** and Multi-Component Catalyst **3.30**

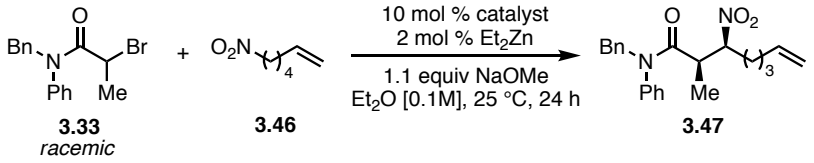

3.33 *racemic* **3.46** **3.47**

Entry	Ni Catalyst	Yield 3.47[a]	d.r 3.47 *syn:anti*	ee 3.47[b] *syn/anti*
1	$NiCl_2$·dme/(*R,R*)-**3.30**	25%	95:05	86/76%
2	(*R,R*)-**3.48**	70%	88:12	86/76%

[a] Yields determined by ^1H NMR using 1,3,5-trimethoxybenzene as an internal standard.

[b] ee determined by HPLC using a chiral stationary phase

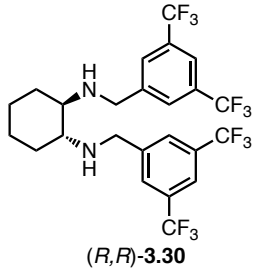

(*R,R*)-**3.30**

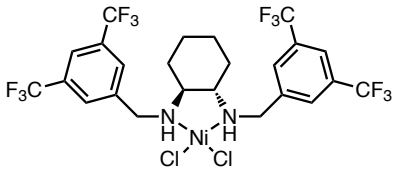

(*R,R*)-**3.48**

Furthermore, I investigated a variety of reductants using single component pre-catalyst (**3.48**), hoping to see if it has effect on enantio- and diastereoselectivity on the formation of β-nitroamides (**3.47**). Single electron reductant such as SmI_2 and strong bases were ineffective as reductants (Table 3.14 entry 1-2). $NaBH_4$ gave trace yield with 87% ee. It is interesting to note that reactive reductant such as $LiAlH_4$ gave (**3.47**) in 99% yield with 84% ee. Several alkyl and aryl Grignard reagents as internal reductant were found to be effective with respect to yield and enantioselectivity, albeit with slightly lower levels of diastereoselection (Table 3.14 entry 5-9). Like organomagnesium reagents, alkyl and aryl zinc reagents worked well except diphenyl zinc which produced (**3.47**) in 24% yield (Table 3.14 entry 10-14). After extensive reductant screen, Et_2Zn was found to be optimal producing (**3.47**) in 88% ee with 88:12 d.r and 78% yield.

Table 3.14: Investigation of Internal Reductants using Single Component Pre-catalyst **3.48**

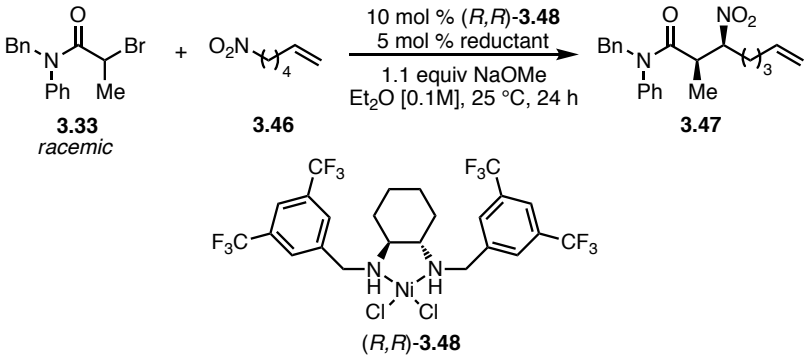

Entry	Reductant	Yield 3.47[a]	d.r 3.47 *syn:anti*	ee 3.47[b] *syn*
1	SmI_2	<1%	-	-
2	NaH	<1%	-	-

3	$NaBH_4$	16%	95:05	87%
4	$LiAlH_4$	99%	74:26	84%
5	MeMgCl	99%	78:22	87%
6	^{i}PrMgCl	92%	76:24	87%
7	BnMgCl	91%	80:20	87%
8	PhMgCl	83%	84:16	84%
9	4-MeO-PhMgCl	97%	78:22	87%
10	BuLi	90%	82:18	87%
11	PhLi	85%	85:15	86%
12[c]	Ph_2Zn	24%	95:05	87%
13[c]	Me_2Zn	82%	86:14	87%
14[c]	Et_2Zn	78%	88:12	88%

[a] Yields determined by ^{1}H NMR using 1,3,5-trimethoxybenzene as an internal standard.

[b] ee determined by HPLC using a chiral stationary phase [c] 1 mol % zinc reagent added

3.6.5 Effect of Temperature

It is well established that several enantioselective reactions perform well under low temperature, encouraged by these precedence, I sought to examine the effect of temperature in the nickel-catalyzed enantioselective *C*-alkylation of nitroalkanes. Gratifyingly, changing the temperature improved ee as well as yield of the product (**3.47**) slightly. For example, at 0 °C the racemic, secondary α-bromoamide (**3.33**) was reacted with prochiral 1-nitrohexene using chiral nickel pre-catalyst (**3.48**) to give (**3.47**) in 90% ee with 80:20 d.r and 87% yield (Table 3.15). However, further lowering temperature adversely affected the yield. Under these heterogeneous reaction conditions the chiral nickel catalyst (**3.48**) could control both the absolute and relative stereochemistry of the β-nitroamides (**3.47**) effectively. The generality of the reaction was studied using this catalytic system at 0 °C unless otherwise mentioned. It is important to mention that the reaction was air sensitive and attempts to run the reaction on the bench top adversely affected the yield. Consequently, the reaction performed in the glove box and we designed a cooling unit and John Famiglietti

(Department's electrical engineer) built it. All the reactions were performed in the glove box at 0 °C using the cooling unit (Figure 3.17).

Figure 3.17: Reaction Set Up in the Glove Box Using Cooling Unit

Table 3.15: Role of Temperature

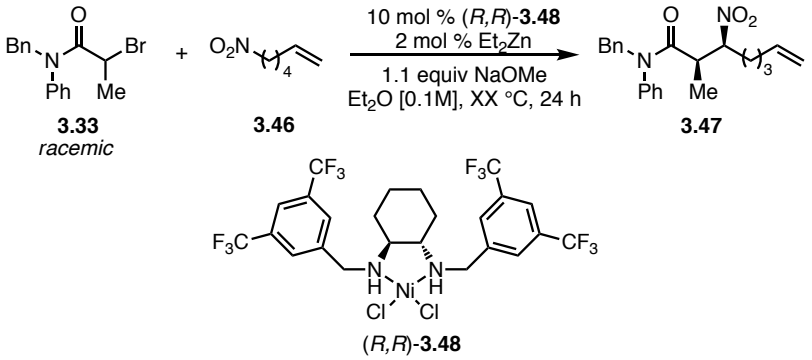

Entry	Temperature °C	Yield 3.47[a]	d.r 3.47 *syn:anti*	ee 3.47[b] *syn/anti*
1	25	74%	86:14	88/76%
2	0	87%	80:20	90/80%
3	–30	34%	78:22	90/79%

[a] Yields determined by ^{1}H NMR using 1,3,5-trimethoxybenzene as an internal standard.

[b] ee determined by HPLC using a chiral stationary phase

3.7 Reaction Scope with Respect to Nitroalkanes

With optimized conditions in hand, we investigated the scope of the nitroalkanes (Figure 3.18). A variety of primary nitroalkanes was subjected to the reaction using racemic *N*-benzyl-2-bromo-*N*-phenylpropionamide as the alkylating reagent. High ee was observed for 1-nitropropane (**3.44**) as well as those with β-branched nitroalkane (**3.49**). Using 10 mol % catalyst loading a variety of functionalized nitroalkanes including alkene, aryl, aryl ether, acetate, free alcohol, ester, free and protected ketone were all alkylated in good to high ee (**3.47, 3.50-3.56**). In all the above cases, modest to high levels of d.r were observed. Nitromethane can also be alkylated albeit with low yield and slightly low ee (**3.57**).

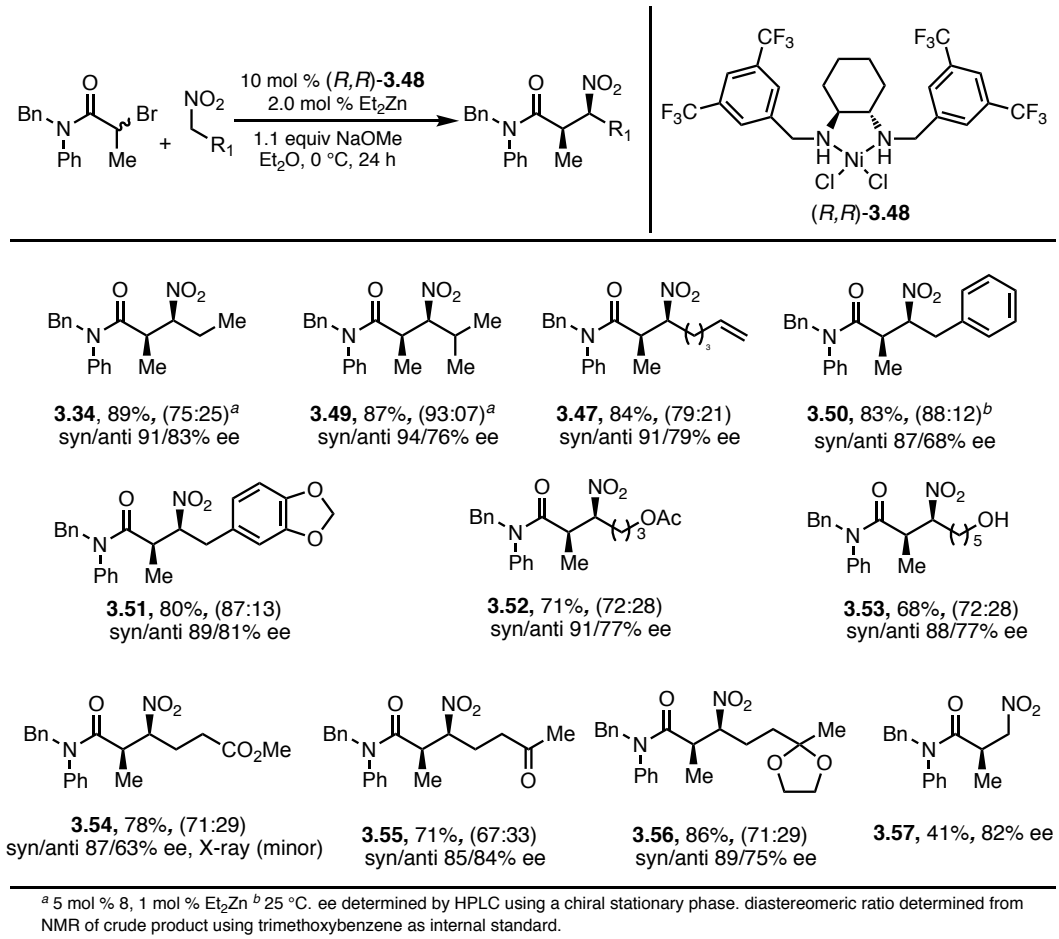

[a] 5 mol % 8, 1 mol % Et_2Zn [b] 25 °C. ee determined by HPLC using a chiral stationary phase. diastereomeric ratio determined from NMR of crude product using trimethoxybenzene as internal standard.

Figure 3.18: Scope of Nitroalkanes in the Nickel-Catalyzed Enantioselective C-Alkylation of Nitroalkanes

3.8 Reaction Scope with Respect to Electrophile and Amide Backbone

The scope of the reaction with respect to the α-bromoamide is broad. Good d.r's and high ee's were observed for amides possessing electron-rich, electron-poor and sterically encumbered groups (**3.58-3.60**, Figure 3.19 top). Importantly, α-bromoamide possessing α-alkyl substituents larger than methyl were also tolerated well with good ee albeit with poor d.r (**3.44, 3.61**, Figure 3.19 bottom). Significantly, several amide back bone including indoline (**3.62**), morpholine (**3.63**), aryl-alkyl

(**3.64**), and synthetically useful Weinreb amide (**3.65**), all performed well with high d.r and high to excellent ee. However, slightly lower level of d.r and ee were observed for nitroalkanes that lack β-branching (**3.65-3.69**) (Figure 3.20).

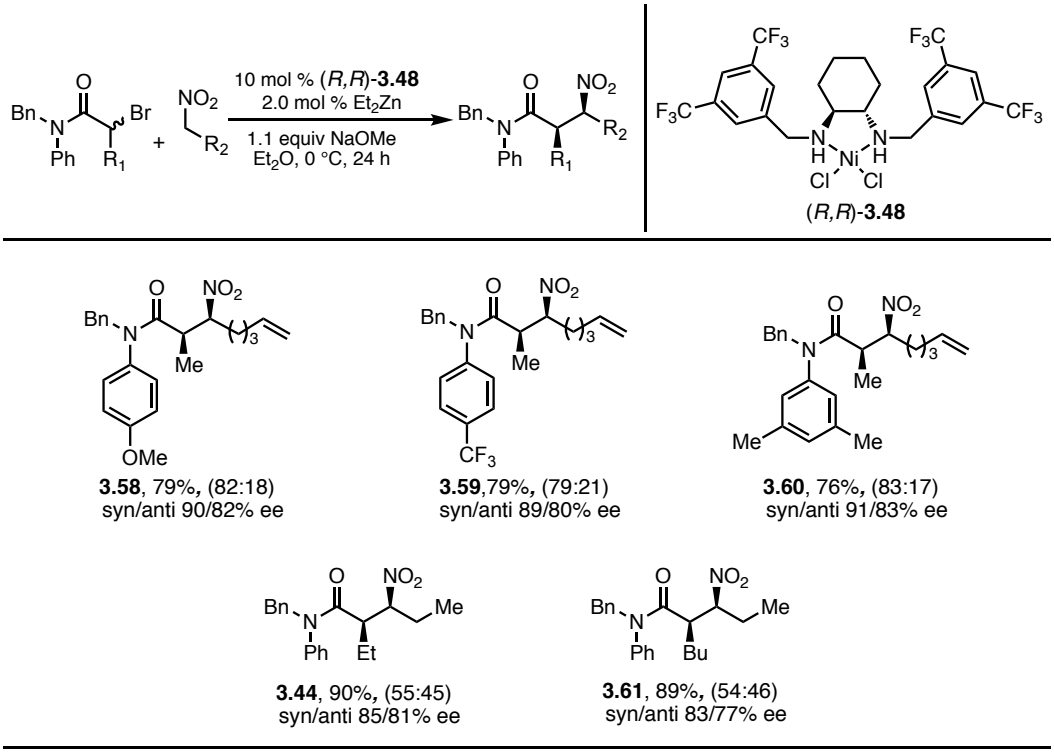

Figure 3.19: Scope of Electrophiles in the Nickel-Catalyzed Enantioselective *C*-Alkylation of Nitroalkanes

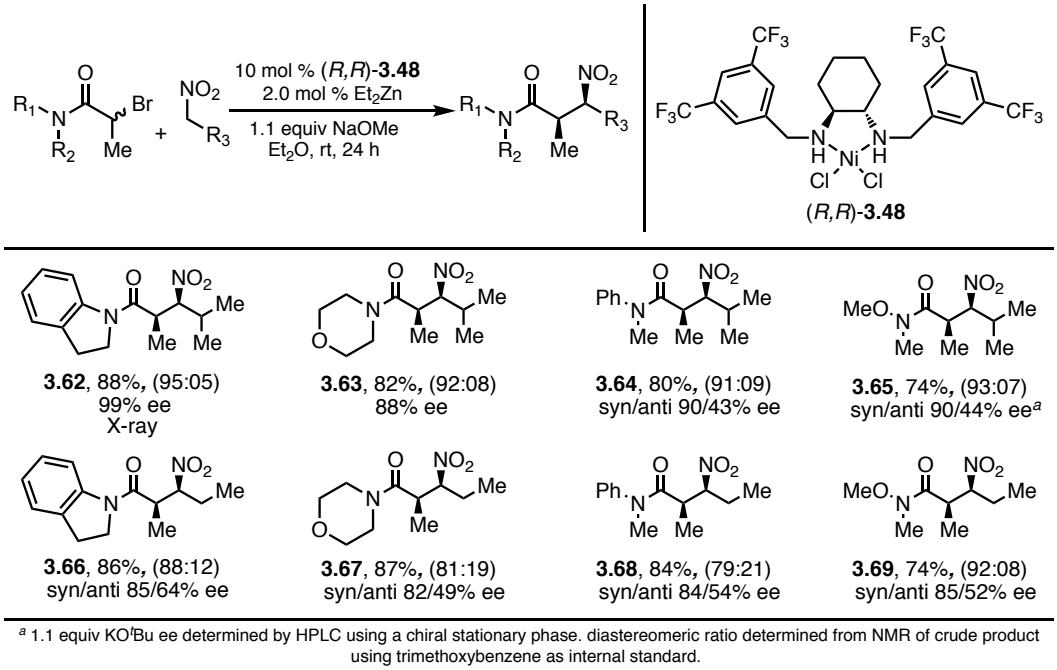

[a] 1.1 equiv KO^{t}Bu ee determined by HPLC using a chiral stationary phase. diastereomeric ratio determined from NMR of crude product using trimethoxybenzene as internal standard.

Figure 3.20: Scope of Amide Backbone in the Nickel-Catalyzed Enantioselective *C*-Alkylation of Nitroalkanes

The reaction exhibits modest to excellent levels of diastereoselectiviy. In several cases, the diastereomers were easily separated by standard column chromatography. The relative and absolute stereochemistry of both diastereomers were determined by X-ray crystallography (**3.54, 3.62**) (see experimental section). The absolute configuration of the other β-nitroamide products were assigned by analogy. Correlation of the structure to their ^{1}H NMR spectra revealed that the *syn*-isomer consistently displayed upfield shift at the hydrogen atom α to the carbonyl group compared to the *anti*-isomer (Figure 3.21). Based on this analysis, we could conclude that the *syn* isomer was the major diastereomer in all cases.

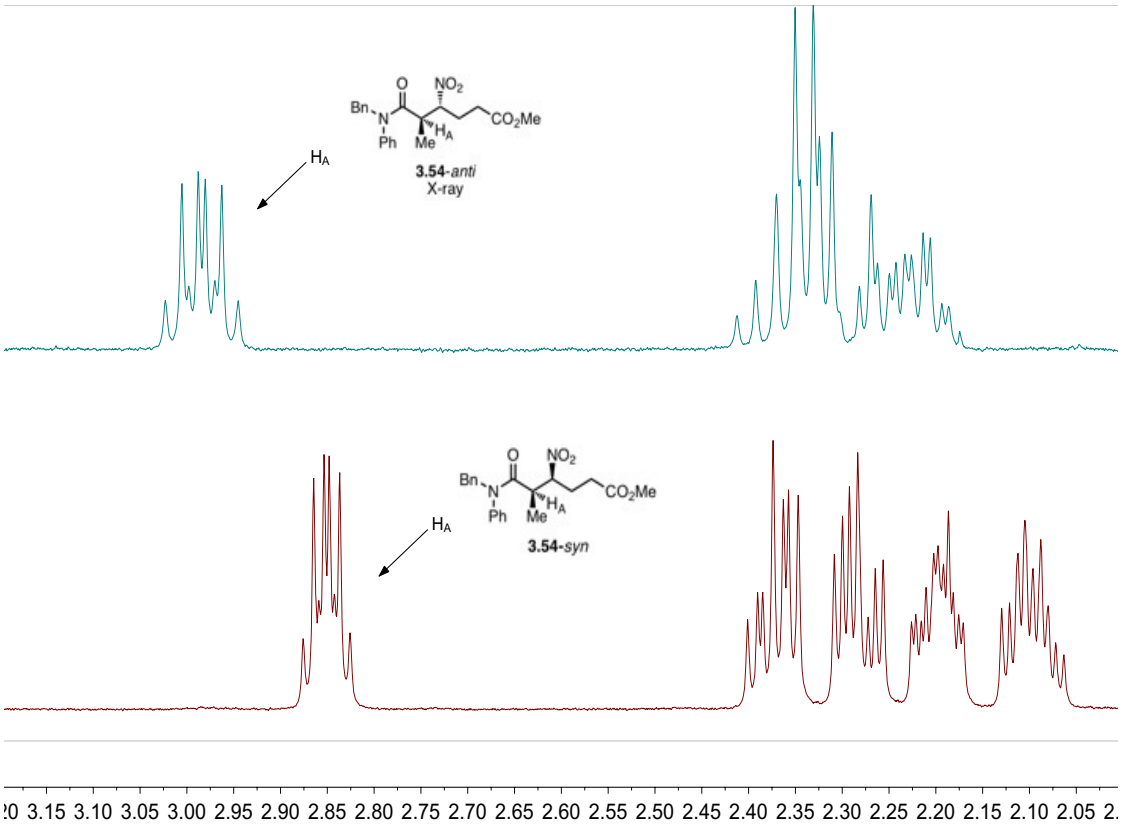

Figure 3.21 ^{1}H NMR spectra of 3.54 *syn* and *anti* diastereomers

3.9 Preliminary Results

Preliminary results suggest that this strategy is applicable to tertiary bromides, providing (**3.3**) with low yield and ee. Interestingly, other preliminary result suggest that this protocol could also be used to alkylate secondary nitroalkanes, albeit with low yield and ee (**3.70, 3.71**) (Figure 3.22). However, these products bear fully substituted nitrogen center, which are challenging to prepare by other methods.

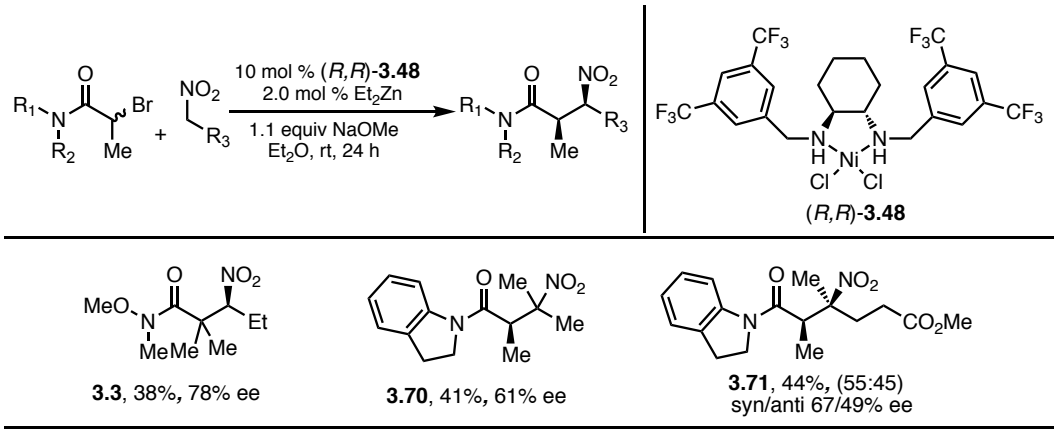

Figure 3.22: Preliminary Results in the Nickel-Catalyzed Enantioselective *C*-Alkylation of Nitroalkanes

3.10 Down Stream Functionalization of Alkylated Products

The enantioenriched β-nitroamide from the alkylation reaction are useful intermediates in the further downstream functionalization. For example, the enantioenriched β-nitroamide can be used as a handle for further C–C bond forming reactions. In 2015, our group published a highly diastereoselective Michael reaction using α-substituted, β-nitrocarbonyls as nucleophiles to afford functional group rich stereodiads containing fully substituted nitrogen-bearing centers (see Chapter 1, section 1.1.3 for discussions).[11] Encouraged by this work, I sought to examine whether these conditions might prove highly diastereoselective for enantioenriched β-nitroamide to form sterically congested, functional group dense nitroalkane with high diastereo- and enantioselectivity. Towards this end, I subjected nitroamide (**3.47**) as a single *syn* diastereomer to the previously optimized diastereoselective Michael addition conditions. The conjugate addition product (**3.72**) was obtained with 91% ee and excellent diastereoslectivity (Table 3.16 entry 1). Interestingly, subjecting mixture

of stereoisomers (79:21 *syn:anti* and 91/82% ee) of nitroamide (**3.47**), produced product (**3.72**) in 89% ee with excellent diastereoselectivity (Table 3.16 entry 2). The relative stereochemistry of product (**3.72**) was assigned based on analogy to our diastereoselective Michael reaction using α-substituted, β-nitrocarbonyls as nucleophiles.[11]

Table 3.16: Diastereoselective Michael Addition of Enantioenriched β-Nitroamide **3.47**

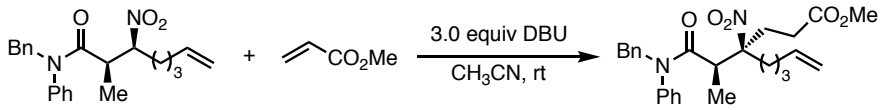

3.47 **3.72**

Entry	**3.47**, d.r	**3.47**, %ee	Yield **3.72**	d.r **3.72** [a] *syn:anti*	ee **3.72**[b] *syn*
1	>95:05	91	84%	>95:05	91
2	79:21	91/82	83%	>95:05	89

[a] diastereomeric ratio determined from ^{1}H NMR of crude product using 1,3,5-trimethoxybenzene as an internal standard.[b] ee determined by HPLC using a chiral stationary phase

Using the diastereomeric and enantiomeric ratios of nitroamide (**3.47**) (Table 3.16 entry 1), I calculated the relative percentage of each stereoisomer subjected into the Michael addition with methyl acrylate (Figure 3.23 left). With the percentage of each stereoisomer known and given the complete diastereoselectivity of the Michael reaction, we could calculate the theoretical enantioselectivity of the resultant product (Figure 3.21 bottom). Since the deprotonation should occur exclusively alpha to the nitro group the stereoconter alpha to the carbonyl should be preserved. The measured enantioselectivity of Michael addition product (**3.72**) (89% ee) closely matched the

theoretical enantioselectivity of the Michael addition product (**3.72**) (88% ee) assuming retention of stereochemistry alpha to the carbonyl group.

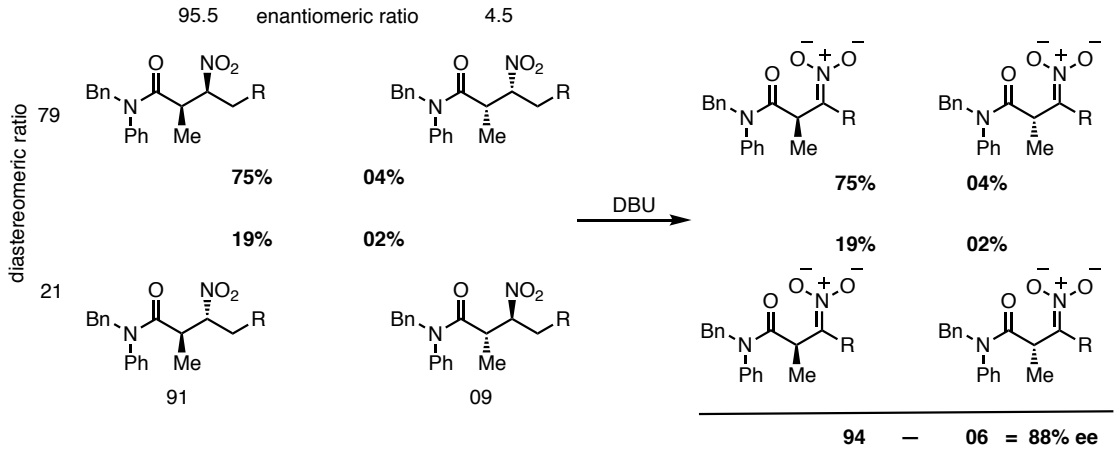

Figure 3.23: Theoretical Enantioselectivity of Michael Addition based on Relative Ratio of Stereoisomers

In 2017, we pusblished mild reaction conditions for the trifluoromethylation of secondary nitroalkanes using a commercially available Umemoto's reagent (Chapter 2).[12] This procedurally simple protocol allows rapid access to highly complex quaternary α-trifluoromethylnitroalkanes in good yields and diastereoselectivity. Inspired by this work, I sought to examine whether these conditions might prove highly diastereoselective for enantioenriched β-nitroamide to form enantioenriched quaternary α-trifluoromethylnitroalkanes with high diastereo- and enantioselectivity. Towards this end, I subjected nitroamide (**3.34**) as a single *syn* diastereomer to the previously optimized trifluromethylation of secondary nitroalkanes conditions. The quaternary α-trifluoromethylated product (**3.73**) was obtained with 90% ee with excellent diastereoslectivity (Table 3.17 entry 1). Similar to the conjugate addition

reaction, subjecting mixture of stereoisomers (76:24 *syn:anti* and 90/84% ee) of nitroamide (**3.34**), produced product (**3.73**) in 86% ee with excellent diastereoselectivity (Table 3.17 entry 2). The relative stereochemistry of product (**3.73**) was assigned based on analogy to our trifluoromethylation of secondary nitroalkanes reactions.[12]

Table 3.17: Synthesis of Enantioenriched Quaternary α-Trifluoromethylnitroalkane (**3.73**)

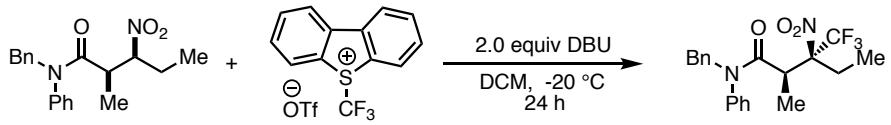

3.34 **3.73**

Entry	**3.34**, d.r	**3.34**, %ee	Yield **3.73**	d.r **3.73** [a] *syn:anti*	ee **3.73** [b] *syn*
1	>95:05	90	>95:05	>95:05	89
2	76:24	90/84	>95:05	>95:05	86

[a] diastereomeric ratio determined from ^{1}H NMR of crude product using 1,3,5-trimethoxybenzene as an internal standard.[b] ee determined by HPLC using a chiral stationary phase

In addition to the conjugate addition and trifluoromethylation reaction, I also subjected enantioenriched β-nitroamide under Tsuji-Trost allylation reactions.[13] For example, the amide (**3.34**) was treated with allyl carbonate (**3.74**) under palladium catalysis affording allylated nitroalkane (**3.75**) with excellent diastereo- and enantioselectivity (Figure 3.24).

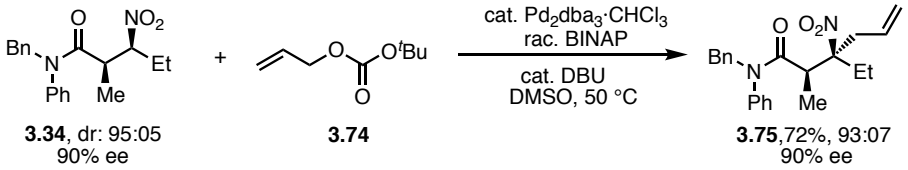

Figure 3.24: Tsuji-Trost Allylation Reaction of Enantioenriched β-Nitroamide

Furthermore, the enantioenriched β-nitroamides (**3.72, 3.73, 3.75**) were transformed to corresponding chiral tertiary amines (**3.76-3.78**) using Zn/AcOH (Figure 3.25). The reduced products are congested, nitrogen-bearing, fully substituted carbon centers, and it is important to note that the ability to functionalize α to the nitro group highlights the importance of this transformation compared to other protocol to prepare β-azacarbonyls such as β-aminocarbonyl that results from Mannich reactions.[14a]

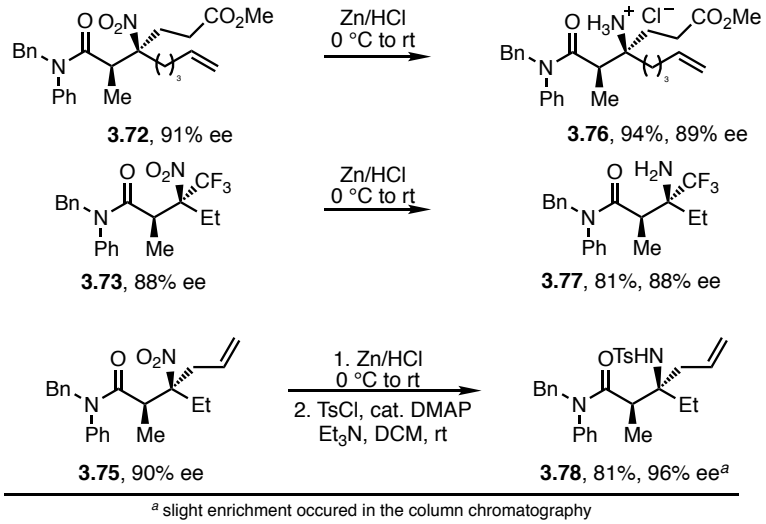

Figure 3.25: Reduction of Alkylated Products

3.11 Investigation of Reaction Mechanism

To investigate the mechanism of the enantioselective *C*-alkylation reaction several experiments were performed. First, when the reaction was run in the presence of 1 equiv TEMPO, a known radical scavenger,[18] no alkylation product (**3.34**) was formed (Figure 3.26 top) and I did not observe the TEMPO adduct. Second, the reaction of substrate (**3.79**), which bears a cyclopropyl ring results exclusively in ring opened product (**3.80**) in 25% yield, suggesting a radical intermediate (Figure 3.26 bottom).[19] Furthermore, 16% ee is encouraging, as it would give opportunity to control the absolute stereochemistry in the *C*-alkylation of nitroalkanes using unactivated electrophiles.

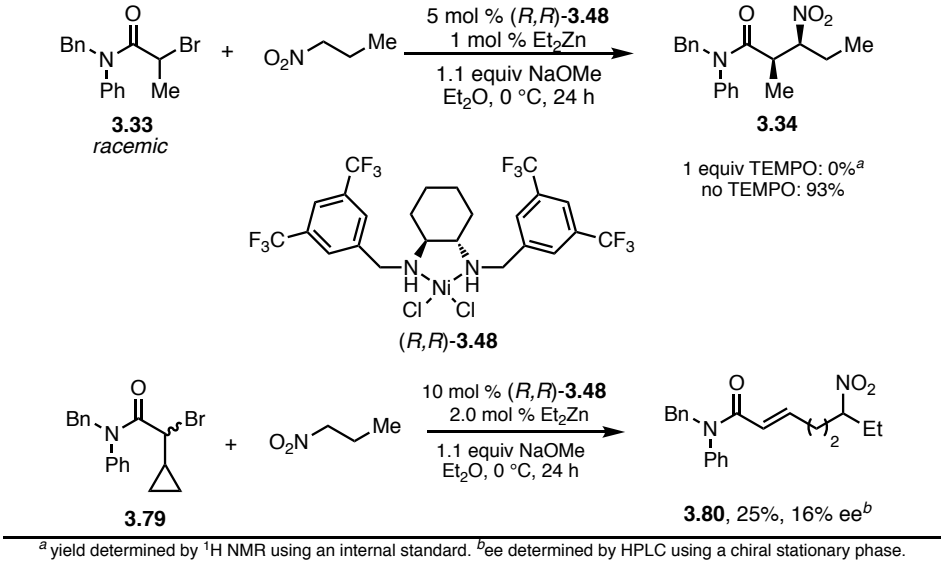

Figure 3.26: Radical Probe Studies in the Nickel-Catalyzed Enantioselective *C*-Alkylation of Nitroalkanes

Third, I examined the stereoconvergence in the reaction. To do this I prepared two enantiomeric α-bromoamide (***R***)-**3.81** and (***S***)- **3.81** and used each isomer in the alkylation of 1-nitropropane using our optimal reaction condition (Figure 3.27). At partial conversion (20 minutes), ^{1}H NMR reavealed a 81:19 mixture of the *syn* and *anti*-isomers and identical enantioselectivity of (**3.66)** in both reaction with slightly different yields. Several implications can be drawn from these results. First, the reaction is stereoconvergent and not stereospecific. This suggests that mechanism of the reaction proceeds through at least one common intermediate (see section 3.2).[3] Second, ee of the product (**3.66)** is controlled by the chirality of the catalyst (**3.48)** rather than substrate (**3.81**). Finally, the ee of the unreacted (**3.81**) at partial conversion is unchanged, which suggests that the breaking of C–Br bond is irreversible in nature. Taken together, the result presented in Figure 3.26 and 3.27 strongly supports a radical based mechanism in this transformation.[16,20]

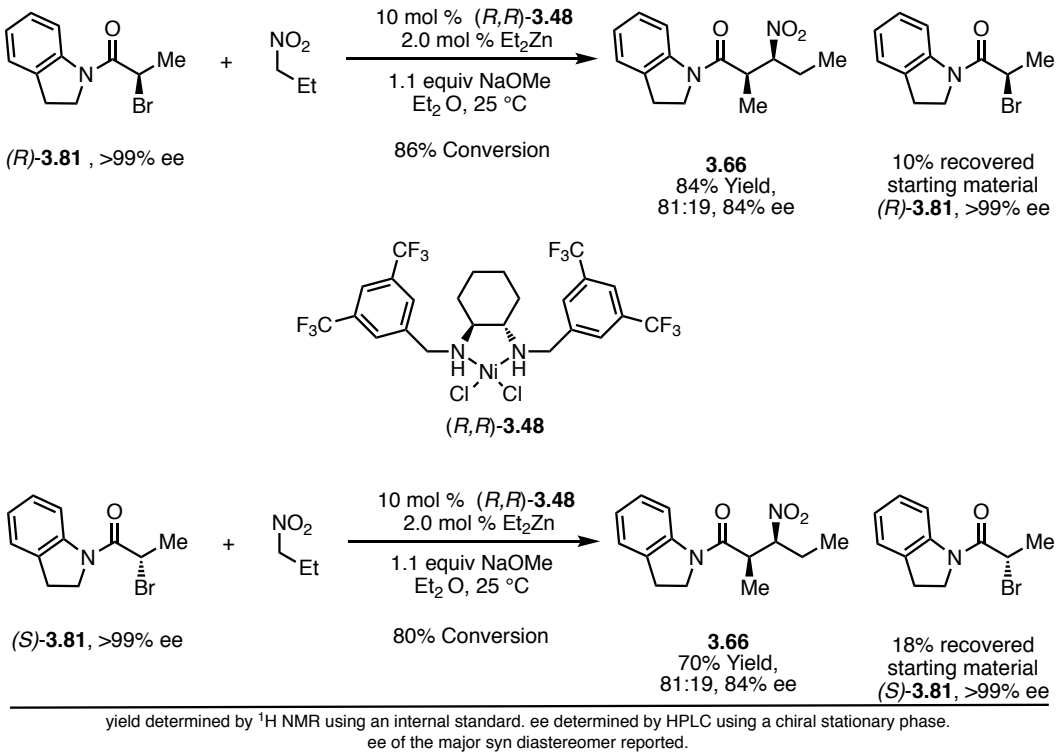

Figure 3.27: Stereoconvergence in the Nickel-Catalyzed Enantioselective *C*-Alkylation of Nitroalkanes

To study the mechanism of nickel-catalyzed enantioselective *C*-alkylation reaction, I investigated the dependence of product enantiomeric excess ee on catalyst ee. To perform this study I prepared enantiomer of the ligand (*S,S*)-**3.30**, and mixed with (*R,R*)- **3.30** ligand to afford 75%, 50%, 25% ee of the catalyst. I subject this into the reaction condition using α-bromoamide (**3.82**) as the electrophile and 1-nitropropane as nucleophile (Table 3.18). A linear correlation was observed by plotting the ee of *syn*-isomer of (**3.69**) (Figure 3.26) against the ee of the catalyst and similar linearity was observed for the *anti*-isomer (**3.69**) (Figure 3.28).[21] This linear relationship between enantiomeric excess and catalyst ee reveals that the active catalyst is likely a monomeric species.

Table 3.18: Study of Product ee and Catalyst ee

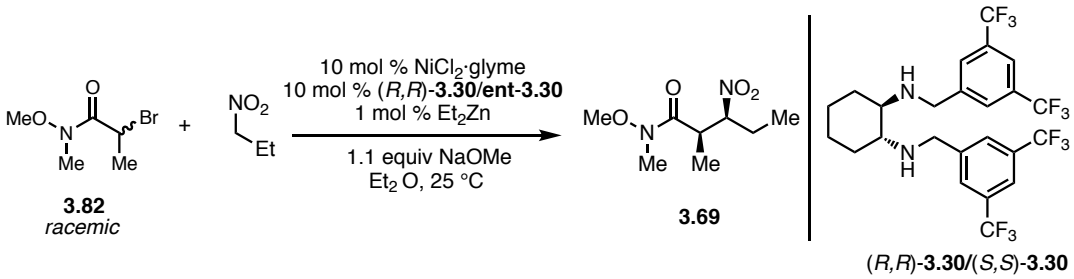

3.82
racemic

(*R,R*)-**3.30**/(*S,S*)-**3.30**

Entry	ee of the Ligand	Yield 3.69[a]	d.r 3.69 *syn:anti*	ee 3.69[b] *syn/anti*
1	100%	77%	88:12	85/42%
2	75%	70%	89:11	64/33%
3	50%	70%	91:09	46/20%
4	25%	71%	90:10	26/10%
5	0%	71%	90:10	0/0%

[a] Yields determined by ^{1}H NMR using 1,3,5-trimethoxybenzene as an internal standard.

[b] ee determined by HPLC using a chiral stationary phase

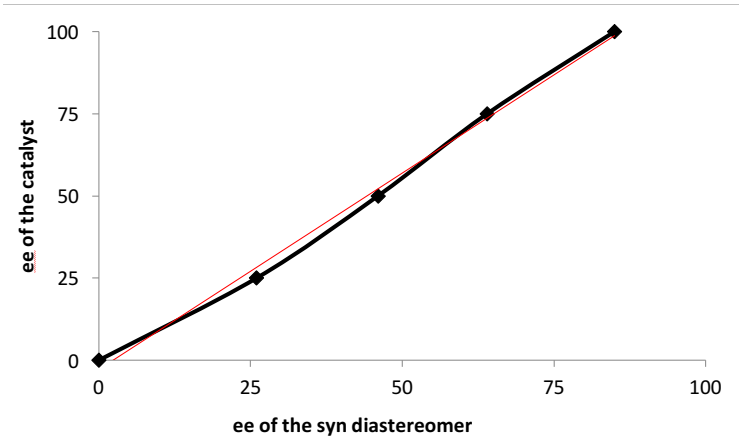

Figure 3.28: Enantiomeric excess of the catalyst Vs enantiomeric excess of the *syn* diatereomer **3.69**

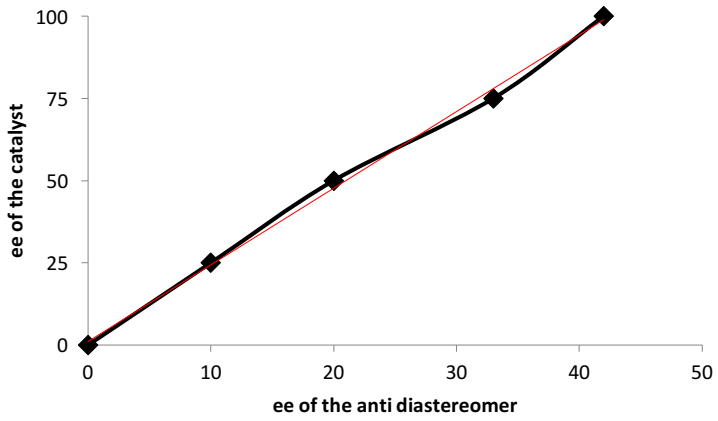

Figure 3.29: Enantiomeric excess of the catalyst Vs enantiomeric excess of the *anti* diatereomer **3.69**

Table 3.19: Revisiting Internal Reductant Screen

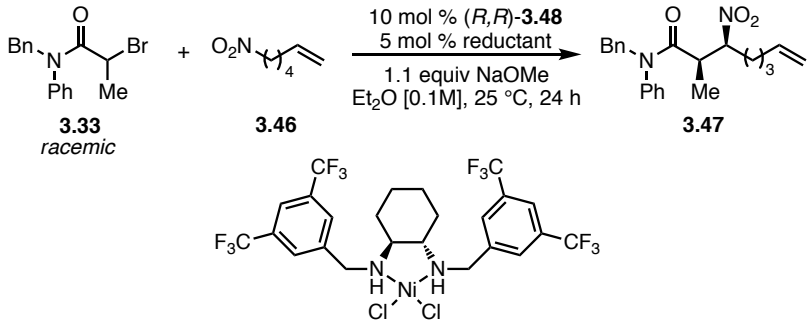

Entry	Reductant	Yield 3.47[a]	d.r 3.47 *syn:anti*	ee 3.47[b] *syn*	By Product
1	BnMgCl	91%	80:20	87%	3.83, trace
2	PhMgCl	83%	84:16	84%	3.84, trace
3	4-MeO-PhMgCl	97%	78:22	87%	3.85,

					trace
4	PhLi	85%	85:15	86%	3.84, trace
5	Et_2Zn (1 mol %)	78%	88:12	88%	-

[a] Yields determined by ^1H NMR using 1,3,5-trimethoxybenzene as an internal standard.

[b] ee determined by HPLC using a chiral stationary phase

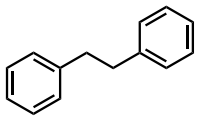

3.83, trace

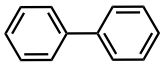

3.84, trace

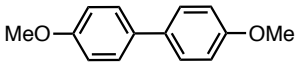

3.85, trace

Table 3.20: Effect of Catalyst Loading

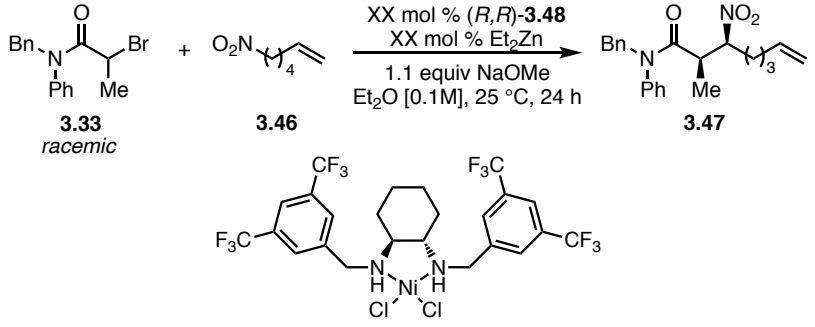

Entry	Catalyst Loading mol %	Et_2Zn mol %	Yield 3.47[a]	d.r 3.47 *syn:anti*	ee 3.47[b] *syn*
1	2.5	0.25	2%	-	-
2	5	0.5	23%	91:9	87%
3	10	1	76%	89:11	87%
4	20	2	90%	77:23	87%
5	2.5	1	64%	81:19	87%
6	5	1	65%	85:15	87%
7	10	1	76%	82:18	87%
8	20	1	48%	96:04	87%

[a] Yields determined by ^1H NMR using 1,3,5-trimethoxybenzene as an internal standard.

[b] ee determined by HPLC using a chiral stationary phase

First, while investigating various internal reductants using single component pre-catalyst (**3.48**), I noticed the formation of trace amount of biaryl and bibenzyl by-products such as **3.83**, **3.84, and 3.85** when using aryl organometallic reductants (Table 3.19 entry 1-4). Second, catalyst loading study shows that high concentration of Ni(II) is necessary for the efficient catalytic system and (Table 3.20 and 3.11, section 3.6.3). It is important to mention that while using Et_2Zn (1 mol %) that the concentration of Ni (0) generated is low, theoretically 9:1 ratio of Ni(II)/Ni(0) produced. Taken together, from Table 3.19 and 3.20, I reasoned that organometallic reagents transmetallate on to Ni(II) species (**3.86**), followed by reductive elimination to afford biaryl product and Ni (0) species (**3.87**). Then Ni (0) presumably, comproportionates[20b,f,22] with high concentration of Ni(II) to afford Ni(I) species (**3.88**), which likely is catalytically active (Figure 3.30). Other possibility of generating Ni (I) species (**3.88**), cannot be ruled out such as Ni (0) abstracting a halogen atom from α-bromocarbonyl to give Ni(I) and alkyl radical, but this would not require excess Ni(II) species.

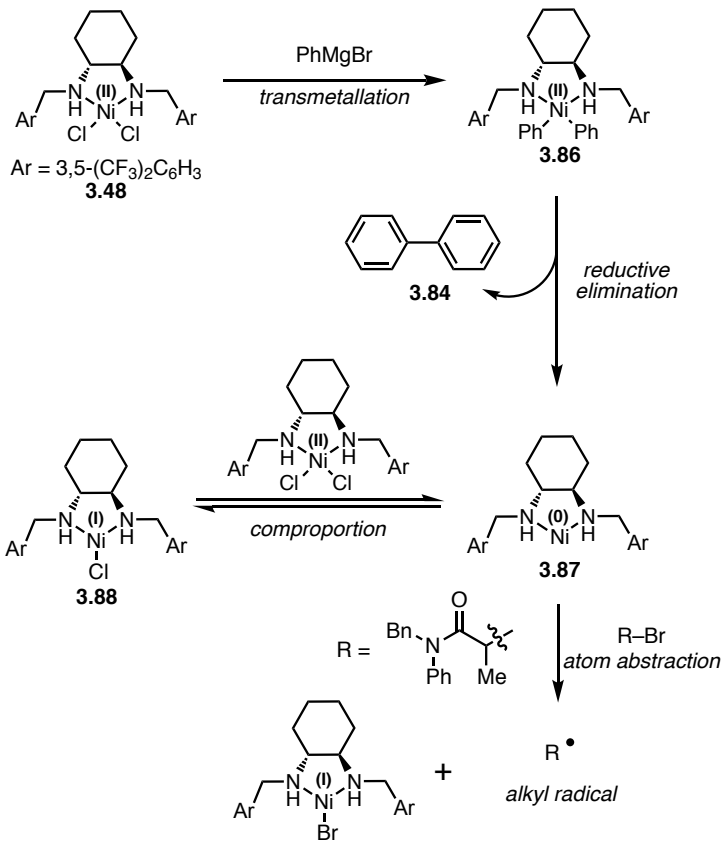

Figure 3.30: Proposed Mechanism for the Generation of Low-Valent Ni Species and Alkyl Radical

Based on these mechanistic studies, and the identification of redox inactive chiral 1,2 diamine ligand (**3.30**), we propose the following Ni^{I}/Ni^{II} catalytic cycle (Figure 3.31). The base quantitatively deprotonates nitroalkane, and generates sodium nitronate anion, which is sparingly soluble in the aprotic reaction medium. Presumably, the insoluble nitronate anion combines with chiral precatalyst (**3.48**) to form the soluble nitro bound nickel (II) complex (**3.89**). Subsequently, transient alkyl radical generated from NiX_2L^*/Et_2Zn (see Figure 3.30) adds to the nitronate anion, which is bound to the nickel (II) complex to give Ni(II) species (**3.90**) via an outer-

sphere mechanism. Then fast single electron transfer from the nitronate radical to Ni(II) species (**3.90**) generates Ni(I) species (**3.91**). The enantioenriched product is released to generate active Ni(I) catalyst (**3.88**), which abstracts a halogen atom from alkyl electrophile to generate alkyl radical and Ni(II) catalyst (**3.48**), which brings more nitronate anion into the liquid phase. We think that the Ni(II) complex (**3.48**) has two roles. First, it is involved in enantioselective nickel catalysis to forge C–C bond. Second it acts as a phase transfer catalyst, where it brings the insoluble nitronate anion from solid phase to liquid phase.

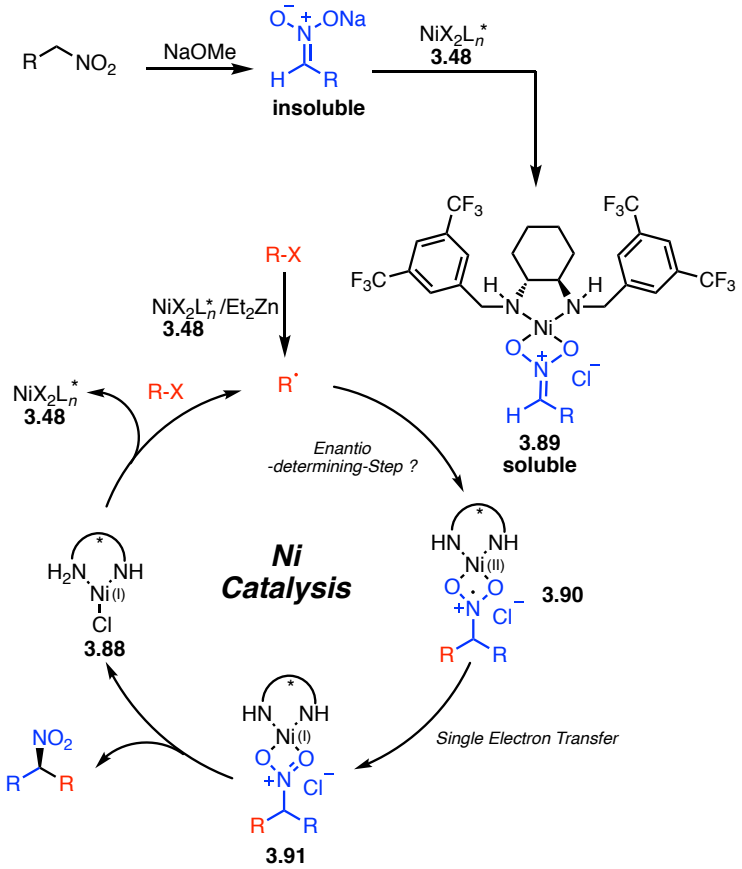

Figure 3.31: Proposed Outer Sphere Mechanism for the Nickel-Catalyzed Enantioselective *C*-Alkylation of Nitroalkanes

We propose an alternative mechanism which involves a Ni^{I}/Ni^{III} catalytic cycle (Figure 3.32). Like the previous mechanism, the chiral precatalyst (**3.48**) brings the insoluble nitronate anion from solid phase to liquid phase. In this case, we propose an inner-sphere mechanism where transient alkyl radical adds to the Ni(II) (**3.48**) center to give stable *O*-bound Ni(III) (**3.92**) species. This Ni(III) species (**3.92**) equilibrates with the less stable, more reactive, *C*-bound Ni(III) species (**3.93**), which reductively eliminates to afford enantioenriched product and active Ni(I) catalyst (**3.88**). The remaining steps are similar to previous outer-sphere mechanism (Figure 3.31). Our current experiments do not allow us to distinguish between outer sphere and inner sphere mechanisms. However, future work in our group will be directed toward exploring fundamental steps of this reaction.

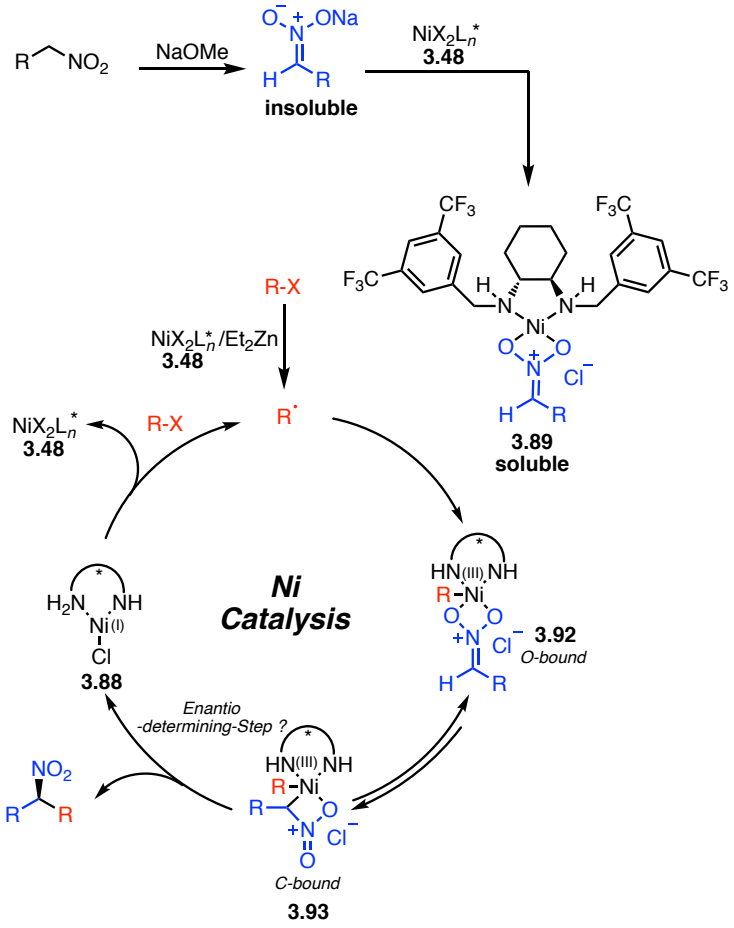

Figure 3.32: Proposed Inner Sphere Mechanism for the Nickel-Catalyzed Enantioselective *C*-Alkylation of Nitroalkanes

3.12 Other Nickel-Catalyzed C-Alkylation of Nitroalkanes Reactions

Our lab developed a general catalytic method for alkylating nitroalkanes using benzyl bromides, α-bromo carbonyls, and α-bromonitriles as alkylating agents, which is a significant advance in the field of nitroalkane *C*-alkylation (Figure 3.33). However, all of these reactions required radical stabilizing groups adjacent to the electrophilic site.[23] Alkyl halides lacking such a stabilization group were not suitable coupling partners under previous copper catalysis. We realized that a method capable

of utilizing non-stabilized alkyl electrophiles would significantly enhance the scope and synthetic utility of nitroalkane alkylation (Figure 3.34).

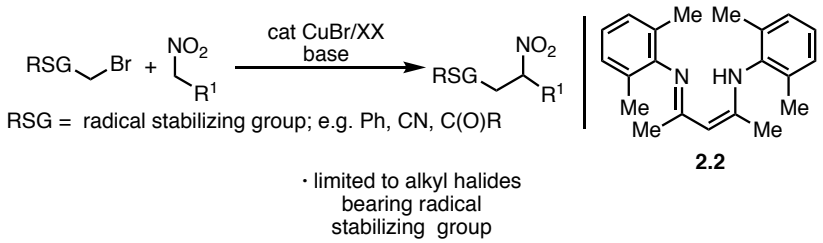

Figure 3.33: Copper-Catalyzed *C*-Alkylation of Nitroalkanes

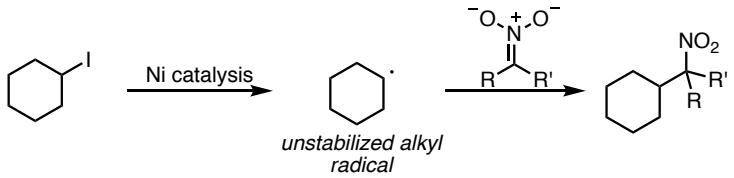

Figure 3.34: Proposed C-alkylation of Nitroalkanes with Unactivated Alkyl Halides Under Nickel Catalysis

Preliminary experiments were focused on alkylating nitroalkanes using cyclohexyl halides as the model substrates. By using catalytic $Ni(COD)_2$/cylohexyl 1,2 diamine (**3.17**), and DBU as a base, no desired product (**3.94**) was formed (Table 3.21 entry 1-2). However, at room temperature a trace amount of desired product (**3.94**) was formed along with cyclohexene by-product (Table 3.21 entry 3). In an attempt to suppress the β-hydride elimination product I used tridentate nitrogen ligand (**3.95**). Gratifyingly, 15% yield of (**3.94**) was produced (Table 3.21 entry 4).

Table 3.21: Initial Studies on Alkylation of 1-nitropropare using Cyclohexyl Iodide

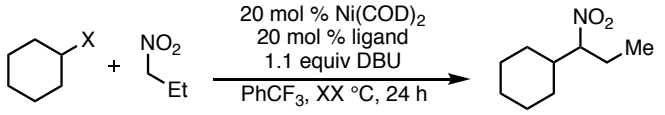

3.94

Entry	X	T °C	Ligand	Yield 3.94[a]
1	Br	–20	3.17	0%
2	I	–20	3.17	0%
3	I	25	3.17	5%
4	I	25	3.95	15%

[a] Yields determined by ^{1}H NMR using 1,3,5-trimethoxybenzene as an internal standard.

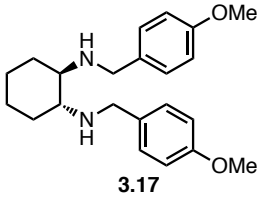

3.17

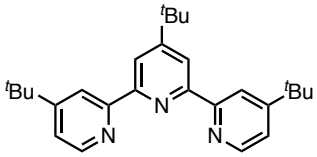

3.95

With this preliminary result for the nickel-catalyzed *C*-alkylation of nitroalkanes using unactivated alkyl halides, my colleague Dr. Sina Razazadeh further optimized the reaction conditions. He found nickel complex (**3.96**) (generated from $NiBr_2$·dme and a redox active bidentate nitrogen ligand such as bathocuproine), and Et_2Zn as the internal reductant catalyzes the *C*-alkylation of nitroalkanes using unactivated alkyl iodides as the alkylating agent. It is important to note that the Et_2Zn, which I discovered in the nickel-catalyzed enantioselective *C*-alkylation of nitroalkanes was also found to be effective for alkylation of nitroalkanes using unactivated alkyl halides.

Dr. Sina Rezazadeh studied the scope of this transformation extensively and found broad scope for both coupling partners. For example, primary alkyl iodides bearing a high degree of functionality (**3.99**, **3.100** and **3.101)** (Figure 3.35) and biologically relevant heterocycles were all tolerated in the reaction (**3.99**, **3.100** and

3.101). Significantly, secondary and tertiary alkyl iodides can also be used in the reaction. A variety of functionalized nitroalkanes (**3.102, 3.103** and **3.106**) can be tolerated in the reaction. For example, nitroalkanes bearing alkenes, acetyl protected alcohols, esters, phthalimides, and Boc-protected amines all provided good yields (**3.102-3.106**). Upon reduction of the nitro group to the corresponding amine, biologically relevant adapromine can be obtained in good yields. This work was communicated in The Journal of the American Chemical Society in 2017.[24]

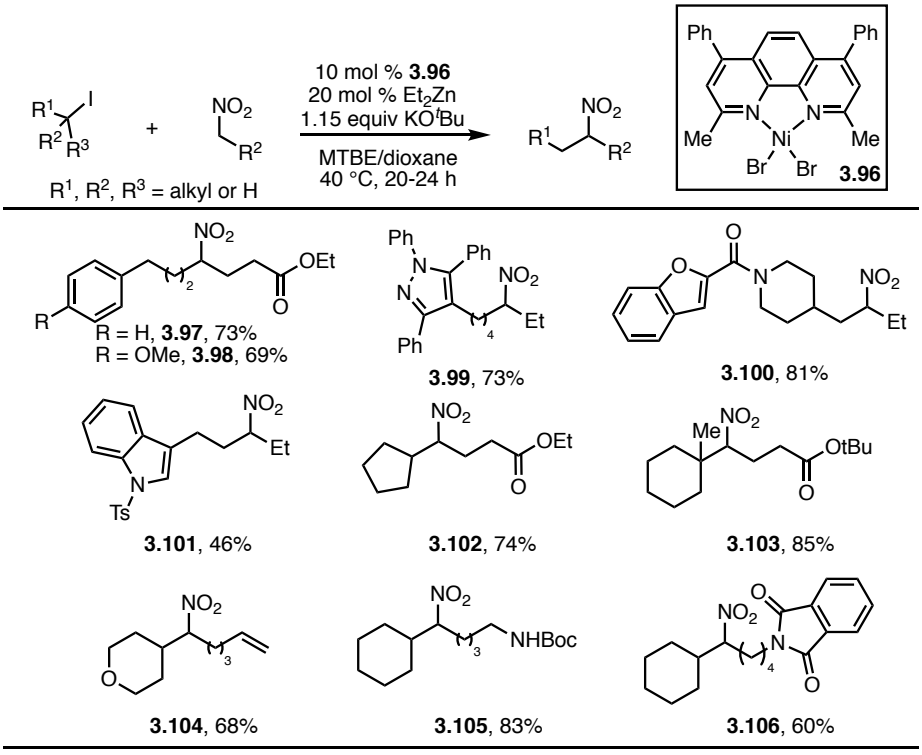

Figure 3.35: Sample Scope of Nickel-Catalyzed C-alkylation of Nitroalkanes Using Unactivated Alkyl Halides

3.13 Conclusion

In conclusion, the first Ni-catalyzed asymmetric *C*-alkylation of nitroalkanes has been developed. This method enables formation of highly enantioenriched β-nitroamide from readily available α-bromoamide and the mild reaction conditions are compatible with wide range of functional groups. Significantly, we showed that the absolute stereocenter α to the nitro group can be controlled. The variety of β-nitroamide are used subsequently synthetic manipulations to form highly enantioenriched products with nitrogen-bearing fully substituted carbon centers. Efforts to expand the scope of this nitroalkylation to secondary nitroalkanes and tertiary electrophiles substrates and to determine the reaction mechanism are underway. Furthermore, I was involved in the development of the first nickel-catalyzed *C*-alkylation of nitroalkanes using unactivated alkyl halides allowed the preparation of a diverse array of complex nitroalkanes using simple starting materials. Significantly, this system allows for the alkylation of primary, secondary, and tertiary alkyl iodides without the requirement of radical stabilizing groups.

3.14 Experimental Section

3.14.1 General Experimental Details

Benzene, dichloromethane, and diethyl ether were dried on alumina according to a published procedure.[25] Trifluorotoluene and dimethyl acetamide were purchased in anhydrous septa sealed bottle. Nickel(II)bromide methoxy ethyl ether, nickel(II) chloride ethylene glycol dimethyl ether, potassium *tert*-butoxide, lithium methoxide, lithium *tert*-butoxide, lithium trimethylsilanolate, potassium trimethylsilanolate, sodium methoxide, potassium methoxide, lithium methoxide and sodium trimethylsilanolate were purchased commercially; the bulk was stored in a N_2 filled

glovebox; samples were removed from the glovebox and stored in a desiccator under air for up to two weeks prior to use. All hot glassware was oven dried for a minimum of two hours or flame-dried under vacuum prior to use. 2-methyl-1-nitropropane,[26] 6-nitrohex-1-ene,[27] 4-nitrobutyl acetate,[28] methyl 4-nitrobutanoate,[29] 5-nitropentan-2-one,[30] 2-methyl-2-(3-nitropropyl)-1,3-dioxolane,[31] (2-nitroethyl)benzene,[23a] 5-(2-nitroethyl)benzo[d][1,3]dioxole,[32] methyl 4-nitropentanoate,[33] 2-bromo-*N*-methoxy-*N*,2-dimethylpropanamide,[23b] allyl *tert*-butyl carbonate,[34] 2-bromo-*N*-methoxy-*N*-methylpropanamide,[35] *N*-benzyl-2-bromo-*N*-phenylpropanamide (**3.33**),[4] *N*-benzyl-2-bromo-*N*-phenylbutanamide (**3.45**),[4] and *N*-benzyl-2-bromo-*N*-phenylhexanamide,[4] and (+)-(*R,R*)-*N,N,N,N*-tetrabenzyl-1,2-diaminocyclohexane (**3.22**)[36] were synthesized according to the published procedures. Bis(1,5-cyclooctadiene) nickel was purchased commercially and stored in a nitrogen filled glovebox freezer at –35 °C. All other substrates and reagents were purchased in highest analytical purity from commercial suppliers and used as received. All NMR yields are reported using 1,3,5-trimethoxybenzene as an internal standard. All reactions were set up using standard Schlenk technique. Reactions were heated with stirring in temperature controlled oil baths and cooled with stirring using Cryo cooling units. “Double manifold” refers to a standard Schlenk-line gas manifold equipped with N_2 and vacuum (ca. 0.1 mm Hg).

3.14.2 Instrumentation and Chromatography

400 MHz ^{1}H, 101 MHz ^{13}C, and 376 MHz ^{19}F spectra were obtained on a 400 MHz FT-NMR spectrometer equipped with a Bruker CryoPlatform. 600 MHz ^{1}H and 151 MHz ^{13}C spectra were obtained on a 600 MHz FTNMR spectrometer equipped with a Bruker SMART probe. ^{13}C spectra were recorded using Attached Proton Test phase pulse sequence; carbons with an odd number of protons are phased down and

those with an even number of protons are phased up.[37] All samples were analyzed in the indicated deutero-solvent and were recorded at ambient temperatures. Chemical shifts are reported in ppm. ^{1}H NMR spectra were calibrated using the residual protio-signal in deutero-solvents as a standard. ^{13}C NMR spectra were calibrated using the deutero-solvent as a standard. IR spectra were recorded on a Nicolet Magma-IR 560 FT-IR spectrometer as thin films on NaCl plates or using KBr pellets. Column chromatography was performed with 40-63 μm silica gel or neutral Al_2O_3 (Brockmann type I, 50-200 μm) with the eluent reported in parentheses. Analytical thin-layer chromatography (TLC) was performed on precoated glass plates and visualized by UV or by staining with $KMnO_4$. GCMS data was collected using an Agilent 6850 series GC and 5973 MS detectors. High resolution MS data was obtained on a Waters GCT Premier spectrometer using chemical ionization (CI) or liquid injection field desorption ionization (LIFDI) or on a Thermo Scientific, Q Exactive model orbitrap using electrospray ionization (ESI).

3.14.3 Procedure for Initial Experiments with DBU as Base:

See notebook pages: DVR01249, DVR01253, DVR01255, DVR01294, DVR01029, DVR02065

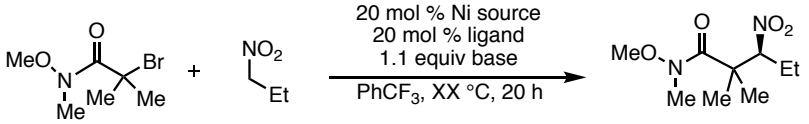

3.1 **3.3**

In a N_2 filled glovebox, to a 15 x 45 mm vial containing a magnetic stir bar was added sequentially Ni source (25 μmol), diamine ligand (25 μmol), base (138 μmol), anhydrous trifluorotoluene (750 μL), 1-nitropropane (13.4 μL, 150 μmol), and

α-bromoamide **3.1** (26.3 mg, 125 μmol). The vial was sealed with a Teflon lined cap and the heterogeneous mixture was stirred at the given temperature for 20 h. After cooling to room temperature, the vials were removed from the glovebox and opened to air. For reaction involving lower temperature the vial was sealed with a septum cap, removed from the glovebox, and submerged in an isopropanol bath at 0 °C or –25 °C chilled using a cryocool. A nitrogen spaghetti line was added and α-bromoamide (**3.1**) (26.3 mg, 125 μmol) was added via syringe using Schlenk technique. The reaction was allowed to continue stirring at 0 °C or –25 °C for 20 h then warmed to room temperature and opened to air. For all reactions 1,3,5-trimethoxybenzene (10.5 mg, 63 μmol) was added and the mixture was diluted with ethyl acetate (ca.1.5 mL). The solution was passed through a plug of celite and concentrated *in vacuo*. The reactions were analyzed by ^{1}H NMR using 1,3,5-trimethoxybenzene as an internal standard to report yields. The product (**3.3**) is a known compound and its spectra are in accordance with literature data.[23b] The enantiomeric excess was determined by chiral HPLC analysis (CHIRALPAK IA, 1.0 mL/min, 1.0% i-PrOH/hexane, λ=220 nm); t_R(major) = 11.341 min, t_R(minor) = 12.722 min.

3.14.4 Synthesis of β-nitroamide:

See notebook page: DVR02093, DVR02100, DVR02121, DVR02127, DVR02131 for using racemic, secondary, α-bromoamide (**3.26**) as electrophile.

See notebook page DVR02136 for kinetic stability study

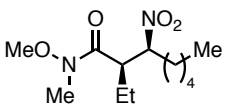

3.28A

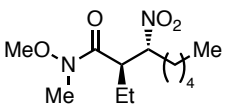

3.28B

In a N_2 filled glovebox, to a 15 x 45 mm vial containing a magnetic stir bar was added sequentially Ni source (25 μmol), diamine ligand (**3.27**) (25 μmol), base (138 μmol),

anhydrous trifluorotoluene (750 μL), and 1-nitrohexane (19.2 μL, 138 μmol). The vial was sealed with a Teflon lined cap removed from the glovebox, and submerged in an isopropanol bath at –20 °C chilled using a cryocool. A nitrogen spaghetti line was added and α-bromoamide (**3.26**) (20 μL, 125 μmol) was added via syringe using Schlenk technique. The reaction was allowed to continue stirring at –20 °C for 20 h then warmed to room temperature and opened to air. 1,3,5-Trimethoxybenzene (10.5 mg, 63 μmol) was added and the mixture was diluted with ethyl acetate (ca.1.5 mL). The solution was passed through a plug of celite and concentrated *in vacuo*. NMR analysis of the crude reaction mixture revealed a 80:20 mixture of *syn* and *anti* isomers. The crude reaction was purified by flash silica gel chromatography (90:10 → 80:20 hexanes : ethyl acetate) to afford two diastereomerically pure products (**3.28**) (25 mg, 77% combined) as clear oil. ^{1}H NMR (600 MHz, $CDCl_3$) δ **3.28A** (*syn*): 4.68 (td, J = 10.7, 2.8 Hz, 1H), 3.78 – 3.70 (m, 8H), 3.42 (td, J = 10.0, 3.7 Hz, 1H), 3.22 (s, 3H), 1.91 (qd, J = 10.2, 5.1 Hz, 1H), 1.71 (ddq, J = 14.7, 9.5, 7.4 Hz, 1H), 1.65 – 1.60 (m, 1H), 1.50 (dddd, J = 13.6, 11.3, 7.5, 3.8 Hz, 1H), 1.34 – 1.18 (m, 6H), 0.92 – 0.83 (m, 6H); ^{13}C NMR (151 MHz, $CDCl_3$) δ **3.28A**: 172.5, 90.6, 61.7, 45.8, 32.3, 32.2, 30.9, 25.5, 23.2, 22.3, 13.9, 10.9; GC/MS (EI) 214.2 (M–NO_2) 200.1 (M–C_2H_6NO) t_R (*syn*) = 10.714 min. ^{1}H NMR (600 MHz, $CDCl_3$) δ **3.28B** (*anti*): 4.85 (td, J = 9.6, 3.7 Hz, 1H), 3.75 (s, 3H), 3.49 (td, J = 9.7, 4.1 Hz, 1H), 3.18 (s, 3H), 1.95 – 1.83 (m, 2H), 1.74 – 1.67 (m, 1H), 1.65 – 1.60 (m, 1H), 1.37 – 1.24 (m, 6H), 0.89 (dt, J = 16.2, 7.2 Hz, 6H); GC/MS (EI) 214.2 (M–NO_2) 200.1 (M–C_2H_6NO) t_R (*anti*) = 10.883 min. The enantiomeric excess was determined to be 85% ee for *syn* isomer by chiral HPLC analysis (CHIRALPAK OD, 1.0 mL/min, 0.5% i-PrOH/hexane, λ=254 nm); t_R(major) = 7.923 min t_R(minor) = 8.415 min. The enantiomeric excess was determined to be

20% ee for *anti* isomer by chiral HPLC analysis (CHIRALPAK OD, 1.0 mL/min, 0.5% i-PrOH/hexane, λ=254 nm); t_R(major) = 14.182 min t_R(minor) = 15.460 min.

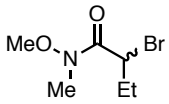

3.26

A hot 250 mL round bottom flask equipped with a magnetic stir bar and rubber septum was attached via needle to a double manifold and cooled under vacuum. The flask was backfilled with N_2 the septum was removed, and N,O-dimethylhydroxylamine·HCl (6.79 g, 69.6 mmol) was added. The septum was replaced, the flask was attached to a double manifold, and evacuated and backfilled with N_2 three times. Anhydrous DCM (120.0 mL), and triethylamine (9.7 mL, 69.6 mmol) were added to the flask sequentially via syringe and the reaction flask was cooled to 0 °C. 2-bromobutyryl bromide (7.0 mL, 58.0 mmol) was added dropwise via syringe. Once the addition is complete, ice bath was removed and the reaction stirred overnight at rt. The septum was removed and the reaction was quenched with 1 M HCl (30.0 mL) and extracted with Et_2O (2x 100 mL). The combined organic layers are washed once with H_2O (50.0 mL). The organic layer was dried over magnesium sulfate, and concentrated *in vacuo*. The crude reaction was purified by flash silica gel chromatography (90:10 hexanes : ethyl acetate) to afford (**3.26**) (8.76 g, 72% Yield) as a clear oil: 1H NMR (600 MHz, $CDCl_3$) δ 4.69 (s, 1H), 3.79 (s, 3H), 3.23 (s, 3H), 2.11 (dp, J = 14.5, 7.3 Hz, 1H), 2.02 (dp, J = 14.8, 7.5 Hz, 1H), 1.00 (t, J = 7.3 Hz, 3H).

3.14.5 Synthesis of Novel Chiral 1,2 Diamine Ligands:

Note: All yields in this section are unoptimized

Novel chiral 1,2 diamine ligands were synthesized based on previously published procedure.[38]

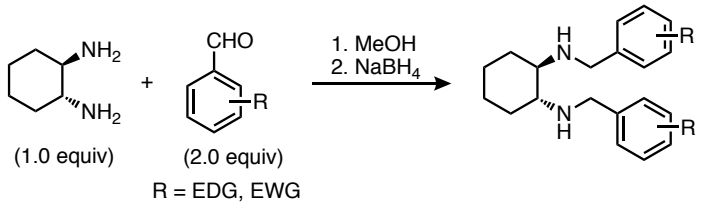

General Protocol A:

A 25 mL oven-dried round-bottom flask equipped with a stirbar and rubber septum is cooled under a stream of nitrogen. The flask was opened to air, (*1R,2R*)-(−)-1,2-Diaminocyclohexane (1.0 equiv) and anhydrous methanol were sequentially added under air. The rubber septum was replaced, purged with nitrogen for ca. 3 min and then aromatic aldehyde (2.0 equiv) was added dropwise over 3 minutes via syringe. The flask was fitted with condenser and refluxed (oil bath, 70 °C) for 1h 30 min with stirring. The reaction was cooled to rt, and reflux condenser was removed. The reaction cooled to 0 °C in an ice-water bath, and $NaBH_4$ (2.1 equiv) was added portionwise under air. After the vigorous effervescence subsided the reaction flask was fitted with condenser and refluxed (oil bath, 70 °C) for 1 h with stirring. The reaction was then cooled to 0 °C in an ice-water bath and quenched the excess $NaBH_4$ by adding H_2O until the bubbling subsides. The aqueous layer extracted with DCM (3x) and combined organic layers were dried over magnesium sulfate, filtered and the filtrate was concentrated in vacuo. The product was purified by silica gel flash chromatography.

Several novel chiral 1,2 diamine ligands were synthesized by reductive amination using sodium triacetoxy borohydride.[39]

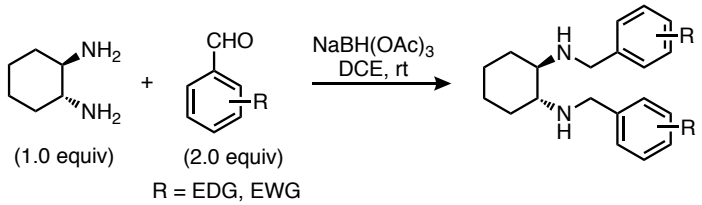

General Protocol B:

A 100 mL oven-dried round-bottom flask equipped with a stirbar and rubber septum is cooled under a stream of nitrogen. The flask was opened to air, (*1R,2R*)-(−)-1,2-Diaminocyclohexane (1.0 equiv) and anhydrous 1,2-dichloroethane were sequentially added under air. The rubber septum was replaced, purged with nitrogen for ca. 3 min and then aromatic aldehyde (2.0 equiv) was added dropwise over 3 minutes via syringe. The rubber septum was removed and $NaBH(OAc)_3$ (2.5 equiv) was added portionwise over 10 minutes, septum replaced and stirred at rt overnight under nitrogen. The reaction mixture was quenched with $NaHCO_3$ extracted with DCM (3x) and combined organic layers were dried over magnesium sulfate, filtered and the filtrate was concentrated *in vacuo*. The product was purified by silica gel flash chromatography.

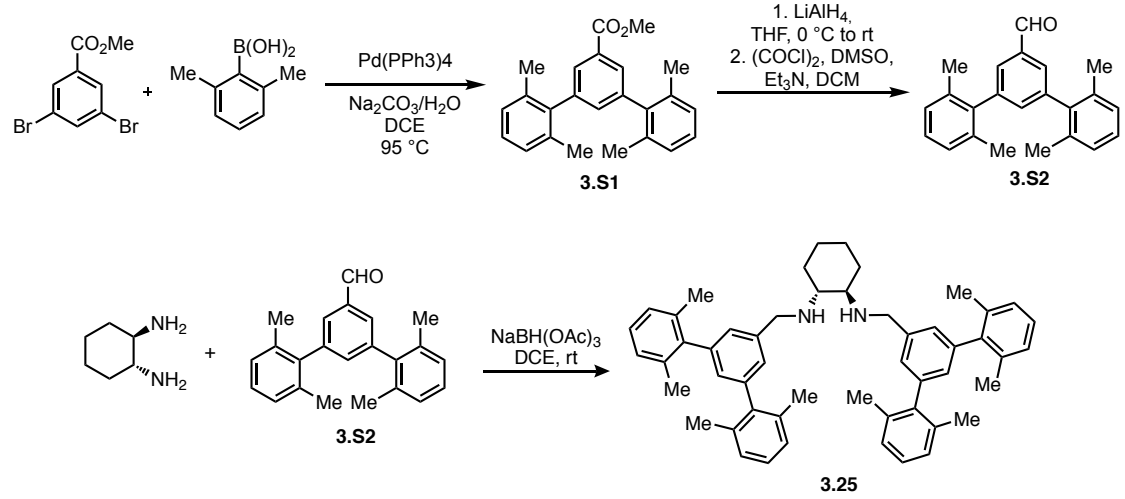

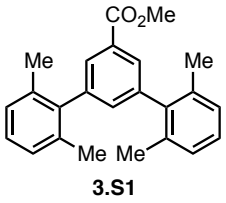

(**3.S1**) A hot 100 mL Schlenk equipped with a magnetic stir bar and a rubber septum was attached to a double manifold and allowed to cool. Once cool, the flask was backfilled with N_2 the septum was replaced, the flask was removed and tetrakis(triphenylphosphine)palladium (0) (0.39 g, 0.34 mmol), methyl 3,5-dibromobenzoate (1.0 g, 3.4 mmol), and 2,6-dimethyl boronic acid (1.22 g, 8.1 mmol), Na_2CO_3 (1.44 g, 13.6 mmol) were added. The septum was replaced, the flask was reattached to the double manifold and evacuated and backfilled with N_2 three times. DME (35 mL) and H_2O (7 mL) were sequentially added via syringe. The resulting suspension was heated in an oil bath at 95 °C for 27 h. Once complete, the reaction was cooled to rt, diluted with H_2O (30 mL) and the contents of the reaction transferred to separatory funnel, extracted with ethyl acetate (2x 50mL), dried over magnesium sulfate and concentrated *in vacuo*. The crude reaction was purified using silica gel chromatography (95:05 hexanes : ethyl acetate) to afford **3.S1** (0.64 g, 55%) as white solid. ^{1}H NMR (600 MHz, $CDCl_3$) δ 7.85 (d, J = 1.6 Hz, 2H), 7.19 – 7.15 (m, 3H), 7.11 (d, J = 7.5 Hz, 4H), 3.92 (s, 3H), 2.07 (s, 12H).

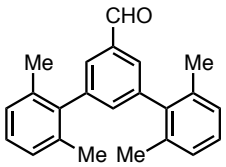

3.S2

(**3.S2**) $LiAlH_4$ (82 mg, 2.17 mmol) was placed in a flame-dried 25 mL round-bottom flask equipped with a magnetic stir bar and a rubber septum and the flask was purged with nitrogen for 10 minutes. Anhydrous THF (5 mL) was added via syringe and the flask was cooled to 0 °C in an ice-water bath. A solution of ester **3.S1** (0.50 g, 1.45 mmol) in anhydrous THF (3 mL) was added dropwise via syringe, the bath was removed, and the resulting grey suspension was allowed to stir at room temperature overnight. The reaction was opened to air, cooled to 0 °C and $NaSO_4 \cdot 10\ H_2O$ (1.0 g) was added slowly and then stirred for 1 h. The reaction, which contains granular precipitate, was filtered through a celite pad, washed with ethyl acetate (20 mL). The solvent was evaporated *in vacuo* to provide the crude alcohol (0.4 g), which was taken on to the oxidation step without further purification.

A flame-dried 25 mL round bottom flask equipped with a magnetic stir bar and a rubber septum was cooled under a stream of nitrogen and charged with anhydrous DCM (1.0 mL) and DMSO (46 μL, 0.64 mmol) via syringe. The mixture was cooled to –78 °C in a dry-ice/acetone bath. The solution of oxalyl chloride (60 μL, 0.70 mmol) in anhydrous DCM (1.0 mL) was added to the flask containing DMSO via syringe and the mixture was allowed to stir for 10 minutes at –78 °C. The crude alcohol (0.19 g, 0.59 mmol) was dissolved in anhydrous DCM (1.0 mL) and this solution was added dropwise into the flask containing DMSO and stirred for 15 minutes at –78 °C. Triethylamine (41 μL, 2.92 mmol) was added via syringe and stirred for 10 minutes at –78 °C. After 10 minutes, the reaction was warmed to room temperature. After 1 h, TLC indicated full conversion of the starting material. The septum was removed and the reaction was quenched with water (10 mL) and diluted

with DCM (10 mL). The layers were separated and the organic layer was washed with water (20 mL) and brine (2x 20 mL). The combined aqueous layers were back-extracted with with DCM (20 mL). The combined organic layers were dried with magnesium sulfate, filtered and the solvent was evaportated *in vacuo* to provide the crude aldehyde **3.S2** (0.148 g), which was taken on to the oxidation step without further purification.

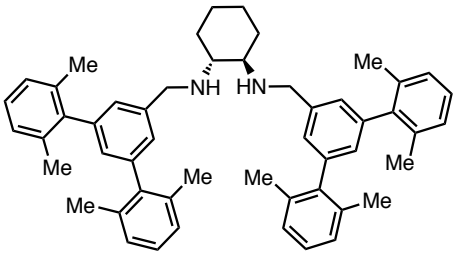

3.25

(**3.25**): According to general protocol B: (*1R,2R*)-(−)-1,2-Diaminocyclohexane (24 mg, 0.21 mmol), **3.S2** (130 mg, 0.41 mmol), and anhydrous 1,2 DCE (1.0 mL) were combined under air and $NaBH(OAc)_3$ (0.11 g, 0.52 mmol) was added portionwise over 10 minutes and stirred at rt overnight. The reaction was worked up according to the general protocol B. The crude reaction was purified by flash silica gel chromatography (98:2 DCM : triethylamine) to afford **3.25** as a white solid (0.11 g, 76%). ^{1}H NMR (600 MHz, $CDCl_3$) δ 7.12 (t, J = 7.5 Hz, 4H), 7.06 (t, J = 7.3 Hz, 8H), 7.03 (d, J = 1.6 Hz, 4H), 6.78 (t, J = 1.6 Hz, 2H), 3.92 (d, J = 13.5 Hz, 2H), 3.78 (d, J = 13.5 Hz, 2H), 2.53 (s, 1H), 2.24 (d, J = 8.8 Hz, 2H), 2.03 (s, 12H), 2.02 (s, 12H), 1.83 (d, J = 29.2 Hz, 2H), 1.66 (d, J = 9.0 Hz, 2H), 1.15 (t, J = 10.4 Hz, 2H), 1.03 (s, 1H), 0.95 (d, J = 11.3 Hz, 2H); ^{13}C NMR (101 MHz, $CDCl_3$) δ 141.72, 141.45, 141.12, 135.85, 135.79, 128.07, 127.19, 127.14, 126.88, 60.59, 50.97, 31.68, 25.01, 20.87.; HRMS (ESI) $(M+H)^+$ m/z calculated for $[C_{52}H_{59}N_2]^+$: 711.4600; found: 711.4659.

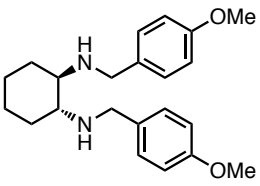

(**3.17**): According to general protocol B: (1R,2R)-(−)-1,2-Diaminocyclohexane (500 mg, 4.4 mmol), 4-Methoxy

benzaldehyde, (1.06 mL, 8.8 mmol), and anhydrous 1,2 DCE (16.0 mL) were combined under air and $NaBH(OAc)_3$ (2.32 g, 11.0 mmol) was added portionwise over 10 minutes and stirred at rt overnight. The reaction was worked up according to the general protocol B. The crude reaction was purified by flash silica gel chromatography (98:2 DCM : triethyl amine) to afford **3.17** as a white solid (1.10 g, 71%). $[\alpha]_D^{25}$=–62.5° (c = 1.00, $CHCl_3$); ^{1}H NMR (400 MHz, $CDCl_3$): δ 7.25 – 7.20 (m, 4H), 6.87 – 6.81 (m, 4H), 3.83 (d, J = 12.9 Hz, 2H), 3.80 (s, 6H), 3.58 (d, J = 12.9 Hz, 2H), 2.27 – 2.18 (m, 2H), 2.15 (dt, J = 13.4, 2.8 Hz, 2H), 1.83 – 1.66 (m, 4H), 1.22 (tdd, J = 9.8, 3.4, 2.0 Hz, 2H), 1.01 (dq, J = 16.3, 6.7, 3.7 Hz, 2H); ^{13}C NMR (101 MHz, $CDCl_3$) δ 164.4, 158.4, 133.2, 129.1, 113.6, 60.7, 55.2, 50.2, 31.5, 25.0; FTIR (cm^{-1}): 3207, 2922, 1612, 1510, 1446, 1246, 1178, 1032, 817; mp = 78-80 °C. HRMS (ESI) $(M+H)^+$ m/z calculated for $[C_{22}H_{31}N_2O_2]^+$: 355.2386; found: 355.2366.

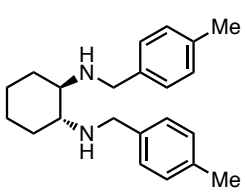

(**3.18**): According to general protocol A: (1R,2R)-(−)-1,2-Diaminocyclohexane (500 mg, 4.4 mmol), 4-Methyl benzaldehyde, (1.04 mL, 8.8 mmol), and anhydrous MeOH (3.0 mL) were combined under air and refluxed for 1:30 h with stirring. The solution allowed to cool to 0 °C in an ice-bath and $NaBH_4$ (347 mg, 9.2 mmol) was added portionwise. After the vigorous effervescence had subsided the mixture was refluxed for 1 h with stirring. The reaction was worked up according to the general protocol A. The crude reaction was purified by flash silica gel chromatography (98:2 DCM : triethyl amine) to afford **3.18** (973 mg, 69%). $[\alpha]_D^{25}$=–78.0° (c = 1.00, $CHCl_3$); ^{1}H NMR (400 MHz, $CDCl_3$): δ 7.20 (d, J = 8.0 Hz, 4H), 7.12 (d, J = 7.8 Hz, 4H), 3.87 (d, J = 13.0 Hz, 2H), 3.62 (d, J = 13.0 Hz, 2H), 2.33 (s, 6H),

2.31 – 2.22 (m, 4H), 2.16 (dq, J = 11.4, 2.4 Hz, 2H), 1.71 (tq, J = 15.8, 6.2, 4.6 Hz, 2H), 1.31 – 1.15 (m, 2H), 1.14 – 0.98 (m, 2H); ^{13}C NMR (101 MHz, $CDCl_3$) δ 137.6, 136.3, 130.0, 128.0, 60.6, 50.4, 31.3, 24.9, 21.1; FTIR (cm^{-1}): 3299, 2924, 1514, 1456, 1355, 1112, 803. HRMS (ESI) $(M+H)^+$ m/z calculated for $[C_{22}H_{31}N_2]^+$: 323.2487; found: 323.2479.

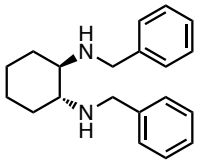

(**3.19**): According to general protocol A: (1R,2R)-(−)-1,2-Diaminocyclohexane (500 mg, 4.4 mmol), Benzaldehyde, (0.89 mL, 8.8 mmol), and anhydrous MeOH (3.0 mL) were combined under air and refluxed for 1:30 h with stirring. The solution allowed to cool to 0 °C in an ice-bath and $NaBH_4$ (347 mg, 9.2 mmol) was added portionwise. After the vigorous effervescence had subsided the mixture was refluxed for 1 h with stirring. The reaction was worked up according to the general protocol A. The crude reaction was purified by flash silica gel chromatography (98:2 DCM : triethyl amine) to afford SX (1.00 g, 78%) as a viscous yellow oil. $[\alpha]_D^{25}$=–83.4° (c = 1.00, $CHCl_3$); ^{1}H NMR (400 MHz, $CDCl_3$): δ 7.29 – 7.21 (m, 8H), 7.21 – 7.15 (m, 2H), 3.84 (d, J = 13.2 Hz, 2H), 3.60 (d, J = 13.1 Hz, 2H), 2.26 – 2.16 (m, 2H), 2.11 (dt, J = 13.2, 2.5 Hz, 2H), 1.85 (s, 2H), 1.66 (dp, J = 9.3, 3.5 Hz, 2H), 1.26 – 1.10 (m, 2H), 1.05 – 0.91 (m, 2H); ^{13}C NMR (101 MHz, $CDCl_3$) δ 141.0, 128.2, 127.9, 126.6, 60.8, 50.8, 31.4, 24.9; FTIR (cm^{-1}): 3300, 2926, 2853, 1603, 1452, 1117,1028, 857, 697. HRMS (ESI) $(M+H)^+$ m/z calculated for $[C_{20}H_{27}N_2]^+$: 295.2174; found: 295.2162.

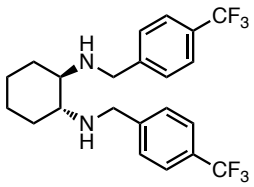

(**3.20**): According to general protocol A: (1R,2R)-(−)-1,2-Diaminocyclohexane (500 mg, 4.4 mmol), 4-(Trifluoromethyl)benzaldehyde, (1.2 mL, 8.8 mmol), and

anhydrous MeOH (3.0 mL) were combined under air and refluxed for 1:30 h with stirring. The solution allowed to cool to 0 °C in an ice-bath and $NaBH_4$ (347 mg, 9.2 mmol) was added portionwise. After the vigorous effervescence had subsided the mixture was refluxed for 1 h with stirring. The reaction was worked up according to the general protocol A. The crude reaction was purified by flash silica gel chromatography (98:2 DCM : triethyl amine) to afford **3.20** (1.41 g, 75%). $[\alpha]_D^{25}$=–62.2° (c = 1.00, $CHCl_3$); ^{1}H NMR (400 MHz, $CDCl_3$): δ 7.56 (d, J = 8.0 Hz, 4H), 7.41 (d, J = 8.0 Hz, 4H), 3.94 (d, J = 13.7 Hz, 2H), 3.71 (d, J = 13.7 Hz, 2H), 2.30 – 2.19 (m, 2H), 2.15 (dt, J = 13.0, 2.4 Hz, 2H), 1.85 (s, 2H), 1.74 (dq, J = 8.4, 3.0 Hz, 2H), 1.32 – 1.14 (m, 2H), 1.12 – 0.95 (m, 2H); ^{13}C NMR (101 MHz, $CDCl_3$) δ 145.1, 129.0 (q, J = 32 Hz), 128.15, 125.2 (q, J = 4 Hz), 124.2 (q, J = 272 Hz), 60.9, 50.3, 31.5, 24.9; ^{19}F NMR (565 MHz, $CDCl_3$) δ -62.4; FTIR (cm^{-1}): 3299, 2931, 1619, 1458, 1328, 1124, 823. HRMS (ESI) $(M+H)^+$ m/z calculated for $[C_{22}H_{25}N_2F_6]^+$: 431.1922; found: 431.1908.

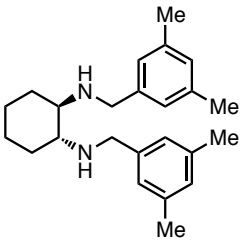

(**3.23**): According to general protocol B: (1R,2R)-(−)-1,2-Diaminocyclohexane (500 mg, 4.38 mmol), 3,5-Dimethylbenzaldehyde, (1.18 mL, 8.77 mmol), and anhydrous 1,2 DCE (16.0 mL) were combined under air and $NaBH(OAc)_3$ (2.32 g, 11.0 mmol) was added portionwise over 10 minutes and stirred at rt overnight. The reaction was worked up according to the general protocol B. The reaction was worked up according to the general protocol B. The crude reaction was purified by flash silica gel chromatography (98:2 DCM : triethyl amine) to afford **3.23** (0.890 mg, 58%) as yellow oil. $[\alpha]_D^{25}$=–59.2° (c = 1.00, $CHCl_3$); ^{1}H NMR (400 MHz,

$CDCl_3$): δ 6.95 (s, 4H), 6.87 (s, 2H), 3.83 (d, J = 12.8 Hz, 2H), 3.58 (d, J = 12.8 Hz, 2H), 2.29 (s, 14H), 2.17 (dt, J = 13.4, 2.5 Hz, 2H), 1.85 (s, 2H), 1.73 (qt, J = 9.7, 4.1 Hz, 2H), 1.33 – 1.18 (m, 2H), 1.15 – 1.00 (m, 2H); ^{13}C NMR (101 MHz, $CDCl_3$) δ 141.0, 137.7, 128.3, 125.8, 61.1, 50.9, 31.6, 25.1, 21.2; FTIR (cm^{-1}): 3300, 2924, 2854, 1607, 1458, 1118, 841. HRMS (ESI) $(M+H)^+$ m/z calculated for $[C_{24}H_{35}N_2]^+$: 351.2800; found: 351.2790.

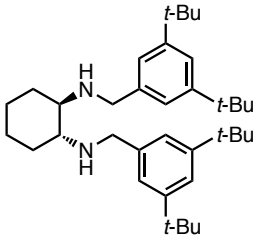

(**3.24**): According to general protocol B: (1R,2R)-(−)-1,2-Diaminocyclohexane (797 mg, 6.99 mmol), 3,5-Di-tert-butylbenzaldehyde, (3.050 g, 14.0 mmol), and anhydrous 1,2 DCE (25.0 mL) were combined under air and $NaBH(OAc)_3$ (3.70 g, 17.5 mmol) was added portionwise over 10 minutes and stirred at rt overnight. The reaction was worked up according to the general protocol B. The crude reaction was purified by flash silica gel chromatography (98:2 DCM : triethyl amine) to **3.24** (2.46 g, 68%). $[\alpha]_D^{25}$=–37.3° (c = 1.00, $CHCl_3$); ^{1}H NMR (400 MHz, $CDCl_3$): δ 7.28 (t, J = 1.9 Hz, 2H), 7.14 (d, J = 1.9 Hz, 4H), 3.90 (d, J = 12.9 Hz, 2H), 3.65 (d, J = 12.9 Hz, 2H), 2.34 – 2.24 (m, 2H), 2.24 – 2.14 (m, 2H), 1.83 (s, 2H), 1.78 – 1.65 (m, 2H), 1.34 – 1.31 (m, 2H), 1.28 (s, 36H), 1.05 (d, J = 11.3 Hz, 2H); ^{13}C NMR (101 MHz, $CDCl_3$) δ 150.5, 140.0, 122.3, 120.7, 61.0, 51.7, 34.7, 31.6, 31.5, 25.0; FTIR (cm^{-1}): 2962, 2361, 1600, 1457, 1248, 871, 713; mp = 56-58 °C. HRMS (ESI) $(M+H)^+$ m/z calculated for $[C_{36}H_{59}N_2]^+$: 519.4678; found: 519.4663.

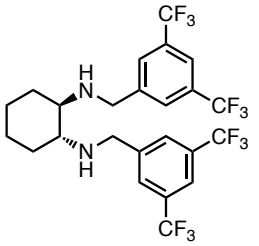

(**3.30**): According to general protocol B: (1R,2R)-(−)-1,2-Diaminocyclohexane (500 mg, 4.38 mmol), 3,5-

Bis(trifluoromethyl)benzaldehyde, (1.44 mL, 8.77 mmol), and anhydrous 1,2 DCE (16.0 mL) were combined under air and $NaBH(OAc)_3$ (2.32 g, 11.0 mmol) was added portionwise over 10 minutes and stirred at rt overnight. The reaction was worked up according to the general protocol B. The crude reaction was purified by flash silica gel chromatography (98:2 DCM : triethyl amine) to afford **3.30** (1.93 g, 78%). Note: Impure fractions can be further purified by recrystallization using $EtOH/H_2O$ mixture. $[\alpha]_D^{25}$=–45.0° (c = 1.00, $CHCl_3$); ^1H NMR (600 MHz, $CDCl_3$): δ 7.78 (s, 4H), 7.74 (s, 2H), 4.01 (d, J = 14.1 Hz, 2H), 3.81 (d, J = 14.0 Hz, 2H), 2.34 – 2.23 (m, 2H), 2.16 (dt, J = 13.9, 2.6 Hz, 2H), 1.86 (s, 2H), 1.75 (dtd, J = 9.8, 6.6, 6.1, 2.8 Hz, 2H), 1.32 – 1.19 (m, 2H), 1.11 – 0.99 (m, 2H); ^{13}C NMR (101 MHz, $CDCl_3$) δ 143.8, 131.6 (q, J = 33 Hz), 128.0, 123.4 (q, J = 273 Hz), 120.9, 61.5, 50.2, 31.6, 24.8; ^{19}F NMR (565 MHz, $CDCl_3$) δ -63.01; FTIR (cm^{-1}): 3258, 2933, 2866, 1493, 1382, 1281, 1127, 705; mp = 66-68 °C. HRMS (ESI) $(M+H)^+$ m/z calculated for $[C_{24}H_{23}N_2F_{12}]^+$: 567.1670; found: 567.1659.

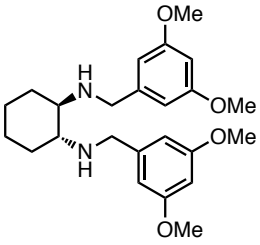

(**3.40**): According to general protocol B: (1R,2R)-(−)-1,2-Diaminocyclohexane (500 mg, 4.38 mmol), 3,5-Dimethoxybenzaldehyde, (1.46 g, 8.77 mmol), and anhydrous 1,2 DCE (16.0 mL) were combined under air and $NaBH(OAc)_3$ (2.32 g, 11.0 mmol) was added portionwise over 10 minutes and stirred at rt overnight. The reaction was worked up according to the general protocol B. The reaction was worked up according to the general protocol B. The crude reaction was purified by flash silica gel chromatography (98:2 DCM : triethyl amine) to afford **3.40** (1.34 g, 74%) as a yellow oil. $[\alpha]_D^{25}$=–54.3° (c = 1.00, $CHCl_3$); ^1H

NMR (400 MHz, $CDCl_3$): δ 6.49 (d, J = 2.3 Hz, 4H), 6.33 (t, J = 2.3 Hz, 2H), 3.88 (d, J = 13.2 Hz, 2H), 3.73 (s, 12H), 3.61 (d, J = 13.3 Hz, 2H), 2.83 (s, 2H), 2.37 – 2.26 (m, 2H), 2.16 (d, J = 13.4, 2.6 Hz, 2H), 1.80 – 1.66 (m, 2H), 1.32 – 1.01 (m, 4H); ^{13}C NMR (101 MHz, $CDCl_3$) δ 160.7, 142.6, 105.8, 98.9, 60.5, 55.1, 50.7, 31.1, 24.8; FTIR (cm^{-1}): 3298, 2930, 2837, 1596, 1461, 1204, 1152,1063, 857. HRMS (ESI) $(M+H)^+$ m/z calculated for $[C_{24}H_{35}N_2O_4]^+$: 415.2597; found: 415.2587.

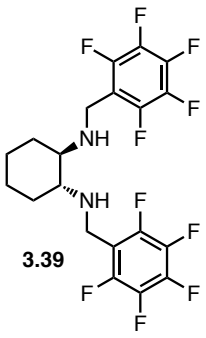

3.39

(**3.39**): According to general protocol B: (*1R,2R*)-(−)-1,2-Diaminocyclohexane (500 mg, 4.38 mmol), 2,3,4,5,6-Pentafluorobenzaldehyde, (1.08 mL, 8.77 mmol), and anhydrous 1,2 DCE (16.0 mL) were combined under air and $NaBH(OAc)_3$ (2.32 g, 11.0 mmol) was added portionwise over 10 minutes and stirred at rt overnight. The reaction was worked up according to the general protocol B. The crude reaction was purified by flash silica gel chromatography (98:2 DCM : triethylamine) to afford **3.39** as a white solid (1.22 g, 59%). $[\alpha]_D^{24}$ = –38.0° (c = 1.00, $CHCl_3$); ^1H NMR (400 MHz, $CDCl_3$): δ 3.94 (d, J = 13.3 Hz, 2H), 3.79 (d, J = 13.2 Hz, 2H), 2.18 – 2.02 (m, 4H), 1.86 – 1.69 (m, 4H), 1.31 – 1.16 (m, 2H), 1.08 – 0.93 (m, 2H); ^{13}C NMR (101 MHz, $CDCl_3$) δ 146.6 – 146.3 (m), 144.1 – 143.9 (m), 141.8 – 141.4 (m), 139.2 – 138.9 (m), 138.8 – 138.4 (m), 136.3 – 135.9 (m), 114.0 – 113.6 (m), 60.6, 37.9, 31.4, 24.8; ^{19}F NMR (565 MHz, $CDCl_3$) δ -144.7 (dd, J = 22.5, 8.5 Hz), -155.9 (t, J = 20.7 Hz), -162.3 (td, J = 22.3, 8.6 Hz); FTIR (cm^{-1}): 3293, 2924, 2851, 1447, 1366, 1134, 888, 727; mp = 44-46 °C. HRMS (ESI) $(M+H)^+$ m/z calculated for $[C_{20}H_{17}N_2F_{10}]^+$: 475.1232; found: 475.1219.

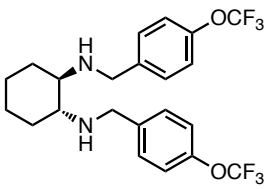

3.43

(**3.43**): According to general protocol B: (*1R,2R*)-(−)-1,2-Diaminocyclohexane (500 mg, 4.38 mmol), 4-(trifluoromethoxy)benzaldehyde, (1.25 mL, 8.77 mmol), and anhydrous 1,2 DCE (16.0 mL) were combined under air and $NaBH(OAc)_3$ (2.32 g, 11.0 mmol) was added portionwise over 10 minutes and stirred at rt overnight. The reaction was worked up according to the general protocol B. The crude reaction was purified by flash silica gel chromatography (98:2 DCM : triethylamine) to afford **3.43** (1.29 g, 64%). $[\alpha]_D^{24}$ = –62.9° (c = 1.00, $CHCl_3$); ^1H NMR (400 MHz, $CDCl_3$): δ 7.35 – 7.29 (m, 4H), 7.18 – 7.12 (m, 4H), 3.89 (d, J = 13.4 Hz, 2H), 3.65 (d, J = 13.4 Hz, 2H), 2.29 – 2.20 (m, 2H), 2.19 – 2.12 (m, 2H), 1.86 (s, 2H), 1.79 – 1.67 (m, 2H), 1.32 – 1.15 (m, 2H), 1.11 – 0.95 (m, 2H); ^{13}C NMR (101 MHz, $CDCl_3$) δ 148.0, 139.8, 129.2, 120.9, 120.4 (q, J = 258 Hz), 60.9, 50.1, 31.5, 24.9; ^{19}F NMR (565 MHz, $CDCl_3$) δ -57.9; FTIR (cm^{-1}): 3300, 2930, 2857, 1508, 1263, 1161, 920, 846. HRMS (ESI) $(M+H)^+$ m/z calculated for $[C_{22}H_{25}N_2O_2F_6]^+$: 463.1743; found: 463.1809.

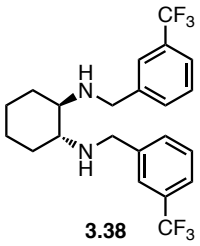

3.38

(**3.38**): According to general protocol B: (*1R,2R*)-(−)-1,2-Diaminocyclohexane (500 mg, 4.38 mmol), 3-(trifluoromethyl)benzaldehyde, (1.17 mL, 8.77 mmol), and anhydrous 1,2 DCE (16.0 mL) were combined under air and $NaBH(OAc)_3$ (2.32 g, 11.0 mmol) was added portionwise over 10 minutes and stirred at rt overnight. The reaction was worked up according to the general protocol B. The crude reaction was purified by flash silica gel chromatography (98:2 DCM : triethylamine) to afford **3.38** (1.35 g, 72%) as a pale yellow oil. $[\alpha]_D^{24}$ = –50.2° (c = 1.00, $CHCl_3$); ^1H

NMR (400 MHz, $CDCl_3$): δ 7.58 (s, 2H), 7.50 (dt, J = 8.3, 1.6 Hz, 4H), 7.41 (t, J = 7.6 Hz, 2H), 3.95 (d, J = 13.5 Hz, 2H), 3.71 (d, J = 13.5 Hz, 2H), 2.31 – 2.21 (m, 2H), 2.17 (dt, J = 13.1, 2.5 Hz, 2H), 1.85 (s, 2H), 1.80 – 1.69 (m, 2H), 1.33 – 1.17 (m, 2H), 1.10 – 0.97 (m, 2H); ^{13}C NMR (101 MHz, $CDCl_3$) δ 142.0, 131.3, 130.6 (q, J = 32 Hz), 128.8, 124.6, 124.2 (q, J = 272 Hz), 123.7, 61.1, 50.5, 31.6, 24.9; ^{19}F NMR (565 MHz, $CDCl_3$) δ - 62.6; FTIR (cm^{-1}): 3298, 2930, 2857, 1449, 1329, 1123, 796, 702. HRMS (ESI) $(M+H)^+$ m/z calculated for $[C_{22}H_{25}N_2F_6]^+$: 431.1743; found: 431.1913.

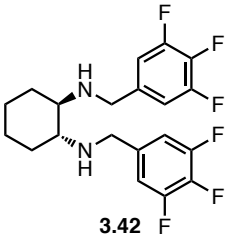

3.42

(**3.42**): According to general protocol B: (*1R,2R*)-(−)-1,2-Diaminocyclohexane (500 mg, 4.38 mmol), 3,4,5-trifluorobenzaldehyde, (0.99 mL, 8.77 mmol), and anhydrous 1,2 DCE (16.0 mL) were combined under air and $NaBH(OAc)_3$ (2.32 g, 11.0 mmol) was added portionwise over 10 minutes and stirred at rt overnight. The reaction was worked up according to the general protocol B. The crude reaction was purified by flash silica gel chromatography (98:2 DCM : triethylamine) to afford **3.42** as a white solid (1.19 g, 68%). $[\alpha]_D^{24} = –66.0°$ (c = 1.00, $CHCl_3$); ^1H NMR (400 MHz, $CDCl_3$): δ 6.99 – 6.90 (m, 4H), 3.82 (d, J = 14.0 Hz, 2H), 3.62 (d, J = 14.0 Hz, 2H), 2.24 – 2.14 (m, 2H), 2.13 – 2.05 (m, 2H), 1.84 – 1.67 (m, 4H), 1.21 (t, J = 11.8, 7.9, 5.9 Hz, 2H), 1.06 – 0.91 (m, 2H); ^{13}C NMR (101 MHz, $CDCl_3$) δ 152.3 (dd, J = 10.0, 3.9 Hz), 149.8 (dd, J = 9.9, 3.9 Hz), 139.7 (t, J = 15.4 Hz), 137.6 – 137.0 (m), 111.5 (d, J = 21.2 Hz), 60.9, 49.7, 31.4, 24.8; ^{19}F NMR (565 MHz, $CDCl_3$) δ –134.8 (d, J = 22 Hz), –163.1 (t, J = 22 Hz); FTIR (cm^{-1}): 3294, 2930, 2863, 1618, 1526, 1444, 1226, 1038, 857; mp = 60-62 °C. HRMS (ESI) $(M+H)^+$ m/z calculated for $[C_{20}H_{21}N_2F_6]^+$: 403.1609; found: 403.1611.

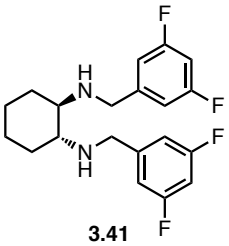

3.41

(**3.41**): According to general protocol B: (*1R,2R*)-(−)-1,2-Diaminocyclohexane (500 mg, 4.38 mmol), 3,5-difluorobenzaldehyde, (0.96 mL, 8.77 mmol), and anhydrous 1,2 DCE (16.0 mL) were combined under air and $NaBH(OAc)_3$ (2.32 g, 11.0 mmol) was added portionwise over 10 minutes and stirred at rt overnight. The reaction was worked up according to the general protocol B. The crude reaction was purified by flash silica gel chromatography (98:2 DCM : triethylamine) to afford **3.41** (1.11 g, 70%) as yellow oil. $[\alpha]_D^{24}$ = –60.0° (c = 1.00, $CHCl_3$); ^{1}H NMR (400 MHz, $CDCl_3$): δ 6.89 – 6.81 (m, 4H), 6.67 (tt, J = 9.0, 2.4 Hz, 2H), 3.87 (d, J = 14.0 Hz, 2H), 3.66 (d, J = 14.0 Hz, 2H), 2.27 – 2.17 (m, 2H), 2.16 – 2.08 (m, 2H), 1.84 (s, 2H), 1.78 – 1.67 (m, 2H), 1.30 – 1.14 (m, 2H), 1.01 (tdd, J = 17.0, 8.4, 4.0 Hz, 2H); ^{13}C NMR (101 MHz, $CDCl_3$) δ 164.2 (d, J = 12.8 Hz), 161.7 (d, J = 12.8 Hz), 145.3 (t, J = 8.5 Hz), 111.4 – 109.6 (m), 102.1 (t, J = 25.5 Hz), 60.8, 50.1, 31.5, 24.8; ^{19}F NMR (565 MHz, $CDCl_3$) δ -110.32; FTIR (cm^{-1}): 2930, 2856, 1652, 1596, 1457, 1315, 1116, 1044, 847. HRMS (ESI) $(M+H)^+$ m/z calculated for $[C_{20}H_{23}N_2F_4]^+$: 366.1719; found: 366.1791.

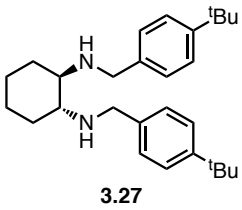

3.27

(**3.27**): According to general protocol A: (1R,2R)-(−)-1,2-Diaminocyclohexane (500 mg, 4.4 mmol), 4-*tert*-butyl benzaldehyde, (2.03 mL, 8.8 mmol), and anhydrous MeOH (3.0 mL) were combined under air and refluxed for 1:30 h with stirring. The solution allowed to cool to 0 °C in an ice-bath and $NaBH_4$ (347 mg, 9.2 mmol) was added portionwise. After the vigorous effervescence had subsided the mixture was refluxed for 1 h with stirring. The reaction was worked up according to

the general protocol A. The crude reaction was purified by flash silica gel chromatography (98:2 DCM : triethyl amine) to afford **3.27** (1.10 g, 62%). ^{1}H NMR (600 MHz, $CDCl_3$) δ 7.33 (d, J = 8.2 Hz, 4H), 7.27 – 7.24 (m, 4H), 3.87 (d, J = 13.0 Hz, 2H), 3.63 (d, J = 13.1 Hz, 2H), 2.33 – 2.23 (m, 2H), 2.17 (dd, J = 9.2, 4.5 Hz, 2H), 1.85 (s, 2H), 1.78 – 1.67 (m, 2H), 1.32 (s, 18H), 1.29 – 1.19 (m, 2H), 1.11 – 0.99 (m, 2H).

3.14.6 General Protocol for Synthesis of Previously Unknown α-bromo amides:

Note: All yields in this section are unoptimized

General Protocol C. A hot round bottom flask equipped with a magnetic stir bar and rubber septum was attached via needle to a double manifold and cooled under vacuum. The flask was evacuated and backfilled with N_2 three times. Anhydrous THF, triethylamine (1.1 quiv), and amine (1.0 equiv) were added to the flask sequentially via syringe and the reaction flask was cooled to 0 °C. α-Bromoacylbromide (1.0 quiv) was added dropwise via syringe. Once the addition is complete, ice bath was removed and the reaction stirred overnight at rt. The septum was removed and the reaction was quenched with 1 M HCl (1x) and extracted with Et_2O (2x). The combined organic layers are washed once with H_2O (1x). The organic layer was dried over magnesium sulfate, and concentrated *in vacuo*. The crude reaction was purified by flash silica gel chromatography.

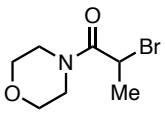

(**3.S3**): According to general protocol C: A hot 500 mL round bottom flask equipped with a magnetic stir bar and rubber septum was attached via needle to a double manifold and cooled under vacuum. The flask was evacuated and backfilled with N_2 three times. Anhydrous THF (104.0 mL), triethylamine (8.0 mL, 57.4 mmol), and morpholine (5.02 mL, 57.4 mmol) were added

to the flask sequentially via syringe and the reaction flask was cooled to 0 °C. 2-Bromopropionyl bromide (5.41 mL, 51.7 mmol) was added dropwise via syringe. Once the addition is complete, ice bath was removed and the reaction stirred overnight at rt. The septum was removed and the reaction was quenched with 1 M HCl (50.0 mL) and extracted with Et_2O (2x 50 mL). The combined organic layers are washed once with H_2O (50.0 mL). The organic layer was dried over magnesium sulfate, and concentrated *in vacuo*. The crude reaction was purified by flash silica gel chromatography (60:40 hexanes : ethyl acetate) to afford **3.S3** (8.3 g, 65%) as a colorless oil: ^{1}H NMR (400 MHz, $CDCl_3$): δ 4.51 (q, J = 6.6 Hz, 1H), 3.83 (ddd, J = 13.3, 5.2, 3.5 Hz, 1H), 3.77 – 3.66 (m, 3H), 3.62 (dt, J = 17.7, 3.8 Hz, 1H), 3.47 (dddd, J = 13.6, 10.6, 6.9, 4.0 Hz, 2H), 1.84 (d, J = 6.6 Hz, 3H); ^{13}C NMR (101 MHz, $CDCl_3$) δ 167.6, 66.6, 66.2, 46.5, 42.5, 37.7, 21.5; FTIR (cm^{-1}): 2970, 2857, 1653, 1434, 1375, 1248, 1115, 1029, 847. HRMS (ESI) $(M+H)^+$ m/z calculated for $[C_7H_{13}NO_2Br]^+$: 222.0051; found: 222.01230.

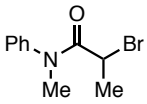

(**3.S4**): According to general protocol C: A hot 250 mL round bottom flask equipped with a magnetic stir bar and rubber septum was attached via needle to a double manifold and cooled under vacuum. The flask was evacuated and backfilled with N_2 three times. Anhydrous THF (50.0 mL), triethylamine (3.8 mL, 27.5 mmol), and N-methylaniline (3.0 mL, 27.5 mmol) were added to the flask sequentially via syringe and the reaction flask was cooled to 0 °C. 2-Bromopropionyl bromide (2.61 mL, 25.0 mmol) was added dropwise via syringe. Once the addition is complete, ice bath was removed and the reaction stirred overnight at rt. The septum was removed and the reaction was quenched with 1 M HCl (50.0 mL) and extracted with Et_2O (2x 50 mL). The combined organic layers are washed

once with H_2O (50.0 mL). The organic layer was dried over magnesium sulfate, and concentrated *in vacuo*. The crude reaction was purified by flash silica gel chromatography (90:10 hexanes : ethyl acetate) to afford **3.S4** (3.75 g, 62%) as off white solid:^{1}H NMR (400 MHz, $CDCl_3$): δ 7.50 – 7.37 (m, 3H), 7.29 (d, J = 7.6 Hz, 2H), 4.27 (q, J = 6.7 Hz, 1H), 3.30 (s, 3H), 1.74 (d, J = 6.7 Hz, 3H); ^{13}C NMR (101 MHz, $CDCl_3$) δ 169.5, 142.8, 129.9, 128.4, 127.1, 39.1, 38.1, 21.8; FTIR (cm^{-1}): 2923, 1668, 1595, 1495, 1388, 1120, 700; mp = 35-37 °C. HRMS (ESI) $(M+H)^+$ m/z calculated for $[C_{10}H_{13}NOBr]^+$: 242.0102; found: 242.0173.

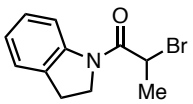

(**3.S5**): According to general protocol C: A hot 250 mL round bottom flask equipped with a magnetic stir bar and rubber septum was attached via needle to a double manifold and cooled under vacuum. The flask was evacuated and backfilled with N_2 three times. Anhydrous THF (50.0 mL), triethylamine (3.8 mL, 27.5 mmol), and indoline (3.08 mL, 27.5 mmol) were added to the flask sequentially via syringe and the reaction flask was cooled to 0 °C. 2-Bromopropionyl bromide (2.61 mL, 25.0 mmol) was added dropwise via syringe. Once the addition is complete, ice bath was removed and the reaction stirred overnight at rt. The septum was removed and the reaction was quenched with 1 M HCl (30.0 mL) and extracted with ethyl acetate (2x 30 mL). The combined organic layers are washed once with H_2O (30.0 mL). The organic layer was dried over magnesium sulfate, and concentrated *in vacuo*. The crude reaction was purified by recrystallization using Ethyl acetate to afford **3.S5** (4.31 g, 68%) as pale brown crystalline solid: ^{1}H NMR (400 MHz, DMSO-d6): δ 8.09 (d, J = 8.0 Hz, 1H), 7.27 (dd, J = 7.5, 1.4 Hz, 1H), 7.18 (t, J = 8.0 Hz, 1H), 7.05 (td, J = 7.4, 1.1 Hz, 1H), 4.98 (q, J = 6.5 Hz, 1H), 4.32 – 4.23 (m, 1H), 4.20 – 4.11 (m, 1H), 3.28 – 3.09 (m, 2H), 1.75 (d, J = 6.4 Hz,

3H); ^{13}C NMR (101 MHz, DMSO-d6) δ 166.9, 142.6, 132.2, 127.1, 125.0, 124.0, 116.4, 47.4, 42.6, 27.4, 21.3; FTIR (cm^{-1}): 2923, 1647, 1594, 1480, 1370, 1162, 758; mp = 138-140 °C. HRMS (ESI) $(M+H)^+$ m/z calculated for $[C_{11}H_{13}NOBr]^+$: 254.0102; found: 254.0169.

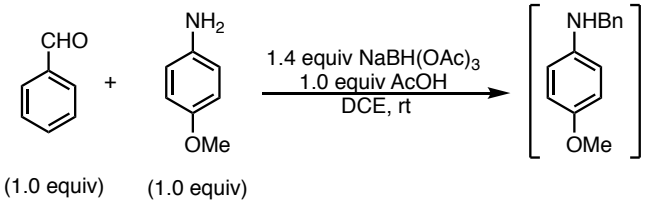

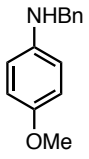

(**3.S6**): A 250 mL oven-dried round-bottom flask equipped with a stir bar and rubber septum is cooled under a stream of nitrogen. The flask was opened to air, 4-methoxy aniline (2.7 mL, 23.6 mmol) and anhydrous 1,2-DCE (80.0 mL) were sequentially added under air. The rubber septum was replaced, purged with nitrogen for ca. 3 min and then benzaldehyde (2.4 mL, 23.6 mmol) was added dropwise over 3 minutes via syringe. The rubber septum was removed, $NaBH(OAc)_3$ (7.0 g, 33 mmol) was added portionwise over 15 minutes, and then acetic acid (1.35 mL, 23.6 mmol) was added slowly via pipette, septum replaced, and stirred at rt overnight under nitrogen. The reaction mixture was quenched with $NaHCO_3$, extracted with DCM (3x 30 mL) and combined organic layers were dried over magnesium sulfate, filtered and the filtrate was concentrated *in vacuo* to afford **3.S6** (5.0g). The product was taken to the next step without further purification.

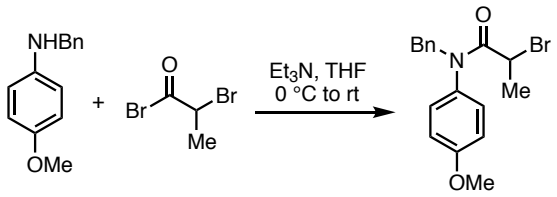

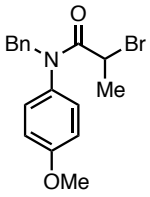

(**3.S7**): A hot 250 mL round bottom flask equipped with a magnetic stir bar and rubber septum was attached via needle to a double manifold and cooled under vacuum. The flask was backfilled with N_2, the septum was removed, and **3.S6** (5.0 g, 23.2 mmol) was added. The septum was replaced, the flask was attached to a double manifold, and evacuated and backfilled with N_2 three times. Anhydrous THF (45.0 mL), and triethylamine (3.56 mL, 25.5 mmol), were added to the flask sequentially via syringe and the reaction flask was cooled to 0 °C. 2-Bromopropionyl bromide (2.42 mL, 23.2mmol) was added dropwise via syringe. Once the addition is complete, ice bath was removed and the reaction stirred overnight at rt. The septum was removed and the reaction was quenched with 1 M HCl (50.0 mL) and extracted with Et_2O (2x 50 mL). The combined organic layers are washed once with H_2O (50.0 mL). The organic layer was dried over magnesium sulfate, and concentrated *in vacuo*. The crude reaction was purified by flash silica gel chromatography (95:05 → 90:10 hexanes : ethyl acetate) to afford **3.S7** (5.25 g, 65%) as a colorless oil: ^{1}H NMR (400 MHz, $CDCl_3$): δ 7.31 – 7.23 (m, 3H), 7.21 – 7.17 (m, 2H), 6.95 (s, 2H), 6.86 – 6.80 (m, 2H), 4.94 (d, J = 14.1 Hz, 1H), 4.75 (d, J = 14.2 Hz, 1H), 4.25 (q, J = 6.7 Hz, 1H), 3.80 (s, 3H), 1.76 (d, J = 6.6 Hz, 3H); ^{13}C NMR (101 MHz, $CDCl_3$) δ 169.7, 159.2, 136.8, 133.4, 129.2, 128.7, 128.3, 127.4, 114.5, 55.3, 53.5, 39.4, 21.6; FTIR (cm^{-1}): 2932, 2850, 1668, 1511, 1444, 1251, 1180, 1038, 838. HRMS (ESI) $(M+H)^+$ m/z calculated for $[C_{17}H_{19}NO_2Br]^+$: 348.0599; found: 348.0593.

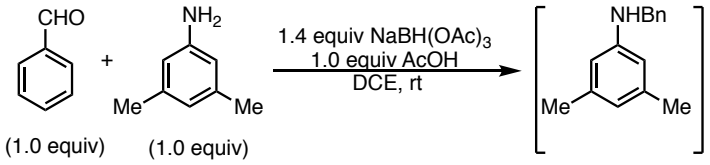

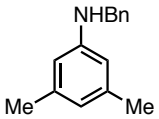

(**3.S8**): A 250 mL oven-dried round-bottom flask equipped with a stir bar and rubber septum is cooled under a stream of nitrogen. The flask was opened to air, 3,5-dimethyl aniline (2.95 mL, 23.6 mmol) and anhydrous 1,2-DCE (80.0 mL) were sequentially added under air. The rubber septum was replaced, purged with nitrogen for ca. 3 min and then benzaldehyde (2.4 mL, 23.6 mmol) was added dropwise over 3 minutes via syringe. The rubber septum was removed, $NaBH(OAc)_3$ (7.0 g, 33 mmol) was added portionwise over 15 minutes, and then acetic acid (1.35 mL, 23.6 mmol) was added slowly via pipette, septum replaced, and stirred at rt overnight under nitrogen. The reaction mixture was quenched with $NaHCO_3$, extracted with DCM (3x 30 mL) and combined organic layers were dried over magnesium sulfate, filtered and the filtrate was concentrated *in vacuo* to afford **3.S8** (4.5 g). The product was taken to the next step without further purification.

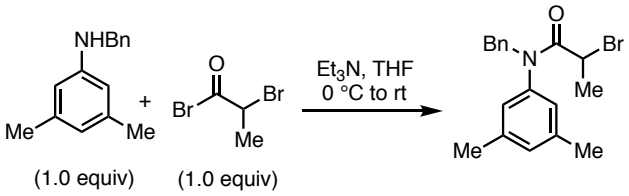

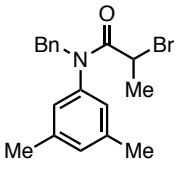

(**3.S9**): A hot 250 mL round bottom flask equipped with a magnetic stir bar and rubber septum was attached via needle to a double manifold and cooled under vacuum. The flask was backfilled with N_2, the septum was removed, and **3.S8** (4.5 g, 21.2 mmol) was added. The septum was replaced, the flask was attached to a double manifold, and

evacuated and backfilled with N_2 three times. Anhydrous THF (40.0 mL), and triethylamine (3.25 mL, 23.3 mmol), were added to the flask sequentially via syringe and the reaction flask was cooled to 0 °C. 2-Bromopropionyl bromide (2.42 mL, 21.2 mmol) was added dropwise via syringe. Once the addition is complete, ice bath was removed and the reaction stirred overnight at rt. The septum was removed and the reaction was quenched with 1 M HCl (50.0 mL) and extracted with Et_2O (2x 50 mL). The combined organic layers are washed once with H_2O (50.0 mL). The organic layer was dried over magnesium sulfate, and concentrated *in vacuo*. The crude reaction was purified by flash silica gel chromatography (95:05 → 90:10 hexanes : ethyl acetate) to afford **3.S9** (4.3 g, 62%) as a viscous yellow oil: ^{1}H NMR (600 MHz, $CDCl_3$): δ 7.31 – 7.22 (m, 3H), 7.23 – 7.18 (m, 2H), 6.96 (s, 1H), 6.66 (s, 2H), 4.94 (d, J = 14.3 Hz, 1H), 4.75 (d, J = 14.3 Hz, 1H), 4.28 (d, J = 6.7 Hz, 1H), 2.26 (s, 6H), 1.76 (d, J = 6.7 Hz, 3H); ^{13}C NMR (101 MHz, $CDCl_3$) δ 169.5, 140.9, 139.3, 136.8, 130.1, 128.6, 128.3, 127.3, 125.5, 53.5, 39.5, 21.8, 21.0; FTIR (cm^{-1}): 2920, 1668, 1594, 1399, 1236, 1184, 1061, 855, 710. HRMS (ESI) $(M+H)^+$ m/z calculated for $[C_{17}H_{17}NO_2Br]^+$: 346.0807; found: 346.0802.

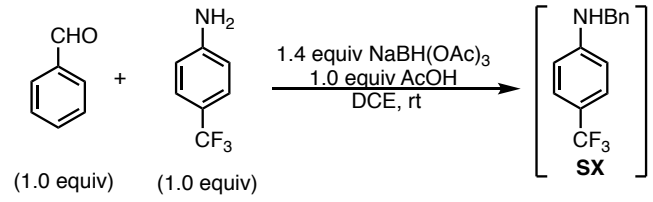

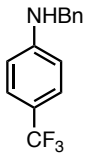

(**3.S10**): A 250 mL oven-dried round-bottom flask equipped with a stir bar and rubber septum is cooled under a stream of nitrogen. The flask was opened to air, 4-(trifluoromethyl) aniline (2.96 mL, 23.6 mmol) and anhydrous 1,2-DCE (80.0 mL) were sequentially added under air. The

rubber septum was replaced, purged with nitrogen for ca. 3 min and then benzaldehyde (2.4 mL, 23.6 mmol) was added dropwise over 3 minutes via syringe. The rubber septum was removed, $NaBH(OAc)_3$ (7.0 g, 33 mmol) was added portionwise over 15 minutes, and then acetic acid (1.35 mL, 23.6 mmol) was added slowly via pipette, septum replaced, and stirred at rt overnight under nitrogen. The reaction mixture was quenched with $NaHCO_3$, extracted with DCM (3x 30 mL) and combined organic layers were dried over magnesium sulfate, filtered and the filtrate was concentrated in vacuo to afford **3.S10** (5.0 g) as a yellow oil. The product was taken to the next step without further purification.

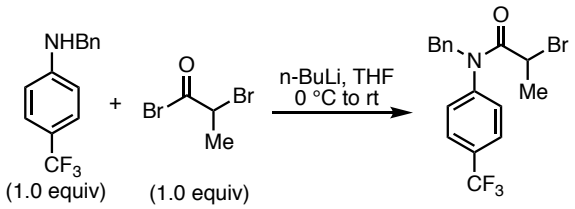

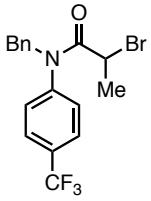

(**3.S11**): A flame-dried 100 mL round-bottomed flask equipped with a magnetic stir bar and a rubber septum was cooled under stream of N_2 for 10 minutes. **3.S10** (5.0 g, 19.9 mmol), and anhydrous THF (40.0 mL) was added sequentially via syringe. The mixture was cooled to 0 °C in an ice bath. n-BuLi (8.64 mL of a 2.60 M solution in hexane, 21.9 mmol) was added to the flask via syringe slowly, and the reaction allowed to stir for 30 minutes at 0 °C. 2-Bromopropionyl bromide (2.3 mL, 21.9 mmol) was added dropwise via syringe. Once the addition is complete, ice bath was removed and the reaction stirred overnight at rt. The septum was removed and the reaction was quenched with saturated NH_4Cl (50.0 mL) and extracted with Et_2O (2x 50 mL). The combined organic layers are washed once with H_2O (50.0 mL). The organic layer was dried over magnesium sulfate, and

concentrated *in vacuo*. The crude reaction was purified by flash silica gel chromatography (95:05 → 90:10 hexanes : ethyl acetate) to afford **3.S11** (2.5 g, 33%) as a pale yellow solid: ^{1}H NMR (600 MHz, $CDCl_3$): δ 7.62 (d, J = 8.2 Hz, 2H), 7.32 – 7.27 (m, 3H), 7.23 – 7.16 (m, 4H), 5.00 (d, J = 14.4 Hz, 1H), 4.80 (d, J = 14.4 Hz, 1H), 4.13 (q, J = 6.6 Hz, 1H), 1.79 (d, J = 6.6 Hz, 3H); ^{13}C NMR (101 MHz, $CDCl_3$) δ 169.2, 144.2, 136.3, 130.8 (q, J = 33 Hz),128.9, 128.8, 128.7,127.9, 126.9, 123.6 (q, J = 273 Hz), 53.6, 39.1, 21.7; ^{19}F NMR (565 MHz, $CDCl_3$) δ -63.6; FTIR (cm^{-1}): 2928, 1672, 1613, 1324, 1169, 1069, 851; mp = 48-50 °C. HRMS (ESI) $(M+H)^+$ m/z calculated for $[C_{17}H_{16}NOBrF_3]^+$: 386.0367; found: 386.0369.

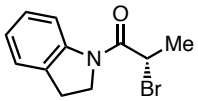

(**3.81**): A hot 100 mL round-bottom flask equipped with a magnetic stir bar and rubber septum was purged with a stream of nitrogen until cool. Indoline (1.1 mL, 9.8 mmol), (S)-(–)-2-bromopropanoic acid (0.88 mL, 9.80 mmol), DCM (33.0 mL), and triethylamine (1.37 mL, 9.8 mmol), were added to the flask sequentially via syringe and the reaction flask was cooled to 0 °C in an ice bath. The rubber septum was removed, HATU (4.1 g, 10.8 mmol) was added portionwise over 3 min, septum replaced and stirred at 0 °C for 2 hours and upon completion (as monitored by TLC) the reaction was quenched with brine (30 mL) and diluted with DCM (30 mL). The resulting biphasic mixture was then transferred to separatory funnel and the layers were separated. The organic layer was washed with brine (2x 30 mL), dried over magnesium sulfate, filtered and concentrated *in vacuo* to give crude product. The crude reaction was purified by recrystallization using DCM to afford **3.81** (1.27 g, 51%) as white crystalline solid: ^{1}H NMR (400 MHz, DMSO-d6): δ 8.09 (d, J = 8.0 Hz, 1H), 7.27 (dd, J = 7.5, 1.4 Hz, 1H), 7.18 (t, J = 8.0 Hz, 1H), 7.05 (td, J = 7.4, 1.1 Hz, 1H), 4.98 (q, J = 6.5 Hz, 1H),

4.32 – 4.23 (m, 1H), 4.20 – 4.11 (m, 1H), 3.28 – 3.09 (m, 2H), 1.75 (d, J = 6.4 Hz, 3H); ^{13}C NMR (101 MHz, DMSO-d6) δ 166.9, 142.6, 132.2, 127.1, 125.0, 124.0, 116.4, 47.4, 42.6, 27.4, 21.3; FTIR (cm^{-1}): 2923, 1647, 1594, 1480, 1370, 1162, 758; mp = 138-140 °C; $[\alpha]_D^{24}$=+143.0° (c = 1.00, $CHCl_3$) HRMS (ESI) $(M+H)^+$ m/z calculated for $[C_{11}H_{13}NOBr]^+$: 254.0102; found: 254.0169.

The *R*-(**3.81**) was prepared based on the above procedure and ^{1}H, ^{13}C, NMR matches with *S*-(**3.81**) except the specific rotation $[\alpha]_D^{24} = -143.0°$.

3.14.7 Synthesis of Radical clock substrate 3.79

Note: All yields in this section are unoptimized

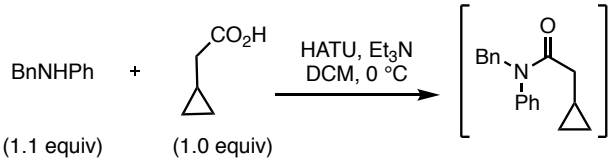

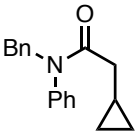

(**3.S12**): A hot 100 mL round bottom flask equipped with a magnetic stir bar and rubber septum was purged with a stream of nitrogen until cool. N-Benzylaniline (2.0 g, 11.0 mmol), cyclopropyl acetic acid (1.0 g, 10.0 mmol), DCM (33.0 mL), and diisopropyl ethylamine (5.2 mL, 30.0 mmol), were added to the flask sequentially via syringe and the reaction flask was cooled to 0 °C in an ice bath. The rubber septum was removed, HATU (4.5 g, 12.0 mmol) was added portionwise over 3 min, septum replaced and stirred at rt for 2 hours and upon completion (as monitored by TLC) the reaction was quenched with brine (30 mL) and diluted with DCM (30 mL). The resulting biphasic mixture was then transferred to separatory funnel and the layers were separated. The organic layer was washed with brine (2x 30 mL), dried over magnesium sulfate, filtered through a glass frit and

concentrated *in vacuo* to give crude product. The crude reaction was partially purified by flash silica gel chromatography (95:05 → 90:10 hexanes : ethyl acetate) to afford of slightly impure **3.S12** (1.72 g). The product was taken to the next step without further purification.

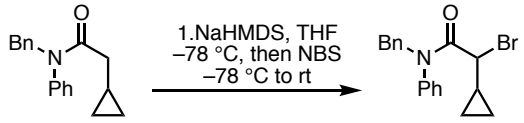

3.79

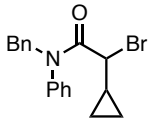

(**3.79**): A flame-dried 100 mL round-bottomed flask equipped with a magnetic stir bar and a rubber septum was cooled under stream of N_2 for 10 minutes. **3.S12** (1.0 g, 3.76 mmol), and anhydrous THF (35 mL) was added sequentially via syringe. The mixture was cooled to –78 °C in a dry-ice/acetone bath. NaHMDS (2.8 mL of a 2.0 M solution in THF, 5.64 mmol) was added to the flask via syringe slowly, and the reaction allowed to stir for 45 minutes at –78 °C. N-Bromosuccinimide (0.8 g, 4.5 mmol) was dissolved in 8 mL THF and then, the solution was added dropwise via syringe. Once the addition is complete, dry-ice/acetone bath was removed and the reaction stirred overnight at rt. The septum was removed and the reaction was quenched with H_2O (50.0 mL) and extracted with EtOAc (2x 100 mL). The combined organic layers are washed once with H_2O (50.0 mL). The organic layer was dried over magnesium sulfate, and concentrated *in vacuo*. The crude reaction was purified by flash silica gel chromatography (95:05 hexanes : ethyl acetate) to afford **3.79** (0.672 g, 52%) as a white solid:^{1}H NMR (400 MHz, $CDCl_3$): δ 7.35 – 7.31 (m, 3H), 7.30 – 7.26 (m, 3H), 7.20 (dd, J = 7.3, 2.2 Hz, 2H), 7.07 – 6.98 (m, 2H), 5.03 (d, J = 14.2 Hz, 1H), 4.77 (d, J = 14.3 Hz, 1H), 3.38 (d, J = 10.3 Hz, 1H), 1.83 (dddd, J = 12.9, 10.0, 8.1, 4.9 Hz, 1H), 0.89 – 0.81 (m, 1H), 0.81 –

0.72 (m, 1H), 0.28 – 0.14 (m, 2H); ^{13}C NMR (101 MHz, $CDCl_3$) δ 168.5, 141.0, 136.7, 129.7, 128.8, 128.6, 128.4, 128.2, 127.5, 53.4, 51.2, 16.1, 9.2, 6.8; FTIR (cm^{-1}): 3062, 1667, 1594, 1498, 1409, 1178, 699; mp = 103-105 °C; HRMS (ESI) $(M+H)^+$ m/z calculated for $[C_{18}H_{19}NOBr]^+$: 344.0572; found: 344.0638.

3.14.8 Synthesis of Starting Nitroalkanes

Note: All yields in this section are unoptimized

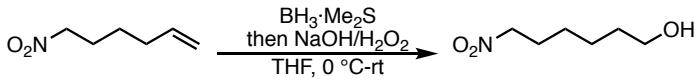

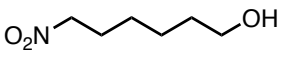

(**3.S13**)A flame-dried 250 mL round bottom flask equipped with a magnetic stir bar and a rubber septum was charged with the 6-nitrohex-1-ene (3.0 g, 23.2 mmol) and the flask was purged with a stream of nitrogen for 5 minutes and cooled to 0 °C in an ice-water bath. Anhydrous THF (100 mL) was added via syringe. Borane-dimethylsulfide complex (~18.0 mL of a 2M solution in THF, 34.8 mmol) was added to the flask slowly via syringe. The mixture was stirred at 0 °C for 25 minutes, then warmed to rt and stirred for 4 hours. The mixture was stirred was cooled to 0 °C in an ice-water bath and 3M NaOH (12 mL, 34.8 mmol) was added slowly via syringe (caution: vigorous gas evolution). Next, 30% aqueous H_2O_2 (4.0 mL) was added via syringe. The mixture was warmed to rt and stirred overnight. The septum was removed, and the mixture was diluted with EtOAc (80 mL) and the layer were separated. The organic layer was washed with brine (50 mL). The combined aqueous layers were extracted with EtOAc (50 mL). The combined organic layers were again washed with brine (50 mL), dried with magnesium sulfate, filtered and concentrated *in vacuo*. The crude reaction was

purified by flash silica gel chromatography (70:30 hexanes : ethyl acetate) to afford **3.S13** (2.5 g, 74% Yield) as a colorless oil: ^{1}H NMR (600 MHz, $CDCl_3$): δ 4.39 (t, J = 7.0 Hz, 2H), 3.65 (t, J = 6.5 Hz, 2H), 2.14 – 1.84 (m, 2H), 1.58 (tdd, J = 6.9, 5.4, 2.6 Hz, 2H), 1.43 (p, J = 3.7 Hz, 4H); ^{13}C NMR (151 MHz, $CDCl_3$) δ 75.5, 62.4, 32.2, 27.3, 26.0, 25.0; FTIR (cm^{-1}): 3355, 2935, 1551, 1434, 1383, 1055, 733. HRMS (ESI) $(M+H)^+$ m/z calculated for $[C_6H_{14}NO_3]^+$: 148.0895; found: 148.0962.

3.14.9 Synthesis of the single-component pre-catalyst 3.48.

A 100 mL oven-dried round-bottom flask equipped with magnetic stir bar was sealed with a septum and cooled under a stream of nitrogen. The septum was partly removed and the diamine ligand (***R,R***)-**3.30** (1.36 g, 2.4 mmol) and anhydrous NiCl2•dme (0.54 g, 2.4 mmol) were added. The septum was replaced and anhydrous Et_2O (64 mL) was added under nitrogen. The reaction mixture was stirred under nitrogen at rt for 24 h. The reaction was concentrated under reduced pressure and the contents were dissolved in DCM (10 mL). The insoluble particles were removed using filtration through filter paper and product recrystallized by vapor diffusion (DCM/hexanes) to afford green crystals. X-ray quality crystals were obtained by slow evaporation of saturated solution of complex (*R,R*)-**3.48** in toluene (Figure 3.36). The complex (*R,R*)-**3.48** crystallized as tetrameric species. To isolate (*R,R*)-**3.48**, the DCM was decanted and the green crystals were washed with hexane. The crystals were transferred to a new vial via spatula and crushed to provide a green powder. The resulting complex (*R,R*)-**3.48** was dried under vacuum to afford 1.43 g, 85 % yield. Anal. Calculated: C, 41.42%; H, 3.48%; N, 4.02%; Found: C, 41.32%; H, 3.15%; N, 4.95%. HRMS (LIFDI) $(M)^+$ m/z, calculated for $[C_{24}H_{22}C_{l2}F_{12}N_2Ni]^+$: 694.0322; found: 694.0334.

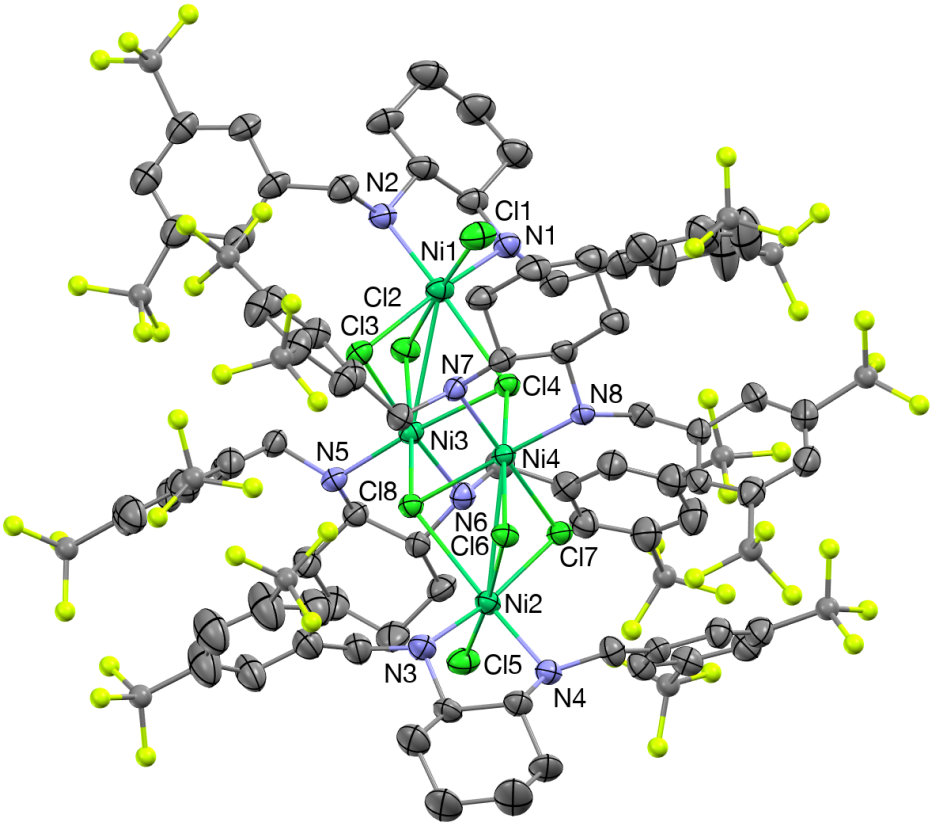

Figure 3.36: X-ray Structure of Single Component Precatalyst (***R,R***)- **3.48**

3.14.10 General Protocol for Asymmetric Alkylation of Nitroalkanes

General Protocol D: Synthesis of enantioenriched β-nitroamide at 0 °C (5 min prestirring): In a nitrogen-filled, moisture and oxygen free glovebox, (*R,R*)-**3.48** (0.1 equiv) and anhydrous Et_2O (4.0 mL) was added into a 20 mL vial (Vial A) containing magnetic stir bar. Vial A was sealed with a Teflon-lined screw cap and the resulting mixture was stirred at rt for 30 min. In a separate 20 mL vial (Vial B, preforming nitronate anion), base (1.1 equiv), nitroalkane (1.2 equiv), anhydrous Et_2O (4.0 mL), and stir bar were added sequentially, and Vial B was capped with a Teflon-lined scew cap. Vial B was then stirred at rt for 5 min. After 5 min, the electrophile (1.0 equiv)

was added as a solid (unless otherwise noted) to Vial B, and Vial B was cooled to 0 °C. Et_2Zn was then added into Vial A, stirred for 2 minutes at rt, and then was cooled to 0 °C. The resulting brown, homogeneous solution in Vial A was transferred to Vial B via pipette; Vial A was rinsed with 2.0 mL Et_2O, and the Et_2O rinse was then transferred into Vial B. The reaction mixture was then stirred vigorously at 0 °C for indiacated time (ca. 20-26h). Once completed, the reaction was warmed to room temperature and removed from the glovebox. The reaction mixture was then opened to air, diluted with Et_2O (10 mL) and filtered through Celite, which was then rinsed with Et_2O (15 mL). The filtrate was concentrated *in vacuo* and the crude reaction was purified by silica gel flash chromatography.

General Protocol E: Synthesis of enantioenriched β-nitroamide at 0 °C (30 min prestirring): In a nitrogen-filled, moisture and oxygen free glovebox, (*R,R*)-**3.48** (0.1 equiv) and anhydrous Et_2O (4.0 mL) was added into a 20 mL vial (Vial A) containing magnetic stir bar. Vial A was sealed with a Teflon-lined screw cap and the resulting mixture was stirred at rt for 30 min. In a separate 20 mL vial (Vial B, preforming nitronate anion), base (1.1 equiv), nitroalkane (1.2 equiv), anhydrous Et_2O (4.0 mL), and stir bar were added sequentially, and Vial B was capped with a Teflon-lined scew cap. Vial B was then stirred at rt for 30 min. After 30 min, the electrophile (1.0 equiv) was added as a solid (unless otherwise noted) to Vial B, and Vial B was cooled to 0 °C. Et_2Zn was then added into Vial A, stirred for 2 minutes at rt, and then was cooled to 0 °C. The resulting brown, homogeneous solution in Vial A was transferred to Vial B via pipette; Vial A was rinsed with 2.0 mL Et_2O, and the Et_2O rinse was then transferred into Vial B. The reaction mixture was then stirred vigorously at 0 °C for

indiacated time (ca. 20-26h). Once completed, the reaction was warmed to room temperature and removed from the glovebox. The reaction mixture was then opened to air, diluted with Et_2O (10 mL) and filtered through Celite, which was then rinsed with Et_2O (15 mL). The filtrate was concentrated *in vacuo* and the crude reaction was purified by silica gel flash chromatography.

General Protocol F: Synthesis of enantioenriched β-nitroamide at rt (5 min prestirring): In a nitrogen-filled, moisture and oxygen free glovebox, (*R,R*)-**3.48** (0.1 equiv) and anhydrous Et_2O (4.0 mL) was added into a 20 mL vial (Vial A) containing magnetic stir bar. Vial A was sealed with a Teflon-lined screw cap and the resulting mixture was stirred at rt for 30 min. In a separate 20 mL vial (Vial B, preforming nitronate anion), base (1.1 equiv), nitroalkane (1.2 equiv), anhydrous Et_2O (4.0 mL), and stir bar were added sequentially, and Vial B was capped with a Teflon-lined screw cap. Vial B was then stirred at rt for 5 min. After the indicated time had passed, the electrophile (1.0 equiv) was added as a solid (unless otherwise noted) to Vial B. Et_2Zn was then added into Vial A, stirred for 2 minutes at rt. The resulting brown, homogeneous solution in Vial A was transferred to Vial B via pipette; Vial A was rinsed with 2.0 mL Et_2O, and the Et_2O rinse was then transferred into Vial B. The reaction mixture was then stirred vigorously at rt for indicated time (ca. 20-26h). Once completed, the reaction was removed from the glovebox. The reaction mixture was then opened to air, diluted with Et_2O (10 mL) and filtered through Celite, which was then rinsed with Et_2O (15 mL). The filtrate was concentrated *in vacuo* and the crude reaction was purified by silica gel flash chromatography.

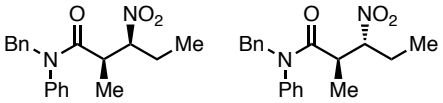

3.34A 75:25 **3.34B**

(**3.34**) According to general protocol D: **3.48** (34.7 mg, 0.05 mmol), *N*-benzyl-2-bromo-*N*-phenylpropionamide (**3.33**, 318 mg, 1.0 mmol), 1-nitropropane (107 μL, 1.2 mmol), sodium methoxide (59.4 mg, 1.1 mmol), diethyl zinc (1 M in hexane, 0.01 mmol, 10 μL) and anhydrous Et_2O (10.0 mL) were combined under N_2 cooled to 0 °C with rapid stirring for 24 h. The reaction was worked up according to the general protocol. NMR analysis of the crude reaction mixture revealed a 75:25 mixture of *syn* and *anti* isomers. The crude reaction was purified by flash silica gel chromatography (95:5 → 90:10 hexanes : ethyl acetate) to afford two diastereomerically pure products **3.34** (290 mg, 89% combined).

3.34A (*SYN*) (91% ee, 221 mg, 68%, clear oil): The enantiomeric excess was determined to be 91% by chiral HPLC analysis (CHIRALPAK IB, 1.0 mL/min, 0.8% i-PrOH/hexane, λ=220 nm); t_R(major) = 13.858 min, t_R(minor) = 15.236 min. $[\alpha]_D^{24}$=–49.2° (c = 1.00, $CHCl_3$); ^{1}H NMR (600 MHz, $CDCl_3$): δ 7.40 – 7.34 (m, 3H), 7.31 – 7.23 (m, 3H), 7.19 – 7.12 (m, 2H), 6.95 – 6.89 (m, 2H), 4.87 (q, 2H), 4.70 (td, J = 10.6, 3.1 Hz, 1H), 2.82 (dq, J = 10.3, 6.7 Hz, 1H), 1.85 (dqd, J = 14.9, 7.5, 3.1 Hz, 1H), 1.77 (ddq, J = 14.3, 10.8, 7.2 Hz, 1H), 1.08 (d, J = 6.6 Hz, 3H), 0.92 (t, J = 7.3 Hz, 3H); ^{13}C NMR (151 MHz, $CDCl_3$) δ 171.9, 141.2, 136.9, 130.0, 128.9, 128.7, 128.5, 128.4, 127.7, 93.4, 53.2, 41.0, 25.8, 15.7, 10.4; FTIR (cm^{-1}): 2974, 2881, 1653, 1545, 1405, 1200, 812, 700. HRMS (ESI) $(M+H)^+$ m/z calculated for $[C_{19}H_{23}N_2O_3]^+$: 327.1703; found: 327.1704.

3.34B (*ANTI*) (83% ee, 70 mg, 21%, off-white solid): The enantiomeric excess was determined to be 83% by chiral HPLC analysis (CHIRALPAK IB, 1.0 mL/min, 0.8% i-PrOH/hexane, λ=220 nm); t_R(major) = 36.585 min, t_R(minor) = 40.556 min. $[\alpha]_D^{24}$=+54.5° (c = 1.00, $CHCl_3$); ^{1}H NMR (600 MHz, $CDCl_3$): δ 7.38 – 7.30 (m, 3H), 7.29 – 7.20 (m, 3H), 7.15 – 7.09 (m, 2H), 7.11 – 7.05 (m, 2H), 4.90 (d, J = 14.3 Hz, 1H), 4.86 (ddd, J = 10.1, 8.7, 3.5 Hz, 1H), 4.78 (d, J = 14.3 Hz, 1H), 3.01 (dq, J = 10.1, 7.0 Hz, 1H), 1.96 (dqd, J = 14.9, 7.5, 3.6 Hz, 1H), 1.67 (ddq, J = 14.7, 8.8, 7.3 Hz, 1H), 1.06 (d, J = 7.0 Hz, 3H), 0.85 (t, J = 7.4 Hz, 3H); ^{13}C NMR (151 MHz, $CDCl_3$) δ 172.9, 141.4, 137.1, 129.6, 128.7, 128.6, 128.4, 128.3, 127.4, 90.5, 53.2, 39.2, 23.9, 14.5, 9.3; FTIR (cm^{-1}): 2975, 1653, 1545, 1407, 1259, 810, 700; mp = 101-103 °C. HRMS (ESI) m/z calculated for $[C_{19}H_{23}N_2O_3]^+$ $(M+H)^+$: 327.1703; found: 327.1704.

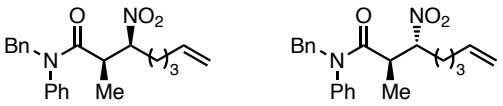

3.47A **79:21** **3.47B**

(**3.47**) According to general protocol D: **3.48** (69.4 mg, 0.1 mmol), *N*-benzyl-2-bromo-*N*-phenylpropionamide (**3.33**, 318 mg, 1.0 mmol), 1-nitrohexene (164 μL, 1.2 mmol), sodium methoxide (59.4 mg, 1.1 mmol), diethyl zinc (1 M in hexane, 0.02 mmol, 20 μL) and anhydrous Et_2O (10.0 mL) were combined under N_2 cooled to 0 °C with rapid stirring for 24 h. The reaction was worked up according to the general protocol. NMR analysis of the crude reaction mixture revealed a 79:21 mixture of *syn* and *anti* isomers. The crude reaction was purified by flash silica gel chromatography (100:0 → 95:05 hexanes : ethyl acetate) to afford two diastereomerically pure products **3.47** (307 mg, 84% combined).

3.47A (*SYN*) (91% ee, 241 mg, 66%, clear oil): The enantiomeric excess was determined to be 91% by chiral HPLC analysis (CHIRALPAK IC, 1.0 mL/min, 2.0% i-PrOH/hexane, λ=210 nm); t_R(major) = 18.968 min, t_R(minor) = 15.837 min. $[\alpha]_D^{24}$=–30.1° (c = 1.00, $CHCl_3$); ^{1}H NMR (600 MHz, $CDCl_3$): δ 7.37 (dp, J = 5.5, 2.0 Hz, 3H), 7.29 – 7.26 (m, 3H), 7.19 – 7.12 (m, 2H), 6.94 – 6.86 (m, 2H), 5.73 (ddt, J = 17.0, 10.2, 6.7 Hz, 1H), 5.06 – 4.93 (m, 3H), 4.81 – 4.70 (m, 2H), 2.81 (dq, J = 10.3, 6.7 Hz, 1H), 2.14 – 1.97 (m, 2H), 1.82 – 1.70 (m, 2H), 1.49 – 1.36 (m, 1H), 1.37 – 1.26 (m, 1H), 1.08 (d, J = 6.6 Hz, 3H); ^{13}C NMR (151 MHz, $CDCl_3$) δ 171.8, 141.2, 137.4, 137.0, 130.0, 129.0, 128.7, 128.5, 128.4, 127.7, 115.5, 91.8, 53.3, 41.1, 32.8, 31.7, 24.9, 15.6; FTIR (cm^{-1}): 3064, 2929, 1653, 1549, 1405, 1262, 915, 701. HRMS (ESI) $(M+H)^+$ m/z calculated for $[C_{22}H_{27}N_2O_3]^+$: 367.2016; found: 327.2014.

3.47B (*ANTI*) (79% ee, 66 mg, 18%, clear oil): The enantiomeric excess was determined to be 79% by chiral HPLC analysis (CHIRALPAK IB, 1.0 mL/min, 0.8% i-PrOH/hexane, λ=210 nm); t_R(major) = 31.082 min, t_R(minor) = 28.802 min. $[\alpha]_D^{24}$=+50.3° (c = 1.00, $CHCl_3$); ^{1}H NMR (600 MHz, $CDCl_3$): δ 7.38 – 7.32 (m, 3H), 7.29 – 7.21 (m, 3H), 7.14 – 7.10 (m, 2H), 7.10 – 7.02 (m, 2H), 5.68 (ddt, J = 16.9, 10.2, 6.7 Hz, 1H), 5.00 – 4.92 (m, 2H), 4.92 – 4.84 (m, 2H), 4.78 (d, J = 14.3 Hz, 1H), 2.99 (dq, J = 10.1, 7.0 Hz, 1H), 2.10 – 1.95 (m, 2H), 1.88 – 1.79 (m, 1H), 1.64 (dtd, J = 14.8, 9.8, 5.1 Hz, 1H), 1.34 (dddt, J = 16.3, 13.5, 10.9, 6.5 Hz, 2H), 1.06 (d, J = 7.0 Hz, 3H); ^{13}C NMR (151 MHz, $CDCl_3$) δ 172.8, 141.3, 137.3, 137.0, 129.6, 128.7, 128.3, 128.3, 127.4, 89.3, 53.1, 39.8, 32.7, 30.0, 24.1, 14.5; FTIR (cm^{-1}): 3064, 2930, 1653, 1548, 1409, 1251, 916, 701. HRMS (ESI) $(M+H)^+$ m/z calculated for $[C_{22}H_{27}N_2O_3]^+$: 367.2016; found: 367.2015.

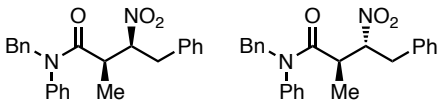

3.50A 88:12 **3.50B**

(**3.50**) According to general protocol F: **3.48** (34.7 mg, 0.05 mmol), *N*-benzyl-2-bromo-*N*-phenylpropionamide (**3.33**, 318 mg, 1.0 mmol), 2-phenylnitroethane (181 mg, 1.2 mmol), sodium methoxide (59.4 mg, 1.1 mmol), diethyl zinc (1 M in hexane, 0.01 mmol, 10 μL) and anhydrous Et_2O (10.0 mL) were combined under N_2 and stirred rapidly at rt for 24 h. The reaction was worked up according to the general protocol. NMR analysis of the crude reaction mixture revealed an 88:12 mixture of *syn* and *anti* isomers. The crude reaction was purified by flash silica gel chromatography (95:05 → 85:15 hexanes : ethyl acetate) to afford two diastereomerically pure products **3.50** (321 mg, 83% combined).

3.50A (*SYN*) (87% ee, 274 mg, 71%, clear oil): The enantiomeric excess was determined to be 87% by chiral HPLC analysis (CHIRALPAK IA, 1.0 mL/min, 5.0% i-PrOH/hexane, λ=220 nm); t_R(major) = 11.475 min, t_R(minor) = 10.712 min. $[\alpha]_D^{24}$=–58.2° (c = 1.00, $CHCl_3$); ^{1}H NMR (600 MHz, $CDCl_3$): δ 7.39 (p, J = 3.5 Hz, 2H), 7.31 – 7.21 (m, 6H), 7.21 – 7.16 (m, 2H), 7.15 – 7.10 (m, 2H), 6.95 (dd, J = 6.6, 3.0 Hz, 2H), 5.04 – 4.94 (m, 2H), 4.83 (d, J = 14.1 Hz, 1H), 3.14 (dd, J = 14.3, 2.9 Hz, 1H), 3.00 – 2.87 (m, 3H), 1.11 (d, J = 6.7 Hz, 3H); ^{13}C NMR (151 MHz, $CDCl_3$) δ 171.7, 141.1, 136.9, 135.4, 128.9, 128.7, 128.6, 128.5, 128.4, 127.7, 127.4, 93.3, 53.3, 41.1, 38.4, 15.5; FTIR (cm^{-1}): 3031, 2980, 1652, 1553, 1456, 1258, 859, 747. HRMS (ESI) $(M+H)^+$ m/z calculated for $[C_{24}H_{25}N_2O_3]^+$: 389.1859; found: 389.1860.

3.50B (*ANTI*) (68% ee, 47 mg, 12%, clear oil): The enantiomeric excess was determined to be 68% by chiral HPLC analysis (CHIRALPAK IA, 1.0 mL/min, 5.0% i-PrOH/hexane, λ=254 nm); t_R(major) = 23.708 min, t_R(minor) = 13.292 min. $[\alpha]_D^{24}$=+46.5° (c = 1.00, $CHCl_3$); ^{1}H NMR (600 MHz, CDCl3): δ 7.35 – 7.28 (m, 3H), 7.27 – 7.20 (m, 6H), 7.14 – 7.09 (m, 2H), 7.04 – 6.98 (m, 4H), 5.09 (td, J = 9.4, 3.8 Hz, 1H), 4.92 (d, J = 14.3 Hz, 1H), 4.75 (d, J = 14.4 Hz, 1H), 3.21 (dd, J = 14.7, 3.8 Hz, 1H), 3.04 (dq, J = 9.7, 6.9 Hz, 1H), 2.91 (dd, J = 14.7, 9.0 Hz, 1H), 1.18 (d, J = 6.9 Hz, 3H); ^{13}C NMR (151 MHz, $CDCl_3$) δ 172.6, 141.3, 137.0, 134.9, 129.6, 128.7, 128.7, 128.7, 128.4, 128.3, 127.4, 127.4, 90.5, 53.1, 39.6, 36.9, 14.6; FTIR (cm^{-1}): 3648, 2360, 1653, 1558, 1456, 1250, 858, 699. HRMS (ESI) $(M+H)^+$ m/z calculated for $[C_{24}H_{25}N_2O_3]^+$: 389.1859; found: 389.1861.

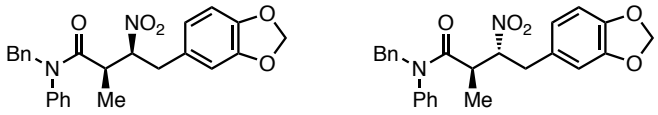

3.51A **87:13** **3.51B**

(**3.51**) According to general protocol D: **3.48** (69.4 mg, 0.1 mmol), *N*-benzyl-2-bromo-*N*-phenylpropionamide (**3.33**, 318 mg, 1.0 mmol), 5-(2-nitroethyl)benzo[1,3]dioxole (234 mg, 1.2 mmol), sodium methoxide (59.4 mg, 1.1 mmol), diethyl zinc (1 M in hexane, 0.02 mmol, 20 μL) and anhydrous Et_2O (10.0 mL) were combined under N_2 cooled to 0 °C with rapid stirring for 24 h. The reaction was worked up according to the general protocol. NMR analysis of the crude reaction mixture revealed a 83:17 mixture of *syn* and *anti* isomers. The crude reaction was purified by flash silica gel chromatography (90:10 → 80:20 hexanes : ethyl acetate) to afford two diastereomerically pure products **3.51** (346 mg, 80% combined).

3.51A (*SYN)* (89% ee, 295 mg, 68%, clear oil): The enantiomeric excess was determined to be 89% by chiral HPLC analysis (CHIRALPAK IA, 1.0 mL/min, 3.0% i-PrOH/hexane, λ=220 nm); t_R(major) = 31.504 min, t_R(minor) = 34.915 min. $[\alpha]_D^{24}$=–77.5° (c = 1.00, $CHCl_3$); ^{1}H NMR (600 MHz, $CDCl_3$): δ 7.44 – 7.36 (m, 3H), 7.32 – 7.25 (m, 3H), 7.19 (dd, J = 7.3, 2.3 Hz, 2H), 7.00 – 6.91 (m, 2H), 6.70 (d, J = 7.9 Hz, 1H), 6.63 (d, J = 1.7 Hz, 1H), 6.57 (dd, J = 7.9, 1.7 Hz, 1H), 5.93 (s, 2H), 4.99 – 4.91 (m, 2H), 4.84 (d, J = 14.1 Hz, 1H), 3.05 (dd, J = 14.2, 2.8 Hz, 1H), 2.92 – 2.84 (m, 2H), 1.11 (d, J = 6.7 Hz, 3H); ^{13}C NMR (151 MHz, $CDCl_3$) δ 171.6, 147.9, 146.9, 141.0, 136.9, 130.0, 129.0, 128.9, 128.8, 128.5, 128.4, 127.7, 121.9, 109.0, 108.4, 101.0, 93.6, 53.3, 41.0, 38.2, 15.5; FTIR (cm^{-1}): 2979, 1652, 1550, 1492, 1249, 1039, 701. HRMS (ESI) $(M+H)^+$ m/z calculated for $[C_{25}H_{25}N_2O_5]^+$: 433.1758; found: 433.1764.

3.51B (*ANTI*) (81% ee, 51 mg, 12%, clear oil): The enantiomeric excess was determined to be 81% by chiral HPLC analysis (CHIRALPAK IB, 1.0 mL/min, 3.0% i-PrOH/hexane, λ=220 nm); t_R(major) = 28.783 min, t_R(minor) = 25.203 min. $[\alpha]_D^{24}$=+6.4° (c = 1.00, $CHCl_3$); ^{1}H NMR (600 MHz, $CDCl_3$): δ 7.36 – 7.29 (m, 3H), 7.27 – 7.20 (m, 3H), 7.14 – 7.09 (m, 2H), 7.05 – 6.97 (m, 2H), 6.65 (d, J = 7.9 Hz, 1H), 6.49 (s, 1H), 6.45 (dd, J = 8.0, 1.7 Hz, 1H), 5.92 (d, 2H), 5.02 (td, J = 9.4, 3.8 Hz, 1H), 4.91 (d, J = 14.3 Hz, 1H), 4.75 (d, J = 14.3 Hz, 1H), 3.12 (dd, J = 14.8, 3.8 Hz, 1H), 3.02 (dq, J = 9.8, 7.0 Hz, 1H), 2.82 (dd, J = 14.7, 9.1 Hz, 1H), 1.16 (d, J = 7.0 Hz, 3H); ^{13}C NMR (151 MHz, $CDCl_3$) δ 172.5, 147.7, 146.9, 141.2, 136.9, 129.6, 128.7, 128.4, 128.3, 128.3, 127.4, 121.9, 109.0, 108.4, 101.0, 90.7, 53.0, 39.6, 36.7, 14.6;

FTIR (cm^{-1}): 2936, 2337, 1653, 1550, 1446, 1250, 1039, 701. HRMS (ESI) $(M+H)^+$ m/z calculated for $[C_{24}H_{25}N_2O_3]^+$: 433.1758; found: 433.1762.

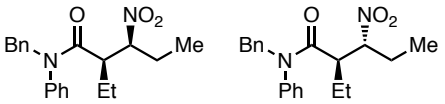

3.44A 55:45 **3.44B**

(**3.44**) According to general protocol D: **3.48** (69.4 mg, 0.1 mmol), *N*-benzyl-2-bromo-*N*-phenylbutanamide (332 mg, 1.0 mmol), 1-nitropropane (107μL, 1.2 mmol), sodium methoxide (59.4 mg, 1.1 mmol), diethyl zinc (1 M in hexane, 0.02 mmol, 20 μL) and anhydrous Et_2O (10.0 mL) were combined under N_2 cooled to 0 °C with rapid stirring for 24 h. The reaction was worked up according to the general protocol. NMR analysis of the crude reaction mixture revealed a 55:45 mixture of *syn* and *anti* isomers. The crude reaction was purified by flash silica gel chromatography (95:05 → 90:10 hexanes : ethyl acetate) to afford two diastereomerically pure products **3.44** (305 mg, 90% combined).

3.44A (*SYN*) (85% ee, 162 mg, 48%, clear oil): The enantiomeric excess was determined to be 85% by chiral HPLC analysis (CHIRALPAK IC, 1.0 mL/min, 3.0% i-PrOH/hexane, λ=220 nm); t_R(major) = 16.928 min, t_R(minor) = 13.016 min. $[\alpha]_D^{24}$=–16.8° (c = 1.00, $CHCl_3$); ^{1}H NMR (600 MHz, $CDCl_3$): δ 7.40 – 7.33 (m, 3H), 7.27 (dd, J = 5.0, 2.0 Hz, 3H), 7.17 (dd, J = 6.5, 2.9 Hz, 2H), 6.95 – 6.89 (m, 2H), 4.90 (q, J = 14.0 Hz, 2H), 4.66 (td, J = 10.0, 4.3 Hz, 1H), 2.83 (td, J = 9.5, 3.9 Hz, 1H), 1.91 – 1.76 (m, 2H), 1.75 – 1.64 (m, 1H), 1.35 (dtd, J = 13.7, 7.4, 4.0 Hz, 1H), 0.91 (t, J = 7.3 Hz, 3H), 0.87 (t, J = 7.5 Hz, 3H); ^{13}C NMR (151 MHz, $CDCl_3$) δ 170.7, 141.0, 137.0, 129.7, 129.1, 129.1, 128.5, 128.4, 127.6, 92.8, 53.5, 46.6, 25.7, 23.9, 10.9, 10.5; FTIR

(cm^{-1}): 2970, 1653, 1549, 1495, 1276, 1079, 701. HRMS (ESI) $(M+H)^+$ m/z calculated for $[C_{25}H_{25}N_2O_5]^+$: 341.1859; found: 341.1854.

3.44B (*ANTI*) (81% ee, 143 mg, 42%, off-white solid): The enantiomeric excess was determined to be 81% by chiral HPLC analysis (CHIRALPAK IF, 1.0 mL/min, 3.0% i-PrOH/hexane, λ=220 nm); t_R(major) = 21.365 min, t_R(minor) = 23.468 min. $[\alpha]_D^{24}$=+51.1° (c = 1.00, $CHCl_3$); ^{1}H NMR (600 MHz, $CDCl_3$): δ 7.36 – 7.29 (m, 3H), 7.28 – 7.20 (m, 3H), 7.16 – 7.12 (m, 2H), 7.09 – 7.02 (m, 2H), 4.91 – 4.83 (m, 3H), 3.00 (ddd, J = 9.7, 7.4, 4.4 Hz, 1H), 1.92 (dqd, J = 14.9, 7.4, 3.4 Hz, 1H), 1.70 (ddq, J = 14.5, 9.6, 7.2 Hz, 1H), 1.60 – 1.46 (m, 2H), 0.86 (t, J = 7.5 Hz, 6H); ^{13}C NMR (151 MHz, $CDCl_3$) δ 171.4, 141.2, 137.1, 129.4, 128.9, 128.8, 128.3, 128.2, 127.4, 90.0, 53.3, 45.0, 23.8, 22.0, 10.6, 9.7; FTIR (cm^{-1}): 2972, 1652, 1546, 1495, 1270, 1079, 700; mp = 88-90 °C. HRMS (ESI) $(M+H)^+$ m/z calculated for $[C_{20}H_{25}N_2O_3]^+$: 341.1859; found: 341.1854.

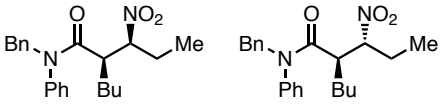

3.61A **54:46** **3.61B**

(**3.61**) According to general protocol D: **3.48** (69.4 mg, 0.1 mmol), *N*-benzyl-2-bromo-*N*-phenylhexanamide (360 mg, 1.0 mmol), 1-nitropropane (107μL, 1.2 mmol), sodium methoxide (59.4 mg, 1.1 mmol), diethyl zinc (1 M in hexane, 0.02 mmol, 20 μL) and anhydrous Et_2O (10.0 mL) were combined under N_2 cooled to 0 °C with rapid stirring for 24 h. The reaction was worked up according to the general protocol. NMR analysis of the crude reaction mixture revealed a 54:46 mixture of *syn* and *anti* isomers. The crude reaction was purified by flash silica gel chromatography (95:05 → 90:10 hexanes : ethyl acetate) to afford

mixture of diastereomers **3.61A** and **3.61B** (327 mg, 89% combined, isolated dr 53:47). The enantiomeric excess was determined to be 83% by chiral HPLC analysis for *SYN* diastereomer, **3.61A** (CHIRALPAK IE, 1.0 mL/min, 3.0% i-PrOH/hexane, λ=254 nm); tR(major) = 13.522 min, tR(minor) = 15.697 min; The enantiomeric excess was determined to be 77% by chiral HPLC analysis for *ANTI* diastereomer, **3.61B** (CHIRALPAK IE, 1.0 mL/min, 3.0% i-PrOH/hexane, λ=254 nm); t_R(major) = 42.670 min, t_R(minor) = 55.276 min. Optical rotation for the mixture of diastereomers **3.61A** and **3.61B** $[\alpha]_D^{24}$=–5.9° (c = 1.00, $CHCl_3$); The reported spectra are for a mixture of two diastereomers ^{1}H NMR (400 MHz, $CDCl_3$) δ 7.41 – 7.30 (m, 7H), 7.29 – 7.22 (m, 4H), 7.20 – 7.11 (m, 5H), 7.04 (d, J = 6.7 Hz, 2H), 6.94 – 6.89 (m, 2H), 4.94 – 4.88 (m, 3H), 4.87 – 4.79 (m, 2H), 4.63 (ddd, J = 9.9, 8.7, 5.6 Hz, 1H), 3.02 (ddd, J = 9.6, 7.8, 4.2 Hz, 1H), 2.85 (td, J = 9.6, 3.2 Hz, 1H), 1.92 (ddt, J = 14.9, 7.5, 3.8 Hz, 1H), 1.87 – 1.78 (m, 2H), 1.77 – 1.64 (m, 2H), 1.55 – 1.45 (m, 1H), 1.45 – 1.34 (m, 1H), 1.32 – 1.22 (m, 2H), 1.17 (td, J = 6.3, 5.1, 2.9 Hz, 7H), 0.94 – 0.80 (m, 12H); ^{13}C NMR (101 MHz, $CDCl_3$) δ 171.7, 170.9, 141.1, 140.9, 137.1, 136.9, 129.7, 129.4, 129.1, 129.1, 128.9, 128.8, 128.6, 128.4, 128.3, 128.2, 127.7, 127.4, 93.1, 90.3, 53.5, 53.3, 45.6, 44.2, 30.7, 28.8, 28.6, 28.2, 25.7, 23.9, 22.9, 22.7, 13.8, 13.8, 10.6, 9.8; FTIR (cm^{-1}): 2958, 1653, 1595, 1495, 1198, 1080, 701. HRMS (ESI) $(M+H)^+$ m/z calculated for $[C_{22}H_{29}N_2O_3]^+$: 369.2172; found: 369.2166.

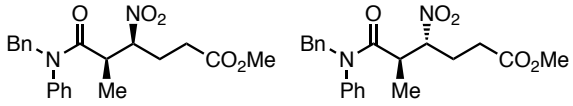

3.54A **71:29** **3.54B**

(**3.54**) According to general protocol E: **3.48** (34.7 mg, 0.05 mmol), *N*-benzyl-2-bromo-*N*-phenylpropionamide (**3.33**, 318 mg, 1.0 mmol), methyl 4-nitrobutyrate (152 μL, 1.2 mmol), sodium methoxide

(59.4 mg, 1.1 mmol), diethyl zinc (1 M in hexane, 0.01 mmol, 10 μL) and anhydrous Et_2O (10.0 mL) were combined under N_2 and stirred rapidly at rt for 24 h. The reaction was worked up according to the general protocol. NMR analysis of the crude reaction mixture revealed a 71:29 mixture of *syn* and *anti* isomers. The crude reaction was purified by flash silica gel chromatography (90:10 → 80:20 hexanes : ethyl acetate) to afford two diastereomerically pure products **3.54** (298 mg, 78% combined).

3.54A (*SYN*) (87% ee, 208 mg, 54%, clear oil): The enantiomeric excess was determined to be 87% by chiral HPLC analysis (CHIRALPAK IA, 1.0 mL/min, 1.5% i-PrOH/hexane, λ=220 nm); t_R(major) = 46.611 min, t_R(minor) = 34.712 min. $[\alpha]_D^{24}$=–27.9° (c = 1.00, $CHCl_3$); ^{1}H NMR (600 MHz, $CDCl_3$): δ 7.40 – 7.35 (m, 3H), 7.30 – 7.26 (m, 3H), 7.19 – 7.14 (m, 2H), 6.96 – 6.92 (m, 2H), 4.90 (d, J = 14.1 Hz, 1H), 4.83 (d, J = 14.1 Hz, 1H), 4.79 (td, J = 10.5, 2.9 Hz, 1H), 3.70 (s, 3H), 2.85 (dq, J = 10.1, 6.7 Hz, 1H), 2.37 (ddd, J = 16.1, 9.7, 6.3 Hz, 1H), 2.28 (ddd, J = 16.5, 9.7, 5.1 Hz, 1H), 2.20 (dddd, J = 16.2, 9.5, 6.3, 2.9 Hz, 1H), 2.14 – 2.05 (m, 1H), 1.09 (d, J = 6.6 Hz, 3H); ^{13}C NMR (101 MHz, $CDCl_3$) δ 171.9, 171.4, 140.9, 136.8, 130.0, 128.9, 128.7, 128.5, 128.3, 127.7, 90.8, 53.2, 51.9, 40.9, 30.4, 27.3, 15.6; FTIR (cm^{-1}): 2950, 1734, 1653, 1550, 1495, 1257, 989, 702. HRMS (ESI) $(M+H)^+$ m/z calculated for $[C_{21}H_{25}N_2O_5]^+$: 385.4320; found: 385.1752.

3.54B (*ANTI*) (63% ee, 90 mg, 24%, off-white solid): The enantiomeric excess was determined to be 63% by chiral HPLC analysis (CHIRALPAK IB, 1.0 mL/min, 5.0% i-PrOH/hexane, λ=254 nm); t_R(major) = 14.988 min, t_R(minor) = 16.460 min. $[\alpha]_D^{24}$=+45.7° (c = 1.00, $CHCl_3$); ^{1}H NMR (600 MHz, $CDCl_3$): δ 7.40 – 7.31 (m, 3H),

7.26 – 7.19 (m, 3H), 7.15 – 7.04 (m, 4H), 4.95 – 4.86 (m, 2H), 4.77 (d, J = 14.3 Hz, 1H), 3.65 (s, 3H), 2.98 (dq, J = 10.0, 7.0 Hz, 1H), 2.43 – 2.15 (m, 3H), 1.89 (dddd, J = 15.1, 10.1, 7.9, 5.2 Hz, 1H), 1.11 (d, J = 7.0 Hz, 3H); ^{13}C NMR (101 MHz, $CDCl_3$) δ 172.5, 172.2, 141.2, 136.9, 129.7, 128.7, 128.4, 127.4, 88.5, 53.1, 51.9, 39.9, 29.6, 25.9, 14.5; FTIR (cm^{-1}): 2951, 1738, 1654, 1549, 1495, 1257, 1079, 702; mp = 97-99 °C. HRMS (ESI) $(M+H)^+$ m/z calculated for $[C_{21}H_{25}N_2O_5]^+$: 385.1758; found: 385.1755. Crystals for X-ray analysis were obtained by slow evaporation of diethyl ether.

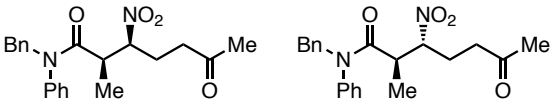

3.55A 67:33 **3.55B**

(**3.55**) According to general protocol E: **3.48** (69.4 mg, 0.1 mmol), *N*-benzyl-2-bromo-*N*-phenylpropionamide (**3.33**, 318 mg, 1.0 mmol), 5-nitro-2-pentanone (157 mg, 1.2 mmol), sodium methoxide (59.4 mg, 1.1 mmol), diethyl zinc (1 M in hexane, 0.02 mmol, 20 μL) and anhydrous Et_2O (10.0 mL) were combined under N_2 cooled to 0 °C with rapid stirring for 24 h. The reaction was worked up according to the general protocol. NMR analysis of the crude reaction mixture revealed a 67:33 mixture of *syn* and *anti* isomers. The crude reaction was purified by flash silica gel chromatography (90:10 → 80:20 hexanes : ethyl acetate) to afford two diastereomerically pure products **3.55** (261 mg, 71% combined).

3.55A (*SYN*) (85% ee, 174 mg, 47%, clear oil): The enantiomeric excess was determined to be 87% by chiral HPLC analysis (CHIRALPAK IA, 1.0 mL/min, 3.0% i-PrOH/hexane, λ=254 nm); t_R(major) = 29.473 min, t_R(minor) = 26.210 min. $[\alpha]_D^{24}$=– 31.4° (c = 1.00, $CHCl_3$); ^{1}H NMR (600 MHz, $CDCl_3$): δ 7.41 – 7.35 (m, 3H), 7.31 –

7.24 (m, 3H), 7.16 (dd, J = 7.4, 2.1 Hz, 2H), 6.99 – 6.94 (m, 2H), 4.90 (d, J = 14.1 Hz, 1H), 4.83 (d, J = 14.1 Hz, 1H), 4.73 (td, J = 10.6, 2.9 Hz, 1H), 2.85 (dq, J = 10.1, 6.6 Hz, 1H), 2.51 (ddd, J = 18.1, 9.9, 5.5 Hz, 1H), 2.37 (ddd, J = 18.1, 10.2, 4.9 Hz, 1H), 2.17 (ddt, J = 14.7, 4.7, 2.2 Hz, 1H), 2.14 (s, 3H), 2.05 – 1.95 (m, 1H), 1.08 (d, J = 6.6 Hz, 3H); ^{13}C NMR (151 MHz, $CDCl_3$) δ 205.7, 171.5, 141.0, 136.8, 130.0, 128.9, 128.7, 128.5, 128.4, 127.7, 91.0, 53.3, 41.0, 39.7, 29.9, 26.1, 15.6; FTIR (cm^{-1}): 2938, 1718, 1653, 1594, 1495, 1256, 1079, 702. HRMS (ESI) $(M+H)^+$ m/z calculated for $[C_{21}H_{25}N_2O_4]^+$: 369.1808; found: 369.1807.

3.55B (*ANTI*) (84% ee, 87 mg, 24%, clear oil): The enantiomeric excess was determined to be 84% by chiral HPLC analysis (CHIRALPAK IA, 1.0 mL/min, 3.0% i-PrOH/hexane, λ=254 nm); t_R(major) = 49.050 min, t_R(minor) = 43.622 min. $[\alpha]_D^{24}$=+66.2° (c = 1.00, $CHCl_3$); ^{1}H NMR (600 MHz, $CDCl_3$): δ 7.38 – 7.32 (m, 3H), 7.28 – 7.21 (m, 3H), 7.13 – 7.09 (m, 2H), 7.09 – 7.05 (m, 2H), 4.88 (d, J = 14.3 Hz, 1H), 4.84 (td, J = 10.3, 3.1 Hz, 1H), 4.78 (d, J = 14.3 Hz, 1H), 2.96 (dq, J = 10.1, 7.0 Hz, 1H), 2.53 (dt, J = 18.5, 7.6 Hz, 1H), 2.42 (ddd, J = 18.4, 8.1, 5.1 Hz, 1H), 2.26 – 2.15 (m, 1H), 2.12 (s, 3H), 1.76 (dddd, J = 15.4, 10.5, 7.9, 5.2 Hz, 1H), 1.11 (d, J = 7.0 Hz, 3H); ^{13}C NMR (151 MHz, $CDCl_3$) δ 206.1, 172.6, 140.9, 136.9, 129.6, 128.7, 128.6, 128.4, 127.4, 88.8, 53.1, 40.2, 38.8, 30.1, 24.7, 14.6; FTIR (cm^{-1}): 2938, 1717, 1653, 1548, 1495, 1256, 1079, 701. HRMS (ESI) $(M+H)^+$ m/z calculated for $[C_{21}H_{25}N_2O_4]^+$: 369.1808; found: 369.1807.

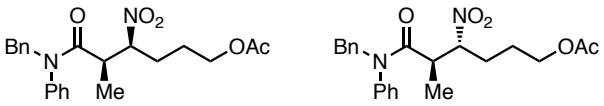

3.52A **72:28** **3.52B**

(**3.52**) According to general protocol E: **3.48** (69.4 mg, 0.1 mmol), *N*-

benzyl-2-bromo-*N*-phenylpropionamide (**3.33**, 318 mg, 1.0 mmol), 4-nitrobutyl acetate (172 μL, 1.2 mmol), sodium methoxide (59.4 mg, 1.1 mmol), diethyl zinc (1 M in hexane, 0.02 mmol, 20 μL) and anhydrous Et_2O (10.0 mL) were combined under N_2 cooled to 0 °C with rapid stirring for 24 h. The reaction was worked up according to the general protocol. NMR analysis of the crude reaction mixture revealed a 72:28 mixture of *syn* and a*nti* isomers. The crude reaction was purified by flash silica gel chromatography (90:10:1 → 80:20:1 hexanes : ethyl acetate : acetic acid) to afford two diastereomerically pure products **3.52** (281 mg, 71% combined).

3.52A (*SYN*) (91% ee, 203 mg, 51%, clear oil): The enantiomeric excess was determined to be 91% by chiral HPLC analysis (CHIRALPAK IB, 1.0 mL/min, 1.0% i-PrOH/hexane, λ=220 nm); t_R(major) = 33.625 min, t_R(minor) = 30.039 min. $[\alpha]_D^{24}$=–14.0° (c = 1.00, $CHCl_3$); ^{1}H NMR (600 MHz, $CDCl_3$): δ 7.40 – 7.34 (m, 3H), 7.29 – 7.23 (m, 3H), 7.18 – 7.13 (m, 2H), 6.95 – 6.89 (m, 2H), 4.90 (d, J = 14.1 Hz, 1H), 4.84 – 4.73 (m, 2H), 4.10 – 3.99 (m, 2H), 2.82 (dq, J = 10.1, 6.7 Hz, 1H), 2.06 (s, 3H), 1.89 – 1.79 (m, 2H), 1.66 (ddq, J = 13.0, 9.3, 6.5 Hz, 1H), 1.55 (ddq, J = 12.8, 9.1, 6.0 Hz, 1H), 1.08 (d, J = 6.6 Hz, 3H); ^{13}C NMR (101 MHz, $CDCl_3$) δ 171.5, 170.9, 140.9, 136.8, 130.0, 128.8, 128.7, 128.4, 128.2, 127.6, 91.3, 63.0, 53.2, 41.0, 29.0, 25.1, 20.9, 15.6; FTIR (cm^{-1}): 2938, 1739, 1654, 1550, 1494, 1240, 1079, 702. HRMS (ESI) $(M+H)^+$ m/z calculated for $[C_{22}H_{27}N_2O_5]^+$: 399.1914; found: 399.1921.

3.52B (*ANTI*) (77% ee, 78 mg, 20%, clear oil): The enantiomeric excess was determined to be 77% by chiral HPLC analysis (CHIRALPAK IA, 1.0 mL/min, 5.0% i-PrOH/hexane, λ=210 nm); t_R(major) = 24.744 min, t_R(minor) = 16.721 min.

$[\alpha]_D^{24}$=+35.6° (c = 1.00, $CHCl_3$); ^1H NMR (600 MHz, $CDCl_3$): δ 7.38 – 7.32 (m, 3H), 7.28 – 7.21 (m, 3H), 7.14 – 7.10 (m, 2H), 7.09 – 7.04 (m, 2H), 4.95 – 4.86 (m, 2H), 4.78 (d, J = 14.3 Hz, 1H), 4.07 – 3.97 (m, 2H), 3.00 (dq, J = 10.1, 7.0 Hz, 1H), 2.01 (s, 3H), 1.98 – 1.88 (m, 1H), 1.78 – 1.67 (m, 1H), 1.65 – 1.53 (m, 2H), 1.08 (d, J = 7.0 Hz, 3H); ^{13}C NMR (101 MHz, $CDCl_3$) δ 172.6, 170.9, 141.1, 136.9, 129.6, 128.6, 128.4, 128.4, 127.4, 88.9, 63.1, 53.1, 39.7, 27.3, 24.4, 20.8, 14.5; FTIR (cm^{-1}): 2938, 1738, 1655, 1549, 1495, 1243, 1074, 702. HRMS (ESI) $(M+H)^+$ m/z calculated for $[C_{22}H_{27}N_2O_5]^+$: 399.1914; found: 399.1923.

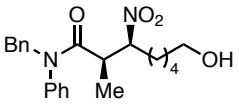

3.53A 72:28

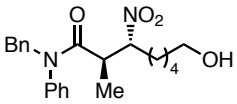

3.53B

(**3.53**) According to general protocol E: **3.48** (69.4 mg, 0.1 mmol), *N*-benzyl-2-bromo-*N*-phenylpropionamide (**3.33**, 318 mg, 1.0 mmol), 6-nitrohexanol (164 μL, 1.2 mmol), sodium methoxide (59.4 mg, 1.1 mmol), diethyl zinc (1 M in hexane, 0.02 mmol, 20 μL) and anhydrous Et_2O (10.0 mL) were combined under N_2 cooled to 0 °C with rapid stirring for 24 h. The reaction was worked up according to the general protocol. NMR analysis of the crude reaction mixture revealed a 72:28 mixture of *syn* and *anti* isomers. The crude reaction was purified by flash silica gel chromatography (85:15:1 → 60:40:1 hexanes : ethyl acetate : acetic acid) to afford two diastereomerically pure products **3.53** (260 mg, 68% combined).

3.53A (*SYN*) (88% ee, 181 mg, 47%, clear oil): The enantiomeric excess was determined to be 88% by chiral HPLC analysis (CHIRALPAK IA, 1.0 mL/min, 5.0% i-PrOH/hexane, λ=210 nm); t_R(minor) = 24.526 min, t_R(major) = 43.331 min. $[\alpha]_D^{24}$=–

28.0° (c = 1.00, $CHCl_3$); ^1H NMR (600 MHz, $CDCl_3$): δ 7.40 – 7.36 (m, 3H), 7.30 – 7.26 (m, 3H), 7.19 – 7.14 (m, 2H), 6.95 – 6.90 (m, 2H), 4.91 (d, J = 14.1 Hz, 1H), 4.81 (d, J = 14.1 Hz, 1H), 4.77 (dt, J = 9.9, 5.0 Hz, 1H), 3.64 (q, J = 6.2 Hz, 2H), 2.81 (dq, J = 10.3, 6.7 Hz, 1H), 1.84 – 1.73 (m, 2H), 1.57 – 1.50 (m, 2H), 1.46 – 1.32 (m, 3H), 1.29 – 1.22 (m, 2H), 1.08 (d, J = 6.7 Hz, 3H); ^{13}C NMR (101 MHz, $CDCl_3$) δ 171.8, 141.0, 136.9, 130.0, 128.9, 128.7, 128.5, 128.3, 127.7, 91.7, 62.6, 53.2, 41.1, 32.2, 25.6, 24.8, 15.6; FTIR (cm^{-1}): 3421, 2935, 2862, 1653, 1549, 1495, 1200, 1077, 701. HRMS (ESI) $(M+H)^+$ m/z calculated for $[C_{22}H_{29}N_2O_4]^+$: 385.2121; found: 385.2129.

3.53B (*ANTI*) (77% ee, 79 mg, 21%, clear oil): The enantiomeric excess was determined to be 77% by chiral HPLC analysis (CHIRALPAK IB, 1.0 mL/min, 5.0% i-PrOH/hexane, λ=210 nm); t_R(major) = 10.167 min, t_R(minor) = 12.878 min. $[\alpha]_D^{24}$=+35.5° (c = 1.00, $CHCl_3$); ^1H NMR (600 MHz, $CDCl_3$): δ 7.30 – 7.23 (m, 2H), 7.21 – 7.12 (m, 4H), 7.06 – 7.01 (m, 2H), 6.98 (d, J = 6.9 Hz, 2H), 4.83 – 4.78 (m, 2H), 4.70 (d, J = 14.3 Hz, 1H), 3.51 (t, J = 6.5 Hz, 2H), 2.91 (dq, J = 10.0, 7.0 Hz, 1H), 1.75 (dtt, J = 14.3, 5.5, 3.3 Hz, 1H), 1.57 (dtd, J = 14.5, 9.5, 5.0 Hz, 1H), 1.47 – 1.39 (m, 2H), 1.35 – 1.13 (m, 4H), 0.98 (d, J = 7.0 Hz, 3H); ^{13}C NMR (101 MHz, $CDCl_3$) δ 172.8, 141.4, 137.1, 129.6, 128.7, 128.6, 128.4, 128.4, 127.4, 89.4, 62.5, 53.2, 39.9, 32.2, 30.7, 25.1, 24.9, 14.6; FTIR (cm^{-1}): 3431, 2933, 2862, 1653, 1548, 1495, 1279, 1074, 701. HRMS (ESI) $(M+H)^+$ m/z calculated for $[C_{22}H_{29}N_2O_4]^+$: 385.2121; found: 385.2127.

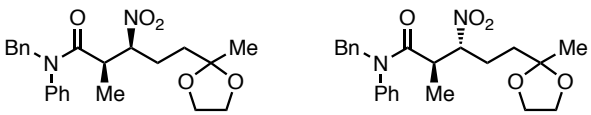

3.56A **71:29** **3.56B**

(**3.56**) According to general protocol E: **3.48** (34.7 mg, 0.05 mmol), *N*-

benzyl-2-bromo-*N*-phenylpropionamide (**3.33**, 318 mg, 1.0 mmol), 2-methyl-2-(3-nitropropyl)-1,3-dioxolane (210 mg, 1.2 mmol), sodium methoxide (59.4 mg, 1.1 mmol), diethyl zinc (1 M in hexane, 0.01 mmol, 10 μL) and anhydrous Et_2O (10.0 mL) were combined under N_2 cooled to 0 °C with rapid stirring for 24 h. The reaction was worked up according to the general protocol. NMR analysis of the crude reaction mixture revealed a 71:29 mixture of s*yn* and *anti* isomers. The crude reaction was purified by flash silica gel chromatography (90:10:1 → 80:20:1 hexanes : ethyl acetate : acetic acid) to afford two diastereomerically pure products **3.56** (353 mg, 86% combined).

3.56A (*SYN*) (89% ee, 249 mg, 61%, clear oil): The enantiomeric excess was determined to be 89% by chiral HPLC analysis (CHIRALPAK IA, 1.0 mL/min, 3.0% i-PrOH/hexane, λ=220 nm); t_R(major) = 24.103 min, t_R(minor) = 16.561min. $[\alpha]_D^{24}$=– 37.3° (c = 1.00, $CHCl_3$); ^{1}H NMR (600 MHz, $CDCl_3$): δ 7.40 – 7.34 (m, 3H), 7.30 – 7.25 (m, 3H), 7.20 – 7.14 (m, 2H), 6.95 – 6.90 (m, 2H), 5.02 (d, J = 14.2 Hz, 1H), 4.83 (td, J = 10.5, 3.0 Hz, 1H), 4.70 (d, J = 14.2 Hz, 1H), 4.00 – 3.84 (m, 4H), 2.81 (dq, J = 10.3, 6.6 Hz, 1H), 1.94 (dddd, J = 13.7, 10.6, 5.9, 3.0 Hz, 1H), 1.84 (dtd, J = 14.6, 10.3, 4.8 Hz, 1H), 1.67 (ddd, J = 14.0, 10.0, 5.9 Hz, 1H), 1.56 – 1.51 (m, 1H), 1.28 (s, 3H), 1.08 (d, J = 6.6 Hz, 3H); ^{13}C NMR (101 MHz, $CDCl_3$) δ 171.7, 141.1, 137.0, 130.0, 128.9, 128.7, 128.5, 128.3, 127.6, 108.9, 91.6, 64.7, 53.2, 41.1, 34.9, 27.0, 24.0, 15.6; FTIR (cm^{-1}): 2982, 1654, 1550, 1495, 1257, 1075, 857, 702. HRMS (ESI) $(M+H)^+$ m/z calculated for $[C_{23}H_{29}N_2O_5]^+$: 413.1998; found: 413.2070.

3.56B (*ANTI*) (75% ee, 104 mg, 25%, off white solid): The enantiomeric excess was determined to be 75% by chiral HPLC analysis (CHIRALPAK IA, 1.0 mL/min, 3.0% i-PrOH/hexane, λ=220 nm); t_R(major) = 36.984 min, t_R(minor) = 22.725 min. $[\alpha]_D^{24}$=+38.1° (c = 1.00, $CHCl_3$); ^{1}H NMR (600 MHz, $CDCl_3$): δ 7.39 – 7.31 (m, 3H), 7.28 – 7.20 (m, 3H), 7.12 (d, 2H), 7.07 (d, J = 7.3 Hz, 2H), 4.94 – 4.86 (m, 2H), 4.78 (d, J = 14.3 Hz, 1H), 3.93 – 3.87 (m, 2H), 3.87 – 3.80 (m, 2H), 2.99 (dq, J = 10.0, 7.0 Hz, 1H), 1.99 (ddt, J = 14.9, 11.4, 4.0 Hz, 1H), 1.78 – 1.67 (m, 1H), 1.63 (td, J = 13.6, 11.1, 4.7 Hz, 1H), 1.59 – 1.50 (m, 1H), 1.24 (s, 3H), 1.08 (d, J = 7.0 Hz, 3H); ^{13}C NMR (101 MHz, $CDCl_3$) δ 172.7, 141.2, 136.9, 129.6, 128.6, 128.5, 128.4, 128.3, 127.4, 108.9, 89.3, 64.6, 53.1, 39.7, 34.2, 25.1, 23.82, 14.5; FTIR (cm^{-1}): 2982, 1655, 1548, 1495, 1257, 858, 701; mp = 107-109 °C. HRMS (ESI) $(M+H)^+$ m/z calculated for $[C_{22}H_{29}N_2O_5]^+$: 413.1998; found: 413.2071.

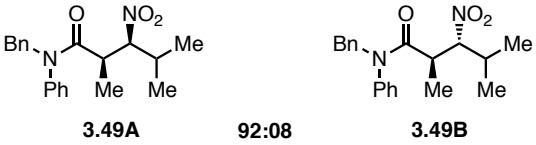

3.49A **92:08** **3.49B**

(**3.49**) According to general protocol D: **3.48** (69.4 mg, 0.1 mmol), *N*-benzyl-2-bromo-*N*-phenylpropionamide (**3.33**, 318 mg, 1.0 mmol), 2-methyl-1-nitropropane (130 µL, 1.2 mmol), sodium methoxide (59.4 mg, 1.1 mmol), diethyl zinc (1 M in hexane, 0.02 mmol, 20 µL) and anhydrous Et_2O (10.0 mL) were combined under N_2 cooled to 0 °C with rapid stirring for 24 h. The reaction was worked up according to the general protocol. NMR analysis of the crude reaction mixture revealed an 92:08 mixture of *syn* and *anti* isomers. The crude reaction was purified by flash silica gel chromatography (95:05 → 90:10 hexanes : ethyl acetate) to afford two diastereomerically pure products **3.49** (295 mg, 87% combined).

3.49A (*SYN*) (94% ee, 270 mg, 80%, clear oil): The enantiomeric excess was determined to be 94% by chiral HPLC analysis (CHIRALPAK IA, 1.0 mL/min, 1.0% i-PrOH/hexane, λ=220 nm); t_R(major) = 17.559 min, t_R(minor) = 22.117 min. $[\alpha]_D^{24}$=–74.1° (c = 1.00, $CHCl_3$); ^{1}H NMR (600 MHz, $CDCl_3$): δ 7.40 – 7.35 (m, 3H), 7.29 – 7.26 (m, 3H), 7.17 – 7.12 (m, 2H), 6.99 – 6.94 (m, 2H), 4.90 (d, J = 14.1 Hz, 1H), 4.82 (d, J = 14.1 Hz, 1H), 4.77 (dd, J = 10.2, 4.7 Hz, 1H), 2.92 (dq, J = 10.2, 6.6 Hz, 1H), 2.15 (pd, J = 6.9, 4.7 Hz, 1H), 1.13 (d, J = 6.6 Hz, 3H), 1.00 (d, J = 6.9 Hz, 3H), 0.84 (d, J = 6.8 Hz, 3H); ^{13}C NMR (101 MHz, $CDCl_3$) δ 171.9, 141.0, 136.9, 129.9, 128.9, 128.7, 128.4, 128.2, 127.6, 96.2, 53.2, 38.4, 30.1, 20.1, 17.0, 16.0; FTIR (cm^{-1}): 2972, 1654, 1545, 1495, 1200, 1079, 701. HRMS (ESI) $(M+H)^+$ m/z calculated for $[C_{20}H_{25}N_2O_3]^+$: 341.1859; found: 341.1849.

3.49B (*ANTI*) (76% ee, 25 mg, 7%, clear oil): The enantiomeric excess was determined to be 76% by chiral HPLC analysis (CHIRALPAK IA, 1.0 mL/min, 5.0% i-PrOH/hexane, λ=220 nm); t_R(major) = 16.688 min, t_R(minor) = 8.950 min. $[\alpha]_D^{24}$=+27.2° (c = 1.00, $CHCl_3$); ^{1}H NMR (600 MHz, $CDCl_3$): δ 7.39 – 7.31 (m, 3H), 7.25 – 7.20 (m, 3H), 7.16 – 7.08 (m, 4H), 4.91 (d, J = 14.3 Hz, 1H), 4.85 (dd, J = 10.7, 2.8 Hz, 1H), 4.77 (d, J = 14.3 Hz, 1H), 3.12 (dq, J = 10.7, 7.0 Hz, 1H), 2.03 (ddq, J = 13.7, 6.8, 3.5, 2.9 Hz, 1H), 1.09 (d, J = 6.9 Hz, 3H), 1.05 (d, J = 7.0 Hz, 3H), 0.68 (d, J = 6.8 Hz, 3H); ^{13}C NMR (101 MHz, $CDCl_3$) δ 173.1, 141.3, 137.0, 129.5, 128.6, 128.4, 128.3, 127.4, 94.0, 53.0, 37.8, 27.8, 20.6, 15.5, 14.6; FTIR (cm^{-1}): 2970, 1655, 1545, 1495, 1259, 1079, 700. HRMS (ESI) $(M+H)^+$ m/z calculated for $[C_{20}H_{25}N_2O_3]^+$: 341.1859; found: 341.1847.

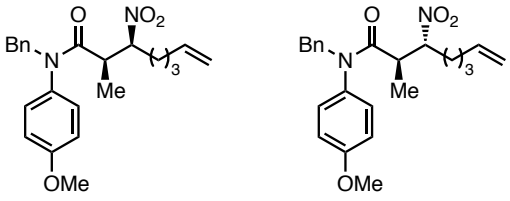

3.58A 82:18 **3.58B**

(**3.58**) According to general protocol D: **3.48** (69.4 mg, 0.1 mmol), *N*-benzyl-2-bromo-*N*-(4-methoxyphenyl)propanamide (**3.S7**, 348 mg, 1.0 mmol), 1-nitrohexene (164 μL, 1.2 mmol), sodium methoxide (59.4 mg, 1.1 mmol), diethyl zinc (1 M in hexane, 0.02 mmol, 20 μL) and anhydrous Et_2O (10.0 mL) were combined under N_2 cooled to 0 °C with rapid stirring for 24 h. The reaction was worked up according to the general protocol. NMR analysis of the crude reaction mixture revealed a 82:18 mixture of *syn* and *anti* isomers. The crude reaction was purified by flash silica gel chromatography (95:05 → 90:10 hexanes : ethyl acetate) to afford two diastereomerically pure products **3.58** (312 mg, 79% combined).

3.58A (*SYN*) (90% ee, 260 mg, 66%, white solid): The enantiomeric excess was determined to be 90% by chiral HPLC analysis (CHIRALPAK IC, 1.0 mL/min, 2.0% i-PrOH/hexane, λ=220 nm); t_R(major) = 29.259 min, t_R(minor) = 22.363 min. $[\alpha]_D^{24}$=–35.4° (c = 1.00, $CHCl_3$); ^{1}H NMR (600 MHz, $CDCl_3$): δ 7.30 – 7.24 (m, 3H), 7.19 – 7.13 (m, 2H), 6.87 – 6.83 (m, 2H), 6.80 (d, J = 9.1 Hz, 2H), 5.73 (ddt, J = 17.0, 10.2, 6.7 Hz, 1H), 5.05 – 4.97 (m, 2H), 4.94 (d, J = 14.0 Hz, 1H), 4.79 – 4.73 (m, 1H), 4.70 (d, J = 14.0 Hz, 1H), 3.82 (s, 3H), 2.84 (dq, J = 10.3, 6.6 Hz, 1H), 2.14 – 1.99 (m, 2H), 1.75 (td, J = 8.1, 6.4 Hz, 2H), 1.47 – 1.38 (m, 1H), 1.32 (dddd, J = 15.1, 13.3, 8.1, 6.6 Hz, 1H), 1.07 (d, J = 6.7 Hz, 3H); ^{13}C NMR (151 MHz, $CDCl_3$) δ 172.1, 159.3, 137.4, 137.1, 133.7, 129.3, 128.9, 128.4, 127.6, 115.4, 115.0, 91.8, 55.4, 53.2, 40.9, 32.7, 31.7, 25.0, 15.5; FTIR (cm^{-1}): 2933, 1653, 1549, 1405, 1250, 1037, 701; mp = 66-68

°C. HRMS (ESI) $(M+H)^+$ m/z calculated for $[C_{23}H_{29}N_2O_4]^+$: 397.2121; found: 397.2103.

3.58B (*ANTI*) (82% ee, 52 mg, 13%, clear oil): The enantiomeric excess was determined to be 82% by chiral HPLC analysis (CHIRALPAK IB, 1.0 mL/min, 0.8% i-PrOH/hexane, λ=254 nm); t_R(major) = 44.576 min, t_R(minor) = 40.614 min. $[\alpha]_D^{24}$=+34.7° (c = 1.00, $CHCl_3$); ^{1}H NMR (600 MHz, $CDCl_3$): δ 7.29 – 7.21 (m, 3H), 7.15 – 7.09 (m, 2H), 6.96 (d, J = 9.2 Hz, 2H), 6.87 – 6.81 (m, 2H), 5.68 (ddt, J = 17.0, 10.3, 6.7 Hz, 1H), 4.99 – 4.93 (m, 2H), 4.88 (td, J = 9.8, 3.4 Hz, 1H), 4.85 (d, J = 14.3 Hz, 1H), 4.74 (d, J = 14.2 Hz, 1H), 3.80 (s, 3H), 3.00 (dq, J = 10.1, 7.0 Hz, 1H), 2.11 – 1.96 (m, 2H), 1.89 – 1.79 (m, 1H), 1.65 (dtd, J = 14.9, 9.7, 5.3 Hz, 1H), 1.42 – 1.29 (m, 2H), 1.05 (d, J = 7.0 Hz, 3H); ^{13}C NMR (151 MHz, $CDCl_3$) δ 173.2, 159.2, 137.3, 137.1, 133.9, 128.8, 128.4, 127.4, 115.5, 114.6, 89.3, 55.3, 53.2, 39.7, 32.7, 30.0, 24.1, 14.5; FTIR (cm^{-1}): 2932, 1653, 1549, 1409, 1250, 916, 700. HRMS (ESI) $(M+H)^+$ m/z calculated for $[C_{23}H_{29}N_2O_4]^+$: 397.2121; found: 397.2103.

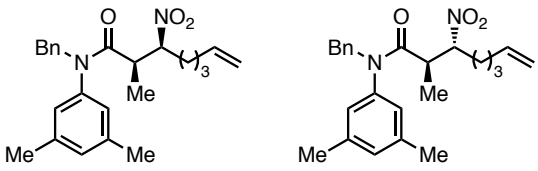

3.60A **83:17** **3.60B**

(**3.60**) According to general protocol D: **3.48** (69.4 mg, 0.1 mmol), 1-nitrohexene (164 μL, 1.2 mmol), *N*-benzyl-2-bromo-*N*-(3,5-dimethylphenyl)propanamide (**3.S9**, 346 mg, 1.0 mmol), sodium methoxide (59.4 mg, 1.1 mmol), diethyl zinc (1 M in hexane, 0.02 mmol, 20 μL) and anhydrous Et_2O (10.0 mL) were combined under N_2 cooled to 0 °C with rapid stirring for 24 h. The reaction was worked up according to the general protocol. NMR analysis of the

crude reaction mixture revealed a 83:17 mixture of *syn* and *anti* isomers. The crude reaction was purified by flash silica gel chromatography (95:05 → 90:10 hexanes : ethyl acetate) to afford two diastereomerically pure products **3.60** (300 mg, 76% combined).

3.60A (*SYN*) (91% ee, 250 mg, 63%, clear oil): The enantiomeric excess was determined to be 91% by chiral HPLC analysis (CHIRALPAK IC, 1.0 mL/min, 2.0% i-PrOH/hexane, λ=220 nm); t_R(major) = 21.293 min, t_R(minor) = 17.692 min. $[\alpha]_D^{24}$=–49.0° (c = 1.00, $CHCl_3$); ^{1}H NMR (600 MHz, $CDCl_3$): δ 7.32 – 7.24 (m, 3H), 7.20 – 7.14 (m, 2H), 6.98 (s, 1H), 6.49 (s, 2H), 5.72 (ddt, J = 17.0, 10.2, 6.7 Hz, 1H), 5.05 – 4.95 (m, 2H), 4.91 (d, J = 14.0 Hz, 1H), 4.82 – 4.73 (m, 1H), 4.71 (d, J = 14.1 Hz, 1H), 2.85 (dq, J = 10.3, 6.7 Hz, 1H), 2.26 (s, 6H), 2.15 – 1.96 (m, 2H), 1.80 – 1.69 (m, 2H), 1.50 – 1.36 (m, 1H), 1.36 – 1.24 (m, 1H), 1.07 (d, J = 6.7 Hz, 3H); ^{13}C NMR (101 MHz, $CDCl_3$) δ 171.7, 141.0, 139.6, 137.4, 137.1, 130.3, 128.9, 128.3, 127.5, 125.8, 115.4, 91.8, 53.2, 40.9, 32.8, 31.7, 24.9, 21.1, 15.7; FTIR (cm^{-1}): 2925, 1653, 1555, 1403, 1217, 915, 711. HRMS (ESI) $(M+H)^+$ m/z calculated for $[C_{24}H_{31}N_2O_3]^+$: 395.2329; found: 395.2312.

3.60B (*ANTI*) (83% ee, 50 mg, 13%, off white solid): The enantiomeric excess was determined to be 83% by chiral HPLC analysis (CHIRALPAK IC, 1.0 mL/min, 8.0% i-PrOH/hexane, λ=254 nm); t_R(major) = 39.319 min, t_R(minor) = 50.571 min. $[\alpha]_D^{24}$=+32.2° (c = 1.00, $CHCl_3$); ^{1}H NMR (600 MHz, $CDCl_3$): δ 7.30 – 7.20 (m, 3H), 7.16 – 7.09 (m, 2H), 6.95 (s, 1H), 6.65 (s, 2H), 5.69 (ddt, J = 17.0, 10.2, 6.7 Hz, 1H), 5.02 – 4.87 (m, 2H), 4.85 (td, 1H), 4.82 (q, 2H), 3.03 (dq, J = 10.0, 7.0 Hz, 1H), 2.26

(s, 6H), 2.13 – 1.94 (m, 2H), 1.90 – 1.76 (m, 1H), 1.72 – 1.59 (m, 1H), 1.44 – 1.28 (m, 2H), 1.06 (d, J = 7.0 Hz, 3H); ^{13}C NMR (101 MHz, $CDCl_3$) δ 172.8, 141.2, 137.4, 137.2, 129.9, 128.6, 128.3, 127.3, 115.5, 89.3, 53.1, 39.8, 32.8, 29.9, 24.2, 21.1, 14.7; FTIR (cm^{-1}): 2924, 1654, 1549, 1406, 1233, 915, 711; mp = 84-86 °C. HRMS (ESI) $(M+H)^+$ m/z calculated for $[C_{24}H_{31}N_2O_3]^+$: 395.2329; found: 395.2310.

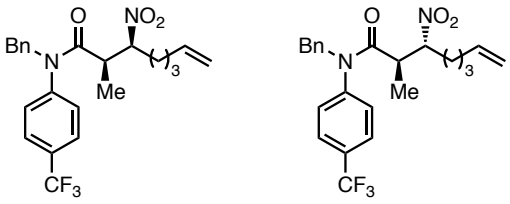

(**3.59**) According to general protocol D: **3.48** (69.4 mg, 0.1 mmol), 1-nitrohexene (164 μL, 1.2 mmol), *N*-benzyl-2-bromo-*N*-(4-(trifluoromethyl)phenyl)propanamide (**3.S11**, 386 mg, 1.0 mmol), sodium methoxide (59.4 mg, 1.1 mmol), diethyl zinc (1 M in hexane, 0.02 mmol, 20 μL) and anhydrous Et_2O (10.0 mL) were combined under N_2 cooled to 0 °C with rapid stirring for 24 h. The reaction was worked up according to the general protocol. NMR analysis of the crude reaction mixture revealed an 79:21 mixture of *syn* and *anti* isomers. The crude reaction was purified by flash silica gel chromatography (95:05 → 90:10 hexanes : ethyl acetate) to afford two diastereomerically pure products **3.59** (342 mg, 79% combined).

3.59A (*SYN*) (89% ee, 274 mg, 63%, off white solid): The enantiomeric excess was determined to be 89% by chiral HPLC analysis (CHIRALPAK IC, 1.0 mL/min, 2.0% i-PrOH/hexane, λ=220 nm); t_R(major) = 12.618 min, t_R(minor) = 10.102 min. $[\alpha]_D^{24}$=–29.7° (c = 1.00, $CHCl_3$); ^{1}H NMR (600 MHz, $CDCl_3$): δ 7.65 (d, J = 8.2 Hz, 2H), 7.33 – 7.27 (m, 3H), 7.18 – 7.12 (m, 2H), 7.04 (d, J = 8.0 Hz, 2H), 5.73 (ddt, J = 17.0, 10.2,

6.7 Hz, 1H), 5.06 – 4.94 (m, 3H), 4.80 – 4.72 (m, 2H), 2.74 (dq, J = 10.0, 6.7 Hz, 1H), 2.16 – 2.00 (m, 2H), 1.76 (dt, J = 9.8, 6.7 Hz, 2H), 1.50 – 1.40 (m, 1H), 1.38 – 1.29 (m, 1H), 1.10 (d, J = 6.7 Hz, 3H); ^{13}C NMR (151 MHz, $CDCl_3$) δ 171.4, 144.3, 137.,4 136.4, 131.0 (q, J = 33 Hz), 129.0, 128.9, 128.7, 128.0, 127.3, 127.2, 123.5 (q, J = 273 Hz), 115.6, 91.5, 53.2, 41.3, 32.8, 31.7, 25.0, 15.6; ^{19}F NMR (565 MHz, $CDCl_3$) δ -62.7; FTIR (cm^{-1}): 2932, 1661, 1555, 1404, 1325, 852, 701; mp = 89-91 °C. HRMS (ESI) $(M+H)^+$ m/z calculated for $[C_{23}H_{26}N_2O_3F_3]^+$: 435.1890; found: 435.1887.

3.59B (*ANTI*) (80% ee, 68 mg, 16%, clear oil): The enantiomeric excess was determined to be 80% by chiral HPLC analysis (CHIRALPAK IC, 1.0 mL/min, 5.0% i-PrOH/hexane, λ=220 nm); t_R(major) = 24.873 min, t_R(minor) = 30.304 min. $[\alpha]_D^{24}$=+37.3° (c = 1.00, $CHCl_3$); ^{1}H NMR (600 MHz, $CDCl_3$): δ 7.63 (d, J = 8.1 Hz, 2H), 7.31 – 7.23 (m, 3H), 7.21 (d, J = 8.0 Hz, 2H), 7.13 – 7.06 (m, 2H), 5.68 (ddt, J = 17.0, 10.3, 6.7 Hz, 1H), 5.03 – 4.93 (m, 2H), 4.93 – 4.86 (m, 2H), 4.79 (d, J = 14.4 Hz, 1H), 2.92 (dq, J = 10.1, 7.0 Hz, 1H), 2.12 – 1.95 (m, 2H), 1.90 – 1.80 (m, 1H), 1.64 (dtd, J = 14.9, 9.8, 5.2 Hz, 1H), 1.42 – 1.28 (m, 2H), 1.07 (d, J = 7.0 Hz, 3H); ^{13}C NMR (151 MHz, $CDCl_3$) δ 172.5, 144.6, 137.2, 136.5, 130.6 (q, J = 33 Hz), 129.1, 128.7, 128.6, 127.8, 126.8, 126.8, 123.6 (q, J = 273 Hz), 115.6, 89.3, 53.1, 40.0, 32.7, 30.0, 24.2, 14.6; ^{19}F NMR (565 MHz, $CDCl_3$) δ -62.6; FTIR (cm^{-1}): 2932, 1661, 1550, 1408, 1325, 853, 700. HRMS (ESI) $(M+H)^+$ m/z calculated for $[C_{23}H_{26}N_2O_3F_3]^+$: 435.1890; found: 435.1887.

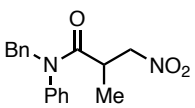

3.57

(**3.57**) According to general protocol D: **3.48** (69.4 mg, 0.1 mmol), *N*-benzyl-2-bromo-*N*-phenylpropionamide (**3.33**, 318 mg, 1.0 mmol), nitromethane (322 μL, 1.2 mmol), sodium methoxide (59.4 mg, 1.1

mmol), diethyl zinc (1 M in hexane, 0.02 mmol, 20μL) and anhydrous Et_2O (10.0 mL) were combined under N_2 cooled to 0 °C with rapid stirring for 24 h. The reaction was worked up according to the general protocol. The crude reaction was purified by flash silica gel chromatography (90:10 hexanes : ethyl acetate) to afford **3.57** (84%ee, 121 mg, 41% Yield) as a white solid. The enantiomeric excess was determined to be 84% by chiral HPLC analysis (CHIRALPAK IA, 1.0 mL/min, 3.0% i-PrOH/hexane, λ=210 nm); t_R(major) = 20.837 min, t_R(minor) = 18.654 min. $[\alpha]_D^{24}$=+73.0° (c = 1.00, $CHCl_3$); ^{1}H NMR (600 MHz, $CDCl_3$): δ 7.38 – 7.31 (m, 3H), 7.30 – 7.22 (m, 3H), 7.19 – 7.14 (m, 2H), 7.13 – 7.07 (m, 2H), 4.97 (dd, J = 14.4, 10.6 Hz, 2H), 4.81 (d, J = 14.3 Hz, 1H), 4.17 (dd, J = 14.4, 4.0 Hz, 1H), 3.18 (dddd, J = 14.1, 10.9, 7.1, 3.9 Hz, 1H), 1.05 (d, J = 7.1 Hz, 3H); ^{13}C NMR (151 MHz, $CDCl_3$) δ 172.5, 141.3, 137.0, 129.7, 128.7, 128.6, 128.4, 128.4, 127.4, 76.7, 53.3, 35.0, 14.9; FTIR (cm^{-1}): 2982, 1653, 1551, 1414, 1380, 1079, 699; mp = 110-112 °C. HRMS (ESI) $(M+H)^+$ m/z calculated for $[C_{23}H_{26}N_2O_3F_3]^+$: 299.1390; found: 299.1386.

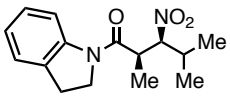

3.62

(**3.62**) According to general protocol F: **3.48** (69.4 mg, 0.1 mmol), 2-bromo-1-(indolin-1-yl) propan-1-one (**3.S5**, 254 mg, 1.0 mmol), 2-methyl-1-nitropropane (128 μL, 1.2 mmol), sodium methoxide (59.4 mg, 1.1 mmol), diethyl zinc (1 M in hexane, 0.02 mmol, 20 μL) and anhydrous Et_2O (10.0 mL) were combined under N_2 and stirred rapidly at rt for 24 h. The reaction was worked up according to the general protocol. NMR analysis of the crude reaction mixture revealed a 95:05 mixture of syn and anti isomers. The crude reaction was purified by flash silica gel chromatography (90:10 hexanes : ethyl acetate) to afford diastereomerically pure product **3.62** (99% ee, 242 mg, 88% Yield) as off-white

solid. The enantiomeric excess was determined to be 99% by chiral HPLC analysis (CHIRALPAK IA, 1.0 mL/min, 1.0% i-PrOH/hexane, λ=254 nm); t_R(major) = 15.458 min, t_R(minor) = 17.698 min. $[\alpha]_D^{24}$=–58.3° (c = 1.00, $CHCl_3$); ^{1}H NMR (400 MHz, DMSO-d6): δ 8.07 (d, J = 8.0 Hz, 1H), 7.26 (d, J = 7.4 Hz, 1H), 7.16 (t, J = 7.8 Hz, 1H), 7.03 (t, J = 7.6 Hz, 1H), 4.73 (dd, J = 8.8, 6.7 Hz, 1H), 4.36 – 4.13 (m, 2H), 3.38 – 3.27 (m, 2H), 3.20 (t, J = 8.4 Hz, 1H), 2.35 – 2.13 (m, J = 6.8 Hz, 1H), 1.17 (d, J = 6.7 Hz, 3H), 0.93 (t, J = 6.8 Hz, 6H); ^{13}C NMR (101 MHz, DMSO-d6) δ 169.9, 142.6, 132.3, 127.0, 124.9, 123.9, 116.5, 95.5, 47.7, 39.5, 29.9, 27.4, 19.0, 17.6, 14.1; FTIR (cm^{-1}): 2970, 1656, 1545, 1482, 1413, 1161, 758; mp = 129-131 °C. HRMS (ESI) $(M+H)^+$ m/z calculated for $[C_{15}H_{21}N_2O_3]^+$: 277.1546; found: 277.1540. Crystals for X-ray analysis were obtained by slow evaporation of diethyl ether.

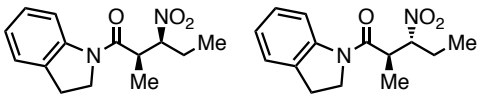

3.66A **88:12** **3.66B**

(**3.66**) According to general protocol F: **3.48** (69.4 mg, 0.1 mmol), 2-bromo-1-(indolin-1-yl) propan-1-one (**3.S5**, 254 mg, 1.0 mmol), 1-nitropropane (108 μL, 1.2 mmol), sodium methoxide (59.4 mg, 1.1 mmol), diethyl zinc (1 M in hexane, 0.02 mmol, 20 μL) and anhydrous Et_2O (10.0 mL) were combined under N_2 and stirred rapidly at rt for 24 h. The reaction was worked up according to the general protocol. NMR analysis of the crude reaction mixture revealed a 88:12 mixture of syn and anti isomers. The crude reaction was purified by flash silica gel chromatography (95:05 → 80:20 hexanes : ethyl acetate) to afford two diastereomerically pure products **3.66** (225 mg, 86% combined).

3.66A (*SYN*) (85% ee, 198mg, 76%, white solid): The enantiomeric excess was determined to be 85% by chiral HPLC analysis (CHIRALPAK IA, 1.0 mL/min, 1.0% i-PrOH/hexane, λ=254 nm); t_R(major) = 17.566 min, t_R(minor) = 21.375 min. $[\alpha]_D^{24}$=–59.4° (c = 1.00, $CHCl_3$); ^{1}H NMR (400 MHz, DMSO-d6): δ 8.09 (d, J = 8.1 Hz, 1H), 7.26 (dd, J = 7.5, 1.5 Hz, 1H), 7.16 (t, J = 7.8, 1.5 Hz, 1H), 7.04 (t, J = 7.4, 1.1 Hz, 1H), 4.68 (td, J = 10.6, 9.3, 3.3 Hz, 1H), 4.33 – 4.14 (m, 2H), 3.29 – 3.21 (m, 1H), 3.18 (t, J = 8.5 Hz, 2H), 1.95 (ddq, J = 14.4, 10.6, 7.2 Hz, 1H), 1.78 (dqd, J = 14.7, 7.5, 3.3 Hz, 1H), 1.16 (d, J = 6.7 Hz, 3H), 0.86 (t, J = 7.3 Hz, 3H); ^{13}C NMR (101 MHz, DMSO-d6) δ 169.8, 142.5, 132.4, 127.0, 124.9, 124.0, 116.5, 92.8, 47.8, 42.0, 27.4, 25.2, 14.4, 10.2; FTIR (cm^{-1}): 2973, 1653, 1548, 1482, 1263, 940, 759; mp = 72-74 °C. HRMS (ESI) $(M+H)^+$ m/z calculated for $[C_{15}H_{21}N_2O_3]^+$: 263.1317; found: 263.1386.

3.66B (*ANTI*) (64% ee, 27 mg, 10%, white solid): The enantiomeric excess was determined to be 64% by chiral HPLC analysis (CHIRALPAK IA, 1.0 mL/min, 5.0% i-PrOH/hexane, λ=220 nm); t_R(major) = 15.807 min, t_R(minor) = 11.990 min. $[\alpha]_D^{24}$=+21.9° (c = 1.00, $CHCl_3$); ^{1}H NMR (400 MHz, DMSO-d6): δ 8.00 (d, J = 8.0 Hz, 1H), 7.25 (d, J = 7.3 Hz, 1H), 7.14 (t, J = 7.7 Hz, 1H), 7.01 (dd, J = 8.1, 6.9 Hz, 1H), 4.86 (td, J = 9.7, 8.3, 3.6 Hz, 1H), 4.21 (ddd, J = 9.6, 7.8, 2.6 Hz, 2H), 3.45 – 3.35 (m, 1H), 3.20 (t, J = 8.5 Hz, 2H), 2.16 – 2.02 (m, 1H), 1.92 – 1.77 (m, 1H), 1.20 (d, J = 6.9 Hz, 3H), 0.89 (t, J = 7.4 Hz, 3H); ^{13}C NMR (101 MHz, DMSO-d6) δ 171.5, 142.6, 132.1, 127.0, 124.9, 123.8, 116.3, 90.1, 47.6, 40.6, 27.4, 23.7, 13.5, 9.2; FTIR (cm^{-1}): 2975, 1655, 1548, 1420, 1278, 1132, 759; mp = 102-104 °C. HRMS (ESI) $(M+H)^+$ m/z calculated for $[C_{15}H_{21}N_2O_3]^+$: 263.1317; found: 263.1391.

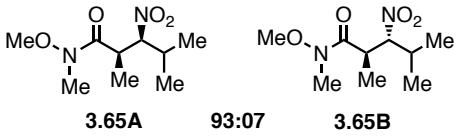

3.65A **93:07** **3.65B**

(**3.65**) According to general protocol F: **3.48** (69.4 mg, 0.1 mmol), 2-bromo-*N*-methoxy-*N*-methylpropanamide (**3.82**, 196 mg, 1.0 mmol), 2-methyl-1-nitropropane (130 μL, 1.2 mmol), potassium tert-butoxide (123 mg, 1.1 mmol), diethyl zinc (1 M in hexane, 0.02 mmol, 20 μL) and anhydrous Et_2O (10.0 mL) were combined under N_2 and stirred rapidly at rt for 24 h. The reaction was worked up according to the general protocol. NMR analysis of the crude reaction mixture revealed a 93:07 mixture of *syn* and *anti* isomers. The crude reaction was purified by flash silica gel chromatography (90:10 hexanes : ethyl acetate) to afford a mixture of diastereomers **3.65** (90% ee, isolated dr 96:04, 161 mg, 74% Yield) as clear oil: The enantiomeric excess was determined to be 90% for **3.65A** by chiral HPLC analysis (CHIRALPAK IB, 1.0 mL/min, 2.0% i-PrOH/hexane, λ=210 nm); t_R(major) = 7.159 min, t_R(minor) = 7.980 min. $[\alpha]_D^{24}$=–22.3° (c = 1.00, $CHCl_3$); The enantiomeric excess was determined to be 44% for **3.65B** by chiral HPLC analysis (CHIRALPAK IB, 1.0 mL/min, 2.0% i-PrOH/hexane, λ=210 nm); t_R(major) = 13.241 min, t_R(minor) = 12.513 min. ^{1}H NMR (400 MHz, $CDCl_3$: mixture of diastereomers; useful diagnostic peaks for each compound are listed. See attached spectra for details): δ **3.65A**: 4.68 (dd, J = 10.4, 5.2 Hz, 1H), 3.75 (s, 3H), 3.58 (dq, J = 10.1, 6.8 Hz, 1H), 3.18 (s, 3H), 2.15 (pd, J = 6.9, 5.3 Hz, 1H), 1.17 (d, J = 6.8 Hz, 3H), 0.97 (dd, J = 6.9, 2.7 Hz, 6H), **3.65B**: 4.81 (dd, J = 11.0, 3.1 Hz, 1H), 1.12 (d, J = 6.9 Hz, 3H); ^{13}C NMR (101 MHz, $CDCl_3$) δ **3.65A**: 173.4, 95.6, 61.7, 36.8, 32.3, 30.2, 19.7, 17.0, 15.4, **3.65B**: 93.1, 61.4, 27.8, 20.6, 13.8; FTIR (cm^{-1}): 2973, 1664, 1548, 1464, 1376, 1178,

996. HRMS (ESI) $(M+H)^+$ m/z calculated for $[C_9H_{19}N_2O_4]^+$: 219.1267; found: 219.1339.

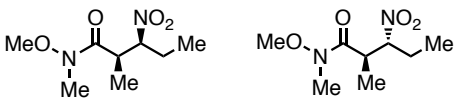

3.69A **92:08** **3.69B**

(**3.69**) According to general protocol F: **3.48** (69.4 mg, 0.1 mmol), 2-bromo-*N*-methoxy-*N*-methylpropanamide (**3.82**, 196 mg, 1.0 mmol), 1-nitropropane (108 μL, 1.2 mmol), sodium methoxide (59.4 mg, 1.1 mmol), diethyl zinc (1 M in hexane, 0.02 mmol, 20 μL) and anhydrous Et_2O (10.0 mL) were combined under N_2 and stirred rapidly at rt for 24 h. The reaction was worked up according to the general protocol. NMR analysis of the crude reaction mixture revealed a 92:08 mixture of *syn* and *anti* isomers. The crude reaction was purified by flash silica gel chromatography (95:05 → 90:10 hexanes : ethyl acetate) to afford a mixture of diastereomers **3.69** (85% ee, isolated dr 93:07, 147 mg, 74% Yield) as clear oil: The enantiomeric excess was determined to be 85% for **3.69A** by chiral HPLC analysis (CHIRALPAK IF, 1.0 mL/min, 2.0% i-PrOH/hexane, λ=210 nm); t_R(major) = 11.489 min, t_R(minor) = 14.258 min. $[\alpha]_D^{24}$=–47.3° (c = 1.00, $CHCl_3$); The enantiomeric excess was determined to be 52% for **3.69B** by chiral HPLC analysis (CHIRALPAK IB, 1.0 mL/min, 2.0% i-PrOH/hexane, λ=210 nm); t_R(major) = 28.742 min, t_R(minor) = 33.026 min. ^{1}H NMR (600 MHz, $CDCl_3$: mixture of diastereomers; useful diagnostic peaks for each compound are listed. See attached spectra for details): δ **3.69A**: 4.63 (td, J = 10.6, 3.0 Hz, 1H), 3.74 (s, 3H), 3.42 (dq, J = 13.3, 6.8 Hz, 1H), 3.20 (s, 3H), 1.89 (ddq, J = 14.4, 10.5, 7.2 Hz, 1H), 1.77 (dqd, J = 14.8, 7.4, 3.0 Hz, 1H), 1.17 (d, J = 6.8 Hz, 3H), 0.94 (t, J = 7.3 Hz, 3H), **3.69B**: 4.81 (td, J = 10.2, 8.7, 3.5 Hz, 1H), 3.78 (s, 3H), 3.52 (dq, J = 8.5 Hz, 1H), 3.18 (s, 3H), 2.08 (ddt, J = 11.0,

7.5, 3.6 Hz, 1H), 0.98 (t, J = 7.4 Hz, 3H), ^{13}C NMR (101 MHz, $CDCl_3$) δ **3.69A**: 172.9, 92.8, 61.8, 39.4, 32.1, 25.9, 15.0, 10.3, **3.69B**: 89.5, 61.4, 38.1, 31.9, 23.9, 13.6, 9.3; FTIR (cm^{-1}): 2975, 1663, 1550, 1462, 1376, 1178, 994. HRMS (ESI) $(M+H)^+$ m/z calculated for $[C_8H_{17}N_2O_4]^+$: 205.1110; found: 205.1183.

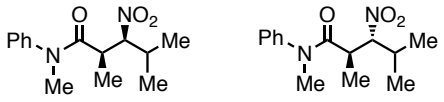

3.64A **91:09** **3.64B**

(**3.64**) According to general protocol F: **3.48** (69.4 mg, 0.1 mmol), 2-bromo-*N*-methyl-*N*-Phenylpropanamide (**3.S4**, 242 mg, 1.0 mmol), 2-methyl-1-nitropropane (128 μL, 1.2 mmol), sodium methoxide (59.4 mg, 1.1 mmol), diethyl zinc (1 M in hexane, 0.02 mmol, 20 μL) and anhydrous Et_2O (10.0 mL) were combined under N_2 and stirred rapidly at rt for 24 h. The reaction was worked up according to the general protocol. NMR analysis of the crude reaction mixture revealed a 91:09 mixture of *syn* and *anti* isomers. The crude reaction was purified by flash silica gel chromatography (90:10:01 hexanes : ethyl acetate : acetic acid) to afford diastereomerically pure product **3.64** (211 mg, 80% combined).

3.64A (*SYN*) (90% ee, 170mg, 64%, clear oil): The enantiomeric excess was determined to be 90% by chiral HPLC analysis (CHIRALPAK ID, 1.0 mL/min, 1.0% i-PrOH/hexane, λ=220 nm); t_R(major) = 15.659 min, t_R(minor) = 17.670 min. $[\alpha]_D^{24}$=–135.2° (c = 1.00, $CHCl_3$); ^{1}H NMR (400 MHz, $CDCl_3$): δ 7.51 – 7.39 (m, 3H), 7.23 – 7.18 (m, 2H), 4.72 (dd, J = 10.3, 4.5 Hz, 1H), 3.27 (s, 3H), 2.99 (dq, J = 10.3, 6.6 Hz, 1H), 2.10 (pd, J = 6.9, 4.5 Hz, 1H), 1.12 (d, J = 6.6 Hz, 3H), 0.99 (d, J = 6.9 Hz, 3H), 0.82 (d, J = 6.8 Hz, 3H); ^{13}C NMR (101 MHz, $CDCl_3$) δ 172.0, 142.9, 130.1, 128.6, 127.0, 96.2, 38.1, 37.7, 30.0, 20.0, 16.9, 15.9; FTIR (cm^{-1}): 2972, 1653, 1541, 1496,

1271, 1032, 703. HRMS (ESI) $(M+H)^+$ m/z calculated for $[C_{14}H_{21}N_2O_3]^+$: 265.1474; found: 265.1536.

3.64B (*ANTI*) (43% ee, 41mg, 16%, combined **3.64A** and **3.64B**, clear oil): The enantiomeric excess was determined to be 43% by chiral HPLC analysis (CHIRALPAK IA, 1.0 mL/min, 5.0% i-PrOH/hexane, λ=220 nm); t_R(major) = 11.390 min, t_R(minor) = 7.949 min. The diastereomer **3.64B** is contaminated with diastereomer **3.64A**: ^{1}H NMR (400 MHz, $CDCl_3$: mixture of diastereomers; useful diagnostic peaks for each compound are listed. See attached spectra for details): δ **3.64A**: 4.72 (dd, J = 10.3, 4.5 Hz, 1H), 3.27 (s, 3H), 2.99 (dq, J = 10.3, 6.6 Hz, 1H), 2.10 (pd, J = 6.9, 4.5 Hz, 1H), 1.12 (d, J = 6.6 Hz, 3H), 0.99 (d, J = 6.8 Hz, 3H), 0.83 (d, J = 6.8 Hz, 3H), **3.64B**: 4.82 (dd, J = 10.7, 2.9 Hz, 1H), 3.23 (s, 3H), 3.16 (dq, J = 10.7, 7.1 Hz, 1H), 2.03 (td, J = 6.9, 2.6 Hz, 1H), 1.08 (d, J = 6.9 Hz, 3H), 1.02 (d, J = 7.0 Hz, 3H), 0.69 (d, J = 6.8 Hz, 3H); ^{13}C NMR (101 MHz, $CDCl_3$) δ **3.64A**: 172.0, 142.9, 130.1, 128.6, 127.0, 96.2, 38.1, 37.7, 30.0, 20.0, 16.9, 15.9, **3.64B**: 173.0, 143.2, 129.8, 128.2, 127.4, 93.9, 37.6, 37.5, 27.8, 20.5, 16.0, 14.5; FTIR (cm^{-1}): 2969, 1654, 1538, 1458, 1274, 1123, 701. HRMS (ESI) $(M+H)^+$ m/z calculated for $[C_{14}H_{21}N_2O_3]^+$: 265. 1474; found: 265.1544.

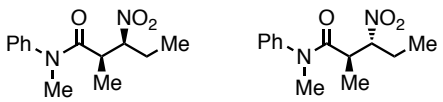

3.68A **79:21** **3.68B**

(**3.68**) According to general protocol F: **3.48** (69.4 mg, 0.1 mmol), 2-bromo-*N*-methyl-*N*-Phenylpropanamide (**3.S4**, 242 mg, 1.0 mmol), 1-nitropropane (108 μL, 1.2 mmol), sodium methoxide (59.4 mg, 1.1 mmol), diethyl zinc (1 M in hexane, 0.02 mmol, 20 μL) and anhydrous Et_2O (10.0 mL) were

combined under N_2 and stirred rapidly at rt for 24 h. The reaction was worked up according to the general protocol. NMR analysis of the crude reaction mixture revealed a 79:21 mixture of *syn* and *anti* isomers. The crude reaction was purified by flash silica gel chromatography (95:05 → 85:15 hexanes : ethyl acetate) to afford two diastereomerically pure products **3.68** (210 mg, 84% combined).

3.68A (*SYN*) (84% ee, 168mg, 67%, clear oil): The enantiomeric excess was determined to be 84% by chiral HPLC analysis (CHIRALPAK IB, 1.0 mL/min, 1.0% i-PrOH/hexane, λ=220 nm); t_R(major) = 13.082 min, t_R(minor) = 14.879 min. $[\alpha]_D^{24}$=–101.1° (c = 1.00, $CHCl_3$); ^{1}H NMR (400 MHz, $CDCl_3$): δ 7.52 – 7.44 (m, 2H), 7.44 – 7.38 (m, 1H), 7.20 – 7.15 (m, 2H), 4.65 (td, J = 10.4, 3.5 Hz, 1H), 3.27 (s, 3H), 2.87 (dq, J = 10.3, 6.7 Hz, 1H), 1.92 – 1.68 (m, 2H), 1.07 (d, J = 6.7 Hz, 3H), 0.91 (t, J = 7.3 Hz, 3H); ^{13}C NMR (101 MHz, $CDCl_3$) δ 171.9, 142.9, 130.2, 128.5, 127.2, 93.4, 40.7, 37.6, 25.8, 15.6, 10.4; FTIR (cm^{-1}): 2974, 1655, 1596, 1549, 1496, 1390, 1120, 1029, 701. HRMS (ESI) $(M+H)^+$ m/z calculated for $[C_{13}H_{19}N_2O_3]^+$: 251.1317; found: 251.1387.

3.68B (*ANTI*) (54% ee, 42mg, 17%, white solid): The enantiomeric excess was determined to be 54% by chiral HPLC analysis (CHIRALPAK IB, 1.0 mL/min, 1.0% i-PrOH/hexane, λ=220 nm); t_R(major) = 27.086 min, t_R(minor) = 33.261 min. $[\alpha]_D^{24}$=+27.5° (c = 1.00, $CHCl_3$); ^{1}H NMR (400 MHz, $CDCl_3$): δ 7.47 (dd, J = 8.2, 7.0 Hz, 2H), 7.41 – 7.37 (m, 1H), 7.34 – 7.29 (m, 2H), 4.81 (td, J = 10.0, 8.9, 3.5 Hz, 1H), 3.23 (s, 3H), 3.05 (dq, J = 10.1, 7.0 Hz, 1H), 1.93 (dqd, J = 14.9, 7.5, 3.5 Hz, 1H), 1.66 (ddq, J = 14.7, 9.0, 7.3 Hz, 1H), 1.04 (d, J = 7.0 Hz, 3H), 0.85 (t, J = 7.4 Hz, 3H); ^{13}C

NMR (101 MHz, $CDCl_3$) δ 172.9, 143.2, 129.9, 128.2, 127.4, 90.5, 39.0, 37.6, 23.9, 14.4, 9.4; FTIR (cm^{-1}): 2975, 1653, 1558, 1446, 1378, 1280, 1071, 709; mp = 95-97 °C. HRMS (ESI) $(M+H)^+$ m/z calculated for $[C_{13}H_{19}N_2O_3]^+$: 251.1317; found: 251.1387.

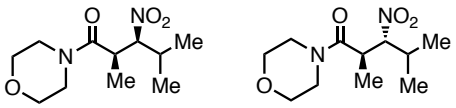

3.63A **92:08** **3.63B**

(**3.63**) According to general protocol F: **3.48** (69.4 mg, 0.1 mmol), α-bromomorpholinopropanamide (**3.S3**, 222 mg, 1.0 mmol), 2-methyl-1-nitropropane (128 μL, 1.2 mmol), sodium methoxide (59.4 mg, 1.1 mmol), diethyl zinc (1 M in hexane, 0.02 mmol, 20 μL) and anhydrous Et_2O (10.0 mL) were combined under N_2 and stirred rapidly at rt for 24 h. The reaction was worked up according to the general protocol. NMR analysis of the crude reaction mixture revealed a 92:08 mixture of *syn* and *anti* isomers. The crude reaction was purified by flash silica gel chromatography (90:10:1 → 80:20:1 hexanes : ethyl acetate : acetic acid) to afford single diastereomer **3.63A** (88% ee, 199 mg, 82%) as clear oil. The enantiomeric excess was determined to be 88% by chiral HPLC analysis (CHIRALPAK IA, 1.0 mL/min, 5.0% i-PrOH/hexane, λ=220 nm); t_R(major) = 8.623 min, t_R(minor) = 10.790 min. $[\alpha]_D^{24}$=–23.0° (c = 1.00, $CHCl_3$); ^1H NMR (400 MHz, $CDCl_3$): δ 4.80 (ddd, J = 10.3, 4.8, 1.3 Hz, 1H), 3.77 – 3.63 (m, 5H), 3.62 – 3.51 (m, 3H), 3.34 (dqd, J = 10.5, 6.9, 1.0 Hz, 1H), 2.20 (dtdd, J = 13.6, 6.8, 4.9, 1.2 Hz, 1H), 1.16 (dd, J = 6.8, 1.3 Hz, 3H), 0.97 (ddd, J = 14.0, 6.9, 1.2 Hz, 6H); ^{13}C NMR (101 MHz, $CDCl_3$) δ 170.6, 95.8, 66.6, 46.1, 42.1, 36.6, 29.8, 19.7, 16.5, 15.7; FTIR (cm^{-1}): 2971, 1639, 1545, 1437, 1226, 1116, 849. HRMS (ESI) $(M+H)^+$ m/z calculated for $[C_{11}H_{21}N_2O_4]^+$: 245.1495; found: 245.1490.

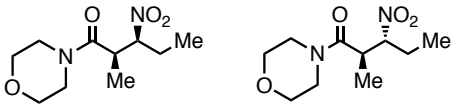

3.67A 81:19 **3.67B**

(**3.67**) According to general protocol F: **3.48** (69.4 mg, 0.1 mmol), α-bromomorpholinopropanamide (**3.S3**, 222 mg, 1.0 mmol), 1-nitropropane (108 μL, 1.2 mmol), sodium methoxide (59.4 mg, 1.1 mmol), diethyl zinc (1 M in hexane, 0.02 mmol, 20 μL) and anhydrous Et_2O (10.0 mL) were combined under N_2 and stirred rapidly at rt for 24 h. The reaction was worked up according to the general protocol. NMR analysis of the crude reaction mixture revealed an 81:19 mixture of *syn* and *anti* isomers. The crude reaction was purified by flash silica gel chromatography (90:10:1 → 75:25:1 hexanes : ethyl acetate : acetic acid) to afford two diastereomerically pure products **3.67** (200 mg, 87% combined).

3.67A (*SYN*) (82% ee, 164mg, 71%, clear oil): The enantiomeric excess was determined to be 82% by chiral HPLC analysis (CHIRALPAK IA, 1.0 mL/min, 5.0% i-PrOH/hexane, λ=220 nm); t_R(major) = 11.920 min, t_R(minor) = 9.460 min. $[\alpha]_D^{24}$=–28.9° (c = 1.00, $CHCl_3$); ^{1}H NMR (400 MHz, $CDCl_3$): δ 4.80 (ddd, J = 10.3, 4.8, 1.3 Hz, 1H), 3.77 – 3.63 (m, 5H), 3.62 – 3.51 (m, 3H), 3.34 (dqd, J = 10.5, 6.9, 1.0 Hz, 1H), 2.20 (dtdd, J = 13.6, 6.8, 4.9, 1.2 Hz, 1H), 1.16 (dd, J = 6.8, 1.3 Hz, 3H), 0.97 (ddd, J = 14.0, 6.9, 1.2 Hz, 6H); ^{13}C NMR (101 MHz, $CDCl_3$) δ 170.6, 95.8, 66.6, 46.1, 42.1, 36.6, 29.8, 19.7, 16.5, 15.7; FTIR (cm^{-1}): 2974, 2858, 1645, 1548, 1457, 1225, 1116, 1028, 813. HRMS (ESI) $(M+H)^+$ m/z calculated for $[C_{10}H_{19}N_2O_4]^+$: 231.1267; found: 231.1337.

3.67B (*ANTI*) (49% ee, 36 mg, 16%, clear oil): The enantiomeric excess was determined to be 49% by chiral HPLC analysis (CHIRALPAK IA, 1.0 mL/min, 5.0% i-PrOH/hexane, λ=220 nm); t_R(major) = 16.599 min, t_R(minor) = 19.398 min. $[\alpha]_D^{24}$=+31.2° (c = 1.00, $CHCl_3$); ^{1}H NMR (600 MHz, $CDCl_3$): δ 4.86 (td, J = 9.8, 8.6, 3.5 Hz, 1H), 3.77 – 3.58 (m, 6H), 3.55 – 3.45 (m, 2H), 3.38 (dq, J = 9.8, 7.2 Hz, 1H), 2.10 (dqd, J = 15.0, 7.5, 3.5 Hz, 1H), 1.85 (ddq, J = 14.7, 8.8, 7.3 Hz, 1H), 1.17 (d, J = 7.2 Hz, 3H), 0.98 (t, J = 7.4 Hz, 3H); ^{13}C NMR (101 MHz, $CDCl_3$) δ 171.56, 90.17, 66.60, 46.18, 42.32, 37.49, 24.05, 14.06, 9.36; FTIR (cm^{-1}): 2974, 2857, 1643, 1548, 1439, 1378, 1115, 809. HRMS (ESI) $(M+H)^+$ m/z calculated for $[C_{10}H_{19}N_2O_4]^+$: 231.1267; found: 231.1340.

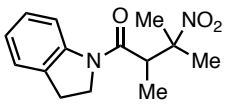

(**3.70**) According to general protocol F: **3.48** (69.4 mg, 0.1 mmol), 2-bromo--(indolin-1-yl) propan-1-one (**3.S5**, 254 mg, 1.0 mmol), 2-nitropropane (108 μL, 1.2 mmol), sodium methoxide (59.4 mg, 1.1 mmol), diethyl zinc (1 M in hexane, 0.02 mmol, 20 μL) and anhydrous Et_2O (10.0 mL) were combined under N_2 and stirred rapidly at rt for 24 h. The reaction was worked up according to the general protocol. The crude reaction was purified by flash silica gel chromatography (95:05 hexanes : ethyl acetate) to afford **3.70** (61%ee, 107 mg, 41%) as white solid. The enantiomeric excess was determined to be 61% by chiral HPLC analysis (CHIRALPAK IA, 1.0 mL/min, 1.0% i-PrOH/hexane, λ=220 nm); t_R(major) = 21.497 min, t_R(minor) = 16.497 min. $[\alpha]_D^{24}$=–18.2° (c = 1.00, $CHCl_3$); ^{1}H NMR (400 MHz, $CDCl_3$): δ 8.20 (d, J = 8.0 Hz, 1H), 7.22 – 7.16 (m, 2H), 7.07 – 7.02 (m, 1H), 4.34 (td, J = 9.7, 7.6 Hz, 1H), 4.15 (td, J = 9.8, 7.2 Hz, 1H), 3.58 (q, J = 7.1

Hz, 1H), 3.33 – 3.17 (m, 2H), 1.78 (s, 3H), 1.75 (s, 3H), 1.27 (d, J = 7.1 Hz, 3H); ^{13}C NMR (101 MHz, $CDCl_3$) δ 170.8, 142.6, 131.4, 127.5, 124.6, 124.1, 117.5, 91.0, 48.6, 45.5, 27.9, 23.9, 13.7; FTIR (cm^{-1}): 2988, 1653, 1539, 1482, 1418, 1264, 757; mp = 126-128 °C. HRMS (ESI) $(M+H)^+$ m/z calculated for $[C_{14}H_{19}N_2O_3]^+$: 263.1317; found: 263.1386.

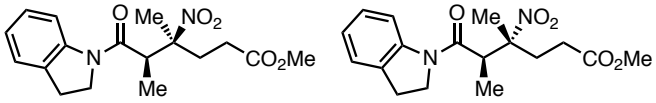

3.71A 55:45 **3.71B**

(**3.71**) According to general protocol F: **3.48** (69.4 mg, 0.1 mmol), 2-bromo-1-(indolin-1-yl) propan-1-one (**3.S5**, 254 mg, 1.0 mmol), 1-nitropropane (108 μL, 1.2 mmol), sodium methoxide (59.4 mg, 1.1 mmol), diethyl zinc (1 M in hexane, 0.02 mmol, 20 μL) and anhydrous Et_2O (10.0 mL) were combined under N_2 and stirred rapidly at rt for 24 h. The reaction was worked up according to the general protocol. NMR analysis of the crude reaction mixture revealed a 56:44 mixture of *syn* and *anti* isomers. The crude reaction was purified by flash silica gel chromatography (90:10 → 80:20 hexanes : ethyl acetate) to afford two diastereomerically pure products **3.71** (157 mg, 44% combined).

3.71A (*SYN*) (67% ee, 81 mg, 24%, clear oil): The enantiomeric excess was determined to be 67% by chiral HPLC analysis (CHIRALPAK IA, 1.0 mL/min, 3.0% i-PrOH/hexane, λ=254 nm); t_R(major) = 15.224 min, t_R(minor) = 13.146 min. $[\alpha]_D^{24}$=–42.1° (c = 1.00, $CHCl_3$); ^{1}H NMR (400 MHz, $CDCl_3$): δ 8.21 (d, 1H), 7.24 – 7.17 (m, 2H), 7.06 (td, J = 7.4, 1.1 Hz, 1H), 4.32 (td, J = 9.8, 7.3 Hz, 1H), 4.16 (td, J = 9.9, 7.0 Hz, 1H), 3.68 – 3.57 (m, 4H), 3.36 – 3.19 (m, 2H), 2.57 – 2.36 (m, 2H), 2.30 – 2.07

(m, 2H), 1.81 (s, 3H), 1.23 (d, J = 7.0 Hz, 3H); ^{13}C NMR (101 MHz, $CDCl_3$) δ 172.2, 169.9, 142.7, 131.5, 127.6, 124.7, 124.4, 117.6, 94.2, 51.9, 48.9, 46.1, 33.2, 28.8, 27.9, 17.1, 13.4; FTIR (cm^{-1}): 2952, 1738, 1656, 1598, 1540, 1481, 1264, 1077, 760. HRMS (ESI) $(M+H)^+$ m/z calculated for $[C_{17}H_{23}N_2O_5]^+$: 335.1529; found: 335.1593.

3.71B (*ANTI*) (49% ee, 66 mg, 20%, clear oil): The enantiomeric excess was determined to be 49% by chiral HPLC analysis (CHIRALPAK IA, 1.0 mL/min, 3.0% i-PrOH/hexane, λ=254 nm); t_R(major) = 24.124 min, t_R(minor) = 19.707 min. $[\alpha]_D^{24}$=+6.1° (c = 1.00, $CHCl_3$); ^{1}H NMR (600 MHz, $CDCl_3$): δ 8.16 (d, J = 8.1 Hz, 1H), 7.23 – 7.13 (m, 2H), 7.02 (t, J = 7.4 Hz, 1H), 4.36 – 4.29 (m, 1H), 4.13 – 4.07 (m, 1H), 3.70 (s, 3H), 3.47 (q, J = 7.2 Hz, 1H), 3.24 (dq, J = 15.7, 9.4 Hz, 2H), 2.46 – 2.33 (m, 3H), 2.32 – 2.24 (m, 1H), 1.86 (s, 3H), 1.33 (d, J = 7.2 Hz, 3H); ^{13}C NMR (101 MHz, $CDCl_3$) δ 172.5, 170.9, 142.7, 131.3, 127.5, 124.5, 124.1, 117.5, 92.8, 52.0, 48.3, 45.4, 33.5, 28.4, 28.0, 18.8, 13.8; FTIR (cm^{-1}): 2952, 1738, 1655, 1598, 1539, 1482, 1263, 1081, 759. HRMS (ESI) $(M+H)^+$ m/z calculated for $[C_{17}H_{23}N_2O_5]^+$: 335.1529; found: 335.1596.

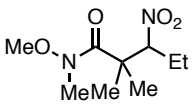

(**3.3**) According to general protocol F: **3.48** (69.4 mg, 0.1 mmol), 2-bromo-*N*-methoxy-N,2-dimethylpropanamide (**3.1**, 210 mg, 1.0 mmol), 1-nitropropane (107 μL, 1.2 mmol), sodium methoxide (59.4 mg, 1.1 mmol), diethyl zinc (1 M in hexane, 0.02 mmol, 20 μL) and anhydrous Et_2O (10.0 mL) were combined under N_2 and stirred rapidly at rt for 24 h. The reaction was worked up according to the general protocol. The crude reaction was purified by flash silica gel chromatography (90:10 hexanes : ethyl acetate) to afford **3.3** (78% ee, 83

mg, 38%) as clear oil. The enantiomeric excess was determined to be 78% by chiral HPLC analysis (CHIRALPAK IA, 1.0 mL/min, 1.0% i-PrOH/hexane, λ=220 nm); t_R(major) = 11.341 min, t_R(minor) = 12.722 min. $[\alpha]_D^{24}$=+29.1° (c = 1.00, $CHCl_3$); ^1H NMR (400 MHz, $CDCl_3$): δ 5.07 (dd, J = 11.6, 2.2 Hz, 1H), 3.73 (s, 3H), 3.19 (s, 3H), 2.10 (ddq, J = 14.3, 11.7, 7.1 Hz, 1H), 1.58 (dqd, J = 14.8, 7.4, 2.2 Hz, 1H), 1.33 (s, 6H), 0.95 (t, J = 7.3 Hz, 3H); ^{13}C NMR (101 MHz, $CDCl_3$) δ 174.6, 94.3, 60.8, 46.5, 34.1, 22.3, 22.1, 20.3, 11.2; FTIR (cm^{-1}): 2976, 1649, 1548, 1462, 1365, 1295, 997. HRMS (ESI) $(M+H)^+$ m/z calculated for $[C_9H_{19}N_2O_4]^+$: 219.1267; found: 219.1331.

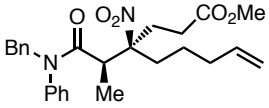

(**3.72**) To a 25 mL round bottom flask equipped with a magnetic stir bar was added **3.47** (Run 1: 200 mg, 0.54 mmol, dr: >95:05, 91% ee), (Run 2: 200 mg, 0.54 mmol, dr: >79:21, 91/82% ee), acetonitrile (5.5 mL), methyl acrylate (147 μL, 1.63 mmol), and DBU (243 μL, 1.63 mmol). The reaction was sealed with a polypropylene cap. The resulting homogenous solution was stirred at rt for 1 h. The reaction was diluted with ethyl acetate (10 mL), washed with brine (2x 10 mL), dried over magnesium sulfate and concentrated in vacuo. NMR analysis of the crude reaction mixture revealed a >95:05 mixture of *syn* and *anti* isomers for both runs. The crude reaction was purified by flash silica gel chromatography (90:10 hexanes : ethyl acetate) to afford **3.72** (Run 1: 91% ee, 205mg, 84% Yield), (Run 2: 89% ee, 202mg, 83% Yield) as a clear oil. The enantiomeric excess was determined to be 91% for Run 1 and 89% for Run 2 by chiral HPLC analysis (CHIRALPAK IF, 1.0 mL/min, 3.0% i-PrOH/hexane, λ=220 nm); t_R(major) = 31.502 min, t_R(minor) = 25.165 min. $[\alpha]_D^{24}$=–30.8° (c = 1.00, $CHCl_3$); ^1H NMR (600 MHz, $CDCl_3$): δ 7.34 (dd, J = 5.2, 2.0 Hz, 1H), 7.26 (d, J = 5.9 Hz, 2H),

7.19 – 7.13 (m, 1H), 6.97 (s, 1H), 5.70 (ddt, J = 17.0, 10.3, 6.7 Hz, 0H), 5.03 – 4.95 (m, 1H), 4.85 (s, 1H), 3.67 (s, 1H), 3.03 (q, J = 7.1 Hz, 0H), 2.48 (ddd, J = 14.1, 10.5, 5.3 Hz, 0H), 2.40 – 2.25 (m, 1H), 2.14 (ddd, J = 14.6, 12.7, 4.1 Hz, 1H), 2.02 (q, J = 7.2 Hz, 1H), 1.95 (ddd, J = 14.6, 12.5, 4.7 Hz, 1H), 1.33 (dddd, J = 19.8, 12.4, 7.2, 4.6 Hz, 0H), 1.26 – 1.16 (m, 1H); ^{13}C NMR (151 MHz, $CDCl_3$) δ 172.8, 171.8, 141.5, 137.4, 137.0, 129.8, 128.9, 128.5, 128.4, 128.3, 127.5, 115.6, 94.9, 53.2, 51.8, 42.4, 34.4, 33.6, 29.0, 28.5, 23.2, 14.3; FTIR (cm^{-1}): 2950, 1738, 1660, 1540, 1403, 1198, 993, 702. HRMS (ESI) $(M+H)^+$ m/z calculated for $[C_{26}H_{33}N_2O_5]^+$: 453.2311; found: 453.2390.

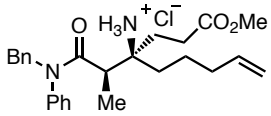

(**3.76**): **3.72** (200 mg, 0.44 mmol), ethyl acetate (13 mL), ethanol (18 mL), and HCl (6 M, 15.8 mmol, 2.64 mL) were added to a 100 mL round-bottom flask equipped with a magnetic stir bar. The flask was cooled to 0 °C and Zn dust (1.44g, 22.1 mmol) was added in 3 portions over 10 minutes under air. The mixture was warmed to room temperature and stirred for 1 h. The resulting mixture was quenched with brine (50 mL) and extracted with ethyl acetate (50mL, 1x). The aqueous layer contains insoluble zinc salts was filtered through celite and back extracted with ethyl acetate (30mL, 3x). The combined organic layer was dried over magnesium sulfate and concentrated in vacuo to afford **3.76** (89%ee, 189mg, 94%) as a white solid. The enantiomeric excess was determined to be 88% by reverse-phase chiral HPLC analysis (CHIRALPAK IF-3, 1.0 mL/min, 10% CH_3CN/water isocratic 1 minute, then 30 minute gradient 35%

CH_3CN/water, 30 minute isocratic 35% CH_3CN/water λ=210 nm); t_R(major) = 38.342 min, t_R(minor) = 41.382 min. $[\alpha]_D^{24}$=–20.3° (c = 1.00, $CHCl_3$); ^{1}H NMR (600 MHz, $CDCl_3$): δ 8.37 (s, 3H), 7.38 (dd, J = 5.1, 1.9 Hz, 3H), 7.28 (dd, J = 5.0, 1.9 Hz, 3H), 7.13 (dd, J = 6.6, 2.9 Hz, 2H), 6.93 (dd, J = 6.4, 2.8 Hz, 2H), 5.67 (ddt, J = 16.9, 10.2, 6.6 Hz, 1H), 4.95 – 4.89 (m, 3H), 4.81 (d, J = 14.0 Hz, 1H), 3.71 (s, 3H), 2.72 (ddd, J = 16.7, 11.3, 5.5 Hz, 1H), 2.41 (q, J = 7.1 Hz, 1H), 2.31 (ddd, J = 16.3, 11.1, 4.8 Hz, 1H), 2.19 (ddd, J = 15.5, 11.1, 5.6 Hz, 1H), 2.09 – 1.92 (m, 2H), 1.93 – 1.72 (m, 3H), 1.27 (d, J = 7.1 Hz, 3H), 1.21 – 1.11 (m, 1H), 0.82 (dh, J = 12.8, 6.3 Hz, 1H); ^{13}C NMR (101 MHz, $CDCl_3$) δ 175.3, 172.8, 140.5, 137.4, 136.2, 130.1, 129.1, 128.9, 128.6, 127.9, 127.8, 115.7, 61.0, 53.1, 52.1, 39.2, 33.0, 31.2, 29.4, 28.0, 21.5, 12.8; FTIR (cm^{-1}): 2942, 1735, 1634, 1592, 1493, 1201, 914, 703; mp = 68-70 °C. HRMS (ESI) $(M)^+$ m/z calculated for $[C_{26}H_{35}N_2O_3]^+$: 423.2642; found: 423.2652.

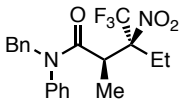

(**3.73**) A hot 25 mL round bottom flask equipped with a magnetic stir bar and a rubber spectrum was attached via needle to a double manifold and cooled under vacuum. Once cooled, the flask was backfilled with N2, the septum was removed, and **3.34** (Run 1: 215 mg, 0.66 mmol, dr: >95:05, 90% ee), (Run 2: 215 mg, 0.66 mmol, dr: 76:24, 90/84% ee), and Umemoto's reagent (344 mg, 0.86 mmol) were added. The septum was replaced, the flask was reattached to a double manifold and evacuated and backfilled with N_2 three times. Anhydrous dichloromethane was added via syringe and the flask was lowered into a precooled –25 °C cooling bath and stirred. DBU (197 μL, 1.32 mmol) was then added dropwise via syringe. The resulting homogenous solution was stirred at –25 °C for 24 h after which the flask was removed from the cooling unit and the septum was

removed. The reaction mixture was washed with brine (10 mL, 1x), dried over magnesium sulfate, and concentrated *in vacuo* onto Celite. The product was purified by silica gel flash chromatography (100:0 → 95:05 hexanes : ethyl acetate) to afford **3.73** (Run 1: 88% ee, 174mg, 67%), (Run 2: 86%ee, 174mg, 67%) as a clear oil. The enantiomeric excess was determined to be 89% for Run 1 and 86% for Run 2 by chiral HPLC analysis (CHIRALPAK IA, 1.0 mL/min, 2.0% i-PrOH/hexane, λ=254 nm); t_R(major) = 9.605 min, t_R(minor) = 6.687 min. $[\alpha]_D^{24}$=–59.1° (c = 1.00, CHCl3); ^{1}H NMR (600 MHz, $CDCl_3$): δ 7.40 – 7.34 (m, 3H), 7.31 – 7.24 (m, 3H), 7.16 – 7.11 (m, 2H), 7.05 – 6.94 (m, 2H), 4.81 (q, 2H), 3.51 (q, J = 7.1 Hz, 1H), 3.07 (dq, J = 15.1, 7.5, 2.5 Hz, 1H), 2.14 (dq, J = 14.9, 7.3 Hz, 1H), 1.31 (d, J = 7.1 Hz, 3H), 1.13 (t, J = 7.3, 3.9 Hz, 3H); ^{13}C NMR (101 MHz, $CDCl_3$) δ 170.1, 140.8, 136.6, 129.7, 128.8, 128.6, 128.4, 127.5, 122.9 (q, J = 288 Hz), 94.9 (q, J = 24 Hz), 53.3, 40.0, 22.9, 14.0, 8.5; ^{19}F NMR (565 MHz, $CDCl_3$) δ - 67.2; FTIR (cm^{-1}): 2986, 1665, 1562, 1495, 1408, 1202, 1120, 824, 701. HRMS (ESI) $(M+H)^+$ m/z calculated for $[C_{20}H_{22}N_2O_3F_3]^+$: 395.1504; found: 395.1568.

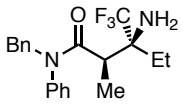

(**3.77**): α-Trifluoromethylnitroalkane **3.73** (190 mg, 0.48 mmol), ethyl acetate (15 mL), ethanol (19 mL), and HCl (6 M, 17.3 mmol, 2.9 mL) were added to a 100 mL round-bottom flask equipped with a magnetic stir bar. The flask was cooled to 0 °C and Zn dust (1.57g, 24.0 mmol) was added in 3 portions over 10 minutes. The mixture was warmed to room temperature and stirred for 1 h. The resulting mixture was quenched with 1.0 M aqueous NaOH (50 mL) and extracted with ethyl acetate (50mL, 1x). The aqueous layer contains insoluble zinc salts was filtered through celite and back extracted with ethyl acetate

(30mL, 3x). The combined organic layer was dried over magnesium sulfate and concentrated *in vacuo* onto Celite. The crude reaction was purified by flash silica gel chromatography (90:10 → 80:20 hexanes : ethyl acetate) to afford **3.77** (88% ee, 142mg, 81% Yield) as a clear oil. The enantiomeric excess was determined to be 88% by chiral HPLC analysis (CHIRALPAK IA, 1.0 mL/min, 5.0% i-PrOH/hexane, λ=220 nm); t_R(major) = 17.099 min, t_R(minor) = 20.364 min. $[\alpha]_D^{24}$=–75.3° (c = 1.00, $CHCl_3$); ^{1}H NMR (600 MHz, $CDCl_3$): δ 7.34 – 7.28 (m, 3H), 7.26 – 7.21 (m, 3H), 7.19 – 7.13 (m, 2H), 6.96 (s, 2H), 4.86 (q, J = 14.2 Hz, 2H), 2.62 (q, J = 6.9 Hz, 1H), 2.24 (s, 2H), 1.66 (dq, J = 15.2, 7.6 Hz, 1H), 1.49 – 1.37 (m, 1H), 1.17 (d, J = 6.9 Hz, 3H), 0.66 (t, J = 7.9, 1.8 Hz, 3H); ^{13}C NMR (101 MHz, $CDCl_3$) δ 174.4, 141.5, 137.1, 129.4, 128.9, 128.3, 128.2, 128.0 (q, J = 288 Hz), 127.3, 60.5 (q, J = 24.1 Hz), 52.8, 35.4, 27.4, 12.9, 7.5; ^{19}F NMR (565 MHz, $CDCl_3$) δ - 74.5; FTIR (cm^{-1}): 3403, 2974, 1656, 1593, 1495, 1403, 1143, 915, 701; mp = 55-57 °C. HRMS (ESI) $(M+H)^+$ m/z calculated for $[C_{20}H_{24}N_2OF_3]^+$: 365.1835; found: 365.1827.

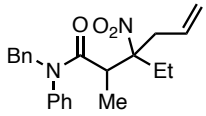

(**3.75**) **3.75** was synthesized by modification of a previously published procedure.[13] A hot 10 mL round bottom flask equipped with a magnetic stir bar and a rubber spectrum was attached via needle to a double manifold and cooled under vacuum. Once cooled, the flask was backfilled with N_2, the septum was removed, and tris(dibenzylideneacetone)dipalladium(0)-chloroform adduct (3.4 mg, 3.3 μmol), (±)-BINAP (6.2 mg, 6.6 μmol), and **3.34** (215 mg, 0.66 mmol, 90% ee) were added. The septum was replaced, the flask was reattached to a double manifold and evacuated and backfilled with N_2 three times. Anhydrous DMSO (0.66 mL) was added via syringe

and the reaction was stirred at rt for 5 minutes. DBU (10 µL, 66 µmol), and *tert*-butyl allyl carbonate (144 µL, 0.79 mmol) were added via syringe. The resulting brown solution was stirred in an oil bath at 50 °C for 48 h. Once complete, the reaction was cooled to rt, opened to air, diluted with ethyl acetate (40 mL) and it was filtered through celite. The filtrate was washed with water (20 mL, 3x). The organic layer was dried over magnesium sulfate and concentrated in vacuo onto Celite. The crude reaction was purified by flash silica gel chromatography (95:05 hexanes : ethyl acetate) to afford **3.75** (90% ee, 178mg, 74%) as a clear oil. The enantiomeric excess was determined to be 90% by chiral HPLC analysis (CHIRALPAK IE, 1.0 mL/min, 3.0% i-PrOH/hexane, λ=254 nm); t_R(major) = 38.353 min, t_R(minor) = 29.727 min. $[\alpha]_D^{24}$=–46.4° (c = 1.00, $CHCl_3$); ^{1}H NMR (600 MHz, $CDCl_3$): δ 7.36 – 7.29 (m, 3H), 7.29 – 7.21 (m, 3H), 7.20 – 7.14 (m, 2H), 7.01 – 6.94 (m, 2H), 5.54 (ddt, J = 17.1, 10.1, 7.0 Hz, 1H), 5.09 (dd, J = 17.2, 1.9 Hz, 1H), 5.02 (d, 1H), 4.86 (q, 2H), 3.04 (q, J = 7.0 Hz, 1H), 2.91 (dd, J = 15.2, 6.7 Hz, 1H), 2.72 (dd, J = 15.2, 7.4 Hz, 1H), 2.35 (dq, J = 14.9, 7.5 Hz, 1H), 1.96 (dq, J = 14.7, 7.4 Hz, 1H), 1.18 (d, J = 7.0 Hz, 3H), 0.86 (t, J = 7.4 Hz, 3H); ^{13}C NMR (101 MHz, $CDCl_3$) δ 172.2, 141.5, 137.1, 131.9, 129.6, 128.9, 128.4, 128.4, 128.3, 127.4, 95.5, 53.1, 41.8, 37.5, 27.7, 14.2, 8.4; FTIR (cm^{-1}): 3063, 2979, 1658, 1594, 1494, 1403, 1245, 924, 702. HRMS (ESI) $(M+H)^+$ m/z calculated for $[C_{22}H_{27}N_2O_3]^+$: 367.2016; found: 367.2005.

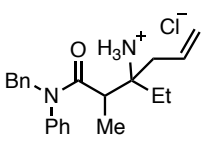

(**3.S14**) **3.75** (350 mg, 0.96 mmol), ethyl acetate (29 mL), ethanol (38 mL), and HCl (6 M, 34.4 mmol, 5.7 mL) were added to a 200 mL round bottom flask equipped with a magnetic stir bar. The flask was cooled to 0 °C and Zn dust (3.125g, 47.8 mmol) was added in 3 portions over 10

minutes. The mixture was warmed to room temperature and stirred for 1 h. The resulting mixture was quenched with brine (100 mL) and extracted with ethyl acetate (80mL, 1x). The aqueous layer contains insoluble zinc salts was filtered through celite and back extracted with ethyl acetate (50 mL, 3x). The combined organic layer was dried over magnesium sulfate and concentrated in vacuo to afford crude (336 mg) as a white solid. The crude material was taken to the next step without further purification.

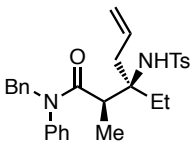

(**3.78**) A hot 10 mL round bottom flask equipped with a magnetic stir bar and rubber septum was attached via needle to a double manifold and cooled under vacuum. The flask was backfilled with N_2, the septum was removed, and the **3.S14** (120 mg, 0.32 mmol), p–toluene sulfonyl chloride (68 mg, 0.35mmol), and 4-(dimethylamino) pyridine (8 mg, 0.064mmol), was added sequentially. The septum was replaced, the flask was attached to a double manifold, and evacuated and backfilled with N_2 three times. Anhydrous dichloromethane (1.6 mL), and triethylamine (90 μL, 0.64 mmol), were added to the flask sequentially via syringe and the reaction stirred at rt for 8 h. The septum was removed and the reaction was diluted with dichloromethane (10.0 mL) and washed with water (10 mL, 2x). The aqueous layer was back extracted with dichloromethane (10 mL, 1x). The organic layers were combined, dried over magnesium sulfate, and concentrated *in vacuo*. The crude reaction was purified by flash silica gel chromatography (90:10 hexanes : ethyl acetate) to afford **3.78** (96% ee, 133mg, 85%) as a white solid. The enantiomeric excess was determined to be 96% by chiral HPLC analysis (CHIRALPAK IB, 1.0 mL/min, 3.0% i-PrOH/hexane, λ=210 nm); t_R(major) = 25.128 min, t_R(minor) = 23.737 min. $[\alpha]_D^{24}$=–11.8° (c = 1.00, $CHCl_3$); ^{1}H NMR (400 MHz, $CDCl_3$): δ 7.76 (d,

2H), 7.51 (s, 1H), 7.37 – 7.31 (m, 4H), 7.29 – 7.26 (m, 2H), 7.24 – 7.20 (m, 2H), 7.16 (dd, J = 6.7, 2.9 Hz, 2H), 6.99 – 6.88 (m, 2H), 5.97 – 5.82 (m, 1H), 5.08 – 4.98 (m, 2H), 4.92 (d, J = 14.1 Hz, 1H), 4.75 (d, J = 14.0 Hz, 1H), 2.39 (s, 3H), 2.38 – 2.26 (m, 2H), 2.20 (dd, J = 14.3, 7.8 Hz, 1H), 1.94 (dq, J = 15.0, 7.5 Hz, 1H), 1.51 – 1.38 (m, 1H), 0.89 (d, J = 6.9 Hz, 3H), 0.31 (t, J = 7.5 Hz, 3H); ^{13}C NMR (101 MHz, $CDCl_3$) δ 175.9, 142.2, 141.5, 141.2, 136.8, 133.7, 129.7, 129.2, 129.0, 128.5, 128.1, 127.6, 127.0, 117.8, 64.0, 52.8, 42.7, 39.8, 29.5, 23.6, 21.5, 13.2, 7.1; FTIR (cm^{-1}): 3220, 2975, 1635, 1594, 1495, 1404, 1340, 1149, 702; mp = 120-122 °C. HRMS (ESI) $(M+H)^+$ m/z calculated for $[C_{29}H_{35}N_2O_3S]^+$: 491.2290; found: 491.2342. Crystals for X-ray analysis were obtained by slow evaporation of diethyl ether.

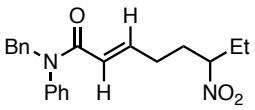

(**3.80**) According to general protocol C: **3.48** (69.4 mg, 0.1 mmol), N-benzyl-2-bromo-2-cyclopropyl-N-phenylacetamide (**3.79**, 222 mg, 1.0 mmol), 1-nitropropane (108 μL, 1.2 mmol), sodium methoxide (59.4 mg, 1.1 mmol), diethyl zinc (1 M in hexane, 0.02 mmol, 20 μL) and anhydrous Et_2O (10.0 mL) were combined under N_2 and stirred rapidly at rt for 24 h. The reaction was worked up according to the general protocol. The crude reaction was purified by flash silica gel chromatography (75:25:01 hexanes : ethyl acetate : acetic acid) to afford **3.80** (16% ee, 87mg, 25%) as a clear oil. The enantiomeric excess was determined to be 16% by chiral HPLC analysis (CHIRALPAK IA, 1.0 mL/min, 5.0% i-PrOH/hexane, λ=220 nm); t_R(major) = 22.898 min, t_R(minor) = 25.021 min. $[\alpha]_D^{24}$=+5.9° (c = 1.00, $CHCl_3$); ^{1}H NMR (400 MHz, $CDCl_3$): δ 7.38 – 7.29 (m, 3H), 7.29 – 7.18 (m, 5H), 7.03 – 6.96 (m, 2H), 6.85 (dt, J =

15.1, 6.9 Hz, 1H), 5.72 (d, J = 15.2 Hz, 1H), 4.96 (s, 2H), 4.32 (tt, J = 9.1, 4.3 Hz, 1H), 2.06 (dtdd, J = 20.8, 14.5, 9.6, 7.7 Hz, 3H), 1.91 (ddt, J = 14.6, 9.3, 7.3 Hz, 1H), 1.80 – 1.64 (m, 2H), 0.91 (t, J = 7.4 Hz, 3H); ^{13}C NMR (101 MHz, $CDCl_3$) δ 165.4, 142.9, 141.7, 137.3, 129.4, 128.6, 128.3, 128.3, 127.8, 127.3, 123.3, 89.2, 53.1, 31.8, 28.4, 27.2, 10.1; FTIR (cm^{-1}): 3063, 2979, 1658, 1594, 1494, 1403, 1245, 924, 702. HRMS (ESI) $(M+H)^+$ m/z calculated for $[C_{21}H_{25}N_2O_3]^+$: 353.1787; found: 353.1844.

3.14.11 Procedure for Stereoconvergence in the Nickel Catalyzed Enantioselective *C*-Alkylation of Nitroalkanes:

Reaction beginning with (*R*)- **3.81**

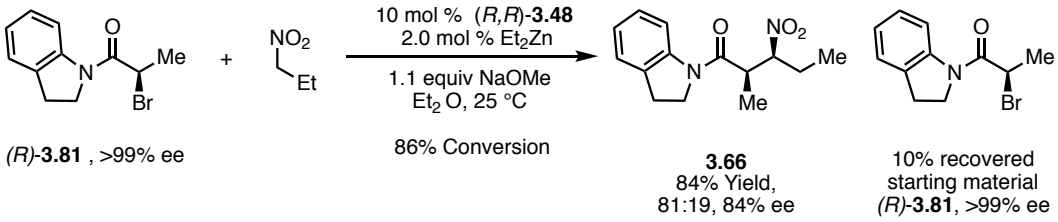

According to general protocol C: **3.48** (17.3 mg, 0.025 mmol), (*R*)-2-bromo-1-(indolin-1-yl) propan-1-one (**3.81**, 64 mg, 0.25 mmol), 1-nitropropane (28 μL, 0.3 mmol), sodium methoxide (14.9 mg, 0.275 mmol), diethyl zinc (1 M in hexane, 0.005 mmol, 5 μL) and anhydrous Et_2O (2.5 mL) were combined under N_2 and stirred rapidly at rt. After 30 min, the reaction was removed from the glovebox and quenched by opening the reaction to air. 1,3,5-trimethoxybenzene (10.5 mg, 0.0625 mmol) was added as an internal standard and the reaction was worked up according to the general protocol C. ^{1}H NMR analysis of the crude reaction mixture revealed a diastereomeric ratio of 81:19 favoring of syn isomer and 86% conversion of starting material (*R*)-**3.81** and 84% yield of **3.66**. The chiral HPLC analysis of starting material (*R*)-**3.81** showed

ee of 99% and a product **3.66** ee of 84%. (CHIRALPAK IA, 1.0 mL/min, 1.0% i-PrOH/hexane, λ=254 nm; starting material (*R*)-**3.81**: t_R(major) = 26.099 min, t_R(minor) = 32.910 min; product **3.66**: t_R(major) = 16.738 min, t_R(minor) = 20.710 min).

Reaction beginning with (*S*)- **3.81**

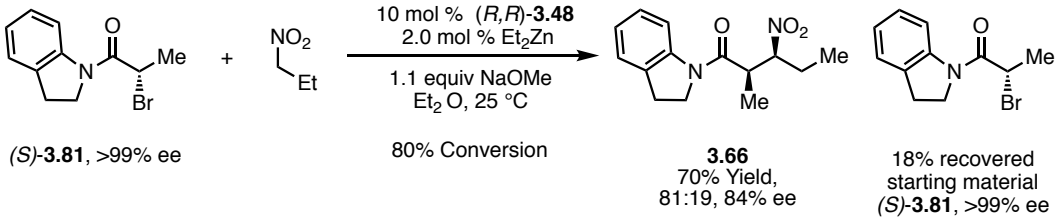

According to general protocol C: **3.48** (17.3 mg, 0.025 mmol), (*S*)-2-bromo-1-(indolin-1-yl) propan-1-one (**3.81**, 64 mg, 0.25 mmol), 1-nitropropane (28 μL, 0.3 mmol), sodium methoxide (14.9 mg, 0.275 mmol), diethyl zinc (1 M in hexane, 0.005 mmol, 5 μL) and anhydrous Et_2O (2.5 mL) were combined under N_2 and stirred rapidly at rt. After 30 min, the reaction was removed from the glovebox and quenched by opening the reaction to air. 1,3,5-trimethoxybenzene (10.5 mg, 0.0625 mmol) was added as an internal standard and the reaction was worked up according to the general protocol C. ^{1}H NMR analysis of the crude reaction mixture revealed a diastereomeric ratio of 81:19 favoring of *syn* isomer and 80% conversion of starting material *(S)*-**3.81** and 70% yield of **3.66**. The chiral HPLC ananlysis of starting material (*S*)-**3.81** showed ee of 99% and a product **3.66** ee of 84%. (CHIRALPAK IA, 1.0 mL/min, 1.0% i-PrOH/hexane, λ=254 nm; starting material (*S*)-**3.81**: t_R(major) = 32.910 min,

t_R(minor) = 26.099 min; product **3.66**: t_R(major) = 16.509 min, t_R(minor) = 20.422 min).

3.14.12 Determination of Stereochemistry of β-nitroamides

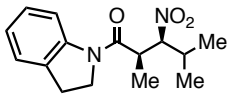

(***R,S***)-**3.62**

The relative and absolute stereochemistry of **3.62** (major diastereomer) was determined by X-ray crystallographic analysis. This compound was prepared using general procedure C from **3.S5** and 2-methyl-1-nitropropane with (***R,R***)-**3.48** as catalyst.

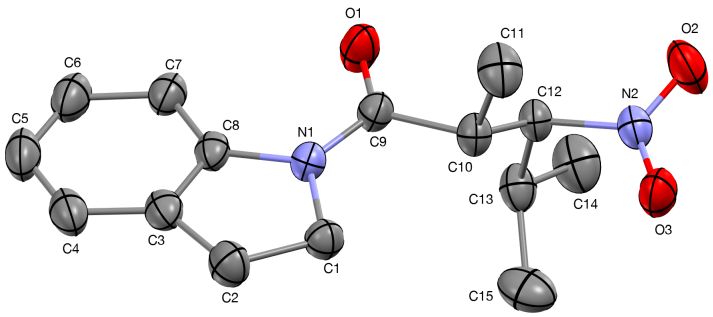

Figure 3.37: Stereochemistry of Major Diastereomer **3.62**

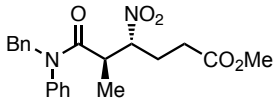

(***R,R***)-**3.54**

The relative and absolute stereochemistry of **3.54** (minor diastereomer) was determined by X-ray crystallographic analysis. This compound was prepared using general procedure B from **3.33** and methyl-4-nitrobutanoate with (***R,R***)-**3.48** as catalyst.

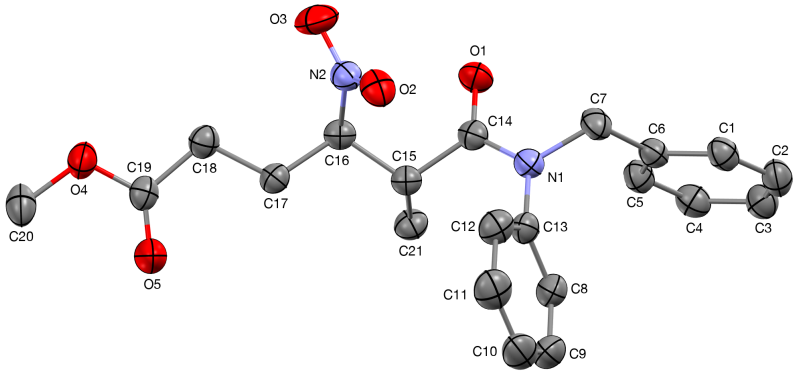

Figure 3.38: Stereochemistry of Minor Diastereomer **3.54**

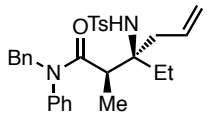

(***R,R***)-**3.78**

The relative and absolute stereochemistry of **3.78** was determined by X-ray crystallographic analysis. This compound was prepared by reducing **3.75** followed by tosylation.

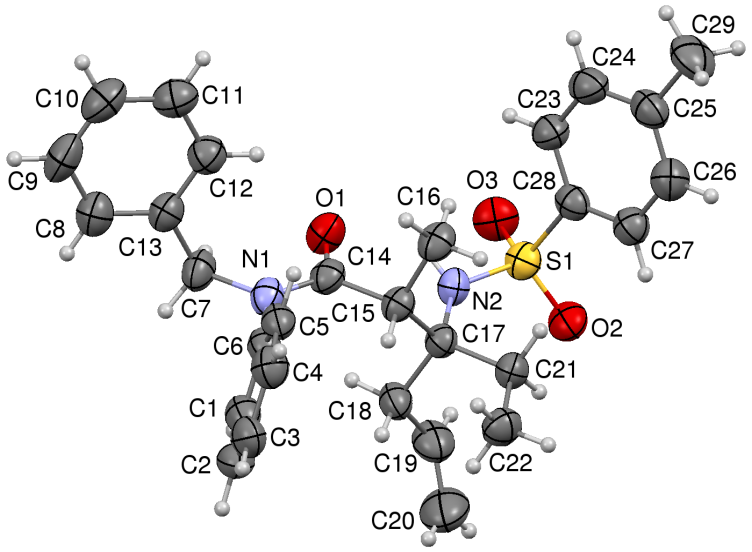

Figure 3.39: Relative and Absolute Stereochemistry of **3.78**

3.14.13 Crystallographic Details:

Crystals were mounted using viscous oil onto a plastic mesh and cooled to the data collection temperature. Data were collected on a Bruker-AXS APEX II DUO CCD diffractometer with with graphite-monochromated Mo-Kα radiation (λ=0.71073 Å) for 59 and Cu-Kα radiation (λ = 1.54178 Å) focused with Goebel mirrors for **3.54**, **3.62** and **3.78**. Unit cell parameters were obtained from 36 data frames, 0.5 º ω, from three different sections of the Ewald sphere. The unit cell parameters, and systematic absences in the diffraction data are consistent with P21 (4) and P21/m (11) for **3.48**; and, uniquely, for P212121 for **3.54**, **3.62** and **3.78**. The non-centrosymmetric space groups are consistent with the chiral compound molecules and they yielded chemically reasonable and computationally stable results of refinement. Refinement of the absolute structure parameters to nil indicates the true hands of the data have been determined. The data were treated with multi-scan absorption corrections.[40] The

structures were solved using intrinsic phasing methods and refined with full-matrix, least-squares procedures on F2.

Compound **3.48** consistently packs inefficiently leading to multiple crystal growth, high mosaicity and disorder at the CF_3 groups. The results herein represent the best of several trials. Two symmetry unique but chemically identical compound molecules and seven cocrystallized toluene solvent molecules were found in the asymmetric unit of **3.48**. In order to converge the chemically reasonable model, the CF_3 groups and toluene solvent molecules were treated as idealized rigid groups and three-dimensional rigid bond restraints were required.

All non-hydrogen atoms were refined with anisotropic displacement parameters. Hydrogen atoms were treated as idealized contributions with geometrically calculated positions and with Uiso equal to 1.2 (or 1.5 for methyl) Ueq of the attached atom. Atomic scattering factors are contained in the SHELXTL program library.[41]

REFERENCES

(1) (a) Kaga, A.; Chiba, S. *ACS Catalysis* **2017**, *7*, 4697. (b) Yan, M.; Lo, J. C.; Edwards, J. T.; Baran, P. S. *J. Am. Chem. Soc.* **2016**, *138*, 12692. (c) Zard, S. Z. *Org. Lett.* **2017**, *19*, 1257.

(2) (a) Bhat, V.; Welin, E. R.; Guo, X.; Stoltz, B. M. *Chem. Rev.* **2017**, *117*, 4528. (b) Cherney, A. H.; Kadunce, N. T.; Reisman, S. E. *Chem. Rev.* **2015**, *115*, 9587.

(3) Choi, J.; Fu, G. C. *Science* **2017**, *356*.

(4) Fischer, C.; Fu, G. C. *J. Am. Chem. Soc.* **2005**, *127*, 4594.

(5) Labinger, J. A. *Organometallics* **2015**, *34*, 4784.

(6) Fu, G. C. *ACS Central Science* **2017**, *3*, 692.

(7) Lundin, P. M.; Fu, G. C. *J. Am. Chem. Soc.* **2010**, *132*, 11027.

(8) Richmond, E.; Moran, J. *Synthesis* **2018**, *50*, 499.

(9) Harper, K. C.; Sigman, M. S. *J. Org. Chem.* **2013**, *78*, 2813.

(10) (a) Hansch, C.; Leo, A.; Taft, R. W. *Chem. Rev.* **1991**, *91*, 165. (b) RajanBabu, T. V.; Radetich, B.; You, K. K.; Ayers, T. A.; Casalnuovo, A. L.; Calabrese, J. C. *J. Org. Chem.* **1999**, *64*, 3429.

(11) Gietter-Burch, A. A. S.; Mitrut, R. E.; Watson, D. A. *Org. Lett.* **2015**, *17*, 5468.

(12) Gietter-Burch, A. A. S.; Devannah, V.; Watson, D. A. *Org. Lett.* **2017**, *19*, 2957.

(13) Maki, K.; Kanai, M.; Shibasaki, M. *Tetrahedron* **2007**, *63*, 4250.

(14) (a) Noble, A.; Anderson, J. C. *Chem. Rev.* **2013**, *113*, 2887. (b) Tramontini, M.; Angiolini, L. *Mannich Bases, Chemistry and Uses*; CRC Press Inc.: Boca

Raton, Fl, 1994. (c) Arend, M.; Westermann, B.; Risch, N. *Angew. Chem., Int. Ed.* **1998**, *37*, 1044. (d) Mukherjee, S.; Yang, J. W.; Hoffmann, S.; List, B. *Chem. Rev.* **2007**, *107*, 5471.

(15) Hie, L.; Ramgren, S. D.; Mesganaw, T.; Garg, N. K. *Org. Lett.* **2012**, *14*, 4182.

(16) (a) Anderson, T. J.; Jones, G. D.; Vicic, D. A. *J. Am. Chem. Soc.* **2004**, *126*, 8100. (b) Hu, X. *Chem. Sci.* **2011**, *2*, 1867. (c) Schley, N. D.; Fu, G. C. *J. Am. Chem. Soc.* **2014**, *136*, 16588.

(17) Evans, D. A.; Mito, S.; Seidel, D. *J. Am. Chem. Soc.* **2007**, *129*, 11583.

(18) (a) Beckwith, A. L. J.; Bowry, V. W.; Ingold, K. U. *J. Am. Chem. Soc.* **1992**, *114*, 4983. (b) Bowry, V. W.; Ingold, K. U. *J. Am. Chem. Soc.* **1992**, *114*, 4992.

(19) (a) Griller, D.; Ingold, K. U. *Acc. Chem. Res.* **1980**, *13*, 317. (b) Newcomb, M. *Tetrahedron* **1993**, *49*, 1151.

(20) (a) Jones, G. D.; McFarland, C.; Anderson, T. J.; Vicic, D. A. *Chem. Commun.* **2005**, 4211. (b) Jones, G. D.; Martin, J. L.; McFarland, C.; Allen, O. R.; Hall, R. E.; Haley, A. D.; Brandon, R. J.; Konovalova, T.; Desrochers, P. J.; Pulay, P.; Vicic, D. A. *J. Am. Chem. Soc.* **2006**, *128*, 13175. (c) Biswas, S.; Weix, D. J. *J. Am. Chem. Soc.* **2013**, *135*, 16192. (d) Breitenfeld, J.; Ruiz, J.; Wodrich, M. D.; Hu, X. *J. Am. Chem. Soc.* **2013**, *135*, 12004. (e) Cornella, J.; Edwards, J. T.; Qin, T.; Kawamura, S.; Wang, J.; Pan, C.-M.; Gianatassio, R.; Schmidt, M.; Eastgate, M. D.; Baran, P. S. *J. Am. Chem. Soc.* **2016**, *138*, 2174. (f) Mohadjer Beromi, M.; Nova, A.; Balcells, D.; Brasacchio, A. M.; Brudvig, G. W.; Guard, L. M.; Hazari, N.; Vinyard, D. J. *J. Am. Chem. Soc.* **2017**, *139*, 922.

(21) Satyanarayana, T.; Abraham, S.; Kagan, H. B. *Angew. Chem., Int. Ed.* **2009**, *48*, 456.

(22) Velian, A.; Lin, S.; Miller, A. J. M.; Day, M. W.; Agapie, T. *J. Am. Chem. Soc.* **2010**, *132*, 6296.

(23) (a) Gildner, P. G.; Gietter, A. A. S.; Cui, D.; Watson, D. A. *J. Am. Chem. Soc.* **2012**, *134*, 9942. (b) Gietter, A. A. S.; Gildner, P. G.; Cinderella, A. P.; Watson, D. A. *Org. Lett.* **2014**, *16*, 3166. (c) Shimkin, K. W.; Gildner, P. G.; Watson, D. A. *Org. Lett.* **2016**, *18*, 988.

(24) Rezazadeh, S.; Devannah, V.; Watson, D. A. *J. Am. Chem. Soc.* **2017**, *139*, 8110.

(25) Pangborn, A. B.; Giardello, M. A.; Grubbs, R. H.; Rosen, R. K.; Timmers, F. J. *Organometallics* **1996**, *15*, 1518.

(26) Skiles, J. W.; Fuchs, V.; Miao, C.; Sorcek, R.; Grozinger, K. G.; Mauldin, S. C.; Vitous, J.; Mui, P. W.; Jacober, S. *J. Med. Chem.* **1992**, *35*, 641.

(27) Marsh, G. P.; Parsons, P. J.; McCarthy, C.; Corniquet, X. G. *Org. Lett.* **2007**, *9*, 2613.

(28) (a) Cho, S.-D.; Chung, J.-W.; Choi, W.-Y.; Kim, S.-K.; Yoon, Y.-J. *J. Heterocycl. Chem.* **1994**, *31*, 1199. (b) Ballini, R.; Barboni, L.; Giarlo, G. *J. Org. Chem.* **2004**, *69*, 6907.

(29) Bobál, P.; Lightner, D. A. *J. Heterocycl. Chem.* **2001**, *38*, 527.

(30) Wahlström, N.; Stensland, B.; Bergman, J. *Tetrahedron* **2004**, *60*, 2147.

(31) Motokura, K.; Fujita, N.; Mori, K.; Mizugaki, T.; Ebitani, K.; Kaneda, K. *J. Am. Chem. Soc.* **2005**, *127*, 9674.

(32) (a) Sinhababu, A. K.; Borchardt, R. T. *Tetrahedron Lett.* **1983**, *24*, 227. (b) Bhattacharjya, A.; Mukhopadhyay, R.; Pakrashi, S. C. *Synthesis* **1985**, *1985*, 886. (c) McNulty, J.; Steere, J. A.; Wolf, S. *Tetrahedron Lett.* **1998**, *39*, 8013.

(33) Ballini, R.; Bosica, G. *Eur. J. Org. Chem.* **1998**, *1998*, 355.

(34) Kraus, J. M.; Gits, H. C.; Silverman, R. B. *Tetrahedron Lett.* **2012**, *53*, 1319.

(35) Donohoe, T. J.; Fishlock, L. P.; Basutto, J. A.; Bower, J. F.; Procopiou, P. A.; Thompson, A. L. *Chem. Commun.* **2009**, 3008.

(36) Arjan, H.; Boyd, E.; Coumbarides, G. S.; Eames, J.; H. Jones, R. V.; Stenson, R. A.; Suggate, M. J. *Tetrahedron Lett.* **2005**, *46*, 1921.

(37) Patt, S. L.; Shoolery, J. N. *J. Magn. Reson.* **1982**, *46*, 535.

(38) Tye, H.; Eldred, C.; Wills, M. *Tetrahedron Lett.* **2002**, *43*, 155.

(39) Abdel-Magid, A. F.; Carson, K. G.; Harris, B. D.; Maryanoff, C. A.; Shah, R. D. *J. Org. Chem.* **1996**, *61*, 3849.

(40) Apex3 software suite; Bruker AXS, I., Madison, WI, 2015.

(41) Sheldrick, G. M. *Acta Crystallogr. Sect. C* **2015**, *71*, 3.

Appendix A

SPECTRAL DATA FOR CHAPTER 2

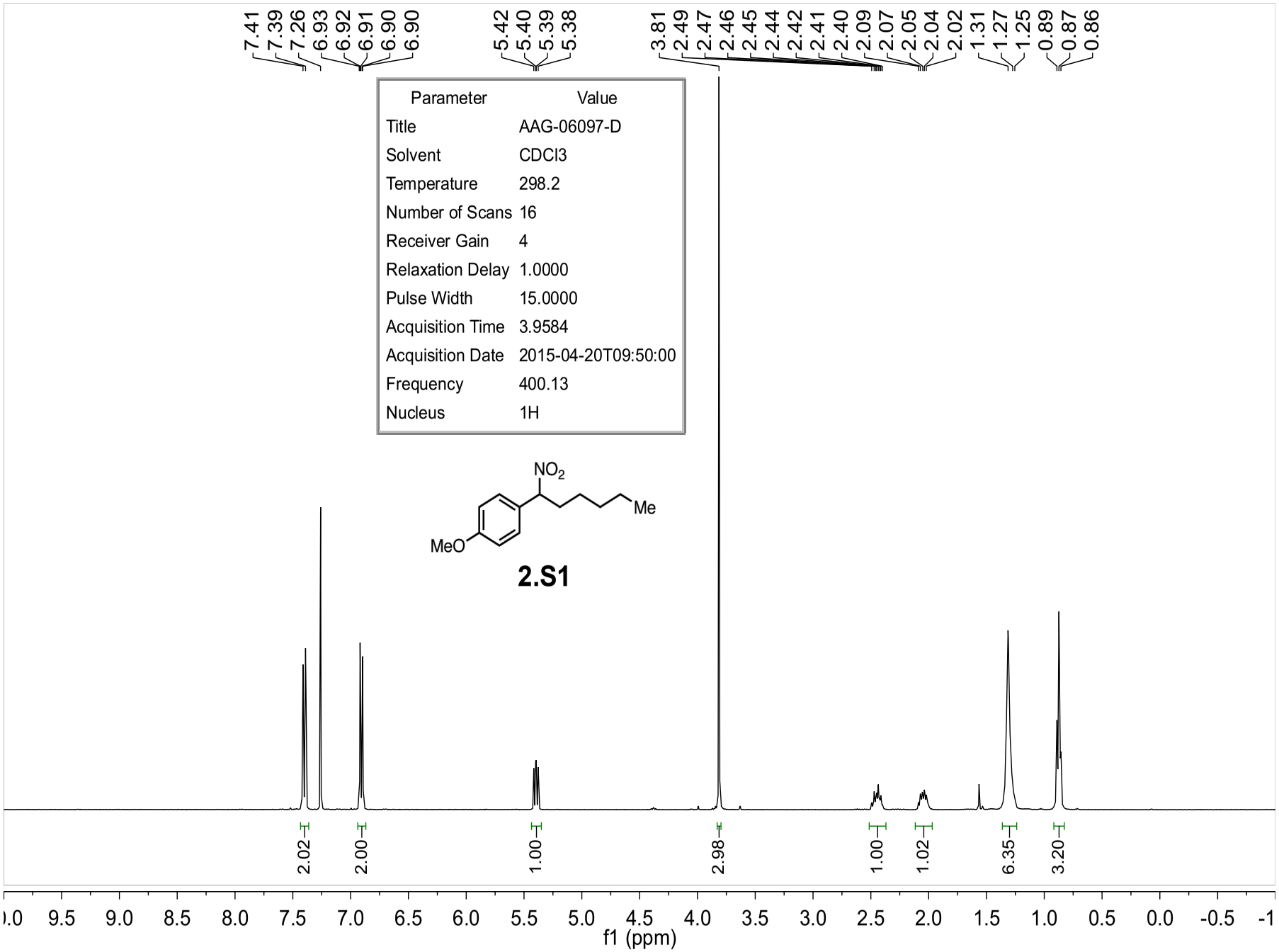
7.41
7.39
7.26
6.93
6.92
6.91
6.90
6.90
5.42
5.40
5.39
5.38
3.81
2.49
2.47
2.46
2.45
2.44
2.42
2.41
2.40
2.09
2.07
2.05
2.04
2.02
1.31
1.27
1.25
0.89
0.87
0.86
Parameter Value
Title AAG-06097-D
Solvent CDCl3
Temperature 298.2
Number of Scans 16
Receiver Gain 4
Relaxation Delay 1.0000
Pulse Width 15.0000
Acquisition Time 3.9584
Acquisition Date 2015-04-20T09:50:00
Frequency 400.13
Nucleus 1H
NO2
Me
MeO
2.S1
2.02
2.00
1.00
2.98
1.00
1.02
6.35
3.20
f1 (ppm)

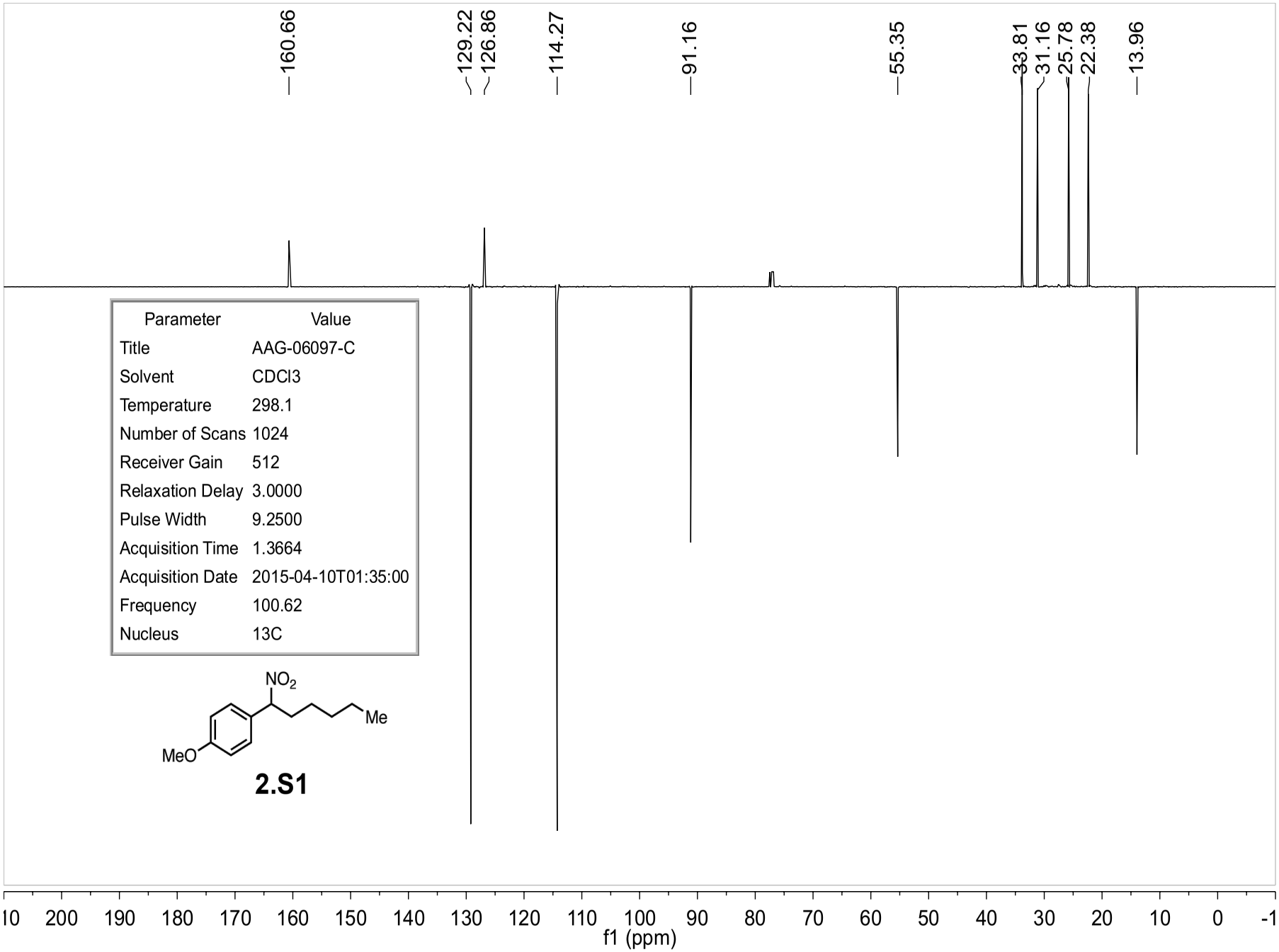
160.66
129.22
126.86
114.27
91.16
55.35
33.81
31.16
25.78
22.38
13.96
Parameter Value
Title AAG-06097-C
Solvent CDCl3
Temperature 298.1
Number of Scans 1024
Receiver Gain 512
Relaxation Delay 3.0000
Pulse Width 9.2500
Acquisition Time 1.3664
Acquisition Date 2015-04-10T01:35:00
Frequency 100.62
Nucleus 13C
NO2
Me
MeO
2.S1
f1 (ppm)

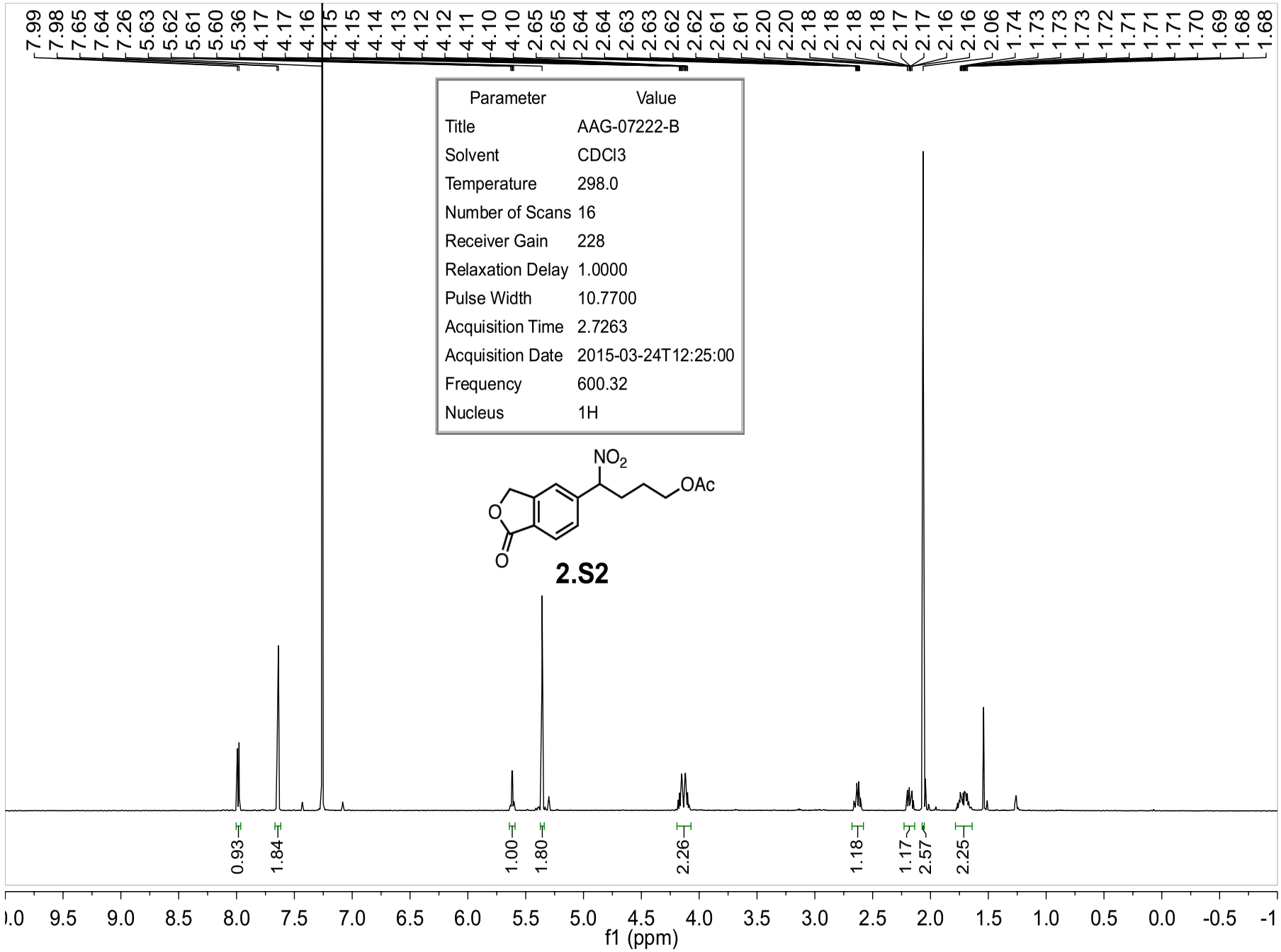
7.99 7.98 7.65 7.64 7.26 5.63 5.62 5.61 5.60 5.36 4.17 4.17 4.16 4.15 4.15 4.14 4.13 4.12 4.12 4.11 4.10 4.10 2.65 2.65 2.64 2.64 2.63 2.63 2.62 2.62 2.61 2.61 2.20 2.20 2.18 2.18 2.18 2.18 2.17 2.17 2.16 2.16 2.06 1.74 1.73 1.73 1.73 1.72 1.71 1.71 1.71 1.70 1.69 1.68 1.68
Parameter Value
Title AAG-07222-B
Solvent CDCl3
Temperature 298.0
Number of Scans 16
Receiver Gain 228
Relaxation Delay 1.0000
Pulse Width 10.7700
Acquisition Time 2.7263
Acquisition Date 2015-03-24T12:25:00
Frequency 600.32
Nucleus 1H
NO2
OAc
O
O
2.S2
0.93 1.84 1.00 1.80 2.26 1.18 1.17 2.57 2.25
f1 (ppm)

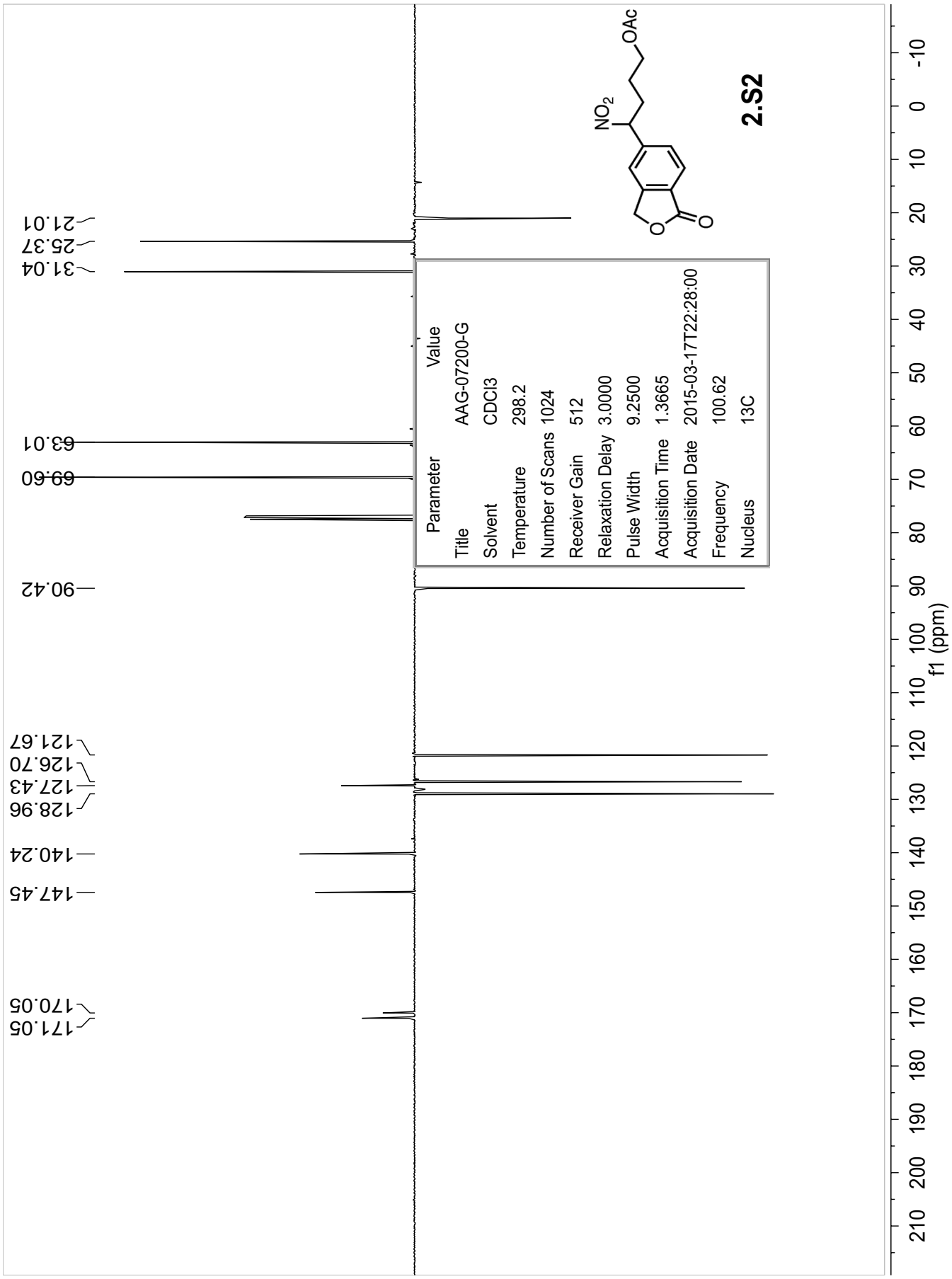
2.S2
NO2
OAc
O
O
Parameter Value
Title AAG-07200-G
Solvent CDCl3
Temperature 298.2
Number of Scans 1024
Receiver Gain 512
Relaxation Delay 3.0000
Pulse Width 9.2500
Acquisition Time 1.3665
Acquisition Date 2015-03-17T22:28:00
Frequency 100.62
Nucleus 13C
21.01
25.37
31.04
63.01
69.60
90.42
121.67
126.70
127.43
128.96
140.24
147.45
170.05
171.05
f1 (ppm)

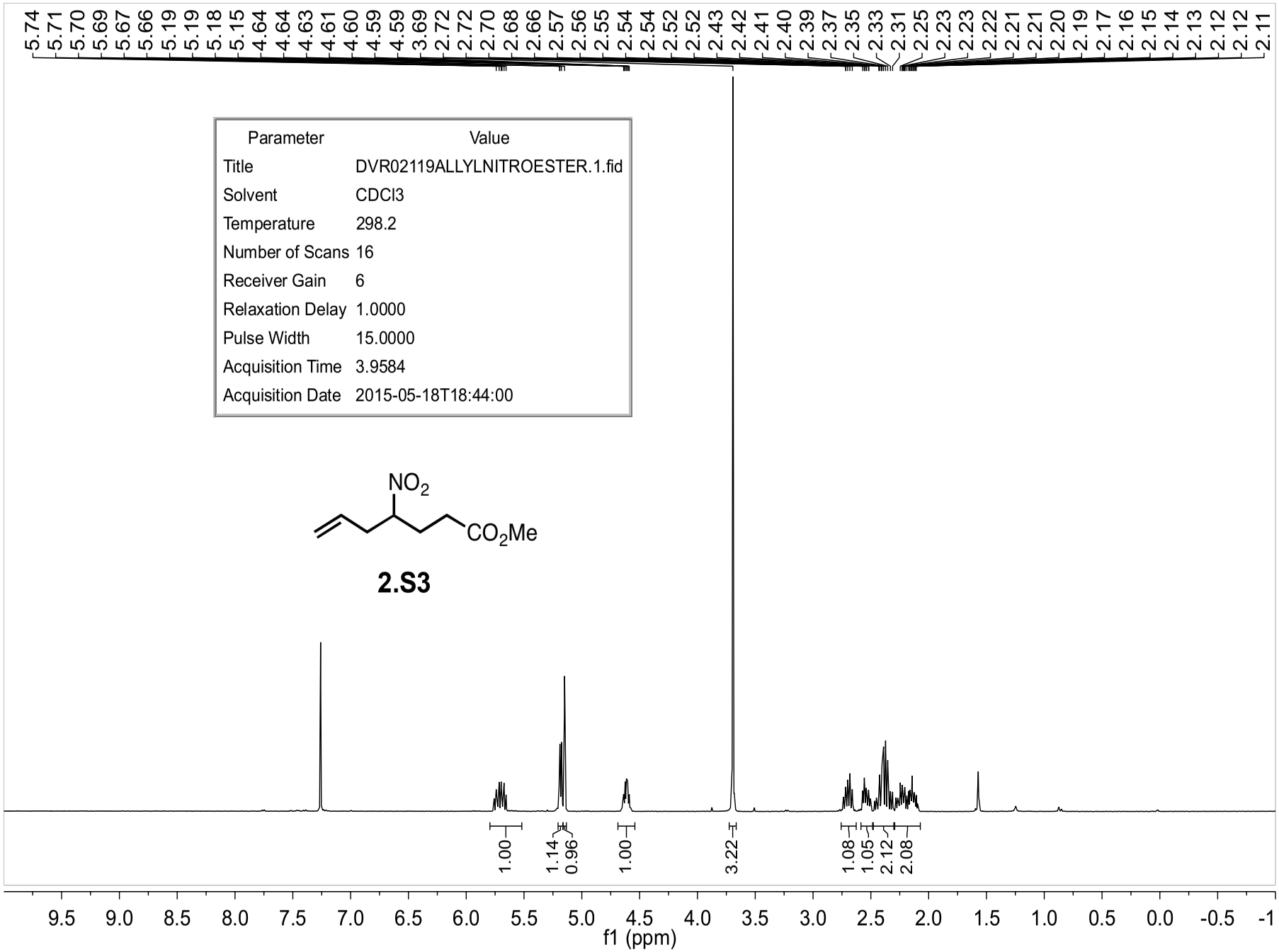
5.74 5.71 5.70 5.69 5.67 5.66 5.19 5.19 5.18 5.15 4.64 4.64 4.63 4.61 4.60 4.59 4.59 3.69 2.72 2.72 2.70 2.68 2.66 2.57 2.56 2.55 2.54 2.54 2.52 2.52 2.43 2.42 2.41 2.40 2.39 2.37 2.35 2.33 2.31 2.25 2.23 2.23 2.22 2.21 2.21 2.20 2.19 2.17 2.16 2.15 2.14 2.13 2.12 2.12 2.11
Parameter Value
Title DVR02119ALLYLNITROESTER.1.fid
Solvent CDCl3
Temperature 298.2
Number of Scans 16
Receiver Gain 6
Relaxation Delay 1.0000
Pulse Width 15.0000
Acquisition Time 3.9584
Acquisition Date 2015-05-18T18:44:00
NO2
CO2Me
2.S3
1.00 1.14 0.96 1.00 3.22 1.08 1.05 2.12 2.08
9.5 9.0 8.5 8.0 7.5 7.0 6.5 6.0 5.5 5.0 4.5 4.0 3.5 3.0 2.5 2.0 1.5 1.0 0.5 0.0 -0.5 -1
f1 (ppm)

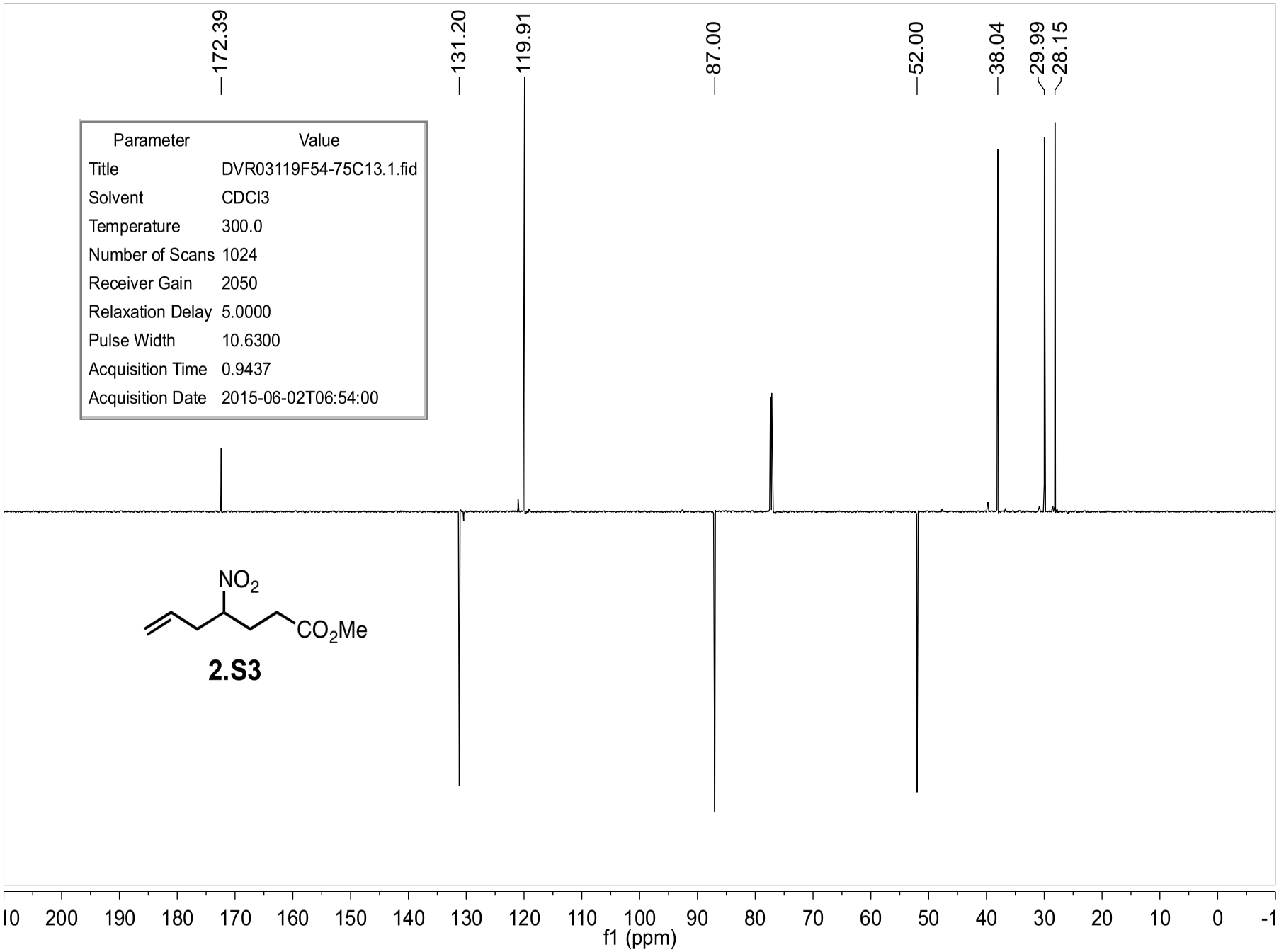
172.39
131.20
119.91
87.00
52.00
38.04
29.99
28.15
Parameter Value
Title DVR03119F54-75C13.1.fid
Solvent CDCl3
Temperature 300.0
Number of Scans 1024
Receiver Gain 2050
Relaxation Delay 5.0000
Pulse Width 10.6300
Acquisition Time 0.9437
Acquisition Date 2015-06-02T06:54:00
NO2
CO2Me
2.S3
f1 (ppm)

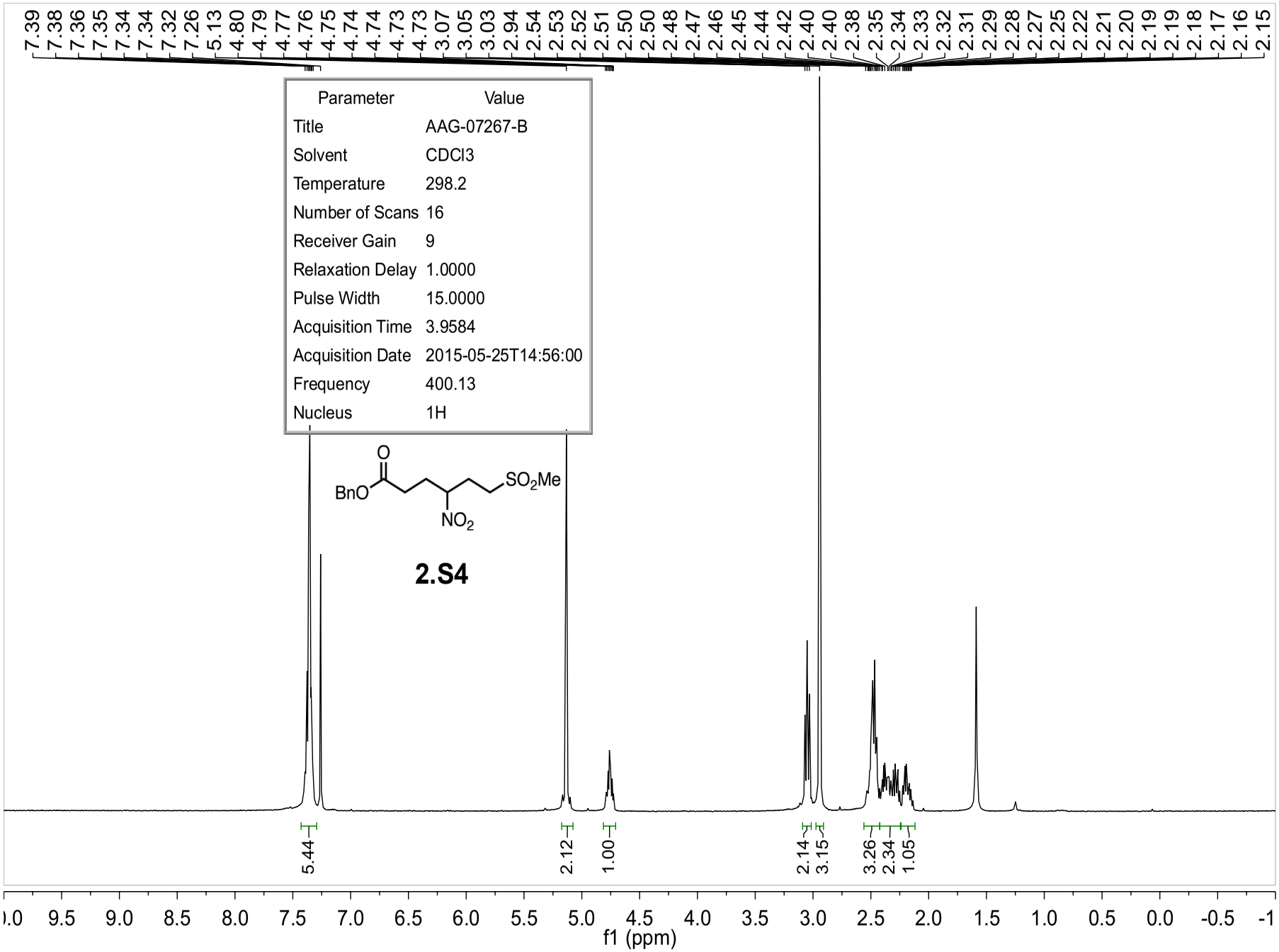
7.39 7.38 7.36 7.35 7.34 7.34 7.32 7.26 5.13 4.80 4.79 4.77 4.76 4.75 4.74 4.74 4.73 4.73 3.07 3.05 3.03 2.94 2.54 2.53 2.52 2.51 2.50 2.50 2.48 2.47 2.46 2.45 2.44 2.42 2.40 2.40 2.38 2.35 2.34 2.33 2.32 2.31 2.29 2.28 2.27 2.25 2.22 2.21 2.20 2.19 2.19 2.18 2.17 2.16 2.15
Parameter Value
Title AAG-07267-B
Solvent CDCl3
Temperature 298.2
Number of Scans 16
Receiver Gain 9
Relaxation Delay 1.0000
Pulse Width 15.0000
Acquisition Time 3.9584
Acquisition Date 2015-05-25T14:56:00
Frequency 400.13
Nucleus 1H
BnO
O
SO2Me
NO2
2.S4
5.44
2.12
1.00
2.14
3.15
3.26
2.34
1.05
f1 (ppm)

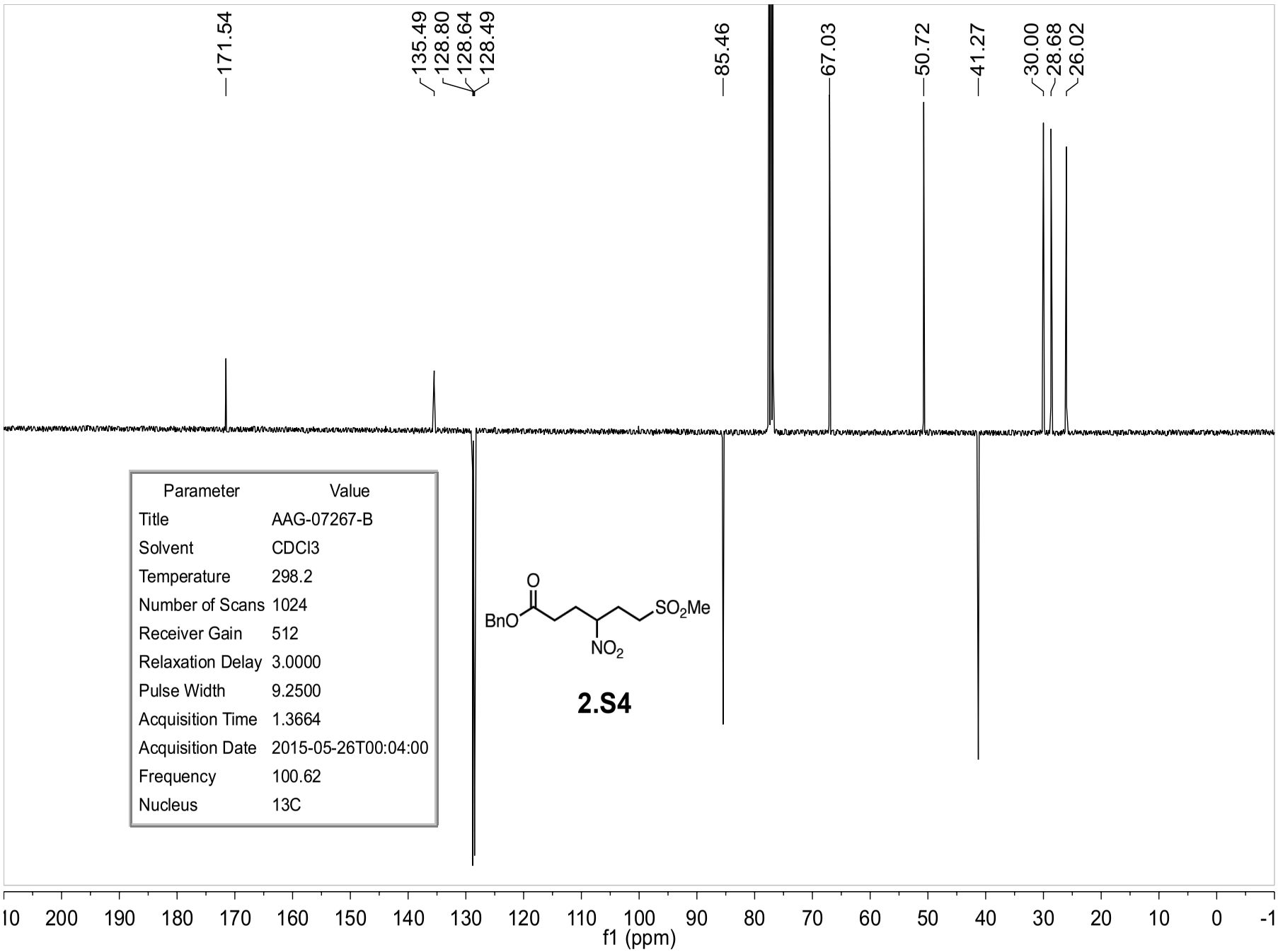
171.54
135.49
128.80
128.64
128.49
85.46
67.03
50.72
41.27
30.00
28.68
26.02
Parameter Value
Title AAG-07267-B
Solvent CDCl3
Temperature 298.2
Number of Scans 1024
Receiver Gain 512
Relaxation Delay 3.0000
Pulse Width 9.2500
Acquisition Time 1.3664
Acquisition Date 2015-05-26T00:04:00
Frequency 100.62
Nucleus 13C
BnO
O
SO2Me
NO2
2.S4
f1 (ppm)

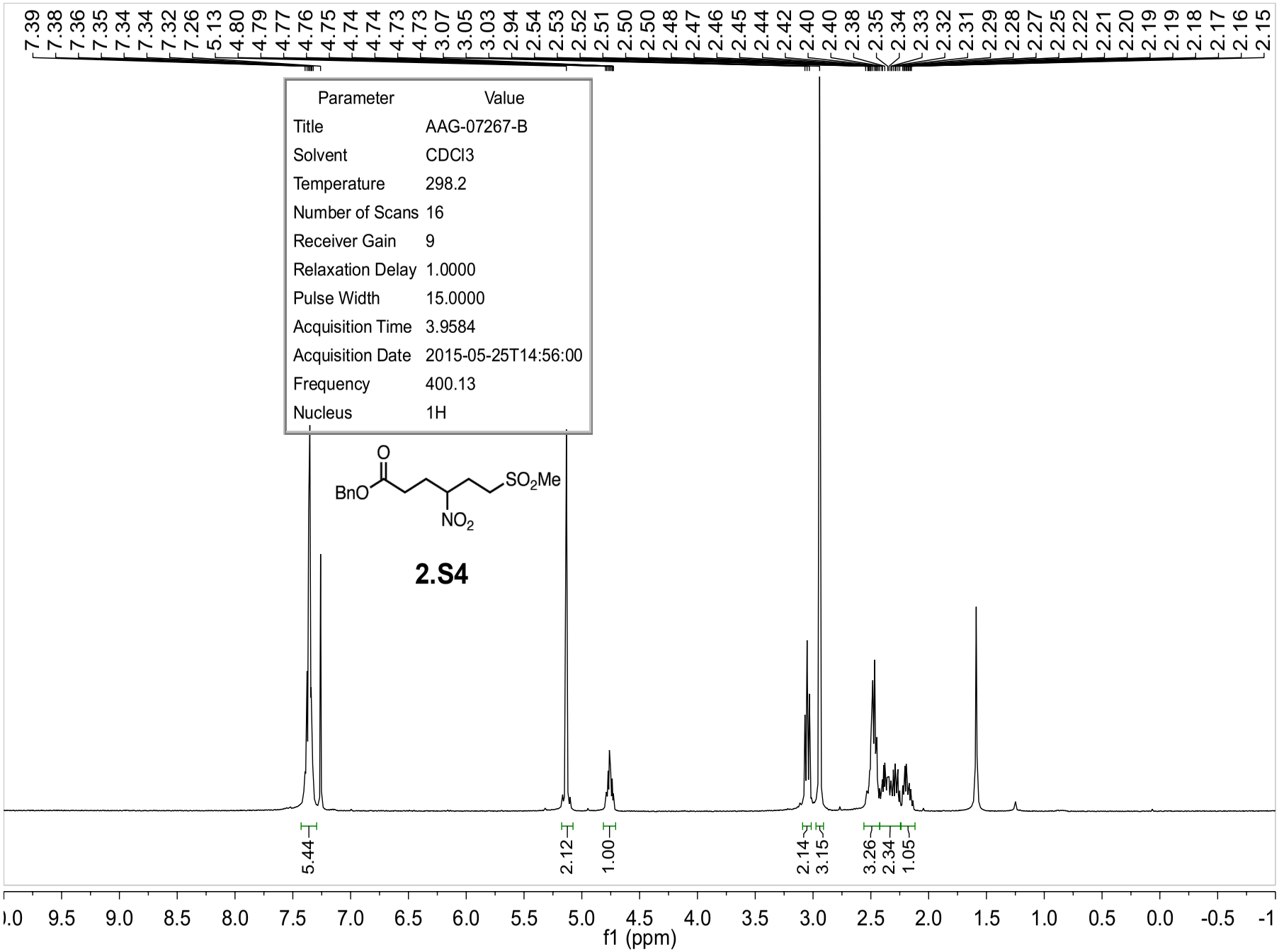
7.39 7.38 7.36 7.35 7.34 7.34 7.32 7.26 5.13 4.80 4.79 4.77 4.76 4.75 4.74 4.74 4.73 4.73 3.07 3.05 3.03 2.94 2.54 2.53 2.52 2.51 2.50 2.50 2.48 2.47 2.46 2.45 2.44 2.42 2.40 2.40 2.38 2.35 2.34 2.33 2.32 2.31 2.29 2.28 2.27 2.25 2.22 2.21 2.20 2.19 2.19 2.18 2.17 2.16 2.15
Parameter Value
Title AAG-07267-B
Solvent CDCl3
Temperature 298.2
Number of Scans 16
Receiver Gain 9
Relaxation Delay 1.0000
Pulse Width 15.0000
Acquisition Time 3.9584
Acquisition Date 2015-05-25T14:56:00
Frequency 400.13
Nucleus 1H
BnO
O
SO2Me
NO2
2.S4
5.44
2.12
1.00
2.14
3.15
3.26
2.34
1.05
f1 (ppm)

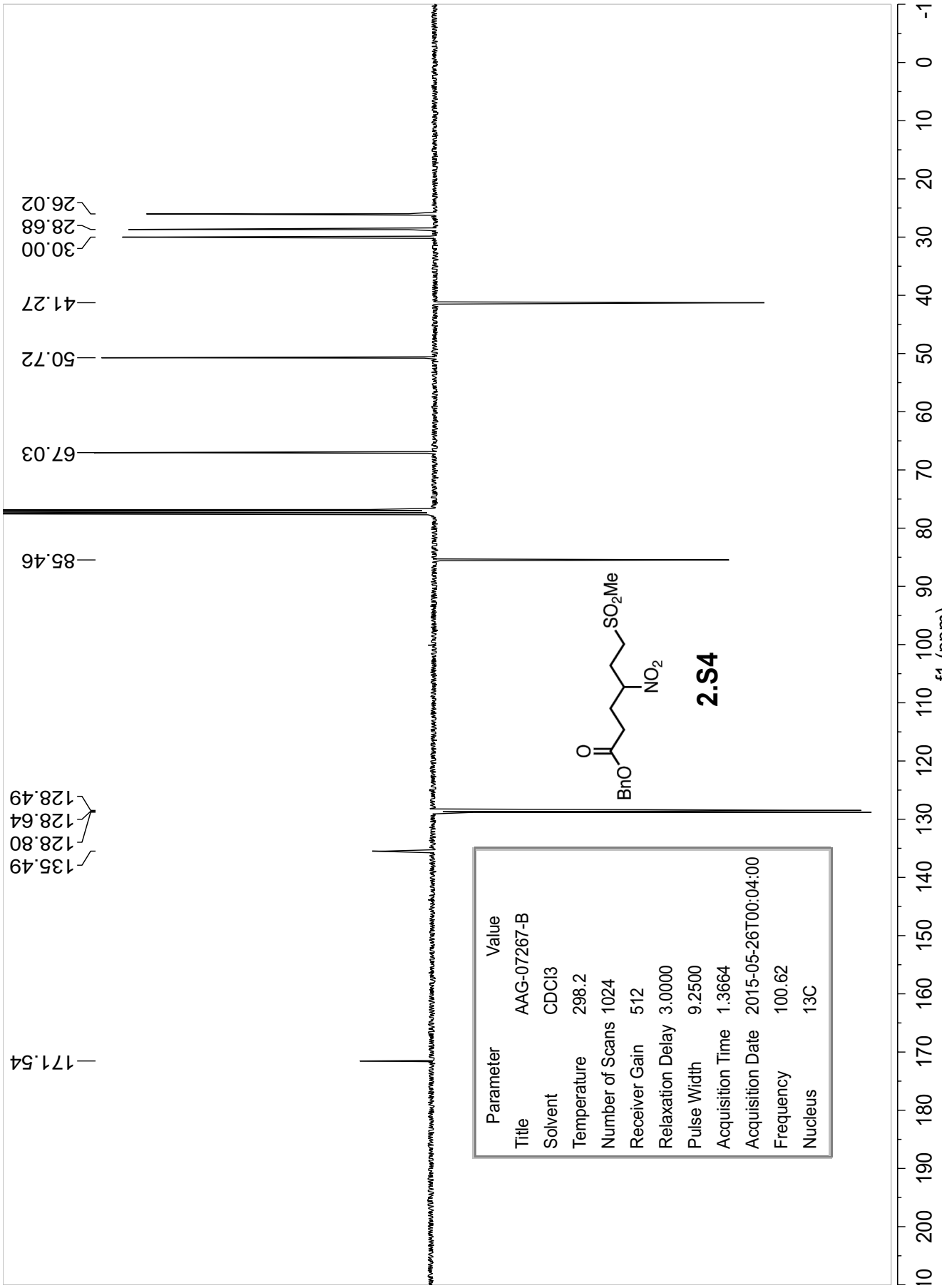
171.54
135.49
128.80
128.64
128.49
85.46
67.03
50.72
41.27
30.00
28.68
26.02
BnO
O
NO2
SO2Me
2.S4
Parameter Value
Title AAG-07267-B
Solvent CDCl3
Temperature 298.2
Number of Scans 1024
Receiver Gain 512
Relaxation Delay 3.0000
Pulse Width 9.2500
Acquisition Time 1.3664
Acquisition Date 2015-05-26T00:04:00
Frequency 100.62
Nucleus 13C
f1 (ppm)

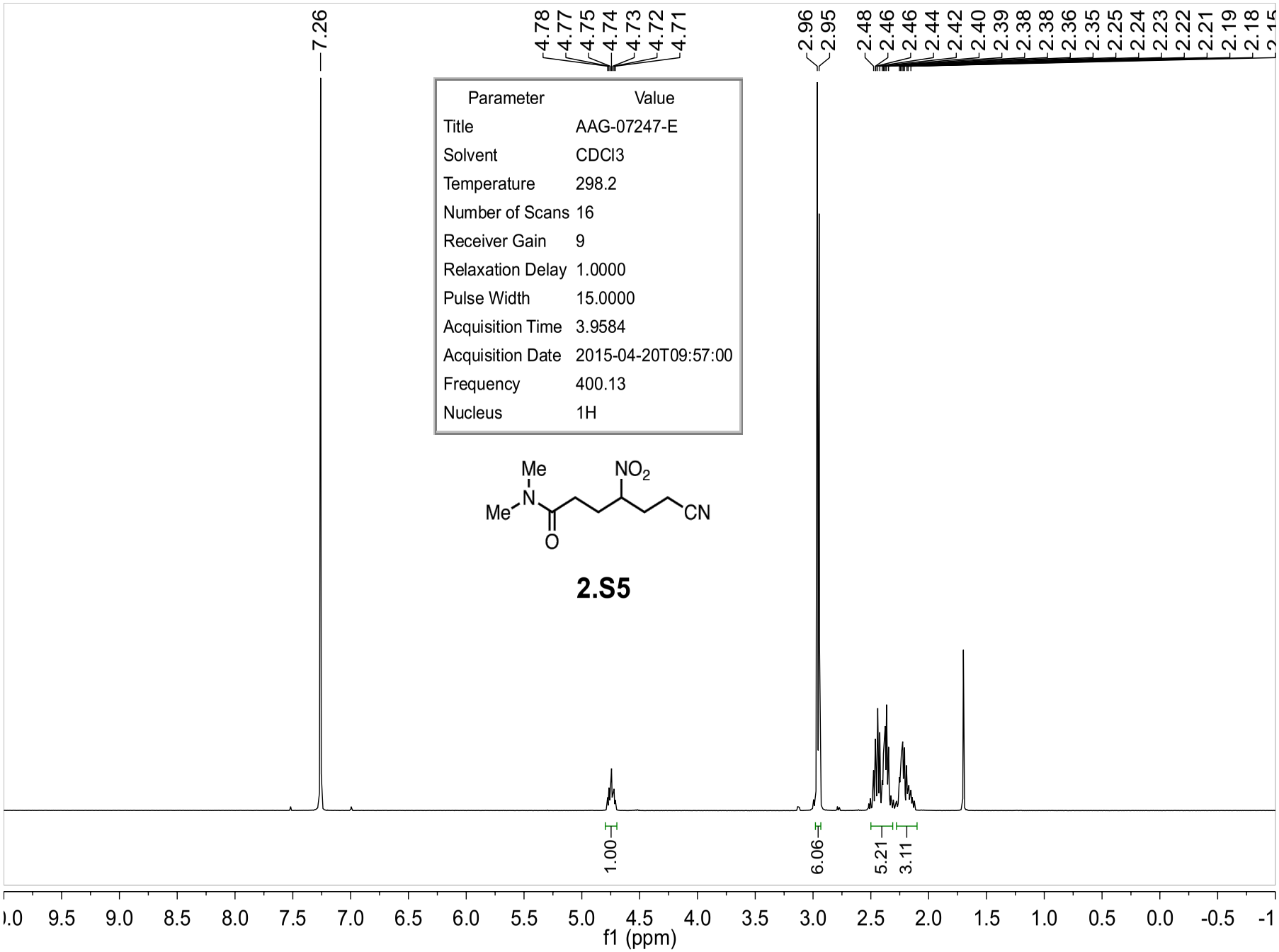
7.26
4.78
4.77
4.75
4.74
4.73
4.72
4.71
2.96
2.95
2.48
2.46
2.46
2.44
2.42
2.40
2.39
2.38
2.38
2.36
2.35
2.25
2.24
2.23
2.22
2.21
2.19
2.18
Parameter Value
Title AAG-07247-E
Solvent CDCl3
Temperature 298.2
Number of Scans 16
Receiver Gain 9
Relaxation Delay 1.0000
Pulse Width 15.0000
Acquisition Time 3.9584
Acquisition Date 2015-04-20T09:57:00
Frequency 400.13
Nucleus 1H
Me
N
Me
NO2
CN
O
2.S5
1.00
6.06
5.21
3.11
f1 (ppm)

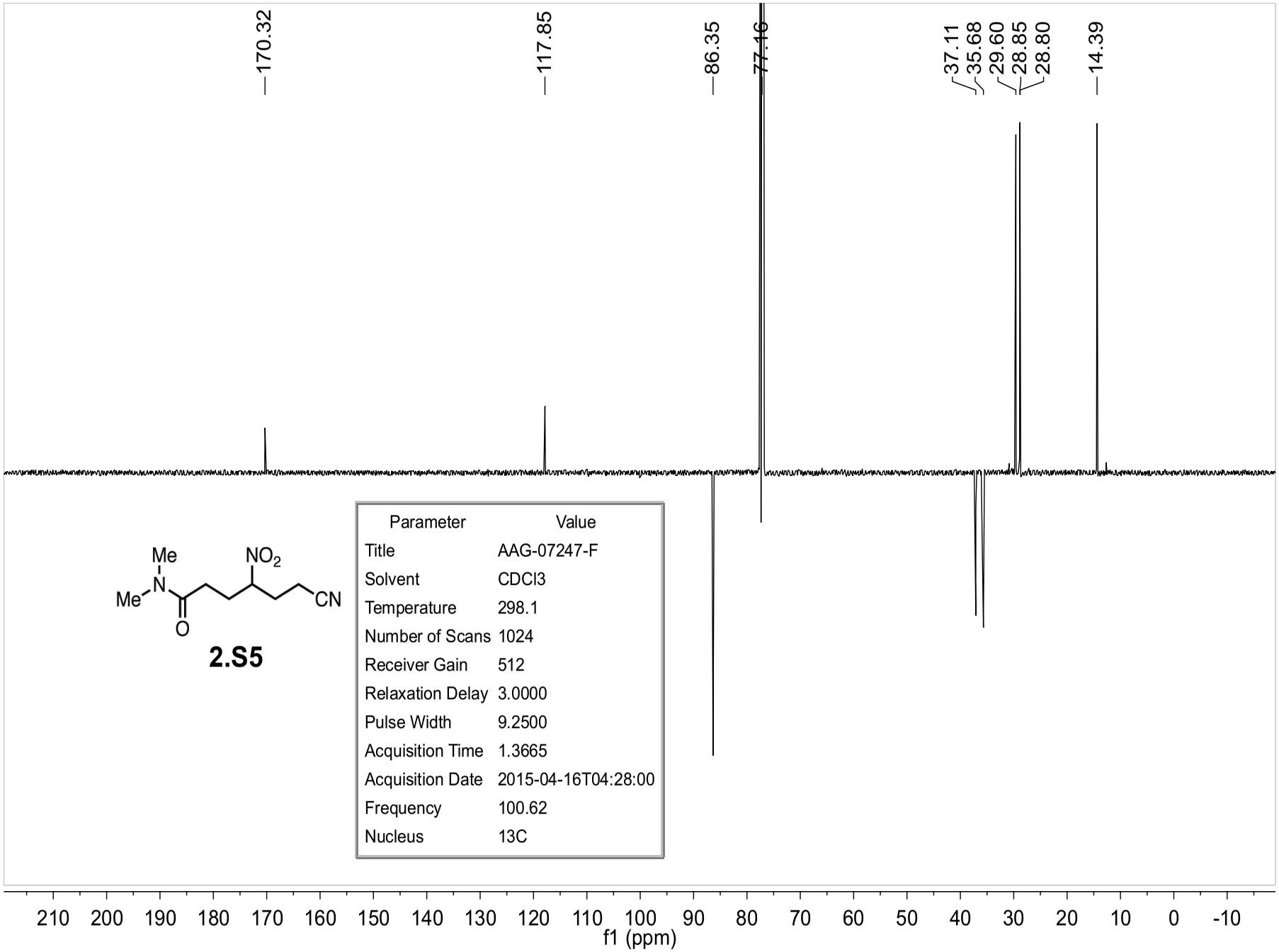
170.32
117.85
86.35
77.16
37.11
35.68
29.60
28.85
28.80
14.39
Me
N
Me
O
NO2
CN
2.S5
Parameter Value
Title AAG-07247-F
Solvent CDCl3
Temperature 298.1
Number of Scans 1024
Receiver Gain 512
Relaxation Delay 3.0000
Pulse Width 9.2500
Acquisition Time 1.3665
Acquisition Date 2015-04-16T04:28:00
Frequency 100.62
Nucleus 13C
210 200 190 180 170 160 150 140 130 120 110 100 90 80 70 60 50 40 30 20 10 0 -10
f1 (ppm)

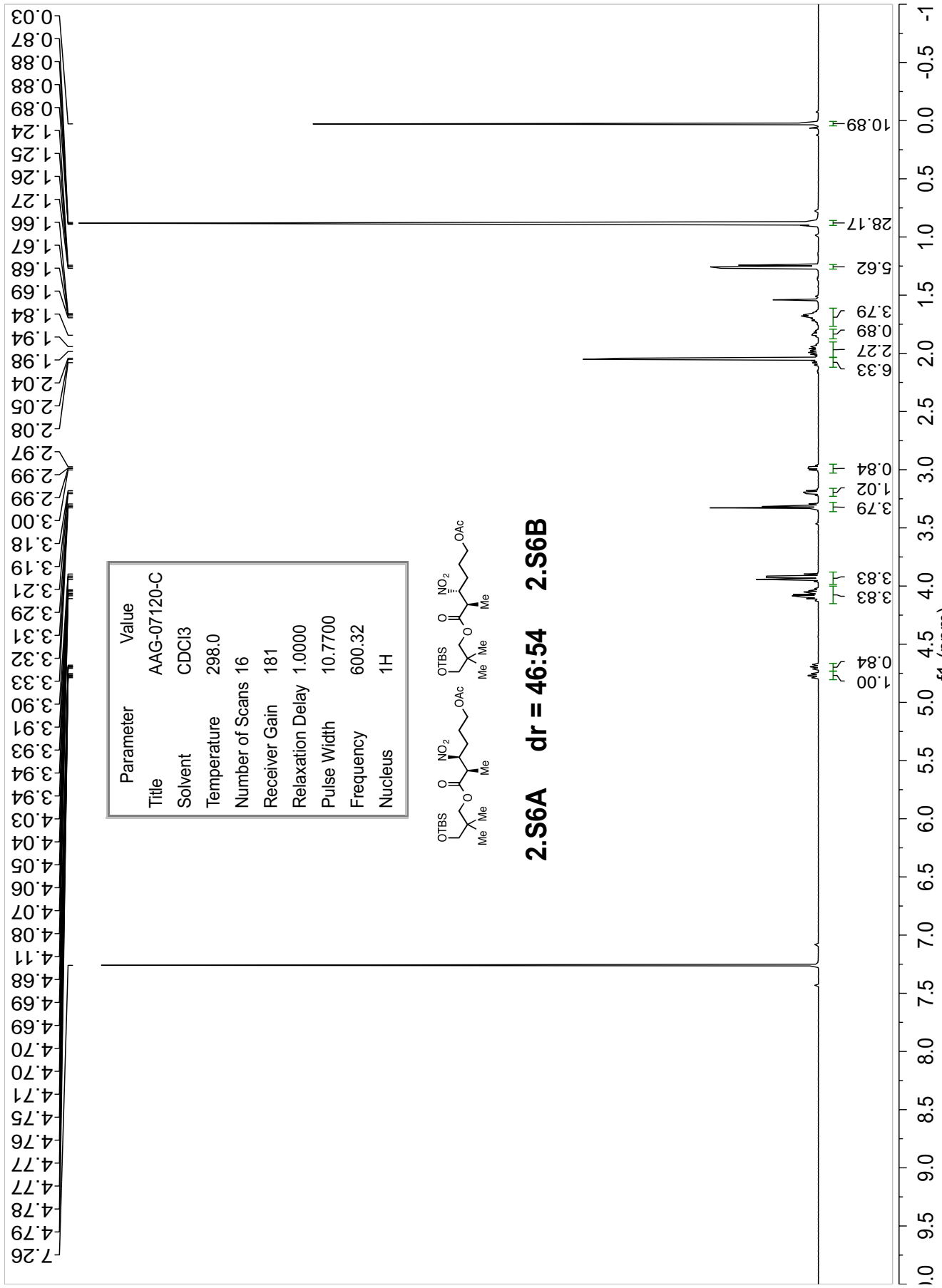
Parameter Value
Title AAG-07120-C
Solvent CDCl3
Temperature 298.0
Number of Scans 16
Receiver Gain 181
Relaxation Delay 1.0000
Pulse Width 10.7700
Frequency 600.32
Nucleus 1H
2.S6A dr = 46:54 2.S6B
f1 (ppm)

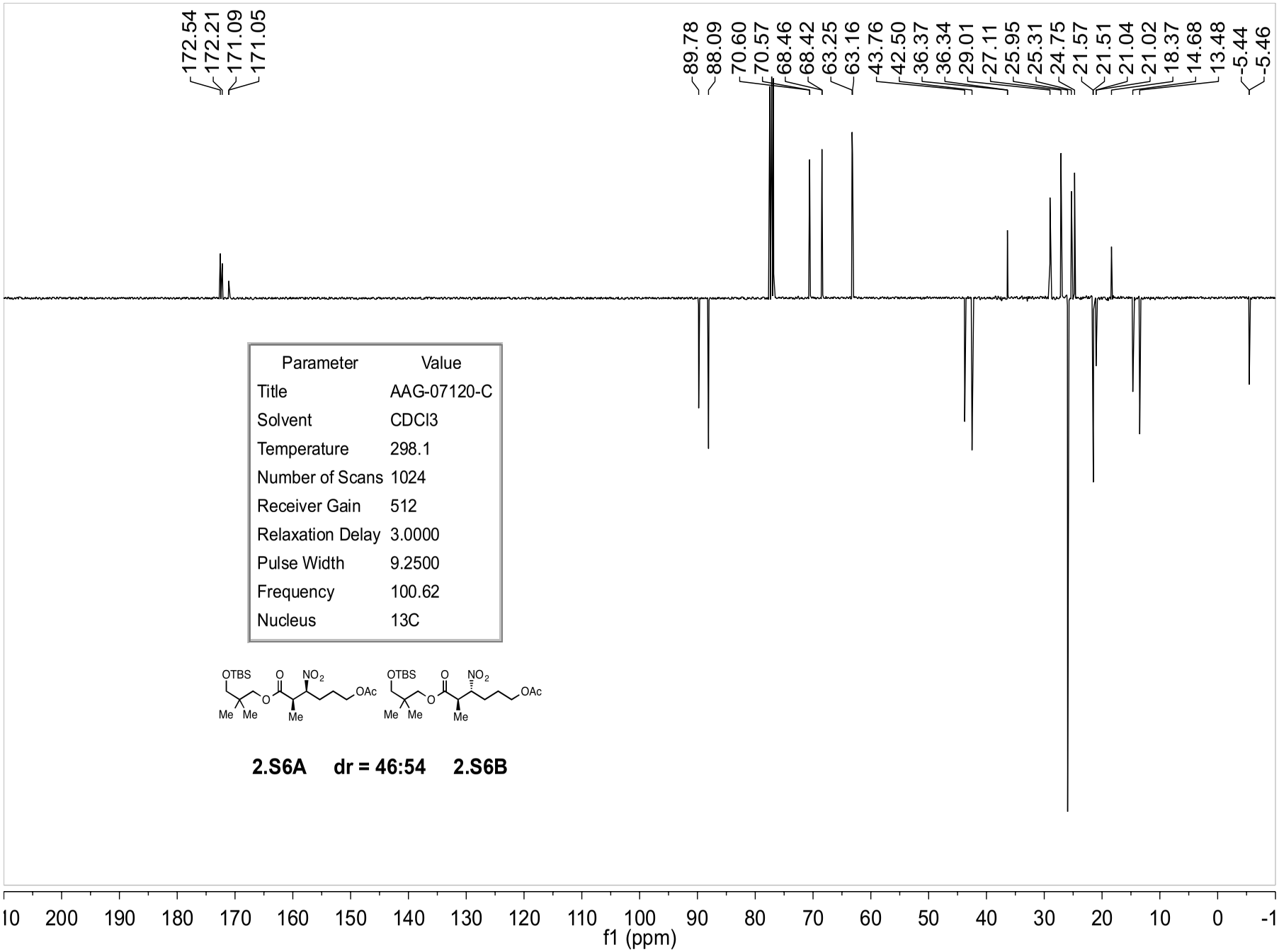
172.54
172.21
171.09
171.05
89.78
88.09
70.60
70.57
68.46
68.42
63.25
63.16
43.76
42.50
36.37
36.34
29.01
27.11
25.95
25.31
24.75
21.57
21.51
21.04
21.02
18.37
14.68
13.48
-5.44
-5.46
Parameter Value
Title AAG-07120-C
Solvent CDCl3
Temperature 298.1
Number of Scans 1024
Receiver Gain 512
Relaxation Delay 3.0000
Pulse Width 9.2500
Frequency 100.62
Nucleus 13C
OTBS
O
NO2
OAc
Me
Me
Me
OTBS
O
NO2
OAc
Me
Me
Me
2.S6A dr = 46:54 2.S6B
f1 (ppm)

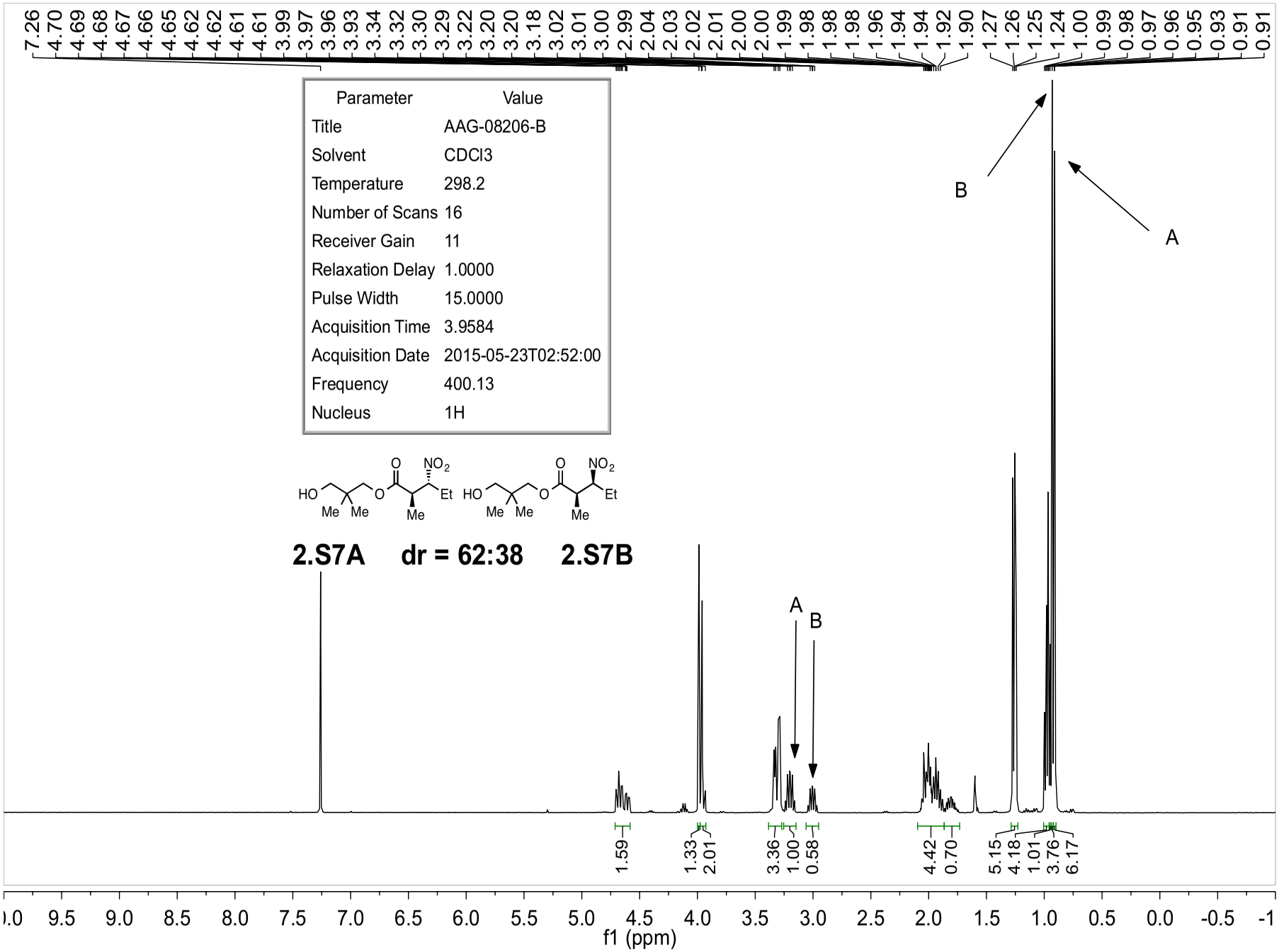
7.26 4.70 4.69 4.68 4.67 4.66 4.65 4.62 4.62 4.61 4.61 3.99 3.97 3.96 3.93 3.34 3.32 3.30 3.29 3.22 3.20 3.20 3.18 3.02 3.01 3.00 2.99 2.04 2.03 2.02 2.01 2.00 2.00 1.99 1.98 1.98 1.98 1.96 1.94 1.94 1.92 1.90 1.27 1.26 1.25 1.24 1.00 0.99 0.98 0.97 0.96 0.95 0.93 0.91 0.91
Parameter Value
Title AAG-08206-B
Solvent CDCl3
Temperature 298.2
Number of Scans 16
Receiver Gain 11
Relaxation Delay 1.0000
Pulse Width 15.0000
Acquisition Time 3.9584
Acquisition Date 2015-05-23T02:52:00
Frequency 400.13
Nucleus 1H
B
A
HO Me Me O O NO2 Et Me
HO Me Me O O NO2 Et Me
2.S7A dr = 62:38 2.S7B
A
B
1.59 1.33 2.01 3.36 1.00 0.58 4.42 0.70 5.15 4.18 1.01 3.76 6.17
f1 (ppm)

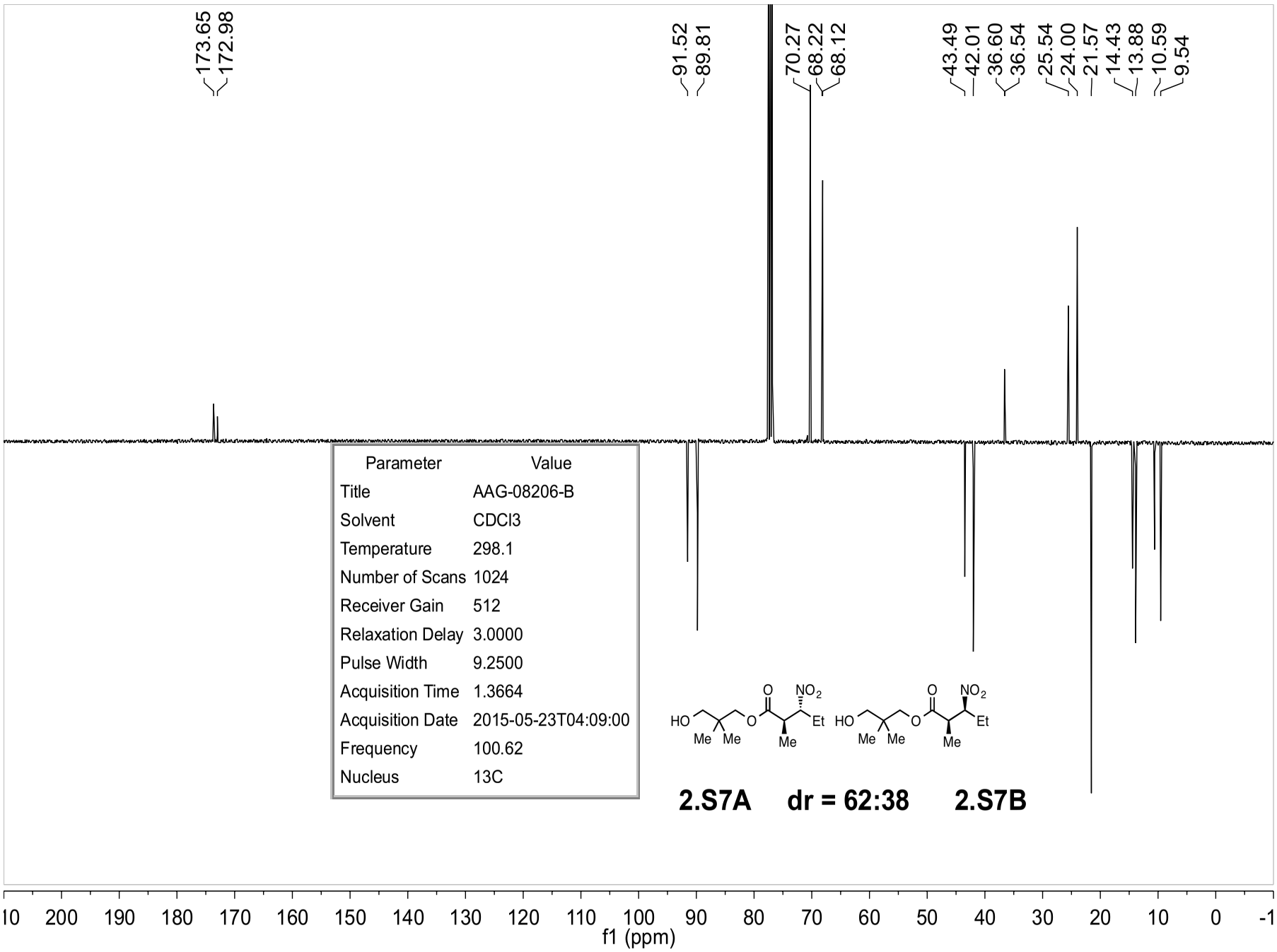
173.65
172.98
91.52
89.81
70.27
68.22
68.12
43.49
42.01
36.60
36.54
25.54
24.00
21.57
14.43
13.88
10.59
9.54
Parameter Value
Title AAG-08206-B
Solvent CDCl3
Temperature 298.1
Number of Scans 1024
Receiver Gain 512
Relaxation Delay 3.0000
Pulse Width 9.2500
Acquisition Time 1.3664
Acquisition Date 2015-05-23T04:09:00
Frequency 100.62
Nucleus 13C
HO
Me Me
O
O
NO2
Et
Me
2.S7A dr = 62:38 2.S7B
f1 (ppm)

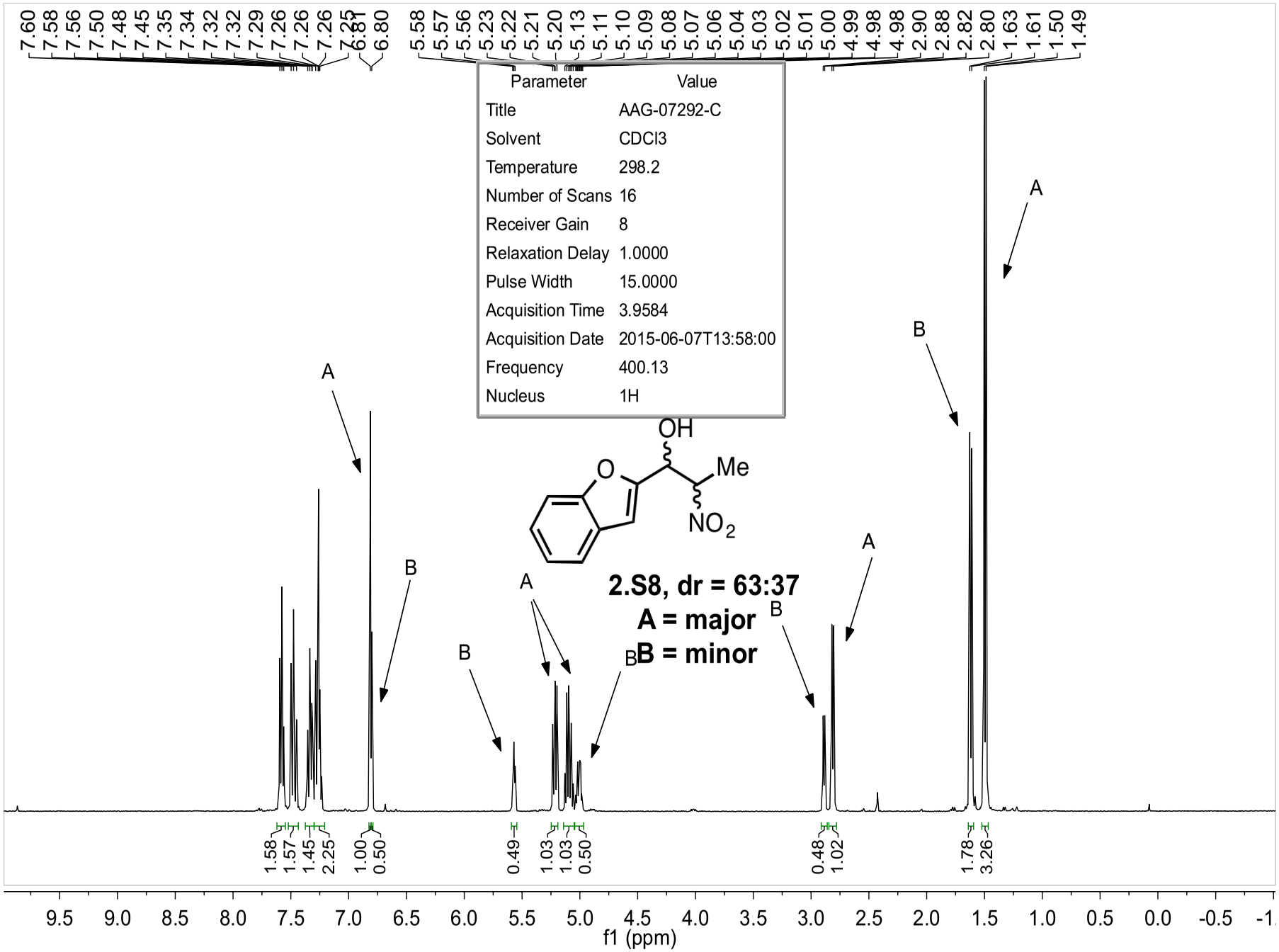
7.60 7.58 7.56 7.50 7.48 7.45 7.35 7.34 7.32 7.32 7.29 7.26 7.26 7.26 7.25 6.81 6.80
5.58 5.57 5.56 5.23 5.22 5.21 5.20 5.13 5.11 5.10 5.09 5.08 5.07 5.06 5.04 5.03 5.02 5.01 5.00 4.99 4.98 4.98 2.90 2.88 2.82 2.80 1.63 1.61 1.50 1.49
Parameter Value
Title AAG-07292-C
Solvent CDCl3
Temperature 298.2
Number of Scans 16
Receiver Gain 8
Relaxation Delay 1.0000
Pulse Width 15.0000
Acquisition Time 3.9584
Acquisition Date 2015-06-07T13:58:00
Frequency 400.13
Nucleus 1H
OH
O
Me
NO2
2.S8, dr = 63:37
A = major
B = minor
A
B
1.58 1.57 1.45 2.25 1.00 0.50 0.49 1.03 1.03 0.50 0.48 1.02 1.78 3.26
9.5 9.0 8.5 8.0 7.5 7.0 6.5 6.0 5.5 5.0 4.5 4.0 3.5 3.0 2.5 2.0 1.5 1.0 0.5 0.0 -0.5
f1 (ppm)

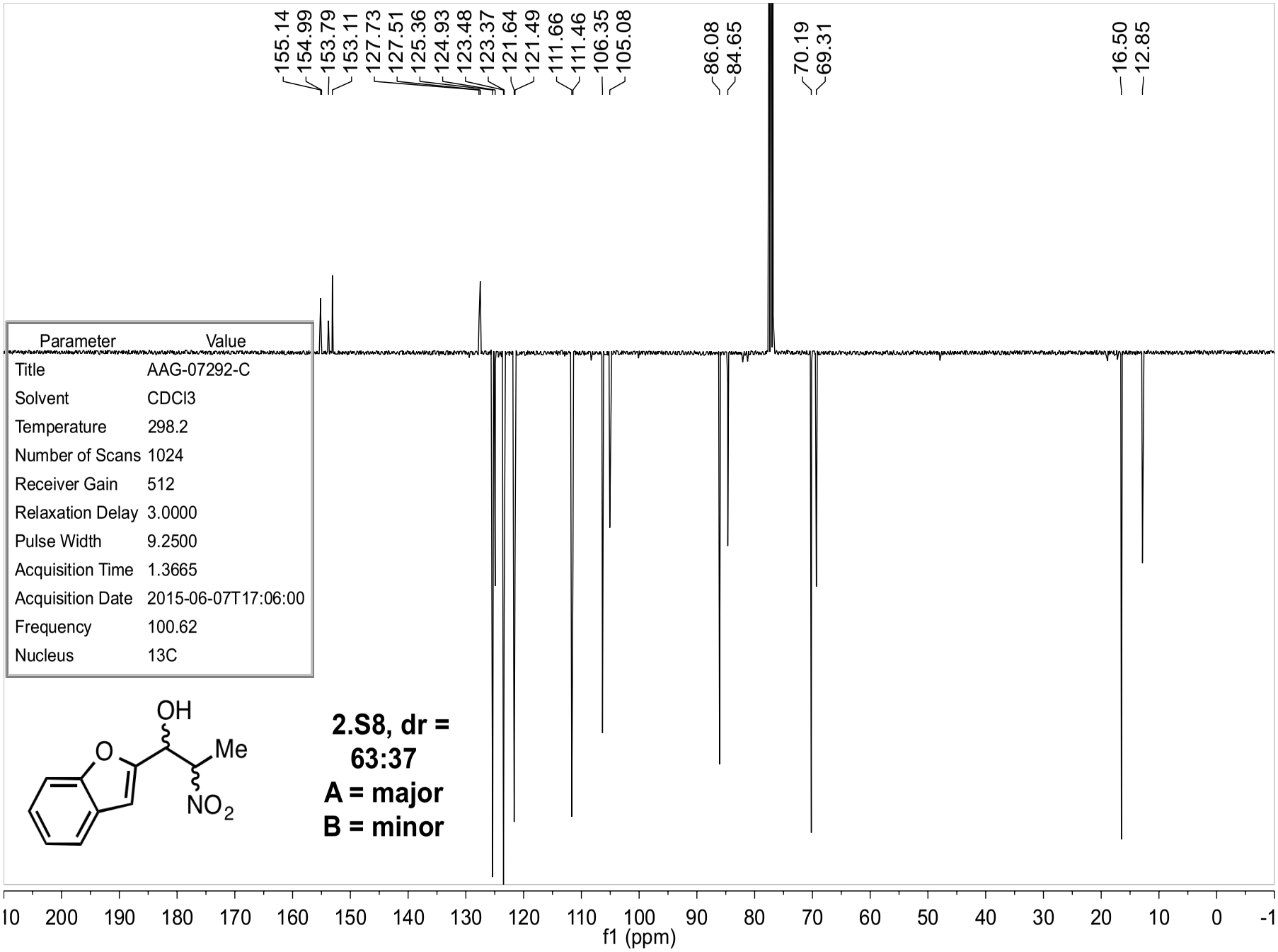
155.14
154.99
153.79
153.11
127.73
127.51
125.36
124.93
123.48
123.37
121.64
121.49
111.66
111.46
106.35
105.08
86.08
84.65
70.19
69.31
16.50
12.85
Parameter Value
Title AAG-07292-C
Solvent CDCl3
Temperature 298.2
Number of Scans 1024
Receiver Gain 512
Relaxation Delay 3.0000
Pulse Width 9.2500
Acquisition Time 1.3665
Acquisition Date 2015-06-07T17:06:00
Frequency 100.62
Nucleus 13C
OH
O
Me
NO2
2.S8, dr = 63:37
A = major
B = minor
f1 (ppm)

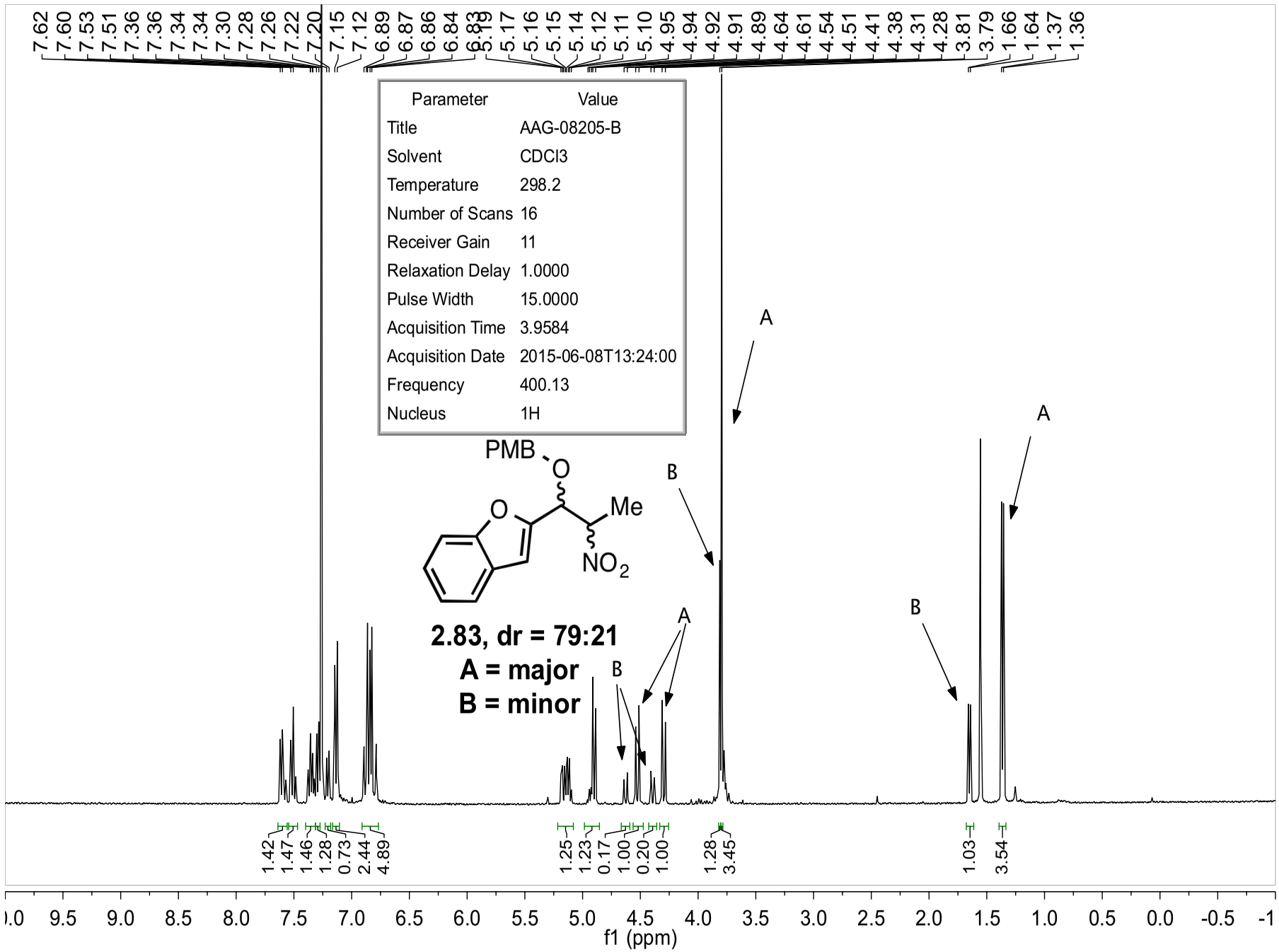
7.62 7.60 7.53 7.51 7.36 7.36 7.34 7.34 7.30 7.28 7.26 7.22 7.20 7.15 7.12 6.89 6.87 6.86 6.84 6.83 5.19 5.17 5.16 5.15 5.14 5.12 5.11 5.10 4.95 4.94 4.92 4.91 4.89 4.64 4.61 4.54 4.51 4.41 4.38 4.31 4.28 3.81 3.79 1.66 1.64 1.37 1.36
Parameter Value
Title AAG-08205-B
Solvent CDCl3
Temperature 298.2
Number of Scans 16
Receiver Gain 11
Relaxation Delay 1.0000
Pulse Width 15.0000
Acquisition Time 3.9584
Acquisition Date 2015-06-08T13:24:00
Frequency 400.13
Nucleus 1H
PMB
O
O
Me
NO2
A
B
2.83, dr = 79:21
A = major
B = minor
1.42 1.47 1.46 1.28 0.73 2.44 4.89 1.25 1.23 0.17 1.00 0.20 1.00 1.28 3.45 1.03 3.54
f1 (ppm)

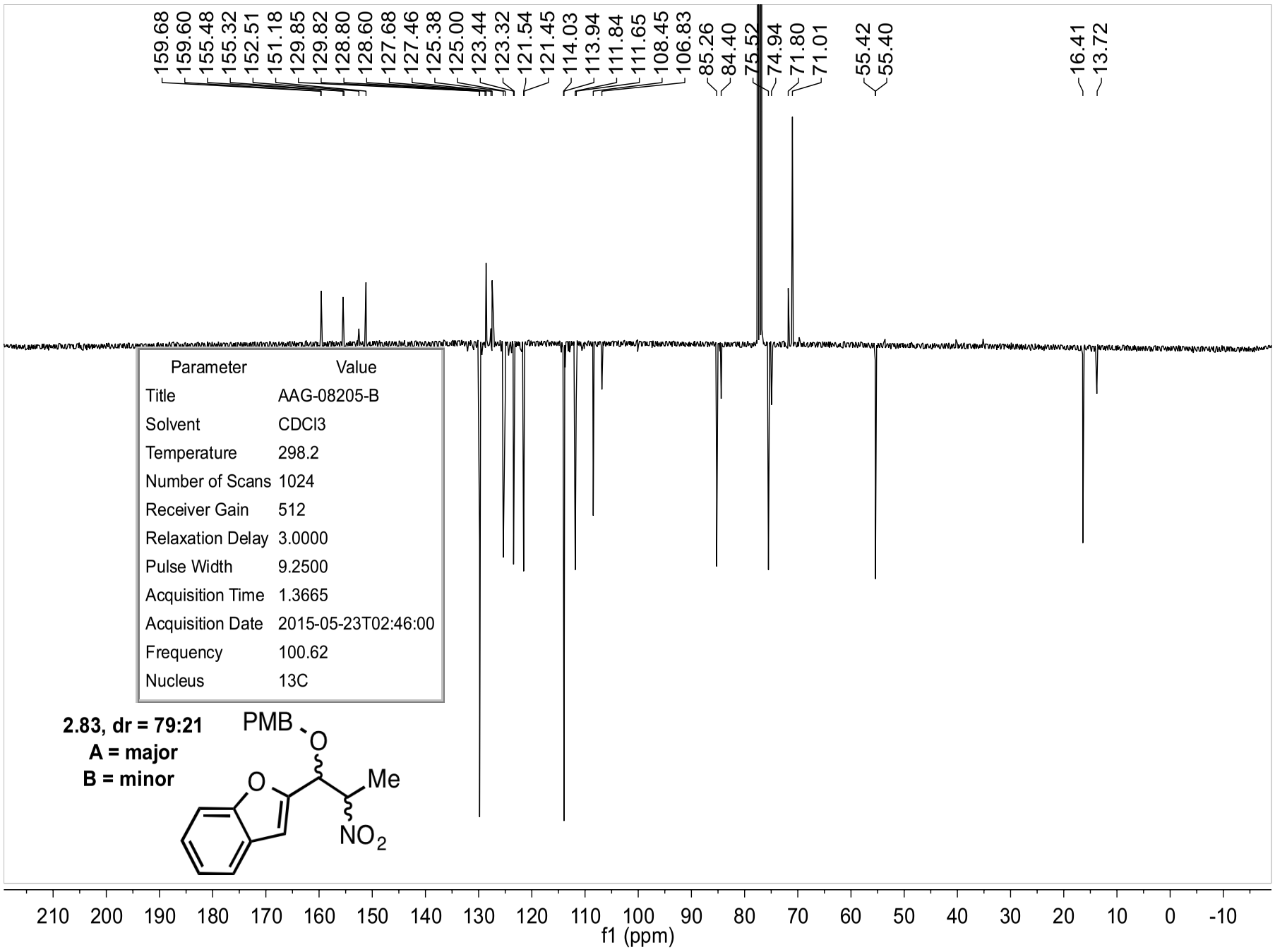
159.68
159.60
155.48
155.32
152.51
151.18
129.85
129.82
128.80
128.60
127.68
127.46
125.38
125.00
123.44
123.32
121.54
121.45
114.03
113.94
111.84
111.65
108.45
106.83
85.26
84.40
75.52
74.94
71.80
71.01
55.42
55.40
16.41
13.72
Parameter Value
Title AAG-08205-B
Solvent CDCl3
Temperature 298.2
Number of Scans 1024
Receiver Gain 512
Relaxation Delay 3.0000
Pulse Width 9.2500
Acquisition Time 1.3665
Acquisition Date 2015-05-23T02:46:00
Frequency 100.62
Nucleus 13C
2.83, dr = 79:21
A = major
B = minor
PMB
O
O
Me
NO2
210 200 190 180 170 160 150 140 130 120 110 100 90 80 70 60 50 40 30 20 10 0 -10
f1 (ppm)

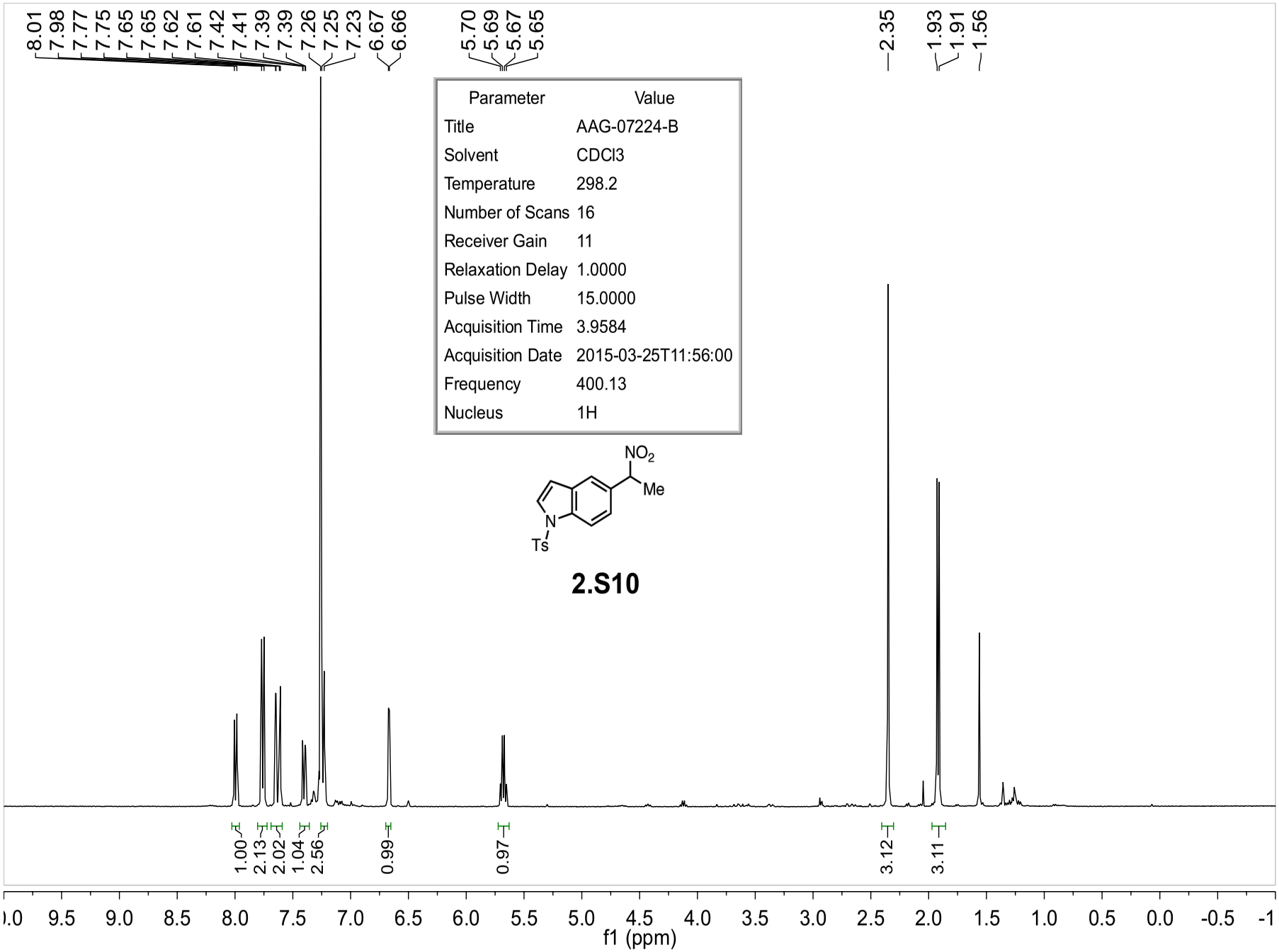
8.01
7.98
7.77
7.75
7.65
7.65
7.62
7.61
7.42
7.41
7.39
7.39
7.26
7.25
7.23
6.67
6.66
5.70
5.69
5.67
5.65
2.35
1.93
1.91
1.56
Parameter Value
Title AAG-07224-B
Solvent CDCl3
Temperature 298.2
Number of Scans 16
Receiver Gain 11
Relaxation Delay 1.0000
Pulse Width 15.0000
Acquisition Time 3.9584
Acquisition Date 2015-03-25T11:56:00
Frequency 400.13
Nucleus 1H
NO2
Me
N
Ts
2.S10
1.00
2.13
2.02
1.04
2.56
0.99
0.97
3.12
3.11
f1 (ppm)

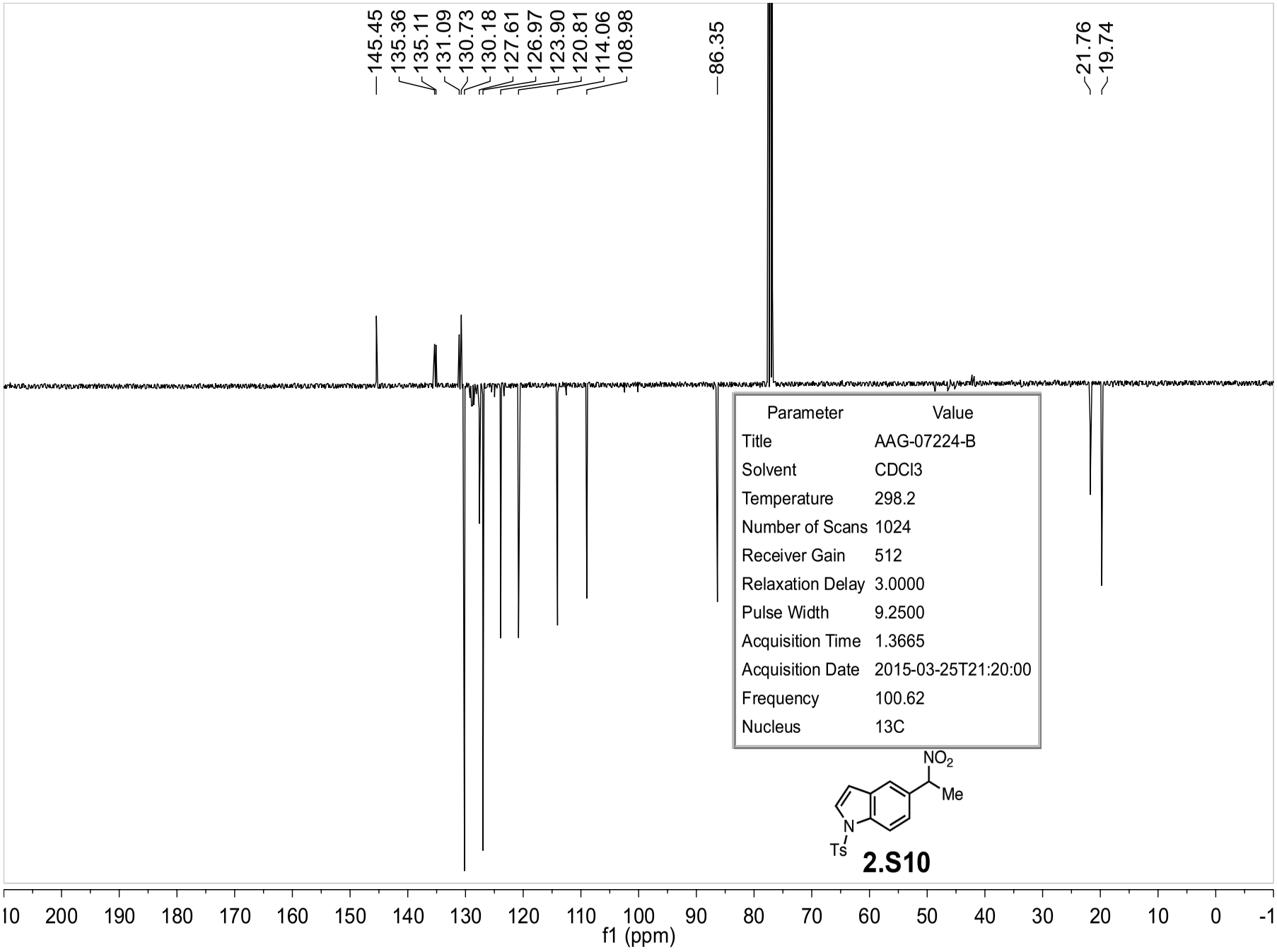
145.45
135.36
135.11
131.09
130.73
130.18
127.61
126.97
123.90
120.81
114.06
108.98
86.35
21.76
19.74
Parameter Value
Title AAG-07224-B
Solvent CDCl3
Temperature 298.2
Number of Scans 1024
Receiver Gain 512
Relaxation Delay 3.0000
Pulse Width 9.2500
Acquisition Time 1.3665
Acquisition Date 2015-03-25T21:20:00
Frequency 100.62
Nucleus 13C
NO2
Me
N
Ts
2.S10
f1 (ppm)

Parameter	Value
1 Title	DVR03295CRD.1.fid
2 Solvent	CDCl3
3 Temperature	298.2
4 Number of Scans	16
5 Receiver Gain	9
6 Relaxation Delay	1.0000
7 Pulse Width	15.0000
8 Spectrometer Frequency	400.13
9 Nucleus	1H

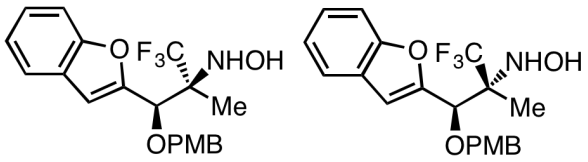

crude-*2.84*
93:07

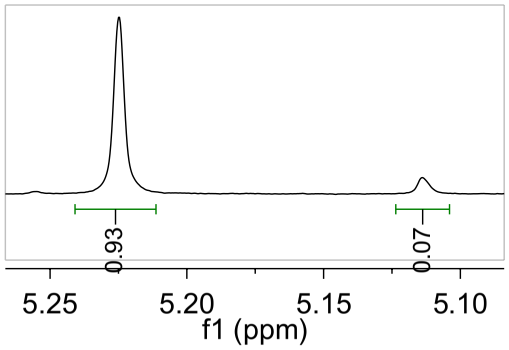

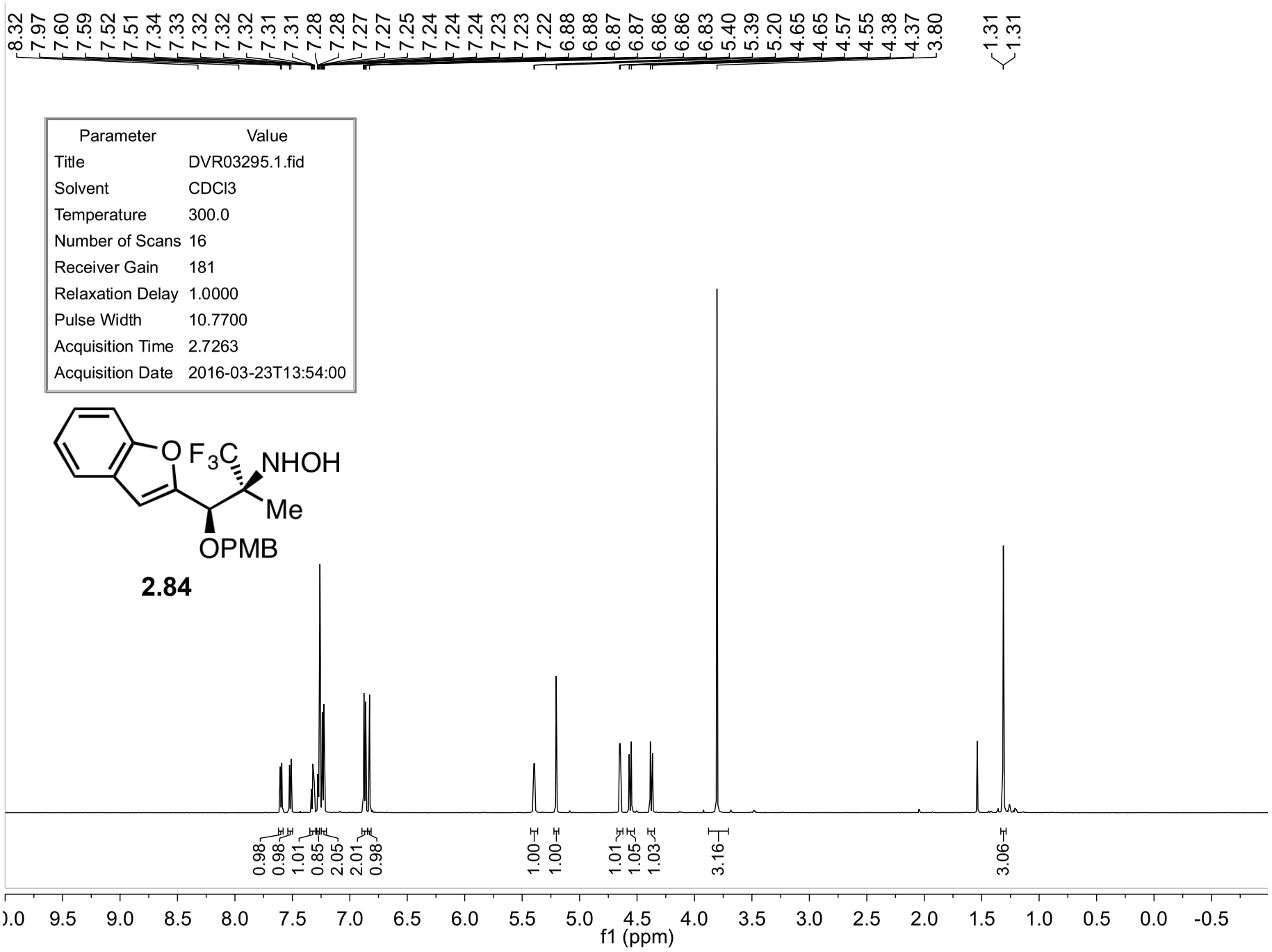
8.32
7.97
7.60
7.59
7.52
7.51
7.34
7.33
7.32
7.32
7.32
7.31
7.31
7.28
7.28
7.27
7.27
7.25
7.24
7.24
7.24
7.23
7.23
7.22
6.88
6.88
6.87
6.87
6.86
6.86
6.83
5.40
5.39
5.20
4.65
4.65
4.57
4.55
4.38
4.37
3.80
1.31
1.31
Parameter Value
Title DVR03295.1.fid
Solvent CDCl3
Temperature 300.0
Number of Scans 16
Receiver Gain 181
Relaxation Delay 1.0000
Pulse Width 10.7700
Acquisition Time 2.7263
Acquisition Date 2016-03-23T13:54:00
O
F3C
NHOH
Me
OPMB
2.84
0.98
0.98
1.01
0.85
2.05
2.01
0.98
1.00
1.00
1.01
1.05
1.03
3.16
3.06
f1 (ppm)

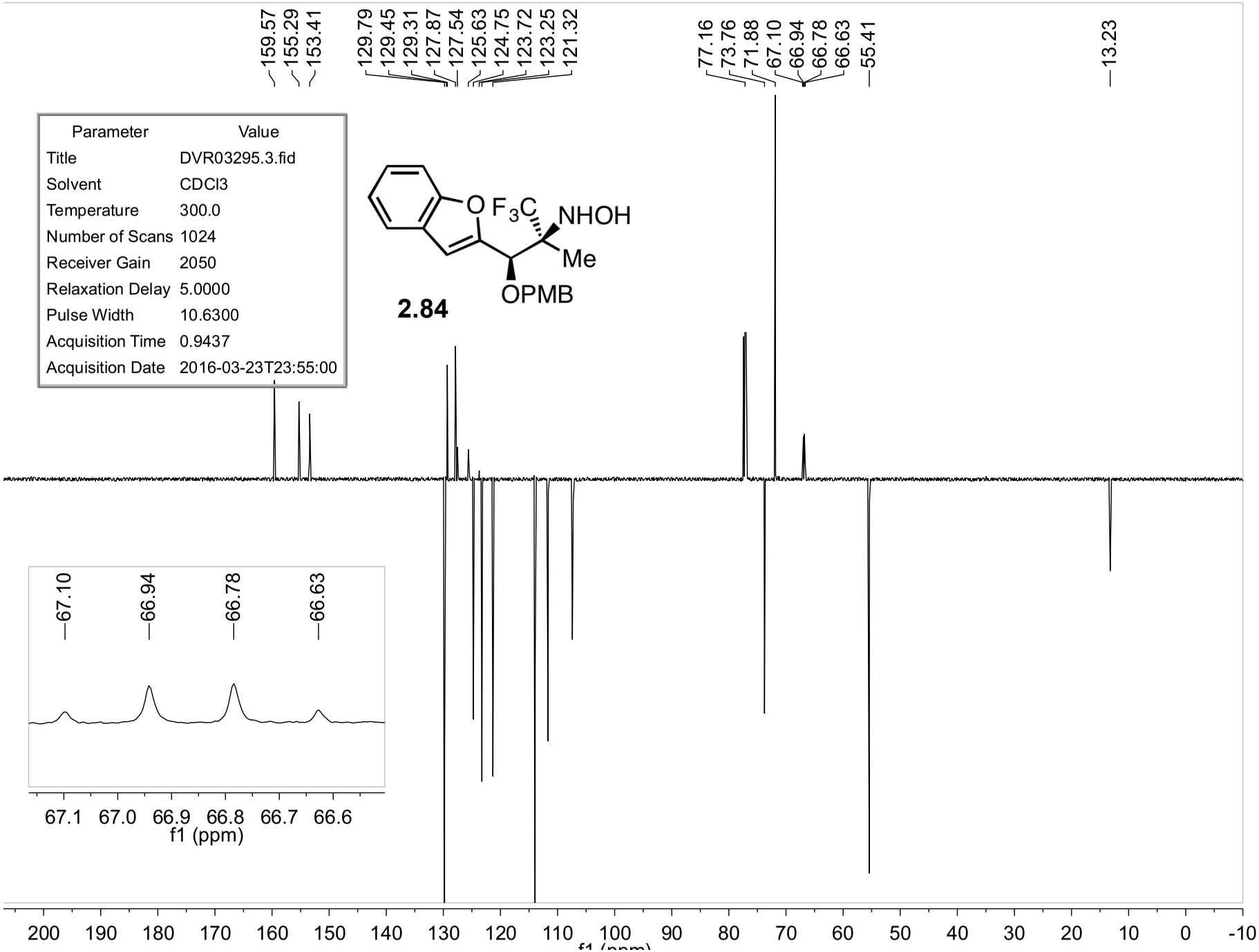
159.57
155.29
153.41
129.79
129.45
129.31
127.87
127.54
125.63
124.75
123.72
123.25
121.32
77.16
73.76
71.88
67.10
66.94
66.78
66.63
55.41
13.23
Parameter Value
Title DVR03295.3.fid
Solvent CDCl3
Temperature 300.0
Number of Scans 1024
Receiver Gain 2050
Relaxation Delay 5.0000
Pulse Width 10.6300
Acquisition Time 0.9437
Acquisition Date 2016-03-23T23:55:00
O
F3C
NHOH
Me
OPMB
2.84
67.1 67.0 66.9 66.8 66.7 66.6
f1 (ppm)
200 190 180 170 160 150 140 130 120 110 100 90 80 70 60 50 40 30 20 10 0 -10

Parameter	Value
Title	DVR03295.2.fid
Solvent	CDCl3
Temperature	300.0
Number of Scans	16
Receiver Gain	362
Relaxation Delay	3.0000
Pulse Width	11.6200
Acquisition Time	0.4893
Acquisition Date	2016-03-23T13:57:00

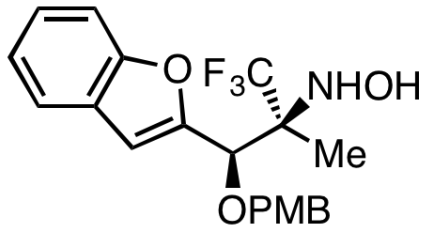

2.84

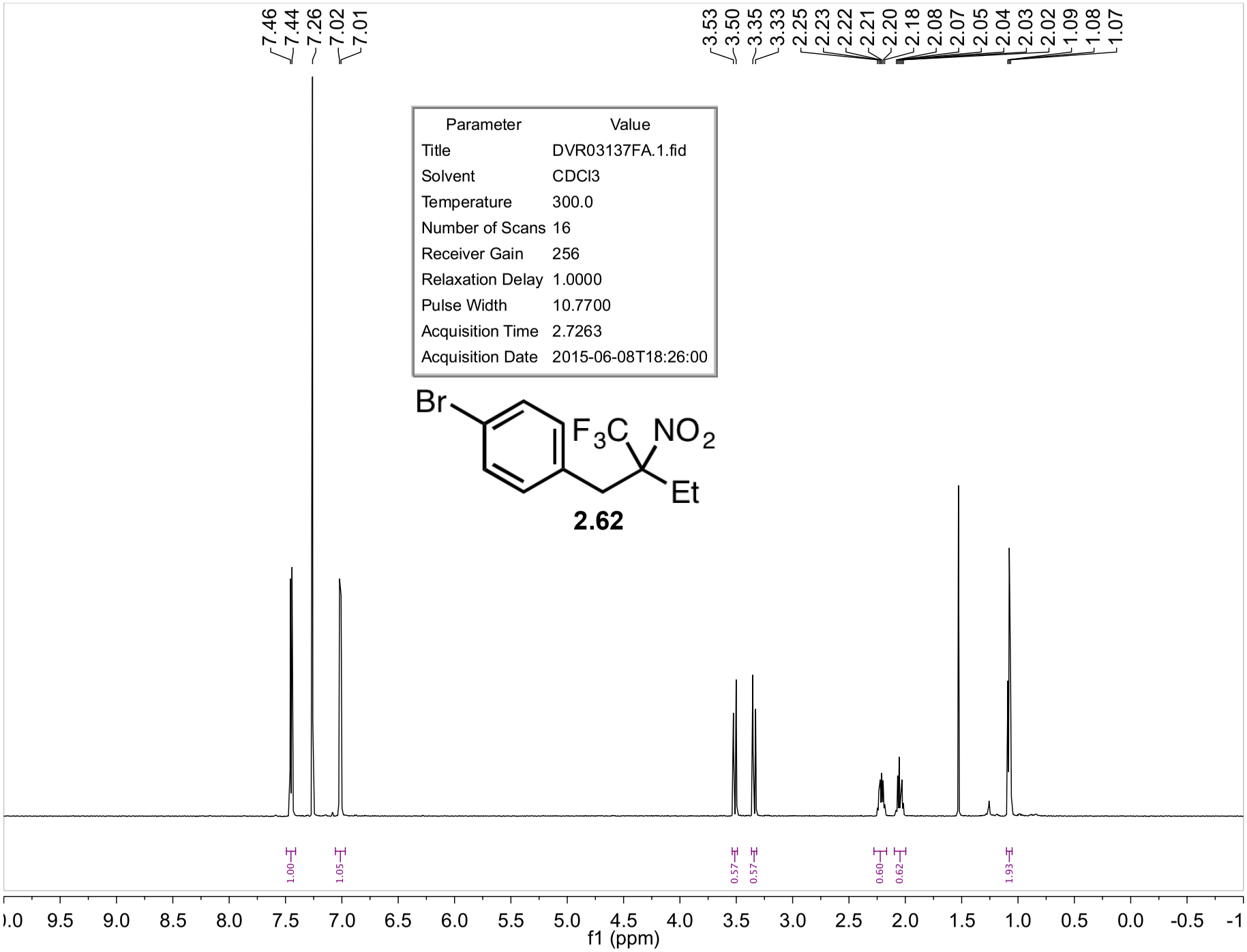
7.46
7.44
7.26
7.02
7.01
3.53
3.50
3.35
3.33
2.25
2.23
2.22
2.21
2.20
2.18
2.08
2.07
2.05
2.04
2.03
2.02
1.09
1.08
1.07
Parameter Value
Title DVR03137FA.1.fid
Solvent CDCl3
Temperature 300.0
Number of Scans 16
Receiver Gain 256
Relaxation Delay 1.0000
Pulse Width 10.7700
Acquisition Time 2.7263
Acquisition Date 2015-06-08T18:26:00
Br
F3C
NO2
Et
2.62
1.00
0.91
0.57
0.57
0.69
0.62
1.93
f1 (ppm)

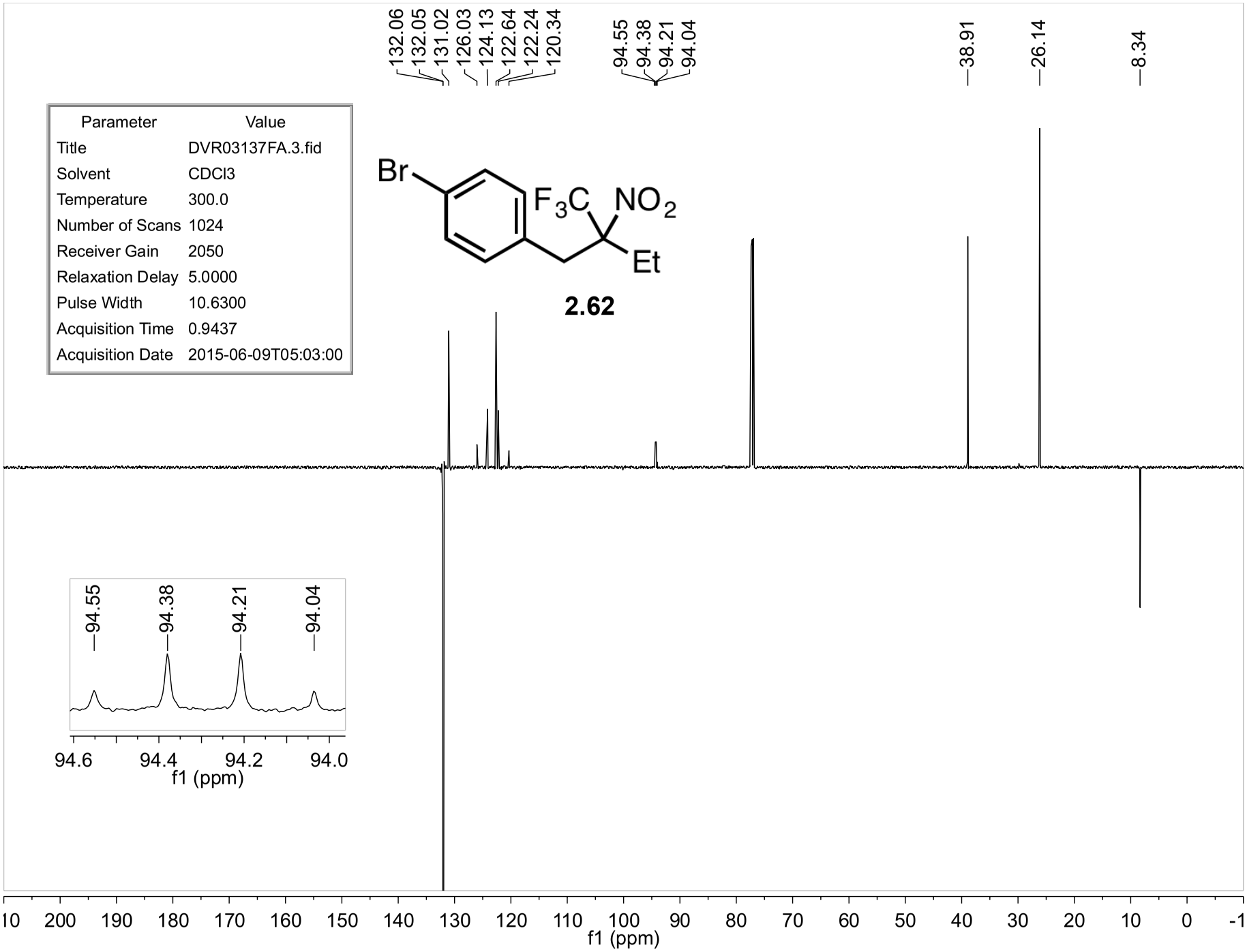
132.06
132.05
131.02
126.03
124.13
122.64
122.24
120.34
94.55
94.38
94.21
94.04
38.91
26.14
8.34
Parameter Value
Title DVR03137FA.3.fid
Solvent CDCl3
Temperature 300.0
Number of Scans 1024
Receiver Gain 2050
Relaxation Delay 5.0000
Pulse Width 10.6300
Acquisition Time 0.9437
Acquisition Date 2015-06-09T05:03:00
Br
F3C
NO2
Et
2.62
94.6
94.4
94.2
94.0
f1 (ppm)
f1 (ppm)

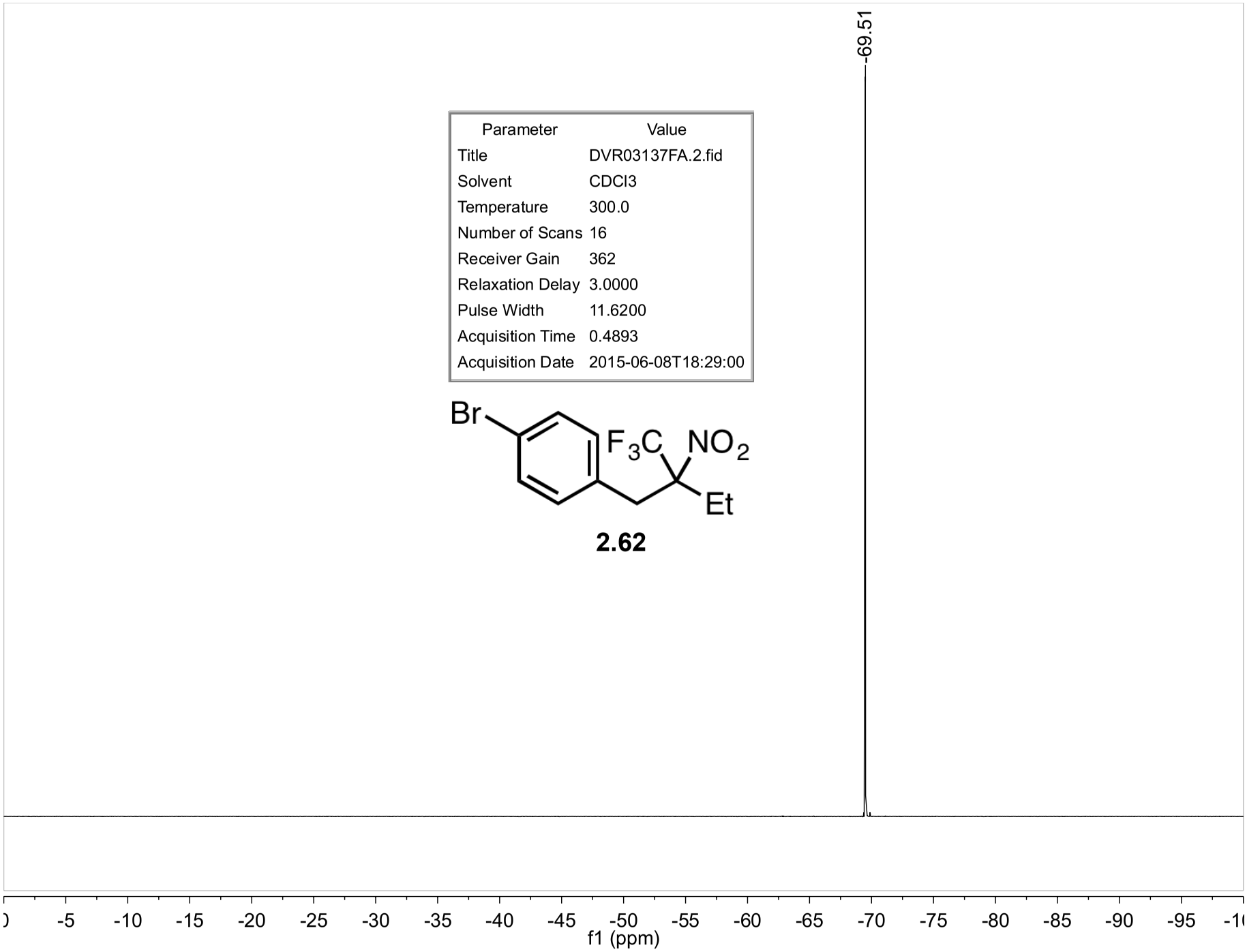
-69.51
Parameter Value
Title DVR03137FA.2.fid
Solvent CDCl3
Temperature 300.0
Number of Scans 16
Receiver Gain 362
Relaxation Delay 3.0000
Pulse Width 11.6200
Acquisition Time 0.4893
Acquisition Date 2015-06-08T18:29:00
Br
F3C
NO2
Et
2.62
-5 -10 -15 -20 -25 -30 -35 -40 -45 -50 -55 -60 -65 -70 -75 -80 -85 -90 -95
f1 (ppm)

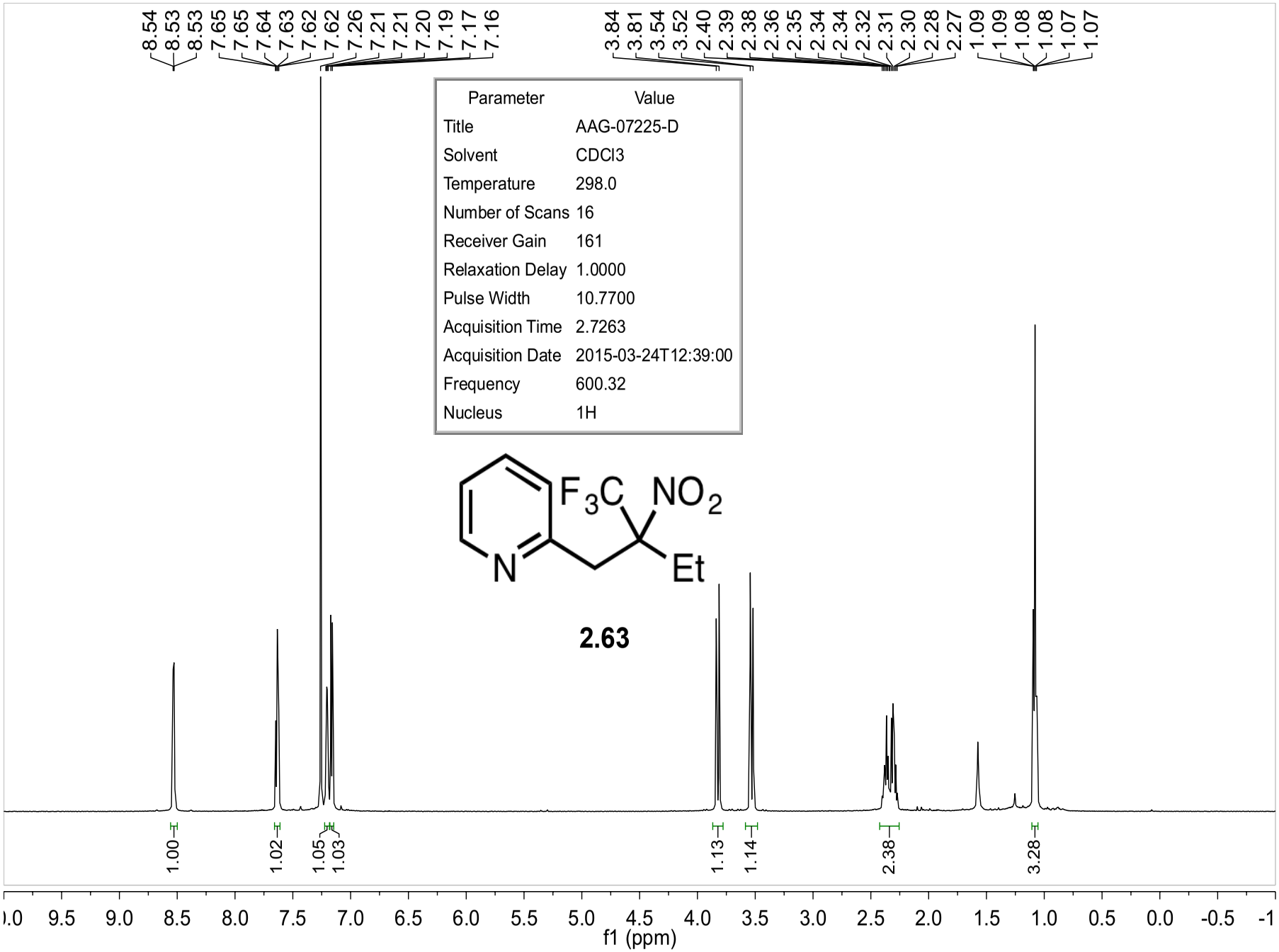
8.54 8.53 8.53 7.65 7.65 7.64 7.63 7.62 7.62 7.26 7.21 7.21 7.20 7.19 7.17 7.16
3.84 3.81 3.54 3.52 2.40 2.39 2.38 2.36 2.35 2.34 2.34 2.32 2.31 2.30 2.28 2.27 1.09 1.09 1.08 1.08 1.07 1.07
Parameter Value
Title AAG-07225-D
Solvent CDCl3
Temperature 298.0
Number of Scans 16
Receiver Gain 161
Relaxation Delay 1.0000
Pulse Width 10.7700
Acquisition Time 2.7263
Acquisition Date 2015-03-24T12:39:00
Frequency 600.32
Nucleus 1H
F3C NO2
N
Et
2.63
1.00 1.02 1.05 1.03 1.13 1.14 2.38 3.28
9.5 9.0 8.5 8.0 7.5 7.0 6.5 6.0 5.5 5.0 4.5 4.0 3.5 3.0 2.5 2.0 1.5 1.0 0.5 0.0 -0.5 -1
f1 (ppm)

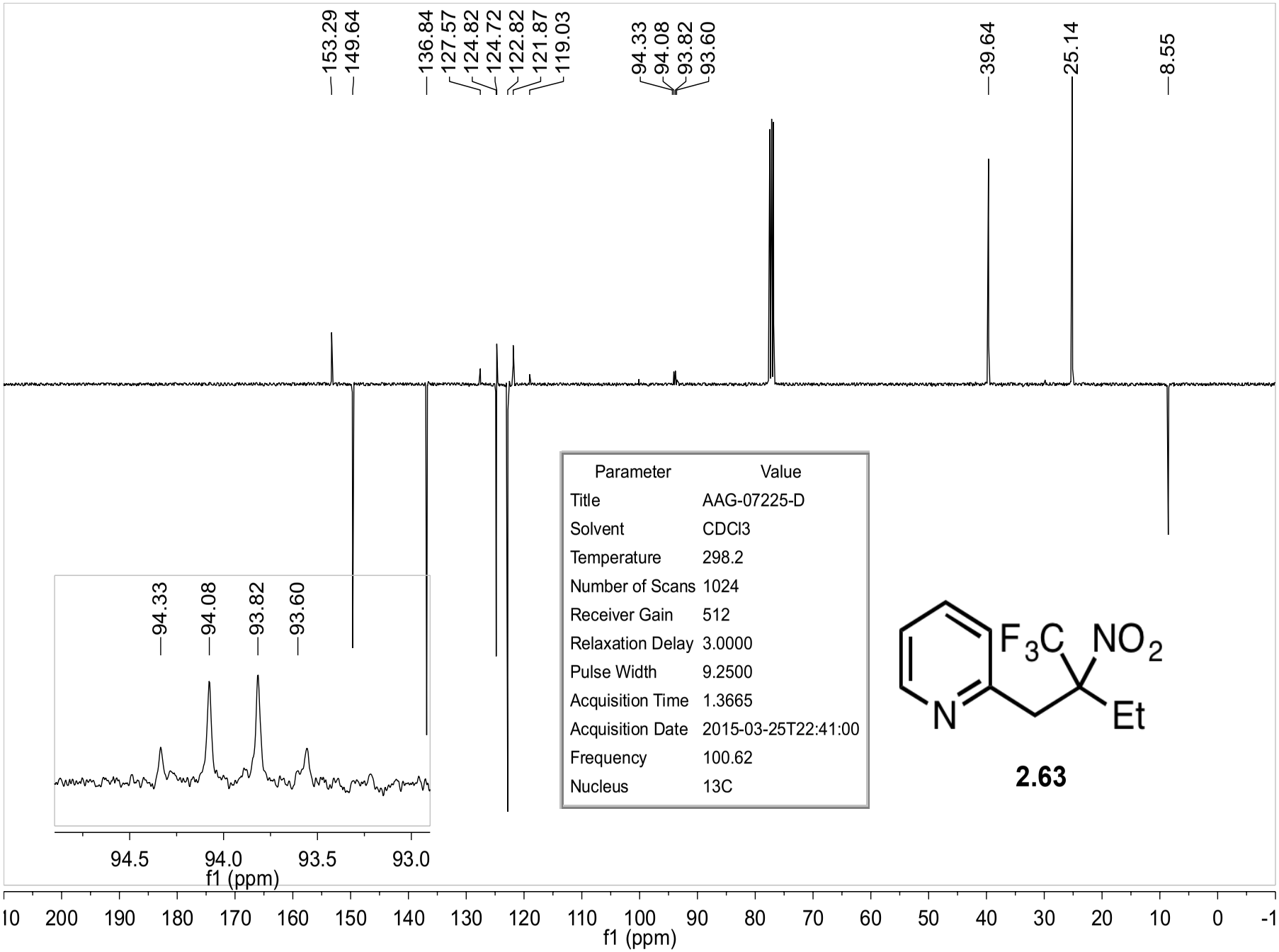
153.29
149.64
136.84
127.57
124.82
124.72
122.82
121.87
119.03
94.33
94.08
93.82
93.60
39.64
25.14
8.55
94.33
94.08
93.82
93.60
94.5
94.0
93.5
93.0
f1 (ppm)
Parameter Value
Title AAG-07225-D
Solvent CDCl3
Temperature 298.2
Number of Scans 1024
Receiver Gain 512
Relaxation Delay 3.0000
Pulse Width 9.2500
Acquisition Time 1.3665
Acquisition Date 2015-03-25T22:41:00
Frequency 100.62
Nucleus 13C
F3C
NO2
N
Et
2.63
f1 (ppm)

Parameter	Value
Title	AAG-07225-D/ 20
Solvent	CDCl3
Temperature	298.0
Number of Scans	16
Receiver Gain	362
Relaxation Delay	3.0000
Pulse Width	11.6200
Acquisition Time	0.4888
Acquisition Date	2015-03-23T22:03:27
Frequency	564.81
Nucleus	19F

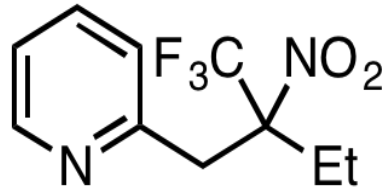

2.63

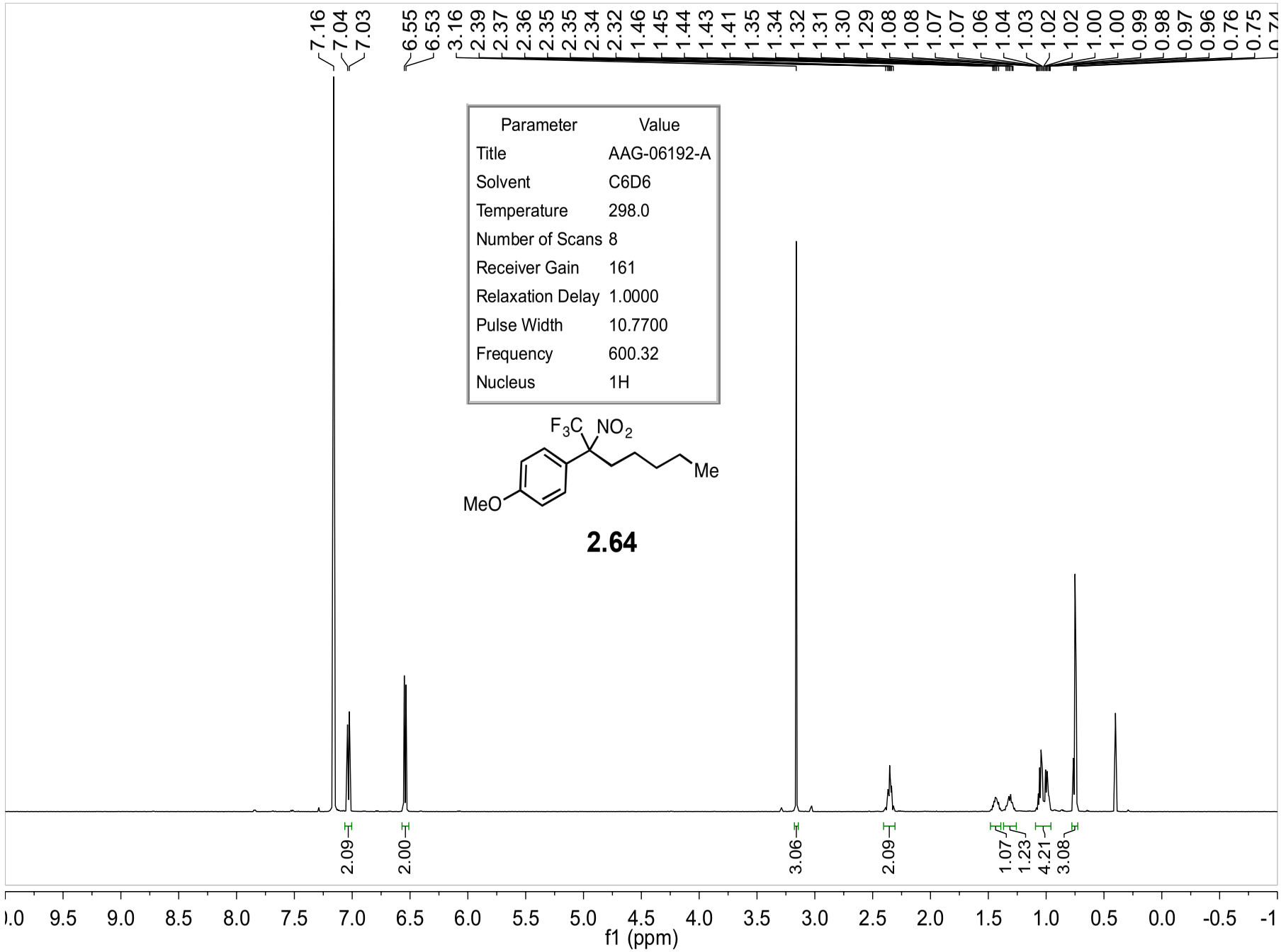
7.16
7.04
7.03
6.55
6.53
3.16
2.39
2.37
2.36
2.35
2.35
2.34
2.32
1.46
1.45
1.44
1.43
1.41
1.35
1.34
1.32
1.31
1.30
1.29
1.08
1.08
1.07
1.07
1.06
1.04
1.03
1.02
1.02
1.00
1.00
0.99
0.98
0.97
0.96
0.76
0.75
Parameter Value
Title AAG-06192-A
Solvent C6D6
Temperature 298.0
Number of Scans 8
Receiver Gain 161
Relaxation Delay 1.0000
Pulse Width 10.7700
Frequency 600.32
Nucleus 1H
F3C NO2
Me
MeO
2.64
2.09
2.00
3.06
2.09
1.07
1.23
4.21
3.08
f1 (ppm)

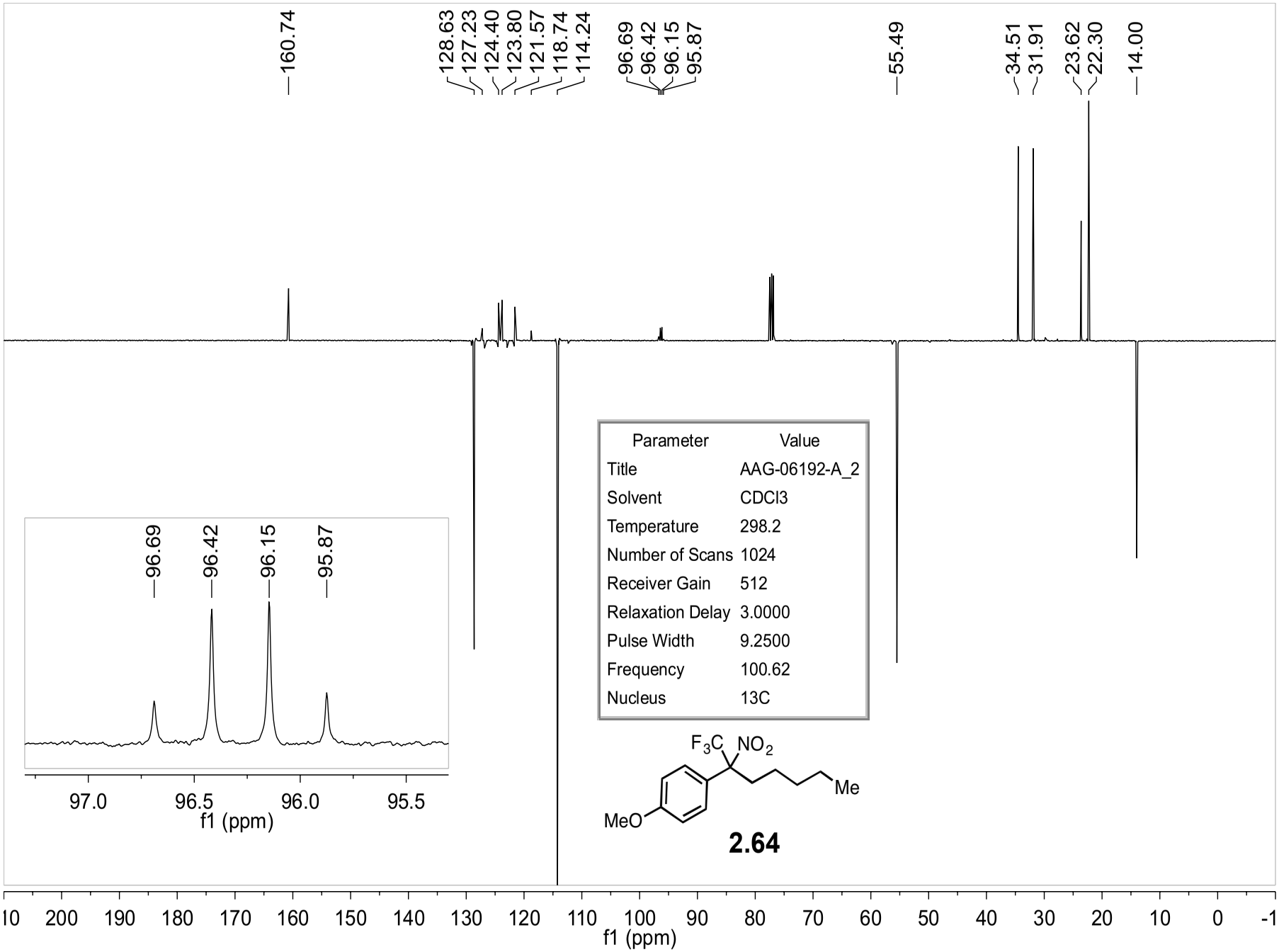
160.74
128.63
127.23
124.40
123.80
121.57
118.74
114.24
96.69
96.42
96.15
95.87
55.49
34.51
31.91
23.62
22.30
14.00
Parameter Value
Title AAG-06192-A_2
Solvent CDCl3
Temperature 298.2
Number of Scans 1024
Receiver Gain 512
Relaxation Delay 3.0000
Pulse Width 9.2500
Frequency 100.62
Nucleus 13C
F3C NO2
Me
MeO
2.64
f1 (ppm)

Parameter	Value
Title	AAG-06192-A
Solvent	CDCl3
Temperature	298.0
Number of Scans	16
Receiver Gain	322
Relaxation Delay	3.0000
Pulse Width	11.6200
Frequency	564.81
Nucleus	19F

2.64

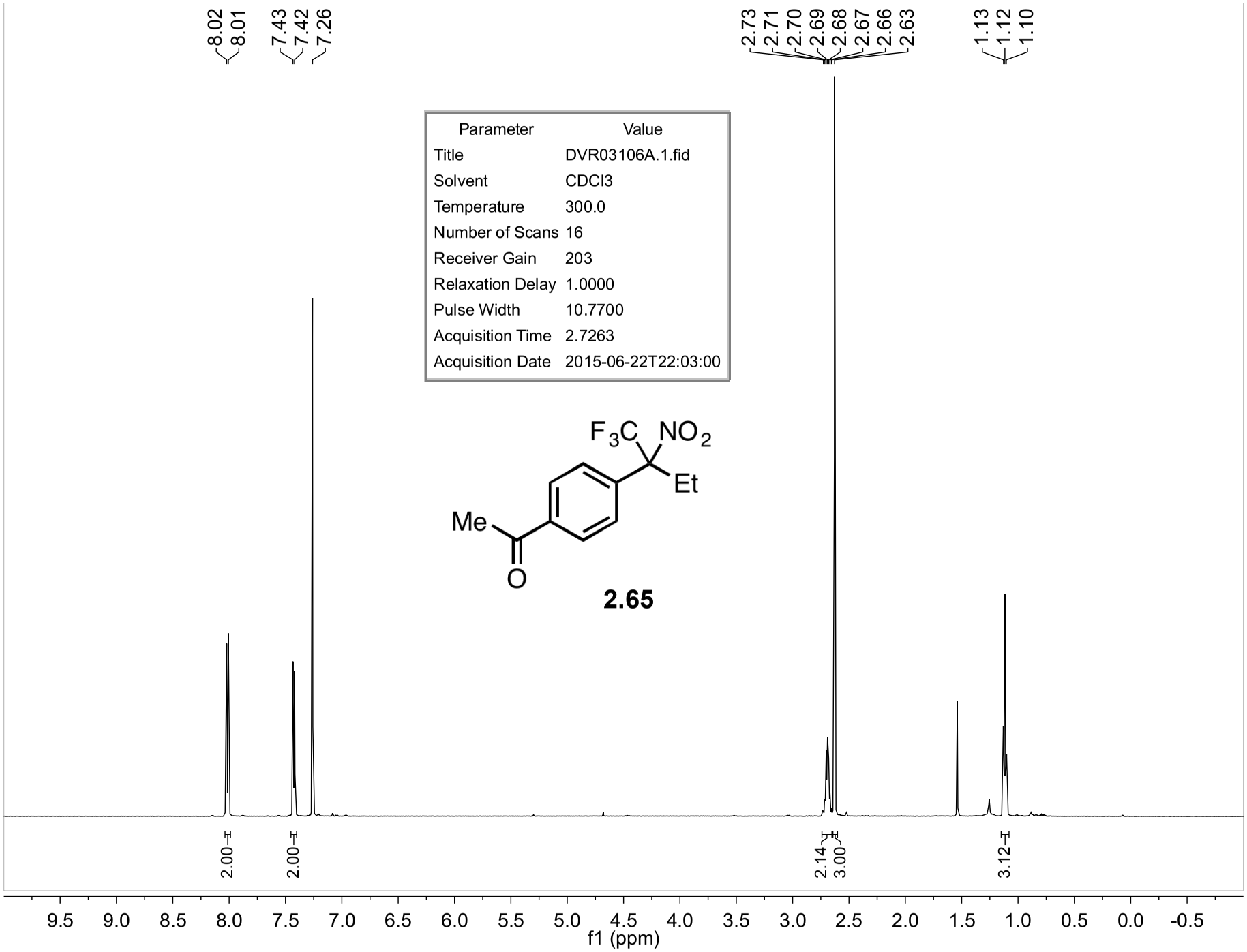
8.02
8.01
7.43
7.42
7.26
2.73
2.71
2.70
2.69
2.68
2.67
2.66
2.63
1.13
1.12
1.10
Parameter Value
Title DVR03106A.1.fid
Solvent CDCl3
Temperature 300.0
Number of Scans 16
Receiver Gain 203
Relaxation Delay 1.0000
Pulse Width 10.7700
Acquisition Time 2.7263
Acquisition Date 2015-06-22T22:03:00
F3C
NO2
Et
Me
O
2.65
2.00
2.00
2.14
3.00
3.12
9.5 9.0 8.5 8.0 7.5 7.0 6.5 6.0 5.5 5.0 4.5 4.0 3.5 3.0 2.5 2.0 1.5 1.0 0.5 0.0 -0.5
f1 (ppm)

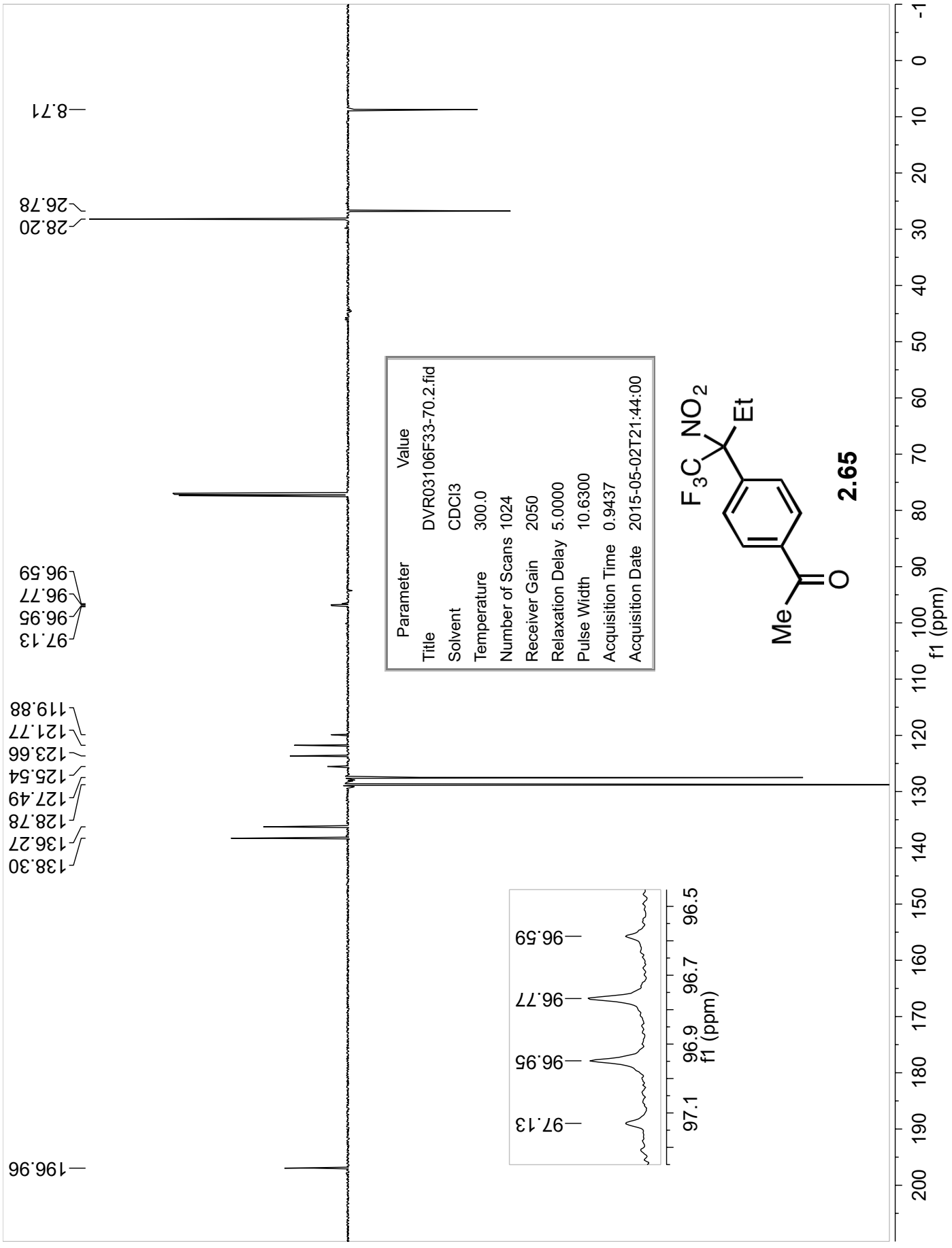
196.96
138.30
136.27
128.78
127.49
125.54
123.66
121.77
119.88
97.13
96.95
96.77
96.59
28.20
26.78
8.71
Parameter Value
Title DVR03106F33-70.2.fid
Solvent CDCl3
Temperature 300.0
Number of Scans 1024
Receiver Gain 2050
Relaxation Delay 5.0000
Pulse Width 10.6300
Acquisition Time 0.9437
Acquisition Date 2015-05-02T21:44:00
F3C
NO2
Et
Me
O
2.65
f1 (ppm)
97.1
96.9
96.7
96.5

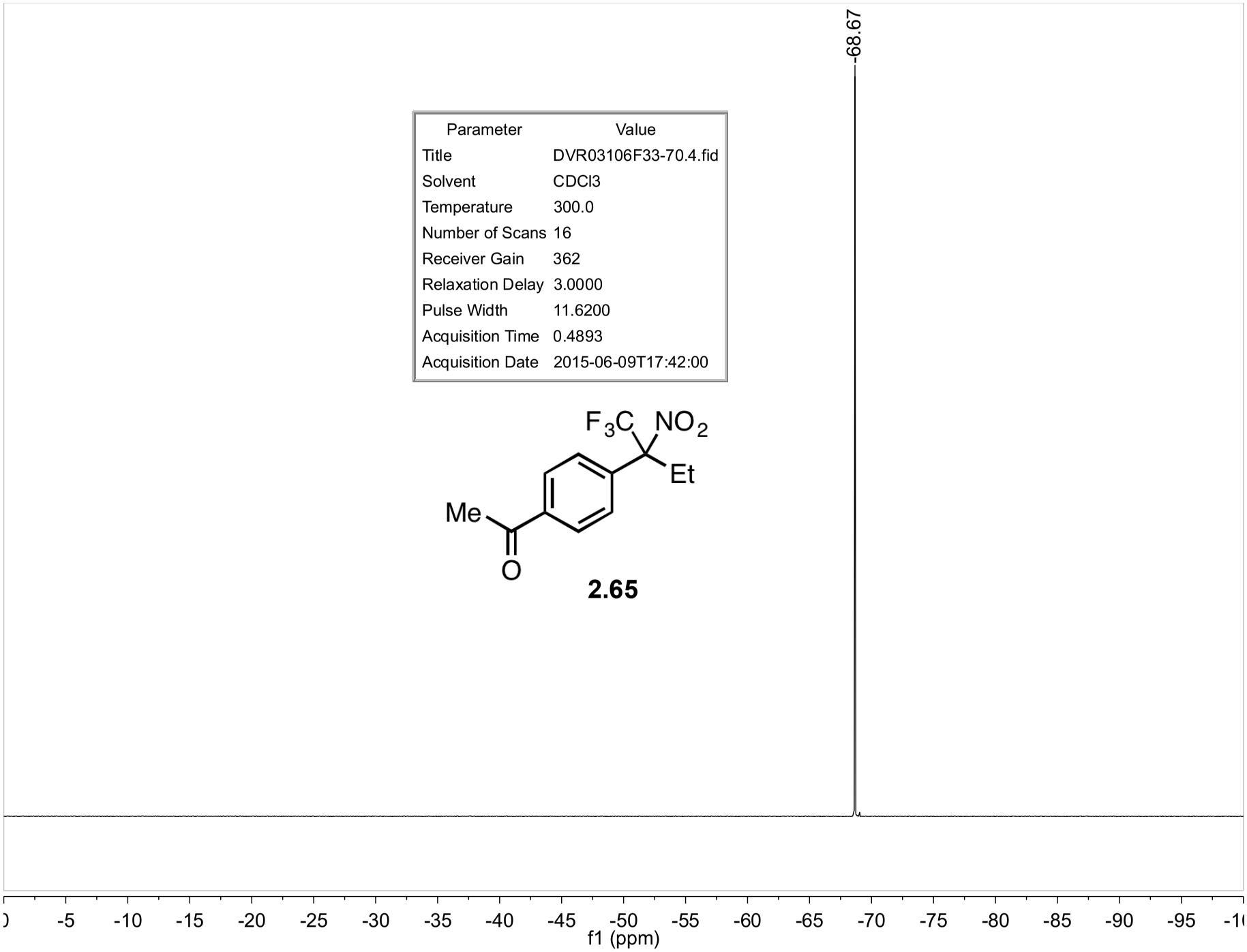
-68.67
Parameter Value
Title DVR03106F33-70.4.fid
Solvent CDCl3
Temperature 300.0
Number of Scans 16
Receiver Gain 362
Relaxation Delay 3.0000
Pulse Width 11.6200
Acquisition Time 0.4893
Acquisition Date 2015-06-09T17:42:00
F3C
NO2
Et
Me
O
2.65
-5 -10 -15 -20 -25 -30 -35 -40 -45 -50 -55 -60 -65 -70 -75 -80 -85 -90 -95
f1 (ppm)

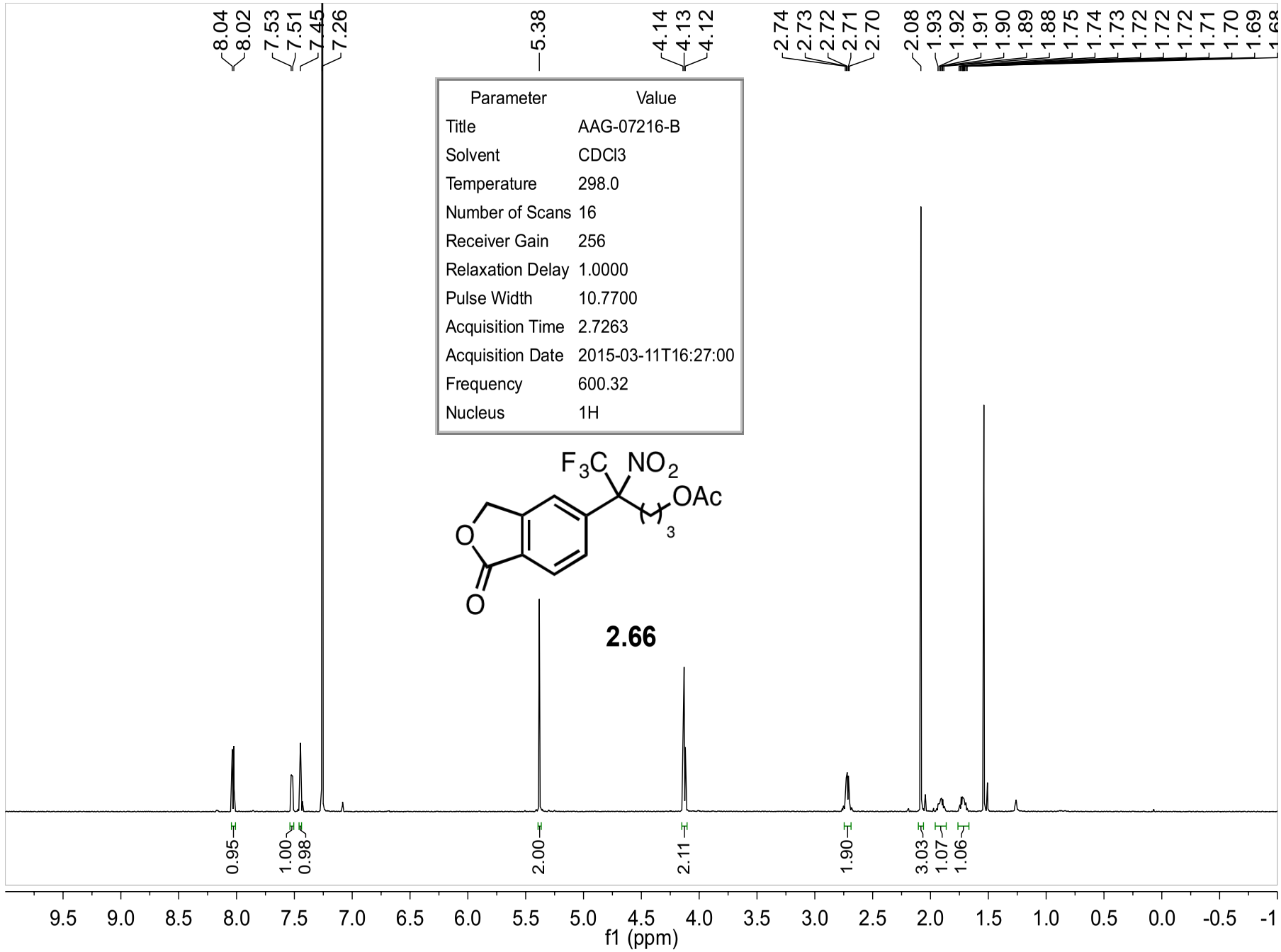
8.04
8.02
7.53
7.51
7.45
7.26
5.38
4.14
4.13
4.12
2.74
2.73
2.72
2.71
2.70
2.08
1.93
1.92
1.91
1.90
1.89
1.88
1.75
1.74
1.73
1.72
1.72
1.72
1.71
1.70
1.69
Parameter Value
Title AAG-07216-B
Solvent CDCl3
Temperature 298.0
Number of Scans 16
Receiver Gain 256
Relaxation Delay 1.0000
Pulse Width 10.7700
Acquisition Time 2.7263
Acquisition Date 2015-03-11T16:27:00
Frequency 600.32
Nucleus 1H
F3C NO2
OAc
3
O
O
2.66
0.95
1.00
0.98
2.00
2.11
1.90
3.03
1.07
1.06
9.5 9.0 8.5 8.0 7.5 7.0 6.5 6.0 5.5 5.0 4.5 4.0 3.5 3.0 2.5 2.0 1.5 1.0 0.5 0.0 -0.5 -1
f1 (ppm)

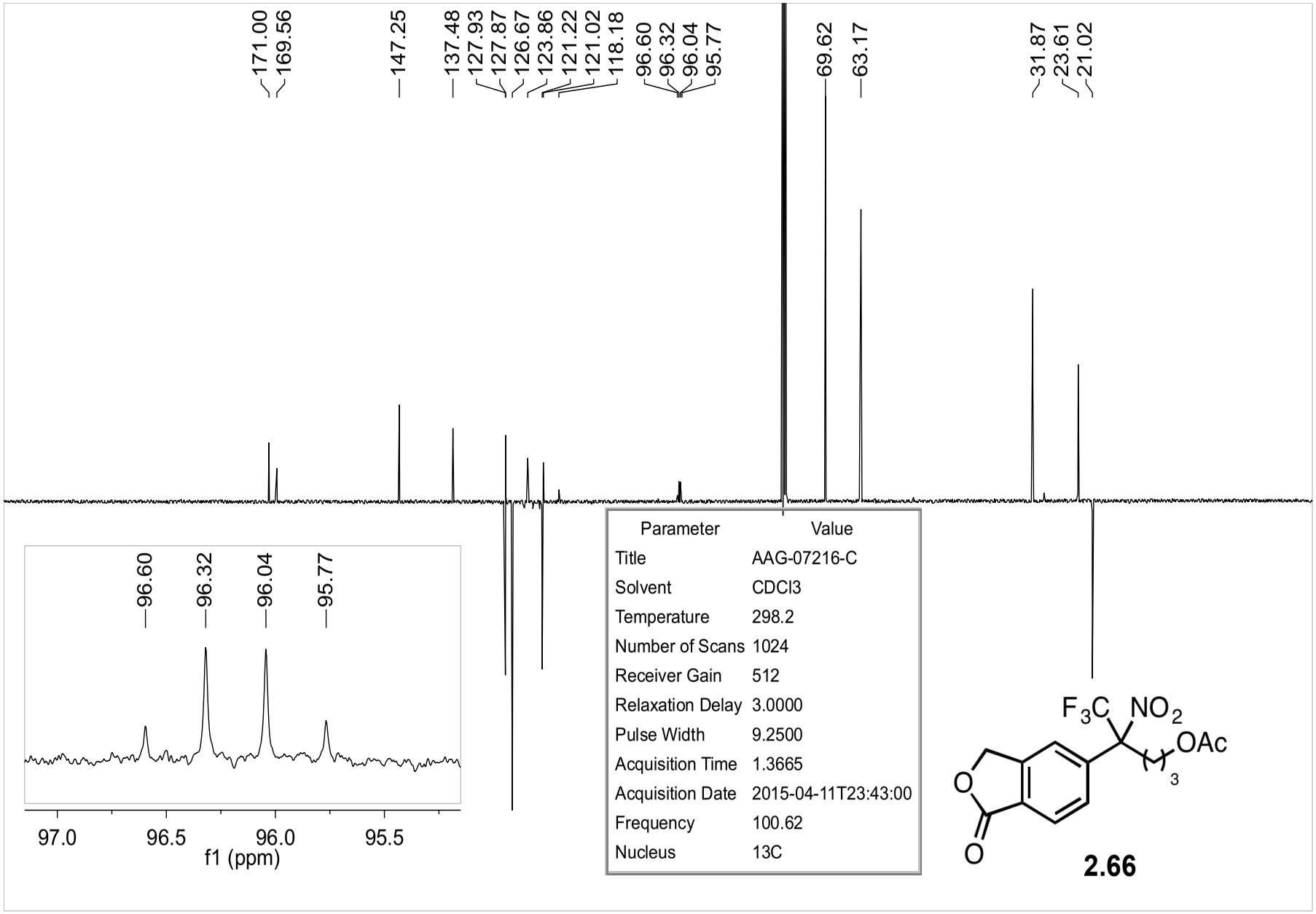
171.00
169.56
147.25
137.48
127.93
127.87
126.67
123.86
121.22
121.02
118.18
96.60
96.32
96.04
95.77
69.62
63.17
31.87
23.61
21.02
f1 (ppm)
Parameter Value
Title AAG-07216-C
Solvent CDCl3
Temperature 298.2
Number of Scans 1024
Receiver Gain 512
Relaxation Delay 3.0000
Pulse Width 9.2500
Acquisition Time 1.3665
Acquisition Date 2015-04-11T23:43:00
Frequency 100.62
Nucleus 13C
F3C NO2
OAc
3
O
O
2.66

Parameter	Value
Title	AAG-07216-B
Solvent	CDCl3
Temperature	298.0
Number of Scans	16
Receiver Gain	362
Relaxation Delay	3.0000
Pulse Width	11.6200
Acquisition Time	0.4893
Acquisition Date	2015-03-11T16:30:00
Frequency	564.81
Nucleus	19F

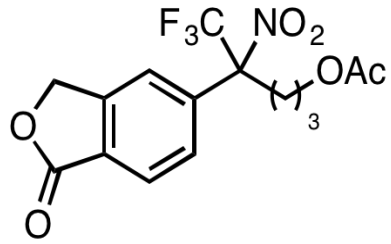

2.66

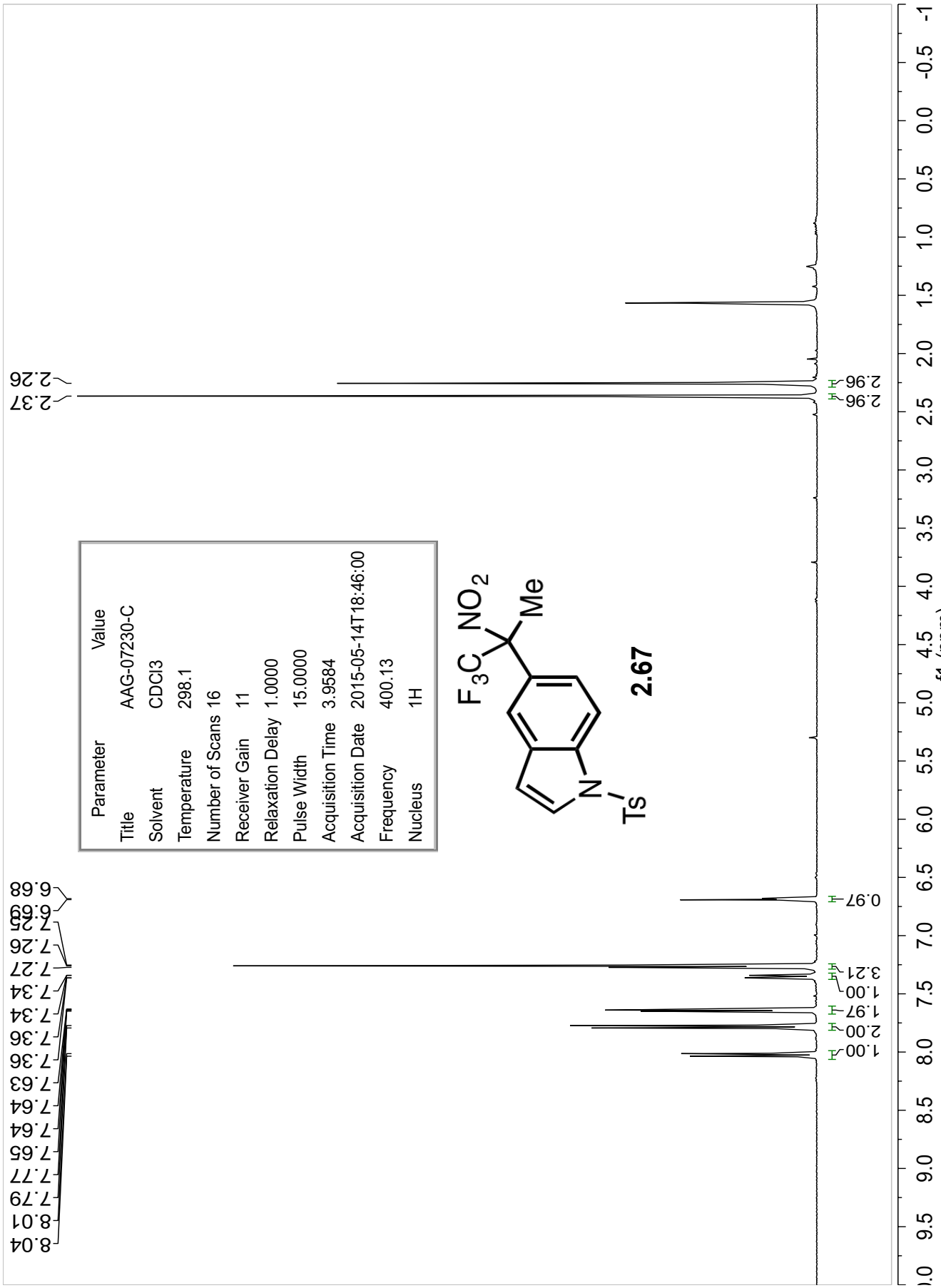
Parameter Value
Title AAG-07230-C
Solvent CDCl3
Temperature 298.1
Number of Scans 16
Receiver Gain 11
Relaxation Delay 1.0000
Pulse Width 15.0000
Acquisition Time 3.9584
Acquisition Date 2015-05-14T18:46:00
Frequency 400.13
Nucleus 1H
F3C NO2
Me
N
Ts
2.67
f1 (ppm)

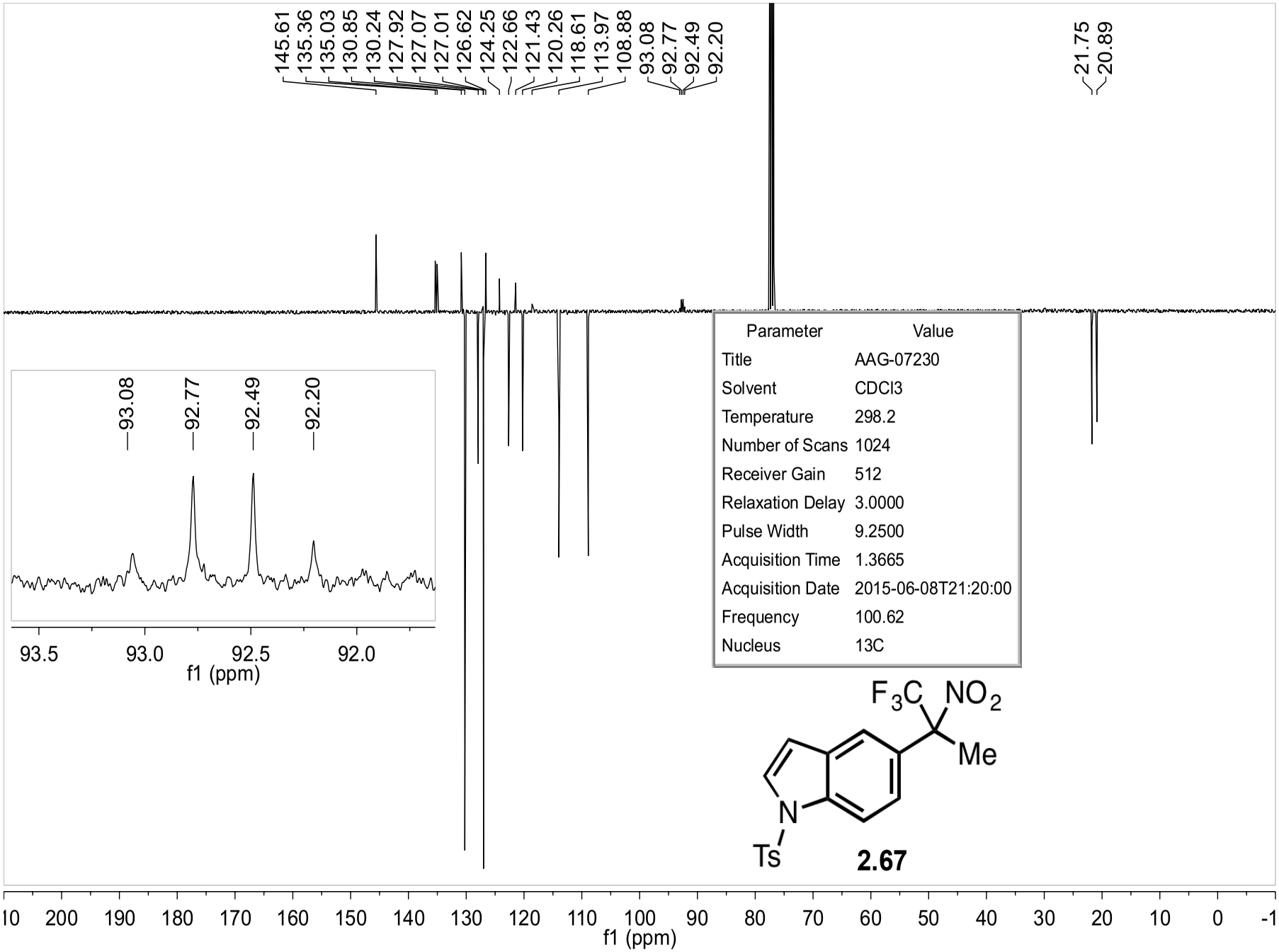
145.61
135.36
135.03
130.85
130.24
127.92
127.07
127.01
126.62
124.25
122.66
121.43
120.26
118.61
113.97
108.88
93.08
92.77
92.49
92.20
21.75
20.89
93.08
92.77
92.49
92.20
93.5
93.0
92.5
92.0
f1 (ppm)
Parameter Value
Title AAG-07230
Solvent CDCl3
Temperature 298.2
Number of Scans 1024
Receiver Gain 512
Relaxation Delay 3.0000
Pulse Width 9.2500
Acquisition Time 1.3665
Acquisition Date 2015-06-08T21:20:00
Frequency 100.62
Nucleus 13C
F3C
NO2
Me
N
Ts
2.67
f1 (ppm)

Parameter	Value
Title	AAG-07230-C
Solvent	CDCl3
Temperature	298.2
Number of Scans	16
Receiver Gain	1626
Relaxation Delay	2.0000
Pulse Width	15.0300
Acquisition Time	0.8717
Acquisition Date	2015-05-14T18:48:00
Frequency	376.46
Nucleus	19F

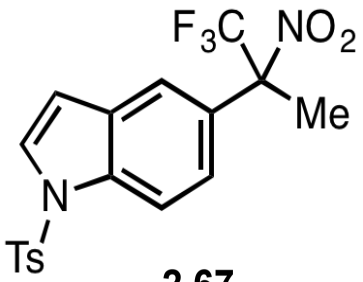

2.67

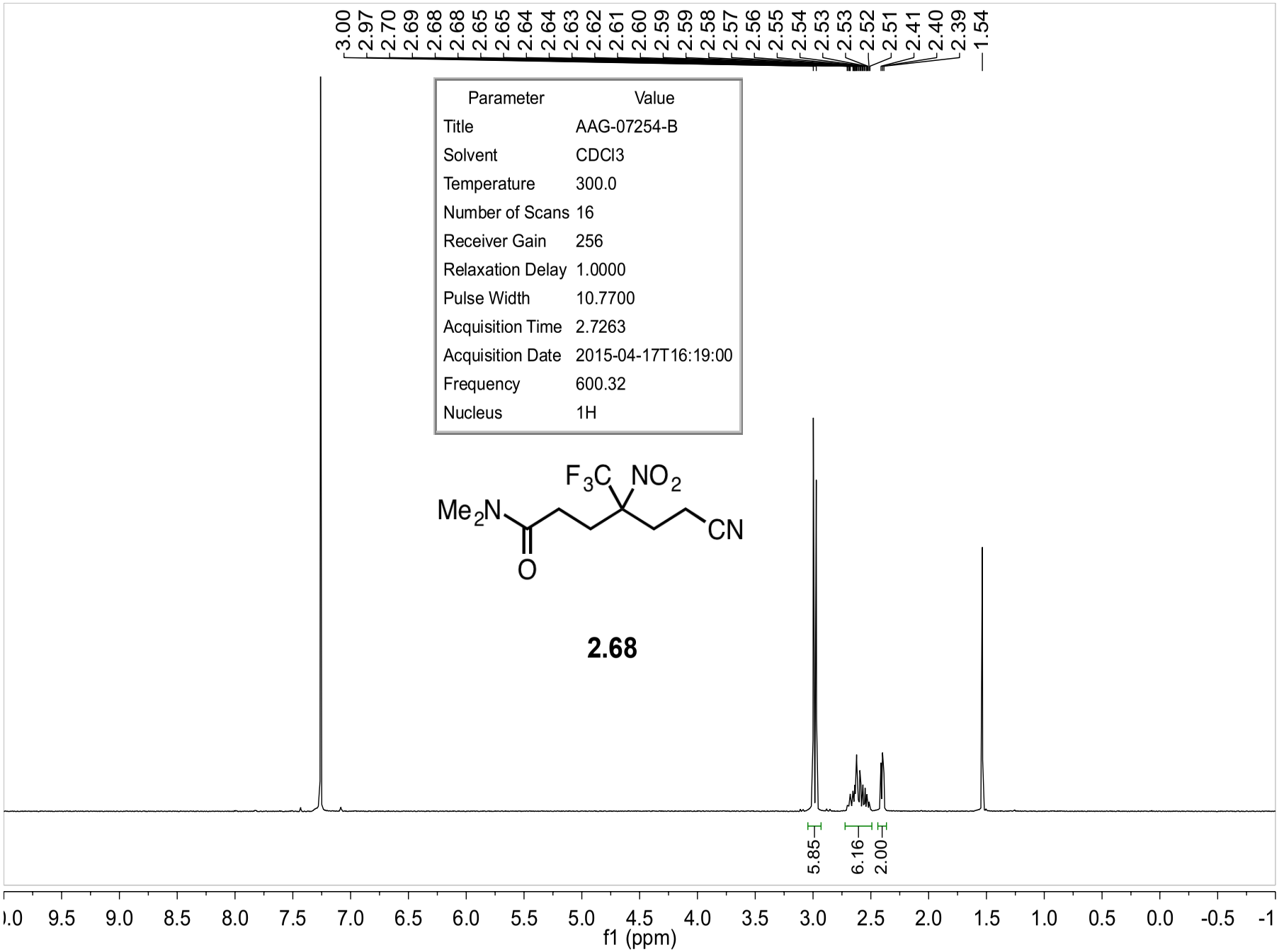
3.00 2.97 2.70 2.69 2.68 2.68 2.65 2.65 2.64 2.64 2.63 2.62 2.61 2.60 2.59 2.59 2.58 2.57 2.56 2.55 2.54 2.53 2.53 2.52 2.51 2.41 2.40 2.39 1.54
Parameter Value
Title AAG-07254-B
Solvent CDCl3
Temperature 300.0
Number of Scans 16
Receiver Gain 256
Relaxation Delay 1.0000
Pulse Width 10.7700
Acquisition Time 2.7263
Acquisition Date 2015-04-17T16:19:00
Frequency 600.32
Nucleus 1H
F3C NO2
Me2N
CN
O
2.68
5.85
6.16
2.00
f1 (ppm)

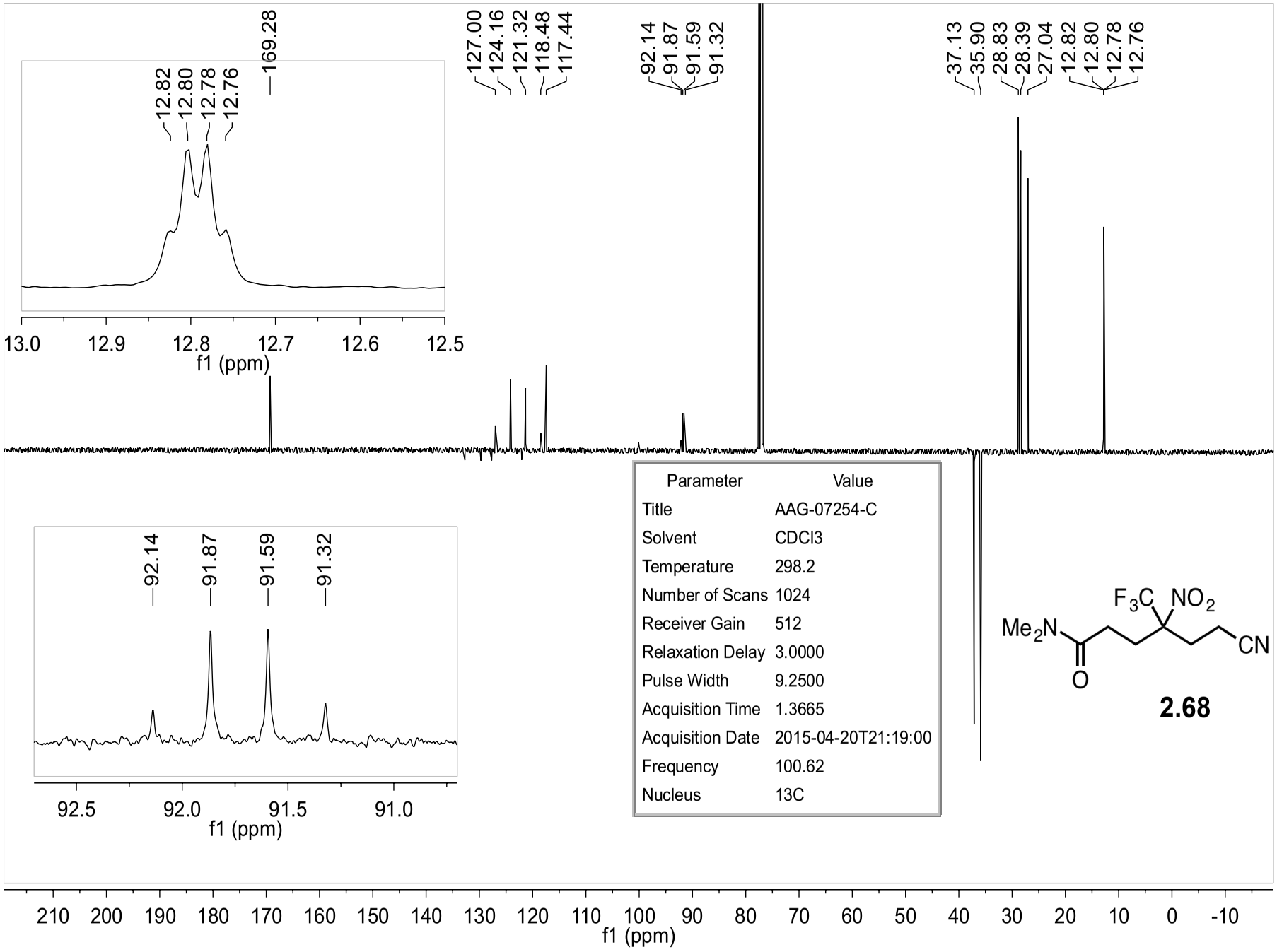
169.28
127.00
124.16
121.32
118.48
117.44
92.14
91.87
91.59
91.32
37.13
35.90
28.83
28.39
27.04
12.82
12.80
12.78
12.76
f1 (ppm)
Parameter Value
Title AAG-07254-C
Solvent CDCl3
Temperature 298.2
Number of Scans 1024
Receiver Gain 512
Relaxation Delay 3.0000
Pulse Width 9.2500
Acquisition Time 1.3665
Acquisition Date 2015-04-20T21:19:00
Frequency 100.62
Nucleus 13C
F3C NO2
Me2N
CN
O
2.68

Parameter	Value
Title	AAG-07254-B
Solvent	CDCl3
Temperature	300.0
Number of Scans	16
Receiver Gain	362
Relaxation Delay	3.0000
Pulse Width	11.6200
Acquisition Time	0.4893
Acquisition Date	2015-04-16T18:22:00
Frequency	564.81
Nucleus	19F

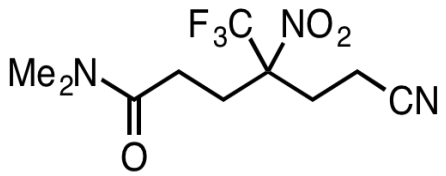

2.68

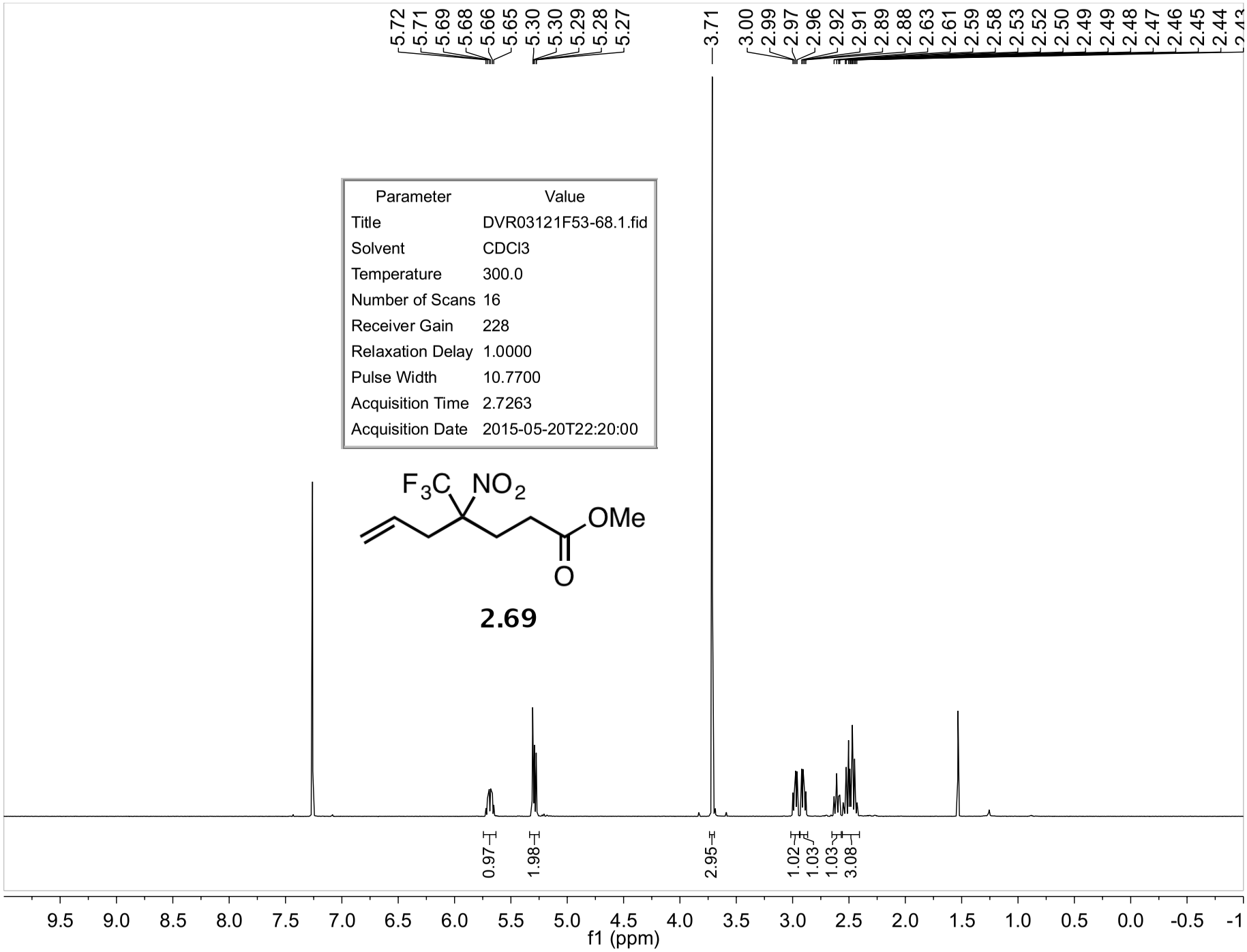
5.72
5.71
5.69
5.68
5.66
5.65
5.30
5.30
5.29
5.28
5.27
3.71
3.00
2.99
2.97
2.96
2.92
2.91
2.89
2.88
2.63
2.61
2.59
2.58
2.53
2.52
2.50
2.49
2.49
2.48
2.47
2.46
2.45
2.44
Parameter Value
Title DVR03121F53-68.1.fid
Solvent CDCl3
Temperature 300.0
Number of Scans 16
Receiver Gain 228
Relaxation Delay 1.0000
Pulse Width 10.7700
Acquisition Time 2.7263
Acquisition Date 2015-05-20T22:20:00
F3C NO2
OMe
O
2.69
0.97
1.98
2.95
1.02
1.03
1.03
3.08
9.5 9.0 8.5 8.0 7.5 7.0 6.5 6.0 5.5 5.0 4.5 4.0 3.5 3.0 2.5 2.0 1.5 1.0 0.5 0.0 -0.5 -1
f1 (ppm)

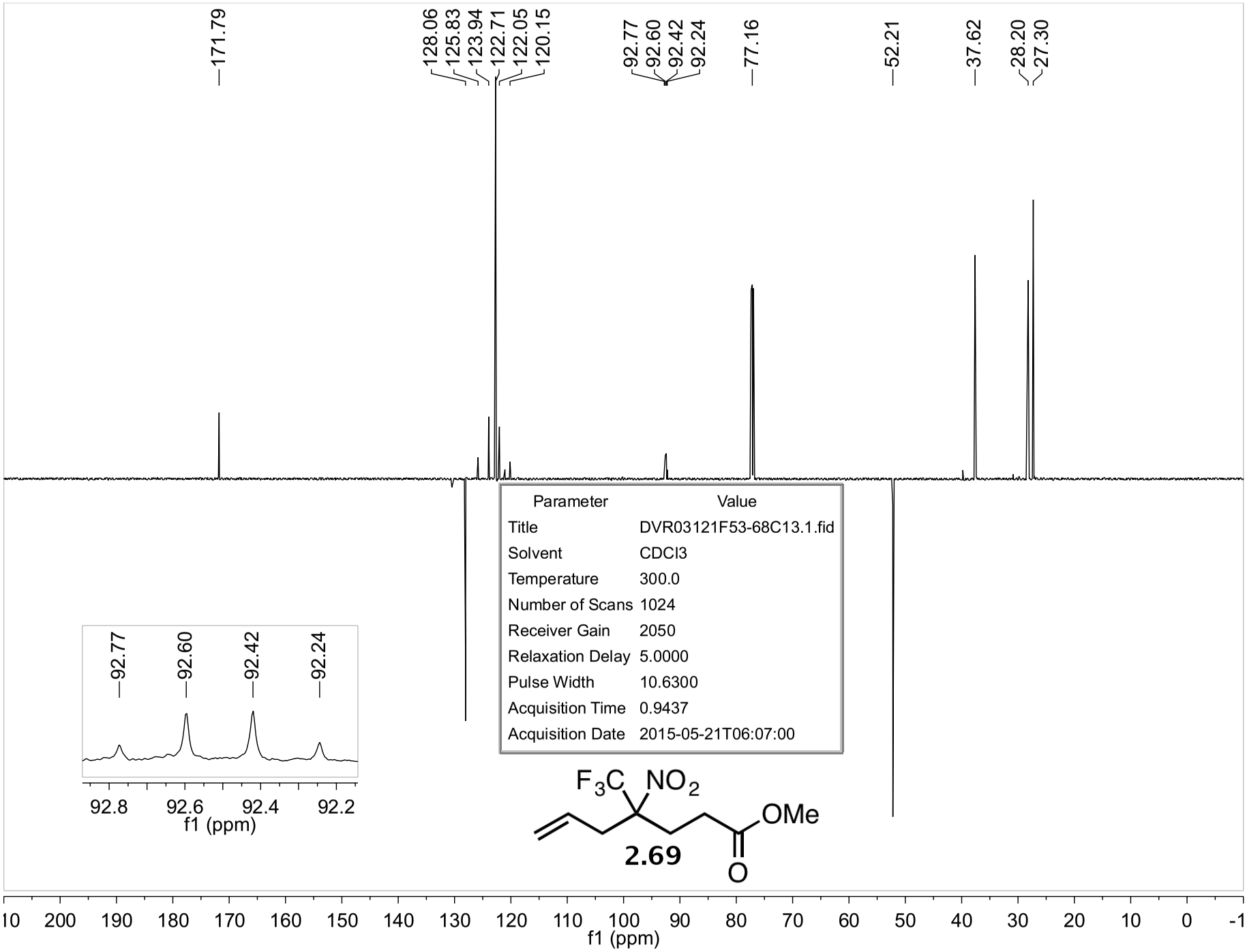
171.79
128.06
125.83
123.94
122.71
122.05
120.15
92.77
92.60
92.42
92.24
77.16
52.21
37.62
28.20
27.30
Parameter Value
Title DVR03121F53-68C13.1.fid
Solvent CDCl3
Temperature 300.0
Number of Scans 1024
Receiver Gain 2050
Relaxation Delay 5.0000
Pulse Width 10.6300
Acquisition Time 0.9437
Acquisition Date 2015-05-21T06:07:00
92.8
92.6
92.4
92.2
f1 (ppm)
F3C
NO2
OMe
O
2.69
f1 (ppm)

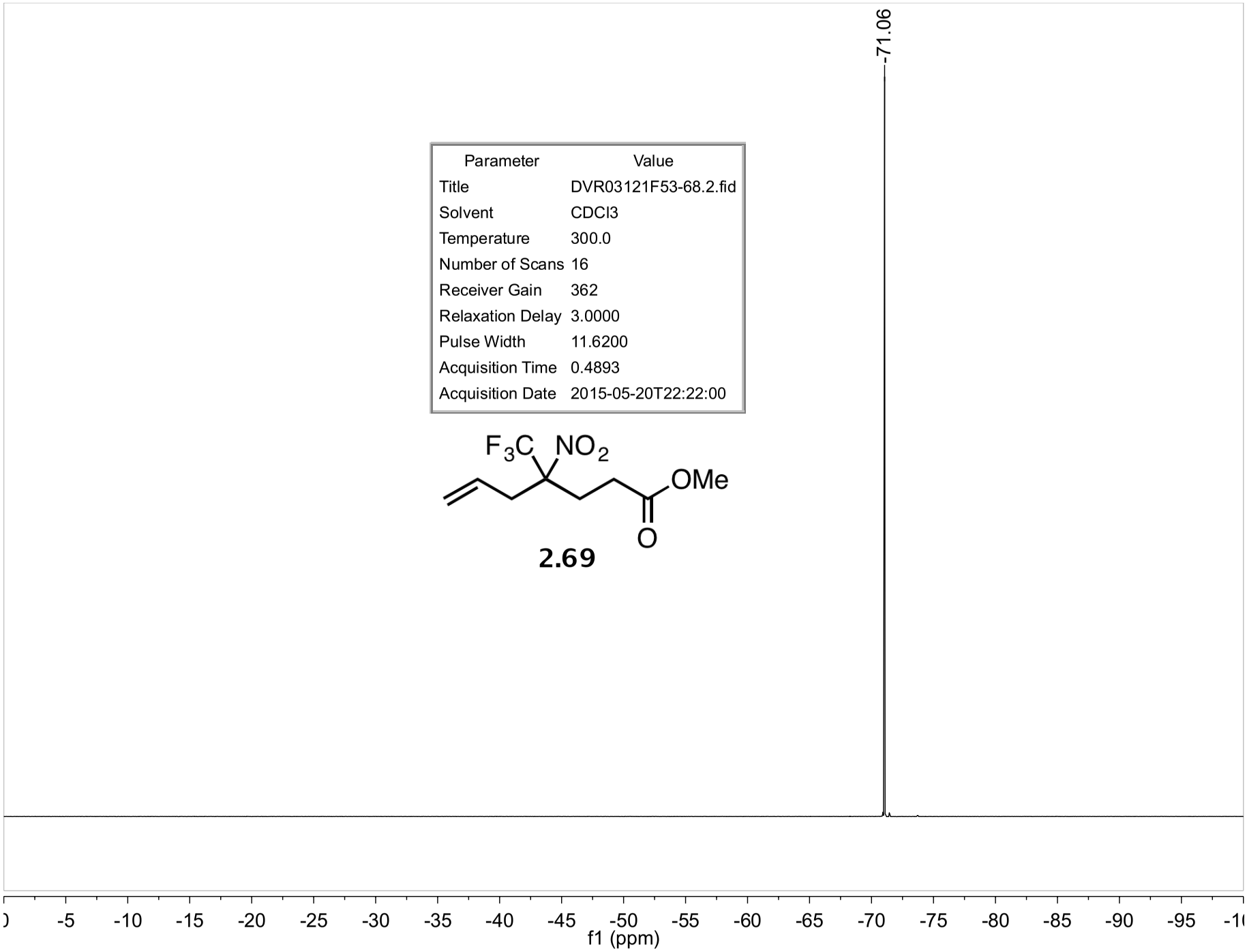
-71.06
Parameter Value
Title DVR03121F53-68.2.fid
Solvent CDCl3
Temperature 300.0
Number of Scans 16
Receiver Gain 362
Relaxation Delay 3.0000
Pulse Width 11.6200
Acquisition Time 0.4893
Acquisition Date 2015-05-20T22:22:00
F3C NO2
OMe
O
2.69
-5 -10 -15 -20 -25 -30 -35 -40 -45 -50 -55 -60 -65 -70 -75 -80 -85 -90 -95
f1 (ppm)

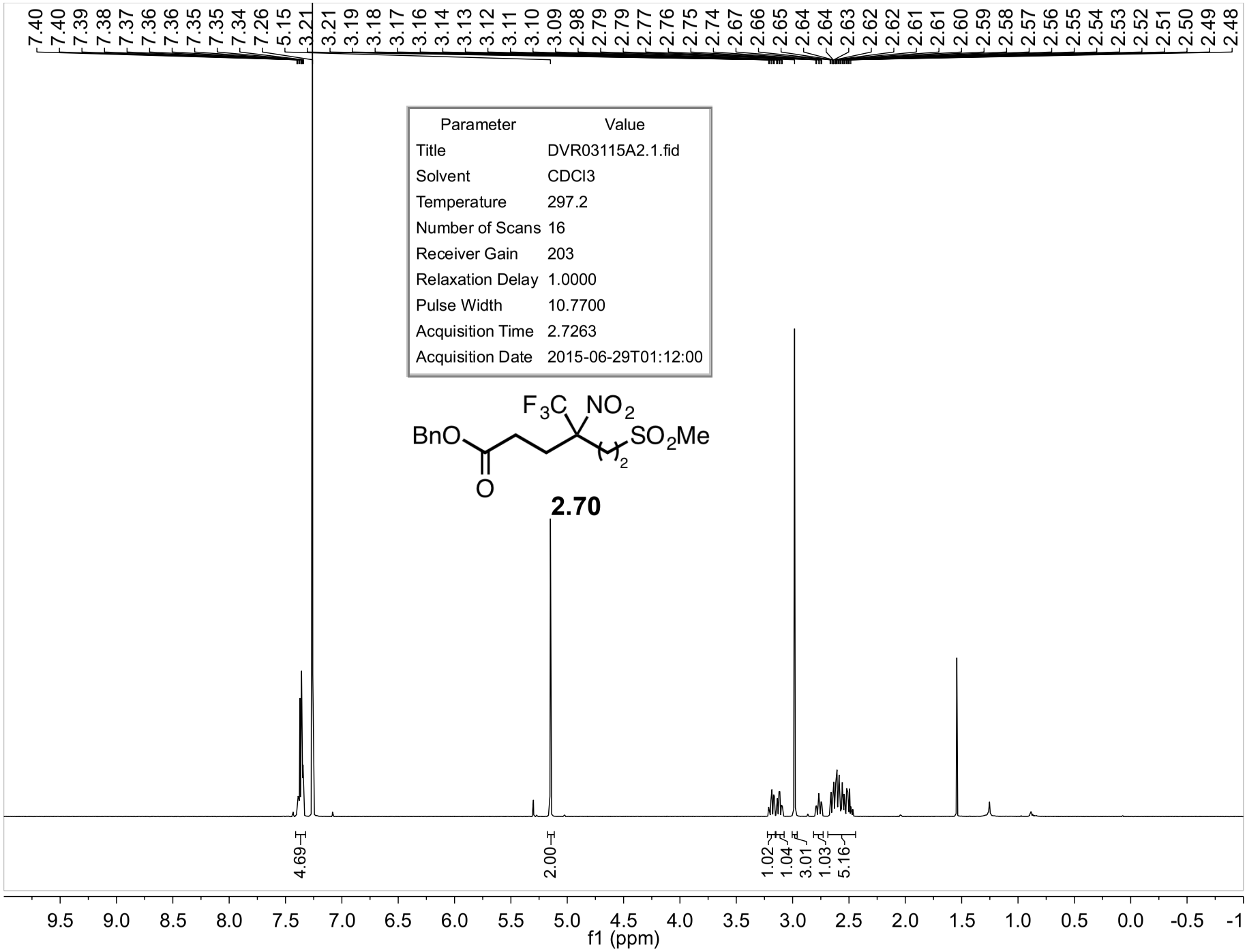
7.40 7.40 7.39 7.38 7.37 7.36 7.36 7.35 7.35 7.34 7.26 5.15 3.21
3.21 3.19 3.18 3.17 3.16 3.14 3.13 3.12 3.11 3.10 3.09 2.98 2.79 2.79 2.77 2.76 2.75 2.74 2.67 2.66 2.65 2.64 2.64 2.63 2.62 2.62 2.61 2.61 2.60 2.59 2.58 2.57 2.56 2.55 2.54 2.53 2.52 2.51 2.50 2.49 2.48
Parameter Value
Title DVR03115A2.1.fid
Solvent CDCl3
Temperature 297.2
Number of Scans 16
Receiver Gain 203
Relaxation Delay 1.0000
Pulse Width 10.7700
Acquisition Time 2.7263
Acquisition Date 2015-06-29T01:12:00
F3C NO2
BnO
SO2Me
2
O
2.70
4.69
2.00
1.02
1.04
3.01
1.03
5.16
9.5 9.0 8.5 8.0 7.5 7.0 6.5 6.0 5.5 5.0 4.5 4.0 3.5 3.0 2.5 2.0 1.5 1.0 0.5 0.0 -0.5 -1
f1 (ppm)

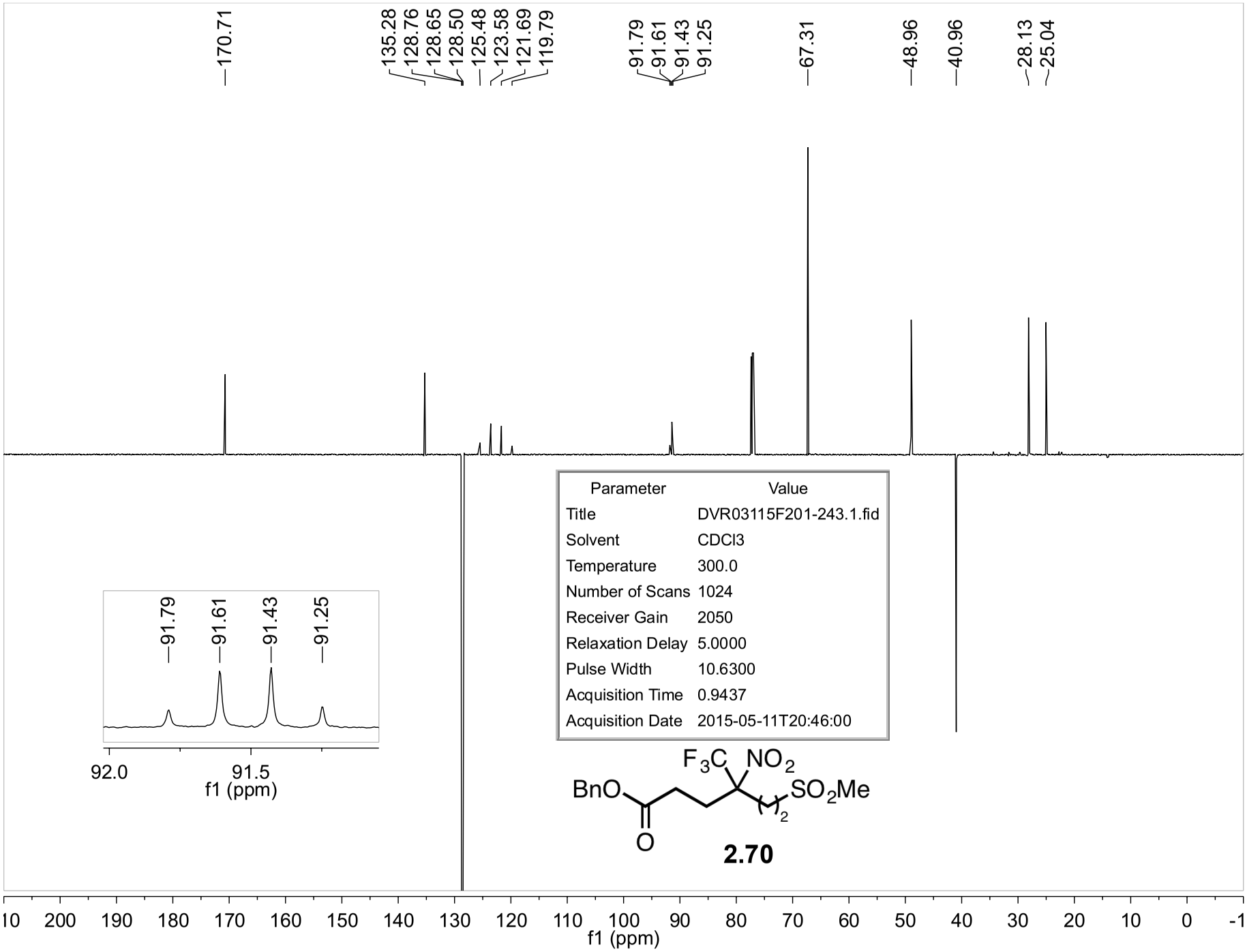
170.71
135.28
128.76
128.65
128.50
125.48
123.58
121.69
119.79
91.79
91.61
91.43
91.25
67.31
48.96
40.96
28.13
25.04
Parameter Value
Title DVR03115F201-243.1.fid
Solvent CDCl3
Temperature 300.0
Number of Scans 1024
Receiver Gain 2050
Relaxation Delay 5.0000
Pulse Width 10.6300
Acquisition Time 0.9437
Acquisition Date 2015-05-11T20:46:00
92.0
91.5
f1 (ppm)
F3C NO2
BnO
SO2Me
O
2.70
f1 (ppm)

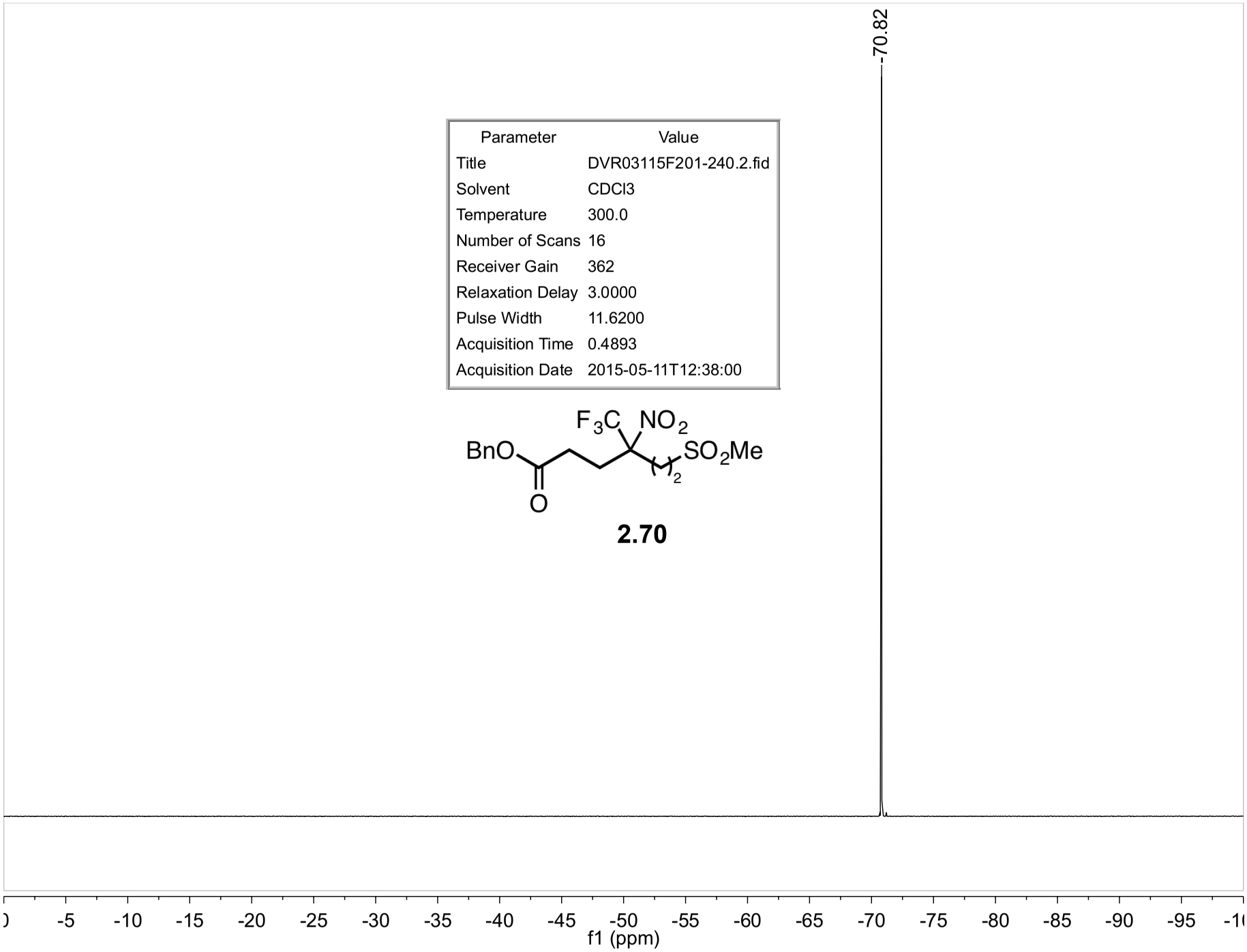
-70.82
Parameter Value
Title DVR03115F201-240.2.fid
Solvent CDCl3
Temperature 300.0
Number of Scans 16
Receiver Gain 362
Relaxation Delay 3.0000
Pulse Width 11.6200
Acquisition Time 0.4893
Acquisition Date 2015-05-11T12:38:00
F3C NO2
BnO
SO2Me
O
2.70
-5 -10 -15 -20 -25 -30 -35 -40 -45 -50 -55 -60 -65 -70 -75 -80 -85 -90 -95
f1 (ppm)

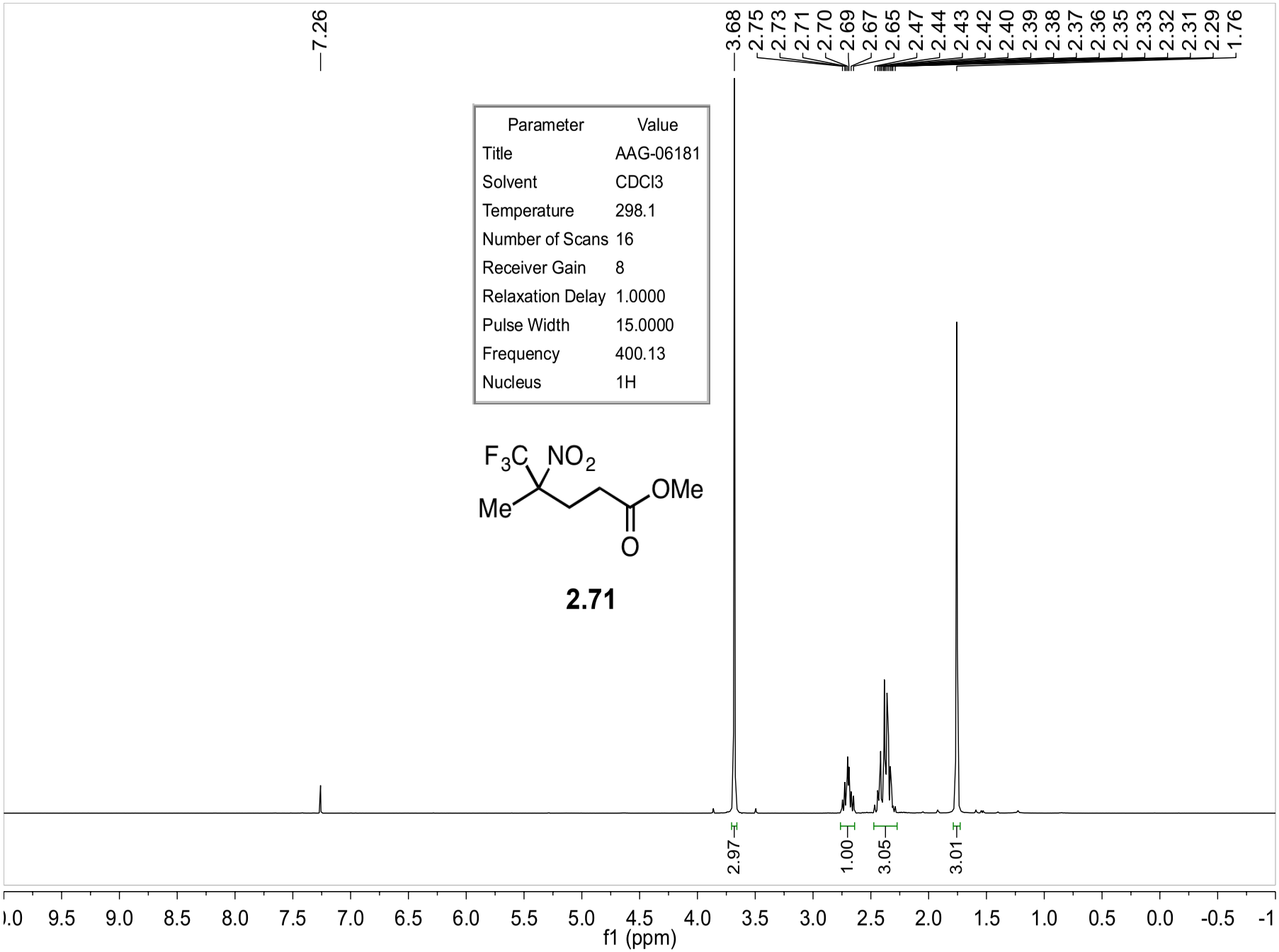
7.26
3.68
2.75
2.73
2.71
2.70
2.69
2.67
2.65
2.47
2.44
2.43
2.42
2.40
2.39
2.38
2.37
2.36
2.35
2.33
2.32
2.31
2.29
1.76
Parameter Value
Title AAG-06181
Solvent CDCl3
Temperature 298.1
Number of Scans 16
Receiver Gain 8
Relaxation Delay 1.0000
Pulse Width 15.0000
Frequency 400.13
Nucleus 1H
F3C NO2
Me
OMe
O
2.71
2.97
1.00
3.05
3.01
f1 (ppm)

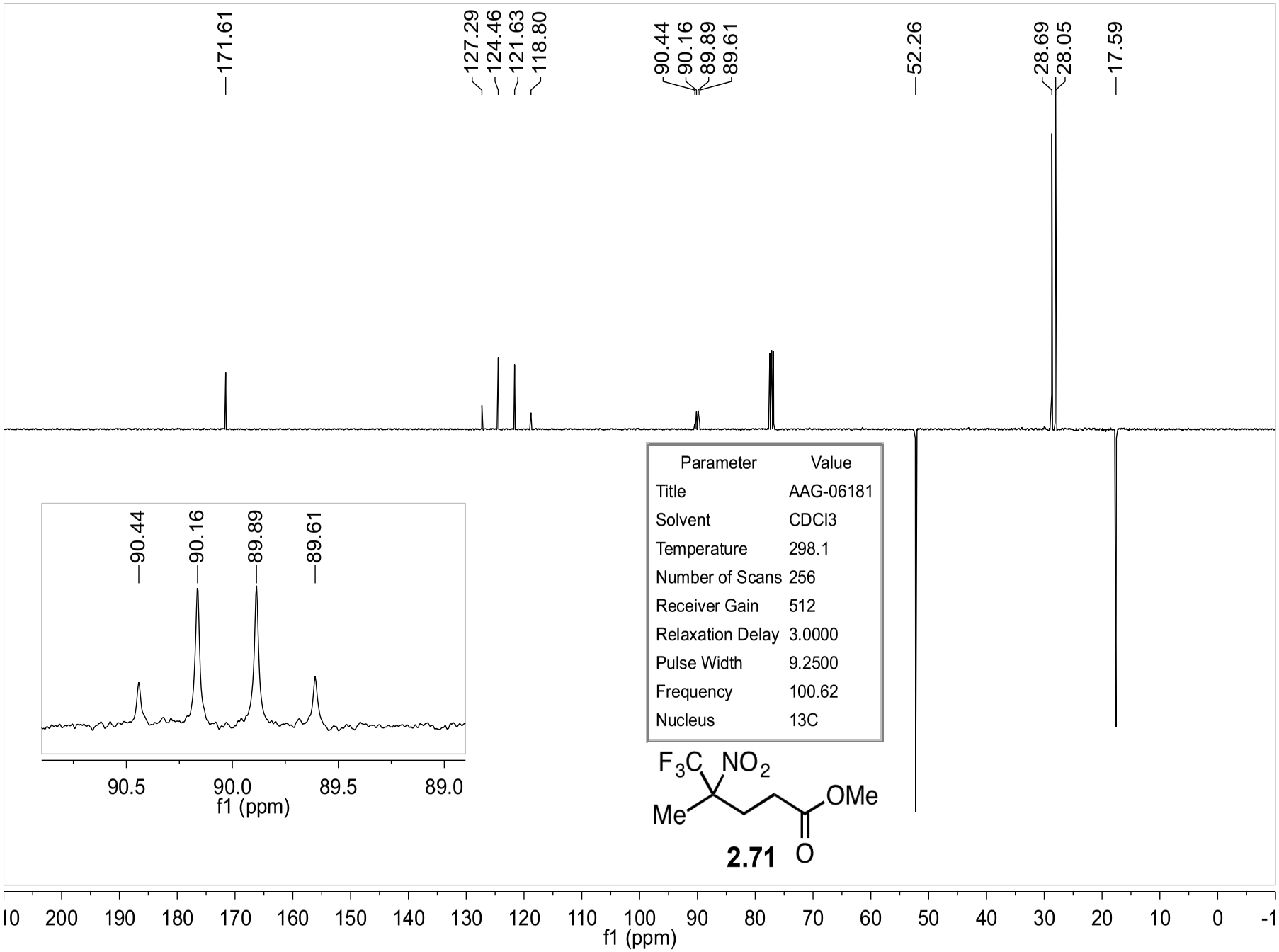
171.61
127.29
124.46
121.63
118.80
90.44
90.16
89.89
89.61
52.26
28.69
28.05
17.59
90.44
90.16
89.89
89.61
90.5
90.0
89.5
89.0
f1 (ppm)
Parameter Value
Title AAG-06181
Solvent CDCl3
Temperature 298.1
Number of Scans 256
Receiver Gain 512
Relaxation Delay 3.0000
Pulse Width 9.2500
Frequency 100.62
Nucleus 13C
F3C NO2
Me
OMe
O
2.71
f1 (ppm)

Parameter	Value
Title	AAG-06181-B
Solvent	CDCl3
Temperature	298.0
Number of Scans	16
Receiver Gain	322
Relaxation Delay	3.0000
Pulse Width	11.6200
Frequency	564.81
Nucleus	19F

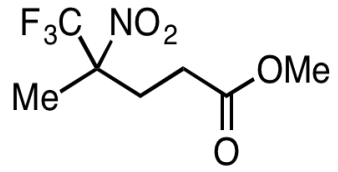

2.71

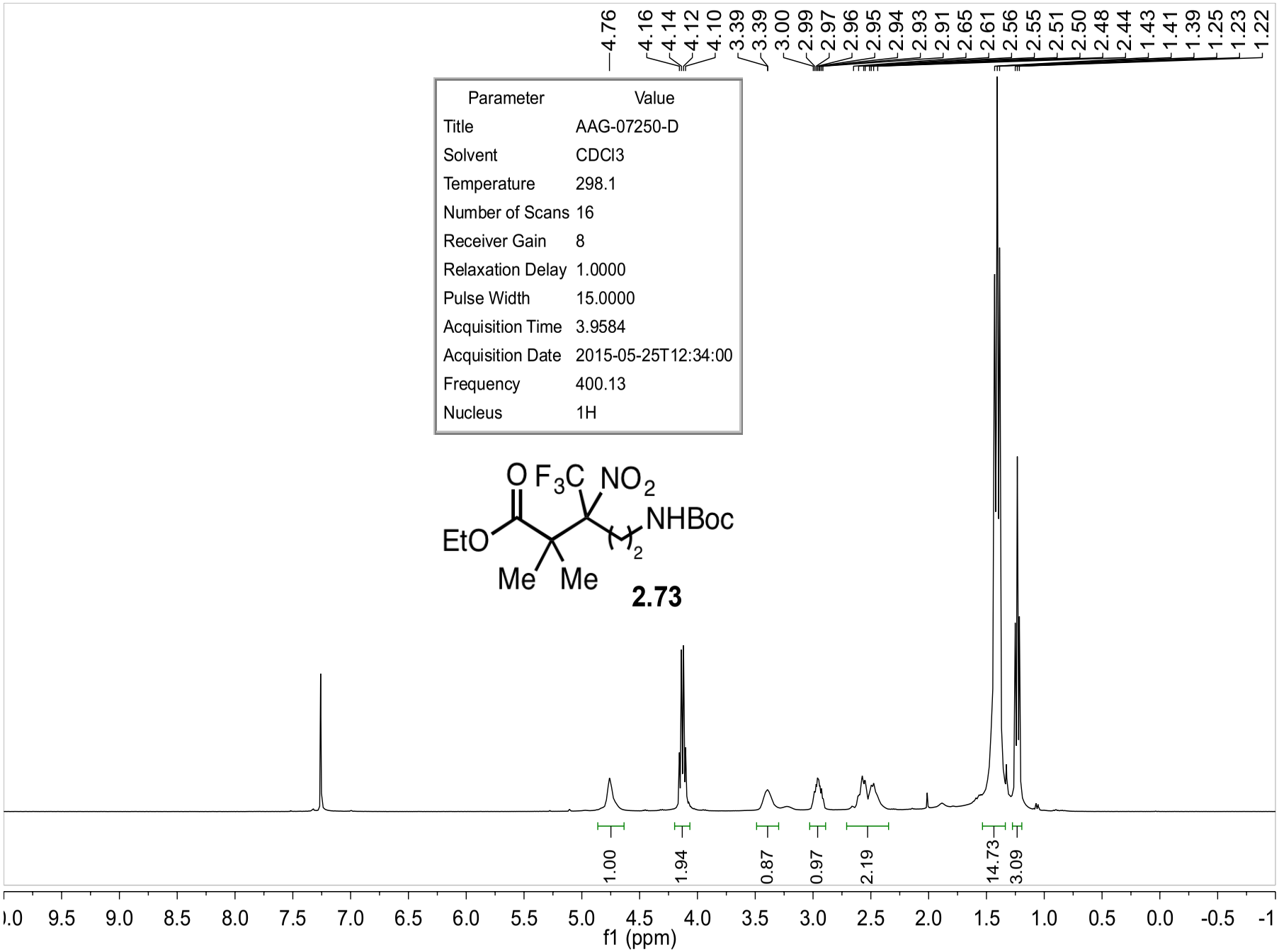
4.76
4.16
4.14
4.12
4.10
3.39
3.39
3.00
2.99
2.97
2.96
2.95
2.94
2.93
2.91
2.65
2.61
2.56
2.55
2.51
2.50
2.48
2.44
1.43
1.41
1.39
1.25
1.23
1.22
Parameter Value
Title AAG-07250-D
Solvent CDCl3
Temperature 298.1
Number of Scans 16
Receiver Gain 8
Relaxation Delay 1.0000
Pulse Width 15.0000
Acquisition Time 3.9584
Acquisition Date 2015-05-25T12:34:00
Frequency 400.13
Nucleus 1H
O
F3C
NO2
NHBoc
EtO
2
Me
Me
2.73
1.00
1.94
0.87
0.97
2.19
14.73
3.09
f1 (ppm)

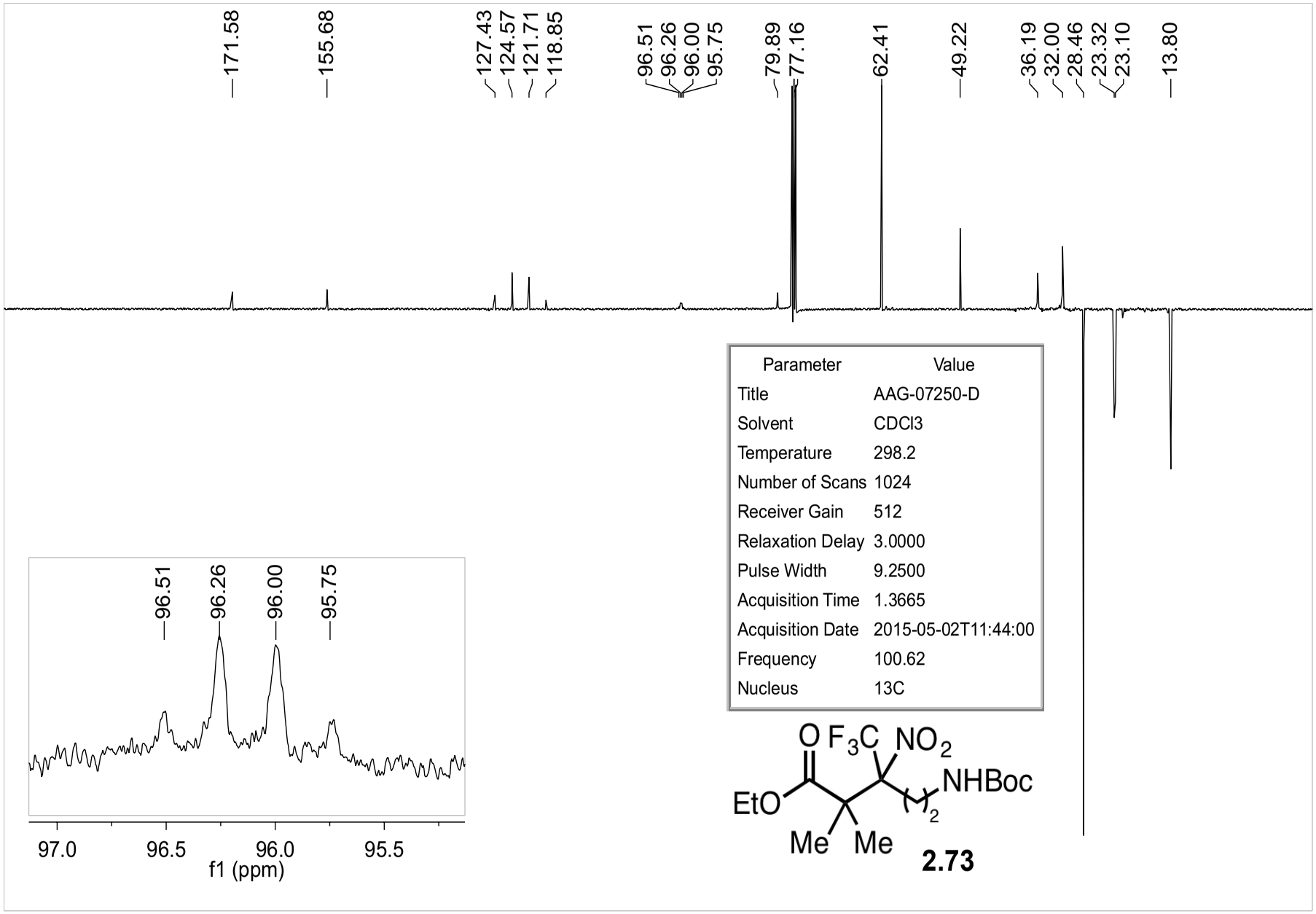
171.58
155.68
127.43
124.57
121.71
118.85
96.51
96.26
96.00
95.75
79.89
77.16
62.41
49.22
36.19
32.00
28.46
23.32
23.10
13.80
Parameter Value
Title AAG-07250-D
Solvent CDCl3
Temperature 298.2
Number of Scans 1024
Receiver Gain 512
Relaxation Delay 3.0000
Pulse Width 9.2500
Acquisition Time 1.3665
Acquisition Date 2015-05-02T11:44:00
Frequency 100.62
Nucleus 13C
97.0
96.5
96.0
95.5
f1 (ppm)
O F3C NO2
NHBoc
EtO
Me Me
2.73
f1 (ppm)

Parameter	Value
Title	AAG-07250-D
Solvent	CDCl3
Temperature	300.0
Number of Scans	16
Receiver Gain	362
Relaxation Delay	3.0000
Pulse Width	11.6200
Acquisition Time	0.4893
Acquisition Date	2015-05-01T11:43:00
Frequency	564.81
Nucleus	19F

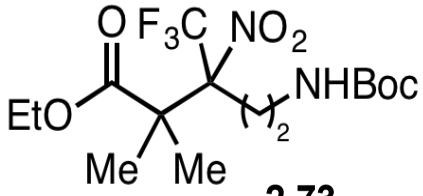

2.73

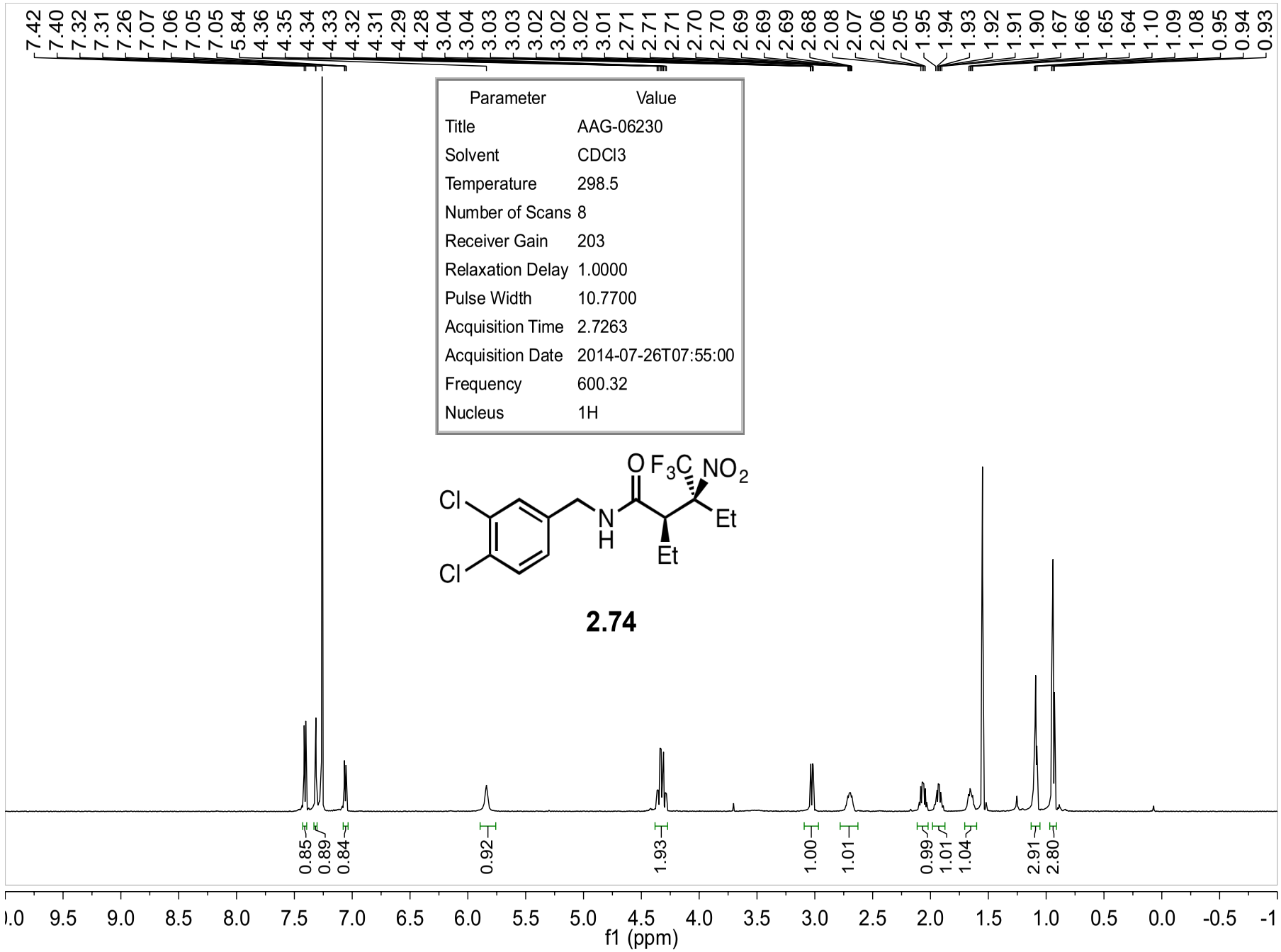
7.42 7.40 7.32 7.31 7.26 7.07 7.06 7.05 7.05 5.84 4.36 4.35 4.34 4.33 4.32 4.31 4.29 4.28 3.04 3.04 3.03 3.03 3.02 3.02 3.02 3.01 2.71 2.71 2.71 2.70 2.70 2.69 2.69 2.69 2.68 2.08 2.07 2.06 2.05 1.95 1.94 1.93 1.92 1.91 1.90 1.67 1.66 1.65 1.64 1.10 1.09 1.08 0.95 0.94 0.93
Parameter Value
Title AAG-06230
Solvent CDCl3
Temperature 298.5
Number of Scans 8
Receiver Gain 203
Relaxation Delay 1.0000
Pulse Width 10.7700
Acquisition Time 2.7263
Acquisition Date 2014-07-26T07:55:00
Frequency 600.32
Nucleus 1H
Cl
Cl
N
H
O
F3C
NO2
Et
Et
2.74
0.85
0.89
0.84
0.92
1.93
1.00
1.01
0.99
1.01
1.04
2.91
2.80
f1 (ppm)

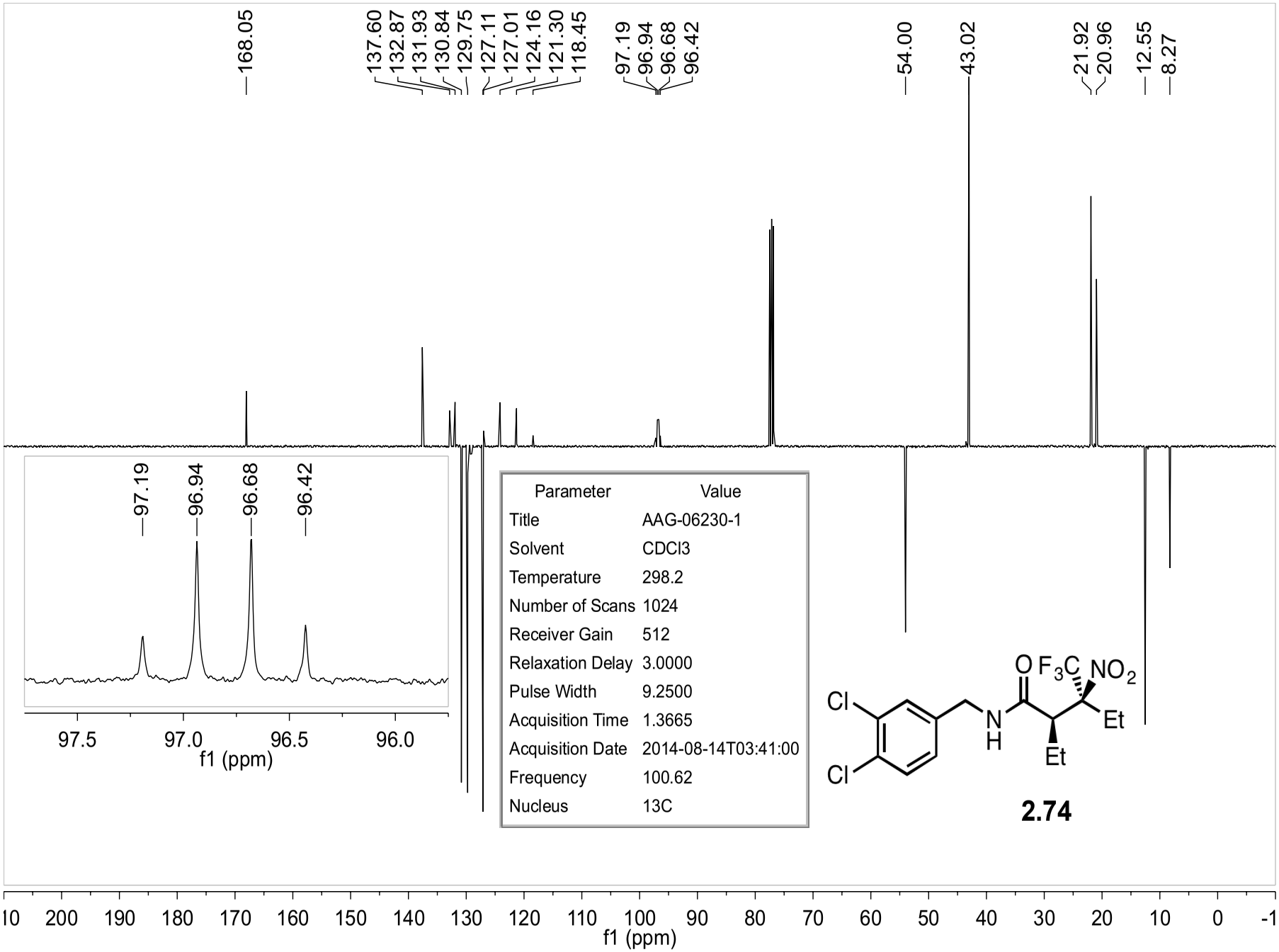
168.05
137.60
132.87
131.93
130.84
129.75
127.11
127.01
124.16
121.30
118.45
97.19
96.94
96.68
96.42
54.00
43.02
21.92
20.96
12.55
8.27
97.19
96.94
96.68
96.42
97.5
97.0
96.5
96.0
f1 (ppm)
Parameter Value
Title AAG-06230-1
Solvent CDCl3
Temperature 298.2
Number of Scans 1024
Receiver Gain 512
Relaxation Delay 3.0000
Pulse Width 9.2500
Acquisition Time 1.3665
Acquisition Date 2014-08-14T03:41:00
Frequency 100.62
Nucleus 13C
O
F3C
NO2
Cl
Cl
N
H
Et
Et
2.74
f1 (ppm)

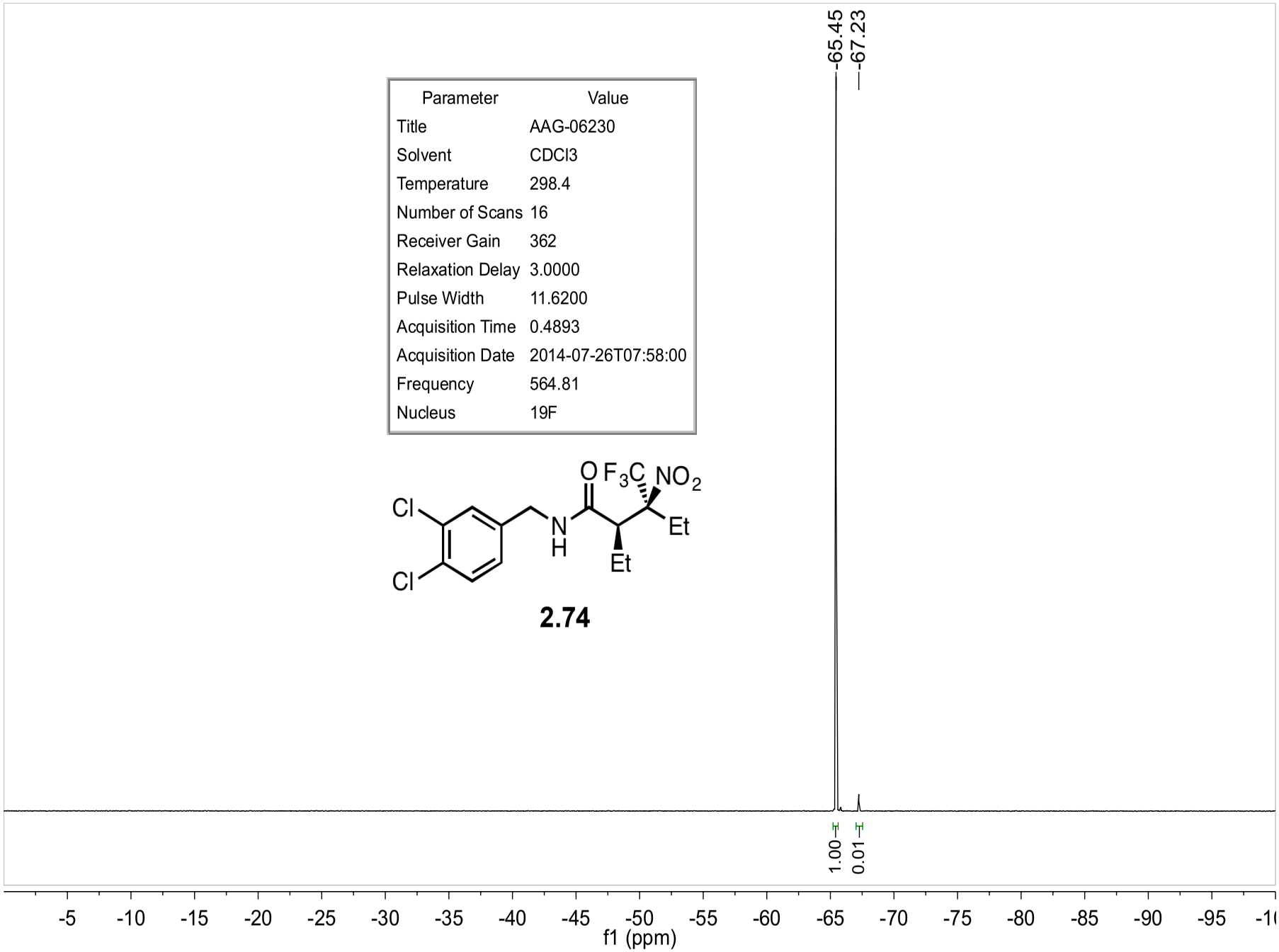

Parameter	Value
Title	AAG-06230
Solvent	CDCl3
Temperature	298.4
Number of Scans	16
Receiver Gain	362
Relaxation Delay	3.0000
Pulse Width	11.6200
Acquisition Time	0.4893
Acquisition Date	2014-07-26T07:58:00
Frequency	564.81
Nucleus	19F

2.74

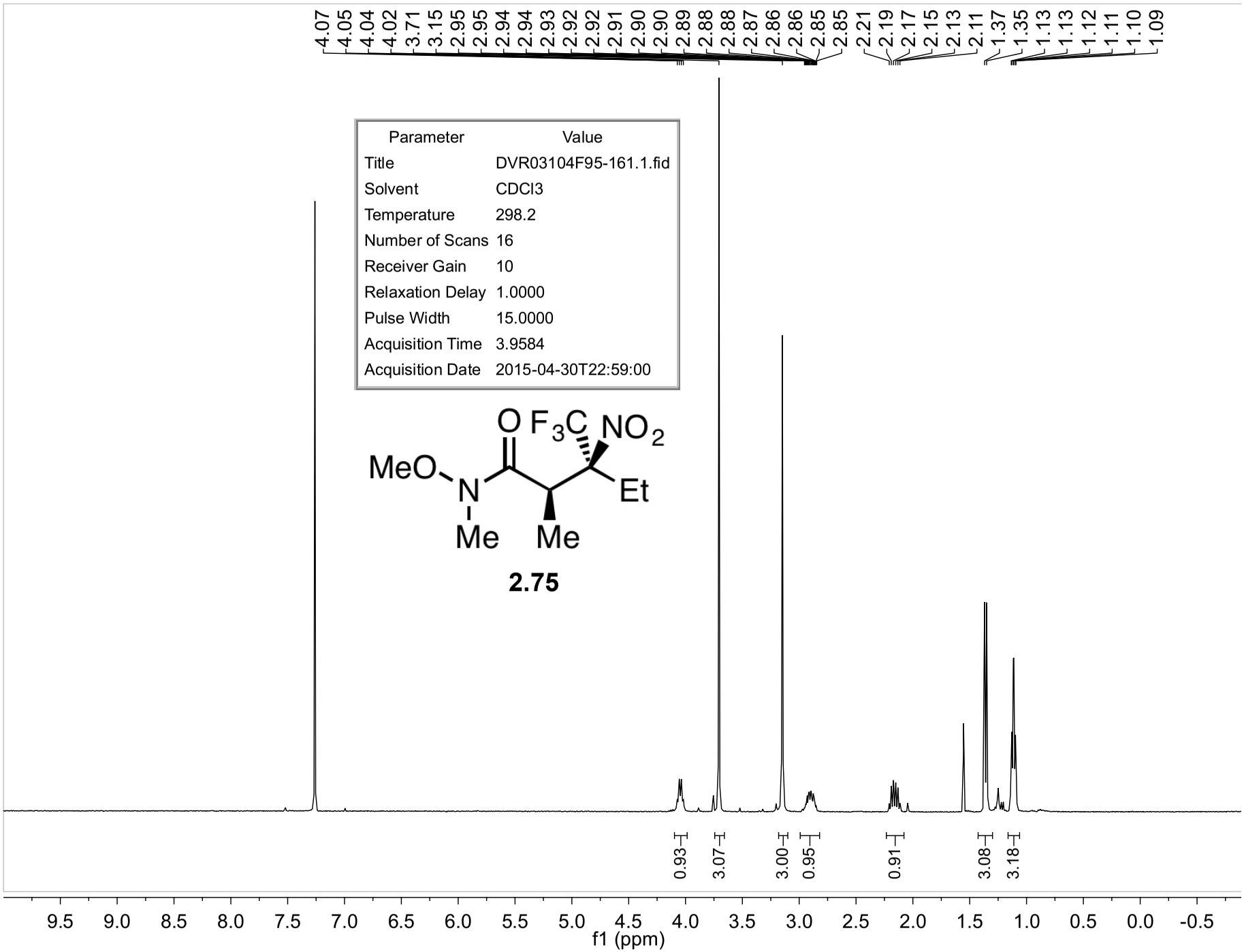
4.07 4.05 4.04 4.02 3.71 3.15 2.95 2.95 2.94 2.94 2.93 2.92 2.92 2.91 2.90 2.90 2.89 2.88 2.88 2.87 2.86 2.86 2.85 2.85 2.21 2.19 2.17 2.15 2.13 2.11 1.37 1.35 1.13 1.13 1.12 1.11 1.10 1.09
Parameter Value
Title DVR03104F95-161.1.fid
Solvent CDCl3
Temperature 298.2
Number of Scans 16
Receiver Gain 10
Relaxation Delay 1.0000
Pulse Width 15.0000
Acquisition Time 3.9584
Acquisition Date 2015-04-30T22:59:00
O F3C NO2
MeO N Et
Me Me
2.75
0.93 3.07 3.00 0.95 0.91 3.08 3.18
9.5 9.0 8.5 8.0 7.5 7.0 6.5 6.0 5.5 5.0 4.5 4.0 3.5 3.0 2.5 2.0 1.5 1.0 0.5 0.0 -0.5
f1 (ppm)

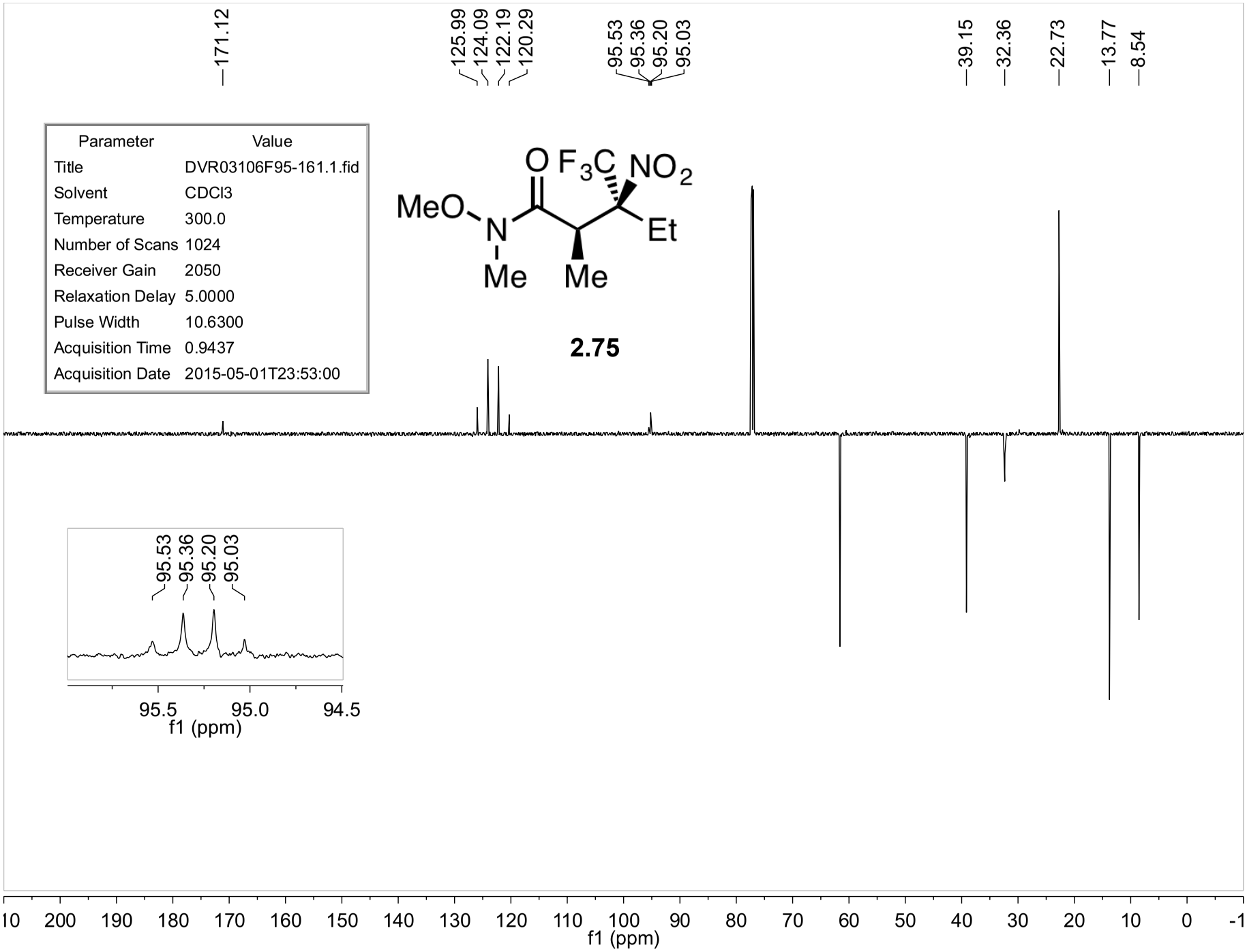
171.12
125.99
124.09
122.19
120.29
95.53
95.36
95.20
95.03
39.15
32.36
22.73
13.77
8.54
Parameter Value
Title DVR03106F95-161.1.fid
Solvent CDCl3
Temperature 300.0
Number of Scans 1024
Receiver Gain 2050
Relaxation Delay 5.0000
Pulse Width 10.6300
Acquisition Time 0.9437
Acquisition Date 2015-05-01T23:53:00
O F3C NO2
MeO N Et
Me Me
2.75
95.5 95.0 94.5
f1 (ppm)
f1 (ppm)

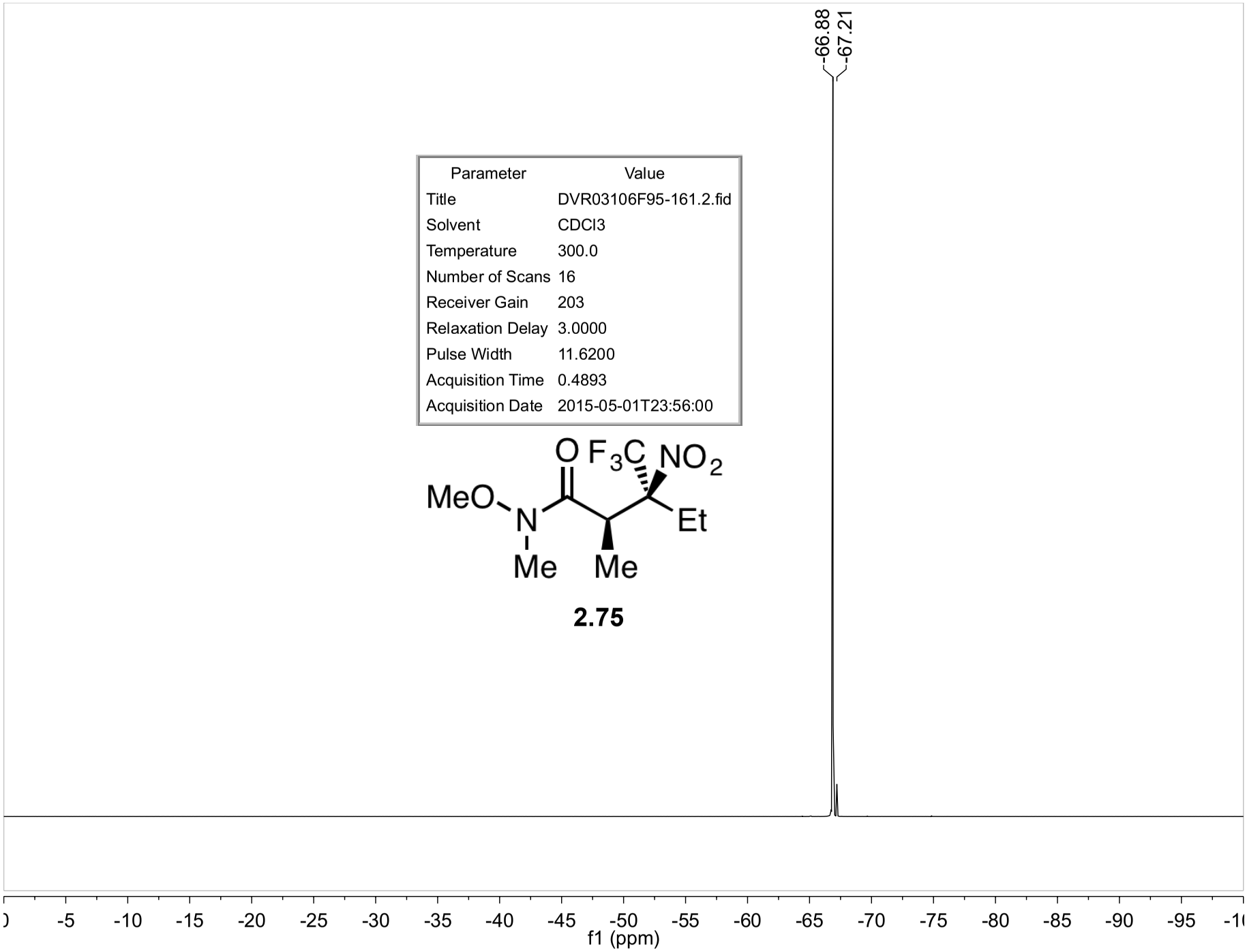
-66.88
-67.21
Parameter Value
Title DVR03106F95-161.2.fid
Solvent CDCl3
Temperature 300.0
Number of Scans 16
Receiver Gain 203
Relaxation Delay 3.0000
Pulse Width 11.6200
Acquisition Time 0.4893
Acquisition Date 2015-05-01T23:56:00
O F3C NO2
MeO N Et
Me Me
2.75
-5 -10 -15 -20 -25 -30 -35 -40 -45 -50 -55 -60 -65 -70 -75 -80 -85 -90 -95
f1 (ppm)

Parameter	Value
1 Title	DVR03126CRD.1.fid
2 Solvent	CDCl3
3 Temperature	300.0
4 Number of Scans	16
5 Receiver Gain	203
6 Relaxation Delay	1.0000
7 Pulse Width	10.7700
8 Spectrometer Frequency	600.32
9 Nucleus	1H

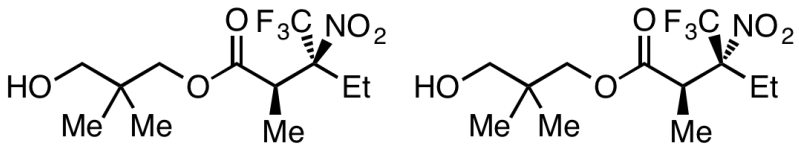

Crude

2.76A dr: 83:17 2.76B

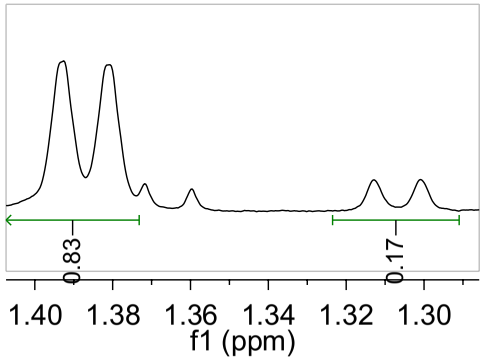

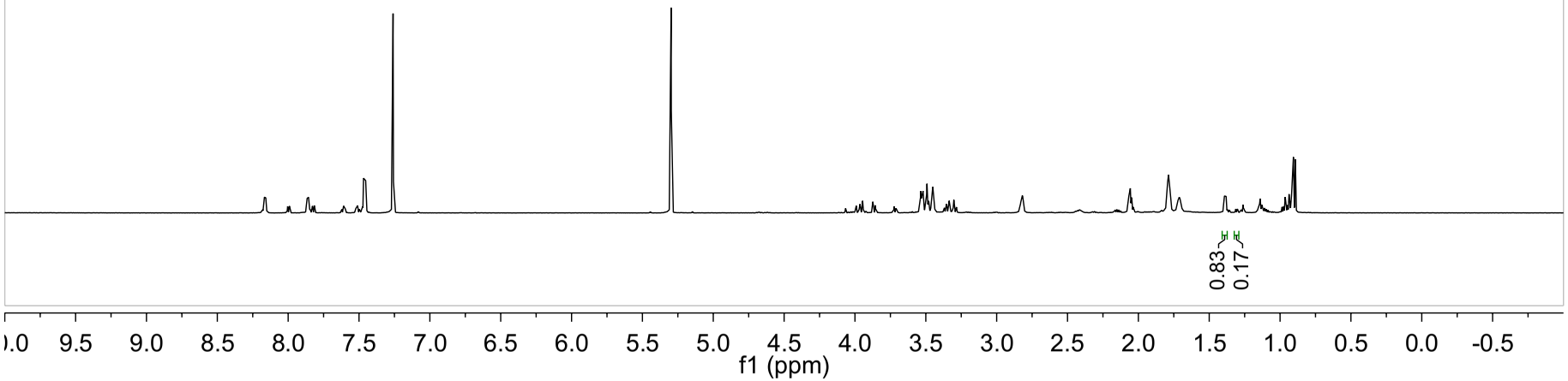

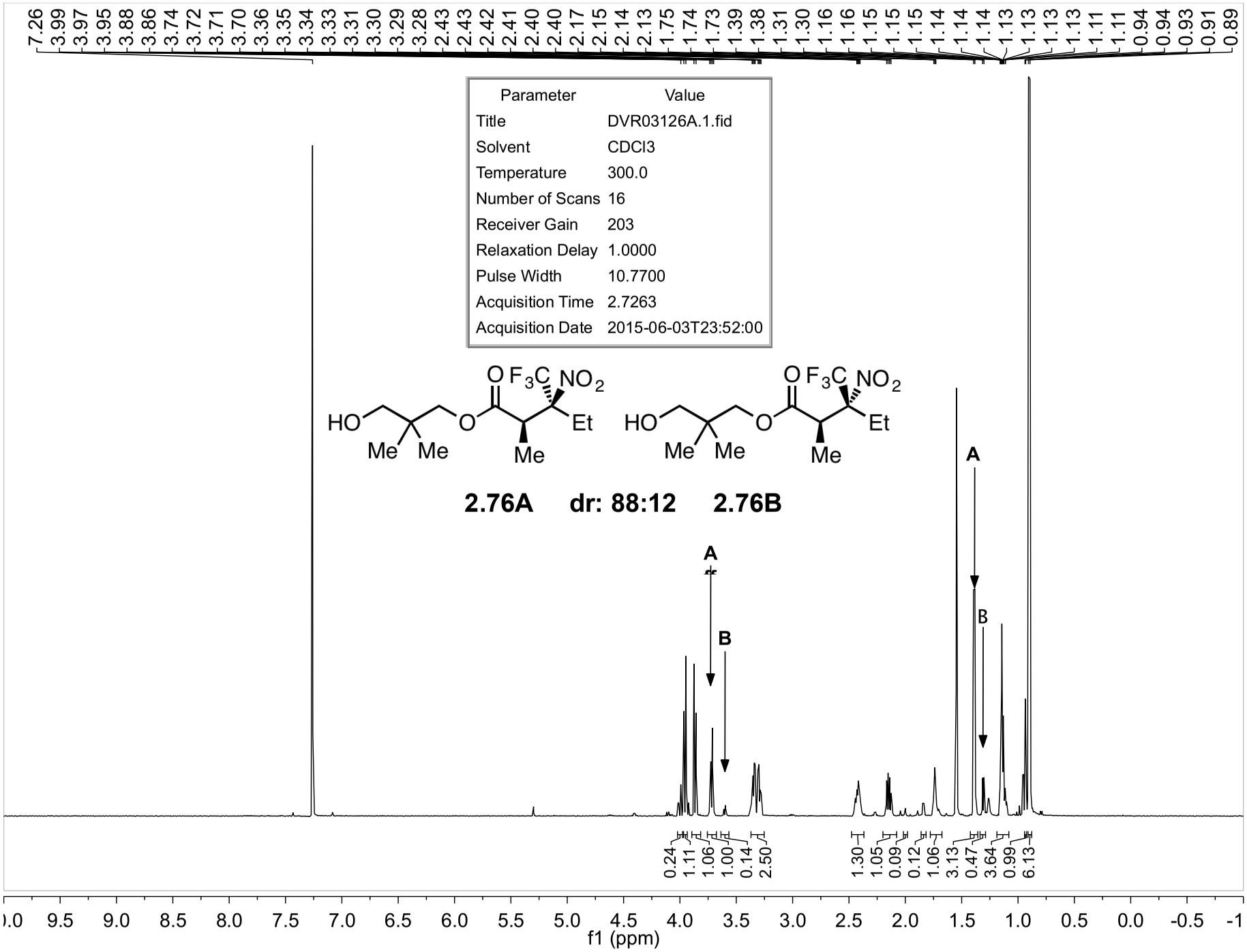
7.26 3.99 3.97 3.95 3.88 3.86 3.74 3.72 3.71 3.70 3.36 3.35 3.34 3.33 3.31 3.30 3.29 3.28 2.43 2.43 2.42 2.41 2.40 2.40 2.17 2.15 2.14 2.13 1.75 1.74 1.73 1.39 1.38 1.31 1.30 1.16 1.16 1.15 1.15 1.15 1.14 1.14 1.14 1.13 1.13 1.13 1.13 1.11 1.11 0.94 0.94 0.93 0.91 0.89
Parameter Value
Title DVR03126A.1.fid
Solvent CDCl3
Temperature 300.0
Number of Scans 16
Receiver Gain 203
Relaxation Delay 1.0000
Pulse Width 10.7700
Acquisition Time 2.7263
Acquisition Date 2015-06-03T23:52:00
HO Me Me O O F3C NO2 Et Me
HO Me Me O O F3C NO2 Et Me
2.76A dr: 88:12 2.76B
A
B
A
B
0.24 1.11 1.06 1.00 0.14 2.50
1.30 1.05 0.09 0.12 1.06 3.13 0.47 3.64 0.99 6.13
f1 (ppm)

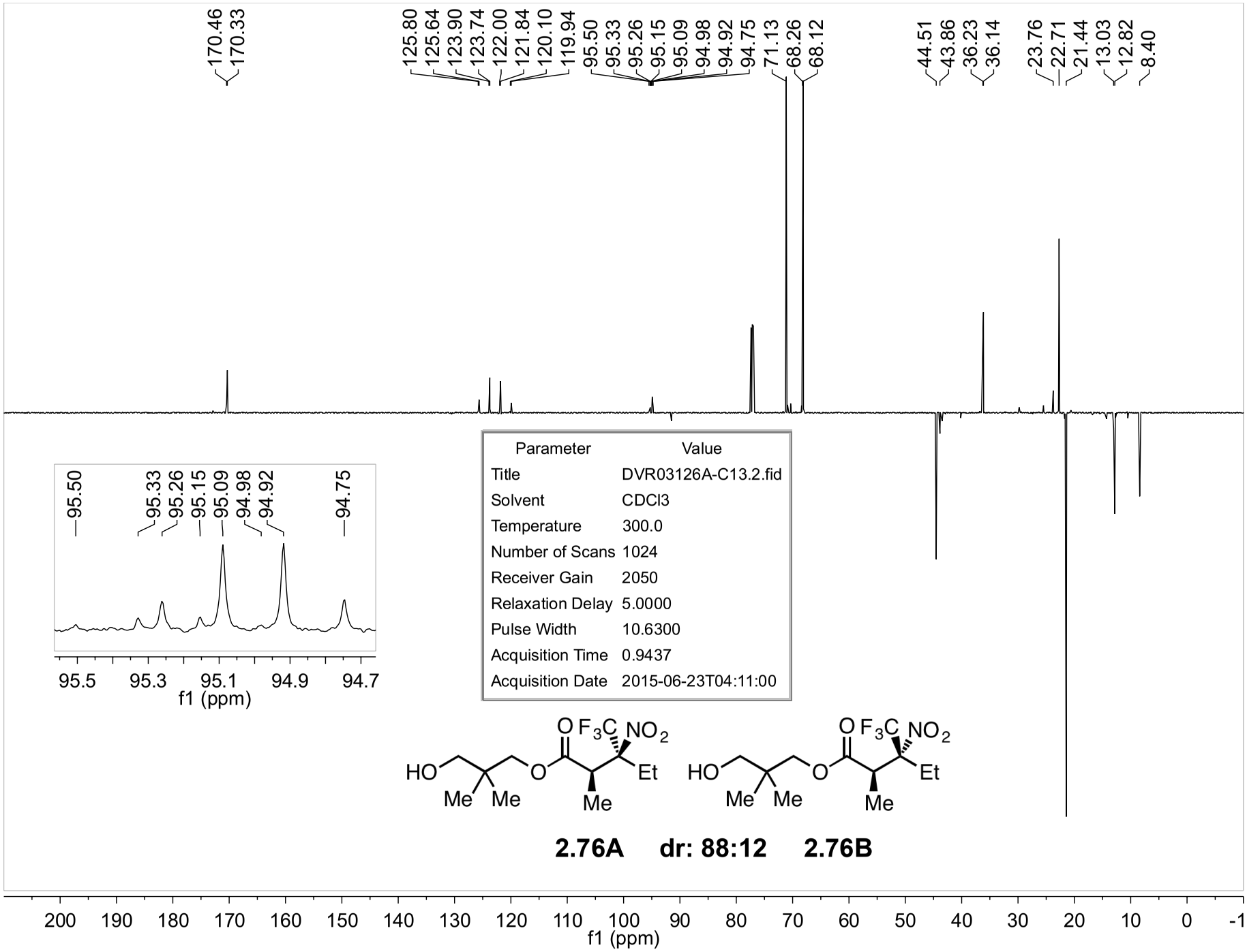
170.46
170.33
125.80
125.64
123.90
123.74
122.00
121.84
120.10
119.94
95.50
95.33
95.26
95.15
95.09
94.98
94.92
94.75
71.13
68.26
68.12
44.51
43.86
36.23
36.14
23.76
22.71
21.44
13.03
12.82
8.40
95.5
95.3
95.1
94.9
94.7
f1 (ppm)
Parameter Value
Title DVR03126A-C13.2.fid
Solvent CDCl3
Temperature 300.0
Number of Scans 1024
Receiver Gain 2050
Relaxation Delay 5.0000
Pulse Width 10.6300
Acquisition Time 0.9437
Acquisition Date 2015-06-23T04:11:00
HO
Me
Me
O
O
F3C
NO2
Et
Me
2.76A dr: 88:12 2.76B
200 190 180 170 160 150 140 130 120 110 100 90 80 70 60 50 40 30 20 10 0 -1
f1 (ppm)

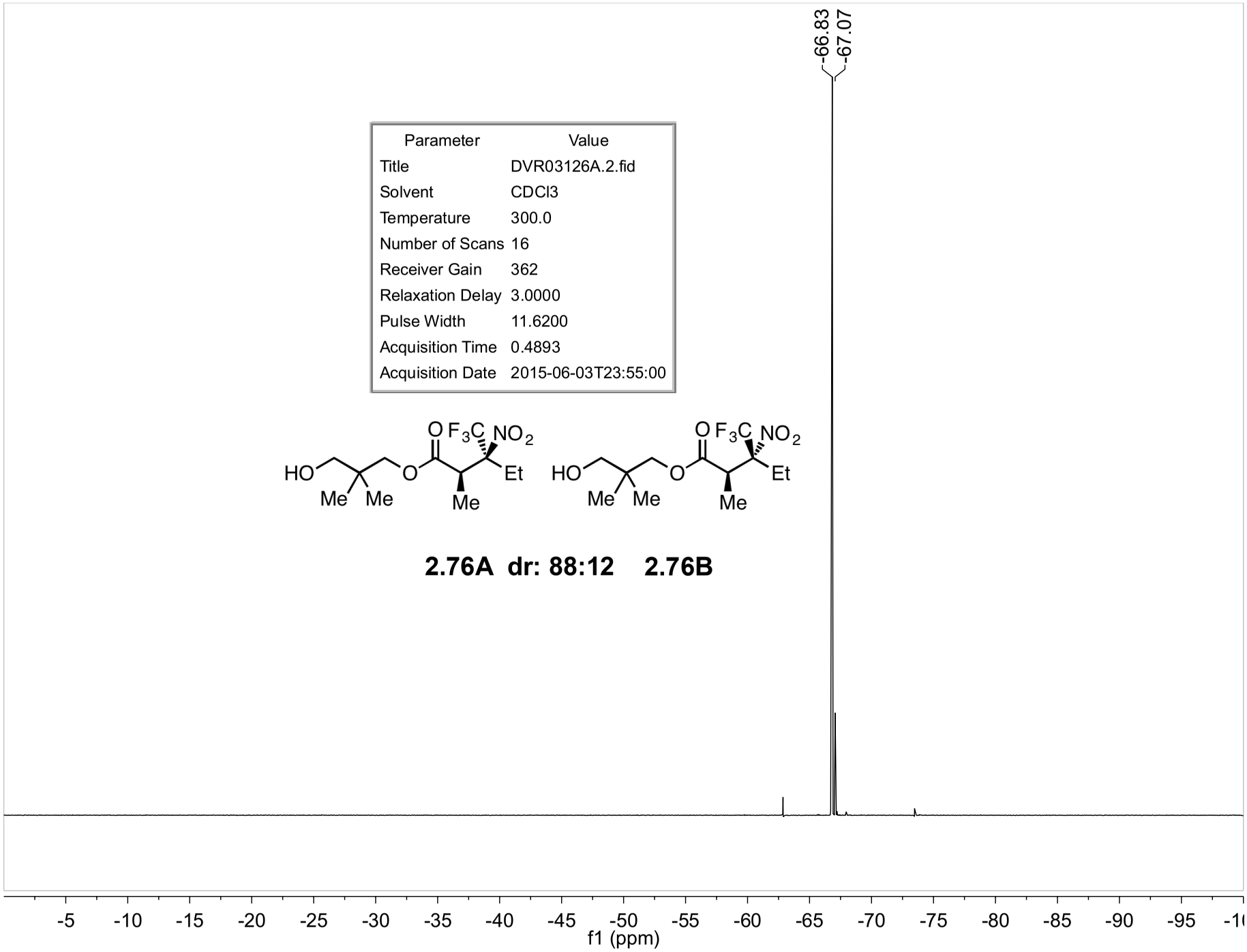
-66.83
-67.07
Parameter Value
Title DVR03126A.2.fid
Solvent CDCl3
Temperature 300.0
Number of Scans 16
Receiver Gain 362
Relaxation Delay 3.0000
Pulse Width 11.6200
Acquisition Time 0.4893
Acquisition Date 2015-06-03T23:55:00
HO
Me Me
O
O F3C NO2
Et
Me
2.76A dr: 88:12 2.76B
-5 -10 -15 -20 -25 -30 -35 -40 -45 -50 -55 -60 -65 -70 -75 -80 -85 -90 -95
f1 (ppm)

Parameter	Value
1 Title	DVR03122CRD.1.fid
2 Solvent	CDCl3
3 Temperature	300.0
4 Number of Scans	16
5 Receiver Gain	144
6 Relaxation Delay	1.0000
7 Pulse Width	10.7700
8 Spectrometer Frequency	600.32
9 Nucleus	1H

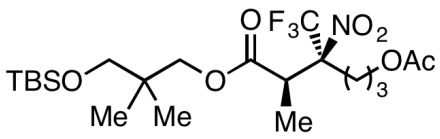

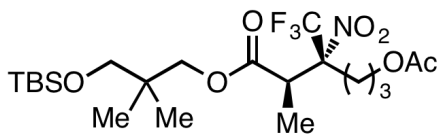

Crude

2.77A dr: 85:15 2.77B

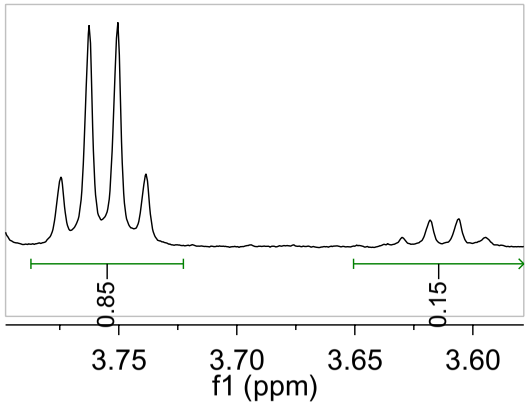

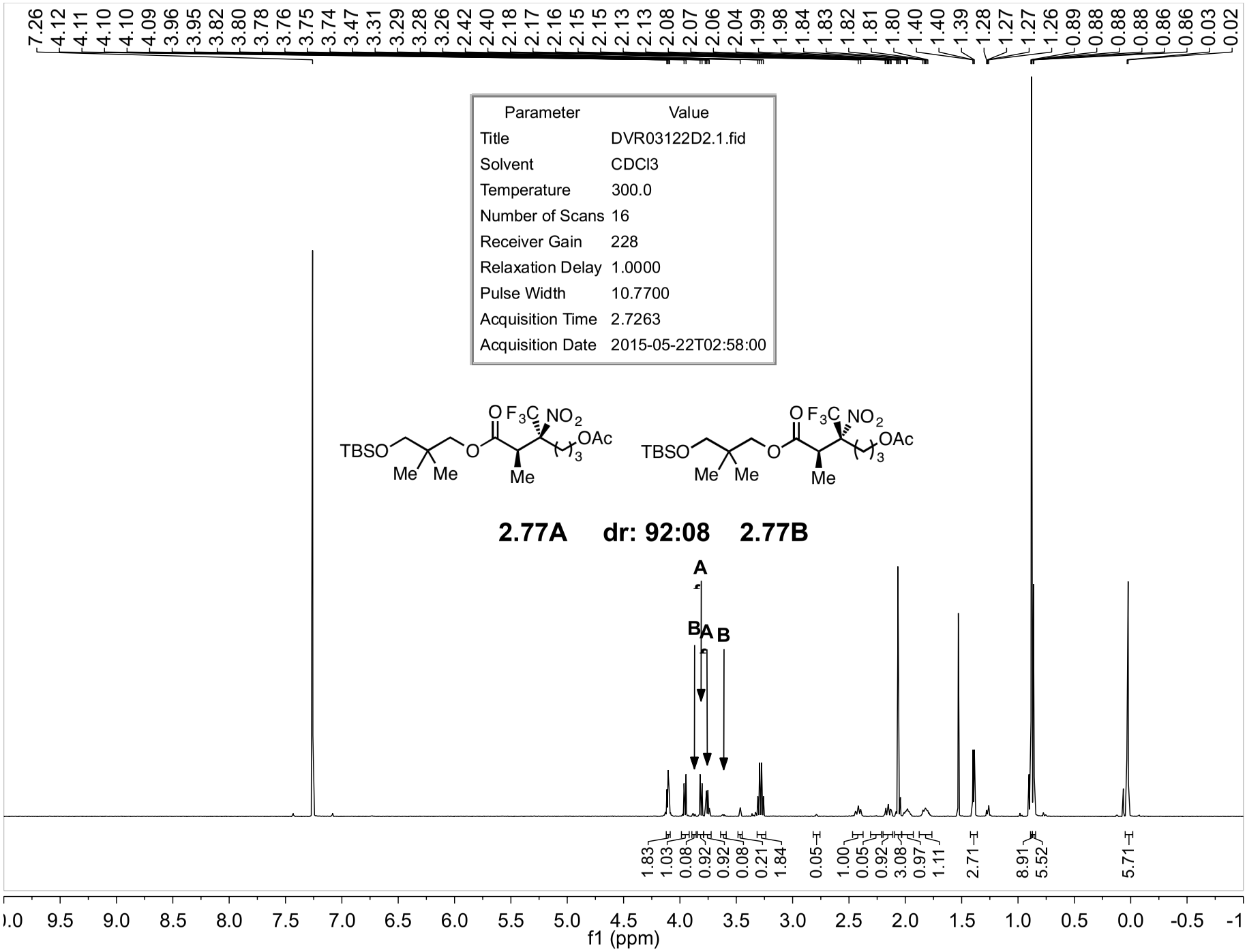
7.26 4.12 4.11 4.10 4.10 4.09 3.96 3.95 3.82 3.80 3.78 3.76 3.75 3.74 3.47 3.31 3.29 3.28 3.26 2.42 2.40 2.18 2.17 2.16 2.15 2.15 2.13 2.13 2.08 2.07 2.06 2.04 1.99 1.98 1.84 1.83 1.82 1.81 1.80 1.40 1.40 1.39 1.28 1.27 1.27 1.26 0.89 0.88 0.88 0.88 0.86 0.86 0.03 0.02
Parameter Value
Title DVR03122D2.1.fid
Solvent CDCl3
Temperature 300.0
Number of Scans 16
Receiver Gain 228
Relaxation Delay 1.0000
Pulse Width 10.7700
Acquisition Time 2.7263
Acquisition Date 2015-05-22T02:58:00
TBSO
Me Me
O
O F3C NO2
OAc
3
Me
2.77A dr: 92:08 2.77B
A
B A B
1.83 1.03 0.08 0.92 0.92 0.08 0.21 1.84 0.05 1.00 0.05 0.92 3.08 0.97 1.11 2.71 8.91 5.52 5.71
f1 (ppm)

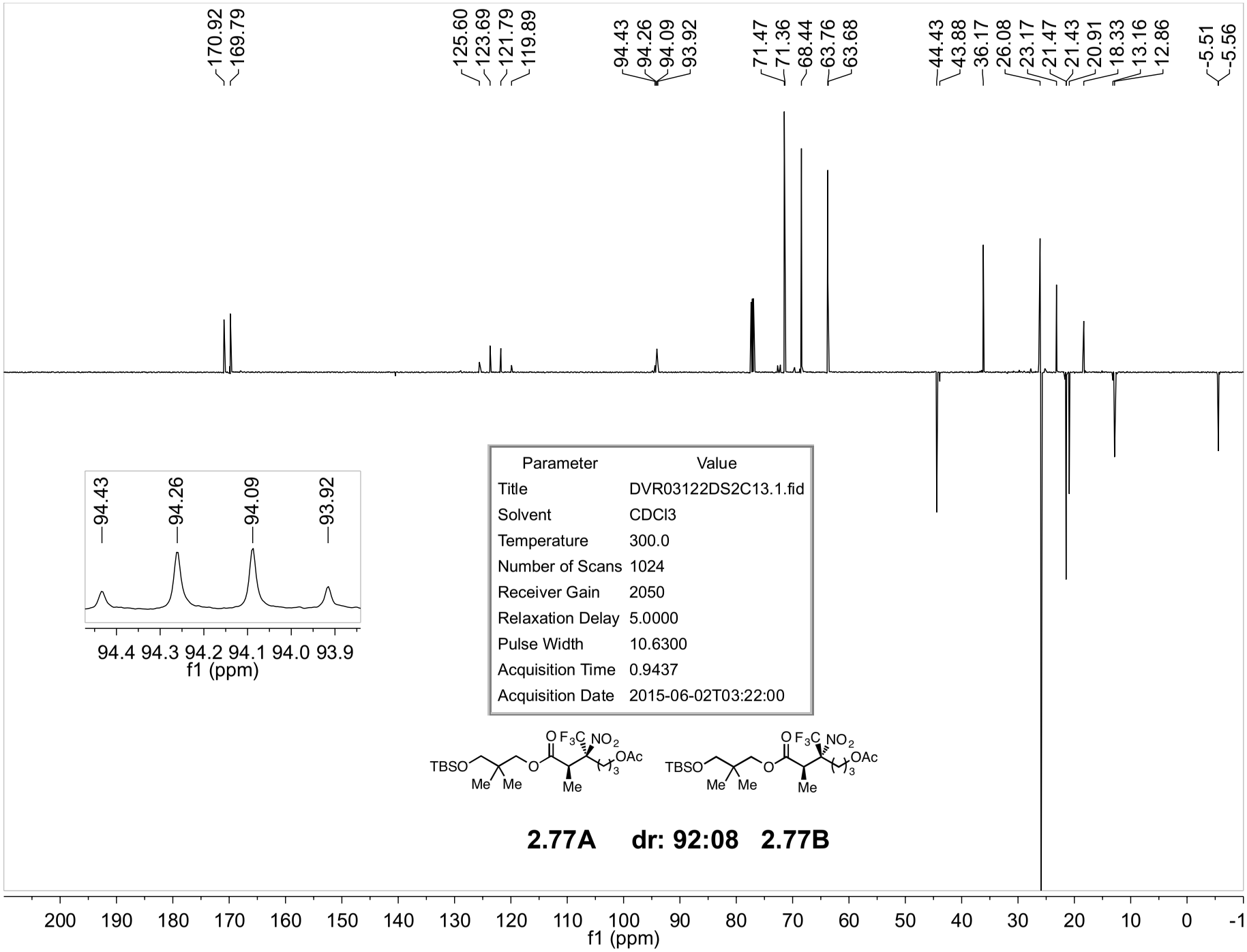
170.92
169.79
125.60
123.69
121.79
119.89
94.43
94.26
94.09
93.92
71.47
71.36
68.44
63.76
63.68
44.43
43.88
36.17
26.08
23.17
21.47
21.43
20.91
18.33
13.16
12.86
-5.51
-5.56
94.4 94.3 94.2 94.1 94.0 93.9
f1 (ppm)
Parameter Value
Title DVR03122DS2C13.1.fid
Solvent CDCl3
Temperature 300.0
Number of Scans 1024
Receiver Gain 2050
Relaxation Delay 5.0000
Pulse Width 10.6300
Acquisition Time 0.9437
Acquisition Date 2015-06-02T03:22:00
TBSO
Me Me
O
O F3C NO2
Me
OAc
3
2.77A dr: 92:08 2.77B
200 190 180 170 160 150 140 130 120 110 100 90 80 70 60 50 40 30 20 10 0 -1
f1 (ppm)

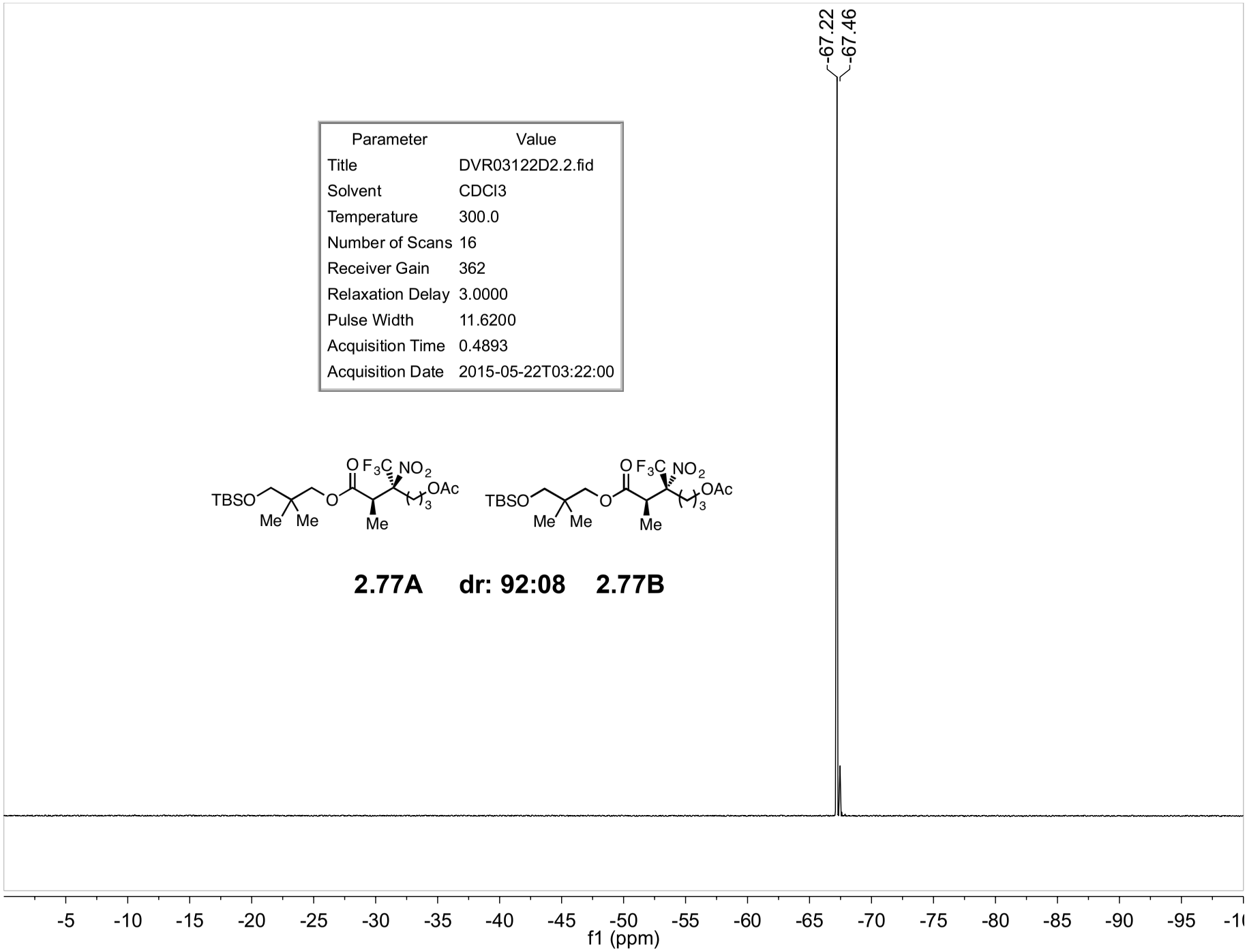
-67.22
-67.46
Parameter Value
Title DVR03122D2.2.fid
Solvent CDCl3
Temperature 300.0
Number of Scans 16
Receiver Gain 362
Relaxation Delay 3.0000
Pulse Width 11.6200
Acquisition Time 0.4893
Acquisition Date 2015-05-22T03:22:00
TBSO
Me Me
O
O F3C NO2
OAc
3
Me
2.77A dr: 92:08 2.77B
-5 -10 -15 -20 -25 -30 -35 -40 -45 -50 -55 -60 -65 -70 -75 -80 -85 -90 -95
f1 (ppm)

Parameter	Value
1 Title	DVR03108CRD.1.fid
2 Solvent	CDCl3
3 Temperature	298.2
4 Number of Scans	16
5 Receiver Gain	10
6 Relaxation Delay	1.0000
7 Pulse Width	15.0000
8 Spectrometer Frequency	400.13
9 Nucleus	1H

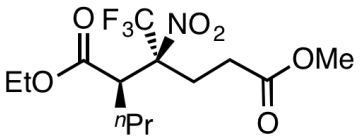

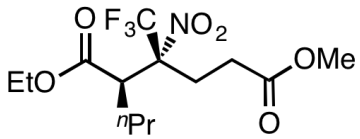

Crude

2.78A dr = 67:33 2.78B

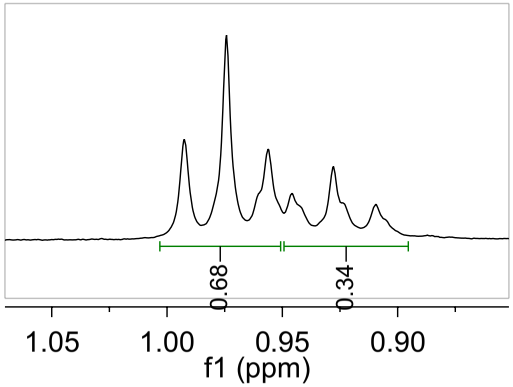

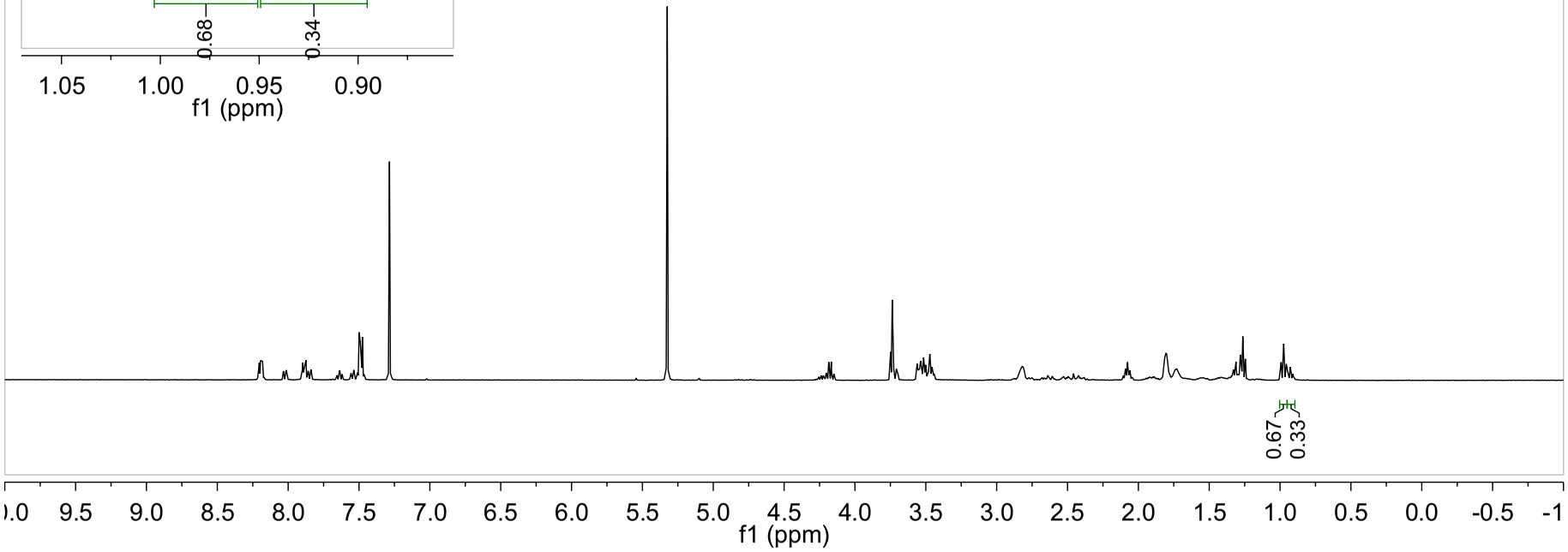

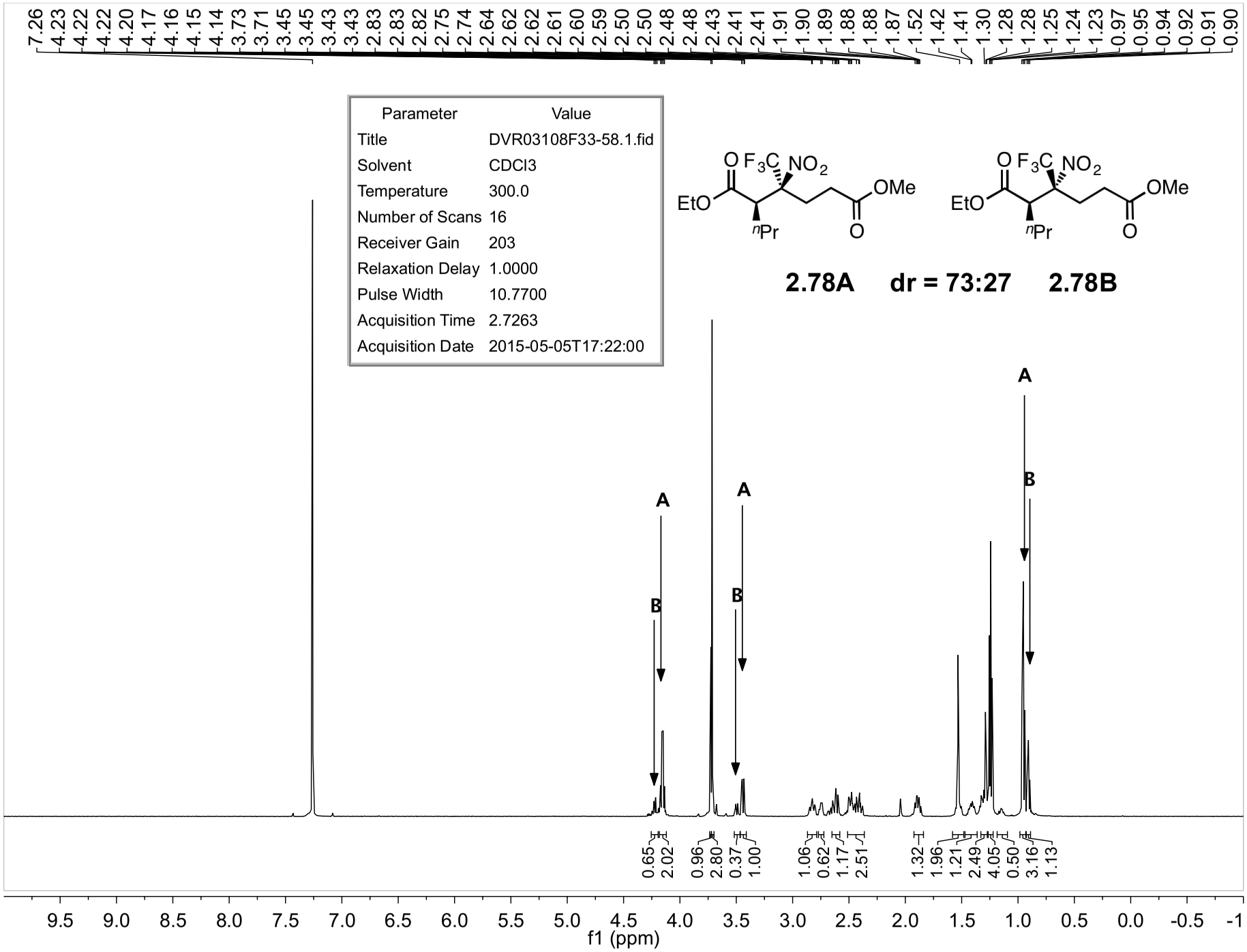
7.26 4.23 4.22 4.22 4.20 4.17 4.16 4.15 4.14 3.73 3.71 3.45 3.45 3.43 3.43 2.83 2.83 2.82 2.75 2.74 2.64 2.62 2.62 2.61 2.60 2.59 2.50 2.50 2.48 2.48 2.43 2.41 2.41 1.91 1.90 1.89 1.88 1.88 1.87 1.52 1.42 1.41 1.30 1.28 1.28 1.25 1.24 1.23 0.97 0.95 0.94 0.92 0.91 0.90
Parameter Value
Title DVR03108F33-58.1.fid
Solvent CDCl3
Temperature 300.0
Number of Scans 16
Receiver Gain 203
Relaxation Delay 1.0000
Pulse Width 10.7700
Acquisition Time 2.7263
Acquisition Date 2015-05-05T17:22:00
EtO
OMe
nPr
2.78A dr = 73:27 2.78B
A
B
0.65 2.02 0.96 2.80 0.37 1.00 1.06 0.62 1.17 2.51 1.32 1.96 1.21 2.49 4.05 0.50 3.16 1.13
9.5 9.0 8.5 8.0 7.5 7.0 6.5 6.0 5.5 5.0 4.5 4.0 3.5 3.0 2.5 2.0 1.5 1.0 0.5 0.0 -0.5 -1
f1 (ppm)

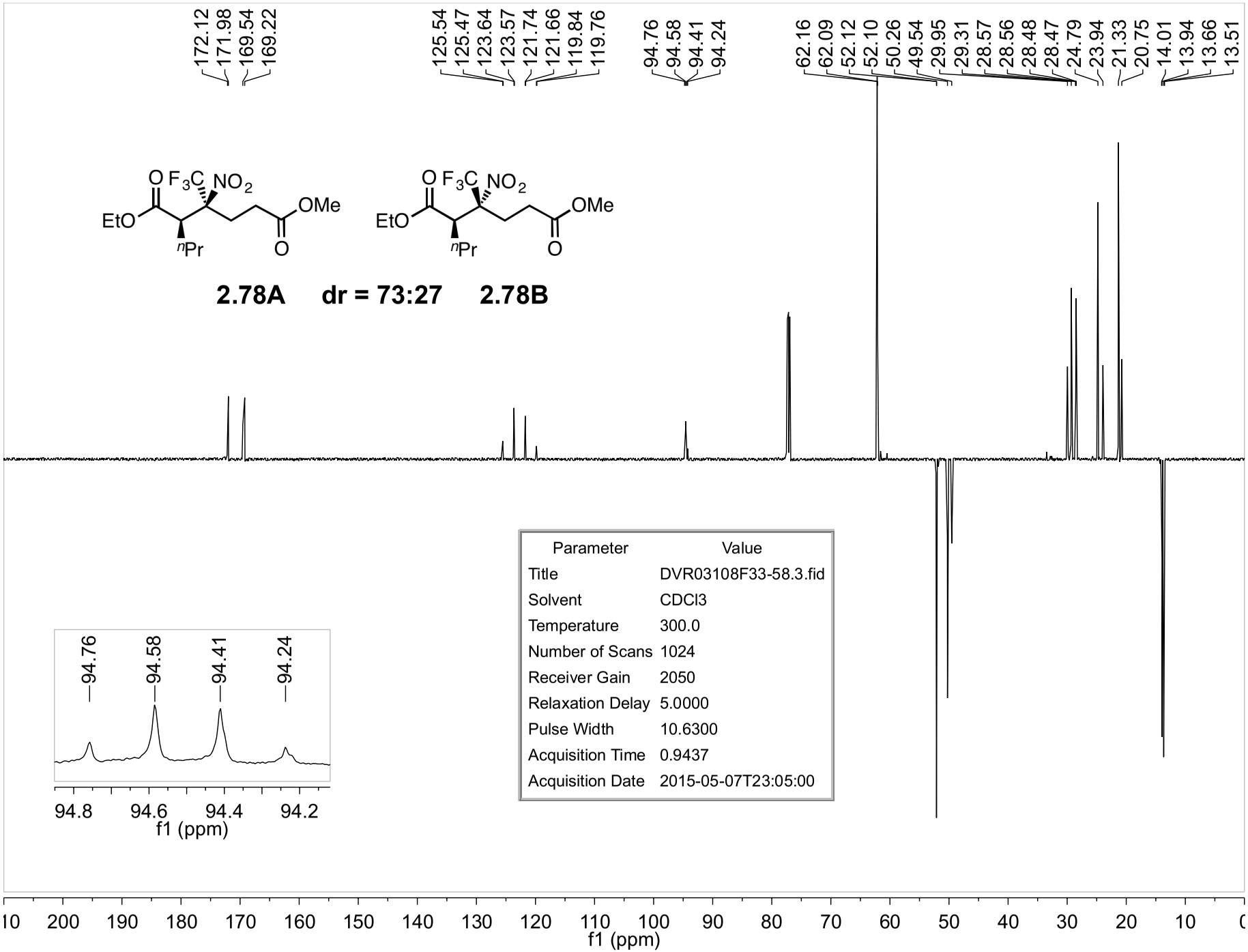
172.12
171.98
169.54
169.22
125.54
125.47
123.64
123.57
121.74
121.66
119.84
119.76
94.76
94.58
94.41
94.24
62.16
62.09
52.12
52.10
50.26
49.54
29.95
29.31
28.57
28.56
28.48
28.47
24.79
23.94
21.33
20.75
14.01
13.94
13.66
13.51
O F3C NO2
EtO
OMe
nPr
O
2.78A dr = 73:27 2.78B
Parameter Value
Title DVR03108F33-58.3.fid
Solvent CDCl3
Temperature 300.0
Number of Scans 1024
Receiver Gain 2050
Relaxation Delay 5.0000
Pulse Width 10.6300
Acquisition Time 0.9437
Acquisition Date 2015-05-07T23:05:00
94.8
94.6
94.4
94.2
f1 (ppm)
f1 (ppm)

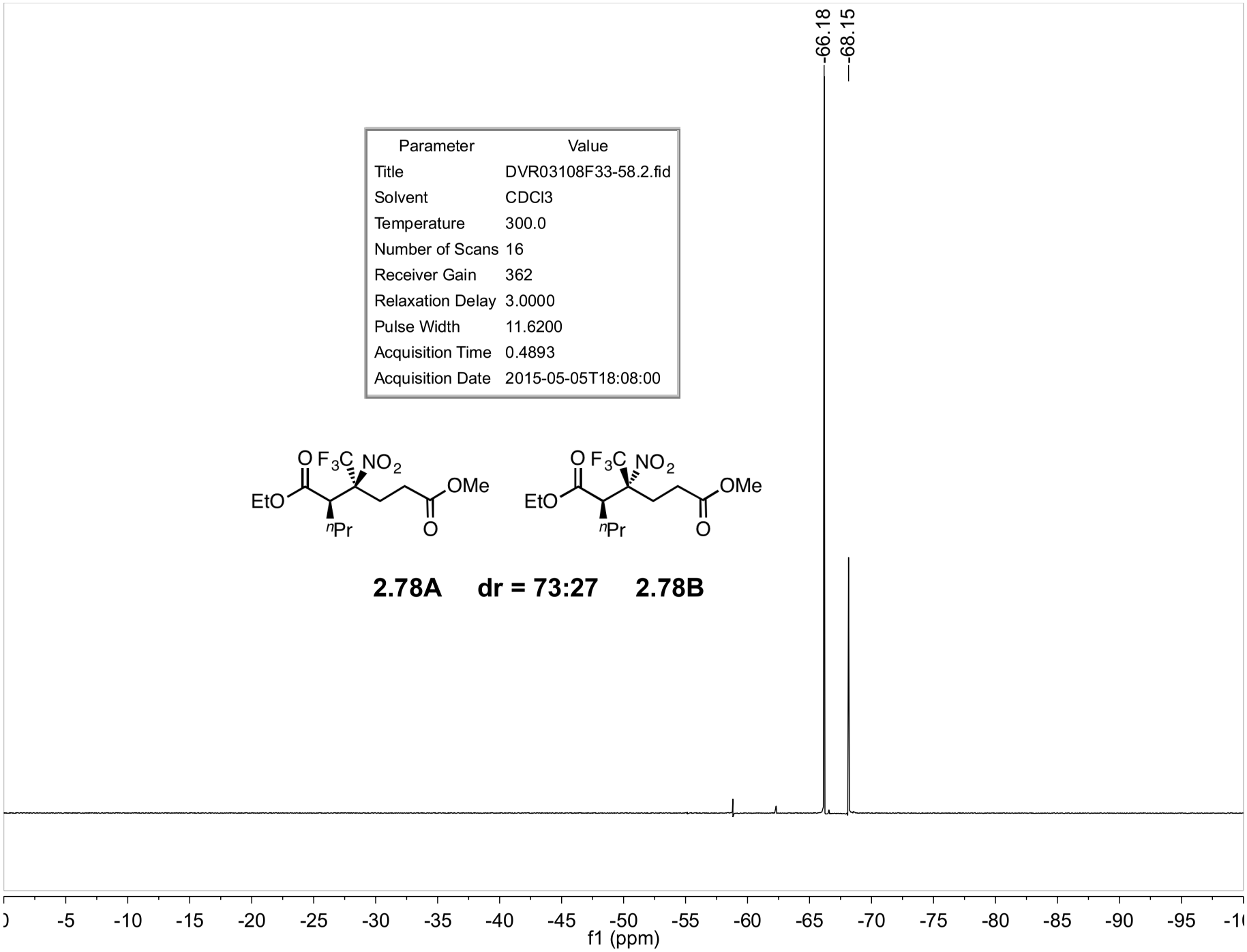
-66.18
-68.15
Parameter Value
Title DVR03108F33-58.2.fid
Solvent CDCl3
Temperature 300.0
Number of Scans 16
Receiver Gain 362
Relaxation Delay 3.0000
Pulse Width 11.6200
Acquisition Time 0.4893
Acquisition Date 2015-05-05T18:08:00
EtO
OMe
nPr
2.78A dr = 73:27 2.78B
f1 (ppm)

Parameter	Value
1 Title	DVR03127CRD.1.fid
2 Solvent	CDCl3
3 Temperature	300.0
4 Number of Scans	16
5 Receiver Gain	228
6 Relaxation Delay	1.0000
7 Pulse Width	10.7700
8 Spectrometer Frequency	600.32
9 Nucleus	1H

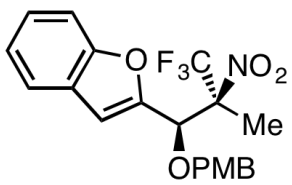

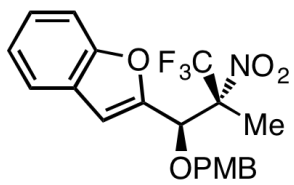

Crude

2.79A dr: 89:11 2.79B

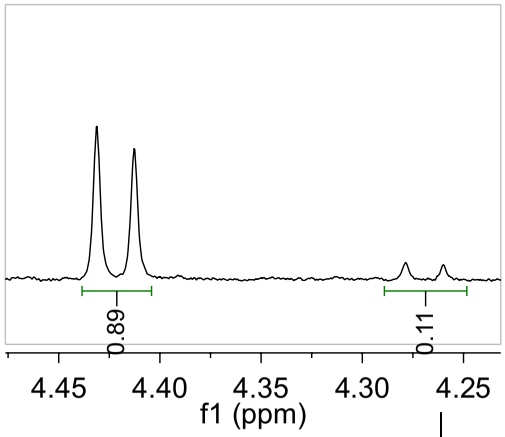

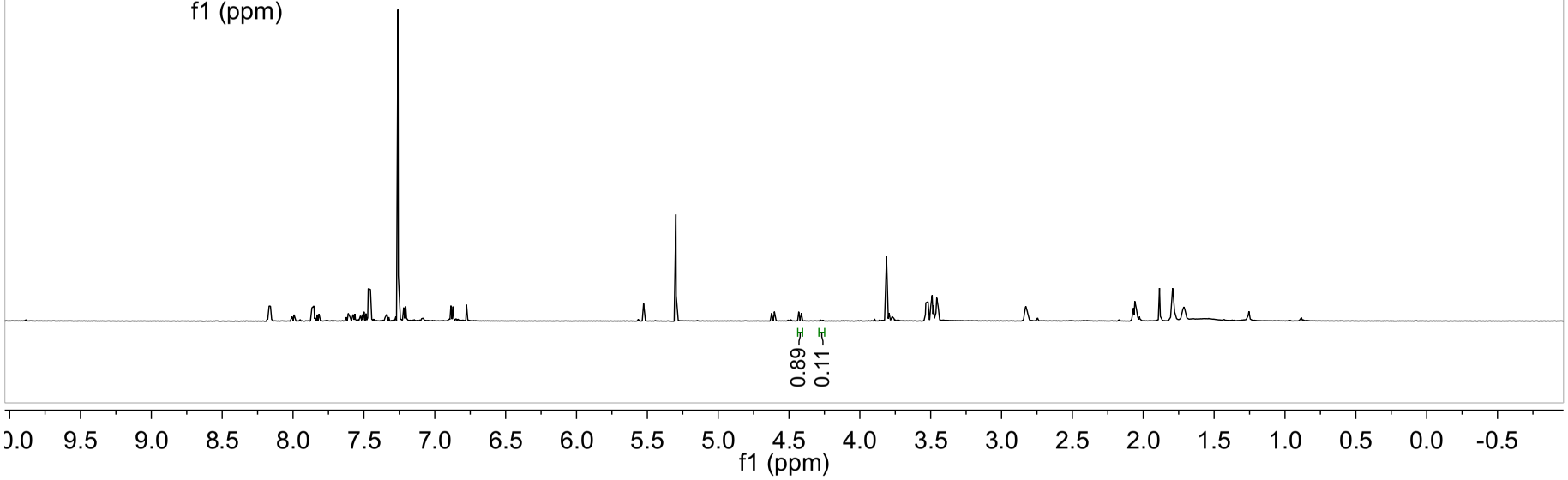

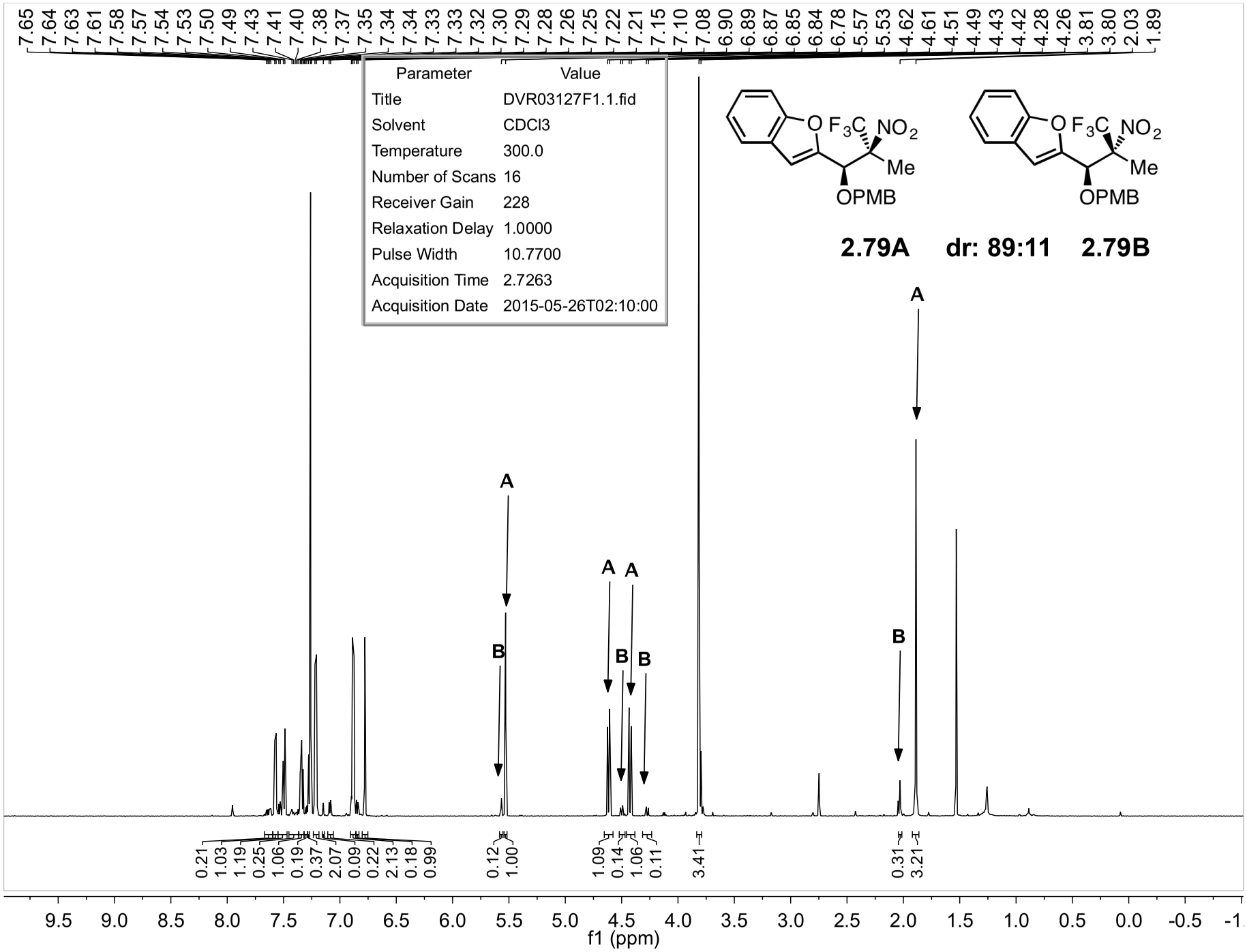
Parameter Value
Title DVR03127F1.1.fid
Solvent CDCl3
Temperature 300.0
Number of Scans 16
Receiver Gain 228
Relaxation Delay 1.0000
Pulse Width 10.7700
Acquisition Time 2.7263
Acquisition Date 2015-05-26T02:10:00
2.79A dr: 89:11 2.79B
OPMB
Me
NO2
F3C
O
A
B
f1 (ppm)

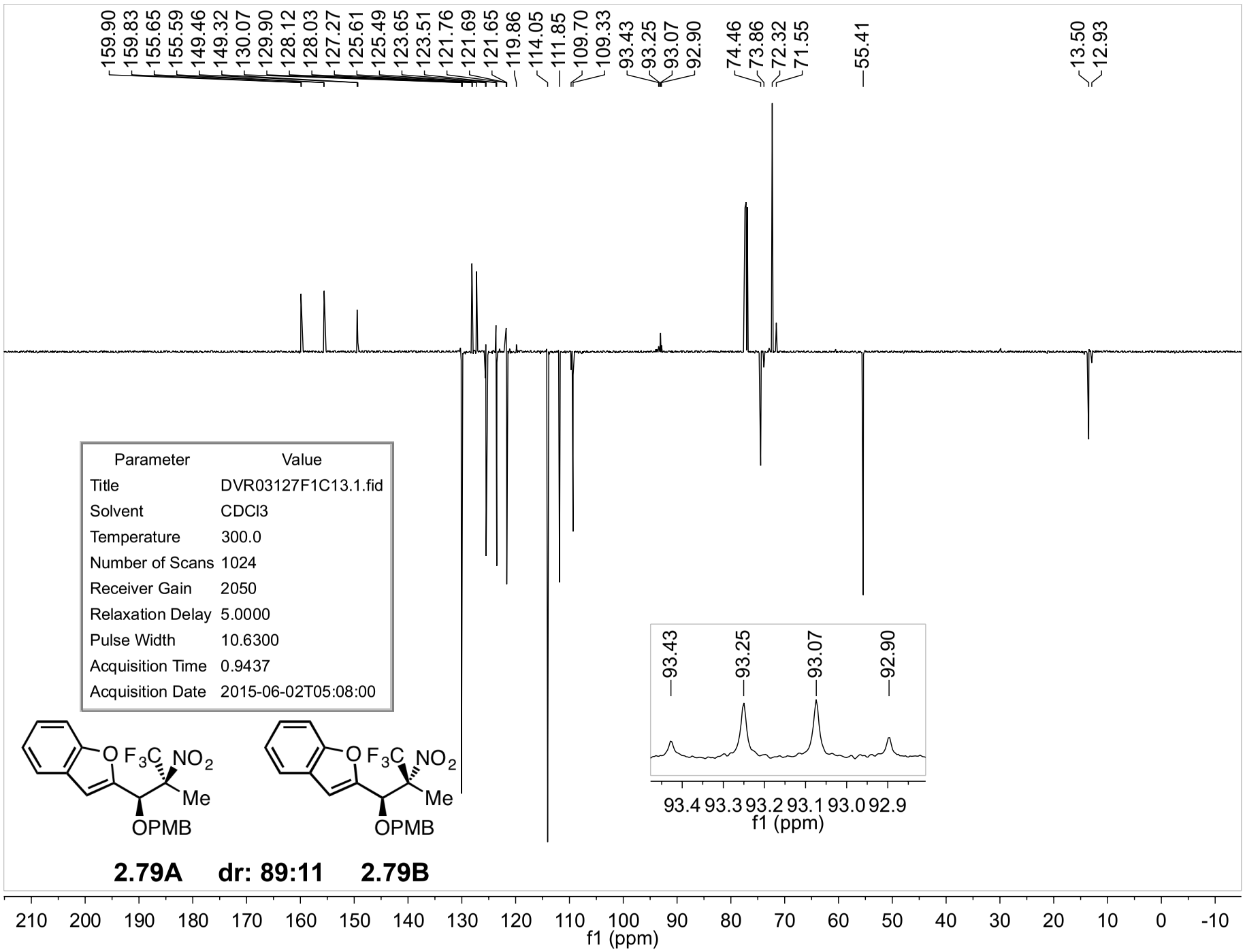
159.90
159.83
155.65
155.59
149.46
149.32
130.07
129.90
128.12
128.03
127.27
125.61
125.49
123.65
123.51
121.76
121.69
121.65
119.86
114.05
111.85
109.70
109.33
93.43
93.25
93.07
92.90
74.46
73.86
72.32
71.55
55.41
13.50
12.93
Parameter Value
Title DVR03127F1C13.1.fid
Solvent CDCl3
Temperature 300.0
Number of Scans 1024
Receiver Gain 2050
Relaxation Delay 5.0000
Pulse Width 10.6300
Acquisition Time 0.9437
Acquisition Date 2015-06-02T05:08:00
93.43
93.25
93.07
92.90
93.4 93.3 93.2 93.1 93.0 92.9
f1 (ppm)
O F3C NO2
Me
OPMB
O F3C NO2
Me
OPMB
2.79A dr: 89:11 2.79B
210 200 190 180 170 160 150 140 130 120 110 100 90 80 70 60 50 40 30 20 10 0 -10
f1 (ppm)

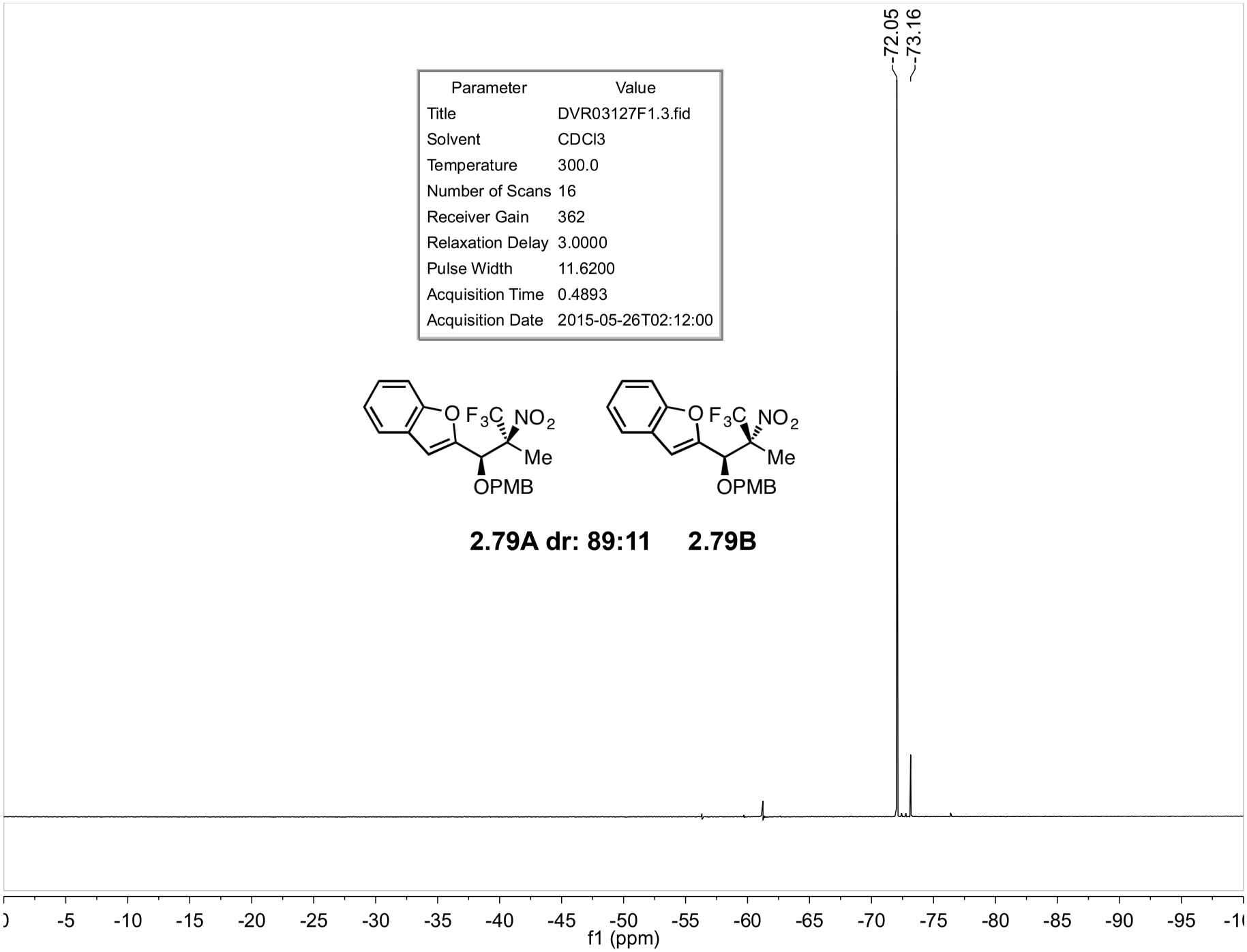
-72.05
-73.16
Parameter Value
Title DVR03127F1.3.fid
Solvent CDCl3
Temperature 300.0
Number of Scans 16
Receiver Gain 362
Relaxation Delay 3.0000
Pulse Width 11.6200
Acquisition Time 0.4893
Acquisition Date 2015-05-26T02:12:00
O F3C NO2
Me
OPMB
O F3C NO2
Me
OPMB
2.79A dr: 89:11 2.79B
-5 -10 -15 -20 -25 -30 -35 -40 -45 -50 -55 -60 -65 -70 -75 -80 -85 -90 -95
f1 (ppm)

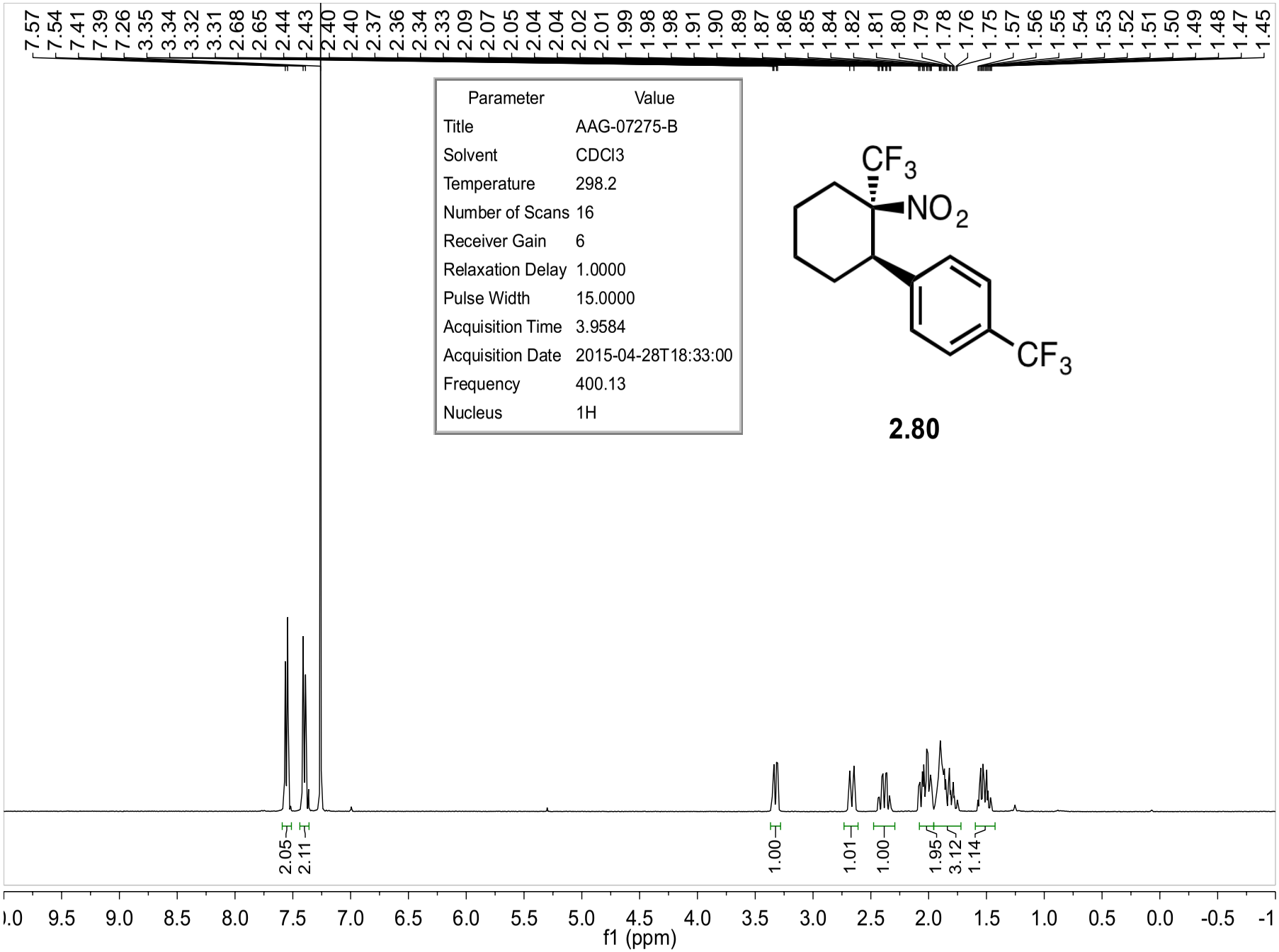
7.57 7.54 7.41 7.39 7.26 3.35 3.34 3.32 3.31 2.68 2.65 2.44 2.43 2.40 2.40 2.37 2.36 2.34 2.33 2.09 2.07 2.05 2.04 2.04 2.02 2.01 1.99 1.98 1.98 1.91 1.90 1.89 1.87 1.86 1.85 1.84 1.82 1.81 1.80 1.79 1.78 1.76 1.75 1.57 1.56 1.55 1.54 1.53 1.52 1.51 1.50 1.49 1.48 1.47 1.45
Parameter Value
Title AAG-07275-B
Solvent CDCl3
Temperature 298.2
Number of Scans 16
Receiver Gain 6
Relaxation Delay 1.0000
Pulse Width 15.0000
Acquisition Time 3.9584
Acquisition Date 2015-04-28T18:33:00
Frequency 400.13
Nucleus 1H
CF3
NO2
CF3
2.80
2.05
2.11
1.00
1.01
1.00
1.95
3.12
1.14
f1 (ppm)

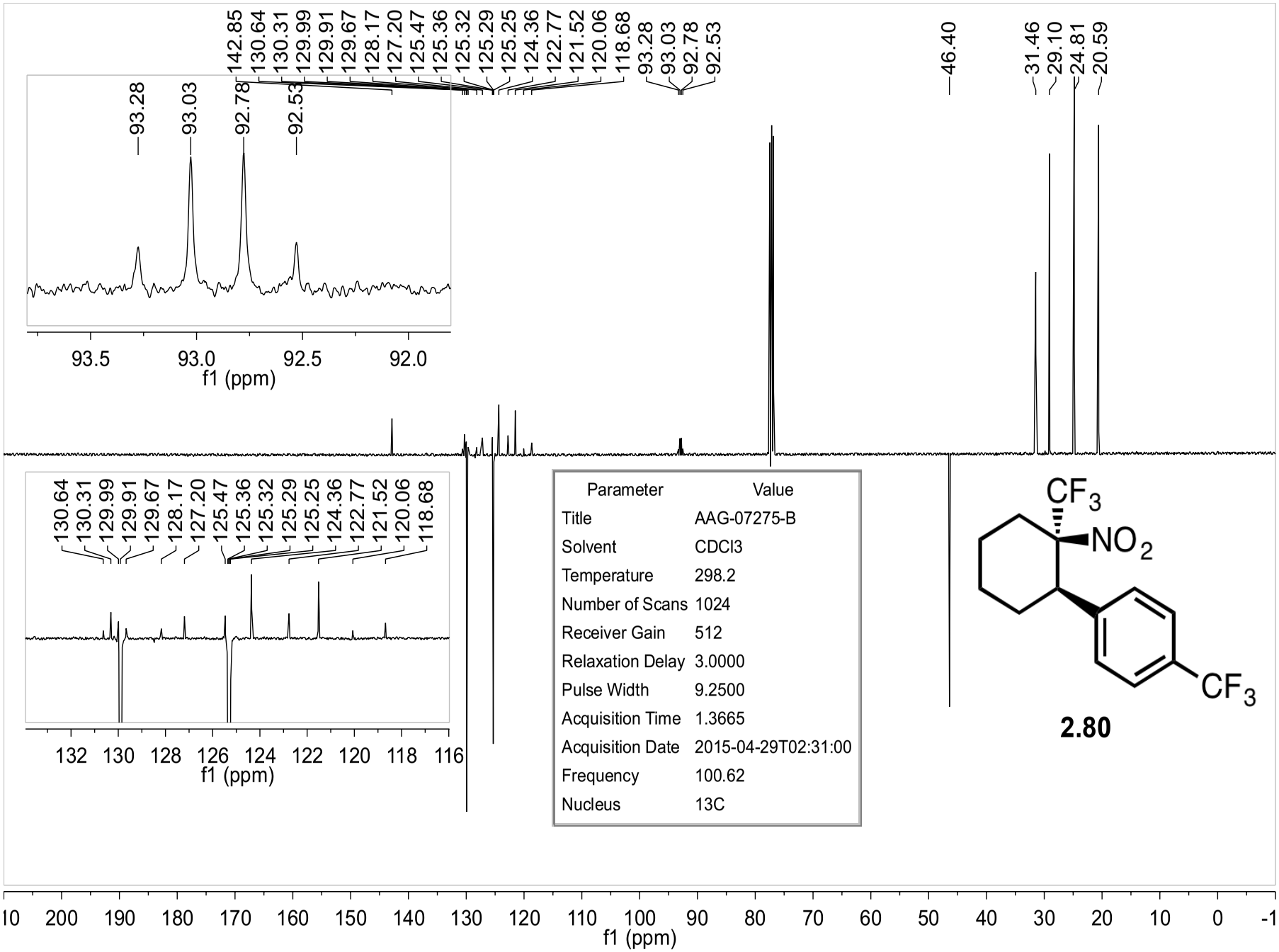
142.85
130.64
130.31
129.99
129.91
129.67
128.17
127.20
125.47
125.36
125.32
125.29
125.25
124.36
122.77
121.52
120.06
118.68
93.28
93.03
92.78
92.53
46.40
31.46
29.10
24.81
20.59
93.5
93.0
92.5
92.0
f1 (ppm)
132
130
128
126
124
122
120
118
116
f1 (ppm)
Parameter Value
Title AAG-07275-B
Solvent CDCl3
Temperature 298.2
Number of Scans 1024
Receiver Gain 512
Relaxation Delay 3.0000
Pulse Width 9.2500
Acquisition Time 1.3665
Acquisition Date 2015-04-29T02:31:00
Frequency 100.62
Nucleus 13C
CF3
NO2
CF3
2.80
f1 (ppm)

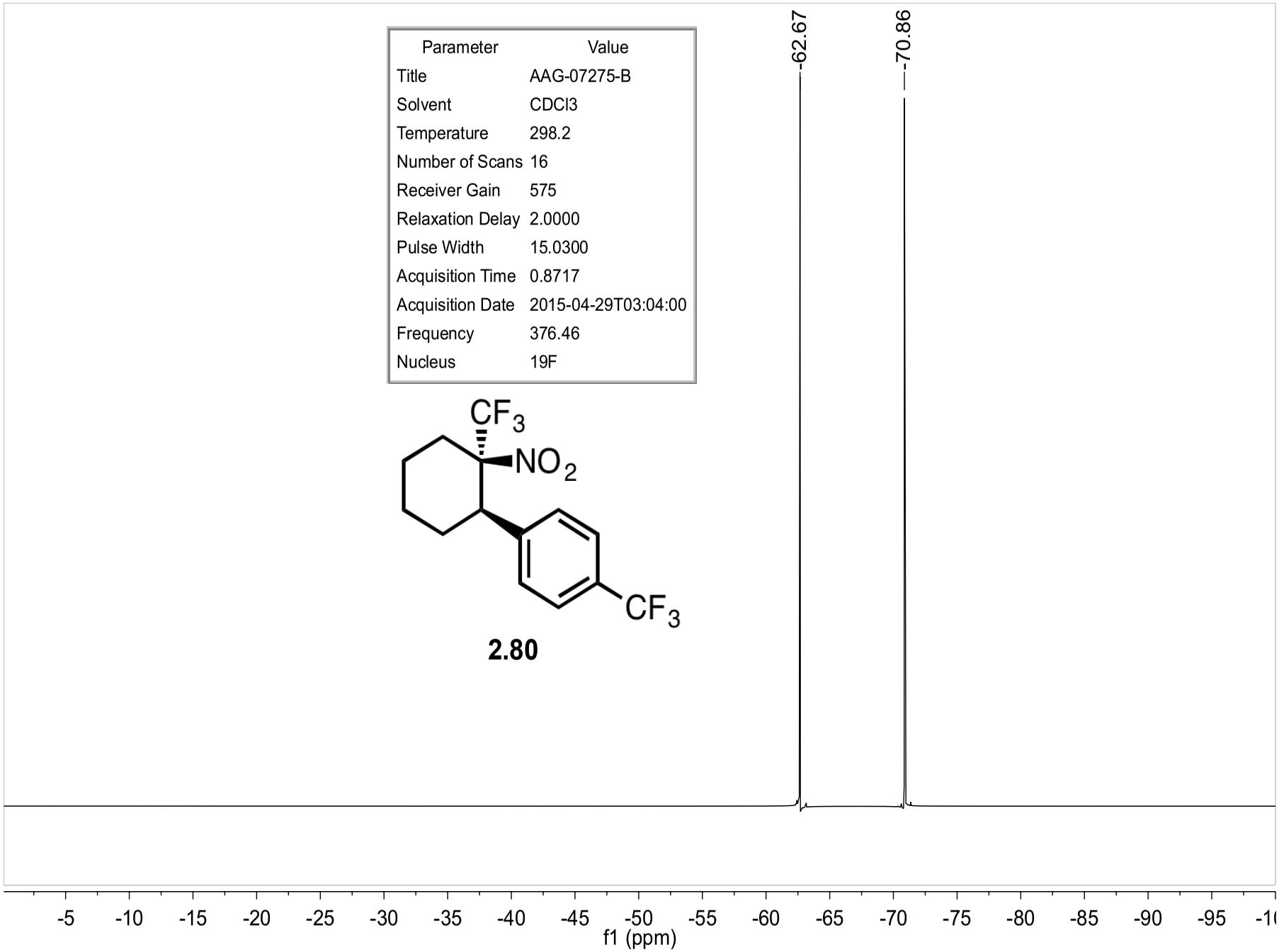
Parameter Value
Title AAG-07275-B
Solvent CDCl3
Temperature 298.2
Number of Scans 16
Receiver Gain 575
Relaxation Delay 2.0000
Pulse Width 15.0300
Acquisition Time 0.8717
Acquisition Date 2015-04-29T03:04:00
Frequency 376.46
Nucleus 19F
CF3
NO2
CF3
2.80
-62.67
-70.86
-5 -10 -15 -20 -25 -30 -35 -40 -45 -50 -55 -60 -65 -70 -75 -80 -85 -90 -95
f1 (ppm)

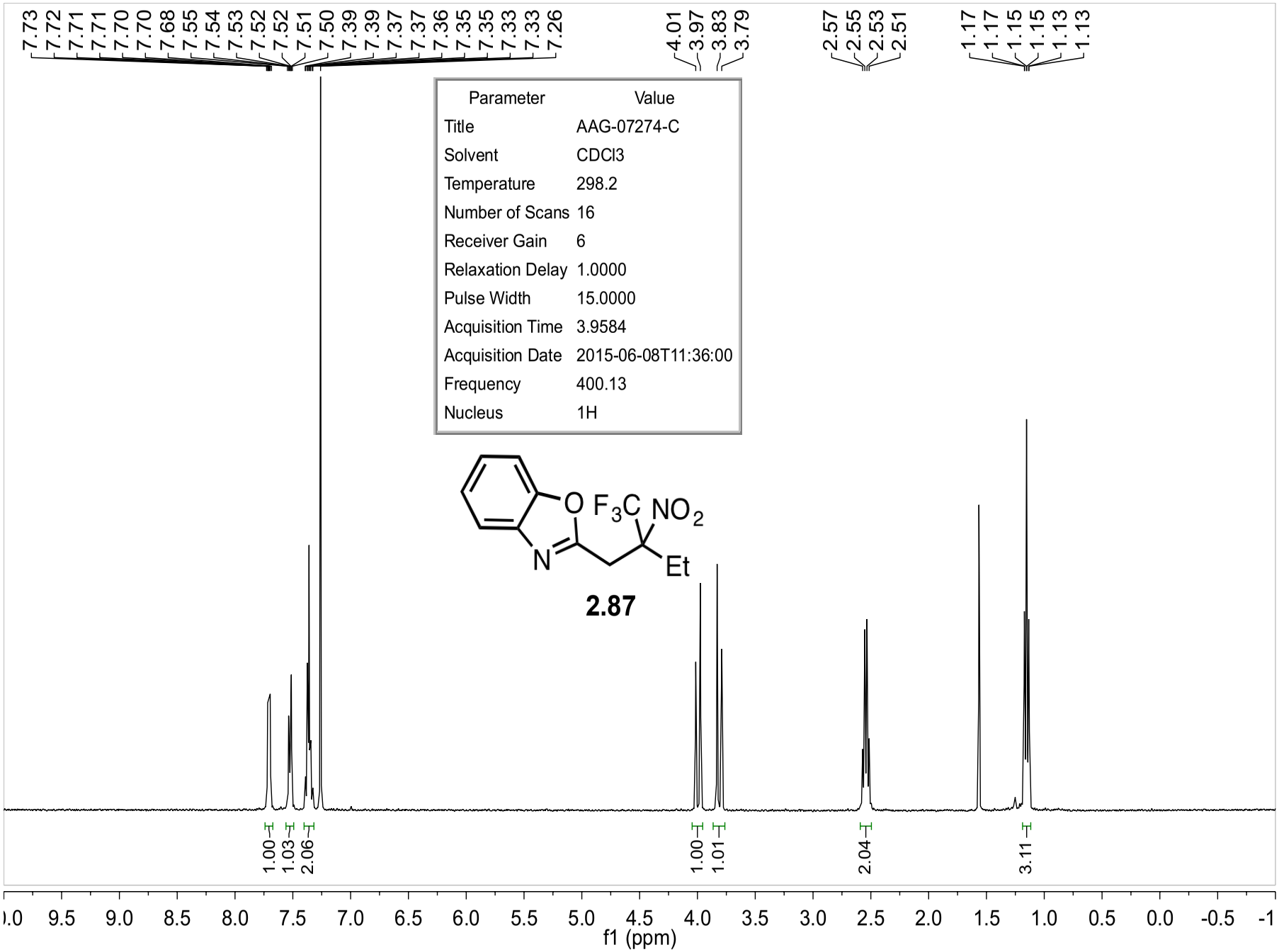
7.73 7.72 7.71 7.71 7.70 7.70 7.68 7.55 7.54 7.53 7.52 7.52 7.51 7.50 7.39 7.39 7.37 7.37 7.36 7.35 7.35 7.33 7.33 7.26
4.01 3.97 3.83 3.79
2.57 2.55 2.53 2.51
1.17 1.17 1.15 1.15 1.13 1.13
Parameter Value
Title AAG-07274-C
Solvent CDCl3
Temperature 298.2
Number of Scans 16
Receiver Gain 6
Relaxation Delay 1.0000
Pulse Width 15.0000
Acquisition Time 3.9584
Acquisition Date 2015-06-08T11:36:00
Frequency 400.13
Nucleus 1H
O
F3C
NO2
N
Et
2.87
1.00 1.03 2.06 1.00 1.01 2.04 3.11
f1 (ppm)

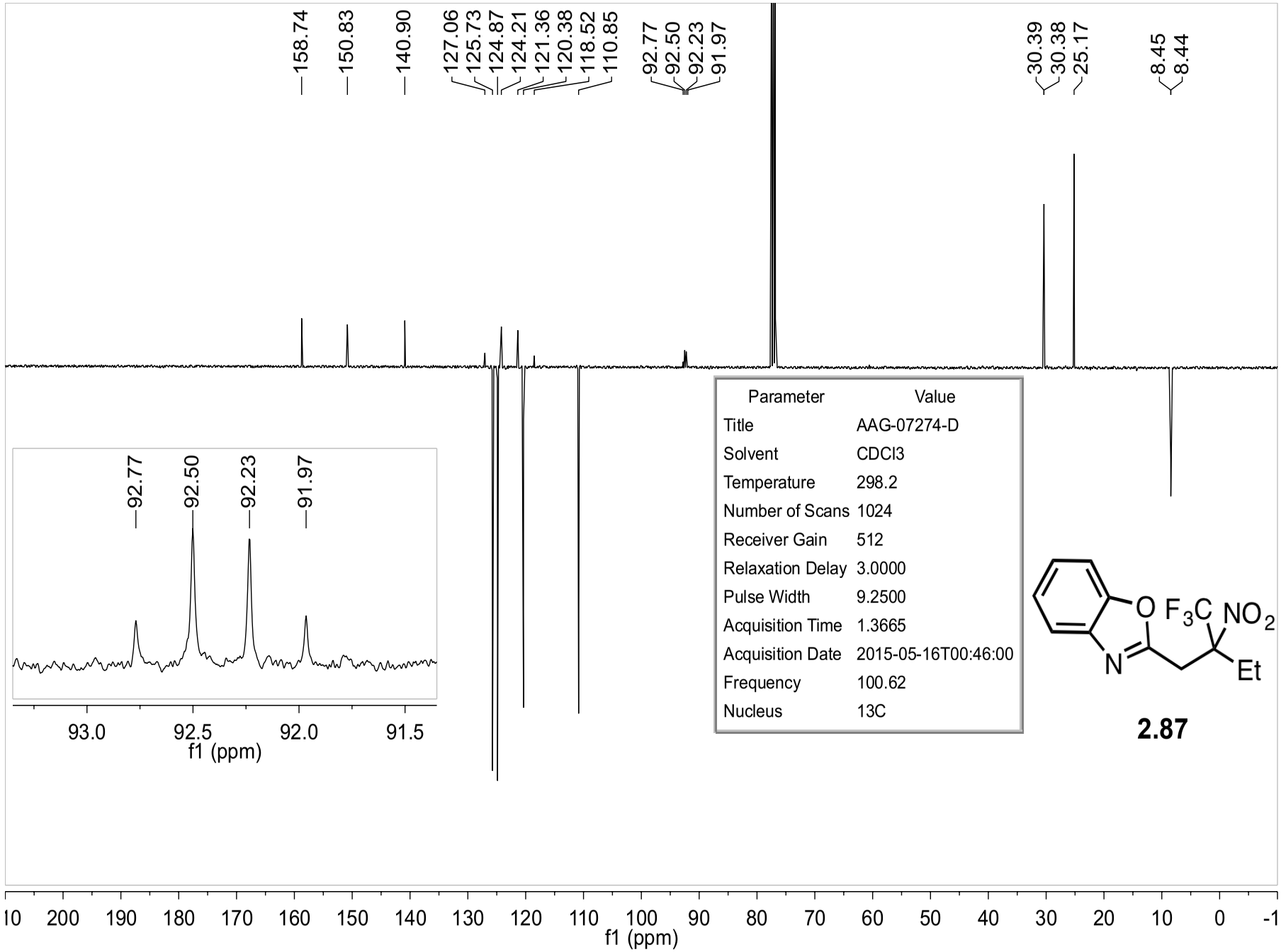
158.74
150.83
140.90
127.06
125.73
124.87
124.21
121.36
120.38
118.52
110.85
92.77
92.50
92.23
91.97
30.39
30.38
25.17
8.45
8.44
92.77
92.50
92.23
91.97
93.0
92.5
92.0
91.5
f1 (ppm)
Parameter Value
Title AAG-07274-D
Solvent CDCl3
Temperature 298.2
Number of Scans 1024
Receiver Gain 512
Relaxation Delay 3.0000
Pulse Width 9.2500
Acquisition Time 1.3665
Acquisition Date 2015-05-16T00:46:00
Frequency 100.62
Nucleus 13C
O
F3C
NO2
N
Et
2.87
f1 (ppm)

Parameter	Value
Title	AAG-07274-D
Solvent	CDCl3
Temperature	298.1
Number of Scans	16
Receiver Gain	1024
Relaxation Delay	2.0000
Pulse Width	15.0300
Acquisition Time	0.8717
Acquisition Date	2015-05-14T19:01:00
Frequency	376.46
Nucleus	19F

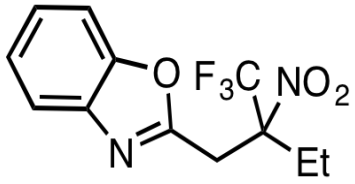

2.87

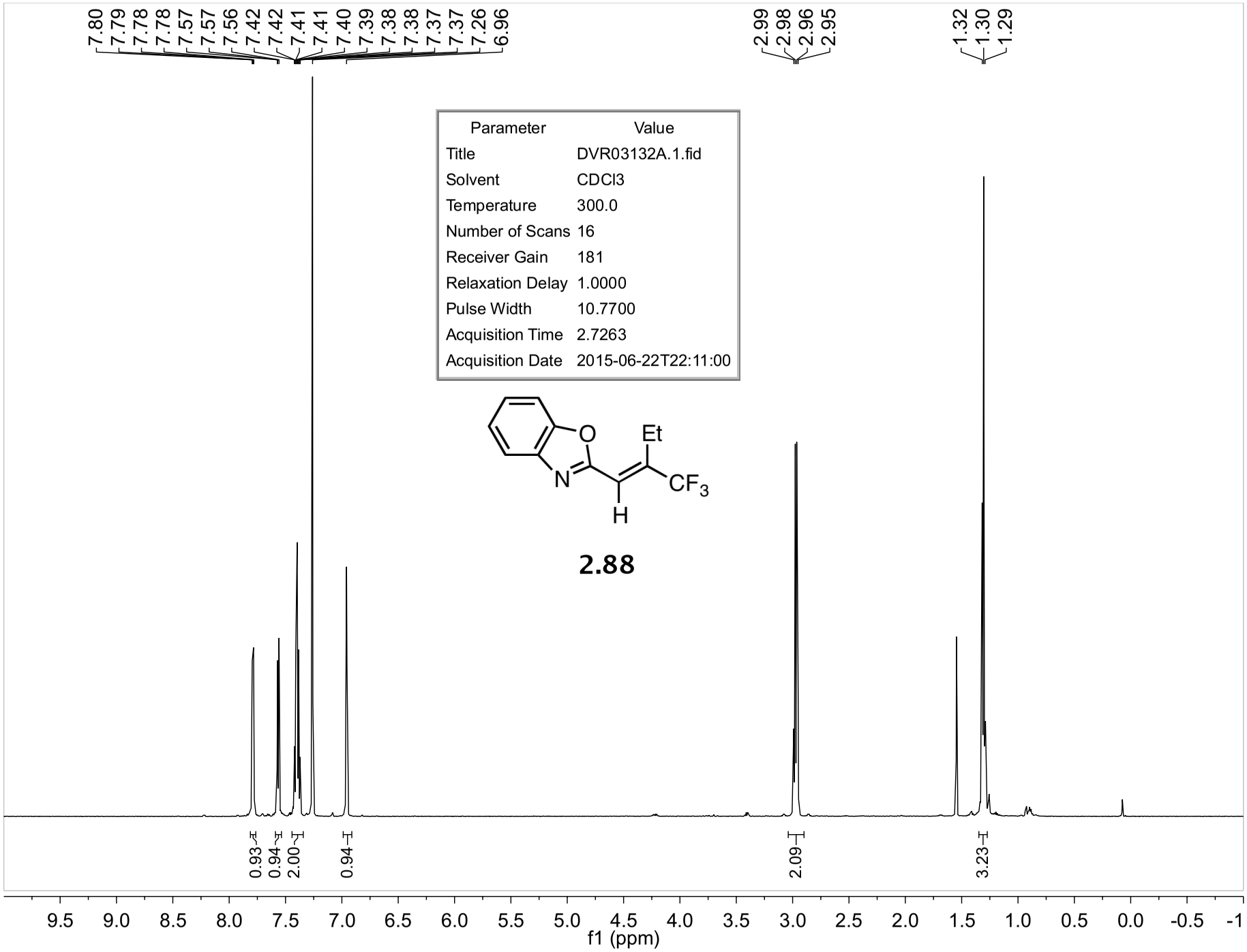
7.80
7.79
7.78
7.78
7.57
7.57
7.56
7.42
7.42
7.41
7.41
7.40
7.39
7.38
7.38
7.37
7.37
7.26
6.96
2.99
2.98
2.96
2.95
1.32
1.30
1.29
Parameter Value
Title DVR03132A.1.fid
Solvent CDCl3
Temperature 300.0
Number of Scans 16
Receiver Gain 181
Relaxation Delay 1.0000
Pulse Width 10.7700
Acquisition Time 2.7263
Acquisition Date 2015-06-22T22:11:00
O
Et
N
CF3
H
2.88
0.93
0.94
2.00
0.94
2.09
3.23
9.5 9.0 8.5 8.0 7.5 7.0 6.5 6.0 5.5 5.0 4.5 4.0 3.5 3.0 2.5 2.0 1.5 1.0 0.5 0.0 -0.5 -1
f1 (ppm)

159.62
150.38
142.92
142.73
142.54
142.35
141.86
126.31
125.06
123.24
120.82
117.33
117.28
117.24
117.19
110.87
21.03
13.23
Parameter Value
Title DVR03132F2C13.1.fid
Solvent CDCl3
Temperature 300.0
Number of Scans 1024
Receiver Gain 2050
Relaxation Delay 5.0000
Pulse Width 10.6300
Acquisition Time 0.9437
Acquisition Date 2015-06-02T22:10:00
Et
CF3
H
O
N
2.88
142.92
142.73
142.54
142.35
142.9 142.7 142.5 142.3
f1 (ppm)
117.33
117.28
117.24
117.19
117.5 117.4 117.3 117.2 117.1
f1 (ppm)
10 200 190 180 170 160 150 140 130 120 110 100 90 80 70 60 50 40 30 20 10 0 -1
f1 (ppm)

Parameter	Value
Title	DVR03132F2.2.fid
Solvent	CDCl3
Temperature	300.0
Number of Scans	16
Receiver Gain	362
Relaxation Delay	3.0000
Pulse Width	11.6200
Acquisition Time	0.4893
Acquisition Date	2015-06-02T16:25:00

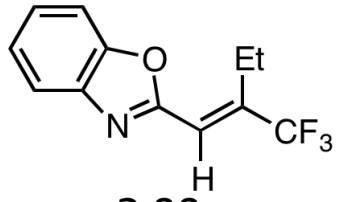

2.88

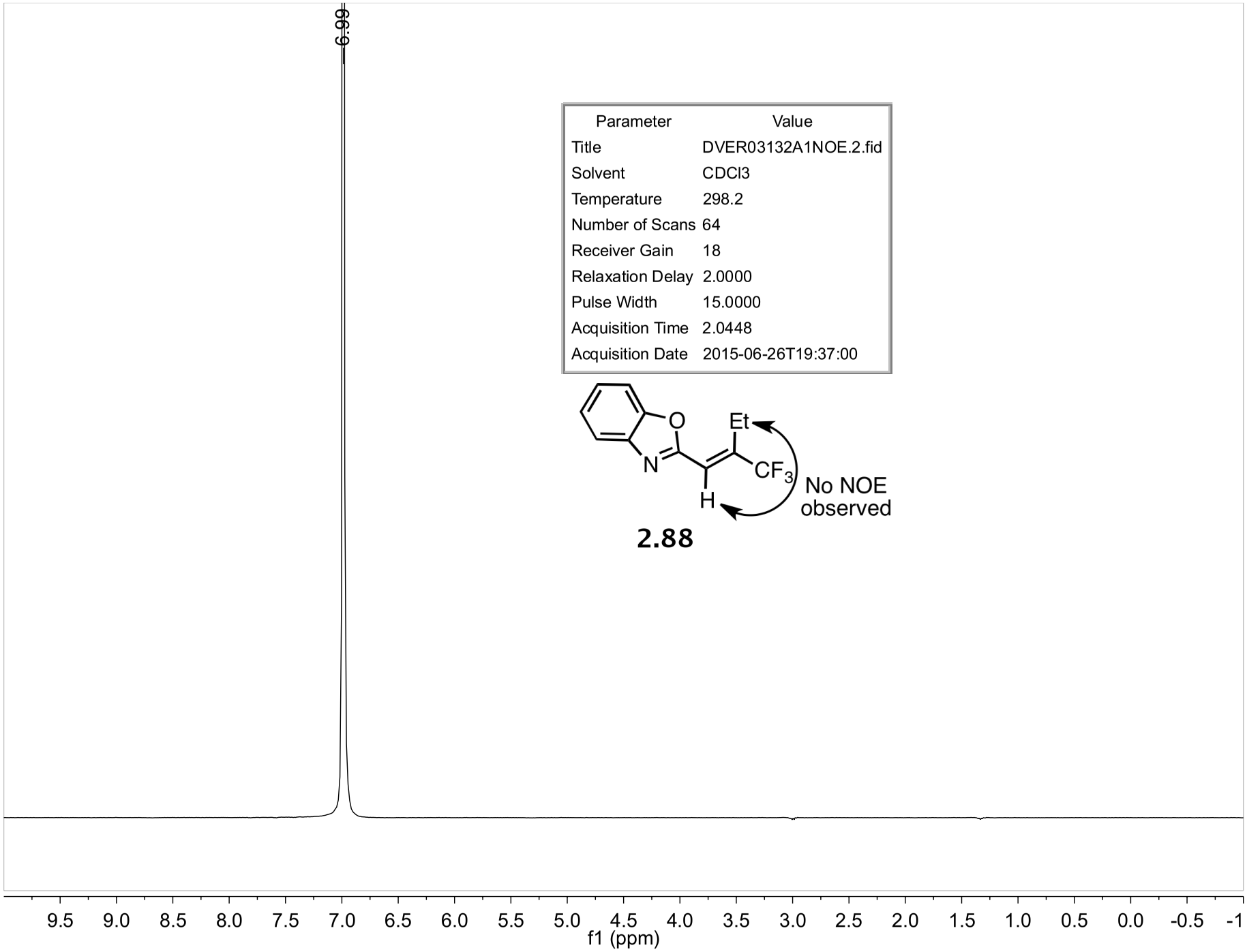

Parameter	Value
Title	DVER03132A1NOE.2.fid
Solvent	CDCl3
Temperature	298.2
Number of Scans	64
Receiver Gain	18
Relaxation Delay	2.0000
Pulse Width	15.0000
Acquisition Time	2.0448
Acquisition Date	2015-06-26T19:37:00

2.88

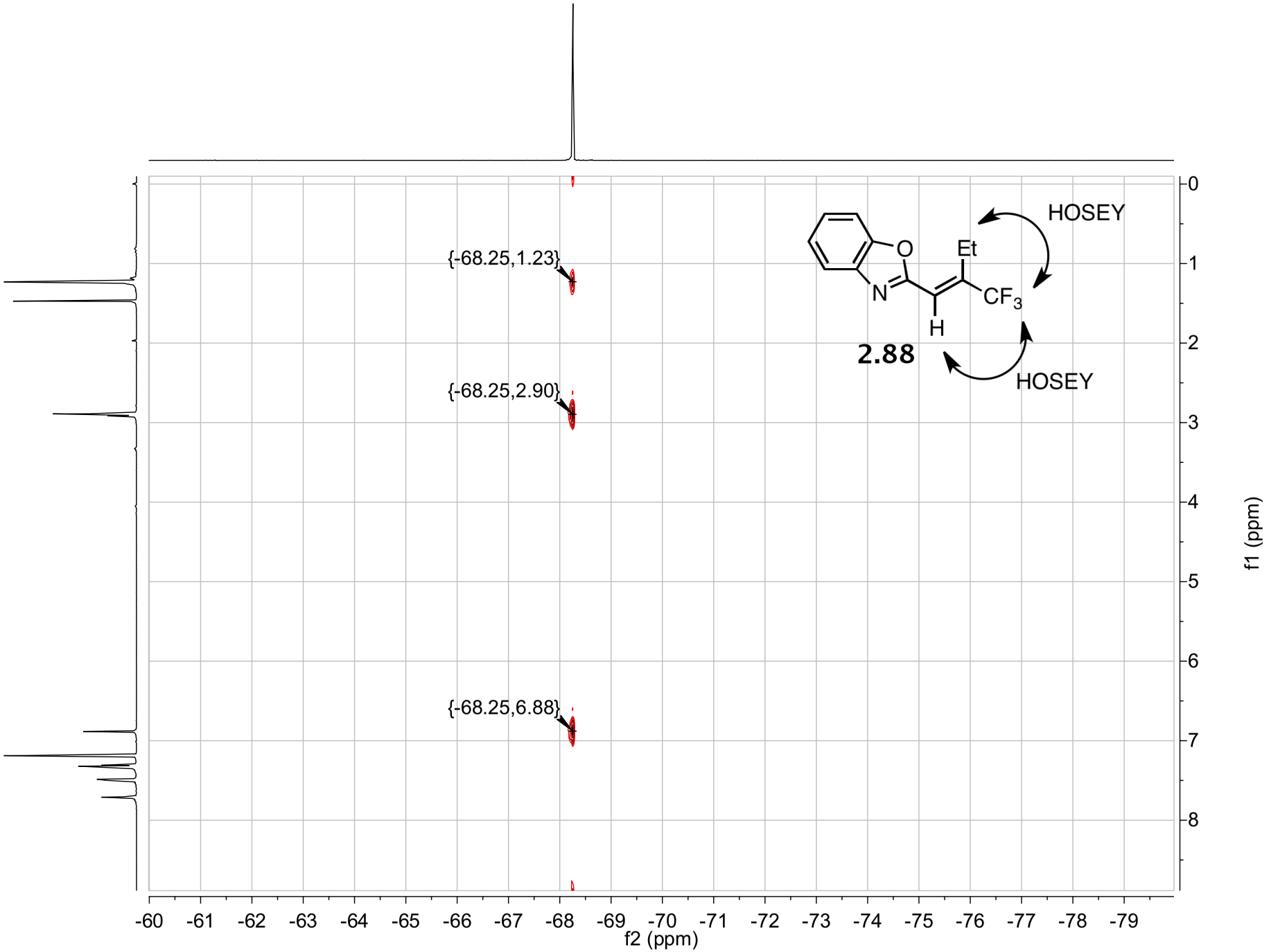
{-68.25,1.23}
{-68.25,2.90}
{-68.25,6.88}
HOSEY
HOSEY
O
N
Et
CF3
H
2.88
-60 -61 -62 -63 -64 -65 -66 -67 -68 -69 -70 -71 -72 -73 -74 -75 -76 -77 -78 -79
f2 (ppm)
0 1 2 3 4 5 6 7 8
f1 (ppm)

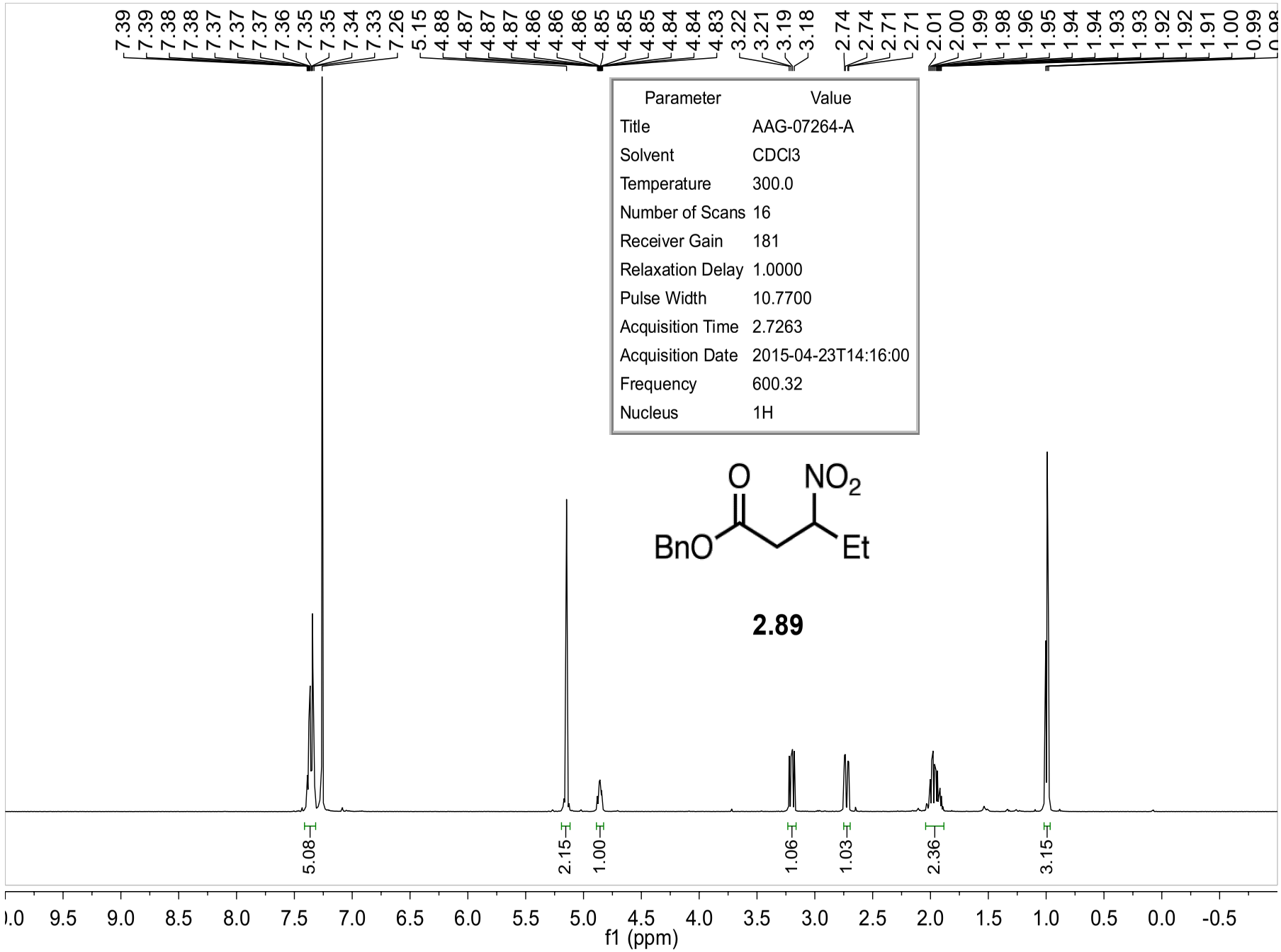
7.39 7.39 7.38 7.38 7.37 7.37 7.37 7.36 7.35 7.35 7.34 7.33 7.26 5.15 4.88 4.87 4.87 4.87 4.86 4.86 4.86 4.85 4.85 4.85 4.84 4.84 4.83 3.22 3.21 3.19 3.18 2.74 2.74 2.71 2.71 2.01 2.00 1.99 1.98 1.96 1.95 1.94 1.94 1.93 1.93 1.92 1.92 1.91 1.00 0.99
Parameter Value
Title AAG-07264-A
Solvent CDCl3
Temperature 300.0
Number of Scans 16
Receiver Gain 181
Relaxation Delay 1.0000
Pulse Width 10.7700
Acquisition Time 2.7263
Acquisition Date 2015-04-23T14:16:00
Frequency 600.32
Nucleus 1H
O
NO2
BnO
Et
2.89
5.08
2.15
1.00
1.06
1.03
2.36
3.15
f1 (ppm)

400

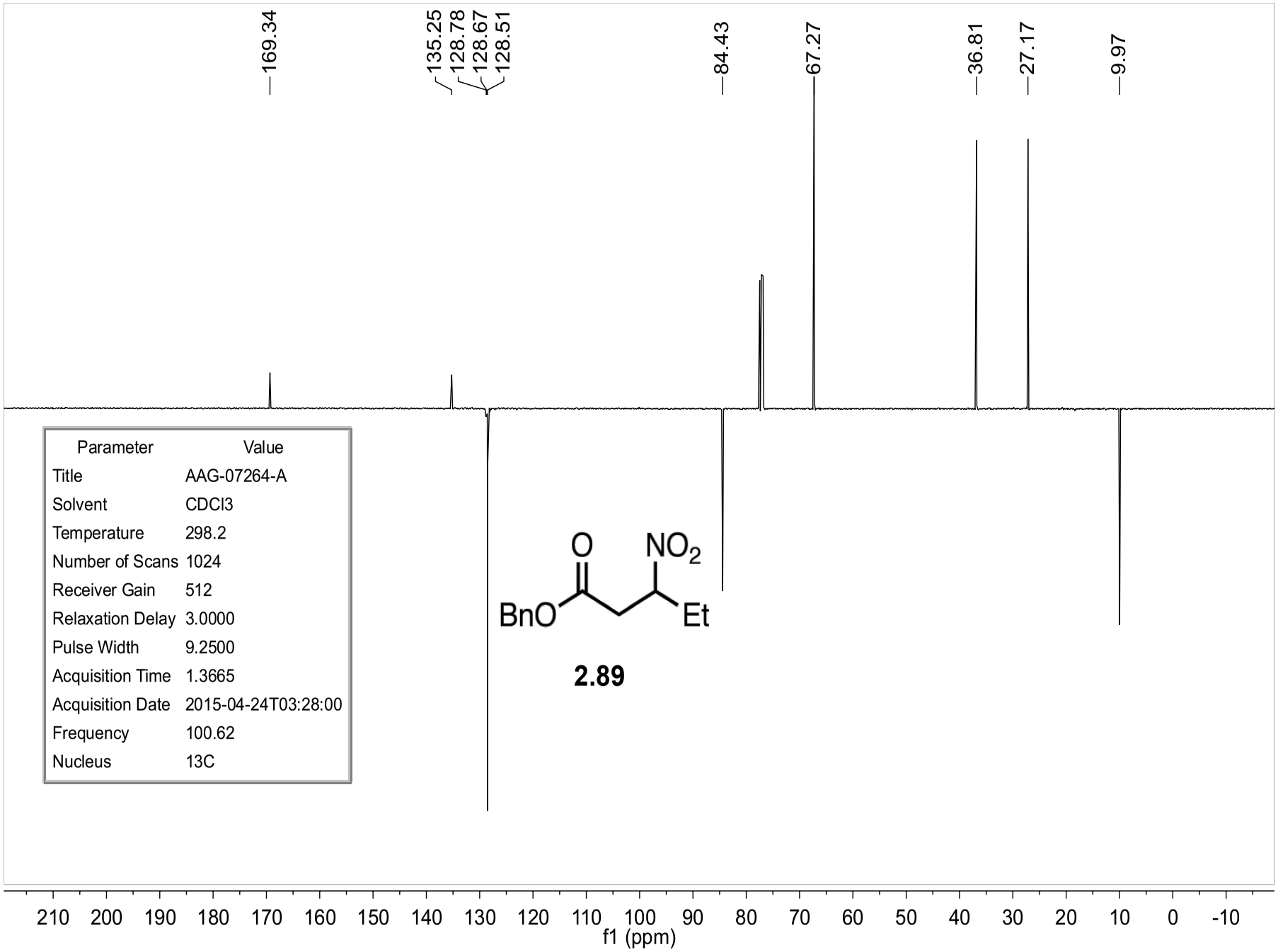
169.34
135.25
128.78
128.67
128.51
84.43
67.27
36.81
27.17
9.97
Parameter Value
Title AAG-07264-A
Solvent CDCl3
Temperature 298.2
Number of Scans 1024
Receiver Gain 512
Relaxation Delay 3.0000
Pulse Width 9.2500
Acquisition Time 1.3665
Acquisition Date 2015-04-24T03:28:00
Frequency 100.62
Nucleus 13C
O
NO2
BnO
Et
2.89
210 200 190 180 170 160 150 140 130 120 110 100 90 80 70 60 50 40 30 20 10 0 -10
f1 (ppm)

Parameter	Value
1 Title	DVR03134CRD.1.fid
2 Solvent	CDCl3
3 Temperature	300.0
4 Number of Scans	16
5 Receiver Gain	161
6 Relaxation Delay	1.0000
7 Pulse Width	10.7700
8 Spectrometer Frequency	600.32
9 Nucleus	1H

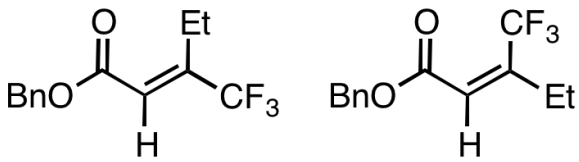

Crude

2.91A E:Z = 88:12 2.91B

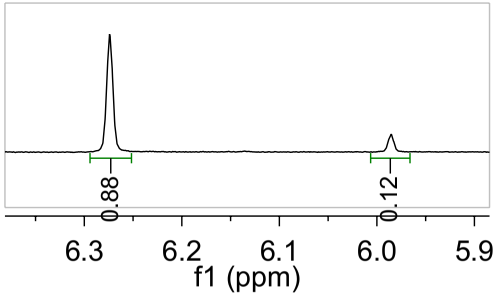

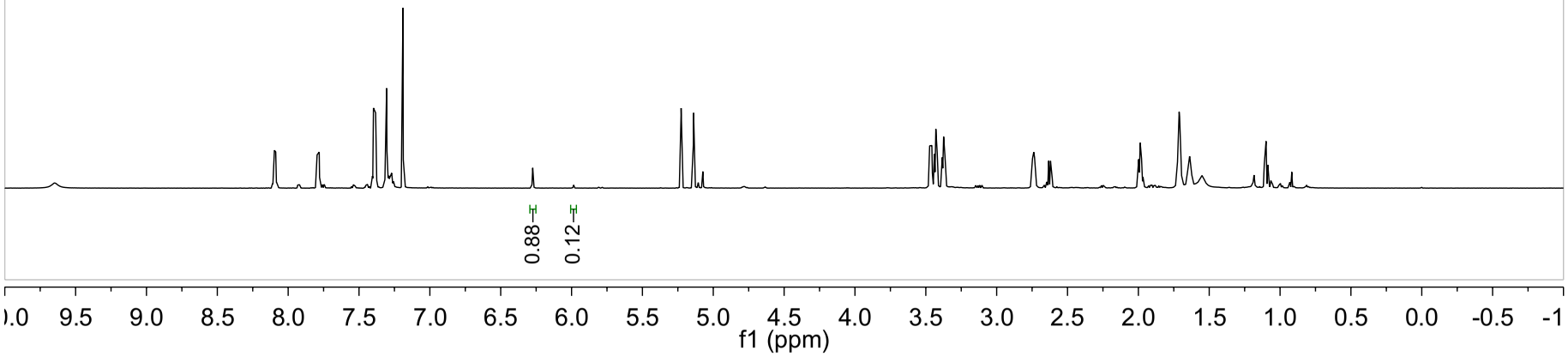

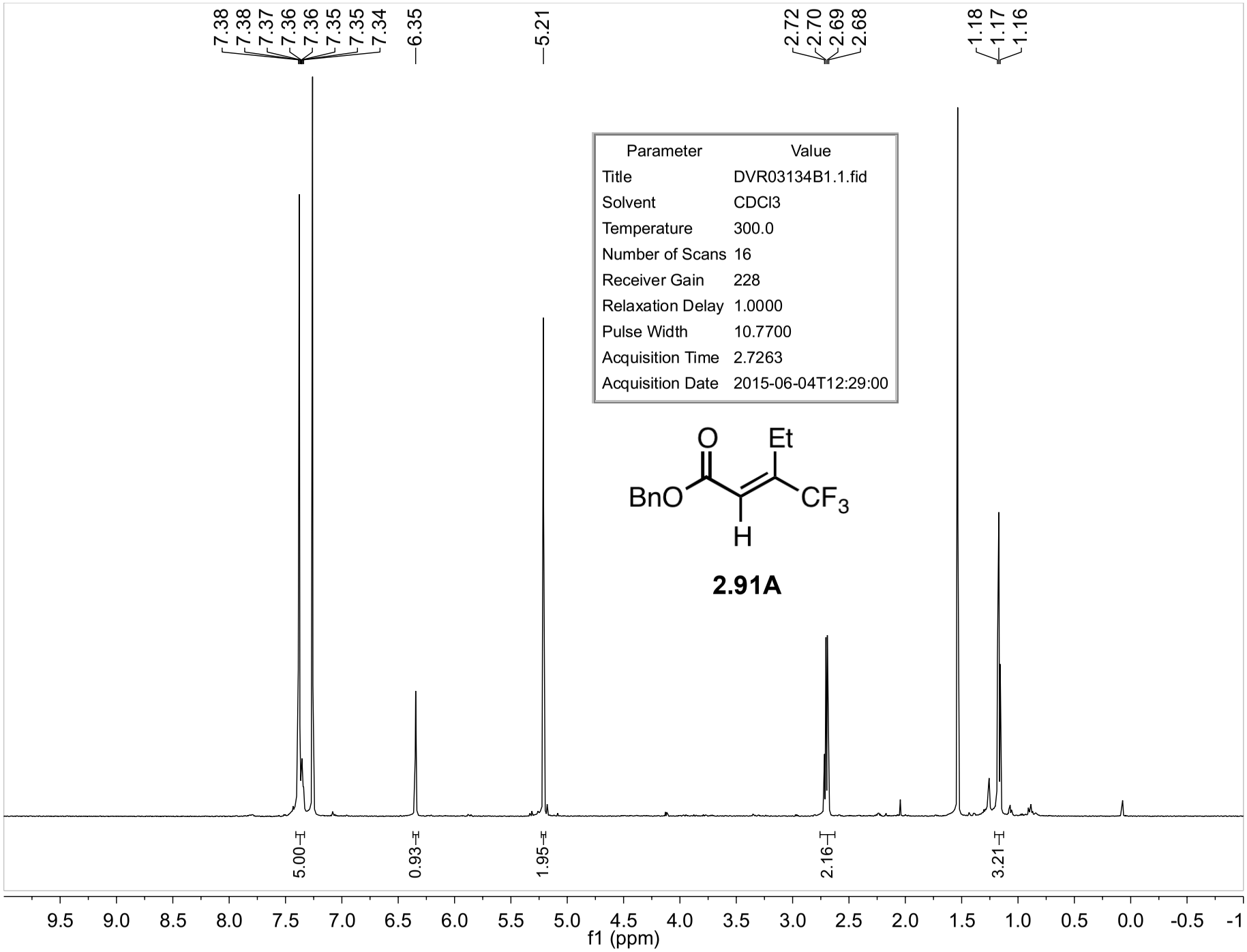
7.38
7.38
7.37
7.36
7.36
7.35
7.35
7.34
6.35
5.21
2.72
2.70
2.69
2.68
1.18
1.17
1.16
Parameter Value
Title DVR03134B1.1.fid
Solvent CDCl3
Temperature 300.0
Number of Scans 16
Receiver Gain 228
Relaxation Delay 1.0000
Pulse Width 10.7700
Acquisition Time 2.7263
Acquisition Date 2015-06-04T12:29:00
O
Et
BnO
CF3
H
2.91A
5.00
0.93
1.95
2.16
3.21
9.5 9.0 8.5 8.0 7.5 7.0 6.5 6.0 5.5 5.0 4.5 4.0 3.5 3.0 2.5 2.0 1.5 1.0 0.5 0.0 -0.5 -1
f1 (ppm)

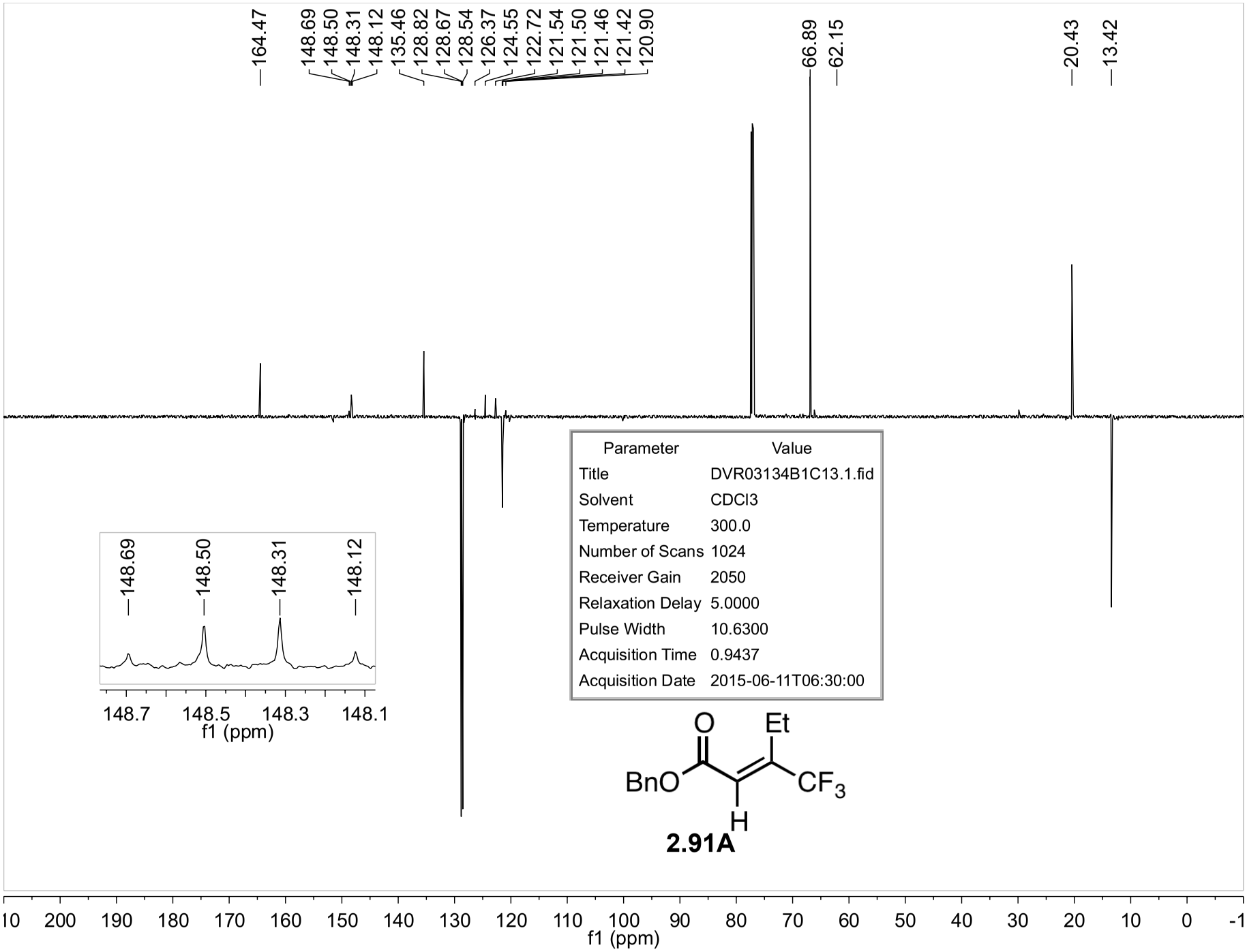
164.47
148.69
148.50
148.31
148.12
135.46
128.82
128.67
128.54
126.37
124.55
122.72
121.54
121.50
121.46
121.42
120.90
66.89
62.15
20.43
13.42
148.69
148.50
148.31
148.12
148.7
148.5
148.3
148.1
f1 (ppm)
Parameter Value
Title DVR03134B1C13.1.fid
Solvent CDCl3
Temperature 300.0
Number of Scans 1024
Receiver Gain 2050
Relaxation Delay 5.0000
Pulse Width 10.6300
Acquisition Time 0.9437
Acquisition Date 2015-06-11T06:30:00
O
Et
BnO
CF3
H
2.91A
10 200 190 180 170 160 150 140 130 120 110 100 90 80 70 60 50 40 30 20 10 0 -1
f1 (ppm)

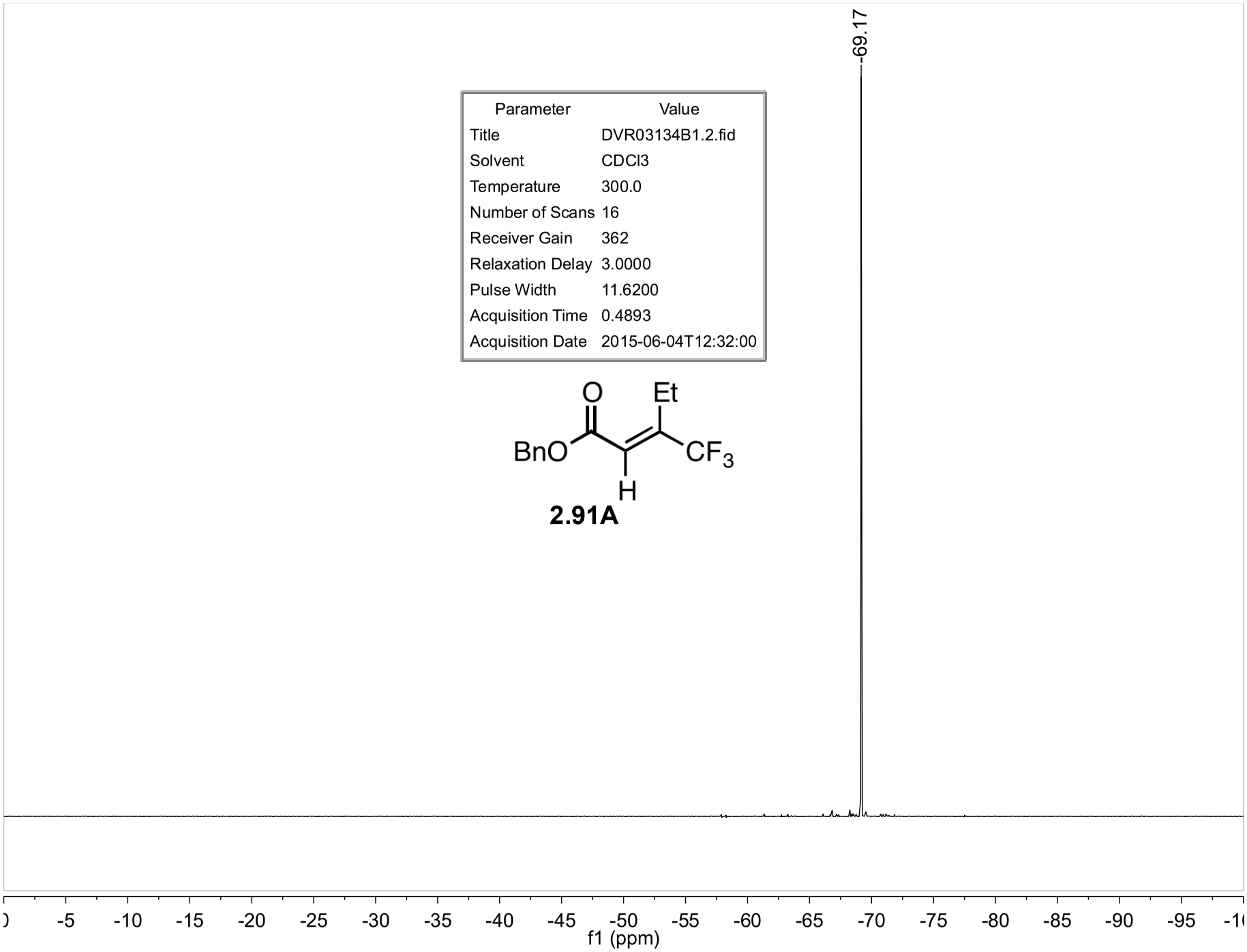
-69.17
Parameter Value
Title DVR03134B1.2.fid
Solvent CDCl3
Temperature 300.0
Number of Scans 16
Receiver Gain 362
Relaxation Delay 3.0000
Pulse Width 11.6200
Acquisition Time 0.4893
Acquisition Date 2015-06-04T12:32:00
O
Et
BnO
CF3
H
2.91A
-5 -10 -15 -20 -25 -30 -35 -40 -45 -50 -55 -60 -65 -70 -75 -80 -85 -90 -95
f1 (ppm)

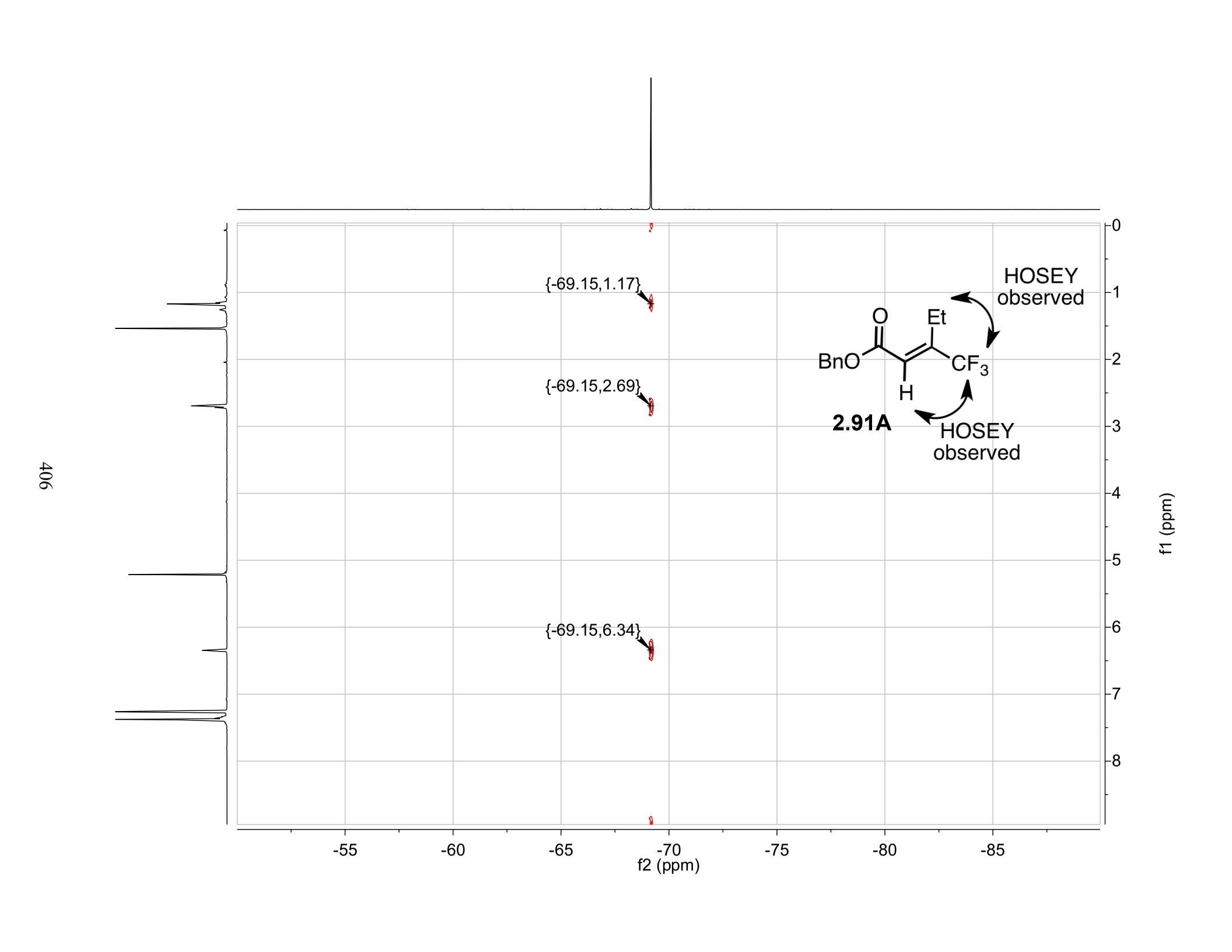
{-69.15,1.17}
{-69.15,2.69}
{-69.15,6.34}
HOSEY observed
O
Et
BnO
CF3
H
2.91A
HOSEY observed
-55
-60
-65
-70
-75
-80
-85
f2 (ppm)
0
1
2
3
4
5
6
7
8
f1 (ppm)
406

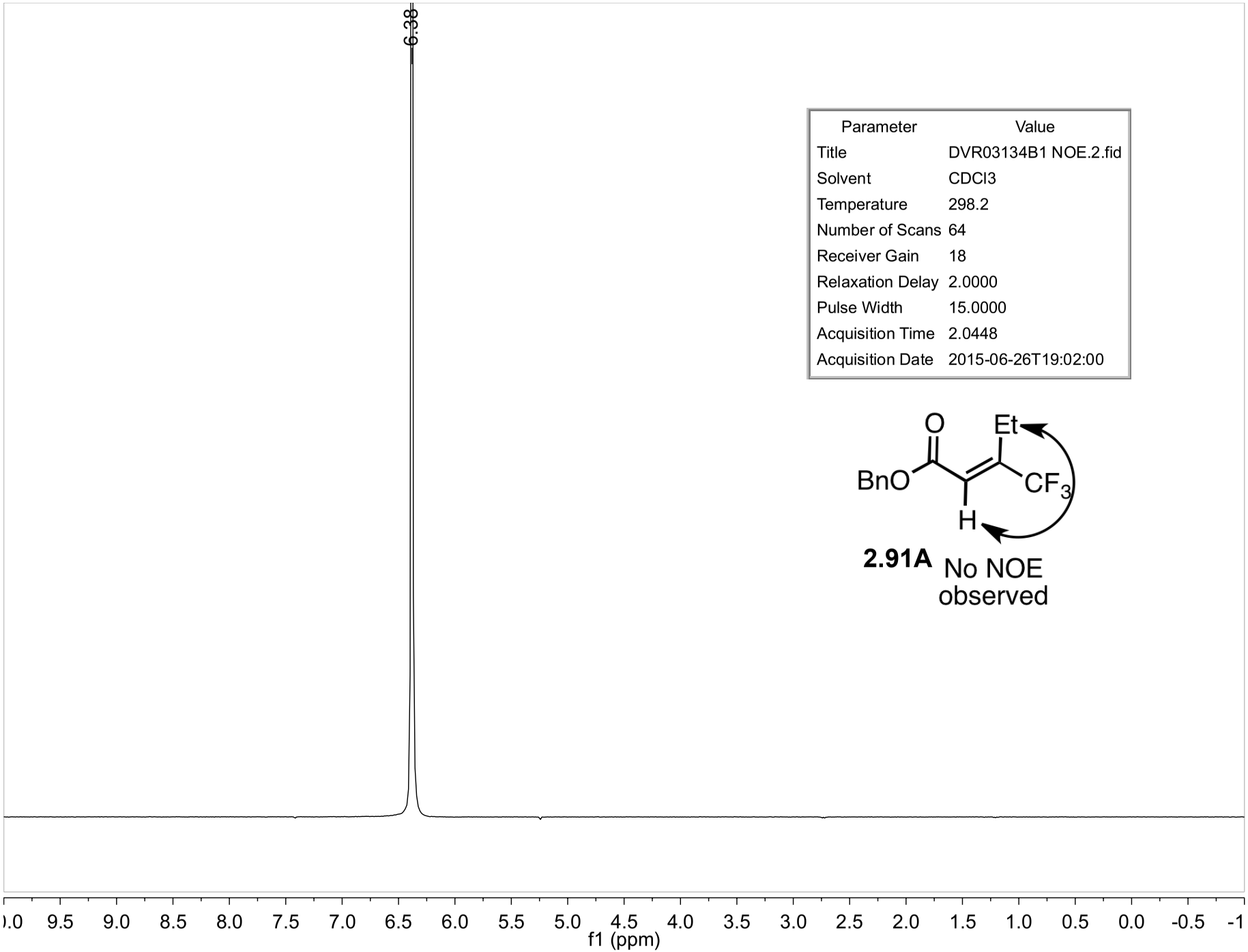

Parameter	Value
Title	DVR03134B1 NOE.2.fid
Solvent	CDCl3
Temperature	298.2
Number of Scans	64
Receiver Gain	18
Relaxation Delay	2.0000
Pulse Width	15.0000
Acquisition Time	2.0448
Acquisition Date	2015-06-26T19:02:00

2.91A No NOE observed

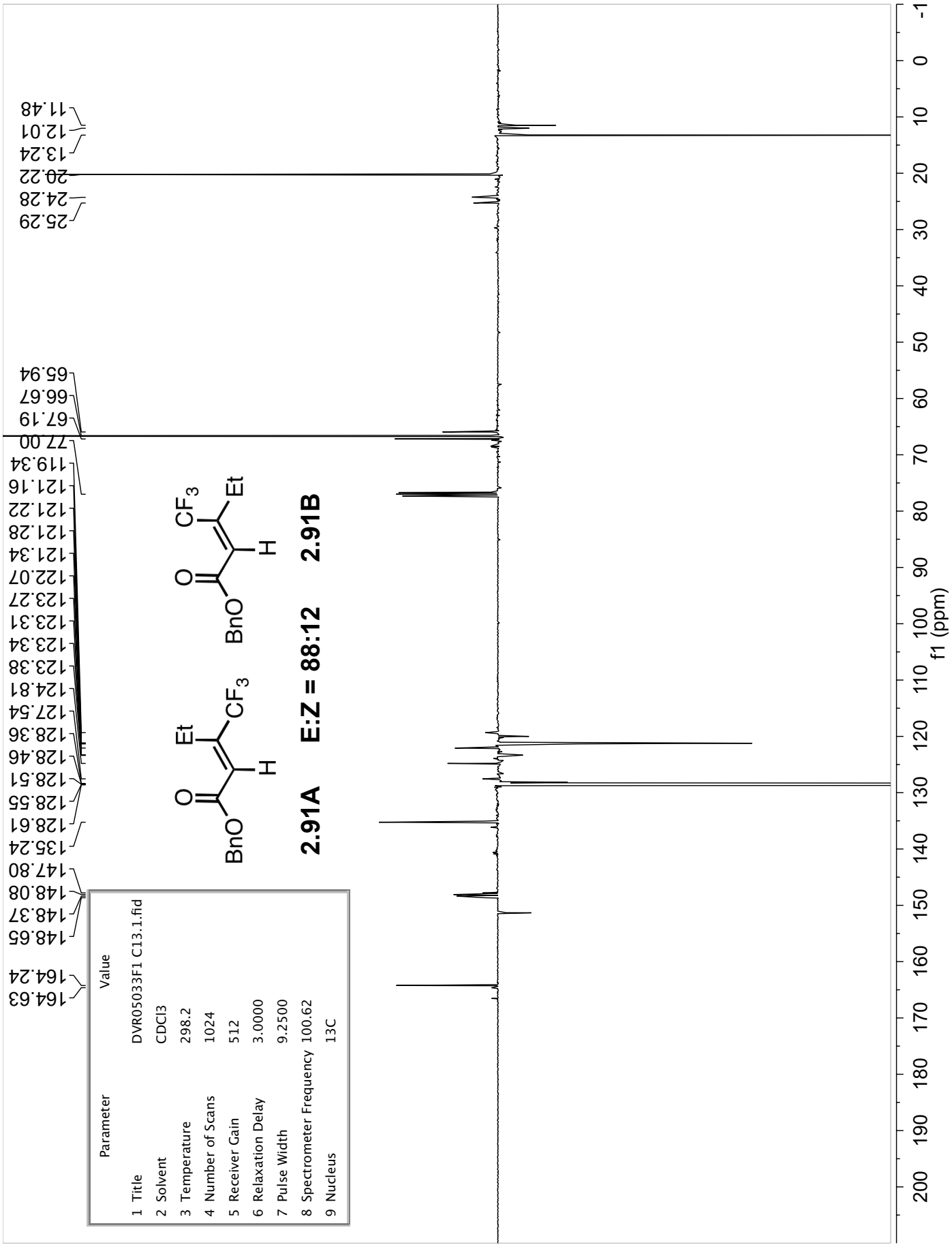
Parameter Value
1 Title DVR05033F1 C13.1.fid
2 Solvent CDCl3
3 Temperature 298.2
4 Number of Scans 1024
5 Receiver Gain 512
6 Relaxation Delay 3.0000
7 Pulse Width 9.2500
8 Spectrometer Frequency 100.62
9 Nucleus 13C
164.63
164.24
148.65
148.37
148.08
147.80
135.24
128.61
128.55
128.51
128.46
128.36
127.54
124.81
123.38
123.34
123.31
123.27
122.07
121.34
121.28
121.22
121.16
119.34
77.00
67.19
66.67
65.94
25.29
24.28
20.22
13.24
12.01
11.48
BnO
O
Et
CF3
H
2.91A E:Z = 88:12 2.91B
f1 (ppm)

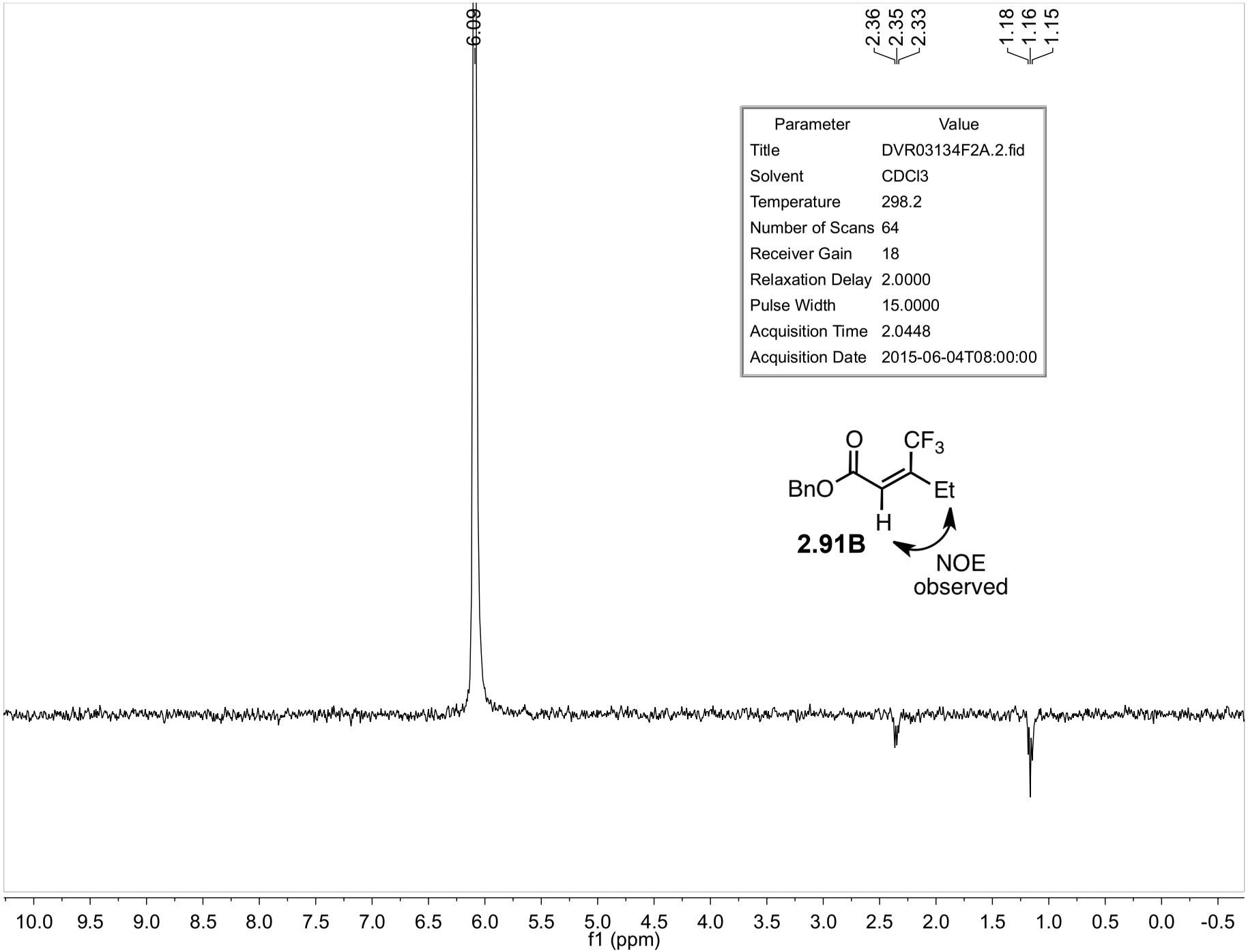
6.09
2.36
2.35
2.33
1.18
1.16
1.15
Parameter Value
Title DVR03134F2A.2.fid
Solvent CDCl3
Temperature 298.2
Number of Scans 64
Receiver Gain 18
Relaxation Delay 2.0000
Pulse Width 15.0000
Acquisition Time 2.0448
Acquisition Date 2015-06-04T08:00:00
O
CF3
BnO
Et
H
2.91B
NOE observed
10.0 9.5 9.0 8.5 8.0 7.5 7.0 6.5 6.0 5.5 5.0 4.5 4.0 3.5 3.0 2.5 2.0 1.5 1.0 0.5 0.0 -0.5
f1 (ppm)

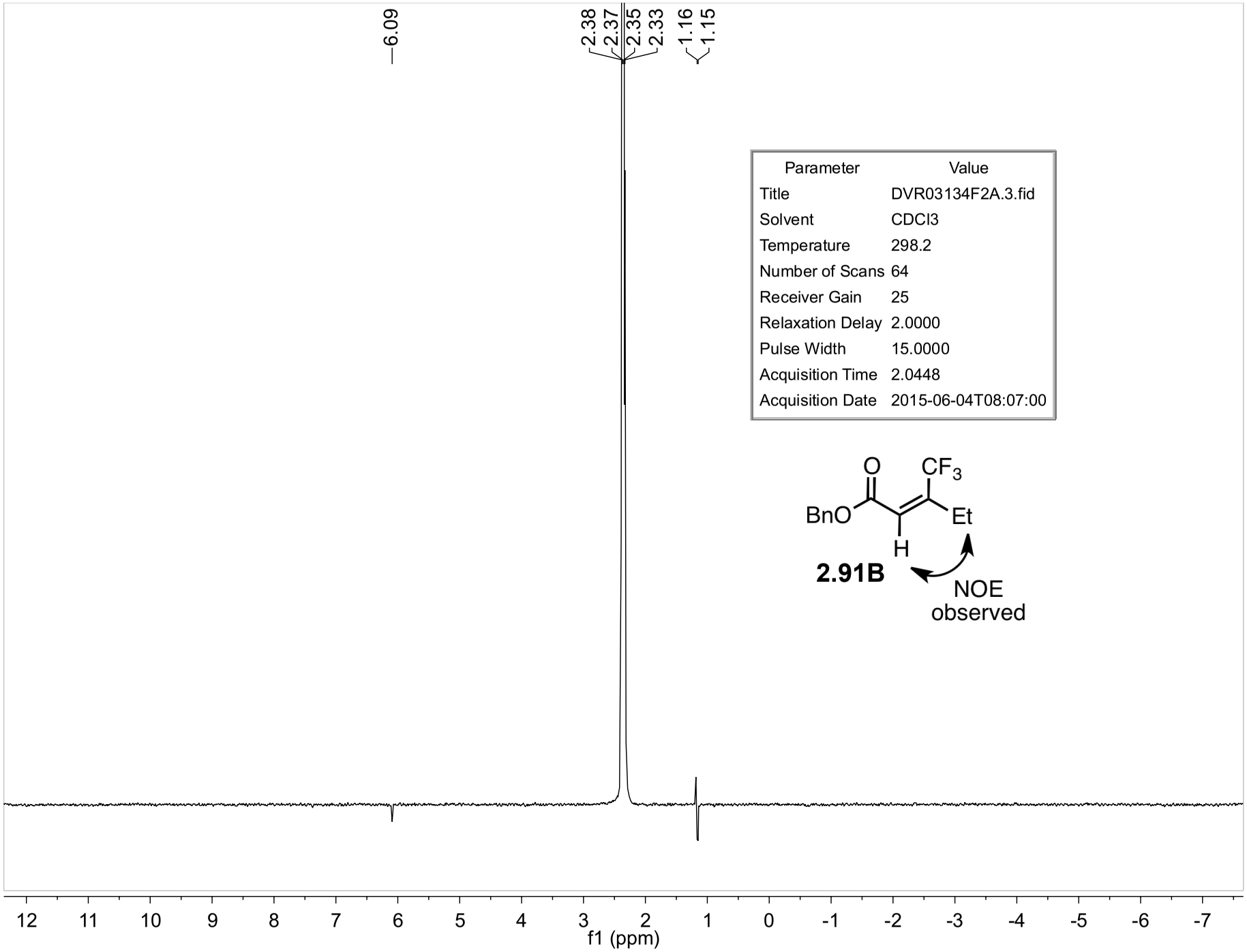
6.09
2.38
2.37
2.35
2.33
1.16
1.15
Parameter Value
Title DVR03134F2A.3.fid
Solvent CDCl3
Temperature 298.2
Number of Scans 64
Receiver Gain 25
Relaxation Delay 2.0000
Pulse Width 15.0000
Acquisition Time 2.0448
Acquisition Date 2015-06-04T08:07:00
O
CF3
BnO
Et
H
2.91B
NOE observed
12 11 10 9 8 7 6 5 4 3 2 1 0 -1 -2 -3 -4 -5 -6 -7
f1 (ppm)

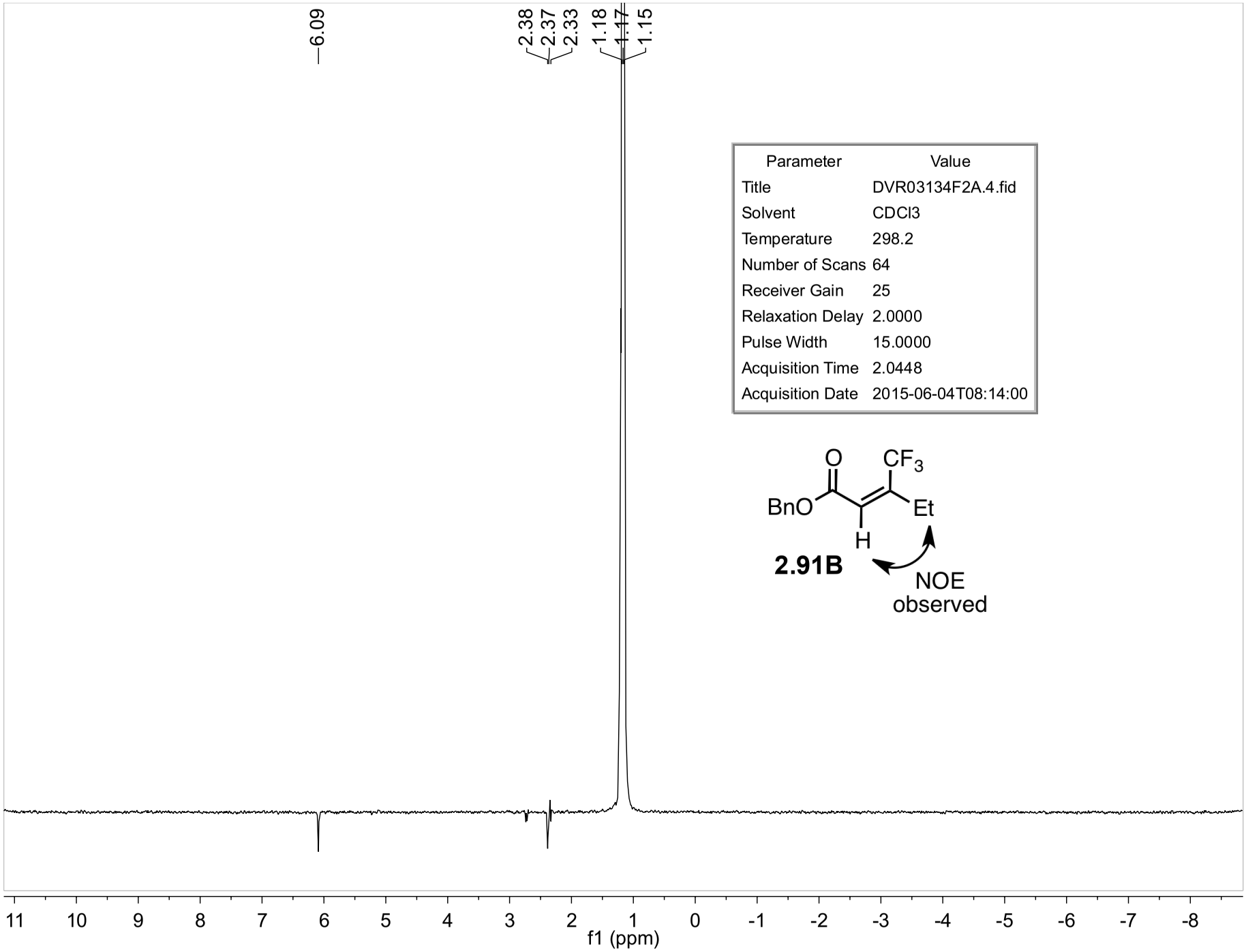
6.09
2.38
2.37
2.33
1.18
1.17
1.15
Parameter Value
Title DVR03134F2A.4.fid
Solvent CDCl3
Temperature 298.2
Number of Scans 64
Receiver Gain 25
Relaxation Delay 2.0000
Pulse Width 15.0000
Acquisition Time 2.0448
Acquisition Date 2015-06-04T08:14:00
O
CF3
BnO
Et
H
2.91B
NOE
observed
11 10 9 8 7 6 5 4 3 2 1 0 -1 -2 -3 -4 -5 -6 -7 -8
f1 (ppm)

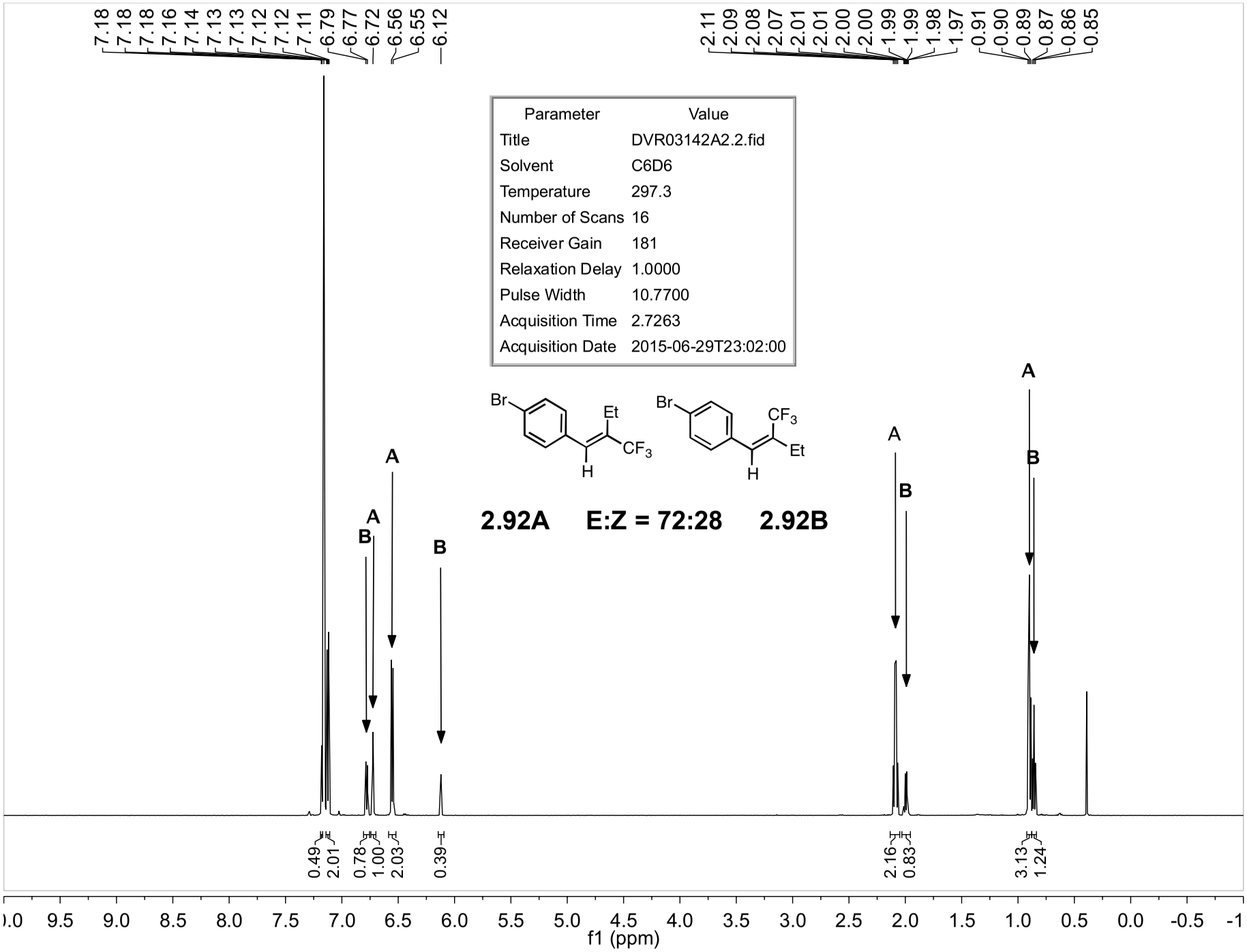
7.18
7.18
7.18
7.16
7.14
7.13
7.13
7.12
7.12
7.11
6.79
6.77
6.72
6.56
6.55
6.12
2.11
2.09
2.08
2.07
2.01
2.01
2.00
2.00
1.99
1.99
1.98
1.97
0.91
0.90
0.89
0.87
0.86
0.85
Parameter Value
Title DVR03142A2.2.fid
Solvent C6D6
Temperature 297.3
Number of Scans 16
Receiver Gain 181
Relaxation Delay 1.0000
Pulse Width 10.7700
Acquisition Time 2.7263
Acquisition Date 2015-06-29T23:02:00
Br
Et
CF3
H
Br
CF3
Et
H
2.92A E:Z = 72:28 2.92B
A
B
A
B
B
A
B
A
B
0.49
2.01
0.78
1.00
2.03
0.39
2.16
0.83
3.13
1.24
f1 (ppm)

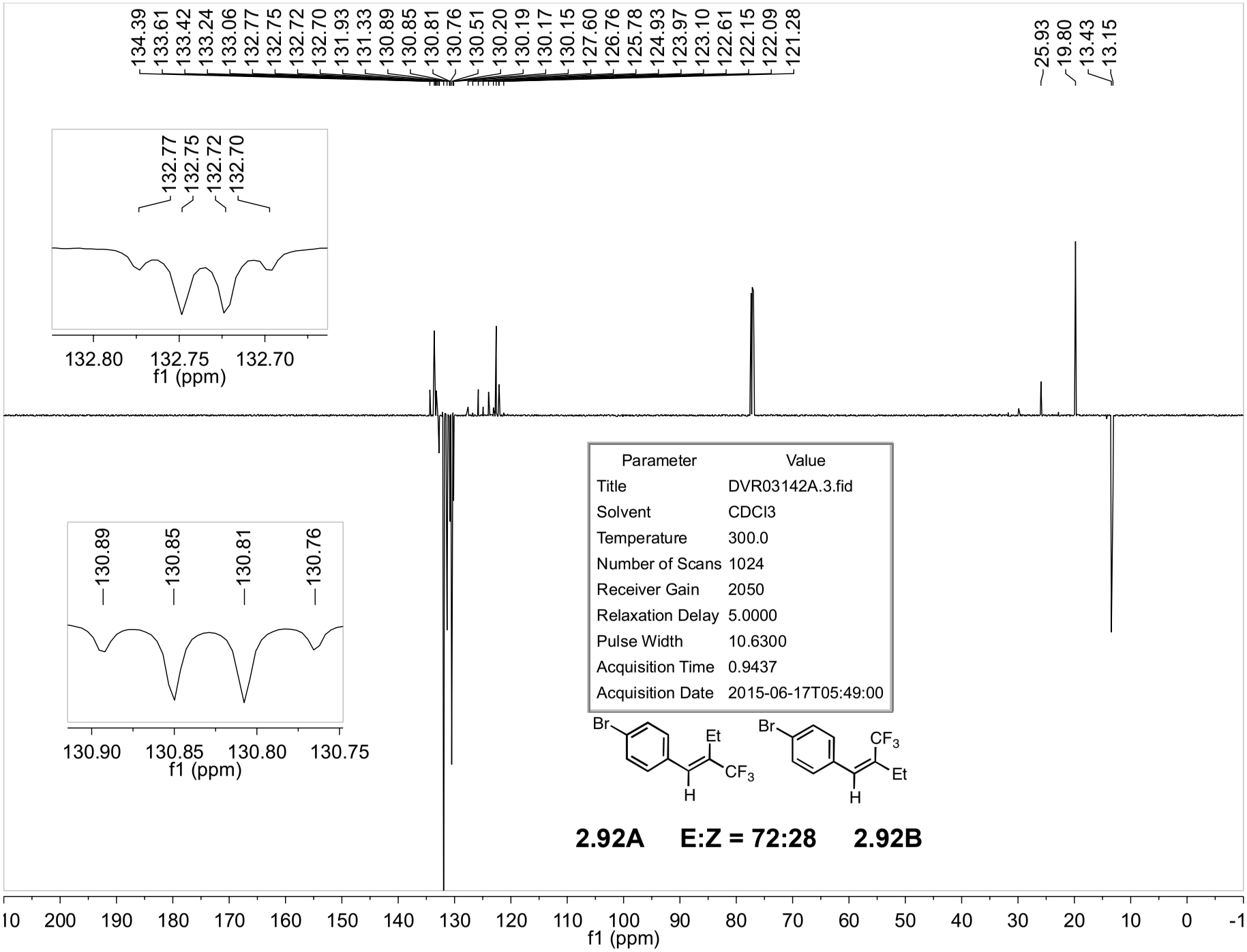
134.39
133.61
133.42
133.24
133.06
132.77
132.75
132.72
132.70
131.93
131.33
130.89
130.85
130.81
130.76
130.51
130.20
130.19
130.17
130.15
127.60
126.76
125.78
124.93
123.97
123.10
122.61
122.15
122.09
121.28
25.93
19.80
13.43
13.15
132.77
132.75
132.72
132.70
132.80
132.75
132.70
f1 (ppm)
130.89
130.85
130.81
130.76
130.90
130.85
130.80
130.75
f1 (ppm)
Parameter Value
Title DVR03142A.3.fid
Solvent CDCl3
Temperature 300.0
Number of Scans 1024
Receiver Gain 2050
Relaxation Delay 5.0000
Pulse Width 10.6300
Acquisition Time 0.9437
Acquisition Date 2015-06-17T05:49:00
Br
Et
CF3
H
Br
CF3
Et
H
2.92A E:Z = 72:28 2.92B
10 200 190 180 170 160 150 140 130 120 110 100 90 80 70 60 50 40 30 20 10 0 -1
f1 (ppm)

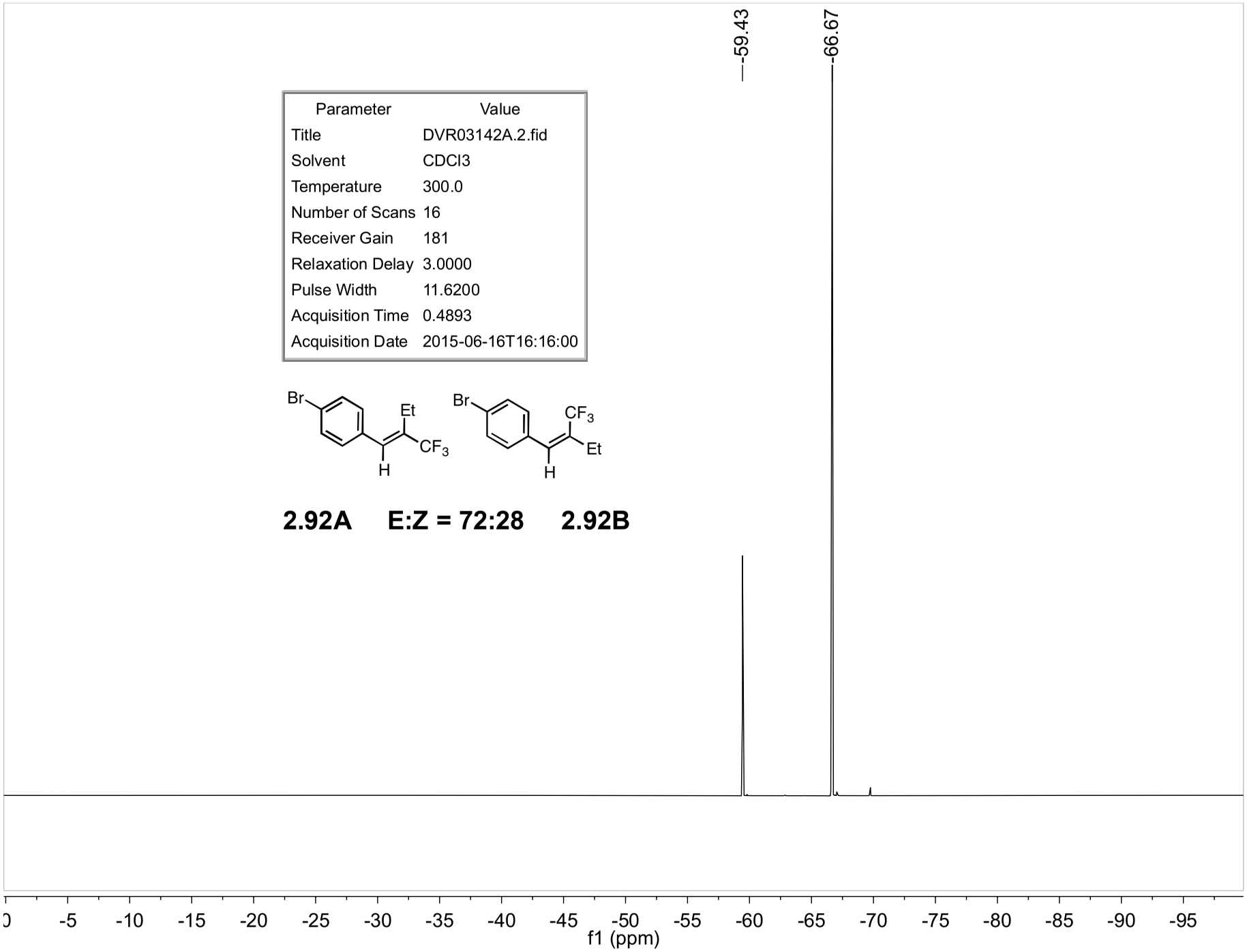
-59.43
-66.67
Parameter Value
Title DVR03142A.2.fid
Solvent CDCl3
Temperature 300.0
Number of Scans 16
Receiver Gain 181
Relaxation Delay 3.0000
Pulse Width 11.6200
Acquisition Time 0.4893
Acquisition Date 2015-06-16T16:16:00
Br
Et
CF3
H
Br
CF3
Et
H
2.92A E:Z = 72:28 2.92B
0 -5 -10 -15 -20 -25 -30 -35 -40 -45 -50 -55 -60 -65 -70 -75 -80 -85 -90 -95
f1 (ppm)

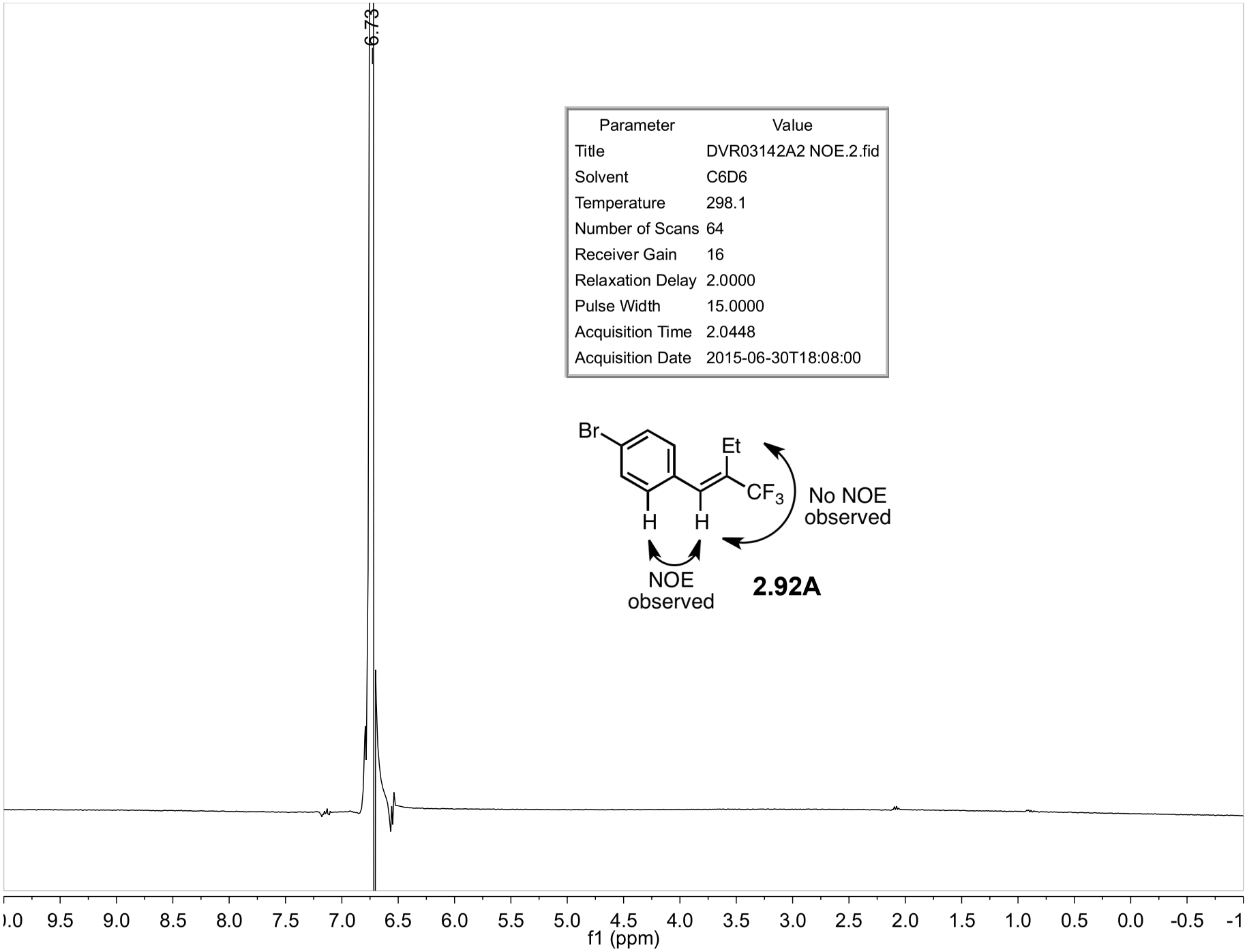
6.73
Parameter Value
Title DVR03142A2 NOE.2.fid
Solvent C6D6
Temperature 298.1
Number of Scans 64
Receiver Gain 16
Relaxation Delay 2.0000
Pulse Width 15.0000
Acquisition Time 2.0448
Acquisition Date 2015-06-30T18:08:00
Br
Et
CF3
H
H
No NOE observed
NOE observed
2.92A
f1 (ppm)

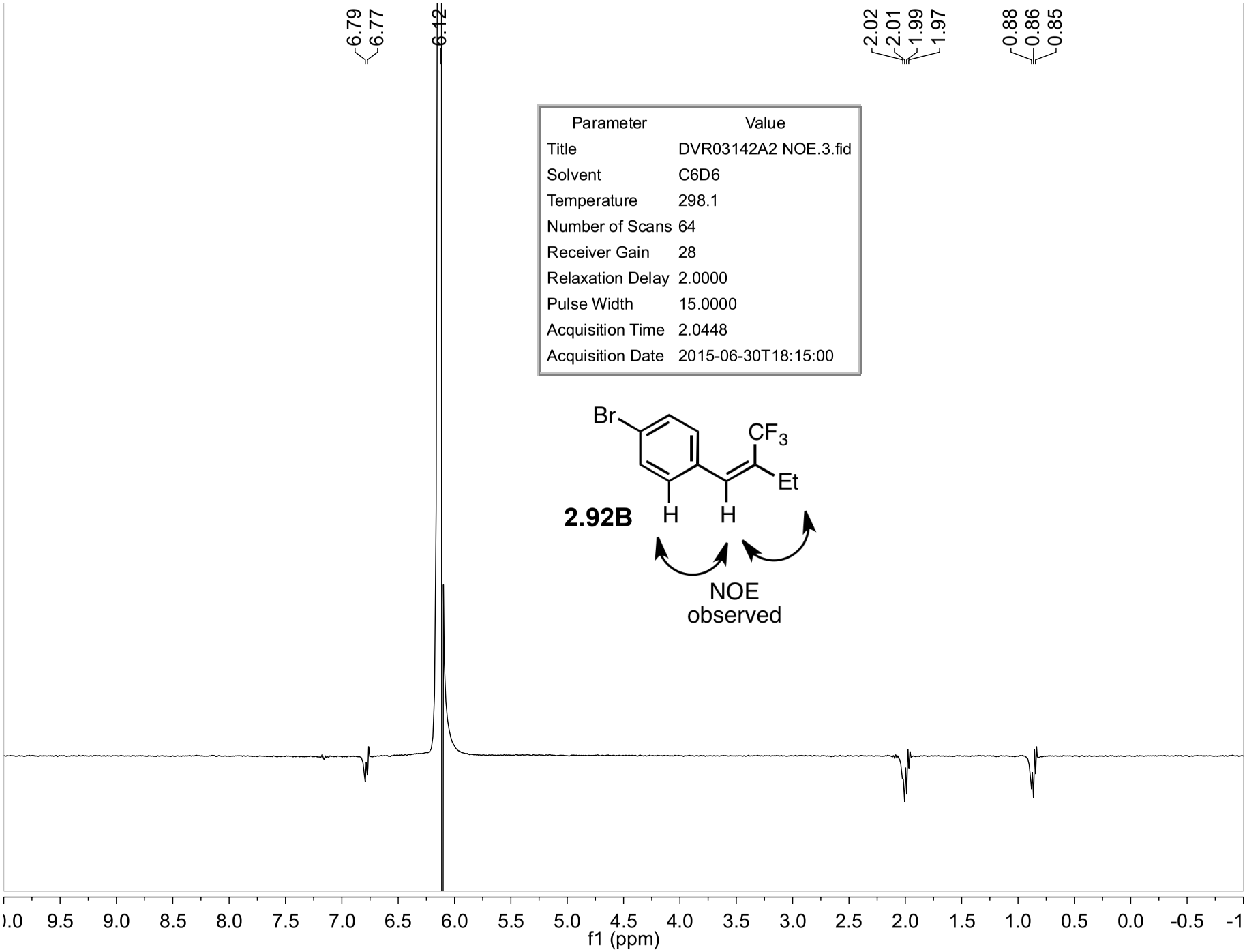
6.79
6.77
6.12
2.02
2.01
1.99
1.97
0.88
0.86
0.85
Parameter Value
Title DVR03142A2 NOE.3.fid
Solvent C6D6
Temperature 298.1
Number of Scans 64
Receiver Gain 28
Relaxation Delay 2.0000
Pulse Width 15.0000
Acquisition Time 2.0448
Acquisition Date 2015-06-30T18:15:00
Br
CF3
Et
H
H
2.92B
NOE
observed
f1 (ppm)

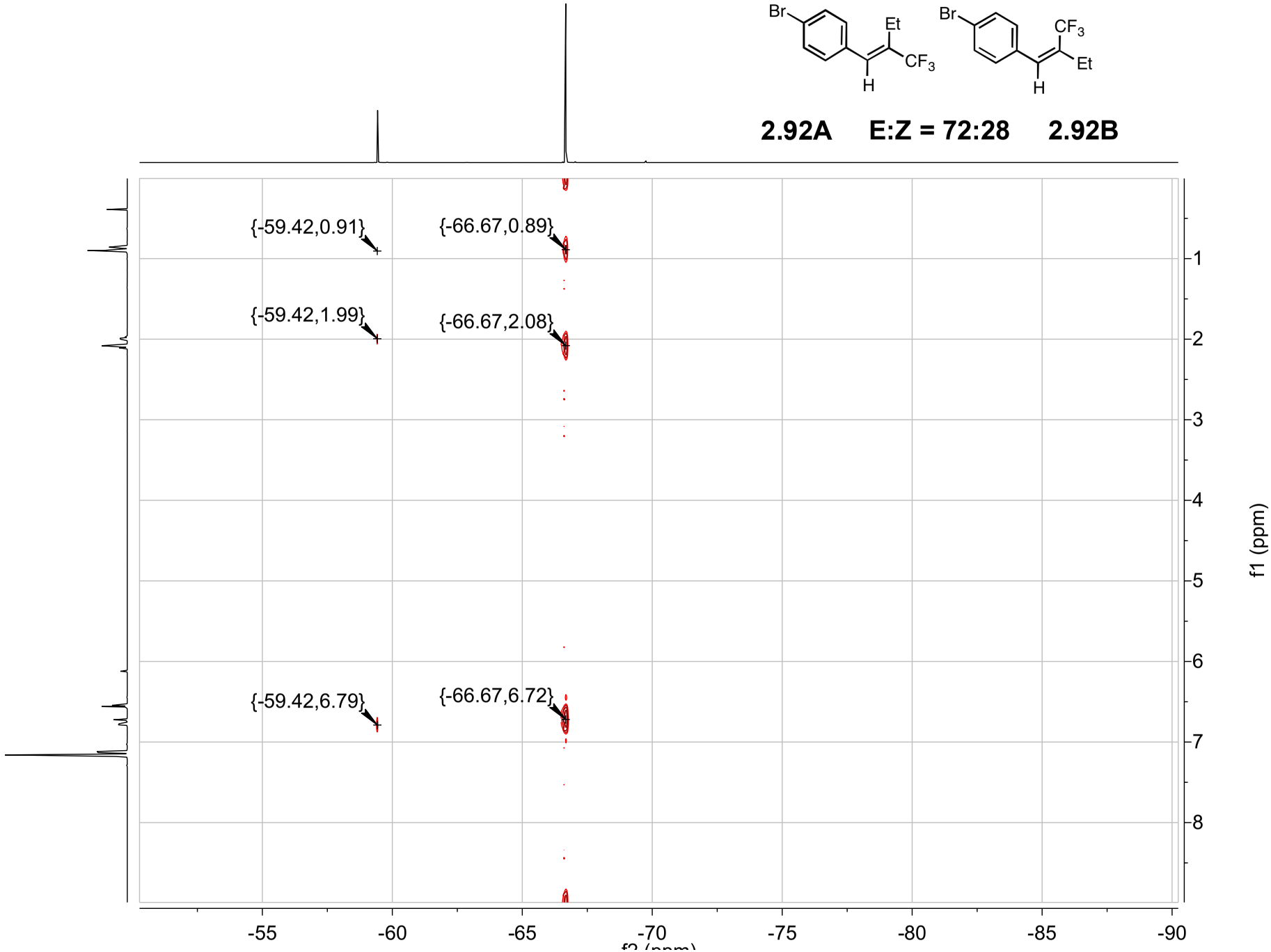
Br
Et
CF3
H
Br
CF3
Et
H
2.92A E:Z = 72:28 2.92B
{-59.42,0.91}
{-66.67,0.89}
{-59.42,1.99}
{-66.67,2.08}
{-59.42,6.79}
{-66.67,6.72}
-55
-60
-65
-70
-75
-80
-85
-90
f2 (ppm)
1
2
3
4
5
6
7
8
f1 (ppm)

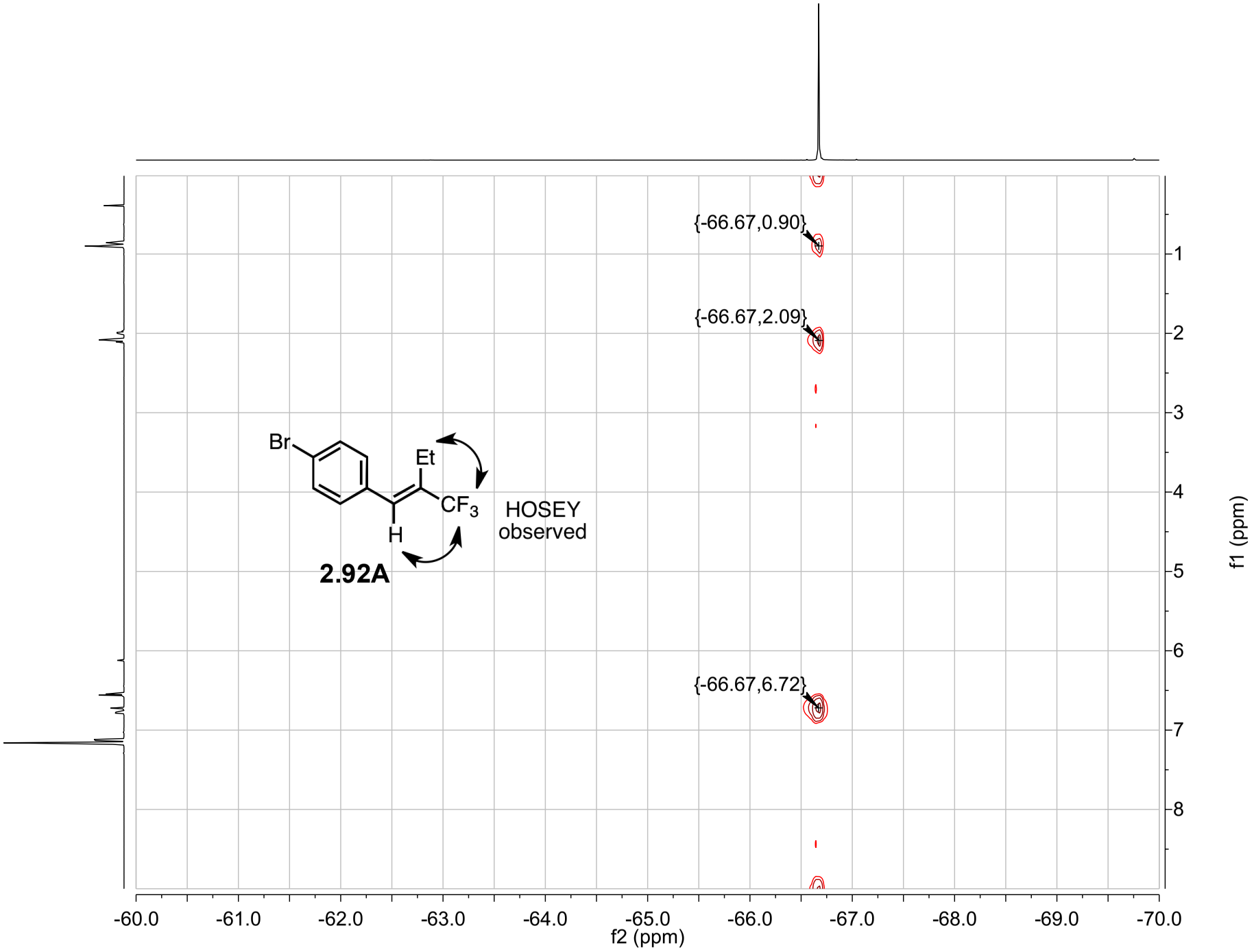
{-66.67,0.90}
{-66.67,2.09}
{-66.67,6.72}
Br
Et
CF3
H
HOSEY
observed
2.92A
-60.0
-61.0
-62.0
-63.0
-64.0
-65.0
-66.0
-67.0
-68.0
-69.0
-70.0
f2 (ppm)
1
2
3
4
5
6
7
8
f1 (ppm)

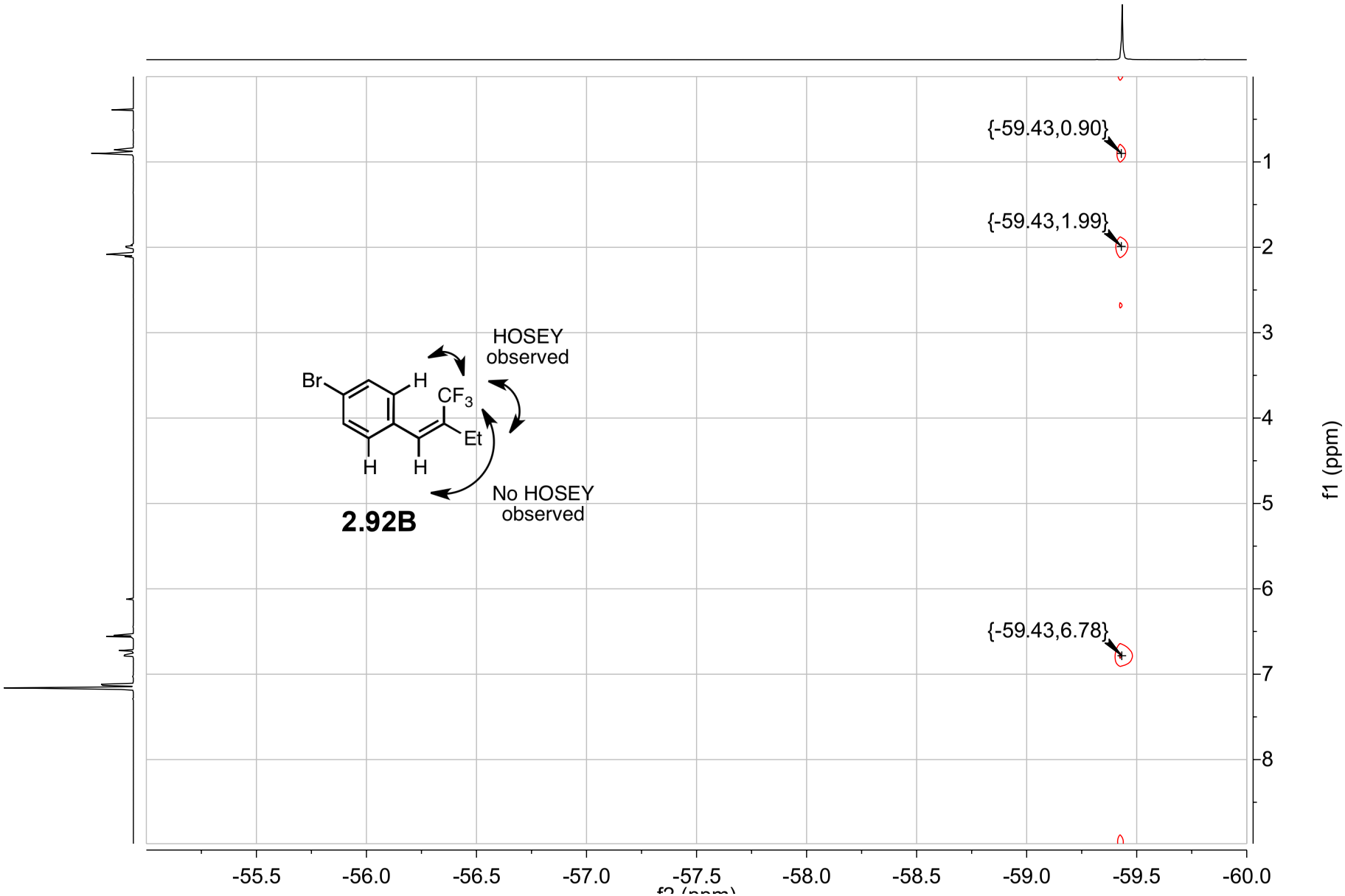
{-59.43,0.90}
{-59.43,1.99}
{-59.43,6.78}
HOSEY
observed
No HOSEY
observed
Br
H
CF3
Et
H
H
2.92B
-55.5
-56.0
-56.5
-57.0
-57.5
-58.0
-58.5
-59.0
-59.5
-60.0
f2 (ppm)
1
2
3
4
5
6
7
8
f1 (ppm)

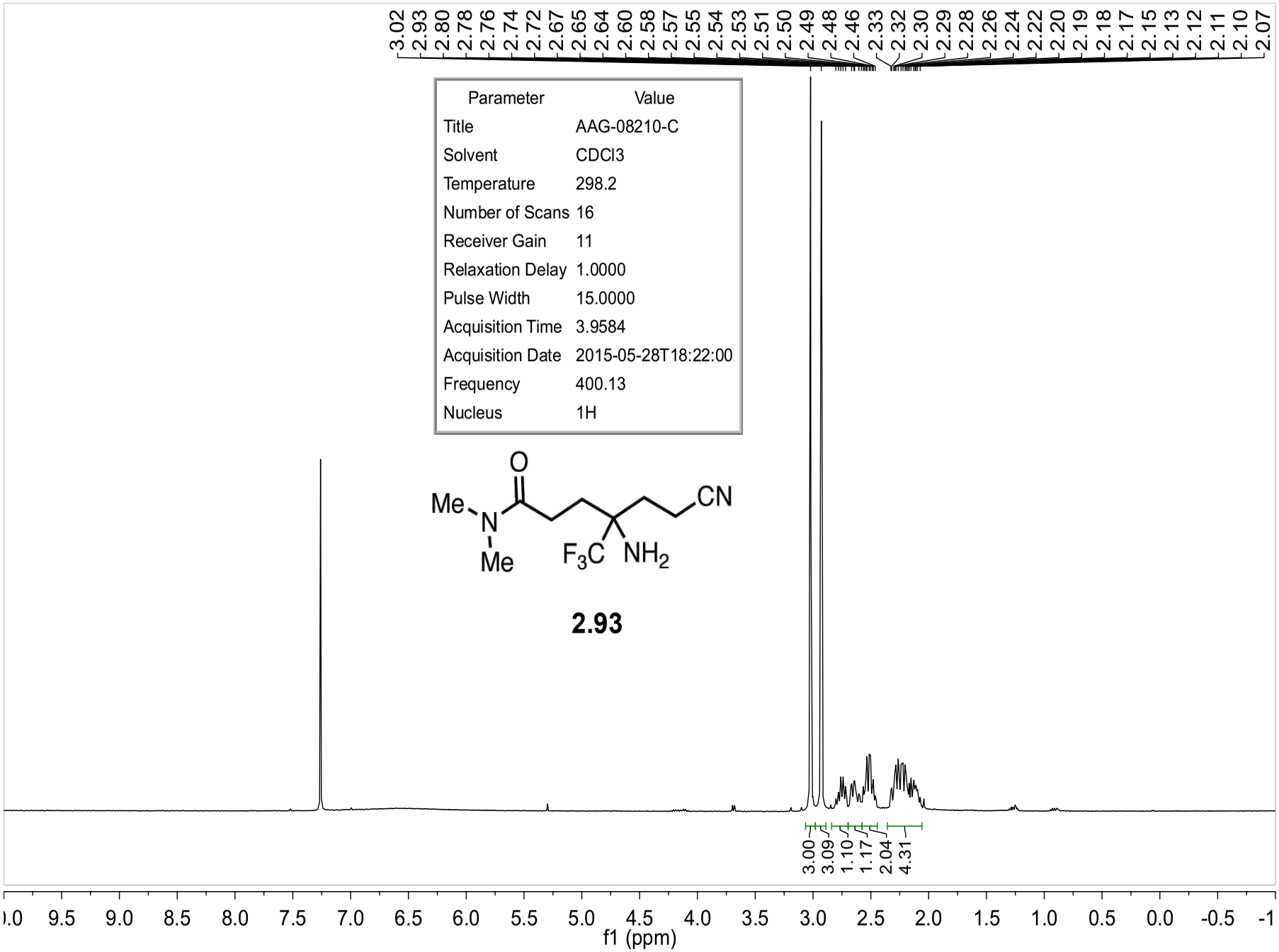
3.02 2.93 2.80 2.78 2.76 2.74 2.72 2.67 2.65 2.64 2.60 2.58 2.57 2.55 2.54 2.53 2.51 2.50 2.49 2.48 2.46 2.33 2.32 2.30 2.29 2.28 2.26 2.24 2.22 2.20 2.19 2.18 2.17 2.15 2.13 2.12 2.11 2.10 2.07
Parameter Value
Title AAG-08210-C
Solvent CDCl3
Temperature 298.2
Number of Scans 16
Receiver Gain 11
Relaxation Delay 1.0000
Pulse Width 15.0000
Acquisition Time 3.9584
Acquisition Date 2015-05-28T18:22:00
Frequency 400.13
Nucleus 1H
O
Me
N
Me
CN
F3C
NH2
2.93
3.00 3.09 1.10 1.17 2.04 4.31
9.5 9.0 8.5 8.0 7.5 7.0 6.5 6.0 5.5 5.0 4.5 4.0 3.5 3.0 2.5 2.0 1.5 1.0 0.5 0.0 -0.5 -1
f1 (ppm)

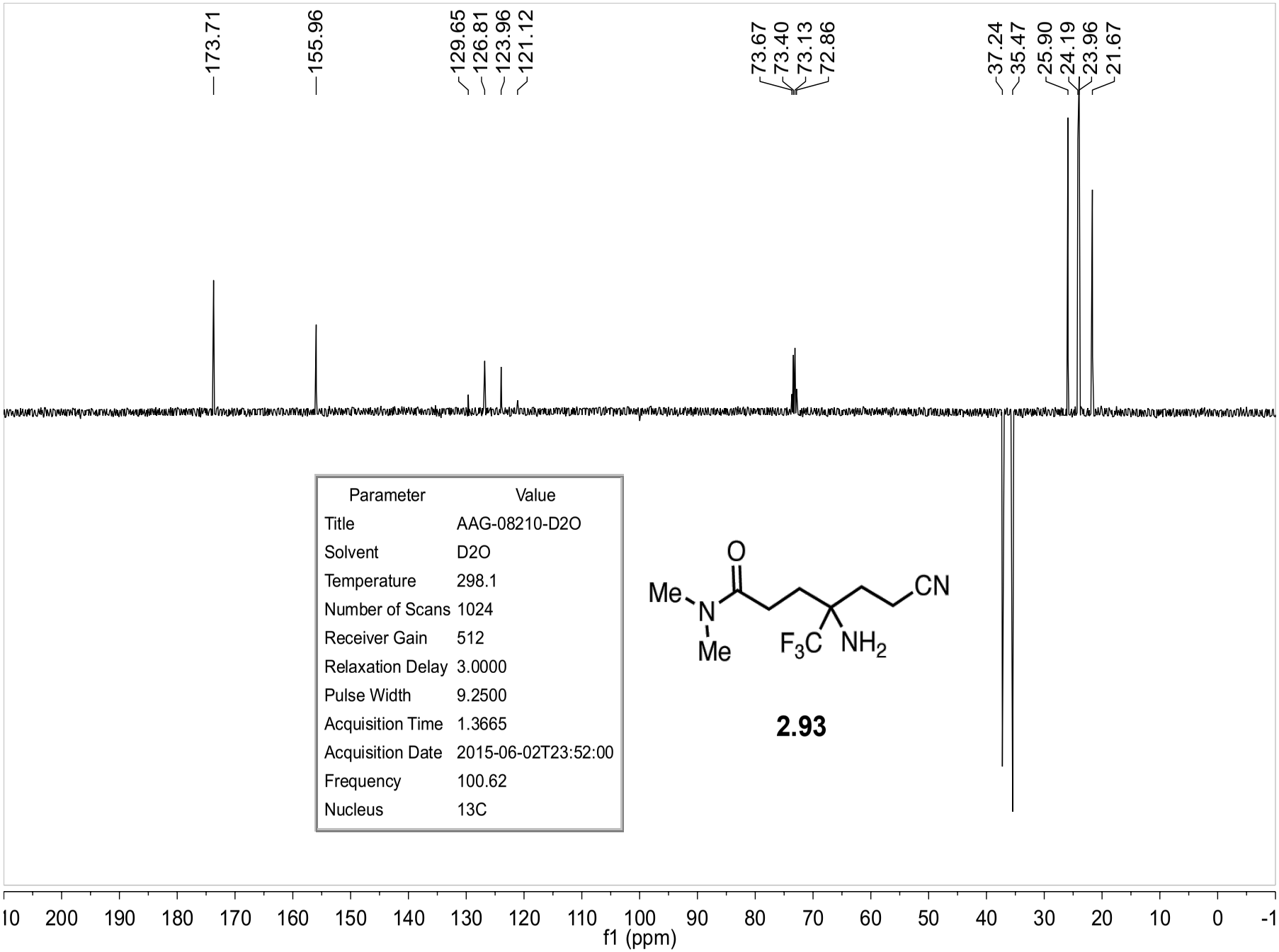

Parameter	Value
Title	AAG-08210-D2O
Solvent	D2O
Temperature	298.1
Number of Scans	1024
Receiver Gain	512
Relaxation Delay	3.0000
Pulse Width	9.2500
Acquisition Time	1.3665
Acquisition Date	2015-06-02T23:52:00
Frequency	100.62
Nucleus	13C

2.93

Parameter	Value
Title	AAG-08210-C
Solvent	CDCl3
Temperature	298.2
Number of Scans	16
Receiver Gain	1626
Relaxation Delay	2.0000
Pulse Width	15.0300
Acquisition Time	0.8717
Acquisition Date	2015-05-28T18:25:00
Frequency	376.46
Nucleus	19F

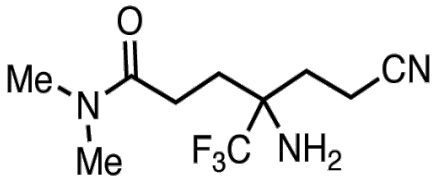

2.93

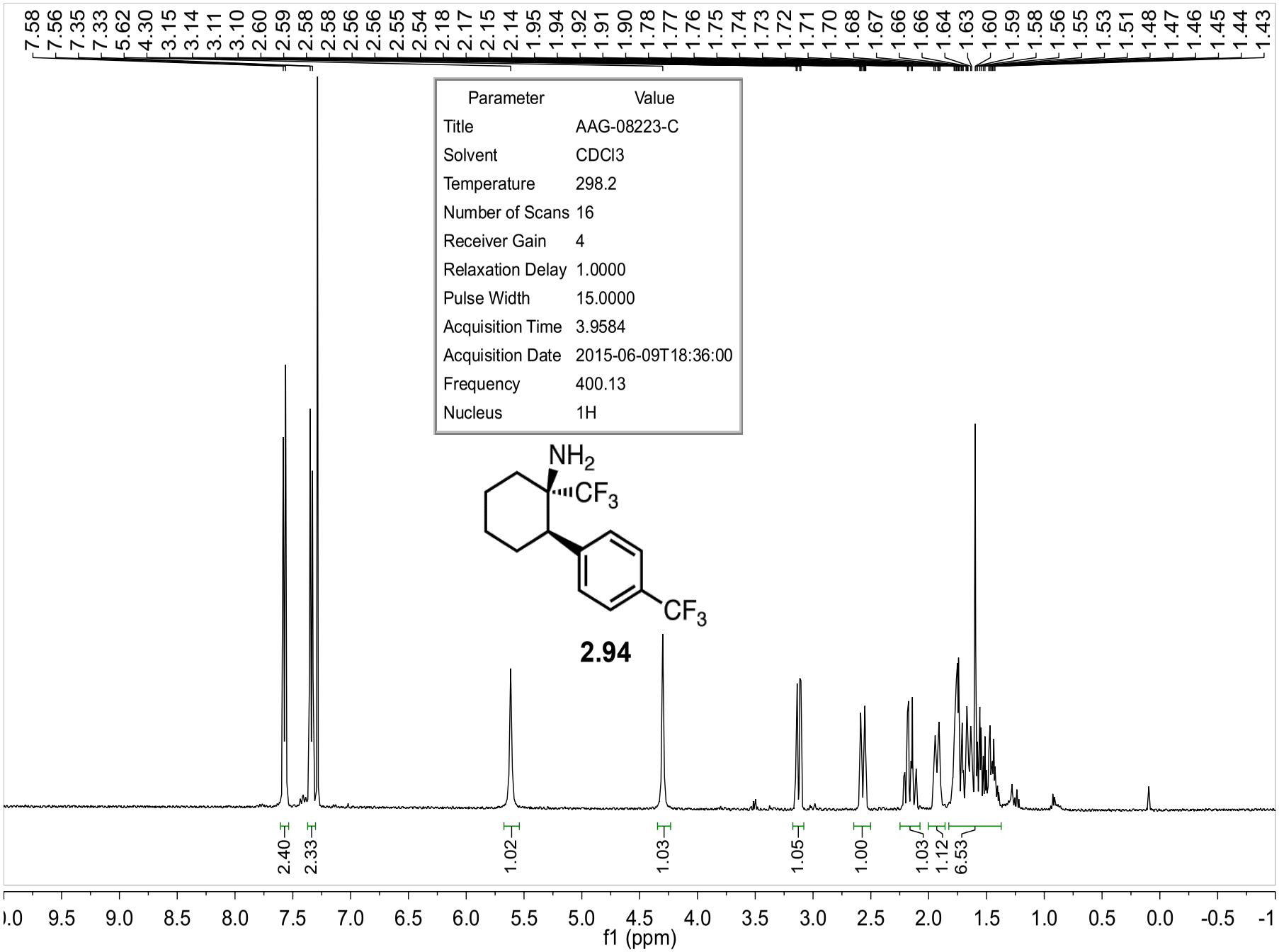
7.58 7.56 7.35 7.33 5.62 4.30 3.15 3.14 3.11 3.10 2.60 2.59 2.58 2.58 2.56 2.56 2.55 2.54 2.18 2.17 2.15 2.14 1.95 1.94 1.92 1.91 1.90 1.78 1.77 1.76 1.75 1.74 1.73 1.72 1.71 1.70 1.68 1.67 1.66 1.66 1.64 1.63 1.60 1.59 1.58 1.56 1.55 1.53 1.51 1.48 1.47 1.46 1.45 1.44 1.43
Parameter Value
Title AAG-08223-C
Solvent CDCl3
Temperature 298.2
Number of Scans 16
Receiver Gain 4
Relaxation Delay 1.0000
Pulse Width 15.0000
Acquisition Time 3.9584
Acquisition Date 2015-06-09T18:36:00
Frequency 400.13
Nucleus 1H
NH2
CF3
CF3
2.94
2.40
2.33
1.02
1.03
1.05
1.00
1.03
1.12
6.53
f1 (ppm)

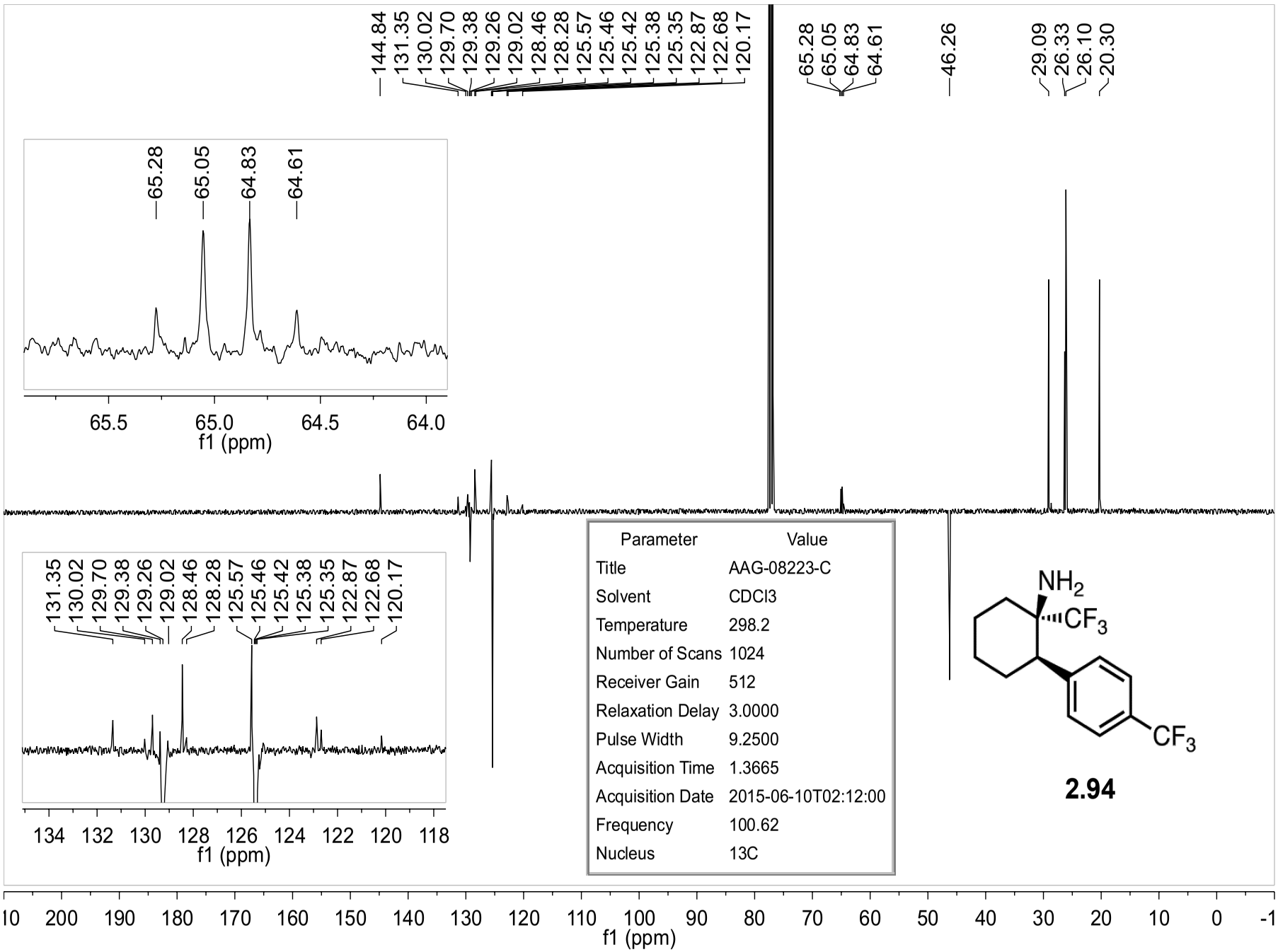
144.84
131.35
130.02
129.70
129.38
129.26
129.02
128.46
128.28
125.57
125.46
125.42
125.38
125.35
122.87
122.68
120.17
65.28
65.05
64.83
64.61
46.26
29.09
26.33
26.10
20.30
65.5
65.0
64.5
64.0
f1 (ppm)
134
132
130
128
126
124
122
120
118
f1 (ppm)
Parameter Value
Title AAG-08223-C
Solvent CDCl3
Temperature 298.2
Number of Scans 1024
Receiver Gain 512
Relaxation Delay 3.0000
Pulse Width 9.2500
Acquisition Time 1.3665
Acquisition Date 2015-06-10T02:12:00
Frequency 100.62
Nucleus 13C
NH2
CF3
CF3
2.94
f1 (ppm)

Parameter	Value
Title	AAG-07223-B
Solvent	CDCl3
Temperature	298.0
Number of Scans	16
Receiver Gain	362
Relaxation Delay	3.0000
Pulse Width	11.6200
Acquisition Time	0.4893
Acquisition Date	2015-03-18T19:13:00
Frequency	564.81
Nucleus	19F

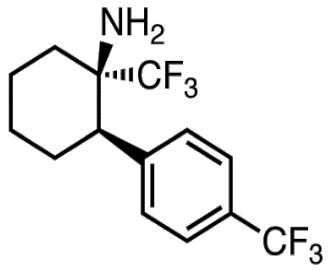

2.94

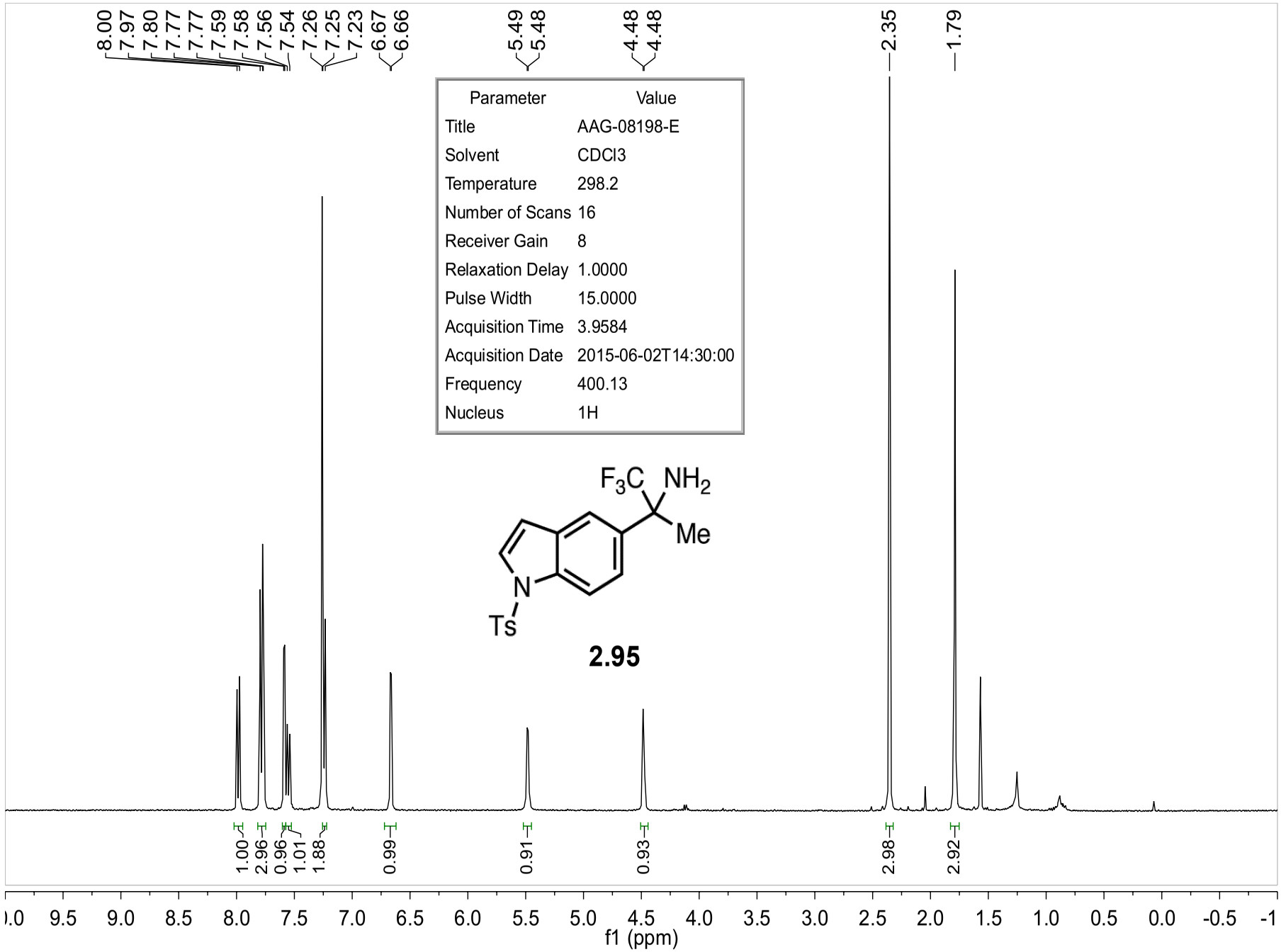
8.00
7.97
7.80
7.77
7.77
7.59
7.58
7.56
7.54
7.26
7.25
7.23
6.67
6.66
5.49
5.48
4.48
4.48
2.35
1.79
Parameter Value
Title AAG-08198-E
Solvent CDCl3
Temperature 298.2
Number of Scans 16
Receiver Gain 8
Relaxation Delay 1.0000
Pulse Width 15.0000
Acquisition Time 3.9584
Acquisition Date 2015-06-02T14:30:00
Frequency 400.13
Nucleus 1H
F3C NH2
Me
N
Ts
2.95
1.00
2.96
0.96
1.01
1.88
0.99
0.91
0.93
2.98
2.92
f1 (ppm)

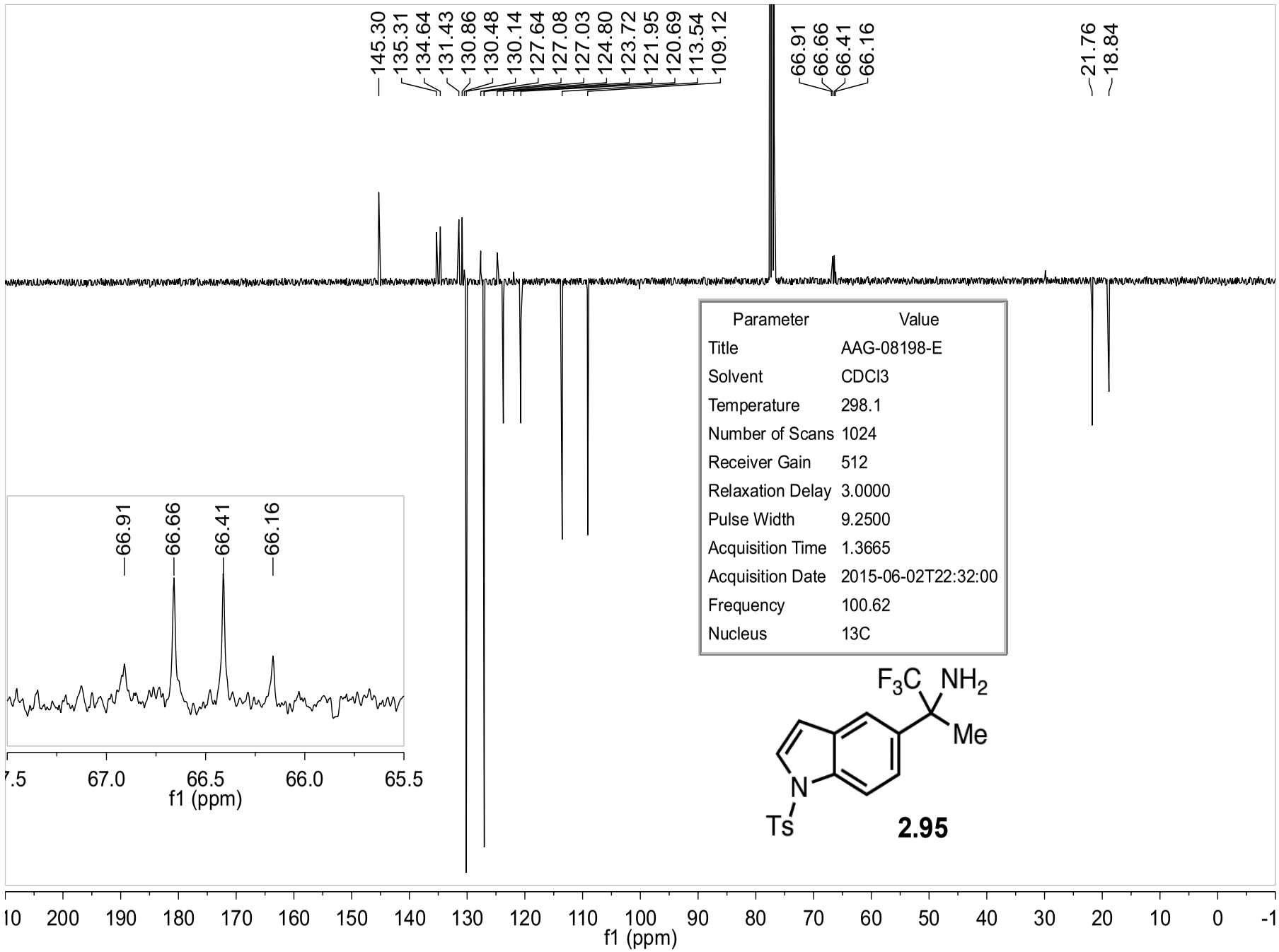
145.30
135.31
134.64
131.43
130.86
130.48
130.14
127.64
127.08
127.03
124.80
123.72
121.95
120.69
113.54
109.12
66.91
66.66
66.41
66.16
21.76
18.84
Parameter Value
Title AAG-08198-E
Solvent CDCl3
Temperature 298.1
Number of Scans 1024
Receiver Gain 512
Relaxation Delay 3.0000
Pulse Width 9.2500
Acquisition Time 1.3665
Acquisition Date 2015-06-02T22:32:00
Frequency 100.62
Nucleus 13C
F3C NH2
Me
N
Ts
2.95
f1 (ppm)

Parameter	Value
Title	AAG-08198-E
Solvent	CDCl3
Temperature	298.1
Number of Scans	16
Receiver Gain	1626
Relaxation Delay	2.0000
Pulse Width	15.0300
Acquisition Time	0.8717
Acquisition Date	2015-06-02T14:33:00
Frequency	376.46
Nucleus	19F

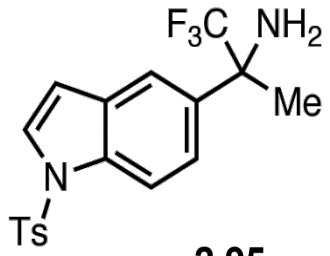

2.95

Appendix B

SPECTRAL DATA FOR CHAPTER 3

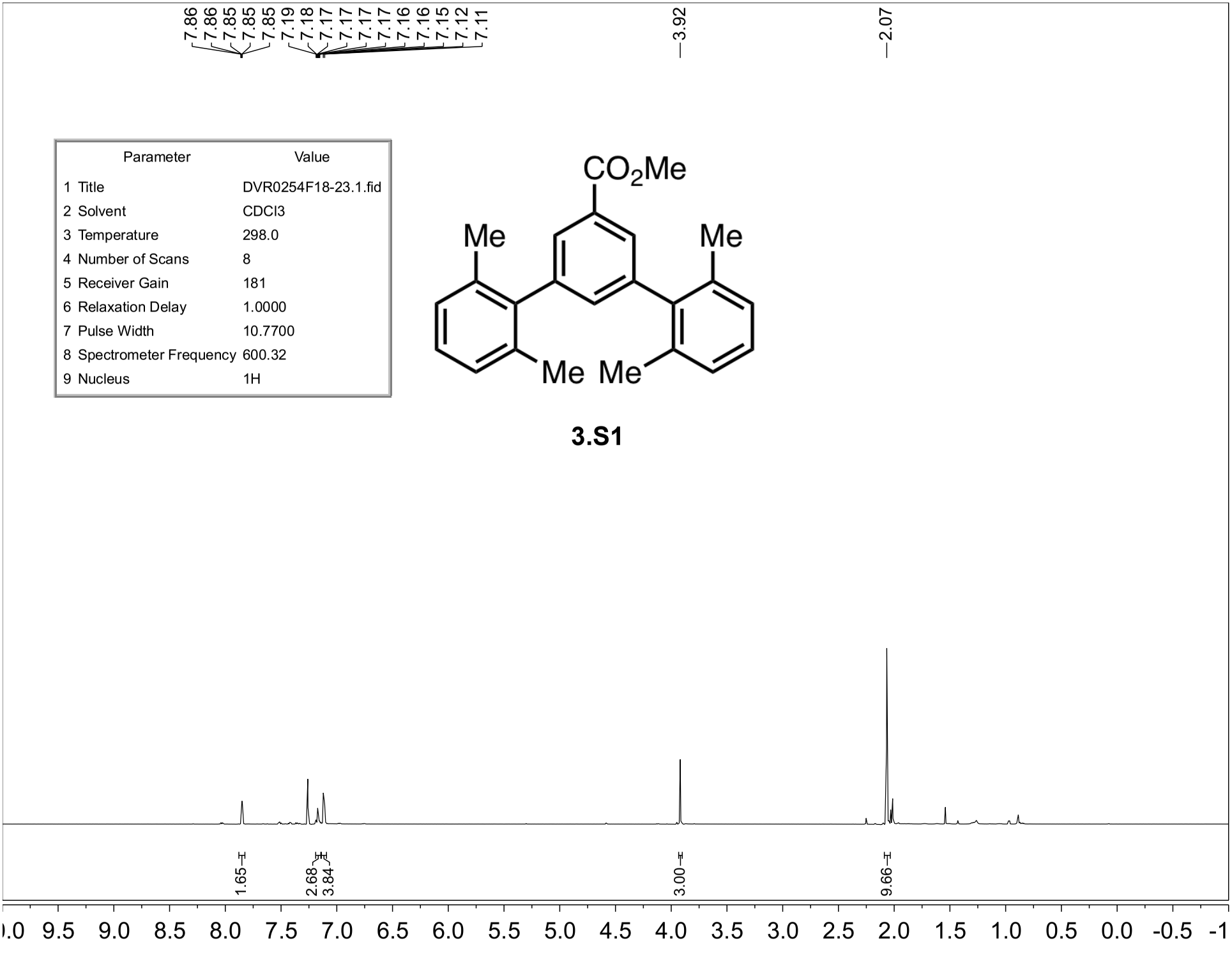
7.86
7.86
7.85
7.85
7.85
7.19
7.18
7.17
7.17
7.17
7.17
7.16
7.16
7.15
7.12
7.11
3.92
2.07
Parameter Value
1 Title DVR0254F18-23.1.fid
2 Solvent CDCl3
3 Temperature 298.0
4 Number of Scans 8
5 Receiver Gain 181
6 Relaxation Delay 1.0000
7 Pulse Width 10.7700
8 Spectrometer Frequency 600.32
9 Nucleus 1H
CO2Me
Me
Me
Me
Me
3.S1
430
1.65
2.68
3.84
3.00
9.66
.0 9.5 9.0 8.5 8.0 7.5 7.0 6.5 6.0 5.5 5.0 4.5 4.0 3.5 3.0 2.5 2.0 1.5 1.0 0.5 0.0 -0.5 -1

Parameter	Value
1 Title	DVR03215.1.fid
2 Solvent	CDCl3
3 Temperature	298.1
4 Number of Scans	16
5 Receiver Gain	9
6 Relaxation Delay	1.0000
7 Pulse Width	15.0000
8 Spectrometer Frequency	400.13
9 Nucleus	1H

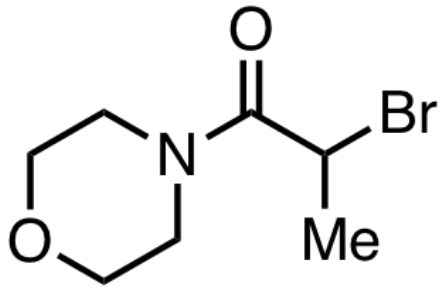

3.S3

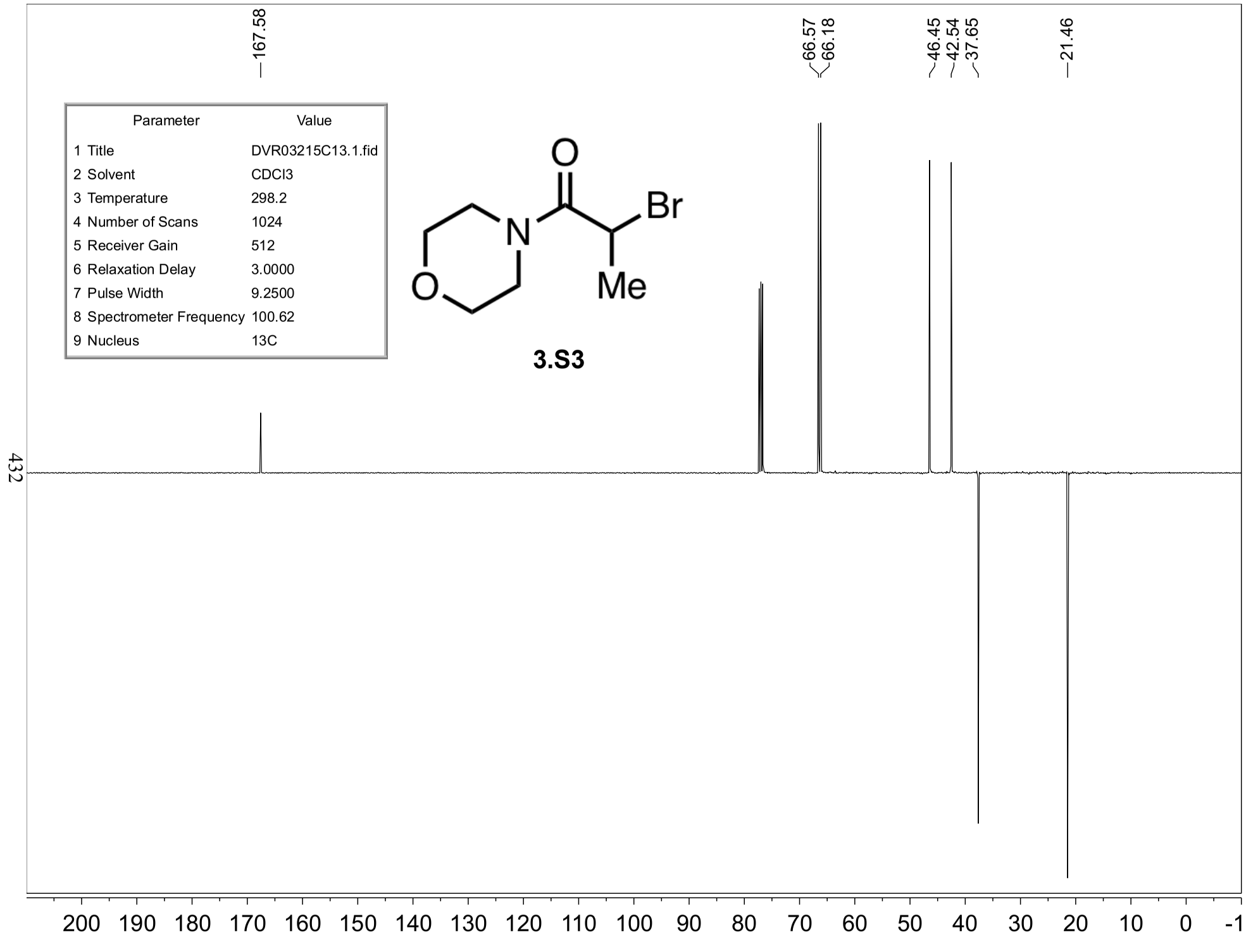
167.58
66.57
66.18
46.45
42.54
37.65
21.46
Parameter Value
1 Title DVR03215C13.1.fid
2 Solvent CDCl3
3 Temperature 298.2
4 Number of Scans 1024
5 Receiver Gain 512
6 Relaxation Delay 3.0000
7 Pulse Width 9.2500
8 Spectrometer Frequency 100.62
9 Nucleus 13C
O
N
O
Br
Me
3.S3
432
200 190 180 170 160 150 140 130 120 110 100 90 80 70 60 50 40 30 20 10 0 -1

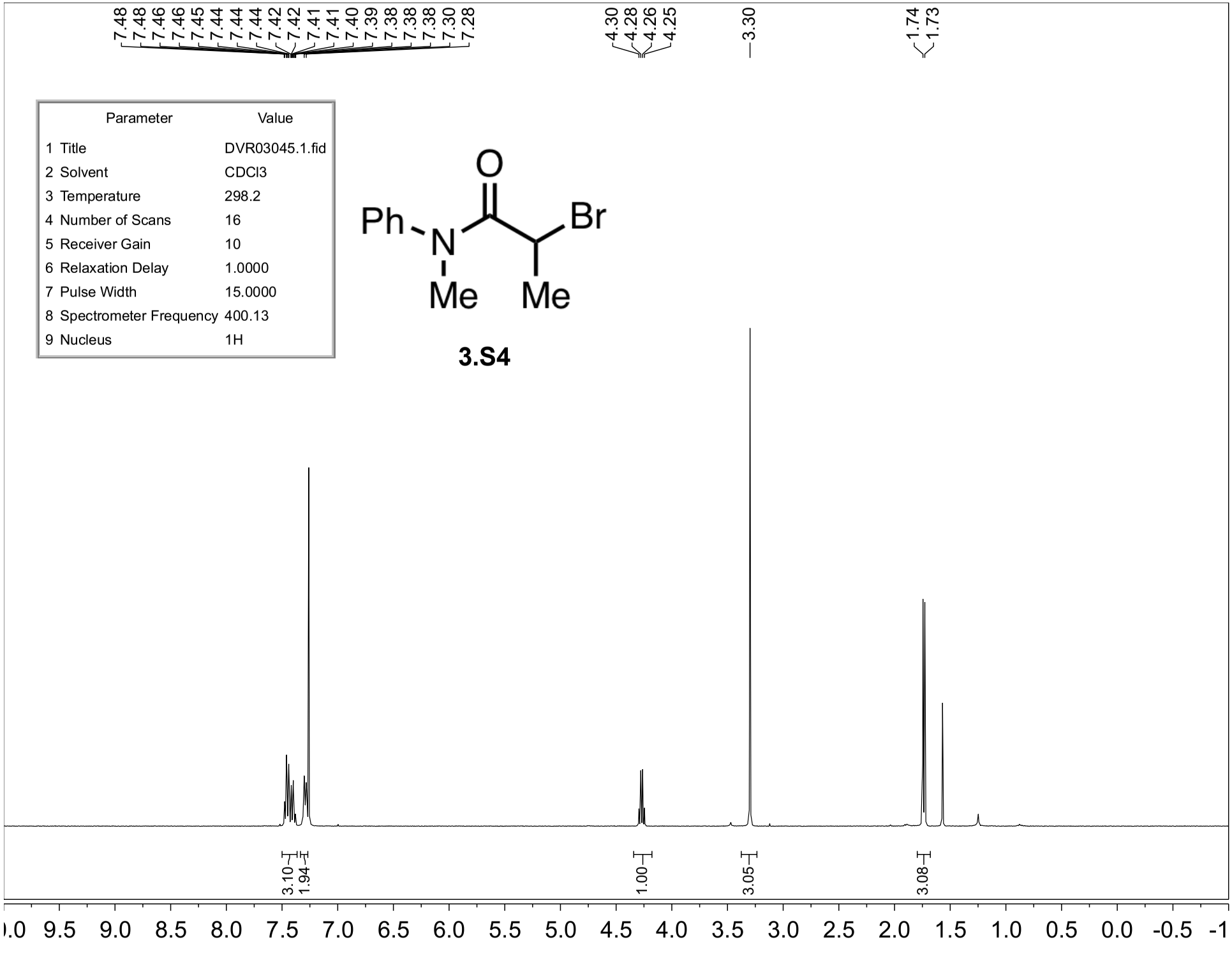
7.48
7.48
7.46
7.46
7.45
7.44
7.44
7.44
7.42
7.42
7.41
7.41
7.40
7.39
7.38
7.38
7.38
7.30
7.28
4.30
4.28
4.26
4.25
3.30
1.74
1.73
Parameter
Value
1 Title
DVR03045.1.fid
2 Solvent
CDCl3
3 Temperature
298.2
4 Number of Scans
16
5 Receiver Gain
10
6 Relaxation Delay
1.0000
7 Pulse Width
15.0000
8 Spectrometer Frequency
400.13
9 Nucleus
1H
O
Ph
N
Br
Me
Me
3.S4
433
3.10
1.94
1.00
3.05
3.08
.0 9.5 9.0 8.5 8.0 7.5 7.0 6.5 6.0 5.5 5.0 4.5 4.0 3.5 3.0 2.5 2.0 1.5 1.0 0.5 0.0 -0.5 -1

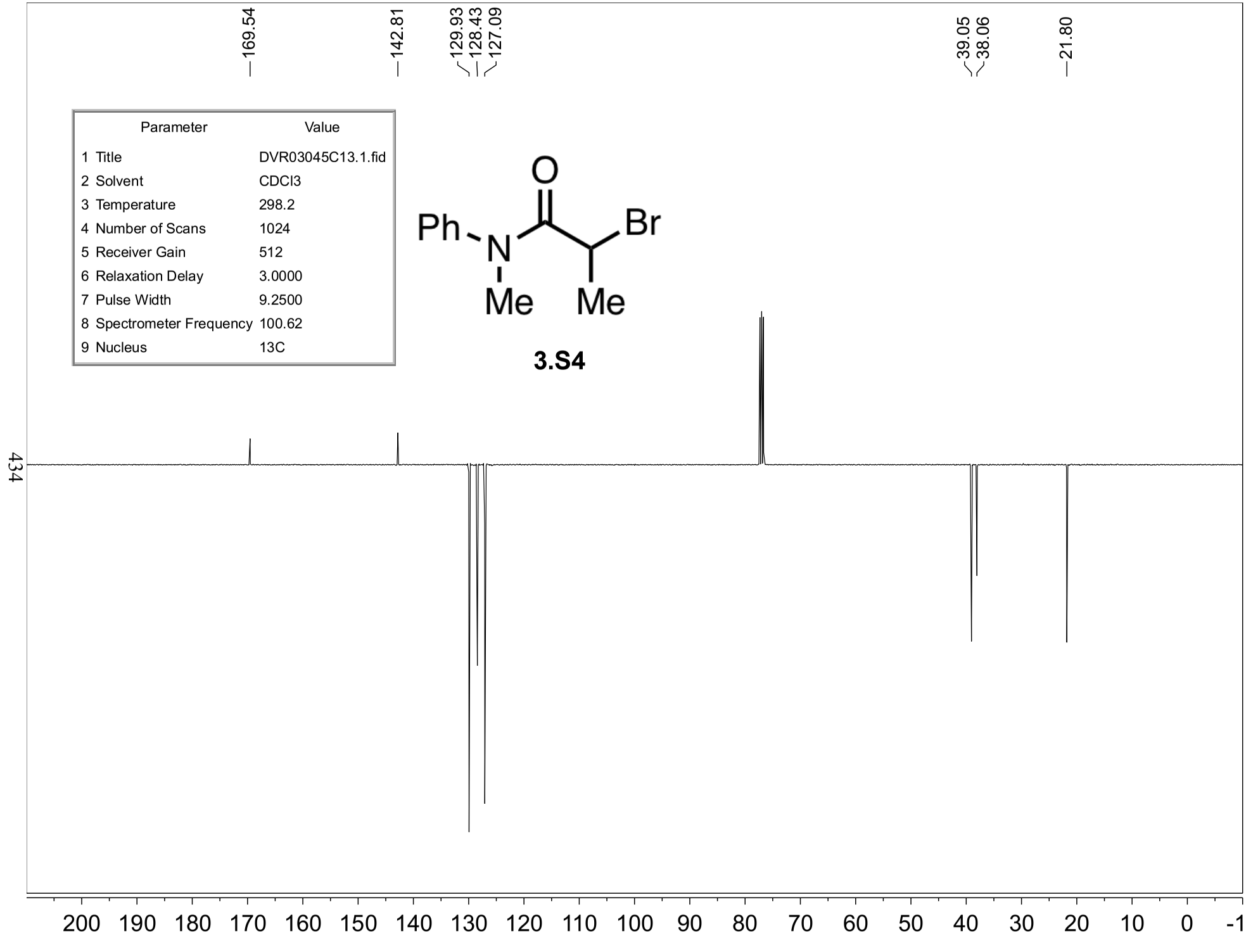
169.54
142.81
129.93
128.43
127.09
39.05
38.06
21.80
Parameter Value
1 Title DVR03045C13.1.fid
2 Solvent CDCl3
3 Temperature 298.2
4 Number of Scans 1024
5 Receiver Gain 512
6 Relaxation Delay 3.0000
7 Pulse Width 9.2500
8 Spectrometer Frequency 100.62
9 Nucleus 13C
O
Ph
N
Br
Me
Me
3.S4
434
200 190 180 170 160 150 140 130 120 110 100 90 80 70 60 50 40 30 20 10 0 -1

Parameter	Value
1 Title	DVR02235.1.fid
2 Solvent	DMSO
3 Temperature	298.2
4 Number of Scans	16
5 Receiver Gain	8
6 Relaxation Delay	1.0000
7 Pulse Width	15.0000
8 Spectrometer Frequency	400.13
9 Nucleus	1H

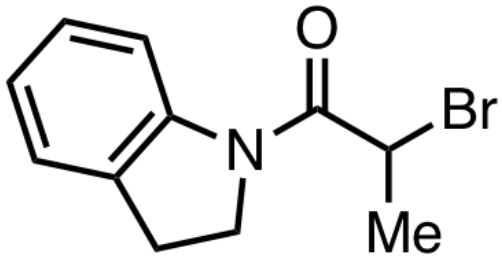

3.S5

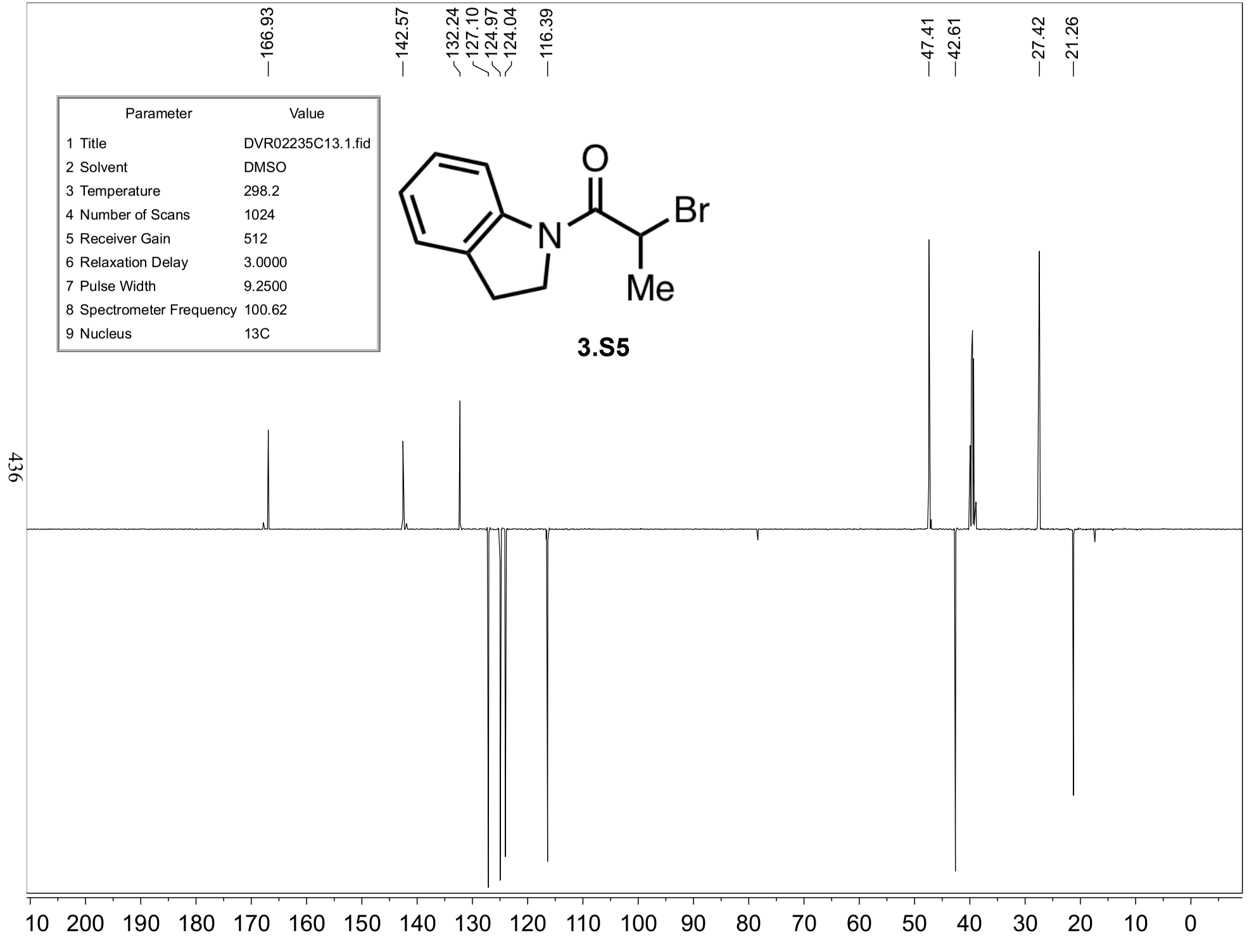
166.93
142.57
132.24
127.10
124.97
124.04
116.39
47.41
42.61
27.42
21.26
Parameter Value
1 Title DVR02235C13.1.fid
2 Solvent DMSO
3 Temperature 298.2
4 Number of Scans 1024
5 Receiver Gain 512
6 Relaxation Delay 3.0000
7 Pulse Width 9.2500
8 Spectrometer Frequency 100.62
9 Nucleus 13C
O
N
Br
Me
3.S5
436
10 200 190 180 170 160 150 140 130 120 110 100 90 80 70 60 50 40 30 20 10 0

Parameter	Value
1 Title	DVR05082A1.1.fid
2 Solvent	CDCl3
3 Temperature	296.9
4 Number of Scans	16
5 Receiver Gain	101
6 Relaxation Delay	1.0000
7 Pulse Width	10.7300
8 Spectrometer Frequency	600.32
9 Nucleus	1H

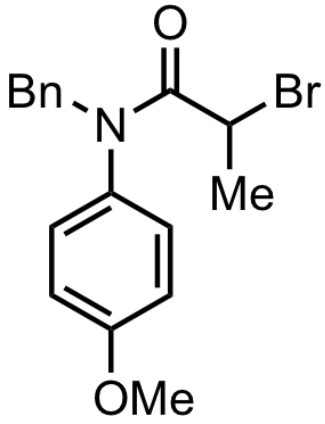

3.S7

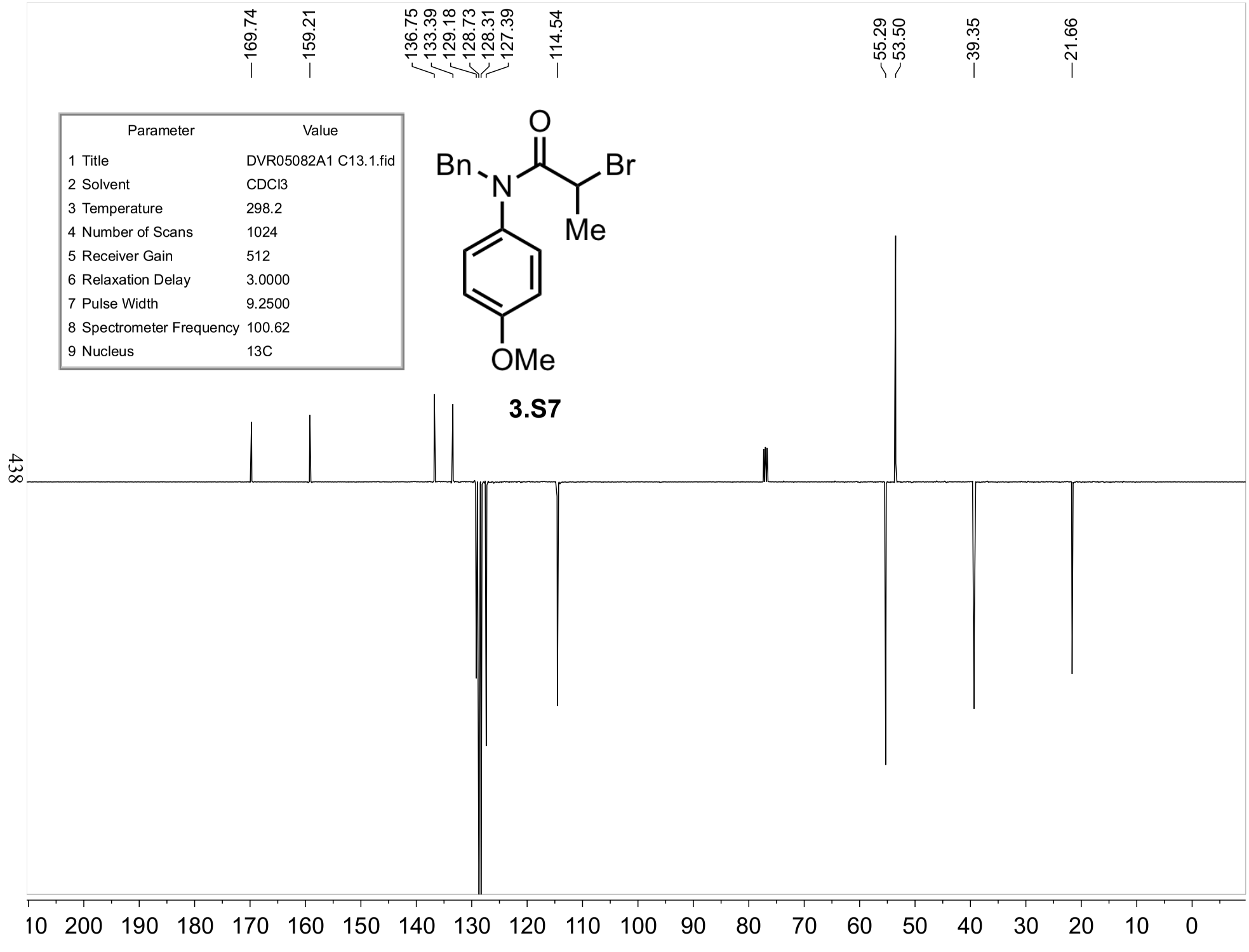
169.74
159.21
136.75
133.39
129.18
128.73
128.31
127.39
114.54
55.29
53.50
39.35
21.66
Parameter Value
1 Title DVR05082A1 C13.1.fid
2 Solvent CDCl3
3 Temperature 298.2
4 Number of Scans 1024
5 Receiver Gain 512
6 Relaxation Delay 3.0000
7 Pulse Width 9.2500
8 Spectrometer Frequency 100.62
9 Nucleus 13C
O
Bn
N
Br
Me
OMe
3.S7
438
10 200 190 180 170 160 150 140 130 120 110 100 90 80 70 60 50 40 30 20 10 0

Parameter	Value
1 Title	DVR05082C1.1.fid
2 Solvent	CDCl3
3 Temperature	296.9
4 Number of Scans	16
5 Receiver Gain	101
6 Relaxation Delay	1.0000
7 Pulse Width	10.7300
8 Spectrometer Frequency	600.32
9 Nucleus	1H

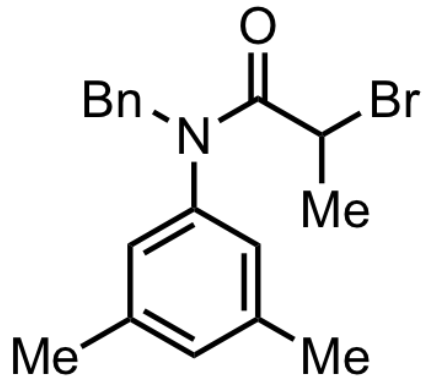

3.S9

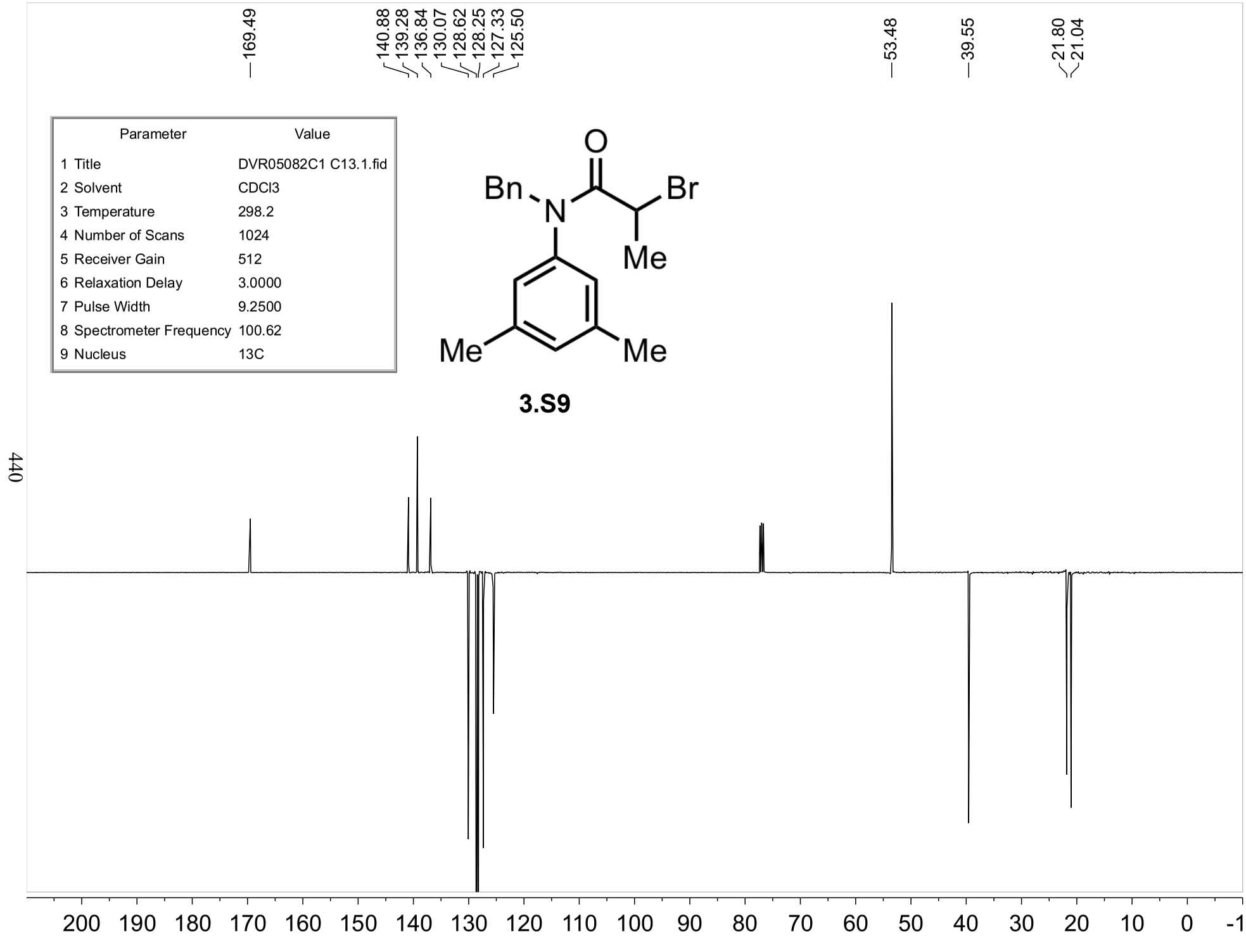
169.49
140.88
139.28
136.84
130.07
128.62
128.25
127.33
125.50
53.48
39.55
21.80
21.04
Parameter Value
1 Title DVR05082C1 C13.1.fid
2 Solvent CDCl3
3 Temperature 298.2
4 Number of Scans 1024
5 Receiver Gain 512
6 Relaxation Delay 3.0000
7 Pulse Width 9.2500
8 Spectrometer Frequency 100.62
9 Nucleus 13C
O
Bn
N
Br
Me
Me
Me
3.S9
440
200 190 180 170 160 150 140 130 120 110 100 90 80 70 60 50 40 30 20 10 0 -1

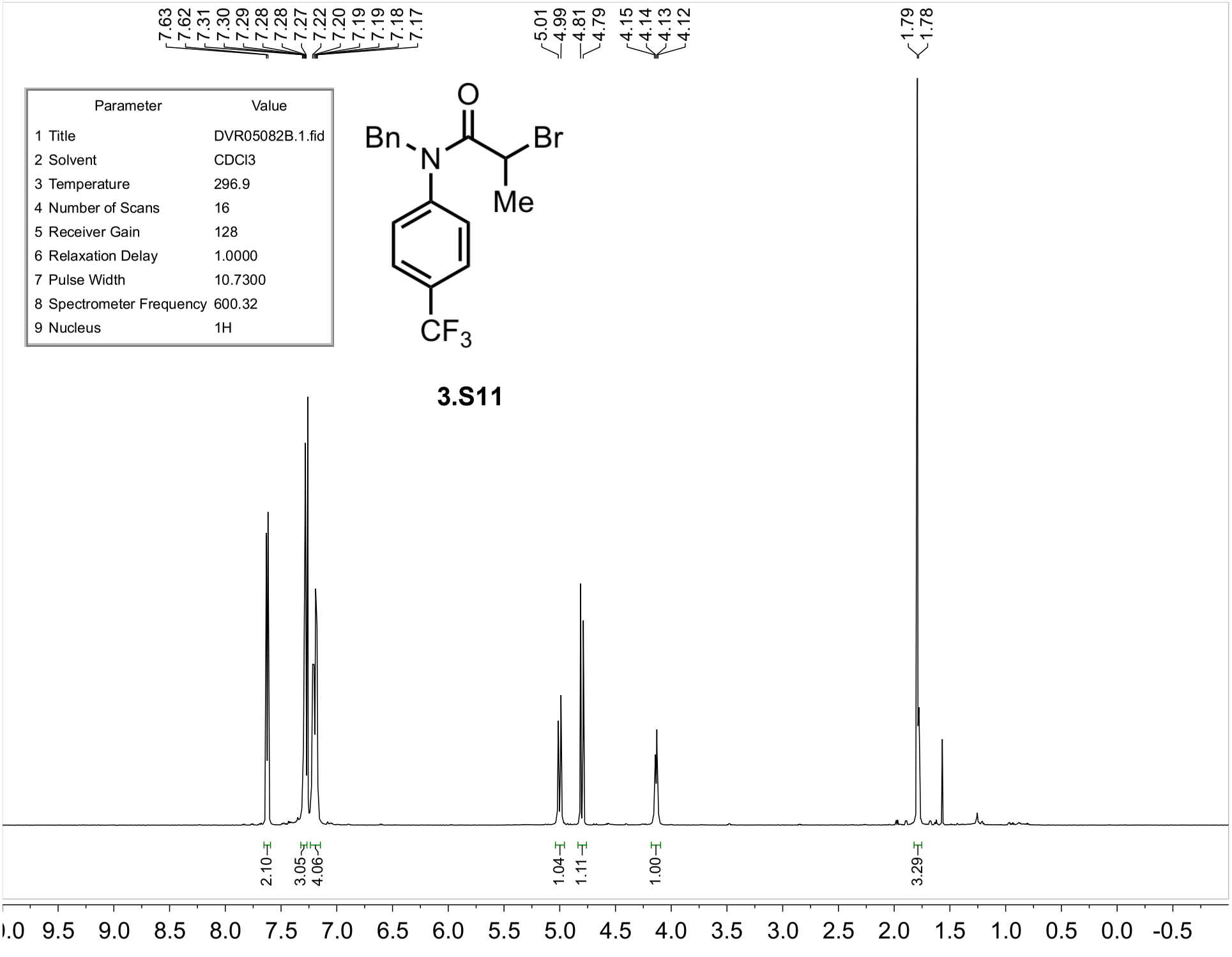
7.63
7.62
7.31
7.30
7.29
7.28
7.28
7.27
7.22
7.20
7.19
7.19
7.18
7.17
5.01
4.99
4.81
4.79
4.15
4.14
4.13
4.12
1.79
1.78
Parameter Value
1 Title DVR05082B.1.fid
2 Solvent CDCl3
3 Temperature 296.9
4 Number of Scans 16
5 Receiver Gain 128
6 Relaxation Delay 1.0000
7 Pulse Width 10.7300
8 Spectrometer Frequency 600.32
9 Nucleus 1H
Bn
N
O
Br
Me
CF3
2.10
3.05
4.06
1.04
1.11
1.00
3.29
9.5 9.0 8.5 8.0 7.5 7.0 6.5 6.0 5.5 5.0 4.5 4.0 3.5 3.0 2.5 2.0 1.5 1.0 0.5 0.0 -0.5

3.S11

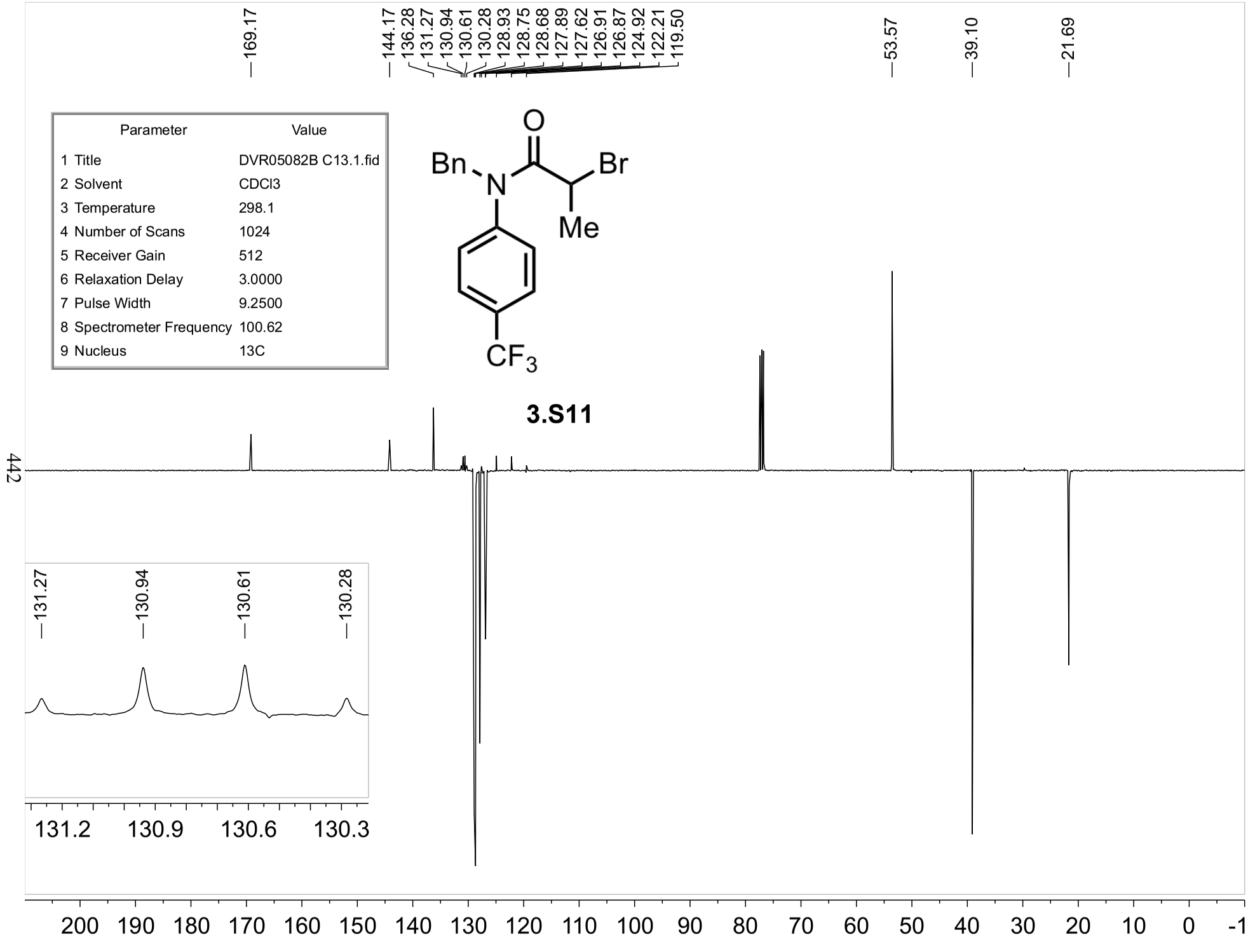
169.17
144.17
136.28
131.27
130.94
130.61
130.28
128.93
128.75
128.68
127.89
127.62
126.91
126.87
124.92
122.21
119.50
53.57
39.10
21.69
Parameter Value
1 Title DVR05082B C13.1.fid
2 Solvent CDCl3
3 Temperature 298.1
4 Number of Scans 1024
5 Receiver Gain 512
6 Relaxation Delay 3.0000
7 Pulse Width 9.2500
8 Spectrometer Frequency 100.62
9 Nucleus 13C
O
Bn
N
Br
Me
CF3
3.S11
442
131.27
130.94
130.61
130.28
131.2
130.9
130.6
130.3
200 190 180 170 160 150 140 130 120 110 100 90 80 70 60 50 40 30 20 10 0 -1

Parameter	Value
1 Title	DVR05082B F19.1.fid
2 Solvent	CDCl3
3 Temperature	297.6
4 Number of Scans	16
5 Receiver Gain	203
6 Relaxation Delay	3.0000
7 Pulse Width	11.6000
8 Spectrometer Frequency	564.81
9 Nucleus	19F

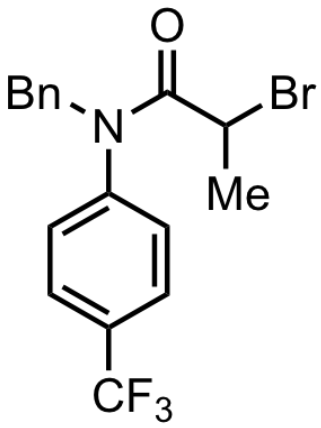

3.S11

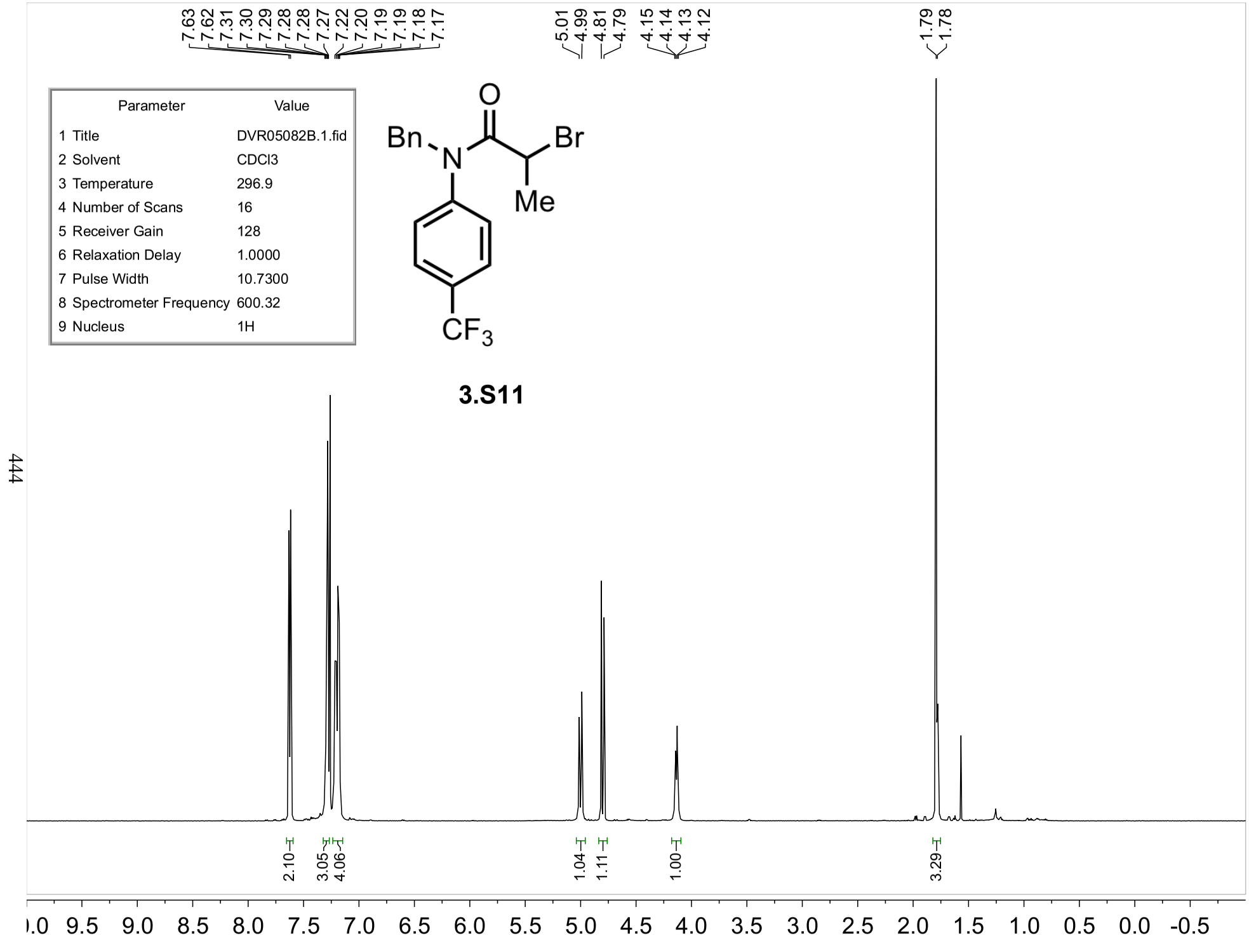
7.63
7.62
7.31
7.30
7.29
7.28
7.28
7.27
7.22
7.20
7.19
7.19
7.18
7.17
5.01
4.99
4.81
4.79
4.15
4.14
4.13
4.12
1.79
1.78
Parameter Value
1 Title DVR05082B.1.fid
2 Solvent CDCl3
3 Temperature 296.9
4 Number of Scans 16
5 Receiver Gain 128
6 Relaxation Delay 1.0000
7 Pulse Width 10.7300
8 Spectrometer Frequency 600.32
9 Nucleus 1H
O
Bn
N
Br
Me
CF3
3.S11
444
2.10
3.05
4.06
1.04
1.11
1.00
3.29
9.5 9.0 8.5 8.0 7.5 7.0 6.5 6.0 5.5 5.0 4.5 4.0 3.5 3.0 2.5 2.0 1.5 1.0 0.5 0.0 -0.5

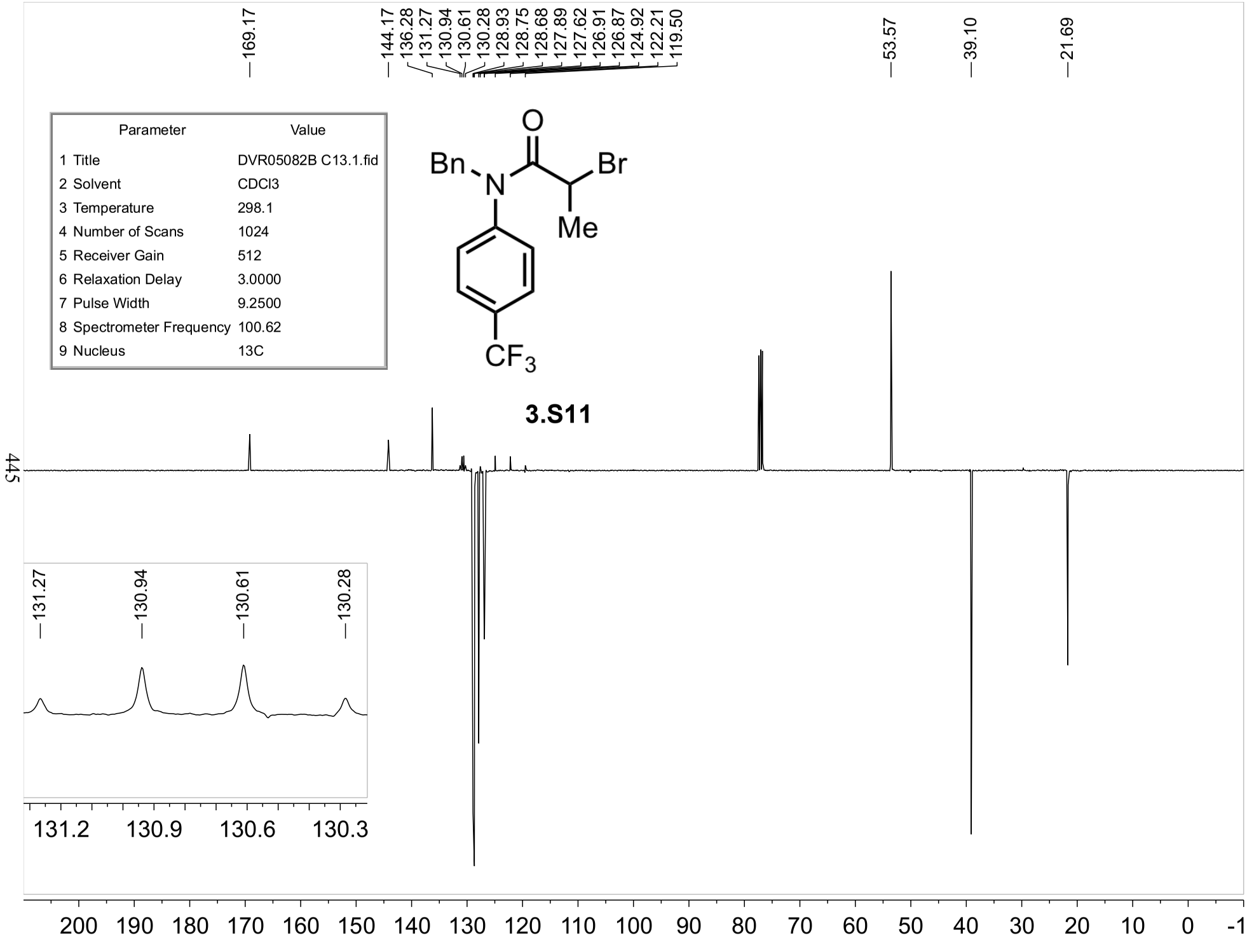
169.17
144.17
136.28
131.27
130.94
130.61
130.28
128.93
128.75
128.68
127.89
127.62
126.91
126.87
124.92
122.21
119.50
53.57
39.10
21.69
Parameter Value
1 Title DVR05082B C13.1.fid
2 Solvent CDCl3
3 Temperature 298.1
4 Number of Scans 1024
5 Receiver Gain 512
6 Relaxation Delay 3.0000
7 Pulse Width 9.2500
8 Spectrometer Frequency 100.62
9 Nucleus 13C
Bn
N
O
Br
Me
CF3
3.S11
445
131.27
130.94
130.61
130.28
131.2
130.9
130.6
130.3
200 190 180 170 160 150 140 130 120 110 100 90 80 70 60 50 40 30 20 10 0 -1

Parameter	Value
1 Title	DVR05082B F19.1.fid
2 Solvent	CDCl3
3 Temperature	297.6
4 Number of Scans	16
5 Receiver Gain	203
6 Relaxation Delay	3.0000
7 Pulse Width	11.6000
8 Spectrometer Frequency	564.81
9 Nucleus	19F

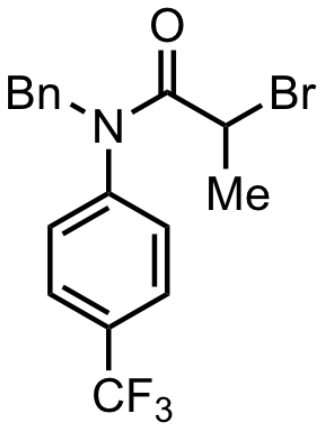

3.S11

Parameter	Value
1 Title	DVR04180AF1.1.fid
2 Solvent	CDCl3
3 Temperature	300.0
4 Number of Scans	16
5 Receiver Gain	128
6 Relaxation Delay	1.0000
7 Pulse Width	10.7300
8 Spectrometer Frequency	600.32
9 Nucleus	1H

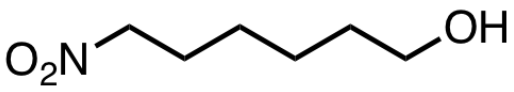

3.S13

Parameter	Value
1 Title	DVR04180AF1 C13.1.fid
2 Solvent	CDCl3
3 Temperature	300.0
4 Number of Scans	1024
5 Receiver Gain	2050
6 Relaxation Delay	5.0000
7 Pulse Width	10.6300
8 Spectrometer Frequency	150.97
9 Nucleus	13C

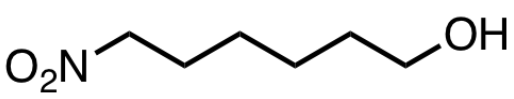

3.S13

Parameter	Value
1 Title	DVR05098D1.1.fid
2 Solvent	CDCl3
3 Temperature	298.2
4 Number of Scans	16
5 Receiver Gain	9
6 Relaxation Delay	1.0000
7 Pulse Width	15.0000
8 Spectrometer Frequency	400.13
9 Nucleus	1H

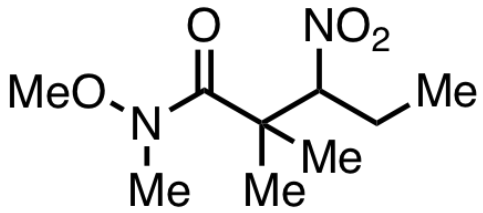

3.3

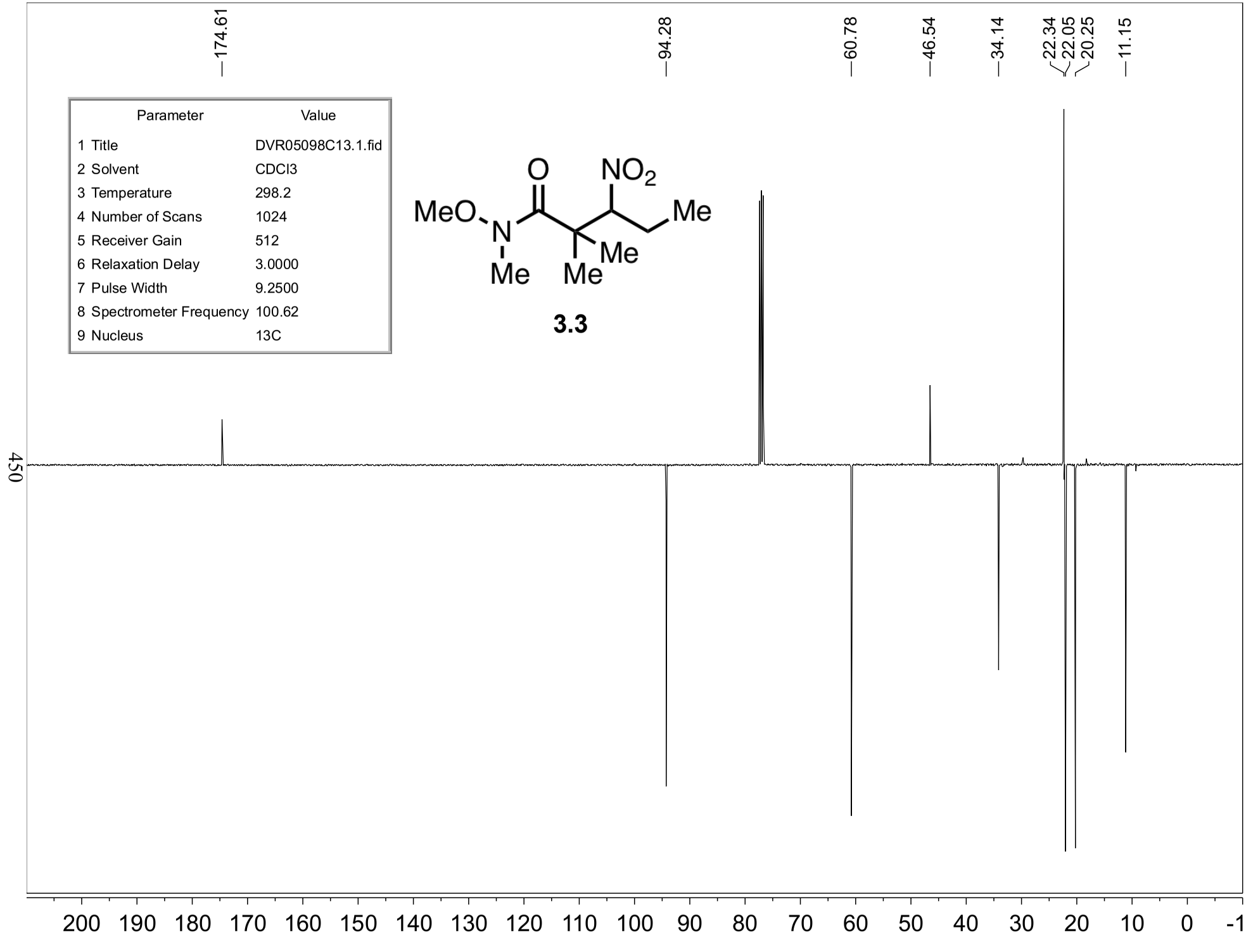
174.61
94.28
60.78
46.54
34.14
22.34
22.05
20.25
11.15
Parameter Value
1 Title DVR05098C13.1.fid
2 Solvent CDCl3
3 Temperature 298.2
4 Number of Scans 1024
5 Receiver Gain 512
6 Relaxation Delay 3.0000
7 Pulse Width 9.2500
8 Spectrometer Frequency 100.62
9 Nucleus 13C
MeO
N
Me
O
NO2
Me
Me
Me
3.3
450
200 190 180 170 160 150 140 130 120 110 100 90 80 70 60 50 40 30 20 10 0 -1

==== Shimadzu LCsolution Analysis Report ====

	C:\LabSolutions\Data\DMM\DVR05098 RAC_6232017_1513 PM_2.lcd
Acquired by	: LC User
Sample Name	: DVR05098 RAC
Sample ID	: DVR05098 RAC
Tray#	: 1
Vail #	: 1
Injection Volume	: 3 uL
Data File Name	: DVR05098 RAC_6232017_1513 PM_2.lcd
Method File Name	: col1_1isoiPA_30min_1ML_220and210.lcm
Batch File Name	: DMM.lcb
Report File Name	: Default.lcr
Data Acquired	: 6/23/2017 3:43:47 PM
Data Processed	: 6/23/2017 4:13:48 PM

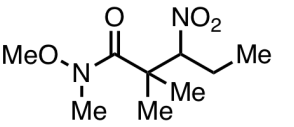

3.3
racemic

<Chromatogram>

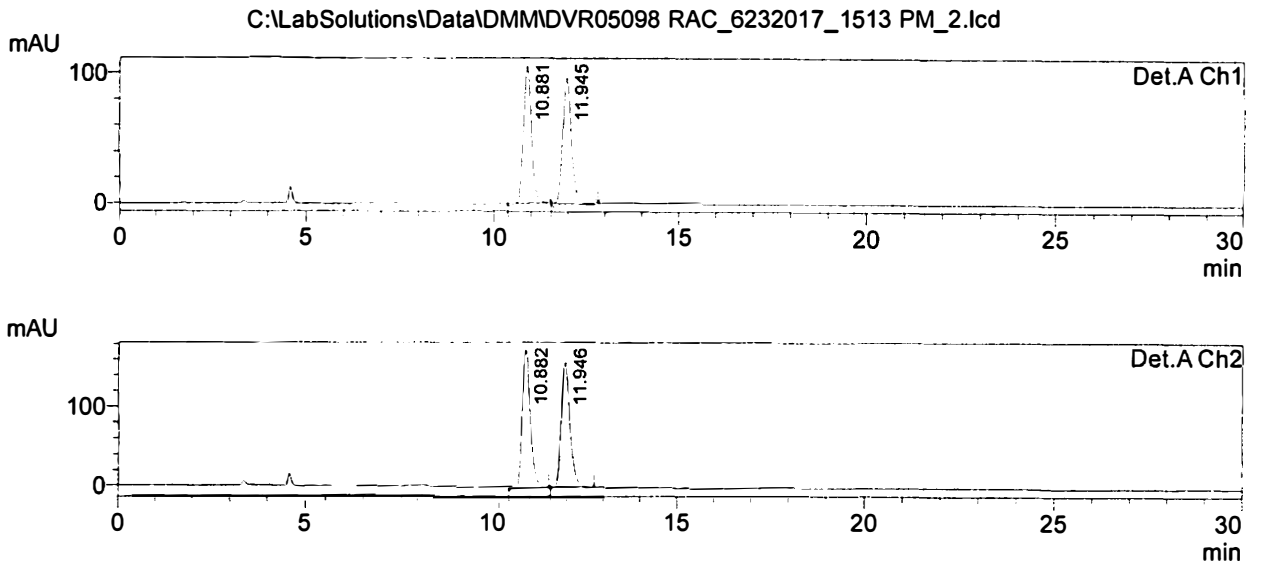

1 Det.A Ch1/220nm
2 Det.A Ch2/210nm

PeakTable

Detector A Ch1 220nm

Peak#	Ret. Time	Area	Height	Area %	Height %
1	10.881	1546789	105485	49.965	52.192
2	11.945	1548959	96625	50.035	47.808
Total		3095748	202110	100.000	100.000

PeakTable

Detector A Ch2 210nm

Peak#	Ret. Time	Area	Height	Area %	Height %
1	10.882	2537933	173332	49.986	52.196
2	11.946	2539398	158750	50.014	47.804
Total		5077332	332082	100.000	100.000

==== Shimadzu LCsolution Analysis Report ====

C:\LabSolutions\Data\DMM\DVR05098_6232017_1513 PM_3.lcd

Acquired by	: LC User
Sample Name	: DVR05098
Sample ID	: DVR05098
Tray#	: 1
Vail #	: 2
Injection Volume	: 3 uL
Data File Name	: DVR05098_6232017_1513 PM_3.lcd
Method File Name	: col1_1isoiPA_30min_1ML_220and210.lcm
Batch File Name	: DMM.lcb
Report File Name	: Default.lcr
Data Acquired	: 6/23/2017 4:14:22 PM
Data Processed	: 6/23/2017 4:44:24 PM

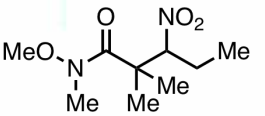

3.3
78% ee

<Chromatogram>

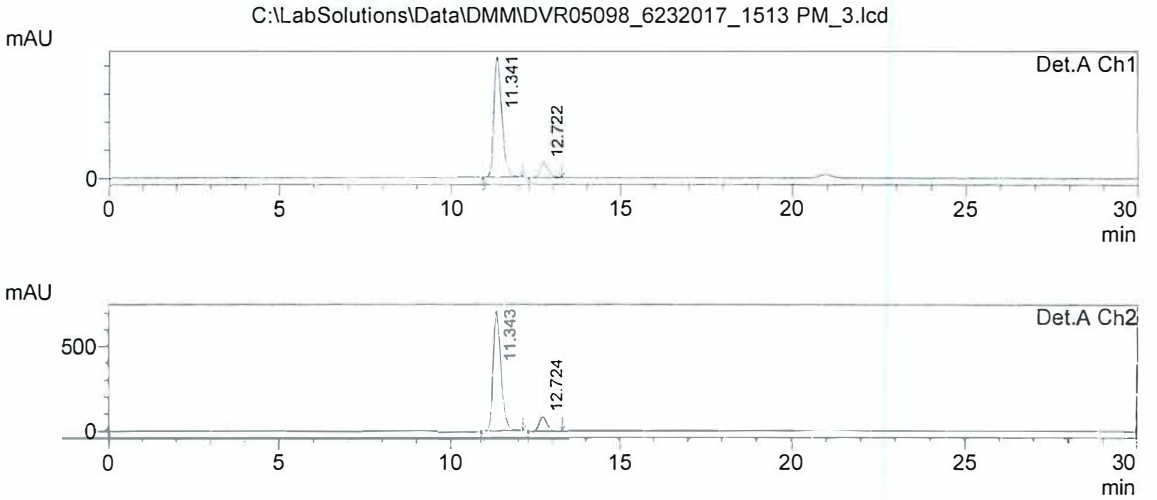

1 Det.A Ch1/220nm
2 Det.A Ch2/210nm

PeakTable

Detector A Ch1 220nm

Peak#	Ret. Time	Area	Height	Area %	Height %
1	11.341	6877766	429717	88.925	89.090
2	12.722	856564	52623	11.075	10.910
Total		7734330	482340	100.000	100.000

PeakTable

Detector A Ch2 210nm

Peak#	Ret. Time	Area	Height	Area %	Height %
1	11.343	11403339	714499	88.999	89.219
2	12.724	1409584	86336	11.001	10.781
Total		12812924	800835	100.000	100.000

Parameter	Value
1 Title	DVR05078B.1.fid
2 Solvent	CDCl3
3 Temperature	298.2
4 Number of Scans	16
5 Receiver Gain	7
6 Relaxation Delay	1.0000
7 Pulse Width	15.0000
8 Spectrometer Frequency	400.13
9 Nucleus	1H

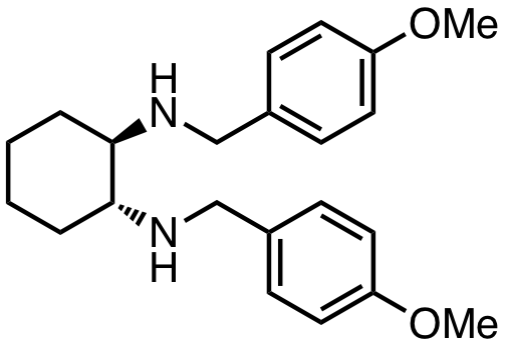

3.17

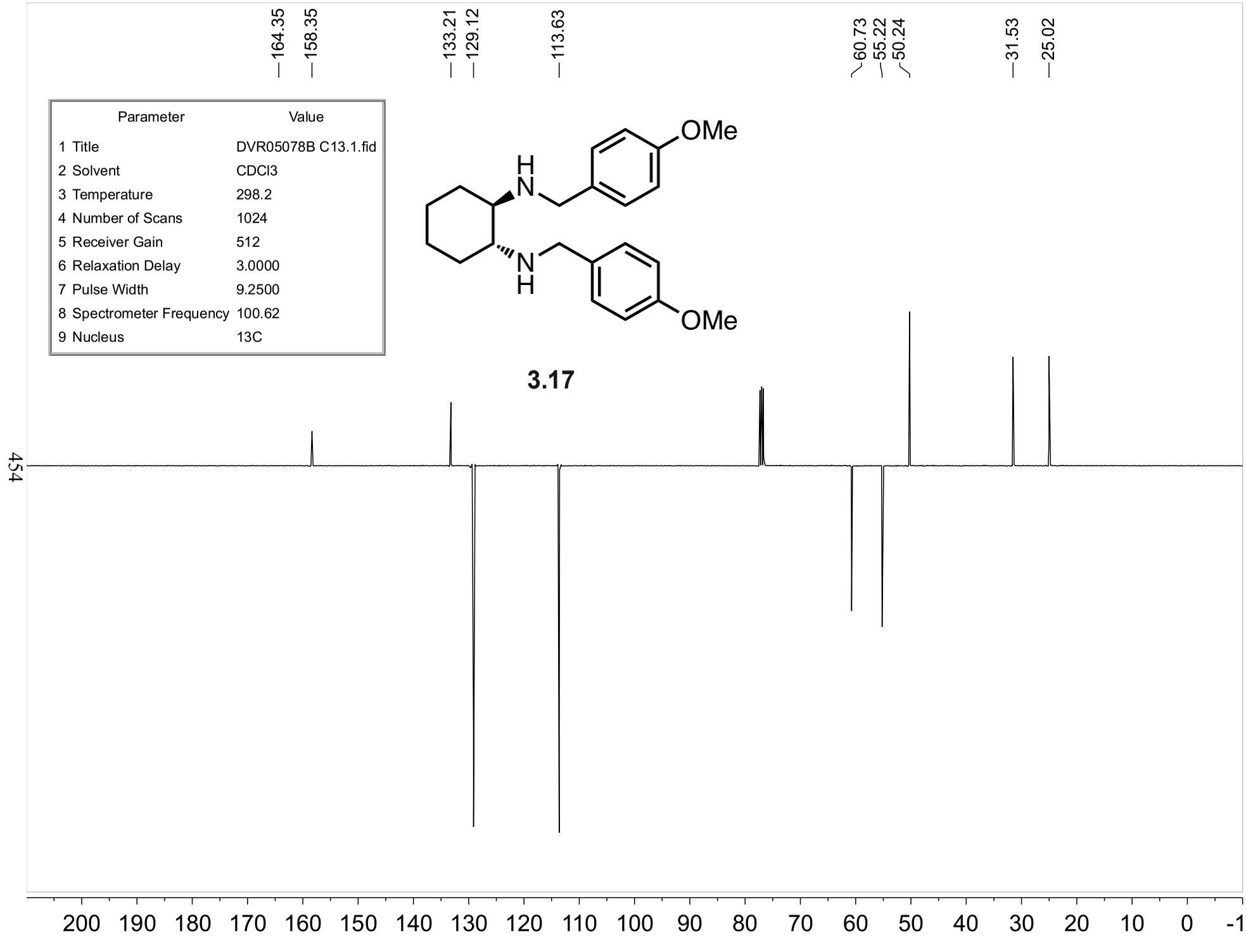
164.35
158.35
133.21
129.12
113.63
60.73
55.22
50.24
31.53
25.02
Parameter Value
1 Title DVR05078B C13.1.fid
2 Solvent CDCl3
3 Temperature 298.2
4 Number of Scans 1024
5 Receiver Gain 512
6 Relaxation Delay 3.0000
7 Pulse Width 9.2500
8 Spectrometer Frequency 100.62
9 Nucleus 13C
OMe
H
N
N
H
OMe
3.17
454
200 190 180 170 160 150 140 130 120 110 100 90 80 70 60 50 40 30 20 10 0 -1

Parameter	Value
1 Title	DVR05078C.1.fid
2 Solvent	CDCl3
3 Temperature	298.2
4 Number of Scans	16
5 Receiver Gain	7
6 Relaxation Delay	1.0000
7 Pulse Width	15.0000
8 Spectrometer Frequency	400.13
9 Nucleus	1H

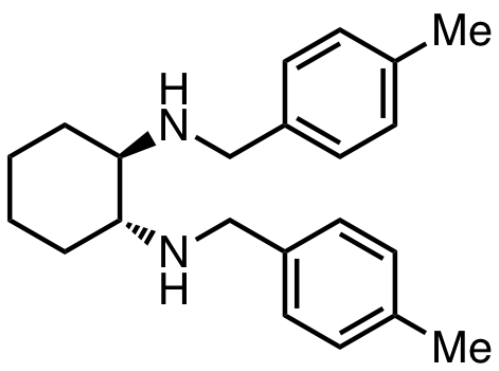

3.18

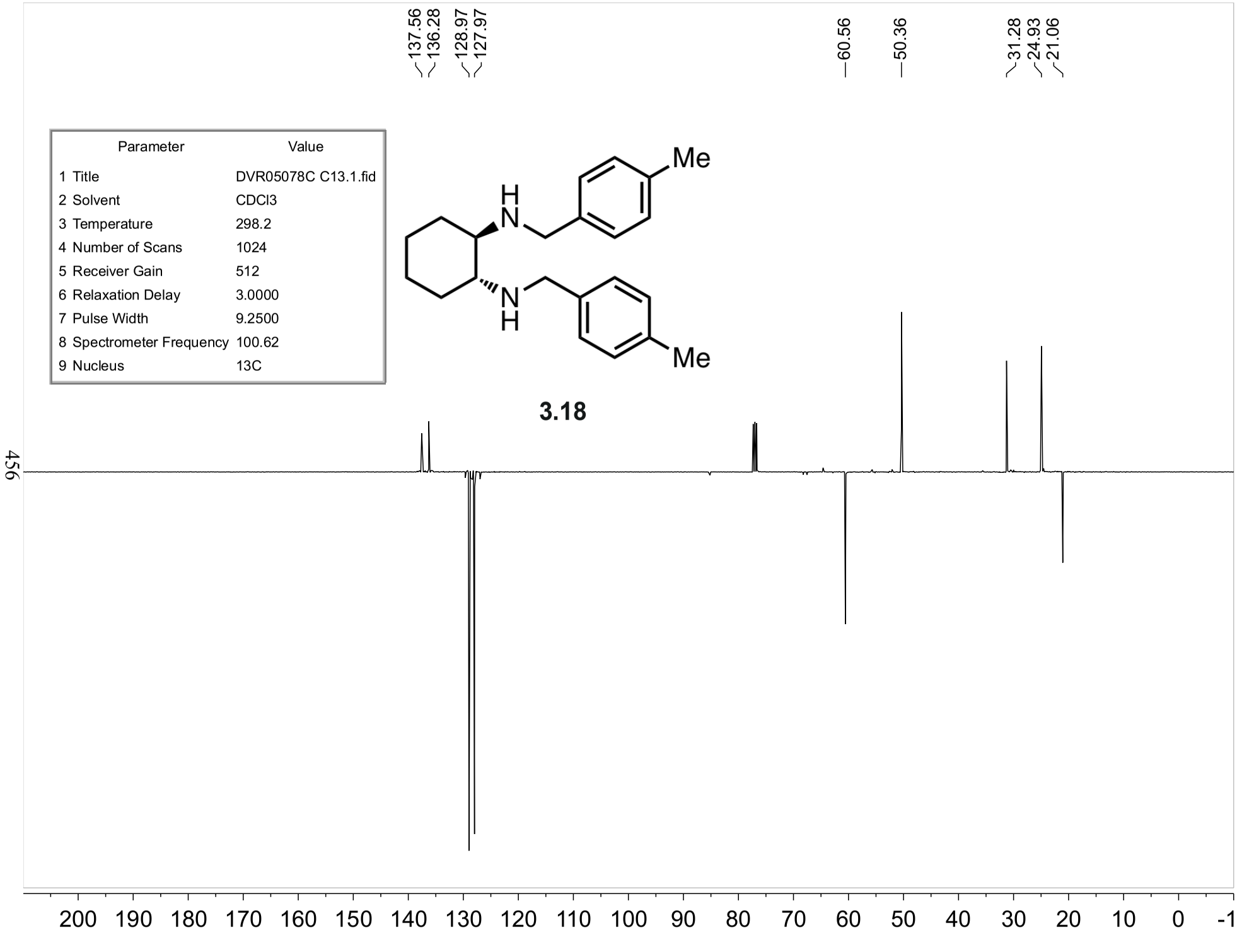
137.56
136.28
128.97
127.97
60.56
50.36
31.28
24.93
21.06
Parameter Value
1 Title DVR05078C C13.1.fid
2 Solvent CDCl3
3 Temperature 298.2
4 Number of Scans 1024
5 Receiver Gain 512
6 Relaxation Delay 3.0000
7 Pulse Width 9.2500
8 Spectrometer Frequency 100.62
9 Nucleus 13C
Me
H
N
N
H
Me
3.18
456
200 190 180 170 160 150 140 130 120 110 100 90 80 70 60 50 40 30 20 10 0 -1

Parameter	Value
1 Title	DVR05078O.1.fid
2 Solvent	CDCl3
3 Temperature	298.2
4 Number of Scans	16
5 Receiver Gain	11
6 Relaxation Delay	1.0000
7 Pulse Width	15.0000
8 Spectrometer Frequency	400.13
9 Nucleus	1H

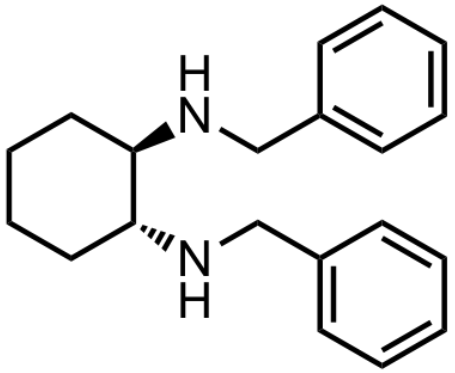

3.19

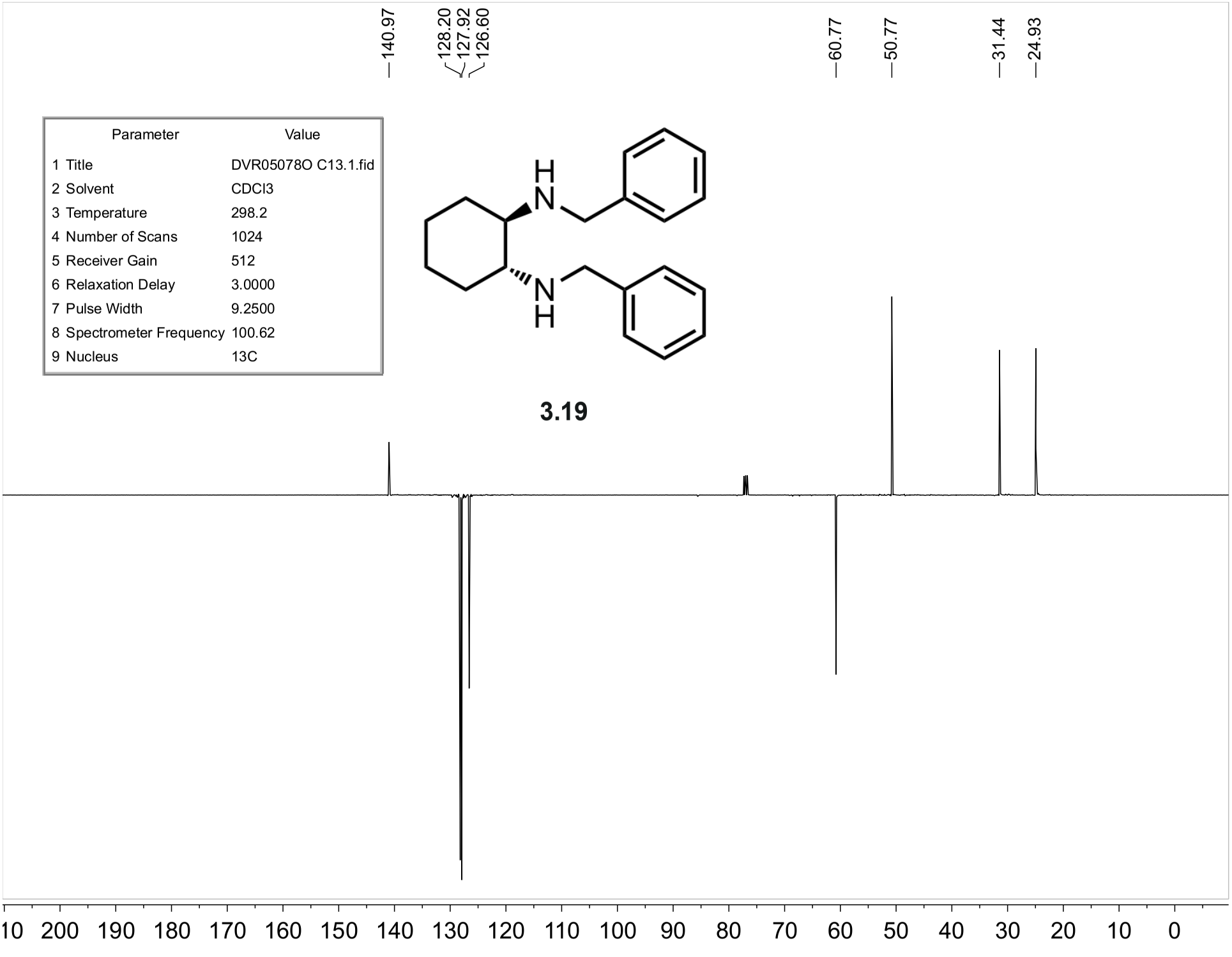
140.97
128.20
127.92
126.60
60.77
50.77
31.44
24.93
Parameter Value
1 Title DVR05078O C13.1.fid
2 Solvent CDCl3
3 Temperature 298.2
4 Number of Scans 1024
5 Receiver Gain 512
6 Relaxation Delay 3.0000
7 Pulse Width 9.2500
8 Spectrometer Frequency 100.62
9 Nucleus 13C
H
N
N
H
3.19
10 200 190 180 170 160 150 140 130 120 110 100 90 80 70 60 50 40 30 20 10 0

Parameter	Value
1 Title	DVR05078D.1.fid
2 Solvent	CDCl3
3 Temperature	298.1
4 Number of Scans	16
5 Receiver Gain	6
6 Relaxation Delay	1.0000
7 Pulse Width	15.0000
8 Spectrometer Frequency	400.13
9 Nucleus	1H

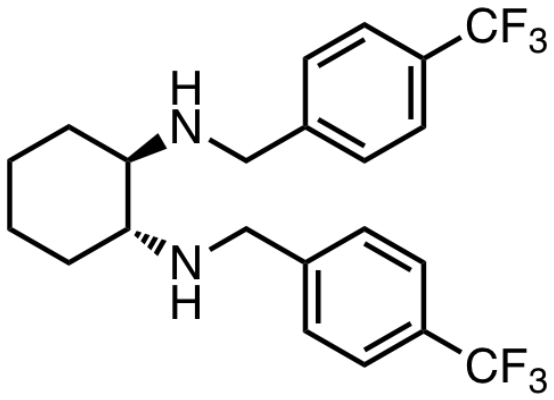

3.20

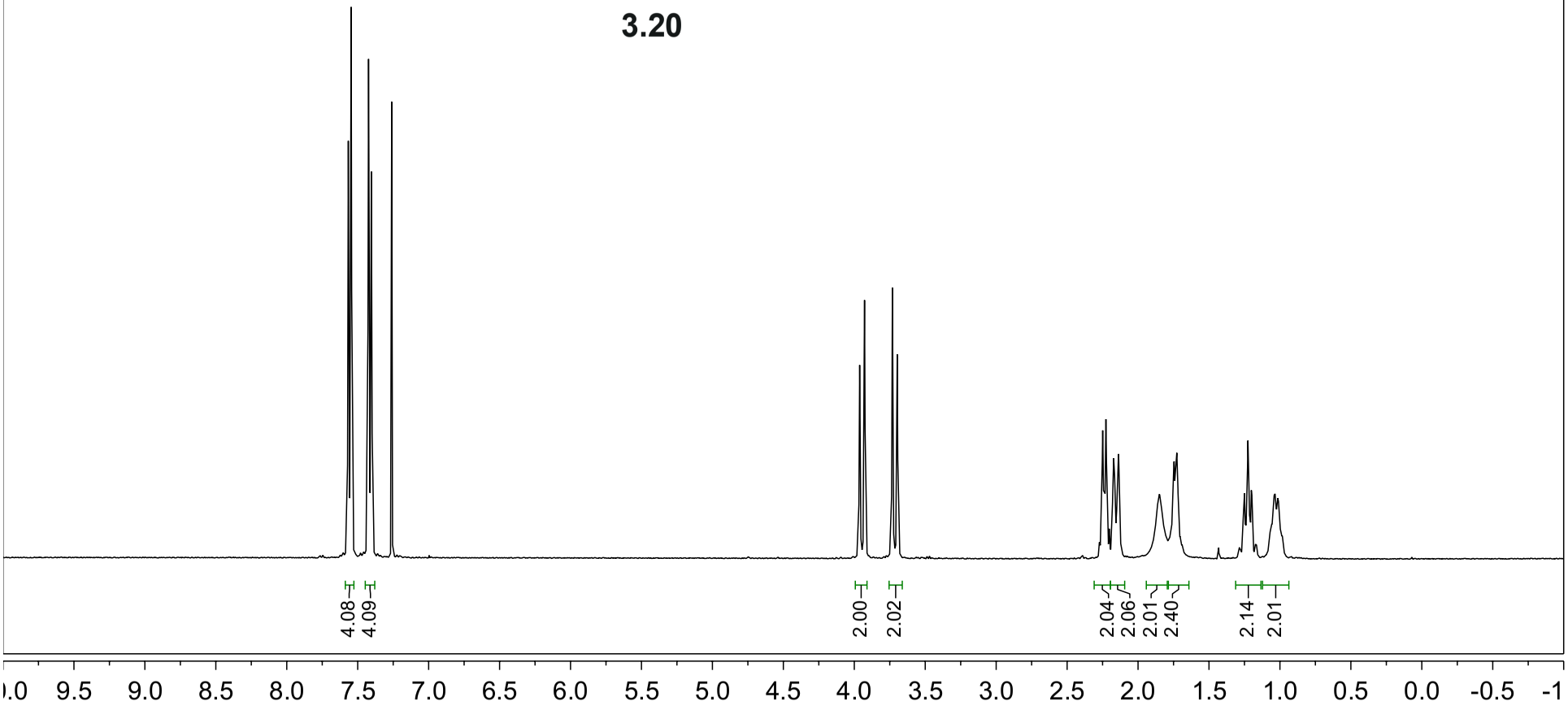

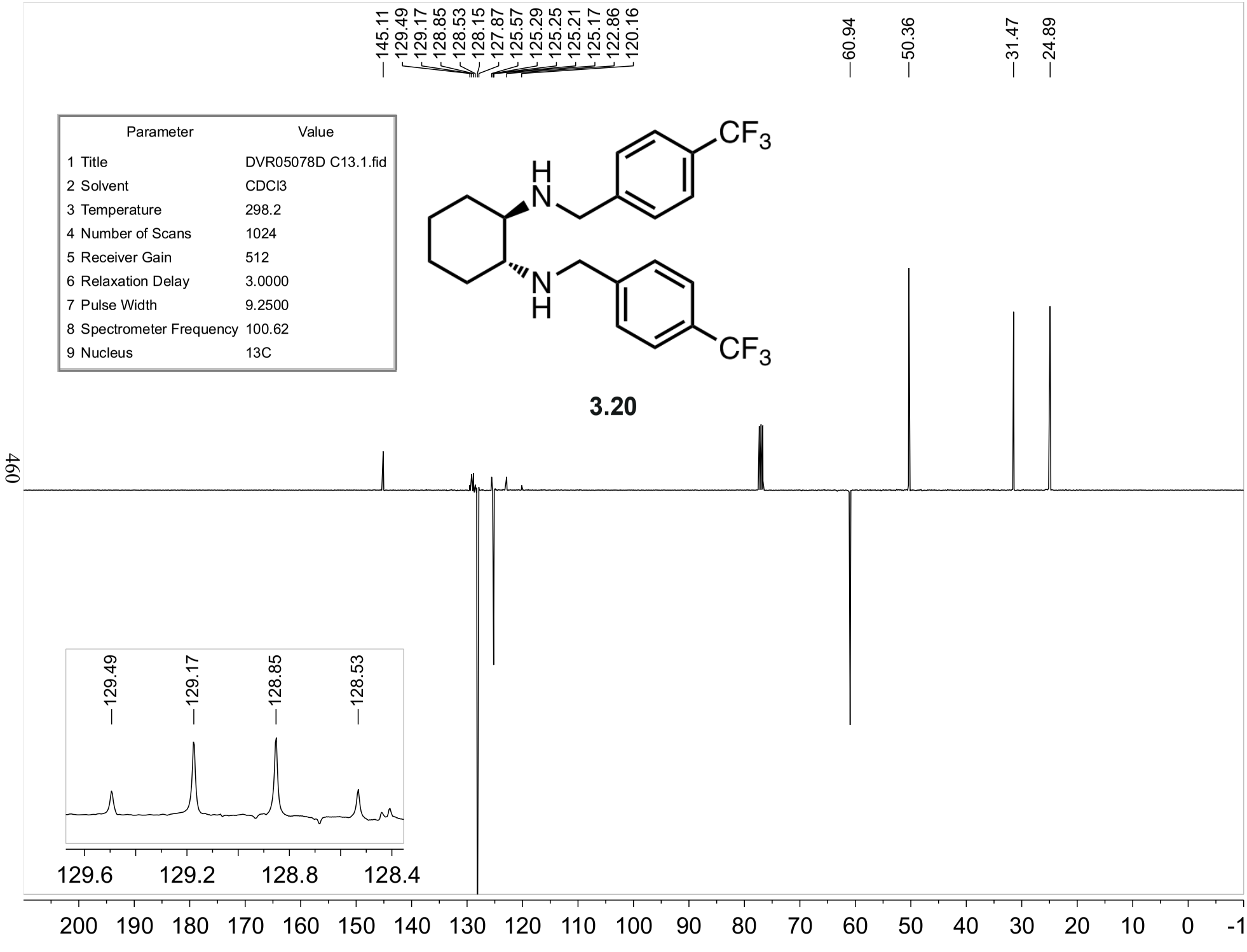
145.11
129.49
129.17
128.85
128.53
128.15
127.87
125.57
125.29
125.25
125.21
125.17
122.86
120.16
60.94
50.36
31.47
24.89
Parameter Value
1 Title DVR05078D C13.1.fid
2 Solvent CDCl3
3 Temperature 298.2
4 Number of Scans 1024
5 Receiver Gain 512
6 Relaxation Delay 3.0000
7 Pulse Width 9.2500
8 Spectrometer Frequency 100.62
9 Nucleus 13C
CF3
H
N
N
H
CF3
3.20
460
129.49
129.17
128.85
128.53
129.6
129.2
128.8
128.4
200 190 180 170 160 150 140 130 120 110 100 90 80 70 60 50 40 30 20 10 0 -1

Parameter	Value
1 Title	DVR05078D F19.1.fid
2 Solvent	CDCl3
3 Temperature	297.5
4 Number of Scans	16
5 Receiver Gain	181
6 Relaxation Delay	3.0000
7 Pulse Width	11.6000
8 Spectrometer Frequency	564.81
9 Nucleus	19F

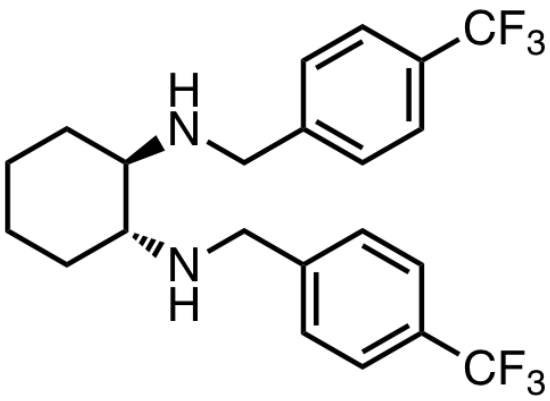

3.20

Parameter	Value
1 Title	DVR05108 1H.1.fid
2 Solvent	CDCl3
3 Temperature	298.2
4 Number of Scans	16
5 Receiver Gain	9
6 Relaxation Delay	1.0000
7 Pulse Width	15.0000
8 Spectrometer Frequency	400.13
9 Nucleus	1H

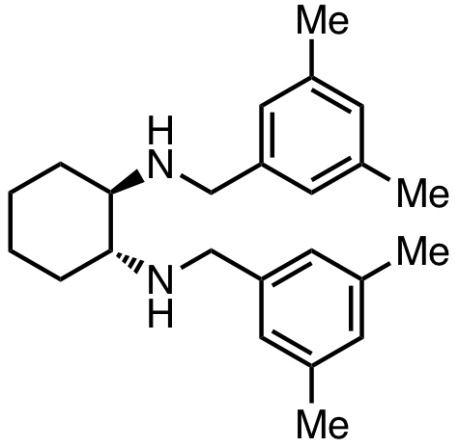

3.23

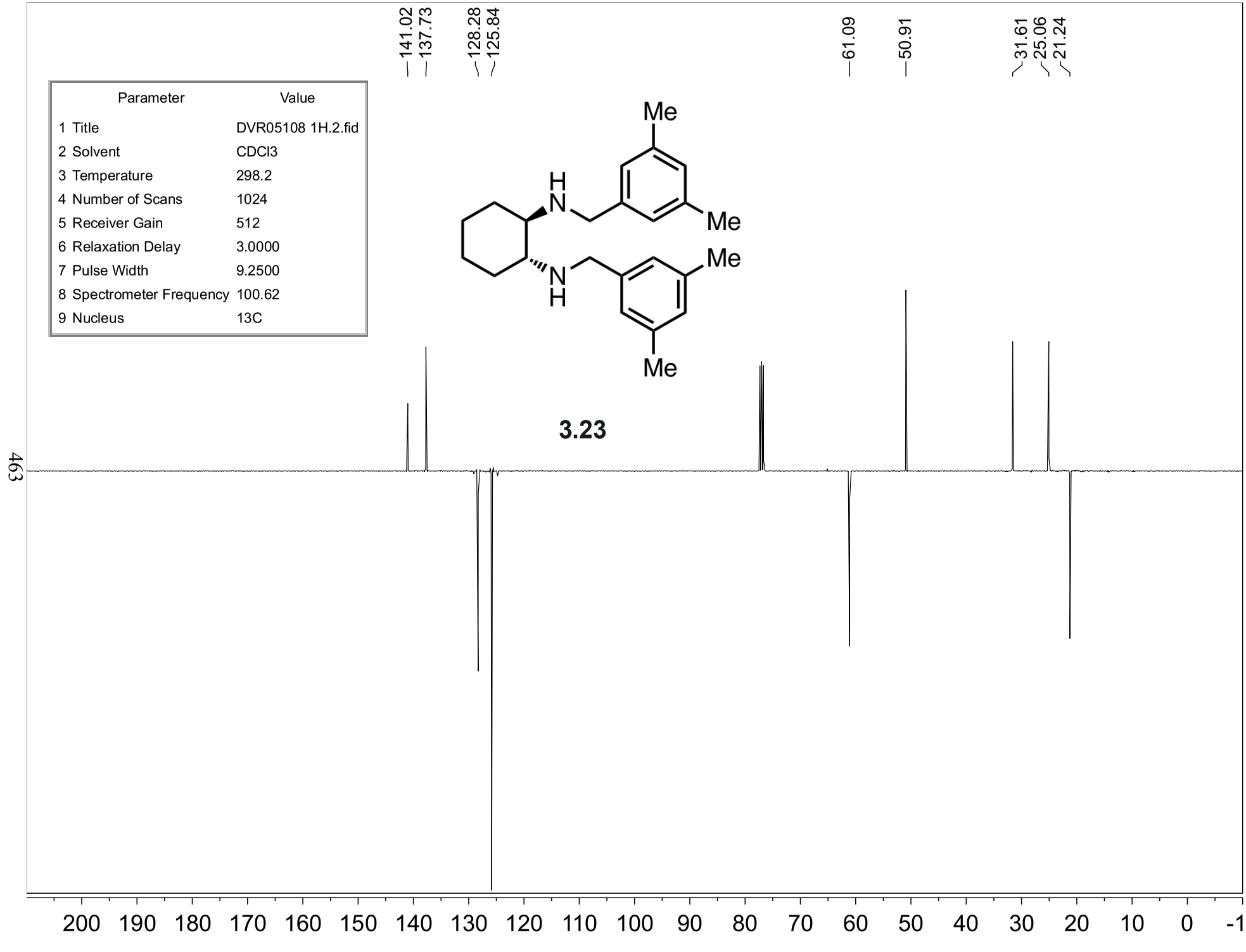
141.02
137.73
128.28
125.84
61.09
50.91
31.61
25.06
21.24
Parameter Value
1 Title DVR05108 1H.2.fid
2 Solvent CDCl3
3 Temperature 298.2
4 Number of Scans 1024
5 Receiver Gain 512
6 Relaxation Delay 3.0000
7 Pulse Width 9.2500
8 Spectrometer Frequency 100.62
9 Nucleus 13C
Me
H
N
Me
Me
N
H
Me
3.23
463
200 190 180 170 160 150 140 130 120 110 100 90 80 70 60 50 40 30 20 10 0 -1

Parameter	Value
1 Title	DVR05078E.1.fid
2 Solvent	CDCl3
3 Temperature	298.2
4 Number of Scans	16
5 Receiver Gain	7
6 Relaxation Delay	1.0000
7 Pulse Width	15.0000
8 Spectrometer Frequency	400.13
9 Nucleus	1H

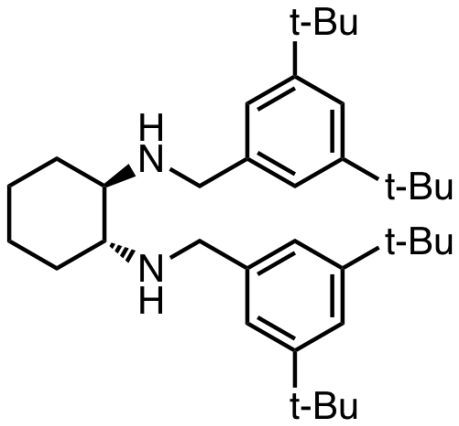

3.24

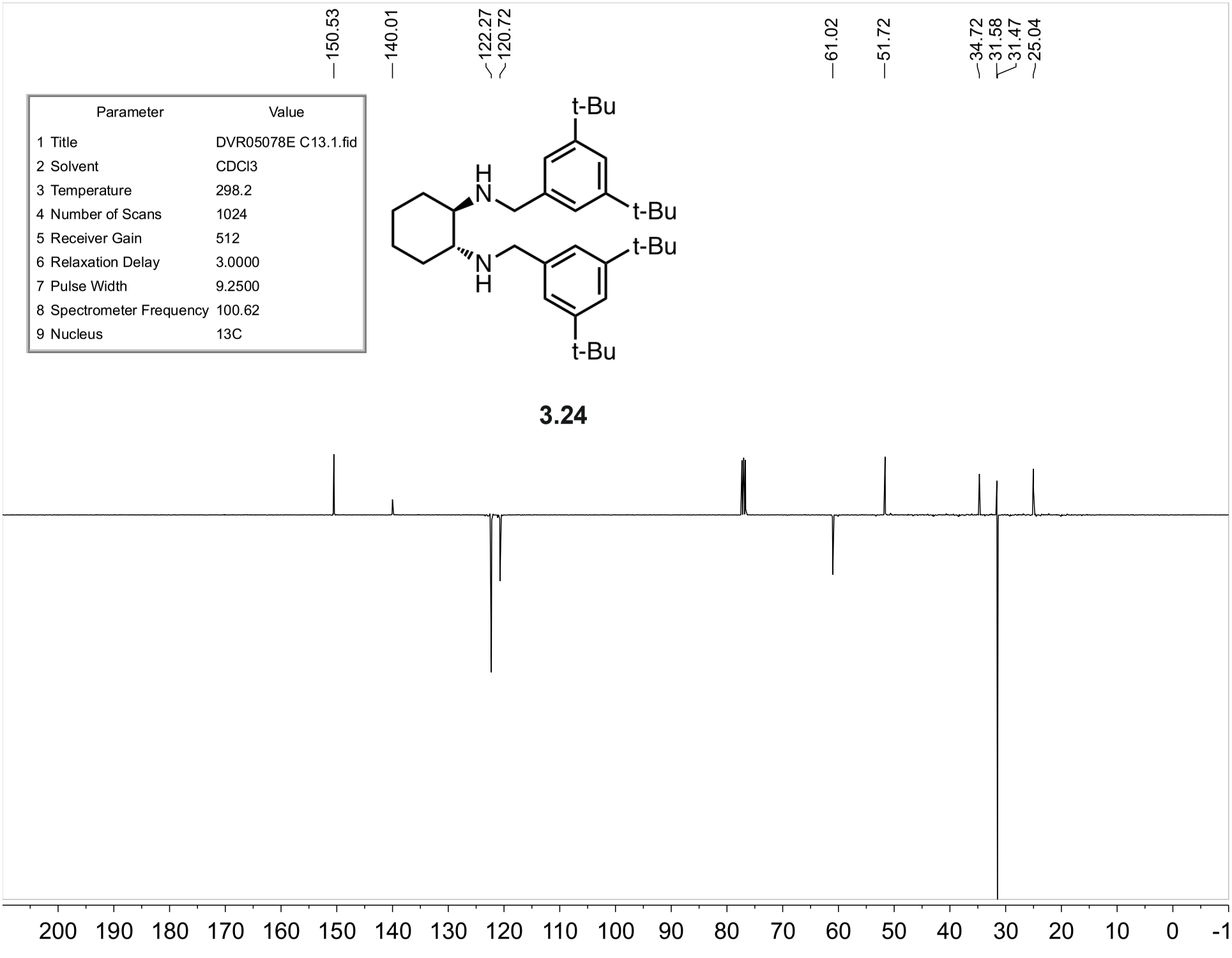
150.53
140.01
122.27
120.72
61.02
51.72
34.72
31.58
31.47
25.04
Parameter Value
1 Title DVR05078E C13.1.fid
2 Solvent CDCl3
3 Temperature 298.2
4 Number of Scans 1024
5 Receiver Gain 512
6 Relaxation Delay 3.0000
7 Pulse Width 9.2500
8 Spectrometer Frequency 100.62
9 Nucleus 13C
t-Bu
t-Bu
t-Bu
t-Bu
H
N
N
H
3.24
200 190 180 170 160 150 140 130 120 110 100 90 80 70 60 50 40 30 20 10 0 -1

Parameter	Value
1 Title	DVR05135BULKY.1.fid
2 Solvent	CDCl3
3 Temperature	300.0
4 Number of Scans	16
5 Receiver Gain	181
6 Relaxation Delay	1.0000
7 Pulse Width	10.5000
8 Spectrometer Frequency	600.32
9 Nucleus	1H

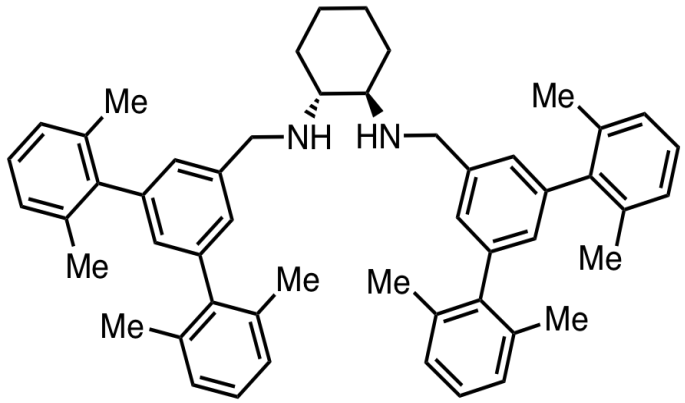

3.25

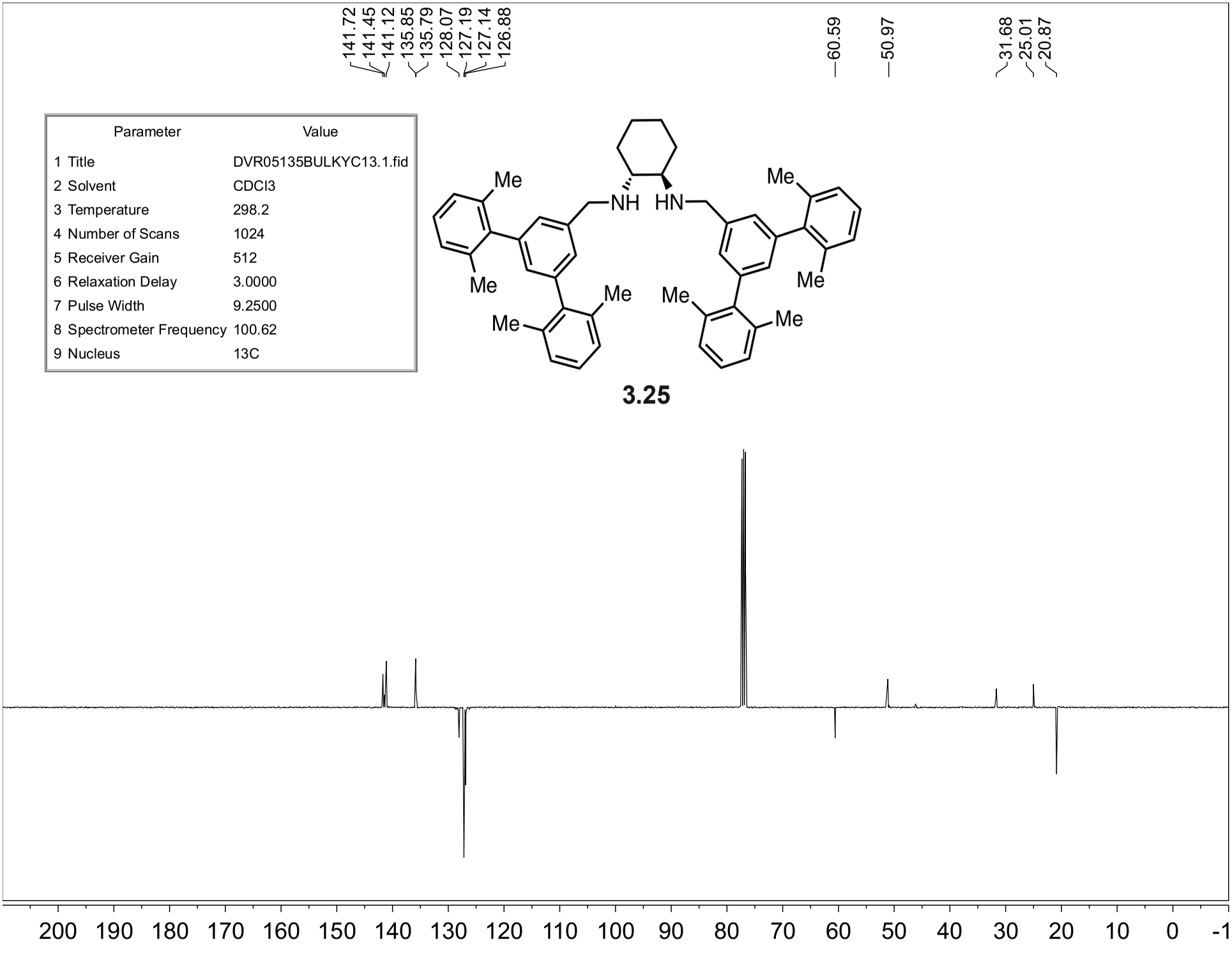
141.72
141.45
141.12
135.85
135.79
128.07
127.19
127.14
126.88
60.59
50.97
31.68
25.01
20.87
Parameter Value
1 Title DVR05135BULKYC13.1.fid
2 Solvent CDCl3
3 Temperature 298.2
4 Number of Scans 1024
5 Receiver Gain 512
6 Relaxation Delay 3.0000
7 Pulse Width 9.2500
8 Spectrometer Frequency 100.62
9 Nucleus 13C
Me
NH
HN
Me
Me
Me
Me
Me
Me
Me
3.25
467
200 190 180 170 160 150 140 130 120 110 100 90 80 70 60 50 40 30 20 10 0 -1

Parameter	Value
1 Title	DVR02205 ETHYL BR WEIREB AMIDE.1.fid
2 Solvent	CDCl3
3 Temperature	298.0
4 Number of Scans	16
5 Receiver Gain	128
6 Relaxation Delay	1.0000
7 Pulse Width	10.7700
8 Spectrometer Frequency	600.32
9 Nucleus	1H

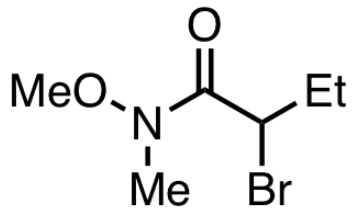

3.26

Parameter	Value
1 Title	DVR01297product.1.fid
2 Solvent	CDCl3
3 Temperature	298.0
4 Number of Scans	8
5 Receiver Gain	101
6 Relaxation Delay	1.0000
7 Pulse Width	10.7700
8 Spectrometer Frequency	600.32
9 Nucleus	1H

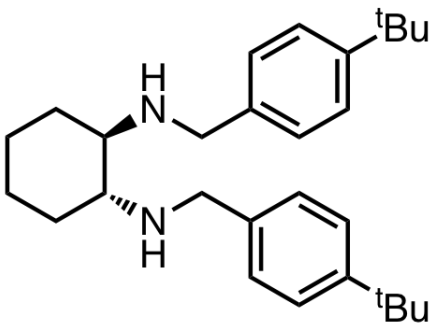

3.27

Parameter	Value
1 Title	DVR02121syn1.1.fid
2 Solvent	CDCl3
3 Temperature	298.0
4 Number of Scans	8
5 Receiver Gain	101
6 Relaxation Delay	1.0000
7 Pulse Width	10.7700
8 Spectrometer Frequency	600.32
9 Nucleus	1H

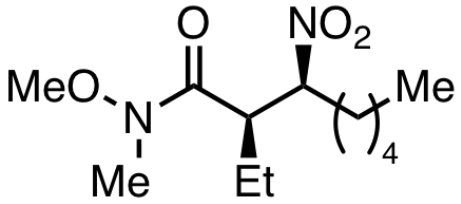

3.28A

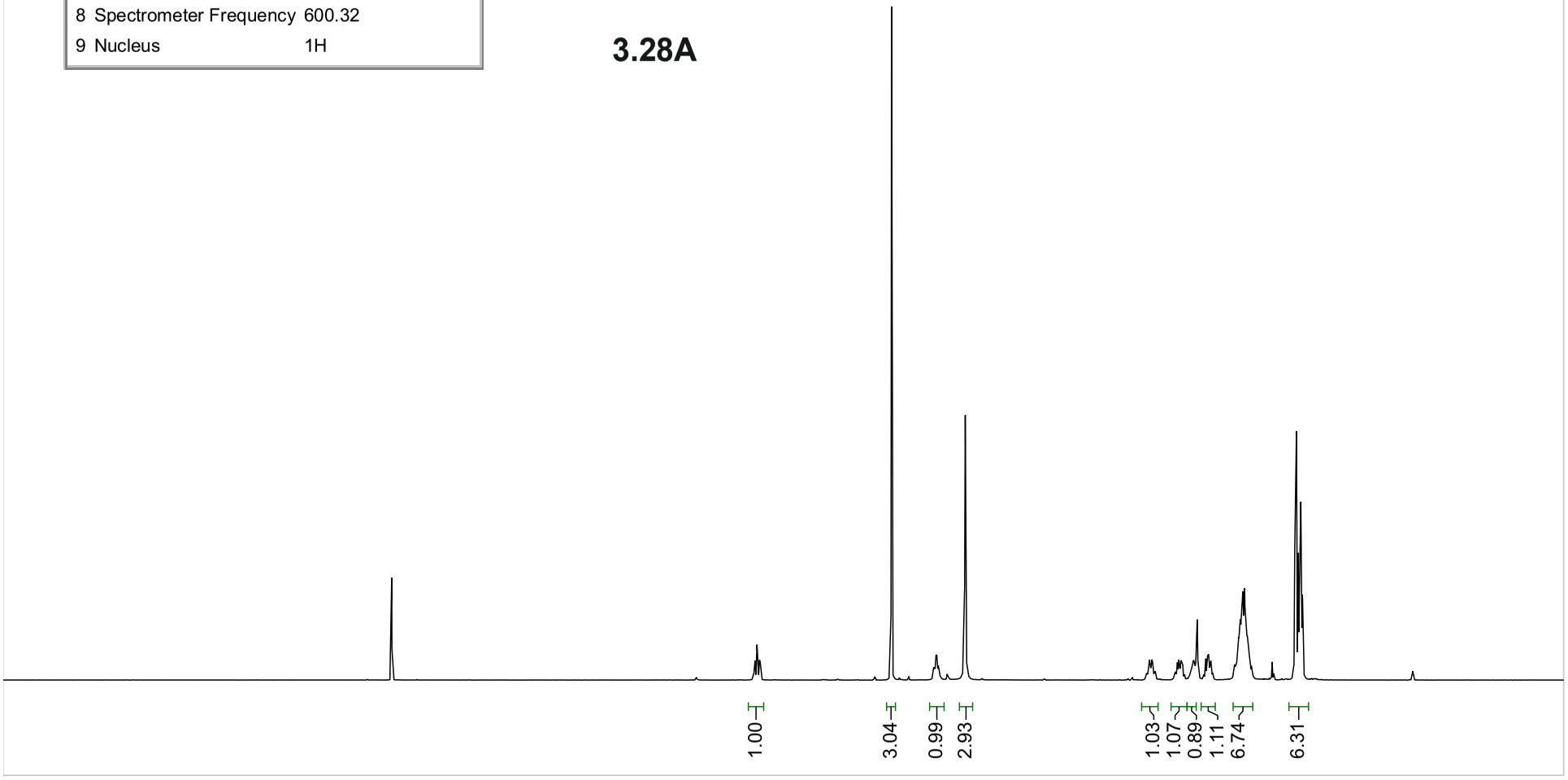

Parameter	Value
1 Title	DVR02121anti1.1.fid
2 Solvent	CDCl3
3 Temperature	298.0
4 Number of Scans	8
5 Receiver Gain	114
6 Relaxation Delay	1.0000
7 Pulse Width	10.7700
8 Spectrometer Frequency	600.32
9 Nucleus	1H

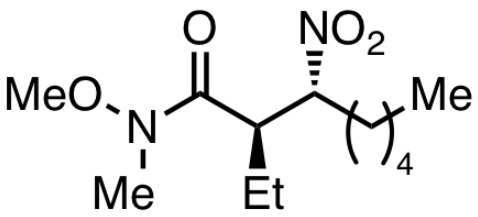

3.28B

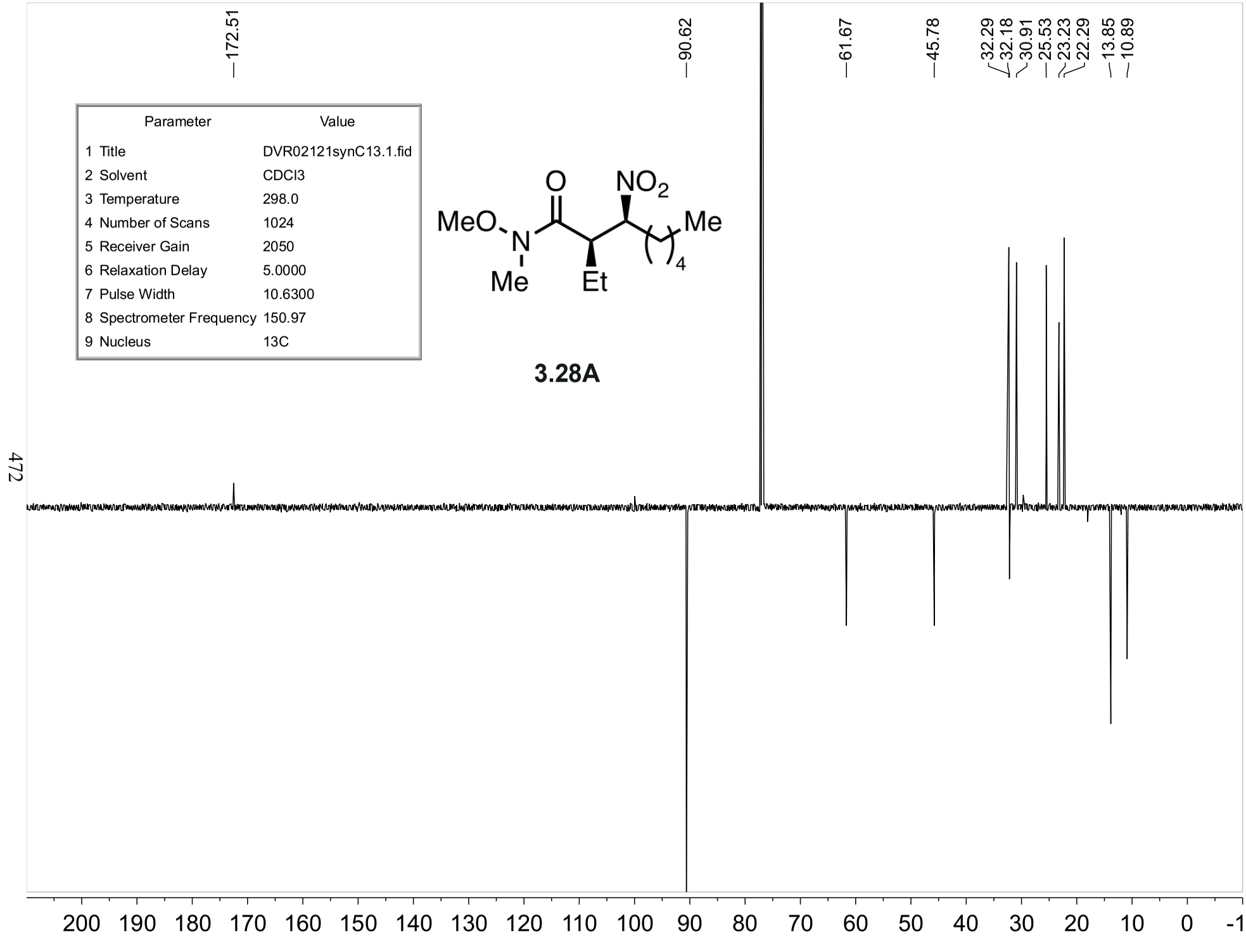
172.51
90.62
61.67
45.78
32.29
32.18
30.91
25.53
23.23
22.29
13.85
10.89
Parameter Value
1 Title DVR02121synC13.1.fid
2 Solvent CDCl3
3 Temperature 298.0
4 Number of Scans 1024
5 Receiver Gain 2050
6 Relaxation Delay 5.0000
7 Pulse Width 10.6300
8 Spectrometer Frequency 150.97
9 Nucleus 13C
MeO
N
Me
O
Et
NO2
Me
4
3.28A
472
200 190 180 170 160 150 140 130 120 110 100 90 80 70 60 50 40 30 20 10 0 -1

Parameter	Value
1 Title	DVR04226.1.fid
2 Solvent	CDCl3
3 Temperature	297.2
4 Number of Scans	16
5 Receiver Gain	57
6 Relaxation Delay	1.0000
7 Pulse Width	10.7700
8 Spectrometer Frequency	600.32
9 Nucleus	1H

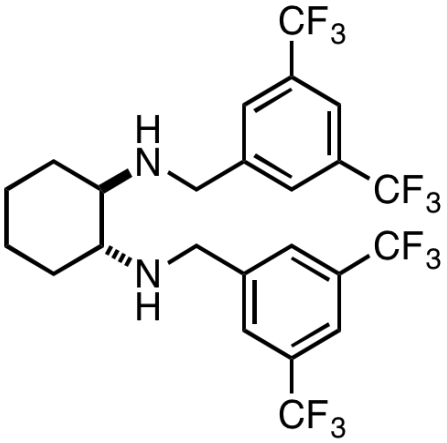

(*R,R*)-3.30

Parameter	Value
1 Title	DVR04226.2.fid
2 Solvent	CDCl3
3 Temperature	297.3
4 Number of Scans	16
5 Receiver Gain	90
6 Relaxation Delay	3.0000
7 Pulse Width	11.6200
8 Spectrometer Frequency	564.81
9 Nucleus	19F

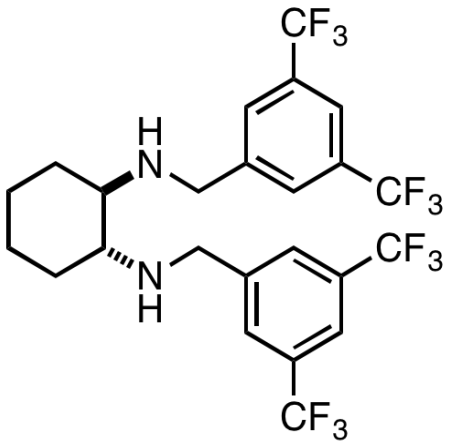

(*R,R*)-3.30

474

Parameter	Value
1 Title	DVR04226.3.fid
2 Solvent	CDCl3
3 Temperature	299.0
4 Number of Scans	1024
5 Receiver Gain	2050
6 Relaxation Delay	5.0000
7 Pulse Width	10.6300
8 Spectrometer Frequency	150.97
9 Nucleus	13C

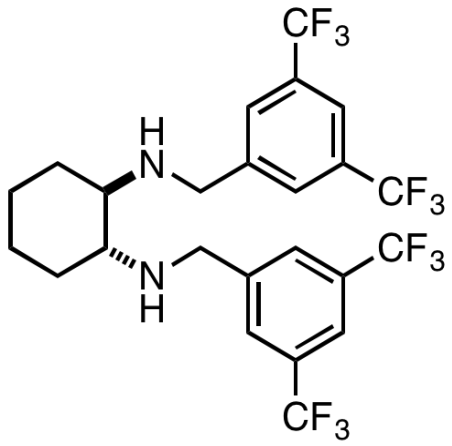

(*R*,*R*)-3.30

475

143.75 131.91 131.69 131.47 131.25 127.99 126.08 124.27 122.47 120.89 120.66 61.47 50.22 31.66 24.84

131.91 131.69 131.47 131.25

132.0 131.8 131.6 131.4 131.2

210 200 190 180 170 160 150 140 130 120 110 100 90 80 70 60 50 40 30 20 10 0 -10

Parameter	Value
1 Title	DVR04263ACRD.1.fid
2 Solvent	CDCl3
3 Temperature	297.5
4 Number of Scans	16
5 Receiver Gain	101
6 Relaxation Delay	1.0000
7 Pulse Width	10.7700
8 Spectrometer Frequency	600.32
9 Nucleus	1H

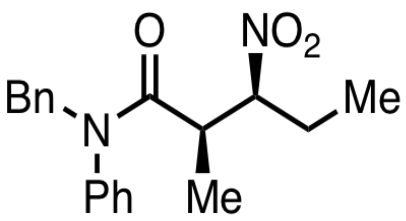

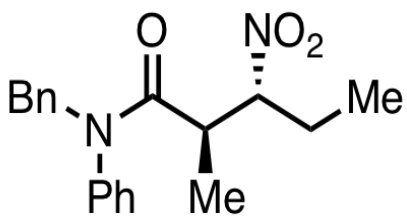

Crude

3.34A **75:25** **3.34B**

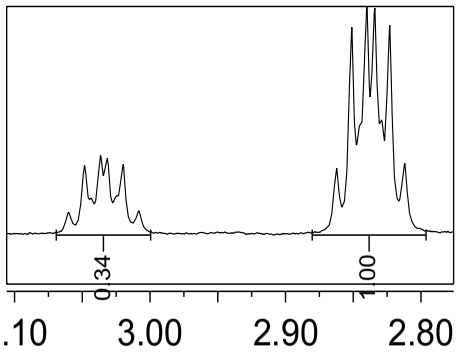

Parameter	Value
1 Title	DVR04135F1.1.fid
2 Solvent	CDCl3
3 Temperature	298.6
4 Number of Scans	16
5 Receiver Gain	181
6 Relaxation Delay	1.0000
7 Pulse Width	10.7700
8 Spectrometer Frequency	600.32
9 Nucleus	1H

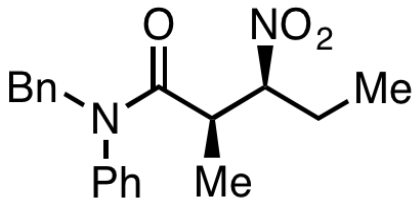

3.34A

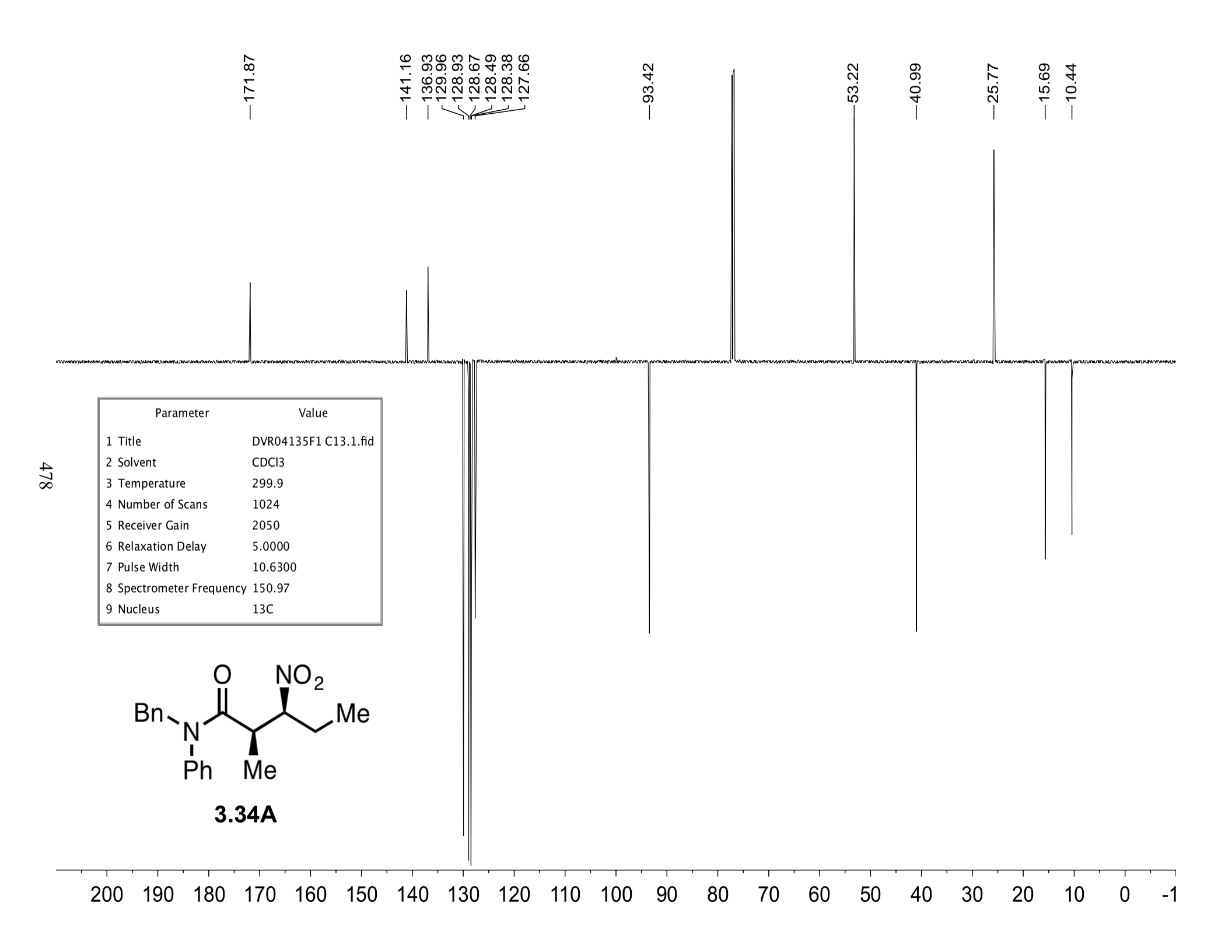
171.87
141.16
136.93
129.96
128.93
128.67
128.49
128.38
127.66
93.42
53.22
40.99
25.77
15.69
10.44
Parameter Value
1 Title DVR04135F1 C13.1.fid
2 Solvent CDCl3
3 Temperature 299.9
4 Number of Scans 1024
5 Receiver Gain 2050
6 Relaxation Delay 5.0000
7 Pulse Width 10.6300
8 Spectrometer Frequency 150.97
9 Nucleus 13C
478
O
NO2
Bn
N
Me
Ph
Me
3.34A
200 190 180 170 160 150 140 130 120 110 100 90 80 70 60 50 40 30 20 10 0 -1

Parameter	Value
1 Title	DVR04135F2.1.fid
2 Solvent	CDCl3
3 Temperature	298.3
4 Number of Scans	16
5 Receiver Gain	256
6 Relaxation Delay	1.0000
7 Pulse Width	10.7700
8 Spectrometer Frequency	600.32
9 Nucleus	1H

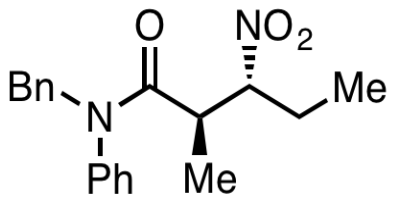

3.34B

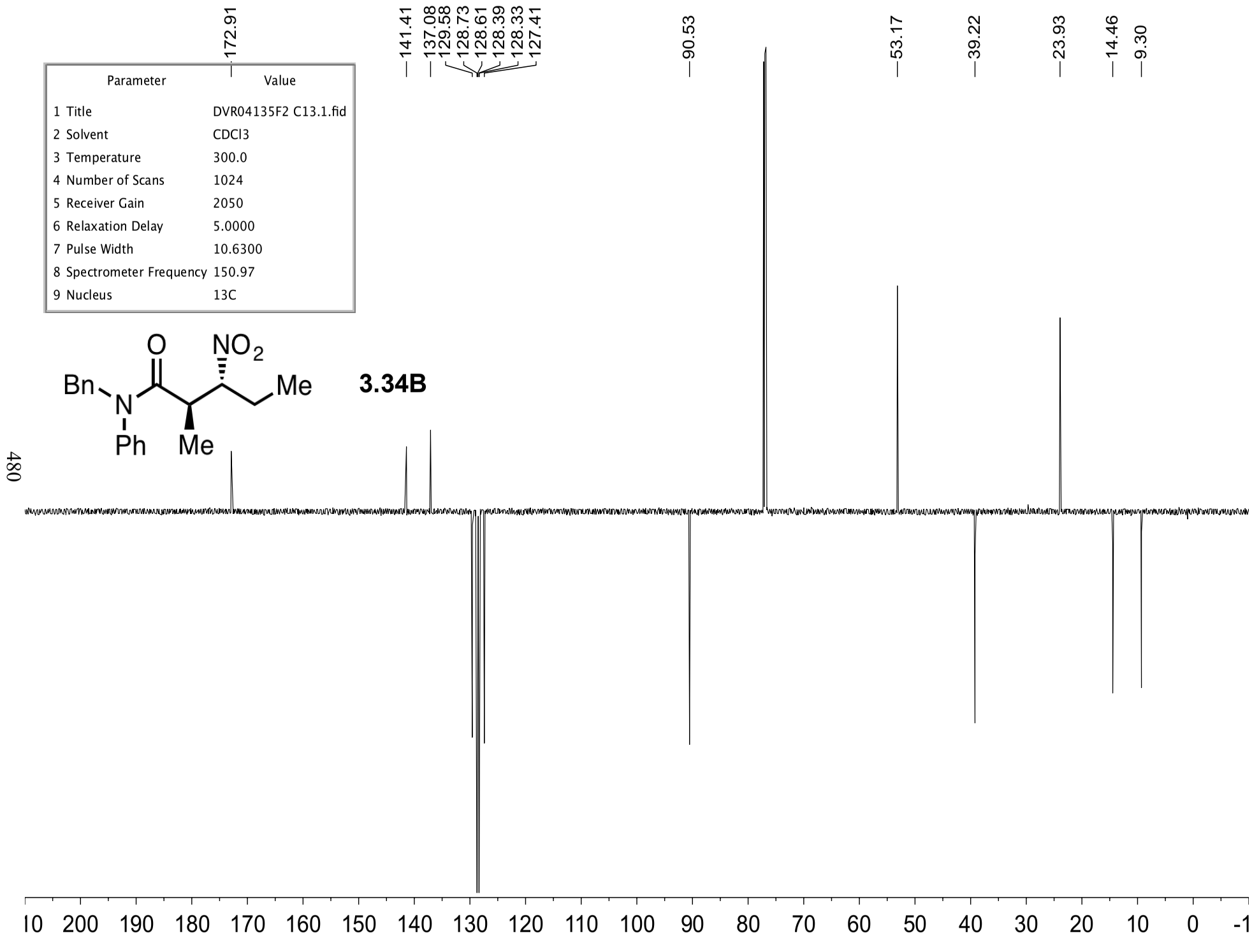
172.91
141.41
137.08
129.58
128.73
128.61
128.39
128.33
127.41
90.53
53.17
39.22
23.93
14.46
9.30
Parameter
Value
1 Title
DVR04135F2 C13.1.fid
2 Solvent
CDCl3
3 Temperature
300.0
4 Number of Scans
1024
5 Receiver Gain
2050
6 Relaxation Delay
5.0000
7 Pulse Width
10.6300
8 Spectrometer Frequency
150.97
9 Nucleus
13C
O
NO2
Bn
N
Ph
Me
Me
3.34B
480
10 200 190 180 170 160 150 140 130 120 110 100 90 80 70 60 50 40 30 20 10 0 -1

==== Shimadzu LCsolution Analysis Report ====

C:\LabSolutions\Data\DMM\DVR04136RAC SYN 3_7142016_1001 AM_3.lcd

Acquired by	: LC User
Sample Name	: DVR04136RAC SYN 3
Sample ID	: DVR04136RAC SYN 3
Tray#	: 1
Vail #	: 6
Injection Volume	: 2 uL
Data File Name	: DVR04136RAC SYN 3_7142016_1001 AM_3.lcd
Method File Name	: col2_0.8isoiPA_30min_1ML_220and210.lcm
Batch File Name	: DMM.lcb
Report File Name	: Default.lcr
Data Acquired	: 7/14/2016 12:14:11 PM
Data Processed	: 7/14/2016 12:44:14 PM

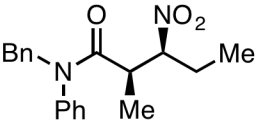

3.34A
racemic

<Chromatogram>

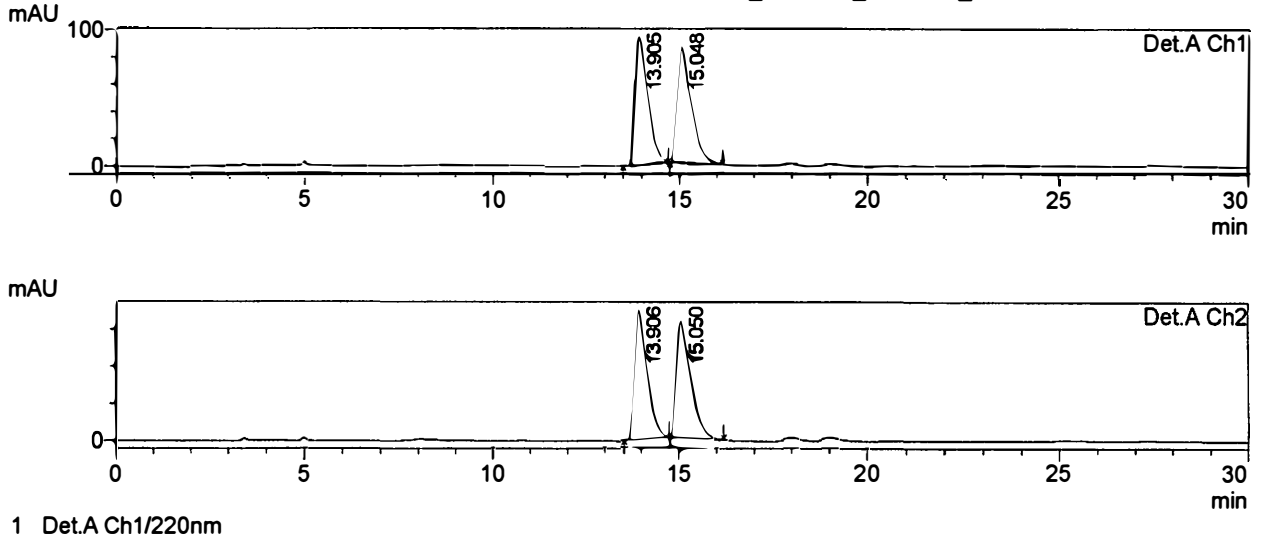

1 Det.A Ch1/220nm
2 Det.A Ch2/210nm

PeakTable

Detector A Ch1 220nm

Peak#	Ret. Time	Area	Height	Area %	Height %
1	13.905	2190844	95013	50.043	52.727
2	15.048	2187053	85184	49.957	47.273
Total		4377897	180197	100.000	100.000

PeakTable

Detector A Ch2 210nm

Peak#	Ret. Time	Area	Height	Area %	Height %
1	13.906	4055770	175507	50.093	52.761
2	15.050	4040646	157140	49.907	47.239
Total		8096415	332647	100.000	100.000

==== Shimadzu LCsolution Analysis Report ====

C:\LabSolutions\Data\DMM\DVR04136 SYN 2_7142016_1001 AM_7.lcd

Acquired by	: LC User
Sample Name	: DVR04136 SYN 2
Sample ID	: DVR04136 SYN 2
Tray#	: 1
Vail #	: 7
Injection Volume	: 2 uL
Data File Name	: DVR04136 SYN 2_7142016_1001 AM_7.lcd
Method File Name	: col2_0.8isoiPA_30min_1ML_220and210.lcm
Batch File Name	: DMM.lcb
Report File Name	: Default.lcr
Data Acquired	: 7/14/2016 1:25:10 PM
Data Processed	: 7/14/2016 1:55:11 PM

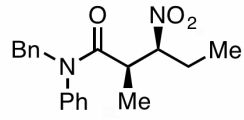

3.34A
91% ee

<Chromatogram>

C:\LabSolutions\Data\DMM\DVR04136 SYN 2_7142016_1001 AM_7.lcd

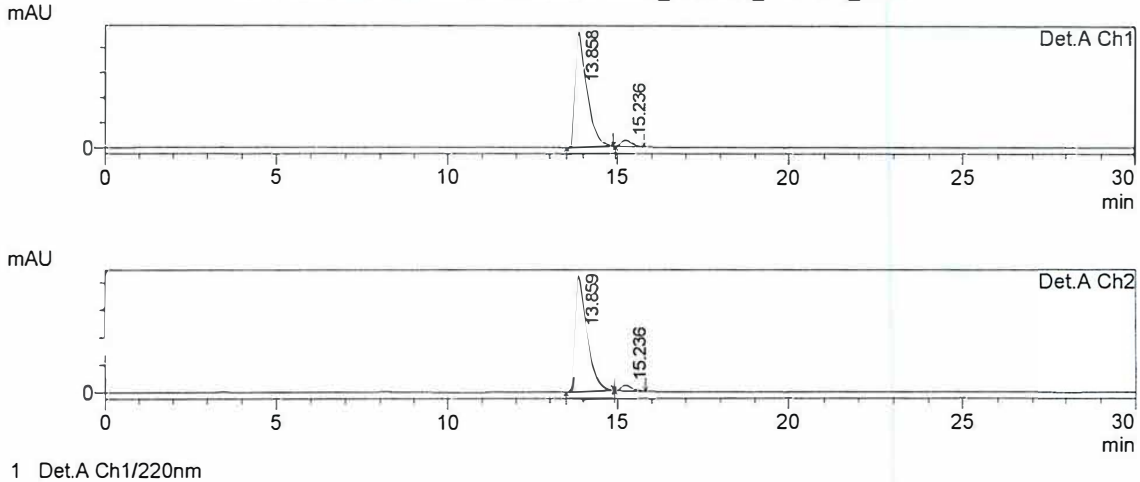

1 Det.A Ch1/220nm
2 Det.A Ch2/210nm

PeakTable

Detector A Ch1 220nm

Peak#	Ret. Time	Area	Height	Area %	Height %
1	13.858	5398412	229800	95.553	95.199
2	15.236	251218	11590	4.447	4.801
Total		5649631	241390	100.000	100.000

PeakTable

Detector A Ch2 210nm

Peak#	Ret. Time	Area	Height	Area %	Height %
1	13.859	9954946	422399	95.449	95.115
2	15.236	474650	21693	4.551	4.885
Total		10429596	444092	100.000	100.000

==== Shimadzu LCsolution Analysis Report ====

C:\LabSolutions\Data\DMM\DVR04135RAC ANTI 3_7162016_1752 PM_2.lcd

Acquired by	: LC User
Sample Name	: DVR04135RAC ANTI 3
Sample ID	: DVR04135RAC ANTI 3
Tray#	: 1
Vail #	: 6
Injection Volume	: 2 uL
Data File Name	: DVR04135RAC ANTI 3_7162016_1752 PM_2.lcd
Method File Name	: col2_0.8isoiPA_45min_1ML_220and210.lcm
Batch File Name	: DMM.lcb
Report File Name	: Default.lcr
Data Acquired	: 7/16/2016 6:38:35 PM
Data Processed	: 7/16/2016 10:46:56 PM

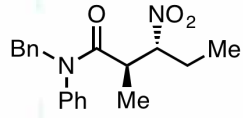

(±)

3.34B
racemic

<Chromatogram>

C:\LabSolutions\Data\DMM\DVR04135RAC ANTI 3_7162016_1752 PM_2.lcd

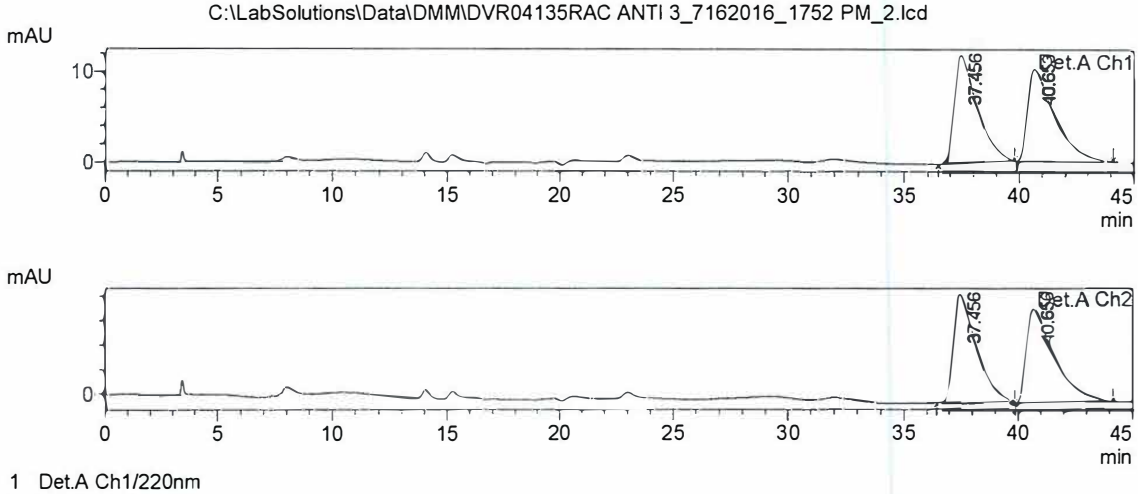

1 Det.A Ch1/220nm
2 Det.A Ch2/210nm

PeakTable

Detector A Ch1 220nm

Peak#	Ret. Time	Area	Height	Area %	Height %
1	37.456	817118	11850	49.593	53.836
2	40.653	830543	10161	50.407	46.164
Total		1647661	22011	100.000	100.000

PeakTable

Detector A Ch2 210nm

Peak#	Ret. Time	Area	Height	Area %	Height %
1	37.456	1545683	22392	49.041	53.793
2	40.656	1606133	19234	50.959	46.207
Total		3151816	41627	100.000	100.000

==== Shimadzu LCsolution Analysis Report ====

C:\LabSolutions\Data\DMM\DVR04135 ANTI 3_7162016_1752 PM_4.lcd

Acquired by	: LC User
Sample Name	: DVR04135 ANTI 3
Sample ID	: DVR04135 ANTI 3
Tray#	: 1
Vail #	: 7
Injection Volume	: 2 uL
Data File Name	: DVR04135 ANTI 3_7162016_1752 PM_4.lcd
Method File Name	: col2_0.8isoiPA_45min_1ML_220and210.lcm
Batch File Name	: DMM.lcb
Report File Name	: Default.lcr
Data Acquired	: 7/16/2016 8:19:26 PM
Data Processed	: 7/16/2016 10:48:54 PM

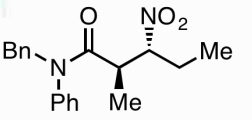

3.34B
83% ee

<Chromatogram>

C:\LabSolutions\Data\DMM\DVR04135 ANTI 3_7162016_1752 PM_4.lcd

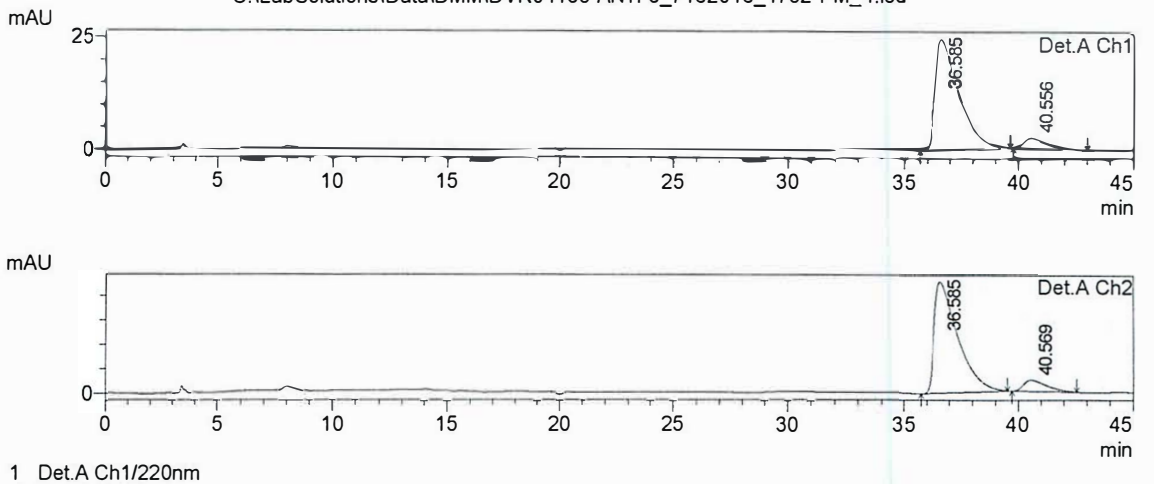

1 Det.A Ch1/220nm
2 Det.A Ch2/210nm

PeakTable

Detector A Ch1 220nm

Peak#	Ret. Time	Area	Height	Area %	Height %
1	36.585	1778887	24567	91.507	91.057
2	40.556	165100	2413	8.493	8.943
Total		1943987	26980	100.000	100.000

PeakTable

Detector A Ch2 210nm

Peak#	Ret. Time	Area	Height	Area %	Height %
1	36.585	3325547	46346	90.964	90.776
2	40.569	330327	4709	9.036	9.224
Total		3655875	51055	100.000	100.000

Parameter	Value
1 Title	DVR05078L.1.fid
2 Solvent	CDCl3
3 Temperature	298.2
4 Number of Scans	16
5 Receiver Gain	10
6 Relaxation Delay	1.0000
7 Pulse Width	15.0000
8 Spectrometer Frequency	400.13
9 Nucleus	1H

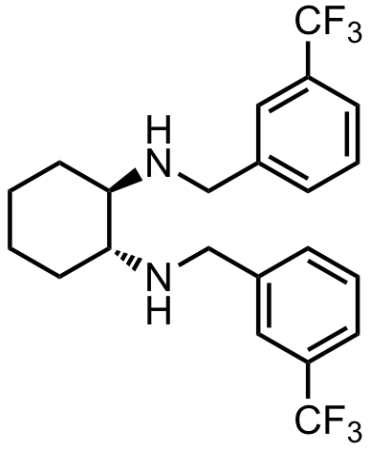

3.38

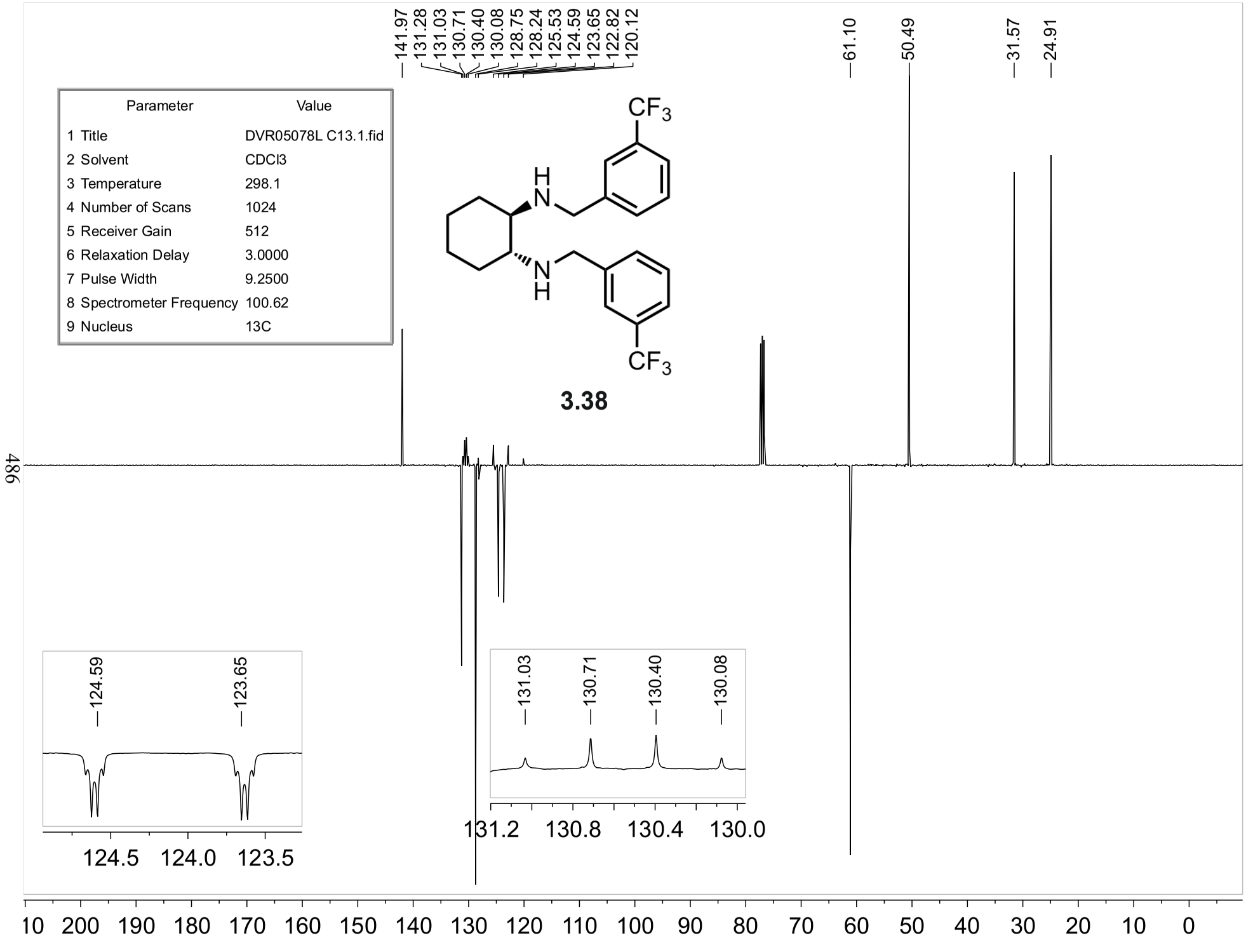
141.97
131.28
131.03
130.71
130.40
130.08
128.75
128.24
125.53
124.59
123.65
122.82
120.12
61.10
50.49
31.57
24.91
Parameter Value
1 Title DVR05078L C13.1.fid
2 Solvent CDCl3
3 Temperature 298.1
4 Number of Scans 1024
5 Receiver Gain 512
6 Relaxation Delay 3.0000
7 Pulse Width 9.2500
8 Spectrometer Frequency 100.62
9 Nucleus 13C
CF3
H
N
N
H
CF3
3.38
486
124.59
123.65
124.5 124.0 123.5
131.03
130.71
130.40
130.08
131.2 130.8 130.4 130.0
10 200 190 180 170 160 150 140 130 120 110 100 90 80 70 60 50 40 30 20 10 0

Parameter	Value
1 Title	DVR05078L F19.1.fid
2 Solvent	CDCl3
3 Temperature	297.4
4 Number of Scans	16
5 Receiver Gain	203
6 Relaxation Delay	3.0000
7 Pulse Width	11.6000
8 Spectrometer Frequency	564.81
9 Nucleus	19F

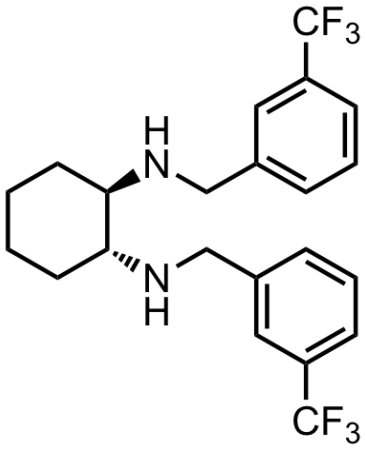

3.38

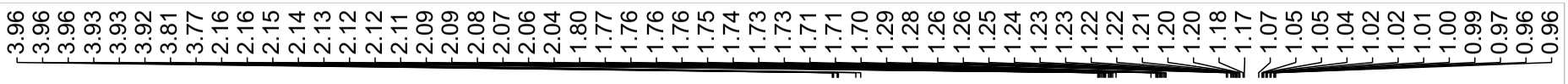

Parameter	Value
1 Title	DVR05078I.1.fid
2 Solvent	CDCl3
3 Temperature	298.2
4 Number of Scans	16
5 Receiver Gain	9
6 Relaxation Delay	1.0000
7 Pulse Width	15.0000
8 Spectrometer Frequency	400.13
9 Nucleus	1H

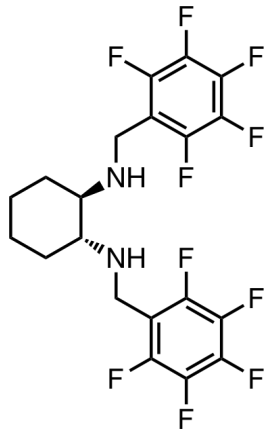

3.39

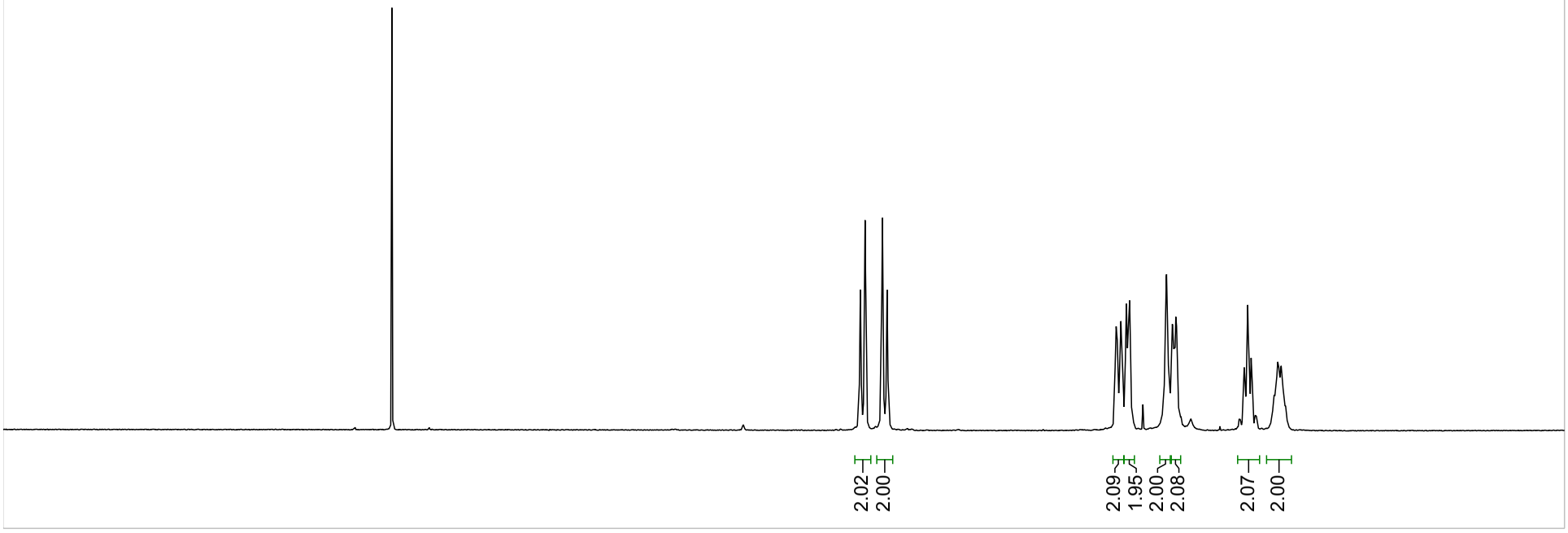

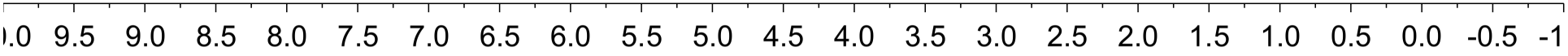

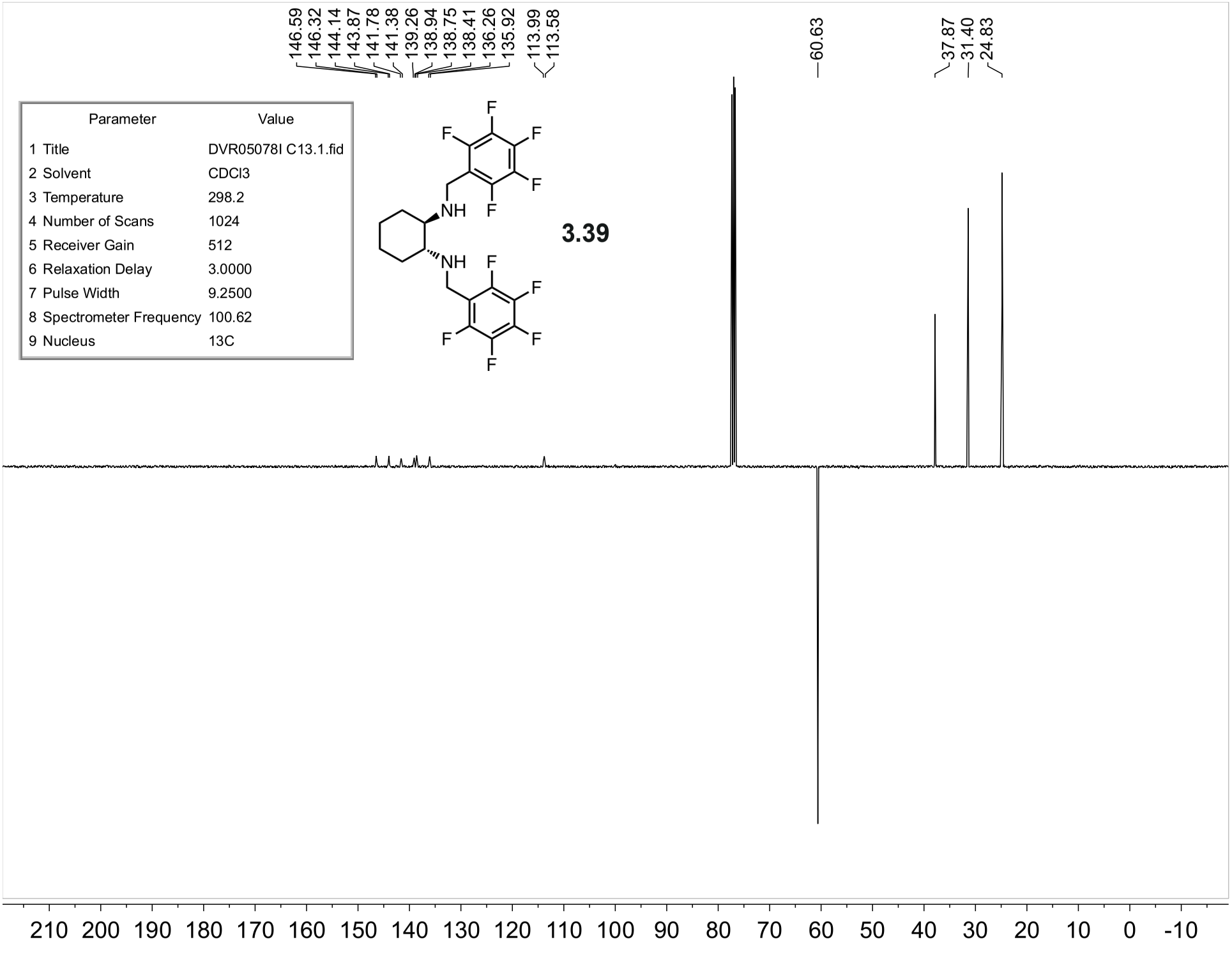
146.59
146.32
144.14
143.87
141.78
141.38
139.26
138.94
138.75
138.41
136.26
135.92
113.99
113.58
60.63
37.87
31.40
24.83
Parameter Value
1 Title DVR05078I C13.1.fid
2 Solvent CDCl3
3 Temperature 298.2
4 Number of Scans 1024
5 Receiver Gain 512
6 Relaxation Delay 3.0000
7 Pulse Width 9.2500
8 Spectrometer Frequency 100.62
9 Nucleus 13C
NH
NH
F
3.39
489
210 200 190 180 170 160 150 140 130 120 110 100 90 80 70 60 50 40 30 20 10 0 -10

Parameter	Value
1 Title	DVR05078I F19.1.fid
2 Solvent	CDCl3
3 Temperature	297.5
4 Number of Scans	16
5 Receiver Gain	456
6 Relaxation Delay	3.0000
7 Pulse Width	11.6000
8 Spectrometer Frequency	564.81
9 Nucleus	19F

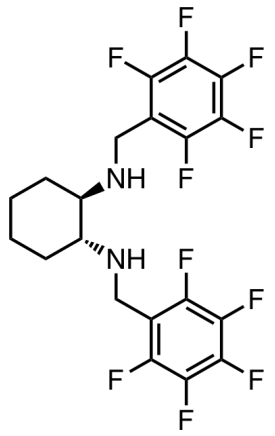

3.39

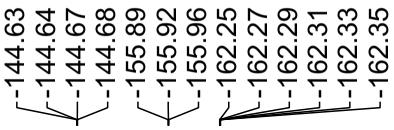

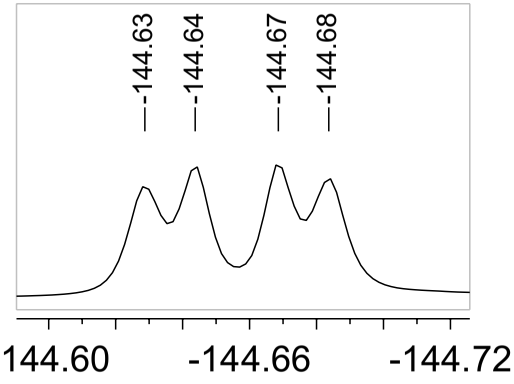

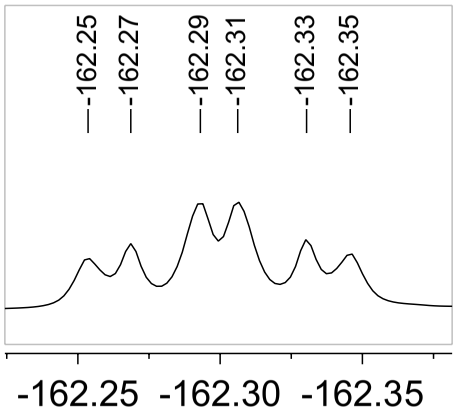

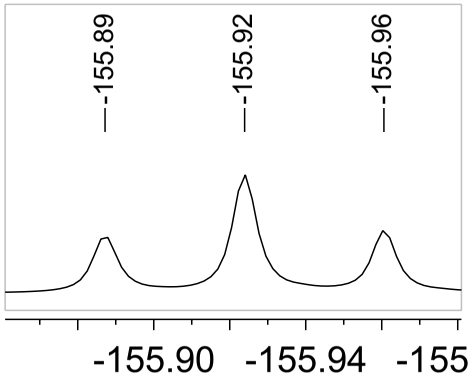

10 0 -10 -20 -30 -40 -50 -60 -70 -80 -90 -100 -110 -120 -130 -140 -150 -160 -170 -180 -190 -200 -210

Parameter	Value
1 Title	DVR05078N.1.fid
2 Solvent	CDCl3
3 Temperature	298.2
4 Number of Scans	16
5 Receiver Gain	9
6 Relaxation Delay	1.0000
7 Pulse Width	15.0000
8 Spectrometer Frequency	400.13
9 Nucleus	1H

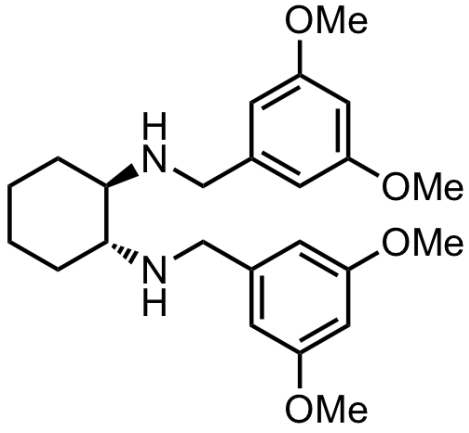

3.40

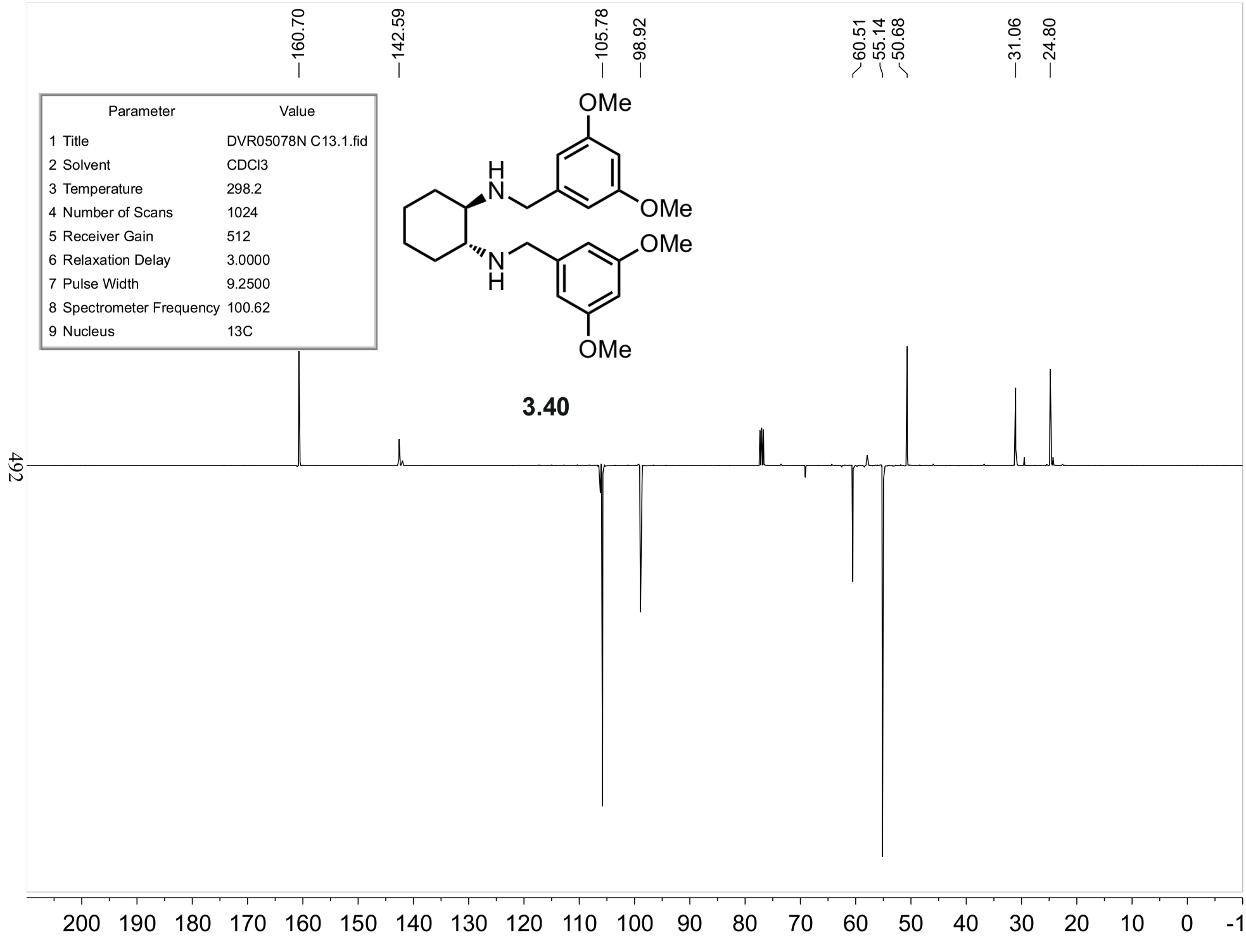
160.70
142.59
105.78
98.92
60.51
55.14
50.68
31.06
24.80
Parameter Value
1 Title DVR05078N C13.1.fid
2 Solvent CDCl3
3 Temperature 298.2
4 Number of Scans 1024
5 Receiver Gain 512
6 Relaxation Delay 3.0000
7 Pulse Width 9.2500
8 Spectrometer Frequency 100.62
9 Nucleus 13C
OMe
OMe
OMe
OMe
H
N
N
H
3.40
492
200 190 180 170 160 150 140 130 120 110 100 90 80 70 60 50 40 30 20 10 0 -1

Parameter	Value
1 Title	DVR05078S.1.fid
2 Solvent	CDCl3
3 Temperature	298.2
4 Number of Scans	16
5 Receiver Gain	9
6 Relaxation Delay	1.0000
7 Pulse Width	15.0000
8 Spectrometer Frequency	400.13
9 Nucleus	1H

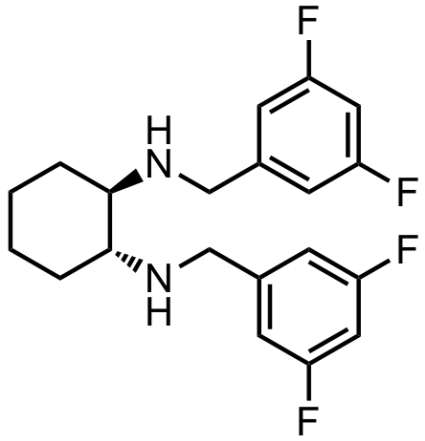

3.41

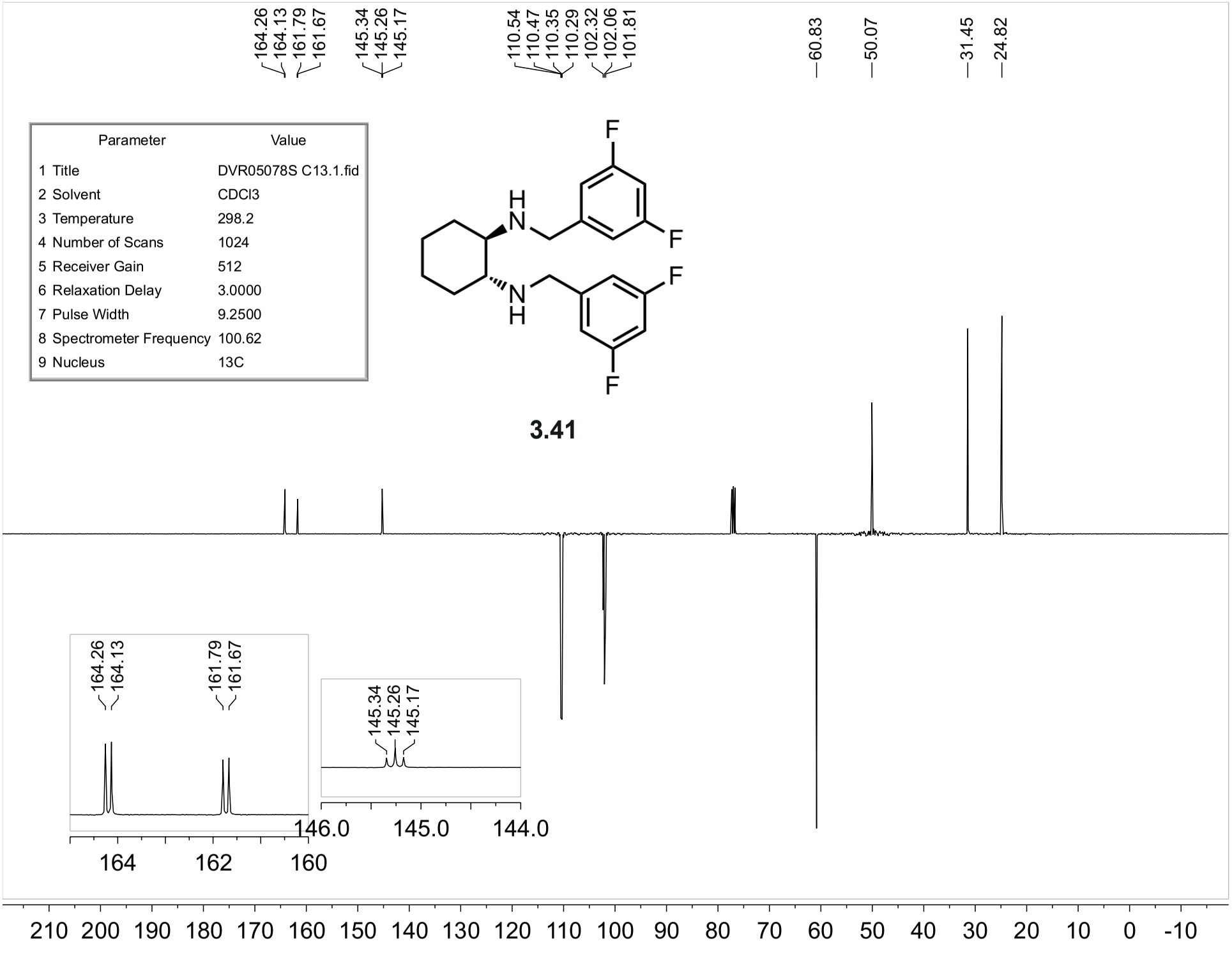
164.26
164.13
161.79
161.67
145.34
145.26
145.17
110.54
110.47
110.35
110.29
102.32
102.06
101.81
60.83
50.07
31.45
24.82
Parameter Value
1 Title DVR05078S C13.1.fid
2 Solvent CDCl3
3 Temperature 298.2
4 Number of Scans 1024
5 Receiver Gain 512
6 Relaxation Delay 3.0000
7 Pulse Width 9.2500
8 Spectrometer Frequency 100.62
9 Nucleus 13C
F
H
N
F
F
H
N
F
3.41
494
164.26
164.13
161.79
161.67
145.34
145.26
145.17
146.0
145.0
144.0
164
162
160
210 200 190 180 170 160 150 140 130 120 110 100 90 80 70 60 50 40 30 20 10 0 -10

Parameter	Value
1 Title	DVR05078S F19.1.fid
2 Solvent	CDCl3
3 Temperature	297.4
4 Number of Scans	16
5 Receiver Gain	203
6 Relaxation Delay	3.0000
7 Pulse Width	11.6000
8 Spectrometer Frequency	564.81
9 Nucleus	19F

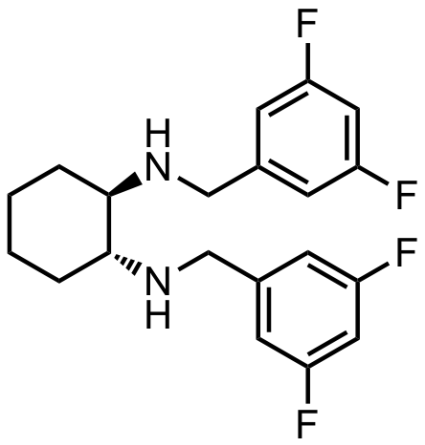

3.41

Parameter	Value
1 Title	DVR05078M.1.fid
2 Solvent	CDCl3
3 Temperature	298.2
4 Number of Scans	16
5 Receiver Gain	9
6 Relaxation Delay	1.0000
7 Pulse Width	15.0000
8 Spectrometer Frequency	400.13
9 Nucleus	1H

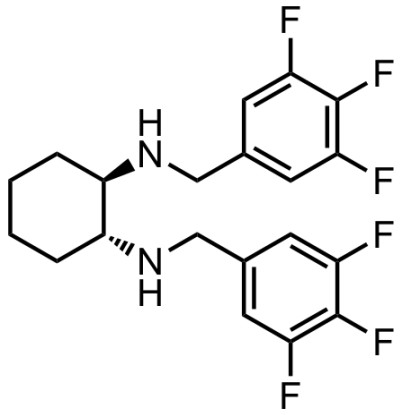

3.42

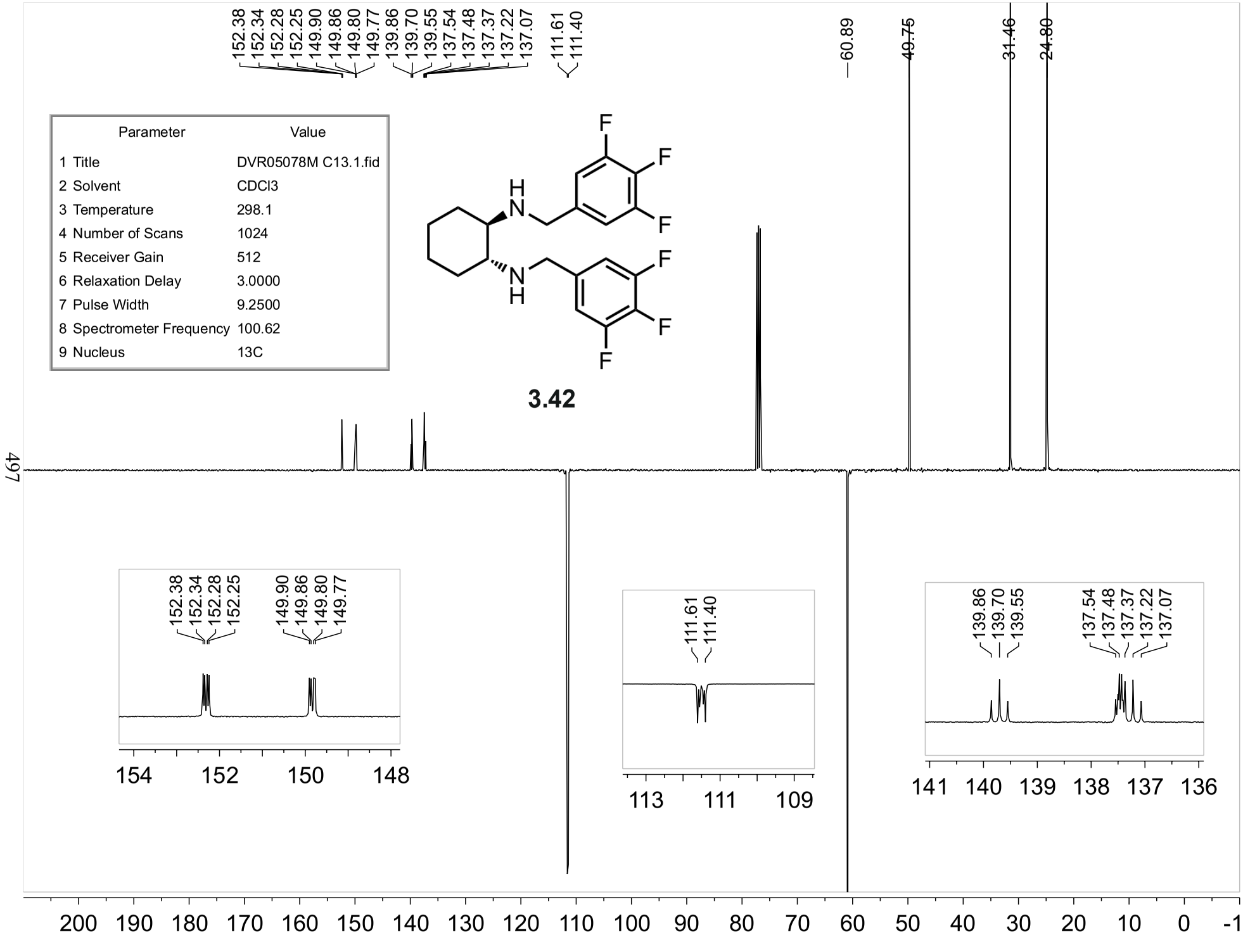
152.38
152.34
152.28
152.25
149.90
149.86
149.80
149.77
139.86
139.70
139.55
137.54
137.48
137.37
137.22
137.07
111.61
111.40
60.89
49.75
31.46
24.80
Parameter Value
1 Title DVR05078M C13.1.fid
2 Solvent CDCl3
3 Temperature 298.1
4 Number of Scans 1024
5 Receiver Gain 512
6 Relaxation Delay 3.0000
7 Pulse Width 9.2500
8 Spectrometer Frequency 100.62
9 Nucleus 13C
3.42
49.7
154 152 150 148
113 111 109
141 140 139 138 137 136
200 190 180 170 160 150 140 130 120 110 100 90 80 70 60 50 40 30 20 10 0 -1

Parameter	Value
1 Title	DVR05078M F19.1.fid
2 Solvent	CDCl3
3 Temperature	297.4
4 Number of Scans	16
5 Receiver Gain	287
6 Relaxation Delay	3.0000
7 Pulse Width	11.6000
8 Spectrometer Frequency	564.81
9 Nucleus	19F

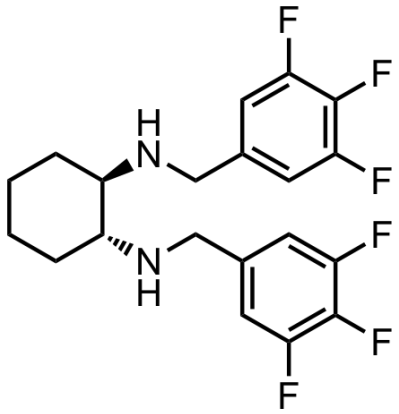

3.42

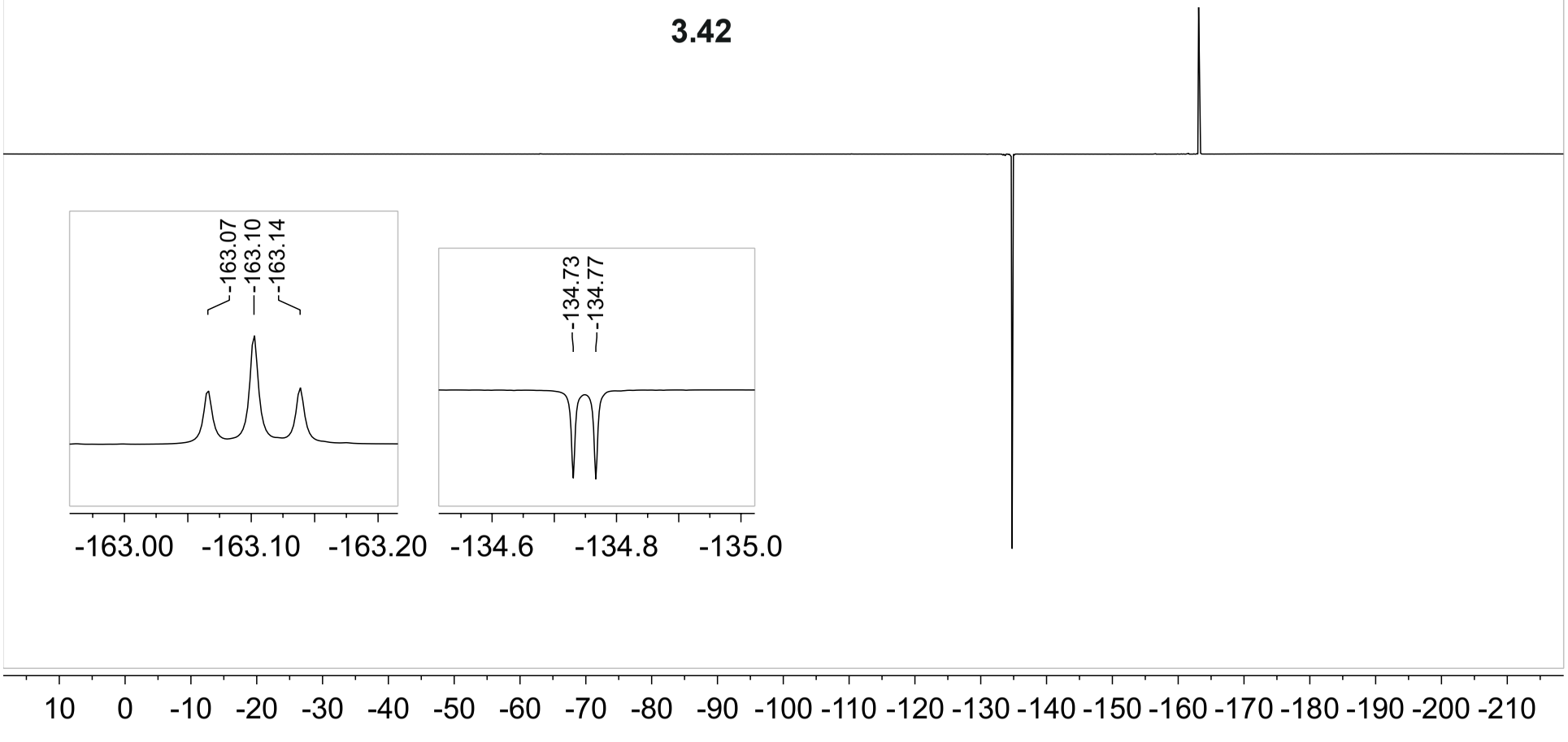

Parameter	Value
1 Title	DVR05078K.1.fid
2 Solvent	CDCl3
3 Temperature	298.2
4 Number of Scans	16
5 Receiver Gain	8
6 Relaxation Delay	1.0000
7 Pulse Width	15.0000
8 Spectrometer Frequency	400.13
9 Nucleus	1H

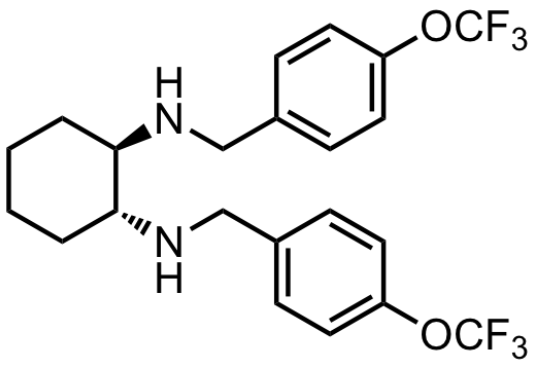

3.43

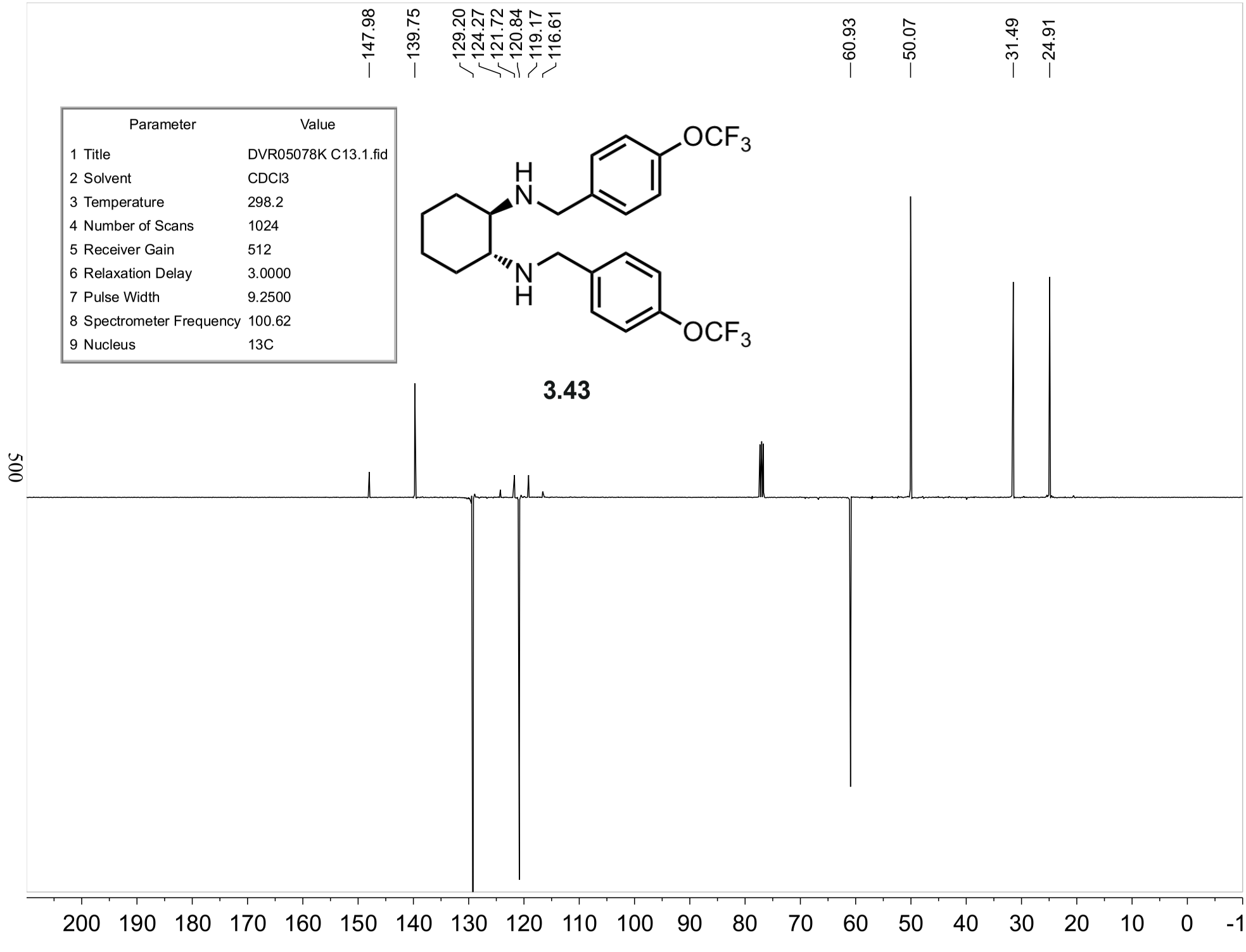
147.98
139.75
129.20
124.27
121.72
120.84
119.17
116.61
60.93
50.07
31.49
24.91
Parameter Value
1 Title DVR05078K C13.1.fid
2 Solvent CDCl3
3 Temperature 298.2
4 Number of Scans 1024
5 Receiver Gain 512
6 Relaxation Delay 3.0000
7 Pulse Width 9.2500
8 Spectrometer Frequency 100.62
9 Nucleus 13C
OCF3
H
N
N
H
OCF3
3.43
500
200 190 180 170 160 150 140 130 120 110 100 90 80 70 60 50 40 30 20 10 0 -1

Parameter	Value
1 Title	DVR05078K F19.1.fid
2 Solvent	CDCl3
3 Temperature	297.5
4 Number of Scans	16
5 Receiver Gain	181
6 Relaxation Delay	3.0000
7 Pulse Width	11.6000
8 Spectrometer Frequency	564.81
9 Nucleus	19F

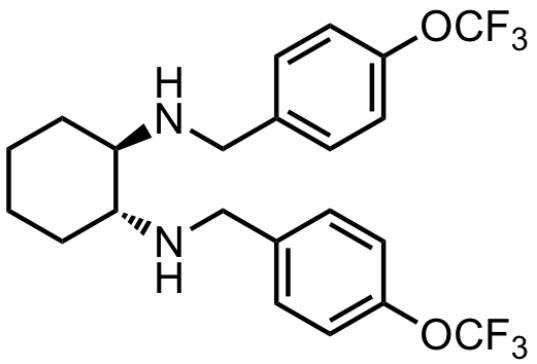

3.43

Parameter	Value
1 Title	DVR04150CRD.1.fid
2 Solvent	CDCl3
3 Temperature	297.9
4 Number of Scans	16
5 Receiver Gain	114
6 Relaxation Delay	1.0000
7 Pulse Width	10.7700
8 Spectrometer Frequency	600.32
9 Nucleus	1H

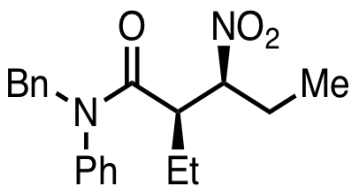

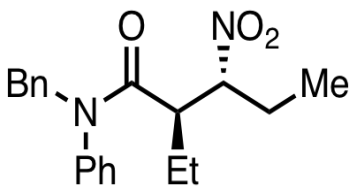

3.44A **Crude** **55:45** **3.44B**

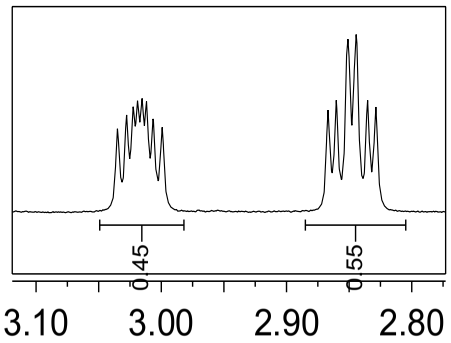

502

Parameter	Value
1 Title	DVR04150D1.1.fid
2 Solvent	CDCl3
3 Temperature	297.2
4 Number of Scans	16
5 Receiver Gain	57
6 Relaxation Delay	1.0000
7 Pulse Width	10.7700
8 Spectrometer Frequency	600.32
9 Nucleus	1H

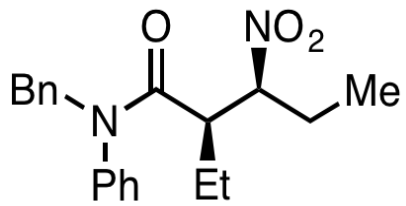

3.44A

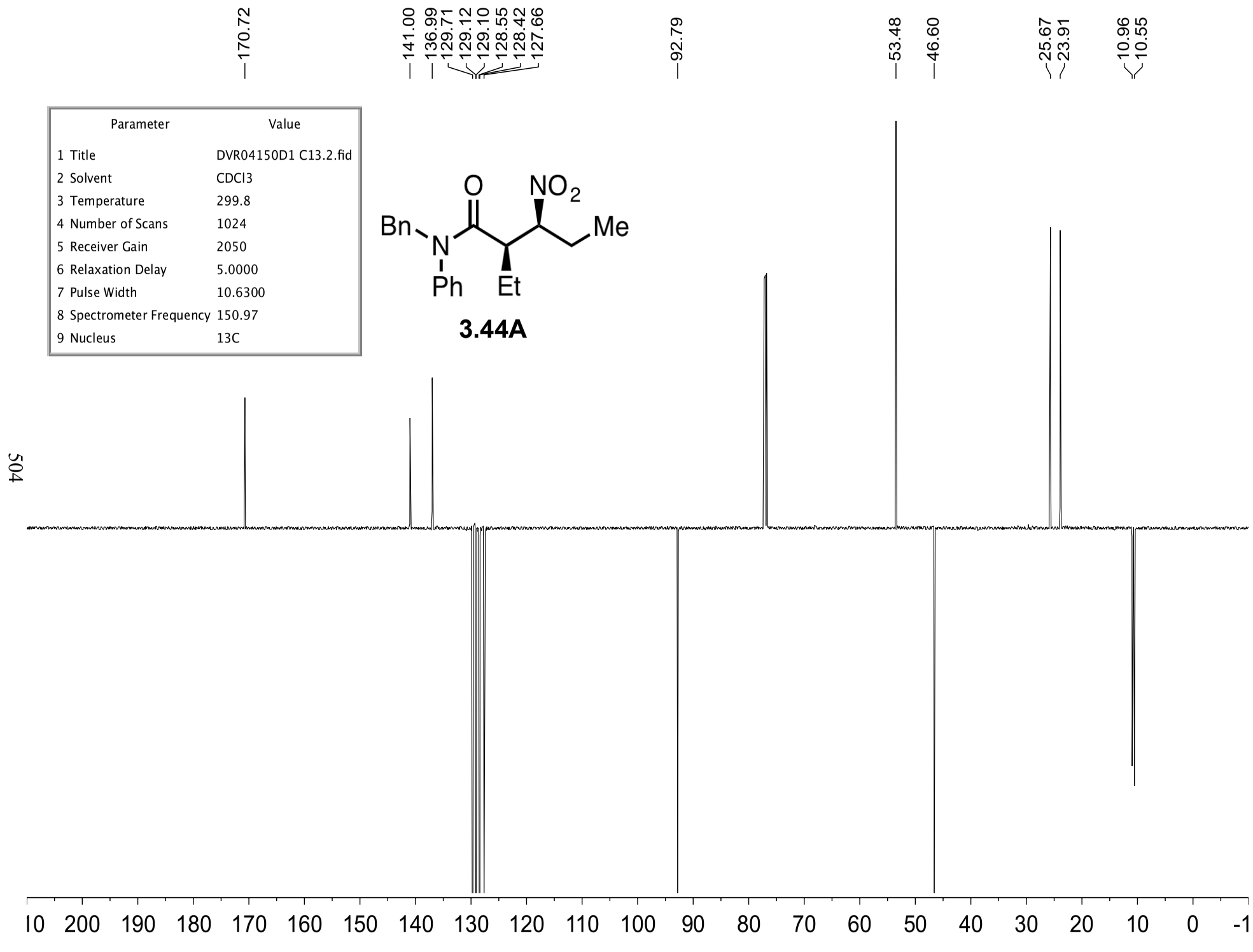
170.72
141.00
136.99
129.71
129.12
129.10
128.55
128.42
127.66
92.79
53.48
46.60
25.67
23.91
10.96
10.55
Parameter
Value
1 Title
DVR04150D1 C13.2.fid
2 Solvent
CDCl3
3 Temperature
299.8
4 Number of Scans
1024
5 Receiver Gain
2050
6 Relaxation Delay
5.0000
7 Pulse Width
10.6300
8 Spectrometer Frequency
150.97
9 Nucleus
13C
O
NO2
Bn
N
Me
Ph
Et
3.44A
504
10 200 190 180 170 160 150 140 130 120 110 100 90 80 70 60 50 40 30 20 10 0 -1

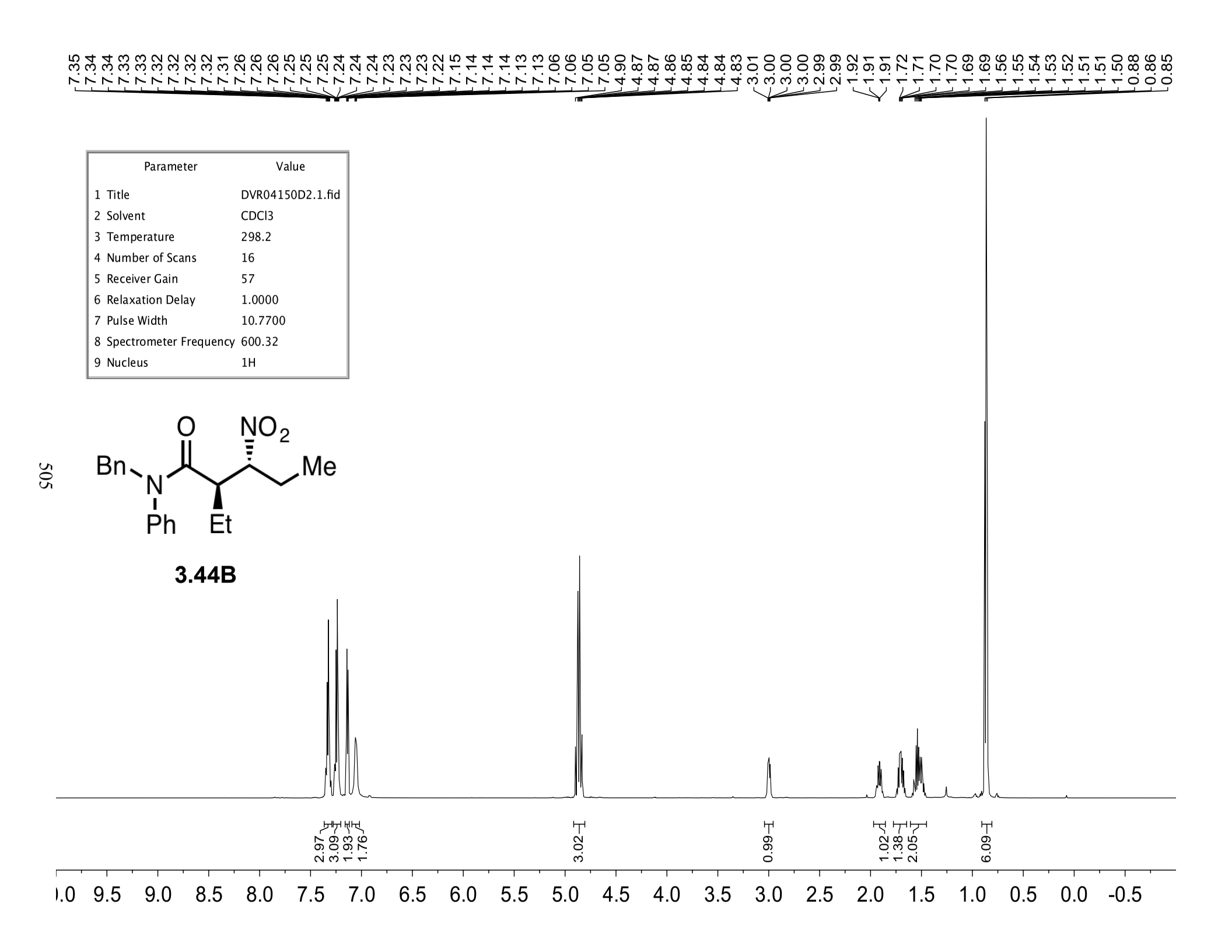
7.35 7.34 7.34 7.33 7.33 7.32 7.32 7.32 7.32 7.31 7.26 7.26 7.26 7.25 7.25 7.25 7.24 7.24 7.24 7.24 7.23 7.23 7.23 7.22 7.15 7.14 7.14 7.14 7.13 7.13 7.06 7.06 7.05 7.05 4.90 4.87 4.87 4.86 4.85 4.84 4.84 4.83 3.01 3.00 3.00 3.00 2.99 2.99 1.92 1.91 1.91 1.72 1.71 1.70 1.70 1.69 1.69 1.56 1.55 1.54 1.53 1.52 1.51 1.51 1.50 0.88 0.86 0.85
Parameter Value
1 Title DVR04150D2.1.fid
2 Solvent CDCl3
3 Temperature 298.2
4 Number of Scans 16
5 Receiver Gain 57
6 Relaxation Delay 1.0000
7 Pulse Width 10.7700
8 Spectrometer Frequency 600.32
9 Nucleus 1H
O
NO2
Bn
N
Me
Ph
Et
3.44B
505
2.97
3.09
1.93
1.76
3.02
0.99
1.02
1.38
2.05
6.09
.0 9.5 9.0 8.5 8.0 7.5 7.0 6.5 6.0 5.5 5.0 4.5 4.0 3.5 3.0 2.5 2.0 1.5 1.0 0.5 0.0 -0.5

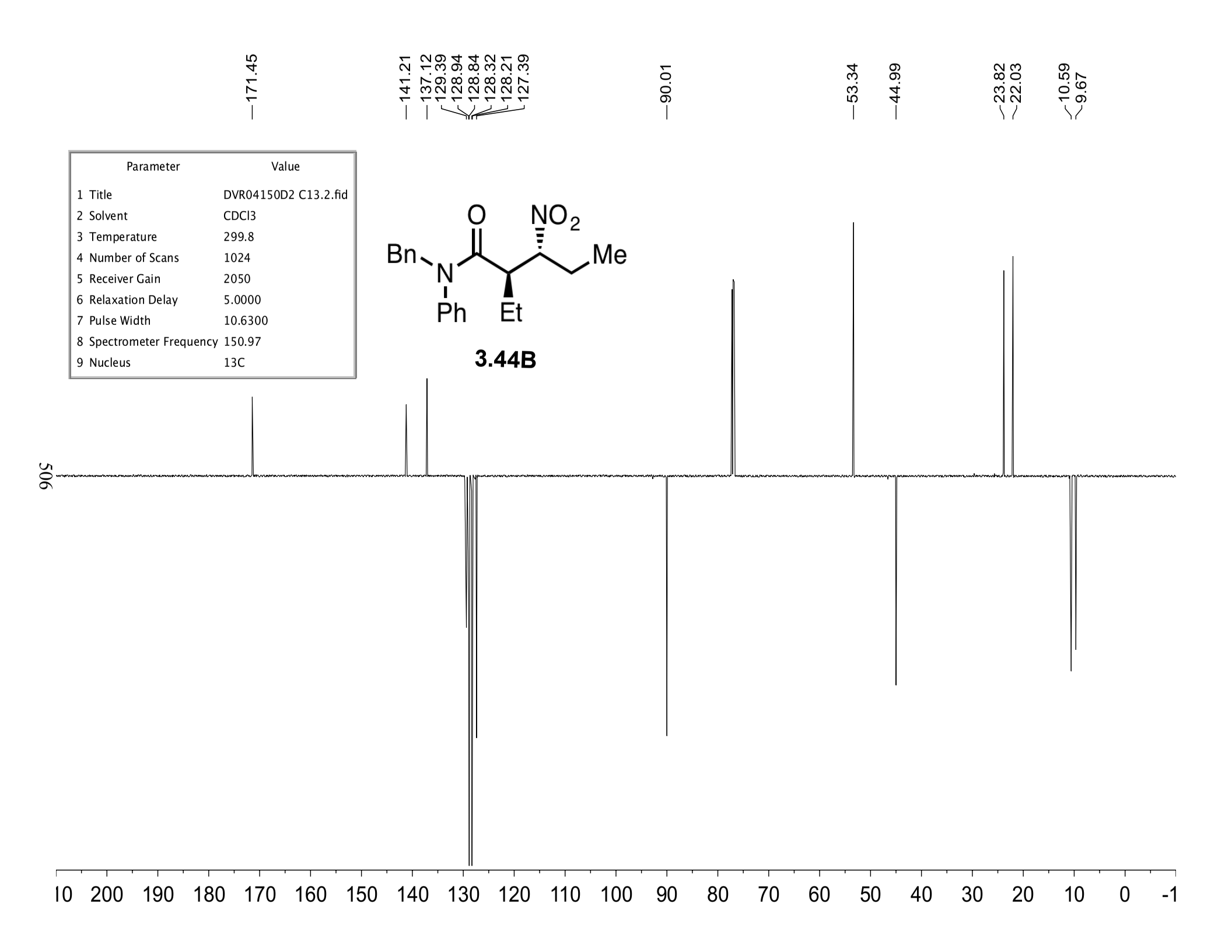
171.45
141.21
137.12
129.39
128.94
128.84
128.32
128.21
127.39
90.01
53.34
44.99
23.82
22.03
10.59
9.67
Parameter
Value
1 Title
DVR04150D2 C13.2.fid
2 Solvent
CDCl3
3 Temperature
299.8
4 Number of Scans
1024
5 Receiver Gain
2050
6 Relaxation Delay
5.0000
7 Pulse Width
10.6300
8 Spectrometer Frequency
150.97
9 Nucleus
13C
O
NO2
Bn
N
Ph
Et
Me
3.44B
506
10 200 190 180 170 160 150 140 130 120 110 100 90 80 70 60 50 40 30 20 10 0 -1

==== Shimadzu LCsolution Analysis Report ====

C:\LabSolutions\Data\DMM\DVR04150 RAC SYN 1_822016_841 AM_25.lcd

Acquired by	: LC User
Sample Name	: DVR04150 RAC SYN 1
Sample ID	: DVR04150 RAC SYN 1
Tray#	: 1
Vail #	: 3
Injection Volume	: 1 uL
Data File Name	: DVR04150 RAC SYN 1_822016_841 AM_25.lcd
Method File Name	: col3_3isoiPA_20min_1ML_220and210.lcm
Batch File Name	: DMM.lcb
Report File Name	: Default.lcr
Data Acquired	: 8/2/2016 7:37:05 PM
Data Processed	: 8/2/2016 7:57:07 PM

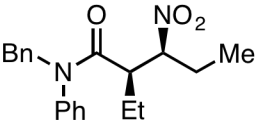

3.44A
racemic

<Chromatogram>

C:\LabSolutions\Data\DMM\DVR04150 RAC SYN 1_822016_841 AM_25.lcd

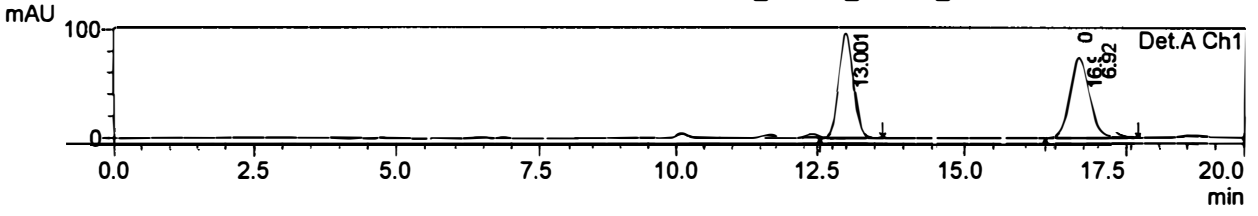

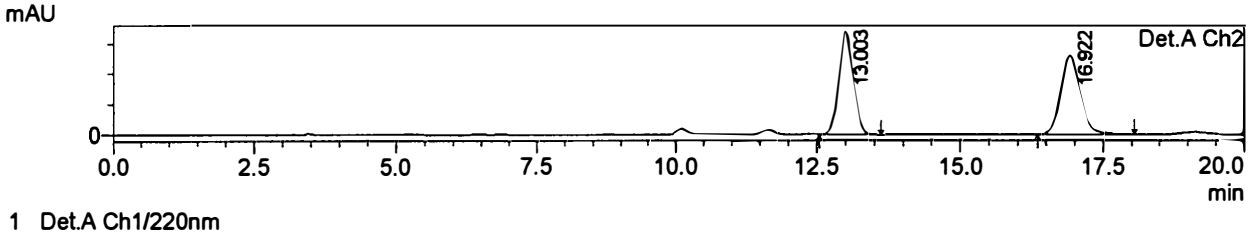

1 Det.A Ch1/220nm
2 Det.A Ch2/210nm

PeakTable

Detector A Ch1 220nm

Peak#	Ret. Time	Area	Height	Area %	Height %
1	13.001	1683886	96541	48.958	56.693
2	16.920	1755548	73745	51.042	43.307
Total		3439434	170286	100.000	100.000

PeakTable

Detector A Ch2 210nm

Peak#	Ret. Time	Area	Height	Area %	Height %
1	13.003	2977086	170612	48.719	56.656
2	16.922	3133617	130525	51.281	43.344
Total		6110703	301138	100.000	100.000

==== Shimadzu LCsolution Analysis Report ====

C:\LabSolutions\Data\DMM\DVR04150 SYN 1_822016_841 AM_29.lcd

Acquired by	: LC User
Sample Name	: DVR04150 SYN 1
Sample ID	: DVR04150 SYN 1
Tray#	: 1
Vail #	: 4
Injection Volume	: 1 uL
Data File Name	: DVR04150 SYN 1_822016_841 AM_29.lcd
Method File Name	: col3_3isoiPA_20min_1ML_220and210.lcm
Batch File Name	: DMM.lcb
Report File Name	: Default.lcr
Data Acquired	: 8/2/2016 8:28:03 PM
Data Processed	: 8/2/2016 8:48:05 PM

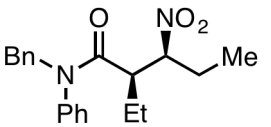

3.44A
85% ee

<Chromatogram>

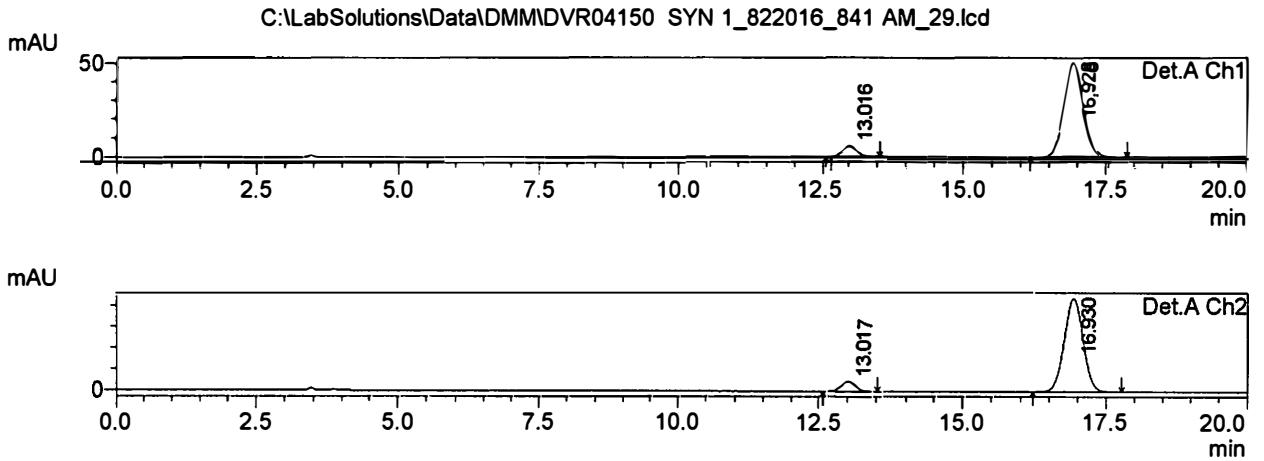

1 Det.A Ch1/220nm
2 Det.A Ch2/210nm

PeakTable

Detector A Ch1 220nm

Peak#	Ret. Time	Area	Height	Area %	Height %
1	13.016	94791	5413	7.531	9.707
2	16.928	1163865	50348	92.469	90.293
Total		1258656	55761	100.000	100.000

PeakTable

Detector A Ch2 210nm

Peak#	Ret. Time	Area	Height	Area %	Height %
1	13.017	166990	9557	7.511	9.698
2	16.930	2056243	88980	92.489	90.302
Total		2223234	98536	100.000	100.000

==== Shimadzu LCsolution Analysis Report ====

C:\LabSolutions\Data\DMM\DVR04150 RAC ANTI 1_812016_1017 AM_1.lcd

Acquired by	: LC User
Sample Name	: DVR04150 RAC ANTI 1
Sample ID	: DVR04150 RAC ANTI 1
Tray#	: 1
Vail #	: 1
Injection Volume	: 1 uL
Data File Name	: DVR04150 RAC ANTI 1_812016_1017 AM_1.lcd
Method File Name	: col6_3isoiPA_30min_1ML_220and210.lcm
Batch File Name	: DMM.lcb
Report File Name	: Default.lcr
Data Acquired	: 8/1/2016 10:48:37 AM
Data Processed	: 8/1/2016 11:18:39 AM

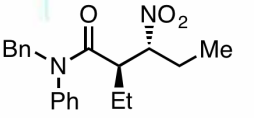

3.44B
racemic

<Chromatogram>

C:\LabSolutions\Data\DMM\DVR04150 RAC ANTI 1_812016_1017 AM_1.lcd

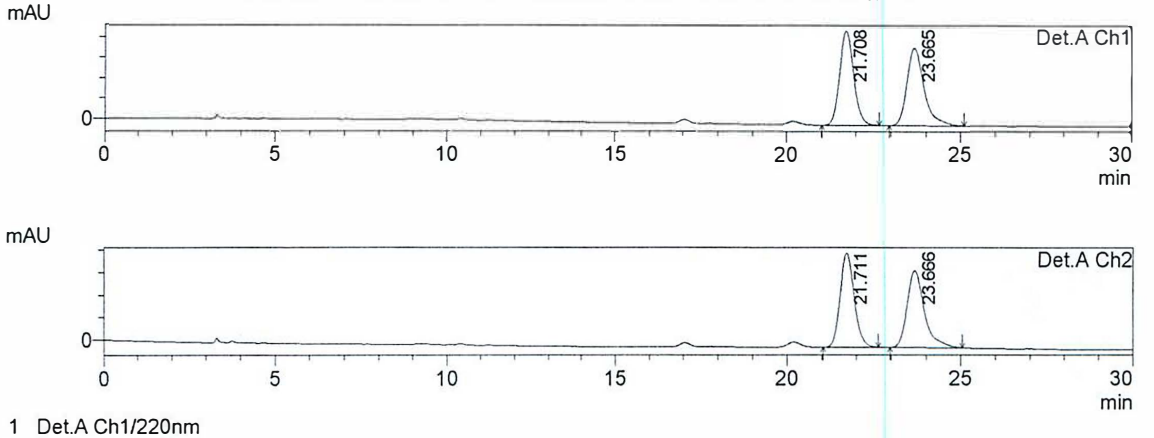

1 Det.A Ch1/220nm
2 Det.A Ch2/210nm

PeakTable

Detector A Ch1 220nm

Peak#	Ret. Time	Area	Height	Area %	Height %
1	21.708	648485	23201	49.674	54.878
2	23.665	656990	19076	50.326	45.122
Total		1305475	42277	100.000	100.000

PeakTable

Detector A Ch2 210nm

Peak#	Ret. Time	Area	Height	Area %	Height %
1	21.711	1182722	41875	49.776	54.948
2	23.666	1193362	34333	50.224	45.052
Total		2376083	76208	100.000	100.000

==== Shimadzu LCsolution Analysis Report ====

C:\LabSolutions\Data\DMM\DVR04150 ANTI_812016_1017 AM_2.lcd

Acquired by	: LC User
Sample Name	: DVR04150 ANTI
Sample ID	: DVR04150 ANTI
Tray#	: 1
Vail #	: 2
Injection Volume	: 1 uL
Data File Name	: DVR04150 ANTI_812016_1017 AM_2.lcd
Method File Name	: col6_3isoiPA_30min_1ML_220and210.lcm
Batch File Name	: DMM.lcb
Report File Name	: Default.lcr
Data Acquired	: 8/1/2016 11:19:14 AM
Data Processed	: 8/1/2016 11:49:14 AM

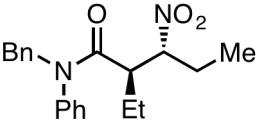

3.44B
81% ee

<Chromatogram>

C:\LabSolutions\Data\DMM\DVR04150 ANTI_812016_1017 AM_2.lcd

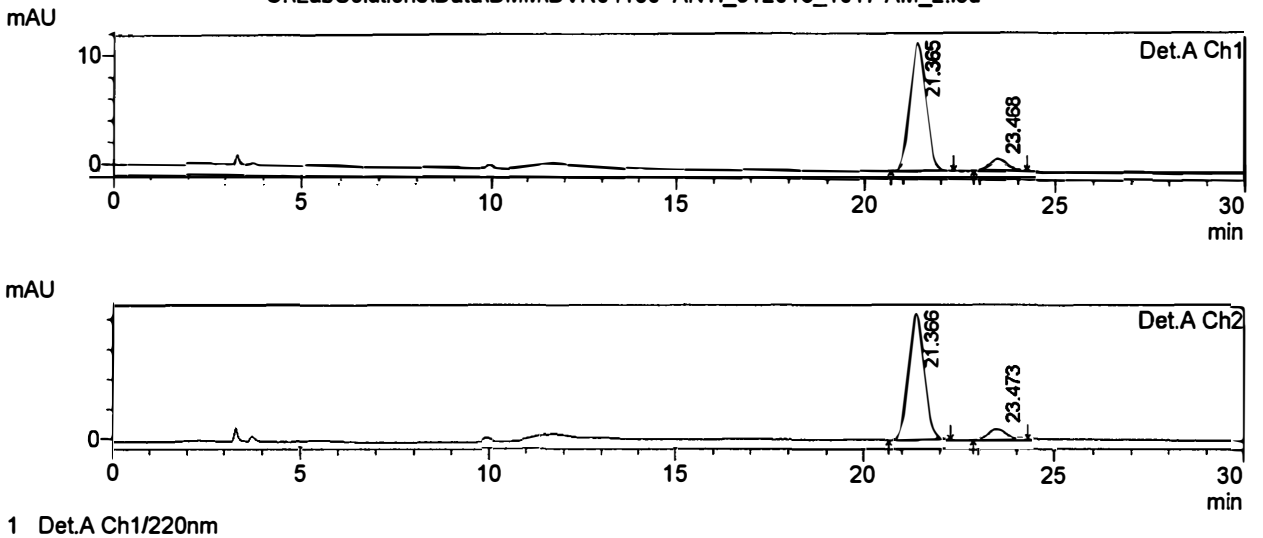

1 Det.A Ch1/220nm
2 Det.A Ch2/210nm

PeakTable

Detector A Ch1 220nm

Peak#	Ret. Time	Area	Height	Area %	Height %
1	21.365	326032	11828	90.671	92.066
2	23.468	33547	1019	9.329	7.934
Total		359579	12847	100.000	100.000

PeakTable

Detector A Ch2 210nm

Peak#	Ret. Time	Area	Height	Area %	Height %
1	21.366	585715	21277	90.446	92.013
2	23.473	61872	1847	9.554	7.987
Total		647587	23124	100.000	100.000

Parameter	Value
1 Title	DVR04130CRD.1.fid
2 Solvent	CDCl3
3 Temperature	297.8
4 Number of Scans	16
5 Receiver Gain	144
6 Relaxation Delay	1.0000
7 Pulse Width	10.7700
8 Spectrometer Frequency	600.32
9 Nucleus	1H

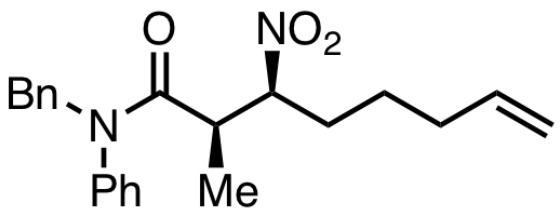

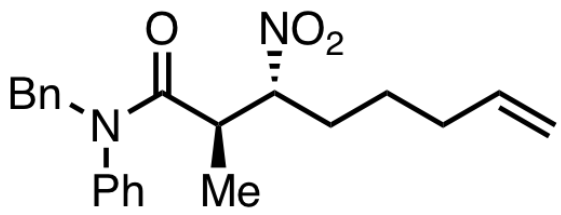

Crude

3.47A **79:21** **3.47B**

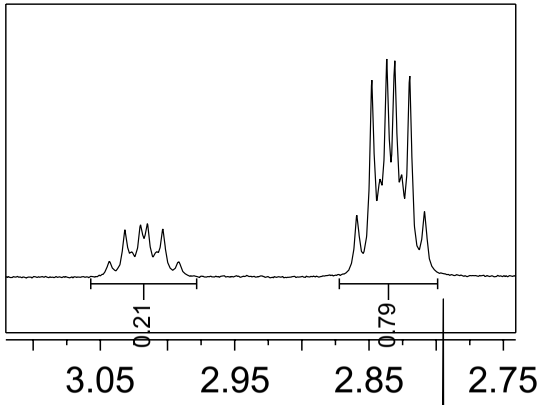

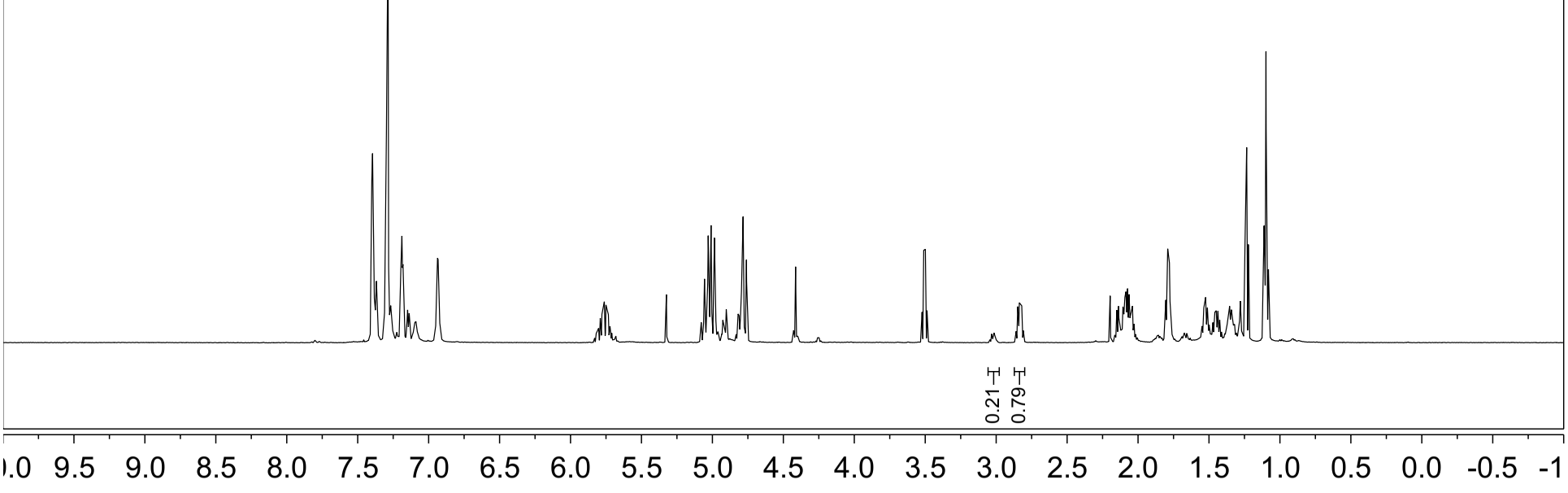

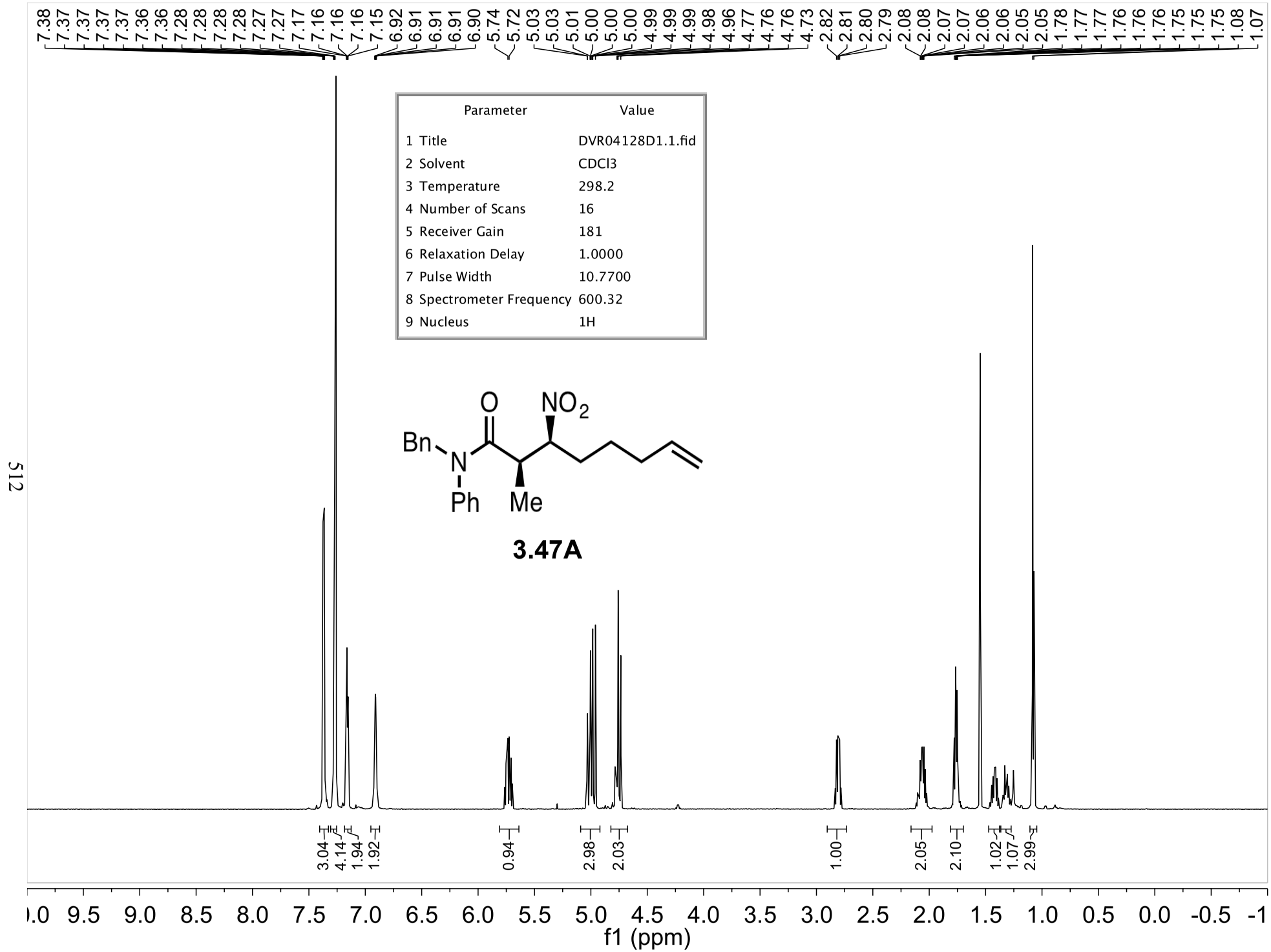
7.38 7.37 7.37 7.37 7.37 7.36 7.36 7.28 7.28 7.28 7.28 7.27 7.27 7.17 7.16 7.16 7.16 7.15 6.92 6.91 6.91 6.91 6.90 5.74 5.72 5.03 5.03 5.01 5.00 5.00 5.00 4.99 4.99 4.99 4.98 4.96 4.77 4.76 4.76 4.73 2.82 2.81 2.80 2.79 2.08 2.08 2.07 2.07 2.06 2.06 2.05 2.05 1.78 1.77 1.77 1.76 1.76 1.76 1.75 1.75 1.75 1.08 1.07
Parameter Value
1 Title DVR04128D1.1.fid
2 Solvent CDCl3
3 Temperature 298.2
4 Number of Scans 16
5 Receiver Gain 181
6 Relaxation Delay 1.0000
7 Pulse Width 10.7700
8 Spectrometer Frequency 600.32
9 Nucleus 1H
O
NO2
Bn
N
Ph
Me
3.47A
3.04 4.14 1.94 1.92 0.94 2.98 2.03 1.00 2.05 2.10 1.02 1.07 2.99
f1 (ppm)

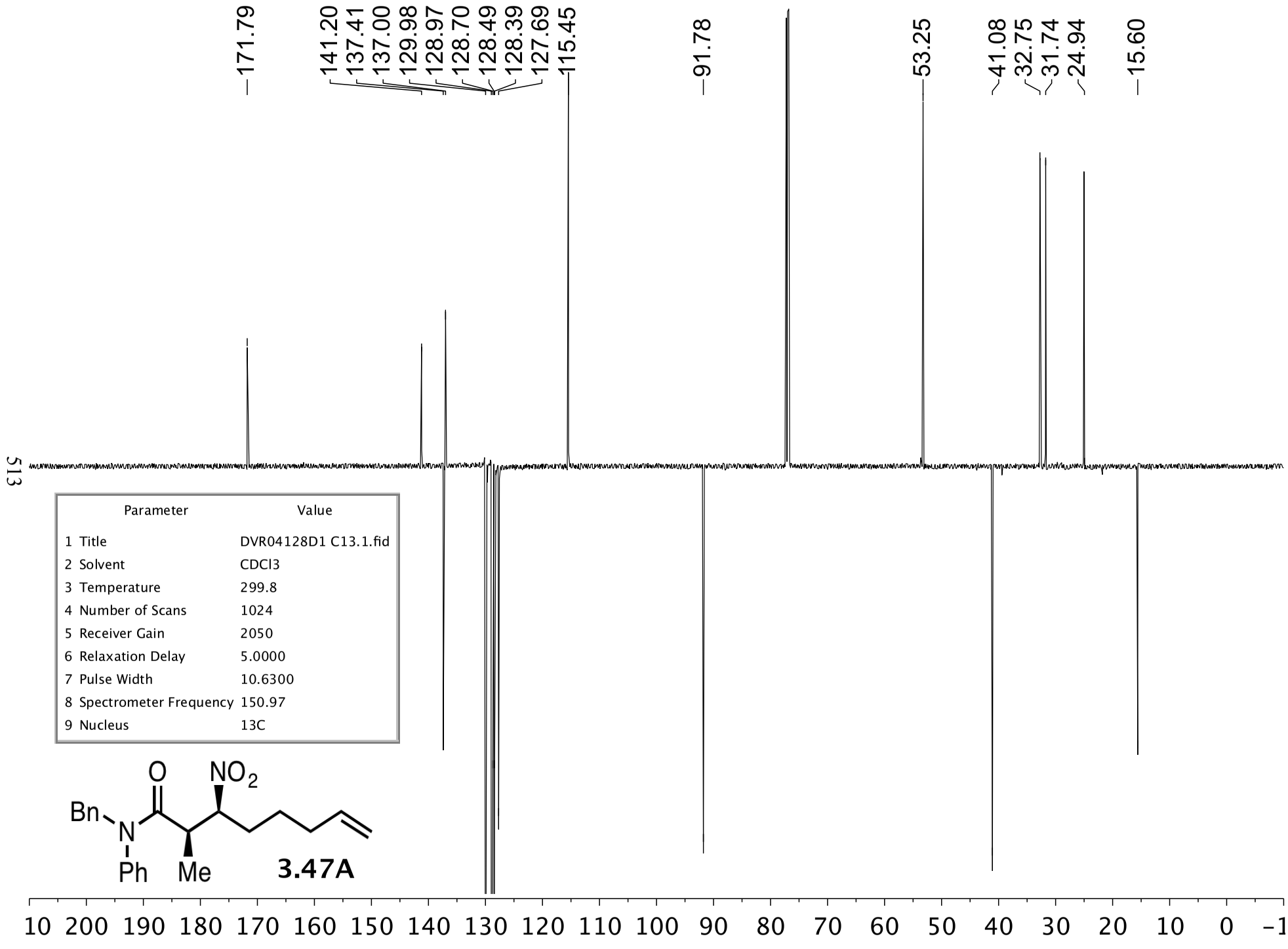
171.79
141.20
137.41
137.00
129.98
128.97
128.70
128.49
128.39
127.69
115.45
91.78
53.25
41.08
32.75
31.74
24.94
15.60
513
Parameter Value
1 Title DVR04128D1 C13.1.fid
2 Solvent CDCl3
3 Temperature 299.8
4 Number of Scans 1024
5 Receiver Gain 2050
6 Relaxation Delay 5.0000
7 Pulse Width 10.6300
8 Spectrometer Frequency 150.97
9 Nucleus 13C
O
NO2
Bn
N
Ph
Me
3.47A
10 200 190 180 170 160 150 140 130 120 110 100 90 80 70 60 50 40 30 20 10 0 -1

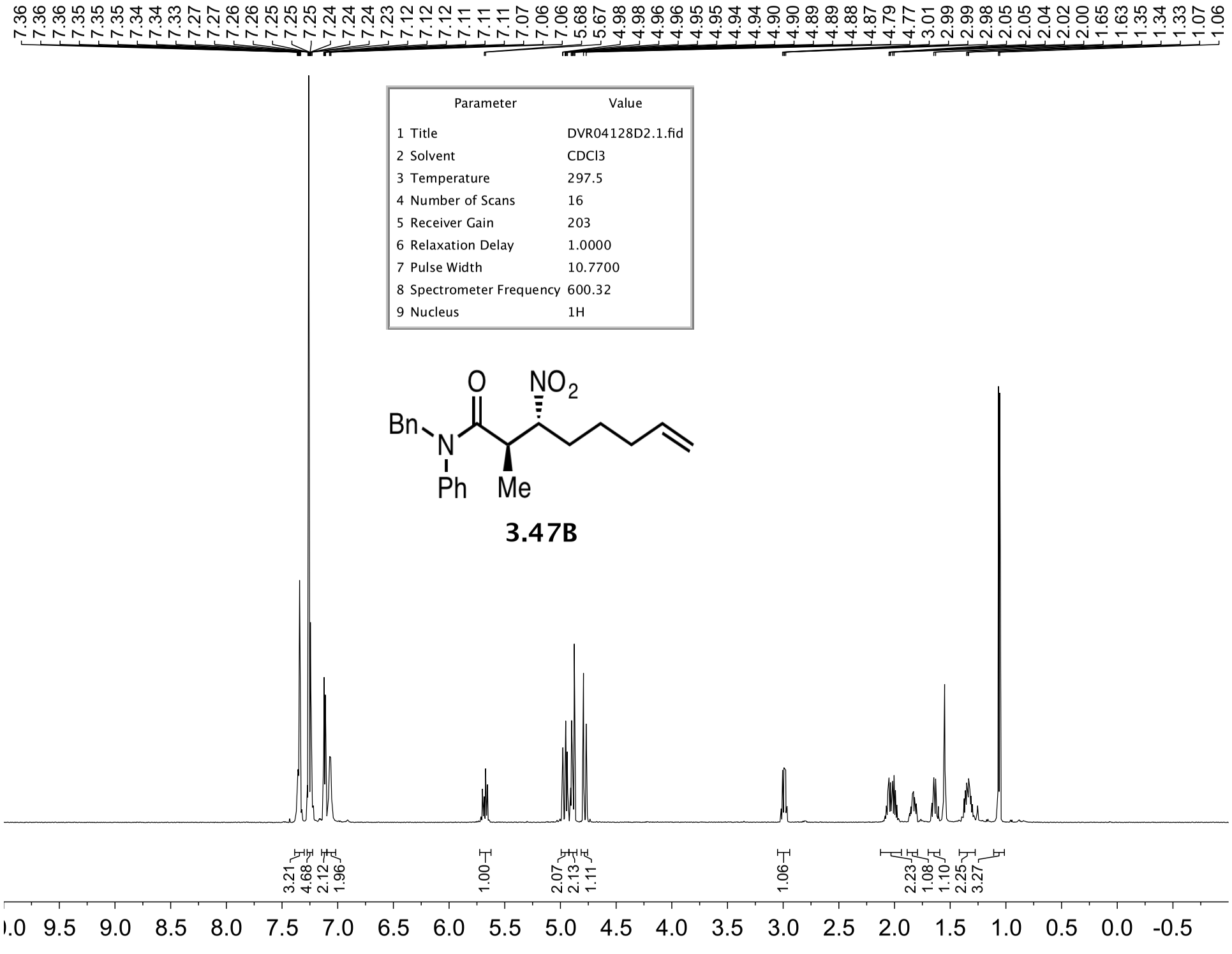
7.36 7.36 7.36 7.35 7.35 7.35 7.34 7.34 7.33 7.27 7.27 7.26 7.26 7.25 7.25 7.25 7.24 7.24 7.24 7.23 7.12 7.12 7.12 7.11 7.11 7.11 7.07 7.06 7.06 5.68 5.67 4.98 4.98 4.96 4.96 4.95 4.95 4.94 4.94 4.90 4.90 4.89 4.89 4.88 4.87 4.79 4.77 3.01 2.99 2.99 2.98 2.05 2.05 2.04 2.02 2.00 1.65 1.63 1.35 1.34 1.33 1.07 1.06
Parameter Value
1 Title DVR04128D2.1.fid
2 Solvent CDCl3
3 Temperature 297.5
4 Number of Scans 16
5 Receiver Gain 203
6 Relaxation Delay 1.0000
7 Pulse Width 10.7700
8 Spectrometer Frequency 600.32
9 Nucleus 1H
O
NO2
Bn
N
Ph
Me
3.47B
3.21 4.68 2.12 1.96 1.00 2.07 2.13 1.11 1.06 2.23 1.08 1.10 2.25 3.27
.0 9.5 9.0 8.5 8.0 7.5 7.0 6.5 6.0 5.5 5.0 4.5 4.0 3.5 3.0 2.5 2.0 1.5 1.0 0.5 0.0 -0.5

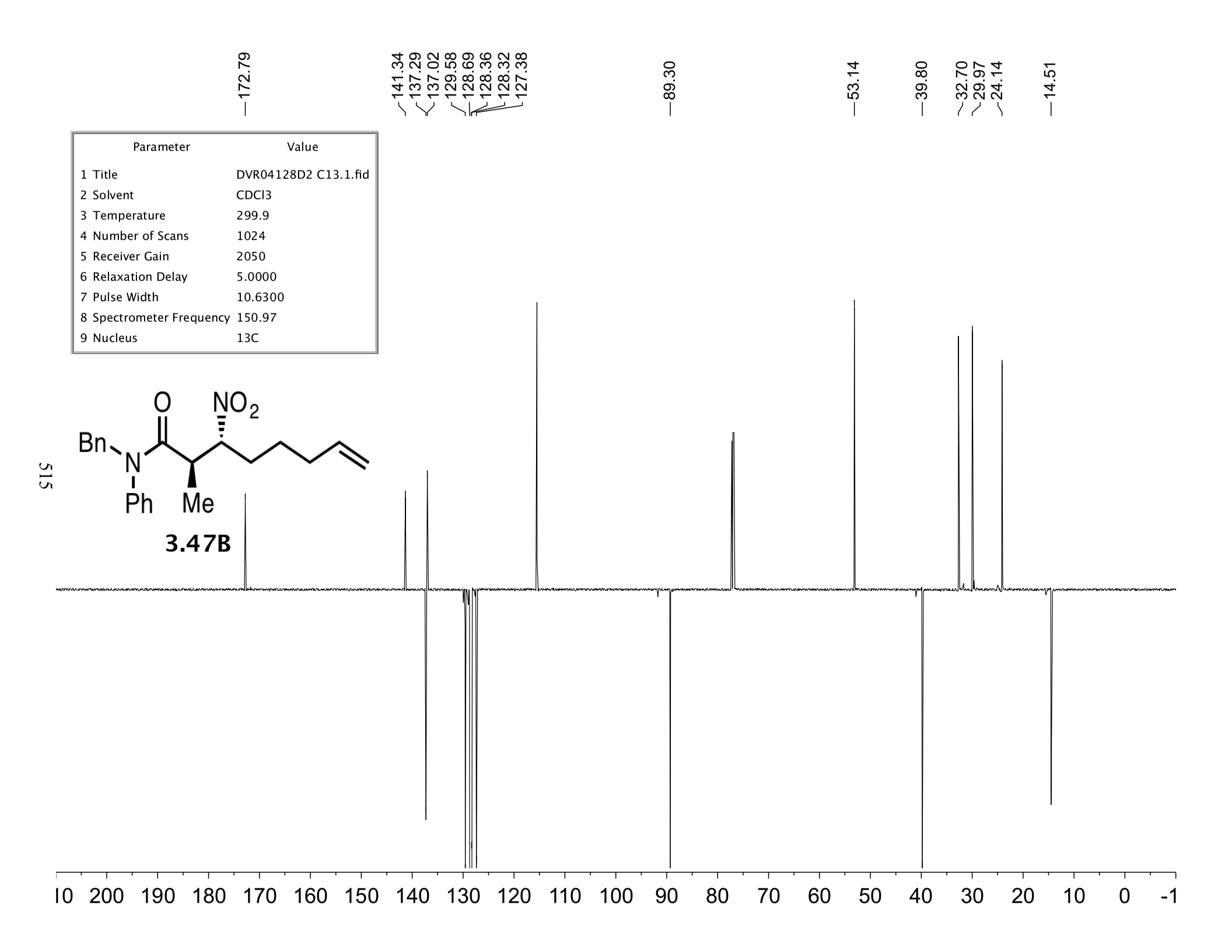
172.79
141.34
137.29
137.02
129.58
128.69
128.36
128.32
127.38
89.30
53.14
39.80
32.70
29.97
24.14
14.51
Parameter Value
1 Title DVR04128D2 C13.1.fid
2 Solvent CDCl3
3 Temperature 299.9
4 Number of Scans 1024
5 Receiver Gain 2050
6 Relaxation Delay 5.0000
7 Pulse Width 10.6300
8 Spectrometer Frequency 150.97
9 Nucleus 13C
O
NO2
Bn
N
Ph
Me
3.47B
515
10 200 190 180 170 160 150 140 130 120 110 100 90 80 70 60 50 40 30 20 10 0 -1

==== Shimadzu LCsolution Analysis Report ====

C:\LabSolutions\Data\DMM\DVR04128RAC D1_7182016_1401 PM_4.lcd

Acquired by	: LC User
Sample Name	: DVR04128RAC D1
Sample ID	: DVR04128RAC D1
Tray#	: 1
Vail #	: 1
Injection Volume	: 3 uL
Data File Name	: DVR04128RAC D1_7182016_1401 PM_4.lcd
Method File Name	: col3_2isoiPA_30min_1ML_254and210.lcm
Batch File Name	: DMM.lcb
Report File Name	: Default.lcr
Data Acquired	: 7/18/2016 3:52:45 PM
Data Processed	: 7/18/2016 4:22:47 PM

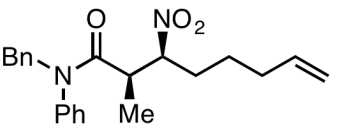

3.47A
racemic

<Chromatogram>

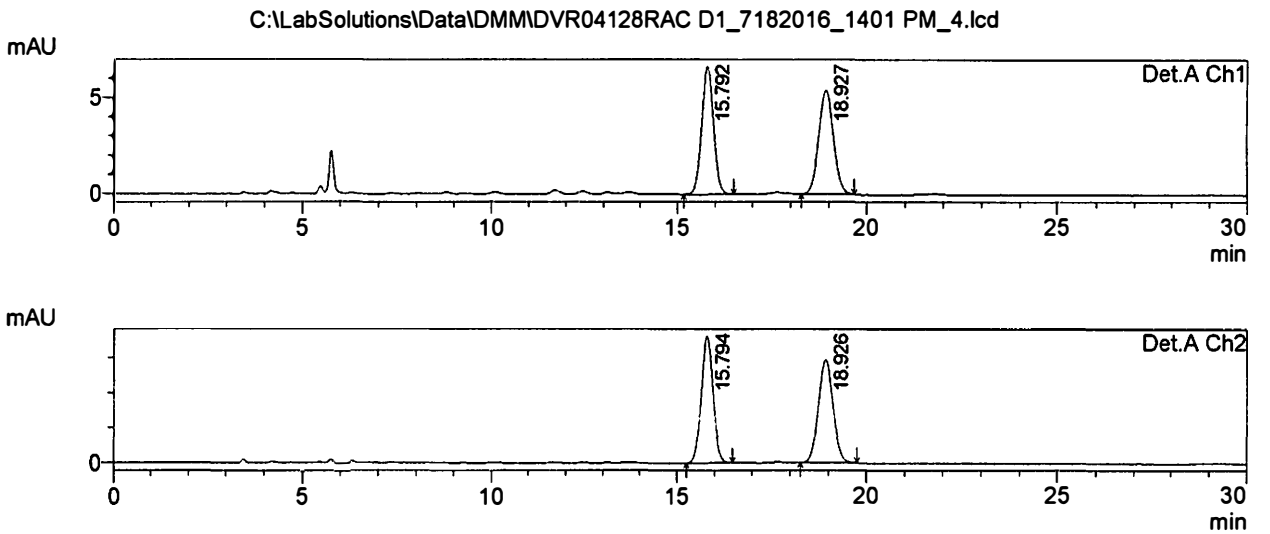

1 Det.A Ch1/254nm
2 Det.A Ch2/210nm

PeakTable

Detector A Ch1 254nm

Peak#	Ret. Time	Area	Height	Area %	Height %
1	15.792	145324	6641	50.250	55.124
2	18.927	143877	5406	49.750	44.876
Total		289200	12047	100.000	100.000

PeakTable

Detector A Ch2 210nm

Peak#	Ret. Time	Area	Height	Area %	Height %
1	15.794	3980250	182070	50.162	55.173
2	18.926	3954586	147927	49.838	44.827
Total		7934836	329997	100.000	100.000

==== Shimadzu LCsolution Analysis Report ====

C:\LabSolutions\Data\DMM\DVR04128 D1_7182016_1401 PM_8.lcd

Acquired by	: LC User
Sample Name	: DVR04128 D1
Sample ID	: DVR04128 D1
Tray#	: 1
Vail #	: 2
Injection Volume	: 3 uL
Data File Name	: DVR04128 D1–7182016_1401 PM_8.lcd
Method File Name	: col3_2isoiPA_30min_1ML_254and210.lcm
Batch File Name	: DMM.lcb
Report File Name	: Default.lcr
Data Acquired	: 7/18/2016 5:03:45 PM
Data Processed	: 7/18/2016 5:33:46 PM

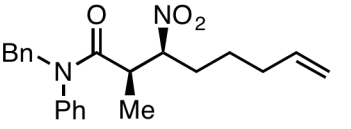

3.47A
90% ee

<Chromatogram>

C:\LabSolutions\Data\DMM\DVR04128 D1–7182016_1401 PM_8.lcd

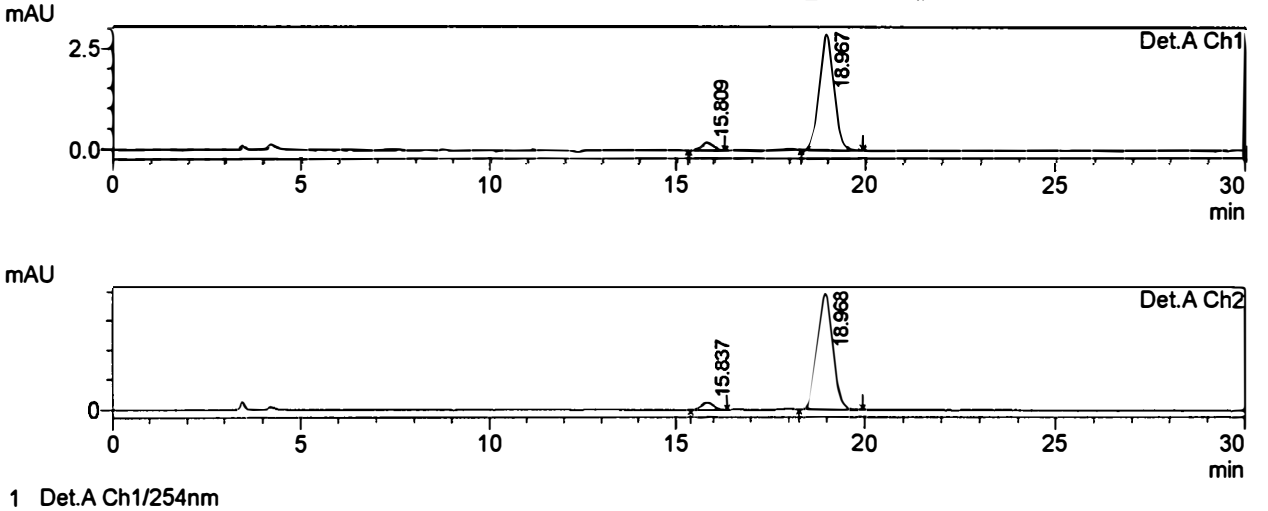

1 Det.A Ch1/254nm
2 Det.A Ch2/210nm

PeakTable

Detector A Ch1 254nm

Peak#	Ret. Time	Area	Height	Area %	Height %
1	15.809	4289	192	5.271	6.220
2	18.967	77076	2897	94.729	93.780
Total		81364	3089	100.000	100.000

PeakTable

Detector A Ch2 210nm

Peak#	Ret. Time	Area	Height	Area %	Height %
1	15.837	104022	4891	4.655	5.792
2	18.968	2130706	79554	95.345	94.208
Total		2234727	84445	100.000	100.000

==== Shimadzu LCsolution Analysis Report ====

C:\LabSolutions\Data\DMM\DVR04128RAC ANTI 2_7192016_1355 PM_2.lcd

Acquired by	: LC User
Sample Name	: DVR04128RAC ANTI 2
Sample ID	: DVR04128RAC ANTI 2
Tray#	: 1
Vail #	: 2
Injection Volume	: 1 uL
Data File Name	: DVR04128RAC ANTI 2_7192016_1355 PM_2.lcd
Method File Name	: col2_0.8isoiPA_45min_1ML_220and210.lcm
Batch File Name	: DMM.lcb
Report File Name	: Default.lcr
Data Acquired	: 7/19/2016 2:25:58 PM
Data Processed	: 7/19/2016 3:11:00 PM

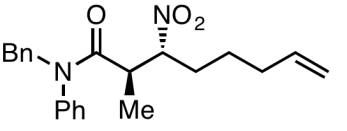

3.47B
racemic

<Chromatogram>

C:\LabSolutions\Data\DMM\DVR04128RAC ANTI 2_7192016_1355 PM_2.lcd

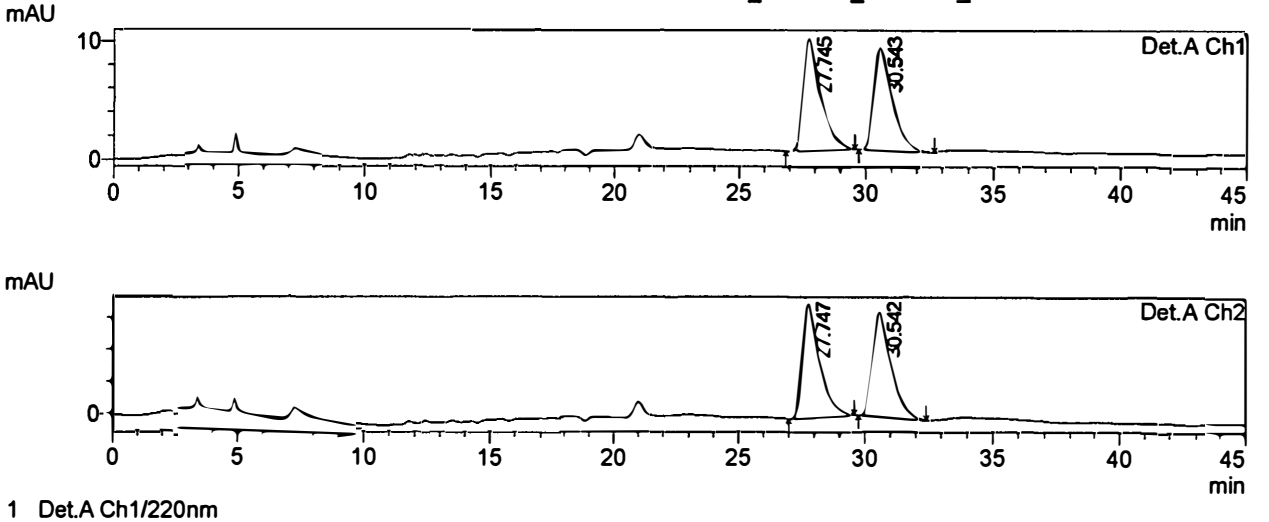

1 Det.A Ch1/220nm
2 Det.A Ch2/210nm

PeakTable

Detector A Ch1 220nm

Peak#	Ret. Time	Area	Height	Area %	Height %
1	27.745	457217	9571	51.168	52.288
2	30.543	436342	8733	48.832	47.712
Total		893559	18304	100.000	100.000

PeakTable

Detector A Ch2 210nm

Peak#	Ret. Time	Area	Height	Area %	Height %
1	27.747	851750	17849	51.218	52.190
2	30.542	811240	16351	48.782	47.810
Total		1662990	34200	100.000	100.000

==== Shimadzu LCsolution Analysis Report ====

C:\LabSolutions\Data\DMM\DVR04128 ANTI D2_7192016_1355 PM_6.lcd

Acquired by	: LC User
Sample Name	: DVR04128 ANTI D2
Sample ID	: DVR04128 ANTI D2
Tray#	: 1
Vail #	: 3
Injection Volume	: 1 uL
Data File Name	: DVR04128 ANTI D2_7192016_1355 PM_6.lcd
Method File Name	: col2_0.8isoiPA_45min_1ML_220and210.lcm
Batch File Name	: DMM.lcb
Report File Name	: Default.lcr
Data Acquired	: 7/19/2016 3:51:55 PM
Data Processed	: 7/19/2016 4:36:58 PM

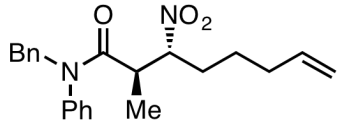

3.47B
80% ee

<Chromatogram>

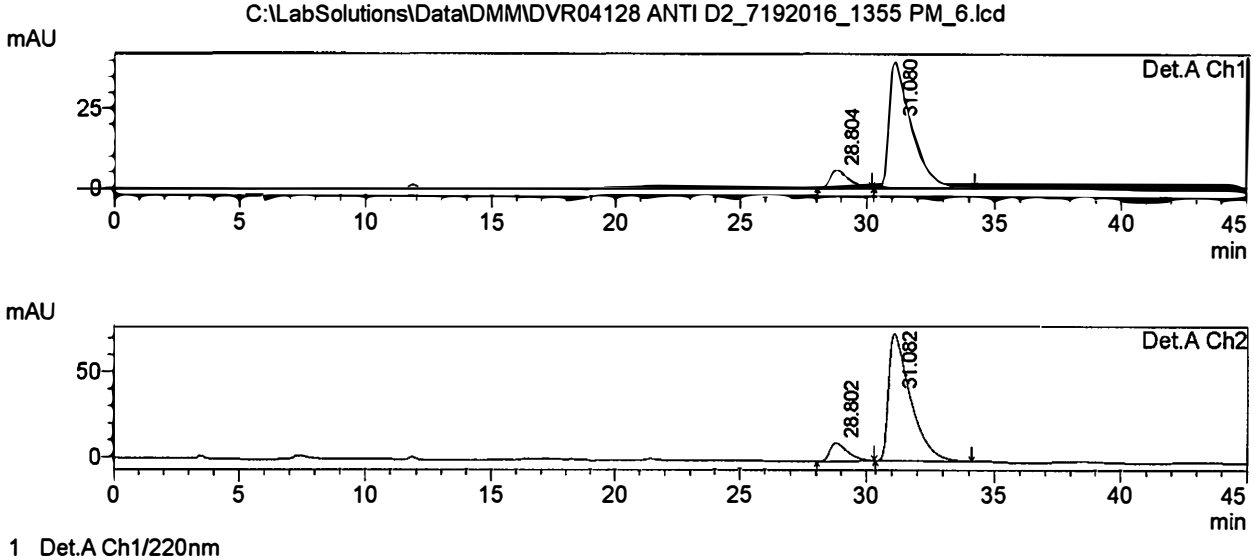

1 Det.A Ch1/220nm
2 Det.A Ch2/210nm

PeakTable

Detector A Ch1 220nm

Peak#	Ret. Time	Area	Height	Area %	Height %
1	28.804	272983	5675	10.343	12.534
2	31.080	2366354	39606	89.657	87.466
Total		2639337	45281	100.000	100.000

PeakTable

Detector A Ch2 210nm

Peak#	Ret. Time	Area	Height	Area %	Height %
1	28.802	521687	10686	10.578	12.586
2	31.082	4409944	74216	89.422	87.414
Total		4931631	84902	100.000	100.000

Parameter	Value
1 Title	DVR04192CRD.1.fid
2 Solvent	CDCl3
3 Temperature	298.1
4 Number of Scans	16
5 Receiver Gain	9
6 Relaxation Delay	1.0000
7 Pulse Width	15.0000
8 Spectrometer Frequency	400.13
9 Nucleus	1H

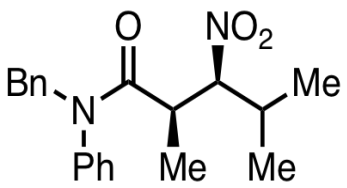

3.49A

Crude

93:07

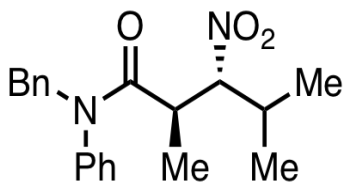

3.49B

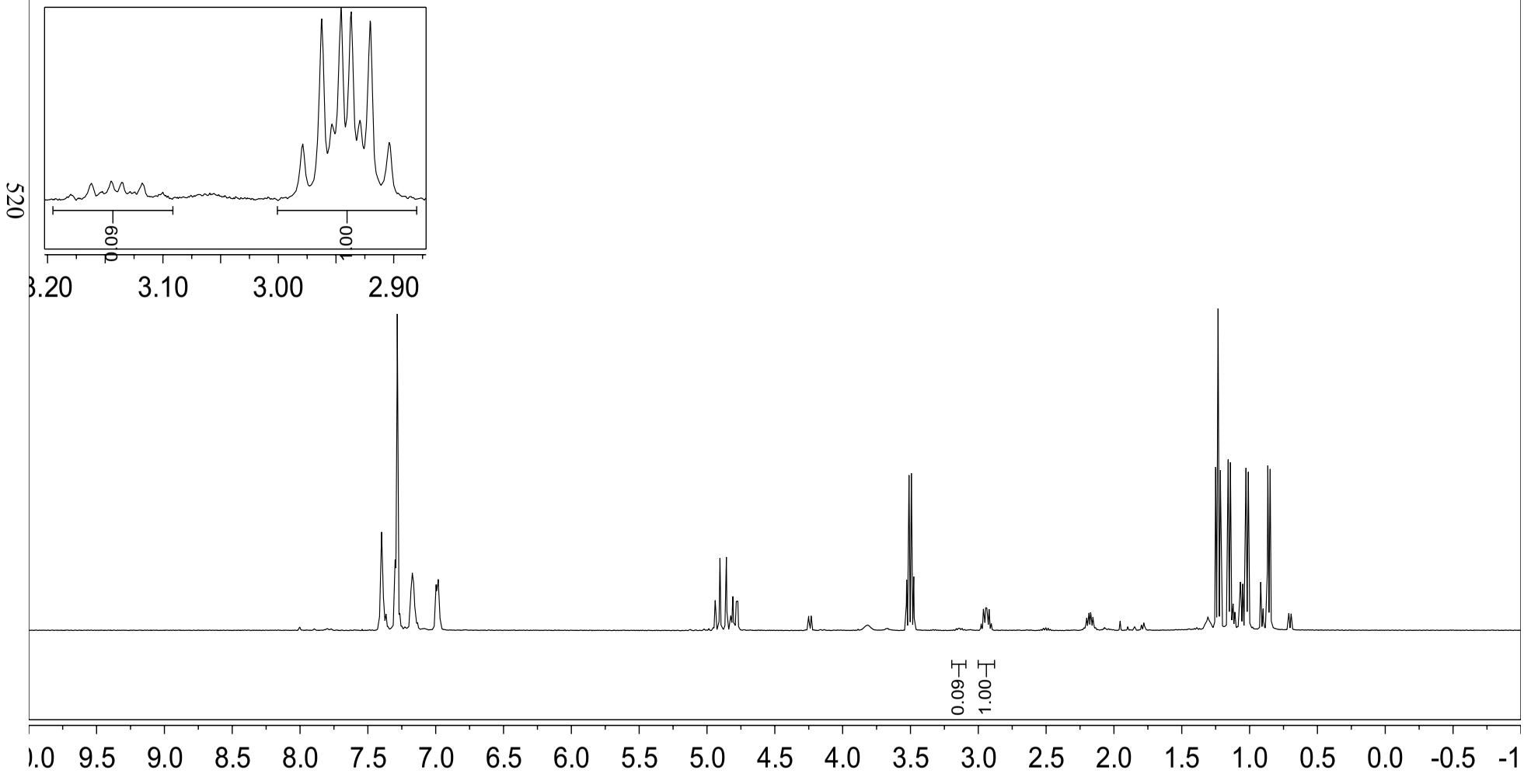

Parameter	Value
1 Title	DVR04192D1.1.fid
2 Solvent	CDCl3
3 Temperature	298.0
4 Number of Scans	16
5 Receiver Gain	181
6 Relaxation Delay	1.0000
7 Pulse Width	10.7700
8 Spectrometer Frequency	600.32
9 Nucleus	1H

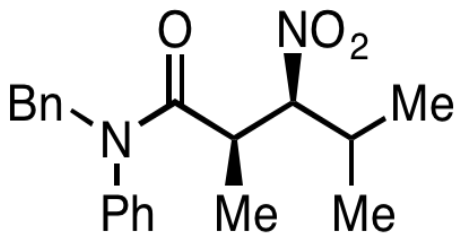

3.49A

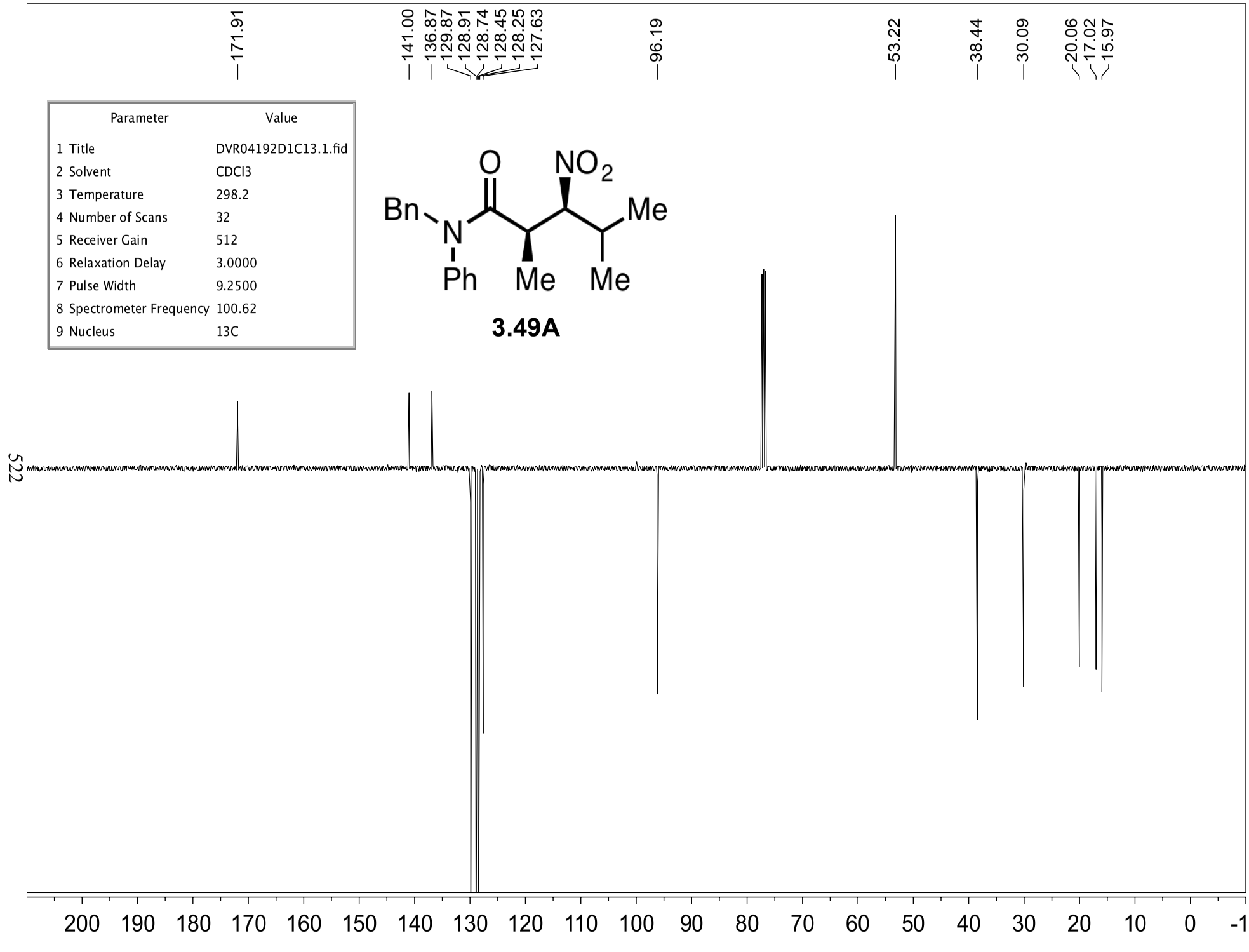
171.91
141.00
136.87
129.87
128.91
128.74
128.45
128.25
127.63
96.19
53.22
38.44
30.09
20.06
17.02
15.97
Parameter
Value
1 Title
DVR04192D1C13.1.fid
2 Solvent
CDCl3
3 Temperature
298.2
4 Number of Scans
32
5 Receiver Gain
512
6 Relaxation Delay
3.0000
7 Pulse Width
9.2500
8 Spectrometer Frequency
100.62
9 Nucleus
13C
O
NO2
Bn
N
Me
Ph
Me
Me
3.49A
522
200
190
180
170
160
150
140
130
120
110
100
90
80
70
60
50
40
30
20
10
0
-1

Parameter	Value
1 Title	DVR04192D2.1.fid
2 Solvent	CDCl3
3 Temperature	298.2
4 Number of Scans	16
5 Receiver Gain	6
6 Relaxation Delay	1.0000
7 Pulse Width	15.0000
8 Spectrometer Frequency	400.13
9 Nucleus	1H

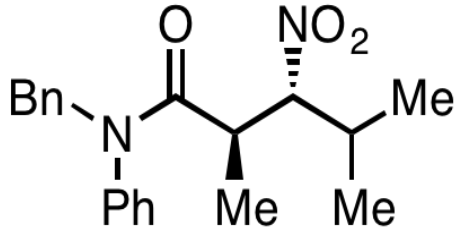

3.49B

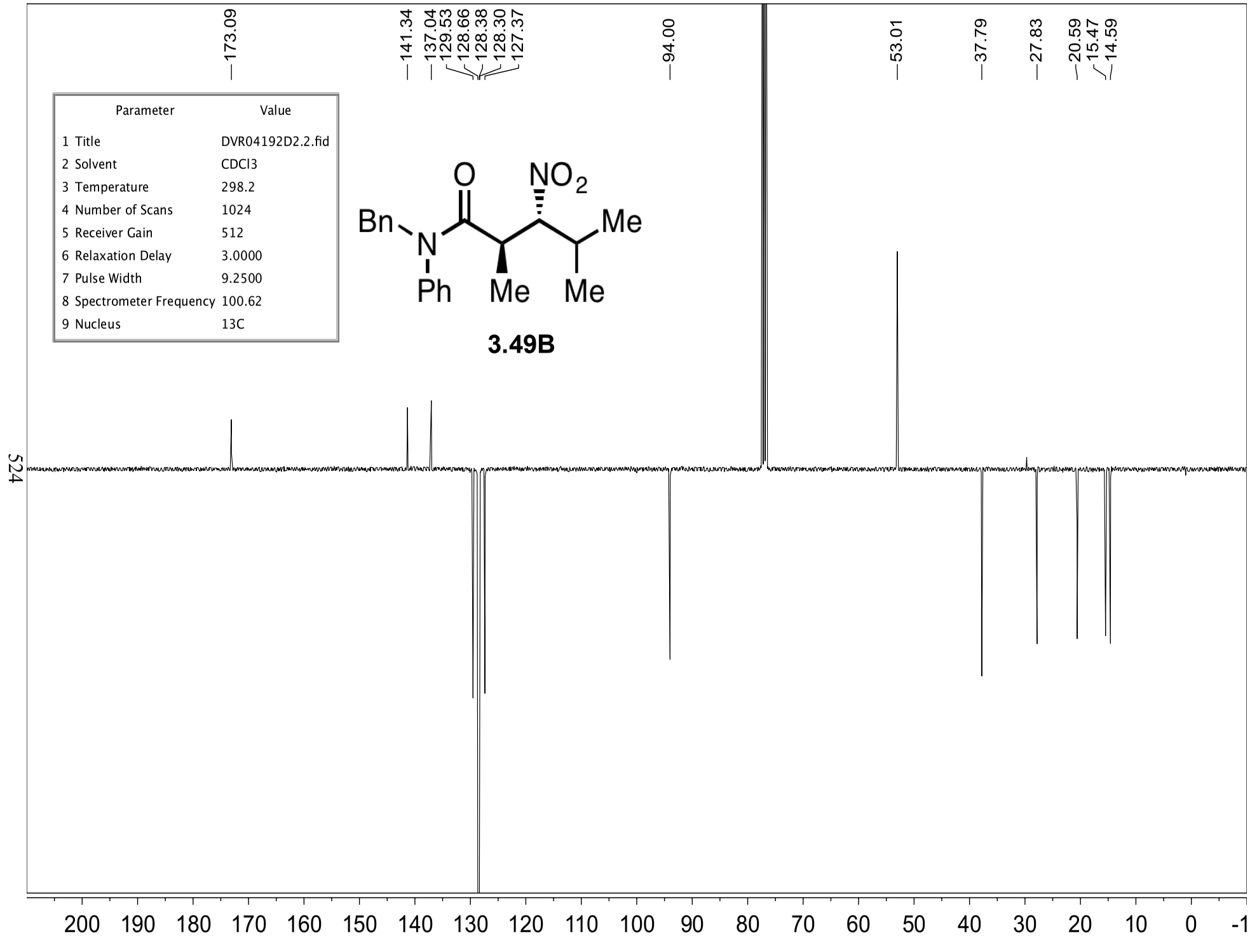
173.09
141.34
137.04
129.53
128.66
128.38
128.30
127.37
94.00
53.01
37.79
27.83
20.59
15.47
14.59
Parameter Value
1 Title DVR04192D2.2.fid
2 Solvent CDCl3
3 Temperature 298.2
4 Number of Scans 1024
5 Receiver Gain 512
6 Relaxation Delay 3.0000
7 Pulse Width 9.2500
8 Spectrometer Frequency 100.62
9 Nucleus 13C
O
NO2
Bn
N
Ph
Me
Me
Me
3.49B
524
200 190 180 170 160 150 140 130 120 110 100 90 80 70 60 50 40 30 20 10 0 -1

==== Shimadzu LCsolution Analysis Report ====

C:\LabSolutions\Data\DMM\DVR04196 RAC SYN1_9262016_954 AM_9.lcd

Acquired by	: LC User
Sample Name	: DVR04196 RAC SYN1
Sample ID	: DVR04196 RAC SYN1
Tray#	: 1
Vail #	: 1
Injection Volume	: 2 uL
Data File Name	: DVR04196 RAC SYN1_9262016_954 AM_9.lcd
Method File Name	: col1_1isoiPA_30min_1ML_220and210.lcm
Batch File Name	: DMM.lcb
Report File Name	: Default.lcr
Data Acquired	: 9/26/2016 2:54:01 PM
Data Processed	: 9/26/2016 3:24:02 PM

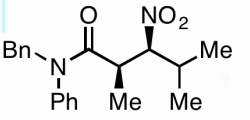

3.49A
racemic
(±) SYN

<Chromatogram>

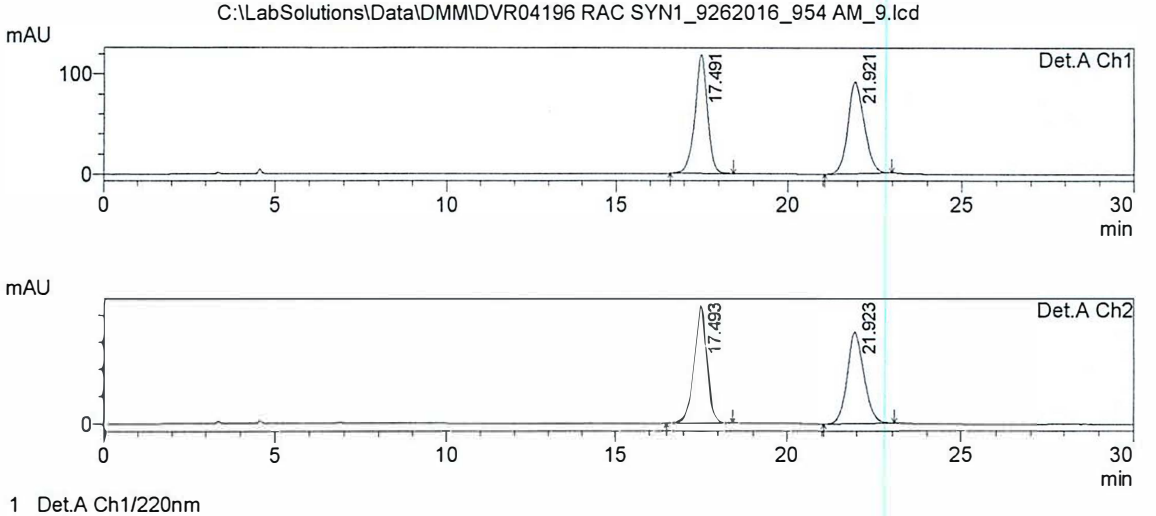

1 Det.A Ch1/220nm
2 Det.A Ch2/210nm

PeakTable

Detector A Ch1 220nm

Peak#	Ret. Time	Area	Height	Area %	Height %
1	17.491	2997080	118652	50.031	56.408
2	21.921	2993359	91694	49.969	43.592
Total		5990440	210346	100.000	100.000

PeakTable

Detector A Ch2 210nm

Peak#	Ret. Time	Area	Height	Area %	Height %
1	17.493	5481415	216292	50.105	56.428
2	21.923	5458508	167013	49.895	43.572
Total		10939923	383305	100.000	100.000

==== Shimadzu LCsolution Analysis Report ====

C:\LabSolutions\Data\DMM\DVR04196 SYN1_9262016_954 AM_1.lcd

Acquired by	: LC User
Sample Name	: DVR04196 SYN1
Sample ID	: DVR04196 SYN1
Tray#	: 1
Vail #	: 2
Injection Volume	: 2 uL
Data File Name	: DVR04196 SYN1_9262016_954 AM_1.lcd
Method File Name	: col1_1isoiPA_30min_1ML_220and210.lcm
Batch File Name	: DMM.lcb
Report File Name	: Default.lcr
Data Acquired	: 9/26/2016 4:04:56 PM
Data Processed	: 9/26/2016 4:34:56 PM

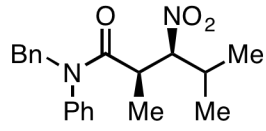

3.49A
94% ee

<Chromatogram>

C:\LabSolutions\Data\DMM\DVR04196 SYN1_9262016_954 AM_1.lcd

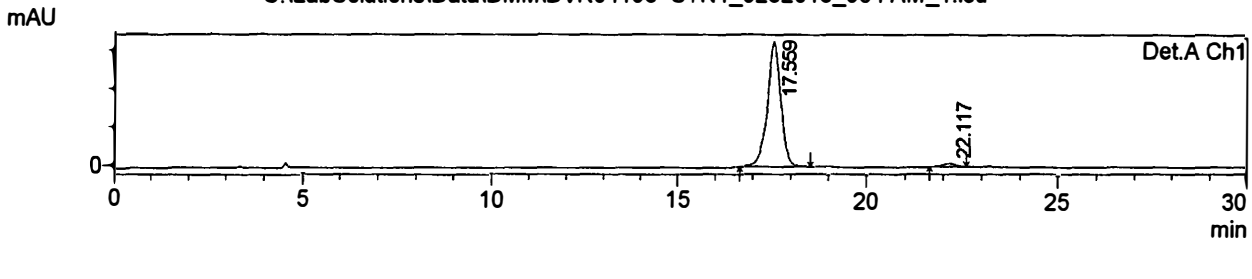

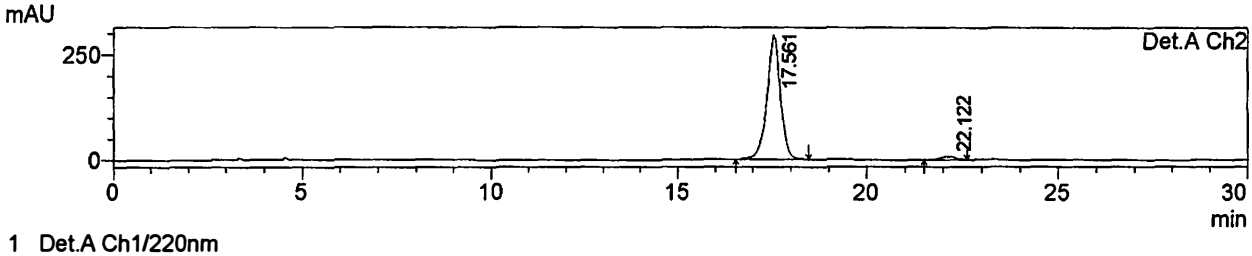

1 Det.A Ch1/220nm
2 Det.A Ch2/210nm

PeakTable

Detector A Ch1 220nm

Peak#	Ret. Time	Area	Height	Area %	Height %
1	17.559	4033823	162734	97.235	97.433
2	22.117	114706	4288	2.765	2.567
Total		4148529	167022	100.000	100.000

PeakTable

Detector A Ch2 210nm

Peak#	Ret. Time	Area	Height	Area %	Height %
1	17.561	7372880	296393	97.038	97.348
2	22.122	225026	8074	2.962	2.652
Total		7597906	304467	100.000	100.000

==== Shimadzu LCsolution Analysis Report ====

C:\LabSolutions\Data\DMM\DVR04192 RAC ANTI _9252016_1431 PM_1.lcd

Acquired by	: LC User
Sample Name	: DVR04192 RAC ANTI
Sample ID	: DVR04192 RAC ANTI
Tray#	: 1
Vail #	: 1
Injection Volume	: 2 uL
Data File Name	: DVR04192 RAC ANTI _9252016_1431 PM_1.lcd
Method File Name	: col1_5isoiPA_30min_1ML_220and210.lcm
Batch File Name	: DMM.lcb
Report File Name	: Default.lcr
Data Acquired	: 9/25/2016 3:04:06 PM
Data Processed	: 9/25/2016 3:34:09 PM

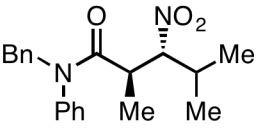

3.49B
racemic

<Chromatogram>

C:\LabSolutions\Data\DMM\DVR04192 RAC ANTI _9252016_1431 PM_1.lcd

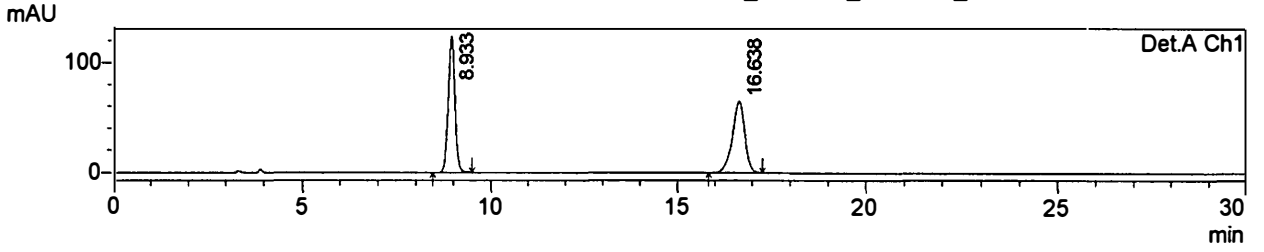

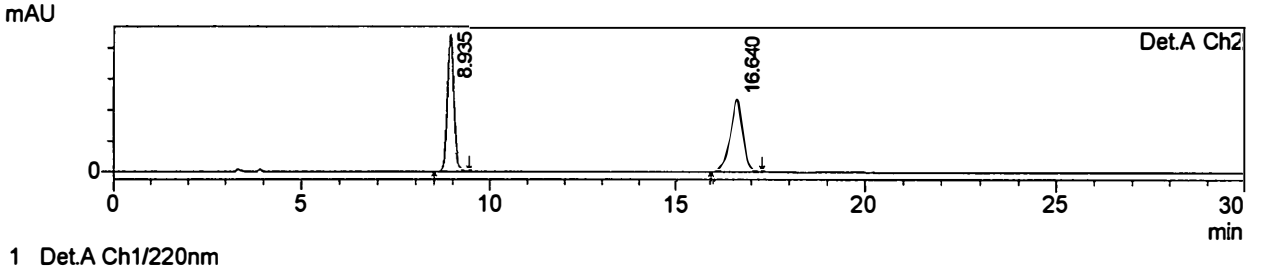

1 Det.A Ch1/220nm
2 Det.A Ch2/210nm

PeakTable

Detector A Ch1 220nm

Peak#	Ret. Time	Area	Height	Area %	Height %
1	8.933	1508239	123366	50.180	65.477
2	16.638	1497399	65044	49.820	34.523
Total		3005638	188411	100.000	100.000

PeakTable

Detector A Ch2 210nm

Peak#	Ret. Time	Area	Height	Area %	Height %
1	8.935	2705991	221558	50.166	65.484
2	16.640	2688042	116781	49.834	34.516
Total		5394033	338339	100.000	100.000

==== Shimadzu LCsolution Analysis Report ====

C:\LabSolutions\Data\DMM\DVR04192 ANTI _9252016_1431 PM_5.lcd

Acquired by	: LC User
Sample Name	: DVR04192 ANTI
Sample ID	: DVR04192 ANTI
Tray#	: 1
Vail #	: 2
Injection Volume	: 2 uL
Data File Name	: DVR04192 ANTI _9252016_1431 PM_5.lcd
Method File Name	: col1_5isoiPA_30min_1ML_220and210.lcm
Batch File Name	: DMM.lcb
Report File Name	: Default.lcr
Data Acquired	: 9/25/2016 4:15:02 PM
Data Processed	: 9/25/2016 4:45:04 PM

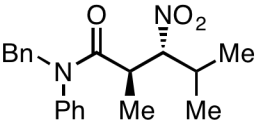

3.49B
76% ee

<Chromatogram>

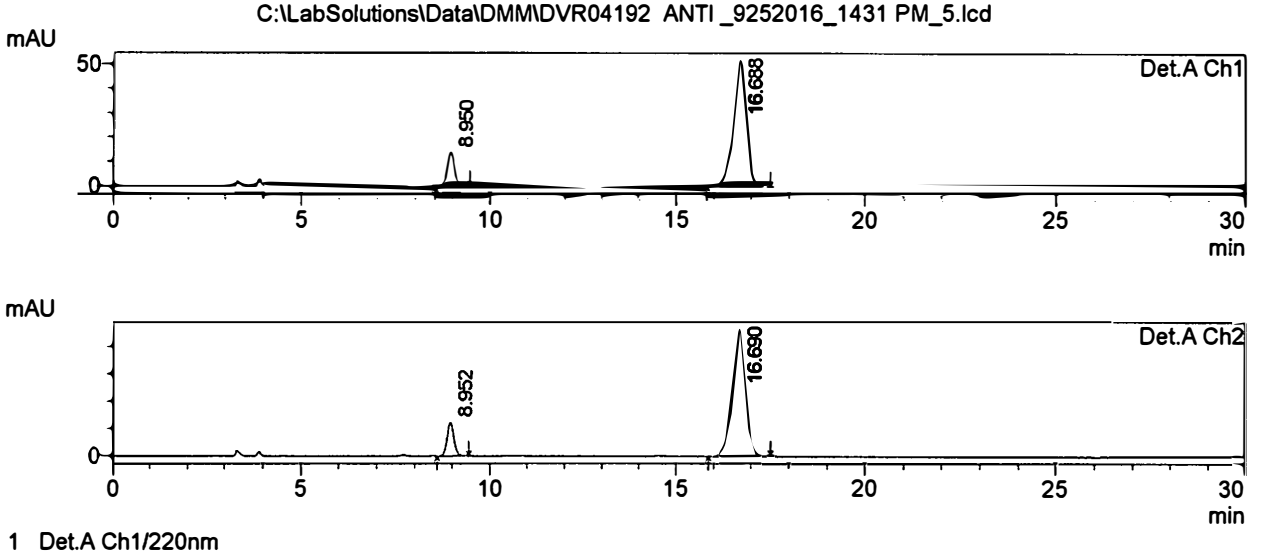

1 Det.A Ch1/220nm
2 Det.A Ch2/210nm

PeakTable

Detector A Ch1 220nm

Peak#	Ret. Time	Area	Height	Area %	Height %
1	8.950	167797	13712	12.237	20.879
2	16.688	1203456	51963	87.763	79.121
Total		1371253	65676	100.000	100.000

PeakTable

Detector A Ch2 210nm

Peak#	Ret. Time	Area	Height	Area %	Height %
1	8.952	302717	24702	12.268	20.922
2	16.690	2164882	93365	87.732	79.078
Total		2467599	118067	100.000	100.000

Parameter	Value
1 Title	DVR04140CRD.1.fid
2 Solvent	CDCl3
3 Temperature	298.1
4 Number of Scans	16
5 Receiver Gain	144
6 Relaxation Delay	1.0000
7 Pulse Width	10.7700
8 Spectrometer Frequency	600.32
9 Nucleus	1H

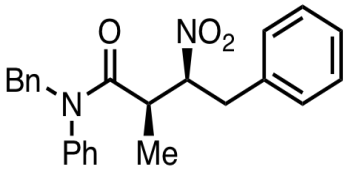

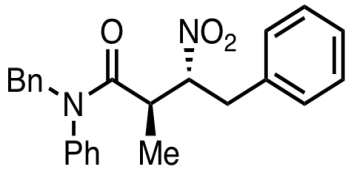

Crude

3.50A **88:12** **3.50B**

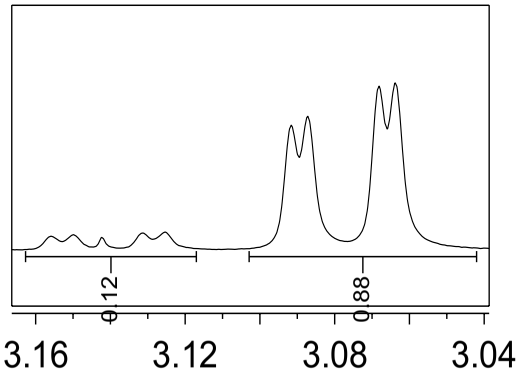

529

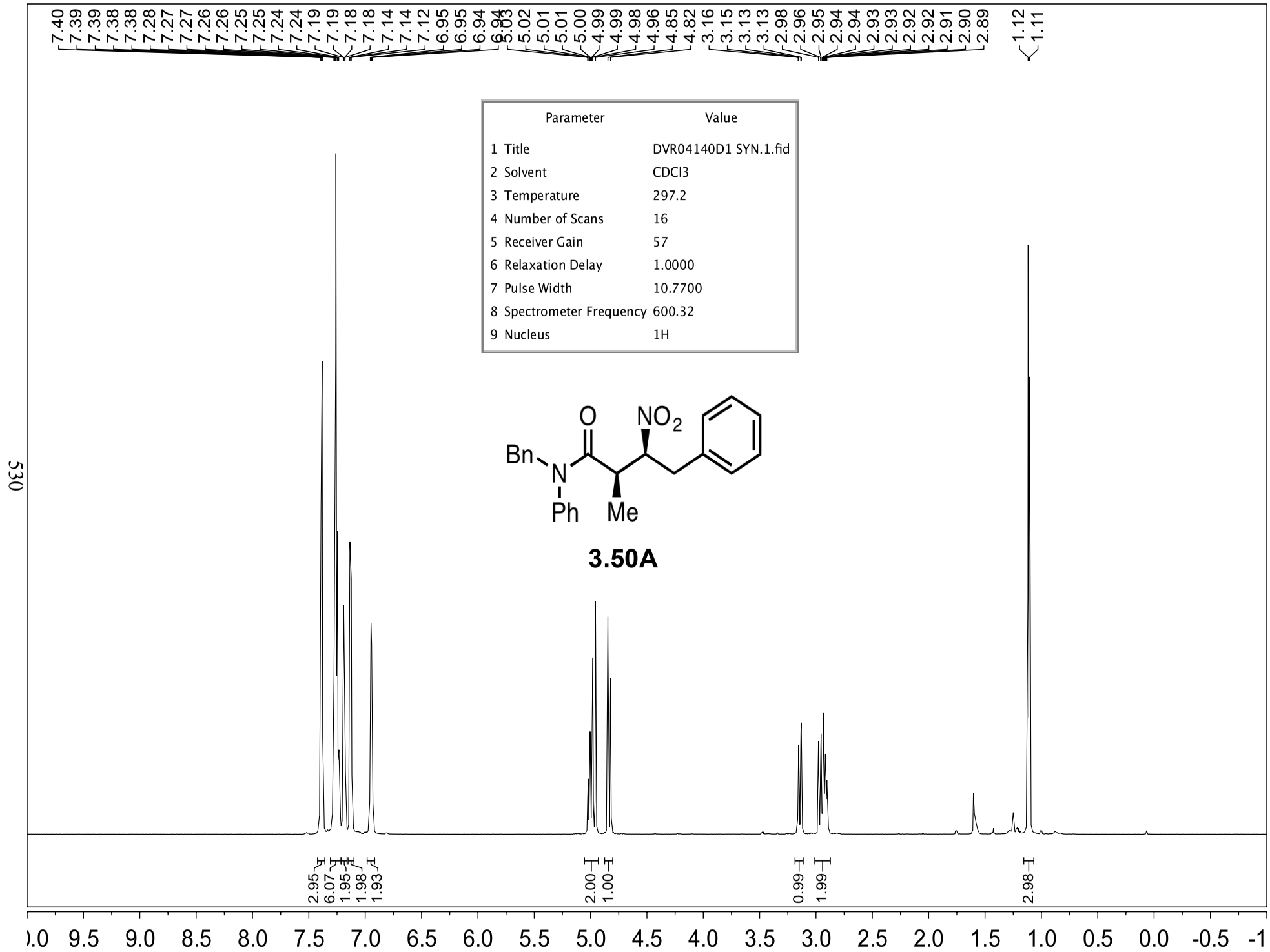
7.40 7.39 7.39 7.38 7.38 7.28 7.27 7.27 7.26 7.26 7.25 7.25 7.24 7.24 7.19 7.19 7.18 7.18 7.14 7.14 7.12 6.95 6.95 6.94 6.93 5.02 5.01 5.01 5.00 4.99 4.99 4.98 4.96 4.85 4.82 3.16 3.15 3.13 3.13 2.98 2.96 2.95 2.94 2.94 2.93 2.93 2.92 2.92 2.91 2.90 2.89 1.12 1.11
Parameter Value
1 Title DVR04140D1 SYN.1.fid
2 Solvent CDCl3
3 Temperature 297.2
4 Number of Scans 16
5 Receiver Gain 57
6 Relaxation Delay 1.0000
7 Pulse Width 10.7700
8 Spectrometer Frequency 600.32
9 Nucleus 1H
O
NO2
Bn
N
Ph
Me
3.50A
530
2.95 6.07 1.95 1.98 1.93 2.00 1.00 0.99 1.99 2.98
.0 9.5 9.0 8.5 8.0 7.5 7.0 6.5 6.0 5.5 5.0 4.5 4.0 3.5 3.0 2.5 2.0 1.5 1.0 0.5 0.0 -0.5 -1

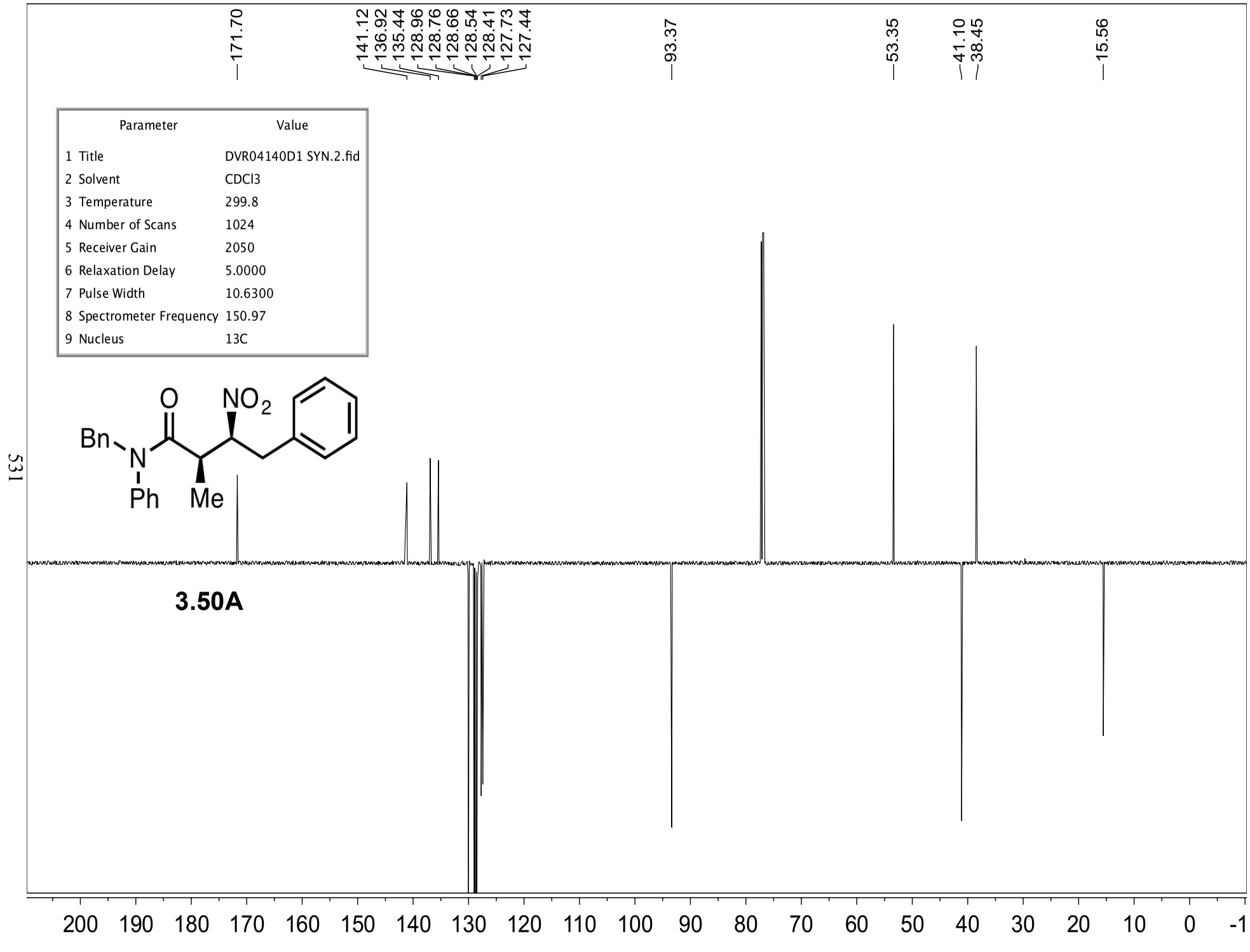
171.70
141.12
136.92
135.44
128.96
128.76
128.66
128.54
128.41
127.73
127.44
93.37
53.35
41.10
38.45
15.56
Parameter Value
1 Title DVR04140D1 SYN.2.fid
2 Solvent CDCl3
3 Temperature 299.8
4 Number of Scans 1024
5 Receiver Gain 2050
6 Relaxation Delay 5.0000
7 Pulse Width 10.6300
8 Spectrometer Frequency 150.97
9 Nucleus 13C
O
NO2
Bn
N
Ph
Me
3.50A
531
200 190 180 170 160 150 140 130 120 110 100 90 80 70 60 50 40 30 20 10 0 -1

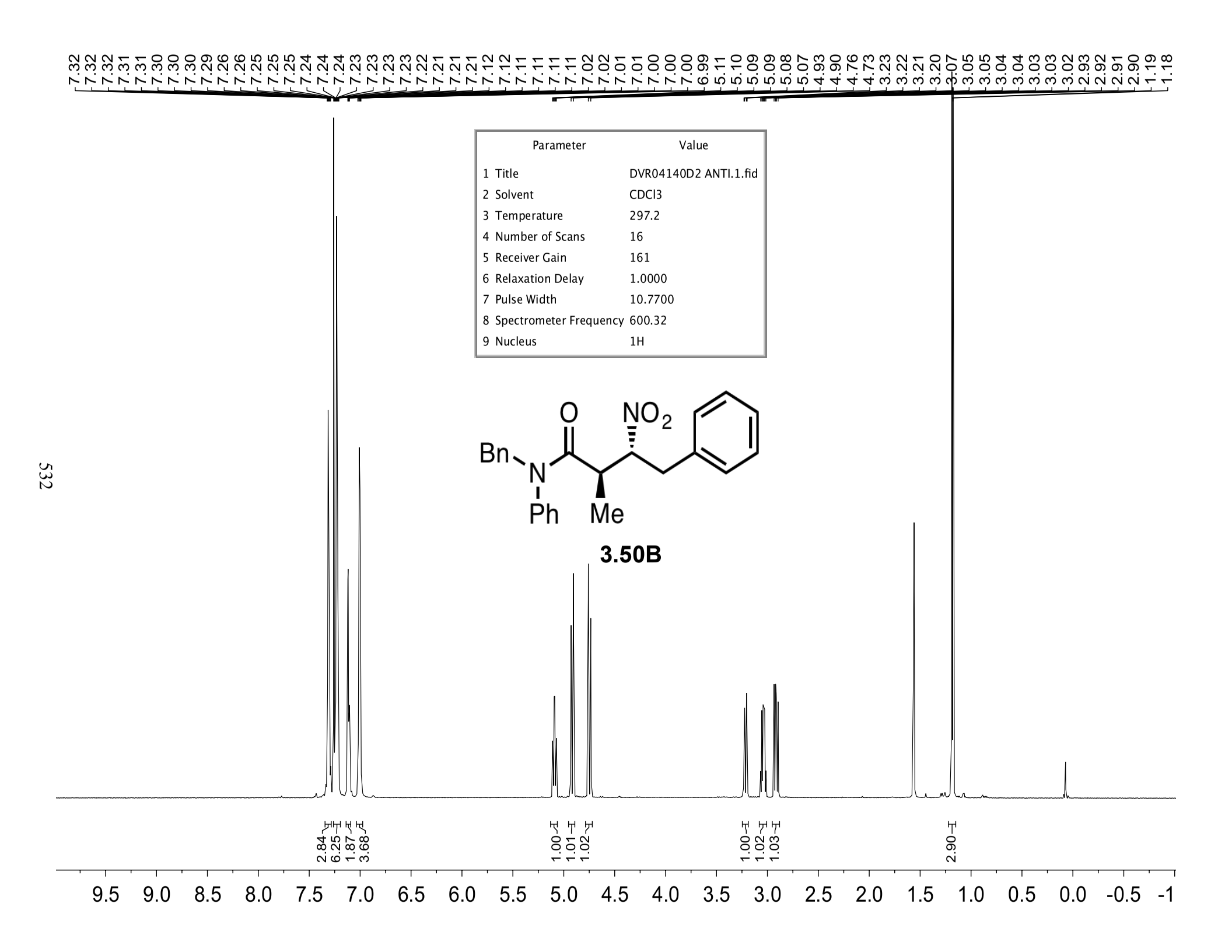
7.32 7.32 7.32 7.31 7.31 7.30 7.30 7.30 7.29 7.26 7.26 7.25 7.25 7.25 7.24 7.24 7.24 7.23 7.23 7.23 7.23 7.22 7.21 7.21 7.21 7.12 7.12 7.11 7.11 7.11 7.11 7.02 7.02 7.01 7.01 7.00 7.00 7.00 6.99 5.11 5.10 5.09 5.09 5.08 5.07 4.93 4.90 4.76 4.73 3.23 3.22 3.21 3.20 3.07 3.05 3.05 3.04 3.04 3.03 3.03 3.02 2.93 2.92 2.91 2.90 1.19 1.18
Parameter Value
1 Title DVR04140D2 ANTI.1.fid
2 Solvent CDCl3
3 Temperature 297.2
4 Number of Scans 16
5 Receiver Gain 161
6 Relaxation Delay 1.0000
7 Pulse Width 10.7700
8 Spectrometer Frequency 600.32
9 Nucleus 1H
O
NO2
Bn
N
Ph
Me
3.50B
532
2.84 6.25 1.87 3.68
1.00 1.01 1.02
1.00 1.02 1.03
2.90
9.5 9.0 8.5 8.0 7.5 7.0 6.5 6.0 5.5 5.0 4.5 4.0 3.5 3.0 2.5 2.0 1.5 1.0 0.5 0.0 -0.5 -1

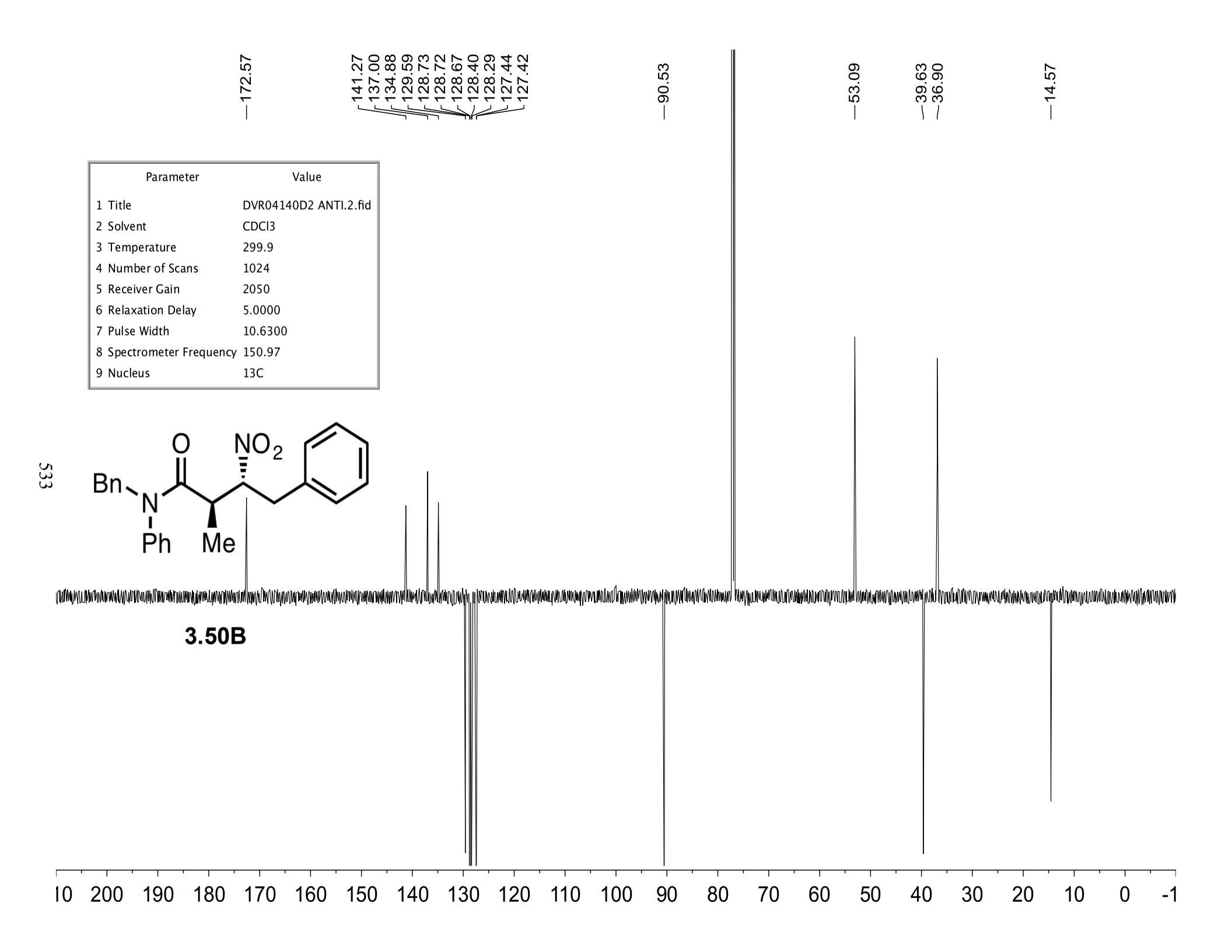
172.57
141.27
137.00
134.88
129.59
128.73
128.72
128.67
128.40
128.29
127.44
127.42
90.53
53.09
39.63
36.90
14.57
Parameter
Value
1 Title
DVR04140D2 ANTI.2.fid
2 Solvent
CDCl3
3 Temperature
299.9
4 Number of Scans
1024
5 Receiver Gain
2050
6 Relaxation Delay
5.0000
7 Pulse Width
10.6300
8 Spectrometer Frequency
150.97
9 Nucleus
13C
O
NO2
Bn
N
Ph
Me
533
3.50B
10 200 190 180 170 160 150 140 130 120 110 100 90 80 70 60 50 40 30 20 10 0 -1

==== Shimadzu LCsolution Analysis Report ====

C:\LabSolutions\Data\DMM\DVR04140 RAC SYN _7202016_1046 AM_2.lcd

Acquired by	: LC User
Sample Name	: DVR04140 RAC SYN
Sample ID	: DVR04140 RAC SYN
Tray#	: 1
Vail #	: 4
Injection Volume	: 3 uL
Data File Name	: DVR04140 RAC SYN _7202016_1046 AM_2.lcd
Method File Name	: col1_5isoiPA_15min_1ML_220and210.lcm
Batch File Name	: DMM.lcb
Report File Name	: Default.lcr
Data Acquired	: 7/20/2016 11:02:13 AM
Data Processed	: 7/20/2016 11:17:14 AM

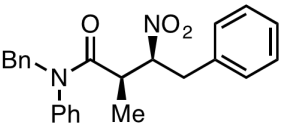

3.50A
racemic

<Chromatogram>

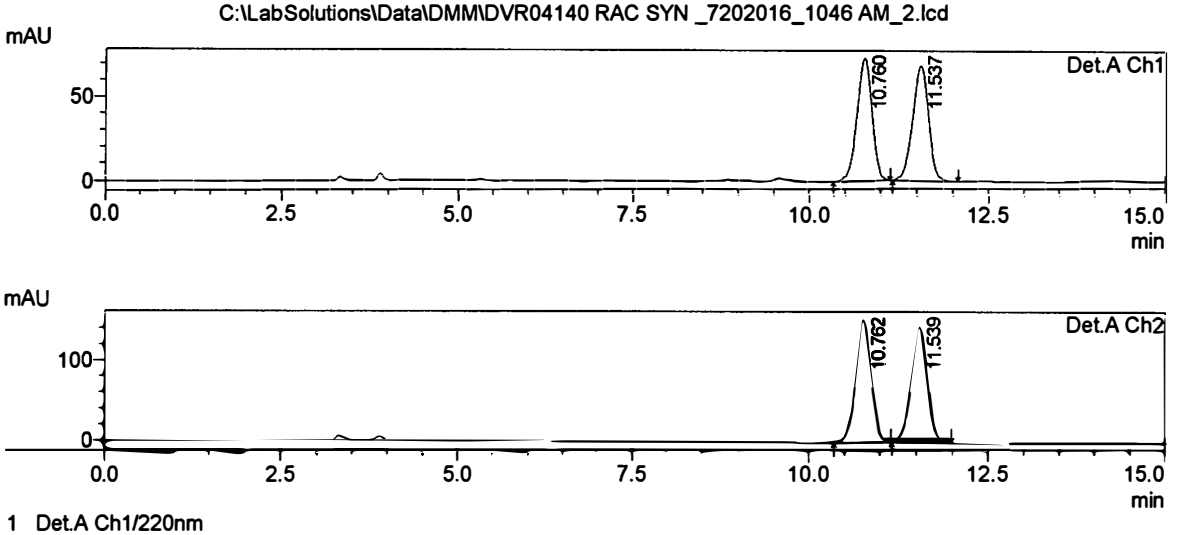

1 Det.A Ch1/220nm
2 Det.A Ch2/210nm

PeakTable

Detector A Ch1 220nm

Peak#	Ret. Time	Area	Height	Area %	Height %
1	10.760	1093144	74436	50.032	51.502
2	11.537	1091760	70093	49.968	48.498
Total		2184904	144529	100.000	100.000

PeakTable

Detector A Ch2 210nm

Peak#	Ret. Time	Area	Height	Area %	Height %
1	10.762	2254340	153508	50.098	51.537
2	11.539	2245525	144353	49.902	48.463
Total		4499866	297861	100.000	100.000

==== Shimadzu LCsolution Analysis Report ====

C:\LabSolutions\Data\DMM\DVR04140 SYN 1_7202016_1046 AM_6.lcd

Acquired by	: LC User
Sample Name	: DVR04140 SYN 1
Sample ID	: DVR04140 SYN 1
Tray#	: 1
Vail #	: 5
Injection Volume	: 3 uL
Data File Name	: DVR04140 SYN 1_7202016_1046 AM_6.lcd
Method File Name	: col1_5isoiPA_15min_1ML_220and210.lcm
Batch File Name	: DMM.lcb
Report File Name	: Default.lcr
Data Acquired	: 7/20/2016 11:43:09 AM
Data Processed	: 7/20/2016 11:58:11 AM

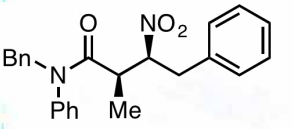

3.50A
87% ee

<Chromatogram>

C:\LabSolutions\Data\DMM\DVR04140 SYN 1_7202016_1046 AM_6.lcd

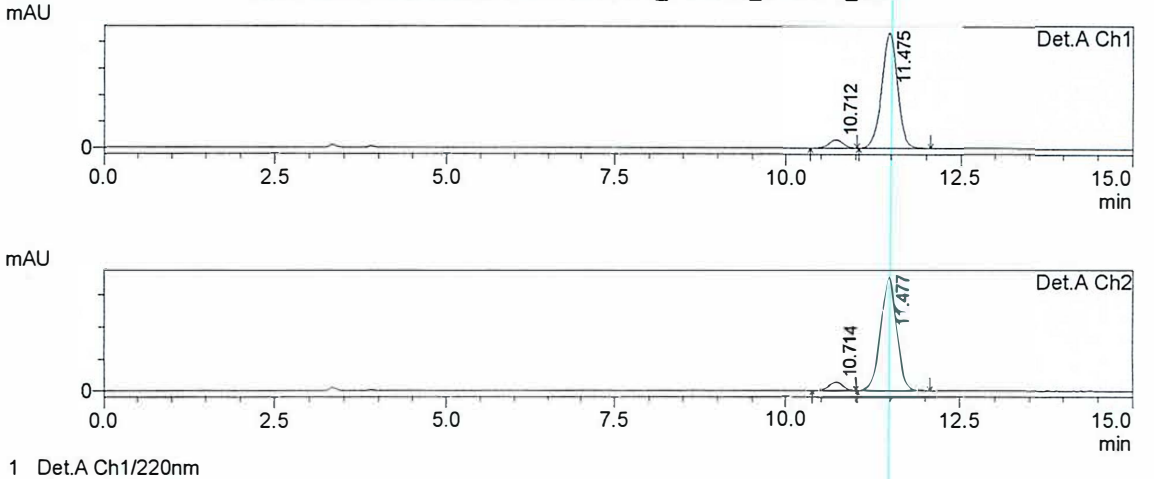

1 Det.A Ch1/220nm
2 Det.A Ch2/210nm

PeakTable

Detector A Ch1 220nm

Peak#	Ret. Time	Area	Height	Area %	Height %
1	10.712	92346	6486	6.370	6.968
2	11.475	1357267	86586	93.630	93.032
Total		1449613	93072	100.000	100.000

PeakTable

Detector A Ch2 210nm

Peak#	Ret. Time	Area	Height	Area %	Height %
1	10.714	189162	13361	6.329	6.961
2	11.477	2799668	178582	93.671	93.039
Total		2988829	191943	100.000	100.000

==== Shimadzu LCsolution Analysis Report ====

C:\LabSolutions\Data\DMM\DVR04140RAC ANTI_7202016_1046 AM_10.lcd

Acquired by	: LC User
Sample Name	: DVR04140RAC ANTI
Sample ID	: DVR04140RAC ANTI
Tray#	: 1
Vail #	: 6
Injection Volume	: 3 uL
Data File Name	: DVR04140RAC ANTI_7202016_1046 AM_10.lcd
Method File Name	: col1_5isoiPA_30min_1ML_254and210.lcm
Batch File Name	: DMM.lcb
Report File Name	: Default.lcr
Data Acquired	: 7/20/2016 12:39:06 PM
Data Processed	: 7/20/2016 1:09:06 PM

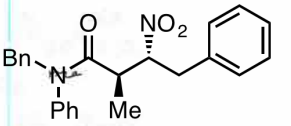

3.50B
racemic

<Chromatogram>

C:\LabSolutions\Data\DMM\DVR04140RAC ANTI_7202016_1046 AM_10.lcd

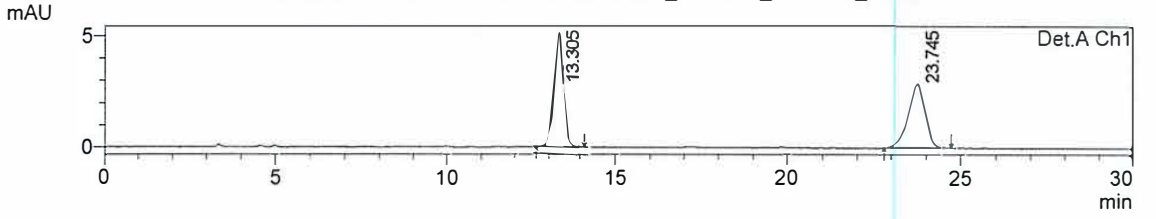

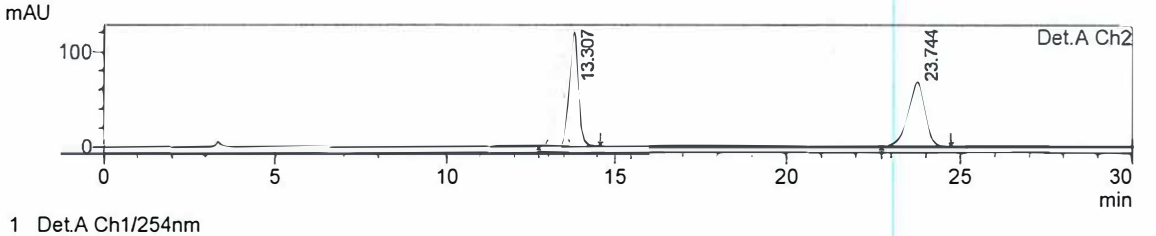

1 Det.A Ch1/254nm
2 Det.A Ch2/210nm

PeakTable

Detector A Ch1 254nm

Peak#	Ret. Time	Area	Height	Area %	Height %
1	13.305	97959	5205	49.970	64.063
2	23.745	98077	2920	50.030	35.937
Total		196036	8124	100.000	100.000

PeakTable

Detector A Ch2 210nm

Peak#	Ret. Time	Area	Height	Area %	Height %
1	13.307	2280277	121019	50.026	64.053
2	23.744	2277909	67917	49.974	35.947
Total		4558186	188936	100.000	100.000

==== Shimadzu LCsolution Analysis Report ====

C:\LabSolutions\Data\DMM\DVR04140 RAC ANTI 1_7202016_1046 AM_14.lcd

Acquired by	: LC User
Sample Name	: DVR04140 RAC ANTI 1
Sample ID	: DVR04140 RAC ANTI 1
Tray#	: 1
Vail #	: 7
Injection Volume	: 3 uL
Data File Name	: DVR04140 RAC ANTI 1_7202016_1046 AM_14.lcd
Method File Name	: col1_5isoiPA_30min_1ML_254and210.lcm
Batch File Name	: DMM.lcb
Report File Name	: Default.lcr
Data Acquired	: 7/20/2016 1:50:02 PM
Data Processed	: 7/20/2016 2:20:04 PM

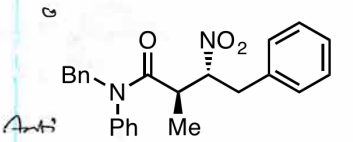

3.50B
67% ee

<Chromatogram>

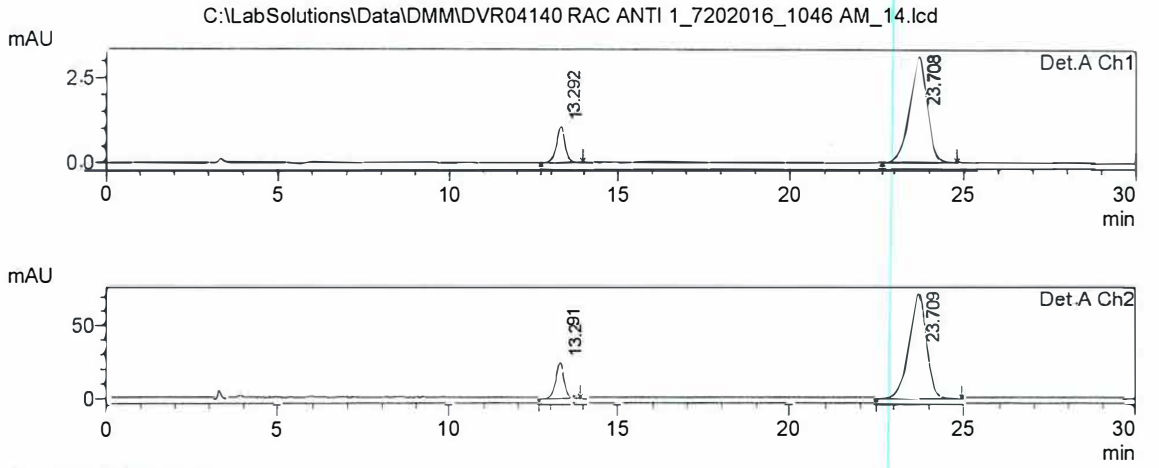

1 Det.A Ch1/254nm
2 Det.A Ch2/210nm

PeakTable

Detector A Ch1 254nm

Peak#	Ret. Time	Area	Height	Area %	Height %
1	13.292	20287	1051	16.159	25.144
2	23.708	105258	3128	83.841	74.856
Total		125544	4179	100.000	100.000

PeakTable

Detector A Ch2 210nm

Peak#	Ret. Time	Area	Height	Area %	Height %
1	13.291	454382	24182	15.632	24.942
2	23.709	2452271	72770	84.368	75.058
Total		2906652	96953	100.000	100.000

Parameter	Value
1 Title	DVR04148CRD.1.fid
2 Solvent	CDCl3
3 Temperature	298.2
4 Number of Scans	16
5 Receiver Gain	9
6 Relaxation Delay	1.0000
7 Pulse Width	15.0000
8 Spectrometer Frequency	400.13
9 Nucleus	1H

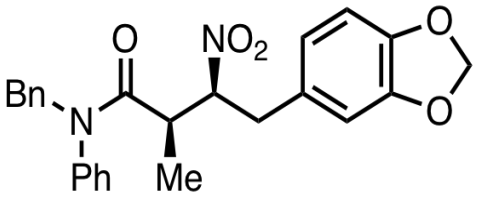

3.51A

Crude

87:13

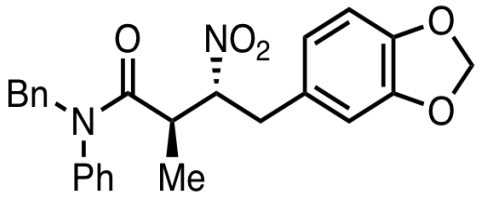

3.51B

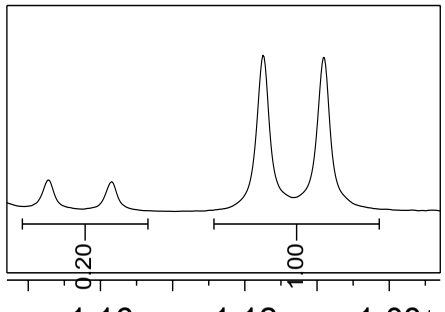

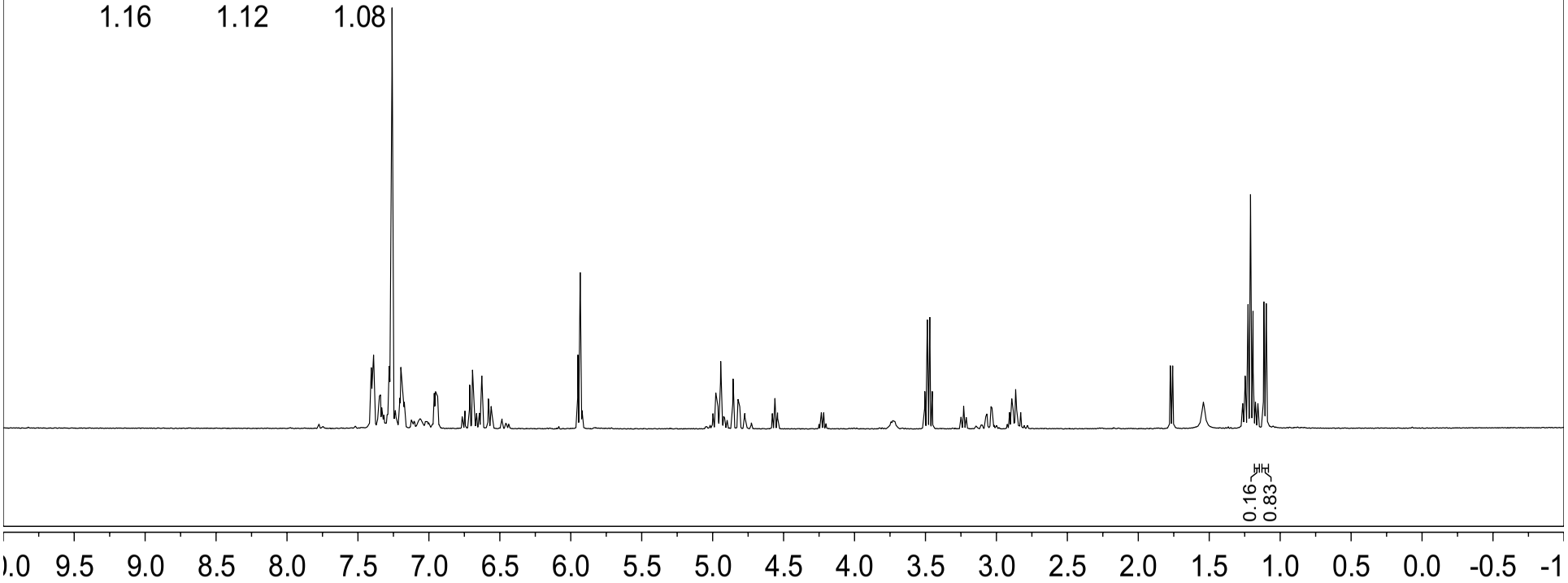

538

Parameter	Value
1 Title	DVR04148AD1.1.fid
2 Solvent	CDCl3
3 Temperature	298.0
4 Number of Scans	16
5 Receiver Gain	203
6 Relaxation Delay	1.0000
7 Pulse Width	10.7700
8 Spectrometer Frequency	600.32
9 Nucleus	1H

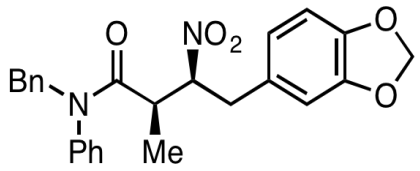

3.51A

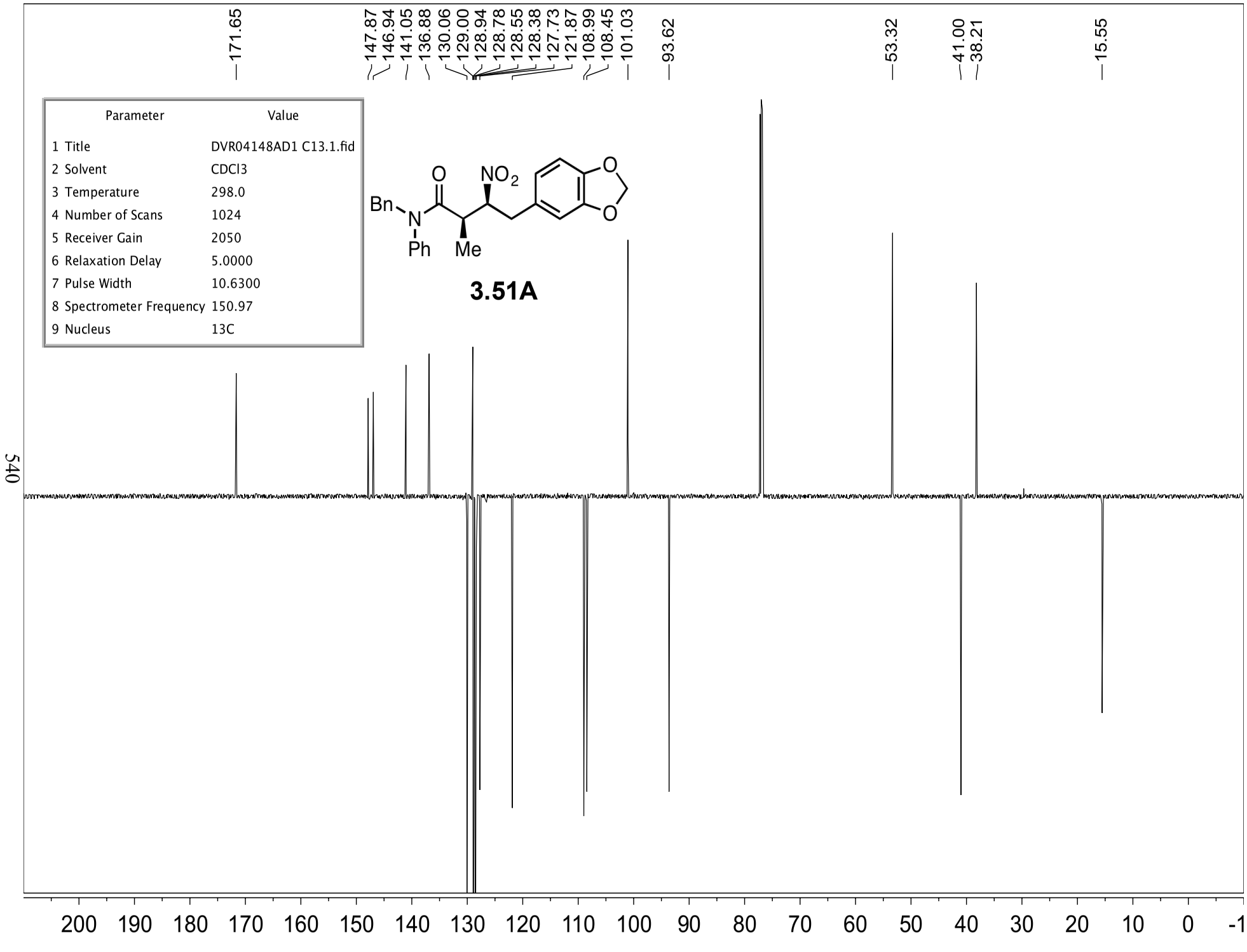
171.65
147.87
146.94
141.05
136.88
130.06
129.00
128.94
128.78
128.55
128.38
127.73
121.87
108.99
108.45
101.03
93.62
53.32
41.00
38.21
15.55
Parameter Value
1 Title DVR04148AD1 C13.1.fid
2 Solvent CDCl3
3 Temperature 298.0
4 Number of Scans 1024
5 Receiver Gain 2050
6 Relaxation Delay 5.0000
7 Pulse Width 10.6300
8 Spectrometer Frequency 150.97
9 Nucleus 13C
Bn
N
Ph
O
NO2
Me
O
O
3.51A
540
200 190 180 170 160 150 140 130 120 110 100 90 80 70 60 50 40 30 20 10 0 -1

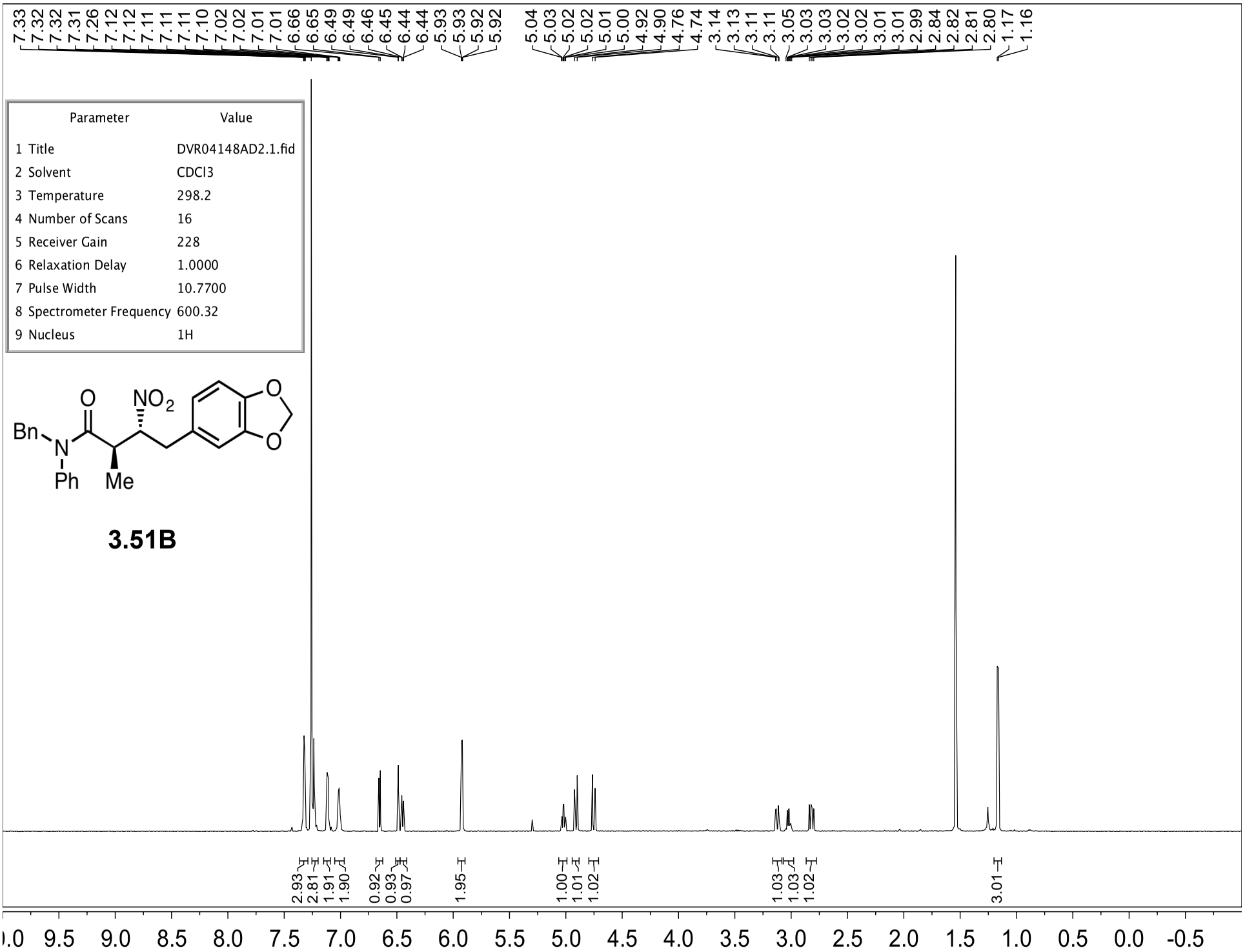
7.33 7.32 7.32 7.31 7.26 7.12 7.12 7.11 7.11 7.11 7.10 7.02 7.02 7.01 7.01 6.66 6.65 6.49 6.49 6.46 6.45 6.44 6.44 5.93 5.93 5.92 5.92 5.04 5.03 5.02 5.02 5.01 5.00 4.92 4.90 4.76 4.74 3.14 3.13 3.11 3.11 3.05 3.03 3.03 3.02 3.02 3.01 3.01 2.99 2.84 2.82 2.81 2.80 1.17 1.16
Parameter Value
1 Title DVR04148AD2.1.fid
2 Solvent CDCl3
3 Temperature 298.2
4 Number of Scans 16
5 Receiver Gain 228
6 Relaxation Delay 1.0000
7 Pulse Width 10.7700
8 Spectrometer Frequency 600.32
9 Nucleus 1H
Bn N Ph Me O NO2 O O
3.51B
2.93 2.81 1.91 1.90 0.92 0.93 0.97 1.95 1.00 1.01 1.02 1.03 1.03 1.02 3.01
1.0 9.5 9.0 8.5 8.0 7.5 7.0 6.5 6.0 5.5 5.0 4.5 4.0 3.5 3.0 2.5 2.0 1.5 1.0 0.5 0.0 -0.5

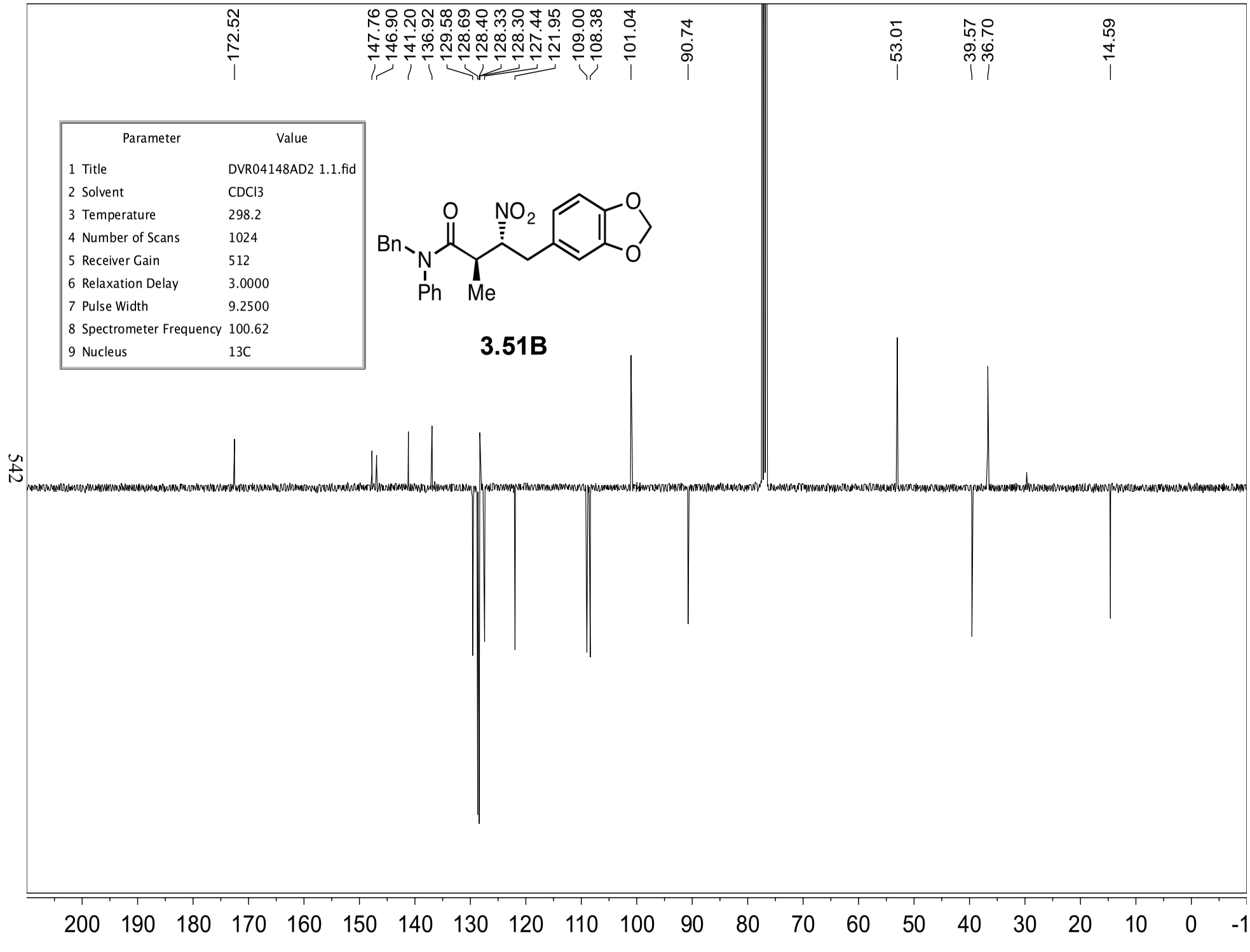
172.52
147.76
146.90
141.20
136.92
129.58
128.69
128.40
128.33
128.30
127.44
121.95
109.00
108.38
101.04
90.74
53.01
39.57
36.70
14.59
Parameter Value
1 Title DVR04148AD2 1.1.fid
2 Solvent CDCl3
3 Temperature 298.2
4 Number of Scans 1024
5 Receiver Gain 512
6 Relaxation Delay 3.0000
7 Pulse Width 9.2500
8 Spectrometer Frequency 100.62
9 Nucleus 13C
Bn
N
Ph
O
NO2
Me
O
O
3.51B
542
200 190 180 170 160 150 140 130 120 110 100 90 80 70 60 50 40 30 20 10 0 -1

==== Shimadzu LCsolution Analysis Report ====

C:\LabSolutions\Data\DMM\DVR04148 RAC D1_7282016_1137 AM_39.lcd

Acquired by	: LC User
Sample Name	: DVR04148 RAC D1
Sample ID	: DVR04148 RAC D1
Tray#	: 1
Vail #	: 2
Injection Volume	: 1 uL
Data File Name	: DVR04148 RAC D1_7282016_1137 AM_39.lcd
Method File Name	: col1_3isoiPA_45min_1ML_220and210.lcm
Batch File Name	: DMM.lcb
Report File Name	: Default.lcr
Data Acquired	: 7/29/2016 3:28:24 AM
Data Processed	: 7/29/2016 4:13:27 AM

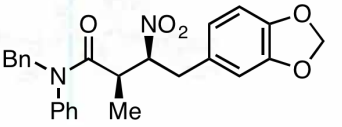

3.51A
racemic

<Chromatogram>

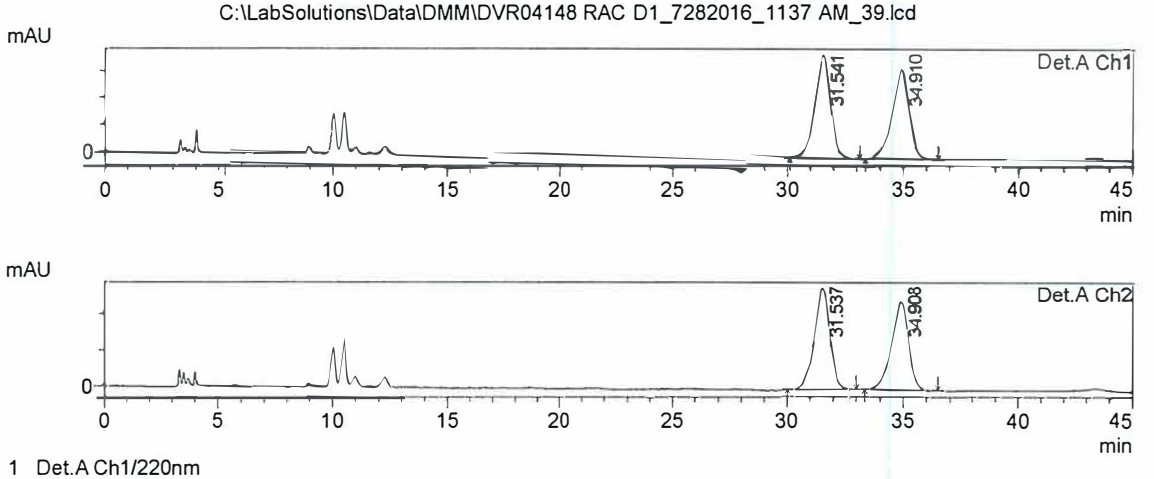

1 Det.A Ch1/220nm
2 Det.A Ch2/210nm

PeakTable

Detector A Ch1 220nm

Peak#	Ret. Time	Area	Height	Area %	Height %
1	31.541	351187	7591	51.175	53.528
2	34.910	335062	6591	48.825	46.472
Total		686249	14182	100.000	100.000

PeakTable

Detector A Ch2 210nm

Peak#	Ret. Time	Area	Height	Area %	Height %
1	31.537	659926	14299	51.196	53.593
2	34.908	629093	12382	48.804	46.407
Total		1289019	26681	100.000	100.000

==== Shimadzu LCsolution Analysis Report ====

C:\LabSolutions\Data\DMM\DVR04148 D1_7282016_1137 AM_43.lcd

Acquired by	: LC User
Sample Name	: DVR04148 D1
Sample ID	: DVR04148 D1
Tray#	: 1
Vail #	: 3
Injection Volume	: 1 uL
Data File Name	: DVR04148 D1_7282016_1137 AM_43.lcd
Method File Name	: col1_3isoiPA_45min_1ML_220and210.lcm
Batch File Name	: DMM.lcb
Report File Name	: Default.lcr
Data Acquired	: 7/29/2016 5:09:21 AM
Data Processed	: 7/29/2016 5:54:23 AM

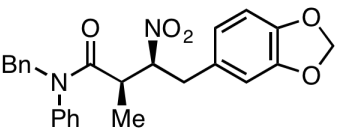

3.51A
89% ee

<Chromatogram>

C:\LabSolutions\Data\DMM\DVR04148 D1_7282016_1137 AM_43.lcd

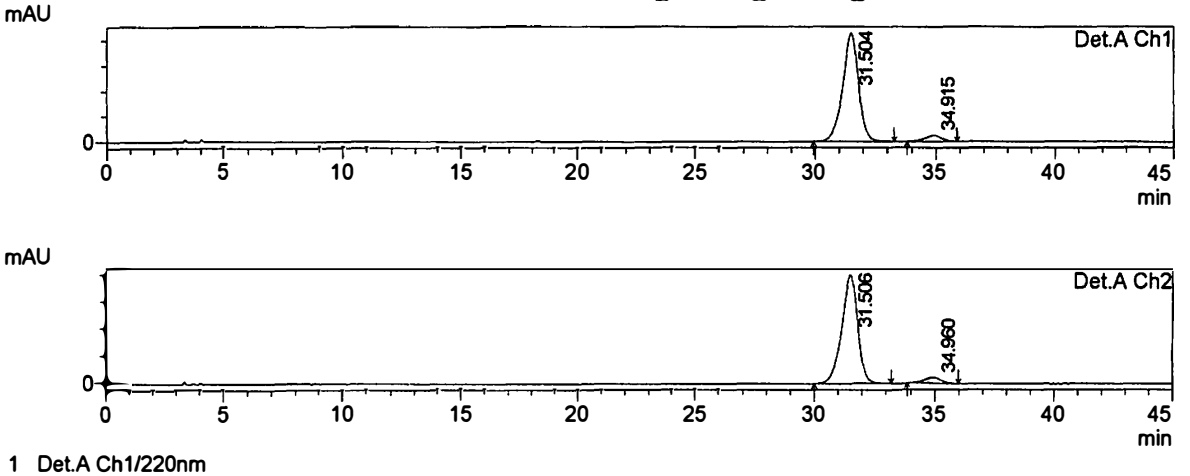

1 Det.A Ch1/220nm
2 Det.A Ch2/210nm

PeakTable

Detector A Ch1 220nm

Peak#	Ret. Time	Area	Height	Area %	Height %
1	31.504	1984056	42980	94.535	94.787
2	34.915	114704	2364	5.465	5.213
Total		2098760	45344	100.000	100.000

PeakTable

Detector A Ch2 210nm

Peak#	Ret. Time	Area	Height	Area %	Height %
1	31.506	3721912	80347	94.562	94.757
2	34.960	214020	4446	5.438	5.243
Total		3935932	84793	100.000	100.000

==== Shimadzu LCsolution Analysis Report ====

	C:\LabSolutions\Data\DMM\DVR04148 RAC D2_7292016_1211 PM_2.lcd
Acquired by	: LC User
Sample Name	: DVR04148 RAC D2
Sample ID	: DVR04148 RAC D2
Tray#	: 1
Vail #	: 2
Injection Volume	: 1 uL
Data File Name	: DVR04148 RAC D2_7292016_1211 PM_2.lcd
Method File Name	: col2_3isoiPA_45min_1ML_220and210.lcm
Batch File Name	: DMM.lcb
Report File Name	: Default.lcr
Data Acquired	: 7/29/2016 12:57:24 PM
Data Processed	: 7/29/2016 1:42:23 PM

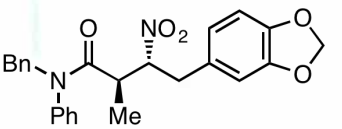

3.51B
racemic

<Chromatogram>

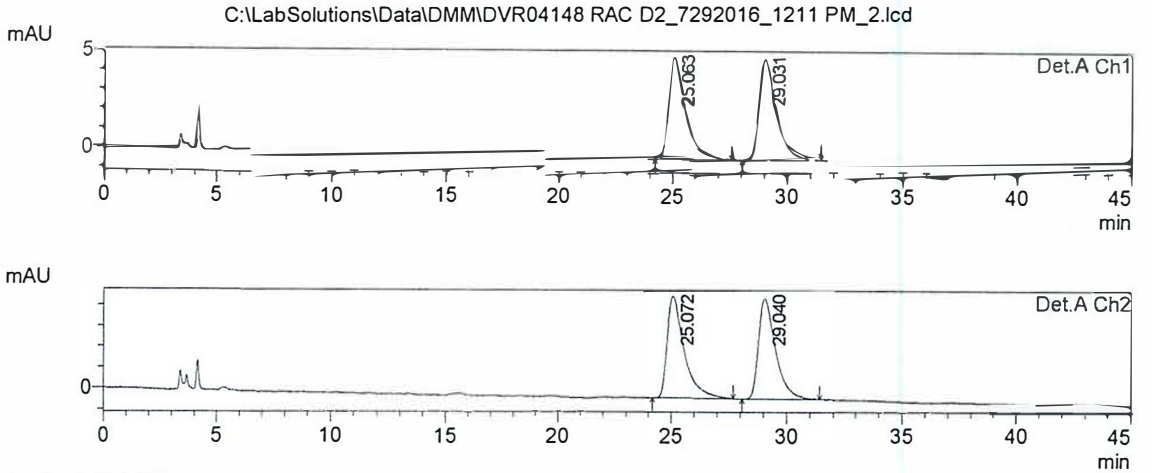

1 Det.A Ch1/220nm
2 Det.A Ch2/210nm

PeakTable

Detector A Ch1 220nm

Peak#	Ret. Time	Area	Height	Area %	Height %
1	25.063	269990	5265	49.936	50.107
2	29.031	270677	5242	50.064	49.893
Total		540666	10507	100.000	100.000

PeakTable

Detector A Ch2 210nm

Peak#	Ret. Time	Area	Height	Area %	Height %
1	25.072	506479	9808	50.801	50.336
2	29.040	490498	9677	49.199	49.664
Total		996977	19485	100.000	100.000

==== Shimadzu LCsolution Analysis Report ====

C:\LabSolutions\Data\DMM\DVR04148 D2_7292016_1211 PM_1.lcd

Acquired by	: LC User
Sample Name	: DVR04148 D2
Sample ID	: DVR04148 D2
Tray#	: 1
Vail #	: 3
Injection Volume	: 1 uL
Data File Name	: DVR04148 D2_7292016_1211 PM_1.lcd
Method File Name	: col2_3isoiPA_45min_1ML_220and210.lcm
Batch File Name	: DMM.lcb
Report File Name	: Default.lcr
Data Acquired	: 7/29/2016 2:39:22 PM
Data Processed	: 7/29/2016 3:24:23 PM

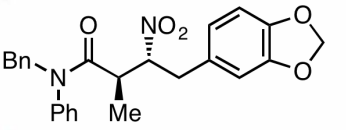

3.51B
80% ee

<Chromatogram>

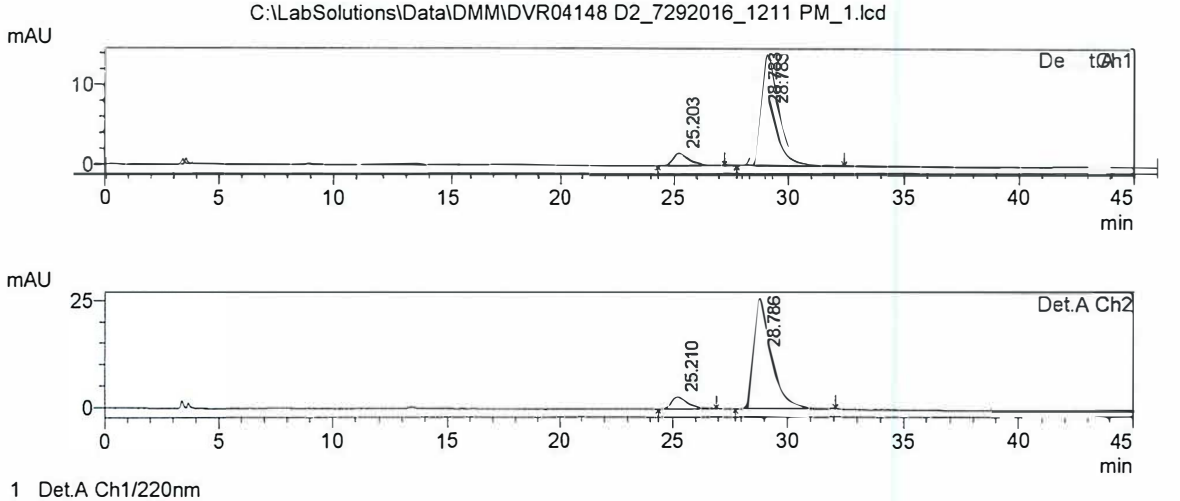

1 Det.A Ch1/220nm
2 Det.A Ch2/210nm

PeakTable

Detector A Ch1 220nm

Peak#	Ret. Time	Area	Height	Area %	Height %
1	25.203	78122	1532	9.695	9.909
2	28.783	727654	13928	90.305	90.091
Total		805775	15460	100.000	100.000

PeakTable

Detector A Ch2 210nm

Peak#	Ret. Time	Area	Height	Area %	Height %
1	25.210	141313	2831	9.455	9.829
2	28.786	1353283	25973	90.545	90.171
Total		1494596	28804	100.000	100.000

Parameter	Value
1 Title	DVR04167CRD.1.fid
2 Solvent	CDCl3
3 Temperature	298.0
4 Number of Scans	16
5 Receiver Gain	128
6 Relaxation Delay	1.0000
7 Pulse Width	10.7700
8 Spectrometer Frequency	600.32
9 Nucleus	1H

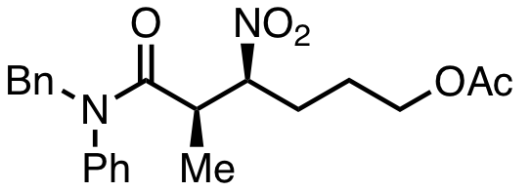

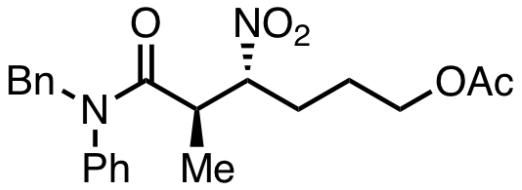

3.52A **Crude** **72:28** **3.52B**

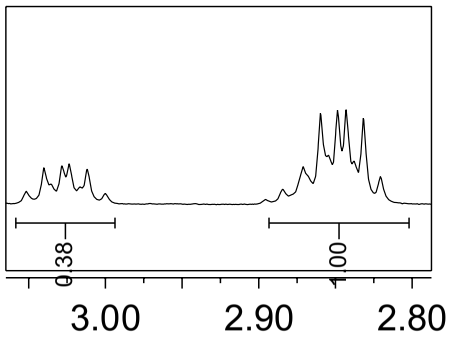

Parameter	Value
1 Title	DVR04167D1.1.fid
2 Solvent	CDCl3
3 Temperature	298.0
4 Number of Scans	16
5 Receiver Gain	128
6 Relaxation Delay	1.0000
7 Pulse Width	10.7700
8 Spectrometer Frequency	600.32
9 Nucleus	1H

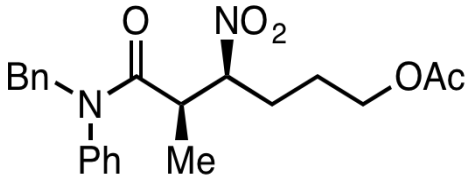

3.52A

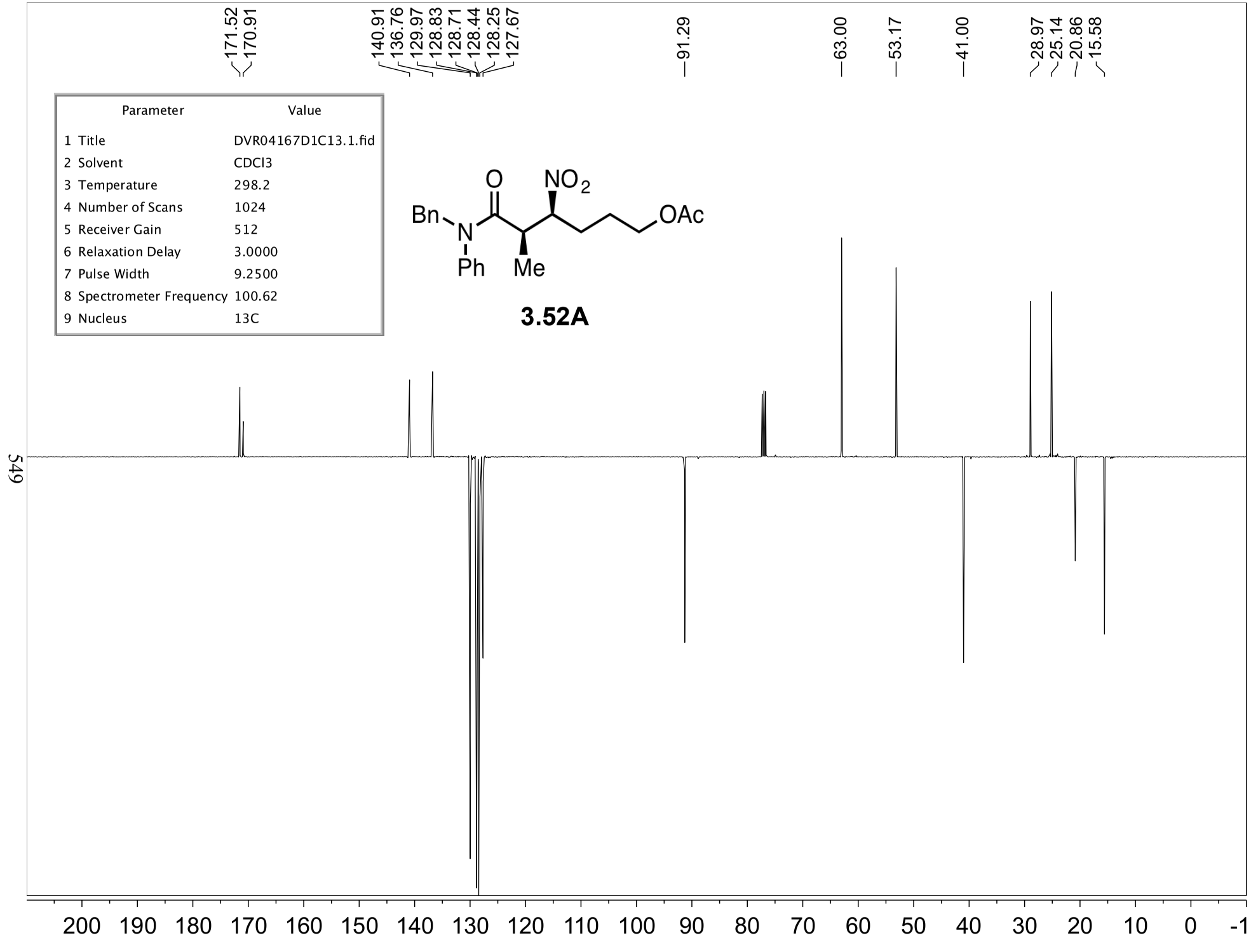
171.52
170.91
140.91
136.76
129.97
128.83
128.71
128.44
128.25
127.67
91.29
63.00
53.17
41.00
28.97
25.14
20.86
15.58
Parameter Value
1 Title DVR04167D1C13.1.fid
2 Solvent CDCl3
3 Temperature 298.2
4 Number of Scans 1024
5 Receiver Gain 512
6 Relaxation Delay 3.0000
7 Pulse Width 9.2500
8 Spectrometer Frequency 100.62
9 Nucleus 13C
O
NO2
Bn
N
OAc
Ph
Me
3.52A
549
200 190 180 170 160 150 140 130 120 110 100 90 80 70 60 50 40 30 20 10 0 -1

Parameter	Value
1 Title	DVR04167D2.1.fid
2 Solvent	CDCl3
3 Temperature	298.0
4 Number of Scans	16
5 Receiver Gain	203
6 Relaxation Delay	1.0000
7 Pulse Width	10.7700
8 Spectrometer Frequency	600.32
9 Nucleus	1H

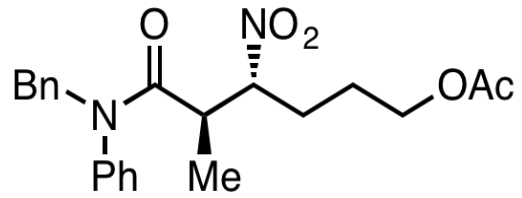

3.52B

550

7.37 7.37 7.36 7.36 7.35 7.35 7.35 7.34 7.12 7.12 7.11 7.11 7.08 7.07 7.06 7.06 4.94 4.93 4.92 4.92 4.90 4.90 4.88 4.80 4.77 4.04 4.03 4.03 4.02 4.02 4.01 4.01 4.00 3.01 3.01 3.00 3.00 2.99 2.99 2.01 1.94 1.94 1.93 1.93 1.92 1.91 1.91 1.90 1.73 1.73 1.72 1.71 1.70 1.61 1.60 1.60 1.59 1.58 1.57 1.57 1.56 1.09 1.07

2.96 3.45 1.99 1.89 2.00 1.03 2.03 1.00 2.89 1.06 1.05 2.08 3.01

9.5 9.0 8.5 8.0 7.5 7.0 6.5 6.0 5.5 5.0 4.5 4.0 3.5 3.0 2.5 2.0 1.5 1.0 0.5 0.0 -0.5 -1

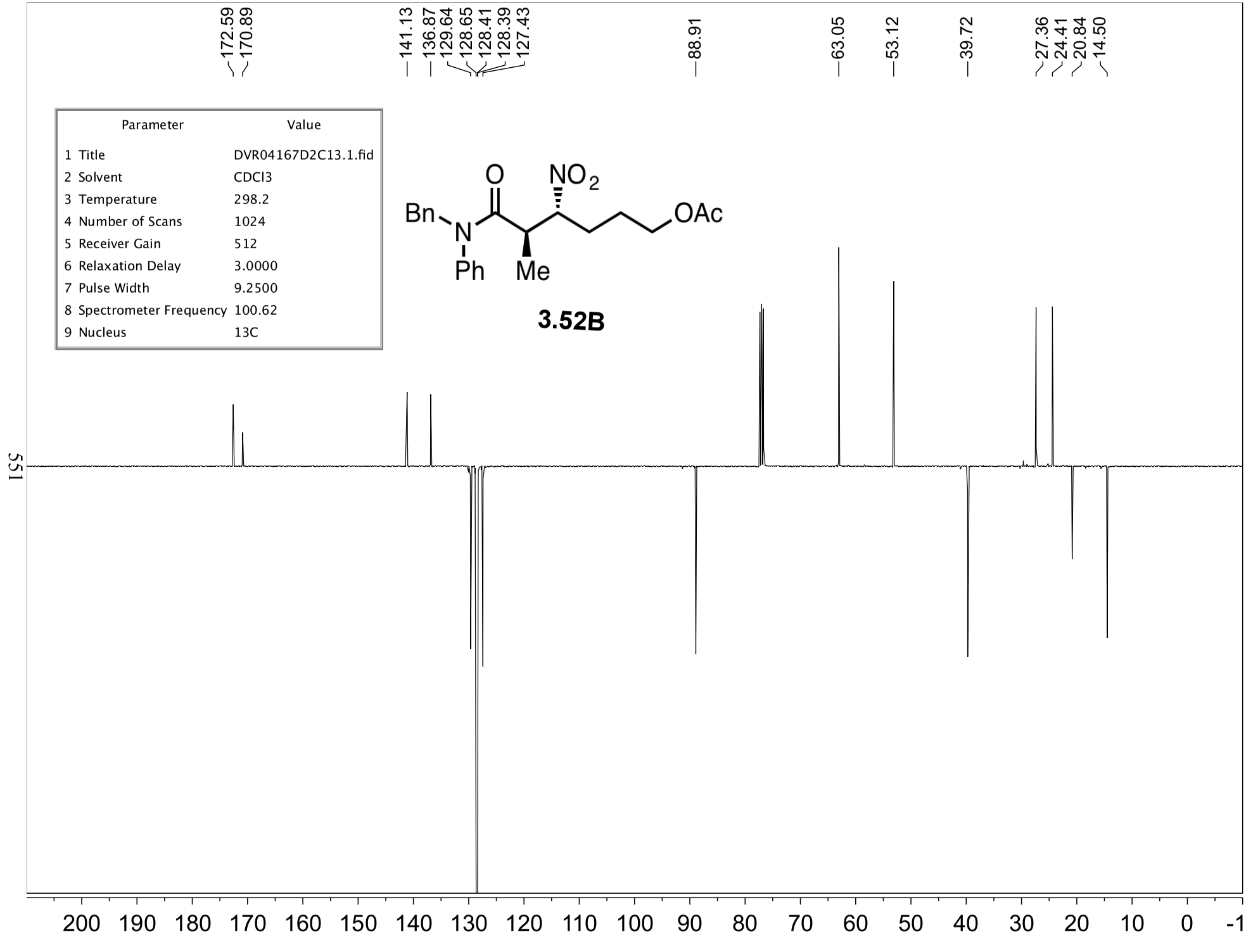
172.59
170.89
141.13
136.87
129.64
128.65
128.41
128.39
127.43
88.91
63.05
53.12
39.72
27.36
24.41
20.84
14.50
Parameter Value
1 Title DVR04167D2C13.1.fid
2 Solvent CDCl3
3 Temperature 298.2
4 Number of Scans 1024
5 Receiver Gain 512
6 Relaxation Delay 3.0000
7 Pulse Width 9.2500
8 Spectrometer Frequency 100.62
9 Nucleus 13C
O
NO2
Bn
N
OAc
Ph
Me
3.52B
200 190 180 170 160 150 140 130 120 110 100 90 80 70 60 50 40 30 20 10 0 -1

==== Shimadzu LCsolution Analysis Report ====

C:\LabSolutions\Data\DMM\DVR04167 D1 RAC_8212016_1521 PM_1.lcd

Acquired by	: LC User
Sample Name	: DVR04167 D1 RAC
Sample ID	: DVR04167 D1 RAC
Tray#	: 1
Vail #	: 1
Injection Volume	: 7 uL
Data File Name	: DVR04167 D1 RAC_8212016_1521 PM_1.lcd
Method File Name	: col2_1isoiPA_45min_1ML_220 and210.lcm
Batch File Name	: DMM.lcb
Report File Name	: Default.lcr
Data Acquired	: 8/21/2016 4:07:01 PM
Data Processed	: 8/21/2016 4:52:04 PM

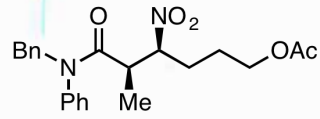

3.52A
racemic

<Chromatogram>

C:\LabSolutions\Data\DMM\DVR04167 D1 RAC_8212016_1521 PM_1.lcd

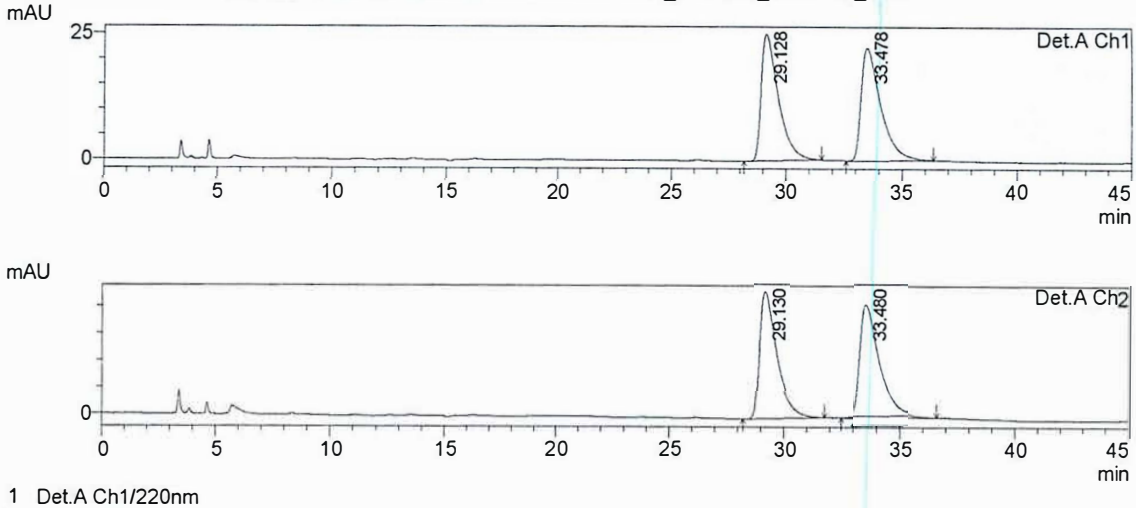

1 Det.A Ch1/220nm
2 Det.A Ch2/210nm

PeakTable

Detector A Ch1 220nm

Peak#	Ret. Time	Area	Height	Area %	Height %
1	29.128	1305476	25180	49.826	52.953
2	33.478	1314597	22372	50.174	47.047
Total		2620073	47552	100.000	100.000

PeakTable

Detector A Ch2 210nm

Peak#	Ret. Time	Area	Height	Area %	Height %
1	29.130	2424328	46353	49.960	52.975
2	33.480	2428165	41147	50.040	47.025
Total		4852493	87501	100.000	100.000

==== Shimadzu LCsolution Analysis Report ====

C:\LabSolutions\Data\DMM\DVR04167 D1_8212016_1521 PM_5.lcd

Acquired by	: LC User
Sample Name	: DVR04167 D1
Sample ID	: DVR04167 D1
Tray#	: 1
Vail #	: 2
Injection Volume	: 2 uL
Data File Name	: DVR04167 D1_8212016_1521 PM_5.lcd
Method File Name	: col2_1isoiPA_45min_1ML_220 and210.lcm
Batch File Name	: DMM.lcb
Report File Name	: Default.lcr
Data Acquired	: 8/21/2016 5:47:58 PM
Data Processed	: 8/21/2016 6:32:59 PM

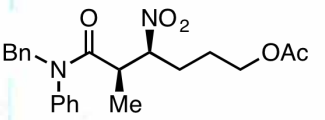

3.52A
91% ee

<Chromatogram>

C:\LabSolutions\Data\DMM\DVR04167 D1_8212016_1521 PM_5.lcd

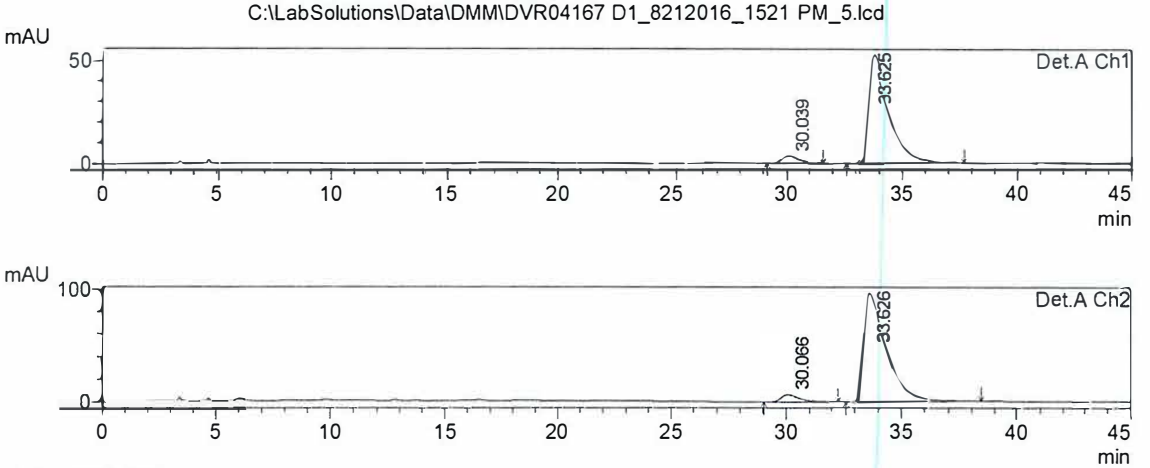

1 Det.A Ch1/220nm
2 Det.A Ch2/210nm

PeakTable

Detector A Ch1 220nm

Peak#	Ret. Time	Area	Height	Area %	Height %
1	30.039	173900	3441	4.744	6.115
2	33.625	3491407	52837	95.256	93.885
Total		3665307	56278	100.000	100.000

PeakTable

Detector A Ch2 210nm

Peak#	Ret. Time	Area	Height	Area %	Height %
1	30.066	365998	6533	5.361	6.313
2	33.626	6460729	96957	94.639	93.687
Total		6826726	103490	100.000	100.000

==== Shimadzu LCsolution Analysis Report ====

C:\LabSolutions\Data\DMM\DVR04167 D2 RAC_8212016_1521 PM_9.lcd

Acquired by	: LC User
Sample Name	: DVR04167 D2 RAC
Sample ID	: DVR04167 D2 RAC
Tray#	: 1
Vail #	: 3
Injection Volume	: 3 uL
Data File Name	: DVR04167 D2 RAC_8212016_1521 PM_9.lcd
Method File Name	: col1_05isoiPA_30min_1ml_254and210.lcm
Batch File Name	: DMM.lcb
Report File Name	: Default.lcr
Data Acquired	: 8/21/2016 7:13:54 PM
Data Processed	: 8/21/2016 7:43:54 PM

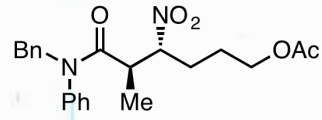

3.52B
racemic

<Chromatogram>

C:\LabSolutions\Data\DMM\DVR04167 D2 RAC_8212016_1521 PM_9.lcd

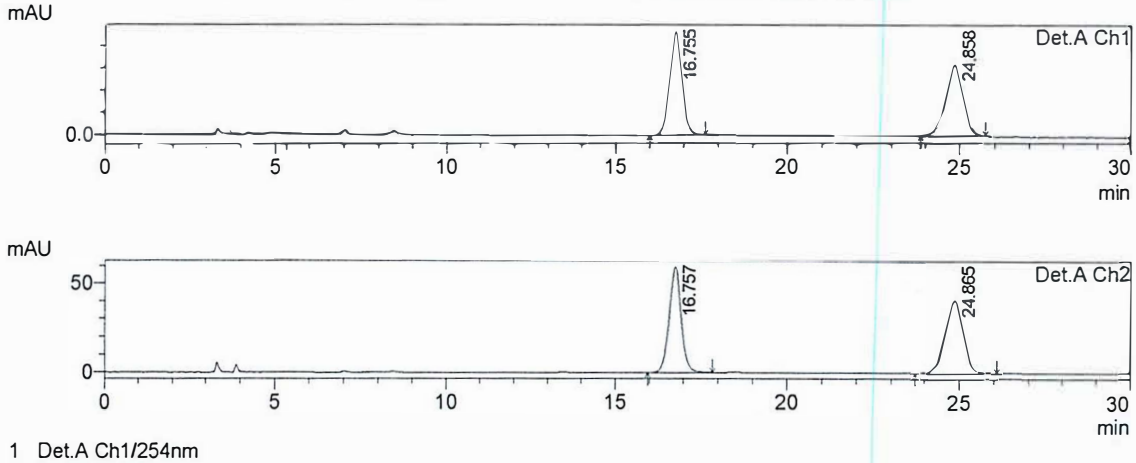

1 Det.A Ch1/254nm
2 Det.A Ch2/210nm

PeakTable

Detector A Ch1 254nm

Peak#	Ret. Time	Area	Height	Area %	Height %
1	16.755	56733	2346	50.344	59.378
2	24.858	55958	1605	49.656	40.622
Total		112690	3951	100.000	100.000

PeakTable

Detector A Ch2 210nm

Peak#	Ret. Time	Area	Height	Area %	Height %
1	16.757	1449925	59478	50.026	59.132
2	24.865	1448408	41106	49.974	40.868
Total		2898332	100584	100.000	100.000

==== Shimadzu LCsolution Analysis Report ====

C:\LabSolutions\Data\DMM\DVR04167 D2_8212016_1521 PM_13.lcd

Acquired by	: LC User
Sample Name	: DVR04167 D2
Sample ID	: DVR04167 D2
Tray#	: 1
Vail #	: 4
Injection Volume	: 3 uL
Data File Name	: DVR04167 D2_8212016_1521 PM_13.lcd
Method File Name	: col1_05isoiPA_30min_1ml_254and210.lcm
Batch File Name	: DMM.lcb
Report File Name	: Default.lcr
Data Acquired	: 8/21/2016 8:24:48 PM
Data Processed	: 8/21/2016 8:54:51 PM

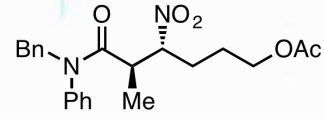

3.52B
76% ee

<Chromatogram>

C:\LabSolutions\Data\DMM\DVR04167 D2_8212016_1521 PM_13.lcd

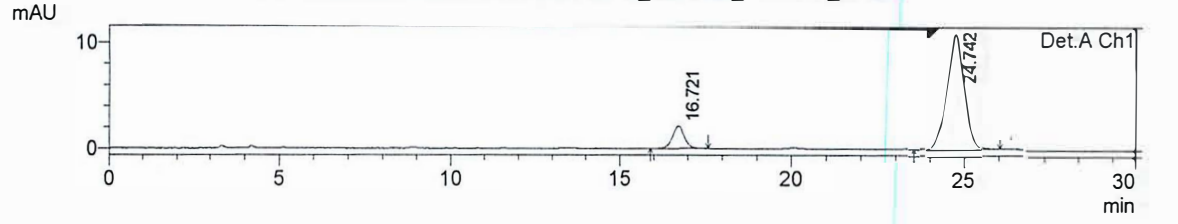

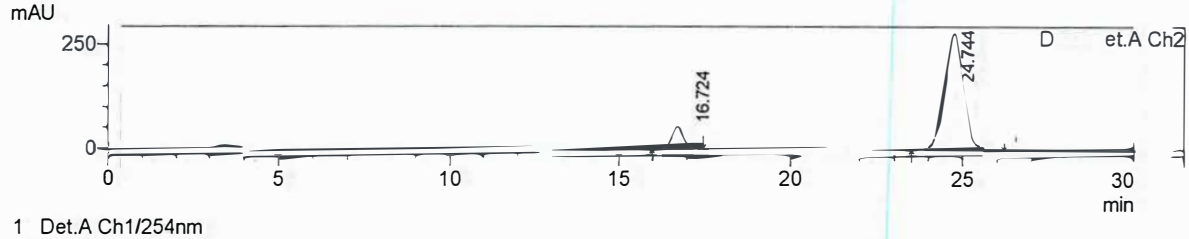

1 Det.A Ch1/254nm
2 Det.A Ch2/210nm

PeakTable

Detector A Ch1 254nm

Peak#	Ret. Time	Area	Height	Area %	Height %
1	16.721	50971	2127	11.753	16.262
2	24.742	382709	10952	88.247	83.738
Tota l		433680	13080	100.000	100.000

PeakTable

Detector A Ch2 210nm

Peak#	Ret. Time	Area	Height	Area %	Height %
1	16.724	1288866	53750	11.620	16.189
2	24.744	9802457	278264	88.380	83.811
Tota l		11091323	332014	100.000	100.000

Parameter	Value
1 Title	DVR04186BCRD.1.fid
2 Solvent	CDCl3
3 Temperature	298.2
4 Number of Scans	64
5 Receiver Gain	8
6 Relaxation Delay	6.0000
7 Pulse Width	15.0000
8 Spectrometer Frequency	400.13
9 Nucleus	1H

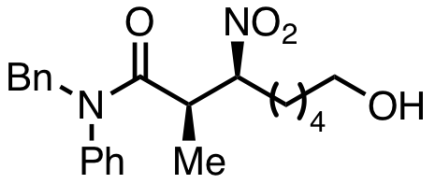

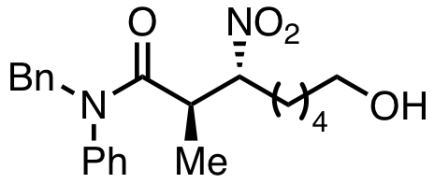

Crude

3.53A **72:28** **3.53B**

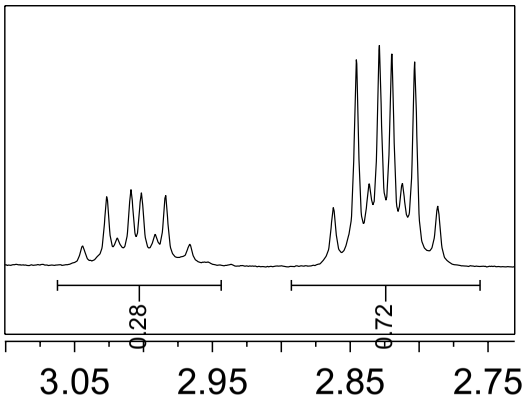

556

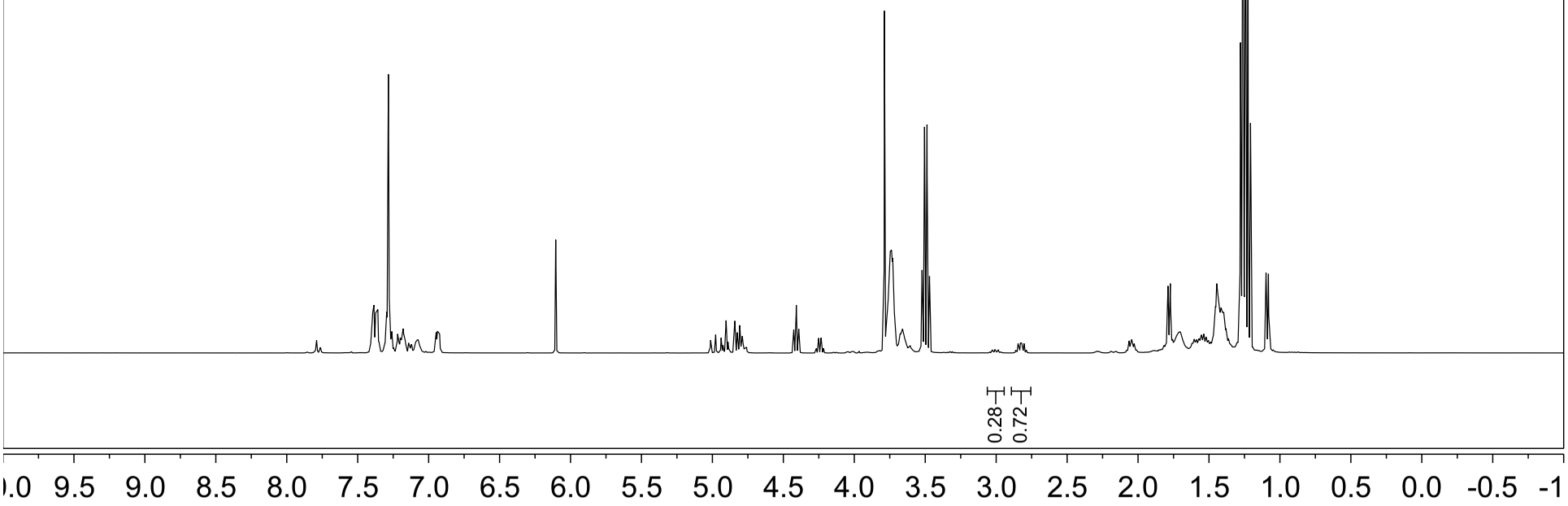

Parameter	Value
1 Title	DVR04186E1-A.1.fid
2 Solvent	CDCl3
3 Temperature	297.1
4 Number of Scans	16
5 Receiver Gain	161
6 Relaxation Delay	1.0000
7 Pulse Width	10.7300
8 Spectrometer Frequency	600.32
9 Nucleus	1H

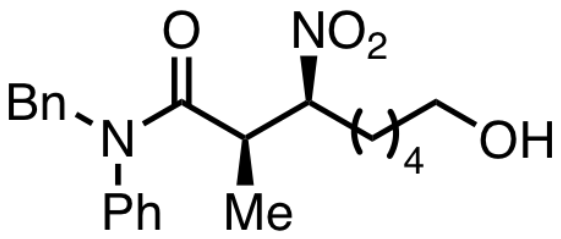

3.53A

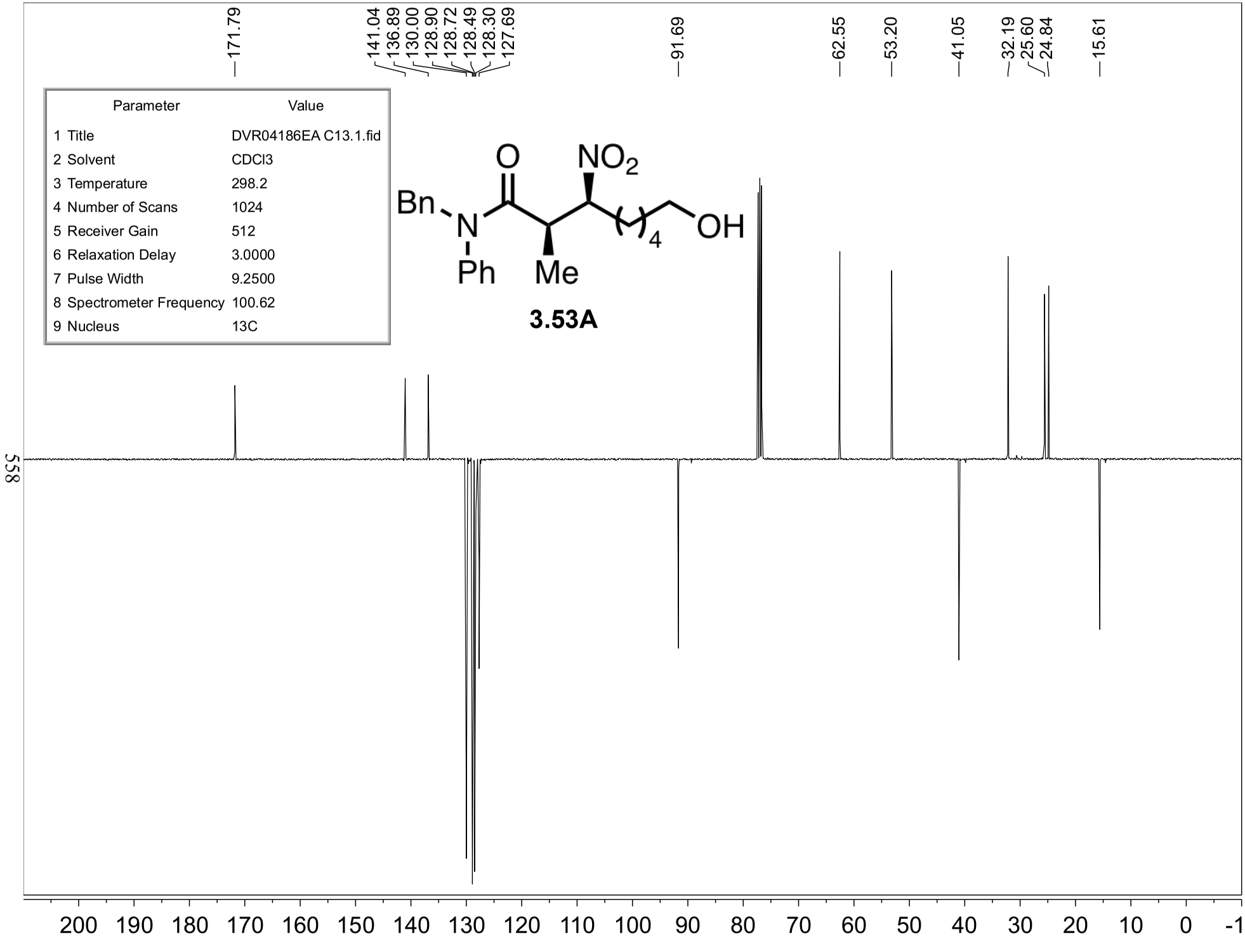
171.79
141.04
136.89
130.00
128.90
128.72
128.49
128.30
127.69
91.69
62.55
53.20
41.05
32.19
25.60
24.84
15.61
Parameter Value
1 Title DVR04186EA C13.1.fid
2 Solvent CDCl3
3 Temperature 298.2
4 Number of Scans 1024
5 Receiver Gain 512
6 Relaxation Delay 3.0000
7 Pulse Width 9.2500
8 Spectrometer Frequency 100.62
9 Nucleus 13C
O
NO2
Bn
N
Ph
Me
4
OH
3.53A
558
200 190 180 170 160 150 140 130 120 110 100 90 80 70 60 50 40 30 20 10 0 -1

Parameter	Value
1 Title	DVR04186G1.2.fid
2 Solvent	CDCl3
3 Temperature	298.5
4 Number of Scans	16
5 Receiver Gain	114
6 Relaxation Delay	1.0000
7 Pulse Width	10.7300
8 Spectrometer Frequency	600.32
9 Nucleus	1H

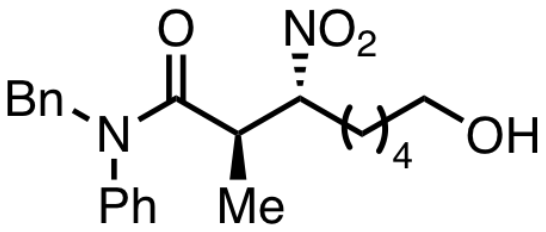

3.53B

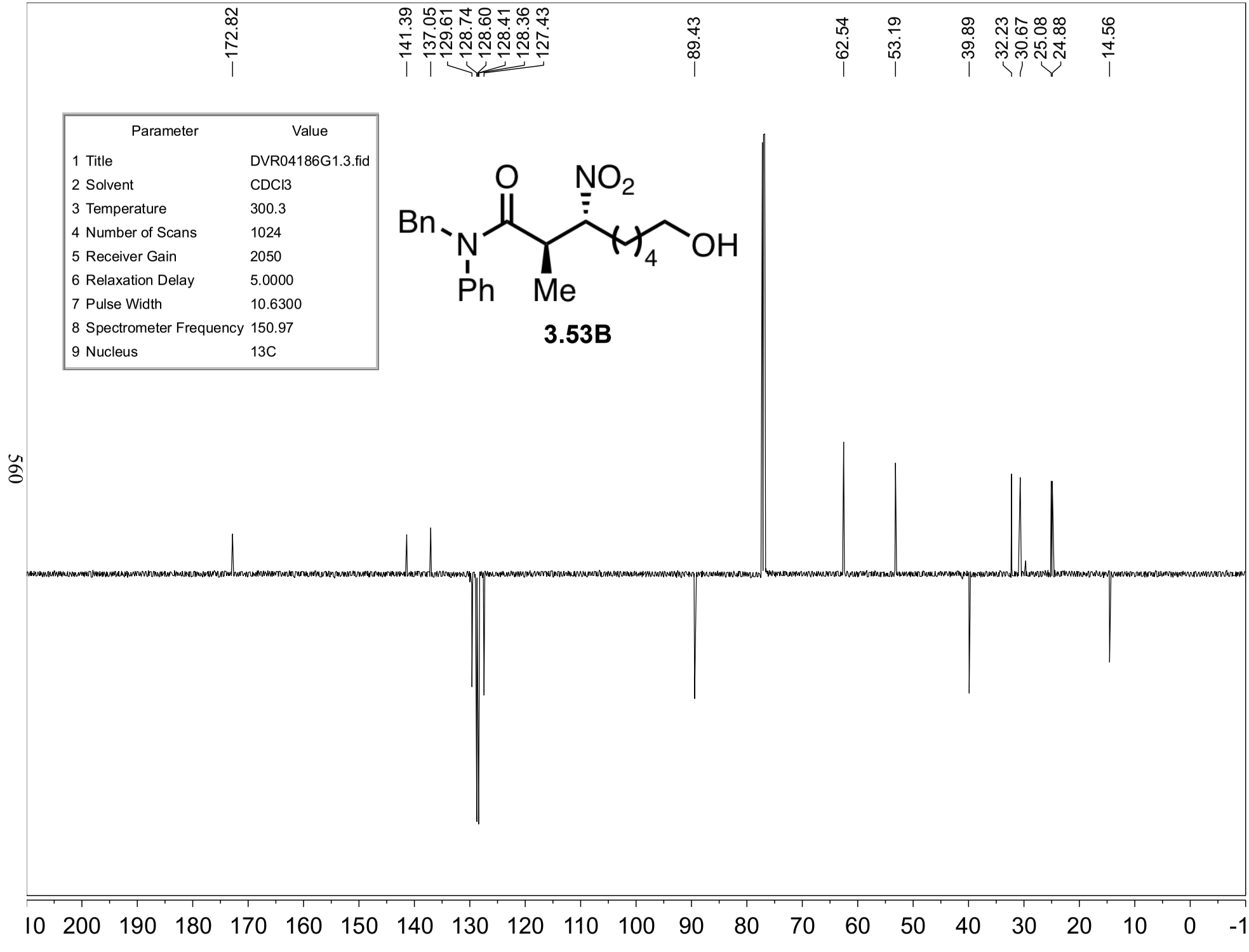
172.82
141.39
137.05
129.61
128.74
128.60
128.41
128.36
127.43
89.43
62.54
53.19
39.89
32.23
30.67
25.08
24.88
14.56
Parameter Value
1 Title DVR04186G1.3.fid
2 Solvent CDCl3
3 Temperature 300.3
4 Number of Scans 1024
5 Receiver Gain 2050
6 Relaxation Delay 5.0000
7 Pulse Width 10.6300
8 Spectrometer Frequency 150.97
9 Nucleus 13C
O
NO2
Bn
N
Ph
Me
4
OH
3.53B
560
10 200 190 180 170 160 150 140 130 120 110 100 90 80 70 60 50 40 30 20 10 0 -1

==== Shimadzu LCsolution Analysis Report ====

C:\LabSolutions\Data\DMM\DVR04186B RAC D1_9182016_1754 PM_2.lcd

Acquired by	: LC User
Sample Name	: DVR04186B RAC D1
Sample ID	: DVR04186B RAC D1
Tray#	: 1
Vail #	: 1
Injection Volume	: 3 uL
Data File Name	: DVR04186B RAC D1_9182016_1754 PM_2.lcd
Method File Name	: col1_5isoiPA_60min_1ML_220and210.lcm
Batch File Name	: DMM.lcb
Report File Name	: Default.lcr
Data Acquired	: 9/18/2016 6:25:08 PM
Data Processed	: 9/18/2016 7:25:09 PM

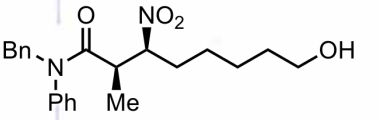

Syn

3.53A
racemic

<Chromatogram>

C:\LabSolutions\Data\DMM\DVR04186B RAC D1_9182016_1754 PM_2.lcd

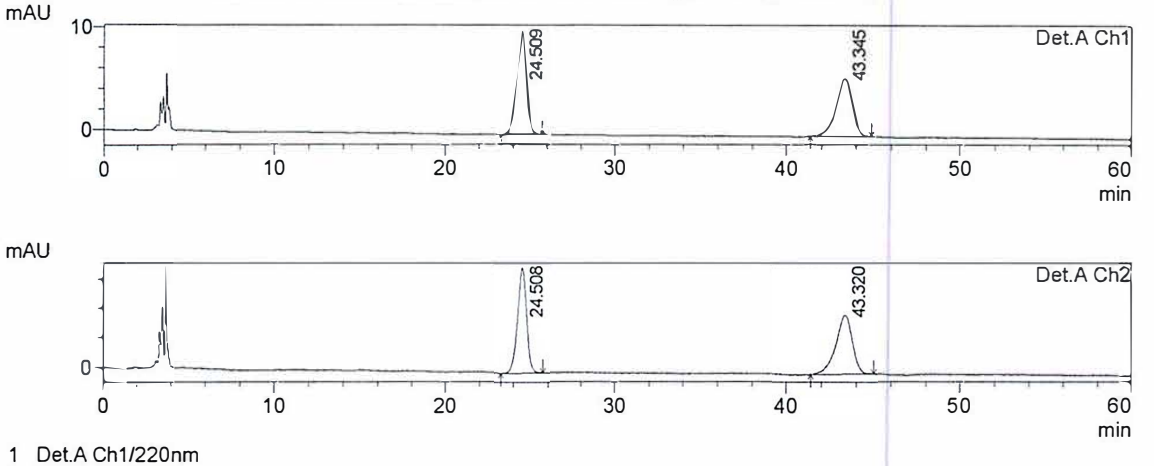

1 Det.A Ch1/220nm
2 Det.A Ch2/210nm

PeakTable

Detector A Ch1 220nm

Peak#	Ret. Time	Area	Height	Area %	Height %
1	24.509	366519	10125	49.929	64.058
2	43.345	367559	5681	50.071	35.942
Total		734078	15806	100.000	100.000

PeakTable

Detector A Ch2 210nm

Peak#	Ret. Time	Area	Height	Area %	Height %
1	24.508	643739	17786	49.731	64.074
2	43.320	650704	9973	50.269	35.926
Total		1294443	27759	100.000	100.000

==== Shimadzu LCsolution Analysis Report ====

C:\LabSolutions\Data\DMM\DVR04186B D1_9182016_1754 PM_6.lcd

Acquired by	: LC User
Sample Name	: DVR04186B D1
Sample ID	: DVR04186B D1
Tray#	: 1
Vail #	: 2
Injection Volume	: 3 uL
Data File Name	: DVR04186B D1_9182016_1754 PM_6.lcd
Method File Name	: col1_5isoiPA_60min_1ML_220and210.lcm
Batch File Name	: DMM.lcb
Report File Name	: Default.lcr
Data Acquired	: 9/18/2016 8:06:04 PM
Data Processed	: 9/18/2016 9:06:05 PM

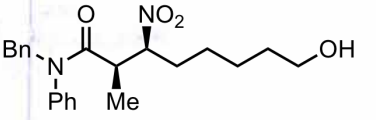

3.53A
88% ee

<Chromatogram>

C:\LabSolutions\Data\DMM\DVR04186B D1_9182016_1754 PM_6.lcd

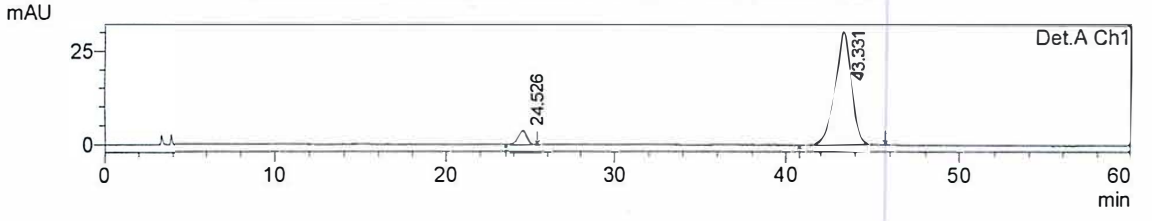

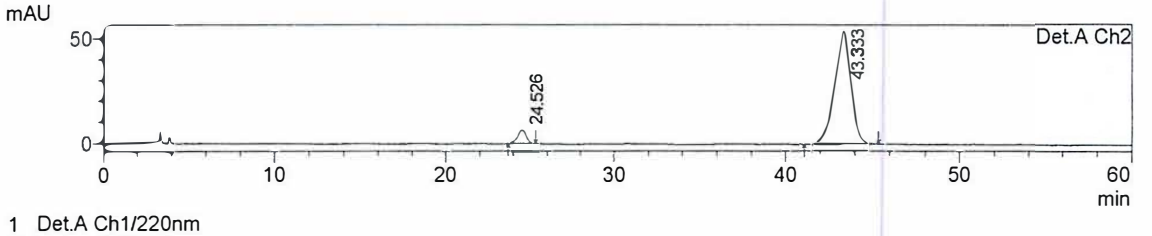

1 Det.A Ch1/220nm
2 Det.A Ch2/210nm

PeakTable

Detector A Ch1 220nm

Peak#	Ret. Time	Area	Height	Area %	Height %
1	24.526	134003	3734	6.313	10.848
2	43.331	1988561	30690	93.687	89.152
Total		2122564	34424	100.000	100.000

PeakTable

Detector A Ch2 210nm

Peak#	Ret. Time	Area	Height	Area %	Height %
1	24.526	229459	6505	6.186	10.782
2	43.333	3479887	53829	93.814	89.218
Total		3709345	60334	100.000	100.000

==== Shimadzu LCsolution Analysis Report ====

C:\LabSolutions\Data\DMM\DVR04186B RAC D2_9182016_1754 PM_10.lcd

Acquired by	: LC User
Sample Name	: DVR04186B RAC D2
Sample ID	: DVR04186B RAC D2
Tray#	: 1
Vail #	: 3
Injection Volume	: 3 uL
Data File Name	: DVR04186B RAC D2_9182016_1754 PM_10.lcd
Method File Name	: col2_15isoiPA_20min_1ML_220and210.lcm
Batch File Name	: DMM.lcb
Report File Name	: Default.lcr
Data Acquired	: 9/18/2016 9:37:02 PM
Data Processed	: 9/18/2016 9:57:02 PM

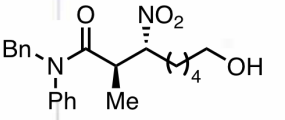

3.53B
racemic

<Chromatogram>

C:\LabSolutions\Data\DMM\DVR04186B RAC D2_9182016_1754 PM_10.lcd

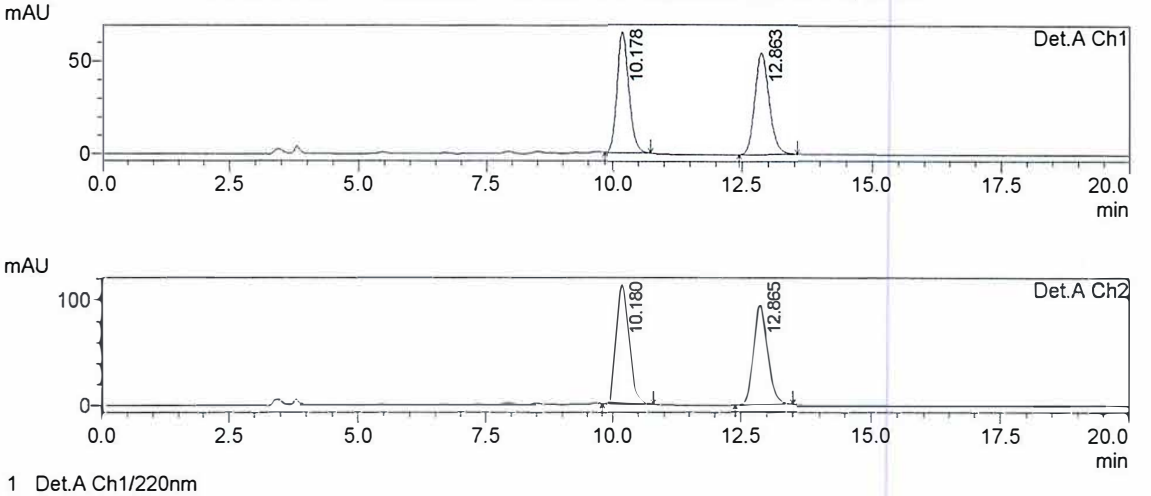

1 Det.A Ch1/220nm
2 Det.A Ch2/210nm

PeakTable

Detector A Ch1 220nm

Peak#	Ret. Time	Area	Height	Area %	Height %
1	10.178	1035088	64444	49.991	54.356
2	12.863	1035462	54116	50.009	45.644
Total		2070550	118559	100.000	100.000

PeakTable

Detector A Ch2 210nm

Peak#	Ret. Time	Area	Height	Area %	Height %
1	10.180	1824405	113225	50.147	54.363
2	12.865	1813704	95049	49.853	45.637
Total		3638109	208274	100.000	100.000

==== Shimadzu LCsolution Analysis Report ====

C:\LabSolutions\Data\DMM\DVR04186B D2_9182016_1754 PM_14.lcd

Acquired by	: LC User
Sample Name	: DVR04186B D2
Sample ID	: DVR04186B D2
Tray#	: 1
Vail #	: 4
Injection Volume	: 3 uL
Data File Name	: DVR04186B D2_9182016_1754 PM_14.lcd
Method File Name	: col2_15isoiPA_20min_1ML_220and210.lcm
Batch File Name	: DMM.lcb
Report File Name	: Default.lcr
Data Acquired	: 9/18/2016 10:27:57 PM
Data Processed	: 9/18/2016 10:47:57 PM

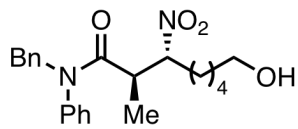

3.53B
78% ee

<Chromatogram>

C:\LabSolutions\Data\DMM\DVR04186B D2_9182016_1754 PM_14.lcd

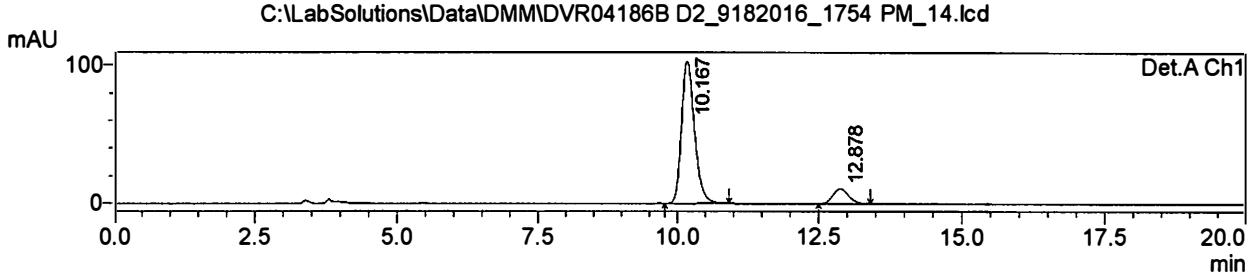

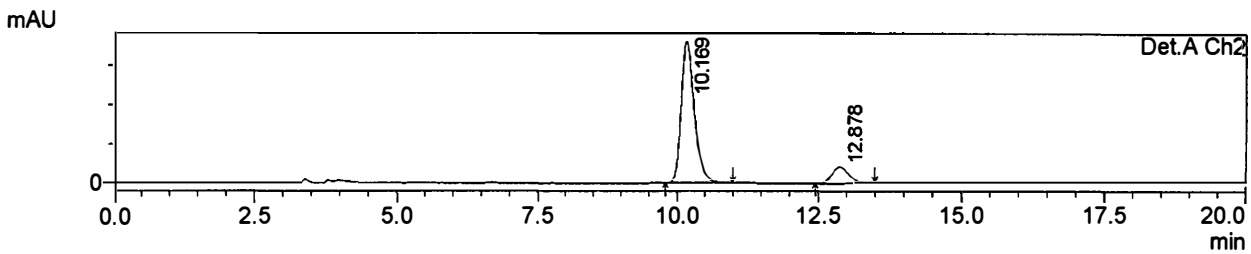

1 Det.A Ch1/220nm
2 Det.A Ch2/210nm

PeakTable

Detector A Ch1 220nm

Peak#	Ret. Time	Area	Height	Area %	Height %
1	10.167	1660610	102762	88.791	90.266
2	12.878	209636	11081	11.209	9.734
Total		1870245	113843	100.000	100.000

PeakTable

Detector A Ch2 210nm

Peak#	Ret. Time	Area	Height	Area %	Height %
1	10.169	2924609	180679	88.656	90.262
2	12.878	374237	19494	11.344	9.738
Total		3298846	200173	100.000	100.000

Parameter	Value
1 Title	DVR04156CRD.1.fid
2 Solvent	CDCl3
3 Temperature	297.6
4 Number of Scans	16
5 Receiver Gain	114
6 Relaxation Delay	1.0000
7 Pulse Width	10.7700
8 Spectrometer Frequency	600.32
9 Nucleus	1H

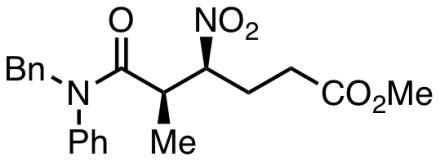

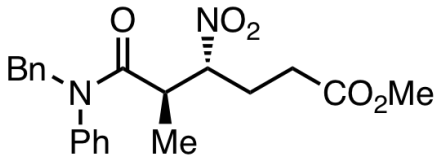

Crude

3.54A **71:29** **3.54B**

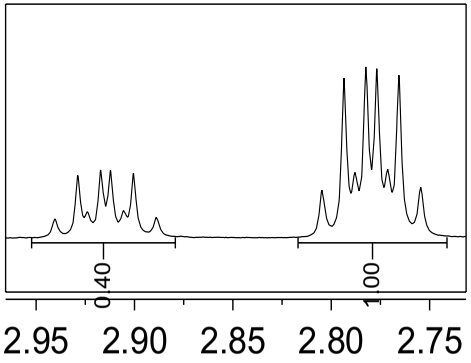

565

Parameter	Value
1 Title	DVR04156D1.2.fid
2 Solvent	CDCl3
3 Temperature	298.0
4 Number of Scans	16
5 Receiver Gain	181
6 Relaxation Delay	1.0000
7 Pulse Width	10.7700
8 Spectrometer Frequency	600.32
9 Nucleus	1H

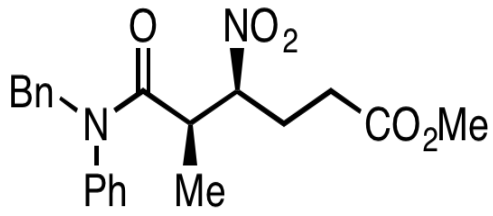

3.54A

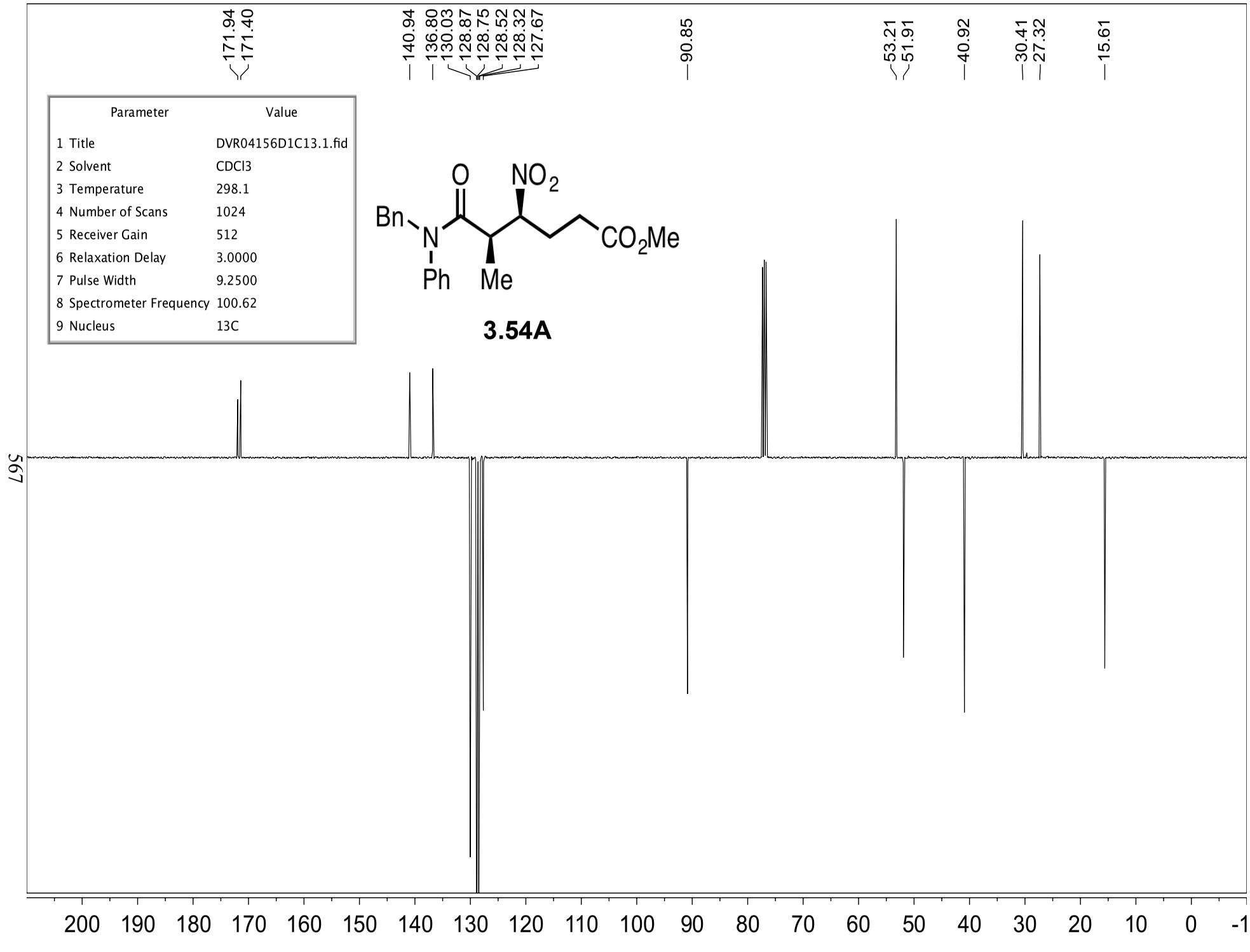
171.94
171.40
140.94
136.80
130.03
128.87
128.75
128.52
128.32
127.67
90.85
53.21
51.91
40.92
30.41
27.32
15.61
Parameter Value
1 Title DVR04156D1C13.1.fid
2 Solvent CDCl3
3 Temperature 298.1
4 Number of Scans 1024
5 Receiver Gain 512
6 Relaxation Delay 3.0000
7 Pulse Width 9.2500
8 Spectrometer Frequency 100.62
9 Nucleus 13C
O
NO2
Bn
N
Ph
Me
CO2Me
3.54A
567
200 190 180 170 160 150 140 130 120 110 100 90 80 70 60 50 40 30 20 10 0 -1

Parameter	Value
1 Title	DVR04156D2.1.fid
2 Solvent	CDCl3
3 Temperature	298.2
4 Number of Scans	16
5 Receiver Gain	13
6 Relaxation Delay	1.0000
7 Pulse Width	15.0000
8 Spectrometer Frequency	400.13
9 Nucleus	1H

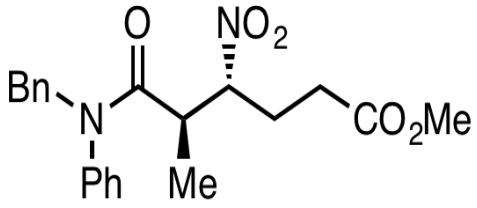

3.54B

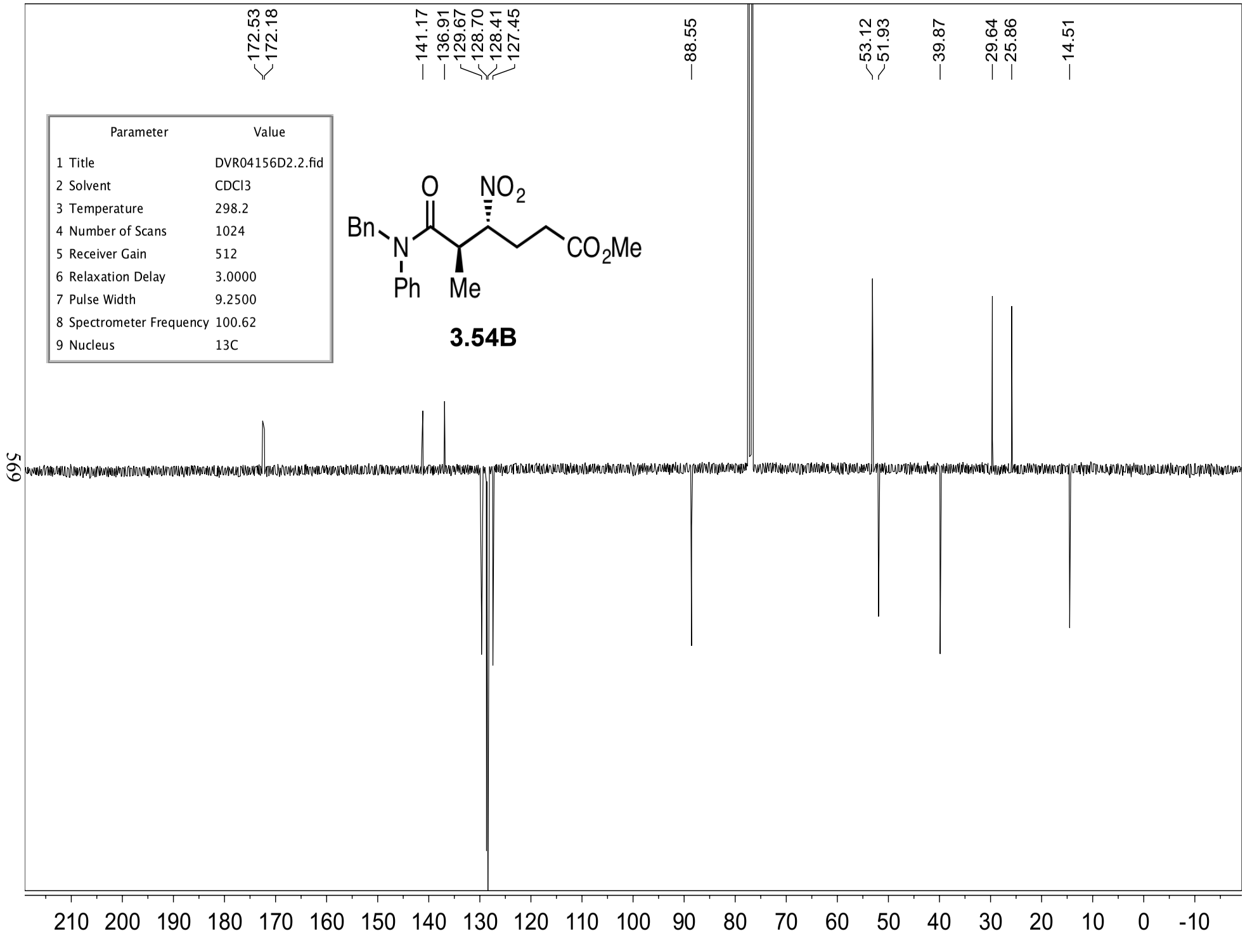
172.53
172.18
141.17
136.91
129.67
128.70
128.41
127.45
88.55
53.12
51.93
39.87
29.64
25.86
14.51
Parameter Value
1 Title DVR04156D2.2.fid
2 Solvent CDCl3
3 Temperature 298.2
4 Number of Scans 1024
5 Receiver Gain 512
6 Relaxation Delay 3.0000
7 Pulse Width 9.2500
8 Spectrometer Frequency 100.62
9 Nucleus 13C
O
NO2
Bn
N
Ph
Me
CO2Me
3.54B
569
210 200 190 180 170 160 150 140 130 120 110 100 90 80 70 60 50 40 30 20 10 0 -10

==== Shimadzu LCsolution Analysis Report ====

C:\LabSolutions\Data\DMM\DVR04153 RAC SYN_8102016_1351 PM_3.lcd

Acquired by	: LC User
Sample Name	: DVR04153 RAC SYN
Sample ID	: DVR04153 RAC SYN
Tray#	: 1
Vail #	: 1
Injection Volume	: 3 uL
Data File Name	: DVR04153 RAC SYN_8102016_1351 PM_3.lcd
Method File Name	: col1_1.5isoiPA_55min_1ml_220and210.lcm
Batch File Name	: DMM.lcb
Report File Name	: Default.lcr
Data Acquired	: 8/10/2016 3:37:04 PM
Data Processed	: 8/10/2016 4:32:07 PM

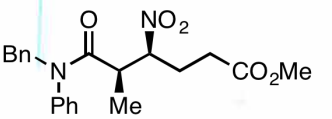

3.54A
racemic

<Chromatogram>

C:\LabSolutions\Data\DMM\DVR04153 RAC SYN_8102016_1351 PM_3.lcd

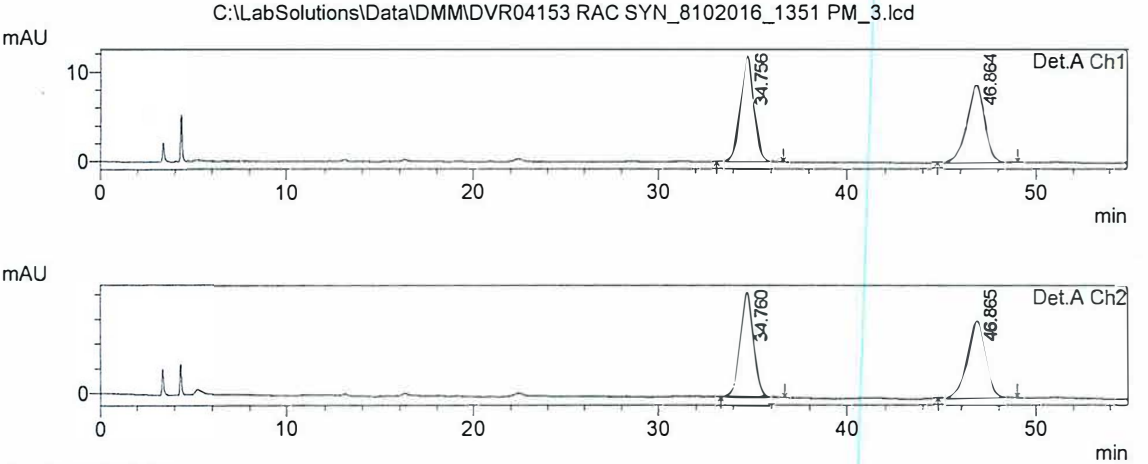

1 Det.A Ch1/220nm
2 Det.A Ch2/210nm

PeakTable

Detector A Ch1 220nm

Peak#	Ret. Time	Area	Height	Area %	Height %
1	34.756	572557	11875	49.859	57.801
2	46.864	575787	8670	50.141	42.199
Total		1148343	20545	100.000	100.000

PeakTable

Detector A Ch2 210nm

Peak#	Ret. Time	Area	Height	Area %	Height %
1	34.760	1036821	21570	49.769	57.706
2	46.865	1046448	15809	50.231	42.294
Total		2083269	37379	100.000	100.000

==== Shimadzu LCsolution Analysis Report ====

C:\LabSolutions\Data\DMM\DVR04156 SYN_8102016_1351 PM_1.lcd

Acquired by	: LC User
Sample Name	: DVR04156 SYN
Sample ID	: DVR04156 SYN
Tray#	: 1
Vail #	: 2
Injection Volume	: 1 uL
Data File Name	: DVR04156 SYN_8102016_1351 PM_1.lcd
Method File Name	: col1_1.5isoiPA_55min_1ml_220and210.lcm
Batch File Name	: DMM.lcb
Report File Name	: Default.lcr
Data Acquired	: 8/10/2016 5:13:02 PM
Data Processed	: 8/10/2016 6:08:03 PM

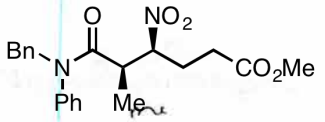

3.54A
87% ee

<Chromatogram>

C:\LabSolutions\Data\DMM\DVR04156 SYN_8102016_1351 PM_1.lcd

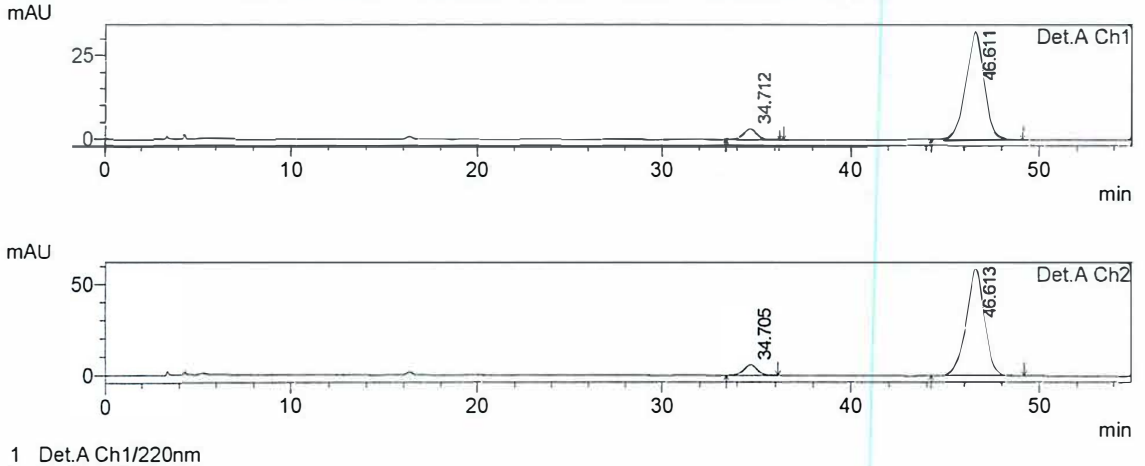

1 Det.A Ch1/220nm
2 Det.A Ch2/210nm

PeakTable

Detector A Ch1 220nm

Peak#	Ret. Time	Area	Height	Area %	Height %
1	34.712	150536	3140	6.474	8.778
2	46.611	2174624	32634	93.526	91.222
Total		2325160	35774	100.000	100.000

PeakTable

Detector A Ch2 210nm

Peak#	Ret. Time	Area	Height	Area %	Height %
1	34.705	279420	5785	6.590	8.862
2	46.613	3960833	59486	93.410	91.138
Total		4240253	65270	100.000	100.000

==== Shimadzu LCsolution Analysis Report ====

C:\LabSolutions\Data\DMM\DVR04153 RAC ANTI1_8122016_859 AM_11.lcd

Acquired by	: LC User
Sample Name	: DVR04153 RAC ANTI1
Sample ID	: DVR04153 RAC ANTI1
Tray#	: 1
Vail #	: 3
Injection Volume	: 2 uL
Data File Name	: DVR04153 RAC ANTI1_8122016_859 AM_11.lcd
Method File Name	: col2_5isoiPA_30min_1ML_254and210.lcm
Batch File Name	: DMM.lcb
Report File Name	: Default.lcr
Data Acquired	: 8/12/2016 8:03:35 PM
Data Processed	: 8/12/2016 8:33:37 PM

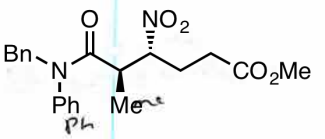

Anti 3.54B
racemic

<Chromatogram>

C:\LabSolutions\Data\DMM\DVR04153 RAC ANTI1_8122016_859 AM_11.lcd

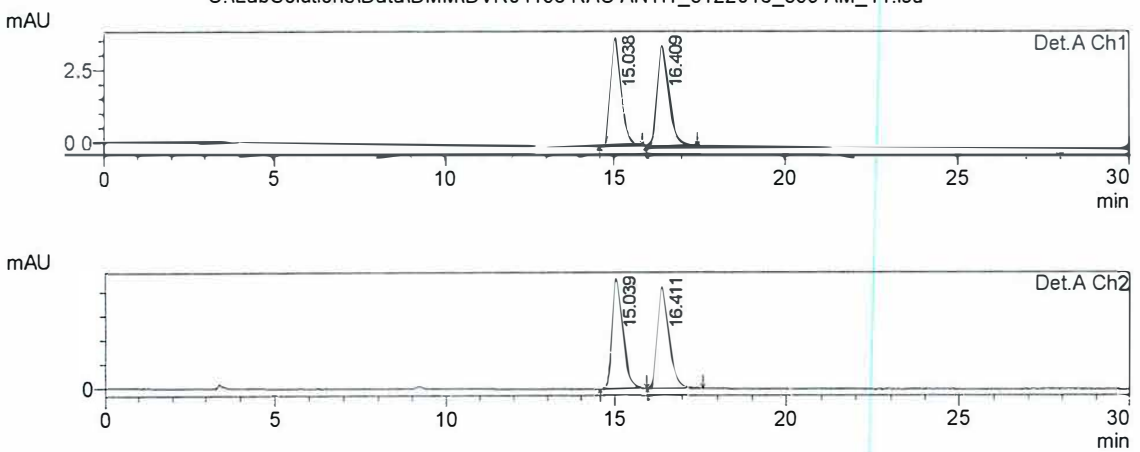

1 Det.A Ch1/254nm
2 Det.A Ch2/210nm

PeakTable

Detector A Ch1 254nm

Peak#	Ret. Time	Area	Height	Area %	Height %
1	15.038	78844	3721	49.687	51.848
2	16.409	79837	3456	50.313	48.152
Total		158681	7177	100.000	100.000

PeakTable

Detector A Ch2 210nm

Peak#	Ret. Time	Area	Height	Area %	Height %
1	15.039	1950335	91811	49.929	51.982
2	16.411	1955899	84808	50.071	48.018
Total		3906234	176619	100.000	100.000

==== Shimadzu LCsolution Analysis Report ====

C:\LabSolutions\Data\DMM\DVR04156 ANTI 1_8122016_859 AM_15.lcd

Acquired by	: LC User
Sample Name	: DVR04156 ANTI 1
Sample ID	: DVR04156 ANTI 1
Tray#	: 1
Vail #	: 4
Injection Volume	: 2 uL
Data File Name	: DVR04156 ANTI 1_8122016_859 AM_15.lcd
Method File Name	: col2_5isoiPA_30min_1ML_254and210.lcm
Batch File Name	: DMM.lcb
Report File Name	: Default.lcr
Data Acquired	: 8/12/2016 9:14:34 PM
Data Processed	: 8/12/2016 9:44:36 PM

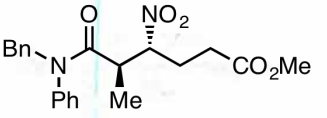

Anti **3.54B**
63% ee

<Chromatogram>

C:\LabSolutions\Data\DMM\DVR04156 ANTI 1_8122016_859 AM_15.lcd

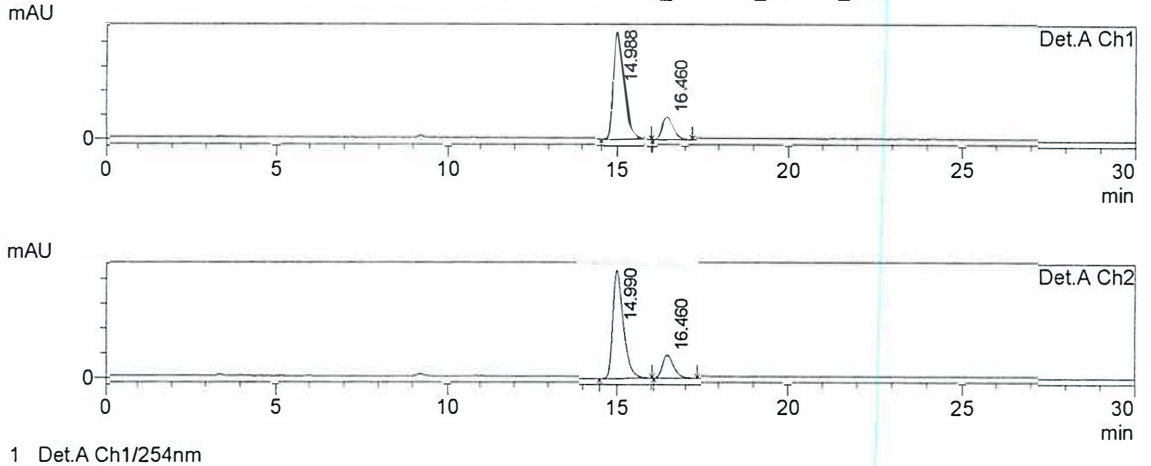

1 Det.A Ch1/254nm
2 Det.A Ch2/210nm

PeakTable

Detector A Ch1 254nm

Peak#	Ret. Time	Area	Height	Area %	Height %
1	14.988	190860	8863	81.634	82.328
2	16.460	42939	1902	18.366	17.672
Total		233799	10765	100.000	100.000

PeakTable

Detector A Ch2 210nm

Peak#	Ret. Time	Area	Height	Area %	Height %
1	14.990	4691540	217336	81.423	82.165
2	16.460	1070383	47175	18.577	17.835
Total		5761923	264510	100.000	100.000

Parameter	Value
1 Title	RS-01-247-crude.1.fid
2 Solvent	CDCl3
3 Temperature	297.1
4 Number of Scans	16
5 Receiver Gain	181
6 Relaxation Delay	1.0000
7 Pulse Width	10.7700
8 Spectrometer Frequency	600.32
9 Nucleus	1H

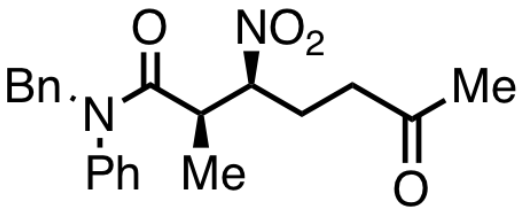

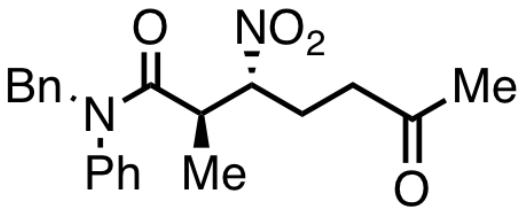

Crude

3.55A **67:33** **3.55B**

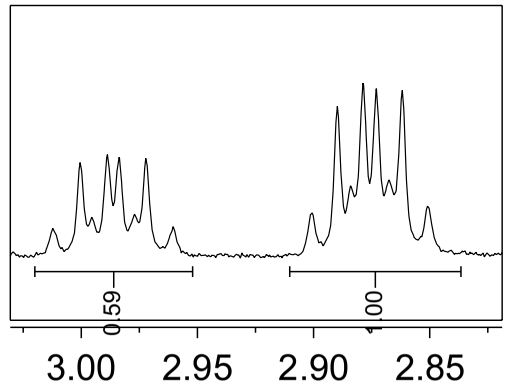

574

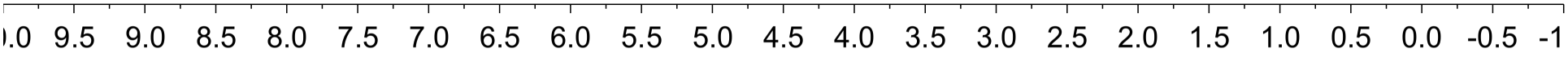

Parameter	Value
1 Title	RS-01-247-C2-D1.1.fid
2 Solvent	CDCl3
3 Temperature	298.0
4 Number of Scans	16
5 Receiver Gain	144
6 Relaxation Delay	1.0000
7 Pulse Width	10.7700
8 Spectrometer Frequency	600.32
9 Nucleus	1H

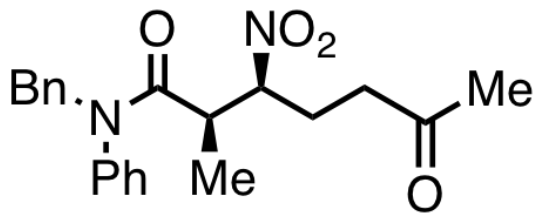

3.55A

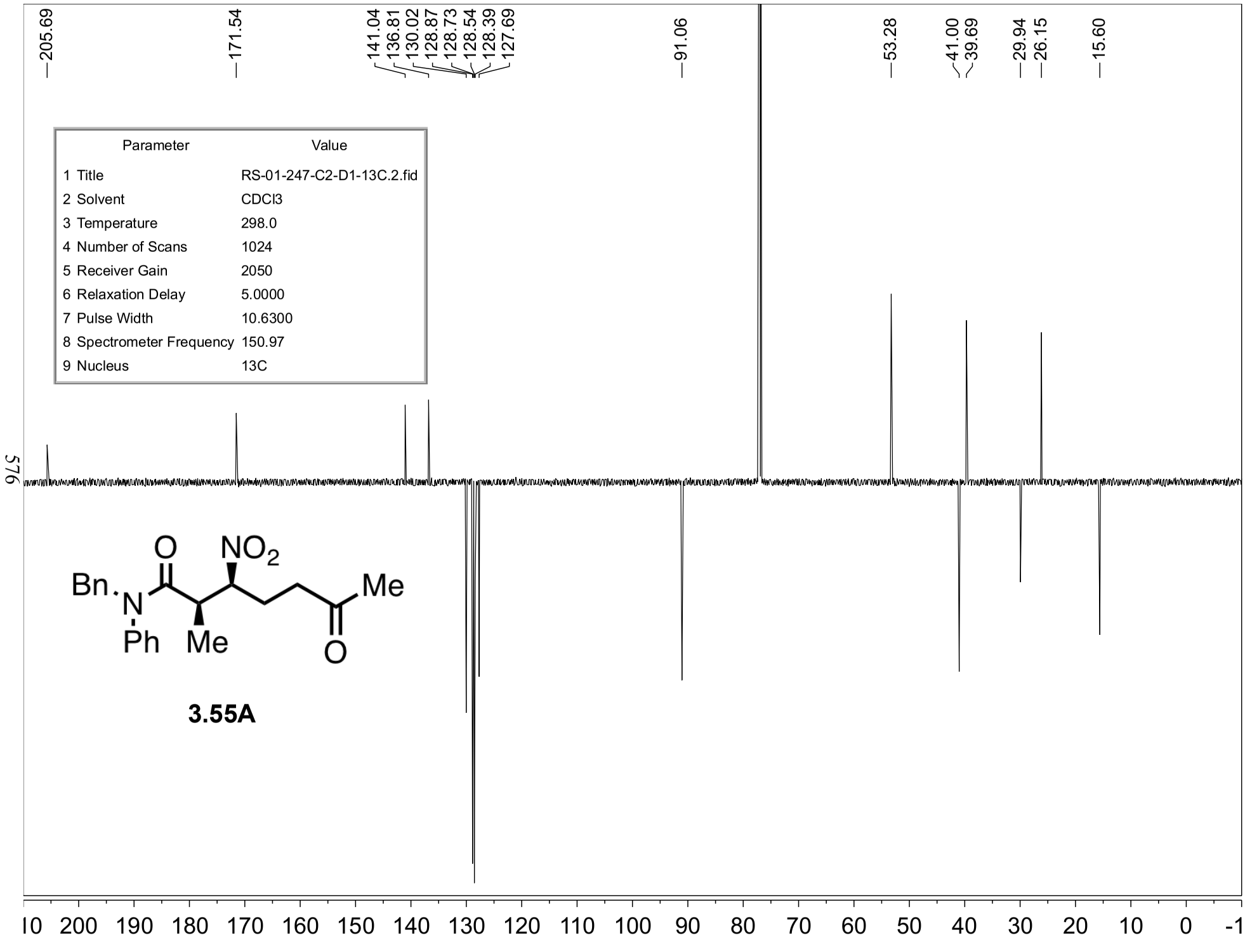
205.69
171.54
141.04
136.81
130.02
128.87
128.73
128.54
128.39
127.69
91.06
53.28
41.00
39.69
29.94
26.15
15.60
Parameter Value
1 Title RS-01-247-C2-D1-13C.2.fid
2 Solvent CDCl3
3 Temperature 298.0
4 Number of Scans 1024
5 Receiver Gain 2050
6 Relaxation Delay 5.0000
7 Pulse Width 10.6300
8 Spectrometer Frequency 150.97
9 Nucleus 13C
576
Bn
N
Ph
Me
O
NO2
Me
O
3.55A
10 200 190 180 170 160 150 140 130 120 110 100 90 80 70 60 50 40 30 20 10 0 -1

Parameter	Value
1 Title	RS-01-247-D2.1.fid
2 Solvent	CDCl3
3 Temperature	297.5
4 Number of Scans	16
5 Receiver Gain	64
6 Relaxation Delay	10.0000
7 Pulse Width	10.7700
8 Spectrometer Frequency	600.32
9 Nucleus	1H

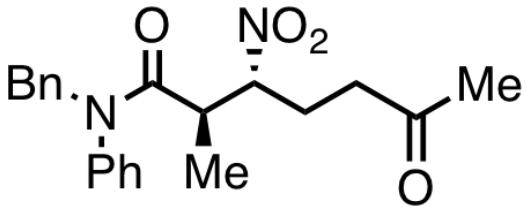

3.55B

206.12
172.63
140.92
136.96
129.64
128.71
128.57
128.41
127.44
88.77
53.13
40.24
38.83
30.06
24.66
14.57

Parameter	Value
1 Title	RS-01-247-D2-13C.1.fid
2 Solvent	CDCl3
3 Temperature	298.0
4 Number of Scans	1024
5 Receiver Gain	2050
6 Relaxation Delay	5.0000
7 Pulse Width	10.6300
8 Spectrometer Frequency	150.97
9 Nucleus	13C

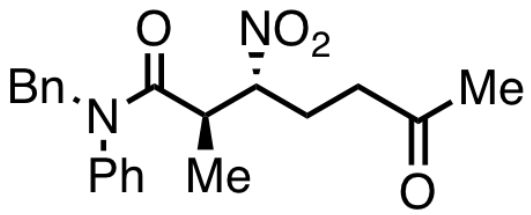

3.55B

10 200 190 180 170 160 150 140 130 120 110 100 90 80 70 60 50 40 30 20 10 0

==== Shimadzu LCsolution Analysis Report ====

C:\LabSolutions\Data\DMM\RS-01-247-RESD1_10272016_853 AM_4.lcd

Acquired by	: LC User
Sample Name	: RS-01-247-RESD1
Sample ID	: RS-01-247-RESD1
Tray#	: 1
Vail #	: 91
Injection Volume	: 3 uL
Data File Name	: RS-01-247-RESD1_10272016_853 AM_4.lcd
Method File Name	: col1_3isoiPA_45min_1ML_254and210.lcm
Batch File Name	: DMM.lcb
Report File Name	: Default.lcr
Data Acquired	: 10/27/2016 10:49:50 AM
Data Processed	: 10/27/2016 11:34:53 AM

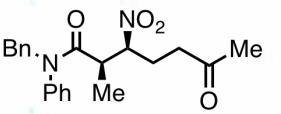

3.55A
racemic

<Chromatogram>

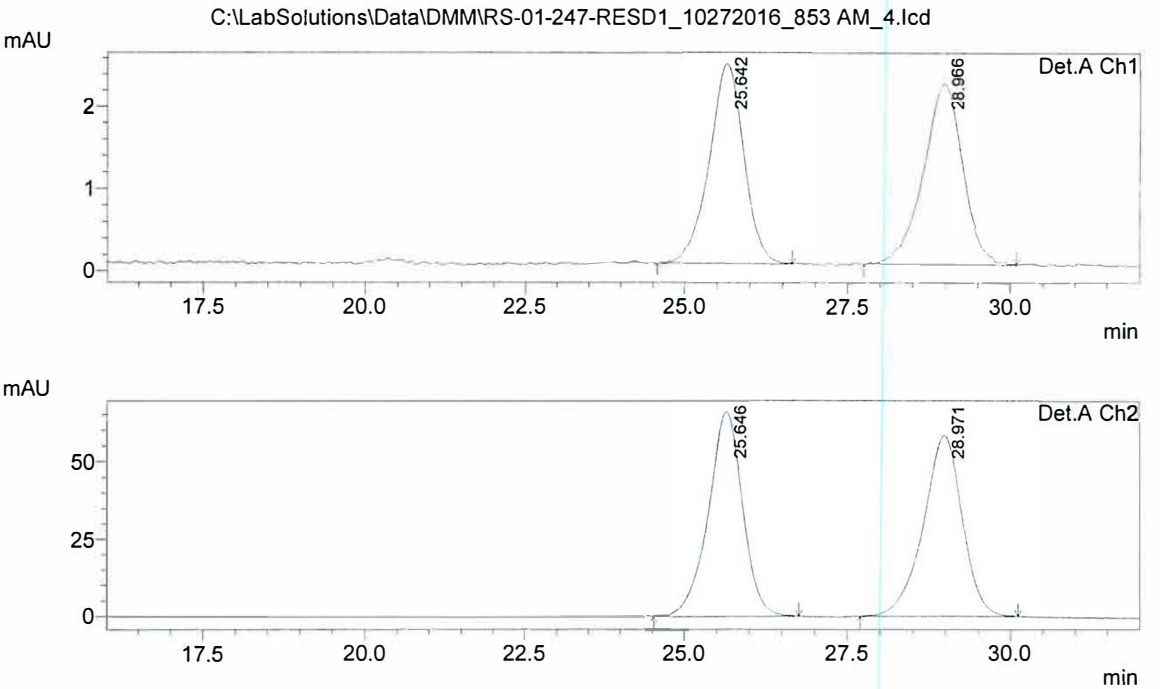

1 Det.A Ch1/254nm
2 Det.A Ch2/210nm

PeakTable

Detector A Ch1 254nm

Peak#	Ret. Time	Area	Height	Area %	Height %
1	25.642	89065	2431	49.047	52.432
2	28.966	92527	2205	50.953	47.568
Total		181592	4636	100.000	100.000

PeakTable

Detector A Ch2 210nm

Peak#	Ret. Time	Area	Height	Area %	Height %
1	25.646	2422797	65652	49.984	53.023
2	28.971	2424345	58167	50.016	46.977
Total		4847142	123819	100.000	100.000

==== Shimadzu LCsolution Analysis Report ====

C:\LabSolutions\Data\DMM\RS-01-247-D1_10242016_2114 PM_4.lcd

Acquired by	: LC User
Sample Name	: RS-01-247-D1
Sample ID	: RS-01-247-D1
Tray#	: 1
Vail #	: 92
Injection Volume	: 3 uL
Data File Name	: RS-01-247-D1_10242016_2114 PM_4.lcd
Method File Name	: col1_3isoiPA_60min_1ML_254and210.lcm
Batch File Name	: DMM.lcb
Report File Name	: Default.lcr
Data Acquired	: 10/24/2016 10:06:00 PM
Data Processed	: 12/20/2016 12:42:13 PM

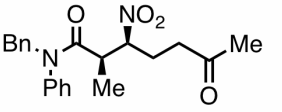

3.55A
85% ee

<Chromatogram>

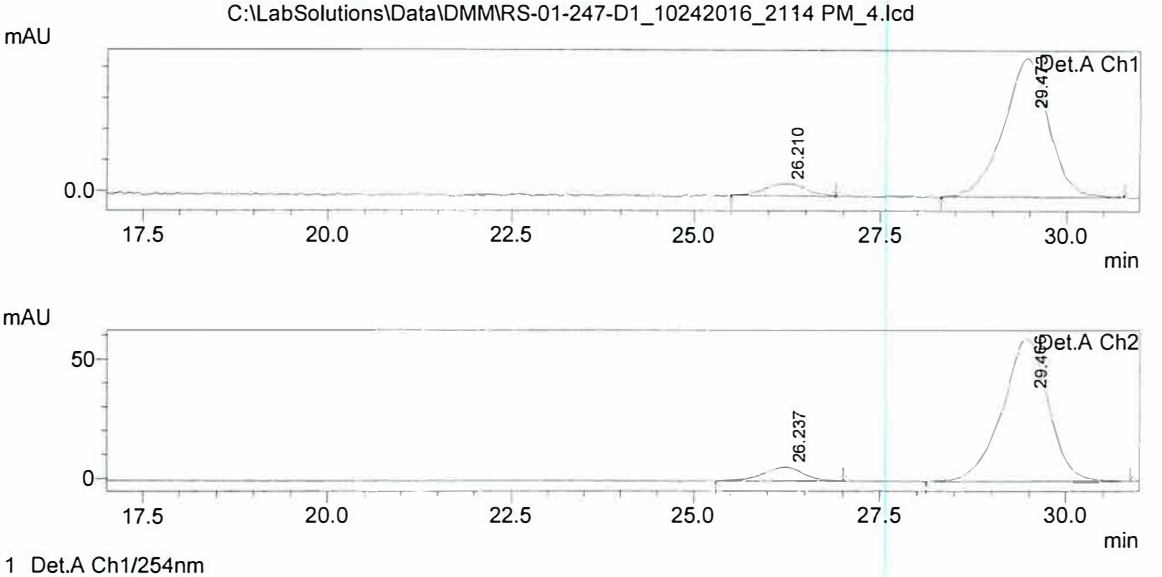

1 Det.A Ch1/254nm
2 Det.A Ch2/210nm

PeakTable

Detector A Ch1 254nm

Peak#	Ret. Time	Area	Height	Area %	Height %
1	26.210	7729	196	7.547	8.102
2	29.473	94683	2225	92.453	91.898
Total		102412	2421	100.000	100.000

PeakTable

Detector A Ch2 210nm

Peak#	Ret. Time	Area	Height	Area %	Height %
1	26.237	210828	5600	7.591	8.553
2	29.466	2566655	59873	92.409	91.447
Total		2777482	65474	100.000	100.000

==== Shimadzu LCsolution Analysis Report ====

C:\LabSolutions\Data\DMM\RS-01-247-RESD2_10272016_853 AM_5.lcd

Acquired by	: LC User
Sample Name	: RS-01-247-RESD2
Sample ID	: RS-01-247-RESD2
Tray#	: 1
Vail #	: 93
Injection Volume	: 3 uL
Data File Name	: RS-01-247-RESD2_10272016_853 AM_5.lcd
Method File Name	: col1_3isoiPA_60min_1ML_254and210.lcm
Batch File Name	: DMM.lcb
Report File Name	: Default.lcr
Data Acquired	: 10/27/2016 12:42:20 PM
Data Processed	: 10/31/2016 8:14:16 AM

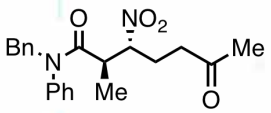

3.55B
racemic

<Chromatogram>

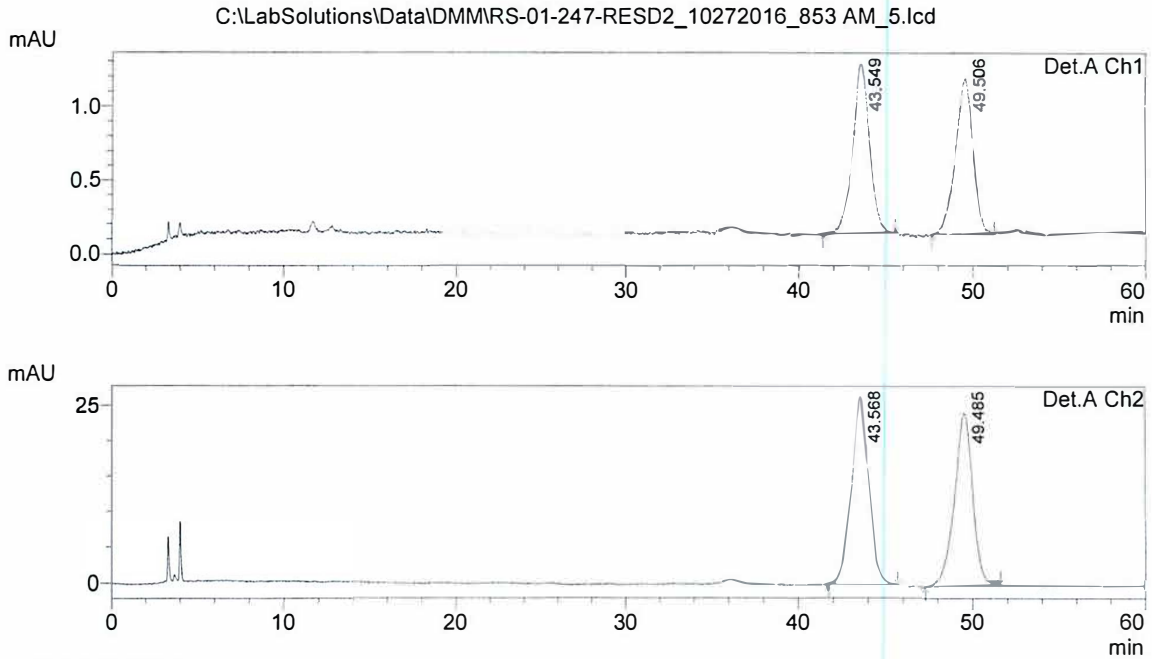

1 Det.A Ch1/254nm
2 Det.A Ch2/210nm

PeakTable

Detector A Ch1 254nm

Peak#	Ret. Time	Area	Height	Area %	Height %
1	43.549	76267	1139	50.922	52.067
2	49.506	73505	1049	49.078	47.933
Total		149773	2188	100.000	100.000

PeakTable

Detector A Ch2 210nm

Peak#	Ret. Time	Area	Height	Area %	Height %
1	43.568	1790765	26534	50.525	52.094
2	49.485	1753536	24401	49.475	47.906
Total		3544301	50935	100.000	100.000

==== Shimadzu LCsolution Analysis Report ====

C:\LabSolutions\Data\DMM\RS-01-247D2_10272016_853 AM_6.lcd

Acquired by	: LC User
Sample Name	: RS-01-247D2
Sample ID	: RS-01-247D2
Tray#	: 1
Vail #	: 94
Injection Volume	: 3 uL
Data File Name	: RS-01-247D2_10272016_853 AM_6.lcd
Method File Name	: col1_3isoiPA_60min_1ML_254and210.lcm
Batch File Name	: DMM.lcb
Report File Name	: Default.lcr
Data Acquired	: 10/27/2016 1:42:57 PM
Data Processed	: 10/31/2016 8:12:11 AM

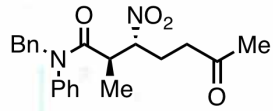

3.55B
84% ee

<Chromatogram>

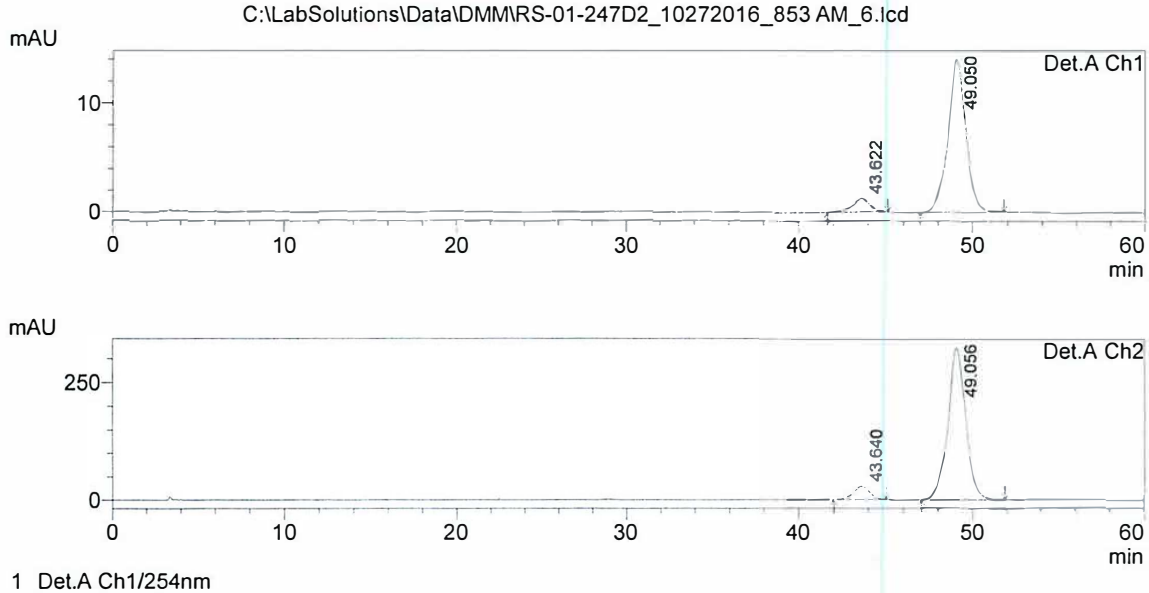

1 Det.A Ch1/254nm
2 Det.A Ch2/210nm

PeakTable

Detector A Ch1 254nm

Peak#	Ret. Time	Area	Height	Area %	Height %
1	43.622	87935	1268	7.909	8.278
2	49.050	1023909	14050	92.091	91.722
Total		1111844	15318	100.000	100.000

PeakTable

Detector A Ch2 210nm

Peak#	Ret. Time	Area	Height	Area %	Height %
1	43.640	1888494	29071	7.384	8.229
2	49.056	23688716	324191	92.616	91.771
Total		25577210	353262	100.000	100.000

Parameter	Value
1 Title	DVR04176CRD.1.fid
2 Solvent	CDCl3
3 Temperature	298.2
4 Number of Scans	16
5 Receiver Gain	4
6 Relaxation Delay	1.0000
7 Pulse Width	15.0000
8 Spectrometer Frequency	400.13
9 Nucleus	1H

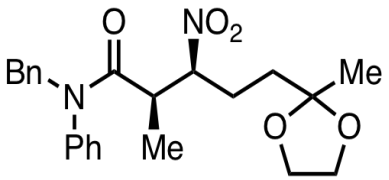

3.56A

Crude

71:29

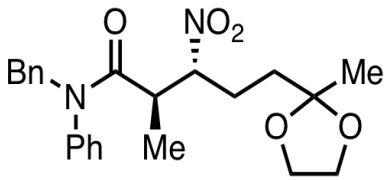

3.56B

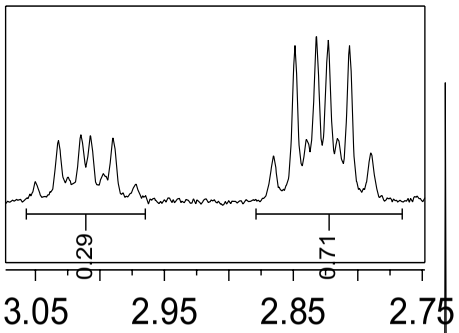

583

Parameter	Value
1 Title	DVR04176D1.1.fid
2 Solvent	CDCl3
3 Temperature	297.3
4 Number of Scans	16
5 Receiver Gain	161
6 Relaxation Delay	1.0000
7 Pulse Width	10.7700
8 Spectrometer Frequency	600.32
9 Nucleus	1H

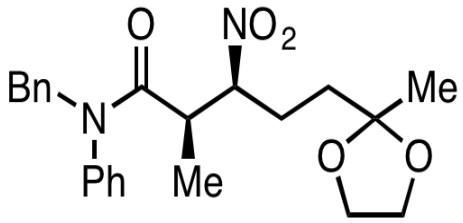

3.56A

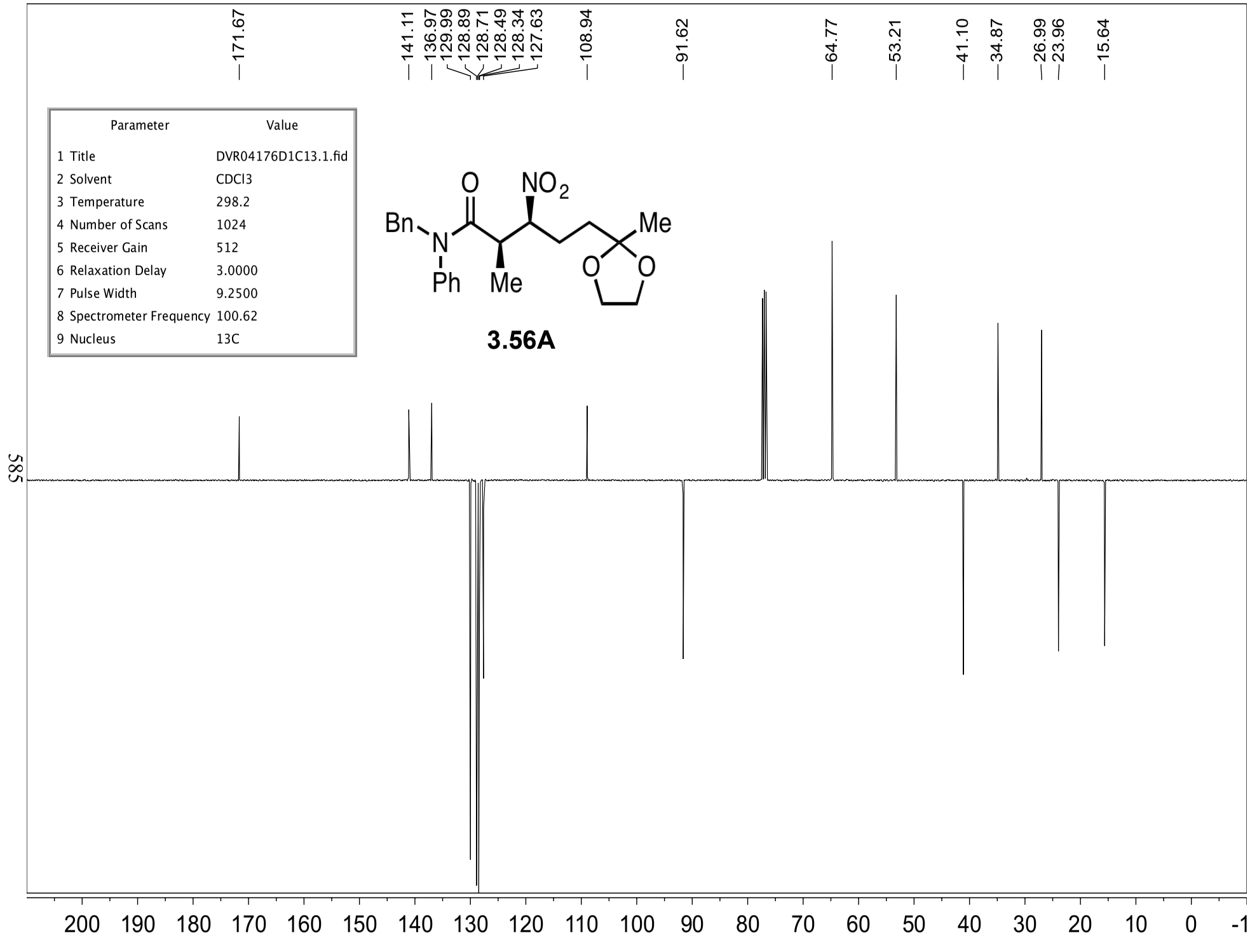
171.67
141.11
136.97
129.99
128.89
128.71
128.49
128.34
127.63
108.94
91.62
64.77
53.21
41.10
34.87
26.99
23.96
15.64
Parameter Value
1 Title DVR04176D1C13.1.fid
2 Solvent CDCl3
3 Temperature 298.2
4 Number of Scans 1024
5 Receiver Gain 512
6 Relaxation Delay 3.0000
7 Pulse Width 9.2500
8 Spectrometer Frequency 100.62
9 Nucleus 13C
O
NO2
Bn
N
Ph
Me
Me
O
O
3.56A
585
200 190 180 170 160 150 140 130 120 110 100 90 80 70 60 50 40 30 20 10 0 -1

Parameter	Value
1 Title	DVR04176D2-2.1.fid
2 Solvent	CDCl3
3 Temperature	297.4
4 Number of Scans	16
5 Receiver Gain	181
6 Relaxation Delay	1.0000
7 Pulse Width	10.7700
8 Spectrometer Frequency	600.32
9 Nucleus	1H

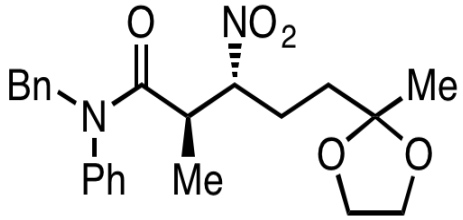

3.56B

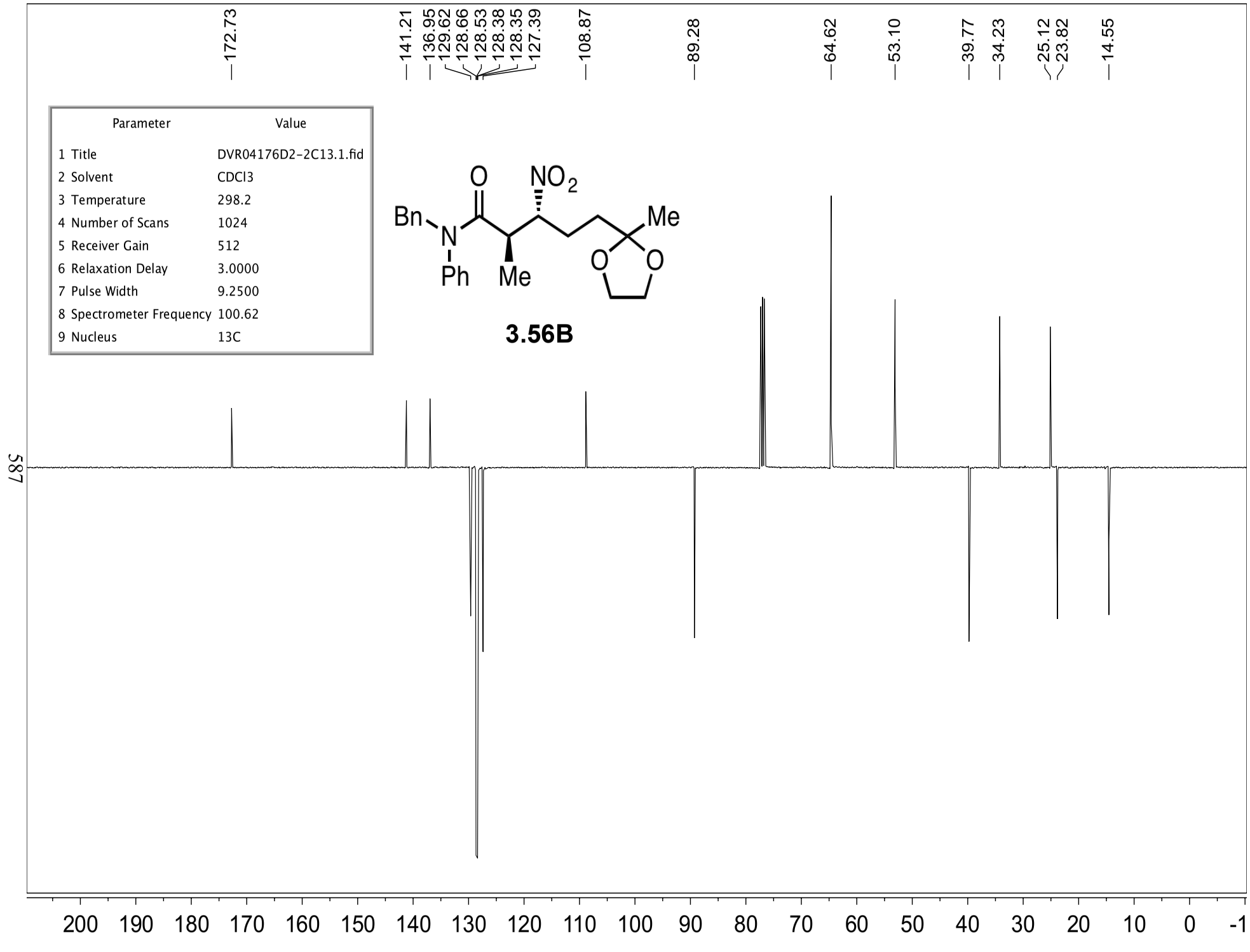
172.73
141.21
136.95
129.62
128.66
128.53
128.38
128.35
127.39
108.87
89.28
64.62
53.10
39.77
34.23
25.12
23.82
14.55
Parameter Value
1 Title DVR04176D2-2C13.1.fid
2 Solvent CDCl3
3 Temperature 298.2
4 Number of Scans 1024
5 Receiver Gain 512
6 Relaxation Delay 3.0000
7 Pulse Width 9.2500
8 Spectrometer Frequency 100.62
9 Nucleus 13C
O
NO2
Bn
N
Ph
Me
Me
O
O
3.56B
587
200 190 180 170 160 150 140 130 120 110 100 90 80 70 60 50 40 30 20 10 0 -1

==== Shimadzu LCsolution Analysis Report ====

C:\LabSolutions\Data\DMM\DVR04176D1 RAC_912016_1826 PM_2.lcd

Acquired by	: LC User
Sample Name	: DVR04176D1 RAC
Sample ID	: DVR04176D1 RAC
Tray#	: 1
Vail #	: 1
Injection Volume	: 2 uL
Data File Name	: DVR04176D1 RAC_912016_1826 PM_2.lcd
Method File Name	: col1_3isoiPA_30min_1ML_220and210.lcm
Batch File Name	: DMM.lcb
Report File Name	: Default.lcr
Data Acquired	: 9/1/2016 6:56:42 PM
Data Processed	: 9/1/2016 7:26:45 PM

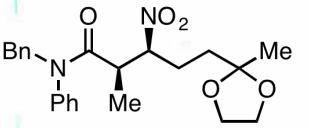

3.56A
racemic

<Chromatogram>

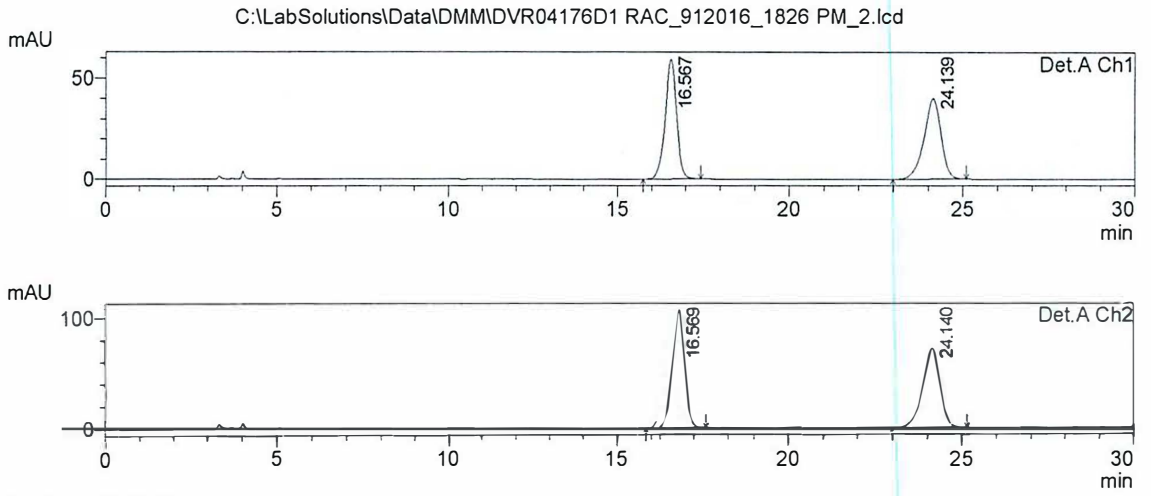

1 Det.A Ch1/220nm
2 Det.A Ch2/210nm

PeakTable

Detector A Ch1 220nm

Peak#	Ret. Time	Area	Height	Area %	Height %
1	16.567	1385353	59416	50.092	59.595
2	24.139	1380273	40283	49.908	40.405
Total		2765626	99700	100.000	100.000

PeakTable

Detector A Ch2 210nm

Peak#	Ret. Time	Area	Height	Area %	Height %
1	16.569	2486420	106893	49.990	59.569
2	24.140	2487449	72551	50.010	40.431
Total		4973869	179444	100.000	100.000

==== Shimadzu LCsolution Analysis Report ====

C:\LabSolutions\Data\DMM\DVR04176D1 SYN_912016_1826 PM_6.lcd

Acquired by	: LC User
Sample Name	: DVR04176D1 SYN
Sample ID	: DVR04176D1 SYN
Tray#	: 1
Vail #	: 2
Injection Volume	: 2 uL
Data File Name	: DVR04176D1 SYN_912016_1826 PM_6.lcd
Method File Name	: col1_3isoiPA_30min_1ML_220and210.lcm
Batch File Name	: DMM.lcb
Report File Name	: Default.lcr
Data Acquired	: 9/1/2016 8:07:38 PM
Data Processed	: 9/1/2016 8:37:39 PM

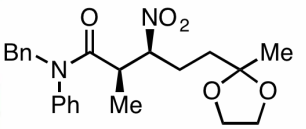

3.56A
89% ee

<Chromatogram>

C:\LabSolutions\Data\DMM\DVR04176D1 SYN_912016_1826 PM_6.lcd

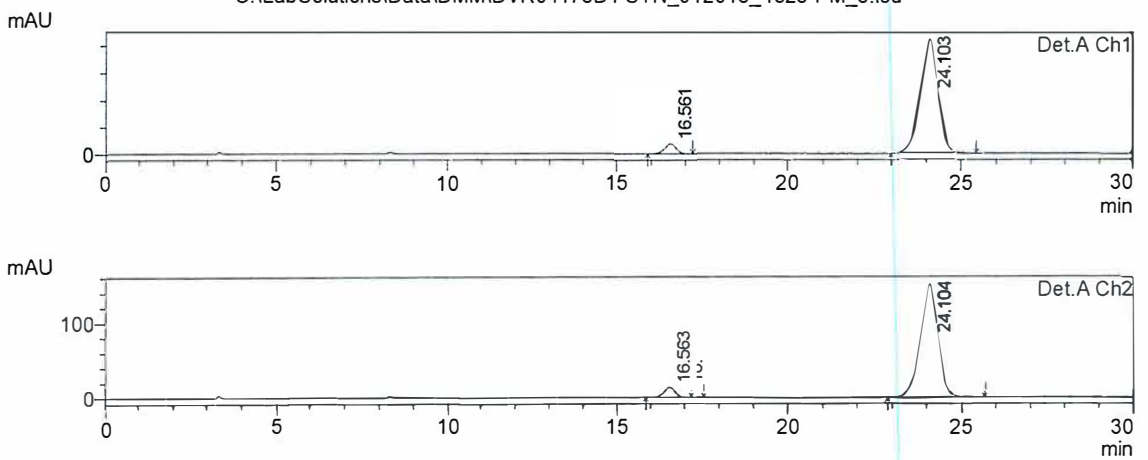

1 Det.A Ch1/220nm
2 Det.A Ch2/210nm

PeakTable

Detector A Ch1 220nm

Peak#	Ret. Time	Area	Height	Area %	Height %
1	16.561	178292	7696	5.702	8.267
2	24.103	2948606	85402	94.298	91.733
Total		3126898	93098	100.000	100.000

PeakTable

Detector A Ch2 210nm

Peak#	Ret. Time	Area	Height	Area %	Height %
1	16.563	320036	13837	5.672	8.257
2	24.104	5321908	153737	94.328	91.743
Total		5641945	167574	100.000	100.000

==== Shimadzu LCsolution Analysis Report ====

C:\LabSolutions\Data\DMM\DVR04176D2 RAC_922016_1106 AM_2.lcd

Acquired by	: LC User
Sample Name	: DVR04176D2 RAC
Sample ID	: DVR04176D2 RAC
Tray#	: 1
Vail #	: 1
Injection Volume	: 2 uL
Data File Name	: DVR04176D2 RAC_922016_1106 AM_2.lcd
Method File Name	: col1_3isoiPA_45min_1ML_220and210.lcm
Batch File Name	: DMM.lcb
Report File Name	: Default.lcr
Data Acquired	: 9/2/2016 11:52:31 AM
Data Processed	: 9/2/2016 12:37:32 PM

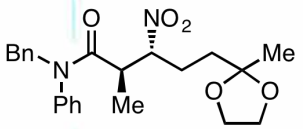

(±) Anti **3.56B racemic**

<Chromatogram>

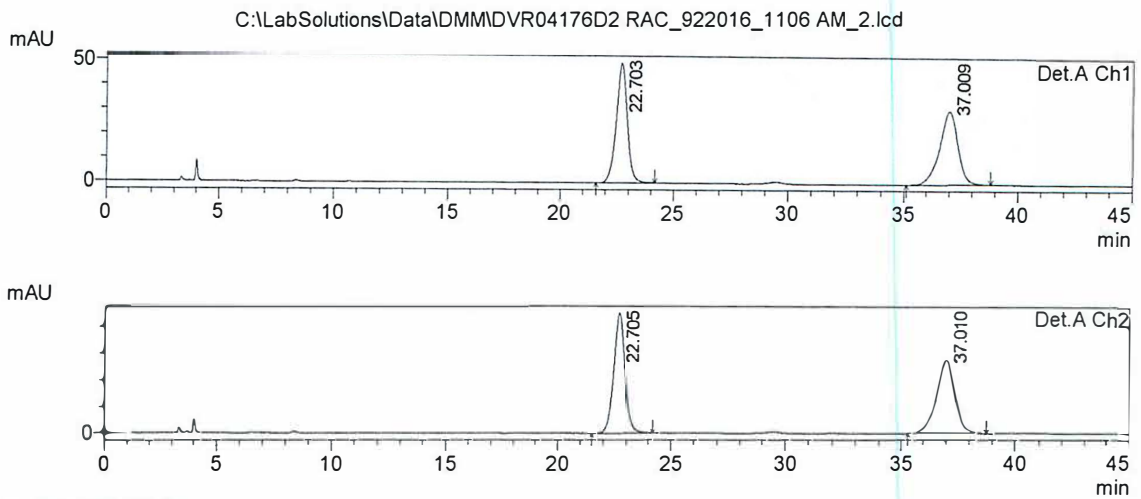

1 Det.A Ch1/220nm
2 Det.A Ch2/210nm

PeakTable

Detector A Ch1 220nm

Peak#	Ret. Time	Area	Height	Area %	Height %
1	22.703	1695439	49784	49.579	61.673
2	37.009	1724221	30939	50.421	38.327
Total		3419661	80723	100.000	100.000

PeakTable

Detector A Ch2 210nm

Peak#	Ret. Time	Area	Height	Area %	Height %
1	22.705	3103114	91134	49.746	61.735
2	37.010	3134829	56487	50.254	38.265
Total		6237943	147621	100.000	100.000

==== Shimadzu LCsolution Analysis Report ====

C:\LabSolutions\Data\DMM\DVR04176D2 anti_922016_1106 AM_6.lcd

Acquired by	: LC User
Sample Name	: DVR04176D2 anti
Sample ID	: DVR04176D2 anti
Tray#	: 1
Vail #	: 2
Injection Volume	: 2 uL
Data File Name	: DVR04176D2 anti_922016_1106 AM_6.lcd
Method File Name	: col1_3isoiPA_45min_1ML_220and210.lcm
Batch File Name	: DMM.lcb
Report File Name	: Default.lcr
Data Acquired	: 9/2/2016 1:33:25 PM
Data Processed	: 9/2/2016 2:18:28 PM

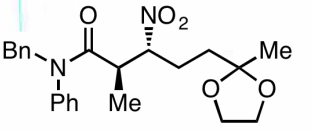

3.56B
75% ee

<Chromatogram>

C:\LabSolutions\Data\DMM\DVR04176D2 anti_922016_1106 AM_6.lcd

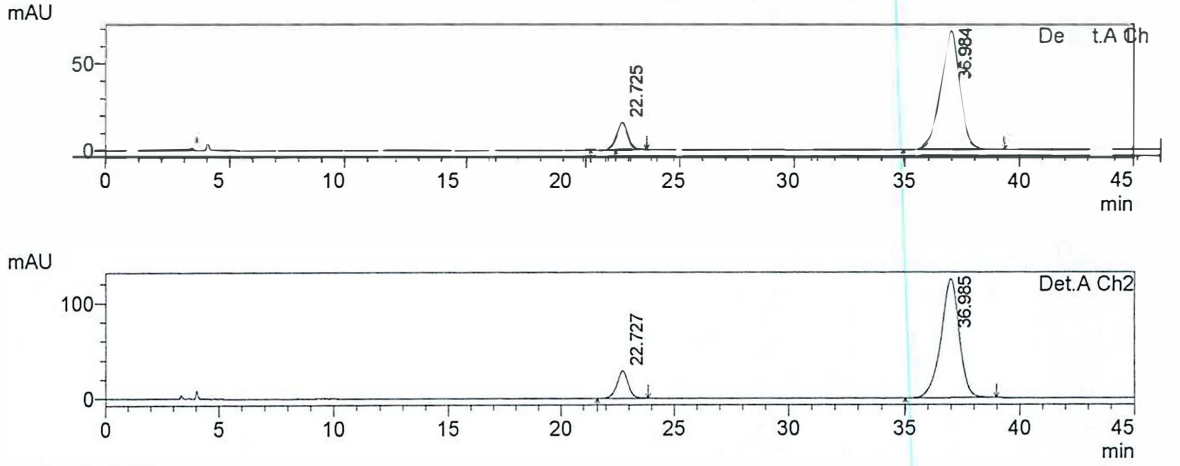

1 Det.A Ch1/220nm
2 Det.A Ch2/210nm

PeakTable

Detector A Ch1 220nm

Peak#	Ret. Time	Area	Height	Area %	Height %
1	22.725	532796	15633	12.406	18.626
2	36.984	3761888	68295	87.594	81.374
Total		4294684	83928	100.000	100.000

PeakTable

Detector A Ch2 210nm

Peak#	Ret. Time	Area	Height	Area %	Height %
1	22.727	982074	28668	12.515	18.662
2	36.985	6865144	124952	87.485	81.338
Total		7847218	153621	100.000	100.000

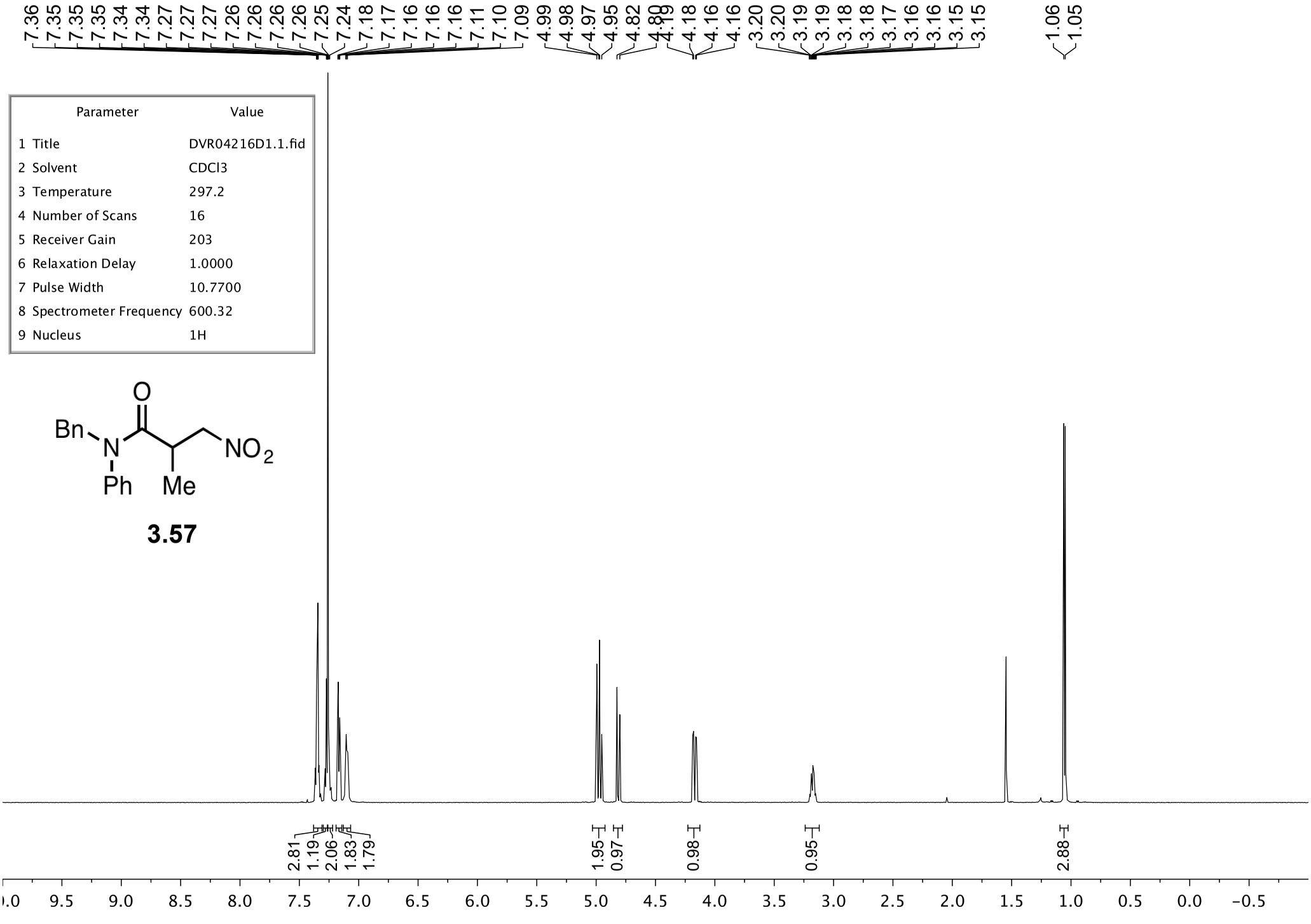
7.36 7.35 7.35 7.35 7.34 7.34 7.27 7.27 7.27 7.26 7.26 7.26 7.26 7.25 7.24 7.18 7.17 7.16 7.16 7.16 7.11 7.10 7.09
4.99 4.98 4.97 4.95 4.82 4.80 4.19 4.18 4.16 4.16
3.20 3.20 3.19 3.19 3.18 3.18 3.17 3.16 3.16 3.15 3.15
1.06 1.05
Parameter Value
1 Title DVR04216D1.1.fid
2 Solvent CDCl3
3 Temperature 297.2
4 Number of Scans 16
5 Receiver Gain 203
6 Relaxation Delay 1.0000
7 Pulse Width 10.7700
8 Spectrometer Frequency 600.32
9 Nucleus 1H
O
Bn
N
NO2
Ph
Me
3.57
2.81 1.19 2.06 1.83 1.79
1.95 0.97 0.98 0.95 2.88
9.5 9.0 8.5 8.0 7.5 7.0 6.5 6.0 5.5 5.0 4.5 4.0 3.5 3.0 2.5 2.0 1.5 1.0 0.5 0.0 -0.5

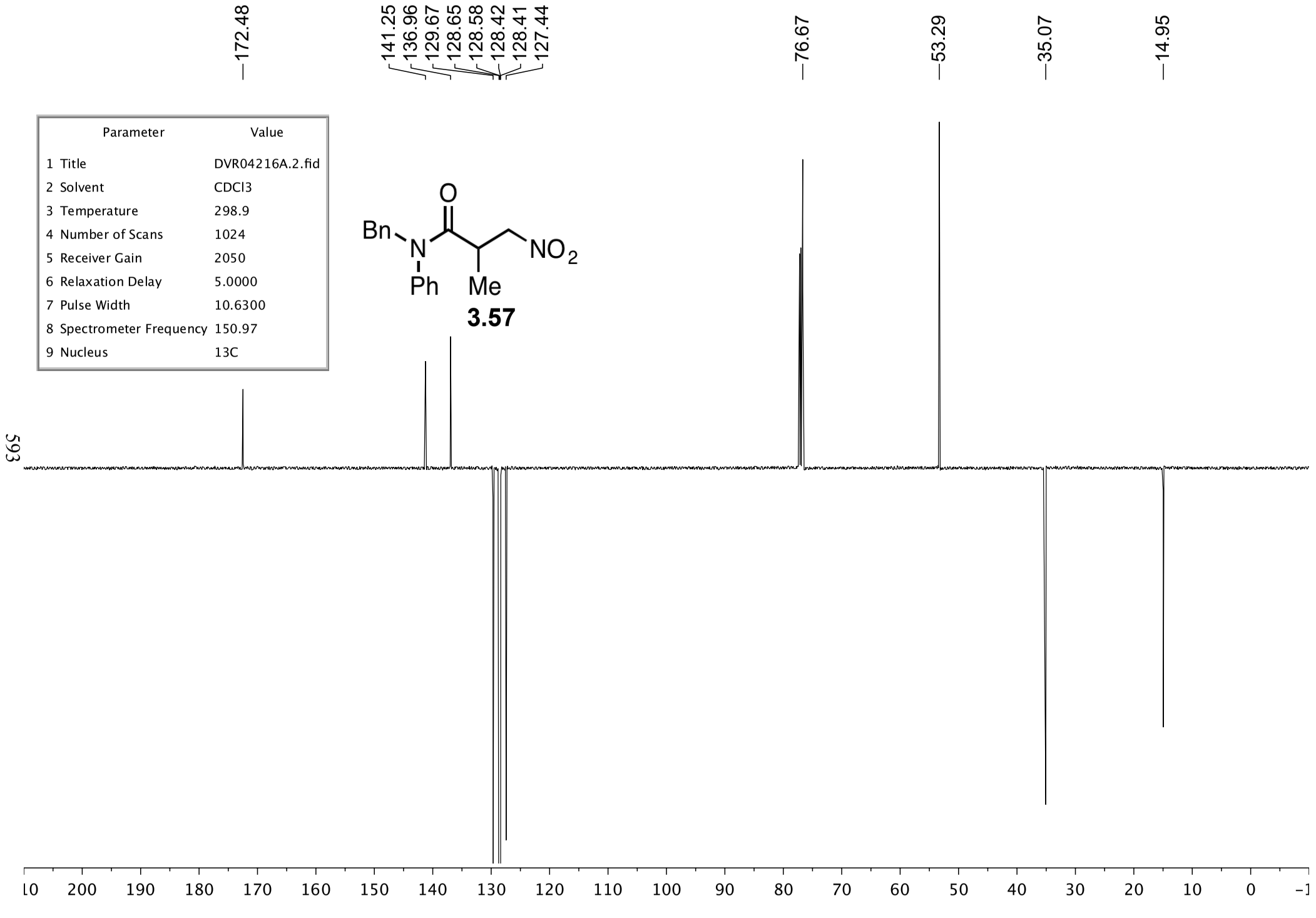
172.48
141.25
136.96
129.67
128.65
128.58
128.42
128.41
127.44
76.67
53.29
35.07
14.95
Parameter Value
1 Title DVR04216A.2.fid
2 Solvent CDCl3
3 Temperature 298.9
4 Number of Scans 1024
5 Receiver Gain 2050
6 Relaxation Delay 5.0000
7 Pulse Width 10.6300
8 Spectrometer Frequency 150.97
9 Nucleus 13C
Bn
N
Ph
O
Me
NO2
3.57
593
200
190
180
170
160
150
140
130
120
110
100
90
80
70
60
50
40
30
20
10
0

==== Shimadzu LCsolution Analysis Report ====

C:\LabSolutions\Data\DMM\DVR04216RAC_10172016_1228 PM_1.lcd

Acquired by	: LC User
Sample Name	: DVR04216RAC
Sample ID	: DVR04216RAC
Tray#	: 1
Vail #	: 2
Injection Volume	: 2 uL
Data File Name	: DVR04216RAC_10172016_1228 PM_1.lcd
Method File Name	: col1_3isoiPA_30min_1ML_220and210.lcm
Batch File Name	: DMM.lcb
Report File Name	: Default.lcr
Data Acquired	: 10/17/2016 8:58:59 PM
Data Processed	: 10/17/2016 9:29:00 PM

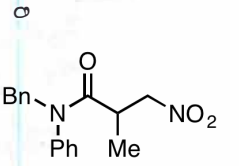

3.57
racemic

<Chromatogram>

C:\LabSolutions\Data\DMM\DVR04216RAC_10172016_1228 PM_1.lcd

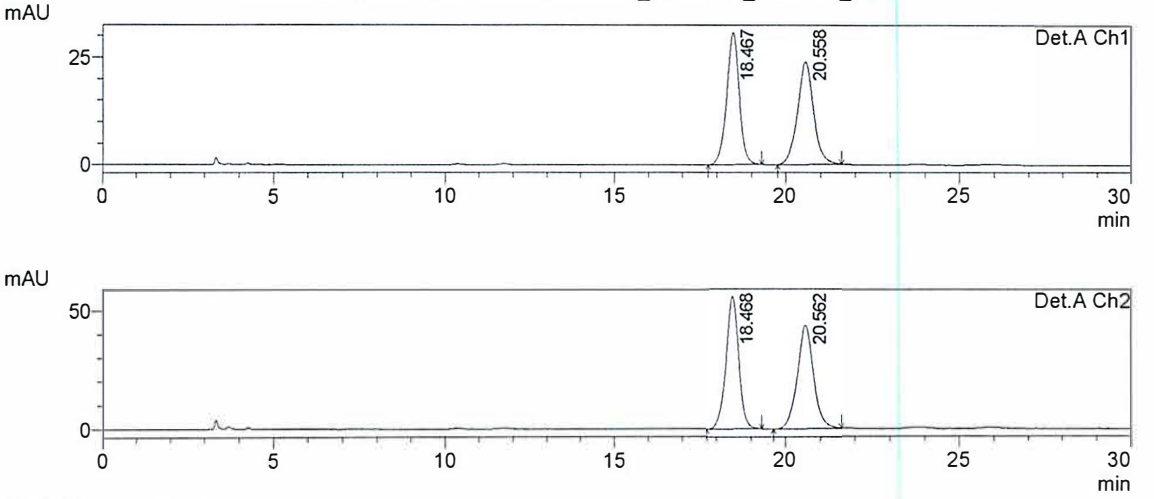

1 Det.A Ch1/220nm
2 Det.A Ch2/210nm

PeakTable

Detector A Ch1 220nm

Peak#	Ret. Time	Area	Height	Area %	Height %
1	18.467	779496	30751	50.358	56.225
2	20.558	768425	23941	49.642	43.775
Total		1547921	54692	100.000	100.000

PeakTable

Detector A Ch2 210nm

Peak#	Ret. Time	Area	Height	Area %	Height %
1	18.468	1419230	56009	50.219	56.182
2	20.562	1406872	43683	49.781	43.818
Total		2826102	99693	100.000	100.000

==== Shimadzu LCsolution Analysis Report ====

C:\LabSolutions\Data\DMM\DVR04216_10152016_2043 PM_2.lcd

Acquired by	: LC User
Sample Name	: DVR04216
Sample ID	: DVR04216
Tray#	: 1
Vail #	: 1
Injection Volume	: 2 uL
Data File Name	: DVR04216_10152016_2043 PM_2.lcd
Method File Name	: col1_3isoiPA_30min_1ML_220and210.lcm
Batch File Name	: DMM.lcb
Report File Name	: Default.lcr
Data Acquired	: 10/15/2016 8:54:06 PM
Data Processed	: 10/15/2016 9:24:09 PM

σ

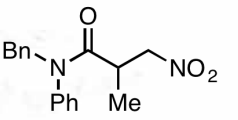

3.57
84% ee

<Chromatogram>

C:\LabSolutions\Data\DMM\DVR04216_10152016_2043 PM_2.lcd

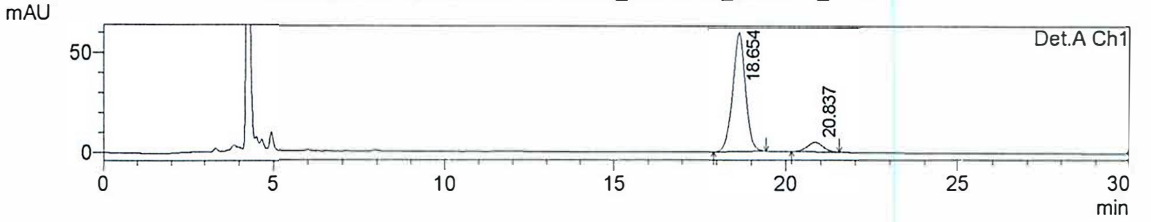

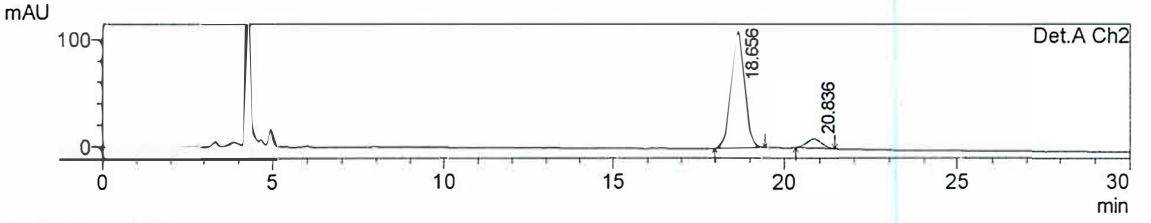

1 Det.A Ch1/220nm
2 Det.A Ch2/210nm

PeakTable

Detector A Ch1 220nm

Peak#	Ret. Time	Area	Height	Area %	Height %
1	18.654	1541824	60100	90.868	92.496
2	20.837	154941	4876	9.132	7.504
Total		1696765	64975	100.000	100.000

PeakTable

Detector A Ch2 210nm

Peak#	Ret. Time	Area	Height	Area %	Height %
1	18.656	2802804	109497	91.979	92.920
2	20.836	244404	8343	8.021	7.080
Total		3047208	117840	100.000	100.000

Parameter	Value
1 Title	DVR04203CRD.1.fid
2 Solvent	CDCl3
3 Temperature	300.0
4 Number of Scans	16
5 Receiver Gain	114
6 Relaxation Delay	1.0000
7 Pulse Width	10.7700
8 Spectrometer Frequency	600.32
9 Nucleus	1H

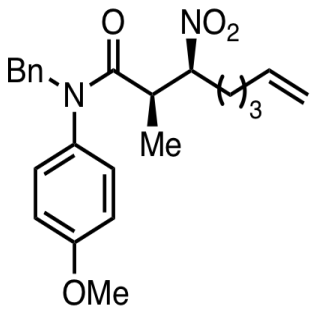

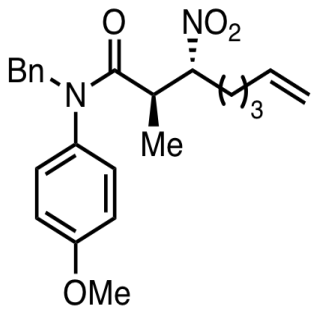

Crude

3.58A **82:12** **3.58B**

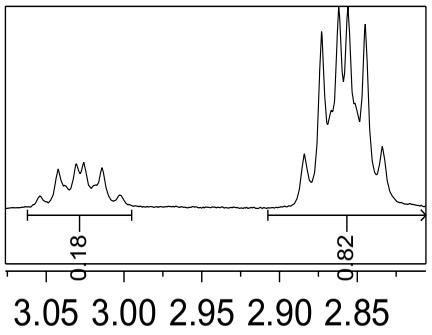

596

Parameter	Value
1 Title	DVR04203D1.1.fid
2 Solvent	CDCl3
3 Temperature	300.0
4 Number of Scans	16
5 Receiver Gain	161
6 Relaxation Delay	1.0000
7 Pulse Width	10.7700
8 Spectrometer Frequency	600.32
9 Nucleus	1H

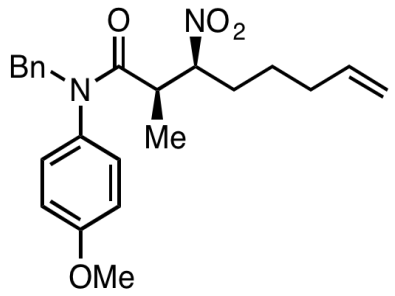

3.58A

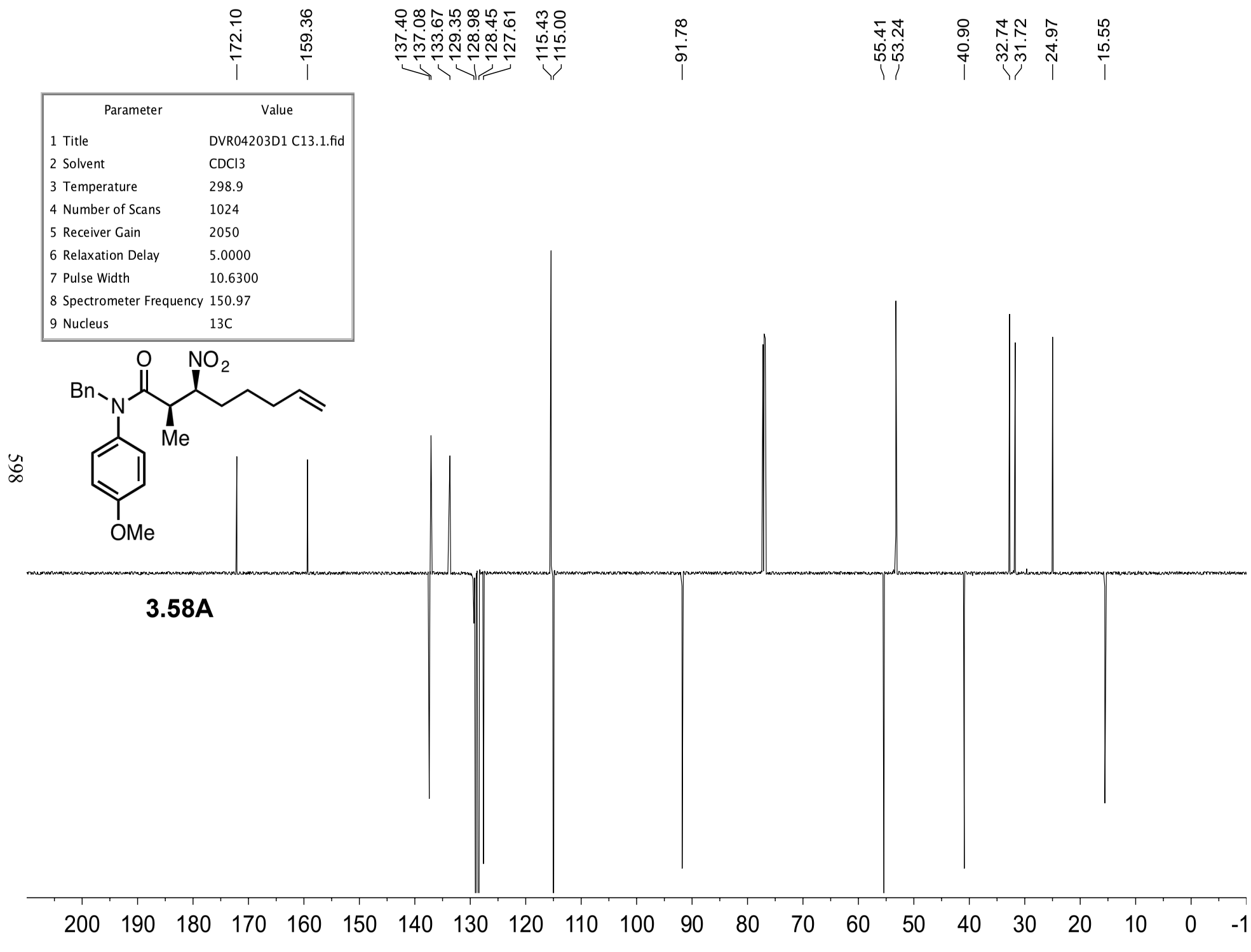
172.10
159.36
137.40
137.08
133.67
129.35
128.98
128.45
127.61
115.43
115.00
91.78
55.41
53.24
40.90
32.74
31.72
24.97
15.55
Parameter Value
1 Title DVR04203D1 C13.1.fid
2 Solvent CDCl3
3 Temperature 298.9
4 Number of Scans 1024
5 Receiver Gain 2050
6 Relaxation Delay 5.0000
7 Pulse Width 10.6300
8 Spectrometer Frequency 150.97
9 Nucleus 13C
O
NO2
Bn
N
Me
OMe
3.58A
598
200 190 180 170 160 150 140 130 120 110 100 90 80 70 60 50 40 30 20 10 0 -1

Parameter	Value
1 Title	DVR04203D2.1.fid
2 Solvent	CDCl3
3 Temperature	300.0
4 Number of Scans	16
5 Receiver Gain	144
6 Relaxation Delay	1.0000
7 Pulse Width	10.7700
8 Spectrometer Frequency	600.32
9 Nucleus	1H

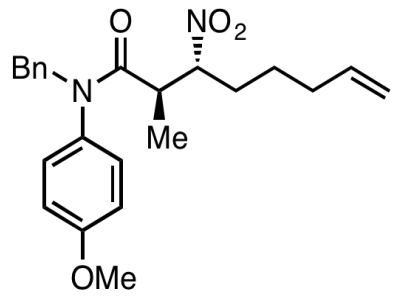

3.58B

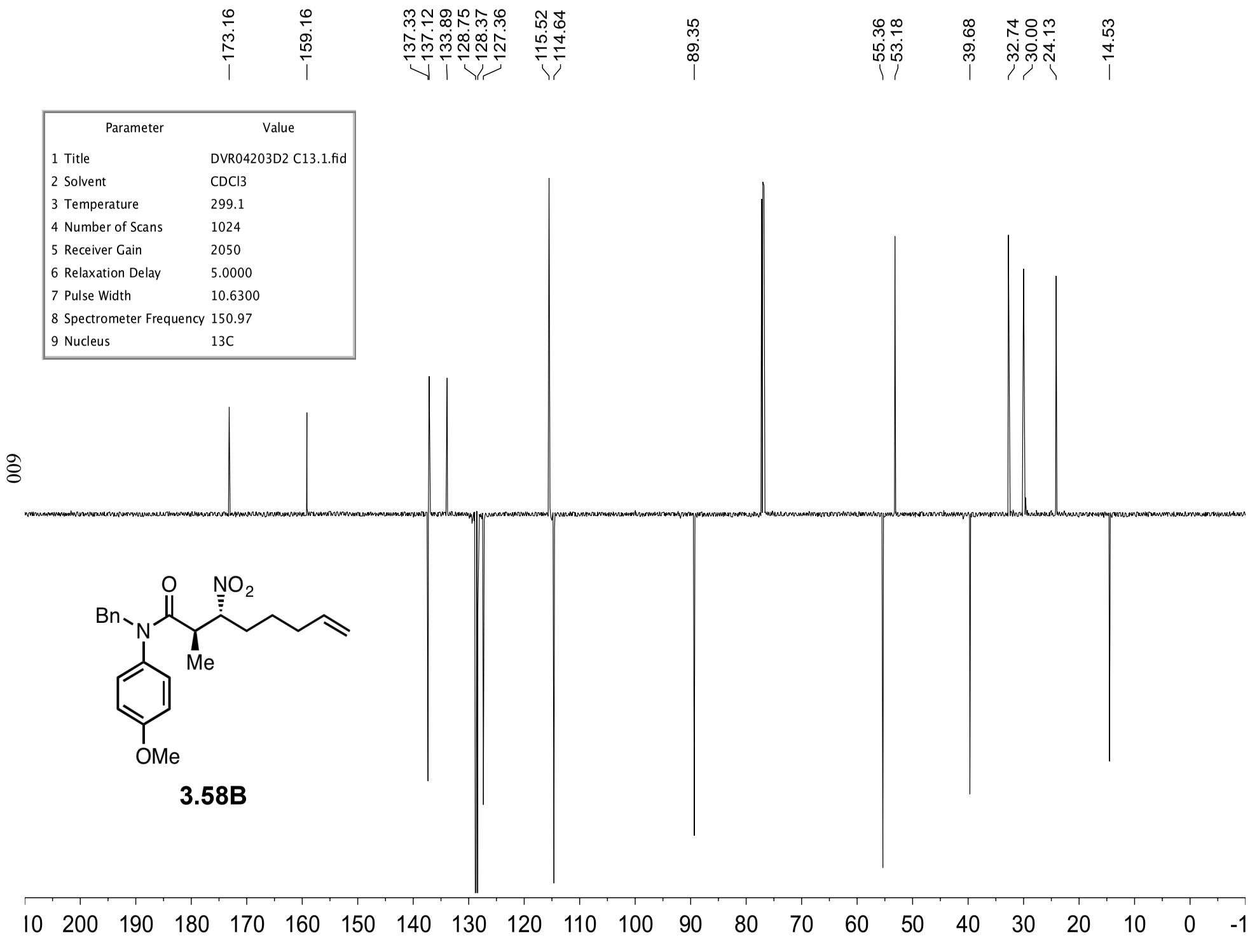
173.16
159.16
137.33
137.12
133.89
128.75
128.37
127.36
115.52
114.64
89.35
55.36
53.18
39.68
32.74
30.00
24.13
14.53
Parameter Value
1 Title DVR04203D2 C13.1.fid
2 Solvent CDCl3
3 Temperature 299.1
4 Number of Scans 1024
5 Receiver Gain 2050
6 Relaxation Delay 5.0000
7 Pulse Width 10.6300
8 Spectrometer Frequency 150.97
9 Nucleus 13C
009
O
NO2
Bn
N
Me
OMe
3.58B
10 200 190 180 170 160 150 140 130 120 110 100 90 80 70 60 50 40 30 20 10 0 -1

==== Shimadzu LCsolution Analysis Report ====

C:\LabSolutions\Data\DMM\DVR04203 RAC SYN_9292016_1421 PM_2.lcd

Acquired by	: LC User
Sample Name	: DVR04203 RAC SYN
Sample ID	: DVR04203 RAC SYN
Tray#	: 1
Vail #	: 1
Injection Volume	: 2 uL
Data File Name	: DVR04203 RAC SYN_9292016_1421 PM_2.lcd
Method File Name	: col3_2isoiPA_45min_1ML_220and210.lcm
Batch File Name	: DMM.lcb
Report File Name	: Default.lcr
Data Acquired	: 9/29/2016 3:07:12 PM
Data Processed	: 9/29/2016 3:52:14 PM

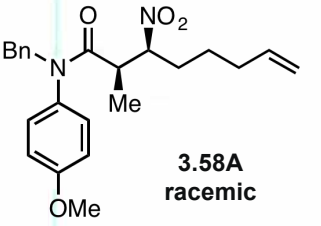

3.58A
racemic

<Chromatogram>

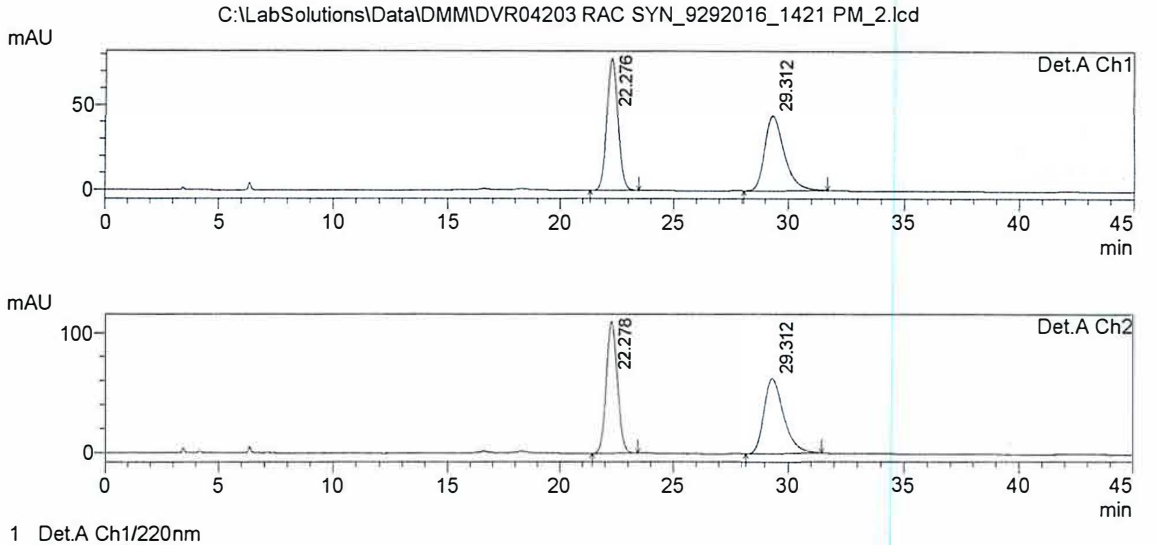

1 Det.A Ch1/220nm
2 Det.A Ch2/210nm

PeakTable

Detector A Ch1 220nm

Peak#	Ret. Time	Area	Height	Area %	Height %
1	22.276	2659822	77815	50.873	63.959
2	29.312	2568546	43848	49.127	36.041
Total		5228369	121663	100.000	100.000

PeakTable

Detector A Ch2 210nm

Peak#	Ret. Time	Area	Height	Area %	Height %
1	22.278	3778750	110421	51.048	63.956
2	29.312	3623583	62230	48.952	36.044
Total		7402333	172651	100.000	100.000

==== Shimadzu LCsolution Analysis Report ====

C:\LabSolutions\Data\DMM\DVR04203D1 _1022016_1418 PM_6.lcd

Acquired by	: LC User
Sample Name	: DVR04203D1
Sample ID	: DVR04203D1
Tray#	: 1
Vail #	: 2
Injection Volume	: 3 uL
Data File Name	: DVR04203D1 _1022016_1418 PM_6.lcd
Method File Name	: col3_2isoiPA_45min_1ML_220and210.lcm
Batch File Name	: DMM.lcb
Report File Name	: Default.lcr
Data Acquired	: 10/2/2016 4:45:26 PM
Data Processed	: 10/2/2016 5:30:28 PM

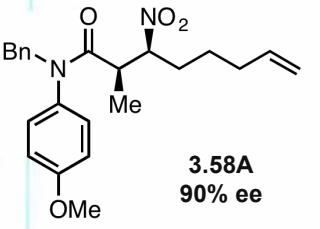

3.58A
90% ee

<Chromatogram>

C:\LabSolutions\Data\DMM\DVR04203D1 _1022016_1418 PM_6.lcd

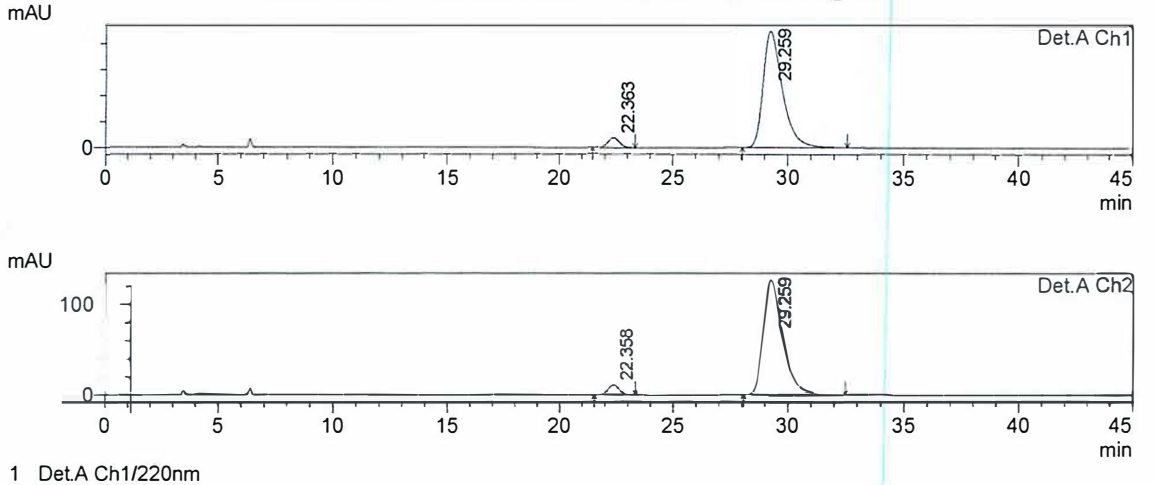

1 Det.A Ch1/220nm
2 Det.A Ch2/210nm

PeakTable

Detector A Ch1 220nm

Peak#	Ret. Time	Area	Height	Area %	Height %
1	22.363	265768	7743	4.856	7.942
2	29.259	5206917	89759	95.144	92.058
Total		5472685	97503	100.000	100.000

PeakTable

Detector A Ch2 210nm

Peak#	Ret. Time	Area	Height	Area %	Height %
1	22.358	377460	11067	4.868	8.003
2	29.259	7376937	127221	95.132	91.997
Total		7754396	138288	100.000	100.000

==== Shimadzu LCsolution Analysis Report ====

C:\LabSolutions\Data\DMM\DVR04203D2 RAC_1022016_1418 PM_10.lcd

Acquired by	: LC User
Sample Name	: DVR04203D2 RAC
Sample ID	: DVR04203D2 RAC
Tray#	: 1
Vail #	: 3
Injection Volume	: 3 uL
Data File Name	: DVR04203D2 RAC_1022016_1418 PM_10.lcd
Method File Name	: col2_0.8isoIPA_60min_1ml_254and210.lcm
Batch File Name	: DMM.lcb
Report File Name	: Default.lcr
Data Acquired	: 10/2/2016 6:11:24 PM
Data Processed	: 10/2/2016 7:11:28 PM

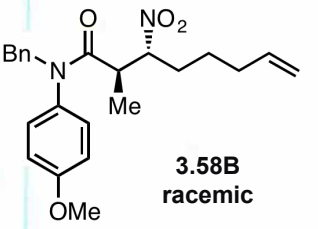

3.58B racemic

<Chromatogram>

C:\LabSolutions\Data\DMM\DVR04203D2 RAC_1022016_1418 PM_10.lcd

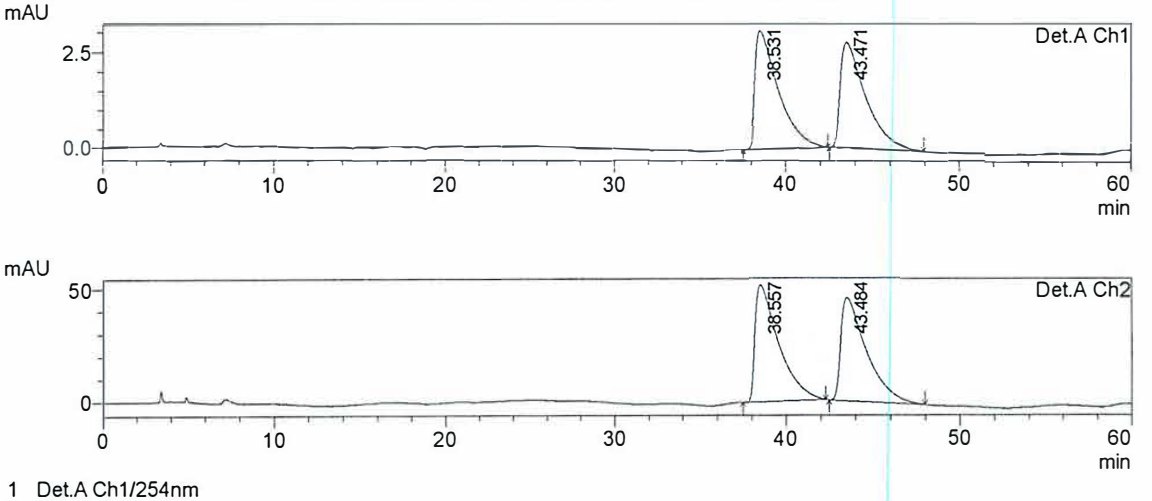

1 Det.A Ch1/254nm
2 Det.A Ch2/210nm

PeakTable

Detector A Ch1 254nm

Peak#	Ret. Time	Area	Height	Area %	Height %
1	38.531	283737	3051	50.830	52.782
2	43.471	274466	2729	49.170	47.218
Total		558203	5780	100.000	100.000

PeakTable

Detector A Ch2 210nm

Peak#	Ret. Time	Area	Height	Area %	Height %
1	38.557	4806533	51199	51.067	53.053
2	43.484	4605717	45307	48.933	46.947
Total		9412251	96505	100.000	100.000

==== Shimadzu LCsolution Analysis Report ====

C:\LabSolutions\Data\DMM\DVR04203D2_1022016_1418 PM_14.lcd

Acquired by	: LC User
Sample Name	: DVR04203D2
Sample ID	: DVR04203D2
Tray#	: 1
Vail #	: 4
Injection Volume	: 3 uL
Data File Name	: DVR04203D2_1022016_1418 PM_14.lcd
Method File Name	: col2_0.8isoIPA_60min_1ml_254and210.lcm
Batch File Name	: DMM.lcb
Report File Name	: Default.lcr
Data Acquired	: 10/2/2016 7:52:23 PM
Data Processed	: 10/2/2016 8:52:25 PM

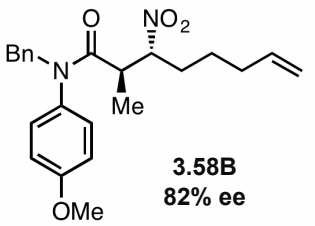

3.58B
82% ee

<Chromatogram>

C:\LabSolutions\Data\DMM\DVR04203D2_1022016_1418 PM_14.lcd

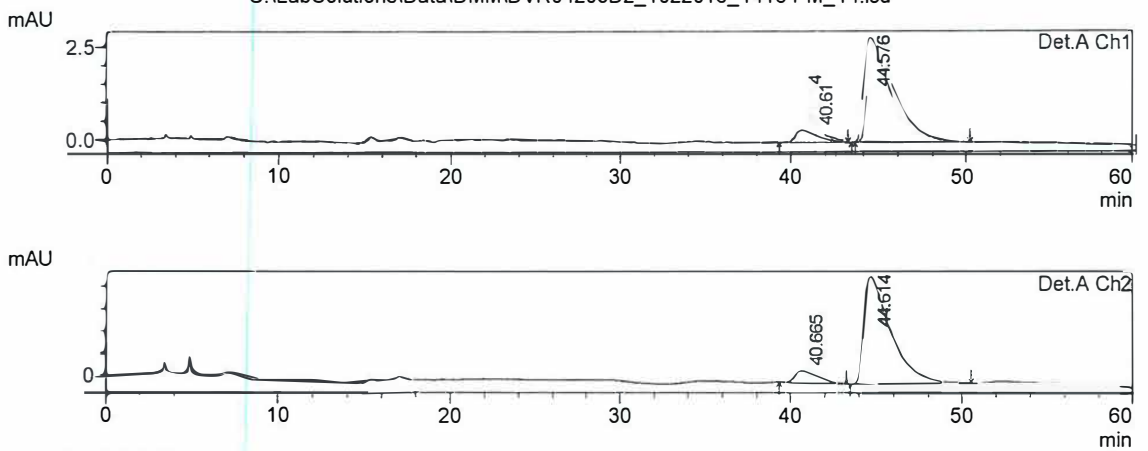

1 Det.A Ch1/254nm
2 Det.A Ch2/210nm

PeakTable

Detector A Ch1 254nm

Peak#	Ret. Time	Area	Height	Area %	Height %
1	40.614	29603	330	8.822	10.432
2	44.576	305968	2835	91.178	89.568
Total		335571	3165	100.000	100.000

PeakTable

Detector A Ch2 210nm

Peak#	Ret. Time	Area	Height	Area %	Height %
1	40.665	474842	5394	8.388	10.157
2	44.614	5186184	47717	91.612	89.843
Total		5661027	53111	100.000	100.000

Parameter	Value
1 Title	DVR04211CRD.1.fid
2 Solvent	CDCl3
3 Temperature	298.1
4 Number of Scans	16
5 Receiver Gain	128
6 Relaxation Delay	1.0000
7 Pulse Width	10.7700
8 Spectrometer Frequency	600.32
9 Nucleus	1H

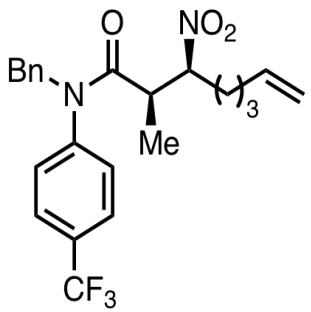

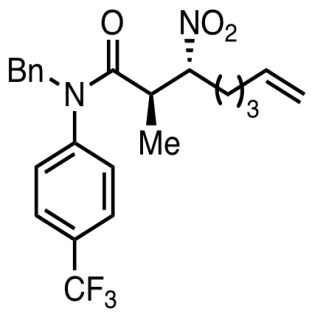

3.59A **Crude** **79:21** **3.59B**

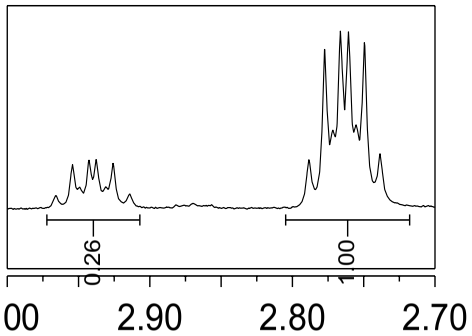

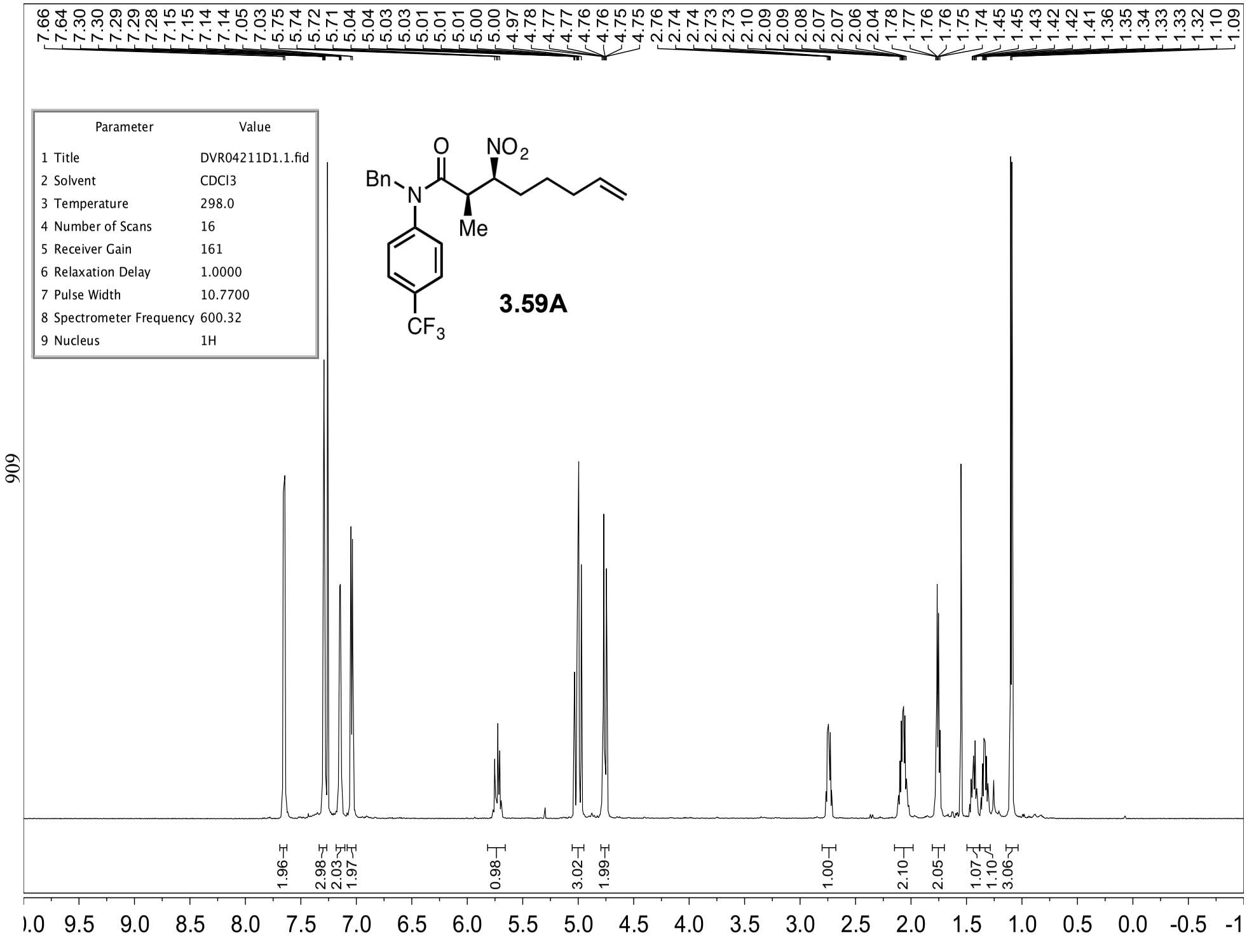
7.66 7.64 7.30 7.30 7.29 7.29 7.28 7.15 7.15 7.14 7.14 7.05 7.03 5.75 5.74 5.72 5.71 5.04 5.04 5.03 5.03 5.01 5.01 5.01 5.00 5.00 4.97 4.78 4.77 4.77 4.76 4.76 4.75 4.75 2.76 2.74 2.74 2.73 2.73 2.10 2.09 2.09 2.08 2.07 2.07 2.06 2.04 1.78 1.77 1.76 1.76 1.75 1.74 1.45 1.45 1.43 1.42 1.42 1.41 1.36 1.35 1.34 1.33 1.33 1.32 1.10 1.09
Parameter Value
1 Title DVR04211D1.1.fid
2 Solvent CDCl3
3 Temperature 298.0
4 Number of Scans 16
5 Receiver Gain 161
6 Relaxation Delay 1.0000
7 Pulse Width 10.7700
8 Spectrometer Frequency 600.32
9 Nucleus 1H
O
NO2
Bn
N
Me
CF3
3.59A
909
1.96 2.98 2.03 1.97 0.98 3.02 1.99 1.00 2.10 2.05 1.07 1.10 3.06
.0 9.5 9.0 8.5 8.0 7.5 7.0 6.5 6.0 5.5 5.0 4.5 4.0 3.5 3.0 2.5 2.0 1.5 1.0 0.5 0.0 -0.5 -1

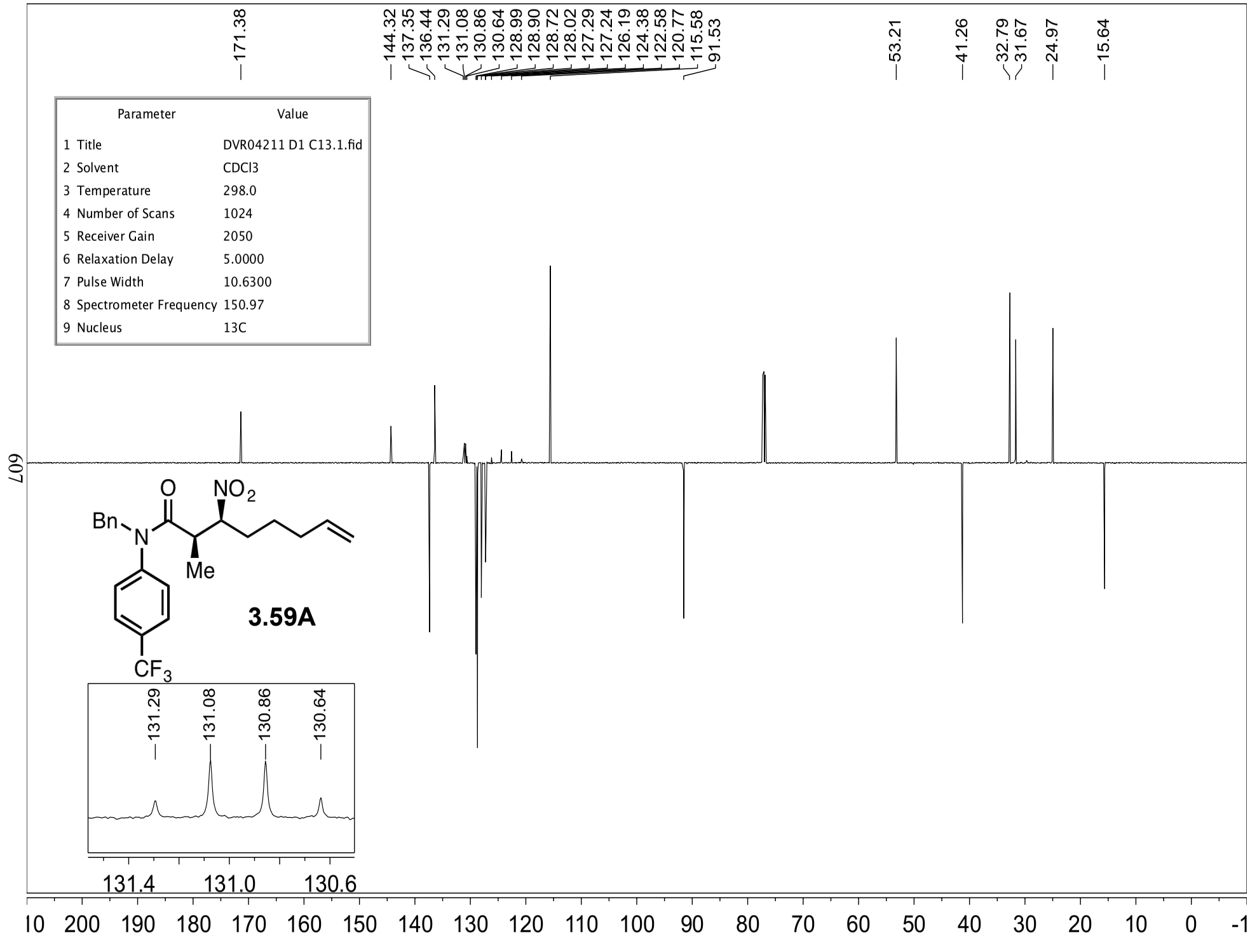
171.38
144.32
137.35
136.44
131.29
131.08
130.86
130.64
128.99
128.90
128.72
128.02
127.29
127.24
126.19
124.38
122.58
120.77
115.58
91.53
53.21
41.26
32.79
31.67
24.97
15.64
Parameter Value
1 Title DVR04211 D1 C13.1.fid
2 Solvent CDCl3
3 Temperature 298.0
4 Number of Scans 1024
5 Receiver Gain 2050
6 Relaxation Delay 5.0000
7 Pulse Width 10.6300
8 Spectrometer Frequency 150.97
9 Nucleus 13C
607
O
NO2
Bn
N
Me
CF3
3.59A
131.29
131.08
130.86
130.64
131.4
131.0
130.6
10 200 190 180 170 160 150 140 130 120 110 100 90 80 70 60 50 40 30 20 10 0 -1

Parameter	Value
1 Title	DVR04211D1 F19.1.fid
2 Solvent	CDCl3
3 Temperature	298.0
4 Number of Scans	16
5 Receiver Gain	406
6 Relaxation Delay	3.0000
7 Pulse Width	11.6200
8 Spectrometer Frequency	564.81
9 Nucleus	19F

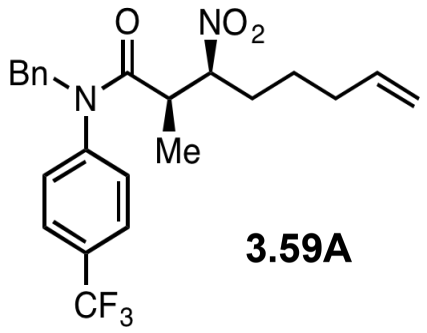

3.59A

-62.68

809

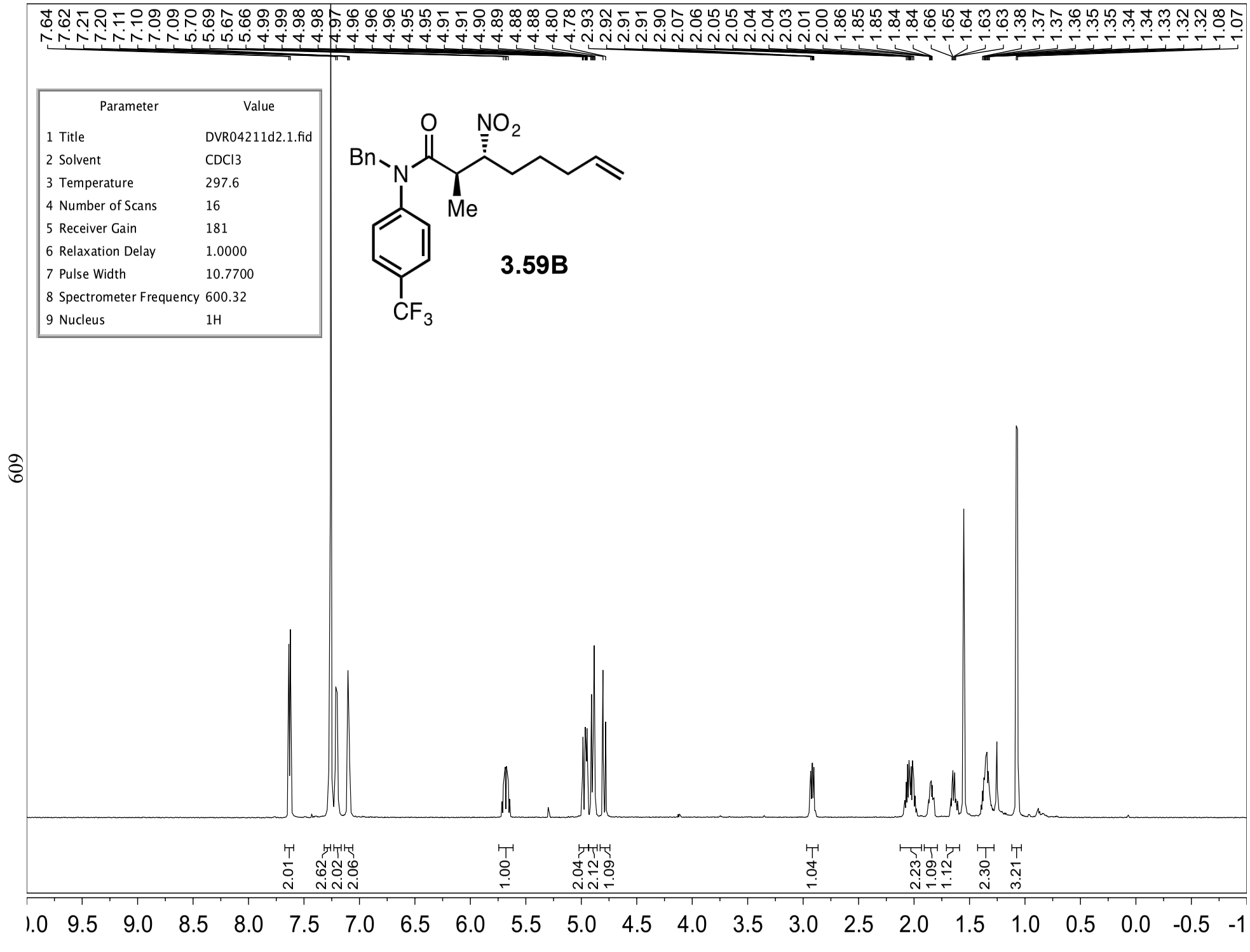
7.64 7.62 7.21 7.20 7.11 7.10 7.09 7.09 5.70 5.69 5.67 5.66 4.99 4.99 4.98 4.98 4.97 4.96 4.96 4.96 4.95 4.95 4.91 4.91 4.90 4.89 4.88 4.88 4.80 4.78 2.93 2.92 2.91 2.91 2.90 2.07 2.06 2.05 2.05 2.04 2.04 2.03 2.01 2.00 1.86 1.85 1.85 1.84 1.84 1.66 1.65 1.64 1.63 1.63 1.38 1.37 1.37 1.36 1.35 1.35 1.34 1.34 1.33 1.32 1.32 1.08 1.07
Parameter Value
1 Title DVR04211d2.1.fid
2 Solvent CDCl3
3 Temperature 297.6
4 Number of Scans 16
5 Receiver Gain 181
6 Relaxation Delay 1.0000
7 Pulse Width 10.7700
8 Spectrometer Frequency 600.32
9 Nucleus 1H
O
NO2
Bn
N
Me
CF3
3.59B
609
2.01 2.62 2.02 2.06 1.00 2.04 2.12 1.09 1.04 2.23 1.09 1.12 2.30 3.21
.0 9.5 9.0 8.5 8.0 7.5 7.0 6.5 6.0 5.5 5.0 4.5 4.0 3.5 3.0 2.5 2.0 1.5 1.0 0.5 0.0 -0.5 -1

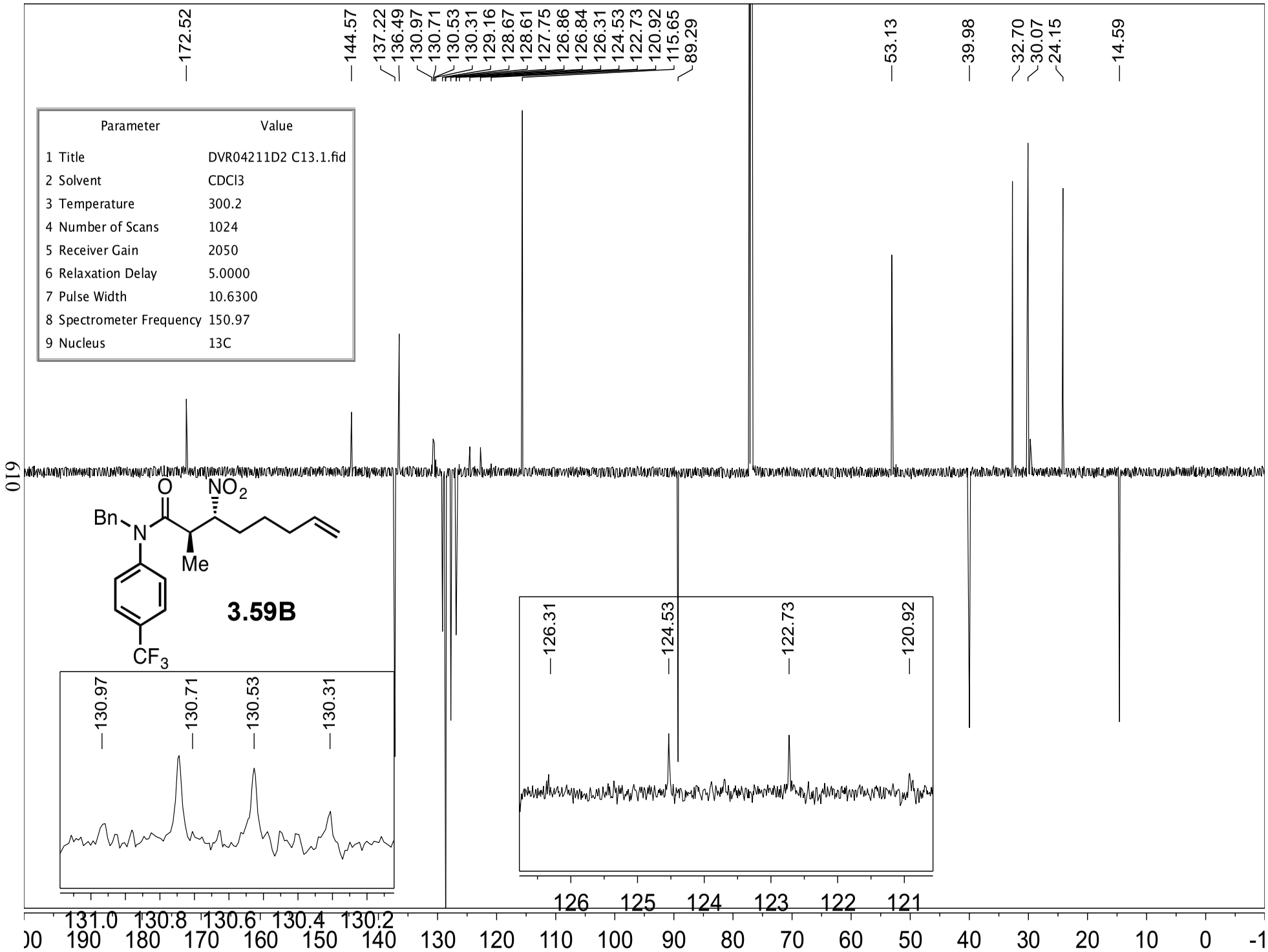
172.52
144.57
137.22
136.49
130.97
130.71
130.53
130.31
129.16
128.67
128.61
127.75
126.86
126.84
126.31
124.53
122.73
120.92
115.65
89.29
53.13
39.98
32.70
30.07
24.15
14.59
Parameter Value
1 Title DVR04211D2 C13.1.fid
2 Solvent CDCl3
3 Temperature 300.2
4 Number of Scans 1024
5 Receiver Gain 2050
6 Relaxation Delay 5.0000
7 Pulse Width 10.6300
8 Spectrometer Frequency 150.97
9 Nucleus 13C
O
NO2
Bn
N
Me
CF3
3.59B
130.97
130.71
130.53
130.31
126.31
124.53
122.73
120.92
131.0 130.8 130.6 130.4 130.2
126 125 124 123 122 121
190 180 170 160 150 140 130 120 110 100 90 80 70 60 50 40 30 20 10 0 -1

Parameter	Value
1 Title	DVR04211D2 F19.1.fid
2 Solvent	CDCl3
3 Temperature	297.6
4 Number of Scans	16
5 Receiver Gain	362
6 Relaxation Delay	3.0000
7 Pulse Width	11.6200
8 Spectrometer Frequency	564.81
9 Nucleus	19F

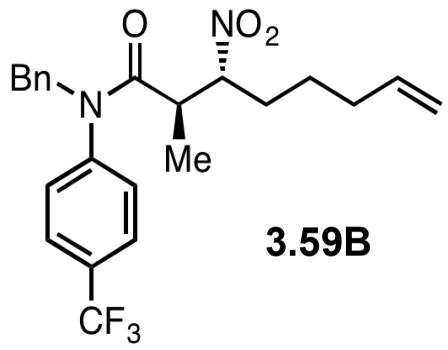

3.59B

==== Shimadzu LCsolution Analysis Report ====

C:\LabSolutions\Data\DMM\DVR04211 RAC D1_1082016_2042 PM_2.lcd

Acquired by	: LC User
Sample Name	: DVR04211 RAC D1
Sample ID	: DVR04211 RAC D1
Tray#	: 1
Vail #	: 1
Injection Volume	: 2 uL
Data File Name	: DVR04211 RAC D1_1082016_2042 PM_2.lcd
Method File Name	: col3_2isoiPA_20min_1ML_220and210.lcm
Batch File Name	: DMM.lcb
Report File Name	: Default.lcr
Data Acquired	: 10/8/2016 9:03:01 PM
Data Processed	: 10/8/2016 9:23:01 PM

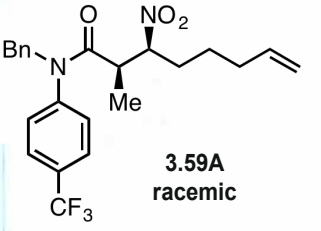

3.59A
racemic

<Chromatogram>

C:\LabSolutions\Data\DMM\DVR04211 RAC D1_1082016_2042 PM_2.lcd

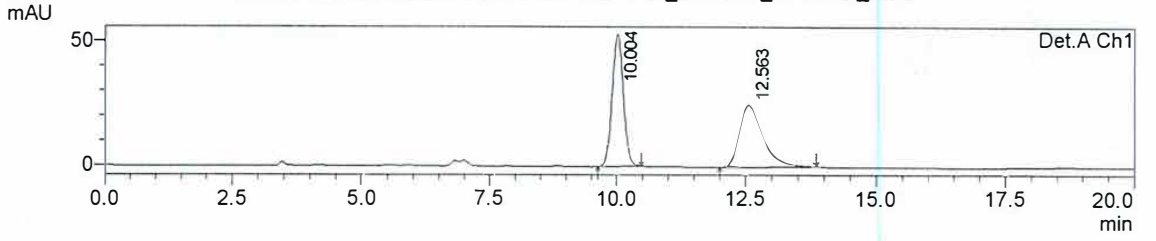

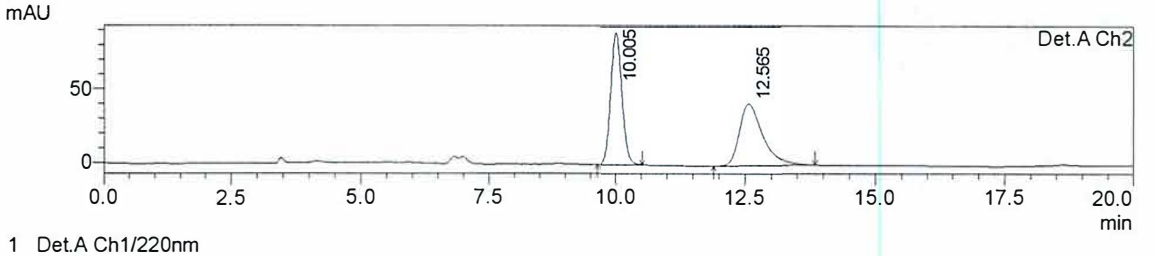

1 Det.A Ch1/220nm
2 Det.A Ch2/210nm

PeakTable

Detector A Ch1 220nm

Peak#	Ret. Time	Area	Height	Area %	Height %
1	10.004	802330	53218	50.985	68.246
2	12.563	771334	24762	49.015	31.754
Total		1573665	77980	100.000	100.000

PeakTable

Detector A Ch2 210nm

Peak#	Ret. Time	Area	Height	Area %	Height %
1	10.005	1348201	89182	50.972	68.225
2	12.565	1296787	41535	49.028	31.775
Total		2644988	130717	100.000	100.000

==== Shimadzu LCsolution Analysis Report ====

C:\LabSolutions\Data\DMM\DVR04211 D1_1082016_2042 PM_6.lcd

Acquired by	: LC User
Sample Name	: DVR04211 D1
Sample ID	: DVR04211 D1
Tray#	: 1
Vail #	: 2
Injection Volume	: 2 uL
Data File Name	: DVR04211 D1_1082016_2042 PM_6.lcd
Method File Name	: col3_2isoiPA_20min_1ML_220and210.lcm
Batch File Name	: DMM.lcb
Report File Name	: Default.lcr
Data Acquired	: 10/8/2016 9:53:54 PM
Data Processed	: 10/8/2016 10:13:55 PM

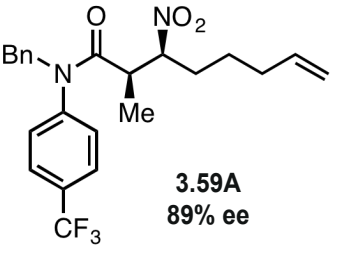

3.59A
89% ee

<Chromatogram>

C:\LabSolutions\Data\DMM\DVR04211 D1_1082016_2042 PM_6.lcd

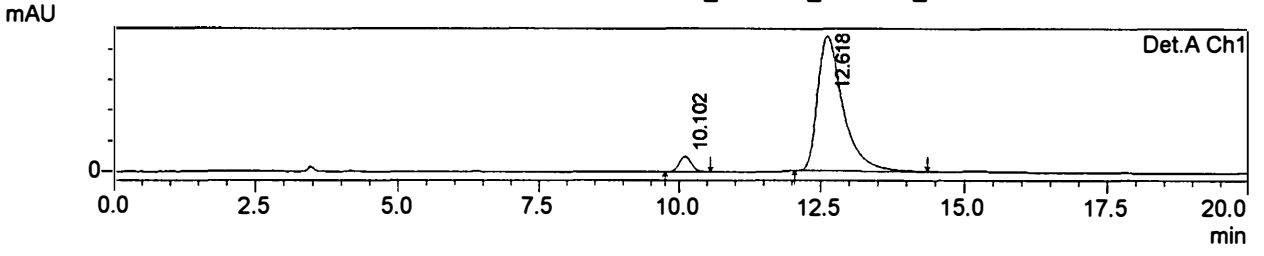

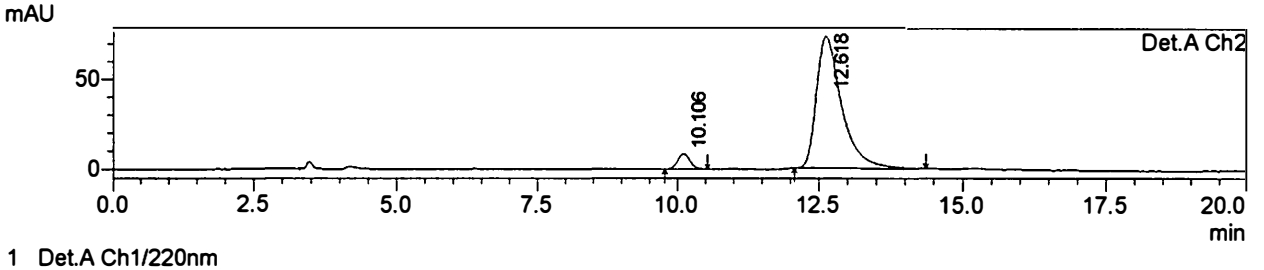

1 Det.A Ch1/220nm
2 Det.A Ch2/210nm

PeakTable

Detector A Ch1 220nm

Peak#	Ret. Time	Area	Height	Area %	Height %
1	10.102	75639	5029	5.271	10.226
2	12.618	1359251	44152	94.729	89.774
Total		1434890	49181	100.000	100.000

PeakTable

Detector A Ch2 210nm

Peak#	Ret. Time	Area	Height	Area %	Height %
1	10.106	126593	8417	5.283	10.226
2	12.618	2269788	73897	94.717	89.774
Total		2396380	82314	100.000	100.000

==== Shimadzu LCsolution Analysis Report ====

C:\LabSolutions\Data\DMM\DVR04211 RAC D2_1082016_2042 PM_10.lcd

Acquired by	: LC User
Sample Name	: DVR04211 RAC D2
Sample ID	: DVR04211 RAC D2
Tray#	: 1
Vail #	: 3
Injection Volume	: 2 uL
Data File Name	: DVR04211 RAC D2_1082016_2042 PM_10.lcd
Method File Name	: col3_5isoiPA_45min_1ML_220and210.lcm
Batch File Name	: DMM.lcb
Report File Name	: Default.lcr
Data Acquired	: 10/8/2016 11:09:50 PM
Data Processed	: 10/8/2016 11:54:51 PM

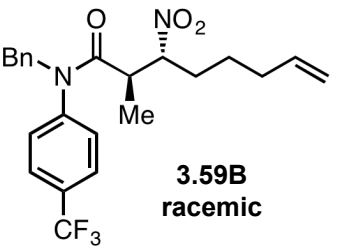

3.59B racemic

<Chromatogram>

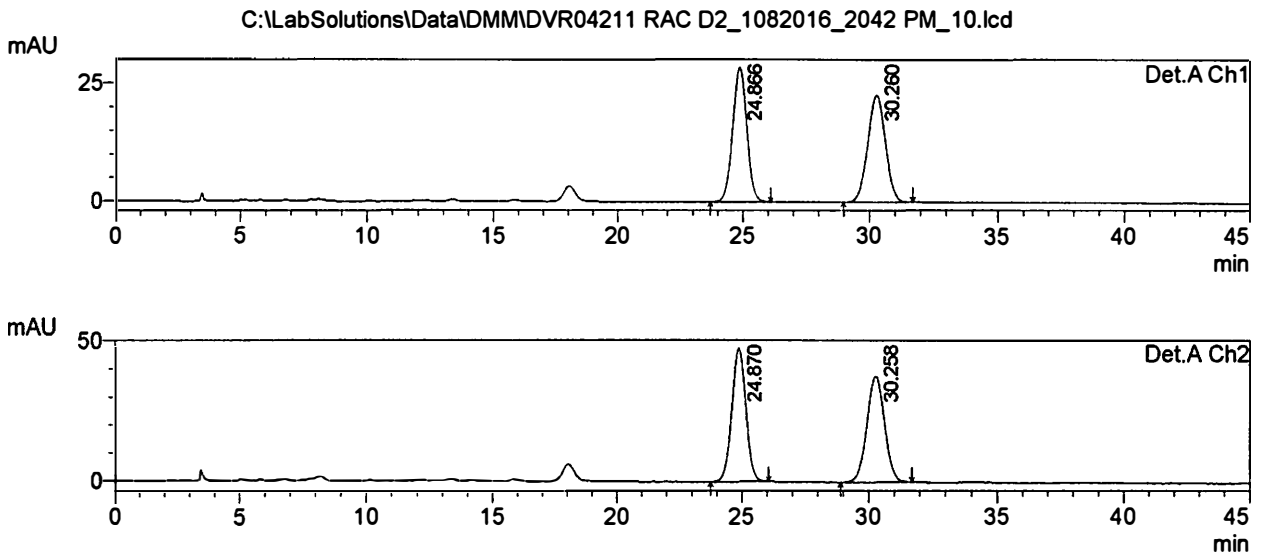

1 Det.A Ch1/220nm
2 Det.A Ch2/210nm

PeakTable

Detector A Ch1 220nm

Peak#	Ret. Time	Area	Height	Area %	Height %
1	24.866	1109817	28443	50.406	55.693
2	30.260	1091922	22628	49.594	44.307
Total		2201739	51071	100.000	100.000

PeakTable

Detector A Ch2 210nm

Peak#	Ret. Time	Area	Height	Area %	Height %
1	24.870	1855855	47618	50.177	55.620
2	30.258	1842744	37995	49.823	44.380
Total		3698599	85612	100.000	100.000

==== Shimadzu LCsolution Analysis Report ====

C:\LabSolutions\Data\DMM\DVR04211 D2_1082016_2042 PM_14.lcd

Acquired by	: LC User
Sample Name	: DVR04211 D2
Sample ID	: DVR04211 D2
Tray#	: 1
Vail #	: 4
Injection Volume	: 2 uL
Data File Name	: DVR04211 D2_1082016_2042 PM_14.lcd
Method File Name	: col3_5isoiPA_45min_1ML_220and210.lcm
Batch File Name	: DMM.lcb
Report File Name	: Default.lcr
Data Acquired	: 10/9/2016 12:50:45 AM
Data Processed	: 10/9/2016 1:35:49 AM

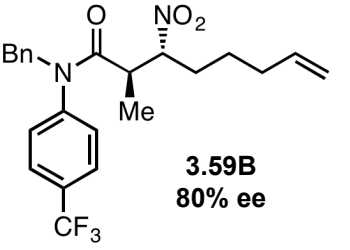

3.59B
80% ee

<Chromatogram>

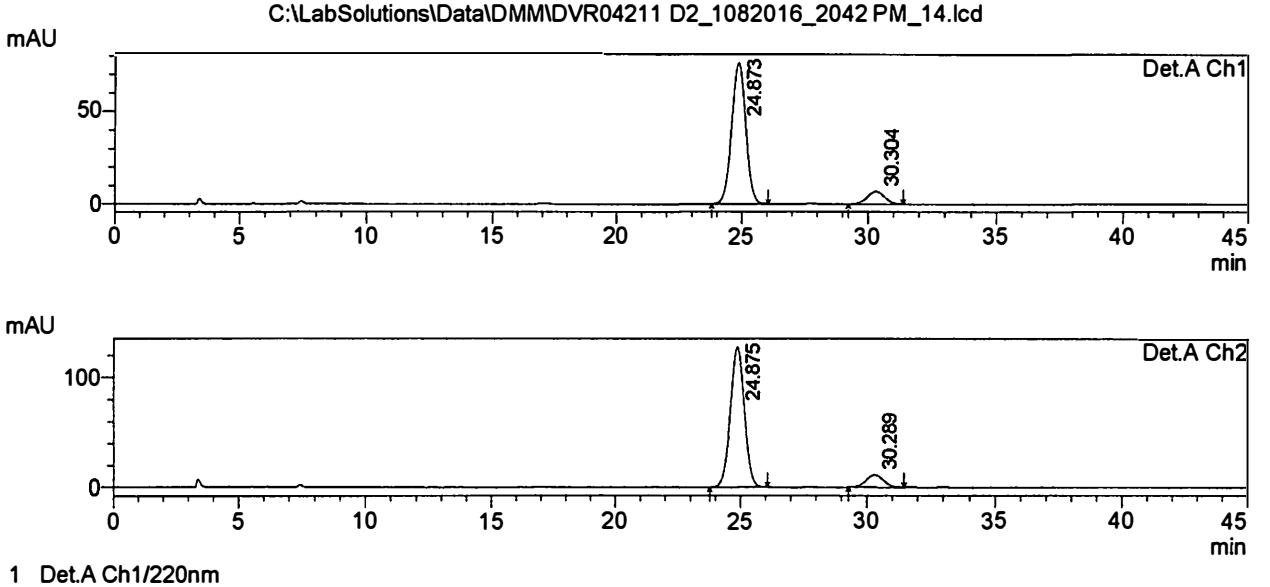

1 Det.A Ch1/220nm
2 Det.A Ch2/210nm

PeakTable

Detector A Ch1 220nm

Peak#	Ret. Time	Area	Height	Area %	Height %
1	24.873	2991187	76619	90.165	91.787
2	30.304	326271	6856	9.835	8.213
Total		3317458	83475	100.000	100.000

PeakTable

Detector A Ch2 210nm

Peak#	Ret. Time	Area	Height	Area %	Height %
1	24.875	5010876	128349	90.308	91.847
2	30.289	537780	11394	9.692	8.153
Total		5548656	139742	100.000	100.000

Parameter	Value
1 Title	DVR04208CRD.1.fid
2 Solvent	CDCl3
3 Temperature	300.0
4 Number of Scans	16
5 Receiver Gain	114
6 Relaxation Delay	1.0000
7 Pulse Width	10.7700
8 Spectrometer Frequency	600.32
9 Nucleus	1H

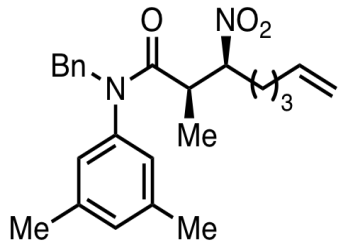

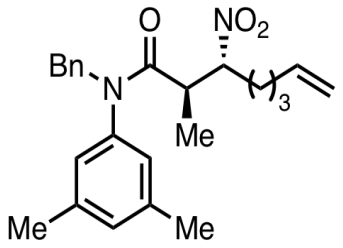

3.60A **Crude** **3.60B**

83:17

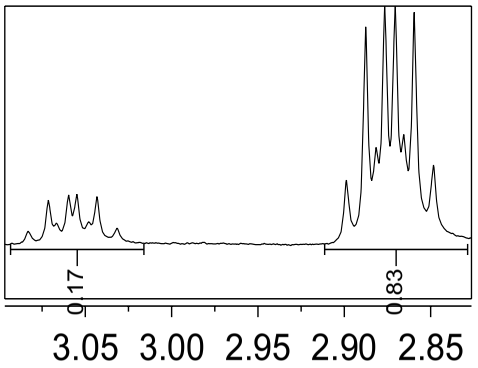

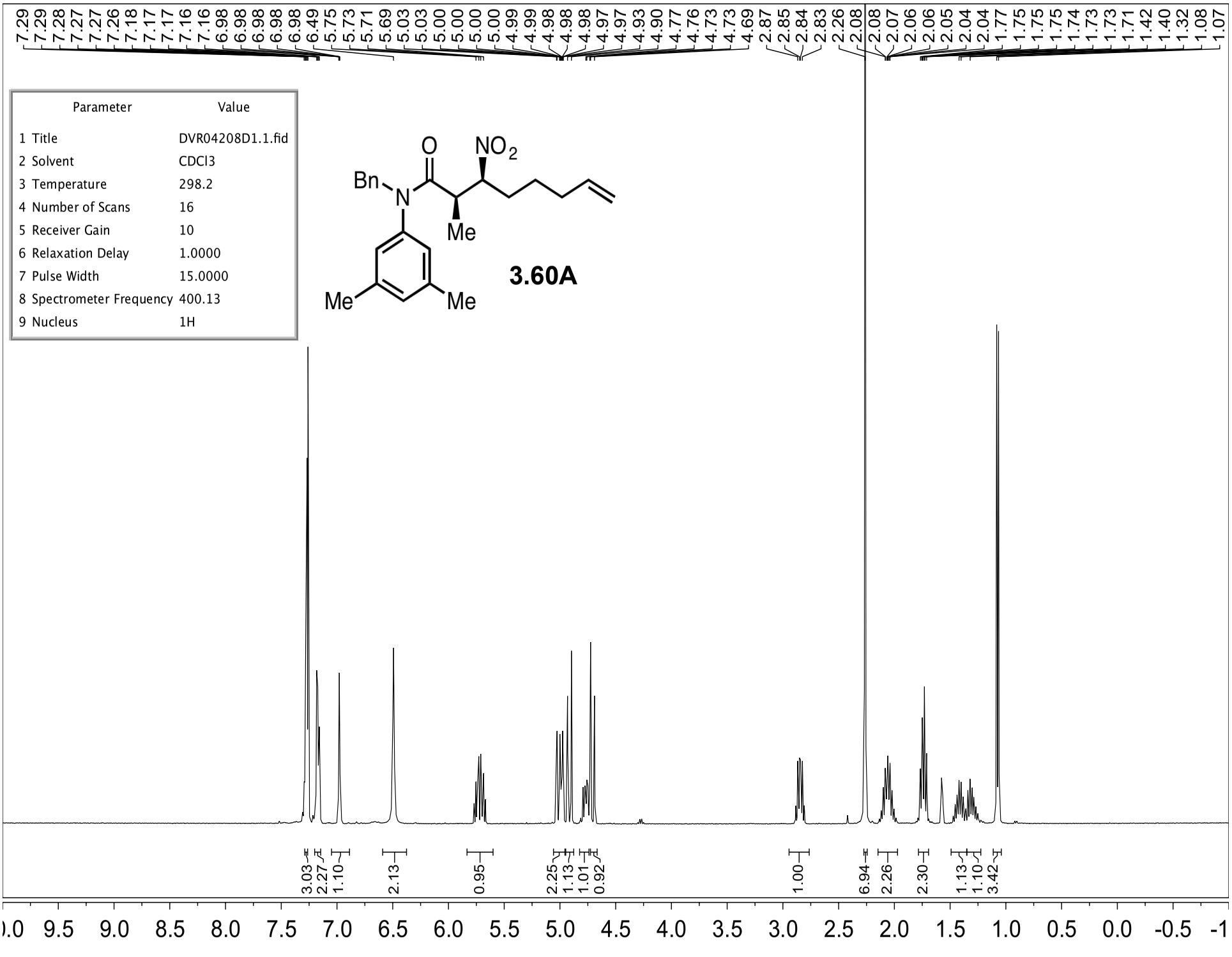
7.29 7.29 7.28 7.27 7.27 7.26 7.18 7.17 7.17 7.16 7.16 6.98 6.98 6.98 6.98 6.98 6.49 5.75 5.73 5.71 5.69 5.03 5.03 5.00 5.00 5.00 5.00 4.99 4.99 4.98 4.98 4.98 4.97 4.97 4.93 4.90 4.77 4.76 4.73 4.73 4.69 2.87 2.85 2.84 2.83 2.26 2.08 2.08 2.07 2.06 2.06 2.05 2.04 2.04 1.77 1.75 1.75 1.75 1.74 1.73 1.73 1.71 1.42 1.40 1.32 1.08 1.07
Parameter Value
1 Title DVR04208D1.1.fid
2 Solvent CDCl3
3 Temperature 298.2
4 Number of Scans 16
5 Receiver Gain 10
6 Relaxation Delay 1.0000
7 Pulse Width 15.0000
8 Spectrometer Frequency 400.13
9 Nucleus 1H
O
NO2
Bn
N
Me
Me
Me
3.60A
3.03 2.27 1.10 2.13 0.95 2.25 1.13 1.01 0.92 1.00 6.94 2.26 2.30 1.13 1.10 3.42
.0 9.5 9.0 8.5 8.0 7.5 7.0 6.5 6.0 5.5 5.0 4.5 4.0 3.5 3.0 2.5 2.0 1.5 1.0 0.5 0.0 -0.5 -1

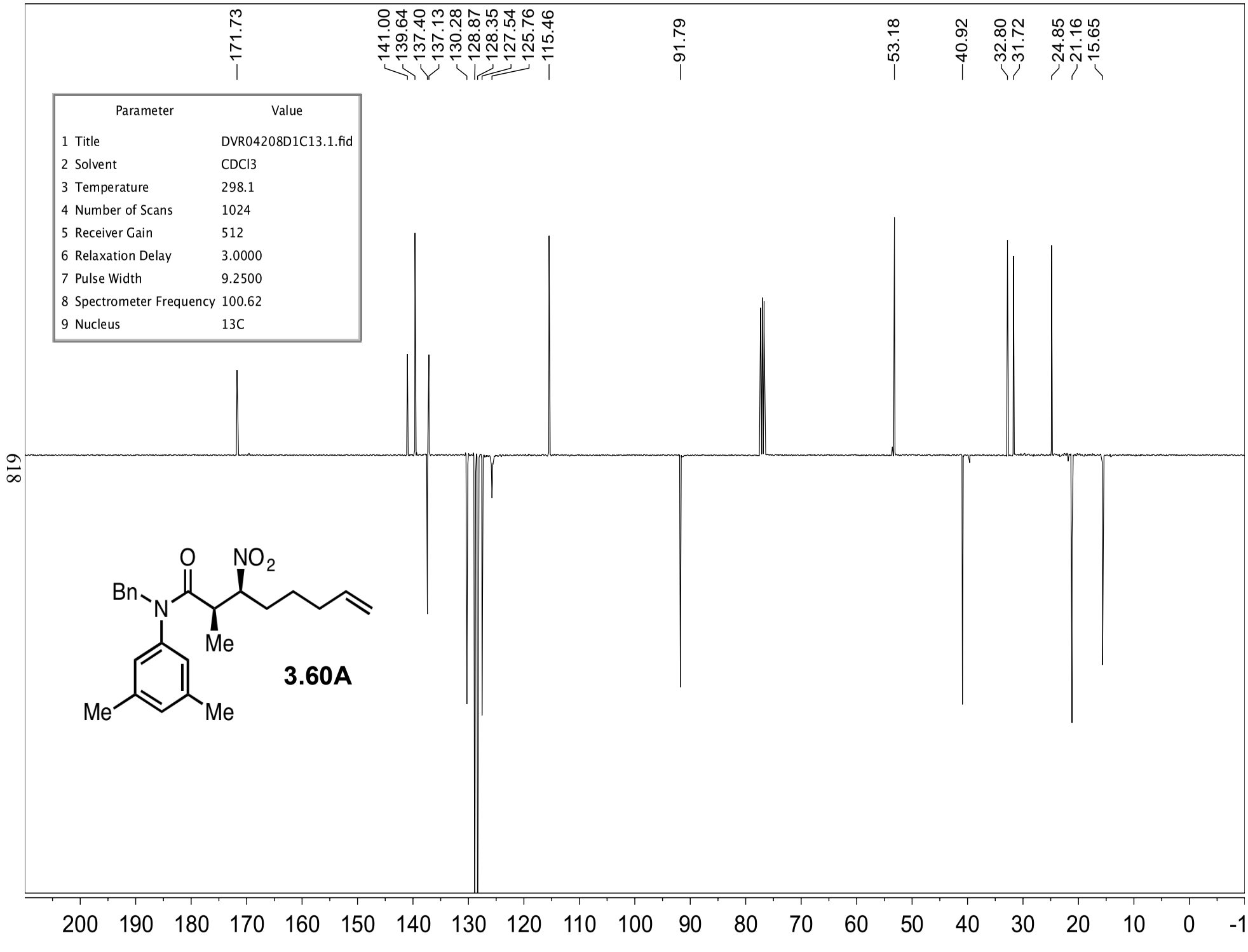
171.73
141.00
139.64
137.40
137.13
130.28
128.87
128.35
127.54
125.76
115.46
91.79
53.18
40.92
32.80
31.72
24.85
21.16
15.65
Parameter Value
1 Title DVR04208D1C13.1.fid
2 Solvent CDCl3
3 Temperature 298.1
4 Number of Scans 1024
5 Receiver Gain 512
6 Relaxation Delay 3.0000
7 Pulse Width 9.2500
8 Spectrometer Frequency 100.62
9 Nucleus 13C
618
O
NO2
Bn
N
Me
Me
Me
3.60A
200 190 180 170 160 150 140 130 120 110 100 90 80 70 60 50 40 30 20 10 0 -1

Parameter	Value
1 Title	DVR04208D2.1.fid
2 Solvent	CDCl3
3 Temperature	298.2
4 Number of Scans	16
5 Receiver Gain	10
6 Relaxation Delay	1.0000
7 Pulse Width	15.0000
8 Spectrometer Frequency	400.13
9 Nucleus	1H

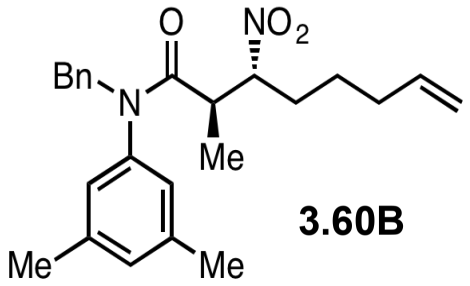

3.60B

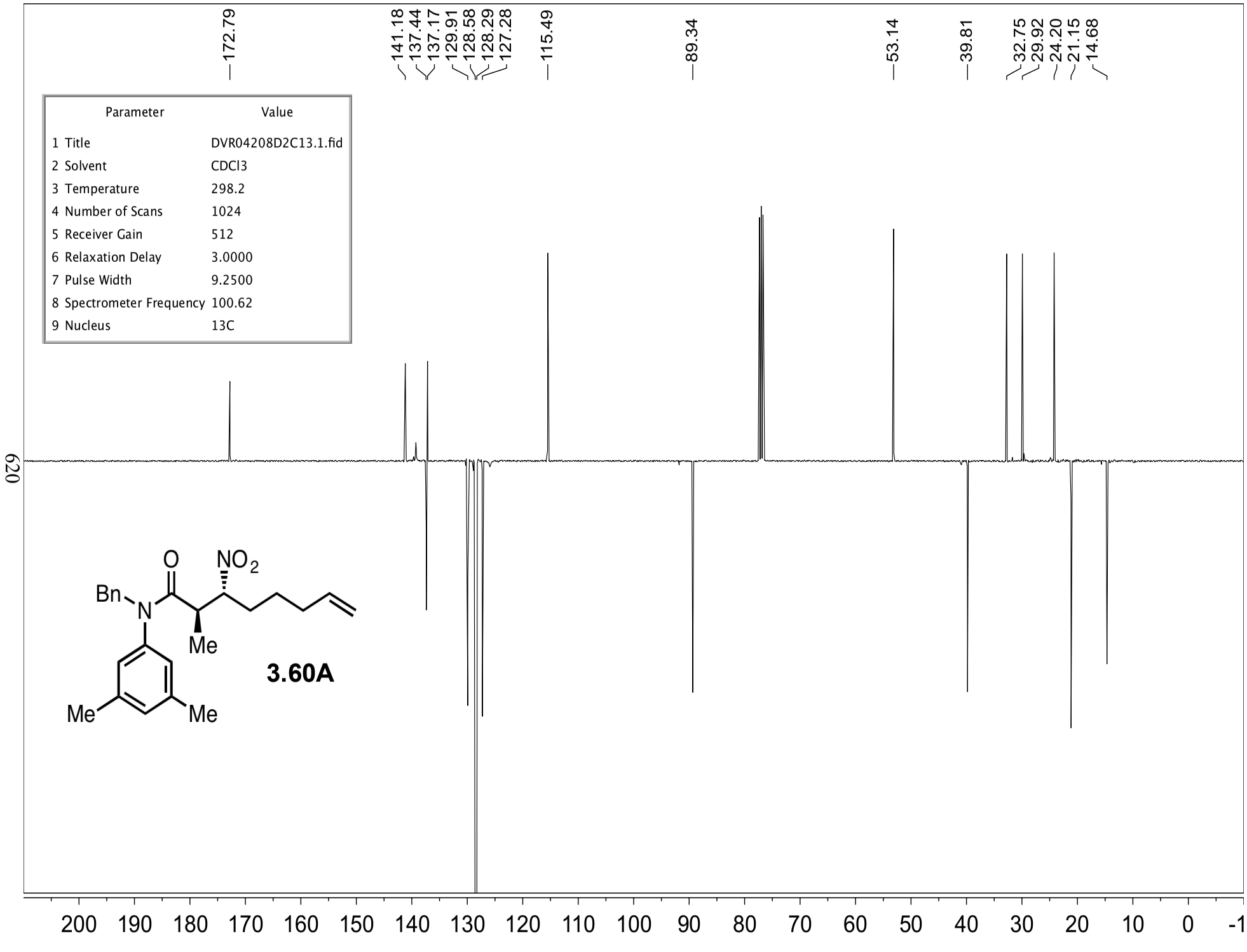
172.79
141.18
137.44
137.17
129.91
128.58
128.29
127.28
115.49
89.34
53.14
39.81
32.75
29.92
24.20
21.15
14.68
620
Parameter Value
1 Title DVR04208D2C13.1.fid
2 Solvent CDCl3
3 Temperature 298.2
4 Number of Scans 1024
5 Receiver Gain 512
6 Relaxation Delay 3.0000
7 Pulse Width 9.2500
8 Spectrometer Frequency 100.62
9 Nucleus 13C
O
NO2
Bn
N
Me
Me
Me
3.60A
200 190 180 170 160 150 140 130 120 110 100 90 80 70 60 50 40 30 20 10 0 -1

==== Shimadzu LCsolution Analysis Report ====

C:\LabSolutions\Data\DMM\DVR04208 RAC SYN_1052016_1934 PM_2.lcd

Acquired by	: LC User
Sample Name	: DVR04208 RAC SYN
Sample ID	: DVR04208 RAC SYN
Tray#	: 1
Vail #	: 1
Injection Volume	: 2 uL
Data File Name	: DVR04208 RAC SYN_1052016_1934 PM_2.lcd
Method File Name	: col3_2isoiPA_30min_1ML_220and210.lcm
Batch File Name	: DMM.lcb
Report File Name	: Default.lcr
Data Acquired	: 10/5/2016 8:04:47 PM
Data Processed	: 10/5/2016 8:34:50 PM

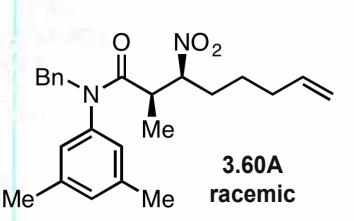

3.60A racemic

<Chromatogram>

C:\LabSolutions\Data\DMM\DVR04208 RAC SYN_1052016_1934 PM_2.lcd

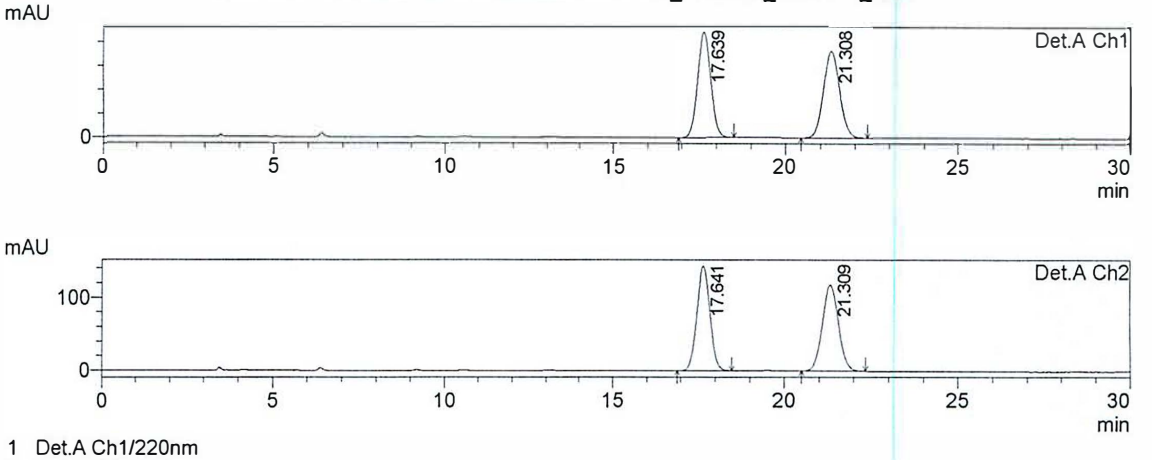

1 Det.A Ch1/220nm
2 Det.A Ch2/210nm

PeakTable

Detector A Ch1 220nm

Peak#	Ret. Time	Area	Height	Area %	Height %
1	17.639	2341462	88122	49.919	54.847
2	21.308	2349054	72547	50.081	45.153
Total		4690517	160669	100.000	100.000

PeakTable

Detector A Ch2 210nm

Peak#	Ret. Time	Area	Height	Area %	Height %
1	17.641	3828553	144185	49.931	54.846
2	21.309	3839066	118705	50.069	45.154
Total		7667619	262890	100.000	100.000

==== Shimadzu LCsolution Analysis Report ====

C:\LabSolutions\Data\DMM\DVR04208 SYN_1052016_1934 PM_6.lcd

Acquired by	: LC User
Sample Name	: DVR04208 SYN
Sample ID	: DVR04208 SYN
Tray#	: 1
Vail #	: 2
Injection Volume	: 2 uL
Data File Name	: DVR04208 SYN_1052016_1934 PM_6.lcd
Method File Name	: col3_2isoiPA_30min_1ML_220and210.lcm
Batch File Name	: DMM.lcb
Report File Name	: Default.lcr
Data Acquired	: 10/5/2016 9:15:42 PM
Data Processed	: 10/5/2016 9:45:44 PM

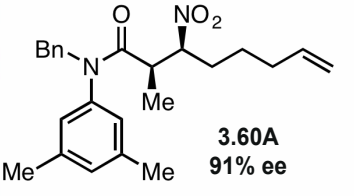

3.60A
91% ee

<Chromatogram>

C:\LabSolutions\Data\DMM\DVR04208 SYN_1052016_1934 PM_6.lcd

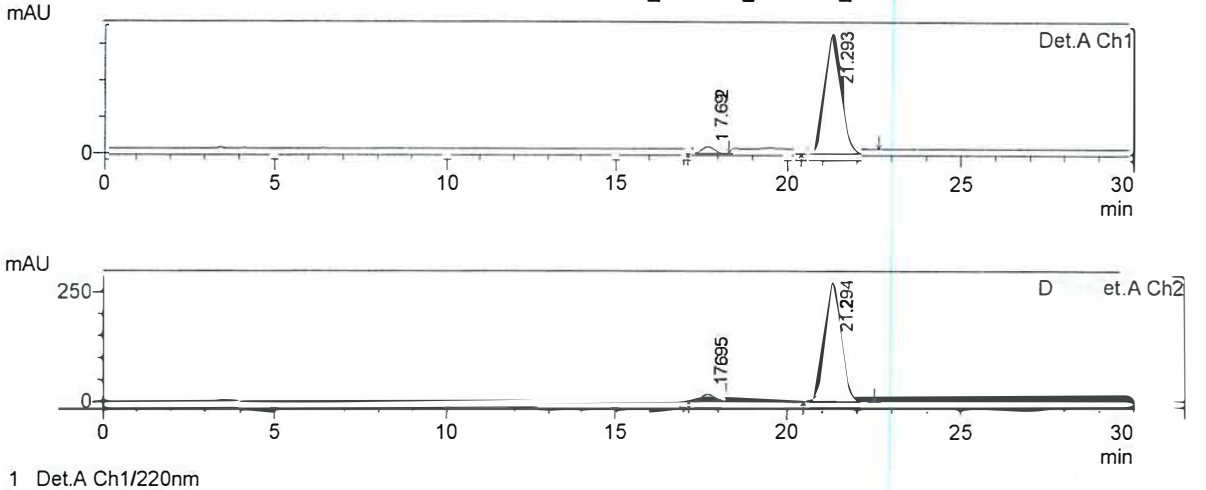

1 Det.A Ch1/220nm
2 Det.A Ch2/210nm

PeakTable

Detector A Ch1 220nm

Peak#	Ret. Time	Area	Height	Area %	Height %
1	17.692	244609	9507	4.360	5.410
2	21.293	5366253	166221	95.640	94.590
Total		5610862	175728	100.000	100.000

PeakTable

Detector A Ch2 210nm

Peak#	Ret. Time	Area	Height	Area %	Height %
1	17.695	399783	15548	4.355	5.400
2	21.294	8780463	272387	95.645	94.600
Total		9180246	287934	100.000	100.000

==== Shimadzu LCsolution Analysis Report ====

C:\LabSolutions\Data\DMM\DVR04208 rac d2_1062016_1716 PM_2.lcd

Acquired by	: LC User
Sample Name	: DVR04208 rac d2
Sample ID	: DVR04208 rac d2
Tray#	: 1
Vail #	: 2
Injection Volume	: 3 uL
Data File Name	: DVR04208 rac d2_1062016_1716 PM_2.lcd
Method File Name	: col3_8isoIPA_60min_1mL_254and280.lcm
Batch File Name	: DMM.lcb
Report File Name	: Default.lcr
Data Acquired	: 10/6/2016 5:46:50 PM
Data Processed	: 10/6/2016 6:46:53 PM

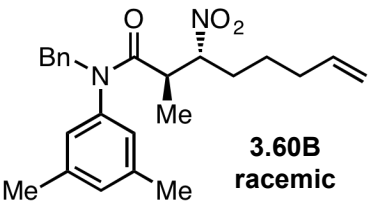

3.60B racemic

<Chromatogram>

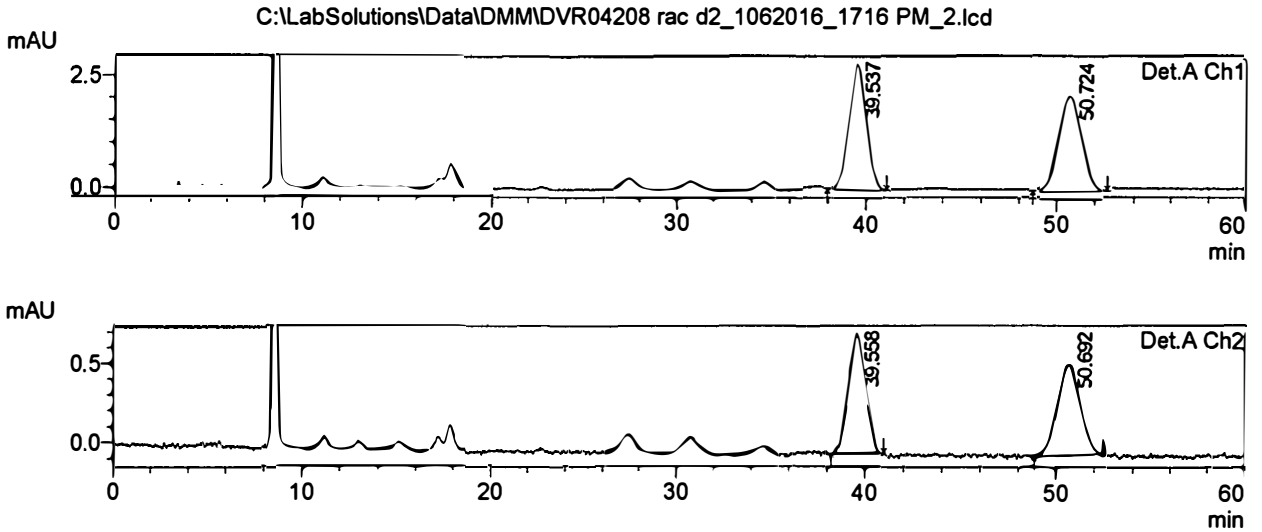

1 Det.A Ch1/254nm
2 Det.A Ch2/280nm

PeakTable

Detector A Ch1 254nm

Peak#	Ret. Time	Area	Height	Area %	Height %
1	39.537	173539	2778	49.844	56.853
2	50.724	174629	2108	50.156	43.147
Total		348168	4886	100.000	100.000

PeakTable

Detector A Ch2 280nm

Peak#	Ret. Time	Area	Height	Area %	Height %
1	39.558	46436	760	49.192	56.765
2	50.692	47963	578	50.808	43.235
Total		94399	1338	100.000	100.000

==== Shimadzu LCsolution Analysis Report ====

C:\LabSolutions\Data\DMM\DVR04208 D2_1062016_1716 PM_6.lcd

Acquired by	: LC User
Sample Name	: DVR04208 D2
Sample ID	: DVR04208 D2
Tray#	: 1
Vail #	: 3
Injection Volume	: 3 uL
Data File Name	: DVR04208 D2_1062016_1716 PM_6.lcd
Method File Name	: col3_8isoIPA_60min_1mL_254and280.lcm
Batch File Name	: DMM.lcb
Report File Name	: Default.lcr
Data Acquired	: 10/6/2016 7:27:44 PM
Data Processed	: 10/6/2016 8:27:45 PM

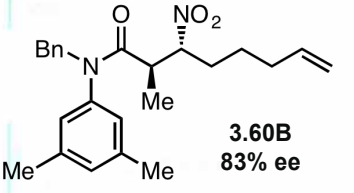

3.60B
83% ee

<Chromatogram>

C:\LabSolutions\Data\DMM\DVR04208 D2_1062016_1716 PM_6.lcd

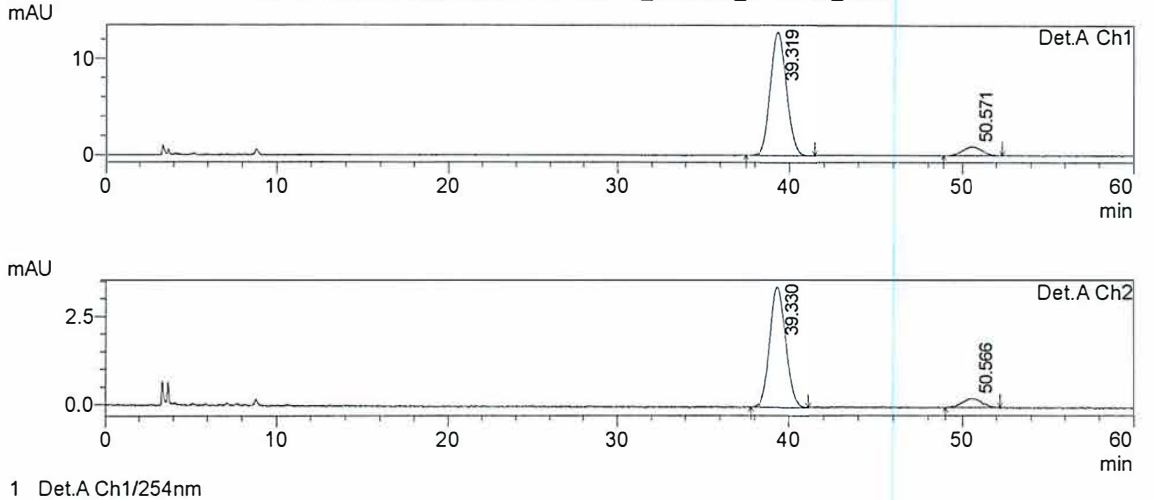

1 Det.A Ch1/254nm
2 Det.A Ch2/280nm

PeakTable

Detector A Ch1 254nm

Peak#	Ret. Time	Area	Height	Area %	Height %
1	39.319	813272	12797	91.477	93.159
2	50.571	75775	940	8.523	6.841
Total		889047	13736	100.000	100.000

PeakTable

Detector A Ch2 280nm

Peak#	Ret. Time	Area	Height	Area %	Height %
1	39.330	219035	3412	91.165	92.897
2	50.566	21228	261	8.835	7.103
Total		240263	3673	100.000	100.000

Parameter	Value
1 Title	RS-01-229-crude.1.fid
2 Solvent	CDCl3
3 Temperature	300.0
4 Number of Scans	16
5 Receiver Gain	32
6 Relaxation Delay	10.0000
7 Pulse Width	10.7700
8 Spectrometer Frequency	600.32
9 Nucleus	1H

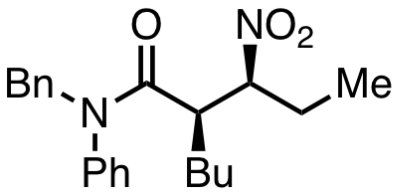

3.61A

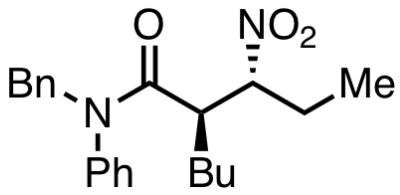

3.61B

Crude

54:46

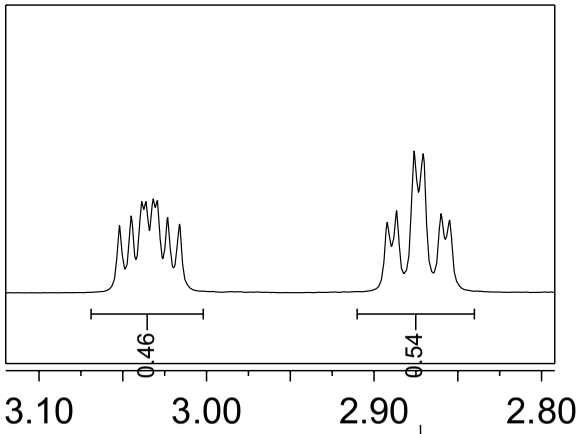

625

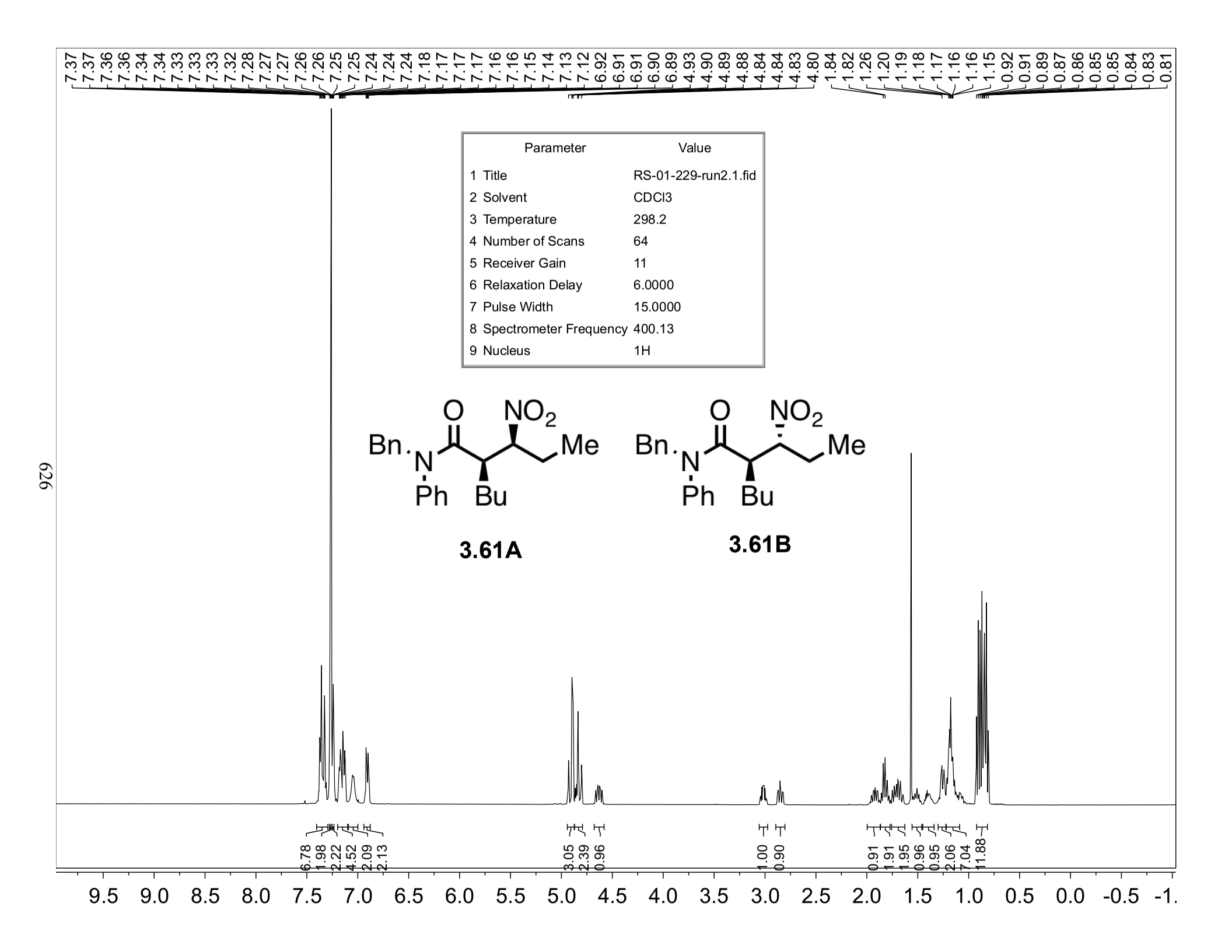
7.37 7.37 7.36 7.36 7.34 7.34 7.33 7.33 7.33 7.32 7.28 7.27 7.27 7.26 7.26 7.25 7.25 7.24 7.24 7.24 7.18 7.17 7.17 7.17 7.16 7.16 7.15 7.14 7.13 7.12 6.92 6.91 6.91 6.90 6.89 4.93 4.90 4.89 4.88 4.84 4.84 4.83 4.80 1.84 1.82 1.26 1.20 1.19 1.18 1.17 1.16 1.16 1.15 0.92 0.91 0.89 0.87 0.86 0.85 0.85 0.84 0.83 0.81
Parameter Value
1 Title RS-01-229-run2.1.fid
2 Solvent CDCl3
3 Temperature 298.2
4 Number of Scans 64
5 Receiver Gain 11
6 Relaxation Delay 6.0000
7 Pulse Width 15.0000
8 Spectrometer Frequency 400.13
9 Nucleus 1H
Bn N Ph O NO2 Me Bu
3.61A
Bn N Ph O NO2 Me Bu
3.61B
626
6.78 1.98 2.22 4.52 2.09 2.13 3.05 2.39 0.96 1.00 0.90 0.91 1.91 1.95 0.96 0.95 2.06 7.04 11.88
9.5 9.0 8.5 8.0 7.5 7.0 6.5 6.0 5.5 5.0 4.5 4.0 3.5 3.0 2.5 2.0 1.5 1.0 0.5 0.0 -0.5 -1.

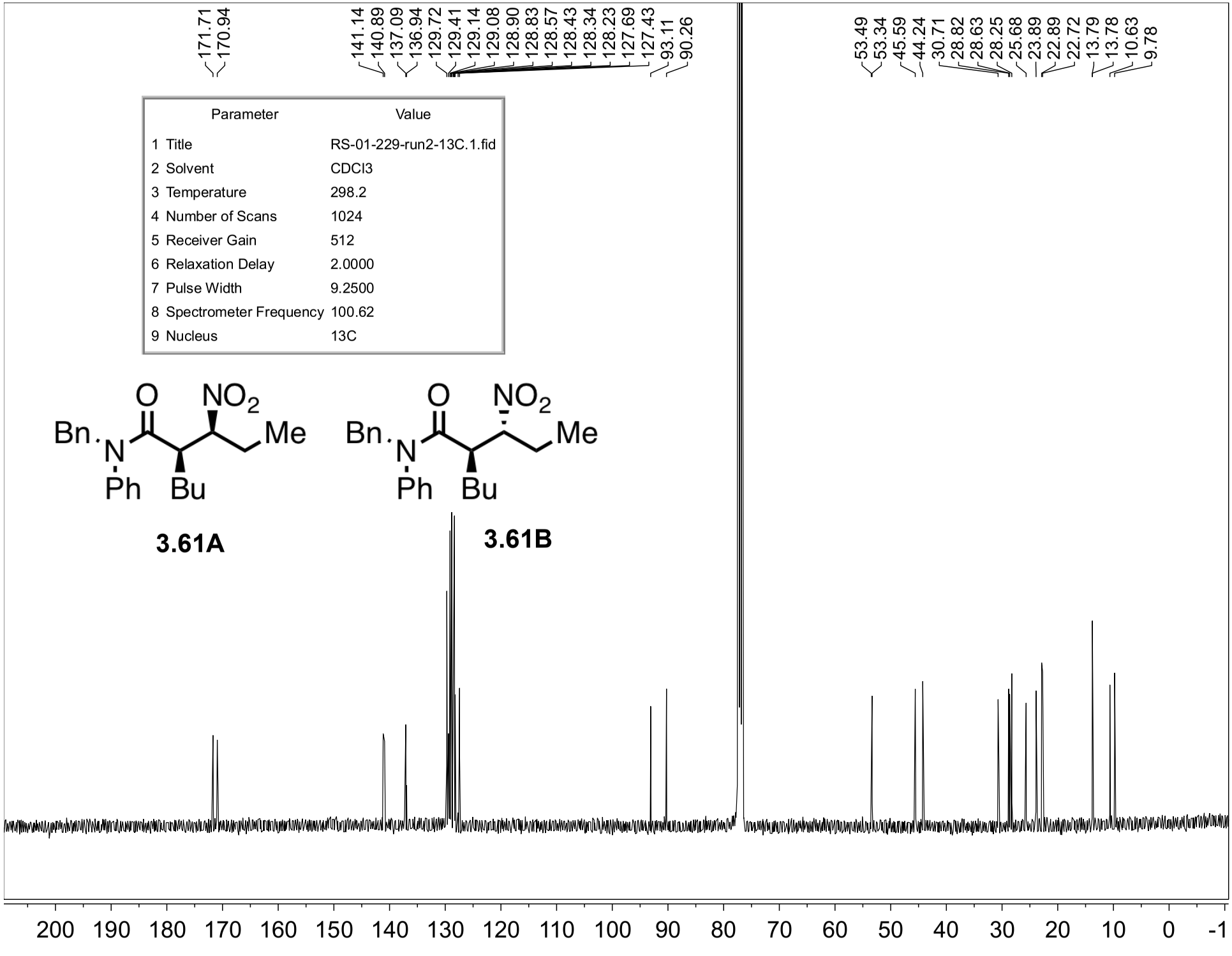
171.71
170.94
141.14
140.89
137.09
136.94
129.72
129.41
129.14
129.08
128.90
128.83
128.57
128.43
128.34
128.23
127.69
127.43
93.11
90.26
53.49
53.34
45.59
44.24
30.71
28.82
28.63
28.25
25.68
23.89
22.89
22.72
13.79
13.78
10.63
9.78
Parameter Value
1 Title RS-01-229-run2-13C.1.fid
2 Solvent CDCl3
3 Temperature 298.2
4 Number of Scans 1024
5 Receiver Gain 512
6 Relaxation Delay 2.0000
7 Pulse Width 9.2500
8 Spectrometer Frequency 100.62
9 Nucleus 13C
Bn
N
Ph
O
NO2
Me
Bu
3.61A
3.61B
200 190 180 170 160 150 140 130 120 110 100 90 80 70 60 50 40 30 20 10 0 -1

==== Shimadzu LCsolution Analysis Report ====

C:\LabSolutions\Data\DMM\RS-01-240-RES_10122016_1001 AM_2.lcd

Acquired by	: LC User
Sample Name	: RS-01-240-RES
Sample ID	: RS-01-240-RES
Tray#	: 1
Vail #	: 91
Injection Volume	: 2 uL
Data File Name	: RS-01-240-RES_10122016_1001 AM_2.lcd
Method File Name	: col5_3isoiPA_60min_1.0ML_254and210.lcm
Batch File Name	: DMM.lcb
Report File Name	: Default.lcr
Data Acquired	: 10/12/2016 10:16:44 AM
Data Processed	: 10/12/2016 11:16:45 AM

<Chromatogram>

C:\LabSolutions\Data\DMM\RS-01-240-RES_10122016_1001 AM_2.lcd

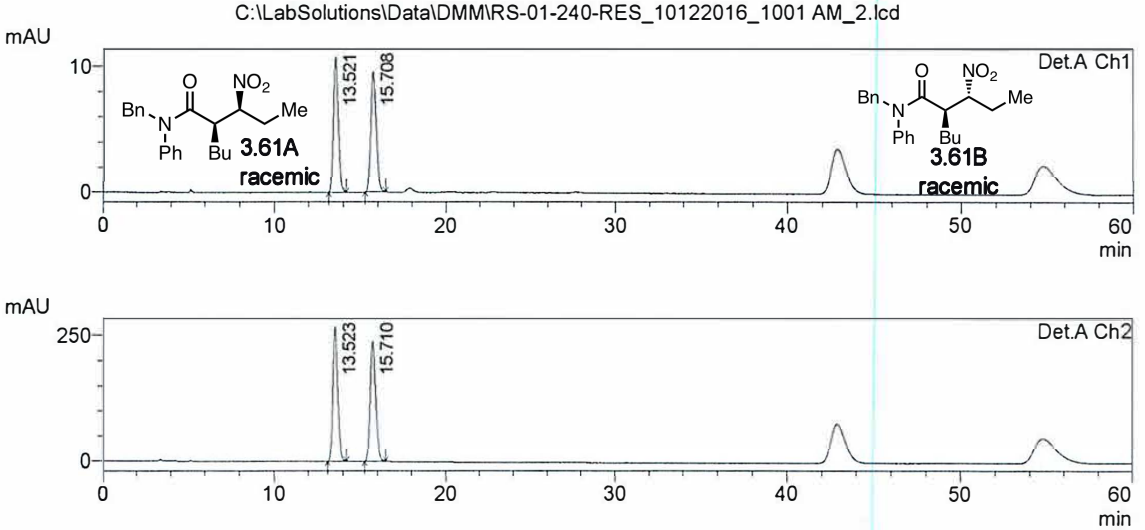

1 Det.A Ch1/254nm
2 Det.A Ch2/210nm

PeakTable

Detector A Ch1 254nm

Peak#	Ret. Time	Area	Height	Area %	Height %
1	13.521	208119	10773	49.292	52.984
2	15.708	214099	9559	50.708	47.016
Total		422218	20332	100.000	100.000

PeakTable

Detector A Ch2 210nm

Peak#	Ret. Time	Area	Height	Area %	Height %
1	13.523	5197100	268121	49.269	52.943
2	15.710	5351355	238314	50.731	47.057
Total		10548455	506435	100.000	100.000

==== Shimadzu LCsolution Analysis Report ====

C:\LabSolutions\Data\DMM\RS-01-229-final_10122016_1001 AM_3.lcd

Acquired by	: LC User
Sample Name	: RS-01-229-final
Sample ID	: RS-01-229-final
Tray#	: 1
Vail #	: 92
Injection Volume	: 3 uL
Data File Name	: RS-01-229-final_10122016_1001 AM_3.lcd
Method File Name	: col5_3isoiPA_60min_1.0ML_254and210.lcm
Batch File Name	: DMM.lcb
Report File Name	: Default.lcr
Data Acquired	: 10/12/2016 11:17:19 AM
Data Processed	: 10/12/2016 12:17:22 PM

<Chromatogram>

C:\LabSolutions\Data\DMM\RS-01-229-final_10122016_1001 AM_3.lcd

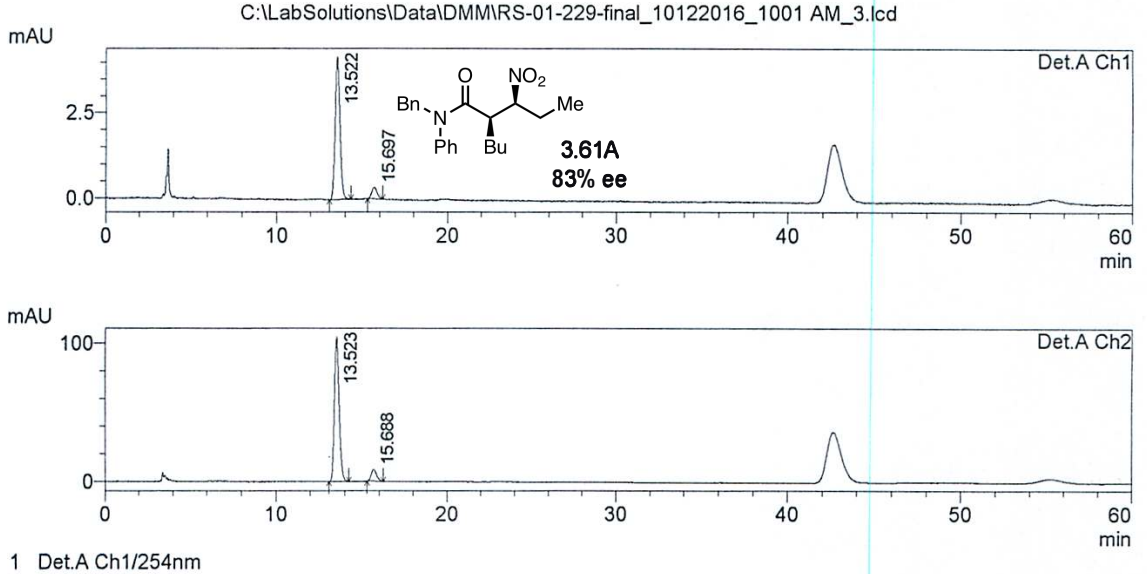

1 Det.A Ch1/254nm
2 Det.A Ch2/210nm

PeakTable

Detector A Ch1 254nm

Peak#	Ret. Time	Area	Height	Area %	Height %
1	13.522	80975	4207	91.552	92.401
2	15.697	7472	346	8.448	7.599
Total		88447	4553	100.000	100.000

PeakTable

Detector A Ch2 210nm

Peak#	Ret. Time	Area	Height	Area %	Height %
1	13.523	2016783	105053	91.495	92.403
2	15.688	187468	8638	8.505	7.597
Total		2204252	113690	100.000	100.000

==== Shimadzu LCsolution Analysis Report ====

C:\LabSolutions\Data\DMM\RS-01-240-RES_10122016_1001 AM_2.lcd

Acquired by	: LC User
Sample Name	: RS-01-240-RES
Sample ID	: RS-01-240-RES
Tray#	: 1
Vail #	: 91
Injection Volume	: 2 uL
Data File Name	: RS-01-240-RES_10122016_1001 AM_2.lcd
Method File Name	: col5_3isoiPA_60min_1.0ML_254and210.lcm
Batch File Name	: DMM.lcb
Report File Name	: Default.lcr
Data Acquired	: 10/12/2016 10:16:44 AM
Data Processed	: 10/12/2016 12:20:03 PM

<Chromatogram>

C:\LabSolutions\Data\DMM\RS-01-240-RES_10122016_1001 AM_2.lcd

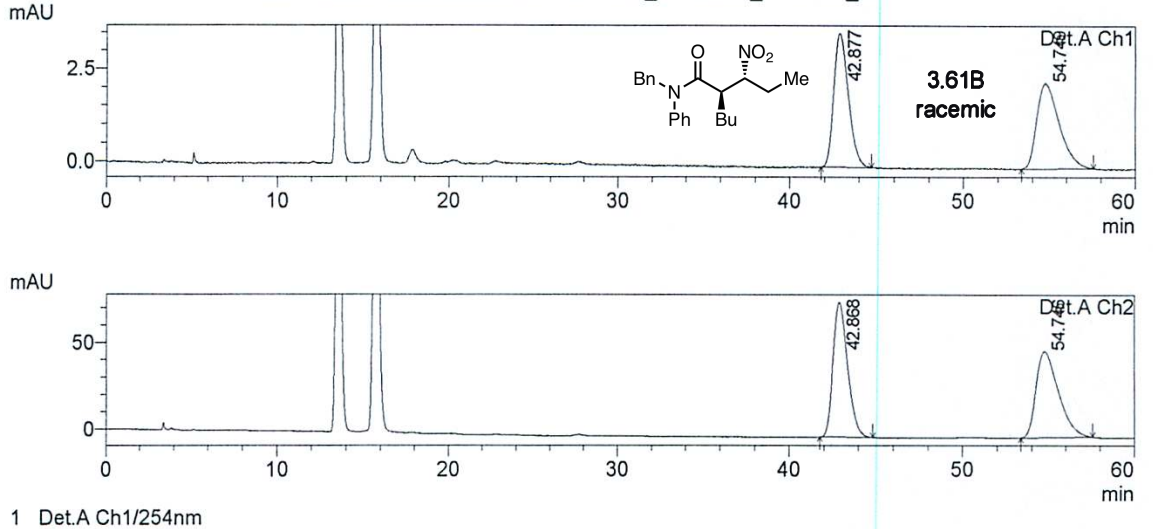

1 Det.A Ch1/254nm
2 Det.A Ch2/210nm

PeakTable

Detector A Ch1 254nm

Peak#	Ret. Time	Area	Height	Area %	Height %
1	42.877	211348	3617	50.119	60.969
2	54.749	210348	2316	49.881	39.031
Total		421696	5933	100.000	100.000

PeakTable

Detector A Ch2 210nm

Peak#	Ret. Time	Area	Height	Area %	Height %
1	42.868	4542037	78030	50.118	61.045
2	54.746	4520585	49793	49.882	38.955
Total		9062621	127824	100.000	100.000

==== Shimadzu LCsolution Analysis Report ====

C:\LabSolutions\Data\DMM\RS-01-229-final_10122016_1001 AM_3.lcd

Acquired by	: LC User
Sample Name	: RS-01-229-final
Sample ID	: RS-01-229-final
Tray#	: 1
Vail #	: 92
Injection Volume	: 3 uL
Data File Name	: RS-01-229-final_10122016_1001 AM_3.lcd
Method File Name	: col5_3isoiPA_60min_1.0ML_254and210.lcm
Batch File Name	: DMM.lcb
Report File Name	: Default.lcr
Data Acquired	: 10/12/2016 11:17:19 AM
Data Processed	: 10/12/2016 12:17:22 PM

<Chromatogram>

C:\LabSolutions\Data\DMM\RS-01-229-final_10122016_1001 AM_3.lcd

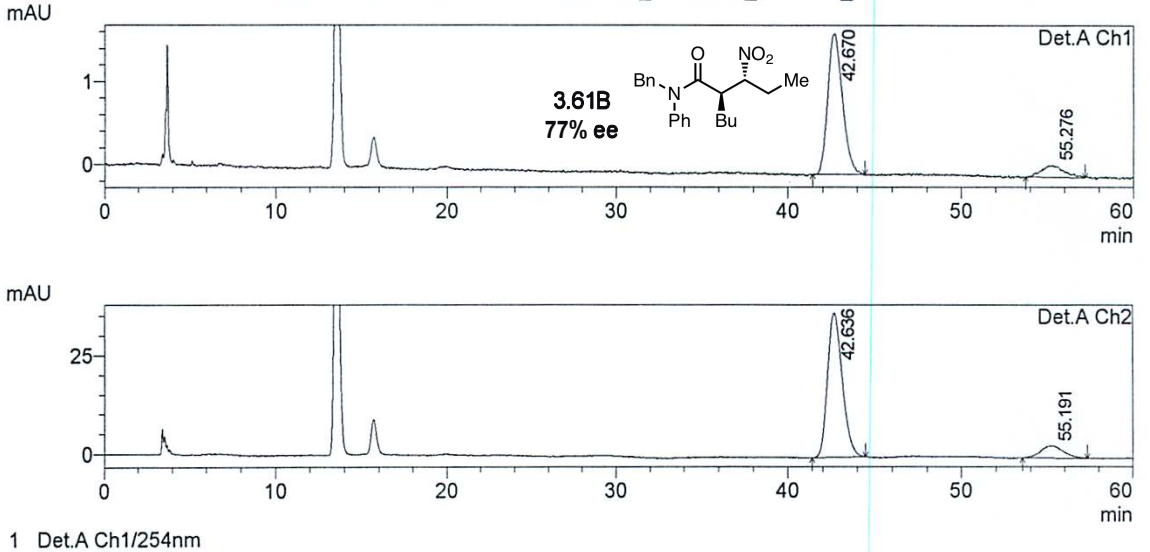

1 Det.A Ch1/254nm
2 Det.A Ch2/210nm

PeakTable

Detector A Ch1 254nm

Peak#	Ret. Time	Area	Height	Area %	Height %
1	42.670	99819	1699	88.563	92.074
2	55.276	12891	146	11.437	7.926
Total		112709	1845	100.000	100.000

PeakTable

Detector A Ch2 210nm

Peak#	Ret. Time	Area	Height	Area %	Height %
1	42.636	2163440	36678	88.746	92.388
2	55.191	274361	3022	11.254	7.612
Total		2437801	39700	100.000	100.000

Parameter	Value
1 Title	DVR05049CRD CDCL3.1.fid
2 Solvent	CDCl3
3 Temperature	298.2
4 Number of Scans	16
5 Receiver Gain	10
6 Relaxation Delay	1.0000
7 Pulse Width	15.0000
8 Spectrometer Frequency	400.13
9 Nucleus	1H

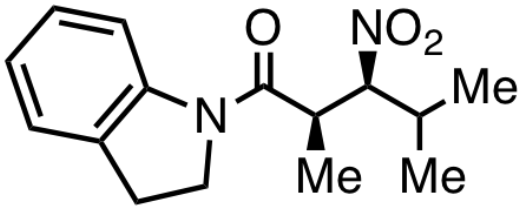

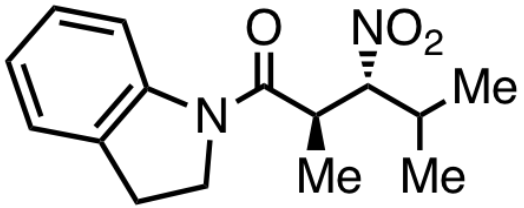

Crude

3.62A 96:04 **3.62B**

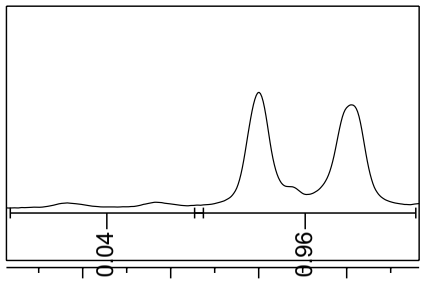

632

Parameter	Value
1 Title	DVR05049 rt.1.fid
2 Solvent	DMSO
3 Temperature	299.4
4 Number of Scans	16
5 Receiver Gain	101
6 Relaxation Delay	1.0000
7 Pulse Width	15.0000
8 Spectrometer Frequency	400.15
9 Nucleus	1H

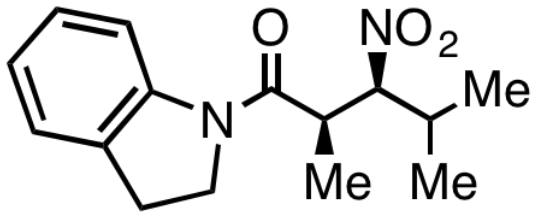

3.62A

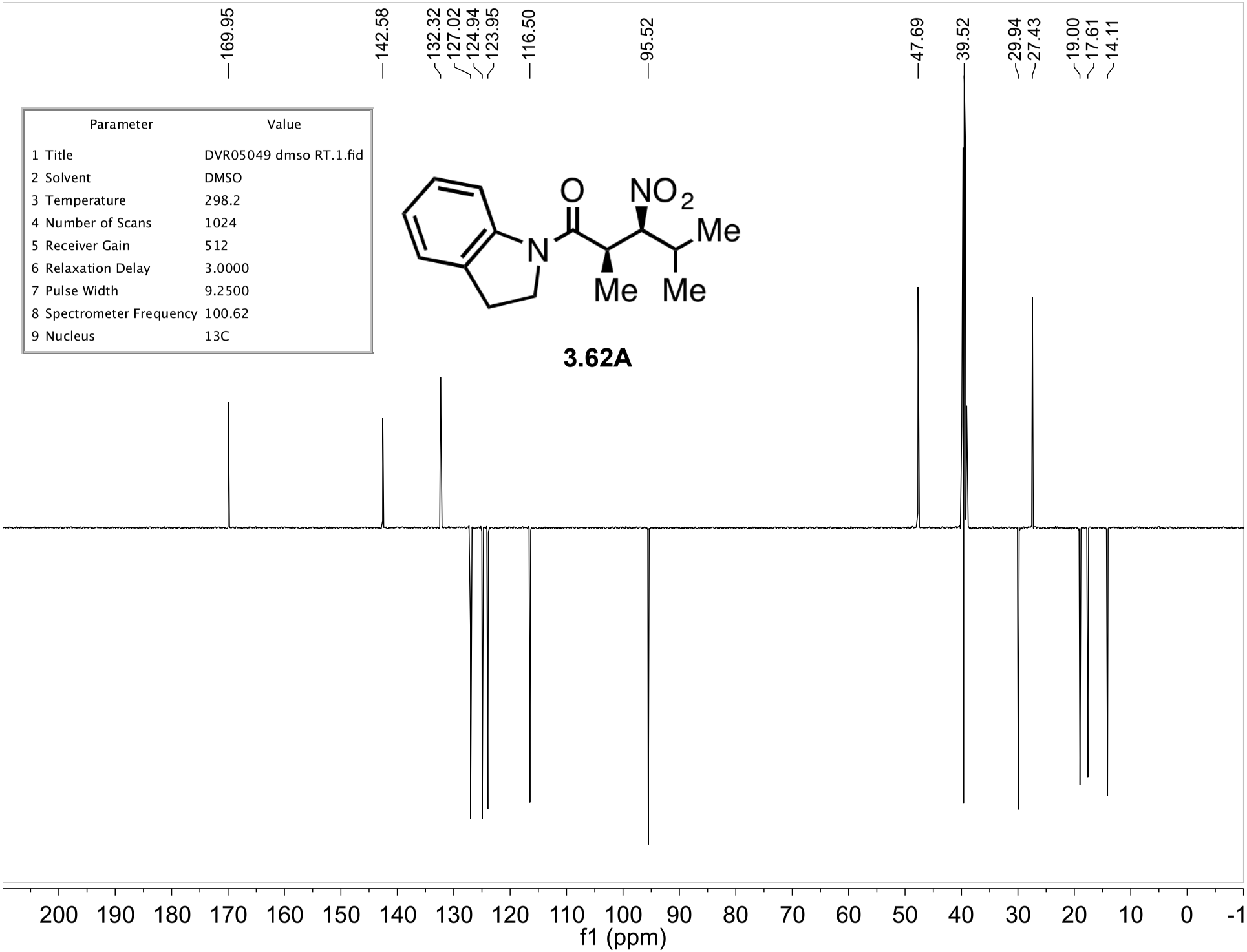
169.95
142.58
132.32
127.02
124.94
123.95
116.50
95.52
47.69
39.52
29.94
27.43
19.00
17.61
14.11
Parameter
Value
1 Title
DVR05049 dmso RT.1.fid
2 Solvent
DMSO
3 Temperature
298.2
4 Number of Scans
1024
5 Receiver Gain
512
6 Relaxation Delay
3.0000
7 Pulse Width
9.2500
8 Spectrometer Frequency
100.62
9 Nucleus
13C
O
NO2
N
Me
Me
Me
3.62A
634
200 190 180 170 160 150 140 130 120 110 100 90 80 70 60 50 40 30 20 10 0 -1
f1 (ppm)

==== Shimadzu LCsolution Analysis Report ====

C:\LabSolutions\Data\DMM\DVR05049RAC_382017_955 AM_5.lcd

Acquired by	: LC User
Sample Name	: DVR05049RAC
Sample ID	: DVR05049RAC
Tray#	: 1
Vail #	: 1
Injection Volume	: 3 uL
Data File Name	: DVR05049RAC_382017_955 AM_5.lcd
Method File Name	: col1_1isoiPA_30min_1ML_254and210.lcm
Batch File Name	: DMM.lcb
Report File Name	: Default.lcr
Data Acquired	: 3/8/2017 12:48:27 PM
Data Processed	: 3/8/2017 1:18:28 PM

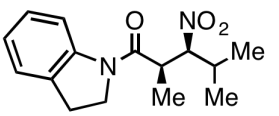

3.62
racemic

<Chromatogram>

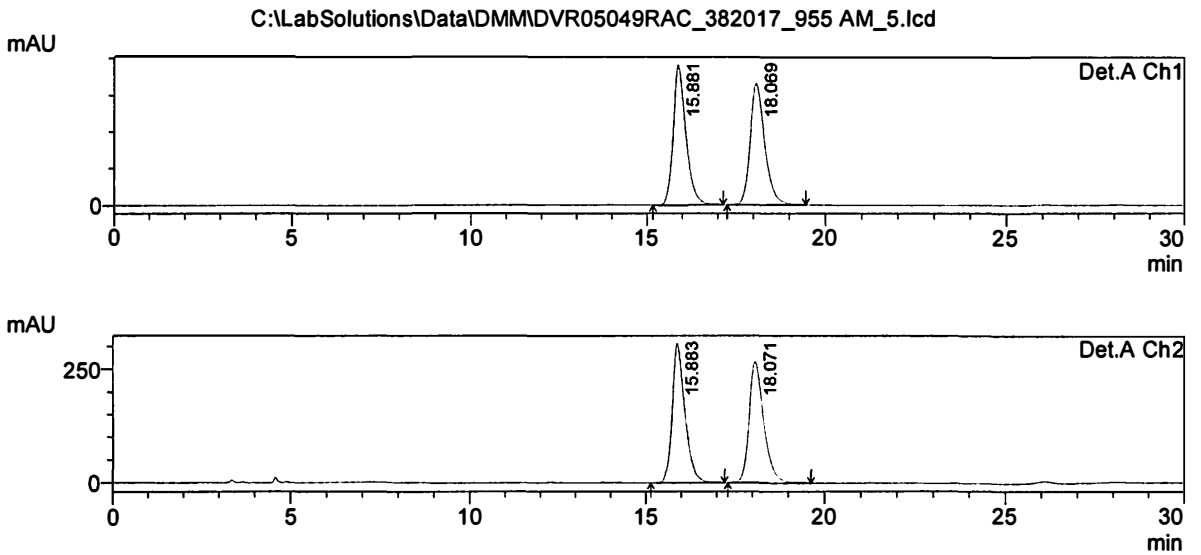

1 Det.A Ch1/254nm
2 Det.A Ch2/210nm

PeakTable

Detector A Ch1 254nm

Peak#	Ret. Time	Area	Height	Area %	Height %
1	15.881	4746999	191118	50.154	53.475
2	18.069	4717929	166282	49.846	46.525
Total		9464928	357400	100.000	100.000

PeakTable

Detector A Ch2 210nm

Peak#	Ret. Time	Area	Height	Area %	Height %
1	15.883	7628150	306467	50.087	53.427
2	18.071	7601695	267148	49.913	46.573
Total		15229845	573615	100.000	100.000

==== Shimadzu LCsolution Analysis Report ====

C:\LabSolutions\Data\DMM\DVR05049 D1_382017_955 AM_9.lcd

Acquired by	: LC User
Sample Name	: DVR05049 D1
Sample ID	: DVR05049 D1
Tray#	: 1
Vail #	: 2
Injection Volume	: 3 uL
Data File Name	: DVR05049 D1_382017_955 AM_9.lcd
Method File Name	: col1_1isoiPA_30min_1ML_254and210.lcm
Batch File Name	: DMM.lcb
Report File Name	: Default.lcr
Data Acquired	: 3/8/2017 1:59:26 PM
Data Processed	: 3/8/2017 2:29:27 PM

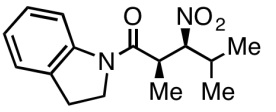

3.62
99% ee

<Chromatogram>

C:\LabSolutions\Data\DMM\DVR05049 D1_382017_955 AM_9.lcd

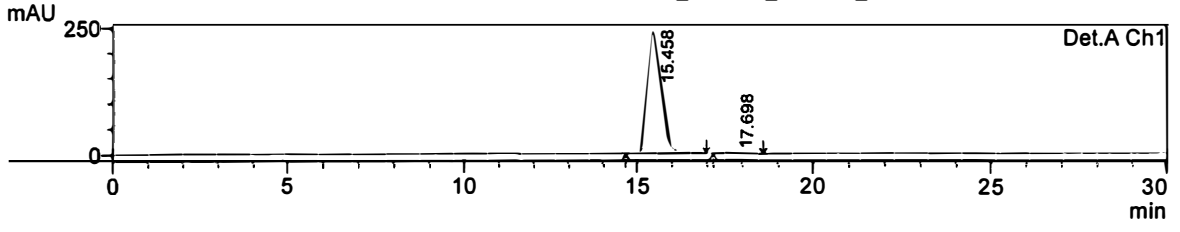

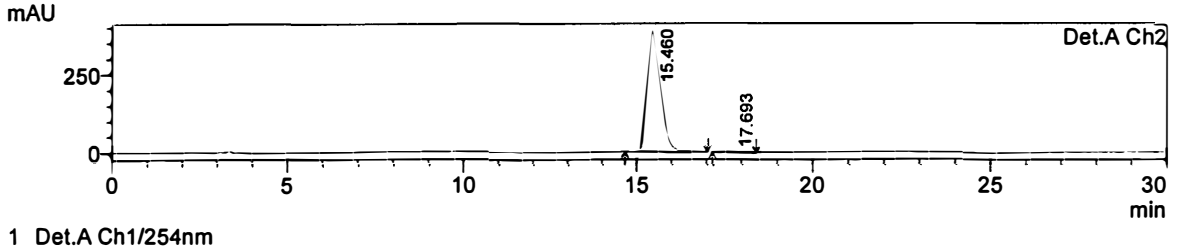

1 Det.A Ch1/254nm
2 Det.A Ch2/210nm

PeakTable

Detector A Ch1 254nm

Peak#	Ret. Time	Area	Height	Area %	Height %
1	15.458	5749436	242233	99.419	99.426
2	17.698	33618	1397	0.581	0.574
Total		5783054	243630	100.000	100.000

PeakTable

Detector A Ch2 210nm

Peak#	Ret. Time	Area	Height	Area %	Height %
1	15.460	9262467	388183	99.470	99.457
2	17.693	49334	2118	0.530	0.543
Total		9311801	390302	100.000	100.000

Parameter	Value
1 Title	DVR05024CRD.1.fid
2 Solvent	CDCl3
3 Temperature	298.0
4 Number of Scans	16
5 Receiver Gain	161
6 Relaxation Delay	1.0000
7 Pulse Width	13.5000
8 Spectrometer Frequency	600.32
9 Nucleus	1H

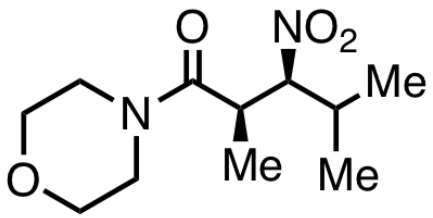

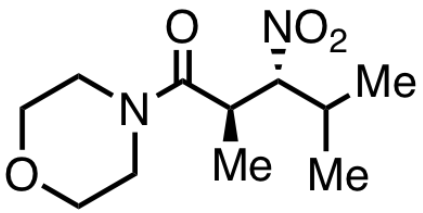

Crude

3.63A **92:08** **3.63B**

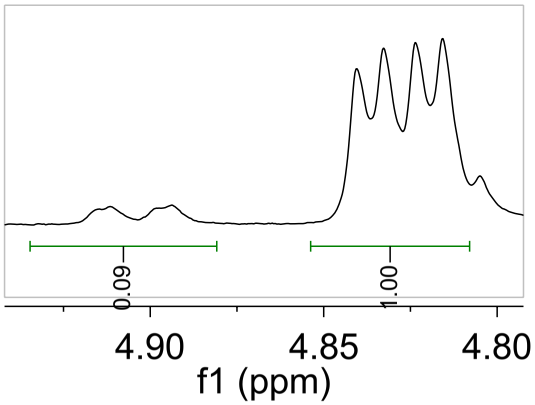

637

Parameter	Value
1 Title	DVR05024D1.1.fid
2 Solvent	CDCl3
3 Temperature	298.2
4 Number of Scans	16
5 Receiver Gain	10
6 Relaxation Delay	1.0000
7 Pulse Width	15.0000
8 Spectrometer Frequency	400.13
9 Nucleus	1H

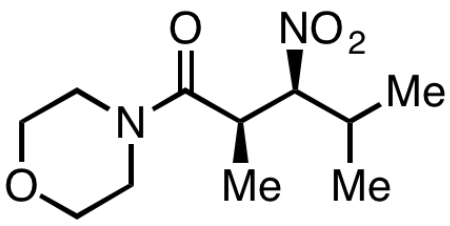

3.63A

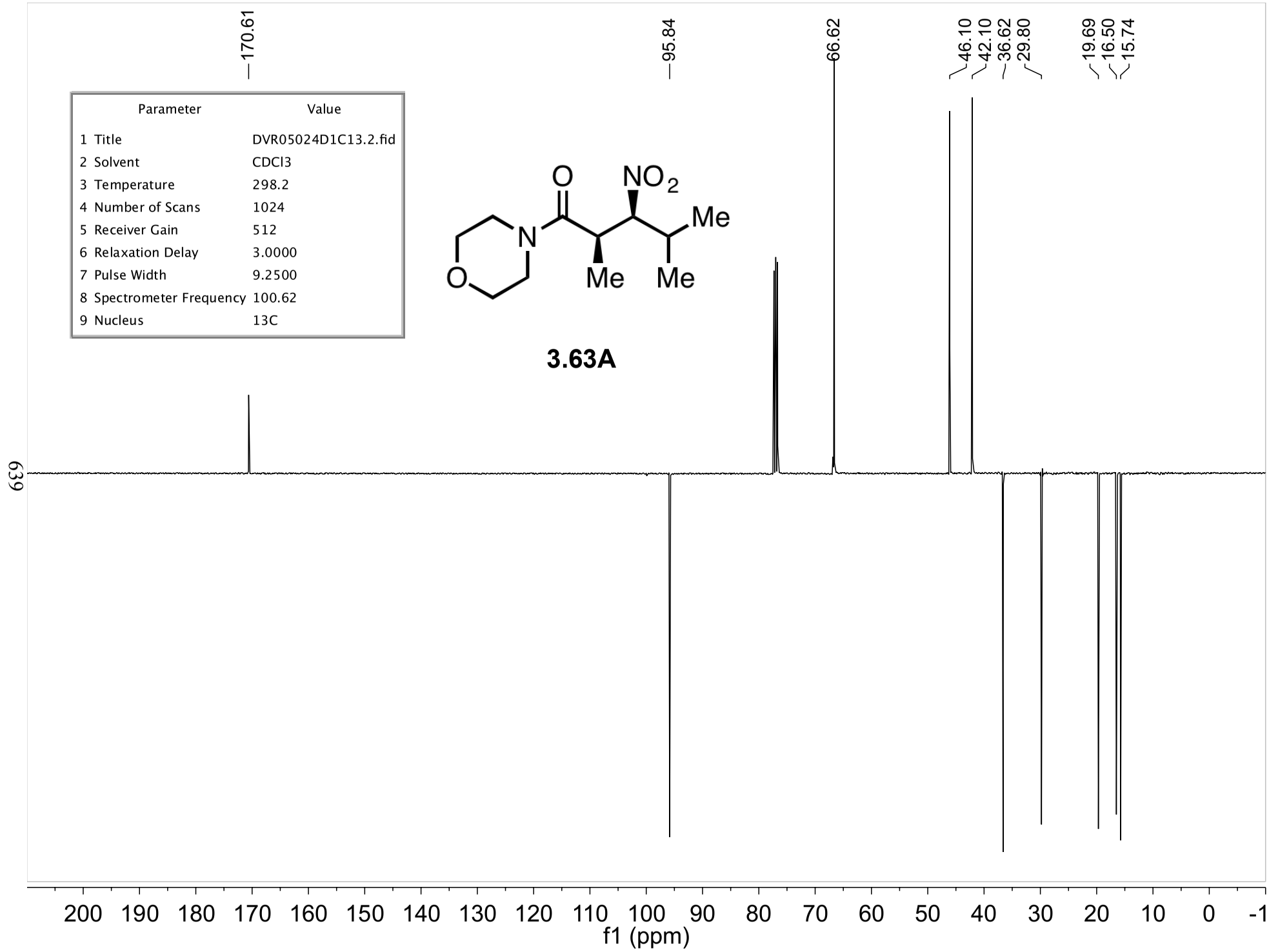
170.61
95.84
66.62
46.10
42.10
36.62
29.80
19.69
16.50
15.74
Parameter Value
1 Title DVR05024D1C13.2.fid
2 Solvent CDCl3
3 Temperature 298.2
4 Number of Scans 1024
5 Receiver Gain 512
6 Relaxation Delay 3.0000
7 Pulse Width 9.2500
8 Spectrometer Frequency 100.62
9 Nucleus 13C
O
NO2
Me
N
O
Me
Me
3.63A
639
200 190 180 170 160 150 140 130 120 110 100 90 80 70 60 50 40 30 20 10 0 -1
f1 (ppm)

==== Shimadzu LCsolution Analysis Report ====

C:\LabSolutions\Data\DMM\DVR05024 RAC COL1_292017_1055 AM_4.lcd

Acquired by	: LC User
Sample Name	: DVR05024 RAC COL1
Sample ID	: DVR05024 RAC COL1
Tray#	: 1
Vail #	: 1
Injection Volume	: 3 uL
Data File Name	: DVR05024 RAC COL1_292017_1055 AM_4.lcd
Method File Name	: col1_5isoiPA_30min_1ML_220and210.lcm
Batch File Name	: DMM.lcb
Report File Name	: Default.lcr
Data Acquired	: 2/9/2017 12:35:22 PM
Data Processed	: 2/9/2017 1:05:25 PM

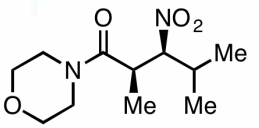

3.63
racemic

<Chromatogram>

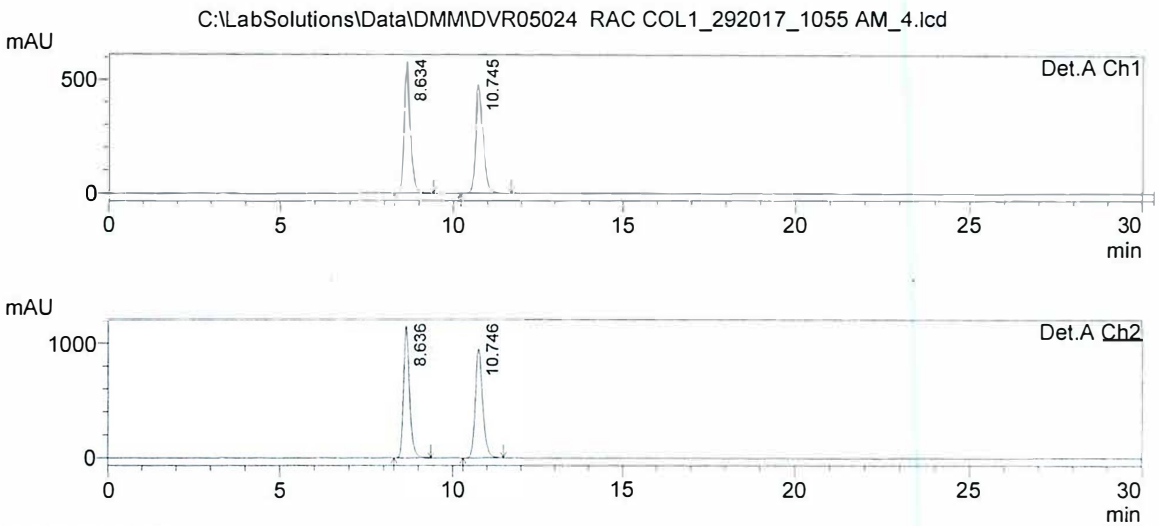

1 Det.A Ch1/220nm
2 Det.A Ch2/210nm

PeakTable

Detector A Ch1 220nm

Peak#	Ret. Time	Area	Height	Area %	Height %
1	8.634	7177016	581006	49.806	54.856
2	10.745	7232806	478140	50.194	45.144
Total		14409822	1059146	100.000	100.000

PeakTable

Detector A Ch2 210nm

Peak#	Ret. Time	Area	Height	Area %	Height %
1	8.636	14177266	1151903	49.779	54.792
2	10.746	14302886	950428	50.221	45.208
Total		28480152	2102331	100.000	100.000

==== Shimadzu LCsolution Analysis Report ====

C:\LabSolutions\Data\DMM\DVR05024 col1_292017_1055 AM_15.lcd

Acquired by	: LC User
Sample Name	: DVR05024 col1
Sample ID	: DVR05024 col1
Tray#	: 1
Vail #	: 2
Injection Volume	: 3 uL
Data File Name	: DVR05024 col1_292017_1055 AM_15.lcd
Method File Name	: col1_5isoiPA_30min_1ML_220and210.lcm
Batch File Name	: DMM.lcb
Report File Name	: Default.lcr
Data Acquired	: 2/10/2017 12:29:01 AM
Data Processed	: 2/10/2017 12:59:03 AM

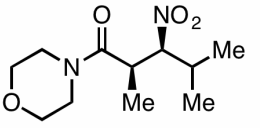

syn **3.63**
88% ee

<Chromatogram>

C:\LabSolutions\Data\DMM\DVR05024 col1_292017_1055 AM_15.lcd

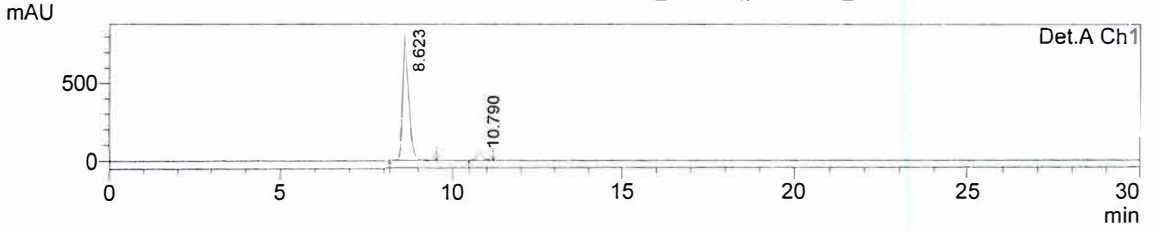

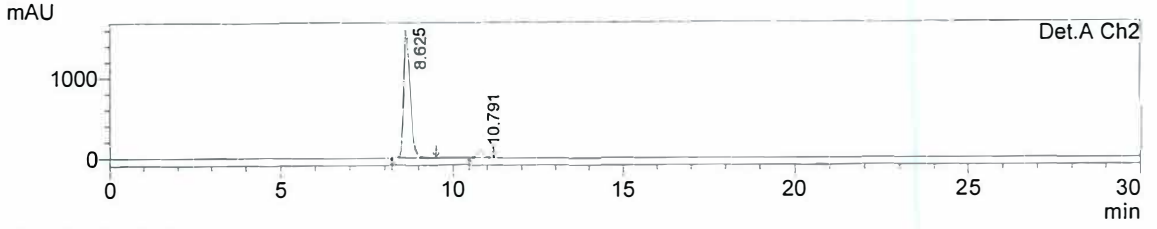

1 Det.A Ch1/220nm
2 Det.A Ch2/210nm

PeakTable

Detector A Ch1 220nm

Peak#	Ret. Time	Area	Height	Area %	Height %
1	8.623	10504819	836720	94.139	94.827
2	10.790	653983	45642	5.861	5.173
Total		11158802	882362	100.000	100.000

PeakTable

Detector A Ch2 210nm

Peak#	Ret. Time	Area	Height	Area %	Height %
1	8.625	20521889	1601647	94.125	94.719
2	10.791	1280955	89297	5.875	5.281
Total		21802844	1690944	100.000	100.000

Parameter	Value
1 Title	DVR05052crd.1.fid
2 Solvent	CDCl3
3 Temperature	297.7
4 Number of Scans	16
5 Receiver Gain	203
6 Relaxation Delay	1.0000
7 Pulse Width	15.0000
8 Spectrometer Frequency	400.15
9 Nucleus	1H

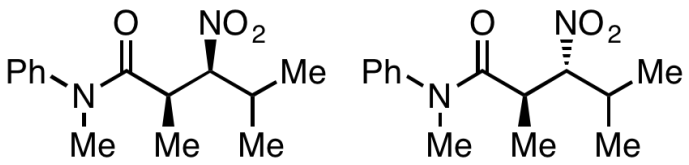

Crude

3.64A **91:09** **3.64B**

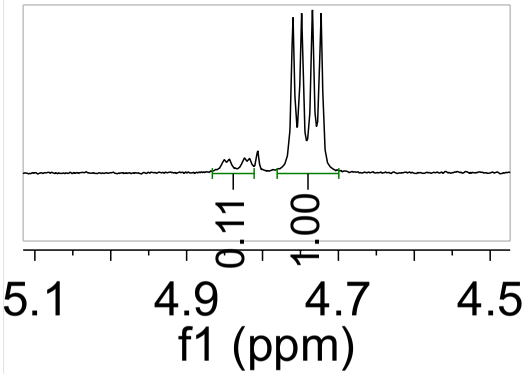

642

Parameter	Value
1 Title	DVR05053D1.1.fid
2 Solvent	CDCl3
3 Temperature	298.1
4 Number of Scans	16
5 Receiver Gain	10
6 Relaxation Delay	1.0000
7 Pulse Width	15.0000
8 Spectrometer Frequency	400.13
9 Nucleus	1H

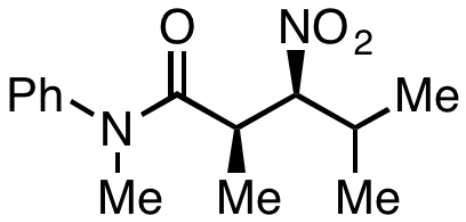

3.64A

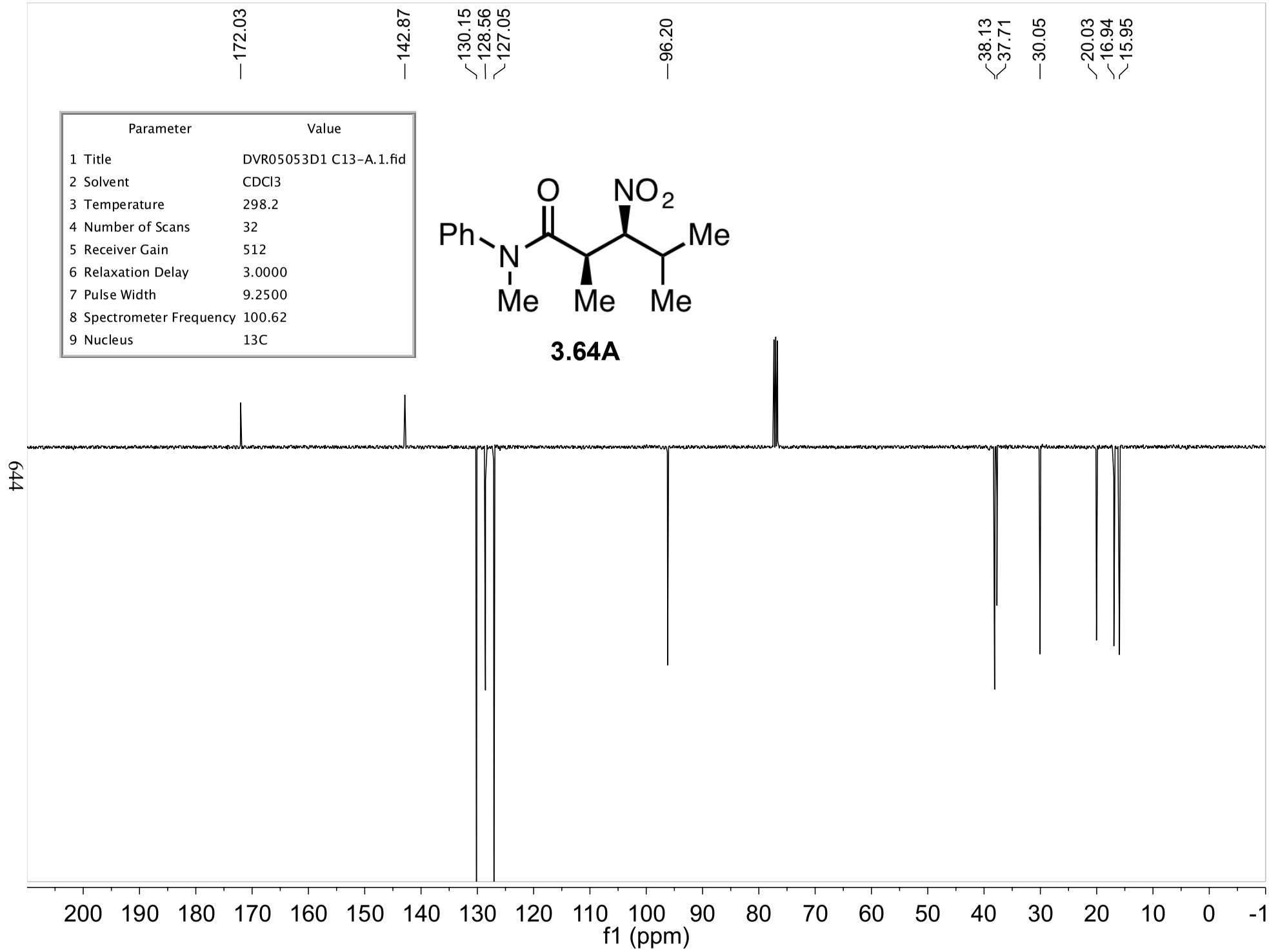
172.03
142.87
130.15
128.56
127.05
96.20
38.13
37.71
30.05
20.03
16.94
15.95
Parameter Value
1 Title DVR05053D1 C13-A.1.fid
2 Solvent CDCl3
3 Temperature 298.2
4 Number of Scans 32
5 Receiver Gain 512
6 Relaxation Delay 3.0000
7 Pulse Width 9.2500
8 Spectrometer Frequency 100.62
9 Nucleus 13C
O
NO2
Ph
N
Me
Me
Me
Me
3.64A
644
200 190 180 170 160 150 140 130 120 110 100 90 80 70 60 50 40 30 20 10 0 -1
f1 (ppm)

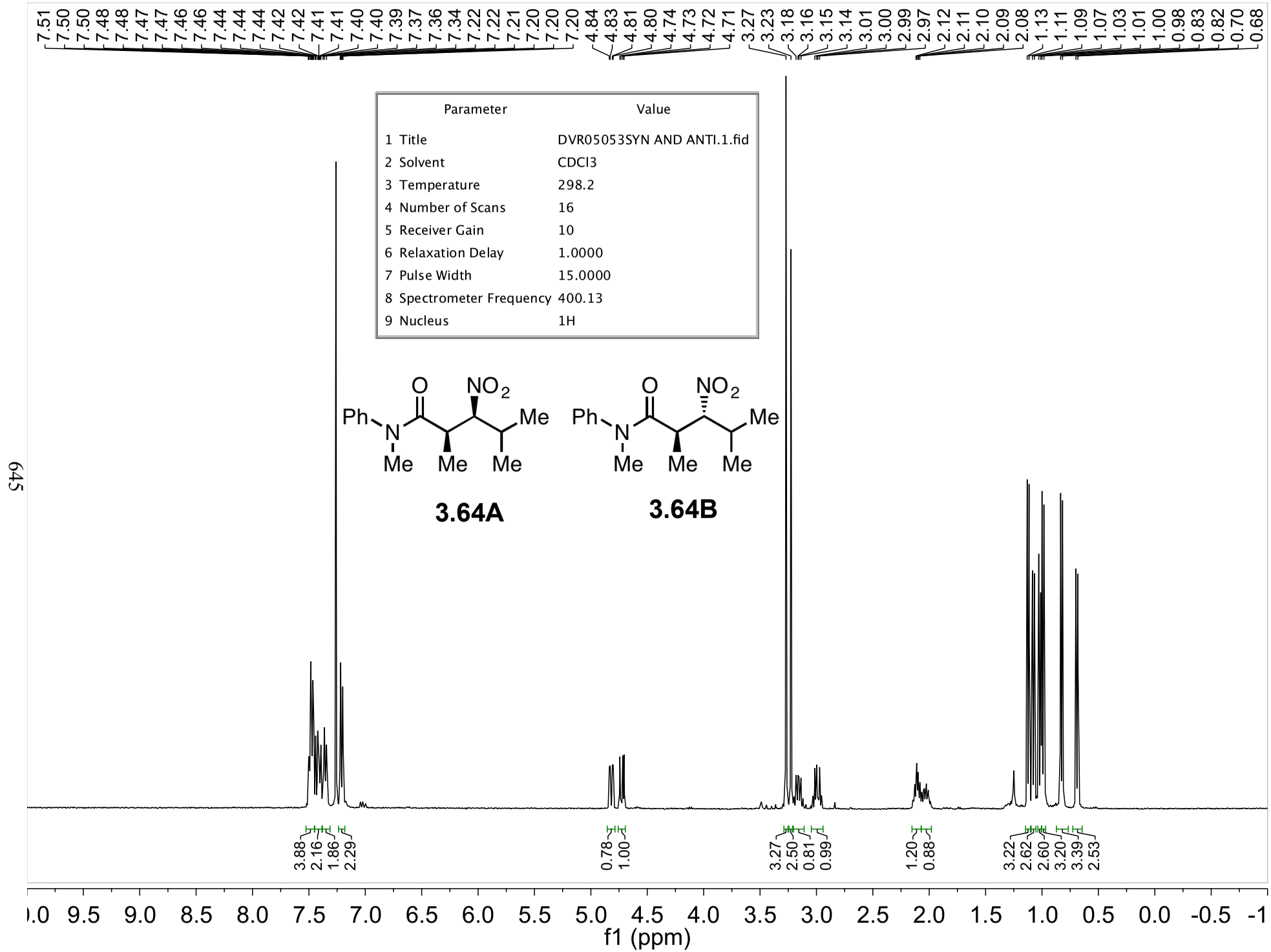
7.51 7.50 7.50 7.48 7.48 7.47 7.47 7.46 7.46 7.44 7.44 7.44 7.42 7.42 7.41 7.41 7.40 7.40 7.39 7.37 7.36 7.34 7.22 7.22 7.21 7.20 7.20 7.20 4.84 4.83 4.81 4.80 4.74 4.73 4.72 4.71 3.27 3.23 3.18 3.16 3.15 3.14 3.01 3.00 2.99 2.97 2.12 2.11 2.10 2.09 2.08 1.13 1.11 1.09 1.07 1.03 1.01 1.00 0.98 0.83 0.82 0.70 0.68
Parameter Value
1 Title DVR05053SYN AND ANTI.1.fid
2 Solvent CDCl3
3 Temperature 298.2
4 Number of Scans 16
5 Receiver Gain 10
6 Relaxation Delay 1.0000
7 Pulse Width 15.0000
8 Spectrometer Frequency 400.13
9 Nucleus 1H
Ph N Me O NO2 Me Me Me
3.64A
Ph N Me O NO2 Me Me Me
3.64B
645
3.88 2.16 1.86 2.29 0.78 1.00 3.27 2.50 0.81 0.99 1.20 0.88 3.22 2.62 2.60 3.20 3.39 2.53
f1 (ppm)

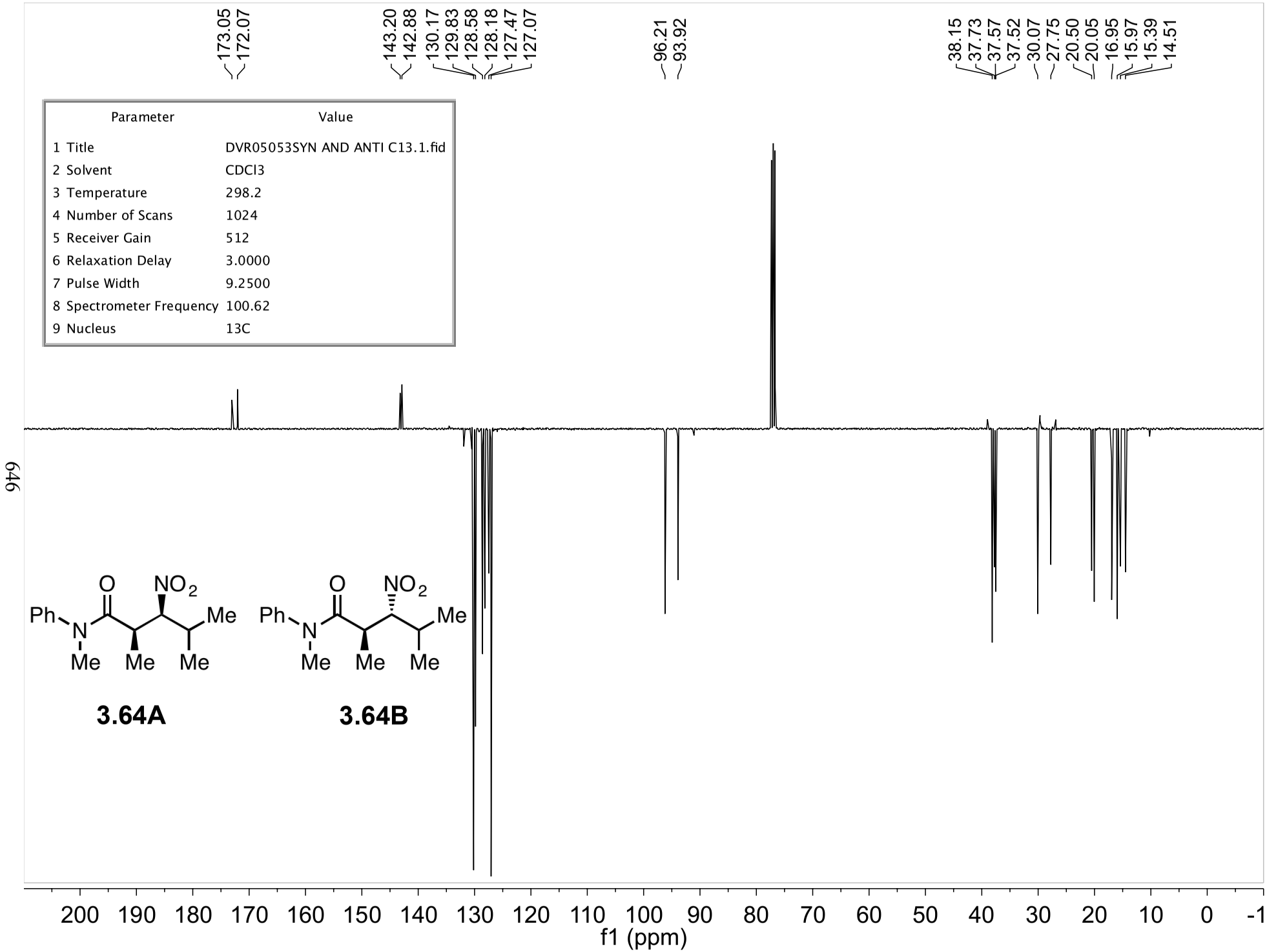
173.05
172.07
143.20
142.88
130.17
129.83
128.58
128.18
127.47
127.07
96.21
93.92
38.15
37.73
37.57
37.52
30.07
27.75
20.50
20.05
16.95
15.97
15.39
14.51
Parameter
Value
1 Title
DVR05053SYN AND ANTI C13.1.fid
2 Solvent
CDCl3
3 Temperature
298.2
4 Number of Scans
1024
5 Receiver Gain
512
6 Relaxation Delay
3.0000
7 Pulse Width
9.2500
8 Spectrometer Frequency
100.62
9 Nucleus
13C
646
Ph
N
O
NO2
Me
Me
Me
Me
Me
3.64A
3.64B
200 190 180 170 160 150 140 130 120 110 100 90 80 70 60 50 40 30 20 10 0 -1
f1 (ppm)

==== Shimadzu LCsolution Analysis Report ====

C:\LabSolutions\Data\DMM\DVR05053 SYN RAC_3222017_1208 PM_2.lcd

Acquired by	: LC User
Sample Name	: DVR05053 SYN RAC
Sample ID	: DVR05053 SYN RAC
Tray#	: 1
Vail #	: 7
Injection Volume	: 3 uL
Data File Name	: DVR05053 SYN RAC_3222017_1208 PM_2.lcd
Method File Name	: col4_1isoiPA_30min_1ML_210and220.lcm
Batch File Name	: DMM.lcb
Report File Name	: Default.lcr
Data Acquired	: 3/22/2017 12:23:51 PM
Data Processed	: 3/22/2017 12:53:54 PM

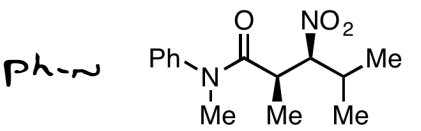

3.64A
racemic

<Chromatogram>

C:\LabSolutions\Data\DMM\DVR05053 SYN RAC_3222017_1208 PM_2.lcd

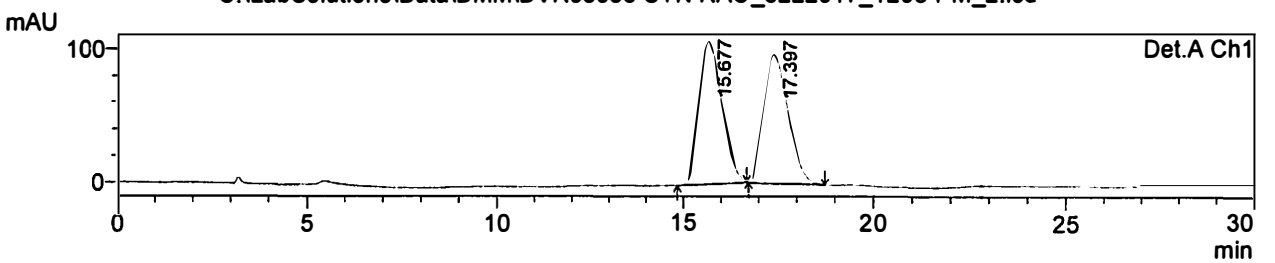

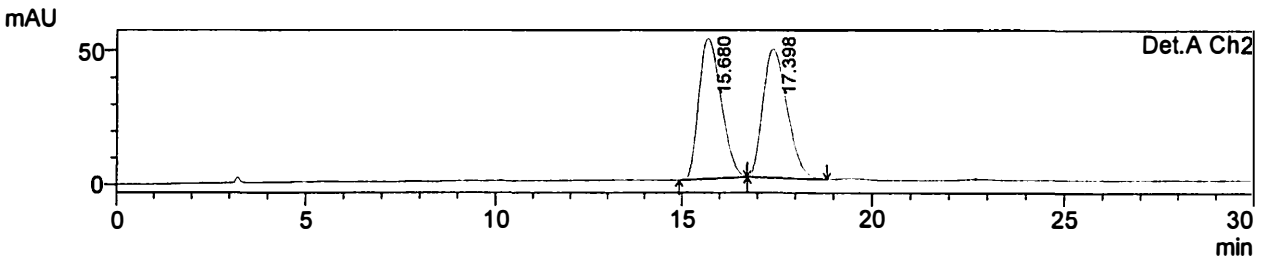

1 Det.A Ch1/210nm
2 Det.A Ch2/220nm

PeakTable

Detector A Ch1 210nm

Peak#	Ret. Time	Area	Height	Area %	Height %
1	15.677	4350073	105559	50.347	52.301
2	17.397	4290082	96271	49.653	47.699
Total		8640155	201830	100.000	100.000

PeakTable

Detector A Ch2 220nm

Peak#	Ret. Time	Area	Height	Area %	Height %
1	15.680	2144959	52093	50.222	52.168
2	17.398	2125976	47763	49.778	47.832
Total		4270935	99856	100.000	100.000

==== Shimadzu LCsolution Analysis Report ====

C:\LabSolutions\Data\DMM\DVR05053R1_3222017_1101 AM_2.lcd

Acquired by	: LC User
Sample Name	: DVR05053R1
Sample ID	: DVR05053R1
Tray#	: 1
Vail #	: 6
Injection Volume	: 3 uL
Data File Name	: DVR05053R1_3222017_1101 AM_2.lcd
Method File Name	: col4_1isoiPA_30min_1ML_210and220.lcm
Batch File Name	: DMM.lcb
Report File Name	: Default.lcr
Data Acquired	: 3/22/2017 11:16:45 AM
Data Processed	: 3/22/2017 11:46:46 AM

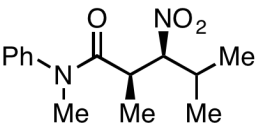

3.64A
90% ee

<Chromatogram>

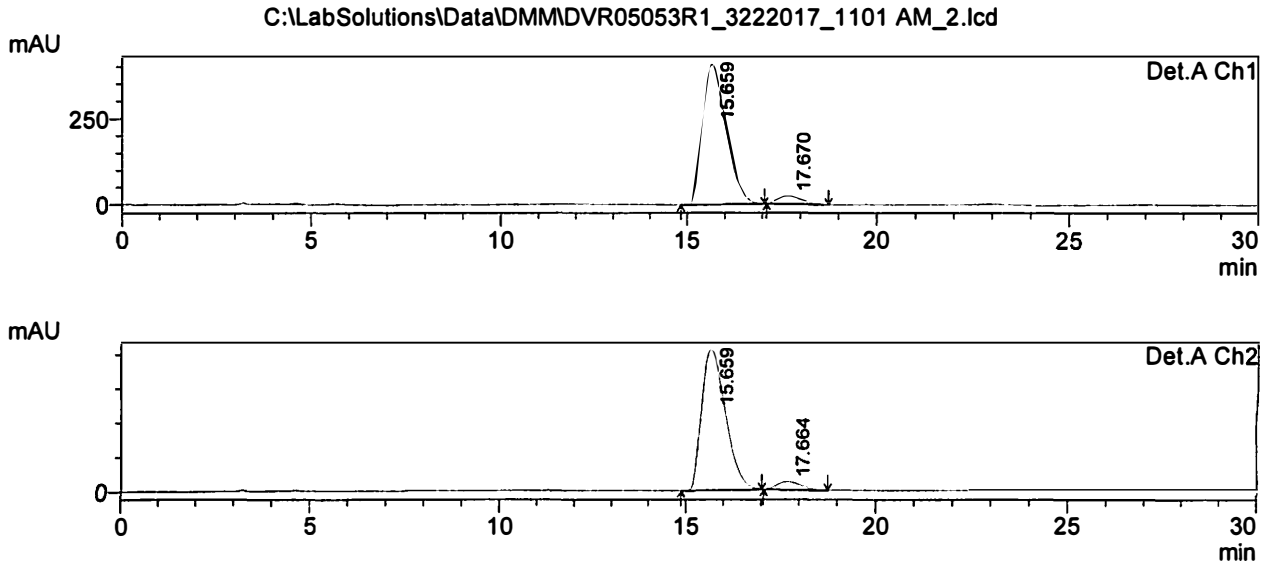

1 Det.A Ch1/210nm
2 Det.A Ch2/220nm

PeakTable

Detector A Ch1 210nm

Peak#	Ret. Time	Area	Height	Area %	Height %
1	15.659	18070828	409433	94.732	94.656
2	17.670	1004850	23116	5.268	5.344
Total		19075678	432549	100.000	100.000

PeakTable

Detector A Ch2 220nm

Peak#	Ret. Time	Area	Height	Area %	Height %
1	15.659	9038728	206005	94.800	94.755
2	17.664	495833	11403	5.200	5.245
Total		9534561	217408	100.000	100.000

==== Shimadzu LCsolution Analysis Report ====

C:\LabSolutions\Data\DMM\DVR05051D2 RAC COL1_3212017_1941 PM_5.lcd

Acquired by	: LC User
Sample Name	: DVR05051D2 RAC COL1
Sample ID	: DVR05051D2 RAC COL1
Tray#	: 1
Vail #	: 5
Injection Volume	: 3 uL
Data File Name	: DVR05051D2 RAC COL1_3212017_1941 PM_5.lcd
Method File Name	: col1_5isoiPA_30min_1ML_220and210.lcm
Batch File Name	: DMM.lcb
Report File Name	: Default.lcr
Data Acquired	: 3/21/2017 8:56:16 PM
Data Processed	: 3/22/2017 11:55:56 AM

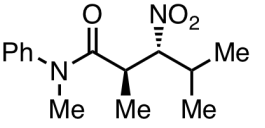

3.64B
racemic

<Chromatogram>

C:\LabSolutions\Data\DMM\DVR05051D2 RAC COL1_3212017_1941 PM_5.lcd

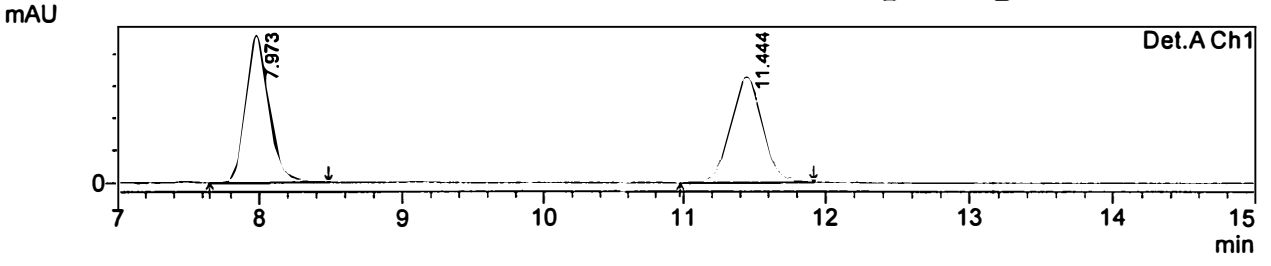

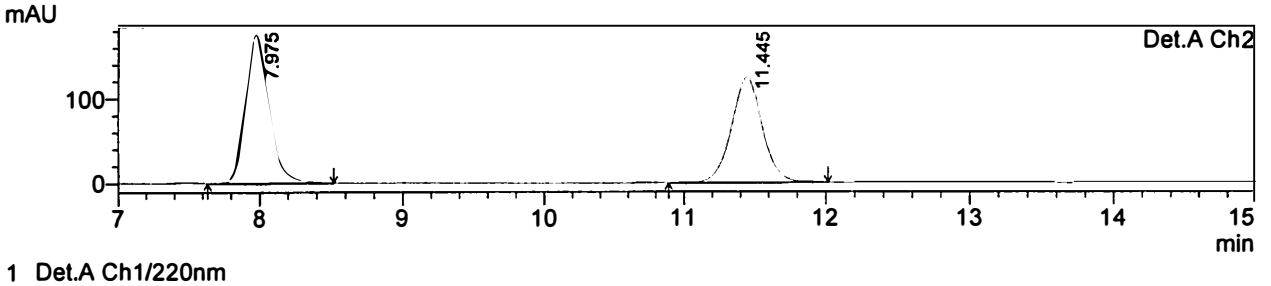

1 Det.A Ch1/220nm
2 Det.A Ch2/210nm

PeakTable

Detector A Ch1 220nm

Peak#	Ret. Time	Area	Height	Area %	Height %
1	7.973	1003185	92461	50.237	58.486
2	11.444	993731	65631	49.763	41.514
Total		1996916	158092	100.000	100.000

PeakTable

Detector A Ch2 210nm

Peak#	Ret. Time	Area	Height	Area %	Height %
1	7.975	1917627	176028	50.094	58.360
2	11.445	1910441	125595	49.906	41.640
Total		3828068	301623	100.000	100.000

==== Shimadzu LCsolution Analysis Report ====

C:\LabSolutions\Data\DMM\DVR05053 ANTI_3222017_1526 PM_6.lcd

Acquired by	: LC User
Sample Name	: DVR05053 ANTI
Sample ID	: DVR05053 ANTI
Tray#	: 1
Vail #	: 2
Injection Volume	: 3 uL
Data File Name	: DVR05053 ANTI_3222017_1526 PM_6.lcd
Method File Name	: col1_5isoiPA_30min_1ML_220and210.lcm
Batch File Name	: DMM.lcb
Report File Name	: Default.lcr
Data Acquired	: 3/22/2017 4:53:20 PM
Data Processed	: 3/22/2017 7:24:22 PM

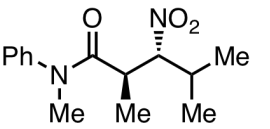

3.64B
43% ee

<Chromatogram>

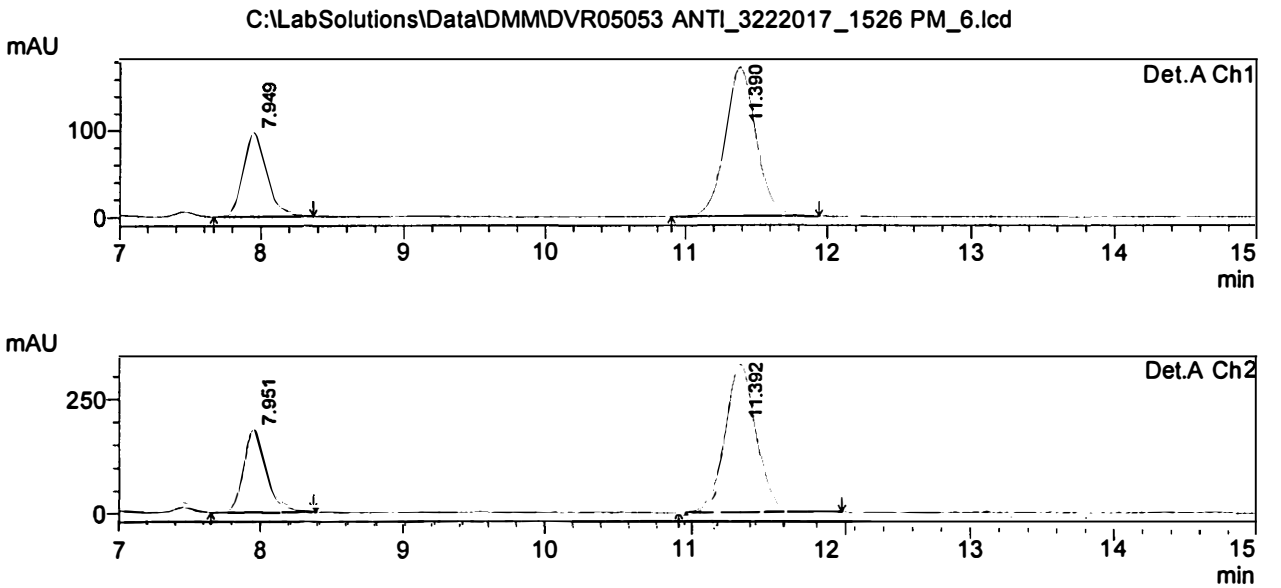

1 Det.A Ch1/220nm
2 Det.A Ch2/210nm

PeakTable

Detector A Ch1 220nm

Peak#	Ret. Time	Area	Height	Area %	Height %
1	7.949	1032740	95668	28.309	35.617
2	11.390	2615418	172937	71.691	64.383
Total		3648159	268605	100.000	100.000

PeakTable

Detector A Ch2 210nm

Peak#	Ret. Time	Area	Height	Area %	Height %
1	7.951	1971180	182055	28.366	35.787
2	11.392	4977953	326658	71.634	64.213
Total		6949133	508713	100.000	100.000

Parameter	Value
1 Title	DVR05096CRD.1.fid
2 Solvent	CDCl3
3 Temperature	297.0
4 Number of Scans	16
5 Receiver Gain	101
6 Relaxation Delay	1.0000
7 Pulse Width	10.7300
8 Spectrometer Frequency	600.32
9 Nucleus	1H

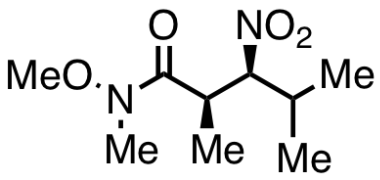

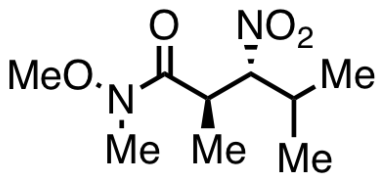

Crude

3.65A **93:07** **3.65B**

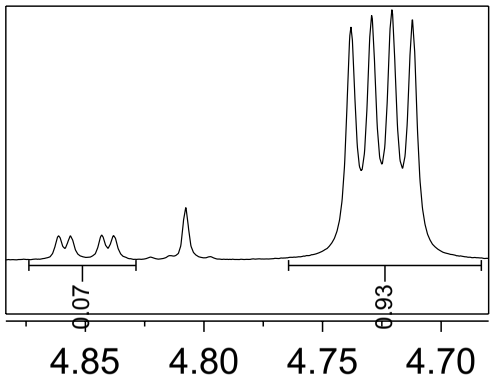

651

Parameter	Value
1 Title	DVR05096D1.1.fid
2 Solvent	CDCl3
3 Temperature	298.2
4 Number of Scans	16
5 Receiver Gain	8
6 Relaxation Delay	1.0000
7 Pulse Width	15.0000
8 Spectrometer Frequency	400.13
9 Nucleus	1H

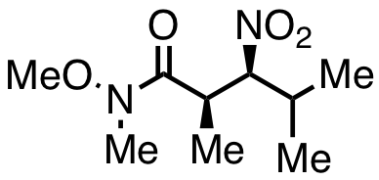

3.65A

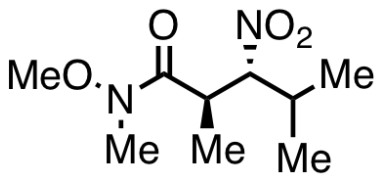

3.65B

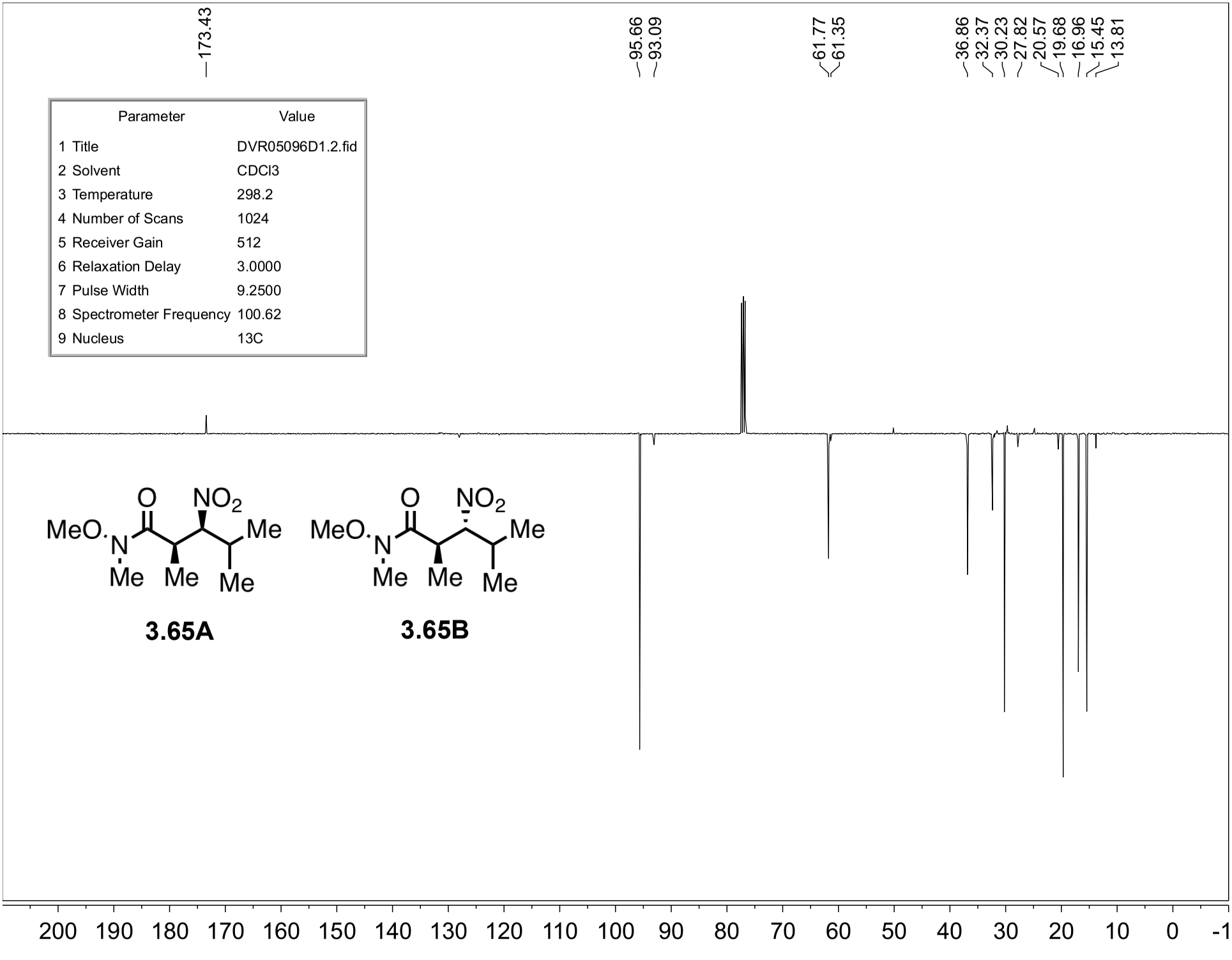
173.43
95.66
93.09
61.77
61.35
36.86
32.37
30.23
27.82
20.57
19.68
16.96
15.45
13.81
Parameter Value
1 Title DVR05096D1.2.fid
2 Solvent CDCl3
3 Temperature 298.2
4 Number of Scans 1024
5 Receiver Gain 512
6 Relaxation Delay 3.0000
7 Pulse Width 9.2500
8 Spectrometer Frequency 100.62
9 Nucleus 13C
653
MeO. N Me Me Me O NO2 Me
3.65A
MeO. N Me Me Me O NO2 Me
3.65B
200 190 180 170 160 150 140 130 120 110 100 90 80 70 60 50 40 30 20 10 0 -1

==== Shimadzu LCsolution Analysis Report ====

C:\LabSolutions\Data\DMM\DVR05096 RAC1_6222017_1847 PM_2.lcd

Acquired by	: LC User
Sample Name	: DVR05096 RAC1
Sample ID	: DVR05096 RAC1
Tray#	: 1
Vail #	: 3
Injection Volume	: 3 uL
Data File Name	: DVR05096 RAC1_6222017_1847 PM_2.lcd
Method File Name	: col2_2isoiPA_20min_1ML_220and210.lcm
Batch File Name	: DMM.lcb
Report File Name	: Default.lcr
Data Acquired	: 6/22/2017 6:58:25 PM
Data Processed	: 6/22/2017 7:18:27 PM

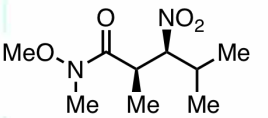

3.65A
racemic

<Chromatogram>

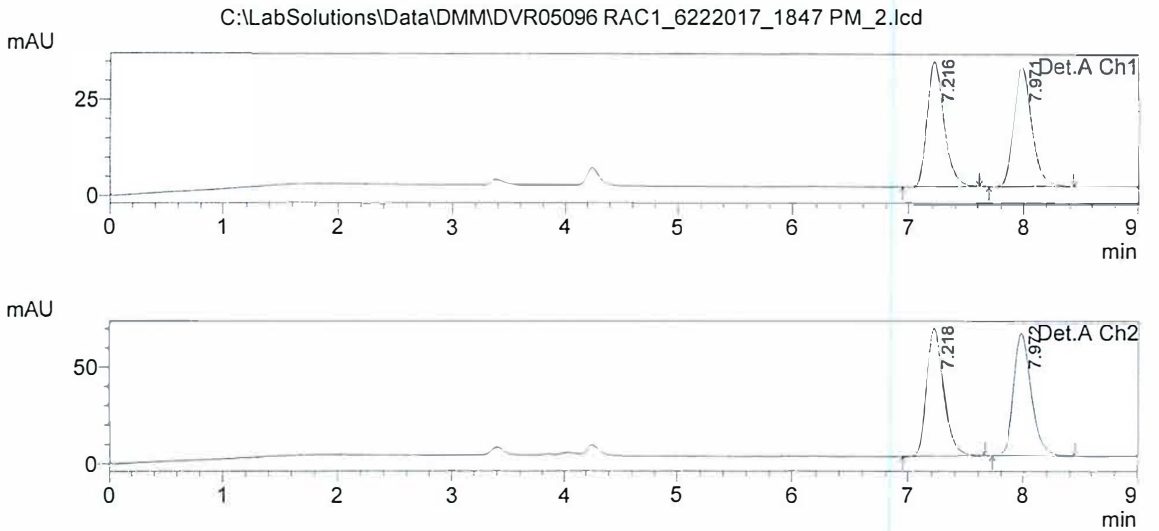

1 Det.A Ch1/220nm
2 Det.A Ch2/210nm

PeakTable

Detector A Ch1 220nm

Peak#	Ret. Time	Area	Height	Area %	Height %
1	7.216	335148	32765	49.851	51.031
2	7.971	337158	31441	50.149	48.969
Total		672306	64206	100.000	100.000

PeakTable

Detector A Ch2 210nm

Peak#	Ret. Time	Area	Height	Area %	Height %
1	7.218	676907	66033	49.917	51.038
2	7.972	679157	63346	50.083	48.962
Total		1356064	129379	100.000	100.000

==== Shimadzu LCsolution Analysis Report ====

C:\LabSolutions\Data\DMM\DVR05096 D1_6222017_1847 PM_3.lcd

Acquired by	: LC User
Sample Name	: DVR05096 D1
Sample ID	: DVR05096 D1
Tray#	: 1
Vail #	: 4
Injection Volume	: 3 uL
Data File Name	: DVR05096 D1_6222017_1847 PM_3.lcd
Method File Name	: col2_2isoiPA_20min_1ML_220and210.lcm
Batch File Name	: DMM.lcb
Report File Name	: Default.lcr
Data Acquired	: 6/22/2017 7:19:00 PM
Data Processed	: 6/22/2017 7:39:02 PM

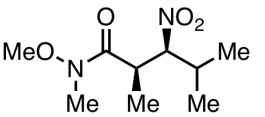

3.65A
90% ee

<Chromatogram>

C:\LabSolutions\Data\DMM\DVR05096 D1_6222017_1847 PM_3.lcd

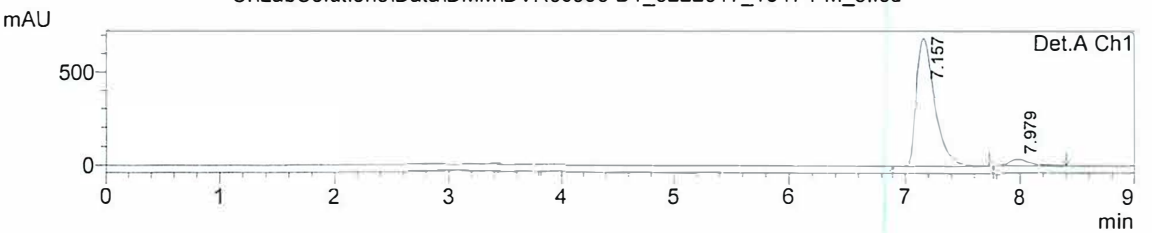

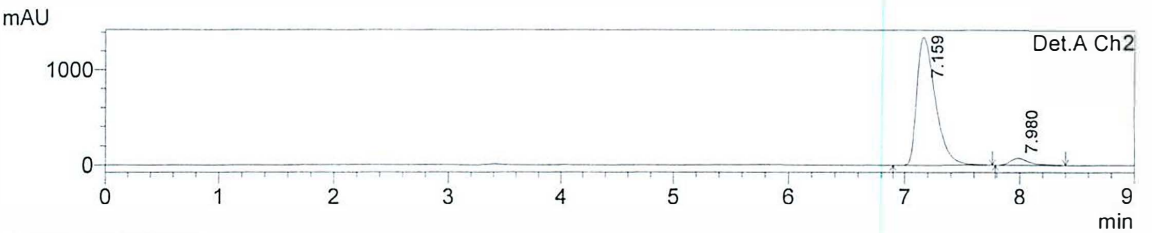

1 Det.A Ch1/220nm
2 Det.A Ch2/210nm

PeakTable

Detector A Ch1 220nm

Peak#	Ret. Time	Area	Height	Area %	Height %
1	7.157	7448257	684968	94.858	95.094
2	7.979	403717	35340	5.142	4.906
Total		7851974	720308	100.000	100.000

PeakTable

Detector A Ch2 210nm

Peak#	Ret. Time	Area	Height	Area %	Height %
1	7.159	14946443	1348215	94.973	94.971
2	7.980	791193	71392	5.027	5.029
Total		15737636	1419607	100.000	100.000

==== Shimadzu LCsolution Analysis Report ====

C:\LabSolutions\Data\DMM\DVR05096 RAC1_6222017_1847 PM_2.lcd

Acquired by	: LC User
Sample Name	: DVR05096 RAC1
Sample ID	: DVR05096 RAC1
Tray#	: 1
Vail #	: 3
Injection Volume	: 3 uL
Data File Name	: DVR05096 RAC1_6222017_1847 PM_2.lcd
Method File Name	: col2_2isoiPA_20min_1ML_220and210.lcm
Batch File Name	: DMM.lcb
Report File Name	: Default.lcr
Data Acquired	: 6/22/2017 6:58:25 PM
Data Processed	: 6/22/2017 8:30:04 PM

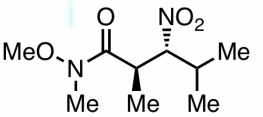

3.65B
racemic

<Chromatogram>

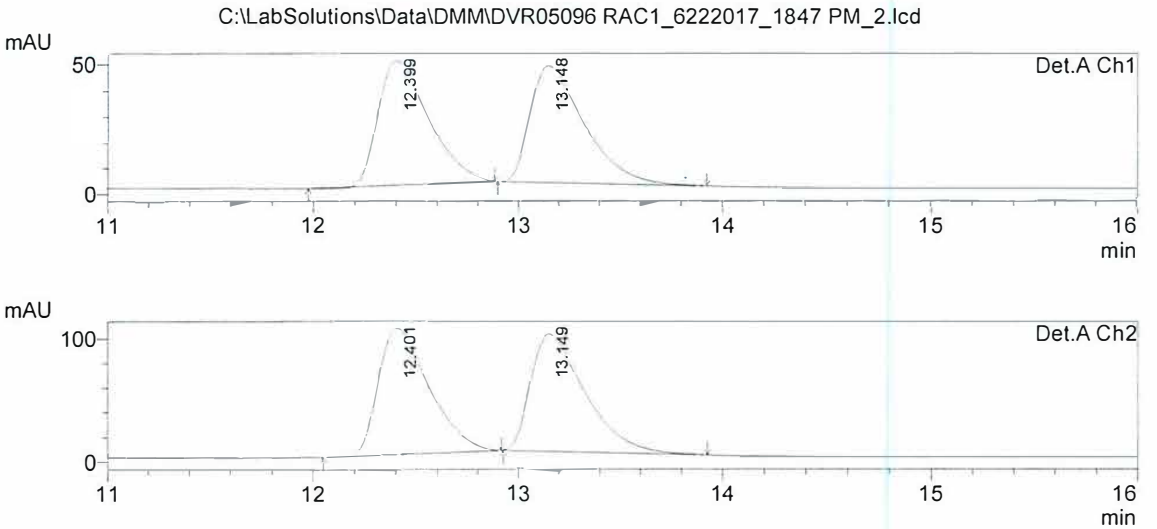

1 Det.A Ch1/220nm
2 Det.A Ch2/210nm

PeakTable

Detector A Ch1 220nm

Peak#	Ret. Time	Area	Height	Area %	Height %
1	12.399	815274	47869	49.467	51.573
2	13.148	832837	44949	50.533	48.427
Total		1648111	92818	100.000	100.000

PeakTable

Detector A Ch2 210nm

Peak#	Ret. Time	Area	Height	Area %	Height %
1	12.401	1753453	102119	49.856	51.741
2	13.149	1763598	95247	50.144	48.259
Total		3517051	197366	100.000	100.000

==== Shimadzu LCsolution Analysis Report ====

C:\LabSolutions\Data\DMM\DVR05096 D1_6222017_1847 PM_3.lcd

Acquired by	: LC User
Sample Name	: DVR05096 D1
Sample ID	: DVR05096 D1
Tray#	: 1
Vail #	: 4
Injection Volume	: 3 uL
Data File Name	: DVR05096 D1_6222017_1847 PM_3.lcd
Method File Name	: col2_2isoiPA_20min_1ML_220and210.lcm
Batch File Name	: DMM.lcb
Report File Name	: Default.lcr
Data Acquired	: 6/22/2017 7:19:00 PM
Data Processed	: 6/22/2017 8:33:52 PM

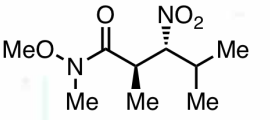

3.65B
44% ee

<Chromatogram>

C:\LabSolutions\Data\DMM\DVR05096 D1_6222017_1847 PM_3.lcd

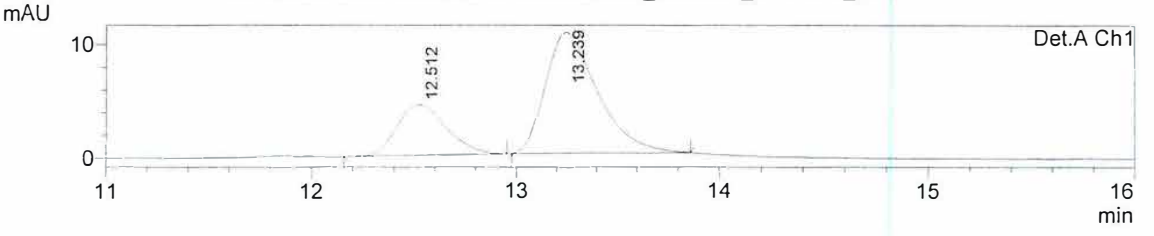

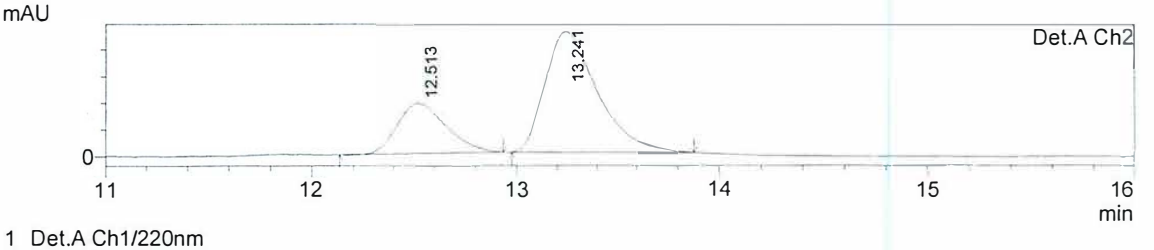

1 Det.A Ch1/220nm
2 Det.A Ch2/210nm

PeakTable

Detector A Ch1 220nm

Peak#	Ret. Time	Area	Height	Area %	Height %
1	12.512	75349	4503	28.007	29.709
2	13.239	193688	10655	71.993	70.291
Total		269037	15158	100.000	100.000

PeakTable

Detector A Ch2 210nm

Peak#	Ret. Time	Area	Height	Area %	Height %
1	12.513	158531	9527	27.733	29.604
2	13.241	413097	22654	72.267	70.396
Total		571628	32180	100.000	100.000

Parameter	Value
1 Title	DVR05054crd 1.1.fid
2 Solvent	CDCl3
3 Temperature	297.8
4 Number of Scans	16
5 Receiver Gain	203
6 Relaxation Delay	1.0000
7 Pulse Width	15.0000
8 Spectrometer Frequency	400.15
9 Nucleus	1H

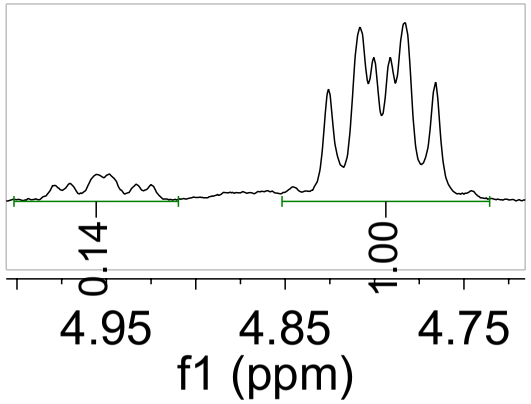

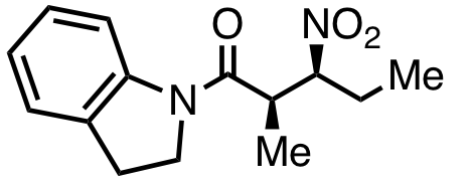

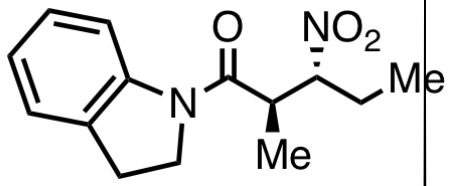

Crude

3.66A **88:12** **3.66B**

Parameter	Value
1 Title	DVR05054D1.1.fid
2 Solvent	DMSO
3 Temperature	298.2
4 Number of Scans	16
5 Receiver Gain	8
6 Relaxation Delay	1.0000
7 Pulse Width	15.0000
8 Spectrometer Frequency	400.13
9 Nucleus	1H

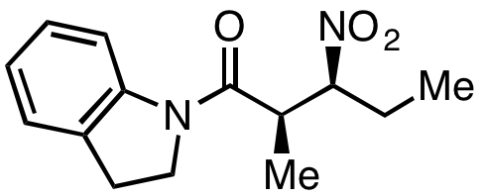

3.66A

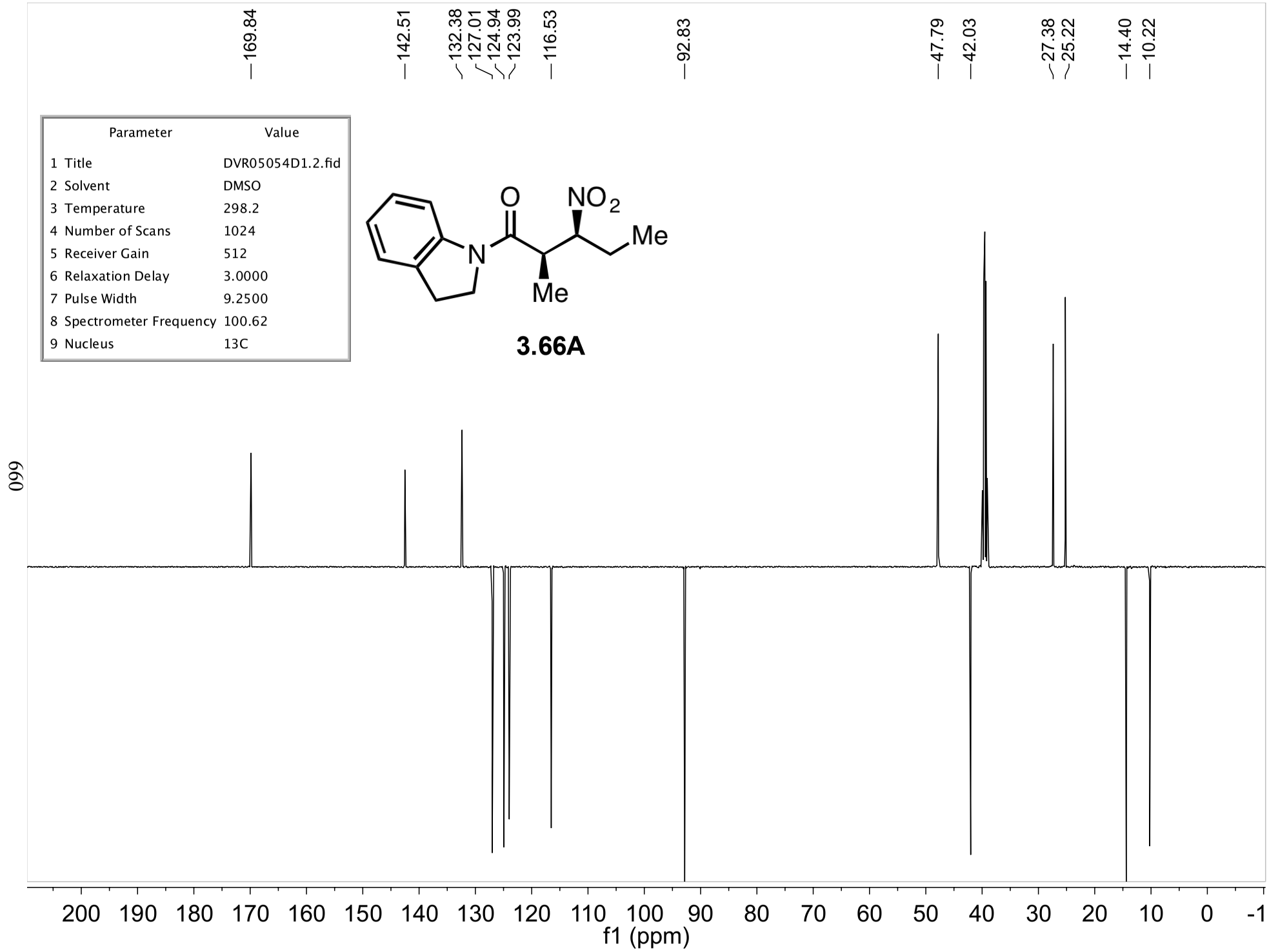
169.84
142.51
132.38
127.01
124.94
123.99
116.53
92.83
47.79
42.03
27.38
25.22
14.40
10.22
Parameter Value
1 Title DVR05054D1.2.fid
2 Solvent DMSO
3 Temperature 298.2
4 Number of Scans 1024
5 Receiver Gain 512
6 Relaxation Delay 3.0000
7 Pulse Width 9.2500
8 Spectrometer Frequency 100.62
9 Nucleus 13C
O
NO2
N
Me
Me
3.66A
099
200 190 180 170 160 150 140 130 120 110 100 90 80 70 60 50 40 30 20 10 0 -1
f1 (ppm)

Parameter	Value
1 Title	DVR05054D2.1.fid
2 Solvent	DMSO
3 Temperature	298.2
4 Number of Scans	16
5 Receiver Gain	6
6 Relaxation Delay	1.0000
7 Pulse Width	15.0000
8 Spectrometer Frequency	400.13
9 Nucleus	1H

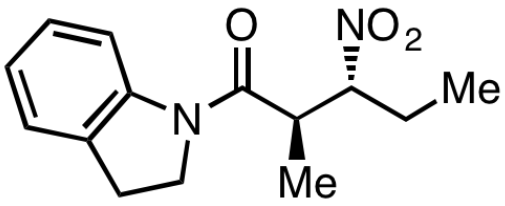

3.66B

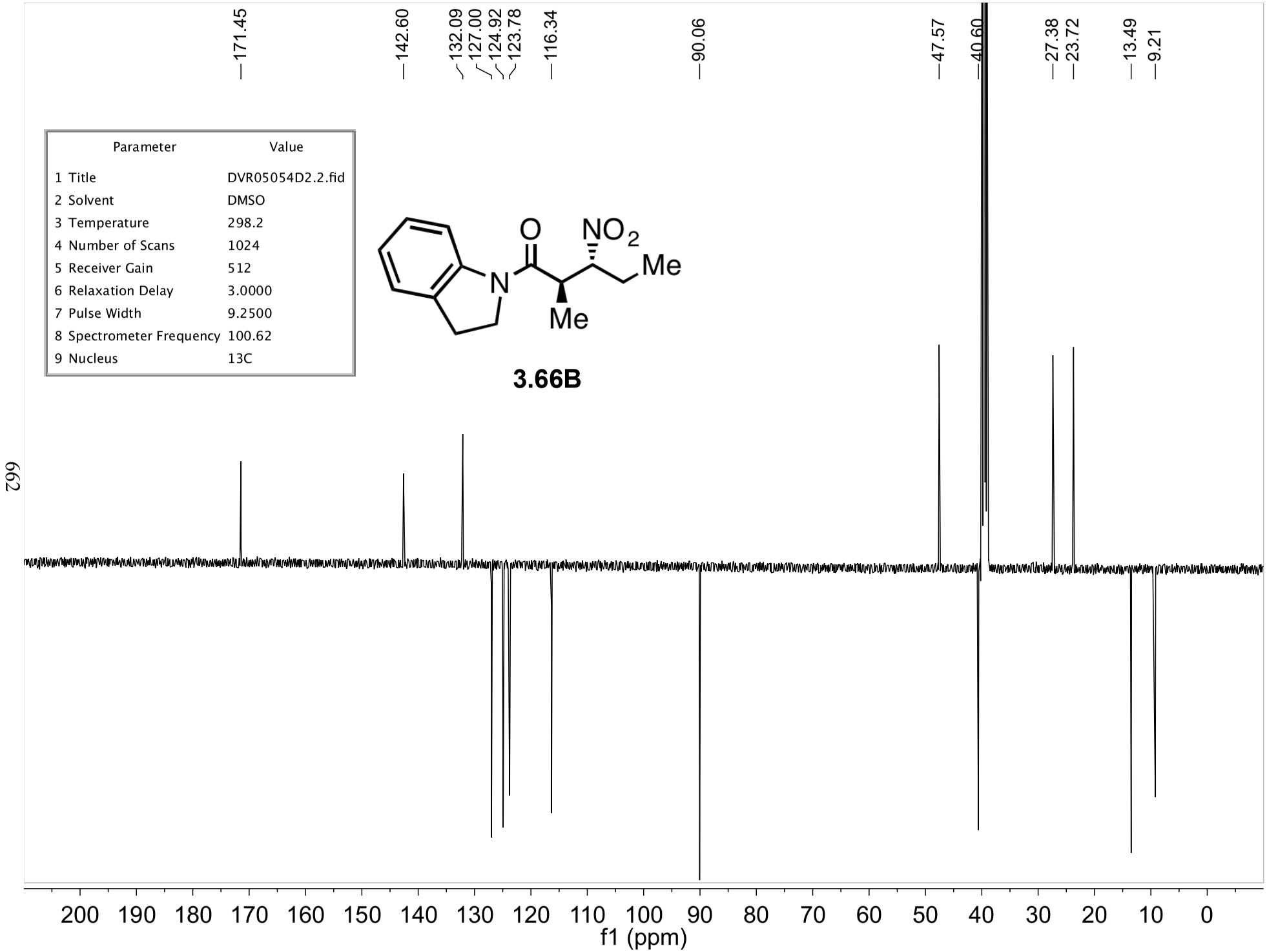
171.45
142.60
132.09
127.00
124.92
123.78
116.34
90.06
47.57
40.60
27.38
23.72
13.49
9.21
Parameter Value
1 Title DVR05054D2.2.fid
2 Solvent DMSO
3 Temperature 298.2
4 Number of Scans 1024
5 Receiver Gain 512
6 Relaxation Delay 3.0000
7 Pulse Width 9.2500
8 Spectrometer Frequency 100.62
9 Nucleus 13C
O
NO2
N
Me
Me
3.66B
662
200 190 180 170 160 150 140 130 120 110 100 90 80 70 60 50 40 30 20 10 0
f1 (ppm)

==== Shimadzu LCsolution Analysis Report ====

C:\LabSolutions\Data\DMM\DVR05057 RAC D1_3232017_1059 AM_2.lcd

Acquired by	: LC User
Sample Name	: DVR05057 RAC D1
Sample ID	: DVR05057 RAC D1
Tray#	: 1
Vail #	: 1
Injection Volume	: 3 uL
Data File Name	: DVR05057 RAC D1_3232017_1059 AM_2.lcd
Method File Name	: col1_1isoiPA_30min_1ML_254and210.lcm
Batch File Name	: DMM.lcb
Report File Name	: Default.lcr
Data Acquired	: 3/23/2017 11:15:40 AM
Data Processed	: 3/23/2017 11:45:42 AM

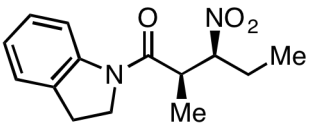

3.66A
racemic

<Chromatogram>

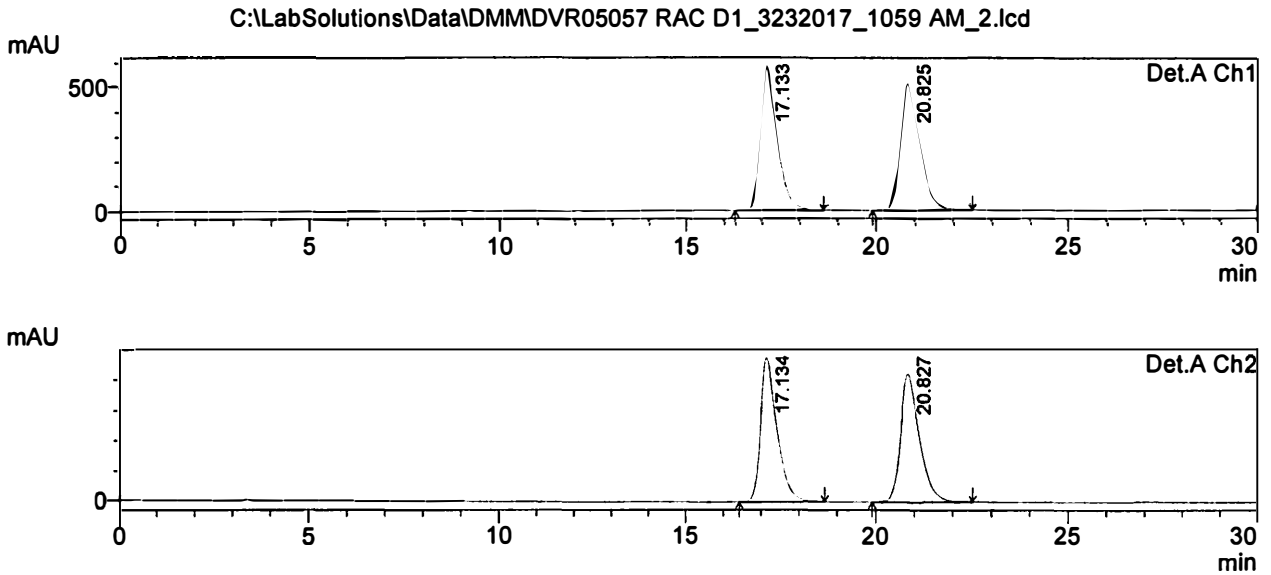

1 Det.A Ch1/254nm
2 Det.A Ch2/210nm

PeakTable

Detector A Ch1 254nm

Peak#	Ret. Time	Area	Height	Area %	Height %
1	17.133	17410414	585976	50.036	53.102
2	20.825	17385493	517516	49.964	46.898
Total		34795906	1103492	100.000	100.000

PeakTable

Detector A Ch2 210nm

Peak#	Ret. Time	Area	Height	Area %	Height %
1	17.134	28484540	949339	49.925	52.982
2	20.827	28569783	842484	50.075	47.018
Total		57054323	1791823	100.000	100.000

==== Shimadzu LCsolution Analysis Report ====

C:\LabSolutions\Data\DMM\DVR05054F1_3212017_1941 PM_1.lcd

Acquired by	: LC User
Sample Name	: DVR05054F1
Sample ID	: DVR05054F1
Tray#	: 1
Vail #	: 4
Injection Volume	: 2 uL
Data File Name	: DVR05054F1_3212017_1941 PM_1.lcd
Method File Name	: col1_1isoiPA_30min_1ML_254and210.lcm
Batch File Name	: DMM.lcb
Report File Name	: Default.lcr
Data Acquired	: 3/21/2017 8:05:18 PM
Data Processed	: 3/22/2017 9:02:54 AM

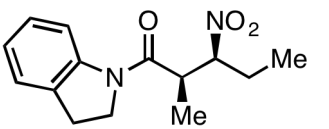

3.66A
85% ee

<Chromatogram>

C:\LabSolutions\Data\DMM\DVR05054F1_3212017_1941 PM_1.lcd

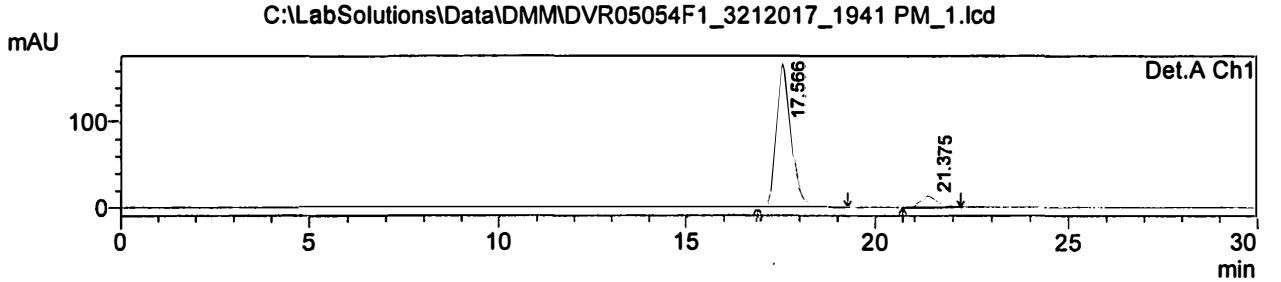

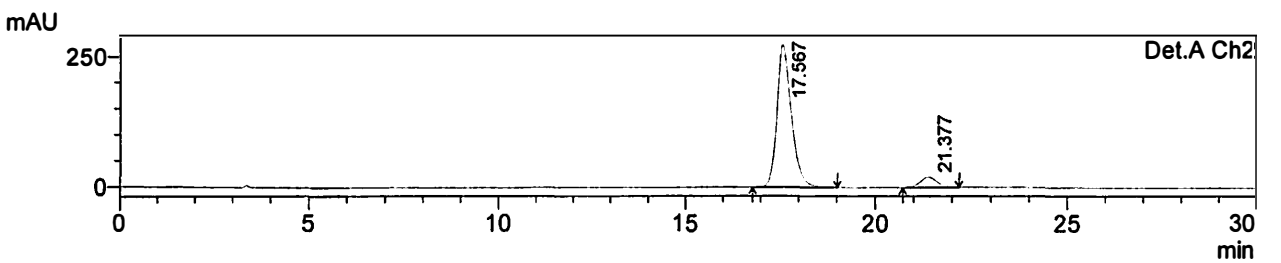

1 Det.A Ch1/254nm
2 Det.A Ch2/210nm

PeakTable

Detector A Ch1 254nm

Peak#	Ret. Time	Area	Height	Area %	Height %
1	17.566	4379186	167345	92.314	93.285
2	21.375	364615	12046	7.686	6.715
Total		4743801	179391	100.000	100.000

✓

PeakTable

Detector A Ch2 210nm

Peak#	Ret. Time	Area	Height	Area %	Height %
1	17.567	7242536	276749	92.329	93.267
2	21.377	601759	19978	7.671	6.733
Total		7844295	296727	100.000	100.000

==== Shimadzu LCsolution Analysis Report ====

C:\LabSolutions\Data\DMM\DVR05056 RAC D2_3232017_1323 PM_4.lcd

Acquired by	: LC User
Sample Name	: DVR05057 RAC D2
Sample ID	: DVR05056 RAC D2
Tray#	: 1
Vail #	: 3
Injection Volume	: 3 uL
Data File Name	: DVR05056 RAC D2_3232017_1323 PM_4.lcd
Method File Name	: col1_5isoiPA_60min_1ML_220and210.lcm
Batch File Name	: DMM.lcb
Report File Name	: Default.lcr
Data Acquired	: 3/23/2017 9:39:19 PM
Data Processed	: 3/23/2017 10:39:19 PM

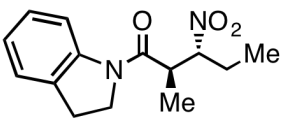

3.66B
racemic

<Chromatogram>

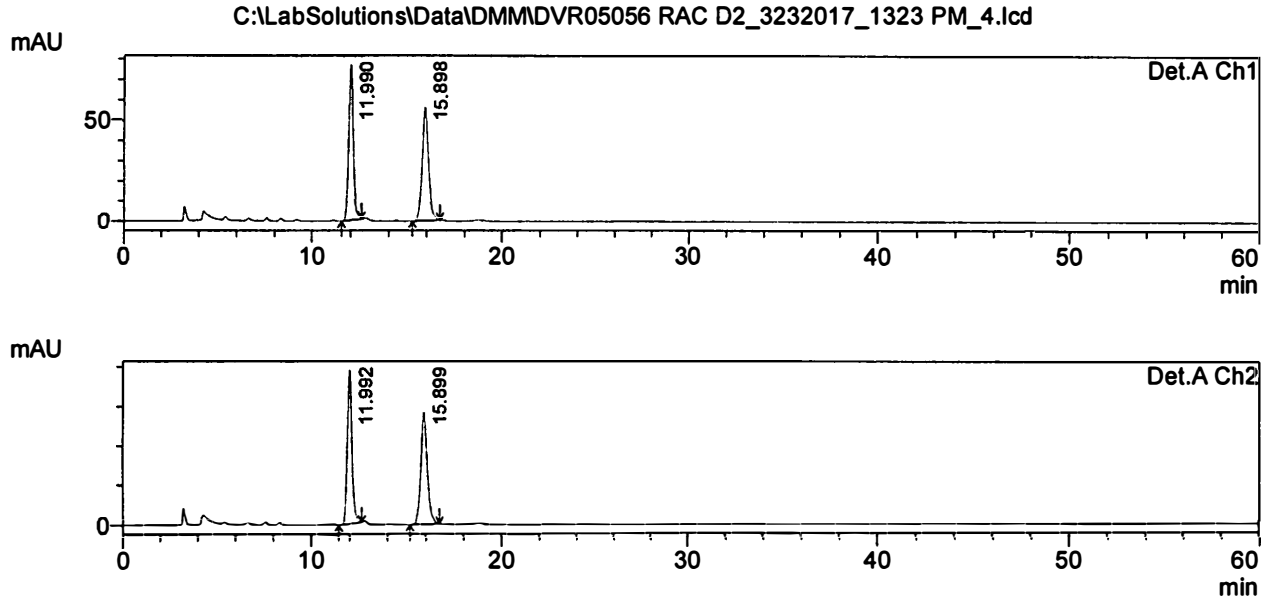

1 Det.A Ch1/220nm
2 Det.A Ch2/210nm

PeakTable

Detector A Ch1 220nm

Peak#	Ret. Time	Area	Height	Area %	Height %
1	11.990	1302409	76793	49.604	57.681
2	15.898	1323191	56341	50.396	42.319
Total		2625600	133134	100.000	100.000

PeakTable

Detector A Ch2 210nm

Peak#	Ret. Time	Area	Height	Area %	Height %
1	11.992	3277661	194717	49.618	57.758
2	15.899	3328124	142408	50.382	42.242
Total		6605785	337125	100.000	100.000

==== Shimadzu LCsolution Analysis Report ====

C:\LabSolutions\Data\DMM\DVR05056 D2_3232017_1323 PM_8.lcd

Acquired by	: LC User
Sample Name	: DVR05057 D2
Sample ID	: DVR05056 D2
Tray#	: 1
Vail #	: 4
Injection Volume	: 3 uL
Data File Name	: DVR05056 D2_3232017_1323 PM_8.lcd
Method File Name	: col1_5isoiPA_60min_1ML_220and210.lcm
Batch File Name	: DMM.lcb
Report File Name	: Default.lcr
Data Acquired	: 3/23/2017 11:20:12 PM
Data Processed	: 3/24/2017 12:20:15 AM

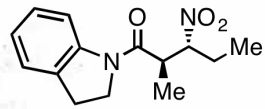

3.66B
64% ee

<Chromatogram>

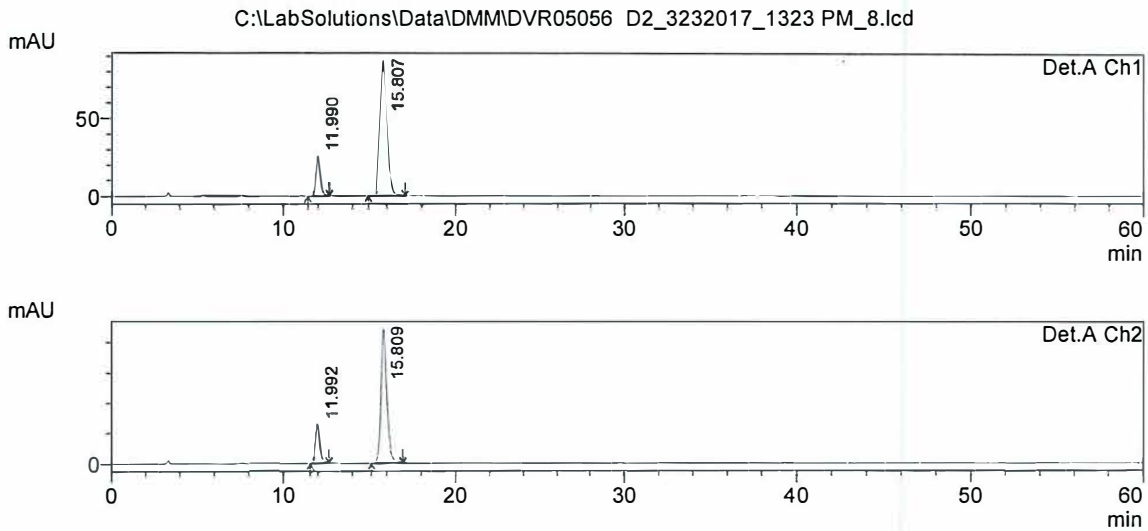

1 Det.A Ch1/220nm
2 Det.A Ch2/210nm

PeakTable

Detector A Ch1 220nm

Peak#	Ret. Time	Area	Height	Area %	Height %
1	11.990	448172	26222	17.777	23.091
2	15.807	2072970	87337	82.223	76.909
Total		2521141	113559	100.000	100.000

PeakTable

Detector A Ch2 210nm

Peak#	Ret. Time	Area	Height	Area %	Height %
1	11.992	1122696	65808	17.661	22.853
2	15.809	5234057	222154	82.339	77.147
Total		6356753	287962	100.000	100.000

Parameter	Value
1 Title	DVR05064CRD.1.fid
2 Solvent	CDCl3
3 Temperature	300.0
4 Number of Scans	16
5 Receiver Gain	161
6 Relaxation Delay	1.0000
7 Pulse Width	13.1400
8 Spectrometer Frequency	600.32
9 Nucleus	1H

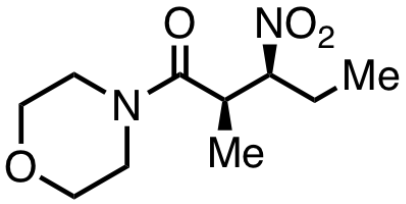

3.67A

Crude

81:19

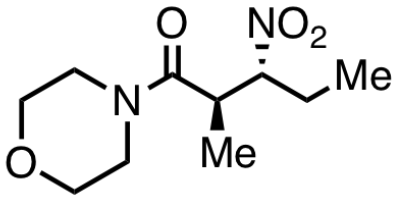

3.67A

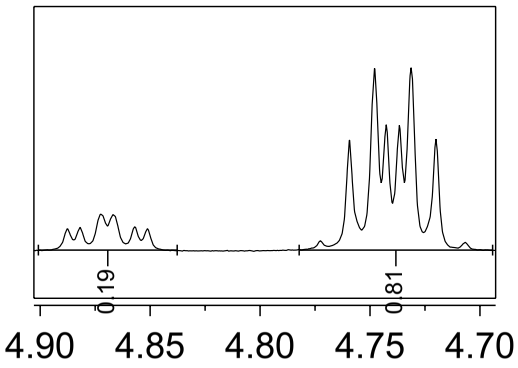

667

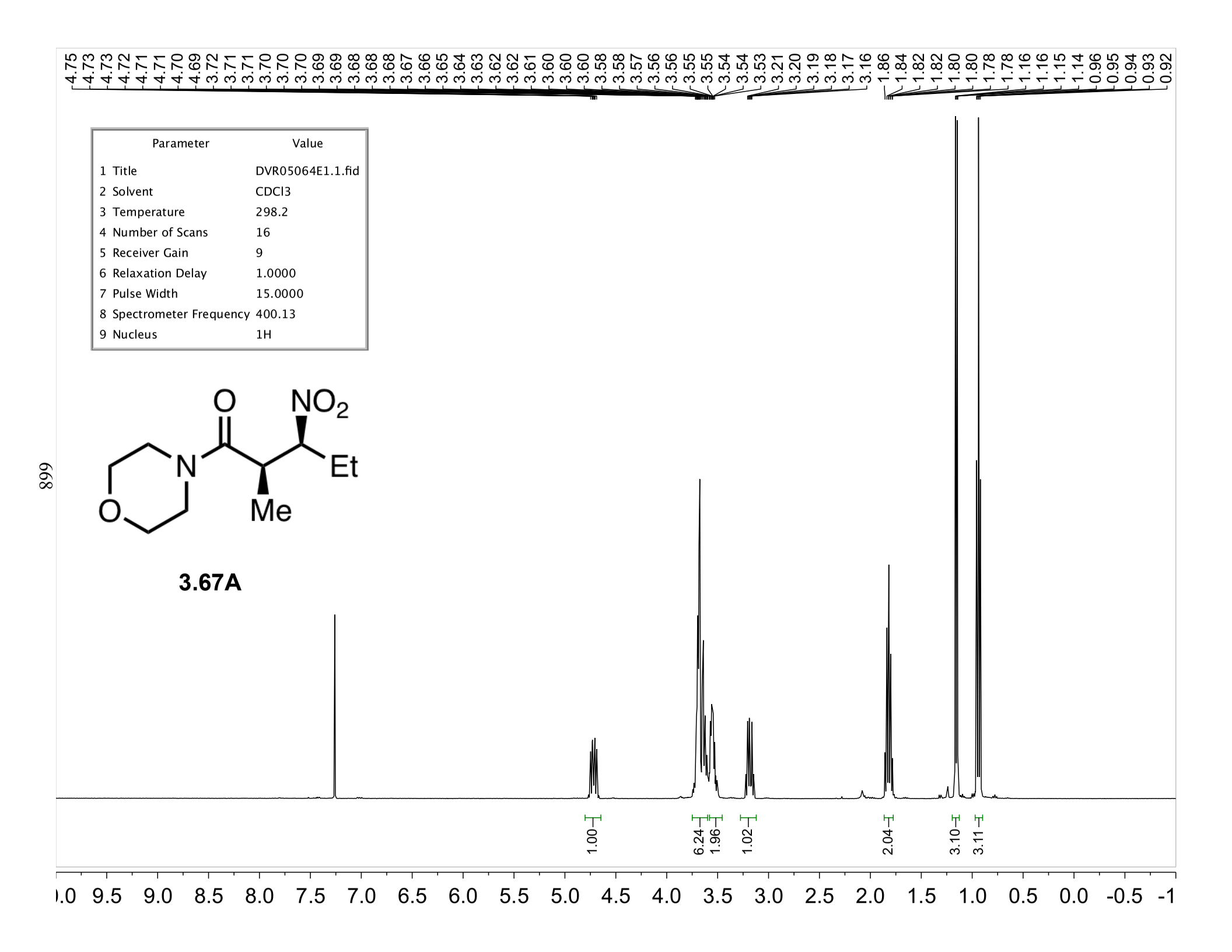
4.75 4.73 4.73 4.72 4.71 4.71 4.70 4.69 3.72 3.71 3.71 3.70 3.70 3.70 3.69 3.69 3.68 3.68 3.68 3.67 3.66 3.65 3.64 3.63 3.62 3.62 3.61 3.60 3.60 3.60 3.58 3.58 3.57 3.56 3.56 3.55 3.55 3.54 3.54 3.53 3.21 3.20 3.19 3.18 3.17 3.16 1.86 1.84 1.82 1.82 1.80 1.80 1.78 1.78 1.16 1.16 1.15 1.14 0.96 0.95 0.94 0.93 0.92
Parameter Value
1 Title DVR05064E1.1.fid
2 Solvent CDCl3
3 Temperature 298.2
4 Number of Scans 16
5 Receiver Gain 9
6 Relaxation Delay 1.0000
7 Pulse Width 15.0000
8 Spectrometer Frequency 400.13
9 Nucleus 1H
O
NO2
N
Et
O
Me
3.67A
899
1.00
6.24
1.96
1.02
2.04
3.10
3.11
.0 9.5 9.0 8.5 8.0 7.5 7.0 6.5 6.0 5.5 5.0 4.5 4.0 3.5 3.0 2.5 2.0 1.5 1.0 0.5 0.0 -0.5 -1

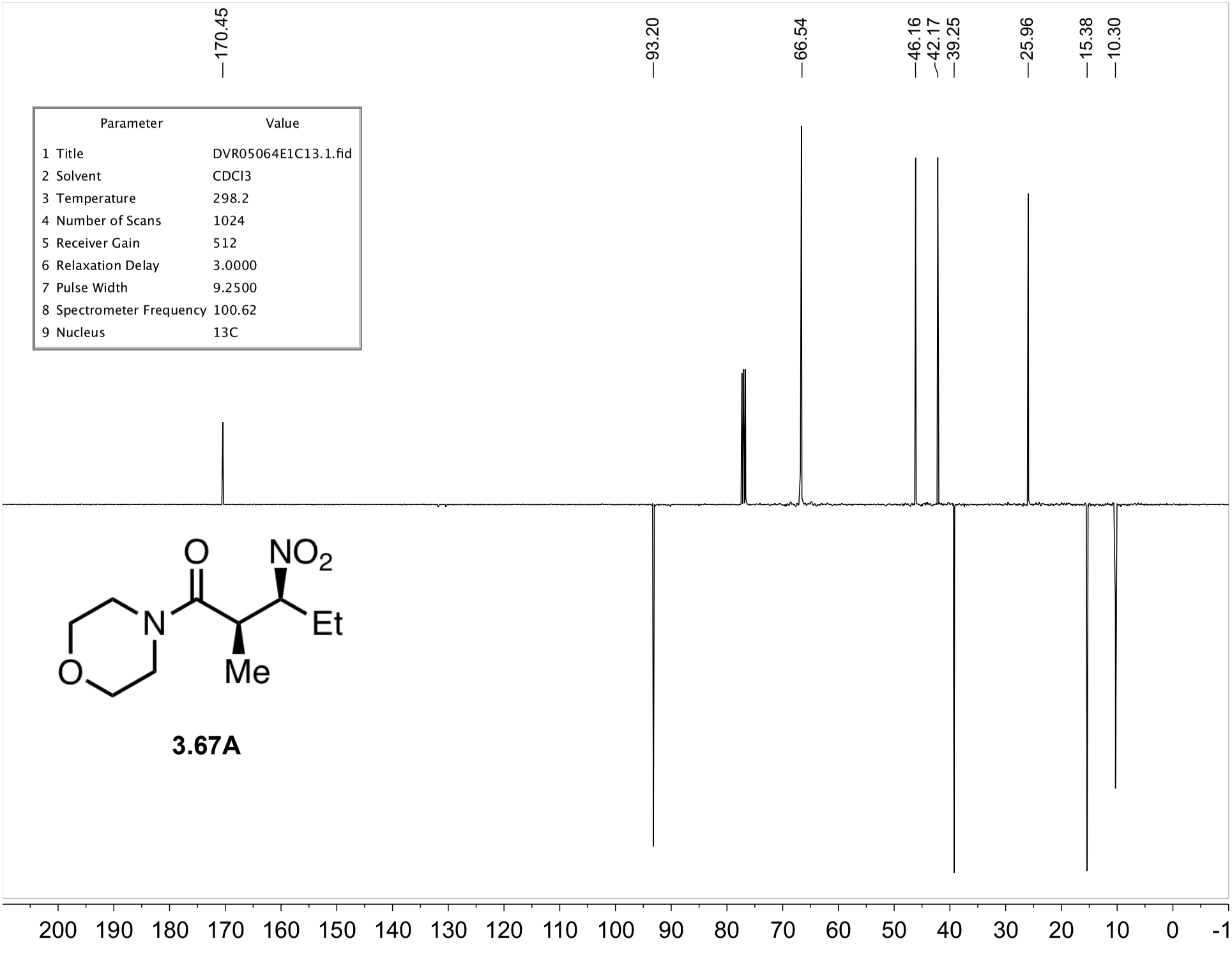
170.45
93.20
66.54
46.16
42.17
39.25
25.96
15.38
10.30
Parameter Value
1 Title DVR05064E1C13.1.fid
2 Solvent CDCl3
3 Temperature 298.2
4 Number of Scans 1024
5 Receiver Gain 512
6 Relaxation Delay 3.0000
7 Pulse Width 9.2500
8 Spectrometer Frequency 100.62
9 Nucleus 13C
699
O
NO2
N
Et
O
Me
3.67A
200 190 180 170 160 150 140 130 120 110 100 90 80 70 60 50 40 30 20 10 0 -1

Parameter	Value
1 Title	DVR05064C2.1.fid
2 Solvent	CDCl3
3 Temperature	300.0
4 Number of Scans	16
5 Receiver Gain	161
6 Relaxation Delay	1.0000
7 Pulse Width	10.7300
8 Spectrometer Frequency	600.32
9 Nucleus	1H

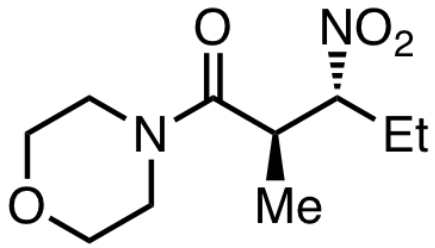

3.67B

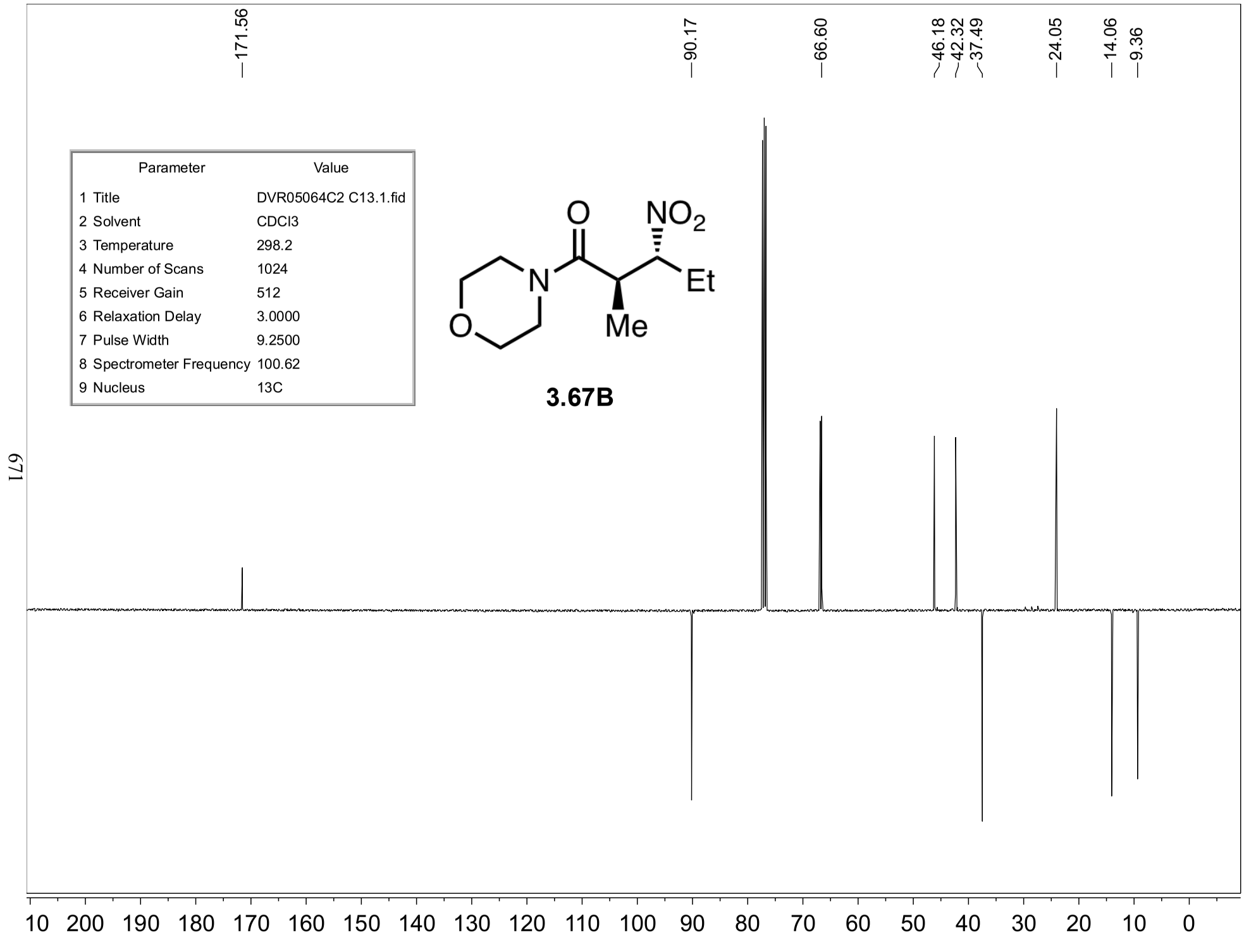
171.56
90.17
66.60
46.18
42.32
37.49
24.05
14.06
9.36
Parameter Value
1 Title DVR05064C2 C13.1.fid
2 Solvent CDCl3
3 Temperature 298.2
4 Number of Scans 1024
5 Receiver Gain 512
6 Relaxation Delay 3.0000
7 Pulse Width 9.2500
8 Spectrometer Frequency 100.62
9 Nucleus 13C
O
NO2
N
Et
O
Me
3.67B
671
10 200 190 180 170 160 150 140 130 120 110 100 90 80 70 60 50 40 30 20 10 0

==== Shimadzu LCsolution Analysis Report ====

C:\LabSolutions\Data\DMM\DVR05062B SYN RAC_4132017_1444 PM_1.lcd

Acquired by	: LC User
Sample Name	: DVR05062B SYN RAC
Sample ID	: DVR05062B SYN RAC
Tray#	: 1
Vail #	: 1
Injection Volume	: 3 uL
Data File Name	: DVR05062B SYN RAC_4132017_1444 PM_1.lcd
Method File Name	: col1_5isoiPA_30min_1ML_220and210.lcm
Batch File Name	: DMM.lcb
Report File Name	: Default.lcr
Data Acquired	: 4/13/2017 4:27:31 PM
Data Processed	: 4/26/2017 8:07:54 PM

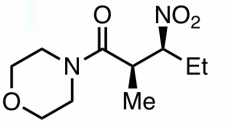

3.67A
racemic

<Chromatogram>

C:\LabSolutions\Data\DMM\DVR05062B SYN RAC_4132017_1444 PM_1.lcd

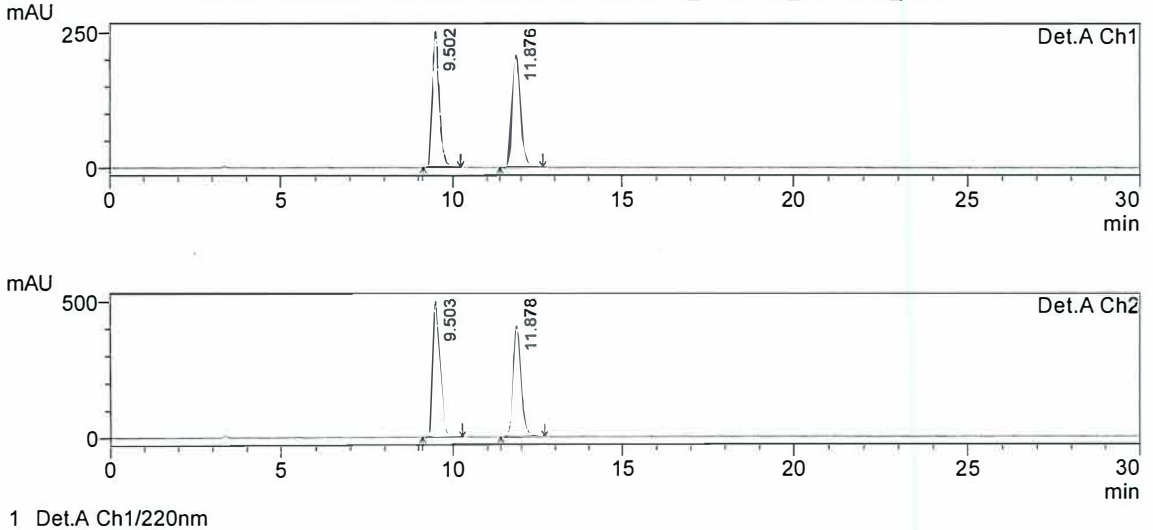

1 Det.A Ch1/220nm
2 Det.A Ch2/210nm

PeakTable

Detector A Ch1 220nm

Peak#	Ret. Time	Area	Height	Area %	Height %
1	9.502	3400093	254233	49.892	54.860
2	11.876	3414842	209185	50.108	45.140
Total		6814935	463417	100.000	100.000

PeakTable

Detector A Ch2 210nm

Peak#	Ret. Time	Area	Height	Area %	Height %
1	9.503	6685168	499845	50.023	54.929
2	11.878	6678977	410134	49.977	45.071
Total		13364145	909979	100.000	100.000

==== Shimadzu LCsolution Analysis Report ====

C:\LabSolutions\Data\DMM\DVR05064SYN_4272017_1056 AM_2.lcd

Acquired by	: LC User
Sample Name	: DVR05064SYN
Sample ID	: DVR05064SYN
Tray#	: 1
Vail #	: 1
Injection Volume	: 3 uL
Data File Name	: DVR05064SYN_4272017_1056 AM_2.lcd
Method File Name	: col1_5isoiPA_35min_1ML_220and210.lcm
Batch File Name	: DMM.lcb
Report File Name	: Default.lcr
Data Acquired	: 4/27/2017 11:12:37 AM
Data Processed	: 4/27/2017 4:51:01 PM

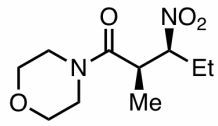

3.67A
82% ee

<Chromatogram>

C:\LabSolutions\Data\DMM\DVR05064SYN_4272017_1056 AM_2.lcd

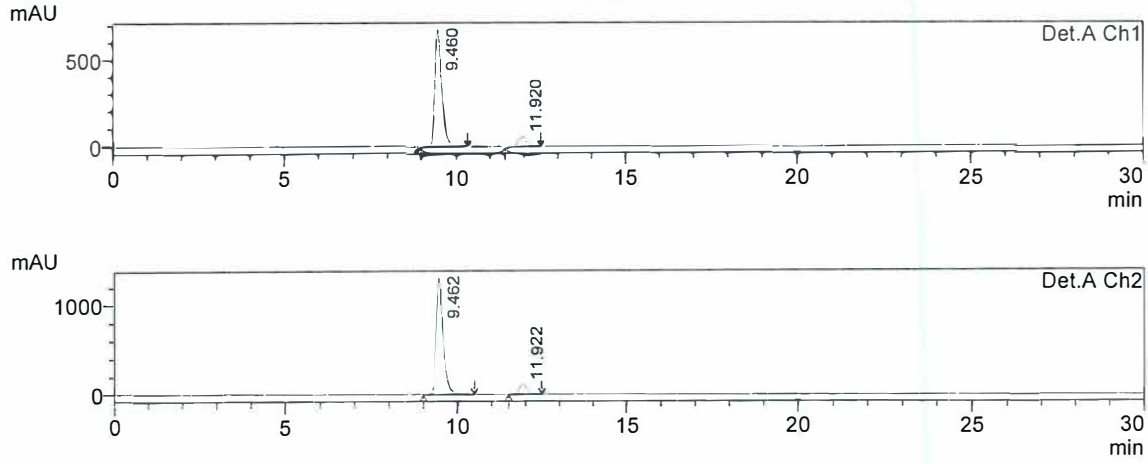

1 Det.A Ch1/220nm
2 Det.A Ch2/210nm

PeakTable

Detector A Ch1 220nm

Peak#	Ret. Time	Area	Height	Area %	Height %
1	9.460	9282986	679090	90.839	92.145
2	11.920	936213	57888	9.161	7.855
Total		10219199	736978	100.000	100.000

PeakTable

Detector A Ch2 210nm

Peak#	Ret. Time	Area	Height	Area %	Height %
1	9.462	18152526	1311597	90.899	92.084
2	11.922	1817481	112747	9.101	7.916
Total		19970007	1424344	100.000	100.000

==== Shimadzu LCsolution Analysis Report ====

C:\LabSolutions\Data\DMM\DVR05064ANTI RAC 2_892017_1946 PM_2.lcd

Acquired by	: LC User
Sample Name	: DVR05064ANTI RAC 2
Sample ID	: DVR05064ANTI RAC 2
Tray#	: 1
Vail #	: 1
Injection Volume	: 5 uL
Data File Name	: DVR05064ANTI RAC 2_892017_1946 PM_2.lcd
Method File Name	: col1_5isoiPA_30min_1ML_220and210.lcm
Batch File Name	: DMM.lcb
Report File Name	: Default.lcr
Data Acquired	: 8/9/2017 7:57:11 PM
Data Processed	: 8/11/2017 11:21:57 AM

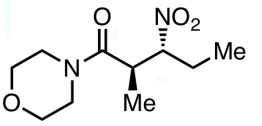

3.67B
racemic

(±)

<Chromatogram>

C:\LabSolutions\Data\DMM\DVR05064ANTI RAC 2_892017_1946 PM_2.lcd

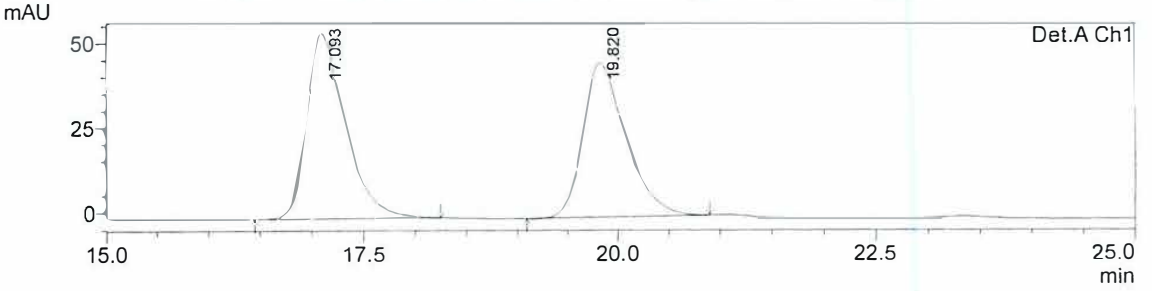

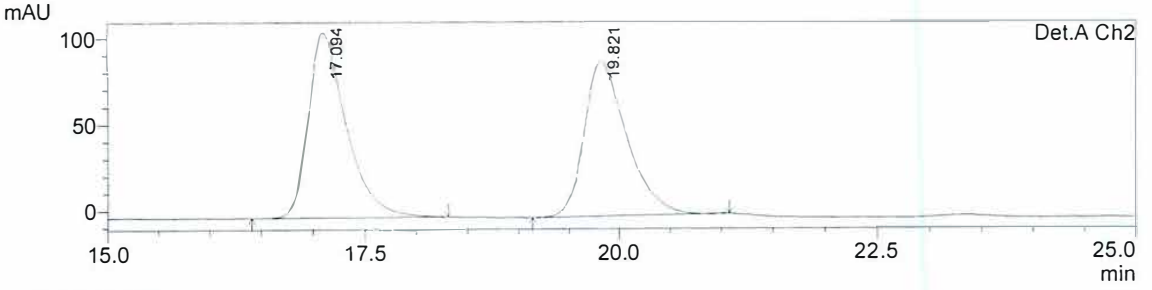

1 Det.A Ch1/220nm
2 Det.A Ch2/210nm

PeakTable

Detector A Ch1 220nm

Peak#	Ret. Time	Area	Height	Area %	Height %
1	17.093	1386247	54558	50.838	54.487
2	19.820	1340558	45572	49.162	45.513
Total		2726805	100130	100.000	100.000

PeakTable

Detector A Ch2 210nm

Peak#	Ret. Time	Area	Height	Area %	Height %
1	17.094	2723976	107119	50.856	54.491
2	19.821	2632268	89461	49.144	45.509
Total		5356244	196580	100.000	100.000

==== Shimadzu LCsolution Analysis Report ====

C:\LabSolutions\Data\DMM\DVR05064 D2-A_8152017_1731 PM_2.lcd

Acquired by	: LC User
Sample Name	: DVR05064 D2-A
Sample ID	: DVR05064 D2-A
Tray#	: 1
Vail #	: 5
Injection Volume	: 5 uL
Data File Name	: DVR05064 D2-A_8152017_1731 PM_2.lcd
Method File Name	: col1_5isoiPA_30min_1ML_220and210.lcm
Batch File Name	: DMM.lcb
Report File Name	: Default.lcr
Data Acquired	: 8/15/2017 5:42:34 PM
Data Processed	: 8/15/2017 6:12:36 PM

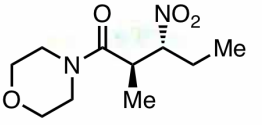

3.67B
48% ee

<Chromatogram>

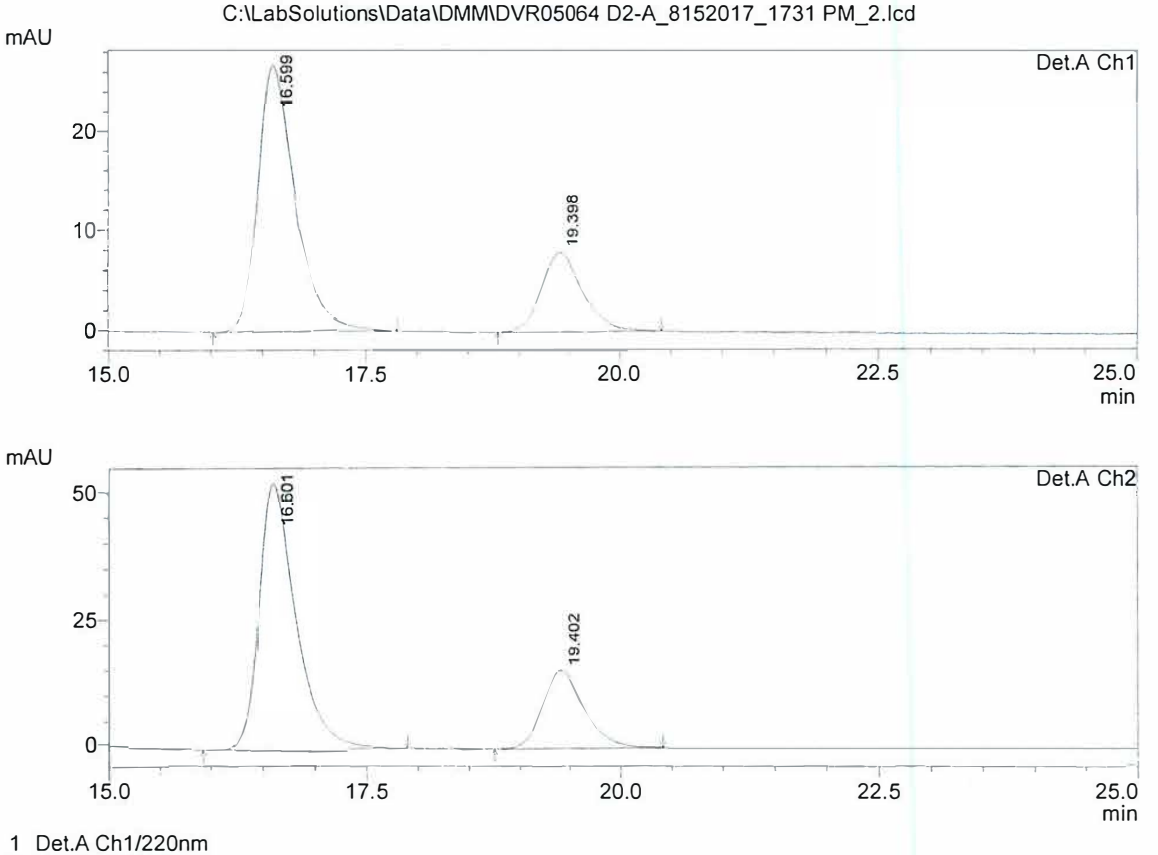

1 Det.A Ch1/220nm
2 Det.A Ch2/210nm

PeakTable

Detector A Ch1 220nm

Peak#	Ret. Time	Area	Height	Area %	Height %
1	16.599	661030	26807	74.380	77.191
2	19.398	227688	7921	25.620	22.809
Total		888718	34728	100.000	100.000

Parameter	Value
1 Title	DVR05063crd.1.fid
2 Solvent	CDCl3
3 Temperature	299.4
4 Number of Scans	8
5 Receiver Gain	181
6 Relaxation Delay	1.0000
7 Pulse Width	15.9700
8 Spectrometer Frequency	400.15
9 Nucleus	1H

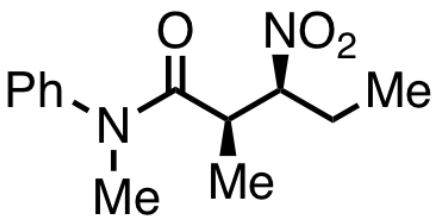

3.68A

Crude

79:21

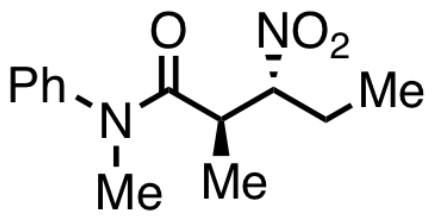

3.68B

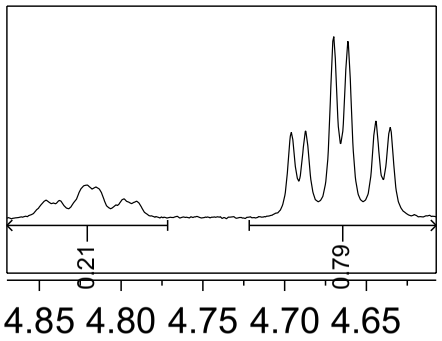

676

Parameter	Value
1 Title	DVR05063C1.2.fid
2 Solvent	CDCl3
3 Temperature	298.1
4 Number of Scans	16
5 Receiver Gain	11
6 Relaxation Delay	1.0000
7 Pulse Width	15.0000
8 Spectrometer Frequency	400.13
9 Nucleus	1H

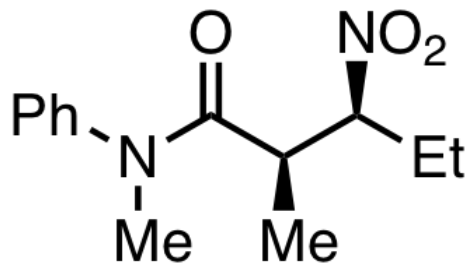

3.68A

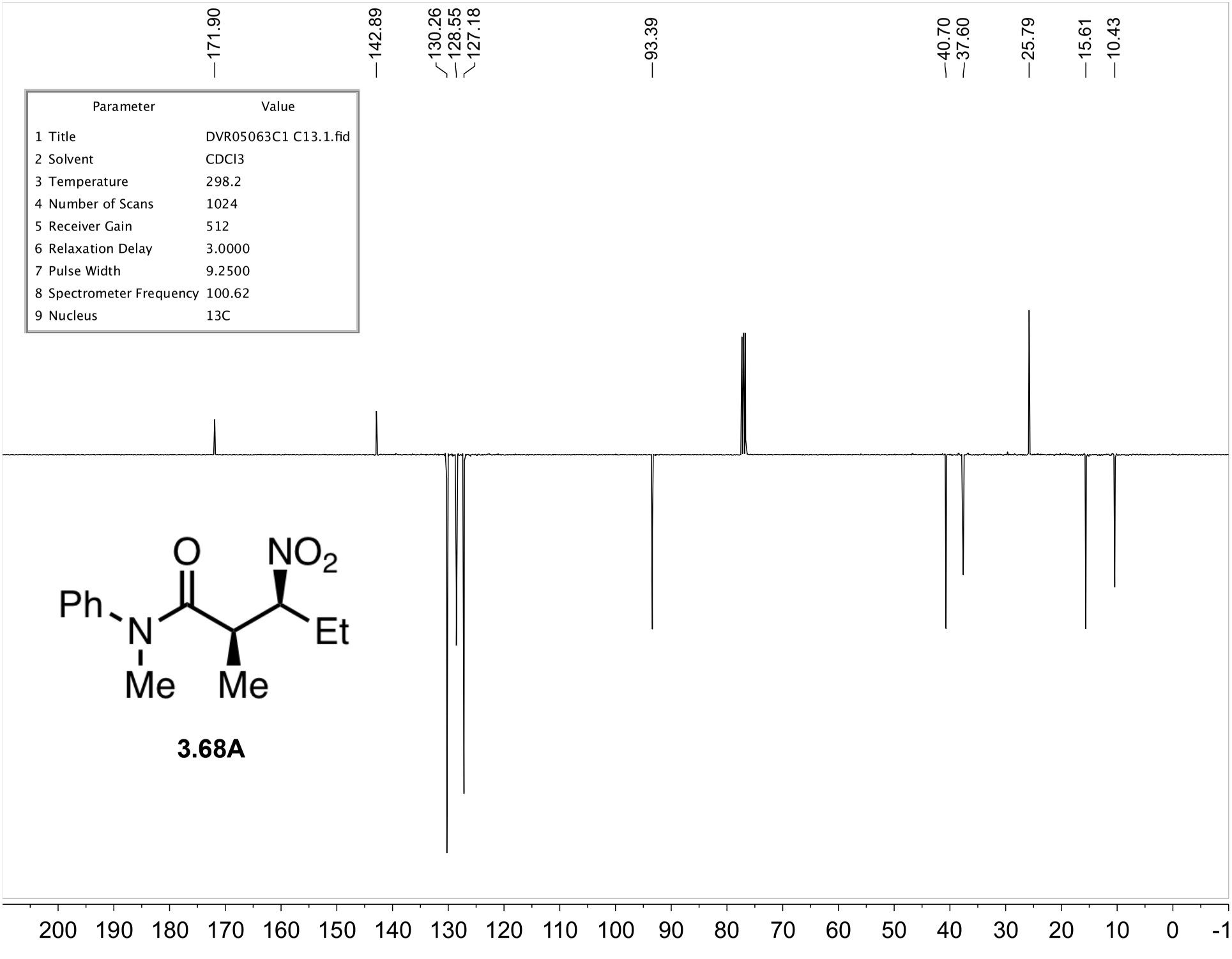
171.90
142.89
130.26
128.55
127.18
93.39
40.70
37.60
25.79
15.61
10.43
Parameter Value
1 Title DVR05063C1 C13.1.fid
2 Solvent CDCl3
3 Temperature 298.2
4 Number of Scans 1024
5 Receiver Gain 512
6 Relaxation Delay 3.0000
7 Pulse Width 9.2500
8 Spectrometer Frequency 100.62
9 Nucleus 13C
678
O
NO2
Ph
N
Et
Me
Me
3.68A
200 190 180 170 160 150 140 130 120 110 100 90 80 70 60 50 40 30 20 10 0 -1

Parameter	Value
1 Title	DVR05063D2.1.fid
2 Solvent	CDCl3
3 Temperature	300.0
4 Number of Scans	16
5 Receiver Gain	144
6 Relaxation Delay	1.0000
7 Pulse Width	10.7300
8 Spectrometer Frequency	600.32
9 Nucleus	1H

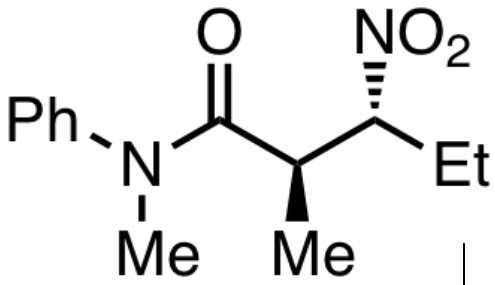

3.68B

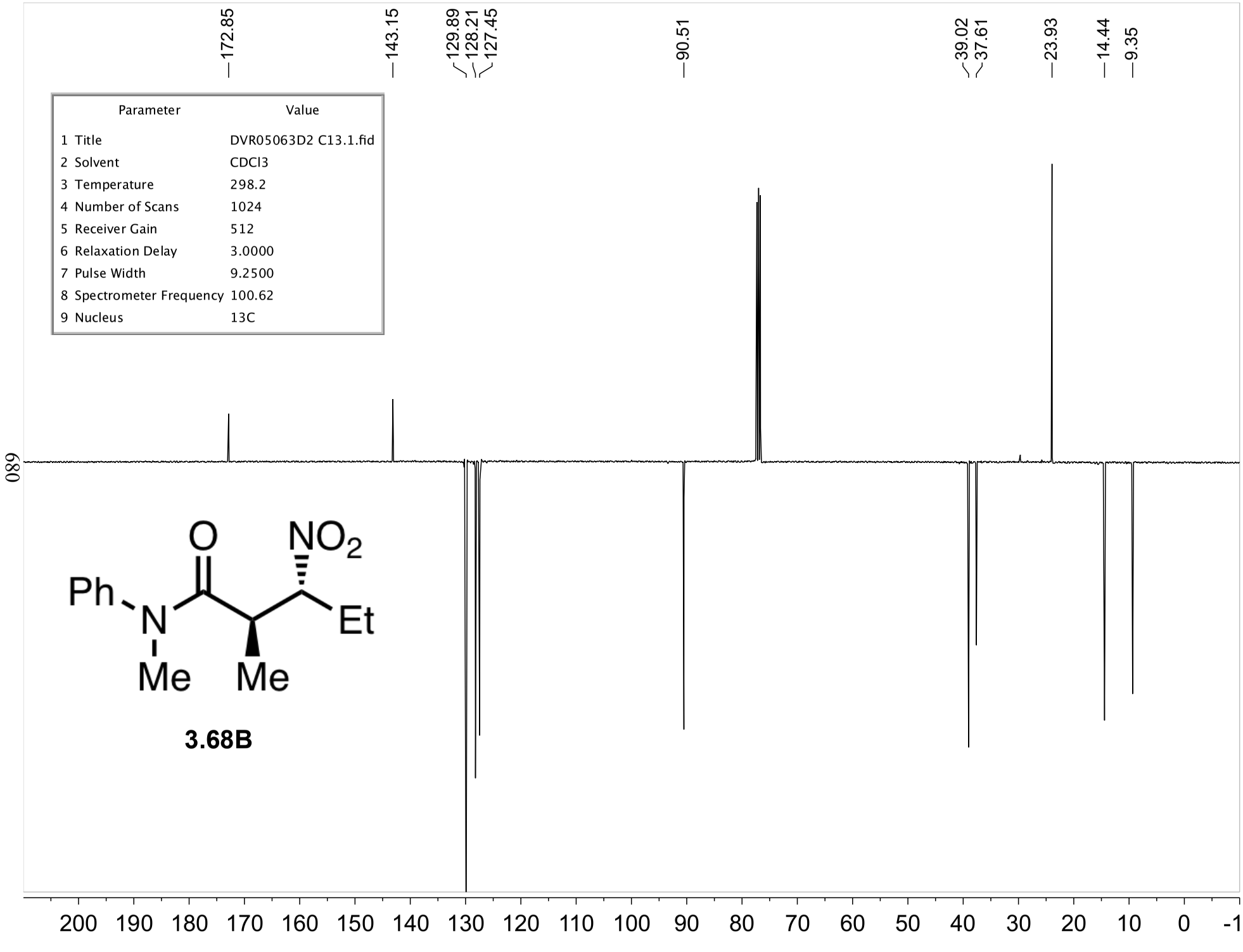
172.85
143.15
129.89
128.21
127.45
90.51
39.02
37.61
23.93
14.44
9.35
Parameter Value
1 Title DVR05063D2 C13.1.fid
2 Solvent CDCl3
3 Temperature 298.2
4 Number of Scans 1024
5 Receiver Gain 512
6 Relaxation Delay 3.0000
7 Pulse Width 9.2500
8 Spectrometer Frequency 100.62
9 Nucleus 13C
089
O
NO2
Ph
N
Et
Me
Me
3.68B
200 190 180 170 160 150 140 130 120 110 100 90 80 70 60 50 40 30 20 10 0 -1

==== Shimadzu LCsolution Analysis Report ====

C:\LabSolutions\Data\DMM\DVR05063 SYN RAC_4142017_1035 AM_4.lcd

Acquired by	: LC User
Sample Name	: DVR05063 SYN RAC
Sample ID	: DVR05063 SYN RAC
Tray#	: 1
Vail #	: 1
Injection Volume	: 3 uL
Data File Name	: DVR05063 SYN RAC_4142017_1035 AM_4.lcd
Method File Name	: col2_1isoiPA_45min_1ML_220 and210.lcm
Batch File Name	: DMM.lcb
Report File Name	: Default.lcr
Data Acquired	: 4/14/2017 12:21:24 PM
Data Processed	: 4/14/2017 9:27:36 PM

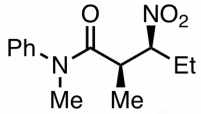

3.68A
racemic
(±) SYN

<Chromatogram>

C:\LabSolutions\Data\DMM\DVR05063 SYN RAC_4142017_1035 AM_4.lcd

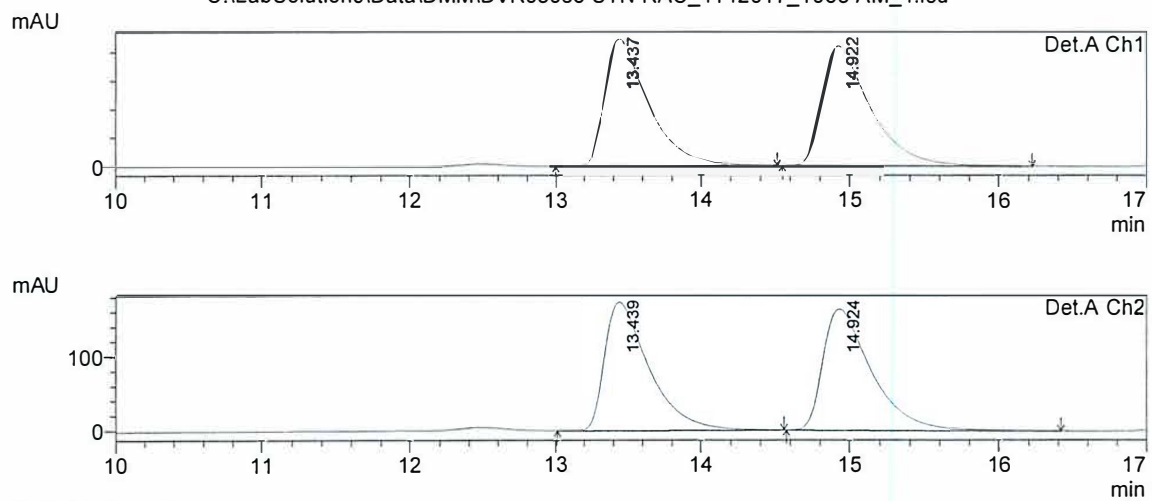

1 Det.A Ch1/220nm
2 Det.A Ch2/210nm

PeakTable

Detector A Ch1 220nm

Peak#	Ret. Time	Area	Height	Area %	Height %
1	13.437	1875039	89147	49.907	51.483
2	14.922	1882004	84011	50.093	48.517
Total		3757042	173158	100.000	100.000

PeakTable

Detector A Ch2 210nm

Peak#	Ret. Time	Area	Height	Area %	Height %
1	13.439	3640912	172661	49.757	51.429
2	14.924	3676496	163067	50.243	48.571
Total		7317407	335728	100.000	100.000

==== Shimadzu LCsolution Analysis Report ====

C:\LabSolutions\Data\DMM\DVR05063 SYN _4142017_1035 AM_5.lcd

Acquired by	: LC User
Sample Name	: DVR05063 SYN
Sample ID	: DVR05063 SYN
Tray#	: 1
Vail #	: 2
Injection Volume	: 3 uL
Data File Name	: DVR05063 SYN _4142017_1035 AM_5.lcd
Method File Name	: col2_1isoiPA_45min_1ML_220 and210.lcm
Batch File Name	: DMM.lcb
Report File Name	: Default.lcr
Data Acquired	: 4/14/2017 1:47:22 PM
Data Processed	: 4/14/2017 9:21:59 PM

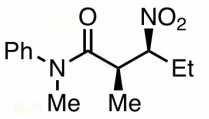

3.68A
84% ee

<Chromatogram>

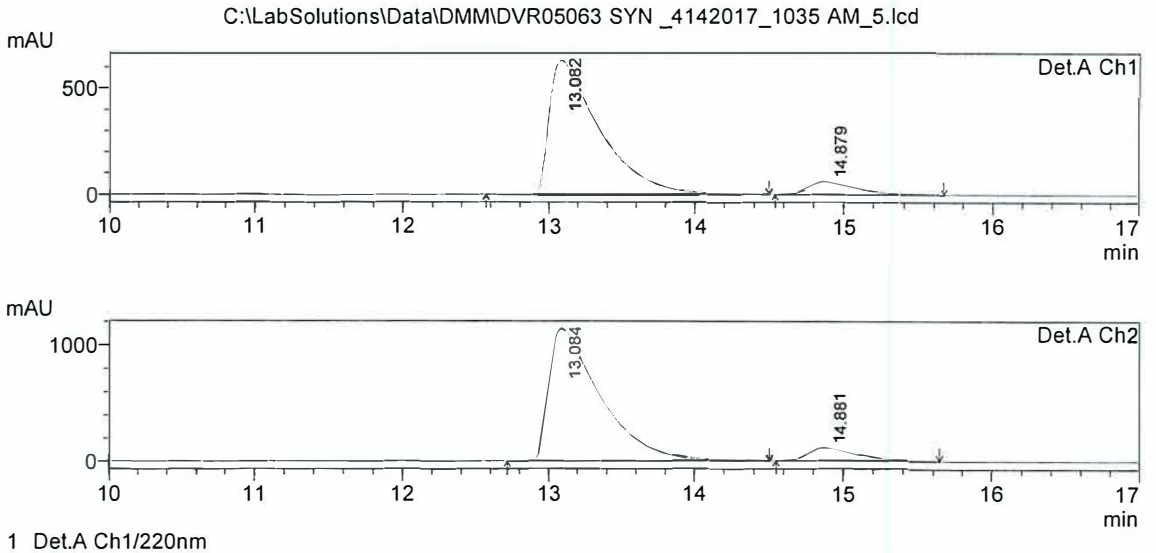

1 Det.A Ch1/220nm
2 Det.A Ch2/210nm

PeakTable

Detector A Ch1 220nm

Peak#	Ret. Time	Area	Height	Area %	Height %
1	13.082	15144440	630793	91.992	91.337
2	14.879	1318328	59830	8.008	8.663
Total		16462767	690623	100.000	100.000

PeakTable

Detector A Ch2 210nm

Peak#	Ret. Time	Area	Height	Area %	Height %
1	13.084	28213573	1139857	91.710	90.757
2	14.881	2550271	116082	8.290	9.243
Total		30763844	1255939	100.000	100.000

==== Shimadzu LCsolution Analysis Report ====

C:\LabSolutions\Data\DMM\DVR05063 ANTI RAC_4142017_1035 AM_6.lcd

Acquired by	: LC User
Sample Name	: DVR05063 ANTI RAC
Sample ID	: DVR05063 ANTI RAC
Tray#	: 1
Vail #	: 3
Injection Volume	: 3 uL
Data File Name	: DVR05063 ANTI RAC_4142017_1035 AM_6.lcd
Method File Name	: col2_1isoiPA_45min_1ML_220 and210.lcm
Batch File Name	: DMM.lcb
Report File Name	: Default.lcr
Data Acquired	: 4/14/2017 3:13:18 PM
Data Processed	: 4/14/2017 3:58:18 PM

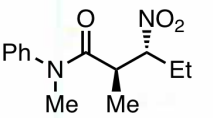

3.68B
racemic

<Chromatogram>

C:\LabSolutions\Data\DMM\DVR05063 ANTI RAC_4142017_1035 AM_6.lcd

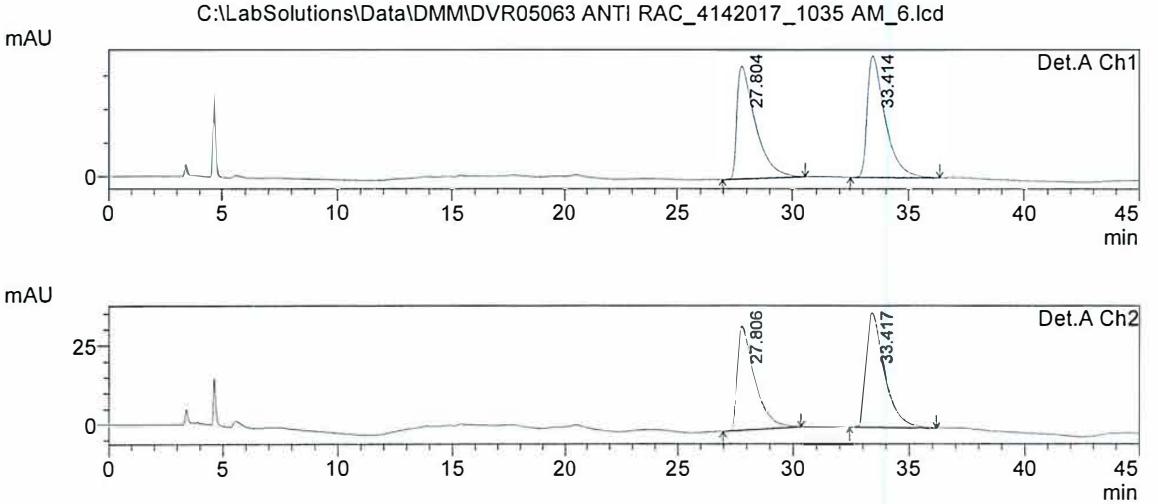

1 Det.A Ch1/220nm
2 Det.A Ch2/210nm

PeakTable

Detector A Ch1 220nm

Peak#	Ret. Time	Area	Height	Area %	Height %
1	27.804	918935	16637	49.096	48.143
2	33.414	952791	17920	50.904	51.857
Total		1871727	34557	100.000	100.000

PeakTable

Detector A Ch2 210nm

Peak#	Ret. Time	Area	Height	Area %	Height %
1	27.806	1751437	32953	47.277	47.555
2	33.417	1953216	36341	52.723	52.445
Total		3704653	69294	100.000	100.000

==== Shimadzu LCsolution Analysis Report ====

C:\LabSolutions\Data\DMM\DVR05063 ANTI_4142017_1035 AM_10.lcd

Acquired by	: LC User
Sample Name	: DVR05063 ANTI
Sample ID	: DVR05063 ANTI
Tray#	: 1
Vail #	: 4
Injection Volume	: 3 uL
Data File Name	: DVR05063 ANTI_4142017_1035 AM_10.lcd
Method File Name	: col2_1isoiPA_45min_1ML_220 and210.lcm
Batch File Name	: DMM.lcb
Report File Name	: Default.lcr
Data Acquired	: 4/14/2017 4:39:16 PM
Data Processed	: 4/14/2017 5:24:17 PM

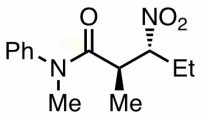

3.68B
54% ee

Anti

<Chromatogram>

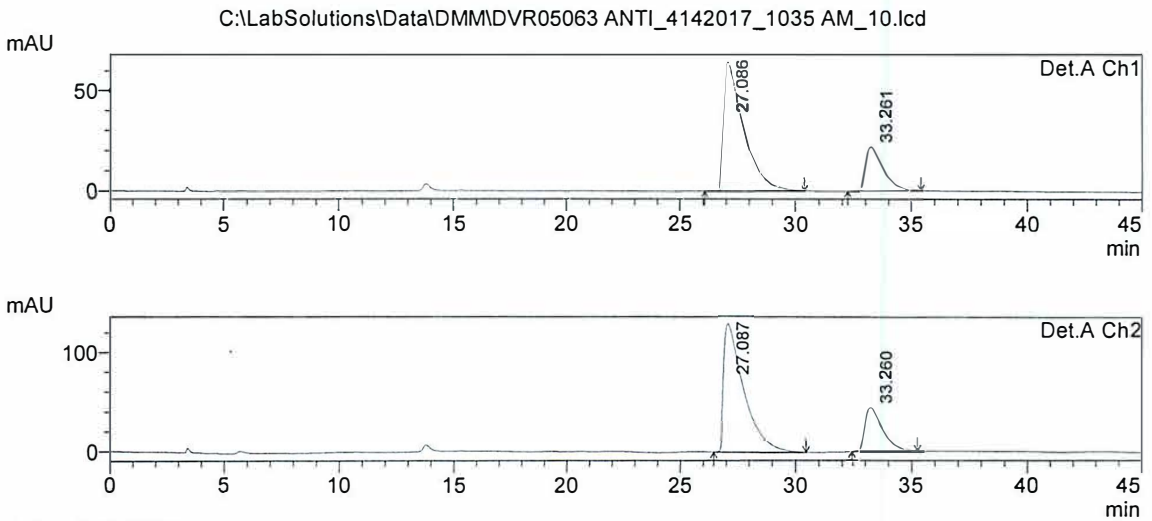

1 Det.A Ch1/220nm
2 Det.A Ch2/210nm

PeakTable

Detector A Ch1 220nm

Peak#	Ret. Time	Area	Height	Area %	Height %
1	27.086	3841588	64821	76.841	74.649
2	33.261	1157821	22014	23.159	25.351
Total		4999409	86835	100.000	100.000

PeakTable

Detector A Ch2 210nm

Peak#	Ret. Time	Area	Height	Area %	Height %
1	27.087	7752624	130001	76.981	74.578
2	33.260	2318221	44313	23.019	25.422
Total		10070845	174314	100.000	100.000

Parameter	Value
1 Title	DVR05058CRD.1.fid
2 Solvent	CDCl3
3 Temperature	300.0
4 Number of Scans	16
5 Receiver Gain	181
6 Relaxation Delay	1.0000
7 Pulse Width	13.1400
8 Spectrometer Frequency	600.32
9 Nucleus	1H

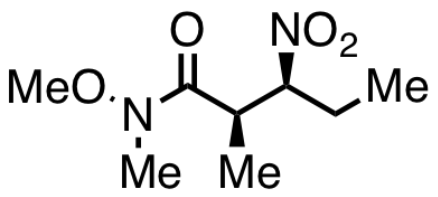

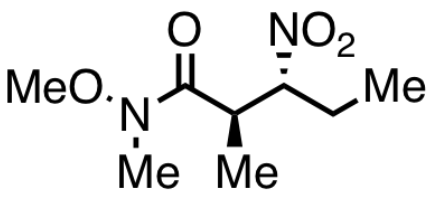

Crude

3.69A **92:08** **3.69B**

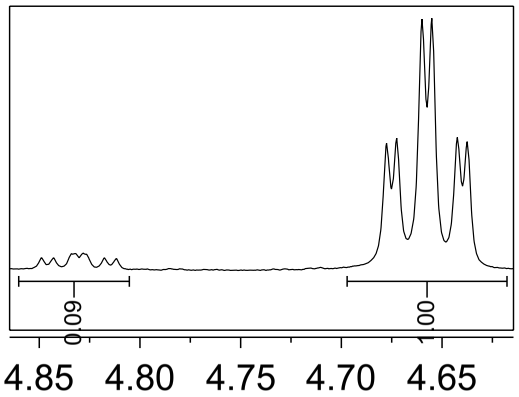

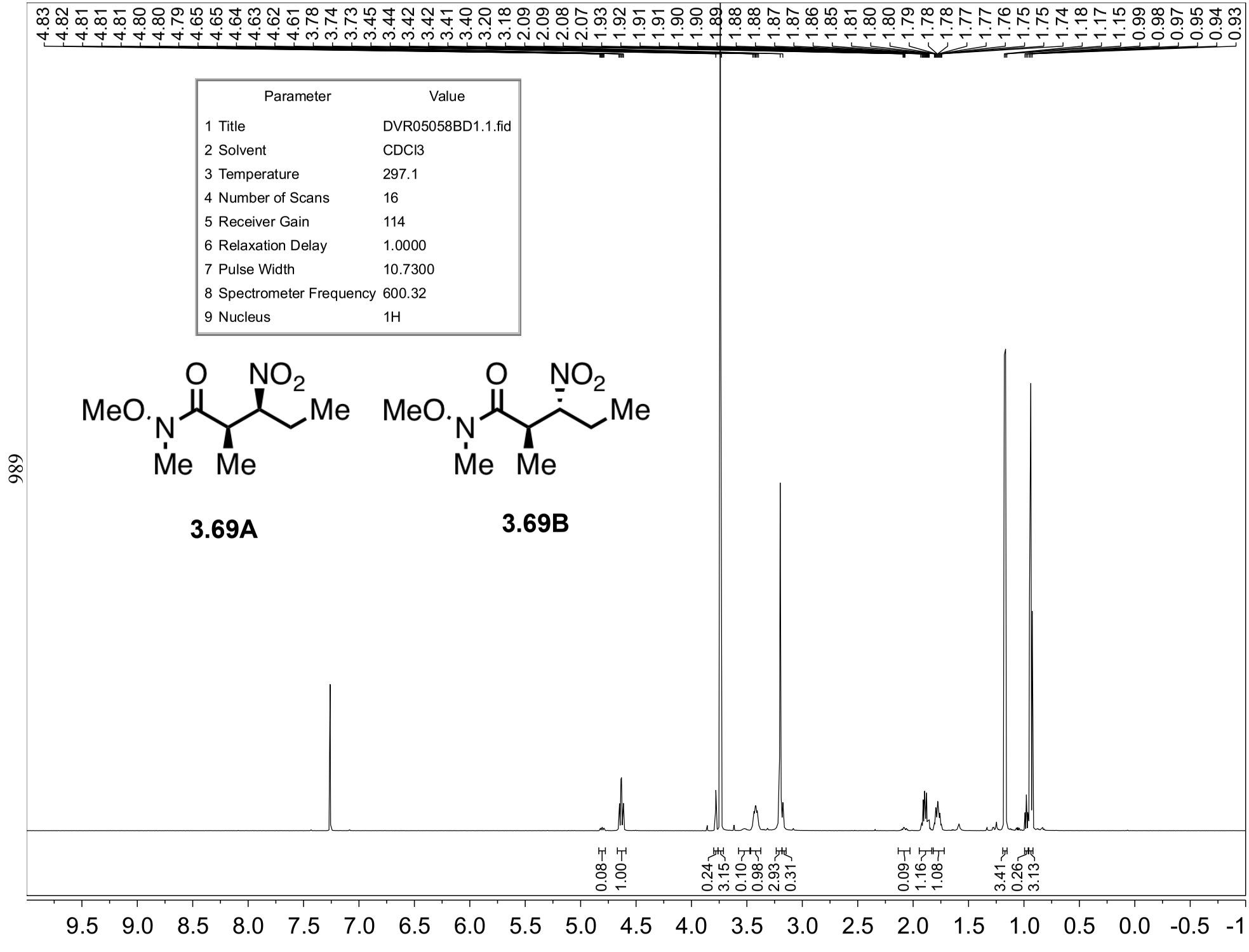
4.83 4.82 4.81 4.81 4.81 4.80 4.80 4.79 4.65 4.65 4.64 4.63 4.62 4.61 3.78 3.74 3.73 3.45 3.44 3.42 3.42 3.41 3.40 3.20 3.18 2.09 2.09 2.08 2.07 1.93 1.92 1.91 1.91 1.90 1.90 1.89 1.88 1.88 1.87 1.87 1.86 1.85 1.81 1.80 1.80 1.79 1.78 1.78 1.77 1.77 1.76 1.75 1.75 1.74 1.18 1.17 1.15 0.99 0.98 0.97 0.95 0.94 0.93
Parameter Value
1 Title DVR05058BD1.1.fid
2 Solvent CDCl3
3 Temperature 297.1
4 Number of Scans 16
5 Receiver Gain 114
6 Relaxation Delay 1.0000
7 Pulse Width 10.7300
8 Spectrometer Frequency 600.32
9 Nucleus 1H
MeO N Me Me O NO2 Me
3.69A
MeO N Me Me O NO2 Me
3.69B
989
0.08 1.00 0.24 3.15 0.10 0.98 2.93 0.31 0.09 1.16 1.08 3.41 0.26 3.13
9.5 9.0 8.5 8.0 7.5 7.0 6.5 6.0 5.5 5.0 4.5 4.0 3.5 3.0 2.5 2.0 1.5 1.0 0.5 0.0 -0.5 -1

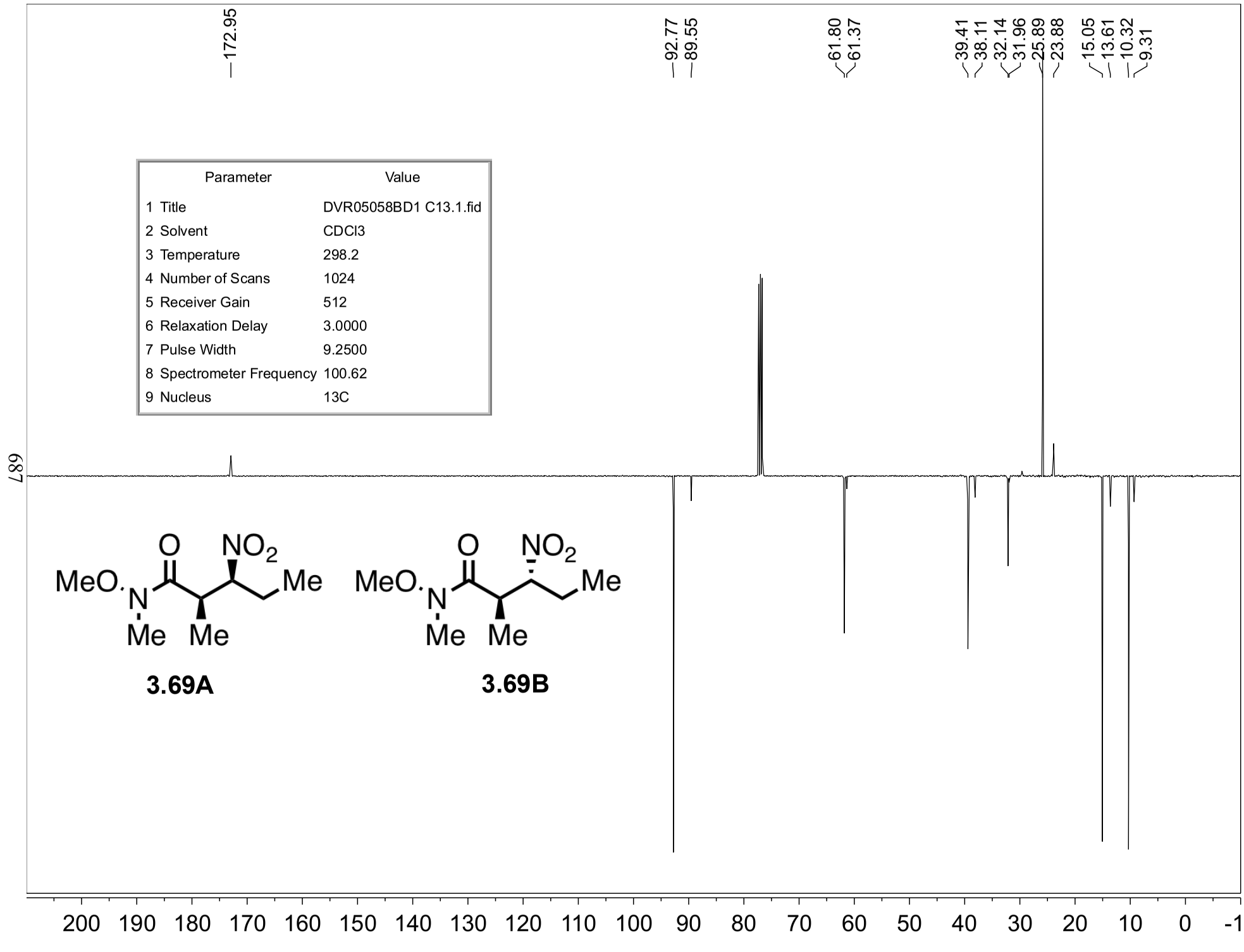
172.95
92.77
89.55
61.80
61.37
39.41
38.11
32.14
31.96
25.89
23.88
15.05
13.61
10.32
9.31
Parameter Value
1 Title DVR05058BD1 C13.1.fid
2 Solvent CDCl3
3 Temperature 298.2
4 Number of Scans 1024
5 Receiver Gain 512
6 Relaxation Delay 3.0000
7 Pulse Width 9.2500
8 Spectrometer Frequency 100.62
9 Nucleus 13C
687
MeO. N Me Me O NO2 Me
3.69A
MeO. N Me Me O NO2 Me
3.69B
200 190 180 170 160 150 140 130 120 110 100 90 80 70 60 50 40 30 20 10 0 -1

==== Shimadzu LCsolution Analysis Report ====

C:\LabSolutions\Data\DMM\DVR05060 F1 RAC_3252017_1721 PM_2.lcd

Acquired by	: LC User
Sample Name	: DVR05060 F1 RAC
Sample ID	: DVR05060 F1 RAC
Tray#	: 1
Vail #	: 2
Injection Volume	: 3 uL
Data File Name	: DVR05060 F1 RAC_3252017_1721 PM_2.lcd
Method File Name	: col6_2isoiPA_45min_1ML_210and220.lcm
Batch File Name	: DMM.lcb
Report File Name	: Default.lcr
Data Acquired	: 3/25/2017 5:32:40 PM
Data Processed	: 5/8/2017 10:08:00 AM

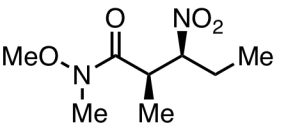

3.69A
racemic

<Chromatogram>

C:\LabSolutions\Data\DMM\DVR05060 F1 RAC_3252017_1721 PM_2.lcd

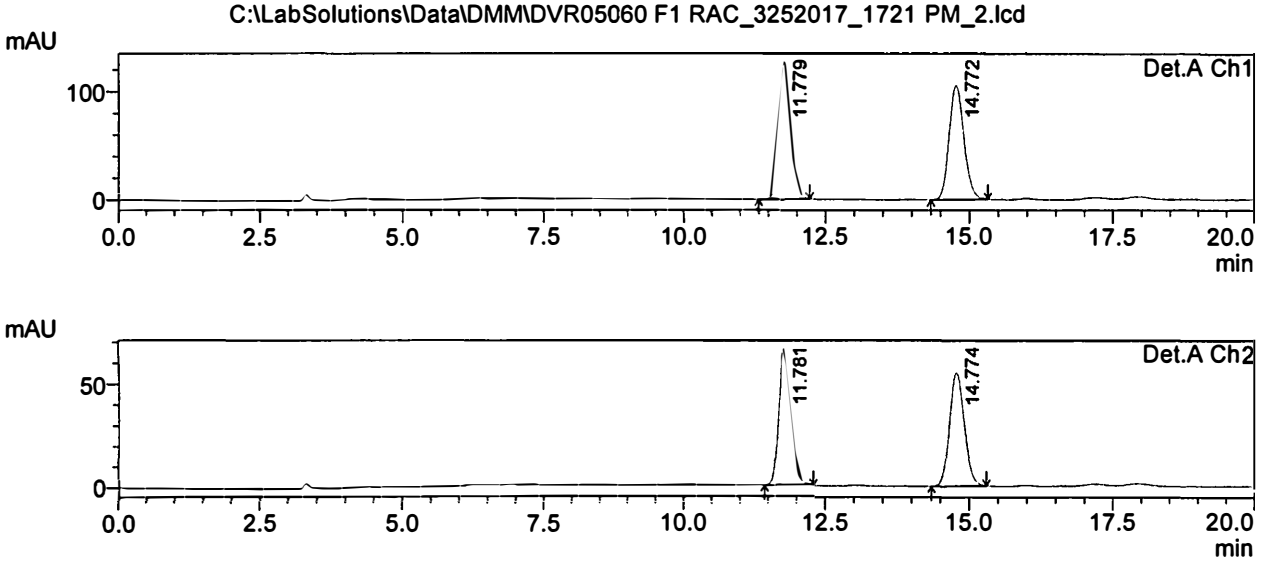

1 Det.A Ch1/210nm
2 Det.A Ch2/220nm

PeakTable

Detector A Ch1 210nm

Peak#	Ret. Time	Area	Height	Area %	Height %
1	11.779	1892057	127392	49.826	54.694
2	14.772	1905263	105526	50.174	45.306
Total		3797320	232918	100.000	100.000

PeakTable

Detector A Ch2 220nm

Peak#	Ret. Time	Area	Height	Area %	Height %
1	11.781	991580	66313	50.039	54.729
2	14.774	990019	54853	49.961	45.271
Total		1981598	121166	100.000	100.000

==== Shimadzu LCsolution Analysis Report ====

C:\LabSolutions\Data\DMM\DVR05058AF2_3302017_1816 PM_5.lcd

Acquired by	: LC User
Sample Name	: DVR05058AF2
Sample ID	: DVR05058AF2
Tray#	: 1
Vail #	: 1
Injection Volume	: 2 uL
Data File Name	: DVR05058AF2_3302017_1816 PM_5.lcd
Method File Name	: col6_2isoiPA_45min_1ML_210and220.lcm
Batch File Name	: DMM.lcb
Report File Name	: Default.lcr
Data Acquired	: 3/30/2017 7:37:52 PM
Data Processed	: 3/30/2017 8:22:54 PM

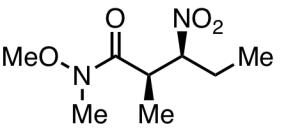

3.69A
85% ee

<Chromatogram>

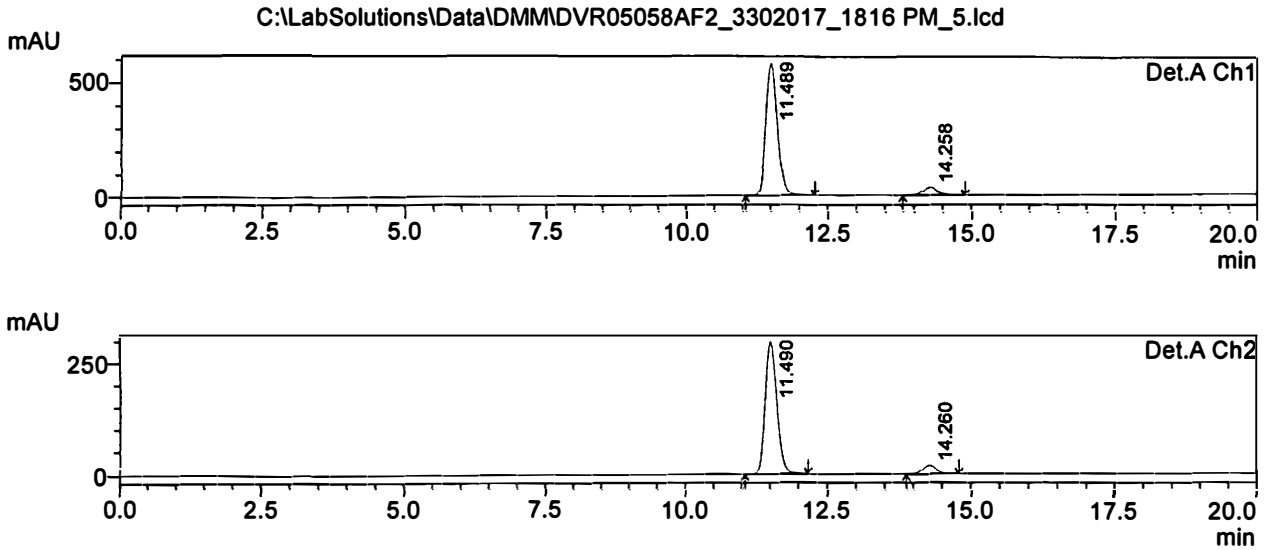

1 Det.A Ch1/210nm
2 Det.A Ch2/220nm

PeakTable

Detector A Ch1 210nm

Peak#	Ret. Time	Area	Height	Area %	Height %
1	11.489	8231186	578832	92.537	93.512
2	14.258	663851	40164	7.463	6.488
Total		8895037	618996	100.000	100.000

PeakTable

Detector A Ch2 220nm

Peak#	Ret. Time	Area	Height	Area %	Height %
1	11.490	4294914	301110	92.621	93.458
2	14.260	342155	21079	7.379	6.542
Total		4637070	322189	100.000	100.000

==== Shimadzu LCsolution Analysis Report ====

C:\LabSolutions\Data\DMM\DVR05060 F1 RAC_3252017_1721 PM_2.lcd

Acquired by	: LC User
Sample Name	: DVR05060 F1 RAC
Sample ID	: DVR05060 F1 RAC
Tray#	: 1
Vail #	: 2
Injection Volume	: 3 uL
Data File Name	: DVR05060 F1 RAC_3252017_1721 PM_2.lcd
Method File Name	: col6_2isoiPA_45min_1ML_210and220.lcm
Batch File Name	: DMM.lcb
Report File Name	: Default.lcr
Data Acquired	: 3/25/2017 5:32:40 PM
Data Processed	: 3/26/2017 4:45:00 PM

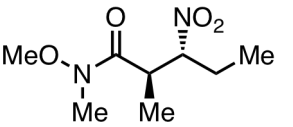

3.69B
racemic

<Chromatogram>

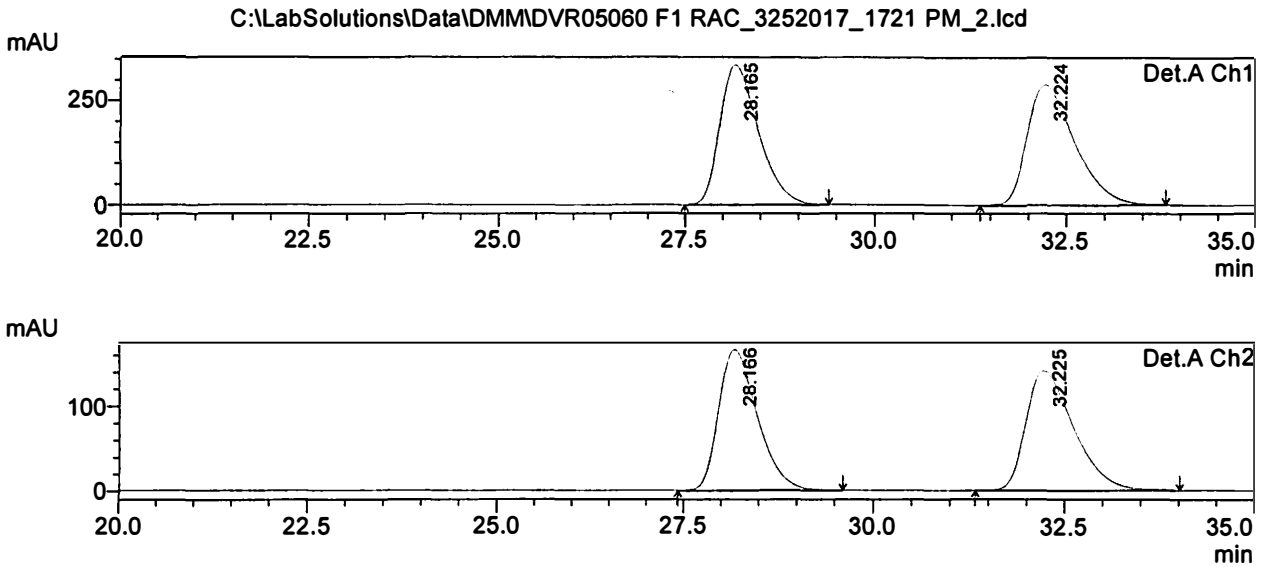

1 Det.A Ch1/210nm
2 Det.A Ch2/220nm

PeakTable

Detector A Ch1 210nm

Peak#	Ret. Time	Area	Height	Area %	Height %
1	28.165	11971890	336483	48.889	53.786
2	32.224	12516074	289114	51.111	46.214
Total		24487965	625597	100.000	100.000

PeakTable

Detector A Ch2 220nm

Peak#	Ret. Time	Area	Height	Area %	Height %
1	28.166	5944017	166301	48.907	53.781
2	32.225	6209711	142920	51.093	46.219
Total		12153728	309221	100.000	100.000

==== Shimadzu LCsolution Analysis Report ====

C:\LabSolutions\Data\DMM\DVR05058 SYN AND ANTI_3252017_1721 PM_8.lcd

Acquired by	: LC User
Sample Name	: DVR05058 SYN AND ANTI
Sample ID	: DVR05058 SYN AND ANTI
Tray#	: 1
Vail #	: 3
Injection Volume	: 3 uL
Data File Name	: DVR05058 SYN AND ANTI_3252017_1721 PM_8.lcd
Method File Name	: col6_2isoiPA_45min_1ML_210and220.lcm
Batch File Name	: DMM.lcb
Report File Name	: Default.lcr
Data Acquired	: 3/25/2017 9:40:09 PM
Data Processed	: 5/8/2017 10:44:10 AM

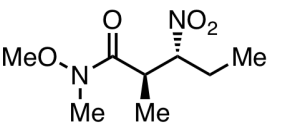

3.69B
52% ee

<Chromatogram>

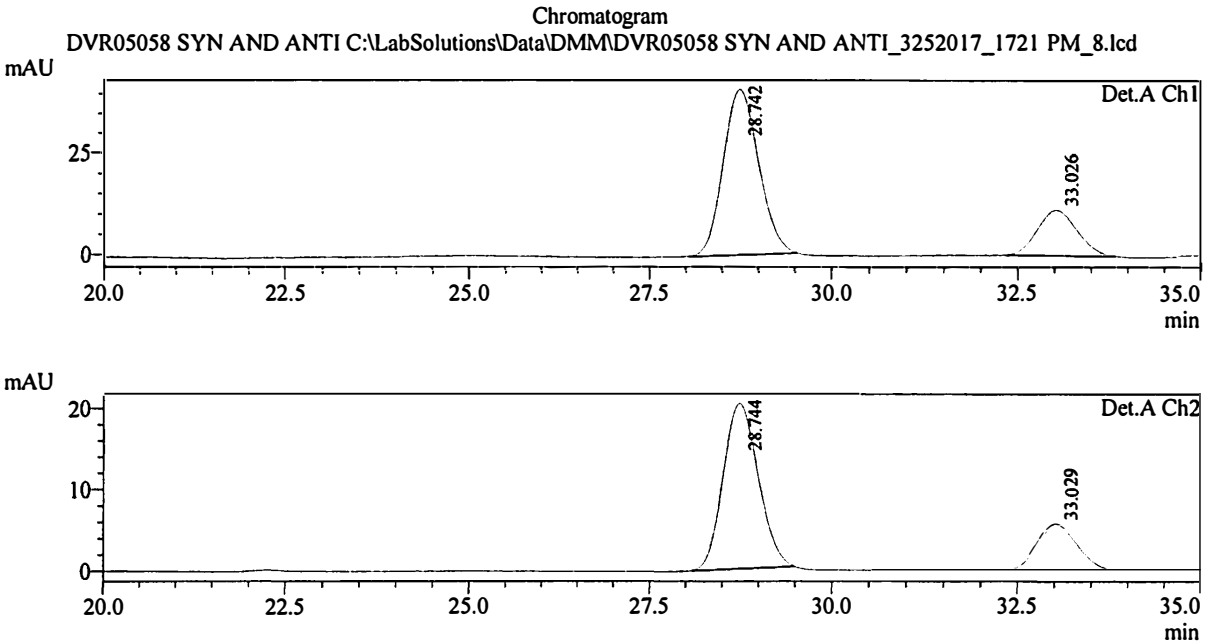

1 Det.A Ch1 / 210nm
2 Det.A Ch2 / 220nm

PeakTable

Detector A Ch1 210nm

Peak#	Ret. Time	Area	Height	Area %	Height %
1	28.742	1395448	41405	76.647	78.632
2	33.026	425178	11252	23.353	21.368
Total		1820626	52656	100.000	100.000

PeakTable

Detector A Ch2 220nm

Peak#	Ret. Time	Area	Height	Area %	Height %
1	28.744	681645	20378	75.992	78.385
2	33.029	215346	5619	24.008	21.615
Total		896991	25998	100.000	100.000

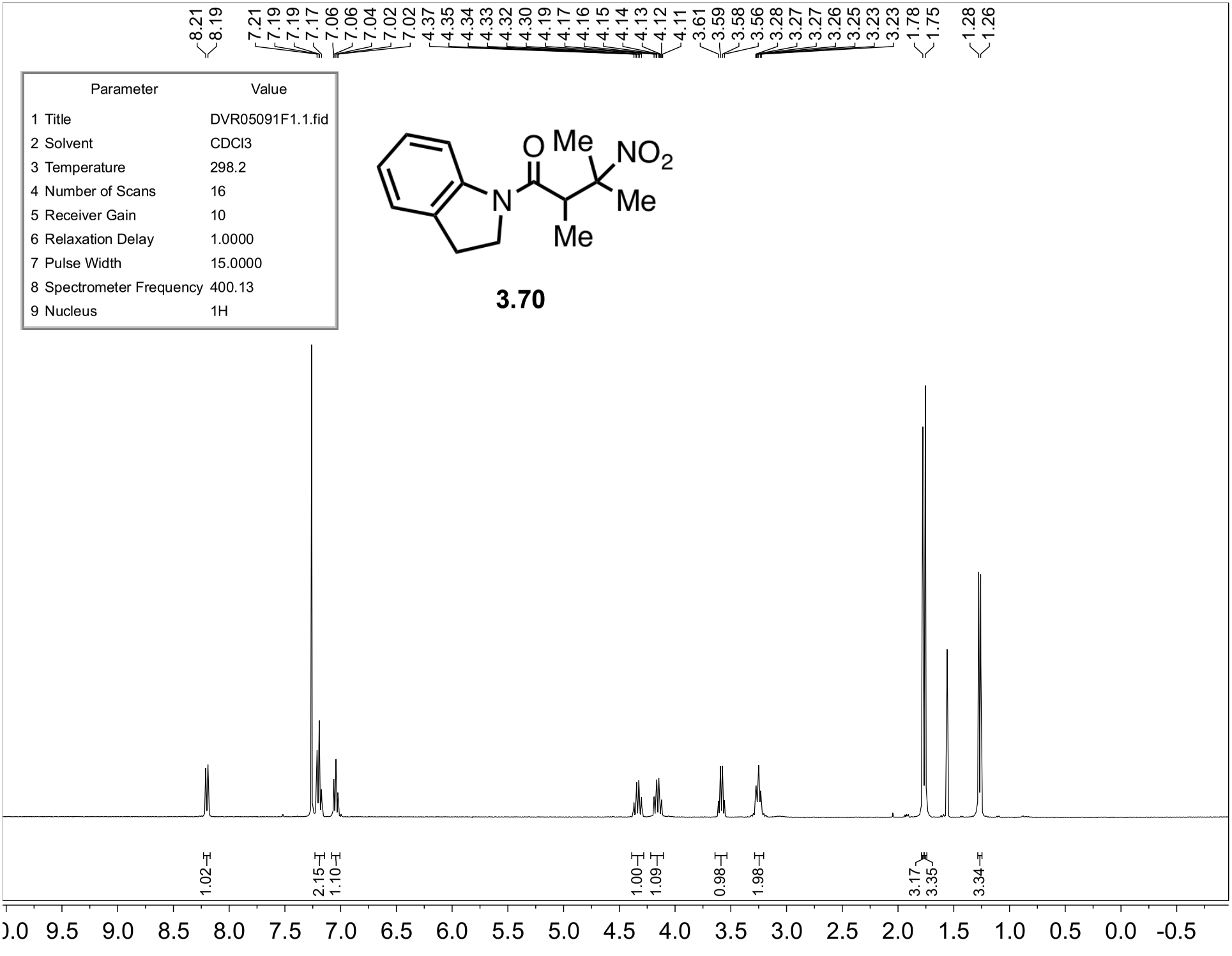
8.21
8.19
7.21
7.19
7.19
7.17
7.06
7.06
7.04
7.02
7.02
4.37
4.35
4.34
4.33
4.32
4.30
4.19
4.17
4.16
4.15
4.14
4.13
4.12
4.11
3.61
3.59
3.58
3.56
3.28
3.27
3.27
3.26
3.25
3.23
3.23
1.78
1.75
1.28
1.26
Parameter Value
1 Title DVR05091F1.1.fid
2 Solvent CDCl3
3 Temperature 298.2
4 Number of Scans 16
5 Receiver Gain 10
6 Relaxation Delay 1.0000
7 Pulse Width 15.0000
8 Spectrometer Frequency 400.13
9 Nucleus 1H
O
Me
NO2
N
Me
Me
3.70
1.02
2.15
1.10
1.00
1.09
0.98
1.98
3.17
3.35
3.34
0.0 9.5 9.0 8.5 8.0 7.5 7.0 6.5 6.0 5.5 5.0 4.5 4.0 3.5 3.0 2.5 2.0 1.5 1.0 0.5 0.0 -0.5

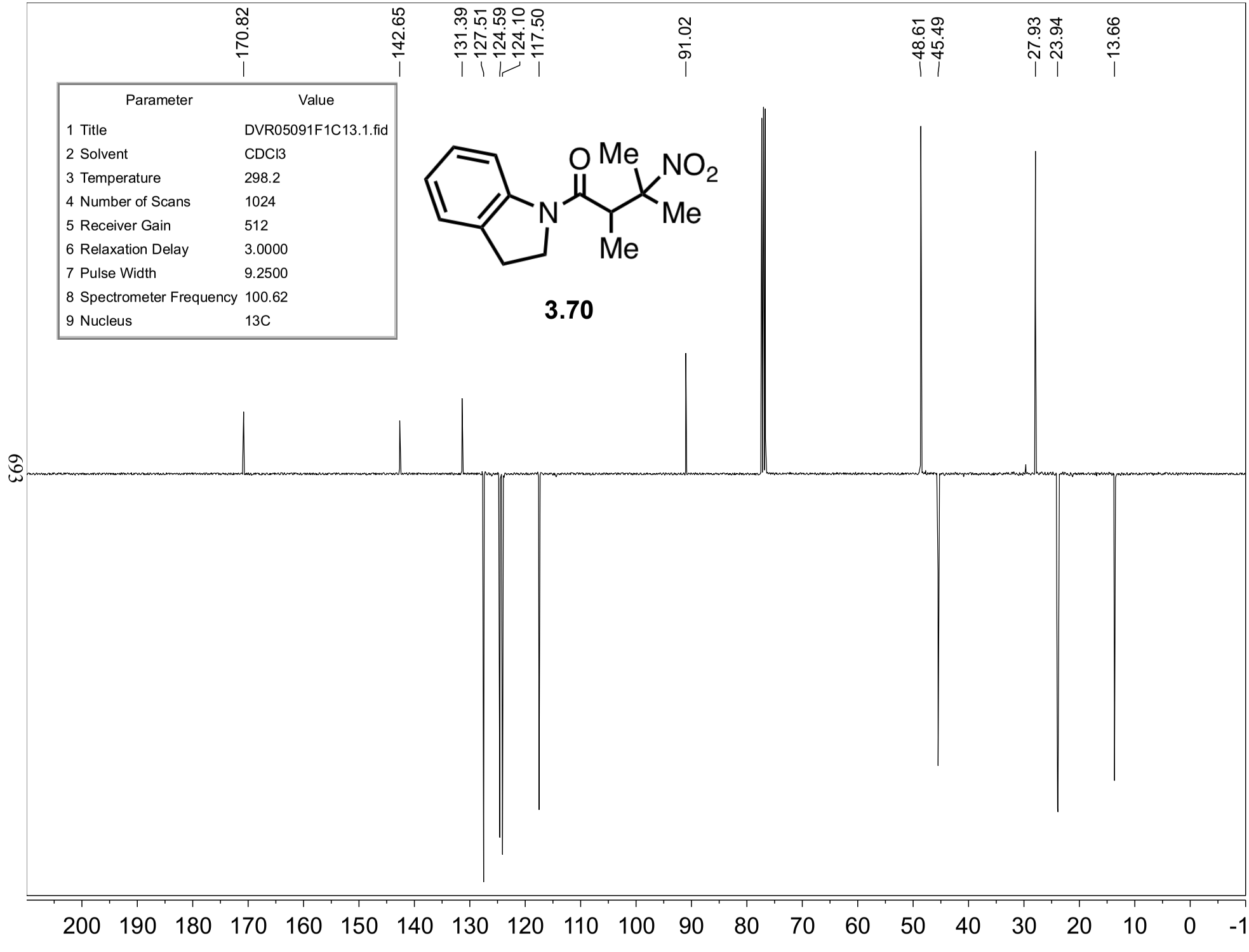
170.82
142.65
131.39
127.51
124.59
124.10
117.50
91.02
48.61
45.49
27.93
23.94
13.66
Parameter Value
1 Title DVR05091F1C13.1.fid
2 Solvent CDCl3
3 Temperature 298.2
4 Number of Scans 1024
5 Receiver Gain 512
6 Relaxation Delay 3.0000
7 Pulse Width 9.2500
8 Spectrometer Frequency 100.62
9 Nucleus 13C
O
Me
NO2
N
Me
Me
3.70
693
200 190 180 170 160 150 140 130 120 110 100 90 80 70 60 50 40 30 20 10 0 -1

==== Shimadzu LCsolution Analysis Report ====

C:\LabSolutions\Data\DMM\DVR05091 rac_6162017_2153 PM_2.lcd

Acquired by	: LC User
Sample Name	: DVR05091 rac
Sample ID	: DVR05091 rac
Tray#	: 1
Vail #	: 1
Injection Volume	: 3 uL
Data File Name	: DVR05091 rac_6162017_2153 PM_2.lcd
Method File Name	: col1_1isoiPA_30min_1ML_220and210.lcm
Batch File Name	: DMM.lcb
Report File Name	: Default.lcr
Data Acquired	: 6/16/2017 10:08:59 PM
Data Processed	: 6/16/2017 10:39:00 PM

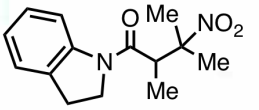

3.70
racemic

(±)

<Chromatogram>

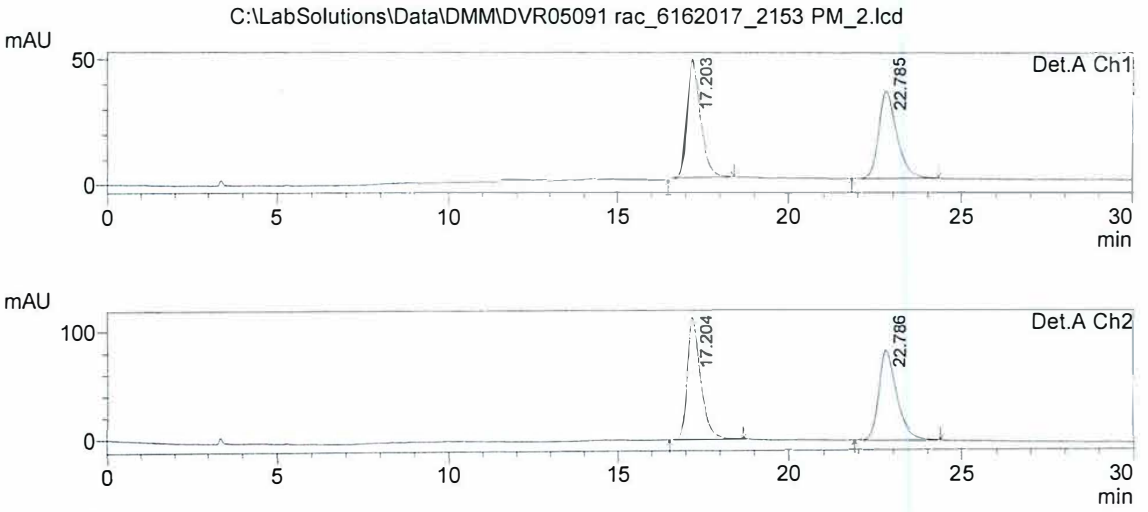

1 Det.A Ch1/220nm
2 Det.A Ch2/210nm

PeakTable

Detector A Ch1 220nm

Peak#	Ret. Time	Area	Height	Area %	Height %
1	17.203	1278229	47202	50.021	57.413
2	22.785	1277175	35013	49.979	42.587
Total		2555404	82214	100.000	100.000

PeakTable

Detector A Ch2 210nm

Peak#	Ret. Time	Area	Height	Area %	Height %
1	17.204	3112654	114185	50.327	57.542
2	22.786	3072236	84254	49.673	42.458
Total		6184890	198439	100.000	100.000

==== Shimądzu LCsolution Analysis Report ====

C:\LabSolutions\Data\DMM\DVR05091 _6162017_2153 PM_6.lcd

Acquired by	: LC User
Sample Name	: DVR05091
Sample ID	: DVR05091
Tray#	: 1
Vail #	: 2
Injection Volume	: 3 uL
Data File Name	: DVR05091 _6162017_2153 PM_6.lcd
Method File Name	: col1_1isoiPA_30min_1ML_220and210.lcm
Batch File Name	: DMM.lcb
Report File Name	: Default.lcr
Data Acquired	: 6/16/2017 11:04:57 PM
Data Processed	: 6/16/2017 11:35:00 PM

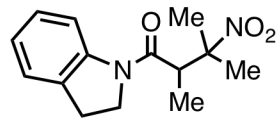

3.70
61% ee

<Chromatogram>

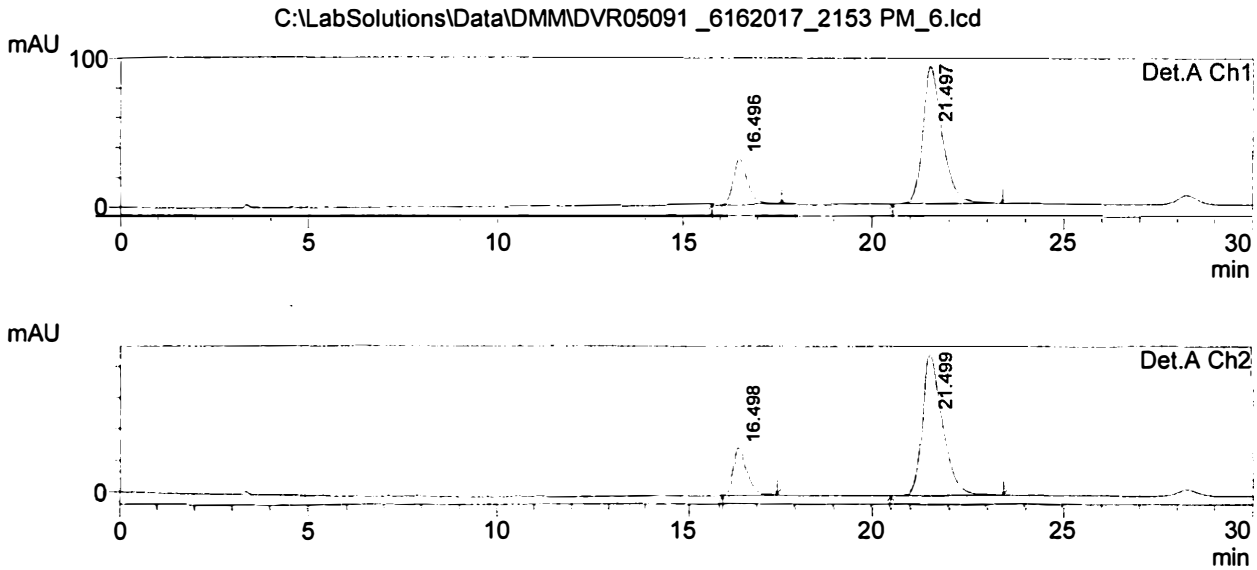

1 Det.A Ch1/220nm
2 Det.A Ch2/210nm

PeakTable

Detector A Ch1 220nm

Peak#	Ret. Time	Area	Height	Area %	Height %
1	16.496	783513	30863	19.410	25.034
2	21.497	3253029	92425	80.590	74.966
Total		4036541	123288	100.000	100.000

PeakTable

Detector A Ch2 210nm

Peak#	Ret. Time	Area	Height	Area %	Height %
1	16.498	1856427	73951	19.108	24.742
2	21.499	7859066	224938	80.892	75.258
Total		9715493	298889	100.000	100.000

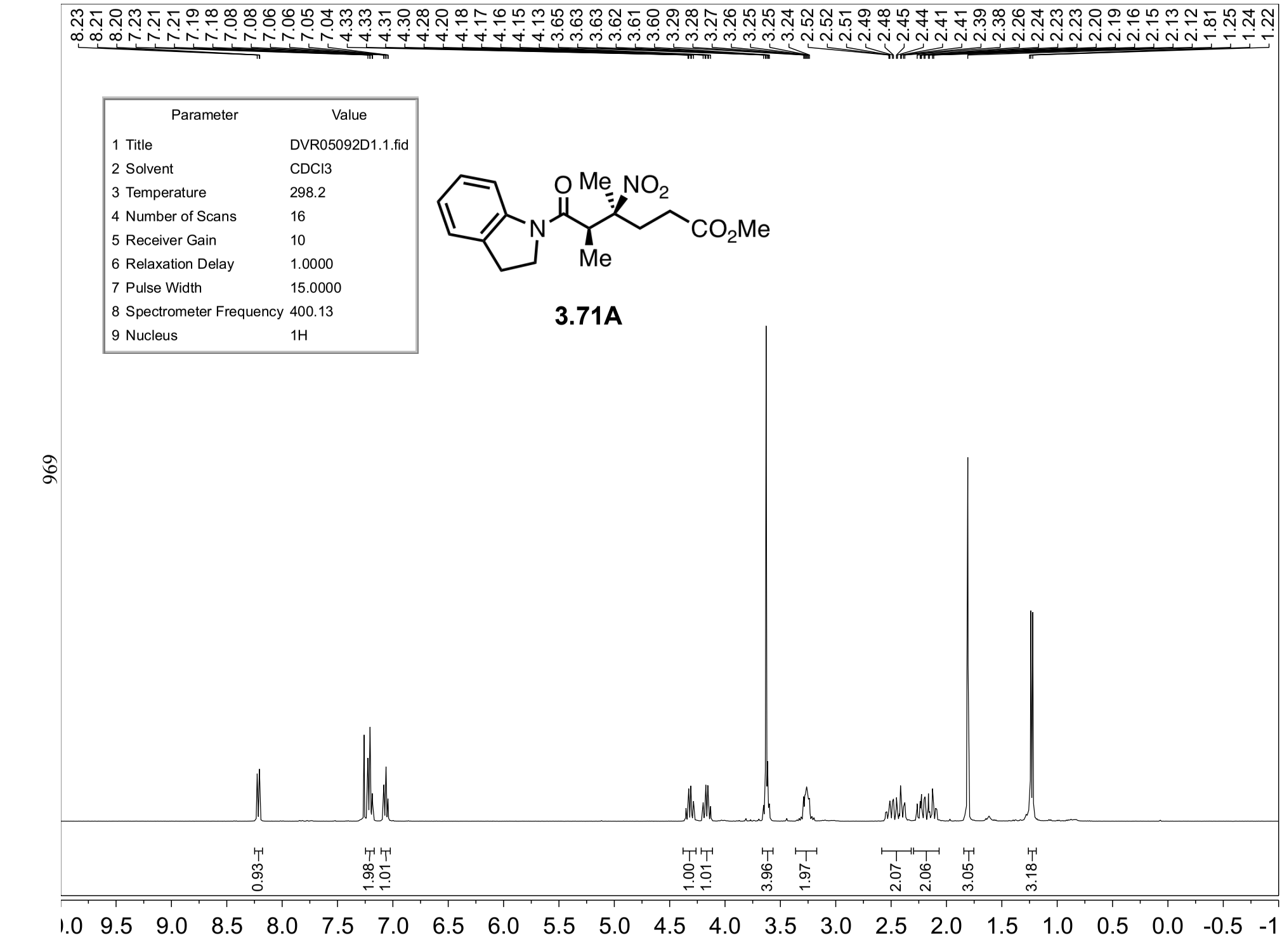
8.23 8.21 8.20 7.23 7.21 7.21 7.19 7.18 7.08 7.08 7.06 7.06 7.05 7.04 4.33 4.33 4.31 4.30 4.28 4.20 4.18 4.17 4.16 4.15 4.13 3.65 3.63 3.63 3.62 3.61 3.60 3.29 3.28 3.27 3.26 3.25 3.25 3.24 2.52 2.52 2.51 2.49 2.48 2.45 2.44 2.41 2.41 2.39 2.38 2.26 2.24 2.23 2.23 2.20 2.19 2.16 2.15 2.13 2.12 1.81 1.25 1.24 1.22
Parameter Value
1 Title DVR05092D1.1.fid
2 Solvent CDCl3
3 Temperature 298.2
4 Number of Scans 16
5 Receiver Gain 10
6 Relaxation Delay 1.0000
7 Pulse Width 15.0000
8 Spectrometer Frequency 400.13
9 Nucleus 1H
O Me NO2
N
CO2Me
Me
3.71A
969
0.93 1.98 1.01 1.00 1.01 3.96 1.97 2.07 2.06 3.05 3.18
.0 9.5 9.0 8.5 8.0 7.5 7.0 6.5 6.0 5.5 5.0 4.5 4.0 3.5 3.0 2.5 2.0 1.5 1.0 0.5 0.0 -0.5 -1

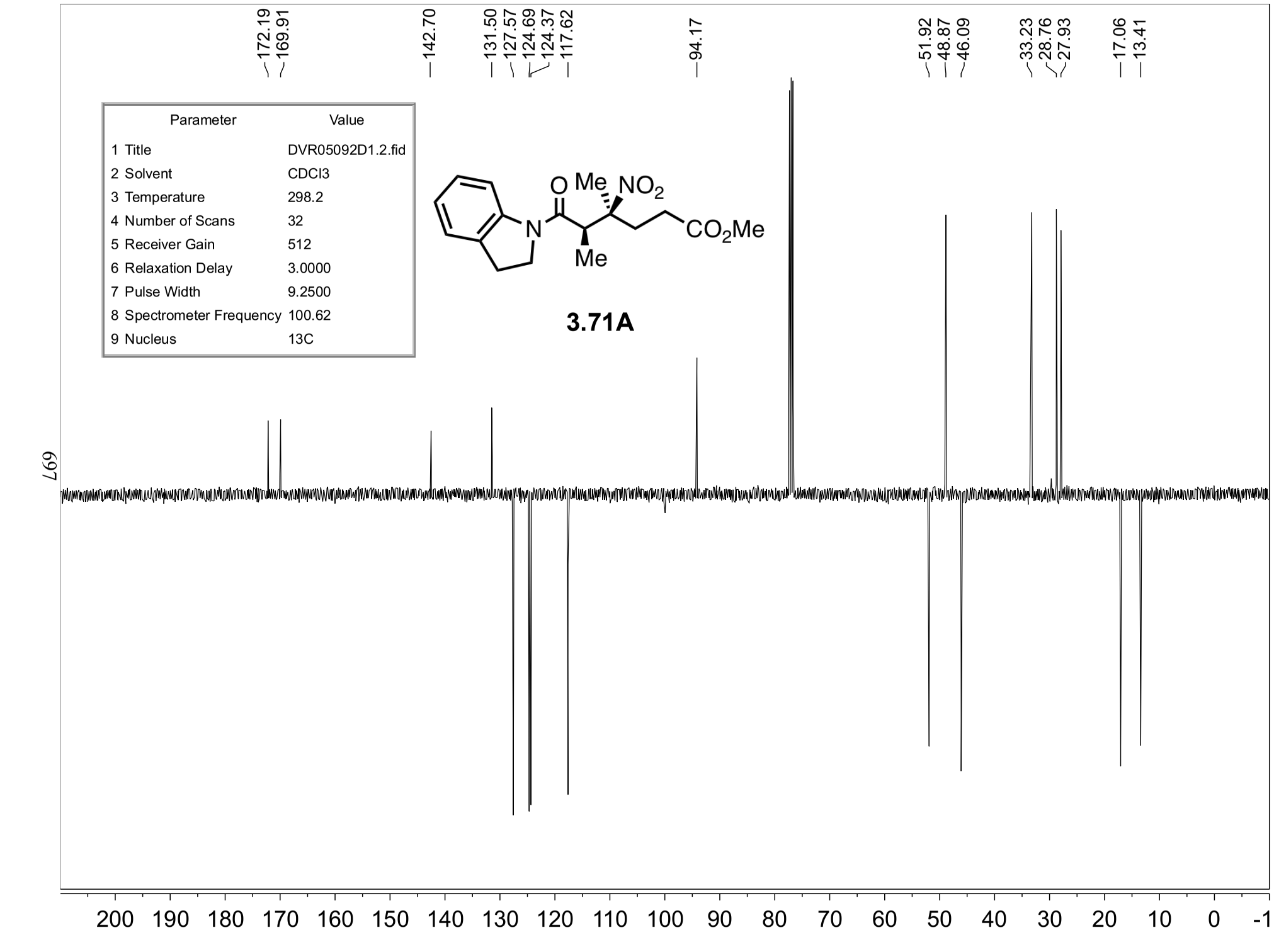
172.19
169.91
142.70
131.50
127.57
124.69
124.37
117.62
94.17
51.92
48.87
46.09
33.23
28.76
27.93
17.06
13.41
Parameter Value
1 Title DVR05092D1.2.fid
2 Solvent CDCl3
3 Temperature 298.2
4 Number of Scans 32
5 Receiver Gain 512
6 Relaxation Delay 3.0000
7 Pulse Width 9.2500
8 Spectrometer Frequency 100.62
9 Nucleus 13C
O
Me
NO2
N
CO2Me
Me
3.71A
697
200 190 180 170 160 150 140 130 120 110 100 90 80 70 60 50 40 30 20 10 0 -1

Parameter	Value
1 Title	DVR05092D2-a.1.fid
2 Solvent	CDCl3
3 Temperature	300.0
4 Number of Scans	16
5 Receiver Gain	144
6 Relaxation Delay	1.0000
7 Pulse Width	10.7300
8 Spectrometer Frequency	600.32
9 Nucleus	1H

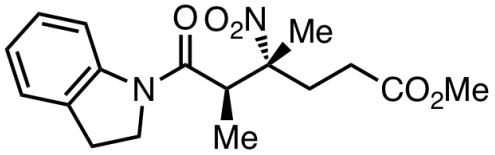

3.71B

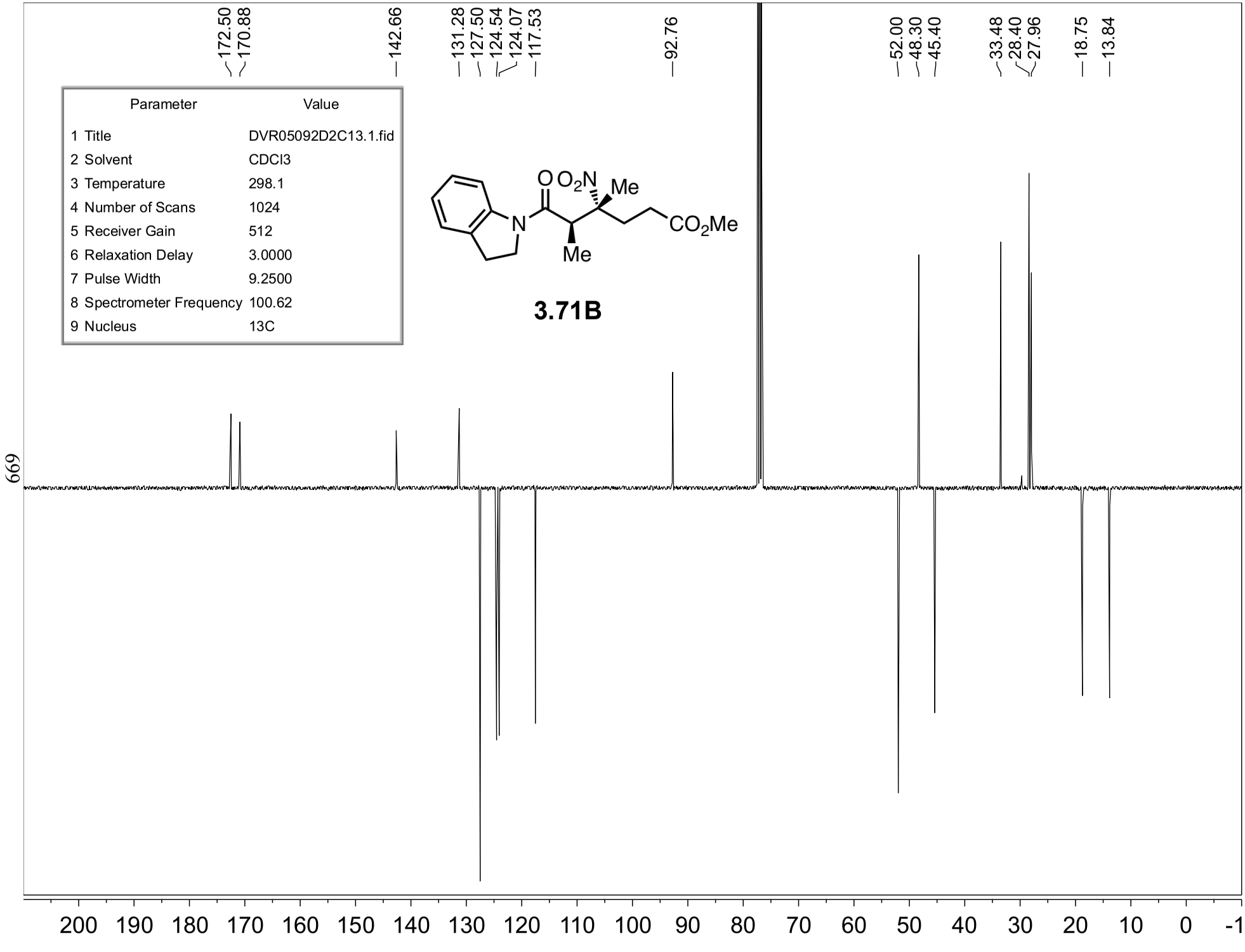
172.50
170.88
142.66
131.28
127.50
124.54
124.07
117.53
92.76
52.00
48.30
45.40
33.48
28.40
27.96
18.75
13.84
Parameter Value
1 Title DVR05092D2C13.1.fid
2 Solvent CDCl3
3 Temperature 298.1
4 Number of Scans 1024
5 Receiver Gain 512
6 Relaxation Delay 3.0000
7 Pulse Width 9.2500
8 Spectrometer Frequency 100.62
9 Nucleus 13C
O
O2N
Me
N
CO2Me
Me
3.71B
669
200 190 180 170 160 150 140 130 120 110 100 90 80 70 60 50 40 30 20 10 0 -1

==== Shimadzu LCsolution Analysis Report ====

C:\LabSolutions\Data\DMM\DVR05092 D2 RAC_6172017_1946 PM_6.lcd

Acquired by	: LC User
Sample Name	: DVR05092 D2 RAC
Sample ID	: DVR05092 D2 RAC
Tray#	: 1
Vail #	: 5
Injection Volume	: 4 uL
Data File Name	: DVR05092 D2 RAC_6172017_1946 PM_6.lcd
Method File Name	: col1_3isoiPA_30min_1ML_254and210.lcm
Batch File Name	: DMM.lcb
Report File Name	: Default.lcr
Data Acquired	: 6/17/2017 10:18:16 PM
Data Processed	: 6/17/2017 10:48:18 PM

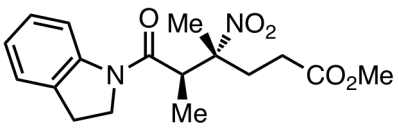

3.71B
racemic

<Chromatogram>

C:\LabSolutions\Data\DMM\DVR05092 D2 RAC_6172017_1946 PM_6.lcd

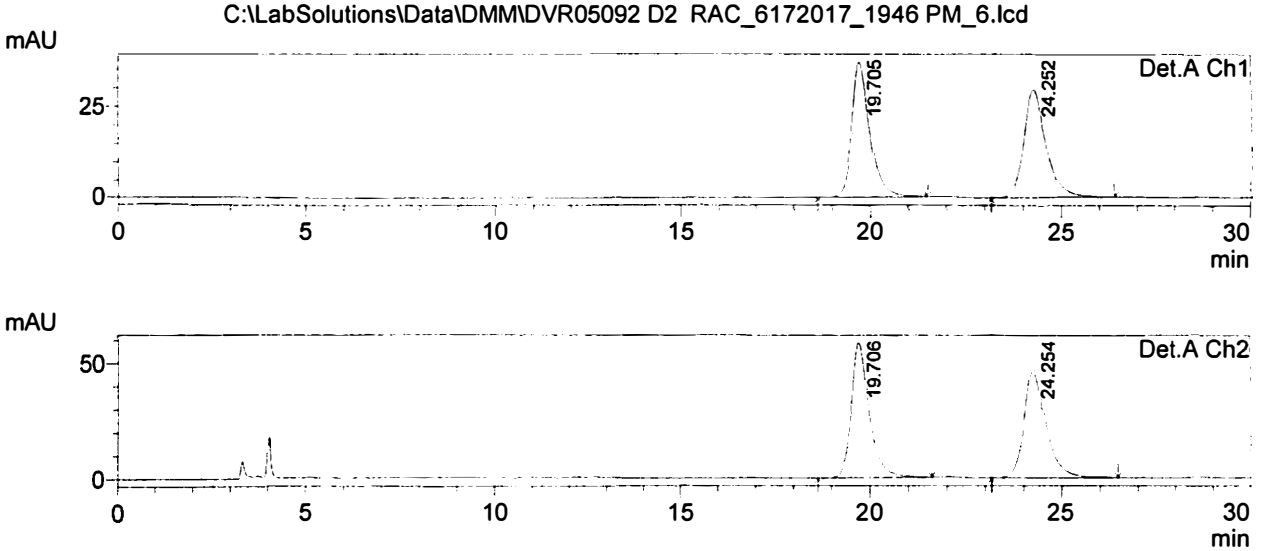

1 Det.A Ch1/254nm
2 Det.A Ch2/210nm

PeakTable

Detector A Ch1 254nm

Peak#	Ret. Time	Area	Height	Area %	Height %
1	19.705	1217550	37219	50.784	55.753
2	24.252	1179977	29538	49.216	44.247
Total		2397527	66757	100.000	100.000

PeakTable

Detector A Ch2 210nm

Peak#	Ret. Time	Area	Height	Area %	Height %
1	19.706	1915901	58821	50.545	55.668
2	24.254	1874552	46844	49.455	44.332
Total		3790453	105665	100.000	100.000

==== Shimadzu LCsolution Analysis Report ====

C:\LabSolutions\Data\DMM\DVR05092 D2_6172017_1946 PM_8.lcd

Acquired by	: LC User
Sample Name	: DVR05092 D2
Sample ID	: DVR05092 D2
Tray#	: 1
Vail #	: 6
Injection Volume	: 4 uL
Data File Name	: DVR05092 D2_6172017_1946 PM_8.lcd
Method File Name	: col1_3isoiPA_30min_1ML_254and210.lcm
Batch File Name	: DMM.lcb
Report File Name	: Default.lcr
Data Acquired	: 6/17/2017 11:18:57 PM
Data Processed	: 6/17/2017 11:49:00 PM

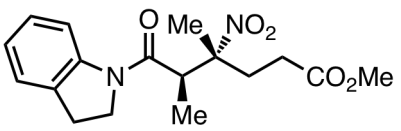

3.71B
48% ee

<Chromatogram>

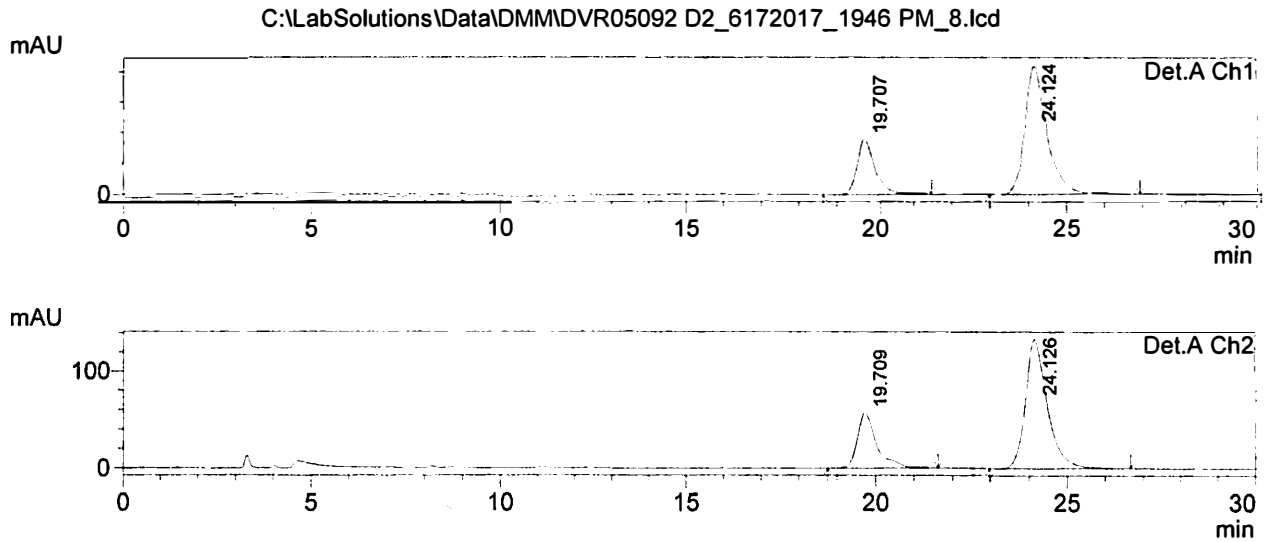

1 Det.A Ch1/254nm
2 Det.A Ch2/210nm

PeakTable

Detector A Ch1 254nm

Peak#	Ret. Time	Area	Height	Area %	Height %
1	19.707	1160996	35980	25.661	29.905
2	24.124	3363385	84334	74.339	70.095
Total		4524381	120314	100.000	100.000

PeakTable

Detector A Ch2 210nm

Peak#	Ret. Time	Area	Height	Area %	Height %
1	19.709	1989404	57153	27.205	29.959
2	24.126	5323123	133617	72.795	70.041
Total		7312526	190771	100.000	100.000

==== Shimadzu LCsolution Analysis Report ====

C:\LabSolutions\Data\DMM\DVR05092 D1 RAC_6172017_1946 PM_2.lcd

Acquired by	: LC User
Sample Name	: DVR05092 D1 RAC
Sample ID	: DVR05092 D1 RAC
Tray#	: 1
Vail #	: 3
Injection Volume	: 4 uL
Data File Name	: DVR05092 D1 RAC_6172017_1946 PM_2.lcd
Method File Name	: col1_3isoiPA_30min_1ML_254and210.lcm
Batch File Name	: DMM.lcb
Report File Name	: Default.lcr
Data Acquired	: 6/17/2017 8:16:52 PM
Data Processed	: 6/17/2017 8:46:53 PM

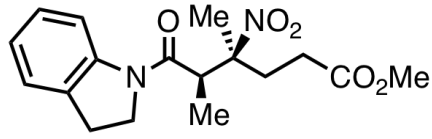

3.71A
racemic

<Chromatogram>

C:\LabSolutions\Data\DMM\DVR05092 D1 RAC_6172017_1946 PM_2.lcd

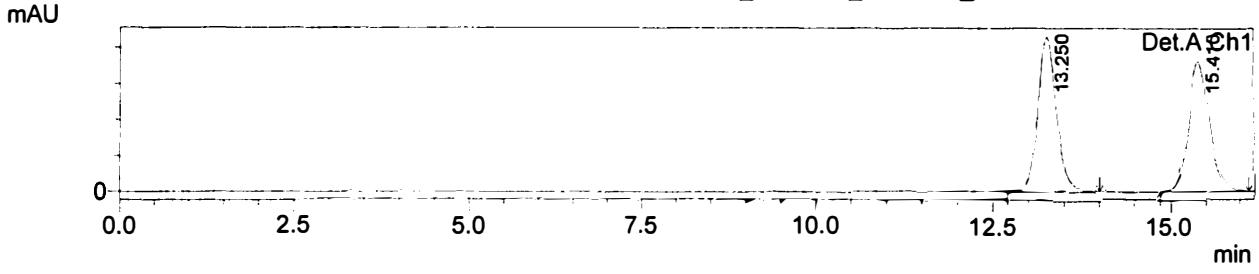

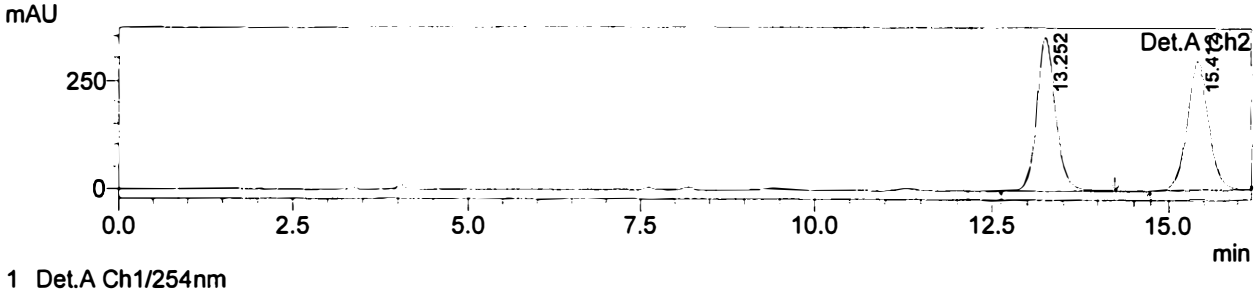

1 Det.A Ch1/254nm
2 Det.A Ch2/210nm

PeakTable

Detector A Ch1 254nm

Peak#	Ret. Time	Area	Height	Area %	Height %
1	13.250	3931393	214397	50.191	54.162
2	15.410	3901537	181450	49.809	45.838
Total		7832930	395847	100.000	100.000

PeakTable

Detector A Ch2 210nm

Peak#	Ret. Time	Area	Height	Area %	Height %
1	13.252	6496471	351300	50.419	54.184
2	15.412	6388544	297041	49.581	45.816
Total		12885016	648342	100.000	100.000

==== Shimadzu LCsolution Analysis Report ====

C:\LabSolutions\Data\DMM\DVR05092 D1 _6172017_1946 PM_4.lcd

Acquired by	: LC User
Sample Name	: DVR05092 D1
Sample ID	: DVR05092 D1
Tray#	: 1
Vail #	: 4
Injection Volume	: 4 uL
Data File Name	: DVR05092 D1 _6172017_1946 PM_4.lcd
Method File Name	: col1_3isoiPA_30min_1ML_254and210.lcm
Batch File Name	: DMM.lcb
Report File Name	: Default.lcr
Data Acquired	: 6/17/2017 9:17:33 PM
Data Processed	: 6/18/2017 8:32:15 PM

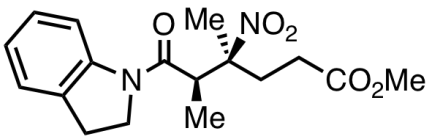

3.71A
67% ee

<Chromatogram>

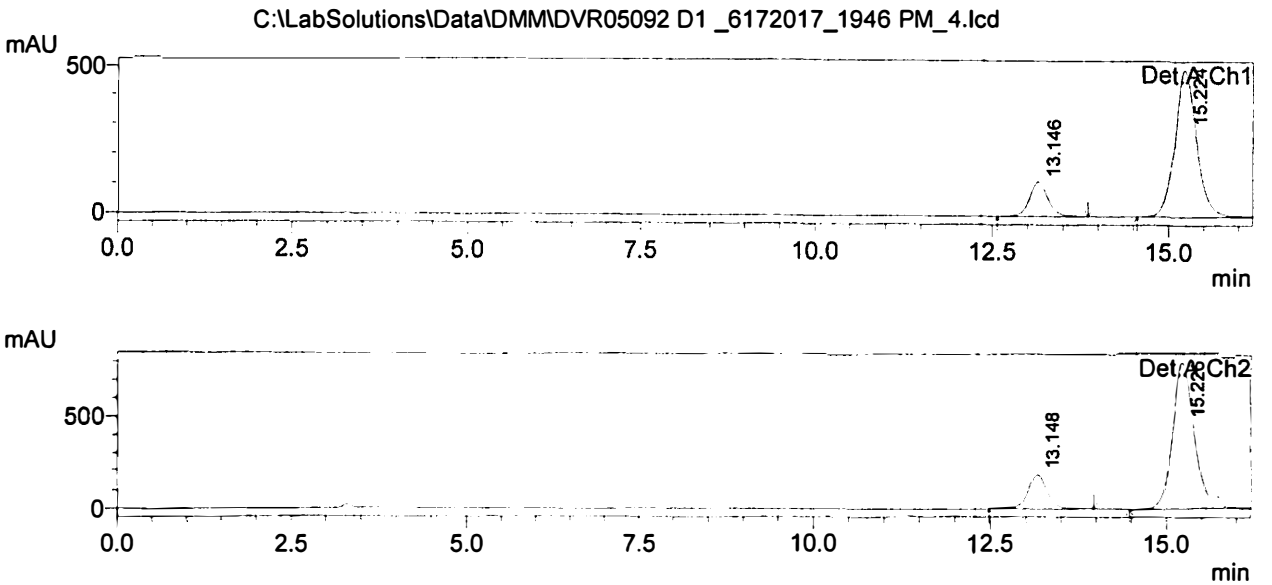

1 Det.A Ch1/254nm
2 Det.A Ch2/210nm

PeakTable

Detector A Ch1 254nm

Peak#	Ret. Time	Area	Height	Area %	Height %
1	13.146	2098119	115398	16.430	18.876
2	15.224	10672153	495958	83.570	81.124
Total		12770272	611356	100.000	100.000

PeakTable

Detector A Ch2 210nm

Peak#	Ret. Time	Area	Height	Area %	Height %
1	13.148	3449008	189265	16.599	19.176
2	15.226	17329891	797699	83.401	80.824
Total		20778900	986964	100.000	100.000

Parameter	Value
1 Title	DVR04232D2.1.fid
2 Solvent	CDCl3
3 Temperature	297.2
4 Number of Scans	16
5 Receiver Gain	228
6 Relaxation Delay	1.0000
7 Pulse Width	10.7700
8 Spectrometer Frequency	600.32
9 Nucleus	1H

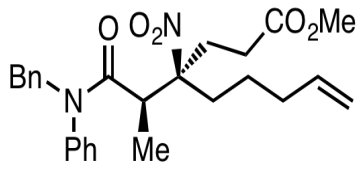

3.72

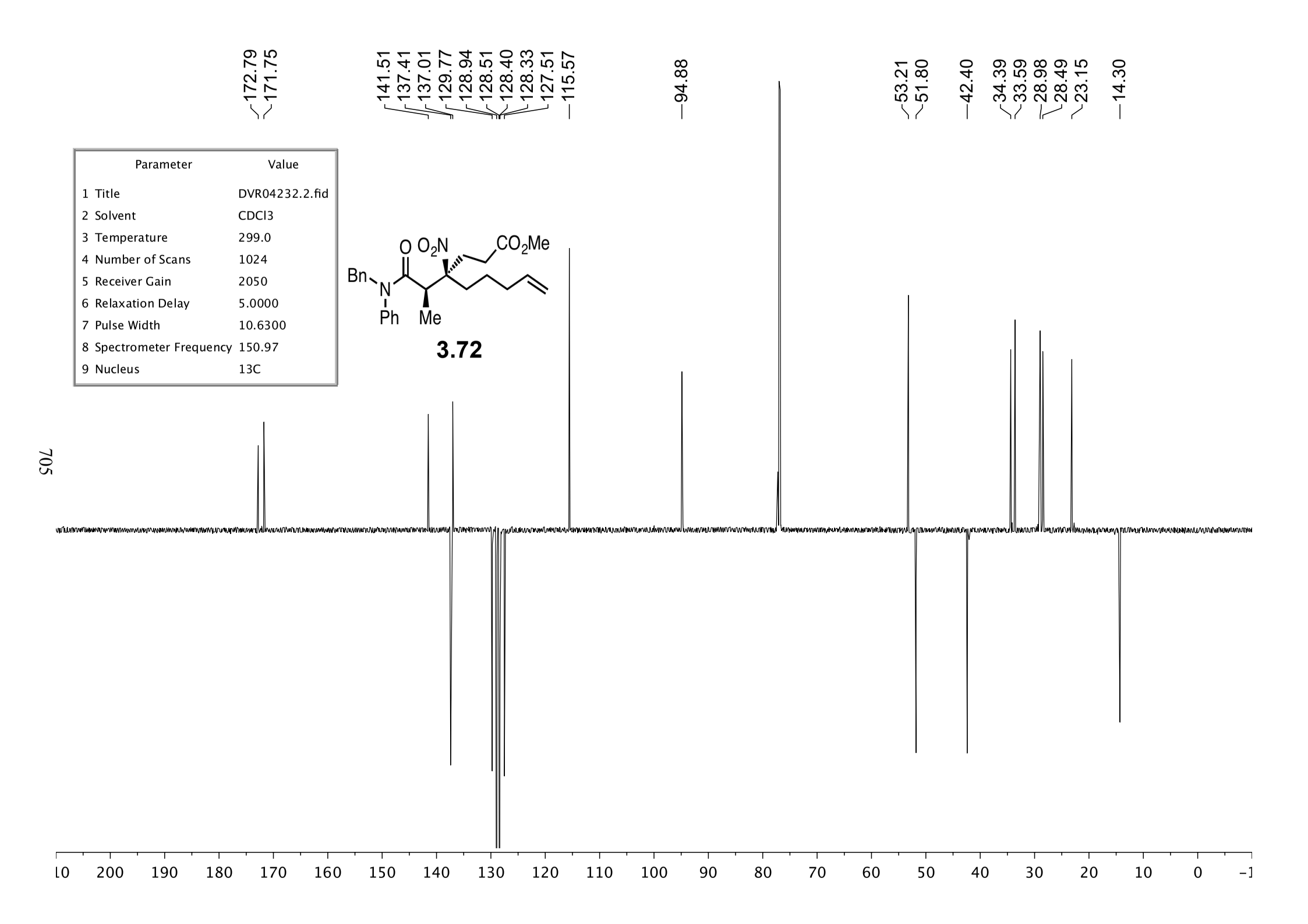
172.79
171.75
141.51
137.41
137.01
129.77
128.94
128.51
128.40
128.33
127.51
115.57
94.88
53.21
51.80
42.40
34.39
33.59
28.98
28.49
23.15
14.30
Parameter Value
1 Title DVR04232.2.fid
2 Solvent CDCl3
3 Temperature 299.0
4 Number of Scans 1024
5 Receiver Gain 2050
6 Relaxation Delay 5.0000
7 Pulse Width 10.6300
8 Spectrometer Frequency 150.97
9 Nucleus 13C
O O2N
CO2Me
Bn
N
Ph
Me
3.72
705
200
190
180
170
160
150
140
130
120
110
100
90
80
70
60
50
40
30
20
10
0

==== Shimadzu LCsolution Analysis Report ====

C:\LabSolutions\Data\DMM\DVR04232 rac 1_10272016_853 AM_2.lcd

Acquired by	: LC User
Sample Name	: DVR04232 rac 1
Sample ID	: DVR04232 rac 1
Tray#	: 1
Vail #	: 2
Injection Volume	: 2 uL
Data File Name	: DVR04232 rac 1_10272016_853 AM_2.lcd
Method File Name	: col6_3isoiPA_36min_1ML_220and210.lcm
Batch File Name	: DMM.lcb
Report File Name	: Default.lcr
Data Acquired	: 10/27/2016 9:29:51 AM
Data Processed	: 10/27/2016 10:05:55 AM

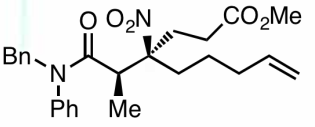

3.72
racemic

<Chromatogram>

C:\LabSolutions\Data\DMM\DVR04232 rac 1_10272016_853 AM_2.lcd

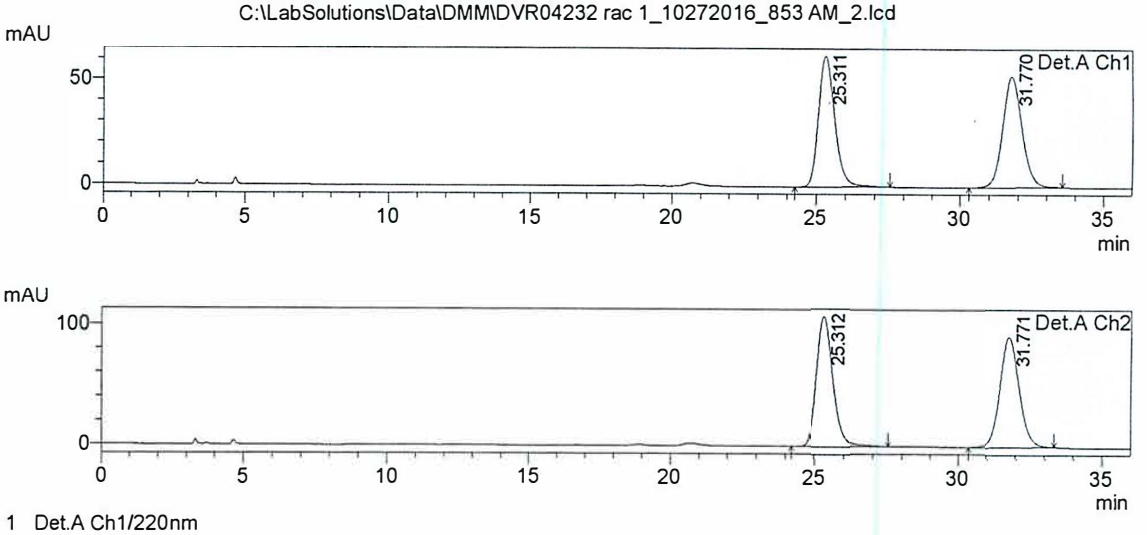

1 Det.A Ch1/220nm
2 Det.A Ch2/210nm

PeakTable

Detector A Ch1 220nm

Peak#	Ret. Time	Area	Height	Area %	Height %
1	25.311	2423234	62422	49.620	54.151
2	31.770	2460372	52853	50.380	45.849
Total		4883607	115274	100.000	100.000

PeakTable

Detector A Ch2 210nm

Peak#	Ret. Time	Area	Height	Area %	Height %
1	25.312	4202740	108032	49.810	54.197
2	31.771	4234796	91299	50.190	45.803
Total		8437535	199331	100.000	100.000

==== Shimadzu LCsolution Analysis Report ====

C:\LabSolutions\Data\DMM\DVR04232 R1_10272016_853 AM_6.lcd

Acquired by	: LC User
Sample Name	: DVR04232 R1
Sample ID	: DVR04232 R1
Tray#	: 1
Vail #	: 3
Injection Volume	: 2 uL
Data File Name	: DVR04232 R1_10272016_853 AM_6.lcd
Method File Name	: col6_3isoiPA_36min_1ML_220and210.lcm
Batch File Name	: DMM.lcb
Report File Name	: Default.lcr
Data Acquired	: 10/27/2016 10:52:50 AM
Data Processed	: 10/27/2016 11:28:52 AM

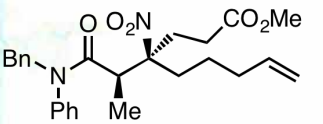

3.72
91% ee

<Chromatogram>

C:\LabSolutions\Data\DMM\DVR04232 R1_10272016_853 AM_6.lcd

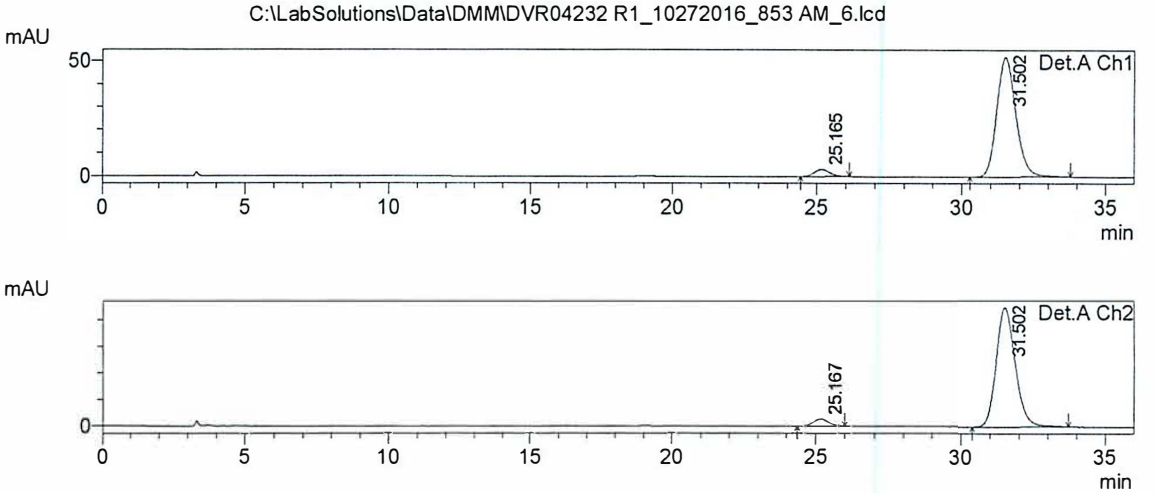

1 Det.A Ch1/220nm
2 Det.A Ch2/210nm

PeakTable

Detector A Ch1 220nm

Peak#	Ret. Time	Area	Height	Area %	Height %
1	25.165	113659	3031	4.515	5.504
2	31.502	2403724	52035	95.485	94.496
Total		2517382	55067	100.000	100.000

PeakTable

Detector A Ch2 210nm

Peak#	Ret. Time	Area	Height	Area %	Height %
1	25.167	199572	5343	4.590	5.606
2	31.502	4148749	89962	95.410	94.394
Total		4348320	95305	100.000	100.000

==== Shimadzu LCsolution Analysis Report ====

C:\LabSolutions\Data\DMM\DVR04233 _10272016_853 AM_29.lcd

Acquired by	: LC User
Sample Name	: DVR04233
Sample ID	: DVR04233
Tray#	: 1
Vail #	: 6
Injection Volume	: 2 uL
Data File Name	: DVR04233 _10272016_853 AM_29.lcd
Method File Name	: col6_3isoiPA_36min_1ML_220and210.lcm
Batch File Name	: DMM.lcb
Report File Name	: Default.lcr
Data Acquired	: 10/28/2016 4:14:37 AM
Data Processed	: 10/28/2016 4:50:38 AM

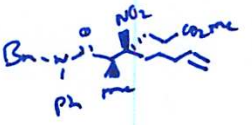

89 % ee

<Chromatogram>

C:\LabSolutions\Data\DMM\DVR04233 _10272016_853 AM_29.lcd

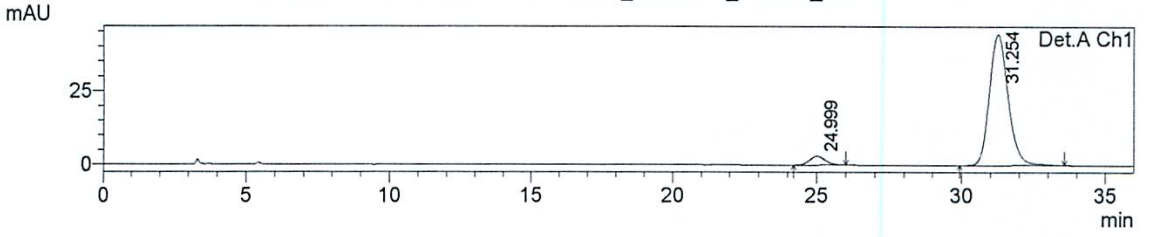

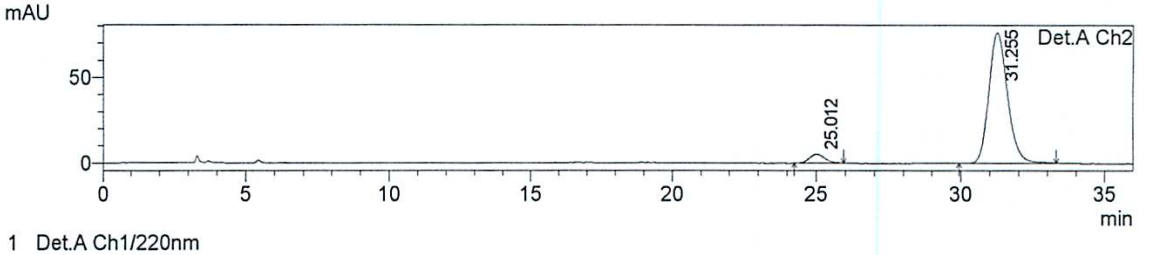

1 Det.A Ch1/220nm
2 Det.A Ch2/210nm

PeakTable

Detector A Ch1 220nm

Peak#	Ret. Time	Area	Height	Area %	Height %
1	24.999	112827	3044	5.315	6.435
2	31.254	2010087	44252	94.685	93.565
Total		2122914	47296	100.000	100.000

PeakTable

Detector A Ch2 210nm

Peak#	Ret. Time	Area	Height	Area %	Height %
1	25.012	191251	5259	5.234	6.440
2	31.255	3462427	76405	94.766	93.560
Total		3653678	81664	100.000	100.000

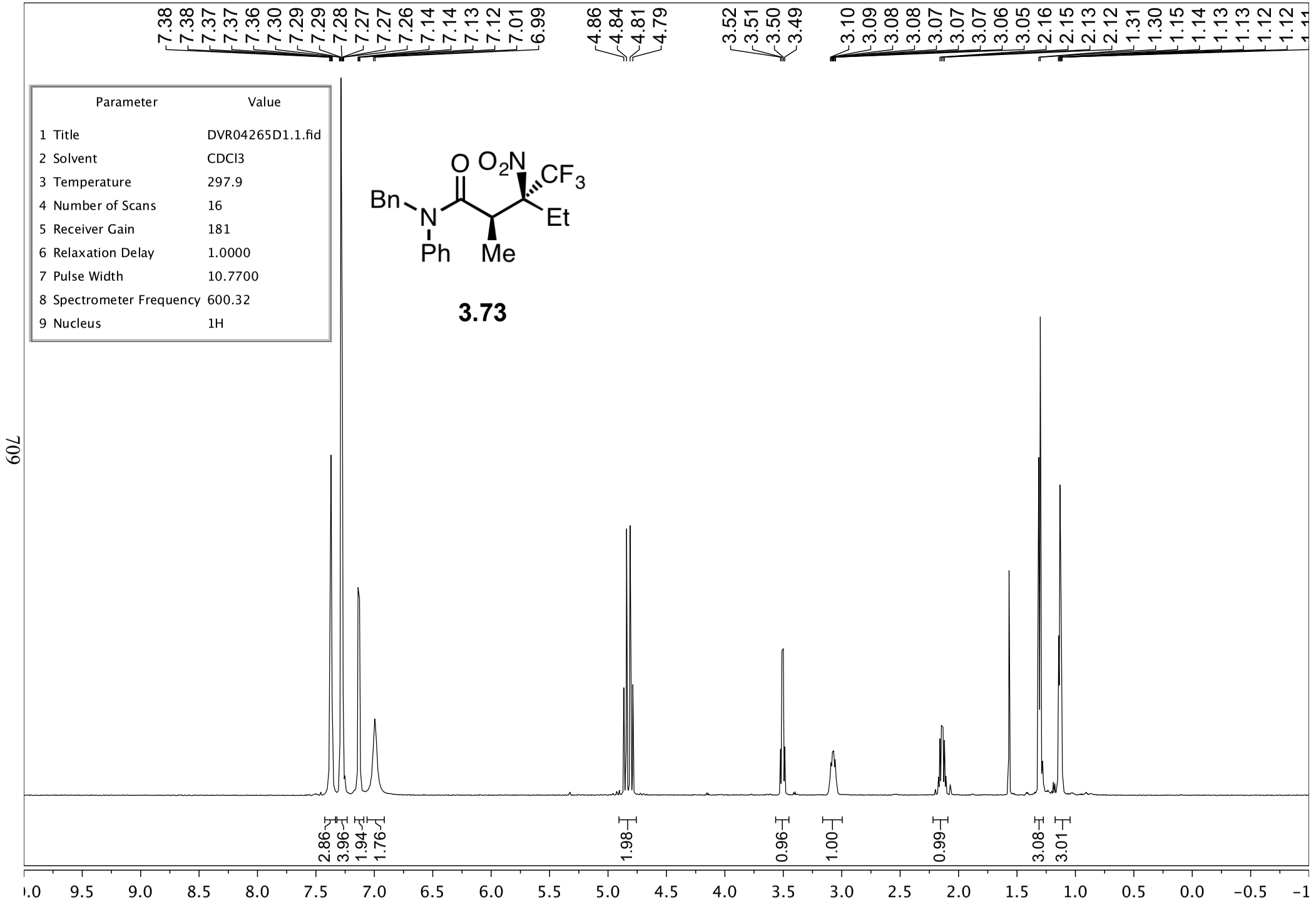
7.38 7.38 7.37 7.37 7.36 7.30 7.29 7.29 7.28 7.27 7.27 7.26 7.14 7.14 7.13 7.12 7.01 6.99
4.86 4.84 4.81 4.79
3.52 3.51 3.50 3.49
3.10 3.09 3.08 3.08 3.07 3.07 3.07 3.06 3.05 2.16 2.15 2.13 2.12 1.31 1.30 1.15 1.14 1.13 1.13 1.12 1.12
Parameter Value
1 Title DVR04265D1.1.fid
2 Solvent CDCl3
3 Temperature 297.9
4 Number of Scans 16
5 Receiver Gain 181
6 Relaxation Delay 1.0000
7 Pulse Width 10.7700
8 Spectrometer Frequency 600.32
9 Nucleus 1H
Bn
N
Ph
O
O2N
CF3
Et
Me
3.73
709
2.86 3.96 1.94 1.76 1.98 0.96 1.00 0.99 3.08 3.01
9.5 9.0 8.5 8.0 7.5 7.0 6.5 6.0 5.5 5.0 4.5 4.0 3.5 3.0 2.5 2.0 1.5 1.0 0.5 0.0 -0.5 -1

Parameter	Value
1 Title	DVR04265D1.2.fid
2 Solvent	CDCl3
3 Temperature	297.9
4 Number of Scans	16
5 Receiver Gain	362
6 Relaxation Delay	3.0000
7 Pulse Width	11.6200
8 Spectrometer Frequency	564.81
9 Nucleus	19F

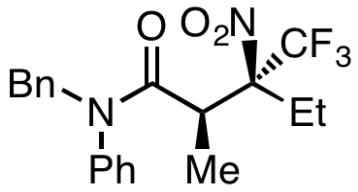

3.73

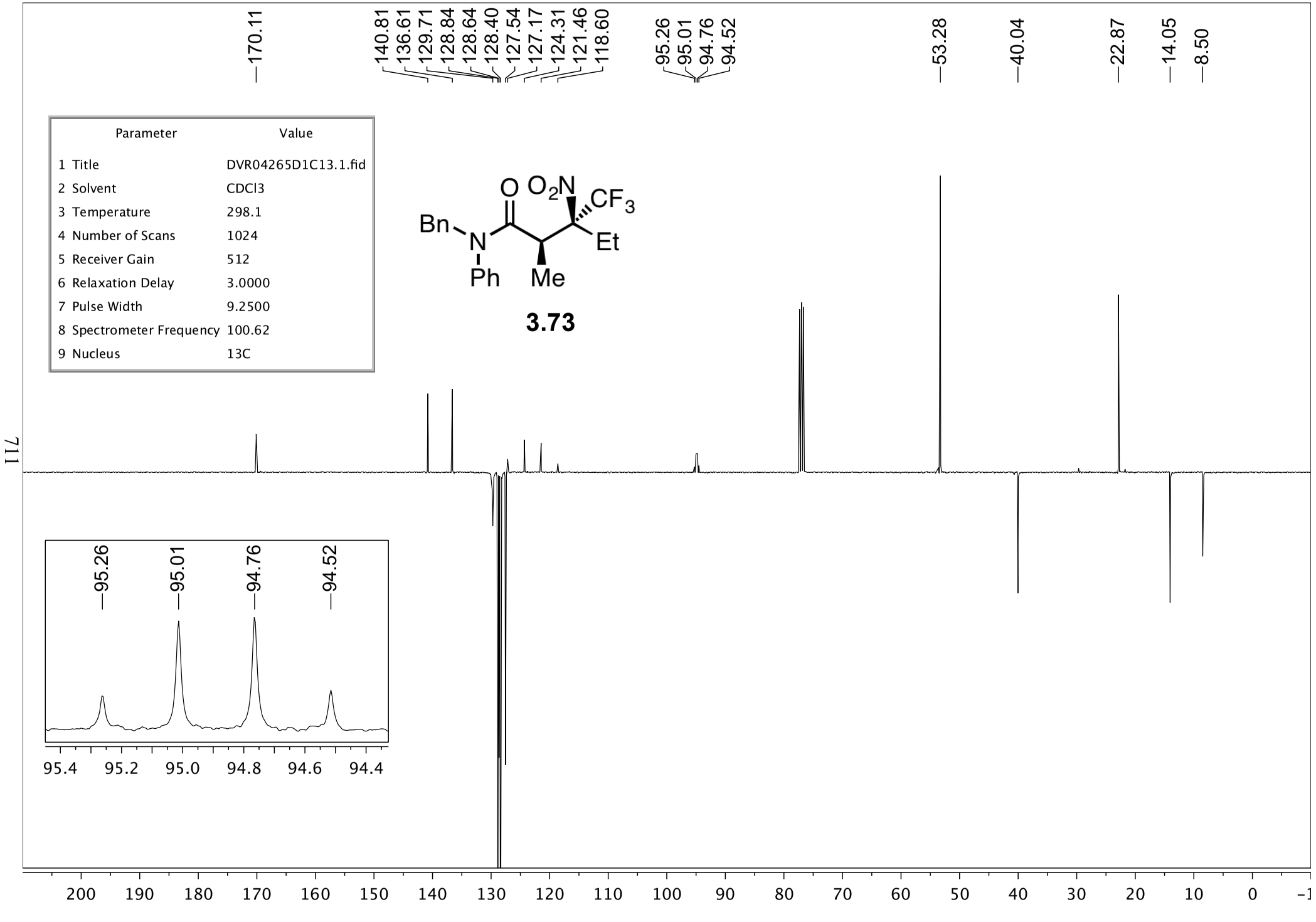
170.11
140.81
136.61
129.71
128.84
128.64
128.40
127.54
127.17
124.31
121.46
118.60
95.26
95.01
94.76
94.52
53.28
40.04
22.87
14.05
8.50
Parameter Value
1 Title DVR04265D1C13.1.fid
2 Solvent CDCl3
3 Temperature 298.1
4 Number of Scans 1024
5 Receiver Gain 512
6 Relaxation Delay 3.0000
7 Pulse Width 9.2500
8 Spectrometer Frequency 100.62
9 Nucleus 13C
Bn
N
Ph
O
O2N
CF3
Et
Me
3.73
711
95.4
95.2
95.0
94.8
94.6
94.4
200
190
180
170
160
150
140
130
120
110
100
90
80
70
60
50
40
30
20
10
0

==== Shimadzu LCsolution Analysis Report ====

C:\LabSolutions\Data\DMM\DVR04264 RAC_11292016_2144 PM_2.lcd

Acquired by	: LC User
Sample Name	: DVR04264 RAC
Sample ID	: DVR04264 RAC
Tray#	: 1
Vail #	: 3
Injection Volume	: 2 uL
Data File Name	: DVR04264 RAC_11292016_2144 PM_2.lcd
Method File Name	: col1_2isoiPA_15min_1ML_254and210.lcm
Batch File Name	: DMM.lcb
Report File Name	: Default.lcr
Data Acquired	: 11/29/2016 9:59:56 PM
Data Processed	: 11/29/2016 10:14:58 PM

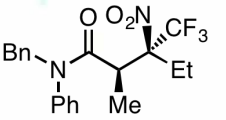

3.73
racemic

<Chromatogram>

C:\LabSolutions\Data\DMM\DVR04264 RAC_11292016_2144 PM_2.lcd

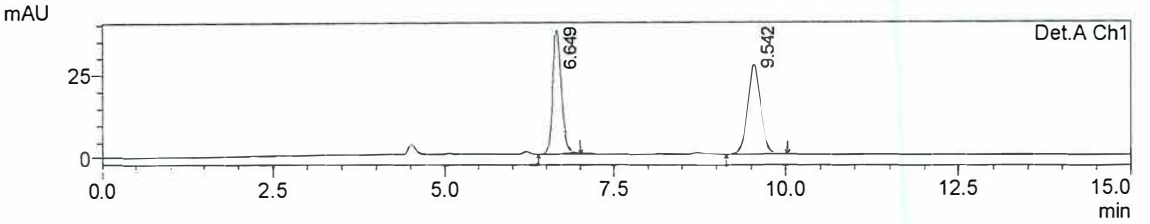

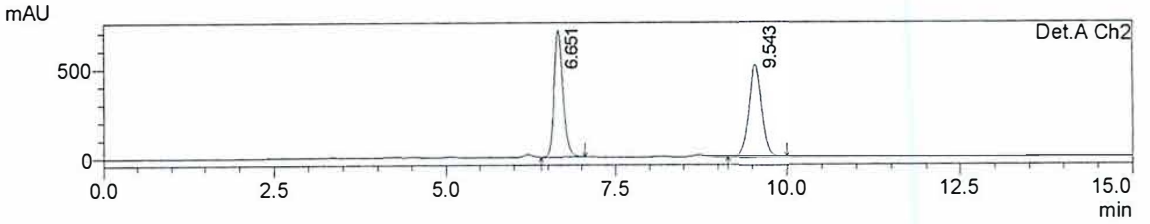

1 Det.A Ch1/254nm
2 Det.A Ch2/210nm

PeakTable

Detector A Ch1 254nm

Peak#	Ret. Time	Area	Height	Area %	Height %
1	6.649	335515	37235	49.726	58.188
2	9.542	339219	26755	50.274	41.812
Total		674734	63990	100.000	100.000

PeakTable

Detector A Ch2 210nm

Peak#	Ret. Time	Area	Height	Area %	Height %
1	6.651	6437992	709044	49.747	58.028
2	9.543	6503513	512864	50.253	41.972
Total		12941504	1221908	100.000	100.000

==== Shimadzu LCsolution Analysis Report ====

C:\LabSolutions\Data\DMM\DVR04264 _11292016_2144 PM_6.lcd

Acquired by	: LC User
Sample Name	: DVR04264
Sample ID	: DVR04264
Tray#	: 1
Vail #	: 4
Injection Volume	: 2 uL
Data File Name	: DVR04264 _11292016_2144 PM_6.lcd
Method File Name	: col1_2isoiPA_15min_1ML_254and210.lcm
Batch File Name	: DMM.lcb
Report File Name	: Default.lcr
Data Acquired	: 11/29/2016 10:40:54 PM
Data Processed	: 11/29/2016 10:55:57 PM

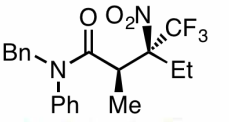

3.73
88% ee

<Chromatogram>

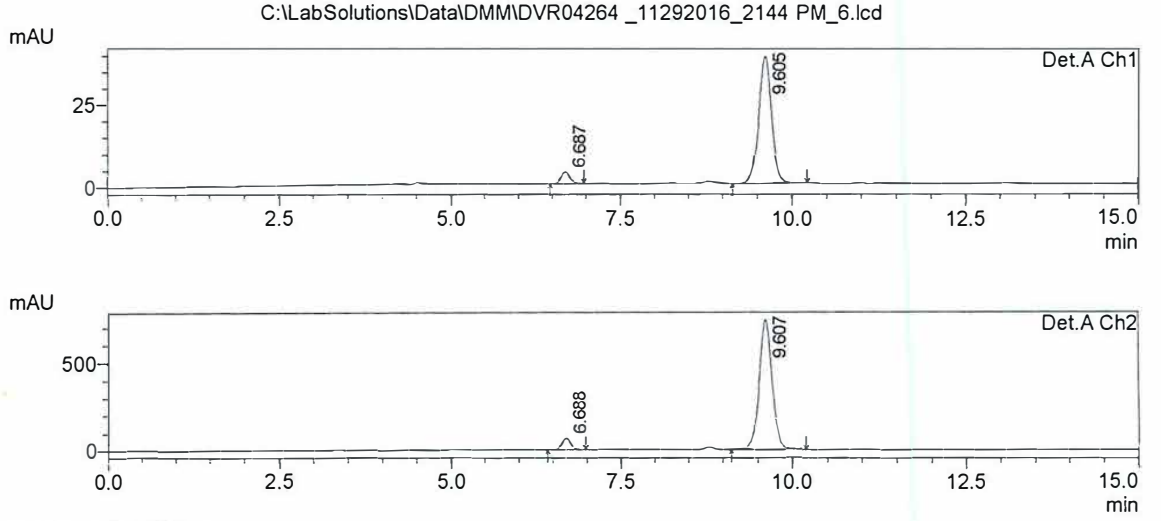

1 Det.A Ch1/254nm
2 Det.A Ch2/210nm

PeakTable

Detector A Ch1 254nm

Peak#	Ret. Time	Area	Height	Area %	Height %
1	6.687	29874	3354	5.685	7.954
2	9.605	495594	38805	94.315	92.046
Total		525468	42159	100.000	100.000

PeakTable

Detector A Ch2 210nm

Peak#	Ret. Time	Area	Height	Area %	Height %
1	6.688	581319	64771	5.780	8.074
2	9.607	9476777	737467	94.220	91.926
Total		10058095	802238	100.000	100.000

==== Shimadzu LCsolution Analysis Report ====

C:\LabSolutions\Data\DMM\DVR04264 RAC 1_11302016_2048 PM_2.lcd

Acquired by	: LC User
Sample Name	: DVR04264 RAC 1
Sample ID	: DVR04264 RAC 1
Tray#	: 1
Vail #	: 3
Injection Volume	: 3 uL
Data File Name	: DVR04264 RAC 1_11302016_2048 PM_2.lcd
Method File Name	: col1_2isoiPA_15min_1ML_254and210.lcm
Batch File Name	: DMM.lcb
Report File Name	: Default.lcr
Data Acquired	: 11/30/2016 9:04:28 PM
Data Processed	: 11/30/2016 9:19:30 PM

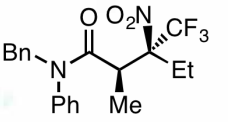

3.73
racemic

<Chromatogram>

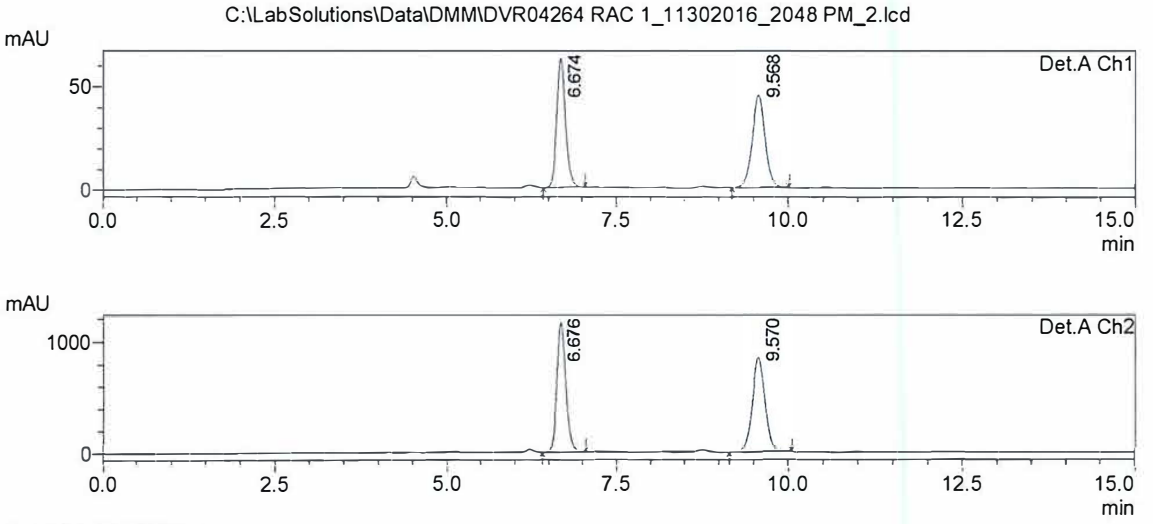

1 Det.A Ch1/254nm
2 Det.A Ch2/210nm

PeakTable

Detector A Ch1 254nm

Peak#	Ret. Time	Area	Height	Area %	Height %
1	6.674	564738	62397	49.815	58.217
2	9.568	568939	44783	50.185	41.783
Total		1133677	107181	100.000	100.000

PeakTable

Detector A Ch2 210nm

Peak#	Ret. Time	Area	Height	Area %	Height %
1	6.676	10644936	1157078	49.477	57.720
2	9.570	10870050	847565	50.523	42.280
Total		21514986	2004643	100.000	100.000

==== Shimadzu LCsolution Analysis Report ====

C:\LabSolutions\Data\DMM\DVR04265_11302016_2048 PM_6.lcd

Acquired by	: LC User
Sample Name	: DVR04265
Sample ID	: DVR04265
Tray#	: 1
Vail #	: 4
Injection Volume	: 2 uL
Data File Name	: DVR04265_11302016_2048 PM_6.lcd
Method File Name	: col1_2isoiPA_15min_1ML_254and210.lcm
Batch File Name	: DMM.lcb
Report File Name	: Default.lcr
Data Acquired	: 11/30/2016 9:45:24 PM
Data Processed	: 11/30/2016 10:00:25 PM

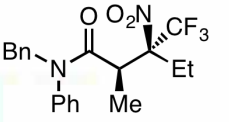

3.73
86% ee

<Chromatogram>

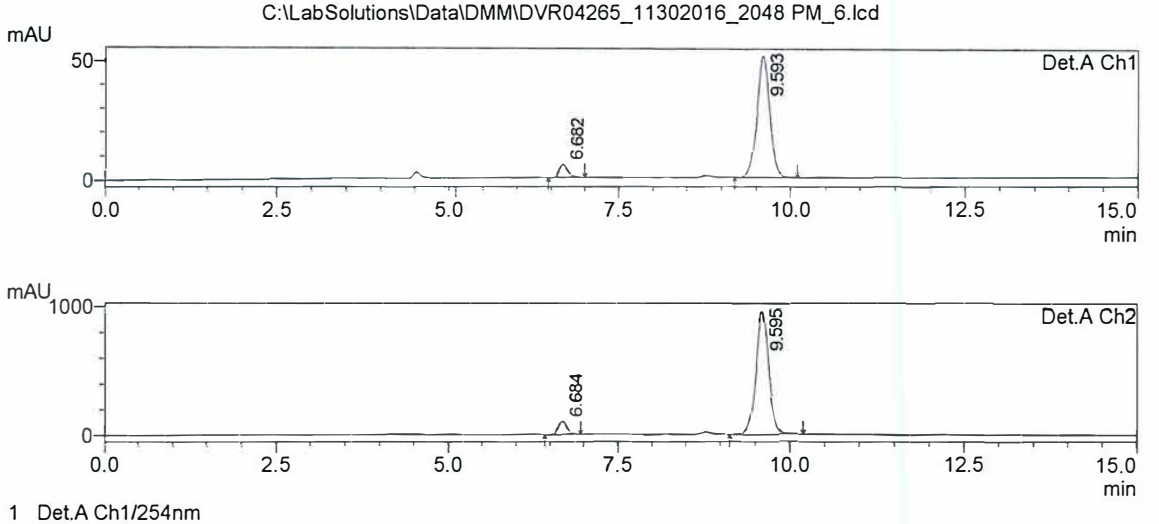

1 Det.A Ch1/254nm
2 Det.A Ch2/210nm

PeakTable

Detector A Ch1 254nm

Peak#	Ret. Time	Area	Height	Area %	Height %
1	6.682	48174	5344	6.812	9.414
2	9.593	659029	51421	93.188	90.586
Total		707203	56765	100.000	100.000

PeakTable

Detector A Ch2 210nm

Peak#	Ret. Time	Area	Height	Area %	Height %
1	6.684	921805	102959	6.845	9.623
2	9.595	12544487	967024	93.155	90.377
Total		13466292	1069984	100.000	100.000

Parameter	Value
1 Title	DVR05004d1.1.fid
2 Solvent	CDCl3
3 Temperature	298.0
4 Number of Scans	16
5 Receiver Gain	203
6 Relaxation Delay	1.0000
7 Pulse Width	10.7700
8 Spectrometer Frequency	600.32
9 Nucleus	1H

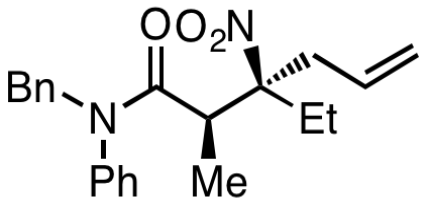

3.75

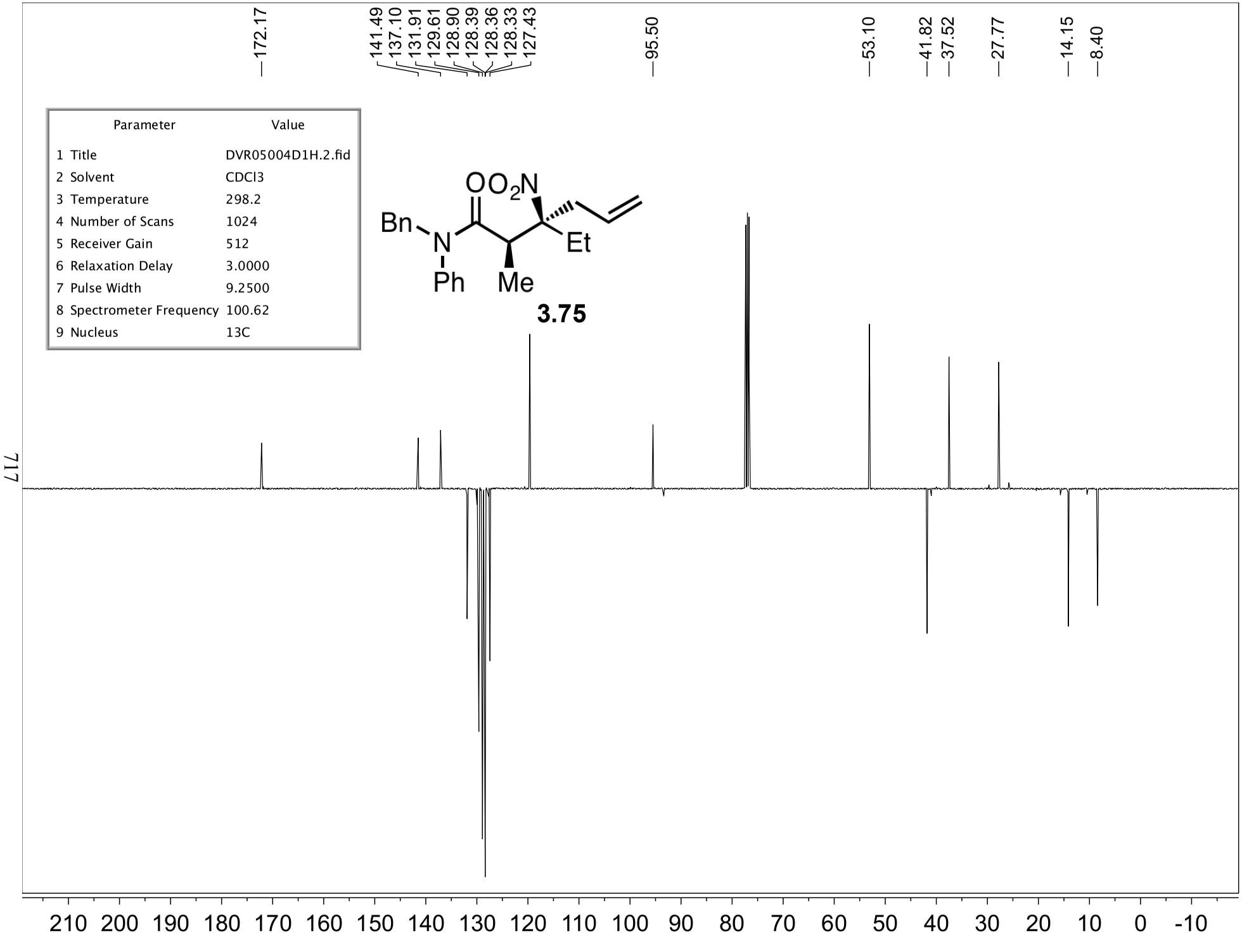
172.17
141.49
137.10
131.91
129.61
128.90
128.39
128.36
128.33
127.43
95.50
53.10
41.82
37.52
27.77
14.15
8.40
Parameter Value
1 Title DVR05004D1H.2.fid
2 Solvent CDCl3
3 Temperature 298.2
4 Number of Scans 1024
5 Receiver Gain 512
6 Relaxation Delay 3.0000
7 Pulse Width 9.2500
8 Spectrometer Frequency 100.62
9 Nucleus 13C
O
O2N
Bn
N
Ph
Me
Et
3.75
717
210 200 190 180 170 160 150 140 130 120 110 100 90 80 70 60 50 40 30 20 10 0 -10

==== Shimadzu LCsolution Analysis Report ====

C:\LabSolutions\Data\DMM\DVR05019 RAC_232017_829 AM_2.lcd

Acquired by	: LC User
Sample Name	: DVR05019 RAC
Sample ID	: DVR05019 RAC
Tray#	: 1
Vail #	: 1
Injection Volume	: 3 uL
Data File Name	: DVR05019 RAC_232017_829 AM_2.lcd
Method File Name	: col5_3isoiPA_45min_1.0ML_254and210.lcm
Batch File Name	: DMM.lcb
Report File Name	: Default.lcr
Data Acquired	: 2/3/2017 9:15:06 AM
Data Processed	: 2/3/2017 10:00:07 AM

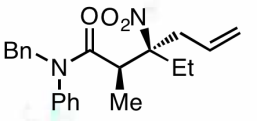

3.75
racemic

<Chromatogram>

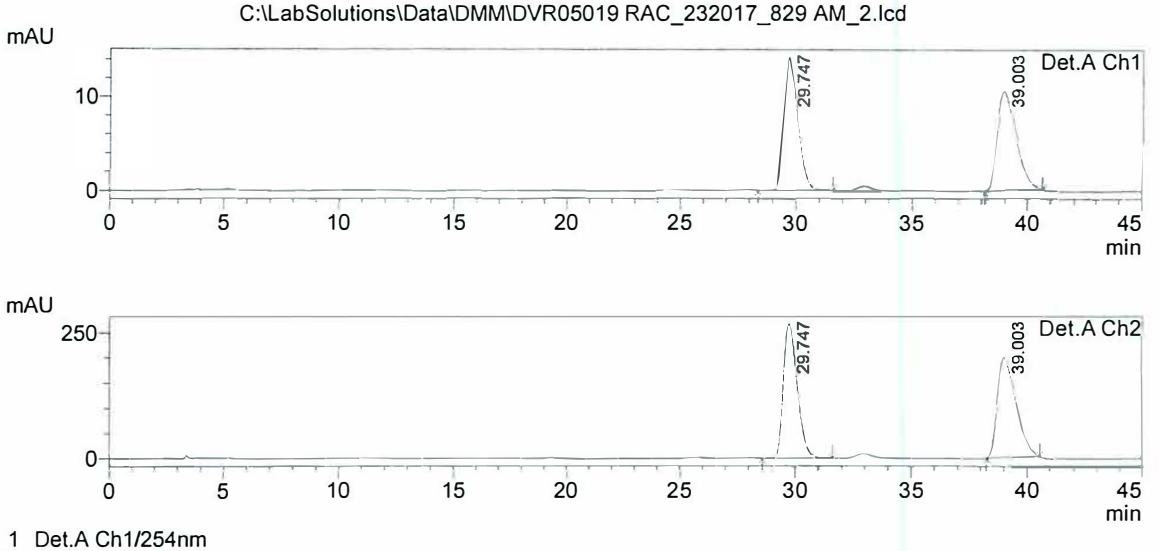

1 Det.A Ch1/254nm
2 Det.A Ch2/210nm

PeakTable

Detector A Ch1 254nm

Peak#	Ret. Time	Area	Height	Area %	Height %
1	29.747	593529	14336	49.395	57.284
2	39.003	608072	10690	50.605	42.716
Total		1201602	25026	100.000	100.000

PeakTable

Detector A Ch2 210nm

Peak#	Ret. Time	Area	Height	Area %	Height %
1	29.747	11134103	267848	50.058	57.486
2	39.003	11108142	198088	49.942	42.514
Total		22242245	465937	100.000	100.000

==== Shimadzu LCsolution Analysis Report ====

C:\LabSolutions\Data\DMM\DVR05019 D1_232017_829 AM_1.lcd

Acquired by	: LC User
Sample Name	: DVR05019 D1
Sample ID	: DVR05019 D1
Tray#	: 1
Vail #	: 2
Injection Volume	: 3 uL
Data File Name	: DVR05019 D1_232017_829 AM_1.lcd
Method File Name	: col5_3isoiPA_45min_1.0ML_254and210.lcm
Batch File Name	: DMM.lcb
Report File Name	: Default.lcr
Data Acquired	: 2/3/2017 10:57:44 AM
Data Processed	: 2/3/2017 11:42:46 AM

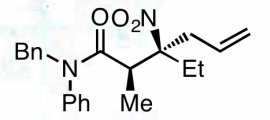

3.75
90% ee

<Chromatogram>

C:\LabSolutions\Data\DMM\DVR05019 D1_232017_829 AM_1.lcd

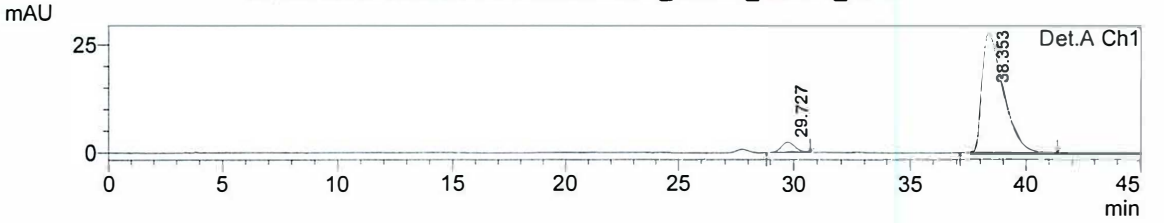

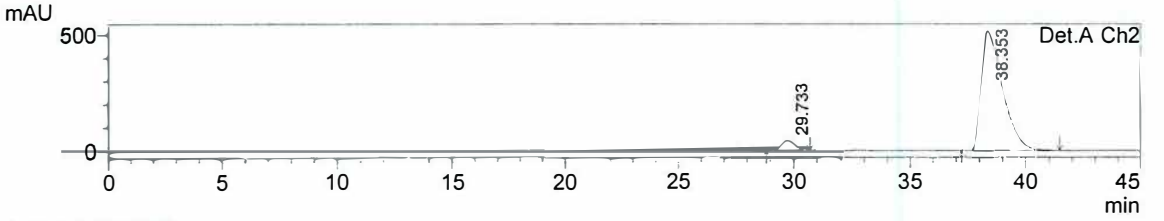

1 Det.A Ch1/254nm
2 Det.A Ch2/210nm

PeakTable

Detector A Ch1 254nm

Peak#	Ret. Time	Area	Height	Area %	Height %
1	29.727	90114	2270	4.872	7.510
2	38.353	1759547	27962	95.128	92.490
Total		1849661	30233	100.000	100.000

PeakTable

Detector A Ch2 210nm

Peak#	Ret. Time	Area	Height	Area %	Height %
1	29.733	1685056	42713	4.901	7.615
2	38.353	32699963	518217	95.099	92.385
Total		34385020	560930	100.000	100.000

Parameter	Value
1 Title	DVR05070A1.1.fid
2 Solvent	CDCl3
3 Temperature	297.0
4 Number of Scans	16
5 Receiver Gain	161
6 Relaxation Delay	1.0000
7 Pulse Width	10.7300
8 Spectrometer Frequency	600.32
9 Nucleus	1H

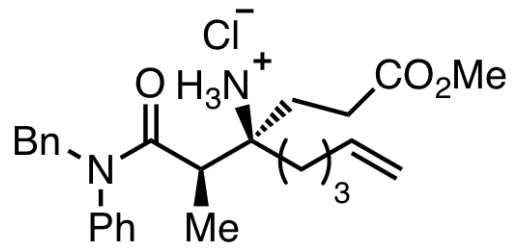

3.76

720

8.37 7.39 7.38 7.38 7.37 7.37 7.36 7.29 7.29 7.28 7.28 7.27 7.27 7.26 7.14 7.14 7.13 7.13 6.94 6.93 6.93 6.92 5.67 5.66 5.64 4.94 4.94 4.94 4.92 4.91 4.91 4.91 4.90 4.90 4.82 4.79 3.71 2.72 2.42 2.40 2.31 2.19 2.02 2.01 1.98 1.97 1.88 1.87 1.82 1.80 1.79 1.77 1.28 1.27

2.85 3.16 3.02 2.12 2.10 1.00 3.01 1.05 3.03 1.01 1.00 1.11 1.06 2.25 3.20 3.28 1.12 1.07

.0 9.5 9.0 8.5 8.0 7.5 7.0 6.5 6.0 5.5 5.0 4.5 4.0 3.5 3.0 2.5 2.0 1.5 1.0 0.5 0.0 -0.5 -1

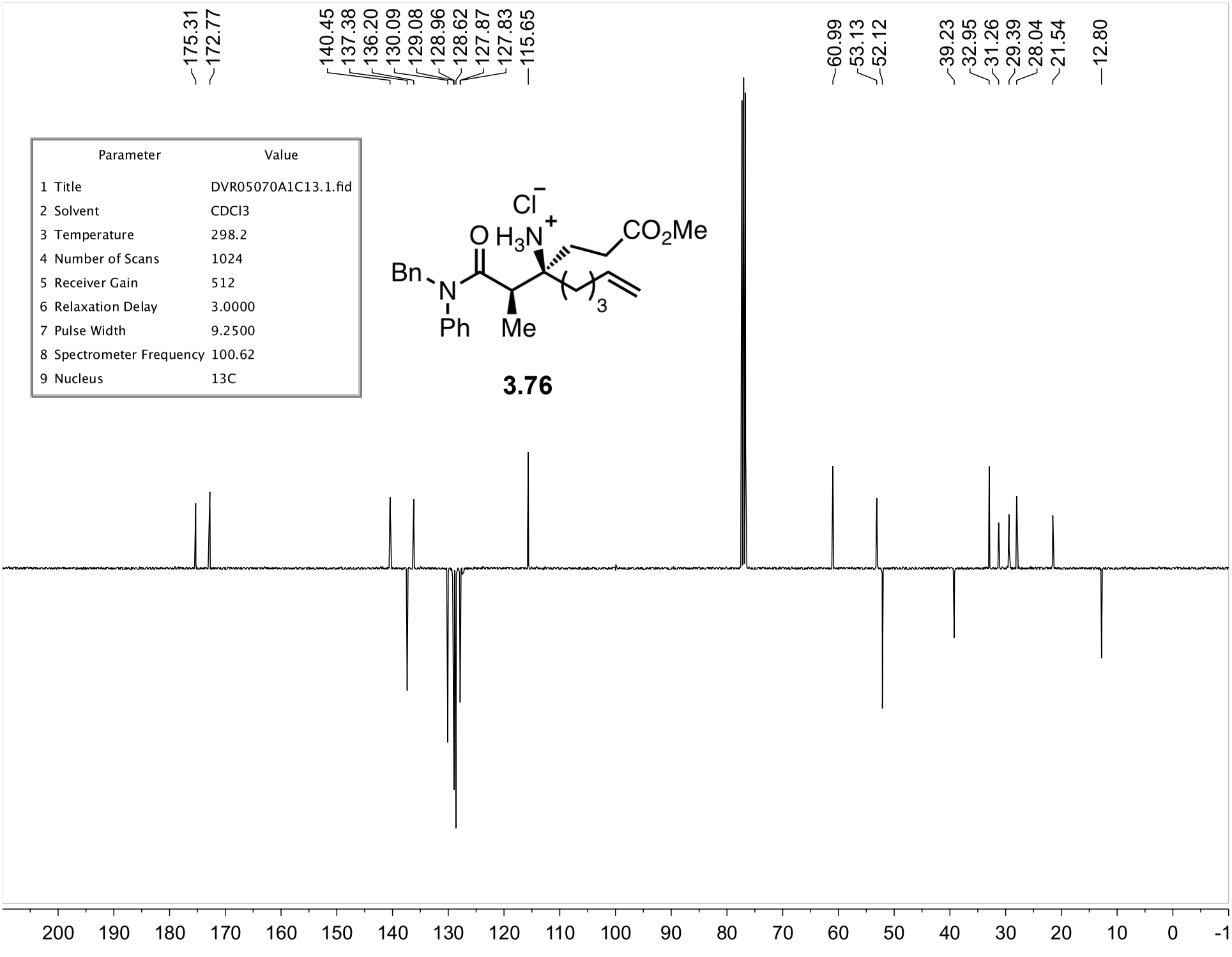
175.31
172.77
140.45
137.38
136.20
130.09
129.08
128.96
128.62
127.87
127.83
115.65
60.99
53.13
52.12
39.23
32.95
31.26
29.39
28.04
21.54
12.80
Parameter
Value
1 Title
DVR05070A1C13.1.fid
2 Solvent
CDCl3
3 Temperature
298.2
4 Number of Scans
1024
5 Receiver Gain
512
6 Relaxation Delay
3.0000
7 Pulse Width
9.2500
8 Spectrometer Frequency
100.62
9 Nucleus
13C
Cl⁻
O
H3N+
CO2Me
Bn
N
Ph
Me
3
3.76
721
200
190
180
170
160
150
140
130
120
110
100
90
80
70
60
50
40
30
20
10
0
-1

Data File C:\Chem32\1\Data\DVR\DVR05065-1 rac IF3 2017-05-10 12-26-42.D
Sample Name: DVR05065-1 rac IF3

==========

Acq. Operator : SYSTEM
Sample Operator : SYSTEM
Acq. Instrument : LC1 Reverse DAD-WPALS Location 21
Injection Date : 5/10/2017 12:27:17 PM
Inj Volume 5.000 µl
Acq. Method : C:\Chem32\1\Methods\BZV_Initial_05mL_lowerslope.M
Last changed : 5/10/2017 12:23:38 PM by SYSTEM
(modified after loading)
Analysis Method : C:\Chem32\1\Methods\BZV_Initial_05mL_lowerslope.M
Last changed : 12/6/2016 3:08:01 PM by SYSTEM
Sample Info : 1 min 10/90 MeCN/water
30 min gradient 35/65 MeCN/H2O
30 min hold 35/65 MeCN/H2O
4 min 90/10 MeCn/H2o Flush
IF-3 rac
1.0 mL/min

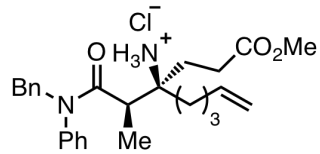

3.76
racemic

Additional Info : Peak(s) manually integrated

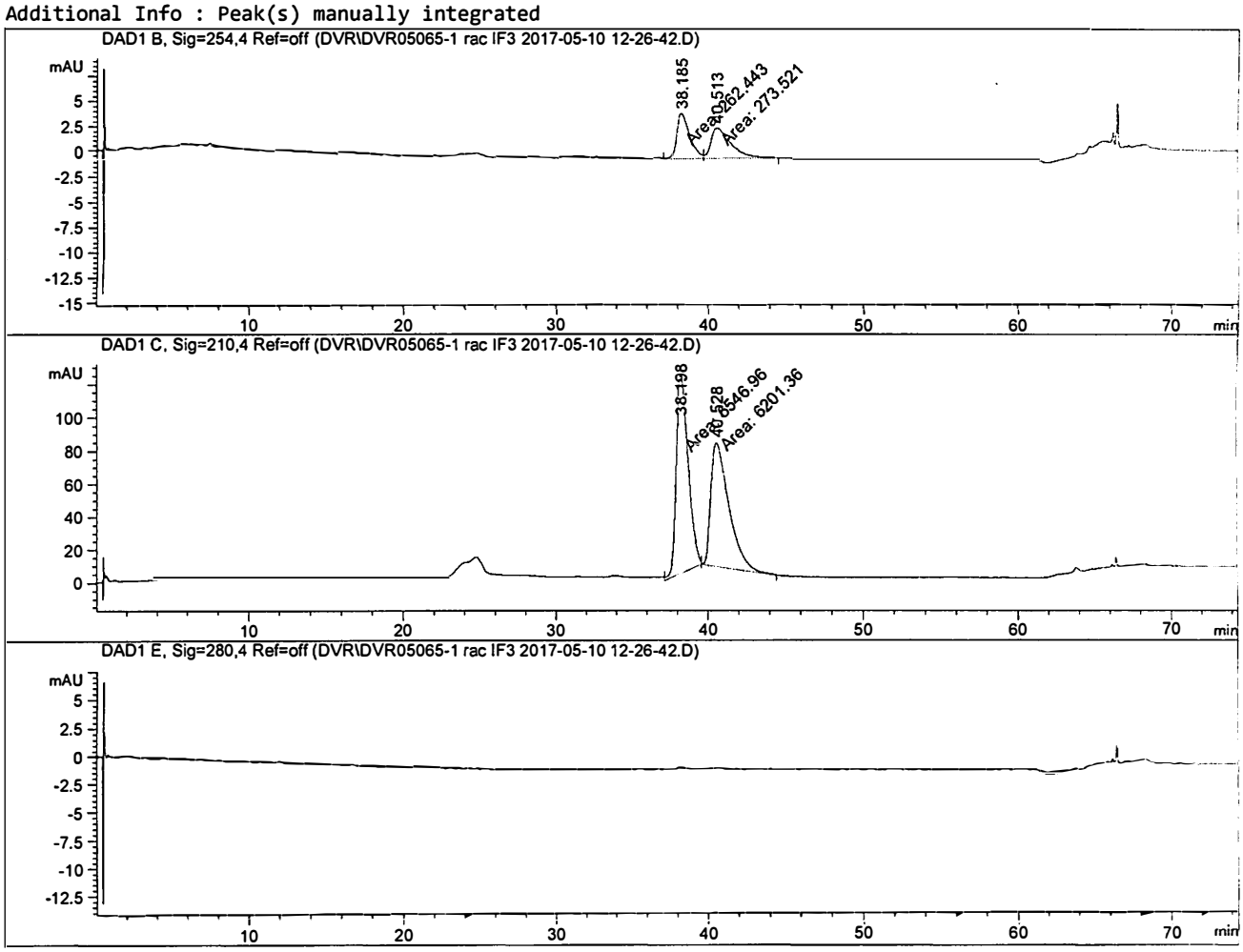

Data File C:\Chem32\1\Data\DVR\DVR05065-1 rac IF3 2017-05-10 12-26-42.D
Sample Name: DVR05065-1 rac IF3

==========

Area Percent Report

==========

Sorted By : Signal
Multiplier : 1.0000
Dilution : 1.0000
Sample Amount: : 5.00000 [ng/ul] (not used in calc.)
Use Multiplier & Dilution Factor with ISTDs

Signal 1: DAD1 B, Sig=254,4 Ref=off

Peak #	RetTime [min]	Type	Width [min]	Area [mAU*s]	Height [mAU]	Area %
1	38.185	MF	0.9771	262.44263	4.47667	48.9665
2	40.513	FM	1.5147	273.52121	3.00964	51.0335

Totals : 535.96384 7.48630

Signal 2: DAD1 C, Sig=210,4 Ref=off

Peak #	RetTime [min]	Type	Width [min]	Area [mAU*s]	Height [mAU]	Area %
1	38.198	MM	0.9071	6546.96143	120.28767	51.3555
2	40.528	MM	1.3773	6201.35938	75.04160	48.6445

Totals : 1.27483e4 195.32926

Signal 3: DAD1 E, Sig=280,4 Ref=off

==========

*** End of Report ***

Data File C:\Chem32\1\Data\DVR\DVR05065-ee IF3 2017-05-10 14-06-22.D
Sample Name: DVR05065-ee IF3

```
==========================================================================
Acq. Operator   : SYSTEM
Sample Operator : SYSTEM
Acq. Instrument : LC1 Reverse DAD-WPALS          Location :   21
Injection Date  : 5/10/2017 2:06:57 PM
                                                 Inj Volume : 5.000 µl
Acq. Method     : C:\Chem32\1\Methods\BZV_Initial_05mL_lowerslope.M
Last changed    : 5/10/2017 2:03:03 PM by SYSTEM
                  (modified after loading)
Analysis Method : C:\Chem32\1\Methods\BZV_Initial_05mL_lowerslope.M
Last changed    : 12/6/2016 3:08:01 PM by SYSTEM
Sample Info     : 1 min 10/90 MeCN/water
                  30 min gradient 35/65 MeCN/H2O
                  30 min hold 35/65 MeCN/H2O
                  4 min 90/10 MeCn/H2o Flush
                  IF-3 rac
                  1.0 mL/min
```

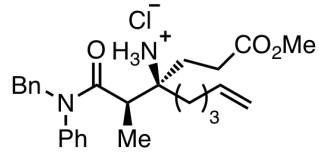

3.76
89% ee

Additional Info : Peak(s) manually integrated

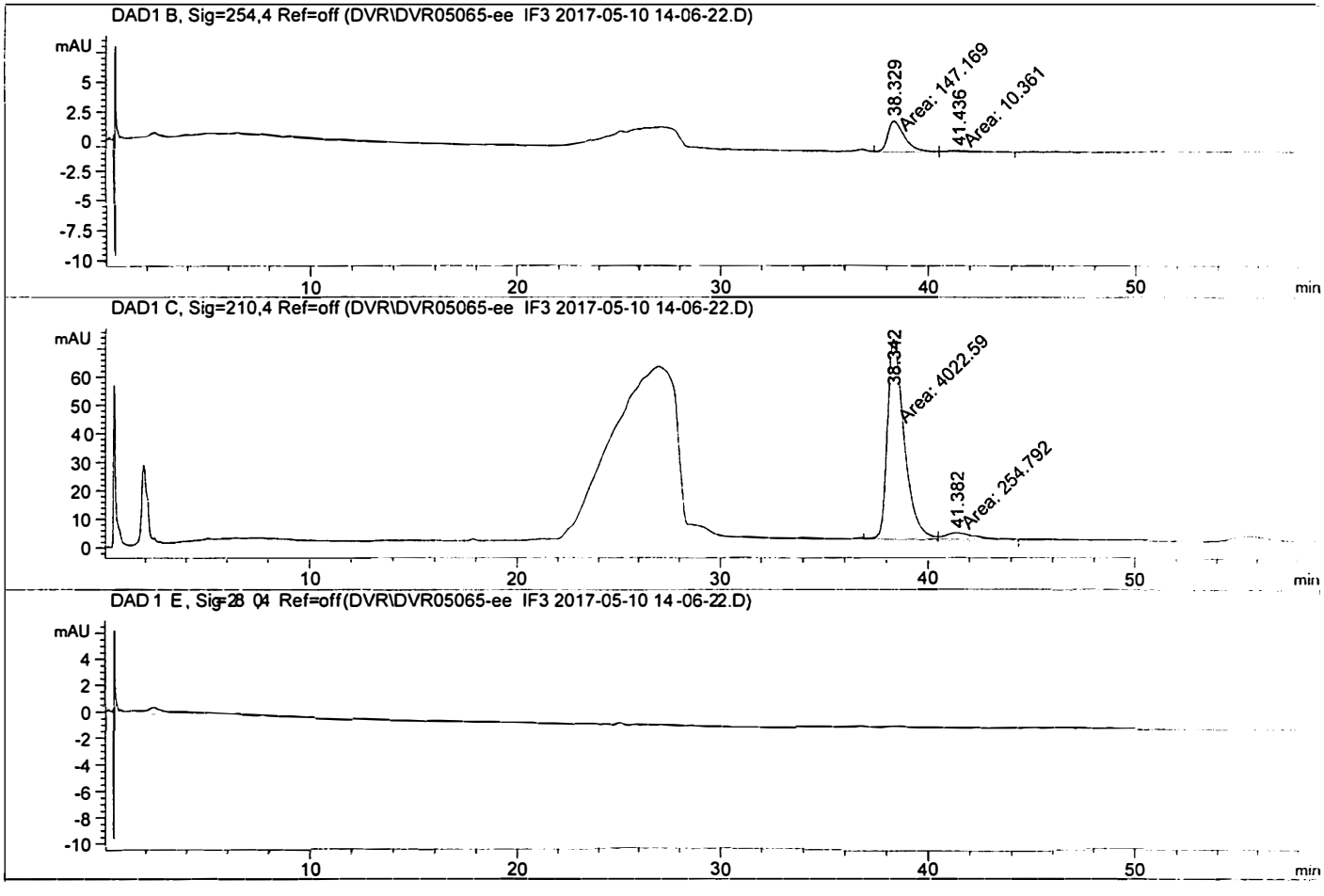

Data File C:\Chem32\1\Data\DVR\DVR05065-ee IF3 2017-05-10 14-06-22.D
Sample Name: DVR05065-ee IF3

==========

Area Percent Report

==========

Sorted By : Signal
Multiplier : 1.0000
Dilution : 1.0000
Sample Amount: : 5.00000 [ng/ul] (not used in calc.)
Use Multiplier & Dilution Factor with ISTDs

Signal 1: DAD1 B, Sig=254,4 Ref=off

Peak #	RetTime [min]	Type	Width [min]	Area [mAU*s]	Height [mAU]	Area %
1	38.329	MF T	0.9395	147.16916	2.61075	93.4228
2	41.436	FM T	1.4913	10.36101	1.15792e-1	6.5772
Totals :				157.53017	2.72654	

Signal 2: DAD1 C, Sig=210,4 Ref=off

Peak #	RetTime [min]	Type	Width [min]	Area [mAU*s]	Height [mAU]	Area %
1	38.342	MF T	1.1691	4022.58813	71.16277	94.0433
2	41.382	FM T	1.6251	254.79185	2.61314	5.9567
Totals :				4277.37999	73.77592	

Signal 3: DAD1 E, Sig=280,4 Ref=off

==========

*** End of Report ***

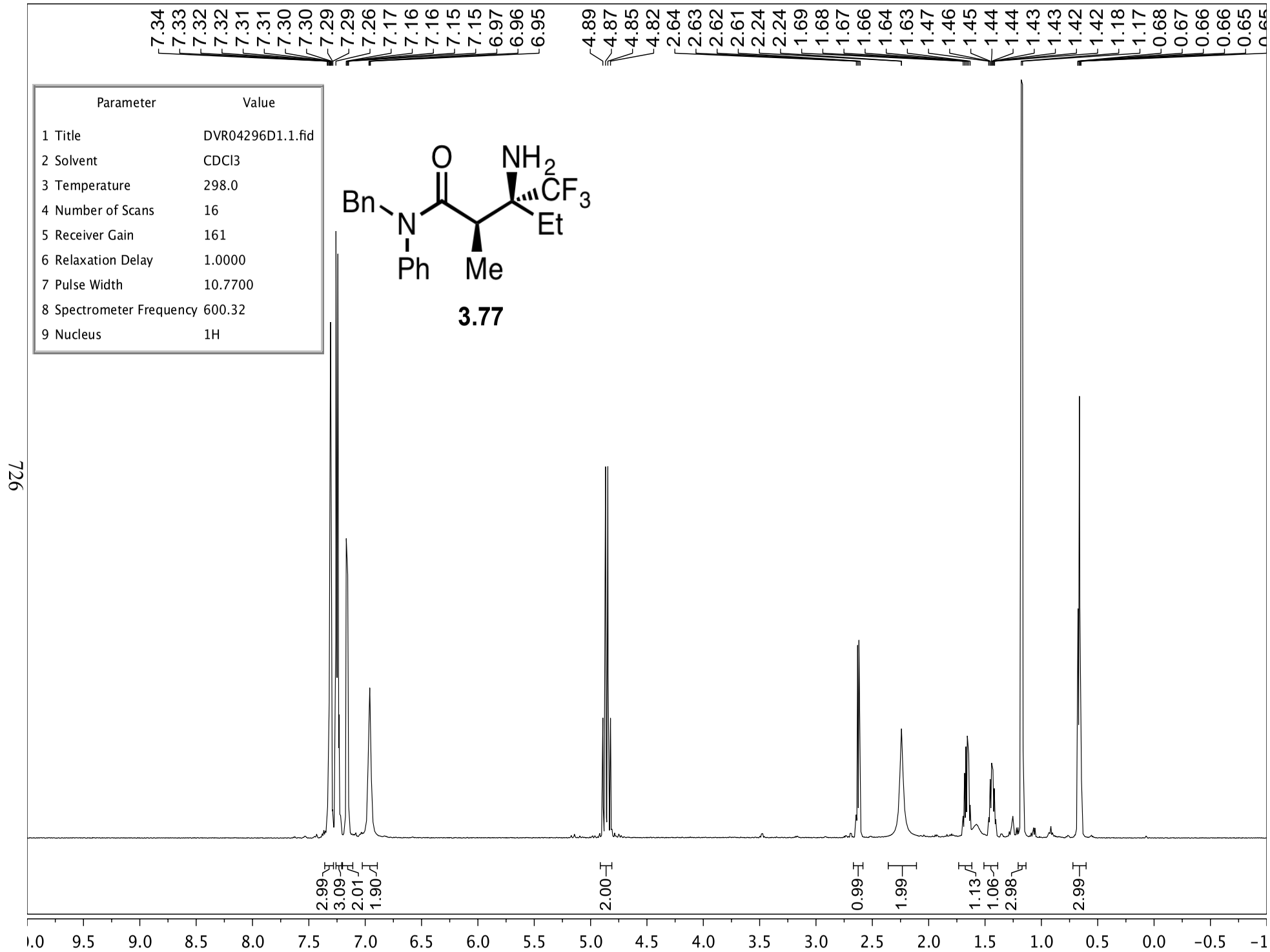
7.34 7.33 7.32 7.32 7.31 7.31 7.30 7.30 7.29 7.29 7.26 7.17 7.16 7.16 7.15 7.15 6.97 6.96 6.95
4.89 4.87 4.85 4.82
2.64 2.63 2.62 2.61 2.24 2.24 1.69 1.68 1.67 1.66 1.64 1.63 1.47 1.46 1.45 1.44 1.44 1.43 1.43 1.42 1.42 1.18 1.17 0.68 0.67 0.66 0.66 0.65
Parameter Value
1 Title DVR04296D1.1.fid
2 Solvent CDCl3
3 Temperature 298.0
4 Number of Scans 16
5 Receiver Gain 161
6 Relaxation Delay 1.0000
7 Pulse Width 10.7700
8 Spectrometer Frequency 600.32
9 Nucleus 1H
O
NH2
CF3
Bn
N
Et
Ph
Me
3.77
726
2.99
3.09
2.01
1.90
2.00
0.99
1.99
1.13
1.06
2.98
2.99
9.5 9.0 8.5 8.0 7.5 7.0 6.5 6.0 5.5 5.0 4.5 4.0 3.5 3.0 2.5 2.0 1.5 1.0 0.5 0.0 -0.5 -1

Parameter	Value
1 Title	DVR04296D1.2.fid
2 Solvent	CDCl3
3 Temperature	298.0
4 Number of Scans	16
5 Receiver Gain	362
6 Relaxation Delay	3.0000
7 Pulse Width	11.6200
8 Spectrometer Frequency	564.81
9 Nucleus	19F

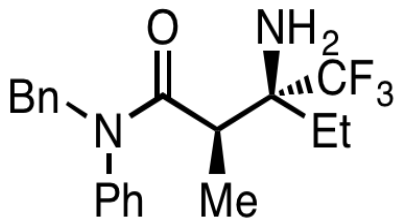

3.77

-74.47

727

0 -5 -10 -15 -20 -25 -30 -35 -40 -45 -50 -55 -60 -65 -70 -75 -80 -85 -90 -95 -1

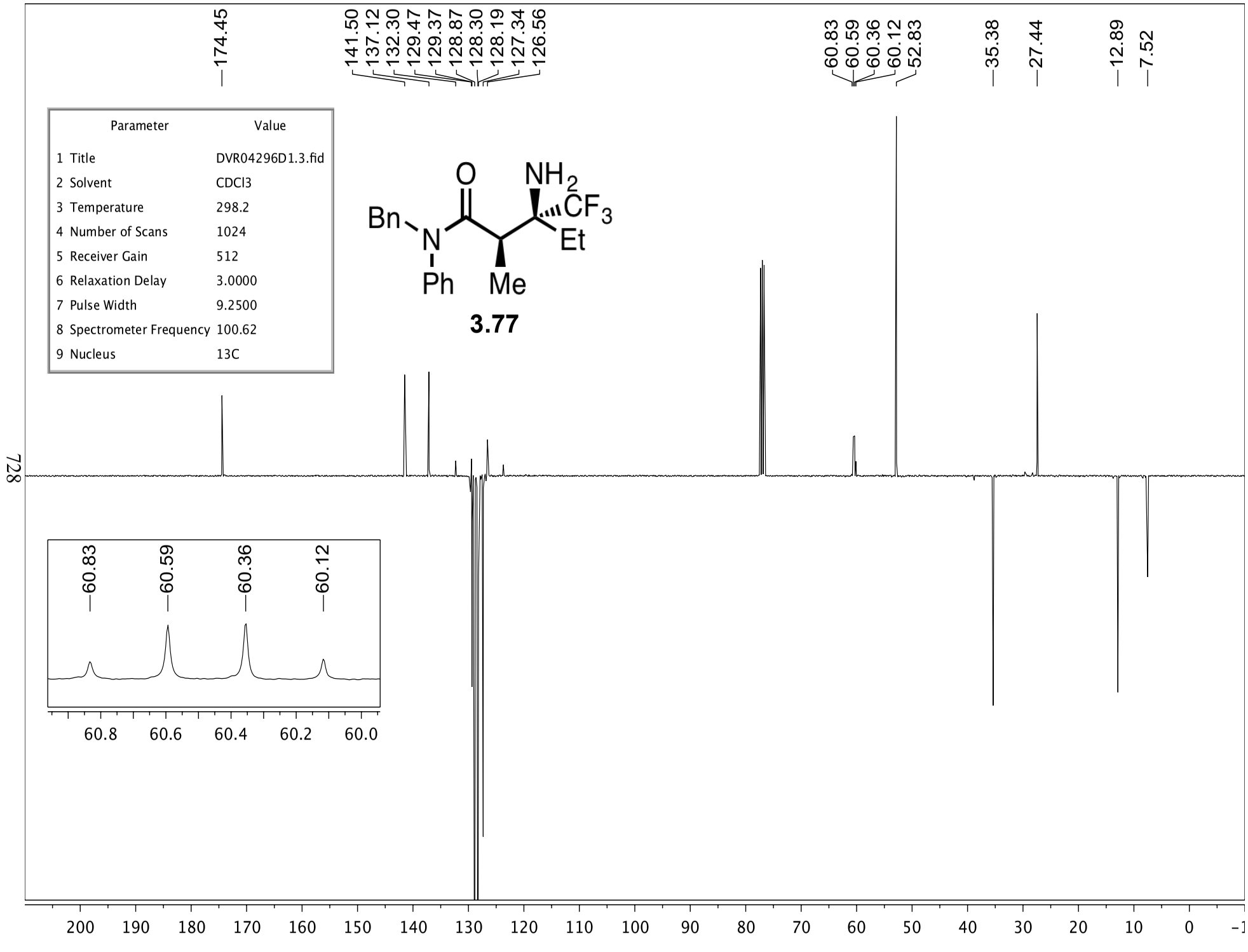
174.45
141.50
137.12
132.30
129.47
129.37
128.87
128.30
128.19
127.34
126.56
60.83
60.59
60.36
60.12
52.83
35.38
27.44
12.89
7.52
Parameter Value
1 Title DVR04296D1.3.fid
2 Solvent CDCl3
3 Temperature 298.2
4 Number of Scans 1024
5 Receiver Gain 512
6 Relaxation Delay 3.0000
7 Pulse Width 9.2500
8 Spectrometer Frequency 100.62
9 Nucleus 13C
O
NH2
CF3
Et
Bn
N
Ph
Me
3.77
728
60.83
60.59
60.36
60.12
60.8
60.6
60.4
60.2
60.0
200
190
180
170
160
150
140
130
120
110
100
90
80
70
60
50
40
30
20
10
0

==== Shimadzu LCsolution Analysis Report ====

C:\LabSolutions\Data\DMM\DVR04296 rac_1122017_1914 PM_2.lcd

Acquired by	: LC User
Sample Name	: DVR04296 rac
Sample ID	: DVR04296 rac
Tray#	: 1
Vail #	: 1
Injection Volume	: 5 uL
Data File Name	: DVR04296 rac_1122017_1914 PM_2.lcd
Method File Name	: col1_5isoiPA_30min_1ML_220and210.lcm
Batch File Name	: DMM.lcb
Report File Name	: Default.lcr
Data Acquired	: 1/12/2017 7:45:40 PM
Data Processed	: 1/12/2017 8:15:42 PM

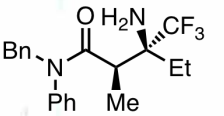

3.77
racemic

<Chromatogram>

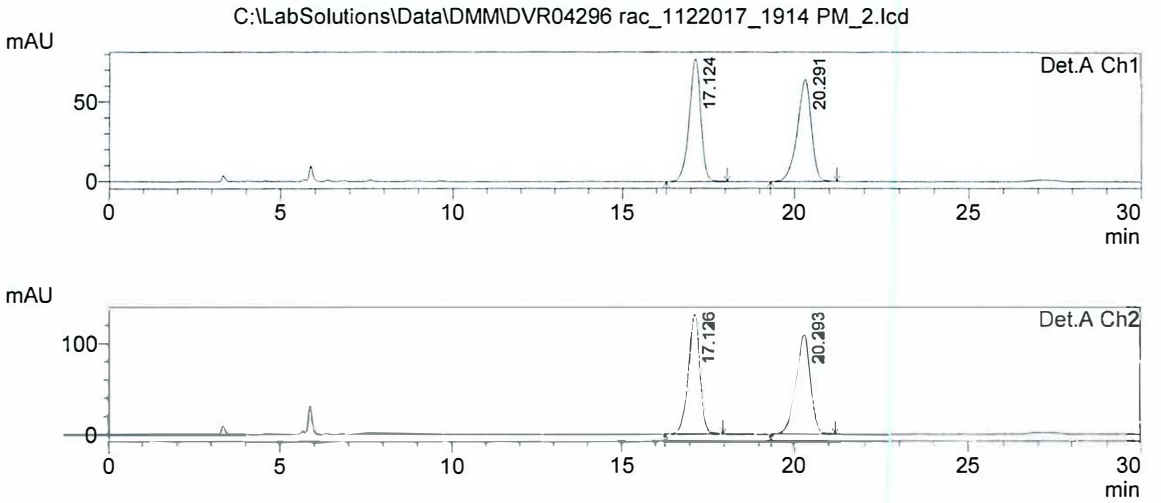

1 Det.A Ch1/220nm
2 Det.A Ch2/210nm

PeakTable

Detector A Ch1 220nm

Peak#	Ret. Time	Area	Height	Area %	Height %
1	17.124	1797024	77416	50.015	54.705
2	20.291	1795951	64098	49.985	45.295
Total		3592976	141514	100.000	100.000

PeakTable

Detector A Ch2 210nm

Peak#	Ret. Time	Area	Height	Area %	Height %
1	17.126	3072160	132476	49.987	54.689
2	20.293	3073760	109758	50.013	45.311
Total		6145919	242234	100.000	100.000

==== Shimadzu LCsolution Analysis Report ====

C:\LabSolutions\Data\DMM\DVR04296 D1_1122017_1914 PM_6.lcd

Acquired by	: LC User
Sample Name	: DVR04296 D1
Sample ID	: DVR04296 D1
Tray#	: 1
Vail #	: 2
Injection Volume	: 5 uL
Data File Name	: DVR04296 D1_1122017_1914 PM_6.lcd
Method File Name	: col1_5isoiPA_30min_1ML_220and210.lcm
Batch File Name	: DMM.lcb
Report File Name	: Default.lcr
Data Acquired	: 1/12/2017 8:56:37 PM
Data Processed	: 1/12/2017 9:26:41 PM

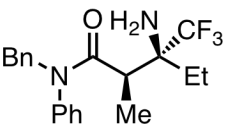

3.77
88% ee

<Chromatogram>

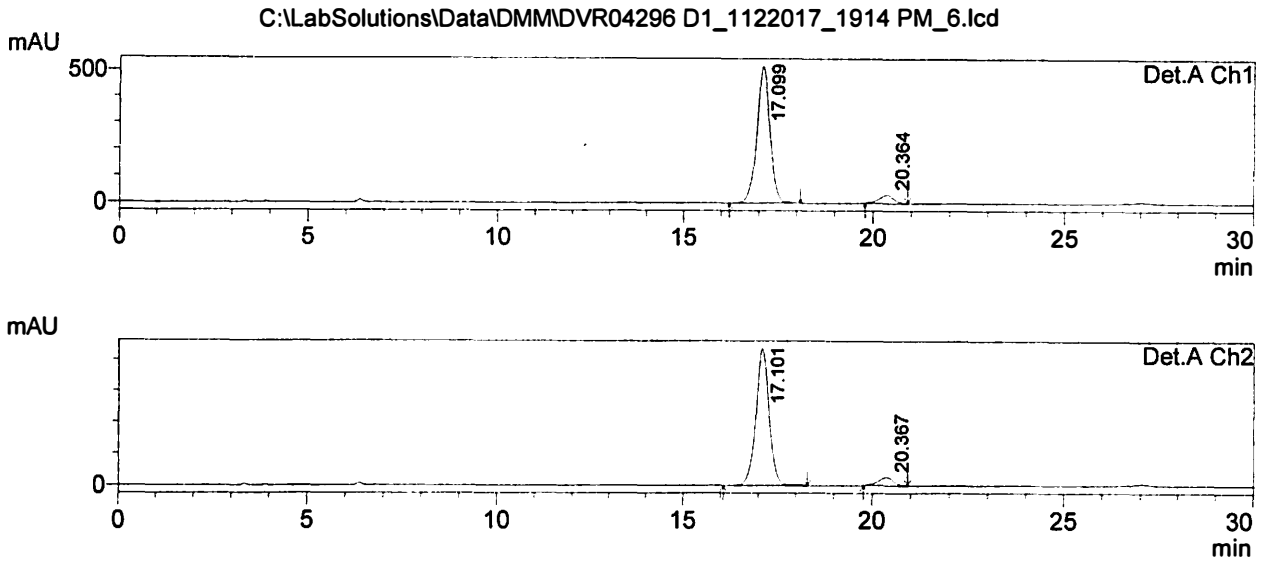

1 Det.A Ch1/220nm
2 Det.A Ch2/210nm

PeakTable

Detector A Ch1 220nm

Peak#	Ret. Time	Area	Height	Area %	Height %
1	17.099	12356691	518103	94.085	94.670
2	20.364	776888	29168	5.915	5.330
Total		13133579	547271	100.000	100.000

PeakTable

Detector A Ch2 210nm

Peak#	Ret. Time	Area	Height	Area %	Height %
1	17.101	21012325	874462	93.919	94.550
2	20.367	1360378	50401	6.081	5.450
Total		22372703	924864	100.000	100.000

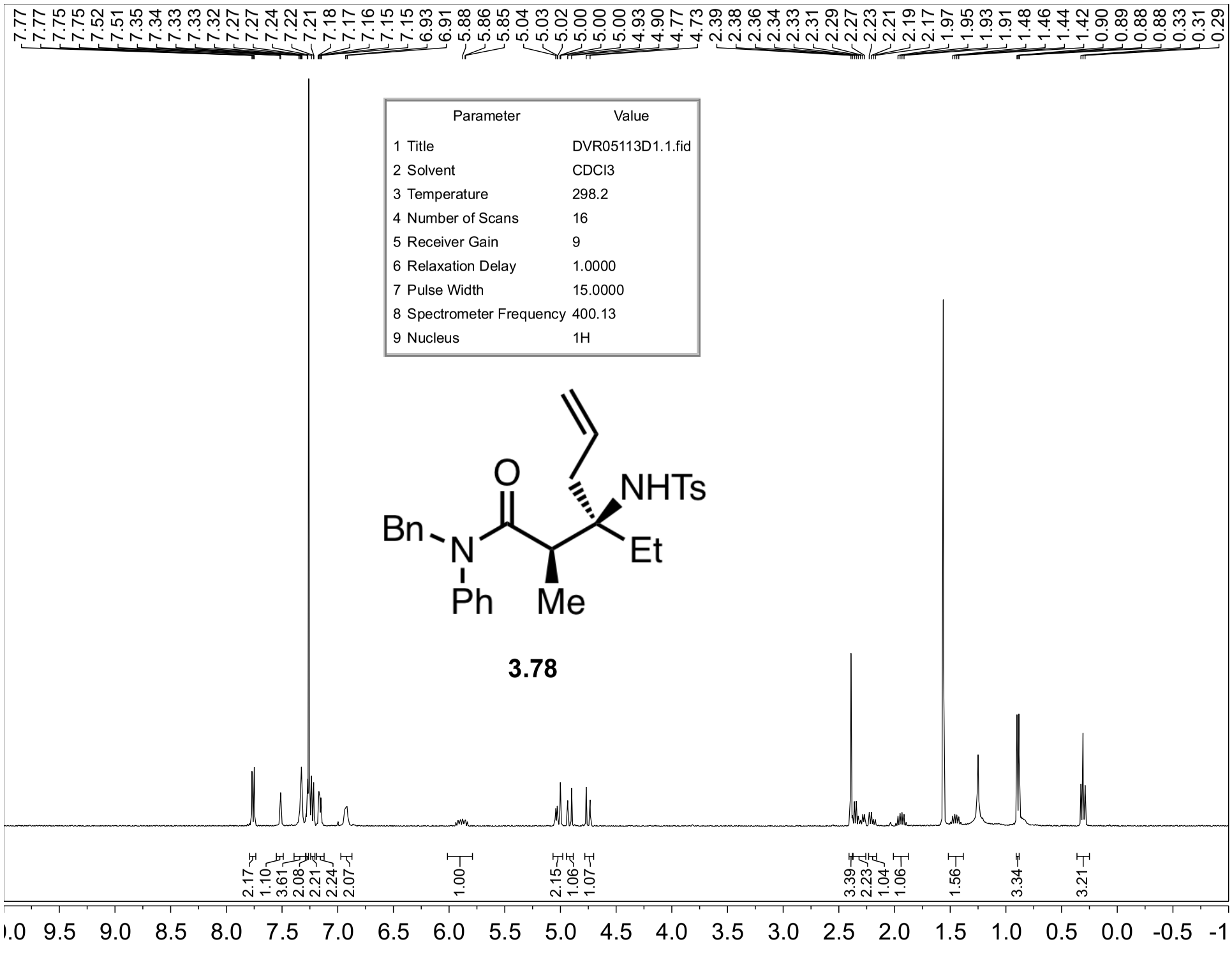
7.77 7.77 7.75 7.75 7.52 7.51 7.35 7.34 7.33 7.33 7.32 7.27 7.27 7.24 7.22 7.21 7.18 7.17 7.16 7.15 7.15 6.93 6.91 5.88 5.86 5.85 5.04 5.03 5.02 5.00 5.00 5.00 4.93 4.90 4.77 4.73 2.39 2.38 2.36 2.34 2.33 2.31 2.29 2.27 2.23 2.21 2.19 2.17 1.97 1.95 1.93 1.91 1.48 1.46 1.44 1.42 0.90 0.89 0.88 0.88 0.33 0.31 0.29
Parameter Value
1 Title DVR05113D1.1.fid
2 Solvent CDCl3
3 Temperature 298.2
4 Number of Scans 16
5 Receiver Gain 9
6 Relaxation Delay 1.0000
7 Pulse Width 15.0000
8 Spectrometer Frequency 400.13
9 Nucleus 1H
O
NHTs
Bn
N
Et
Ph
Me
3.78
2.17 1.10 3.61 2.08 2.21 2.24 2.07 1.00 2.15 1.06 1.07 3.39 2.23 1.04 1.06 1.56 3.34 3.21
.0 9.5 9.0 8.5 8.0 7.5 7.0 6.5 6.0 5.5 5.0 4.5 4.0 3.5 3.0 2.5 2.0 1.5 1.0 0.5 0.0 -0.5 -1

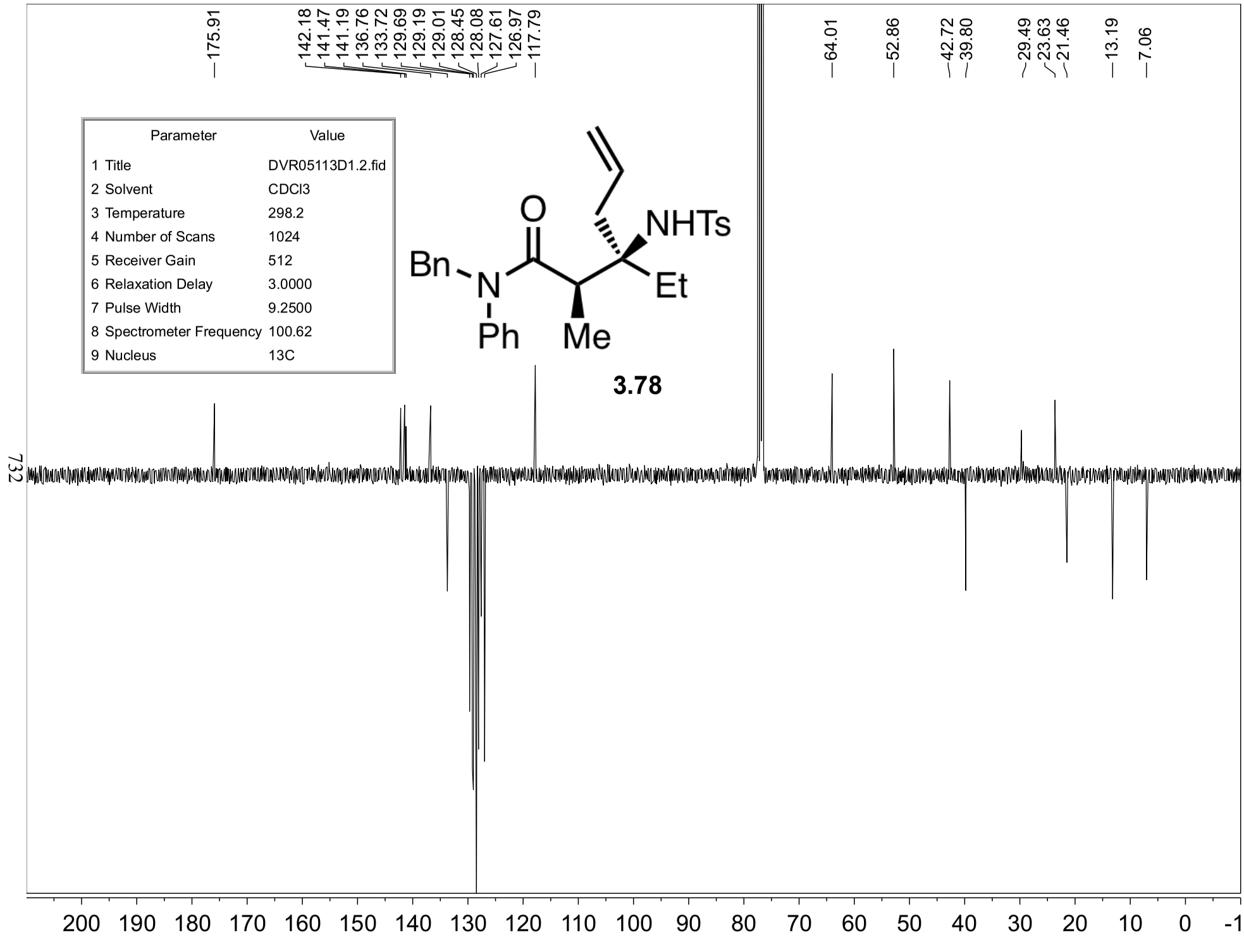
175.91
142.18
141.47
141.19
136.76
133.72
129.69
129.19
129.01
128.45
128.08
127.61
126.97
117.79
64.01
52.86
42.72
39.80
29.49
23.63
21.46
13.19
7.06
Parameter Value
1 Title DVR05113D1.2.fid
2 Solvent CDCl3
3 Temperature 298.2
4 Number of Scans 1024
5 Receiver Gain 512
6 Relaxation Delay 3.0000
7 Pulse Width 9.2500
8 Spectrometer Frequency 100.62
9 Nucleus 13C
O
NHTs
Bn
N
Et
Ph
Me
3.78
732
200 190 180 170 160 150 140 130 120 110 100 90 80 70 60 50 40 30 20 10 0 -1

==== Shimadzu LCsolution Analysis Report ====

C:\LabSolutions\Data\DMM\DVR05112 RAC COL2_7312017_1816 PM_6.lcd

Acquired by	: LC User
Sample Name	: DVR05112 RAC COL2
Sample ID	: DVR05112 RAC COL2
Tray#	: 1
Vail #	: 1
Injection Volume	: 4 uL
Data File Name	: DVR05112 RAC COL2_7312017_1816 PM_6.lcd
Method File Name	: col2_3isoiPA_45min_1ML_220and210.lcm
Batch File Name	: DMM.lcb
Report File Name	: Default.lcr
Data Acquired	: 7/31/2017 7:33:04 PM
Data Processed	: 8/28/2017 9:09:03 AM

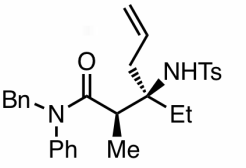

3.78
racemic

<Chromatogram>

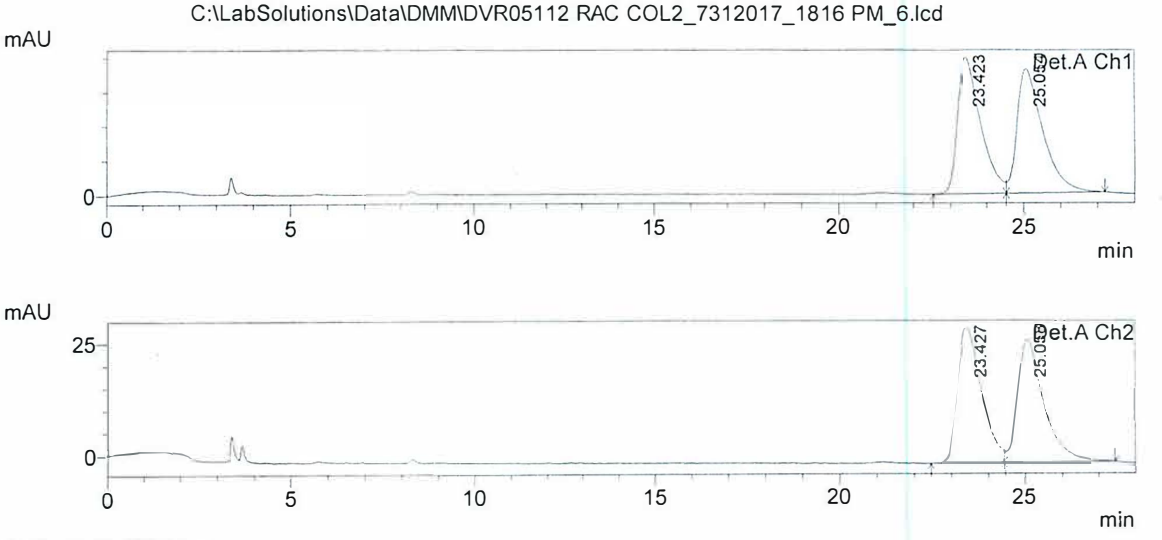

1 Det.A Ch1/220nm
2 Det.A Ch2/210nm

PeakTable

Detector A Ch1 220nm

Peak#	Ret. Time	Area	Height	Area %	Height %
1	23.423	887881	19932	50.195	52.288
2	25.054	880972	18187	49.805	47.712
Total		1768853	38119	100.000	100.000

PeakTable

Detector A Ch2 210nm

Peak#	Ret. Time	Area	Height	Area %	Height %
1	23.427	1346497	30425	49.495	52.327
2	25.058	1373982	27719	50.505	47.673
Total		2720479	58143	100.000	100.000

==== Shimadzu LCsolution Analysis Report ====

C:\LabSolutions\Data\DMM\DVR05113 R1_812017_1914 PM_3.lcd

Acquired by	: LC User
Sample Name	: DVR05113 R1
Sample ID	: DVR05113 R1
Tray#	: 1
Vail #	: 3
Injection Volume	: 5 uL
Data File Name	: DVR05113 R1_812017_1914 PM_3.lcd
Method File Name	: col2_3isoiPA_45min_1ML_254and210.lcm
Batch File Name	: DMM.lcb
Report File Name	: Default.lcr
Data Acquired	: 8/1/2017 8:30:52 PM
Data Processed	: 8/28/2017 9:06:53 AM

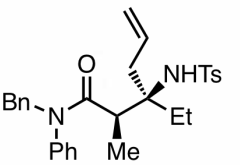

3.78
96% ee

<Chromatogram>

C:\LabSolutions\Data\DMM\DVR05113 R1_812017_1914 PM_3.lcd

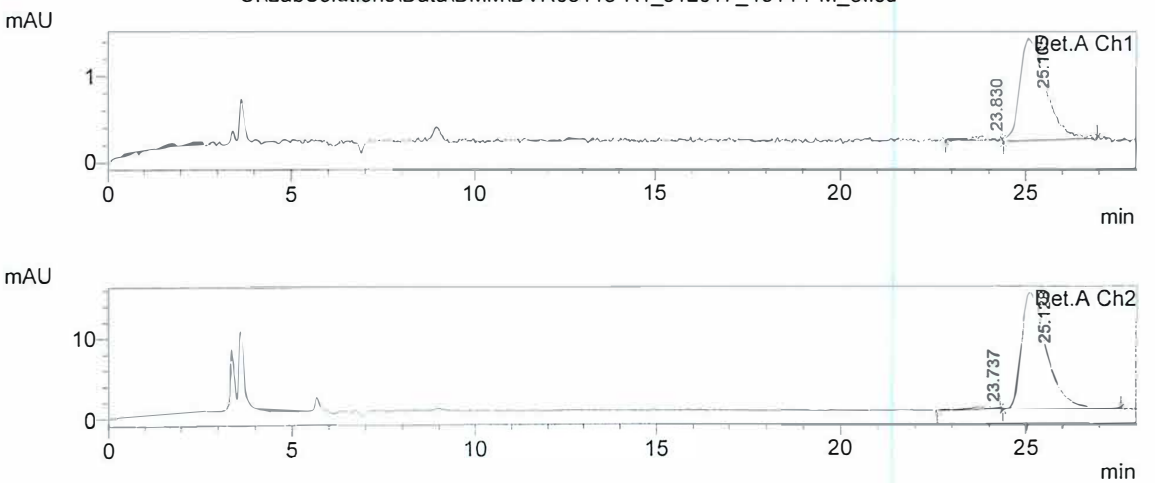

1 Det.A Ch1/254nm
2 Det.A Ch2/210nm

PeakTable

Detector A Ch1 254nm

Peak#	Ret. Time	Area	Height	Area %	Height %
1	23.830	1431	50	2.515	4.018
2	25.105	55484	1190	97.485	95.982
Total		56915	1240	100.000	100.000

PeakTable

Detector A Ch2 210nm

Peak#	Ret. Time	Area	Height	Area %	Height %
1	23.737	13302	305	1.922	2.063
2	25.128	678853	14504	98.078	97.937
Total		692155	14810	100.000	100.000

Parameter	Value
1 Title	DVR04259H1.1.fid
2 Solvent	CDCl3
3 Temperature	298.2
4 Number of Scans	16
5 Receiver Gain	10
6 Relaxation Delay	1.0000
7 Pulse Width	15.0000
8 Spectrometer Frequency	400.13
9 Nucleus	1H

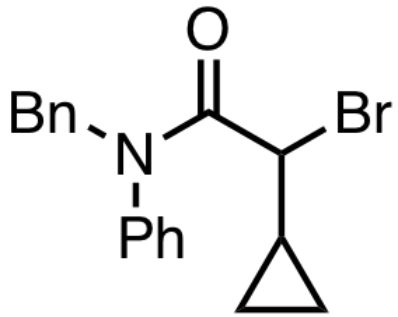

3.79

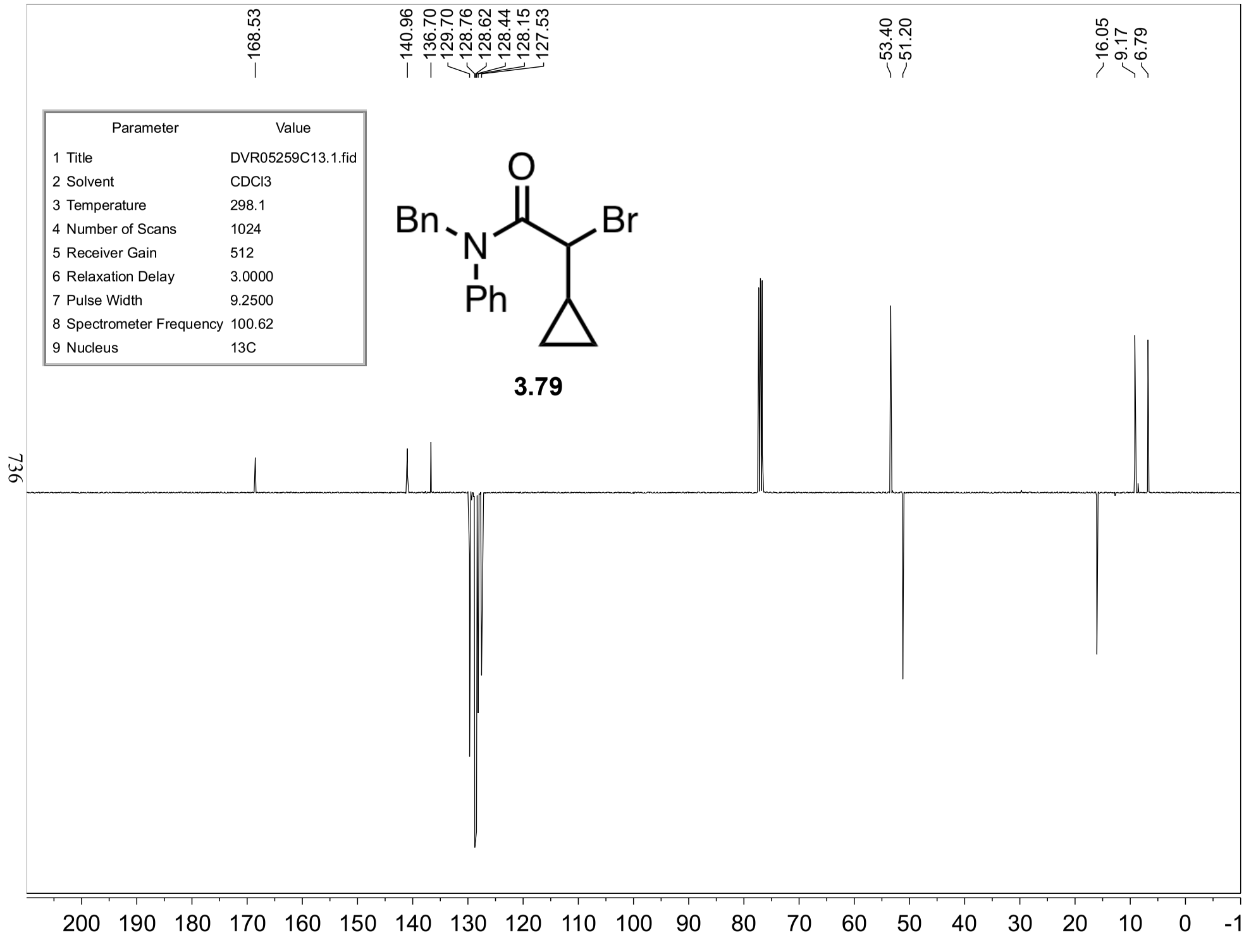
168.53
140.96
136.70
129.70
128.76
128.62
128.44
128.15
127.53
53.40
51.20
16.05
9.17
6.79
Parameter
Value
1 Title
DVR05259C13.1.fid
2 Solvent
CDCl3
3 Temperature
298.1
4 Number of Scans
1024
5 Receiver Gain
512
6 Relaxation Delay
3.0000
7 Pulse Width
9.2500
8 Spectrometer Frequency
100.62
9 Nucleus
13C
O
Bn
N
Ph
Br
3.79
736
200 190 180 170 160 150 140 130 120 110 100 90 80 70 60 50 40 30 20 10 0 -1

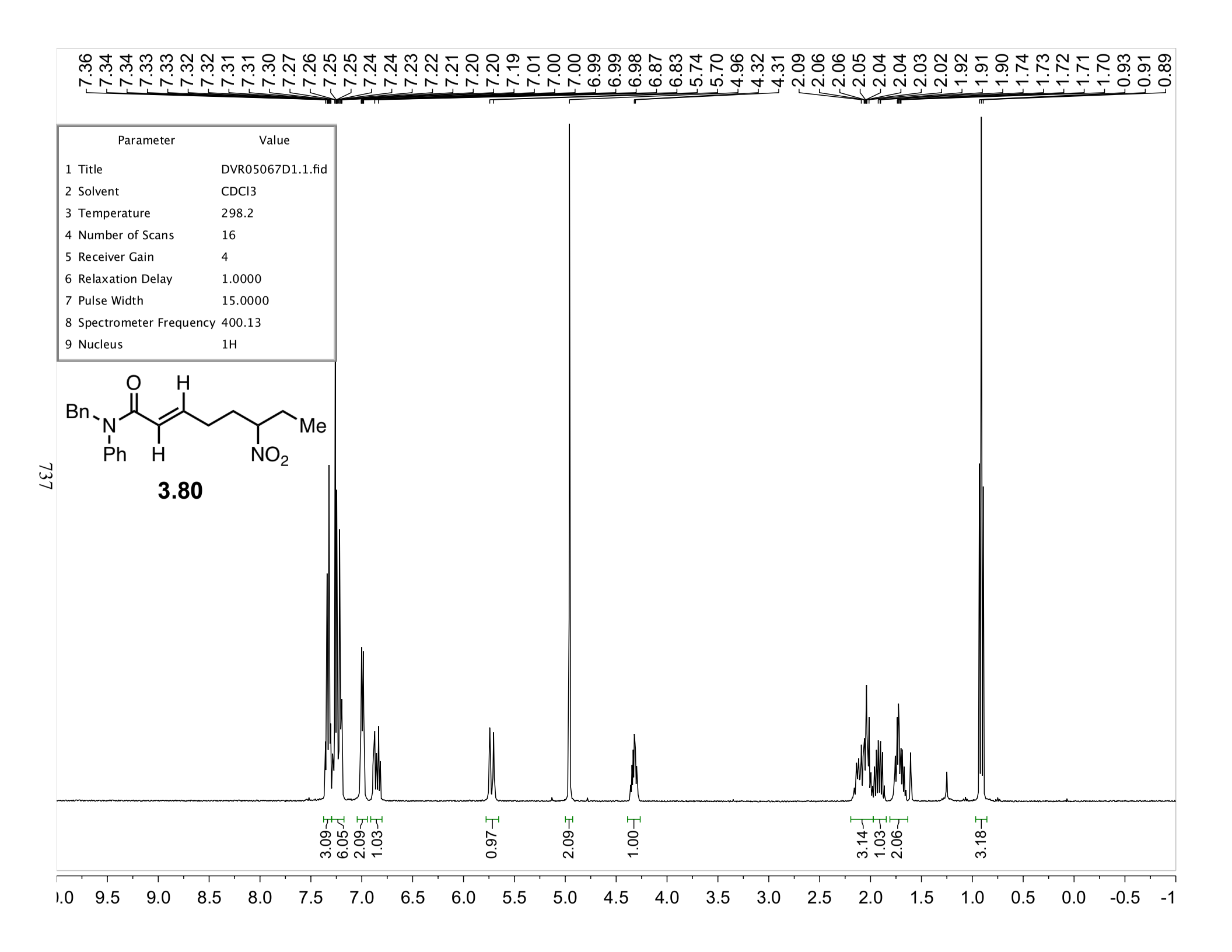
7.36 7.34 7.34 7.33 7.33 7.32 7.32 7.31 7.31 7.30 7.27 7.26 7.25 7.25 7.24 7.24 7.23 7.22 7.21 7.20 7.20 7.19 7.01 7.00 7.00 6.99 6.99 6.98 6.87 6.83 5.74 5.70 4.96 4.32 4.31 2.09 2.06 2.06 2.05 2.04 2.04 2.03 2.02 1.92 1.91 1.90 1.74 1.73 1.72 1.71 1.70 0.93 0.91 0.89
Parameter Value
1 Title DVR05067D1.1.fid
2 Solvent CDCl3
3 Temperature 298.2
4 Number of Scans 16
5 Receiver Gain 4
6 Relaxation Delay 1.0000
7 Pulse Width 15.0000
8 Spectrometer Frequency 400.13
9 Nucleus 1H
Bn
N
Ph
O
H
H
Me
NO2
3.80
737
3.09
6.05
2.09
1.03
0.97
2.09
1.00
3.14
1.03
2.06
3.18
9.5 9.0 8.5 8.0 7.5 7.0 6.5 6.0 5.5 5.0 4.5 4.0 3.5 3.0 2.5 2.0 1.5 1.0 0.5 0.0 -0.5 -1

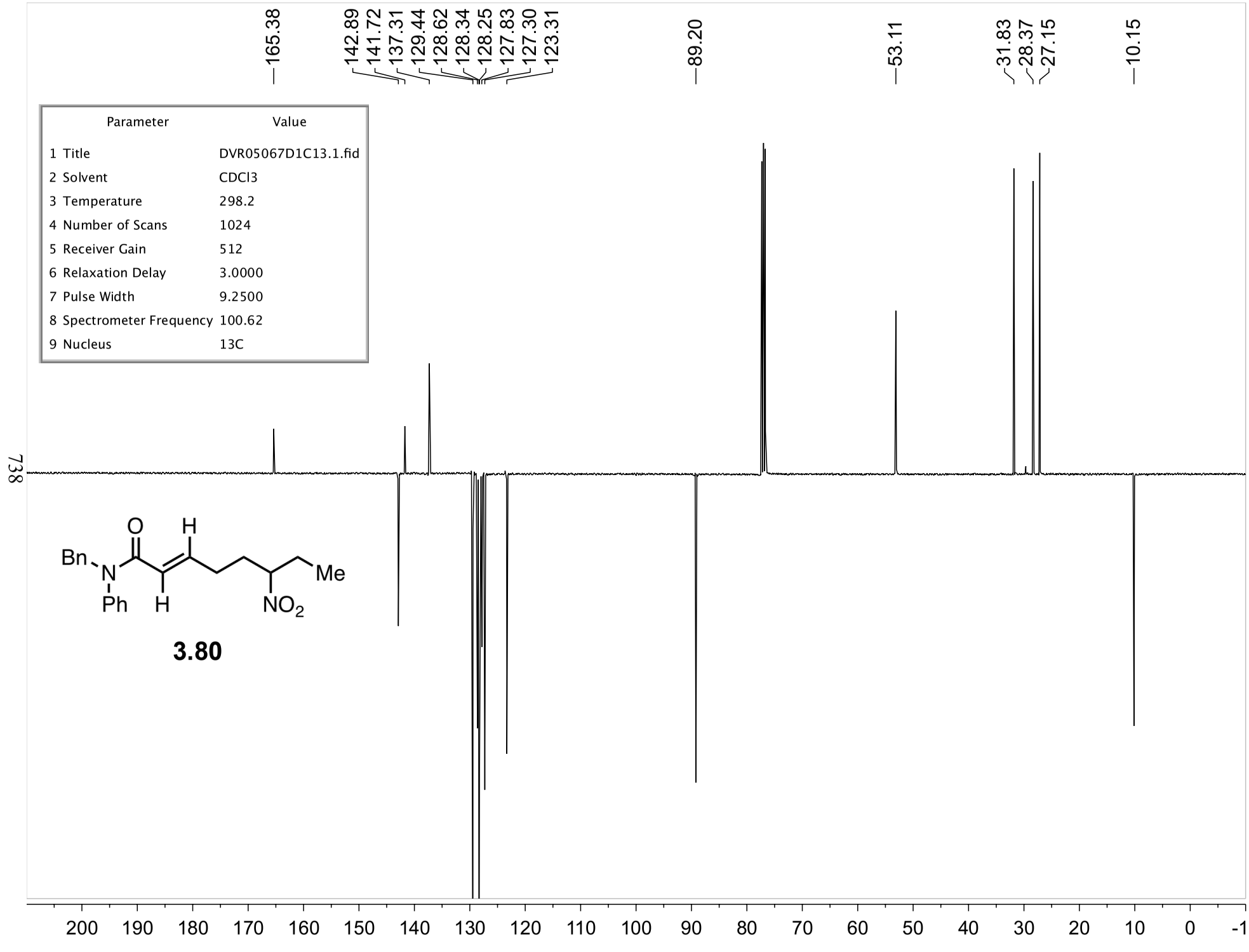
165.38
142.89
141.72
137.31
129.44
128.62
128.34
128.25
127.83
127.30
123.31
89.20
53.11
31.83
28.37
27.15
10.15
Parameter Value
1 Title DVR05067D1C13.1.fid
2 Solvent CDCl3
3 Temperature 298.2
4 Number of Scans 1024
5 Receiver Gain 512
6 Relaxation Delay 3.0000
7 Pulse Width 9.2500
8 Spectrometer Frequency 100.62
9 Nucleus 13C
738
Bn
N
Ph
O
H
H
Me
NO2
3.80
200 190 180 170 160 150 140 130 120 110 100 90 80 70 60 50 40 30 20 10 0 -1

==== Shimadzu LCsolution Analysis Report ====

C:\LabSolutions\Data\DMM\DVR04261_11282016_2040 PM_2.lcd

Acquired by	: LC User
Sample Name	: DVR04261
Sample ID	: DVR04261
Tray#	: 1
Vail #	: 1
Injection Volume	: 3 uL
Data File Name	: DVR04261_11282016_2040 PM_2.lcd
Method File Name	: col1_5isoiPA_30min_1ML_220and210.lcm
Batch File Name	: DMM.lcb
Report File Name	: Default.lcr
Data Acquired	: 11/28/2016 9:51:02 PM
Data Processed	: 11/29/2016 10:15:06 AM

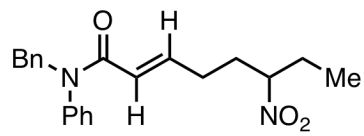

3.80
racemic

<Chromatogram>

C:\LabSolutions\Data\DMM\DVR04261_11282016_2040 PM_2.lcd

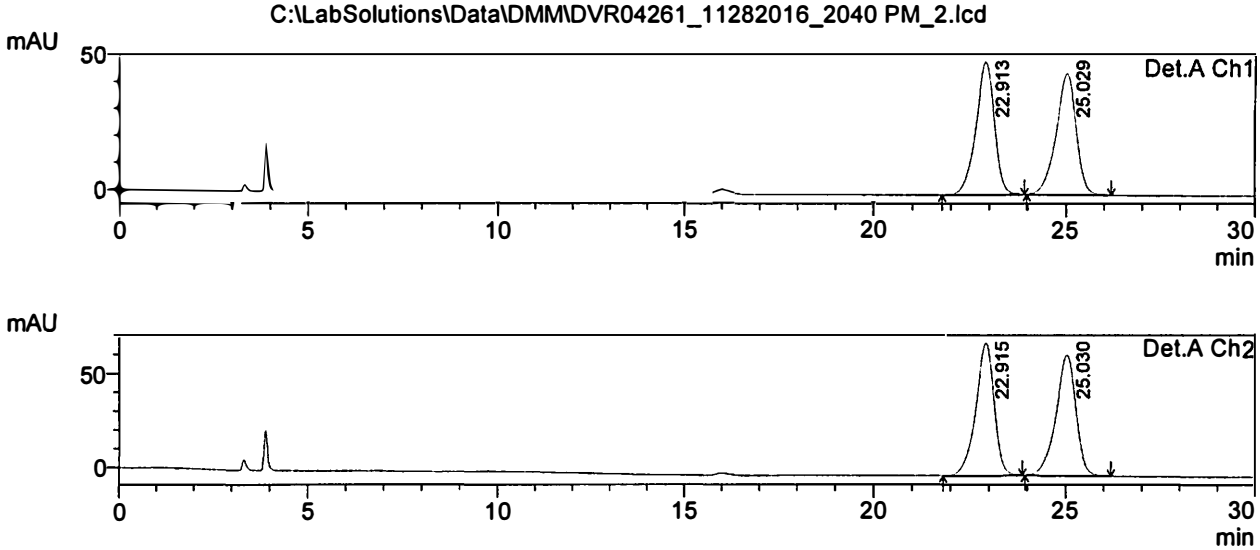

1 Det.A Ch1/220nm
2 Det.A Ch2/210nm

PeakTable

Detector A Ch1 220nm

Peak#	Ret. Time	Area	Height	Area %	Height %
1	22.913	1640779	49207	50.076	52.291
2	25.029	1635815	44896	49.924	47.709
Total		3276593	94103	100.000	100.000

PeakTable

Detector A Ch2 210nm

Peak#	Ret. Time	Area	Height	Area %	Height %
1	22.915	2351690	70527	50.093	52.300
2	25.030	2342912	64325	49.907	47.700
Total		4694603	134852	100.000	100.000

==== Shimadzu LCsolution Analysis Report ====

C:\LabSolutions\Data\DMM\DVR04258 COL1_11232016_1332 PM_10.lcd

Acquired by	: LC User
Sample Name	: DVR04258 COL1
Sample ID	: DVR04258 COL1
Tray#	: 1
Vail #	: 1
Injection Volume	: 3 uL
Data File Name	: DVR04258 COL_1 11232016 1332 PM 1 0.lcd
Method File Name	: col1_5isoiPA 30min 1_ML 220and210.lcm
Batch File Name	: DMM.lcb
Report File Name	: Default.lcr
Data Acquired	: 11/23/2016 8:08:57 PM
Data Processed	: 11/28/2016 10:02:36 AM

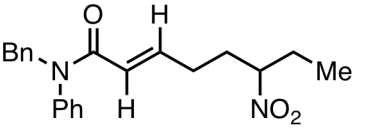

3.80
16% ee

<Chromatogram>

C:\LabSolutions\Data\DMM\DVR04258 COL1_11232016_1332 PM_10.lcd

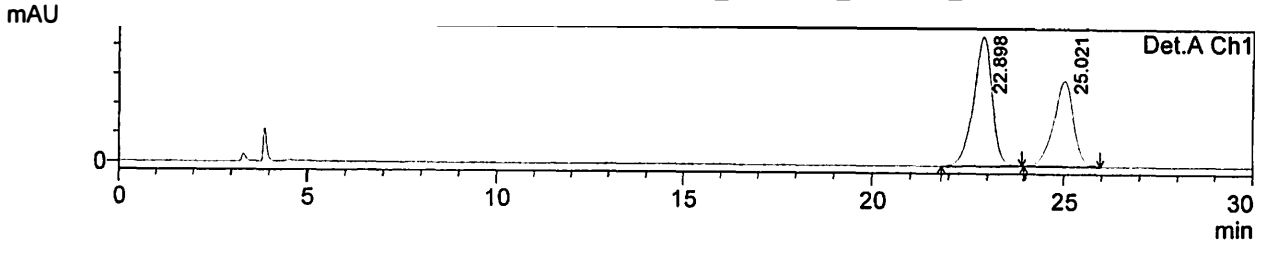

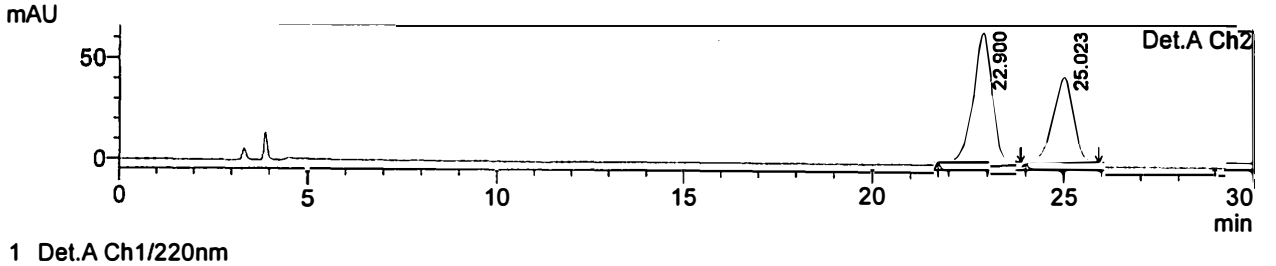

1 Det.A Ch1/220nm
2 Det.A Ch2/210nm

PeakTable

Detector A Ch1 220nm

Peak#	Ret. Time	Area	Height	Area %	Height %
1	22.898	1498085	44612	58.180	60.219
2	25.021	1076816	29471	41.820	39.781
Total		2574901	74083	100.000	100.000

PeakTable

Detector A Ch2 210nm

Peak#	Ret. Time	Area	Height	Area %	Height %
1	22.900	2140251	63852	58.118	60.128
2	25.023	1542333	42341	41.882	39.872
Total		3682584	106193	100.000	100.000

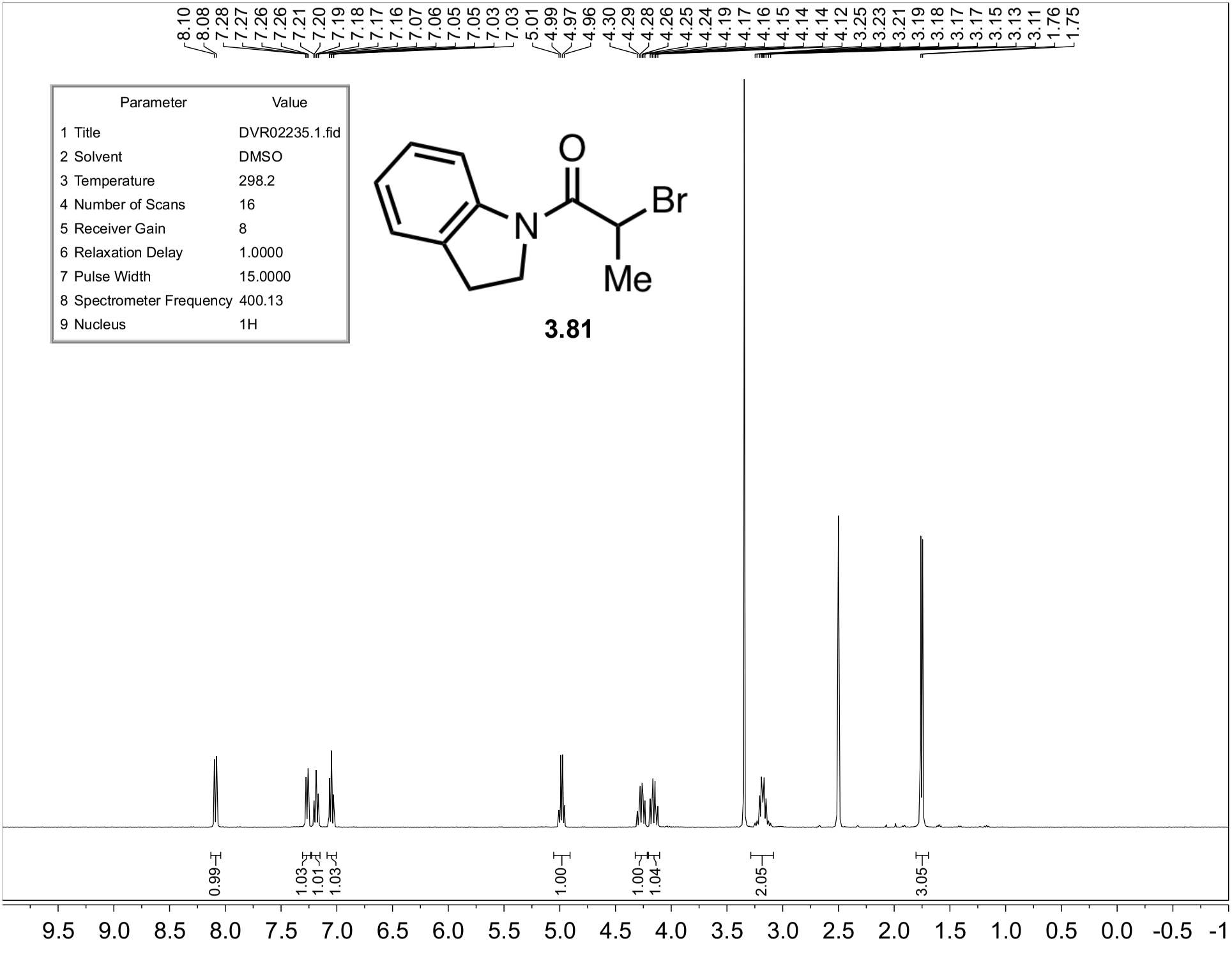
8.10 8.08 7.28 7.27 7.26 7.26 7.21 7.20 7.19 7.18 7.17 7.16 7.07 7.06 7.05 7.05 7.03 7.03 5.01 4.99 4.97 4.96 4.30 4.29 4.28 4.26 4.25 4.24 4.19 4.17 4.16 4.15 4.14 4.14 4.12 3.25 3.23 3.21 3.19 3.18 3.17 3.17 3.15 3.13 3.11 1.76 1.75
Parameter Value
1 Title DVR02235.1.fid
2 Solvent DMSO
3 Temperature 298.2
4 Number of Scans 16
5 Receiver Gain 8
6 Relaxation Delay 1.0000
7 Pulse Width 15.0000
8 Spectrometer Frequency 400.13
9 Nucleus 1H
O
N
Br
Me
3.81
0.99 1.03 1.01 1.03 1.00 1.00 1.04 2.05 3.05
9.5 9.0 8.5 8.0 7.5 7.0 6.5 6.0 5.5 5.0 4.5 4.0 3.5 3.0 2.5 2.0 1.5 1.0 0.5 0.0 -0.5 -1

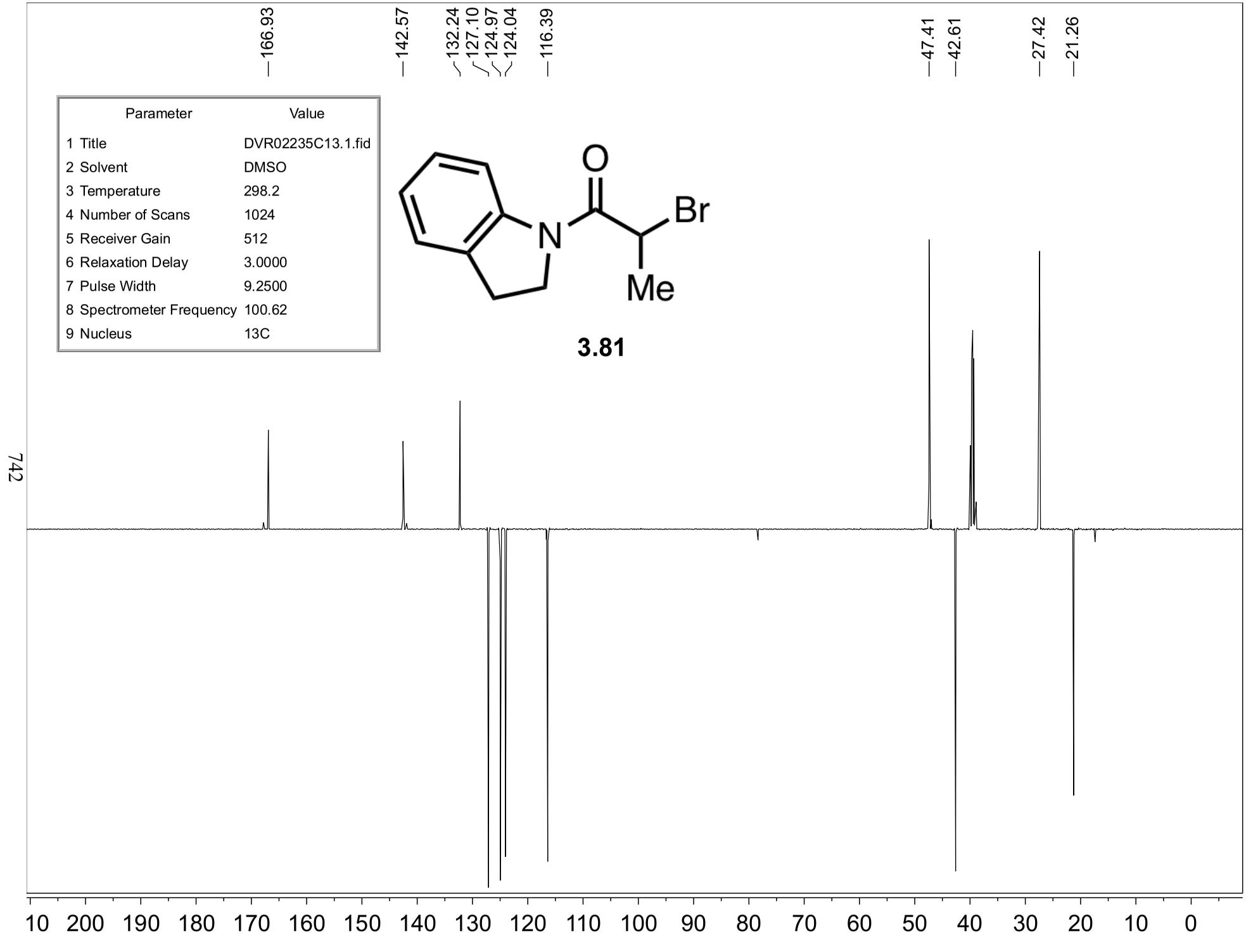
166.93
142.57
132.24
127.10
124.97
124.04
116.39
47.41
42.61
27.42
21.26
Parameter Value
1 Title DVR02235C13.1.fid
2 Solvent DMSO
3 Temperature 298.2
4 Number of Scans 1024
5 Receiver Gain 512
6 Relaxation Delay 3.0000
7 Pulse Width 9.2500
8 Spectrometer Frequency 100.62
9 Nucleus 13C
O
N
Br
Me
3.81
742
10 200 190 180 170 160 150 140 130 120 110 100 90 80 70 60 50 40 30 20 10 0

==== Shimadzu LCsolution Analysis Report ====

C:\LabSolutions\Data\DMM\DVR05088 RAC_682017_1612 PM_3.lcd

Acquired by	: LC User
Sample Name	: DVR05088 RAC
Sample ID	: DVR05088 RAC
Tray#	: 1
Vail #	: 3
Injection Volume	: 5 uL
Data File Name	: DVR05088 RAC_682017_1612 PM_3.lcd
Method File Name	: col1_1isoiPA_70min_1ML_254and210.lcm
Batch File Name	: DMM.lcb
Report File Name	: Default.lcr
Data Acquired	: 6/8/2017 6:14:24 PM
Data Processed	: 6/8/2017 7:34:27 PM

(±)

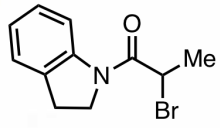

racemic-3.81

<Chromatogram>

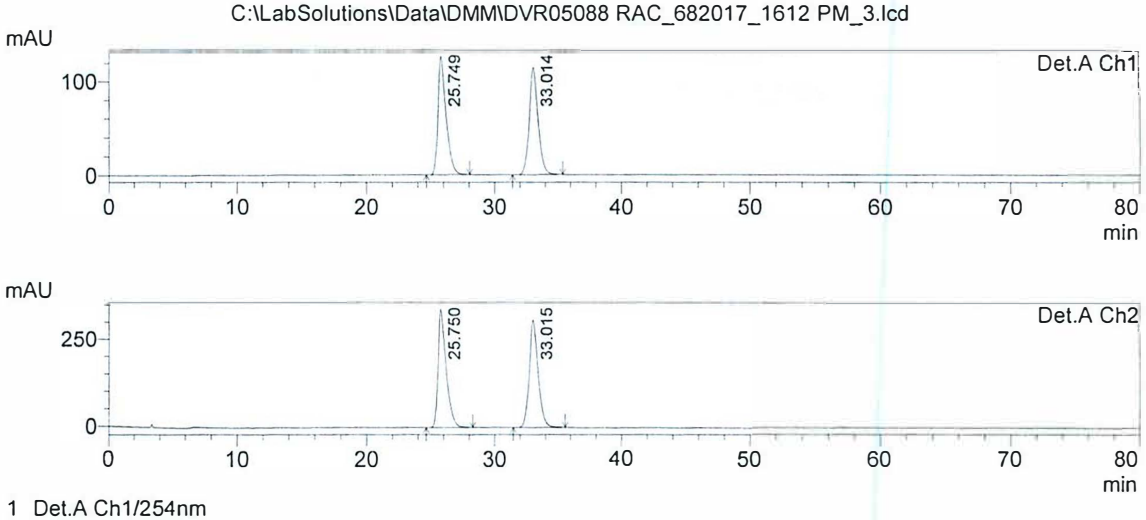

1 Det.A Ch1/254nm
2 Det.A Ch2/210nm

PeakTable

Detector A Ch1 254nm

Peak#	Ret. Time	Area	Height	Area %	Height %
1	25.749	5523757	126927	50.001	52.473
2	33.014	5523525	114965	49.999	47.527
Total		11047282	241892	100.000	100.000

PeakTable

Detector A Ch2 210nm

Peak#	Ret. Time	Area	Height	Area %	Height %
1	25.750	14973238	341657	49.948	52.416
2	33.015	15004329	310163	50.052	47.584
Total		29977568	651820	100.000	100.000

==== Shimadzu LCsolution Analysis Report ====

C:\LabSolutions\Data\DMM\DVR05080 CROP2_5312017_1028 AM_4.lcd

Acquired by	: LC User
Sample Name	: DVR05080 CROP2
Sample ID	: DVR05080 CROP2
Tray#	: 1
Vail #	: 1
Injection Volume	: 7 uL
Data File Name	: DVR05080 CROP2_5312017_1028 AM_4.lcd
Method File Name	: col1_1isoiPA_45min_1ML_220and210.lcm
Batch File Name	: DMM.lcb
Report File Name	: Default.lcr
Data Acquired	: 5/31/2017 12:20:55 PM
Data Processed	: 5/31/2017 1:05:56 PM

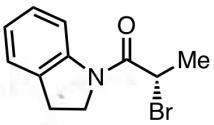

(*S*)-3.81, >99% ee

<Chromatogram>

C:\LabSolutions\Data\DMM\DVR05080 CROP2_5312017_1028 AM_4.lcd

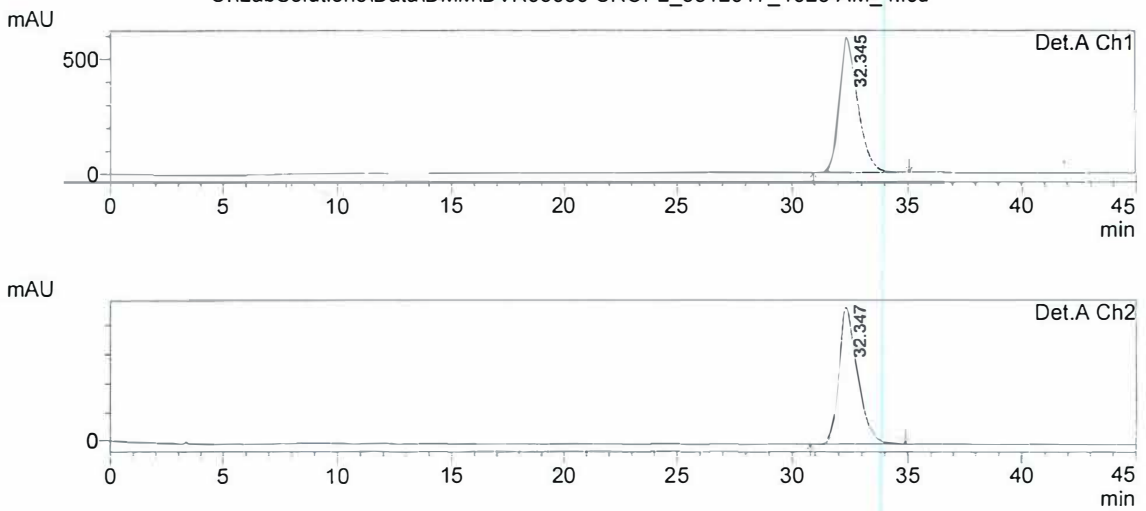

1 Det.A Ch1/220nm
2 Det.A Ch2/210nm

PeakTable

Detector A Ch1 220nm

Peak#	Ret. Time	Area	Height	Area %	Height %
1	32.345	31626570	585635	100.000	100.000
Total		31626570	585635	100.000	100.000

PeakTable

Detector A Ch2 210nm

Peak#	Ret. Time	Area	Height	Area %	Height %
1	32.347	50981975	932861	100.000	100.000
Total		50981975	932861	100.000	100.000

==== Shimadzu LCsolution Analysis Report ====

C:\LabSolutions\Data\DMM\DVR05085 CROP1_612017_1219 PM_2.lcd

Acquired by	: LC User
Sample Name	: DVR05085 CROP1
Sample ID	: DVR05085 CROP1
Tray#	: 1
Vail #	: 1
Injection Volume	: 5 uL
Data File Name	: DVR05085 CROP1_612017_1219 PM_2.lcd
Method File Name	: col1_1isoiPA_45min_1ML_220and210.lcm
Batch File Name	: DMM.lcb
Report File Name	: Default.lcr
Data Acquired	: 6/1/2017 12:29:48 PM
Data Processed	: 6/1/2017 1:14:50 PM

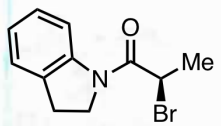

(*R*)-3.81, >99% ee

<Chromatogram>

C:\LabSolutions\Data\DMM\DVR05085 CROP1_612017_1219 PM_2.lcd

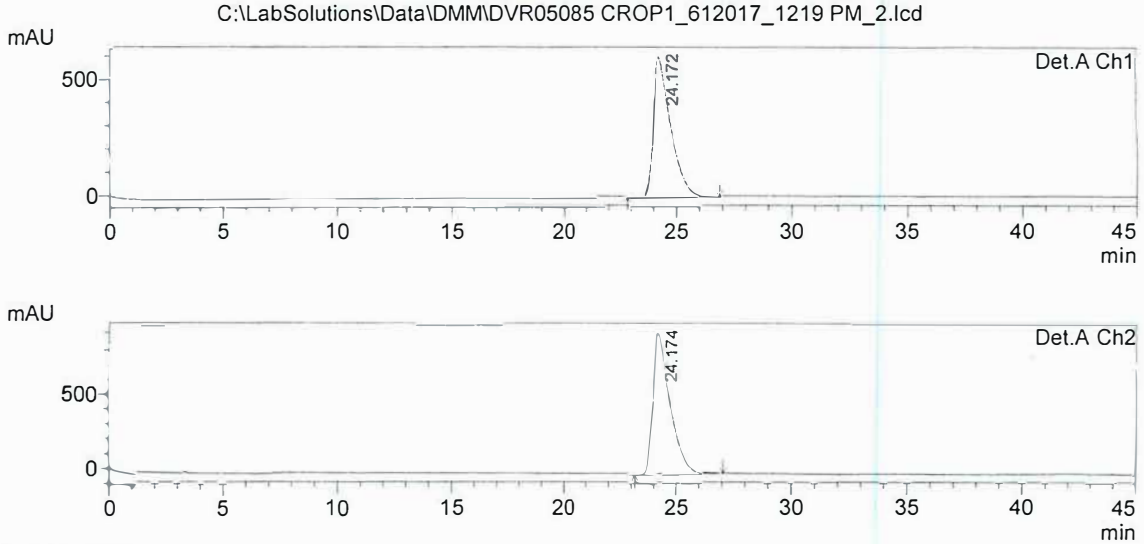

1 Det.A Ch1/220nm
2 Det.A Ch2/210nm

PeakTable

Detector A Ch1 220nm

Peak#	Ret. Time	Area	Height	Area %	Height %
1	24.172	31383329	603604	100.000	100.000
Total		31383329	603604	100.000	100.000

PeakTable

Detector A Ch2 210nm

Peak#	Ret. Time	Area	Height	Area %	Height %
1	24.174	50736042	961453	100.000	100.000
Total		50736042	961453	100.000	100.000

==== Shimadzu LCsolution Analysis Report ====

C:\LabSolutions\Data\DMM\DVR05088B_682017 1612 PM_2.lcd

Acquired by	: LC User
Sample Name	: DVR05088B
Sample ID	: DVR05088B
Tray#	: 1
Vail #	: 2
Injection Volume	: 3 uL
Data File Name	: DVR05088B_682017_1612 PM_2.lcd
Method File Name	: col1_1isoiPA_70min_1ML_254and210.lcm
Batch File Name	: DMM.lcb
Report File Name	: Default.lcr
Data Acquired	: 6/8/2017 4:28:27 PM
Data Processed	: 6/8/2017 5:58:36 PM

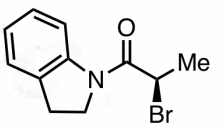

using (*R*)-3.81, >99% ee

<Chromatogram>

C:\LabSolutions\Data\DMM\DVR05088B_682017_1612 PM_2.lcd

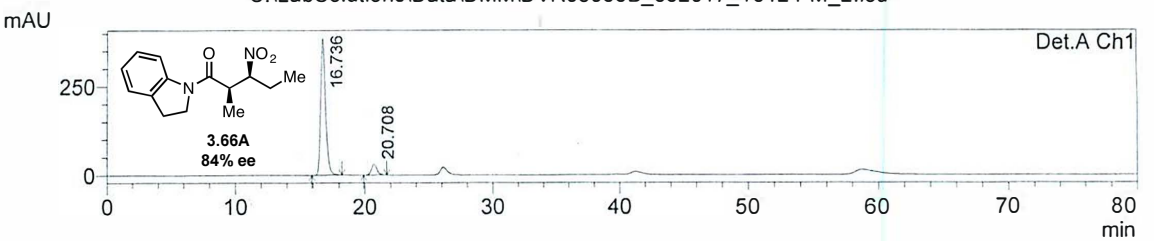

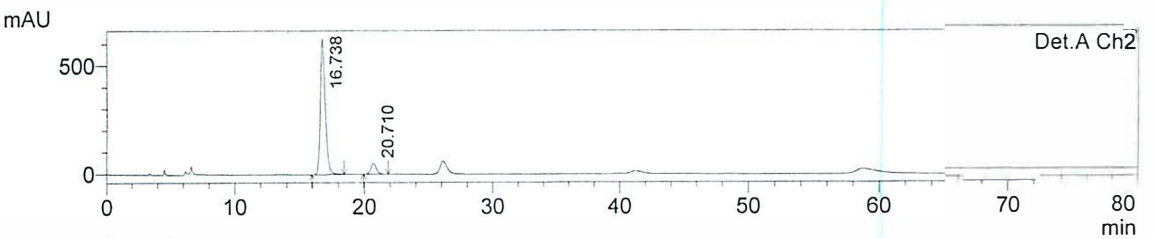

1 Det.A Ch1/254nm
2 Det.A Ch2/210nm

PeakTable

Detector A Ch1 254nm

Peak#	Ret. Time	Area	Height	Area %	Height %
1	16.736	9966909	385908	91.608	92.589
2	20.708	913061	30889	8.392	7.411
Total		10879970	416797	100.000	100.000

PeakTable

Detector A Ch2 210nm

Peak#	Ret. Time	Area	Height	Area %	Height %
1	16.738	16383132	628903	91.531	92.486
2	20.710	1515871	51098	8.469	7.514
Total		17899003	680001	100.000	100.000

==== Shimadzu LCsolution Analysis Report ====

C:\LabSolutions\Data\DMM\DVR05088B_682017_1612 PM_2.lcd

Acquired by	: LC User
Sample Name	: DVR05088B
Sample ID	: DVR05088B
Tray#	: 1
Vail #	: 2
Injection Volume	: 3 uL
Data File Name	: DVR05088B_682017_1612 PM_2.lcd
Method File Name	: col1_1isoiPA_70min_1ML_254and210.lcm
Batch File Name	: DMM.lcb
Report File Name	: Default.lcr
Data Acquired	: 6/8/2017 4:28:27 PM
Data Processed	: 6/8/2017 5:59:42 PM

<Chromatogram>

C:\LabSolutions\Data\DMM\DVR05088B_682017_1612 PM_2.lcd

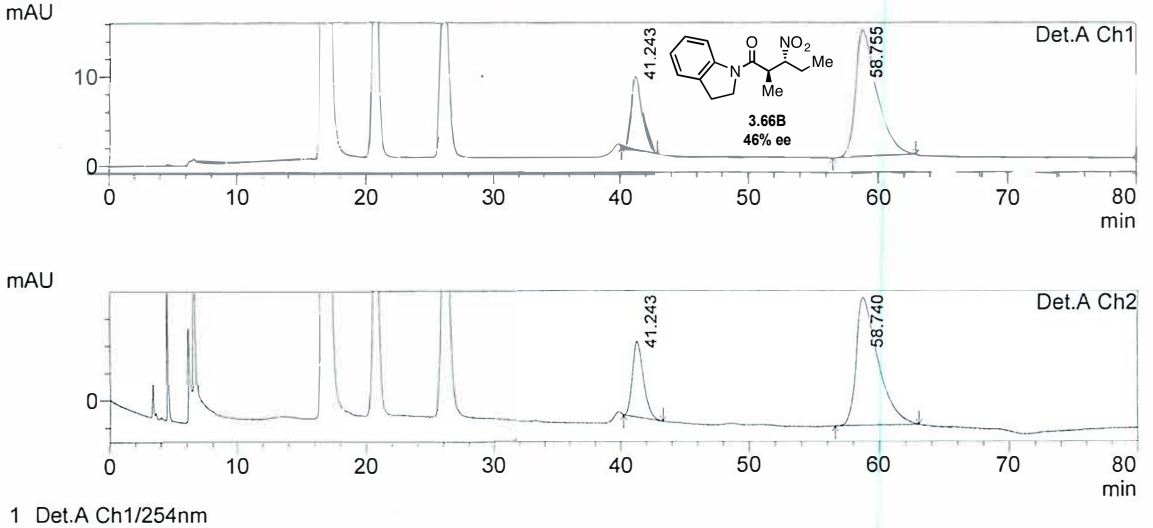

1 Det.A Ch1/254nm
2 Det.A Ch2/210nm

PeakTable

Detector A Ch1 254nm

Peak#	Ret. Time	Area	Height	Area %	Height %
1	41.243	486573	8311	22.758	36.765
2	58.755	1651498	14295	77.242	63.235
Total		2138071	22606	100.000	100.000

PeakTable

Detector A Ch2 210nm

Peak#	Ret. Time	Area	Height	Area %	Height %
1	41.243	823845	13760	23.287	37.186
2	58.740	2713945	23242	76.713	62.814
Total		3537790	37002	100.000	100.000

==== Shimadzu LCsolution Analysis Report ====

C:\LabSolutions\Data\DMM\DVR05088B_682017_1612 PM_2.lcd

Acquired by	: LC User
Sample Name	: DVR05088B
Sample ID	: DVR05088B
Tray#	: 1
Vail #	: 2
Injection Volume	: 3 uL
Data File Name	: DVR05088B_682017_1612 PM_2.lcd
Method File Name	: col1_1isoiPA_70min_1ML_254and210.lcm
Batch File Name	: DMM.lcb
Report File Name	: Default.lcr
Data Acquired	: 6/8/2017 4:28:27 PM
Data Processed	: 6/8/2017 5:48:30 PM

<Chromatogram>

C:\LabSolutions\Data\DMM\DVR05088B_682017_1612 PM_2.lcd

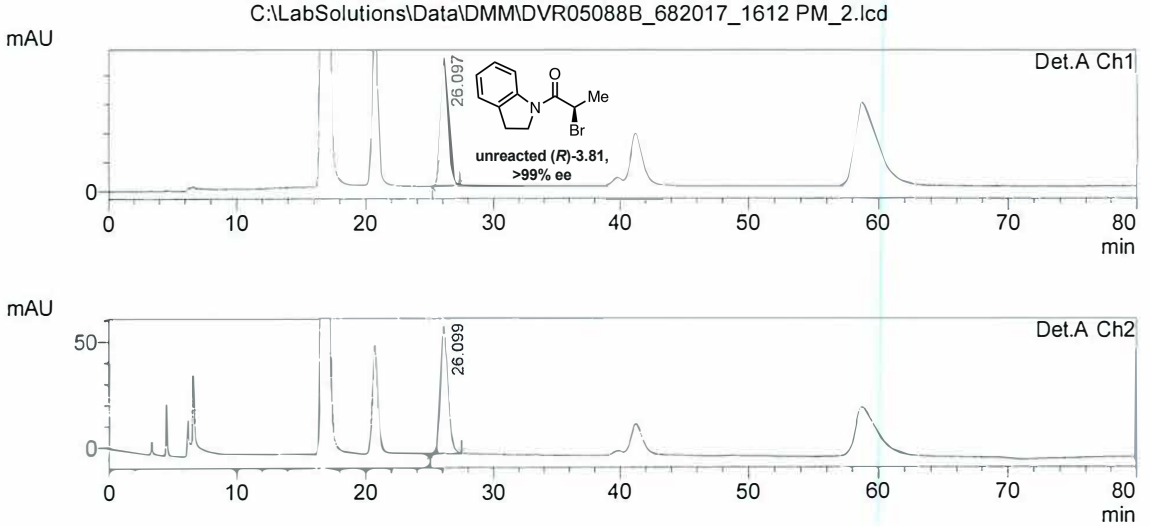

1 Det.A Ch1/254nm
2 Det.A Ch2/210nm

PeakTable

Detector A Ch1 254nm

Peak#	Ret. Time	Area	Height	Area %	Height %
1	26.097	827395	22041	100.000	100.000
Total		827395	22041	100.000	100.000

PeakTable

Detector A Ch2 210nm

Peak#	Ret. Time	Area	Height	Area %	Height %
1	26.099	2270685	60158	100.000	100.000
Total		2270685	60158	100.000	100.000

==== Shimadzu LCsolution Analysis Report ====

C:\LabSolutions\Data\DMM\DVR05088A_682017_1113 AM_2.lcd

Acquired by	: LC User
Sample Name	: DVR05088A
Sample ID	: DVR05088A
Tray#	: 1
Vail #	: 1
Injection Volume	: 3 uL
Data File Name	: DVR05088A_682017_1113 AM_2.lcd
Method File Name	: col1_1isoiPA_70min_1ML_254and210.lcm
Batch File Name	: DMM.lcb
Report File Name	: Default.lcr
Data Acquired	: 6/8/2017 11:28:54 AM
Data Processed	: 6/8/2017 5:33:03 PM

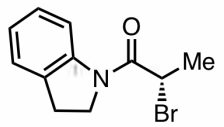

using (*S*)-3.81, >99% ee

<Chromatogram>

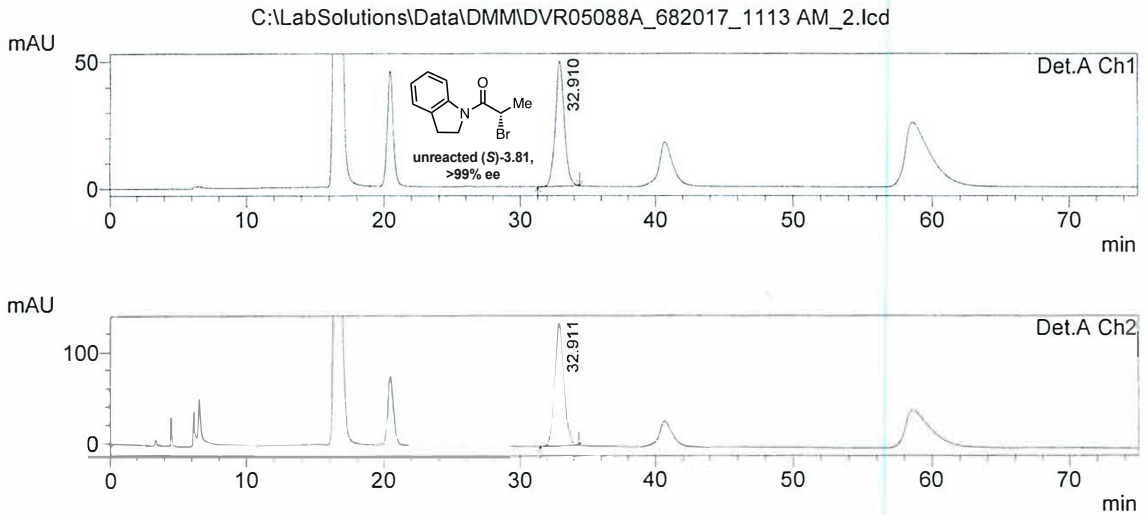

1 Det.A Ch1/254nm
2 Det.A Ch2/210nm

PeakTable

Detector A Ch1 254nm

Peak#	Ret. Time	Area	Height	Area %	Height %
1	32.910	2257829	49329	100.000	100.000
Total		2257829	49329	100.000	100.000

PeakTable

Detector A Ch2 210nm

Peak#	Ret. Time	Area	Height	Area %	Height %
1	32.911	6129378	133936	100.000	100.000
Total		6129378	133936	100.000	100.000

==== Shimadzu LCsolution Analysis Report ====

C:\LabSolutions\Data\DMM\DVR05088A_682017_1113 AM_2.lcd

Acquired by	: LC User
Sample Name	: DVR05088A
Sample ID	: DVR05088A
Tray#	: 1
Vail #	: 1
Injection Volume	: 3 uL
Data File Name	: DVR05088A_682017_1113 AM_2.lcd
Method File Name	: col1_1isoiPA_70min_1ML_254and210.lcm
Batch File Name	: DMM.lcb
Report File Name	: Default.lcr
Data Acquired	: 6/8/2017 11:28:54 AM
Data Processed	: 6/8/2017 12:48:55 PM

<Chromatogram>

C:\LabSolutions\Data\DMM\DVR05088A_682017_1113 AM_2.lcd

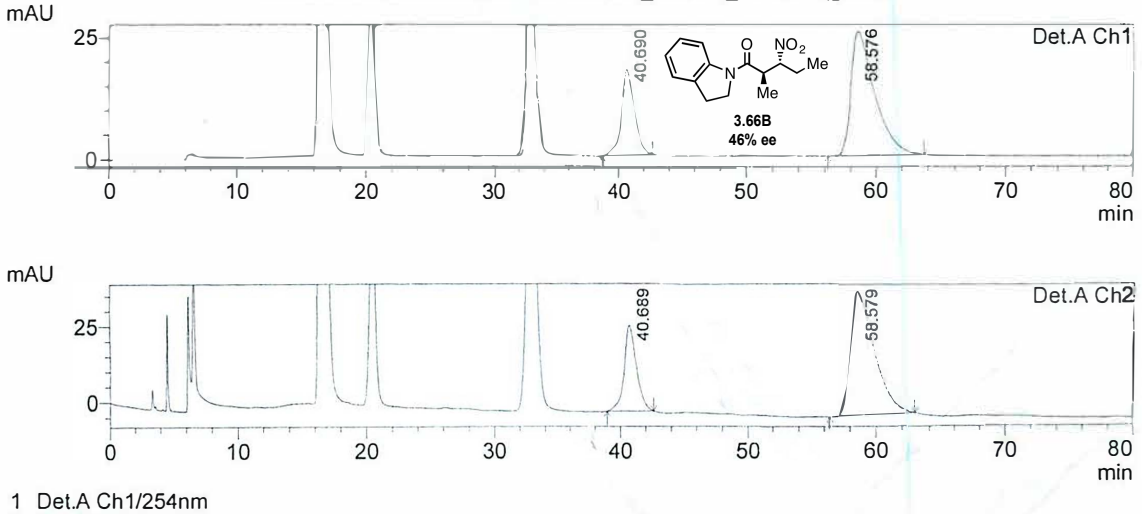

1 Det.A Ch1/254nm
2 Det.A Ch2/210nm

PeakTable

Detector A Ch1 254nm

Peak#	Ret. Time	Area	Height	Area %	Height %
1	40.690	1200115	17509	27.142	40.781
2	58.576	3221427	25425	72.858	59.219
Total		4421542	42935	100.000	100.000

PeakTable

Detector A Ch2 210nm

Peak#	Ret. Time	Area	Height	Area %	Height %
1	40.689	1897306	28196	27.003	40.638
2	58.579	5128882	41187	72.997	59.362
Total		7026188	69384	100.000	100.000

==== Shimadzu LCsolution Analysis Report ====

C:\LabSolutions\Data\DMM\DVR05088A_682017_1113 AM_2.lcd

Acquired by	: LC User
Sample Name	: DVR05088A
Sample ID	: DVR05088A
Tray#	: 1
Vail #	: 1
Injection Volume	: 3 uL
Data File Name	: DVR05088A_682017_1113 AM_2.lcd
Method File Name	: col1_1isoiPA_70min_1ML_254and210.lcm
Batch File Name	: DMM.lcb
Report File Name	: Default.lcr
Data Acquired	: 6/8/2017 11:28:54 AM
Data Processed	: 6/8/2017 12:48:55 PM

<Chromatogram>

C:\LabSolutions\Data\DMM\DVR05088A_682017_1113 AM_2.lcd

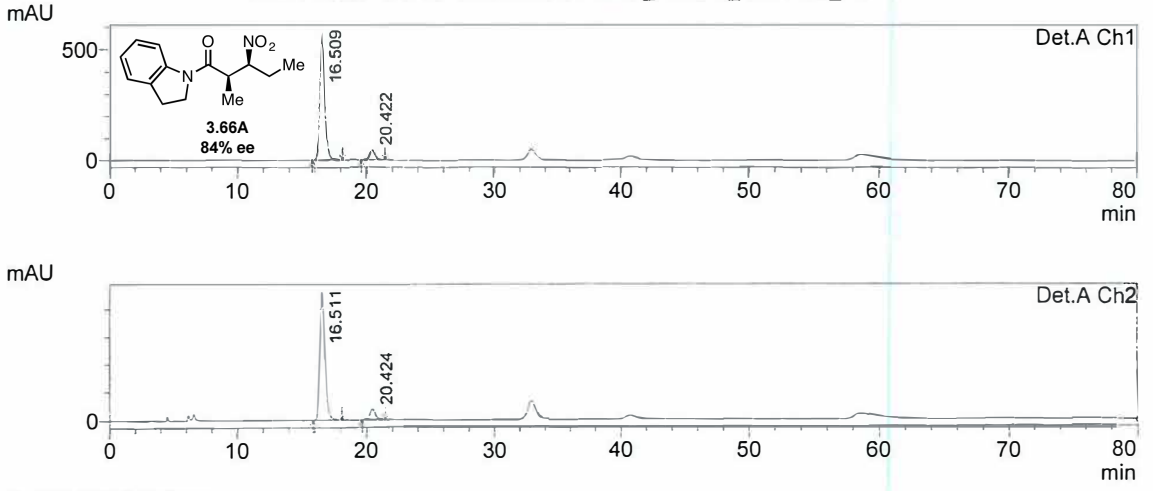

1 Det.A Ch1/254nm
2 Det.A Ch2/210nm

PeakTable

Detector A Ch1 254nm

Peak#	Ret. Time	Area	Height	Area %	Height %
1	16.509	14896468	575351	91.767	92.689
2	20.422	1336390	45383	8.233	7.311
Total		16232859	620734	100.000	100.000

PeakTable

Detector A Ch2 210nm

Peak#	Ret. Time	Area	Height	Area %	Height %
1	16.511	24214155	924284	91.633	92.488
2	20.424	2210874	75070	8.367	7.512
Total		26425029	999354	100.000	100.000

Appendix C

PERMISSION LETTERS

Title: Trifluoromethylation of Secondary Nitroalkanes

Author: Amber A. S. Gietter-Burch, Vijayarajan Devannah, Donald A. Watson

Publication: Organic Letters

Publisher: American Chemical Society

Date: Jun 1, 2017

PERMISSION/LICENSE IS GRANTED FOR YOUR ORDER AT NO CHARGE

This type of permission/license, instead of the standard Terms & Conditions, is sent to you because no fee is being charged for your order. Please note the following:

- Permission is granted for your request in both print and electronic formats, and translations.
- If figures and/or tables were requested, they may be adapted or used in part.
- Please print this page for your records and send a copy of it to your publisher/graduate school.
- Appropriate credit for the requested material should be given as follows: "Reprinted (adapted) with permission from (COMPLETE REFERENCE CITATION). Copyright (YEAR) American Chemical Society." Insert appropriate information in place of the capitalized words.
- One-time permission is granted only for the use specified in your request. No additional uses are granted (such as derivative works or other editions). For any other uses, please submit a new request.

Title: Nickel-Catalyzed C-Alkylation of Nitroalkanes with Unactivated Alkyl Iodides

Author: Sina Rezazadeh, Vijayarajan Devannah, Donald A. Watson

Publication: Journal of the American Chemical Society

Publisher: American Chemical Society

Date: Jun 1, 2017

PERMISSION/LICENSE IS GRANTED FOR YOUR ORDER AT NO CHARGE

This type of permission/license, instead of the standard Terms & Conditions, is sent to you because no fee is being charged for your order. Please note the following:

- Permission is granted for your request in both print and electronic formats, and translations.
- If figures and/or tables were requested, they may be adapted or used in part.
- Please print this page for your records and send a copy of it to your publisher/graduate school.
- Appropriate credit for the requested material should be given as follows: "Reprinted (adapted) with permission from (COMPLETE REFERENCE CITATION). Copyright (YEAR) American Chemical Society." Insert appropriate information in place of the capitalized words.
- One-time permission is granted only for the use specified in your request. No additional uses are granted (such as derivative works or other editions). For any other uses, please submit a new request.